THE UNIVERSITY OF CHICAGO

# TRANSITION METAL CATALYZED C−C ACTIVATION: NATURAL PRODUCT SYNTHESIS AND POLYMER DEGRADATION

A DISSERTATION SUBMITTED TO

THE FACULTY OF THE DIVISION OF THE PHYSICAL SCIENCES

IN CANDIDACY FOR THE DEGREE OF

DOCTOR OF PHILOSOPHY

DEPARTMENT OF CHEMISTRY

BY

YIBIN XUE

CHICAGO, ILLINOIS

DECEMBER 2022

To my family

TABLE OF CONTENT

LIST OF SCHEMES ..... vii

LIST OF FIGURES ..... xii

LIST OF TABLES ..... xxx

LIST OF ABBREVIATIONS ..... xxxvi

ACKNOWLEDGEMENT ..... xlv

Chapter 1: Deconstructive Synthesis of Bridged and Fused Rings via Transition Metal-Catalyzed "Cut-and-Sew" Reactions of Benzocyclobutenones and Cyclobutanones ..... 1

1.1. Introduction ..... 1

1.2. Method Development ..... 3

1.2.1 (4+2) "Cut-and-Sew" Reaction of Benzocyclobutenone ..... 3

1.2.2 (4+2) "Cut-and-Sew" Reaction of Cyclobutanone ..... 10

1.2.3 (4+2−1) "Cut-and-Sew" Reaction of Benzocyclobutenone and Cyclobutanone ..... 16

1.2.4 (4+1) "Cut-and-Sew" Reaction of Benzocyclobutenone and Cyclobutanone ..... 18

1.3. Application in Total Synthesis ..... 21

1.3.1 Total Synthesis of Cycloinumakiol (Proposed Structure) ..... 22

1.3.2 Enantioselective Total Synthesis of (−)-Cycloclavine ..... 23

1.3.3 Enantioselective Total Synthesis of (−)-Thebainone A ..... 25

1.4. Summary and Outlook ..... 28

1.5. References ..... 30

Chapter 2: Total Synthesis of Penicibilaenes via C−C Activaton-Enabled Deconstruction and Desaturation Relay-Mediated C−H Functionalization ..... 37

2.1. Introduction..... 37

2.2. First Generation Route..... 39

2.3. Second Generation Route ..... 71

2.4. Third Generation Route ..... 93

2.5. Conclusion .....118

2.6. Experimental.....118

2.6.1 General Information .....118

2.6.2 Experimental Procedure and Characterization Data.....119

2.6.3 Comparison of Spectroscopic Data of the Natural and Synthetic Products ..... 200

2.6.4 Crystal Data and Structure Refinement..... 205

2.6.5 NMR Spectra..... 210

2.7. References..... 270

Chapter 3: Catalytic Activation of Unstrained C(aryl)−C(alkyl) Bonds in 2,2'-Methylenediphenols ..... 281

3.1. Introduction..... 281

3.2. Discovery and Optimization..... 284

3.3. Substrate Scope and Applications..... 288

3.4. Mechanism Study ..... 293

3.5. Conclusion ..... 300

3.6. Experimental ..... 301

3.7. NMR Spectra ..... 414

3.8. References ..... 548

Chapter 4: Mono-Directed Catalytic Activation of Unstrained C(Aryl)−C(Alkyl) Bonds in α-Methyl Phenols ..... 556

4.1. Introduction ..... 556

4.2. Discovery and Optimization ..... 561

4.3. Conclusion ..... 579

4.4. Experimental ..... 580

4.5. NMR Spectra ..... 591

4.6. References ..... 610

LIST OF SCHEMES

**Scheme 1.1.** "Cut-and-Sew" Reaction of Benzocyclobutenone and Cyclobutanone, and Their Applications. ..... 3

**Scheme 1.2.** Rhodium Catalyzed (4+2) "Cut-and-Sew" Reaction between Benzocyclobutenone and Alkene. ..... 5

**Scheme 1.3.** Rhodium Catalyzed Asymmetric (4+2) "Cut-and-Sew" Reaction between Benzocyclobutenone and Alkene. ..... 6

**Scheme 1.4.** Rhodium Catalyzed (4+2) "Cut-and-Sew" Reaction between Benzocyclobutenone and Alkyne. ..... 7

**Scheme 1.5.** Cobalt Catalyzed (4+2) "Cut-and-Sew" Reaction between Benzocyclobutenone and Alkyne. ..... 8

**Scheme 1.6.** Rhodium Catalyzed Asymmetric (4+2) "Cut-and-Sew" Reaction between Benzocyclobutenone and Imine. ..... 9

**Scheme 1.7.** Rhodium Catalyzed Asymmetric (4+2) "Cut-and-Sew" Reaction between Benzocyclobutenone and Ketone/Aldehyde. ..... 9

**Scheme 1.8.** Murakami's Pioneer Work on Rhodium Catalyzed (4+2) "Cut-and-Sew" Reaction between Cyclobutanone and Alkene. ..... 11

**Scheme 1.9.** Transient Directing Group Enabled Rhodium Catalyzed (4+2) "Cut-and-Sew" Reaction between Cyclobutanone and Alkene. ..... 12

**Scheme 1.10.** Rhodium Catalyzed (4+2) "Cut-and-Sew" Reaction between Cyclobutanone and Alkene/Ketone/Aldehyde. ..... 13

**Scheme 1.11.** Rhodium Catalyzed (4+2) "Cut-and-Sew" Reaction between Cyclobutanone and Alkyne. ..... 14

**Scheme 1.12.** Rhodium Catalyzed (4+2) "Cut-and-Sew" Reaction between $\alpha$-Branched Cyclobutanone and Alkyne. ..... 15

**Scheme 1.13.** Rhodium Catalyzed Asymmetric (4+2) "Cut-and-Sew" Reaction between $\alpha$-Branched Cyclobutanone and Alkyne. ..... 16

**Scheme 1.14.** Rhodium Catalyzed (4+2−1) "Cut-and-Sew" Reaction between Benzocyclobutenone and Alkyne. ..... 17

**Scheme 1.15.** Rhodium Catalyzed (4+2−1) "Cut-and-Sew" Reaction between Cyclobutenone and Alkene. ..... 18

**Scheme 1.16.** Rhodium Catalyzed (4+1) "Cut-and-Sew" Reaction between Benzocyclobutenone and Styrene ..... 19

**Scheme 1.17.** Rhodium Catalyzed (4+1) "Cut-and-Sew" Reaction between Cyclobutenone and Allene. ..... 21

**Scheme 1.18.** Total Synthesis of Cycloinumakiol (Proposed Structure) ..... 23

**Scheme 1.19.** Enantioselective Total Synthesis of (−)-Cycloclavine. ..... 25

**Scheme 1.20.** Deconstructive Asymmetric Total Synthesis of (−)-Thebainone A. ..... 28

**Scheme 2.1.** Approach for Terpene Synthesis ..... 38

**Scheme 2.2.** Retrosyntic Analysis of First Generation Route ..... 39

**Scheme 2.3.** Synthesis of Triene **2.7** ..... 40

**Scheme 2.4.** Alternative Route to Construct Cyclobutanone **2.6**. ..... 41

**Scheme 2.5.** Synthesis of stannane **2.15** and dichlorocyclobutanone **2.22**. ..... 42

**Scheme 2.6.** Protection of Double Bond. ..... 45

**Scheme 2.7.** Preparation of Epoxide **2.24**. ..... 46

**Scheme 2.8.** Proposed Mechanism of Rearrangement from **2.24** to **2.27**. ..... 48

**Scheme 2.9.** Synthesis of Cyclobutanone **2.36** (Initial Route). ..... 49

**Scheme 2.10.** Synthesis of Cyclobutanone **2.36** (Optimized Route). ..... 50

**Scheme 2.11.** Proposed Mechanism for Generation of Lactone **2.47**. ..... 54

**Scheme 2.12.** Preparation of Methyl Ether Tethered Cyclobutanone **2.52**. ..... 55

**Scheme 2.13.** Preparation of Methyl Ether Tethered Cyclobutanone **2.54**. ..... 57

**Scheme 2.14.** Design of Ester Linker. ..... 58

**Scheme 2.15.** Preparation of Cyclobutanone **2.62**. ..... 59

**Scheme 2.16.** Preparation of Ketal **2.68** through Three-Components Coupling. ..... 60

**Scheme 2.17.** Linker Effect in the "cut-and-sew" reaction. ..... 67

**Scheme 2.18.** Proposed Retrosynthetic Analysis Enabled by "Cut-and-Sew" Reaction of Ester Tethered Cyclobutanone. ..... 68

**Scheme 2.19.** Preparation of Cyclobutanone **2.75**. ..... 68

**Scheme 2.20.** Preparation of Cyclobutanone **2.91**. ..... 70

**Scheme 2.21.** The Second Generation Strategy to Synthesize Penicibilaenes. ..... 71

**Scheme 2.22.** Preparation of Cyclobutanone **2.95**. ..... 72

**Scheme 2.23.** Gram-Scale "Cut-and-Sew" Reaction of Cyclobutanone **2.95**. ..... 81

**Scheme 2.24.** Total Synthesis of Penicibilaenes through "Cut-and-Sew" Reaction of Cyclobutanone **2.110**..... 83

**Scheme 2.25.**Approach to Prepare Cyclobutanone **2.110**. ..... 84

**Scheme 2.26.** Total Synthesis of Penicibilaenes through "Cut-and-Sew" Reaction of Cyclobutanone **2.118**..... 85

**Scheme 2.27.** Preparation of Alcohol **2.124**. ..... 85

**Scheme 2.28.** Preparation of Cyclobutanone **2.118**..... 86

**Scheme 2.29.** Side Products Analysis on "Cut-and-Sew" Reaction of Cyclobutanone **2.118**. .... 93

**Scheme 2.30.** Retrosynthetic Analysis (Third Generation Route). ..... 94

**Scheme 2.31.** X-Ray Structure of hydrazone **2.139**. ..... 97

**Scheme 2.32.** Approach to Install Oxygen on C4 through Schönecker−Baran Oxidation. ..... 97

**Scheme 2.33.** Preparation of *O*-Methyl Oxime **2.143**. ..... 98

**Scheme 2.34.** Approach to Install Oxygen on C4 through 1,5-HAT. ..... 99

**Scheme 2.35.** Approach to Install Oxygen on C4 through Hartwig C−H hydroxylation. ..... 101

**Scheme 2.36.** Approach to Install Oxygen on C4 through Gevorgyan C−H Functionalization. 102

**Scheme 2.37.** Methylation of Protection of Enone **2.167**..... 108

**Scheme 2.38.** Oxidation of Ketone **2.175** and Methylation of Ketone **2.177**. .....113

**Scheme 2.39.** Preparation of Diol through Hoveyda *β*-Boration. .....113

**Scheme 2.40.** Saegusa Oxidation of Silyl Enol Ether **2.183** and **2.184**. .....115

**Scheme 2.41.** Synthesis of Penicibilaenes A and B. .....117

**Scheme 3.1.** TM-mediated C(aryl)−C(alkyl) Bond Activation. ..... 283

**Scheme 3.2.** Gram-Scale Synthesis and One-Pot Synthesis..... 291

**Scheme 3.3.** C−C Cleavage of Oligomers. ..... 292

**Scheme 3.4.** C−C Cleavage of Novolacs..... 293

**Scheme 3.5.** Preparation of Intermediate [Rh(**3.2g**)Cl]$_2$. ..... 294

**Scheme 3.6.** Mechanism Studies on Complex **3.5**. ..... 295

**Scheme 3.7.** Deuterium Labeling. ..... 296

**Scheme 3.8.** Kenetic Order Measurement. ..... 297

**Scheme 3.9.** Proposed Catalytic Cycles and Computed Energies (Path A). ..... 298

**Scheme 3.10.** Proposed Catalytic Cycles and Computed Energies (Path B). ..... 299

**Scheme 4.1.** Bidentate Ligand Chelation-Assisted Unstained C−C Bond Activation via Oxidative Addition. ..... 558

**Scheme 4.2.** Monodentate Ligand Chelation-Assisted Unstained C−C Bond Activation. ..... 560

**Scheme 4.3.** Mono-Directed Catalytic C−C Activation. ..... 561

**Scheme 4.4.** Preparation of Phosphinite **4.2a**. ..... 561

**Scheme 4.5.** Preparation of Phosphinite **4.6a**. ..... 570

**Scheme 4.6.** C−C Activation of Phosphinite **4.5a** with bidentate NHC ligands. ..... 573

**Scheme 4.7.** C−C Activation of Phosphinite **4.5a** (Adding Catalyst in Two Batches). ..... 577

**Scheme 4.8.** Preparation of Phosphinite **4.5b**..... 577

**Scheme 4.9.** Preliminary Substrate Scope. ..... 579

LIST OF FIGURES

**Figure 2.1.** $^{1}$H-NMR Spectrum of **2.20** in $CDCl_3$, 500 MHz ..... 211

**Figure 2.2.** $^{1}$H-NMR Spectrum of **2.22** in $CDCl_3$, 500 MHz ..... 211

**Figure 2.3.** $^{1}$H-NMR Spectrum of **2.16** in $CDCl_3$, 500 MHz ..... 212

**Figure 2.4.** $^{1}$H-NMR Spectrum of **2.6** in $CDCl_3$, 500 MHz ..... 212

**Figure 2.5.** $^{13}$C-NMR Spectrum of **2.6** in $CDCl_3$, 101 MHz ..... 213

**Figure 2.6.** $^{1}$H-NMR Spectrum of **2.24** in $CDCl_3$, 500 MHz ..... 213

**Figure 2.7.** $^{13}$C-NMR Spectrum of **2.24** in $CDCl_3$, 101 MHz ..... 214

**Figure 2.8.** $^{1}$H-NMR Spectrum of **2.27** in $CDCl_3$, 500 MHz ..... 214

**Figure 2.9.** $^{13}$C-NMR Spectrum of **2.27** in $CDCl_3$, 101 MHz ..... 215

**Figure 2.10.** $^{1}$H-NMR Spectrum of **2.31** in $CDCl_3$, 500 MHz ..... 215

**Figure 2.11.** $^{1}$H-NMR Spectrum of **2.32** in $CDCl_3$, 500 MHz ..... 216

**Figure 2.12.** $^{1}$H-NMR Spectrum of **2.33** in $CDCl_3$, 500 MHz ..... 216

**Figure 2.13.** $^{1}$H-NMR Spectrum of **2.34** in $CDCl_3$, 500 MHz ..... 217

**Figure 2.14.** $^{1}$H-NMR Spectrum of **2.35** in $CDCl_3$, 500 MHz ..... 217

**Figure 2.15.** $^{1}$H-NMR Spectrum of **2.36** in $CDCl_3$, 500 MHz ..... 218

**Figure 2.16.** $^{13}$C-NMR Spectrum of **2.36** in $CDCl_3$, 101 MHz ..... 218

**Figure 2.17.** $^{1}$H-NMR Spectrum of **2.38** in $CDCl_3$, 500 MHz ..... 219

**Figure 2.18.** $^{1}$H-NMR Spectrum of **2.39** in $CDCl_3$, 500 MHz ..... 219

**Figure 2.19.** $^{1}$H-NMR Spectrum of **2.40** in $CDCl_3$, 500 MHz ..... 220

**Figure 2.20.** $^{1}$H-NMR Spectrum of **2.41** in $CDCl_3$, 500 MHz ..... 220

**Figure 2.21.** $^{1}$H-NMR Spectrum of **2.42** in $CDCl_3$, 500 MHz ..... 221

**Figure 2.22.** $^{1}$H-NMR Spectrum of **2.43** in $CDCl_3$, 500 MHz ..... 221

**Figure 2.23.** $^{1}$H-NMR Spectrum of **2.44** in $CDCl_3$, 500 MHz ..... 222

**Figure 2.24.** $^{1}$H-NMR Spectrum of **2.51** in $CDCl_3$, 500 MHz ..... 222

**Figure 2.25.** $^{1}$H-NMR Spectrum of **2.52** in $CDCl_3$, 500 MHz ..... 223

**Figure 2.26.** $^{13}$C-NMR Spectrum of **2.52** in $CDCl_3$, 101 MHz ..... 223

**Figure 2.27.** $^{1}$H-NMR Spectrum of **2.54** in $CDCl_3$, 500 MHz ..... 224

**Figure 2.28.** $^{1}$H-NMR Spectrum of **2.65** in $CDCl_3$, 500 MHz ..... 224

**Figure 2.29.** $^{1}$H-NMR Spectrum of **2.67** in $CDCl_3$, 500 MHz ..... 225

**Figure 2.30.** $^{13}$C-NMR Spectrum of **2.67** in $CDCl_3$, 126 MHz ..... 225

**Figure 2.31.** $^{1}$H-NMR Spectrum of **2.68** in $CDCl_3$, 500 MHz ..... 226

**Figure 2.32.** $^{13}$C-NMR Spectrum of **2.68** in $CDCl_3$, 101 MHz ..... 226

**Figure 2.33.** $^{1}$H-NMR Spectrum of **2.62** in $CDCl_3$, 500 MHz ..... 227

**Figure 2.34.** $^{13}$C-NMR Spectrum of **2.62** in $CDCl_3$, 101 MHz ..... 227

**Figure 2.35.** $^{1}$H-NMR Spectrum of **2.73** in $CDCl_3$, 500 MHz ..... 228

**Figure 2.36.** $^{13}$C-NMR Spectrum of **2.73** in $CDCl_3$, 101 MHz ..... 228

**Figure 2.37.** $^{1}$H-NMR Spectrum of **2.78** in $CDCl_3$, 500 MHz ..... 229

**Figure 2.38.** $^{1}$H-NMR Spectrum of **2.79** in $CDCl_3$, 500 MHz ..... 229

**Figure 2.39.** $^{1}$H-NMR Spectrum of **2.80** in $CDCl_3$, 500 MHz ..... 230

**Figure 2.40.** $^{1}$H-NMR Spectrum of **2.81** in $CDCl_3$, 500 MHz ..... 230

**Figure 2.41.** $^{1}$H-NMR Spectrum of **2.82** in $CDCl_3$, 500 MHz ..... 231

**Figure 2.42.** $^{1}$H-NMR Spectrum of **2.75** in $CDCl_3$, 500 MHz ..... 231

**Figure 2.43.** $^{13}$C-NMR Spectrum of **2.75** in $CDCl_3$, 101 MHz ..... 232

**Figure 2.44.** $^{1}$H-NMR Spectrum of **2.91** in $CDCl_3$, 500 MHz ..... 232

**Figure 2.45.** $^{1}$H-NMR Spectrum of **2.95** in $CDCl_3$, 500 MHz ..... 233

**Figure 2.46.** $^{13}$C-NMR Spectrum of **2.95** in $CDCl_3$, 101 MHz ..... 233

**Figure 2.47.** $^{1}$H-NMR Spectrum of **2.99** in $CDCl_3$, 500 MHz ..... 234

**Figure 2.48.** $^{13}$C-NMR Spectrum of **2.99** in $CDCl_3$, 101 MHz ..... 234

**Figure 2.49.** $^{1}$H-NMR Spectrum of **S2.2** in $CDCl_3$, 500 MHz ..... 235

**Figure 2.50.** $^{13}$C-NMR Spectrum of **S2.2** in $CDCl_3$, 101 MHz ..... 235

**Figure 2.51.** $^{1}$H-NMR Spectrum of **2.100** in $CDCl_3$, 500 MHz ..... 236

**Figure 2.52.** $^{13}$C-NMR Spectrum of **2.100** in $CDCl_3$, 101 MHz ..... 236

**Figure 2.53.** $^{1}$H-NMR Spectrum of **2.101** in $CDCl_3$, 500 MHz ..... 237

**Figure 2.54.** $^{13}$C-NMR Spectrum of **2.101** in $CDCl_3$, 101 MHz ..... 237

**Figure 2.55.** $^{1}$H-NMR Spectrum of **DG4** in $CDCl_3$, 500 MHz ..... 238

**Figure 2.56.** $^{13}$C-NMR Spectrum of **DG4** in $CDCl_3$, 101 MHz ..... 238

**Figure 2.57.** $^{1}$H-NMR Spectrum of **2.113** in $CDCl_3$, 500 MHz ..... 239

**Figure 2.58.** $^{1}$H-NMR Spectrum of **2.114** in $CDCl_3$, 500 MHz ..... 239

**Figure 2.59.** $^{1}$H-NMR Spectrum of **2.115** in $CDCl_3$, 500 MHz ..... 240

**Figure 2.60.** $^{1}$H-NMR Spectrum of **2.116** in $CDCl_3$, 500 MHz ..... 240

**Figure 2.61.** $^{1}$H-NMR Spectrum of **2.124** in $CDCl_3$, 500 MHz ..... 241

**Figure 2.62.** $^{1}$H-NMR Spectrum of **2.129** in $CDCl_3$, 500 MHz ..... 241

**Figure 2.63.** $^{1}$H-NMR Spectrum of **2.118** in $CDCl_3$, 500 MHz ..... 242

**Figure 2.64.** $^{13}$C-NMR Spectrum of **2.118** in $CDCl_3$, 101 MHz ..... 242

**Figure 2.65.** $^{1}$H-NMR Spectrum of **2.117** in $CDCl_3$, 500 MHz ..... 243

**Figure 2.66.** $^{1}$H-NMR Spectrum of **2.136** in $CDCl_3$, 500 MHz ..... 243

**Figure 2.67.** $^{13}$C-NMR Spectrum of **2.136** in $CDCl_3$, 101 MHz ..... 244

**Figure 2.68.** $^{1}$H-NMR Spectrum of **2.135** in $CDCl_3$, 500 MHz ..... 244

**Figure 2.69.** $^{13}$C-NMR Spectrum of **2.135** in $CDCl_3$, 101 MHz ..... 245

**Figure 2.70.** $^{1}$H-NMR Spectrum of **2.139** in $CDCl_3$, 500 MHz ..... 245

**Figure 2.71.** $^{13}$C-NMR Spectrum of **2.139** in $CDCl_3$, 101 MHz ..... 246

**Figure 2.72.** $^{1}$H-NMR Spectrum of **2.142** in $CDCl_3$, 500 MHz ..... 246

**Figure 2.73.** $^{13}$C-NMR Spectrum of **2.142** in $CDCl_3$, 101 MHz ..... 247

**Figure 2.74.** $^{1}$H-NMR Spectrum of **2.143** in $CDCl_3$, 500 MHz ..... 247

**Figure 2.75.** $^{1}$H-NMR Spectrum of **2.147** in $CDCl_3$, 500 MHz ..... 248

**Figure 2.76.** $^{13}$C-NMR Spectrum of **2.147** in $CDCl_3$, 101 MHz ..... 248

**Figure 2.77.** $^{1}$H-NMR Spectrum of **2.148** in $CDCl_3$, 500 MHz ..... 249

**Figure 2.78.** $^{13}$C-NMR Spectrum of **2.148** in $CDCl_3$, 101 MHz ..... 249

**Figure 2.79.** $^{1}$H-NMR Spectrum of **2.148** in $C_6D_6$, 500 MHz ..... 250

**Figure 2.80.** COSY Spectrum of **2.148** in $C_6D_6$ ..... 250

**Figure 2.81.** NOESY Spectrum of **2.148** in $C_6D_6$ ..... 251

**Figure 2.82.** $^{1}$H-NMR Spectrum of **2.151** in $CDCl_3$, 500 MHz ..... 251

**Figure 2.83.** $^{1}$H-NMR Spectrum of **2.152** in $CDCl_3$, 500 MHz ..... 252

**Figure 2.84.** $^{1}$H-NMR Spectrum of **2.153** in $CDCl_3$, 500 MHz ..... 252

**Figure 2.85.** $^{1}$H-NMR Spectrum of **2.154** in $CDCl_3$, 500 MHz ..... 253

**Figure 2.86.** $^{1}$H-NMR Spectrum of **2.160** in $CDCl_3$, 500 MHz ..... 253

**Figure 2.87.** $^{1}$H-NMR Spectrum of **2.161** in $CDCl_3$, 500 MHz ..... 254

**Figure 2.88.** $^{1}$H-NMR Spectrum of **2.162** in $CDCl_3$, 500 MHz ..... 254

**Figure 2.89.** $^{13}$C-NMR Spectrum of **2.162** in $CDCl_3$, 101 MHz ..... 255

**Figure 2.90.** DEPT135-NMR Spectrum of **2.162** in $CDCl_3$, 126 MHz ..... 255

**Figure 2.91.** COSY-NMR Spectrum of **2.162** in $CDCl_3$, 126 MHz ..... 256

**Figure 2.92.** $^{1}$H-NMR Spectrum of **2.163** in $CDCl_3$, 500 MHz ..... 256

**Figure 2.93.** $^{1}$H-NMR Spectrum of **2.166** in $CDCl_3$, 500 MHz ..... 257

**Figure 2.94.** $^{1}$H-NMR Spectrum of **2.167** in $CDCl_3$, 500 MHz ..... 257

**Figure 2.95.** $^{1}$H-NMR Spectrum of **2.170** in $CDCl_3$, 500 MHz ..... 258

**Figure 2.96.** $^{1}$H-NMR Spectrum of **2.172** in $CDCl_3$, 500 MHz ..... 258

**Figure 2.97.** $^{13}$C-NMR Spectrum of **2.172** in $CDCl_3$, 101 MHz ..... 259

**Figure 2.98.** $^{1}$H-NMR Spectrum of **2.173** in $CDCl_3$, 500 MHz ..... 259

**Figure 2.99.** $^{13}$C-NMR Spectrum of **2.173** in $CDCl_3$, 101 MHz ..... 260

**Figure 2.100.** $^{1}$H-NMR Spectrum of **2.175** in $CDCl_3$, 500 MHz ..... 260

**Figure 2.101.** $^{1}$H-NMR Spectrum of **2.177** in $CDCl_3$, 500 MHz ..... 261

**Figure 2.102.** $^{13}$C-NMR Spectrum of **2.177** in $CDCl_3$, 101 MHz ..... 261

**Figure 2.103.** $^{1}$H-NMR Spectrum of **2.179** in $CDCl_3$, 500 MHz ..... 262

**Figure 2.104.** $^{13}$C-NMR Spectrum of **2.179** in $CDCl_3$, 101 MHz ..... 262

**Figure 2.105.** DEPT135-NMR Spectrum of **2.179** in $CDCl_3$, 101 MHz ..... 263

**Figure 2.106.** $^{11}$B-NMR Spectrum of **2.179** in $CDCl_3$, 128 MHz ..... 263

**Figure 2.107.** $^{1}$H-NMR Spectrum of **2.178** in $CDCl_3$, 500 MHz ..... 264

**Figure 2.108.** $^{13}$C-NMR Spectrum of **2.178** in $CDCl_3$, 101 MHz ..... 264

**Figure 2.109.** $^{1}$H-NMR Spectrum of **2.134** in $CDCl_3$, 500 MHz ..... 265

**Figure 2.110.** $^{13}$C-NMR Spectrum of **2.134** in $CDCl_3$, 101 MHz ..... 265

**Figure 2.111.** $^{1}$H-NMR Spectrum of **2.183** in $CDCl_3$, 500 MHz ..... 266

**Figure 2.112.** $^{1}$H-NMR Spectrum of **2.185** in $CDCl_3$, 500 MHz ..... 266

**Figure 2.113.** $^{13}$C-NMR Spectrum of **2.185** in $CDCl_3$, 101 MHz ..... 267

**Figure 2.114.** $^{1}$H-NMR Spectrum of **2.188** in $CDCl_3$, 500 MHz ..... 267

**Figure 2.115.** $^{13}$C-NMR Spectrum of **2.188** in $CDCl_3$, 101 MHz ..... 268

**Figure 2.116.** $^{1}$H-NMR Spectrum of **2.1** in acetone-D6, 500 MHz ..... 268

**Figure 2.117.** $^{13}$C-NMR Spectrum of **2.1** in acetone-D6, 101 MHz ..... 269

**Figure 2.118.** $^{1}$H-NMR Spectrum of **2.2** in $CDCl_3$, 500 MHz ..... 269

**Figure 2.118.** $^{13}$C-NMR Spectrum of **2.2** in $CDCl_3$, 101 MHz ..... 270

**Figure 3.1.** GPC-MALS Chromatography of Compound **3.1ab**..... 392

**Figure 3.2.** MALDI-TOF Spectra of Compound **3.1ab**. ..... 393

**Figure 3.3.** GPC-MALS Chromatography of Compound **3.1ac**. ..... 402

**Figure 3.4.** GPC-MALS Chromatography of Product Mixture. ..... 404

**Figure 3.5.** General GC-MS Chromatography of Product Mixture. ..... 405

**Figure 3.6.** Mass Spectra of Peak A (Retention Time = 4.600 min). ..... 405

**Figure 3.7.** Mass Spectra of Peak B (Retention Time = 4.977 min). ..... 405

**Figure 3.8.** Mass Spectra of Peak C (Retention Time = 8.441 min). ..... 406

**Figure 3.9.** Mass Spectra of Peak D (Retention Time = 8.645 min). ..... 406

**Figure 3.10.** Mass Spectra of Peak E (Retention Time = 8.875 min). ..... 407

**Figure 3.11.** Mass Spectra of Peak F (Retention Time = 9.099 min). ..... 407

**Figure 3.12.** $^{31}$P-NMR Spectrum of the Product Mixture in $CDCl_3$, 162 MHz, 8 scans ..... 408

**Figure 3.13.** $^{1}$H-NMR Spectrum of **3.1b** in $CDCl_3$, 400 MHz..... 414

**Figure 3.14.** $^{13}$C-NMR Spectrum of **3.1b** in $CDCl_3$, 101 MHz..... 414

**Figure 3.15.** $^{1}$H-NMR Spectrum of **3.1c** in $CDCl_3$, 400 MHz ..... 415

**Figure 3.16.** $^{13}$C-NMR Spectrum of **3.1c** in $CDCl_3$, 101 MHz ..... 415

**Figure 3.17.** $^{1}$H-NMR Spectrum of **3.1d** in $CDCl_3$, 400 MHz..... 416

**Figure 3.18.** $^{13}$C-NMR Spectrum of **3.1d** in $CDCl_3$, 101 MHz..... 416

**Figure 3.19.** $^{1}$H-NMR Spectrum of **3.1e** in $CDCl_3$, 400 MHz ..... 417

**Figure 3.20.** $^{13}$C-NMR Spectrum of **3.1e** in $CDCl_3$, 101 MHz ..... 417

**Figure 3.21.** $^{1}$H-NMR Spectrum of **3.1g** in $CDCl_3$, 400 MHz ..... 418

**Figure 3.22.** $^{13}$C-NMR Spectrum of **3.1g** in $CDCl_3$, 101 MHz ..... 418

**Figure 3.23.** $^{1}$H-NMR Spectrum of **3.1h** in $CDCl_3$, 400 MHz ..... 419

**Figure 3.24.** $^{13}$C-NMR Spectrum of **3.1h** in $CDCl_3$, 101 MHz ..... 419

**Figure 3.25.** $^{1}$H-NMR Spectrum of **3.1i** in $CDCl_3$, 400 MHz ..... 420

**Figure 3.26.** $^{13}$C-NMR Spectrum of **3.1i** in $CDCl_3$, 101 MHz ..... 420

**Figure 3.27.** $^{1}$H-NMR Spectrum of **3.1j** in $CDCl_3$, 400 MHz ..... 421

**Figure 3.28.** $^{13}$C-NMR Spectrum of **3.1j** in $CDCl_3$, 101 MHz ..... 421

**Figure 3.29.** $^{1}$H-NMR Spectrum of **3.1k** in $CDCl_3$, 400 MHz ..... 422

**Figure 3.30.** $^{13}$C-NMR Spectrum of **3.1k** in $CDCl_3$, 101 MHz ..... 422

**Figure 3.31.** $^{1}$H-NMR Spectrum of **3.1l** in DMSO-d6, 400 MHz ..... 423

**Figure 3.32.** $^{13}$C-NMR Spectrum of **3.1l** in DMSO-d6, 101 MHz ..... 423

**Figure 3.33.** $^{19}$F-NMR Spectrum of **3.1l** in DMSO-d6, 376 MHz ..... 424

**Figure 3.34.** $^{1}$H-NMR Spectrum of **3.1m** in $CDCl_3$, 400 MHz ..... 425

**Figure 3.35.** $^{13}$C-NMR Spectrum of **3.1m** in $CDCl_3$, 101 MHz ..... 425

**Figure 3.36.** $^{1}$H-NMR Spectrum of **3.1n** in $CDCl_3$, 400 MHz ..... 426

**Figure 3.37.** $^{13}$C-NMR Spectrum of **3.1n** in $CDCl_3$, 101 MHz ..... 426

**Figure 3.38.** $^{1}$H-NMR Spectrum of **3.1o** in $CDCl_3$, 400 MHz ..... 427

**Figure 3.39.** $^{13}$C-NMR Spectrum of **3.1o** in $CDCl_3$, 101 MHz ..... 427

**Figure 3.40.** $^{1}$H-NMR Spectrum of **3.1p** in $CDCl_3$, 400 MHz ..... 428

**Figure 3.41.** $^{13}$C-NMR Spectrum of **3.1p** in $CDCl_3$, 101 MHz ..... 428

**Figure 3.42.** $^{1}$H-NMR Spectrum of **3.1q** in $CDCl_3$, 400 MHz ..... 429

**Figure 3.43.** $^{13}$C-NMR Spectrum of **3.1q** in $CDCl_3$, 101 MHz ..... 429

**Figure 3.44.** $^{1}$H-NMR Spectrum of **3.1r** in DMSO-d6, 500 MHz ..... 430

**Figure 3.45.** $^{13}$C-NMR Spectrum of **3.1r** in DMSO-d6, 126 MHz ..... 430

**Figure 3.46.** $^{1}$H-NMR Spectrum of **3.1s** in $CDCl_3$, 400 MHz ..... 431

**Figure 3.47.** $^{13}$C-NMR Spectrum of **3.1s** in $CDCl_3$, 101 MHz ..... 431

**Figure 3.48.** $^{1}$H-NMR Spectrum of **3.1u** in $CDCl_3$, 400 MHz ..... 432

**Figure 3.49.** $^{13}$C-NMR Spectrum of **3.1u** in $CDCl_3$, 101 MHz ..... 432

**Figure 3.50.** $^{1}$H-NMR Spectrum of **3.1v** in $CDCl_3$, 400 MHz ..... 433

**Figure 3.51.** $^{13}$C-NMR Spectrum of **3.1v** in $CDCl_3$, 101 MHz ..... 433

**Figure 3.52.** $^{1}$H-NMR Spectrum of **3.1w** in $CDCl_3$, 400 MHz ..... 434

**Figure 3.53.** $^{13}$C-NMR Spectrum of **3.1w** in $CDCl_3$, 101 MHz ..... 434

**Figure 3.54.** $^{1}$H-NMR Spectrum of **3.1x** in $CDCl_3$, 400 MHz ..... 435

**Figure 3.55.** $^{13}$C-NMR Spectrum of **3.1x** in $CDCl_3$, 101 MHz ..... 435

**Figure 3.56.** $^{1}$H-NMR Spectrum of **3.2a** in $C_6D_6$, 500 MHz ..... 436

**Figure 3.57.** $^{13}$C-NMR Spectrum of **3.2a** in $C_6D_6$, 125 MHz ..... 436

**Figure 3.58.** $^{31}$P-NMR Spectrum of **3.2a** in $C_6D_6$, 202 MHz ..... 437

**Figure 3.59.** $^{1}$H-NMR Spectrum of **3.2b** in $C_6D_6$, 500 MHz ..... 438

**Figure 3.60.** $^{13}$C-NMR Spectrum of **3.2b** in $C_6D_6$, 125 MHz ..... 438

**Figure 3.61.** $^{31}$P-NMR Spectrum of **3.2b** in $C_6D_6$, 202 MHz ..... 439

**Figure 3.62.** $^{1}$H-NMR Spectrum of **3.2c** in $C_6D_6$, 500 MHz ..... 440

**Figure 3.63.** $^{13}$C-NMR Spectrum of **3.2c** in $C_6D_6$, 125 MHz ..... 440

**Figure 3.64.** $^{31}$P-NMR Spectrum of **3.2c** in $C_6D_6$, 202 MHz ..... 441

**Figure 3.65.** $^{1}$H-NMR Spectrum of **3.2d** in $C_6D_6$, 500 MHz ..... 442

**Figure 3.66.** $^{13}$C-NMR Spectrum of **3.2d** in $C_6D_6$, 125 MHz ..... 442

**Figure 3.67.** $^{31}$P-NMR Spectrum of **3.2d** in $C_6D_6$, 202 MHz ..... 443

**Figure 3.68.** $^{1}$H-NMR Spectrum of **3.2e** in $CDCl_3$, 500 MHz ..... 444

**Figure 3.69.** $^{13}$C-NMR Spectrum of **3.2e** in $CDCl_3$, 125 MHz ..... 444

**Figure 3.70.** $^{31}$P-NMR Spectrum of **3.2e** in $CDCl_3$, 202 MHz ..... 445

**Figure 3.71.** $^{1}$H-NMR Spectrum of **3.2f** in $C_6D_6$, 500 MHz ..... 446

**Figure 3.72.** $^{13}$C-NMR Spectrum of **3.2f** in $C_6D_6$, 125 MHz ..... 446

**Figure 3.73.** $^{31}$P-NMR Spectrum of **3.2f** in $C_6D_6$, 202 MHz ..... 447

**Figure 3.74.** $^{1}$H-NMR Spectrum of **3.2g** in $CDCl_3$, 500 MHz ..... 448

**Figure 3.75.** $^{13}$C-NMR Spectrum of **3.2g** in $CDCl_3$, 125 MHz ..... 448

**Figure 3.76.** $^{31}$P-NMR Spectrum of **3.2g** in $CDCl_3$, 202 MHz ..... 449

**Figure 3.77.** $^{1}$H-NMR Spectrum of **3.2h** in $CDCl_3$, 500 MHz ..... 450

**Figure 3.78.** $^{13}$C-NMR Spectrum of **3.2h** in $CDCl_3$, 125 MHz ..... 450

**Figure 3.79.** $^{31}$P-NMR Spectrum of **3.2h** in $CDCl_3$, 202 MHz ..... 451

**Figure 3.80.** $^{1}$H-NMR Spectrum of **3.2i** in $C_6D_6$, 500 MHz ..... 452

**Figure 3.81.** $^{13}$C-NMR Spectrum of **3.2i** in $C_6D_6$, 125 MHz ..... 452

**Figure 3.82.** $^{31}$P-NMR Spectrum of **3.2i** in $C_6D_6$, 202 MHz ..... 453

**Figure 3.83.** $^{1}$H-NMR Spectrum of **3.2j** in $CDCl_3$, 400 MHz ..... 454

**Figure 3.84.** $^{13}$C-NMR Spectrum of **3.2j** in $CDCl_3$, 100 MHz ..... 454

**Figure 3.85.** $^{31}$P-NMR Spectrum of **3.2j** in $CDCl_3$, 202 MHz ..... 455

**Figure 3.86.** $^{1}$H-NMR Spectrum of **3.2k** in $CDCl_3$, 500 MHz ..... 456

**Figure 3.87.** $^{13}$C-NMR Spectrum of **3.2k** in $CDCl_3$, 126 MHz ..... 456

**Figure 3.88.** $^{31}$P-NMR Spectrum of **3.2k** in $CDCl_3$, 202 MHz ..... 457

**Figure 3.89.** $^{1}$H-NMR Spectrum of **3.2l** in $CDCl_3$, 500 MHz ..... 458

**Figure 3.90.** $^{13}$C-NMR Spectrum of **3.2l** in $CDCl_3$, 126 MHz ..... 458

**Figure 3.91.** $^{19}$F-NMR Spectrum of **3.2l** in $CDCl_3$, 470 MHz ..... 459

**Figure 3.92.** $^{31}$P-NMR Spectrum of **3.2l** in $CDCl_3$, 202 MHz ..... 459

**Figure 3.93.** $^{1}$H-NMR Spectrum of **3.2m** in $CDCl_3$, 400 MHz ..... 460

**Figure 3.94.** $^{13}$C-NMR Spectrum of **3.2m** in $CDCl_3$, 101 MHz ..... 460

**Figure 3.95.** $^{31}$P-NMR Spectrum of **3.2m** in $CDCl_3$, 202 MHz ..... 461

**Figure 3.96.** $^{1}$H-NMR Spectrum of **3.2n** in $CDCl_3$, 500 MHz ..... 462

**Figure 3.97.** $^{13}$C-NMR Spectrum of **3.2n** in $CDCl_3$, 126 MHz ..... 462

**Figure 3.98.** $^{31}$P-NMR Spectrum of **3.2n** in $CDCl_3$, 202 MHz ..... 463

**Figure 3.99.** $^{1}$H-NMR Spectrum of **3.2o** in $CDCl_3$, 500 MHz ..... 464

**Figure 3.100.** $^{13}$C-NMR Spectrum of **3.2o** in $CDCl_3$, 126 MHz ..... 464

**Figure 3.101.** $^{31}$P-NMR Spectrum of **3.2o** in $CDCl_3$, 202 MHz ..... 465

**Figure 3.102.** $^{1}$H-NMR Spectrum of **3.2p** in $CDCl_3$, 500 MHz ..... 466

**Figure 3.103.** $^{13}$C-NMR Spectrum of **3.2p** in $CDCl_3$, 126 MHz ..... 466

**Figure 3.104.** $^{31}$P-NMR Spectrum of **3.2p** in $CDCl_3$, 202 MHz ..... 467

**Figure 3.105.** $^{1}$H-NMR Spectrum of **3.2q** in $CDCl_3$, 500 MHz ..... 468

**Figure 3.106.** $^{13}$C-NMR Spectrum of **3.2q** in $CDCl_3$, 126 MHz ..... 468

**Figure 3.107.** $^{31}$P-NMR Spectrum of **3.2q** in $CDCl_3$, 202 MHz ..... 469

**Figure 3.108.** $^{1}$H-NMR Spectrum of **3.2r** in $CDCl_3$, 500 MHz ..... 470

**Figure 3.109.** $^{13}$C-NMR Spectrum of **3.2r** in $CDCl_3$, 126 MHz ..... 470

**Figure 3.110.** $^{31}$P-NMR Spectrum of **3.2r** in $CDCl_3$, 202 MHz ..... 471

**Figure 3.111.** $^{1}$H-NMR Spectrum of **3.2s** in $CDCl_3$, 500 MHz ..... 472

**Figure 3.112.** $^{13}$C-NMR Spectrum of **3.2s** in $CDCl_3$, 126 MHz ..... 472

**Figure 3.113.** $^{31}$P-NMR Spectrum of **3.2s** in $CDCl_3$, 202 MHz ..... 473

**Figure 3.114.** $^{1}$H-NMR Spectrum of **3.2t** in $C_6D_6$, 400 MHz ..... 474

**Figure 3.115.** $^{13}$C-NMR Spectrum of **3.2t** in $C_6D_6$, 101 MHz ..... 474

**Figure 3.116.** $^{31}$P-NMR Spectrum of **3.2t** in $C_6D_6$, 202 MHz ..... 475

**Figure 3.117.** $^{1}$H-NMR Spectrum of **3.2t'** in $C_6D_6$, 500 MHz ..... 476

**Figure 3.118.** $^{13}$C-NMR Spectrum of **3.2t'** in $C_6D_6$, 126 MHz ..... 476

**Figure 3.119.** $^{31}$P-NMR Spectrum of **3.2t'** in $C_6D_6$, 202 MHz ..... 477

**Figure 3.120.** $^{1}$H-NMR Spectrum of **3.2u** in $C_6D_6$, 400 MHz ..... 478

**Figure 3.121.** $^{13}$C-NMR Spectrum of **3.2u** in $C_6D_6$, 101 MHz ..... 478

**Figure 3.122.** $^{31}$P-NMR Spectrum of **3.2u** in $C_6D_6$, 162 MHz ..... 479

**Figure 3.123.** $^{1}$H-NMR Spectrum of **3.2v** in $C_6D_6$, 400 MHz ..... 480

**Figure 3.124.** $^{13}$C-NMR Spectrum of **3.2v** in $C_6D_6$, 101 MHz ..... 480

**Figure 3.125.** $^{31}$P-NMR Spectrum of **3.2v** in $C_6D_6$, 162 MHz ..... 481

**Figure 3.126.** $^{1}$H-NMR Spectrum of **3.2w** in $C_6D_6$, 400 MHz ..... 482

**Figure 3.127.** $^{13}$C-NMR Spectrum of **3.2w** in $C_6D_6$, 101 MHz ..... 482

**Figure 3.128.** $^{31}$P-NMR Spectrum of **3.2w** in $C_6D_6$, 162 MHz ..... 483

**Figure 3.129.** $^{1}$H-NMR Spectrum of **3.2x** in $C_6D_6$, 500 MHz ..... 484

**Figure 3.130.** $^{13}$C-NMR Spectrum of **3.2x** in $C_6D_6$, 126 MHz ..... 484

**Figure 3.131.** $^{31}$P-NMR Spectrum of **3.2x** in $C_6D_6$, 202 MHz ..... 485

**Figure 3.132.** $^{1}$H-NMR Spectrum of **3.3a** in $CDCl_3$, 400 MHz ..... 486

**Figure 3.133.** $^{13}$C-NMR Spectrum of **3.3a** in $CDCl_3$, 101 MHz ..... 486

**Figure 3.134.** $^{1}$H-NMR Spectrum of **3.4a** in $CDCl_3$, 400 MHz ..... 487

**Figure 3.135.** $^{13}$C-NMR Spectrum of **3.4a** in $CDCl_3$, 101 MHz ..... 487

**Figure 3.136.** $^{1}$H-NMR Spectrum of **3.3b** in $CDCl_3$, 500 MHz ..... 488

**Figure 3.137.** $^{13}$C-NMR Spectrum of **3.3b** in $CDCl_3$, 126 MHz ..... 488

**Figure 3.138.** $^{1}$H-NMR Spectrum of **3.4b** in $CDCl_3$, 500 MHz ..... 489

**Figure 3.139.** $^{13}$C-NMR Spectrum of **3.4b** in $CDCl_3$, 126 MHz ..... 489

**Figure 3.140.** $^{1}$H-NMR Spectrum of **3.3c** in $CDCl_3$, 500 MHz ..... 490

**Figure 3.141.** $^{13}$C-NMR Spectrum of **3.3c** in $CDCl_3$, 126 MHz ..... 490

**Figure 3.142.** $^{1}$H-NMR Spectrum of **3.4c** in $CDCl_3$, 500 MHz ..... 491

**Figure 3.143.** $^{13}$C-NMR Spectrum of **3.4c** in $CDCl_3$, 126 MHz ..... 491

**Figure 3.144.** $^{1}$H-NMR Spectrum of **3.3d** in $CDCl_3$, 500 MHz ..... 492

**Figure 3.145.** $^{13}$C-NMR Spectrum of **3.3d** in $CDCl_3$, 126 MHz ..... 492

**Figure 3.146.** $^{1}$H-NMR Spectrum of **3.4d** in $CDCl_3$, 500 MHz ..... 493

**Figure 3.147.** $^{13}$C-NMR Spectrum of **3.4d** in $CDCl_3$, 126 MHz ..... 493

**Figure 3.148.** $^{1}$H-NMR Spectrum of **3.3e** in $CDCl_3$, 500 MHz ..... 494

**Figure 3.149.** $^{13}$C-NMR Spectrum of **3.3e** in $CDCl_3$, 126 MHz ..... 494

**Figure 3.150.** $^{1}$H-NMR Spectrum of **3.4e** in $CDCl_3$, 500 MHz ..... 495

**Figure 3.151.** $^{13}$C-NMR Spectrum of **3.4e** in $CDCl_3$, 126 MHz ..... 495

**Figure 3.152.** $^{1}$H-NMR Spectrum of **3.3f** in $CDCl_3$, 500 MHz ..... 496

**Figure 3.153.** $^{13}$C-NMR Spectrum of **3.3f** in $CDCl_3$, 126 MHz ..... 496

**Figure 3.154.** $^{1}$H-NMR Spectrum of **3.4f** in $CDCl_3$, 500 MHz ..... 497

**Figure 3.155.** $^{13}$C-NMR Spectrum of **3.4f** in $CDCl_3$, 126 MHz ..... 497

**Figure 3.156.** $^{1}$H-NMR Spectrum of **3.3g** in $CDCl_3$, 500 MHz ..... 498

**Figure 3.157.** $^{13}$C-NMR Spectrum of **3.3g** in $CDCl_3$, 126 MHz ..... 498

**Figure 3.158.** $^{1}$H-NMR Spectrum of **3.4g** in $CDCl_3$, 500 MHz ..... 499

**Figure 3.159.** $^{13}$C-NMR Spectrum of **3.4g** in $CDCl_3$, 126 MHz ..... 499

**Figure 3.160.** $^{1}$H-NMR Spectrum of **3.3h** in $CDCl_3$, 400 MHz ..... 500

**Figure 3.161.** $^{13}$C-NMR Spectrum of **3.3h** in $CDCl_3$, 101 MHz ..... 500

**Figure 3.162.** $^{1}$H-NMR Spectrum of **3.4h** in $CDCl_3$, 400 MHz ..... 501

**Figure 3.163.** $^{13}$C-NMR Spectrum of **3.4h** in $CDCl_3$, 101 MHz ..... 501

**Figure 3.164.** $^{1}$H-NMR Spectrum of **3.3i** in $CDCl_3$, 500 MHz ..... 502

**Figure 3.165.** $^{13}$C-NMR Spectrum of **3.3i** in $CDCl_3$, 126 MHz ..... 502

**Figure 3.166.** $^{1}$H-NMR Spectrum of **3.4i** in $CDCl_3$, 500 MHz ..... 503

**Figure 3.167.** $^{13}$C-NMR Spectrum of **3.4i** in $CDCl_3$, 126 MHz ..... 503

**Figure 3.168.** $^{1}$H-NMR Spectrum of **3.3j** in $CDCl_3$, 500 MHz ..... 504

**Figure 3.169.** $^{13}$C-NMR Spectrum of **3.3j** in $CDCl_3$, 126 MHz ..... 504

**Figure 3.170.** $^{1}$H-NMR Spectrum of **3.4j** in $CDCl_3$, 400 MHz ..... 505

**Figure 3.171.** $^{13}$C-NMR Spectrum of **3.4j** in $CDCl_3$, 126 MHz ..... 505

**Figure 3.172.** $^{1}$H-NMR Spectrum of **3.3k** in $CDCl_3$, 500 MHz ..... 506

**Figure 3.173.** $^{13}$C-NMR Spectrum of **3.3k** in $CDCl_3$, 126 MHz ..... 506

**Figure 3.174.** $^{1}$H-NMR Spectrum of **3.4k** in $CDCl_3$, 500 MHz ..... 507

**Figure 3.175.** $^{13}$C-NMR Spectrum of **3.4k** in $CDCl_3$, 126 MHz ..... 507

**Figure 3.176.** $^{1}$H-NMR Spectrum of **3.3l** in $CDCl_3$, 500 MHz ..... 508

**Figure 3.177.** $^{13}$C-NMR Spectrum of **3.3l** in $CDCl_3$, 126 MHz ..... 508

**Figure 3.178.** $^{19}$F-NMR Spectrum of **3.3l** in $CDCl_3$, 470 MHz ..... 509

**Figure 3.179.** $^{1}$H-NMR Spectrum of **3.4l** in $CDCl_3$, 500 MHz ..... 510

**Figure 3.180.** $^{13}$C-NMR Spectrum of **3.4l** in $CDCl_3$, 126 MHz..... 510

**Figure 3.181.** $^{19}$F-NMR Spectrum of **3.4l** in $CDCl_3$, 470 MHz .....511

**Figure 3.182.** $^{1}$H-NMR Spectrum of **3.3m** in $CDCl_3$, 400 MHz..... 512

**Figure 3.183.** $^{13}$C-NMR Spectrum of **3.3m** in $CDCl_3$, 101 MHz ..... 512

**Figure 3.184.** $^{1}$H-NMR Spectrum of **3.4m** in $CDCl_3$, 400 MHz..... 513

**Figure 3.185.** $^{13}$C-NMR Spectrum of **3.4m** in $CDCl_3$, 101 MHz ..... 513

**Figure 3.186.** $^{1}$H-NMR Spectrum of **3.3n** in $CDCl_3$, 500 MHz..... 514

**Figure 3.187.** $^{13}$C-NMR Spectrum of **3.3n** in $CDCl_3$, 126 MHz..... 514

**Figure 3.188.** $^{1}$H-NMR Spectrum of **3.4n** in $CDCl_3$, 500 MHz..... 515

**Figure 3.189.** $^{13}$C-NMR Spectrum of **3.4n** in $CDCl_3$, 126 MHz..... 515

**Figure 3.190.** $^{1}$H-NMR Spectrum of **3.3o** in $CDCl_3$, 500 MHz..... 516

**Figure 3.191.** $^{13}$C-NMR Spectrum of **3.3o** in $CDCl_3$, 126 MHz..... 516

**Figure 3.192.** $^{1}$H-NMR Spectrum of **3.4o** in $CDCl_3$, 400 MHz..... 517

**Figure 3.193.** $^{13}$C-NMR Spectrum of **3.4o** in $CDCl_3$, 101 MHz..... 517

**Figure 3.194.** $^{1}$H-NMR Spectrum of **3.3q** in $CDCl_3$, 500 MHz..... 518

**Figure 3.195.** $^{13}$C-NMR Spectrum of **3.3q** in $CDCl_3$, 126 MHz..... 518

**Figure 3.196.** $^{1}$H-NMR Spectrum of **3.4q** in $CDCl_3$, 500 MHz..... 519

**Figure 3.197.** $^{13}$C-NMR Spectrum of **3.4q** in $CDCl_3$, 126 MHz..... 519

**Figure 3.198.** $^{1}$H-NMR Spectrum of **3.3r** in $CDCl_3$, 500 MHz ..... 520

**Figure 3.199.** $^{13}$C-NMR Spectrum of **3.3r** in $CDCl_3$, 126 MHz ..... 520

**Figure 3.200.** $^{1}$H-NMR Spectrum of **3.4r** in $CDCl_3$, 500 MHz ..... 521

**Figure 3.201.** $^{13}$C-NMR Spectrum of **3.4r** in $CDCl_3$, 126 MHz ..... 521

**Figure 3.202.** $^{1}$H-NMR Spectrum of **3.3s** in $CDCl_3$, 500 MHz ..... 522

**Figure 3.203.** $^{13}$C-NMR Spectrum of **3.3s** in $CDCl_3$, 126 MHz ..... 522

**Figure 3.204.** $^{1}$H-NMR Spectrum of **3.4s** in $CDCl_3$, 500 MHz ..... 523

**Figure 3.205.** $^{13}$C-NMR Spectrum of **3.4s** in $CDCl_3$, 101 MHz ..... 523

**Figure 3.206.** $^{1}$H-NMR Spectrum of **3.4t** in $CDCl_3$, 400 MHz..... 524

**Figure 3.207.** $^{13}$C-NMR Spectrum of **3.4t** in $CDCl_3$, 101 MHz ..... 524

**Figure 3.208.** $^{1}$H-NMR Spectrum of **3.3t'** in $CDCl_3$, 500 MHz ..... 525

**Figure 3.209.** $^{13}$C-NMR Spectrum of **3.3t'** in $CDCl_3$, 126 MHz ..... 525

**Figure 3.210.** $^{1}$H-NMR Spectrum of **3.4t'** in $CDCl_3$, 500 MHz ..... 526

**Figure 3.211.** $^{13}$C-NMR Spectrum of **3.4t'** in $CDCl_3$, 126 MHz ..... 526

**Figure 3.212.** $^{1}$H-NMR Spectrum of **3.3u** in $CDCl_3$, 400 MHz..... 527

**Figure 3.213.** $^{13}$C-NMR Spectrum of **3.3u** in $CDCl_3$, 101 MHz..... 527

**Figure 3.214.** $^{1}$H-NMR Spectrum of **3.4u** in $CDCl_3$, 400 MHz..... 528

**Figure 3.215.** $^{13}$C-NMR Spectrum of **3.4u** in $CDCl_3$, 101 MHz..... 528

**Figure 3.216.** $^{1}$H-NMR Spectrum of **3.3v** in $CDCl_3$, 500 MHz..... 529

**Figure 3.217.** $^{13}$C-NMR Spectrum of **3.3v** in $CDCl_3$, 101 MHz..... 529

**Figure 3.218.** $^{1}$H-NMR Spectrum of **3.4v** in $CDCl_3$, 500 MHz..... 530

**Figure 3.219.** $^{13}$C-NMR Spectrum of **3.4v** in $CDCl_3$, 101 MHz..... 530

**Figure 3.220.** $^{1}$H-NMR Spectrum of **S3.19** in DMSO-d6, 500 MHz ..... 531

**Figure 3.221.** $^{13}$C-NMR Spectrum of **S3.19** in DMSO-d6, 101 MHz ..... 531

**Figure 3.222.** $^{1}$H-NMR Spectrum of **3.1z** in $CDCl_3$, 500 MHz ..... 532

**Figure 3.223.** $^{13}$C-NMR Spectrum of **3.1z** in CDCl3, 101 MHz ..... 532

**Figure 3.224.** $^{1}$H-NMR Spectrum of **S3.21** in $CDCl_3$, 500 MHz..... 533

**Figure 3.225.** $^{13}$C-NMR Spectrum of **S3.21** in CDCl3, 101 MHz..... 533

**Figure 3.226.** $^{1}$H-NMR Spectrum of **3.1aa** in $CDCl_3$, 500 MHz ..... 534

**Figure 3.227.** $^{13}$C-NMR Spectrum of **3.1aa** in $CDCl_3$, 101 MHz ..... 534

**Figure 3.228.** $^{1}$H-NMR Spectrum of **3.2y** in $C_6D_6$, 500 MHz ..... 535

**Figure 3.229.** $^{13}$C-NMR Spectrum of **3.2y** in $C_6D_6$, 126 MHz ..... 535

**Figure 3.230.** $^{31}$P-NMR Spectrum of **3.2y** in $C_6D_6$, 162 MHz ..... 536

**Figure 3.231.** $^{1}$H-NMR Spectrum of **3.2z** in $C_6D_6$, 500 MHz ..... 537

**Figure 3.232.** $^{13}$C-NMR Spectrum of **3.2z** in $C_6D_6$, 101 MHz ..... 537

**Figure 3.233.** $^{31}$P-NMR Spectrum of **3.2z** in $C_6D_6$, 162 MHz ..... 538

**Figure 3.234.** $^{1}$H-NMR Spectrum of **3.2aa** in $C_6D_6$, 500 MHz ..... 539

**Figure 3.235.** $^{13}$C-NMR Spectrum of **3.2aa** in $C_6D_6$, 126 MHz ..... 539

**Figure 3.236.** $^{31}$P-NMR Spectrum of **3.2aa** in $C_6D_6$, 202 MHz ..... 540

**Figure 3.237.** $^{1}$H-NMR Spectrum of **3.1t** in $CDCl_3$, 400 MHz ..... 541

**Figure 3.238.** $^{13}$C-NMR Spectrum of **3.1t** in $CDCl_3$, 101 MHz ..... 541

**Figure 3.239.** $^{1}$H-NMR Spectrum of **[Rh(3.2g)Cl]$_2$** in $C_6D_6$, 500 MHz ..... 542

**Figure 3.240.** $^{13}$C-NMR Spectrum of **[Rh(3.2g)Cl]$_2$** in $C_6D_6$, 126 MHz ..... 542

**Figure 3.241.** $^{31}$P-NMR Spectrum of **[Rh(3.2g)Cl]$_2$** in $C_6D_6$, 202 MHz ..... 543

**Figure 3.242.** $^{1}$H-NMR Spectrum of **3.5** in $C_6D_6$, 500 MHz ..... 544

**Figure 3.243.** $^{31}$P-NMR Spectrum of **3.5** in $C_6D_6$, 202 MHz ..... 544

**Figure 3.244.** $^{1}$H-NMR Spectrum of **3.1g-*d*** in $CDCl_3$, 400 MHz ..... 545

**Figure 3.245.** $^{13}$C-NMR Spectrum of **3.1g-*d*** in $CDCl_3$, 101 MHz ..... 545

**Figure 3.246.** $^{1}$H-NMR Spectrum of **3.3g-*d*** in $CDCl_3$, 400 MHz ..... 546

**Figure 3.247.** $^{13}$C-NMR Spectrum of **3.3g-*d*** in $CDCl_3$, 101 MHz ..... 546

**Figure 3.248.** $^{1}$H-NMR Spectrum of **3.4g-*d*** in $CDCl_3$, 400 MHz ..... 547

**Figure 3.249.** $^{13}$C-NMR Spectrum of **3.4g-*d*** in $CDCl_3$, 101 MHz ..... 547

**Figure 4.1.** Kinetic Profile on C−C Activation of Phosphinite **4.5a**. ..... 574

**Figure 4.2.** $^{1}$H-NMR Spectrum of **4.1c** in $CDCl_3$, 500 MHz ..... 592

**Figure 4.3.** $^{13}$C-NMR Spectrum of **4.1c** in $CDCl_3$, 101 MHz ..... 592

**Figure 4.4.** $^{19}$F-NMR Spectrum of **4.1c** in $CDCl_3$, 376 MHz ..... 593

**Figure 4.5.** $^{1}$H-NMR Spectrum of **4.1d** in $CDCl_3$, 500 MHz ..... 594

**Figure 4.6.** $^{13}$C-NMR Spectrum of **4.1d** in $CDCl_3$, 101 MHz ..... 594

**Figure 4.7.** $^{1}$H-NMR Spectrum of **4.1e** in $CDCl_3$, 400 MHz ..... 595

**Figure 4.8.** $^{13}$C-NMR Spectrum of **4.1e** in $CDCl_3$, 101 MHz ..... 595

**Figure 4.9.** $^{1}$H-NMR Spectrum of **4.5a** in $C_6D_6$, 500 MHz ..... 596

**Figure 4.10.** $^{13}$C-NMR Spectrum of **4.5a** in $C_6D_6$, 126 MHz ..... 596

**Figure 4.11.** $^{31}$P-NMR Spectrum of **4.5a** in $C_6D_6$, 202 MHz ..... 597

**Figure 4.12.** $^{1}$H-NMR Spectrum of **4.5b** in $C_6D_6$, 500 MHz ..... 598

**Figure 4.13.** $^{31}$P-NMR Spectrum of **4.5b** in $C_6D_6$, 202 MHz ..... 598

**Figure 4.14.** $^{1}$H-NMR Spectrum of **4.5c** in $C_6D_6$, 500 MHz ..... 599

**Figure 4.15.** $^{13}$C-NMR Spectrum of **4.5c** in $C_6D_6$, 126 MHz ..... 599

**Figure 4.16.** $^{31}$P-NMR Spectrum of **4.5c** in $C_6D_6$, 202 MHz ..... 600

**Figure 4.17.** $^{19}$F-NMR Spectrum of **4.5c** in $C_6D_6$, 470 MHz ..... 600

**Figure 4.18.** $^{1}$H-NMR Spectrum of **4.5e** in $C_6D_6$, 500 MHz ..... 601

**Figure 4.19.** $^{13}$C-NMR Spectrum of **4.5e** in $C_6D_6$, 126 MHz ..... 601

**Figure 4.20.** $^{31}$P-NMR Spectrum of **4.5e** in $C_6D_6$, 202 MHz ..... 602

**Figure 4.21.** $^{1}$H-NMR Spectrum of **4.3a** in $CDCl_3$, 500 MHz ..... 603

**Figure 4.22.** $^{13}$C-NMR Spectrum of **4.3a** in $CDCl_3$, 126 MHz ..... 603

**Figure 4.23.** $^{1}$H-NMR Spectrum of **4.1a** in $CDCl_3$, 500 MHz ..... 604

**Figure 4.24.** $^{13}$C-NMR Spectrum of **4.1a** in $CDCl_3$, 126 MHz ..... 604

**Figure 4.25.** $^{1}$H-NMR Spectrum of **4.3b** in $CDCl_3$, 500 MHz ..... 605

**Figure 4.26.** $^{13}$C-NMR Spectrum of **4.3b** in $CDCl_3$, 126 MHz ..... 605

**Figure 4.27.** $^{1}$H-NMR Spectrum of **4.1b** in $CDCl_3$, 500 MHz ..... 606

**Figure 4.28.** $^{13}$C-NMR Spectrum of **4.1b** in $CDCl_3$, 126 MHz ..... 606

**Figure 4.29.** $^{1}$H-NMR Spectrum of **4.3c** in $CDCl_3$, 400 MHz ..... 607

**Figure 4.30.** $^{13}$C-NMR Spectrum of **4.3c** in $CDCl_3$, 101 MHz ..... 607

**Figure 4.31.** $^{19}$F-NMR Spectrum of **4.3c** in $CDCl_3$, 376 MHz ..... 608

**Figure 4.32.** $^{1}$H-NMR Spectrum of **4.3e** in $CDCl_3$, 400 MHz ..... 609

**Figure 4.33.** $^{13}$C-NMR Spectrum of **4.3e** in $CDCl_3$, 101 MHz ..... 609

LIST OF TABLES

**Table 2.1.** Dechloronation of Compound **2.22**. ..... 42

**Table 2.2.** Stille coupling of Stannane **2.15** and Acetate **2.16**. ..... 43

**Table 2.3.** Catalysts Screening on "Cut-and-Sew" Reaction of Cyclobutanone **2.6**. ..... 44

**Table 2.4.** Ligands and Directing Groups Screening on "Cut-and-Sew" Reaction of Cyclobutanone **2.6**..... 45

**Table 2.5.** Catalyst Screening on "Cut-and-Sew" Reaction of Cyclobutanone **2.24**..... 46

**Table 2.6.** Ligand Screening on "Cut-and-Sew" Reaction of Cyclobutanone **2.24**. ..... 47

**Table 2.7.** Catalysts Screening on "Cut-and-Sew" Reaction of Cyclobutanone **2.36**. ..... 51

**Table 2.8.** Ligands Screening on "Cut-and-Sew" Reaction of Cyclobutanone **2.36**..... 51

**Table 2.9.** Ligands Screening on "Cut-and-Sew" Reaction of Cyclobutanone **2.36** (No Directing Group, Part I). ..... 52

**Table 2.10.** Ligands Screening on "Cut-and-Sew" Reaction of Cyclobutanone **2.36** (No Directing Group, Part II). ..... 53

**Table 2.11.** Ligands Screening on "Cut-and-Sew" Reaction of Cyclobutanone **2.36** (No Directing Group, Part II). ..... 54

**Table 2.12.** Ligands Screening on "Cut-and-Sew" Reaction of Cyclobutanone **2.52**..... 55

**Table 2.13.** Catalysts Screening on "Cut-and-Sew" Reaction of Cyclobutanone **2.52**. ..... 56

**Table 2.14.** Ligands Screening on "Cut-and-Sew" Reaction of Cyclobutanone **2.52** (Toluene as Solvent). ..... 56

**Table 2.15.** Ligands Screening on "Cut-and-Sew" Reaction of Cyclobutanone **2.52** (Cationic Rhodium). ..... 57

**Table 2.16.** Initial Screening on "Cut-and-Sew" Reaction of Cyclobutanone **2.62**. ..... 61

**Table 2.17.** Temperature Screening on “Cut-and-Sew” Reaction of Cyclobutanone **2.62**..... 61

**Table 2.18.** Ligand Screening on “Cut-and-Sew” Reaction of Cyclobutanone **2.62**. ..... 62

**Table 2.19.** Catalysts Screening on “Cut-and-Sew” Reaction of Cyclobutanone **2.62**. ..... 62

**Table 2.20.** Solvent Screening on “Cut-and-Sew” Reaction of Cyclobutanone **2.62**. ..... 63

**Table 2.21.** Solvent Screening on “Cut-and-Sew” Reaction of Cyclobutanone **2.62** (150 °C). .. 63

**Table 2.22.** Ligands Screening on “Cut-and-Sew” Reaction of Cyclobutanone **2.62** (Cationic Rhodium). ..... 64

**Table 2.23.** Ligands Screening on “Cut-and-Sew” Reaction of Cyclobutanone **2.62** (Cationic Rhodium, 130 °C). ..... 65

**Table 2.24.** Additives Screening on “Cut-and-Sew” Reaction of Cyclobutanone **2.62**. ..... 66

**Table 2.25.** Attempts on “Cut-and-Sew” Reaction of Cyclobutanone **2.75**. ..... 69

**Table 2.26.** Attempts on “Cut-and-Sew” Reaction of Cyclobutanone **2.91**. ..... 70

**Table 2.27.** “Cut-and-Sew” Reaction of Cyclobutanone **2.95**. ..... 73

**Table 2.28.** Lewis Acid Screening on “Cut-and-Sew” Reaction of Cyclobutanone **2.95**. ..... 74

**Table 2.29.** Control Experiments on “Cut-and-Sew” Reaction of Cyclobutanone **2.95**. ..... 75

**Table 2.30.** Directing Group Equivalence Screening on “Cut-and-Sew” Reaction of Cyclobutanone **2.95**. ..... 76

**Table 2.31.** Directing Group Equivalence and Reaction Time Screening on “Cut-and-Sew” Reaction of Cyclobutanone **2.95**. ..... 76

**Table 2.32.** Directing Group Screening on “Cut-and-Sew” Reaction of Cyclobutanone **2.95**. ... 77

**Table 2.33.** Brønsted Acid Screening on “Cut-and-Sew” Reaction of Cyclobutanone **2.95**..... 78

**Table 2.34.** Concentration Screening on “Cut-and-Sew” Reaction of Cyclobutanone **2.95**. ..... 79

**Table 2.35.** Solvent Screening on “Cut-and-Sew” Reaction of Cyclobutanone **2.95**. ..... 79

**Table 2.36.** Solvent Screening on “Cut-and-Sew” Reaction of Cyclobutanone **2.95** (140 °C). .. 80

**Table 2.37.** Solvent Screening on “Cut-and-Sew” Reaction of Cyclobutanone **2.95** (5 mol% catalyst loading). ..... 80

**Table 2.38.** Preliminary Substrate Scope of the “Cut-and-Sew” Reaction of Ester-Tethered Cyclobutanones. ..... 82

**Table 2.39.** Preparation of Cyclobutanone **2.94a** through Pauson-Khand Reaction. ..... 83

**Table 2.40.** Catalyst Screening on “Cut-and-Sew” Reaction of Cyclobutanone **2.118**. ..... 87

**Table 2.41.** Ligands Screening on “Cut-and-Sew” Reaction of Cyclobutanone **2.118**. ..... 88

**Table 2.42.** Ligand Equivalence Screening on “Cut-and-Sew” Reaction of Cyclobutanone **2.118**. ..... 89

**Table 2.43.** Solvent Screening on “Cut-and-Sew” Reaction of Cyclobutanone **2.118**..... 90

**Table 2.44.** Base Additives Screening on “Cut-and-Sew” Reaction of Cyclobutanone **2.118**..... 90

**Table 2.45.** Lewis Acids Screening on “Cut-and-Sew” Reaction of Cyclobutanone **2.118**. ..... 91

**Table 2.46.** Concentration Screening on “Cut-and-Sew” Reaction of Cyclobutanone **2.118**. ..... 91

**Table 2.47.** Directing Groups Screening on “Cut-and-Sew” Reaction of Cyclobutanone **2.118**. 92

**Table 2.48.** Hydrolysis of Ester **2.99**. ..... 95

**Table 2.49.** Decarboxylation of Carboxylic Acid **2.136**. ..... 96

**Table 2.50.** Approach to Install Oxygen on C4 through Sanford’s C−H Oxygenation. ..... 98

**Table 2.51.** Methylation of Ketone **2.135**. ..... 100

**Table 2.52.** Attemps to Prepare sulfonyl amide **2.157**. ..... 103

**Table 2.53.** Reduction of Ketone **2.135**. ..... 104

**Table 2.54.** Preparation of Sulfonyl Amide **2.161**. ..... 105

**Table 2.55.** Du Bois C−H Amination of Sulfonyl Amide **2.161**. ..... 105

**Table 2.56.** Attempts to Prepare Ketone **2.165**..... 106

**Table 2.57.** Preparation of Silyl Enol Ether **2.166**..... 107

**Table 2.58.** Preparation of enone **2.167**..... 107

**Table 2.59.** Attemps on Hydroboration-Oxidation of Ketal **2.167**..... 108

**Table 2.60.** Desaturation of Ketone **2.135**..... 109

**Table 2.61.** One-Step Desaturation of Ketone **2.135**.....110

**Table 2.62.** Optimization on Stahl Oxidation of Ketone **2.135** (Part I). .....111

**Table 2.63.** Optimization on Stahl Oxidation of Ketone **2.135** (Part II). .....111

**Table 2.64.** Silylation of Enone **2.173**. .....112

**Table 2.65.** Meylation of Ketone **2.175**. .....112

**Table 2.66.** Oxidation of Diol **2.178**.....114

**Table 2.67.** Preparation of Silyl Enol Ether **2.183**.....115

**Table 2.68.** One-Step Desaturation of Ketone **2.134**.....116

**Table 2.69.** Conjugated Methylation of Enone **2.185**.....117

**Table 2.70.** Comparison of the $^{1}$H-NMR (Acetone-D6) Data of the Synthetic Penicibilaene A (**2.1**) ..... 201

**Table 2.71.** Comparison of the $^{13}$C-NMR (Acetone-D6) Data of the Synthetic Penicibilaene A (**2.1**) ..... 202

**Table 2.72.** Comparison of the $^{1}$H-NMR ($CDCl_3$) Data of the Synthetic Penicibilaene B (**2.2**) 203

**Table 2.73.** Comparison of the $^{1}$H-NMR ($CDCl_3$) Data of the Synthetic Penicibilaene B (**2.2**) 204

**Table 3.1.** Control Experiments..... 286

**Table 3.2**. Exploring the Limits of the Hydrogenolysis of C(aryl)−C(alkyl) Bonds.[a] ..... 287

**Table 3.3**. Substrate Scope.[a] ..... 290

**Table 3.4.** High Catalyst Loading Experiment. ..... 297

**Table 3.5.** Molecular Weight of Compound **3.1ab**. ..... 392

**Table 3.6.** Molecular Weight of Compound **3.1ac**. ..... 403

**Table 3.7.** Molecular Weight of Product Mixture. ..... 404

**Table 4.1.** Catalysts Screening on C−C Activation of Phosphinite **4.2a**. ..... 562

**Table 4.2.** Preparation of Phosphinite **4.5a**. ..... 563

**Table 4.3.** Initial Attempts on C−C Activation of Phosphinite **4.5a**. ..... 563

**Table 4.4.** Catalysts Screening on C−C Activation of Phosphinite **4.5a**. ..... 564

**Table 4.5.** Temperature Screening on C−C Activation of Phosphinite **4.5a**. ..... 565

**Table 4.6.** Ligands Screening on C−C Activation of Phosphinite **4.5a**. ..... 566

**Table 4.7.** Solvent Screening on C−C Activation of Phosphinite **4.5a**. ..... 567

**Table 4.8.** Reaction Time, Temperature and Concentration Screening on C−C Activation of Phosphinite **4.5a**. ..... 568

**Table 4.9.** Additives Screening on C−C Activation of Phosphinite **4.5a**. ..... 569

**Table 4.10.** Ligands Screening on C−C Activation of Phosphinite **4.5a** (Cationic Ruthenium). 569

**Table 4.11.** Temperature Screening on C−C Activation of Phosphinite **4.5a** (Cationic Ruthenium). ..... 570

**Table 4.12.** C−C Activation of Phosphinite **4.6a**. ..... 571

**Table 4.13.** Additives Screening on C−C Activation of Phosphinite **4.5a** (Part 2). ..... 572

**Table 4.14.** Reductant Screening on C−C Activation of Phosphinite **4.5a**. ..... 572

**Table 4.15.** Kinetic Studies on C−C Activation of Phosphinite **4.5a**. ..... 574

**Table 4.16.** Additives Screening on C−C Activation of Phosphinite **4.5a** (Part 3). ..... 575

**Table 4.17.** Additives Screening on C−C Activation of Phosphinite **4.5a** (Part 4). ..... 576

**Table 4.18.** Additives Screening on C−C Activation of Phosphinite **4.5a** (Part 5). ..... 577

**Table 4.19.** Solvent Screening on C−C Activation of Phosphinite **4.5b**. ..... 578

# LIST OF ABBREVIATIONS

| | |
|---|---|
| Ac | Acetyl |
| acac | Acetylacetonate |
| Ad | Adamantyl |
| Ar | Aryl |
| 9-BBN | 9-Borabicyclo[3.3.1]nonane |
| BHT | 3,5-Di-*tert*-4-butylhydroxytoluene |
| BIPHEP | 2,2′-Bis(diphenylphosphino)-1,1′-biphenyl |
| Bn | Benzyl |
| Boc | *tert*-Butoxycarbonyl |
| BPY | 2,2'-Bipyridine |
| BQ | *p*-Benzoquinone |
| Bu | Butyl |
| Bz | Benzoyl |
| cat. | Catalytic / catalyst |
| COD | 1,5-Cyclooctadienyl |

| | |
|---|---|
| COE | Cyclooctene |
| COT | Cyclooctatetraene |
| CSA | Camphor-10-sulfonic acid |
| Cy | Cyclohexyl |
| δ | Chemical shift |
| DAC | Diallyl carbonate |
| dba | Dibenzylideneacetone |
| DBU | 1,8-Diazabicyclo[5.4.0]undec-7-ene |
| DCE | 1,2-Dichloroethane |
| DCM | Dichloromethane |
| dCypb | 1,4-Bis(dicyclohexylphosphino)butane |
| dCype | 1,2-Bis(dicyclohexylphosphino)ethane |
| dCypm | Bis(dicyclohexylphosphino)methane |
| deCO | Decarbonylation |
| DFB | Difluorobenzene |
| dfppe | 1,2-Bis[bis(pentafluorophenyl)phosphino]ethane |

| | |
|---|---|
| DG | Directing group |
| DIAD | Diisopropyl azodicarboxylate |
| DIBAL-H | Diisobutylaluminum hydride |
| DIC | *N*,*N*'-Diisopropylcarbodiimide |
| DIPA | Diisopropylamine |
| DIPEA | *N*,*N*-Diisopropylethylamine |
| DMAc | *N*,*N*-Dimethylacetamide |
| DMAP | 4-(Dimethylamino)pyridine |
| DME | 1,2-Dimethoxyethane |
| DMF | *N*,*N*-Dimethylformamide |
| DMP | Dess-Martin periodinane |
| DMPU | *N, N'*-Dimethylpropyleneurea |
| DMS | Dimethyl sulfide |
| DMSO | Dimethylsulphoxide |
| DNPH | 2,4-Dinitrophenylhydrazine |
| DPEphos | (Oxydi-2,1-phenylene)bis(diphenylphosphine) |

| | |
|---|---|
| dppb | 1,4-Bis(diphenylphosphino)butane |
| dppbz (dppbenz) | 1,2-Bis(diphenylphosphino)benzene |
| dppe | 1,2-Bis(diphenylphosphino)ethane |
| dppf | 1,1'-Bis(diphenylphosphino)ferrocene |
| dppm | Bis(diphenylphosphino)methane |
| dppp | 1,3-Bis(diphenylphosphino)propane |
| dpppe | 1,5-Bis(diphenylphosphino)pentane |
| DTBMP | 2,6-Di-*tert*-butyl-4-methylpyridine |
| EA | Ethyl acetate |
| EDC (EDCI) | *N*-(3-Dimethylaminopropyl)-*N'*-ethylcarbodiimide hydrochloride |
| ee | Enantiomeric excess |
| esp | α,α,α',α'-Tetramethyl-1,3-benzenedipropionic acid |
| Et | Ethyl |
| equiv | Equivalent |
| GC | Gas chromatography |

| | |
|---|---|
| GPC | Gel permeation chromatography |
| 1,5-HD | 1,5-Hexadiene |
| HMDS | Hexamethyldisilazane |
| HMPA | Hexamethylphosphoramide |
| HOBt | 1-Hydroxybenzotriazole |
| HRMS | High-resolution mass spectrometry |
| IBX | 2-Iodoxybenzoic acid |
| IMes | 1,3-Bis(2,4,6-trimethylphenyl)-1,3-dihydro-2H-imidazol-2-ylidene |
| *i*-Pr | Isopropyl |
| IPr | 1,3-Bis(2,6-diisopropylphenyl)-1,3-dihydro-2H-imidazol-2-ylidene |
| IR | Infrared |
| LDA | Lithium diisopropylamide |
| *m* | Meta |
| MALS | Multi-Angle Light Scattering Detection |

| | |
|---|---|
| mCPBA | *meta*-Chloroperoxybenzoic acid |
| Me | Methyl |
| $Me_4Phen$ | 3,4,7,8-Tetramethyl-1,10-phenanthroline |
| Mes | Mesityl |
| MOM | Methoxymethyl |
| MPO | 4-Methoxypyridine *N*-oxide |
| Ms | Methanesulphonyl |
| NBD | 2,5-Norbornadiene |
| NBE | 2-Norbornene |
| NBS | *N*-Bromosuccinimide |
| *n*-Bu | *normal*-Butyl |
| n.d. | No desired product |
| NHPI | *N*-Hydroxyphthalimide |
| NIS | *N*-Iodosuccinimide |
| NMM | 4-Methylmorpholine |
| NMO | 4-Methylmorpholine *N*-oxide |

| | |
|---|---|
| NMP | 1-Methyl-2-pyrrolidinone |
| NMR | Nuclear magnetic resonance |
| *n*-Pr | *normal*-Propyl |
| n.r. | No reaction |
| Ns | Nitrobenzenesulphonyl |
| *o* | Ortho |
| *p* | Para |
| PCC | Pyridinium chlorochromate |
| pdt | Product |
| Ph | Phenyl |
| PIDA | (Diacetoxyiodo)benzene |
| pin | pinacolato |
| Piv | Pivaloyl |
| PMP | 1,2,2,6,6-Pentamethylpiperidine |
| PPTS | Pyridinium *p*-toluenesulfonate |
| PTSA | *p*-Toluenesulfonic acid |

| | |
|---|---|
| Py | Pyridine |
| RT | Room temperature |
| SIMes | 1,3-Bis(2,4,6-trimethylphenyl)-4,5-dihydroimidazol-2-ylidene |
| SIPr | 1,3-Bis(2,6-di-*i*-propylphenyl)imidazolidin-2-ylidene |
| s.m. | Starting material |
| TBAF | Tetrabutylammonium fluoride |
| TBAI | Tetrabutylammonium iodide |
| TBDPS | *tert*-Butyldiphenylsilyl |
| TBHP | *tert*-Butyl hydroperoxide |
| TBS | *tert*-Butyldimethylsilyl |
| *t*-Bu | *tert*-Butyl |
| TEA | Triethylamine |
| TEMPO | 2,2,6,6-Tetramethylpiperidine 1-oxyl |
| Tf | Trifluoromethanesulphonyl |

| | |
|---|---|
| TFA | Trifluoroacetic acid |
| TFP | Tri(2-furyl)phosphine |
| THF | Tetrahydrofuran |
| TIPS | Triisopropylsilyl |
| TLC | Thin-layer chromatography |
| TMEDA | *N*,*N*,*N'*,*N'*-Tetramethylethylenediamine |
| TMP | 2,2,6,6-Tetramethylpiperidine |
| TMS | Trimethylsilyl |
| TMTU | Tetramethylthiourea |
| Tol | Tolyl |
| TPAP | Tetrapropylammonium perruthenate |
| Ts | *para*-Toluenesulphonyl |

ACKNOWLEDGEMENT

First, I would like to thank my advisor, Professor Guangbin Dong, for giving me such an opportunity to join his lab and pursue organic chemistry research here. I really thank Guangbin's managing style, which as his favorite motto said, "Hire the best people……then get out of their way". When I first join the lab, I told Gunagbin that I was really interested in total synthesis and want to do research on this area. Although our group is majorly working on methodology research, Guangbin still encourage me to do the things I would like to. During my Ph.D. study, Guangbin never stop me to try my own ideas and force me to trying something else, which ignite my passion towards organic chemistry research. Guangbin also always gave me the critical suggestions and encourage me every time I encountered some problems in my research, which helps me a lot during the past five years. As a team leader, Guangbin also build a very nice environment in our group, which inherit the academic tradition of the University of Chicago. On the occasion of leaving this lab, I am really grateful that I have the lucky to join this lab and appreciate what Guangbin did in the past.

Secondly, I would like to thank Professor Tuoping Luo, my undergraduate research advisor. Professor Tuoping Luo is one of the most talented young organic chemists. I not only learned organic chemistry knowledge in his lab, but also infected by his enthusiasm on the research. He is always my model during my learning.

Thirdly, I would like to thank Mr. Yamin Zhang, who teach me chemistry in the high school. During this period, I first encountered organic chemistry and found a way I wanted to walk on.

I would also like to thank my committee members, Professor Viresh Rawal and Professor Scott Snyder, for attending my dissertation defense, and generously providing the their critical

feedback. I also really appreciate their recommendation letters on my behalf, which offer a huge help during my job searching.

I am also very grateful to thank committee members for my candidacy exam, Professor Stuart Rowan, Professor Luping Yu and Professor Scott Snyder, for their supporting and suggestions on my research and career.

I would like to express my gratitude on everyone in total synthesis and C−C subgroups in our lab: Jiaxin Xie, Sihua Hou, Saiyong Pan, Brent Billett, Jun Zhu, Ziqiang Rong, Ying Xia, Lin Deng, Tatsuhiro Tsukamoto, Xuan Yu, Xukai Zhou, Congjun Yu, Shusuke Ochi, Rui Zhang, Cole Wagner and Zining Zhang. Some of them are nice coworkers on my projects. They gave me many valuable suggestions on my research and I believe I cannot finish any project without the help from these smart co-workers. I especially appreciate Jiaxin Xie, who also works on total synthesis projects in our lab. Jiaxin teach me many things on experiments and offered numerous creative and insightful discussions during my Ph.D. study. I am also grateful to him for bringing me from airport to lab on the first day I came Chicago. Sihua Hou is a big brother in total synthesis and C−C subgroups and I would like to thank him for his suggestions on my project as well as holding the parties and the activities. Jun and Rui are both nice co-workers and I am glad to collaborate with them to finish C(aryl)−C(alkyl) activation project.

I would also like to thank two undergraduate students working with me, Benjamin Ratchford and Arjuna Parsad, who are all smart and talented young people. I also learned a lot during teaching them, and I appreciate the material they prepared, which effectively cut down the time I need to finish a project.

I want to express my appreciation to all the other past and present members of the Dong group: Zhongxing Huang, Gang Li, Likun Jin, Dong Xing, Zhe Dong, Yan Xu, Feipeng Liu, Pengfei Liu, Xiaoyang Chen, Jianchun Wang, Ki-Young Yoon, Chengpeng Wang, Yun Zhou, Ming Chen, Alexander Rago, Renhe Li, Won Jun Jang, Zhao Wu, Pingluan Wang, Hairong Lyu, Bo Zhou, Jiangliang Yin, Xin Liu, Qiqiang Xie, Jingfeng Huo, Woohyun Jo, Shinyoung Choi, Miao Chen, Daniel Pyle and Zhijie Chen. I especially thank to Renhe Li, who came from the same city as me and shareed the same hood with me as well for one year. I also miss the happy hour with Yan Xu, Jianchun Wang and Chengpeng Wang to play the video game. I would like to thank Major Pengfei Zheng and Pingluan Wang for exploring the restaurants in Chicago.

Besides, I would like to thank people who offering help on the machines and materials: Antoni Jurkiewicz (NMR), Josh Kurutz (NMR), Jin Qin (Masspec), Guangchang Zhou (Masspec), Ki-Young Yoon (XRD), Shusuke Ochi (XRD), Xin Liu (XRD), Philip Griffin (GPC-MALS), Andreas Henke (Novolacs), Michael Reedy (Technical support) and Laura Luburich (Technical support).

I also want to thank friends outside the Dong Group: Xuanyu Feng, Yiyang Luo, Zuyu Qiao, Pei Qu, Yun Zhang and Chang Liu, for the happy time with them over the past years.

The last word of acknowledgement that I have saves is for my family. I deeply thank my mom, dad, grandma and grandpa for their trust and love. I cannot have any achievements without their understanding and support. I dedicated this thesis to them.

Yibin Xue

*University of Chicago*

August 2022

# CHAPTER 1

## Deconstructive Synthesis of Bridged and Fused Rings via Transition Metal-Catalyzed "Cut-and-Sew" Reactions of Benzocyclobutenones and Cyclobutanones

### 1.1. Introduction

Transition metal (TM)-catalyzed carbon−carbon bond (C−C) activation has been emerging from organometallic curiosity to useful synthetic tools.[1] After numerous of efforts in the past decades, the "inert" C−C bond can be cleavage by transition metal to form more active carbon−metal (C−M) bonds in catalytic manner, which enable the following functionalization of the C−C bond. Comparing to well-developed C−H activation, a unique character of C−C activation is the potential to reconstruct carbon skeleton, which provides new strategies to synthetic community to synthesize complex natural products.

Among all the C−C activation methodologies, "cut-and-sew" reaction,[2] the transition-metal catalyzed C−C activation followed by insertion of an unsaturated 2π unit, has been found useful for constructing various bridged and fused rings which are ubiquitous in natural products. Two types of the most well-applied substrates for "cut-and-sew" reactions are benzocyclobutenone and cyclobutanone, since the internal strain in the four-membered ring can facilitate oxidative addition

of transition metal into C−C bonds (Scheme 1.1A).[3] The first catalytic intramolecular "cut-and-sew" reaction between cyclobutanone and alkenes was developed by Murakami and co-workers in 2002.[4] Inspired by the elegant work of Murakami, our group successfully realized the "cut-and-sew" reaction between benzocyclobutenone and alkene in 2012.[5] Up to date, many different types of "cut-and-sew" reaction of benzocyclobutenone and cyclobutanone have been developed, including 1) (4+2) or (4+2−1) cycloaddition between benzocyclobutenone and 2π unit to construct [m.n.0] fused rings; 2) (4+1) cycloaddition between benzocyclobutenone and alkene to construct 2-indanone; 3) (4+2) cycloaddition between $\alpha$-branched cyclobutanone and 2π unit to construct [m.n.0] fused rings; 4) (4+2), (4+2−1) or (4+1) cycloaddition between $\beta$-branched cyclobutanone and 2π unit to construct [m.n.1] bridged rings.

[m.n.0] fused rings and [m.n.1] bridged ring systems are abundant in many bioactive natural products, such as terpenes, alkaloids and steroids. As a powerful tools to construct [m.n.0] and [m.n.1] ring system, "cut-and-sew" strategy has been applied to several complex natural product syntheses, including total synthesis of cycloinumakiol (**1.1**, proposed structure),[6] cycloclavine (**1.2**),[7] xylanigripones A (**1.3**),[8] galanthamine (**1.4**),[9] morphine-family alkaloids (**1.5**−**1.7**)[10] and penicibilaenes (**1.8**, **1.9**)[11] (Scheme 1.1B). In this chapter, we summarize the diverse reactivities of "cut-and-sew" reaction of benzocyclobutenone and cyclobutanone, as well as the representative total synthesis of alkaloids and terpenes enabled by "cut-and-sew" reaction during the past 10 years in our laboratory.

**Scheme 1.1.** "Cut-and-Sew" Reaction of Benzocyclobutenone and Cyclobutanone, and Their Applications.

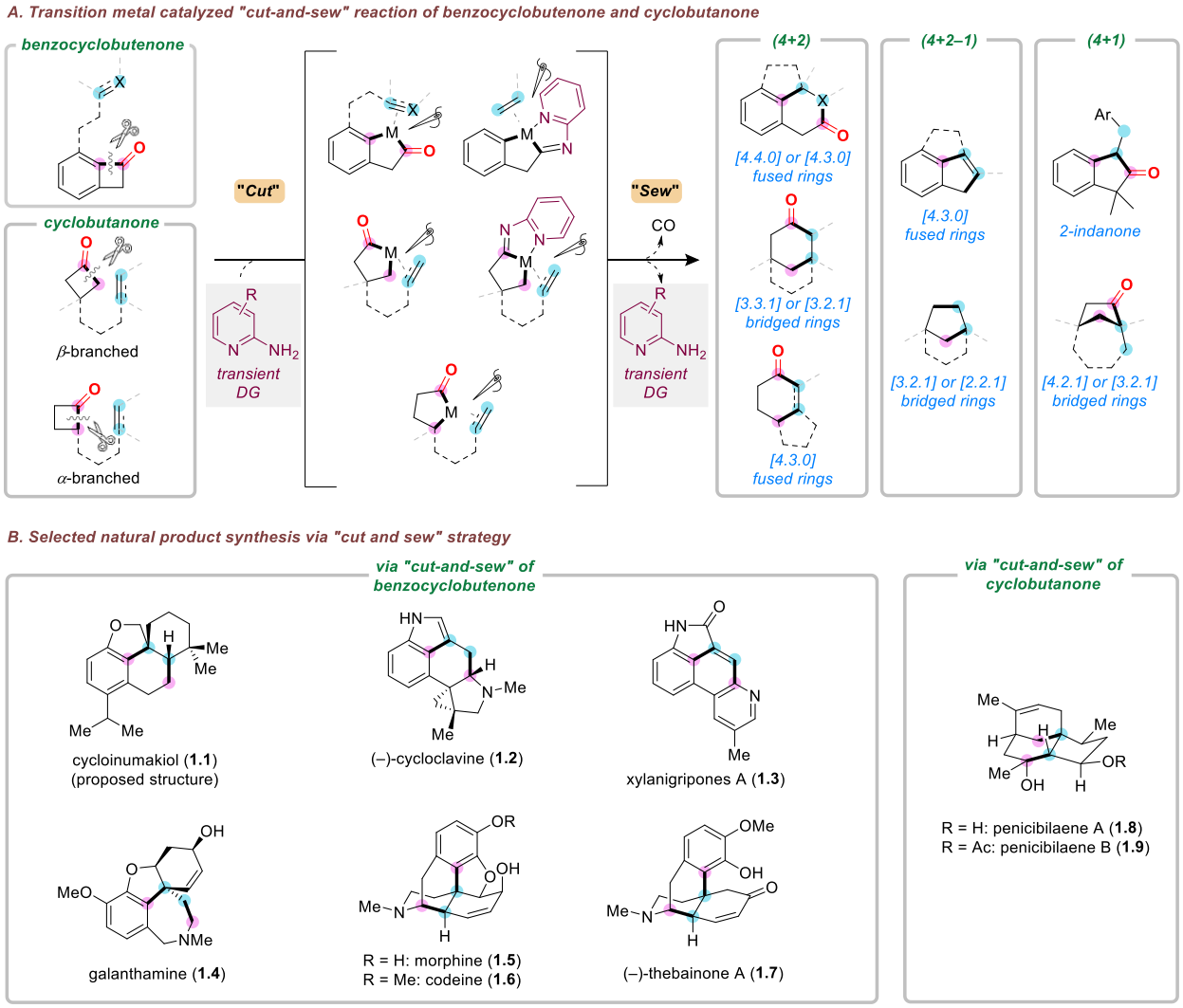


## 1.2. Method Development

### 1.2.1 (4+2) "Cut-and-Sew" Reaction of Benzocyclobutenone

Benzocyclobutenone is a kind of readily available compounds contains four-membered cyclobutanone motif,[12] which can be easily prepared from [2+2] cycloaddition[13] or some other transformations.[14] The C−C activation of benzocyclobutenone was facilitated by the ring strain in four-membered ring. Thus, benzocyclobutenone was proved to be an excellent substrate for "cut-

and-sew" transformation, such as (4+2) "cut-and-sew" reaction. The first intramolecular "cut-and-sew" reaction between benzocyclobutenone and alkene was accomplished by our group in 2012 (Scheme 1.2A).[5] This method shows good functional group tolerance (Scheme 1.2C), such as ester and protected alcohol. Besides, this method not only works on less sterically hindered mono- and 1,1-di-substituted alkene, but also delivers moderate to good yield for 1,2-di- or tri-substituted alkene. The "cut-and-sew" reaction between benzocyclobutenone and alkene can also be enantioselective with DTBM-segphos as ligand (Scheme 1.3A).[15] The asymmetric version of "cut-and-sew" reaction also shown great functional group tolerance and delivers high enantioselectivity for most of the substrates (Scheme 1.3B).

After detailed computational and experimental study on this reaction, we proposed a "rhodium migration" mechanism for this transformation (Scheme 1.2B).[16] Instead of directly oxidative addition into C(aryl)−C(carbonyl) bond in benzocyclobutenone **1.10** to generate more thermodynamically stable intermediate **1.14**, oxidative addition of less hindered C(alkyl)−C(carbonyl) bond to generate intermediate **1.12** is more kinetically feasible. Intermediate **1.12** can readily undergo $\alpha$-elimination to give carbonyl complex **1.13**, followed by CO-reinsertion to deliver complex **1.14**. Finally, migration insertion of alkene into C(aryl)−C(carbonyl) bond gives seven-membered metallacycle **1.15**, followed by reductive elimination to release final product **1.11**.

**Scheme 1.2.** Rhodium Catalyzed (4+2) "Cut-and-Sew" Reaction between Benzocyclobutenone and Alkene.

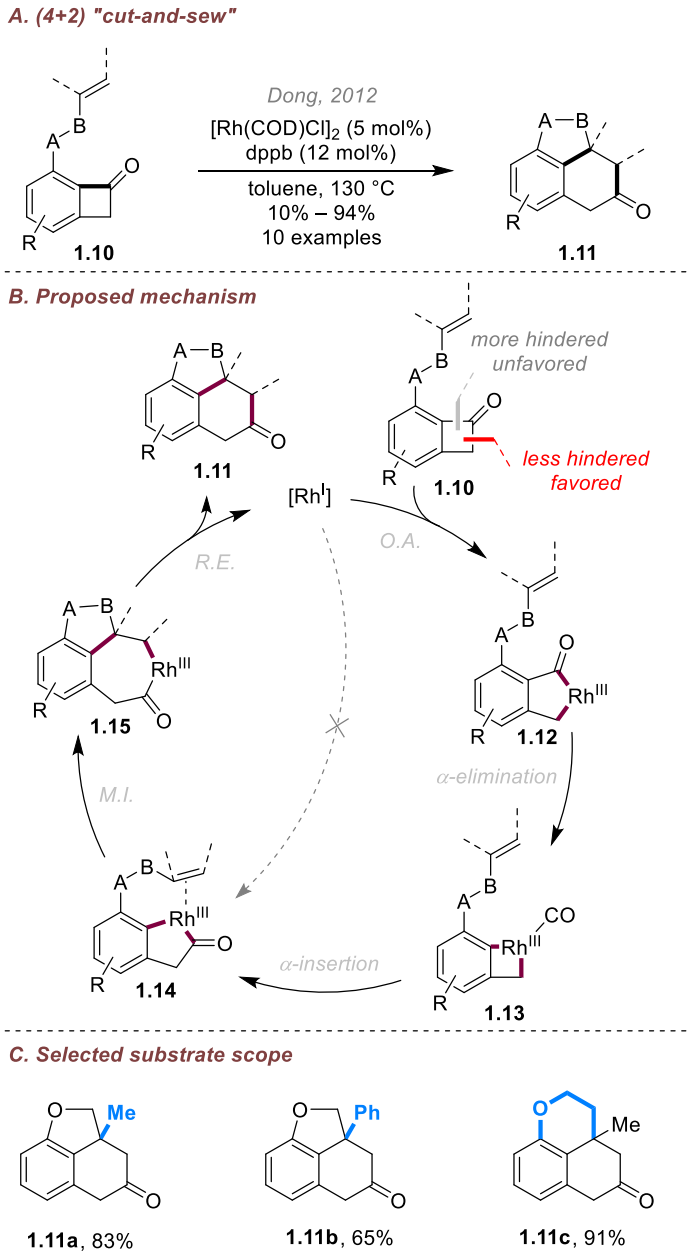

**Scheme 1.3.** Rhodium Catalyzed Asymmetric (4+2) "Cut-and-Sew" Reaction between Benzocyclobutenone and Alkene.

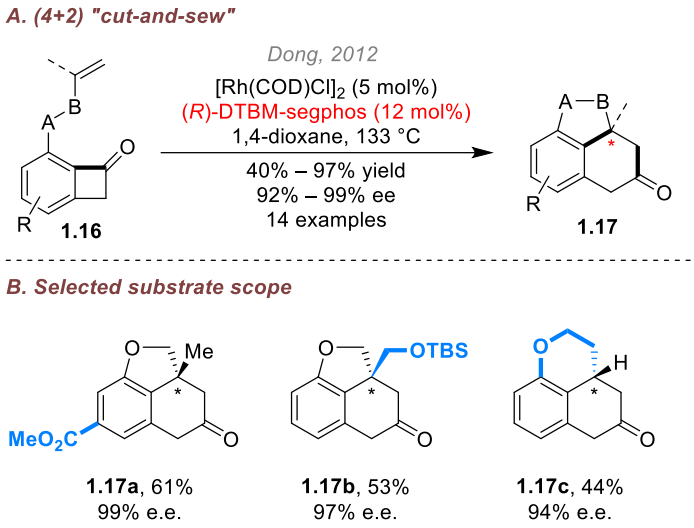


In 2014, our group developed "cut-and-sew" reaction between benzocyclobutenone and alkyne.[17] Driven by aromatization, the initial ketone product would undergo keto-enol tautomerization to generate 2-naphthol (Scheme 1.4). To our delight, in 2018 we found the same type of reaction can be catalyzed by first-row metal, cobalt (Scheme 1.5A), which is much more abundant and cheaper than rhodium catalyst.[18] Using $Co_2(CO)_8$ as the catalyst, (4+2) "cut-and-sew" reaction between benzocyclobutenone and alkyne can deliver 2-naphthol **1.21** or enol **1.22**. Comparing with rhodium catalyzed condition, cobalt catalysis even shows higher efficiency on some substrate, such as the substrate with methyl alkyne or enyne, which can deliver 2-naphthol **1.21a** and **1.21b** (Scheme 1.5B). It worth to notice that the rhodium catalysis and cobalt catalysis go through different reaction pathway. Rhodium condition initiated by oxidative addition into less hindered C(carbonyl)−C(alkyl) bond, then undergo carbonyl exclusion/reinsertion to get formally C(carbonyl)−C(aryl) bond activation product. Whereas cobalt catalyst can directly undergo oxidative addition into C(carbonyl)−C(aryl) bond, which "directed" by alkyne via alkyne-cobalt

complex. The special mechanism of cobalt catalysis enabled some unprecedented “cut-and-sew” reactions, such as the (4+2) “cut-and-sew” between substituted benzocyclobutenone and alkyne to give enone **1.22a**. For comparison, the substituents on the ketone α position inhibit the oxidative addition of C(carbonyl)−C(aryl) bond, which give no desired “cut-and-sew” product under rhodium condition.

**Scheme 1.4.** Rhodium Catalyzed (4+2) “Cut-and-Sew” Reaction between Benzocyclobutenone and Alkyne.

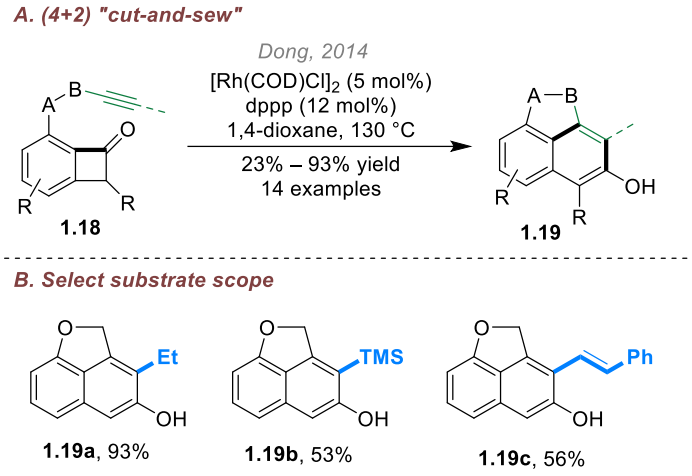

**Scheme 1.5.** Cobalt Catalyzed (4+2) "Cut-and-Sew" Reaction between Benzocyclobutenone and Alkyne.

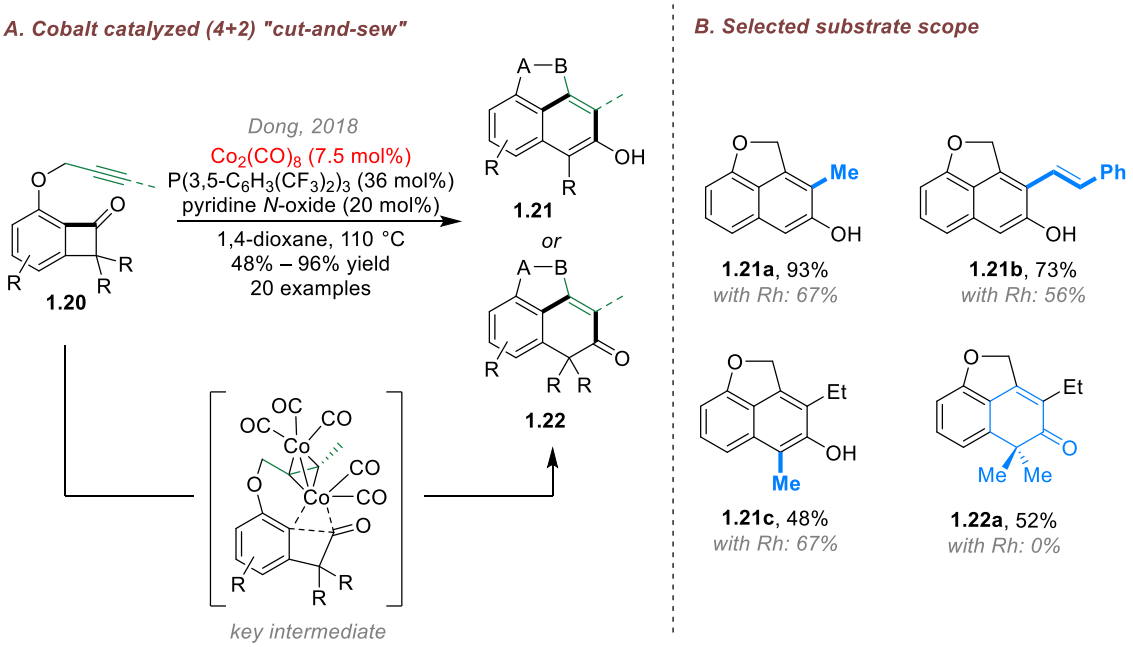


Besides carbon−carbon multiple bond, polar carbon−hetero double bond can also serve as 2π unit in "cut-and-sew" reaction. In 2016, our group developed asymmetrical "cut-and-sew" reaction between benzocyclobutenone and imine (Scheme 1.6A).[19] In this work, the combination of two chiral ligands can deliver both high yield and high enantioselectivity of chiral lactam product (Scheme 1.6B). Similar as imine, ketone can also serve as 2π unit in this type of "cut-and-sew" reaction (Scheme 1.7A).[20] After generation of initial (4+2) cycloaddition product, the lactone ring can be spontaneously opened through a elimination, which driven by the aromatization to form benzofuran **1.26** (Scheme 1.7B).

**Scheme 1.6.** Rhodium Catalyzed Asymmetric (4+2) "Cut-and-Sew" Reaction between Benzocyclobutenone and Imine.

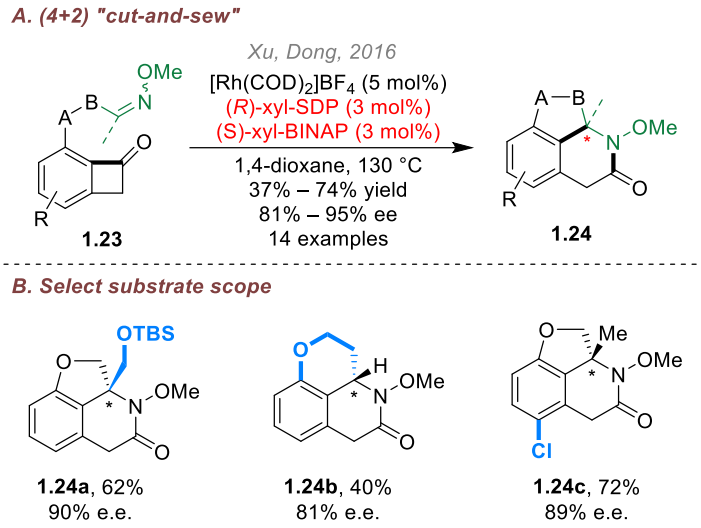


**Scheme 1.7.** Rhodium Catalyzed Asymmetric (4+2) "Cut-and-Sew" Reaction between Benzocyclobutenone and Ketone/Aldehyde.

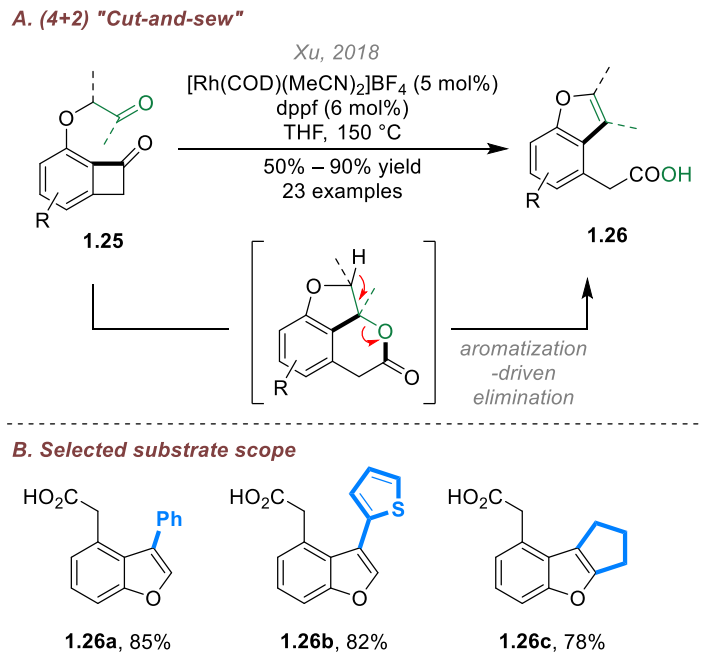

### 1.2.2 (4+2) "Cut-and-Sew" Reaction of Cyclobutanone

Both $\beta$-branched and $\alpha$-branched cyclobutanone can undergo (4+2) "cut-and-sew" reaction with 2π unsaturated unit to give bridged or fused bicycles. The pioneer work by Murakami shown that the cationic rhodium can catalyze "cut-and-sew" reaction between benzene-tethered cyclobutanone and alkene, albeit the scope of their method is limited (Scheme 1.8).[4] In 2012, utilizing amino pyridine as transient directing group, our group accomplished nitrogen- or malonate-tethered "cut-and-sew" reaction between cyclobutanone and alkene to construct bicyclo[3.3.1] bridged ring system, which is difficult to be constructed by traditional type II intramolecular Diels-Alder (IMDA) reaction (Scheme 1.9A).[21] The reaction started from condensation between amino pyridine and cyclobutanone **1.29** to form imine **1.31** (Scheme 1.9B). Directed by pyridine, the rhodium(I) catalyst can undergo oxidative addition to give metallocycle **1.32**, followed by migratory insertion of alkene and reductive elimination to give imine **1.34**. Finally, in-situ hydrolysis of imine **1.34** delivers the ketone **1.30** and regenerate amino pyridine. Our method shown a broad substrate scope (Scheme 1.9C), and acid-sensitive functional group such as silyl ether in **1.30b** can be well tolerated. In particular, the linker in this reaction can be largely expanded using our method, shorter linker in **1.30e** and malonate linker in **1.30f** also delivered cyclized product in moderate yield.

**Scheme 1.8.** Murakami's Pioneer Work on Rhodium Catalyzed (4+2) "Cut-and-Sew" Reaction between Cyclobutanone and Alkene.

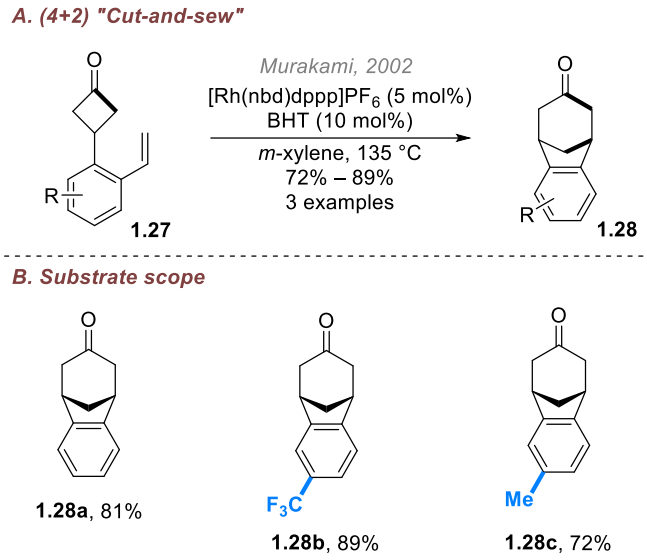

**Scheme 1.9.** Transient Directing Group Enabled Rhodium Catalyzed (4+2) "Cut-and-Sew" Reaction between Cyclobutanone and Alkene.

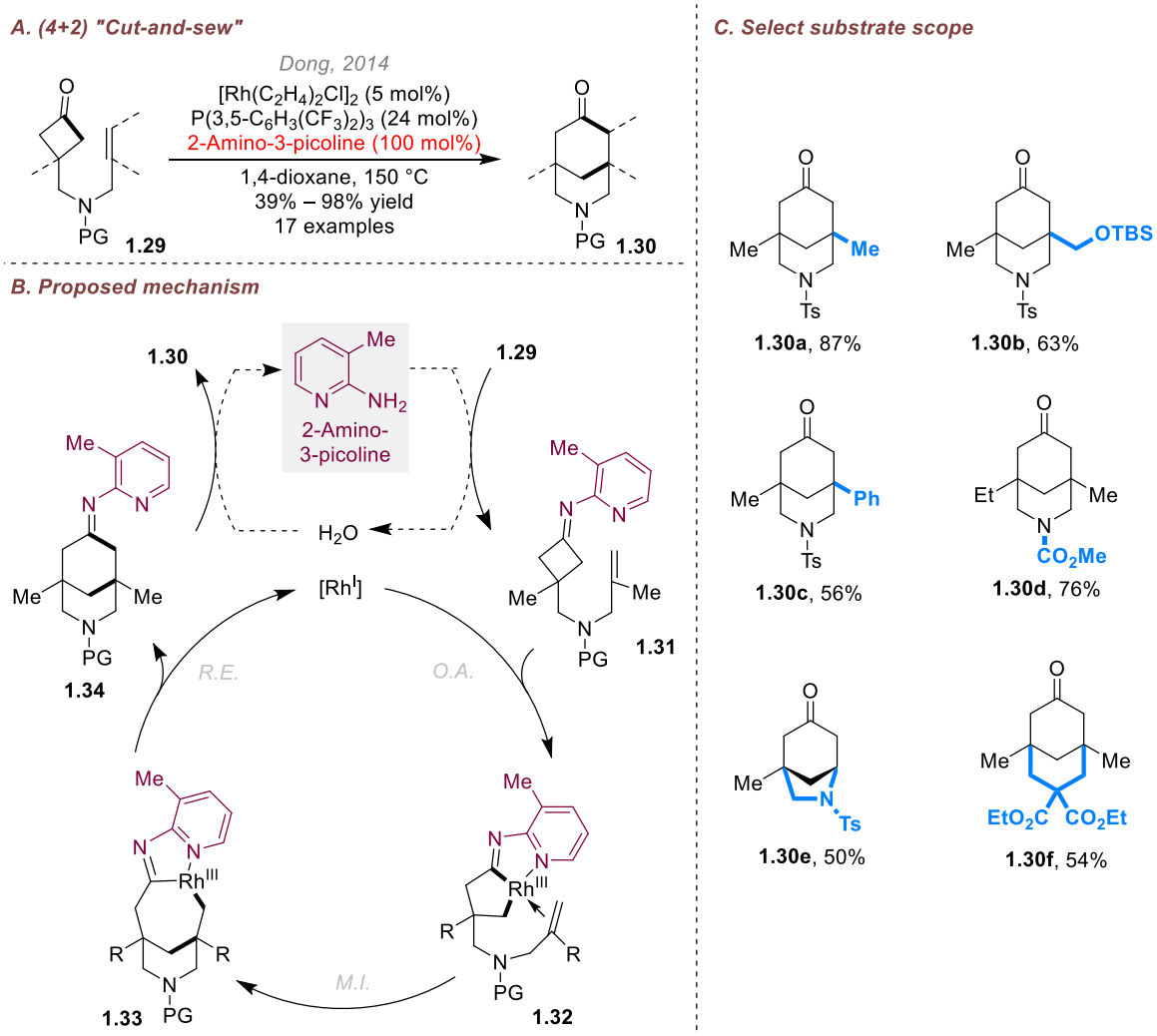


In 2014, Cramer group found that high enantioselectivity can be achieved in (4+2) "cut-and-sew" reaction between benzene-tethered cyclobutanone and alkene with DTBM-segphos as ligand (Scheme 1.10).[22] Besides alkene, ketone can also serve as the 2π unit in this work.[23] In 2020, our group developed the enantioselective "cut-and-sew" reaction between cyclobutanone and alkyne (Scheme 1.11A).[24] The detailed calculation study reveals that the rhodium-stabilized anti-Bredt double bond would be generated at first, and then a rhodium-catalyzed hydride migration can

deliver the final product. The enone product typically have a more thermodynamically favored *E* double bond (Scheme 1.11B). However, kinetically favored *Z* product became predominated with oxygen linkage in **1.40c**, due to the reaction was run under room temperature in this entry.

**Scheme 1.10.** Rhodium Catalyzed (4+2) "Cut-and-Sew" Reaction between Cyclobutanone and Alkene/Ketone/Aldehyde.

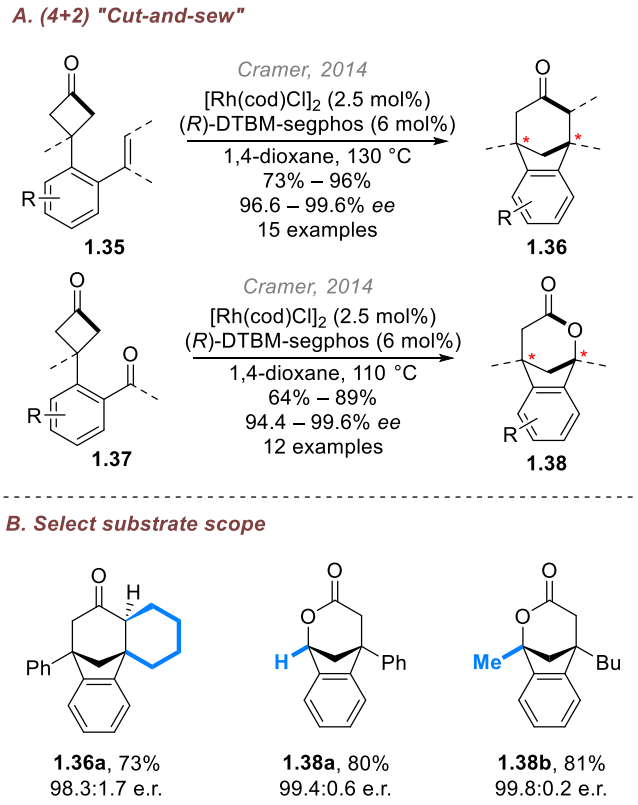

**Scheme 1.11.** Rhodium Catalyzed (4+2) "Cut-and-Sew" Reaction between Cyclobutanone and Alkyne.

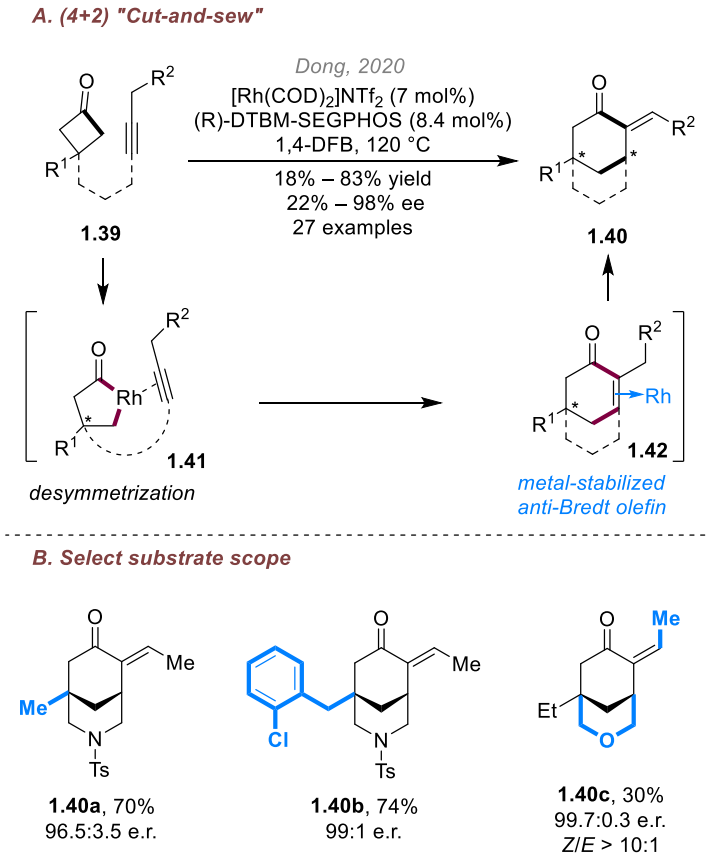


In addition to $\beta$-branched cyclobutanone, $\alpha$-branched cyclobutanone can also undergo "cut-and-sew" reaction with 2π unit. In 2018, our group found that the "cut-and-sew" reaction between $\alpha$-branched cyclobutanone and alkyne can be utilized to construct [4.3.0] fused enone (Scheme 1.12A).[25] Similar to "cut-and-sew" reaction of benzocyclobutenone, we proposed that the rhodium(I) catalyst tend to undergo oxidative addition with less sterically hindered C−C bond in cyclobutanone **1.43** to give complex **1.45**, followed by CO elimination and reinsertion to generate thermodynamically more stable metallocycle **1.47** (Scheme 1.12C). The sequential migratory insertion and reductive elimination finally delivers the cyclized product **1.44**. Besides alkyl and phenyl alkyne, TMS protected alkyne also works under the standard condition (Scheme 1.12B).

With DTBM-segphos as ligand, we can also realize kinetic resolution of $\alpha$-branched cyclobutanone **1.49** (Scheme 1.13A), to give high yield and enantioselectivity of cyclized product **1.50** with fused rings (Scheme 1.13B).[26]

**Scheme 1.12.** Rhodium Catalyzed (4+2) "Cut-and-Sew" Reaction between $\alpha$-Branched Cyclobutanone and Alkyne.

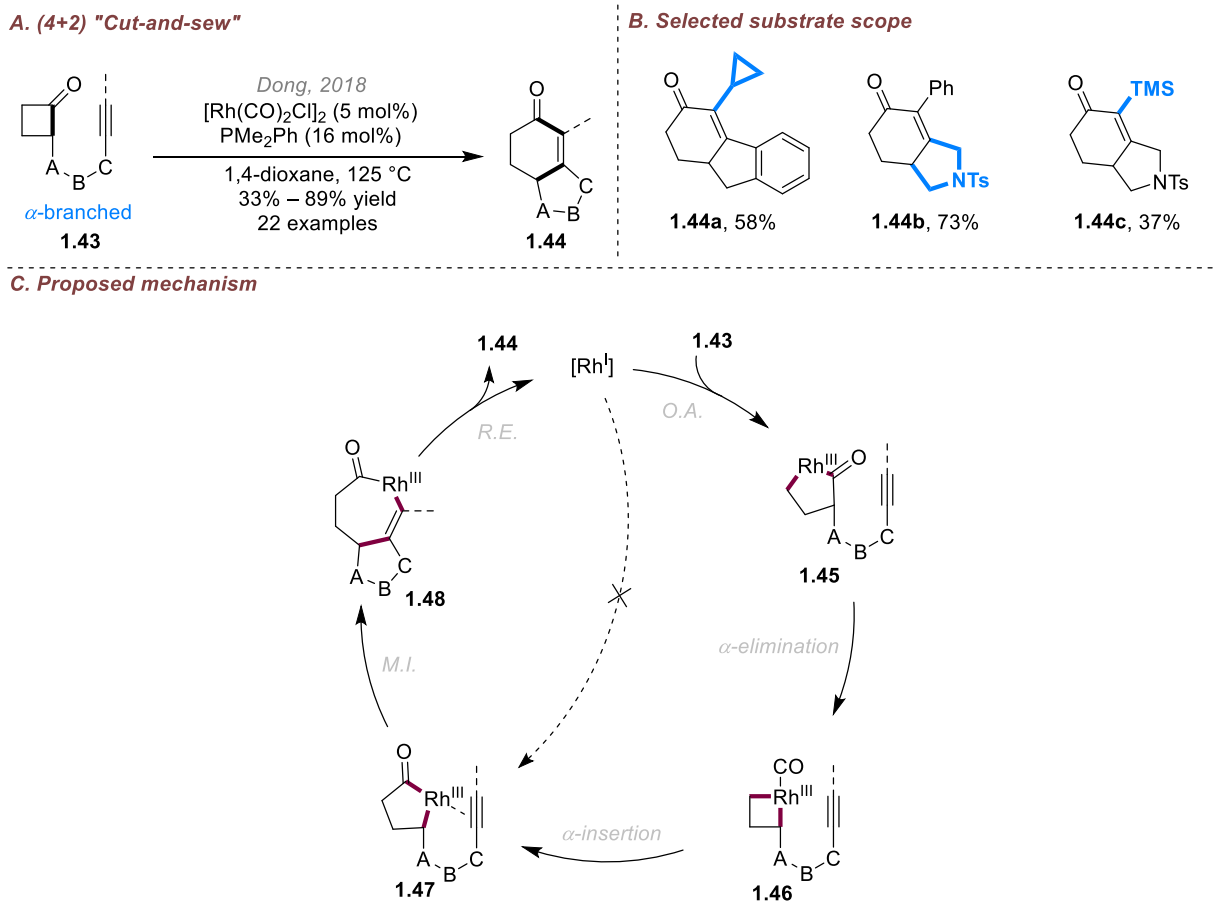

**Scheme 1.13.** Rhodium Catalyzed Asymmetric (4+2) "Cut-and-Sew" Reaction between α-Branched Cyclobutanone and Alkyne.

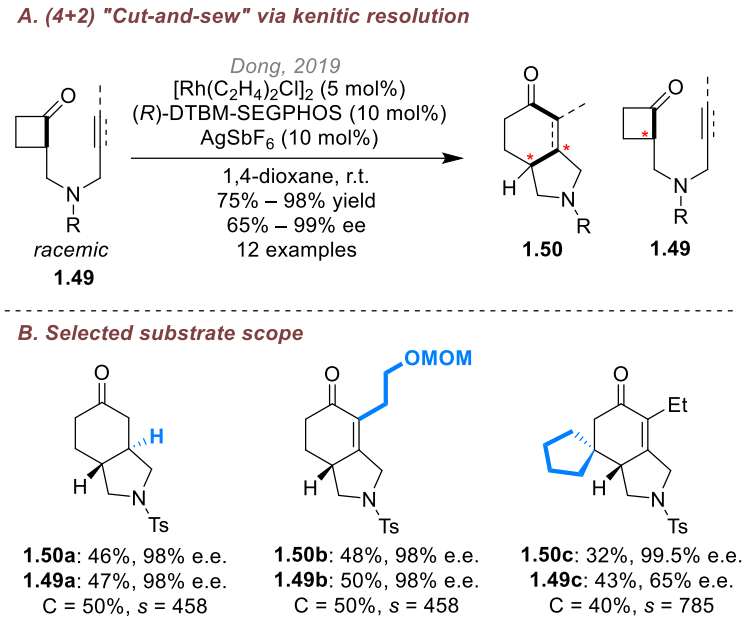


### 1.2.3 (4+2−1) "Cut-and-Sew" Reaction of Benzocyclobutenone and Cyclobutanone

Besides (4+2) "cut-and-sew" reaction, other "cut-and-sew" reaction such as (4+2−1) cycloaddition can also be utilized to construct bridged or fused ring system. In 2014, our group found that substituted indene can be prepared through (4+2−1) reaction between benzocyclobutenone and alkyne when refluxing in xylene (Scheme 1.14A).[17] From mechanism aspect, the initial stage of (4+2−1) "cut-and-sew" reaction is the same as (4+2) "cut-and-sew" reaction, which started with oxidation addition of rhodium(I) into less hindered C(carbonyl)−C(alkyl) bond in benzocyclobutenone **1.51** followed by α-carbon elimination to generate metallocycle **1.54** (Scheme 1.14B). Afterward, instead of CO reinsertion, the CO ligand in complex **1.54** would dissociate to give complex **1.55** in (4+2−1) "cut-and-sew" reaction due to high temperature applied in this reaction. Finally, alkyne migratory insertion and reductive elimination of complex **1.55** delivers the indene product **1.52**. The substrate scope of this reaction

is similar to related (4+2) "cut-and-sew" reaction, which can well tolerate alkyl alkyne in **1.52a**, phenyl alkyne in **1.52b** and longer linkage in **1.52c** (Scheme 1.14C).

**Scheme 1.14.** Rhodium Catalyzed (4+2−1) "Cut-and-Sew" Reaction between Benzocyclobutenone and Alkyne.

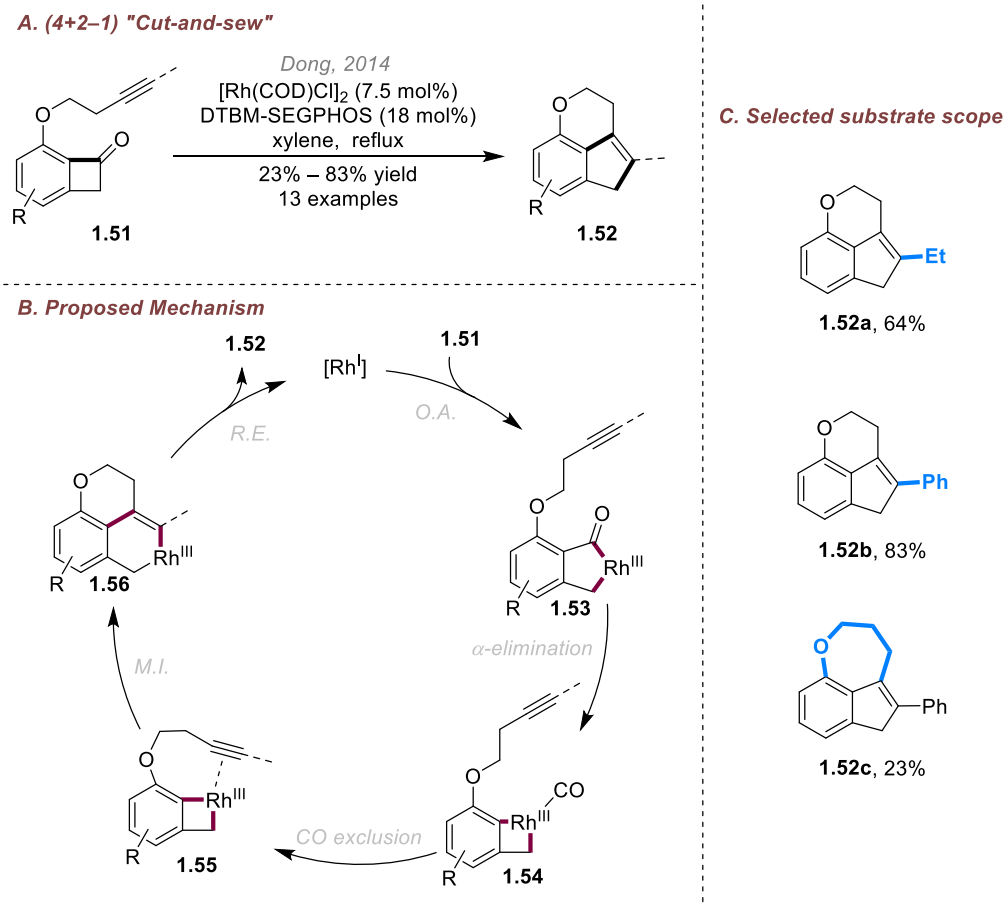


Similar to benzocyclobutenone, (4+2−1) cycloaddition between saturated cyclobutanone and alkene (Scheme 1.15A) was also accomplished under high temperature to construct bridged cyclopentane (Scheme 1.15B).[27] The monodentate bulky Buchwald ligand plays a key role in this reaction, which not only promote CO exclusion, but also prevent the coordination of more than one phosphine ligand, and that resulting unsaturation of the metal center should promote olefin coordination.

**Scheme 1.15.** Rhodium Catalyzed (4+2−1) "Cut-and-Sew" Reaction between Cyclobutenone and Alkene.

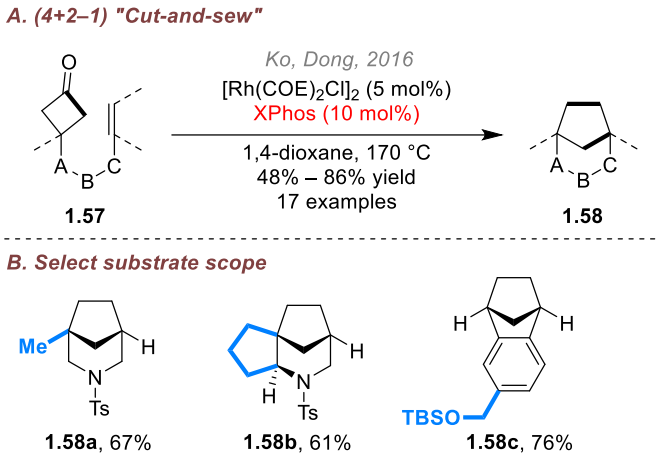


### 1.2.4 (4+1) "Cut-and-Sew" Reaction of Benzocyclobutenone and Cyclobutanone

Although intramolecular "cut-and-sew" reaction of benzocyclobutenone and cyclobutanone has been well developed, the intermolecular "cut-and-sew" reaction is still very rare up to now. Recently, during our exploration on an intermolecular "cut-and-sew" reaction between benzocyclobutenone and styrene, to our surprise, (4+1) product 2-indanone instead of (4+2) product 2-tetralone was found to be the major product in this reaction (Scheme 1.16A).[28] Utilization of "ligandless" cationic rhodium catalyst was crucial for both reactivity and selectivity towards (4+1) product. Our method exhibited a broad substrate scope on both benzocyclobutenone and styrene parts (Scheme 1.16C), which facilitated construction of multi-substituted 2-indanone. Interestingly, the reverse selectivity between (4+1) and (4+2) was observed when adding BNDHP as a ligand in this reaction.

A $\beta$-H elimination mechanism was proposed to explain the unique selectivity of this intermolecular "cut-and-sew" reaction (Scheme 1.16B). Oxidative addition of rhodium(I) into sterically less hinder C(carbonyl)−C(aryl) bond of imine derived from 2,2-disubstituted

benzocyclobutenone **1.60** and amino pyridine **DG1** gave metallacycle **1.62**. And insertion of styrene **1.59** into C(aryl)−Rh bond delivered seven-membered metallacycle **1.63**. The selectivity between (4+1) and (4+2) product comes from competition between *β*-H elimination and reductive elimination of key intermediate **1.63**. The calculation study shown that the *β*-H elimination pathway is overall favored by 2.5 kcal/mol kinetically. The relatively small energy difference between two pathways indicated that the selectivity of this intermolecular "cut-and-sew" reaction sensitive to reactant and ligand, which supported by our experimental observation.

**Scheme 1.16.** Rhodium Catalyzed (4+1) "Cut-and-Sew" Reaction between Benzocyclobutenone and Styrene.

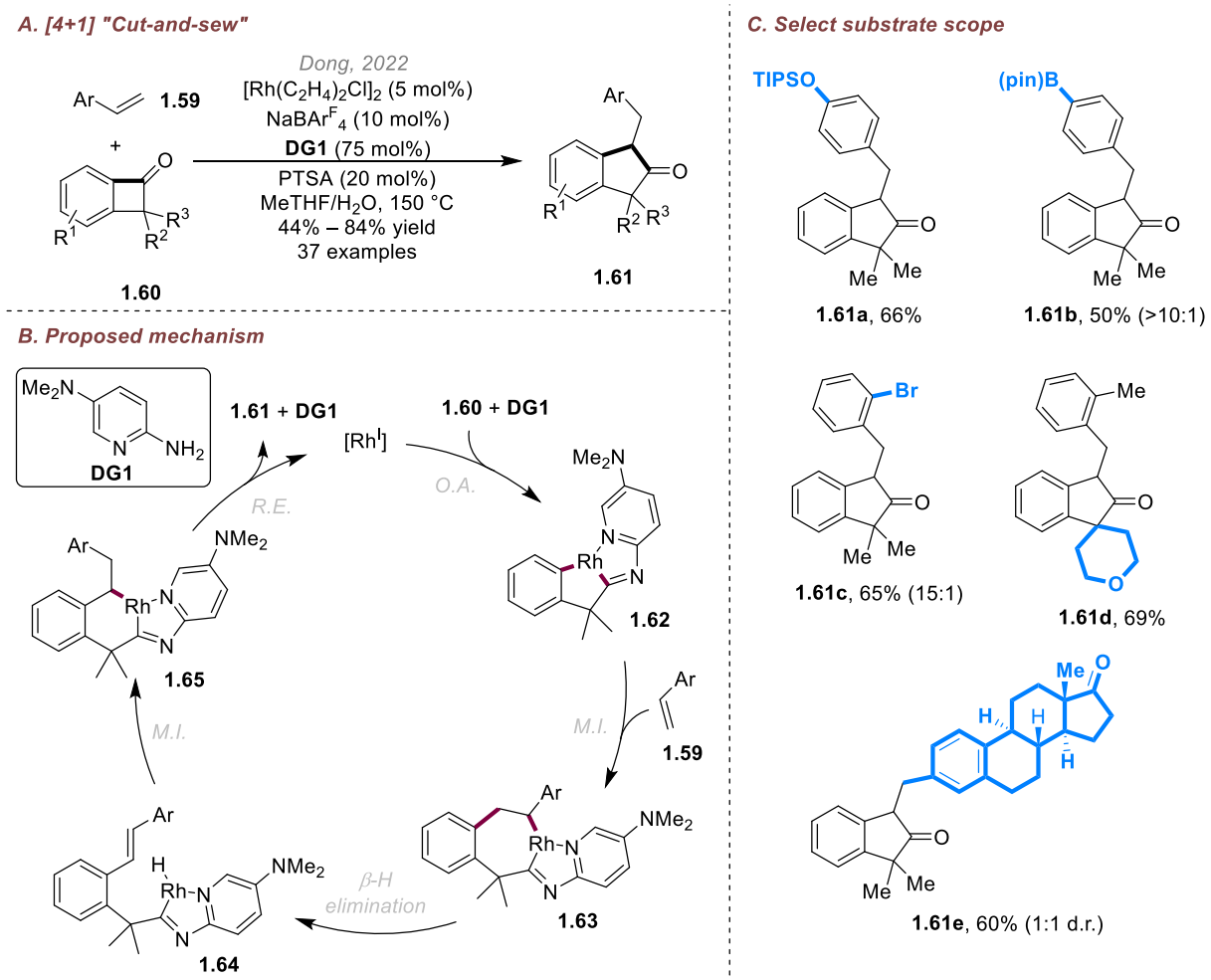

In 2015, our group developed a (4+1) "cut-and-sew" cycloaddition between cyclobutanones and allenes, which can be utilized to construction [4.2.1] and [3.2.1] bicycles (Scheme 1.17A).[29] This method shows a broad substrate scope on both cyclobutanone and allene part (Scheme 1.17C). Based on experimental mechanism study, a unique mechanism was proposed to explain the special reactivity of allene (Scheme 1.17B). The reaction starts from the oxidation addition of Rh(I) into the α-C−C bond of cyclobutanone **1.66** to give intermediate **1.68**, in which allene coordinated to rhodium center. This is followed by migratory insertion of acyl group into allene to generate allyl-rhodium complex **1.69**, which then undergoes *β*-H elimination to give diene **1.70**. There are two possible routes after this step, either C−H or C−C migratory insertion followed by reductive elimination can generate product **1.67**.

**Scheme 1.17.** Rhodium Catalyzed (4+1) "Cut-and-Sew" Reaction between Cyclobutenone and Allene.

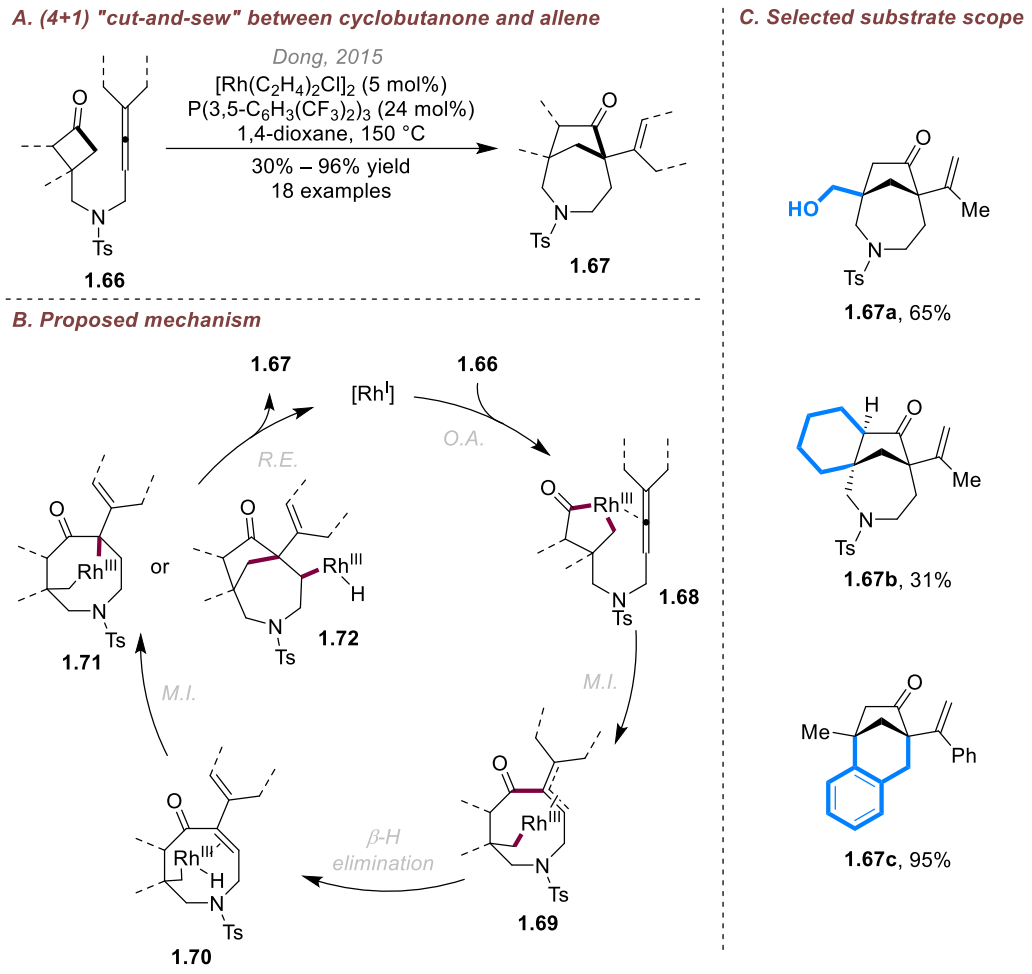


## 1.3. Application in Total Synthesis

As a powerful method to construct [m.n.0] fused ring and [m.n.1] bridged ring system, "cut-and-sew" strategy has been applied in many natural product synthesis.[30] In this section, we will highlight the total synthesis of alkaloids and terpenes enabled by "cut-and-sew" strategy finished in our group in past 10 years.

### 1.3.1 Total Synthesis of Cycloinumakiol (Proposed Structure)

Isolated from extracts of *podocarpus latifolius*, cycloinumakiol (**1.1**) is a unique diterpenoid in inumakiol family, which exhibited a distinct proposed chemical structure from other natural products in this family.[31] First, its oxygen substituent on the aromatic ring is *para* instead of *meta* or *ortho* to the isopropyl group; second, cycloinumakiol contained an unusual tetracyclic skeleton feature a dihydrofuran ring, along with an quaternary carbon center on C10.

A synthetic route based on "cut-and-sew" strategy was proposed to construct the special skeleton of cycloinumakiol (Scheme 1.18A).[6] We envisioned that the isopropyl group on the phenyl ring can be introduced by am arene functionalization. Meanwhile. The C5 stereocenter could be easily epimerized since it located on ketone α position to trace back to ketone **1.73**. A "cut-and-sew" reaction between benzocyclobutenone and alkene can be utilized to construct the tetracyclic skeleton in ketone **1.73** from ketone **1.74**. Finally, ketone **1.74** can be synthesize from two simple fragments **1.75** and **1.76** in a convergent way.

The Mitsunobu reaction between compound **1.75** and **1.76** delivered ketone **1.74** in 90% yield (Scheme 1.18B). although the "cut-and-sew" reaction between benzocyclobutenone and alkene has been developed, the insertion of sterically hindered tri-substituted alkene is still challenged. No desired product ketone **1.73** was observed under previous optimized condition. After condition screening, we found that using electron-deficient rhodium is crucial for this transformation. The $[Rh(CO)_2Cl]_2/P(C_6F_5)_3$ combination was found to be optimal for this "cut-and-sew" reaction, which can deliver ketone **1.73** in 66% yield. The installation of isopropyl group on phenyl ring was accomplished in 2 steps, including a bromination and an one-pot Suzuki coupling/hydrogenation. Ketone **1.78** was epimerized and converted to olefin **1.79** in 4 steps, and a following hydrogenation furnished the proposed structure of cycloinumakiol (**1.1**). Using "cut-

and-sew" strategy, we accomplished the first total synthesis of proposed structure of cycloinumakiol (**1.1**) in 9 steps from simple starting materials compounds **1.75** and **1.76**, which enable us to revise the proposed structure of cycloinumakiol.

**Scheme 1.18.** Total Synthesis of Cycloinumakiol (Proposed Structure)

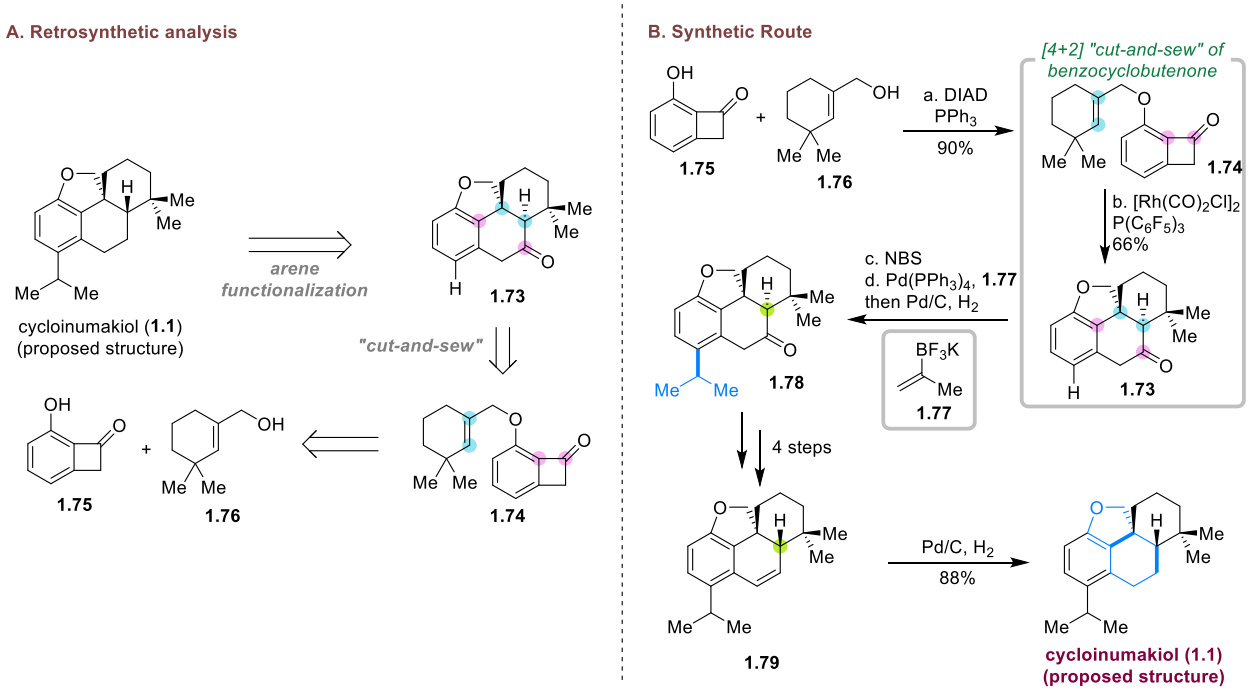


### 1.3.2 Enantioselective Total Synthesis of (−)-Cycloclavine

Isolated from the seeds of *Ipomoea hildebrandtii* by Hofmann and co-workers in1969[32] and later from *Aspergillus japonicas* in 1982,[33] cycloclavine (**1.2**) is a special indole alkaloids in ergot alkaloids family, as the only member contains a cyclopropane ring in this family. Although the full biological profile of cycloclavine has not been established, a preliminary study shows that cycloclavine exhibits promising activities on insecticidal and antiparasitic properties. From structural aspect, cycloclavine processes a penta-cyclic core with unique [3.1.0] structural motif. A sterically congested cyclopropane and three contiguous chiral centers including two adjacent quaternary carbons bring the significant challenge for asymmetric total synthesis of cycloclavine.

To develop a concise, efficient and enantioselective route towards (−)-cycloclavine, we proposed a synthetic plan using "cut-and-sew" strategy (Scheme 1.19A).[7] From retrosynthetic viewpoint, we envisioned that the D ring of cycloclavine can be constructed by reductive amination from ketone **1.80**, and the cyclopropane E ring can be established by rhodium catalyzed cyclopropanation between 1,1-disubstituted alkene and $\alpha$-diazoketone, which can be readily prepared from ketone **1.81a**. Finally, the 6-6-5 fused ring system (A/B/C rings) is expected to be constructed by an asymmetric nitrogen-tethered "cut-and-sew" reaction of benzocyclobutenone **1.82**, which can be easily prepared from diphenol **1.83** through benzyne [2+2] cycloaddition.

"Cut-and-sew" reaction precursor benzocyclobutenone **1.73** was prepared from commercially available diphenol **1.83** in 3 steps (Scheme 19B). After detailed condition optimization, we found that the combination of cationic rhodium $[Rh(COD)_2]BF_4$ and DTBM-segphos can efficiently catalyze the desired "cut-and-sew" reaction to give desired ketone **1.81a** in 95% yield and 97.5% e.e. This nitrogen-tethered "cut-and-sew" reaction between benzocyclobutenone and alkene shown broad substrate scope and good functional group tolerance, giving high yields and excellent enantioselectivity (Scheme 1.19C).

After the "cut-and-sew" step, diazo-transfer of ketone **1.72** selectively delivered $\alpha$-diazo ketone **1.78** in 92% yield. The next challenge is to efficiently construct tetrasubstituted cyclopropane E ring in cycloclavine. To avoid the possible side reaction, the reaction was run under low temperature and with less hindered 2-methylallyl chloride **1.79** as olefin substrate, which gave desired cyclopropane product **1.71** in 85% yield and 5.8:1 diastereoselectivity.[34] In the end game, azide substitution, Boc deprotection and oxidation gave indole **1.80**, followed by sequential aza-Wittig/reduction/reductive amination delivered (−)-cycloclavine (**1.2**) in 78% yield and >20:1 diastereoselectivity. Comparing to prior synthetic works to cycloclavine, our "cut-and-sew"

approach accomplished asymmetric total synthesis of (−)-cycloclavine in 10 steps with 30% overall yield, which pave the way for further biological study on this natural product.

**Scheme 1.19.** Enantioselective Total Synthesis of (−)-Cycloclavine.

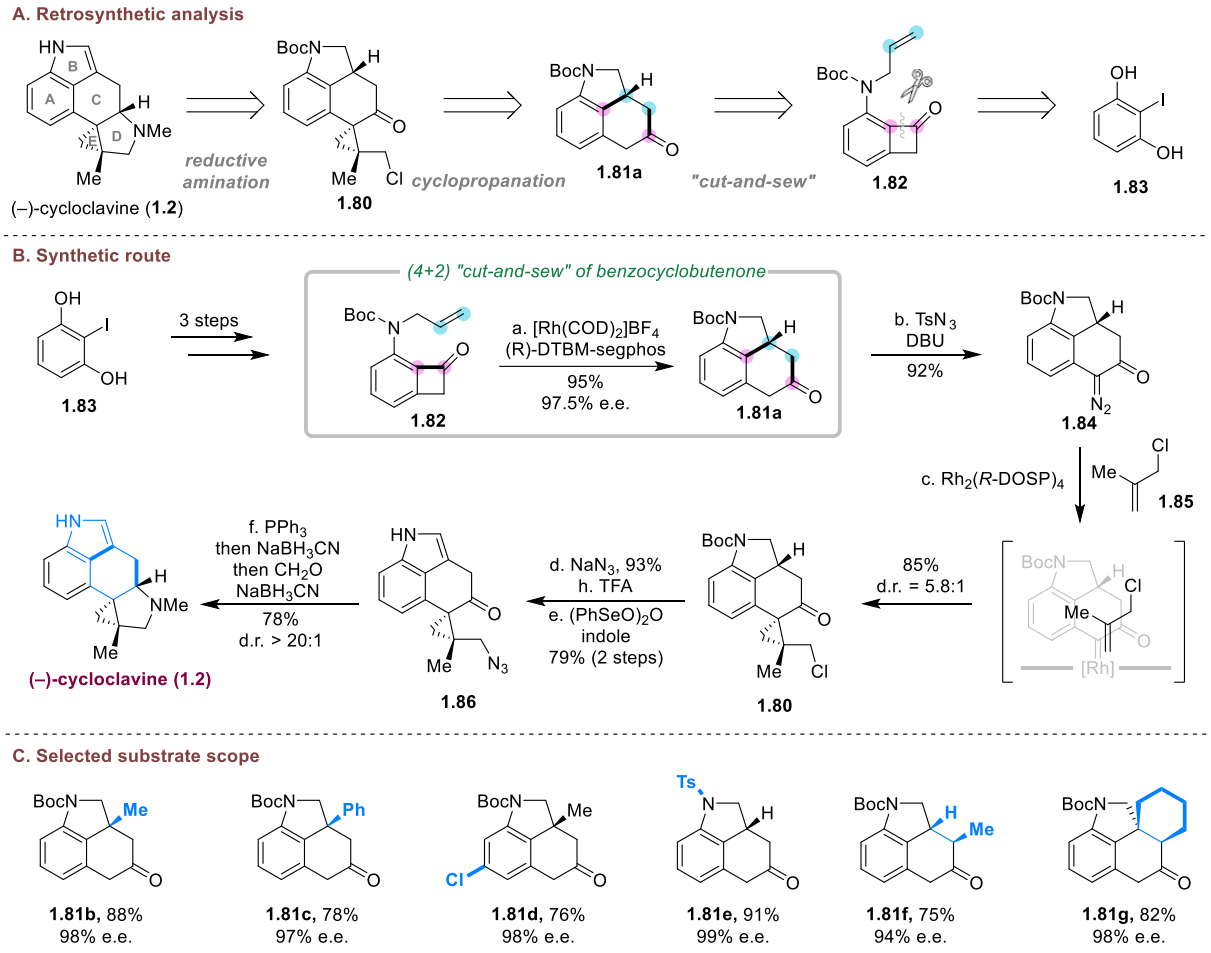


### 1.3.3 Enantioselective Total Synthesis of (−)-Thebainone A

Morphine (**1.5**) and its congeners are among the oldest and most studied alkaloid natural products. Many of them exhibit potent neurological and immunological activity.[35] From structural aspect, morphine-family alkaloids typically have a unique poly-bridged/fused ring system, a quaternary center and a basic tertiary amine moiety and a 1,2,3,4-tetrasubstituted arene. Thebainone A (**1.7**) is a unique morphine-family alkaloids which contains an enone-containing C

rings. It has been used as a precursor to synthesize morphine (**1.5**) and codeine (**1.6**) by Gates and co-workers.[36]

The key strategy in our total synthesis of (±)-thebainone A is *deconstructive synthesis* enabled by "cut-and-sew" reaction, which builds new structures through bond cleavage of easily accessible moieties (Scheme 1.20A).[10] From retrosynthetic viewpoint, we first cut C−N bonds in D ring through a deconstructive C−O bond cleavage of ether **1.87a**. As the key intermediate in our synthesis, tetracycle **1.87a**, which contains the fused A/B/C rings, a 2-tetralone moiety along with a quaternary carbon center, can be readily accessible by a rhodium catalyzed "cut-and-sew" reaction from ketone **1.88**. Finally, ketone **1.88** can be convergently synthesized from commercially available starting materials **1.89** and **1.90**.

The substrate of key "cut-and-sew" reaction, ketone **1.88**, can be prepared from compounds **1.89** and **1.90** in 4 steps LLS (Scheme 1.20B). Although there has been several reports on oxygen tethered "cut-and-sew" reaction between benzocyclobutenone and alkene, "cut-and-sew" reaction of compound **1.88** is still challenged due to the presence of a acid-sensitive ketal, a sterically hindered trisubstituted olefin and a relatively long linker. After condition screening, $[Rh(COD)_2]NTf_2$ was found to be the optimized pre-catalyst, with DTBM-segphos as the optimized asymmetric ligand and 1,2-difluorobenzene as solvent, which can deliver 80% yield of ketone **1.87a** in 97:3 e.r. The optimized condition shown broad substrate scope on bulky olefins, aromatic substitutions and linkers (Scheme 20C). Enabled by "cut-and-sew" reaction, we not only constructed all the C−C bonds in the natural product, but also set the correct stereochemistry on the quaternary carbon center.

With ketone **1.87a** in hand, the next phase is cleavage of C−O bond and constructing C−N bonds in D ring. C−O bond in ketone **1.87a** was cleavage to give bromide **1.91** in 4 steps. A sequential ketone protection, $S_N2$ amination and de-acylation of ketone **1.87a** can be achieved in one pot and 76% yield, followed by elimination of secondary alcohol by Martin's sulfurane to generate amine **1.97**. The final D ring of thebainone A can be constructed by a radical-induced hydroamination of alkene, which initiated by generation of amine radical through sodium naphthalenide reduction of tosyl amine **1.97**. Finally, selective deprotection of middle phenol methyl ether in ketone **1.98** by NaSEt delivered phenol **1.99**, followed by desaturation through palladium-catalyzed Stahl's oxidation[37] furnished (−)-thebainone A (**1.7**). Phenol **1.99** is also a known precursor to morphine (**1.5**) and codeine (**1.6**).[38] In summary, the first enantioselective total synthesis of (−)-thebainone A (**1.7**) was achieved in 13 (and 14) steps with 4.7% (and 7.2%) overall yield from commercial available starting materials. The efficiency of our synthesis comes from deconstructive strategy through rhodium-catalyzed "cut-and-sew" reaction, which enable us to set up initial chirality and all the carbon cycles of natural product in one step.

**Scheme 1.20.** Deconstructive Asymmetric Total Synthesis of (−)-Thebainone A.

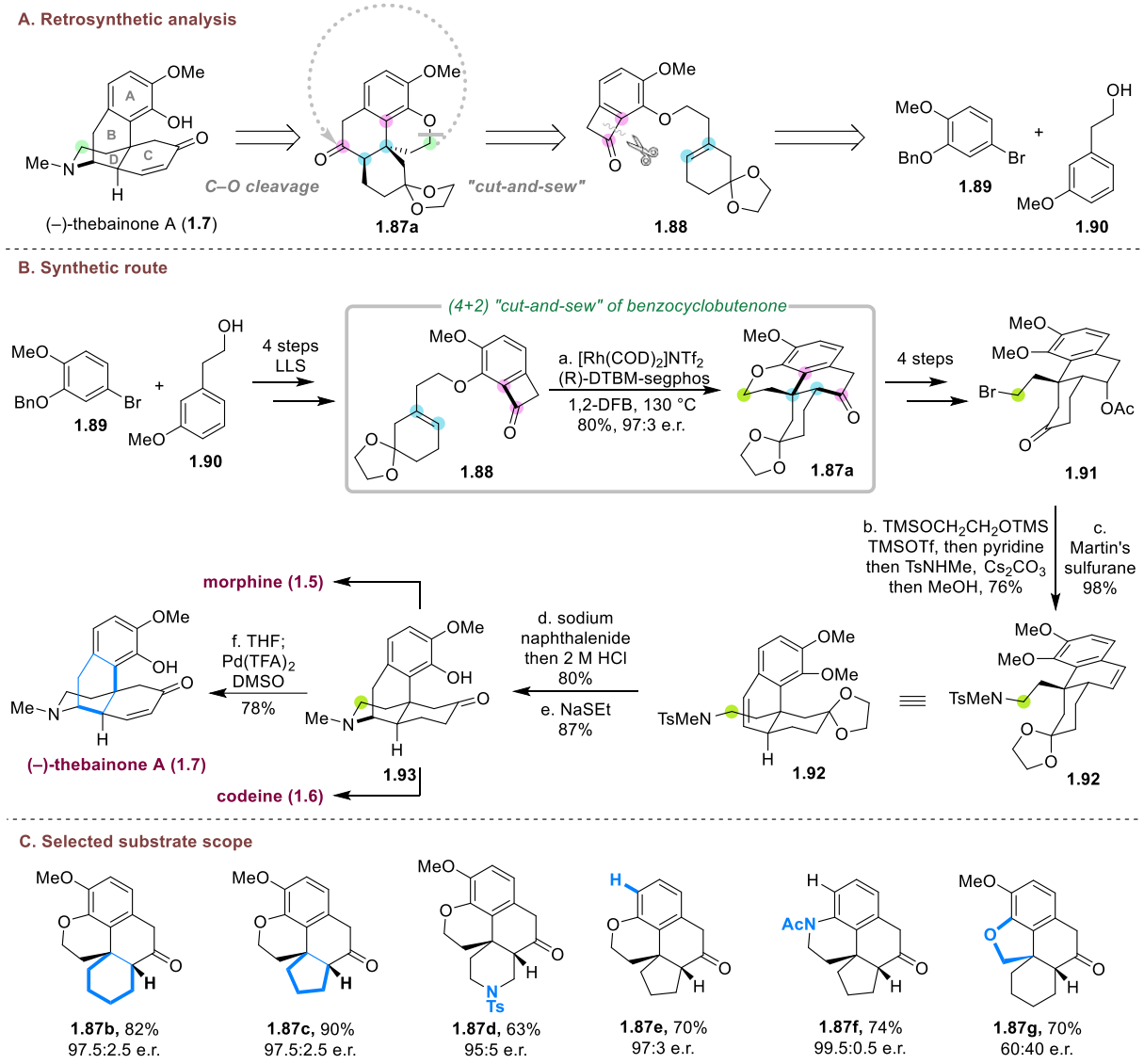


## 1.4. Summary and Outlook

In this chapter, we have summarized our efforts on development of rhodium catalyzed "cut-and-sew" reaction of benzocyclobutenone and cyclobutanone, as well as the total synthesis of complex alkaloids and terpenoids utilizing "cut-and-sew" strategy. Diverse types of cycloaddition can be achieved by "cut-and-sew" reaction, including (4+2), (4+2−1) and (4+1) cycloaddition. The

"cut-and-sew" reaction brings new thoughts and possibilities to construct [m.n.0] fused rings and [m.n.1] bridged rings, which enable us to develop concise and efficient ways to synthesize natural products. Comparing to the traditional approach of cycloaddition, our method not only can construct some inaccessible ring system by IMDA such as [3.3.1] bicycle, but also remains a ketone moiety after cycloaddition, which can serve as a handle for further functionalization.

Rhodium catalyzed "cut-and-sew" reaction of benzocyclobutenone and cyclobutanone has shown its efficiency in construction of carbon skeleton in natural products. Nitrogen-tethered "cut-and-sew" reaction of benzocyclobutenone enables the fast establishing of northern ring system in cycloclavine in a catalytic and enantioselective way. And the challenged tetrasubstituted cyclopropane ring can be constructed by a rhodium catalyzed cyclopropanation between alkene and α-diazo ketone, which is prepared from the product of "cut-and-sew" reaction in one step. In total synthesis of thebainone A, all the carbon−carbon bonds can be furnished after "cut-and-sew" step, and a following deconstructive C−O bond cleavage and C−N bond formation construct the final heterocycle in natural product. Together, these works demonstrate that "cut-and-sew" reaction of benzocyclobutenone and cyclobutanone provides a new strategy to construct complex scaffold in natural products containing fused/bridged ring systems. Although there are still many challenges in "cut-and-sew" reaction, hopefully our continuous cultivation on this area can afford a useful tool in organic synthesis.

(Some contents of this chapter were published in *Acc. Chem. Res.* **2022**, DOI: 10.1021/acs.accounts.2c00400)

## 1.5. References

1. (a) Nakao, Y. Metal-mediated C–CN Bond Activation in Organic Synthesis. *Chem. Rev.* **2021,** *121*, 327-344. (b) Murakami, M.; Ito, Y. Cleavage of Carbon—Carbon Single Bonds by Transition Metals. In *Activation of Unreactive Bonds and Organic Synthesis*, Murai, S.; Alper, H.; Gossage, R. A.; Grushin, V. V.; Hidai, M.; Ito, Y.; Jones, W. D.; Kakiuchi, F.; van Koten, G.; Lin, Y. S.; Mizobe, Y.; Murai, S.; Murakami, M.; Richmond, T. G.; Sen, A.; Suginome, M.; Yamamoto, A., Eds. Springer Berlin Heidelberg: Berlin, Heidelberg, 1999; pp 97-129. (c) van der Boom, M. E.; Milstein, D. Cyclometalated Phosphine-Based Pincer Complexes: Mechanistic Insight in Catalysis, Coordination, and Bond Activation. *Chem. Rev.* **2003,** *103*, 1759-1792. (d) Jun, C.-H. Transition metal-catalyzed carbon–carbon bond activation. *Chem. Soc. Rev.* **2004,** *33*, 610-618. (e) Tobisu, M.; Chatani, N. Catalytic reactions involving the cleavage of carbon–cyano and carbon–carbon triple bonds. *Chem. Soc. Rev.* **2008,** *37*, 300-307. (f) Chen, F.; Wang, T.; Jiao, N. Recent Advances in Transition-Metal-Catalyzed Functionalization of Unstrained Carbon–Carbon Bonds. *Chem. Rev.* **2014,** *114*, 8613-8661. (g) Souillart, L.; Cramer, N. Catalytic C–C Bond Activations via Oxidative Addition to Transition Metals. *Chem. Rev.* **2015,** *115*, 9410-9464. (h) Fumagalli, G.; Stanton, S.; Bower, J. F. Recent Methodologies That Exploit C–C Single-Bond Cleavage of Strained Ring Systems by Transition Metal Complexes. *Chem. Rev.* **2017,** *117*, 9404-9432. (i) Song, F.; Gou, T.; Wang, B.-Q.; Shi, Z.-J. Catalytic activations of unstrained C–C bond involving organometallic intermediates. *Chem. Soc. Rev.* **2018,** *47*, 7078-7115. (j) Deng, L.; Dong, G. Carbon–Carbon Bond Activation of Ketones. *Trends Chem.* **2020,** *2*, 183-198. (k) Xia, Y.; Dong, G. Temporary or removable directing groups enable activation of unstrained C–C bonds. *Nat. Rev. Chem.* **2020,** *4*, 600-614. (l) Murakami, M.; Ishida, N. Cleavage of Carbon–Carbon σ-Bonds of Four-Membered Rings. *Chem. Rev.* **2021,** *121*, 264-299.

2. Chen, P.-h.; Billett, B. A.; Tsukamoto, T.; Dong, G. “Cut and Sew” Transformations via Transition-Metal-Catalyzed Carbon–Carbon Bond Activation. *ACS Catal.* **2017,** *7*, 1340-1360.

3. Chen, J.; Zhou, Q.; Fang, H.; Lu, P. Dancing on Ropes - Enantioselective Functionalization of Preformed Four-Membered Carbocycles. *Chin. J. Chem* . **2022,** *40*, 1346-1358.

4. Murakami, M.; Itahashi, T.; Ito, Y. Catalyzed Intramolecular Olefin Insertion into a Carbon−Carbon Single Bond. *J. Am. Chem. Soc.* **2002,** *124*, 13976-13977.

5. Xu, T.; Dong, G. Rhodium-Catalyzed Regioselective Carboacylation of Olefins: A C□C Bond Activation Approach for Accessing Fused-Ring Systems. *Angew. Chem., Int. Ed.* **2012,** *51*, 7567-7571.

6. Xu, T.; Dong, G. Coupling of Sterically Hindered Trisubstituted Olefins and Benzocyclobutenones by C□C Activation: Total Synthesis and Structural Revision of Cycloinumakiol. *Angew. Chem., Int. Ed.* **2014,** *53*, 10733-10736.

7. Deng, L.; Chen, M.; Dong, G. Concise Synthesis of (−)-Cycloclavine and (−)-5-epi-Cycloclavine via Asymmetric C–C Activation. *J. Am. Chem. Soc.* **2018,** *140*, 9652-9658.

8. Qiu, B.; Li, X.-T.; Zhang, J.-Y.; Zhan, J.-L.; Huang, S.-P.; Xu, T. Catalytic Enantioselective Synthesis of 3,4-Polyfused Oxindoles with Quaternary All-Carbon Stereocenters: A Rh-Catalyzed C–C Activation Approach. *Org. Lett.* **2018,** *20*, 7689-7693.

9. Zhang, Y.; Shen, S.; Fang, H.; Xu, T. Total Synthesis of Galanthamine and Lycoramine Featuring an Early-Stage C–C and a Late-Stage Dehydrogenation via C–H Activation. *Org. Lett.* **2020,** *22*, 1244-1248.

10. Hou, S.-H.; Prichina, A. Y.; Dong, G. Deconstructive Asymmetric Total Synthesis of Morphine-Family Alkaloid (−)-Thebainone A. *Angew. Chem., Int. Ed.* **2021,** *60*, 13057-13064.

11. Xue, Y.; Dong, G. Total Synthesis of Penicibilaenes via C–C Activation-Enabled Skeleton Deconstruction and Desaturation Relay-Mediated C–H Functionalization. *J. Am. Chem. Soc.* **2021,** *143*, 8272-8277.

12. (a) Flores-Gaspar, A.; Martin, R. Recent Advances in the Synthesis and Application of Benzocyclobutenones and Related Compounds. *Synthesis* **2013,** *45*, 563-580. (b) Chen, P.-h.; Dong, G. Cyclobutenones and Benzocyclobutenones: Versatile Synthons in Organic Synthesis. *Chem. - Eur. J.* **2016,** *22*, 18290-18315.

13. (a) Mariet, N.; Ibrahim-Ouali, M.; Santelli, M. First [2+2]-cycloaddition of a 3,4-didehydropyridine and a ketene dialkyl acetal. *Tetrahedron Lett.* **2002,** *43*, 5789-5791. (b) Im, G. Y. J.; Bronner, S. M.; Goetz, A. E.; Paton, R. S.; Cheong, P. H. Y.; Houk, K. N.; Garg, N. K. Indolyne Experimental and Computational Studies: Synthetic Applications and Origins of Selectivities of Nucleophilic Additions. *J. Am. Chem. Soc.* **2010,** *132*, 17933-17944. (c) Chen, P. H.; Savage, N. A.; Dong, G. Concise synthesis of functionalized benzocyclobutenones. *Tetrahedron* **2014,** *70*, 4135-4146.

14. (a) Aidhen, I. S.; Ahuja, J. R. A novel synthesis of benzocyclobutenones. *Tetrahedron Lett.* **1992,** *33*, 5431-5432. (b) Álvarez-Bercedo, P.; Flores-Gaspar, A.; Correa, A.; Martin, R. Pd-Catalyzed Intramolecular Acylation of Aryl Bromides via C−H Functionalization: A Highly Efficient Synthesis of Benzocyclobutenones. *J. Am. Chem. Soc.* **2010,** *132*, 466-467. (c) Flores-Gaspar, A.; Gutiérrez-Bonet, Á.; Martin, R. N-Heterocyclic Carbene Dichotomy in Pd-Catalyzed Acylation of Aryl Chlorides via C–H Bond Functionalization. *Org. Lett.* **2012,** *14*, 5234-5237. (d) Yano, T.; Kawasaki, T.; Yuhki, T.; Ishida, N.; Murakami, M. Synthetic Approach to Benzocyclobutenones Using Visible Light and a Phosphonate Auxiliary. *Org. Lett.* **2018,** *20*, 1224-1227.

15. Xu, T.; Ko, H. M.; Savage, N. A.; Dong, G. Highly Enantioselective Rh-Catalyzed Carboacylation of Olefins: Efficient Syntheses of Chiral Poly-Fused Rings. *J. Am. Chem. Soc.* **2012,** *134*, 20005-20008.

16. Lu, G.; Fang, C.; Xu, T.; Dong, G.; Liu, P. Computational Study of Rh-Catalyzed Carboacylation of Olefins: Ligand-Promoted Rhodacycle Isomerization Enables Regioselective C–C Bond Functionalization of Benzocyclobutenones. *J. Am. Chem. Soc.* **2015,** *137*, 8274-8283.

17. Chen, P.-h.; Xu, T.; Dong, G. Divergent Syntheses of Fused β-Naphthol and Indene Scaffolds by Rhodium-Catalyzed Direct and Decarbonylative Alkyne–Benzocyclobutenone Couplings. *Angew. Chem., Int. Ed.* **2014,** *53*, 1674-1678.

18. Zhu, Z.; Li, X.; Chen, S.; Chen, P.-h.; Billett, B. A.; Huang, Z.; Dong, G. Cobalt-Catalyzed Intramolecular Alkyne/Benzocyclobutenone Coupling: C–C Bond Cleavage via a Tetrahedral Dicobalt Intermediate. *ACS Catal.* **2018,** *8*, 845-849.

19. Deng, L.; Xu, T.; Li, H.; Dong, G. Enantioselective Rh-Catalyzed Carboacylation of C═N Bonds via C–C Activation of Benzocyclobutenones. *J. Am. Chem. Soc.* **2016,** *138*, 369-374.

20. Sun, T.; Zhang, Y.; Qiu, B.; Wang, Y.; Qin, Y.; Dong, G.; Xu, T. Rhodium(I)-Catalyzed Carboacylation/Aromatization Cascade Initiated by Regioselective C−C Activation of Benzocyclobutenones. *Angew. Chem., Int. Ed.* **2018,** *57*, 2859-2863.

21. Ko, H. M.; Dong, G. Cooperative activation of cyclobutanones and olefins leads to bridged ring systems by a catalytic [4 + 2] coupling. *Nat. Chem.* **2014,** *6*, 739-744.

22. Souillart, L.; Parker, E.; Cramer, N. Highly Enantioselective Rhodium(I)-Catalyzed Activation of Enantiotopic Cyclobutanone C□C Bonds. *Angew. Chem., Int. Ed.* **2014,** *53*, 3001-3005.

23. Souillart, L.; Cramer, N. Highly Enantioselective Rhodium(I)-Catalyzed Carbonyl Carboacylations Initiated by C□C Bond Activation. *Angew. Chem., Int. Ed.* **2014,** *53*, 9640-9644.

24. Hou, S.-H.; Yu, X.; Zhang, R.; Deng, L.; Zhang, M.; Prichina, A. Y.; Dong, G. Enantioselective Type II Cycloaddition of Alkynes via C–C Activation of Cyclobutanones: Rapid and Asymmetric Construction of [3.3.1] Bridged Bicycles. *J. Am. Chem. Soc.* **2020,** *142*, 13180-13189.

25. Deng, L.; Jin, L.; Dong, G. Fused-Ring Formation by an Intramolecular "Cut-and-Sew" Reaction between Cyclobutanones and Alkynes. *Angew. Chem., Int. Ed.* **2018,** *57*, 2702-2706.

26. Deng, L.; Fu, Y.; Lee, S. Y.; Wang, C.; Liu, P.; Dong, G. Kinetic Resolution via Rh-Catalyzed C–C Activation of Cyclobutanones at Room Temperature. *J. Am. Chem. Soc.* **2019,** *141*, 16260-16265.

27. Zhou, X.; Ko, H. M.; Dong, G. Synthesis of Bridged Cyclopentane Derivatives by Catalytic Decarbonylative Cycloaddition of Cyclobutanones and Olefins. *Angew. Chem., Int. Ed.* **2016,** *55*, 13867-13871.

28. Ochi, S.; Zhang, Z.; Xia, Y.; Dong, G. Rhodium-Catalyzed (4+1) Cycloaddition between Benzocyclobutenones and Styrene-Type Alkenes. *Angew. Chem., Int. Ed.* **2022,** *61*, e202202703.

29. Zhou, X.; Dong, G. (4+1) vs (4+2): Catalytic Intramolecular Coupling between Cyclobutanones and Trisubstituted Allenes via C–C Activation. *J. Am. Chem. Soc.* **2015,** *137*, 13715-13721.

30. (a) Murakami, M.; Ishida, N. Potential of Metal-Catalyzed C–C Single Bond Cleavage for Organic Synthesis. *J. Am. Chem. Soc.* **2016,** *138*, 13759-13769. (b) Wang, B.; Perea, M. A.; Sarpong, R. Transition Metal-Mediated C−C Single Bond Cleavage: Making the Cut in Total Synthesis. *Angew. Chem., Int. Ed.* **2020,** *59*, 18898-18919.

31. Devkota, K. P.; Ratnayake, R.; Colburn, N. H.; Wilson, J. A.; Henrich, C. J.; McMahon, J. B.; Beutler, J. A. Inhibitors of the Oncogenic Transcription Factor AP-1 from Podocarpus latifolius. *J. Nat. Prod.* **2011,** *74*, 374-377.

32. Stauffacher, D.; Niklaus, P.; Tscherter, H.; Weber, H. P.; Hofmann, A. Cycloclavin, ein neues alkaloid aus Ipomoea hildebrandtii vatke—71: Mutterkornalkaloide. *Tetrahedron* **1969,** *25*, 5879-5887.

33. Furuta, T.; Koike, M.; Abe, M. Isolation of Cycloclavine from the Culture Broth of Aspergillus japonicus SAITO. *Agricultural and Biological Chemistry* **1982,** *46*, 1921-1922.

34. Davies, H. M. L.; Nagashima, T.; Klino, J. L. Stereoselectivity of Methyl Aryldiazoacetate Cyclopropanations of 1,1-Diarylethylene. Asymmetric Synthesis of a Cyclopropyl Analogue of Tamoxifen. *Org. Lett.* **2000,** *2*, 823-826.

35. Blakemore, P. R.; White, J. D. Morphine, the Proteus of organic molecules. *Chem. Commun.* **2002**, 1159-1168.

36. (a) Gates, M.; Tschudi, G. THE SYNTHESIS OF MORPHINE. *J. Am. Chem. Soc.* **1952,** *74*, 1109-1110. (b) Gates, M.; Tschudi, G. The Synthesis of Morphine. *J. Am. Chem. Soc.* **1956,** *78*, 1380-1393.

37. Diao, T.; Wadzinski, T. J.; Stahl, S. S. Direct aerobic α,β-dehydrogenation of aldehydes and ketones with a Pd(TFA)2/4,5-diazafluorenone catalyst. *Chem. Sci.* **2012,** *3*, 887-891.

38. (a) Weller, D. D.; Rapoport, H. A practical synthesis of codeine from dihydrothebainone. *J. Med. Chem.* **1976,** *19*, 1171-1175. (b) Rice, K. C. A rapid, high-yield conversion of codeine to morphine. *J. Med. Chem.* **1977,** *20*, 164-165. (c) Rice, K. C. Synthetic opium alkaloids and derivatives. A short total synthesis of (.+-.)-dihydrothebainone, (.+-.)-dihydrocodeinone, and

(.+-.)-nordihydrocodeinone as an approach to a practical synthesis of morphine, codeine, and congeners. *J. Org. Chem.* **1980,** *45*, 3135-3137.

# CHAPTER 2

## Total Synthesis of Penicibilaenes via C−C Activaton-Enabled Deconstruction and Desaturation Relay-Mediated C−H Functionalization

### 2.1. Introduction

Terpenes and their derivatives have been a rich source of therapeutic agents, agrochemicals, and fragrances. In addition, they often exhibit intriguing and complex chemical structures, such as bridged/fused rings and diverse substitutions. As such, terpenes have been highly attractive target molecules in the synthetic community.[1] Inspired by the biosynthesis of terpenes, a "two-phase" strategy has been advanced by Baran and coworkers, leading to a number of elegant total syntheses since 2009.[2] This strategy involves a cyclase phase to first build the carbon backbone from a linear or less com-plex precursor, followed by an oxidase phase to install oxygen functionalities at proper positions (Scheme 2.1.A). Notably, in the cyclase phase, polyene cyclization and various cycloadditions such as Diels−Alder reaction and Robinson annulation, are commonly employed for synthesizing multi-ring systems. On the other hand, the transition metal-catalyzed C−C activation[3] of cyclic ketones followed by insertion of an un-saturated 2π-unit, namely a "cut-and-sew" process,[4] has been found useful for constructing various bridged and fused rings. In addition,

the resulting carbonyl moiety could provide a convenient handle for site-selective C−H functionalization.[5] Thus, terpene synthesis could also be envisioned to go through a closely related but complementary strategy, which utilizes C−C activation to construct the core skeleton[6] and then ketone-directed or mediated C−H functionalization to introduce the substituents (Scheme 2.1.B). Comparing to the "two-phase" strategy, one subtle difference with this "C−C/C−H" approach is that not all carbons in the terpene core need to be introduced in the "C−C" stage as some carbon substituents can be installed in the later "C−H" stage. Herein, we describe a proof-of-concept of utilizing this "C−C/C−H" strategy in a concise total synthesis of penicibilaenes A (**2.1**) and B (**2.2**).

**Scheme 2.1.** Approach for Terpene Synthesis

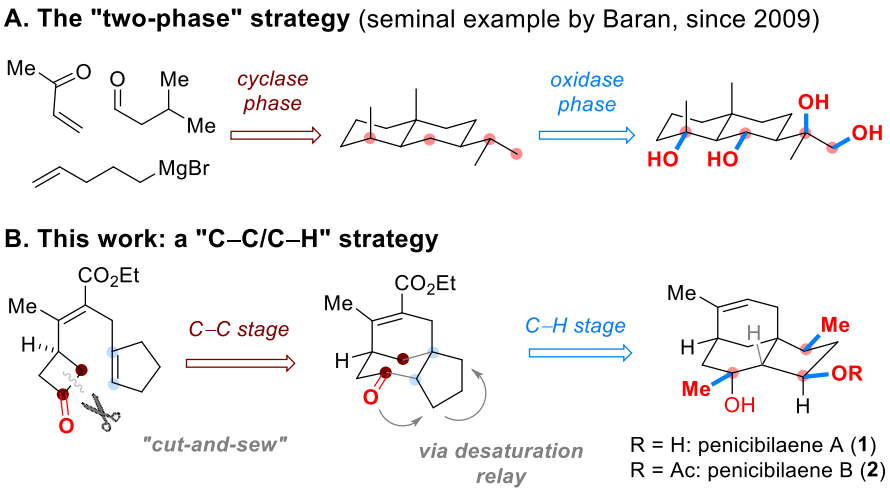


Isolated from a marine fugus *Penicillium bilaiae* MA-267 by Wang and coworkers in 2014, sesquiterpene penicibilaenes A (**2.1**) and B (**2.2**) display selective and potent activity against the plant pathogenic fungus *Colletotrichum gloeosporioides* that are responsible for anthracnose in many fruits and vegetables.[7] In particular, penicibilaene B even shows better efficacy than broad-spectrum antibiotic zeocin. To the best of our knowledge, total synthesis of penicibilaenes had not been reported before our work published. These sesquiterpenes possess interesting chemical

structures, including a tricyclo[6.3.1.$0^{1,5}$]dodecane skeleton constituted by [3.3.1] bridged and [4.3.0] fused junctions, as well as five adjacent stereocenters with one being all-carbon quaternary. Of note, the substitutions on the tricyclic skeleton exhibit a 1,3,5-triad pattern.

## 2.2. First Generation Route

To efficiently synthesize penicibilaenes A and B, we proposed a "cut-and-sew" pathway to construct these two natural products (Scheme 2.2). For retrosynthetic viewpoint, the C14 methyl group in penicibilaenes A and B can be introduced in a late-stage methylation of β-hydroxyl ketone **2.3**, which can be constructed from an intramolecular aldol rection of aldehyde **2.4**. The [3.3.1] skeleton in compound **2.4** is expected to be furnished by "cut-and-sew" reaction from cyclobutanone **2.5**. In order to test the key "cut-and-sew" reaction, cyclobutanone **2.6** was designed as an model substrate, which is proposed to be synthesized from triene **2.7** through a regioselective [2+2] cycloaddition with ketene. Triene **2.7** is expected to be prepared by coupling between bromide **2.8** and hydrazone **2.9**.

**Scheme 2.2.** Retrosyntic Analysis of First Generation Route

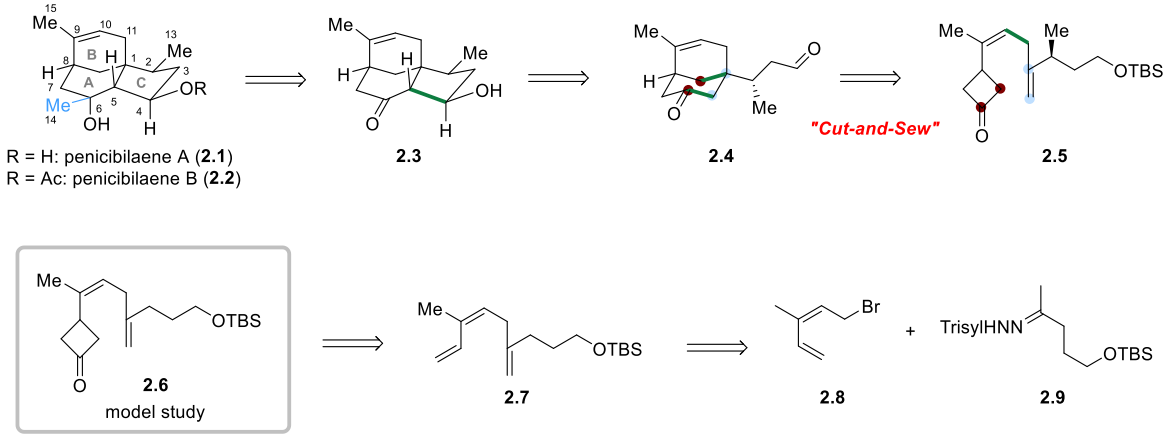


Following the reported procedure,[8] bromide **2.8** could be prepared from alcohol **2.10** in three step sequence (Scheme 2.3). On the other hand, hydrazone **2.9** could be synthesized from ketone

**2.13** in 2 steps. However, the Shapiro reaction between bromide **2.8** and hydrazone **2.9** only give triene **2.7** in 27% yield after several trials. Considering the difficulty of preparing triene **2.7** and the potential selectivity issue for the following [2+2] cycloaddition, we decide to change a route to synthesis cyclobutanone **2.6**.

**Scheme 2.3.** Synthesis of Triene **2.7**

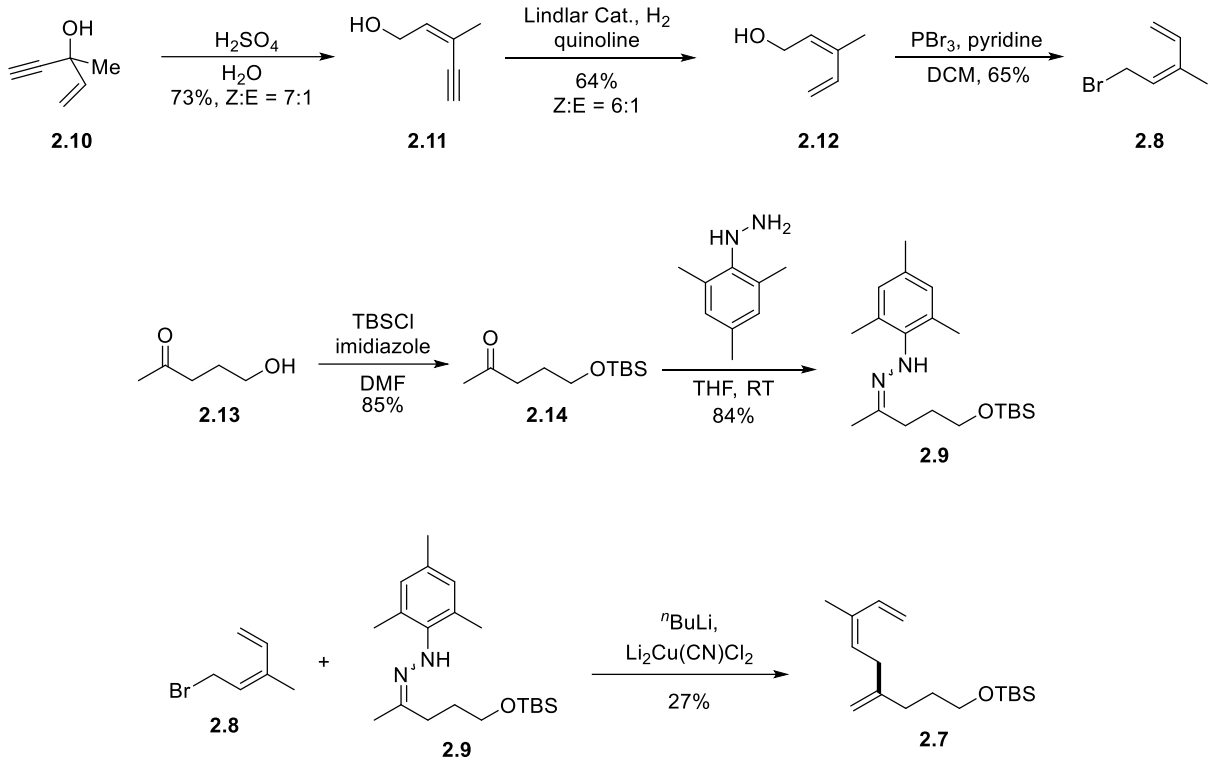


To solve the possible selectivity issue of [2+2] cycloaddition of triene **2.7**, an alternative route to cyclobutanone **2.6** was proposed (Scheme 2.4). Cyclobutanone **2.6** was proposed to be prepared from Stille coupling between organic stannane **2.15** and acetate **2.16**. Acetate **2.16** was planed to be synthesized from a regioselective [2+2] cycloaddition of diene **2.12**.

**Scheme 2.4.** Alternative Route to Construct Cyclobutanone **2.6**.

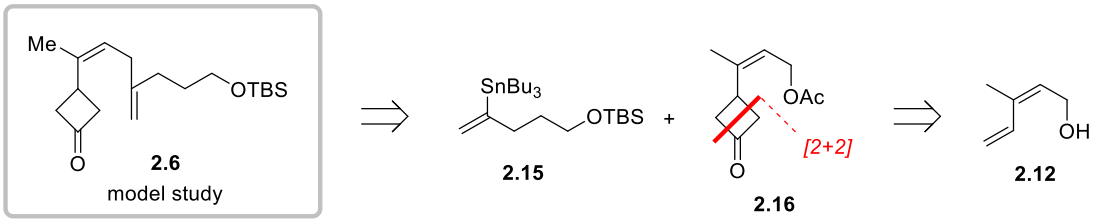


The stannane **2.15** was initially prepared from hydrazone **2.9** through Shapiro reaction (Scheme 2.5). However, this reaction suffered from the low yield. A more convenient way to synthesize stannane **2.15** was found later from alkyne **2.17**. Simply protection of alcohol **2.17** afforded alkyne **2.18**. A nickel catalyzed hydroiodination[9] of alkyne **2.18** furnished iodide **2.19**, which was treated with n-butyl lithium and $Bu_3SnCl$ to give stannane **2.15**. The new route enabled the gram-scale and high-yield preparation of stannane **2.15** from commercially available alkyne **2.17**.

On the other hand, acylation of alcohol **2.12** gave acetate **2.20**, which readily underwent [2+2] cycloaddition with dichloroketene in a regioselective manner to give compound **2.22**. The dichloroketene was selectively reacted with the less hindered double bond in diene to deliver the desired selectivity. Although the compound **2.22** could be converted to cyclobutanone **2.16** using classic reduction method in high yield (entry 1, Table 2.1), the internal alkene was totally isomerized to a 1:1 *Z*/*E* mixture. After condition screening, we found that using zinc as reductant along with a weaker acid $NH_4Cl$ under room temperature can afford cyclobutanone **2.16** in moderate yield and remain with Z alkene (Z/E = 4:1) in the product (entry 2, Table 2.1). The higher yield and *Z*/*E* ratio was achieved when shorten the reaction time to 1 h (entry 3, Table 2.1).

**Scheme 2.5.** Synthesis of stannane **2.15** and dichlorocyclobutanone **2.22**.

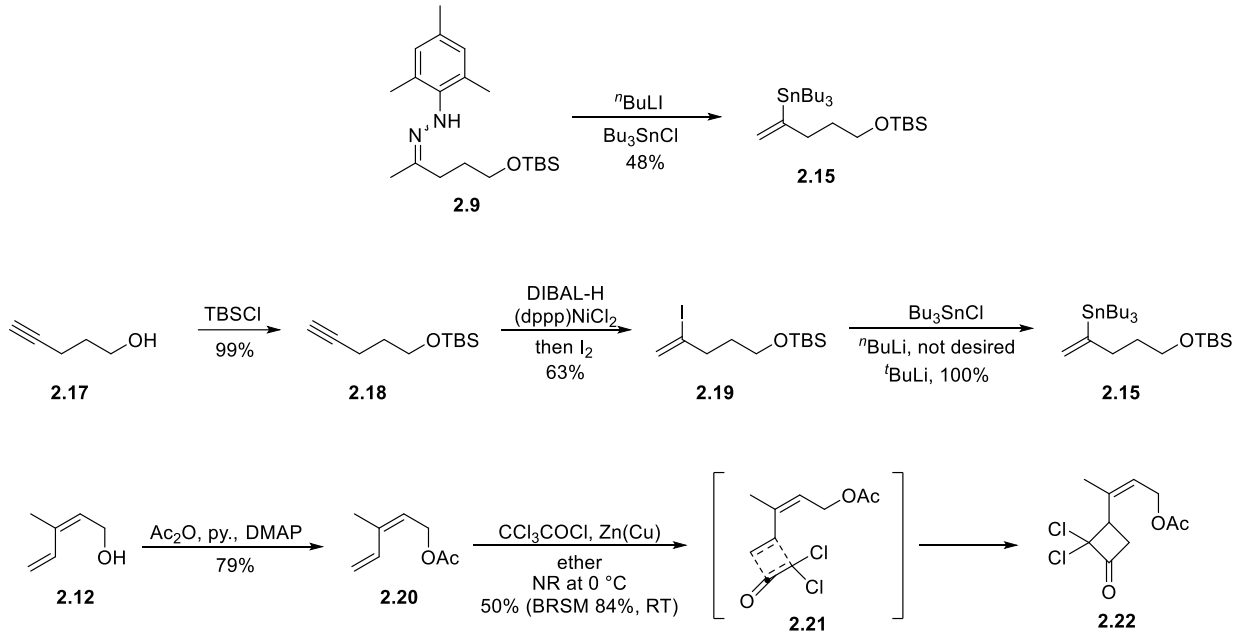


**Table 2.1.** Dechloronation of Compound **2.22**.

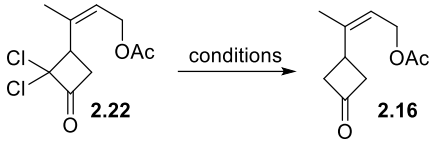


| Entry | Conditions | Scale | Yield | Z:E |
|---|---|---|---|---|
| 1 | Zn, AcOH, 75 °C | 50 mg | quantitive | 1:1 |
| 2 | Zn, $NH_4Cl$, MeOH, rt. overnight | 50 mg | 63% | 4:1 |
| 3 | Zn, $NH_4Cl$, MeOH, rt., 1 h | 10 g | 75% | 8:1 |

With two coupling precursors, stannane **2.15** and acetate **2.16** in hand, we started to screen the Stille coupling (Table 2.2). Some reported conditions[10] of Stille coupling of acetate and stannane (entry 1-2, Table 2.2) with do not work on our substrates. Trace amount of coupling product **2.6** was observed when the temperature raised to 70 °C (entry 3, Table 2.2), and 51% yield of compound **2.6** was obtained when the reaction temperature was further increased to 80 °C (entry 4, Table 2.2). Unfortunately, the reaction yield was not further improved after screening different

palladium pre-catalysts (entry 5-10, Table 2.2), solvents (entry 11-12, Table 2.2) and additives (entry 13-18, Table 2.2).

**Table 2.2.** Stille coupling of Stannane **2.15** and Acetate **2.16**.

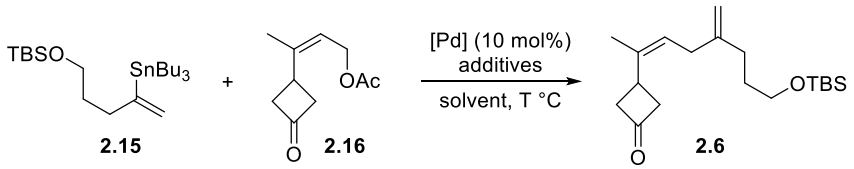


| Entry | [Pd] | Additive | Solvent | Temperature | Time | Yield |
|---|---|---|---|---|---|---|
| 1 | $Pd(dba)_2$ | 3 equiv. LiCl | DMF | 40 °C | 2 h | n.d. |
| 2 | $Pd(PPh_3)_4$ | 0.2 equiv. CuI + 3 equiv. LiCl | DMSO | 60 °C | 2 h | n.d. |
| 3 | $Pd(dba)_2$ | 3 equiv. LiCl | DMF | 70 °C | 2 h | low conversion |
| 4 | $Pd(dba)_2$ | 3 equiv. LiCl | DMF | 80 °C | 2 h | 51% |
| 5 | $Pd(dba)_2$ | 3 equiv. LiCl | DMF | 80 °C | 16 h | 29% (16 h) |
| 6 | $Pd(OAc)_2$ | 3 equiv. LiCl | DMF | 80 °C | 16 h | n.d. (16 h) |
| 7 | $Pd(PPh_3)_4$ | 3 equiv. LiCl | DMF | 80 °C | 16 h | n.r. (16 h) |
| 8 | $Pd(PPh_3)_2Cl_2$ | 3 equiv. LiCl | DMF | 80 °C | 16 h | n.r. (16 h) |
| 9 | $[Pd(allyl)Cl]_2$ | 3 equiv. LiCl | DMF | 80 °C | 16 h | 24% (16 h) |
| 10 | $Pd(OAc)_2 + AsPh_3$ | 3 equiv. LiCl | DMF | 80 °C | 16 h | n.d. (16 h) |
| 11 | $Pd(dba)_2$ | 3 equiv. LiCl | NMP | 80 °C | 2 h | 31% |
| 12 | $Pd(dba)_2$ | 3 equiv. LiCl | THF | 80 °C | 2 h | n.d. |
| 13 | $Pd(dba)_2$ | 3 equiv. CsF | DMF | 80 °C | 2 h | n.d. |
| 14 | $Pd(dba)_2$ | 0.2 equiv. CuI | DMF | 80 °C | 2 h | n.d. |
| 15 | $Pd(dba)_2$ | 0.2 equiv. CuI + 3 equiv. LiCl | DMF | 80 °C | 2 h | 44% |
| 16 | $Pd(dba)_2$ | 0.2 equiv. CuI + 3 equiv. CsF | DMF | 80 °C | 2 h | n.d. |
| 17 | $Pd(dba)_2$ | 1 equiv. LiCl | DMF | 80 °C | 2 h | 40% |
| 18 | $Pd(dba)_2$ | 10 equiv. LiCl | DMF | 80 °C | 2 h | 35% |

With "cut-and-sew" reaction precursor cyclobutanone **2.6** in hand, we started to explore the key "cut-and-sew" reaction. However, the standard "cut-and-sew" condition reported in the literature[11] did not work well with cyclobutanone **2.6** as substrate, which did not deliver any cyclized product **2.23** (entry 1, Table 2.3). Different rhodium pre-catalysts were then examined, which were not fruitful (entry 2-11, Table 2.3). The aminopyridine played an important role in this reaction, decarbonylated product cyclopropane was observed in the absence of aminopyridine directing groups (entry 1, Table 2.4). Diverse ligands were also screened, including NHC ligands

(entry 5-6), bidentate ligands (entry 7, 14, 15, Table 2.4) and monodentate ligands (entry 8-13). However, no desired product **2.23** was observed under these conditions.

**Table 2.3.** Catalysts Screening on "Cut-and-Sew" Reaction of Cyclobutanone **2.6**.

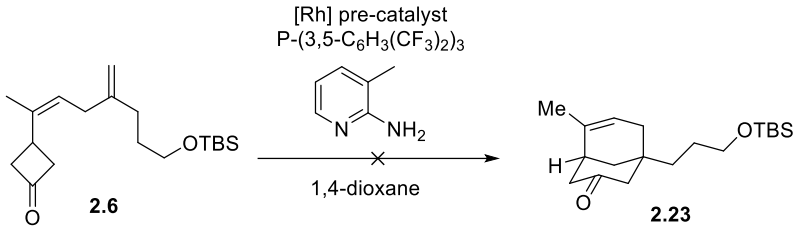


| Entry | [Rh] pre-catalyst | Temperature | Result |
|---|---|---|---|
| 1 | $[Rh(C_2H_4)_2Cl]_2$ | 150 °C | n.d. |
| 2 | $[Rh(cod)Cl]_2$ | 150 °C | n.r. |
| 3 | $[Rh(cod)Cl]_2$ | 160 °C | n.r. |
| 4 | $[Rh(cod)Cl]_2$ | 170 °C | n.d. |
| 5 | $[Rh(cod)Cl]_2$ | 180 °C | decomposed |
| 6 | $[Rh(cod)OH]_2$ | 170 °C | n.r. |
| 7 | $Rh(PPh_3)_3Cl$ | 170 °C | n.r. |
| 8 | $[Rh(coe)_2Cl]_2$ | 150 °C | n.r. |
| 9 | $[Rh(CO)_2Cl]_2$ | 150 °C | n.r. |
| 10 | $[Rh(CH_3CN)_2(cod)]BF_4$ | 150 °C | n.d. |
| 11 | $[Rh(dppb)(cod)]BF_4$ | 150 °C | n.d. |

**Table 2.4.** Ligands and Directing Groups Screening on "Cut-and-Sew" Reaction of Cyclobutanone **2.6**.

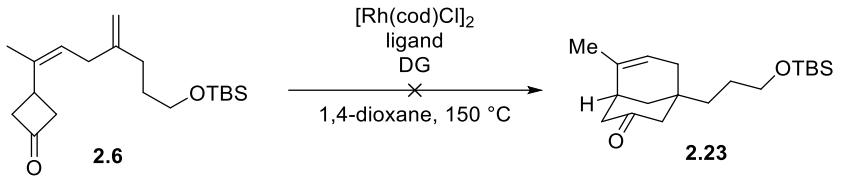


**2.6** **2.23**

| Entry | Ligand | DG | Result |
|---|---|---|---|
| 1 | P-(3,5-$C_6H_3(CF_3)_2)_3$ | none | decarbonylation |
| 2 | P-(3,5-$C_6H_3(CF_3)_2)_3$ | 2-aminopyridine | n.r. |
| 3 | P-(3,5-$C_6H_3(CF_3)_2)_3$ | 6-methyl-2-aminopyridine | n.r. |
| 4 | none | 3-methyl-2-aminopyridine | ring expansion? |
| 5 | IPr | 3-methyl-2-aminopyridine | n.r. |
| 6 | IMes | 3-methyl-2-aminopyridine | n.r. |
| 7 | BINAP | 3-methyl-2-aminopyridine | decarbonylation |
| 8 | XPhos | 3-methyl-2-aminopyridine | ring expansion? |
| 9 | P(*p*-$C_6H_4F)_3$ | 3-methyl-2-aminopyridine | n.r. |
| 10 | $PCy_3$ | 3-methyl-2-aminopyridine | n.r. |
| 11 | $PPh_3$ | 3-methyl-2-aminopyridine | n.d. |
| 12 | P($C_6F_5)_3$ | 3-methyl-2-aminopyridine | n.r. |
| 13 | P$(OPh)_3$ | 3-methyl-2-aminopyridine | n.d. |
| 14 | dppb | 3-methyl-2-aminopyridine | decomposed |
| 15 | dppf | 3-methyl-2-aminopyridine | decomposed |

The current results of "cut-and-sew" condition screening revealed that the alkene linker is too labile, which underwent double bond migration and many other side reactions. Thus, we planed to protect the C=C double bond in the linker to epoxide or ether, which proposed to be sufficient stable under typical "cut-and-sew" conditions (Scheme 2.6).

**Scheme 2.6.** Protection of Double Bond.

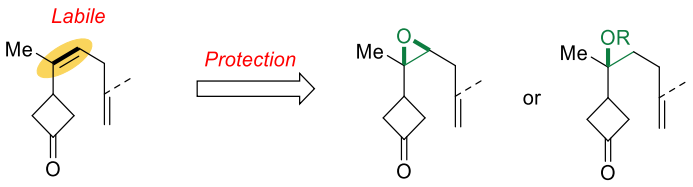

Epoxidation of cyclobutanone **2.6** selectively occurred on more electron-rich trisubstituted alkene to deliver epoxide **2.24** (Scheme 2.7). With epoxide linked cyclobutanone **2.24** in hand, we started to examine different combinations of catalyst and ligand to find out a proper condition which can give cyclized product **2.25**. Screening of catalysts did not deliver any promising result, including different rhodium (entry 1-5, Table 2.5) and nickel catalysts (entry 6-7, Table 2.5).

**Scheme 2.7.** Preparation of Epoxide **2.24**.

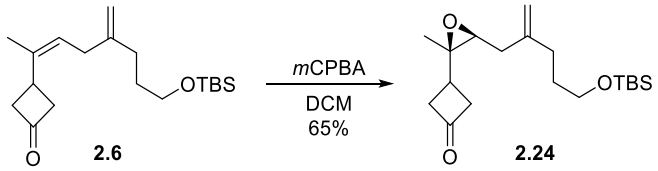


**Table 2.5.** Catalyst Screening on "Cut-and-Sew" Reaction of Cyclobutanone **2.24**.

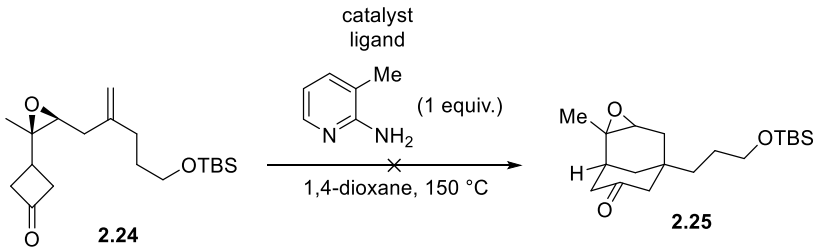


| Entry | Catalyst (10 mol%) | Ligand (22 mol%) | Result |
|---|---|---|---|
| 1 | $[Rh(cod)_2Cl]_2$ | P-(3,5-$C_6H_3(CF_3)_2)_3$ | N.R. |
| 2 | $[Rh(coe)_2Cl]_2$ | P-(3,5-$C_6H_3(CF_3)_2)_3$ | N.R. |
| 3 | $[Rh(C_2H_4)_2Cl]_2$ | P-(3,5-$C_6H_3(CF_3)_2)_3$ | N.R. |
| 4 | $[Rh(CO)_2Cl]_2$ | P-(3,5-$C_6H_3(CF_3)_2)_3$ | N.R. |
| 5 | $[Rh(nbd)_2]BF_4$ (20 mol%) | P-(3,5-$C_6H_3(CF_3)_2)_3$ | decomposed |
| 6 | $Ni(COD)_2$ | $PCy_3$ | N.R. |
| 7 | $Ni(COD)_2$ (No DG) | $PCy_3$ | N.R. |

Besides catalysts, diverse types of ligands were also screened (Table 2.6). Although none of the monodentate phosphine ligands, bidentate phosphine ligands, Buchward ligand or NHC ligand could give desired bicycle **2.25**, some interesting side products were generated under specific

entries. Decarbonylation product **2.26** was observed when using dppe as the ligand (entry 4, Table 2.6), and lactone **2.27** (entry 8, Table 2.6) was isolated with dppp as the ligand in this reaction. We proposed that this transformation contained a carbon cation rearrangement (Scheme 2.8). After cleavage of α-C−C bond in cyclobutanone, the epoxide could attack the carbonyl group in intermediate **2.28** and substitute rhodium to give intermediate **2.29**. The following Wagner–Meerwein rearrangement terminated by rhodium elimination delivered lactone **2.30**. Finally, double bond migration enabled the formation of conjugated lactone **2.27**.

**Table 2.6.** Ligand Screening on "Cut-and-Sew" Reaction of Cyclobutanone **2.24**.

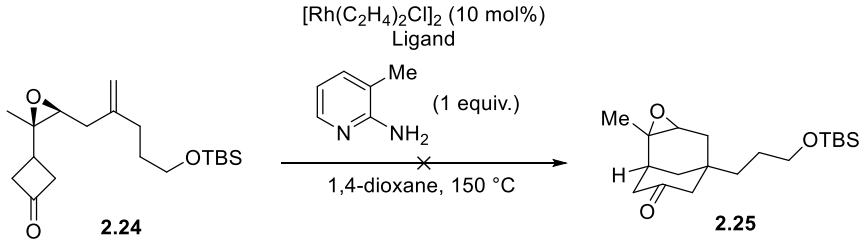


| Entry | Ligand | Result | Entry | Ligand | Result |
|---|---|---|---|---|---|
| 1 | none | N.R. | 15 | $P(OMe)_3$ (22 mol%) | N.D. |
| 2 | $PPh_3$ (22 mol%) | N.R. | 16 | $PMe_3$ (22 mol%) | N.D. |
| 3 | $P(OPh)_3$ (22 mol%) | N.D. | 17 | STBM-SEGPHOS (11 mol%) | Decomposed |
| 4 | dppe (11 mol%) | **2.26** observed | 18 | DM-SEGPHOS (11 mol%) | Decomposed |
| 5 | $AsPh_3$ (22 mol%) | N.R. | 19 | BIPHEP (11 mol%) | Decomposed |
| 6 | $P(OiPr)_3$ (22 mol%) | N.R. | 20 | dppf (11 mol%) | Decomposed |
| 7 | dppm (11 mol%) | N.R. | 21 | $P(2\text{-furan})_3$ (22 mol%) | N.R. |
| 8 | dppp (11 mol%) | **2.27** observed | 22 | $P(4\text{-}CF_3\text{-}C_6H_4)_3$ (22 mol%) | N.R. |
| 9 | $P^tBu_3$ (22 mol%) | N.D. | 23 | $P(C_6F_5)_3$ (22 mol%) | N.R. |
| 10 | XPhos (11 mol%) | N.R. | 24 | $PCy_3$ (22 mol%) | N.R. |
| 11 | SPhos (11 mol%) | N.D. | 25 | dppb (11 mol%) | N.R. |
| 12 | TMTU (22 mol%) | N.R. | 26 | BINAP (11 mol%) | Decomposed |
| 13 | $PMe_2Ph$ (22 mol%) | N.D. | 27 | IPr (22 mol%) | Decomposed |
| 14 | $PEt_3$ (22 mol%) | N.D. | 28 | IMes (22 mol%) | N.R. |

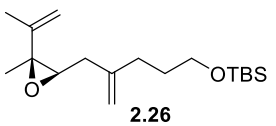

2.26

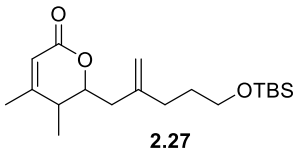

2.27

**Scheme 2.8.** Proposed Mechanism of Rearrangement from **2.24** to **2.27**.

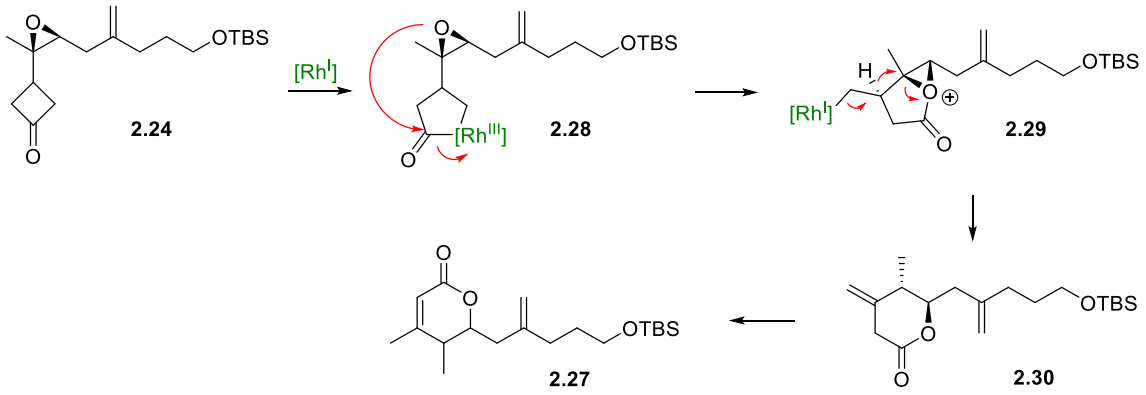


Since the epoxide tethered cyclobutanone cannot deliver the desired "cut-and-sew" product, we then tested silyl ether linked cyclobutanone **2.36**. The initial route to prepare cyclobutanone **2.36** was started from previously prepared cyclobutanone **2.6** (Scheme 2.9). Cyclobutanone **2.6** was treated by PTSA and $HC(OMe)_3$ to give compound **2.31**, followed by protection of alcohol to generate ketal **2.32**. The epoxidation of ketal **2.32** also prefer more substituted double bond to deliver epoxide **2.33**, which readily reduced by $LiAlH_4$ to afford tertiary alcohol **2.34**.

**Scheme 2.9.** Synthesis of Cyclobutanone **2.36** (Initial Route).

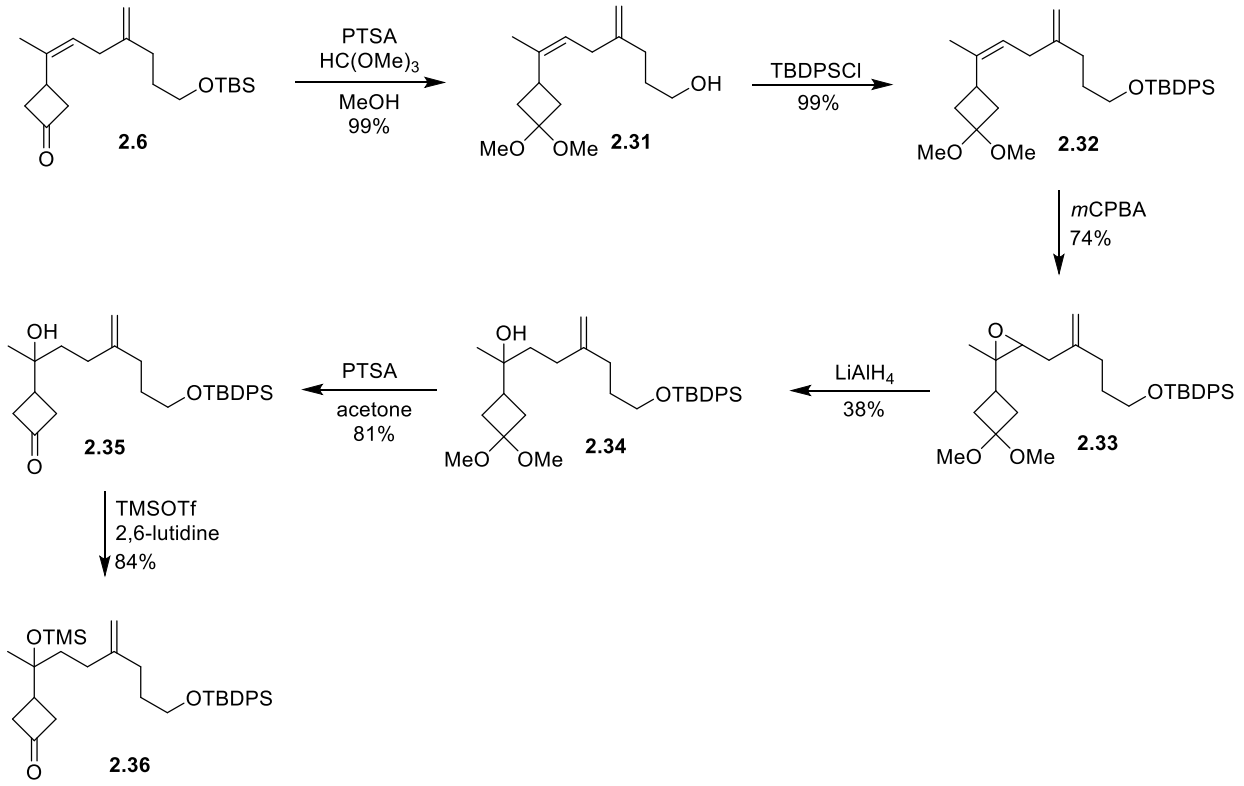


Although we have successfully got cyclobutanone **2.36**, but the initial synthetic route required 12 steps to access cyclobutanone **2.36** from commercially available starting materials, which caused huge difficulties to accumulate enough amount of material for key "cut-and-sew" reaction screening. Thus, we proposed and realized a more efficient route to construct cyclobutanone **2.36** (Scheme 2.10). The commercially available carboxylic acid **2.37** was converted to Weinreb amide **2.38**, followed by protection of ketone to deliver amide **2.39**. On the other hand, commercially available alkyne **2.17** was converted to vinyl iodide **2.19** in 2 steps (refer to Scheme 2.5). Iodide **2.19** underwent lithium-iodide exchange with *t*BuLi, followed by treatment with ethylene oxide furnished alcohol **2.40**. Sequential iodization/lithium-iodide exchange of alcohol **2.40** followed by treating with Weinreb amide **2.39** generate ketone **2.42**, which was attacked by methyl lithium to give alcohol **2.43**. Finally, global deprotection followed by reprotection of two hydroxyl groups

delivered cyclobutanone **2.36**. The optimized route was 3 steps shorter than the initial route, meanwhile delivered higher total yield. The new synthetic route was also much easier to scale up comparing to the original one.

**Scheme 2.10.** Synthesis of Cyclobutanone **2.36** (Optimized Route).

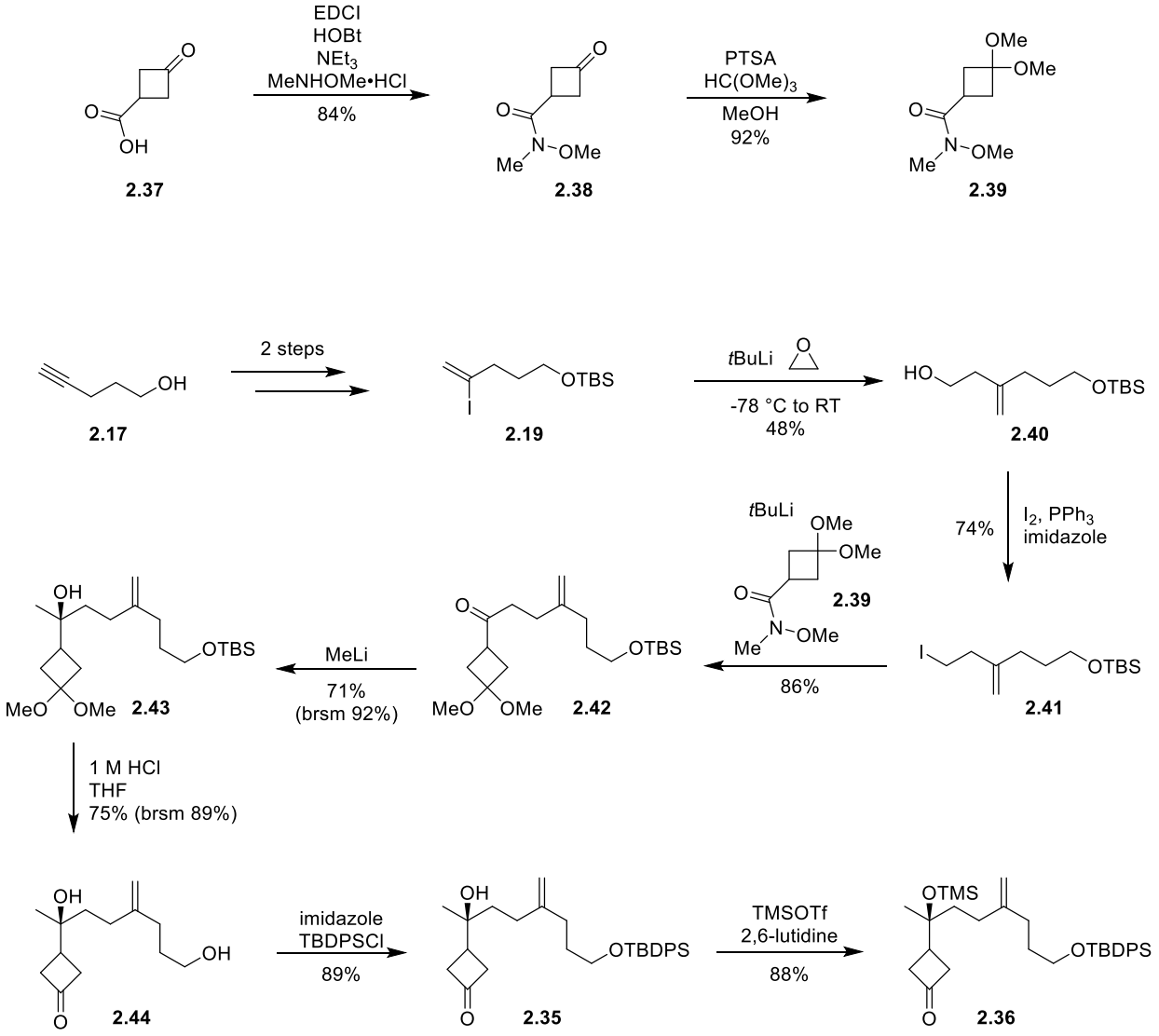


With cyclobutanone **2.36** in hand, we started to explore the suitable condition for the "cut-and-sew" reaction. Different rhodium catalysts (with or without ligands) were screened, but none of the conditions delivered the desired cyclized product **2.45** (Table 2.7). It worth to mention that

decarbonylated product, cyclopropane **2.46**, was observed when using $[Rh(COE)_2Cl]_2$ as pre-catalyst (entry 7, Table 2.7), which indicated that the C−C activation of cyclobutanone happened. Screening of different ligands were also not fruitful, only decarbonylation side products could be observed (Table 2.8).

**Table 2.7.** Catalysts Screening on "Cut-and-Sew" Reaction of Cyclobutanone **2.36**.

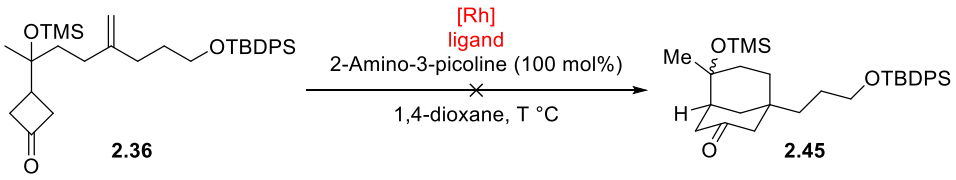


| Entry | [Rh] (20 mol%) | Ligand (22 mol%) | Temperature | Result |
|---|---|---|---|---|
| 1 | $[Rh(C_2H_4)_2Cl]_2$ | $P(3,5\text{-}C_6H_3(CF_3)_2)_3$ | 150 °C | N.D. |
| 2 | $[Rh(COD)Cl]_2$ | $P(3,5\text{-}C_6H_3(CF_3)_2)_3$ | 150 °C | N.R. |
| 3 | $[Rh(COE)_2Cl]_2$ | $P(3,5\text{-}C_6H_3(CF_3)_2)_3$ | 150 °C | N.D. |
| 4 | $[Rh(CH_3CN)_2(COD)]BF_4$ | $P(3,5\text{-}C_6H_3(CF_3)_2)_3$ | 150 °C | N.R. |
| 5 | $[Rh(CO)_2Cl]_2$ | $P(3,5\text{-}C_6H_3(CF_3)_2)_3$ | 150 °C | N.R. |
| 6 | $[Rh(COD)Cl]_2$ | / | 130 °C | N.D. |
| 7 | $[Rh(COE)_2Cl]_2$ | / | 130 °C | **2.46** observed |
| 8 | $[Rh(C_2H_4)_2Cl]_2$ | / | 130 °C | N.R. |
| 9 | $[Rh(COD)_2]BF_4$ | / | 130 °C | N.D. |
| 10 | $[Rh(CH_3CN)_2(COD)]BF_4$ | / | 130 °C | N.D. |
| 11 | $[Rh(COD)Cl]_2$ | / | 150 °C | N.D. |
| 12 | $[Rh(COD)_2]BF_4$ | / | 150 °C | N.D. |

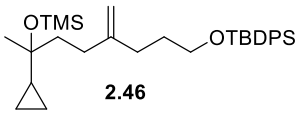


**Table 2.8.** Ligands Screening on "Cut-and-Sew" Reaction of Cyclobutanone **2.36**.

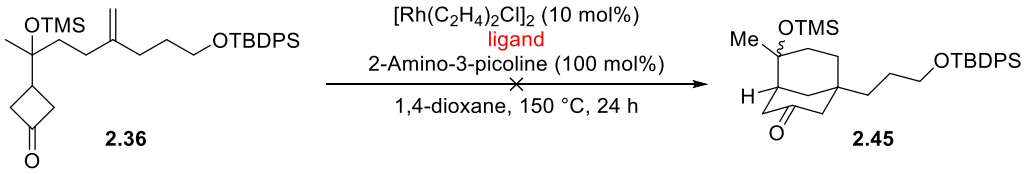


| Entry | Ligand (45 mol%) | Result | Entry | Ligand (20 mol%) | Result |
|---|---|---|---|---|---|
| 1 | $PPh_3$ | N.R. | 7 | SPhos | N.D. |
| 2 | TFP | N.D. | 8 | XPhos | N.R. |
| 3 | $P(C_6F_5)_3$ | N.R. | 9 | RuPhos | Decarbonylation |
| 4 | $P(4\text{-}C_6H_4CF_3)_3$ | N.D. | 10 | tBuXPhos | N.R. |
| 5 | $P(4\text{-}C_6H_4F)_3$ | N.D. | 11 | BrettPhos | N.R. |
| 6 | $P(3,5\text{-}C_6H_3(CF_3)_2)_3$ | N.D. | 12 | DavePhos | Decarbonylation |

It has been proved that the C−C activation of cyclobutanone readily occur without directing group.[12] Thus, multiple conditions without directing groups were screened (Table 2.9, 2.10). Although still no desired product was detected, we found that decarbonylation became much easier with the absence of directing groups. Under some conditions, the TMS protecting group were removed.

**Table 2.9.** Ligands Screening on "Cut-and-Sew" Reaction of Cyclobutanone **2.36** (No Directing Group, Part I).

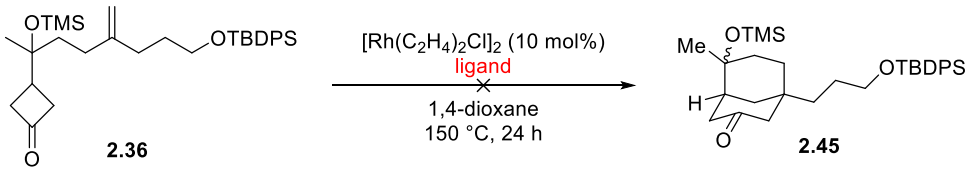


| Entry | Ligand (22 mol%) | Result | Entry | Ligand (22 mol%) | Result |
|---|---|---|---|---|---|
| 1 | SPhos | Decarbonylation | 16 | $PMe_2Ph$ | N.D. |
| 2 | XPhos | N.R. | 17 | $PMePh_2$ | N.R. |
| 3 | $PPh_3$ | Decarbonylation | 18 | P(*o*-tol)$_3$ | N.D. |
| 4 | $P(OPh)_3$ | TMS removed | 19 | P(*t*Bu)$_3$ | N.D. |
| 5 | $P(OMe)_3$ | TMS removed | 20 | dppm | Decarbonylation |
| 6 | $P(C_6F_5)_3$ | TMS removed | 21 | dppe | Decarbonylation |
| 7 | $P(4\text{-}C_6H_4F)_3$ | TMS removed; decarbonylation | 22 | dppp | Decarbonylation |
| 8 | $P(4\text{-}C_6H_4CF_3)_3$ | TMS removed; decarbonylation | 23 | dppb | Decarbonylation |
| 9 | $P(3,5\text{-}C_6H_3(CF_3)_2)_3$ | N.R. | 24 | dppf | Decarbonylation |
| 10 | TFP | TMS removed | 25 | dpppe | N.R. |
| 11 | $AsPh_3$ | TMS removed | 26 | dfppe | N.D. |
| 12 | $SbPh_3$ | TMS removed | 27 | BINAP | Decarbonylation |
| 13 | $PMe_3$ | N.D. | 28 | DPEPhos | Decarbonylation |
| 14 | $PCy_3$ | Decarbonylation | 29 | dppbenz | N.D. |
| 15 | P(*n*Bu)$_3$ | Decarbonylation | 30 | BIPHEP | Decarbonylation |

**Table 2.10.** Ligands Screening on "Cut-and-Sew" Reaction of Cyclobutanone **2.36** (No Directing Group, Part II).

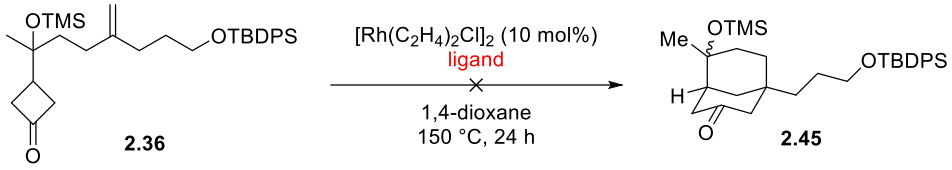


| Entry | Ligand (40 mol%) | Result | Entry | Ligand (40 mol%) | Result |
|---|---|---|---|---|---|
| 1 | $PPh_3$ | N.R. | 9 | $AsPh_3$ | Decarbonylation |
| 2 | $P(OPh)_3$ | TMS removed; decarbonylation | 10 | $PMe_3$ | Decarbonylation |
| 3 | $P(OMe)_3$ | TMS removed | 11 | $PCy_3$ | Decarbonylation |
| 4 | $P(C_6F_5)_3$ | TMS removed; decarbonylation | 12 | $P(n\text{Bu})_3$ | Decarbonylation |
| 5 | $P(4\text{-}C_6H_4F)_3$ | Decarbonylation | 13 | $PMe_2Ph$ | Decarbonylation |
| 6 | $P(4\text{-}C_6H_4CF_3)_3$ | Decarbonylation | 14 | $PMePh_2$ | N.R. |
| 7 | $P(3,5\text{-}C_6H_3(CF_3)_2)_3$ | Decarbonylation | 15 | $P(4\text{-}MeOC_6H_4)_3$ | Decarbonylation |
| 8 | TFP | Decarbonylation | 16 | $P(o\text{-tol})_3$ | Decarbonylation |

Besides the neutral rhodium catalysts, the cationic rhodium catalysts were also able to catalyze C−C activation of cyclobutanone.[13] Comparing to neutral rhodium catalysts, cationic rhodium catalysts typically has higher reactivity on C−C oxidative addition and double bond migratory insertion. Thus, we screened different ligands and temperatures with cationic rhodium catalyst, $[Rh(COD)_2]BF_4$, as catalyst (Table 2.11). However, the starting material decomposed under these conditions. Lower temperature only reduced the conversion of the substrate. One possible side product under these conditions is lactone **2.47**. We proposed that TMS deprotection and rhodium oxidative addition of cyclobutanone **2.36** delivered metallocycle **2.48** (Scheme 2.11). The hydroxyl group in **2.48** could kicked off rhodium through acyl substitution to give intermediate **2.49**, which readily underwent protonation to generate lactone **2.47a**. Considering rhodium catalyst can promote double bond migration, **2.47b** and **2.47c** also formed.

**Table 2.11.** Ligands Screening on "Cut-and-Sew" Reaction of Cyclobutanone **2.36** (No Directing Group, Part II).

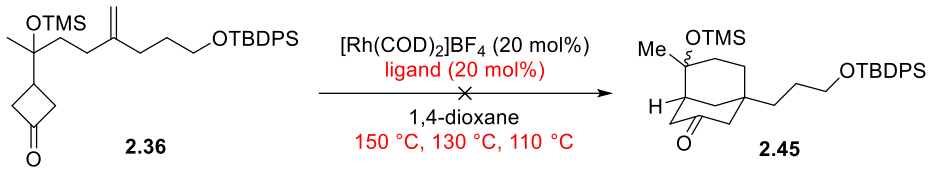


| Entry | Ligand | Result | Entry | Ligand | Result |
|---|---|---|---|---|---|
| 1 | dppm | Decomposed | 6 | dpppe | Decomposed |
| 2 | dppe | Decomposed | 7 | dfppe | Decomposed |
| 3 | dppp | Decarbonylation | 8 | BINAP | Decomposed |
| 4 | dppb | Decomposed | 9 | DPEPhos | Decomposed |
| 5 | dppf | Decomposed | 10 | dppbenz | Decomposed |

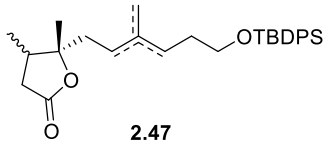


possible side product

**Scheme 2.11.** Proposed Mechanism for Generation of Lactone **2.47**.

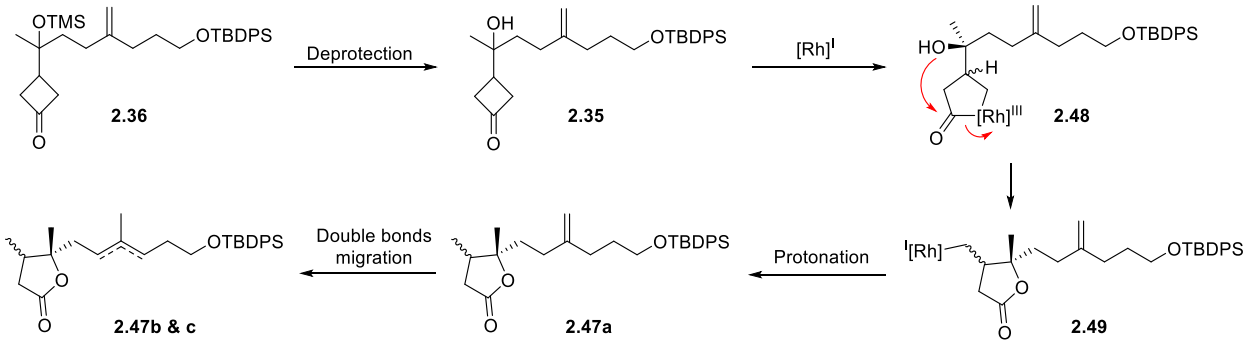


Based on current results, the TMS protecting group in cyclobutanone **2.36** was not stable enough, which made nucleophilic attack to be favored than alkene migratory insertion. Thus, we decided to change the protecting group on the tertiary alcohol to methyl group, which is one of the most stable protecting group of alcohol. Preparation of methyl ether tethered cyclobutanone **2.52** was also started from alkyne **2.17**. Alkyne **2.17** was converted to alcohol **2.43** in 6 steps (see

Scheme 2.10 for detail), followed by deprotection by TBAF to give diol **2.50**. Double methylation of diol **2.50** afforded ketal **2.51** in 84% yield with potassium hydride as base. Finally, deprotection of ketal by aqueous hydrochloride acid furnished cyclobutanone **2.52**.

**Scheme 2.12.** Preparation of Methyl Ether Tethered Cyclobutanone **2.52**.

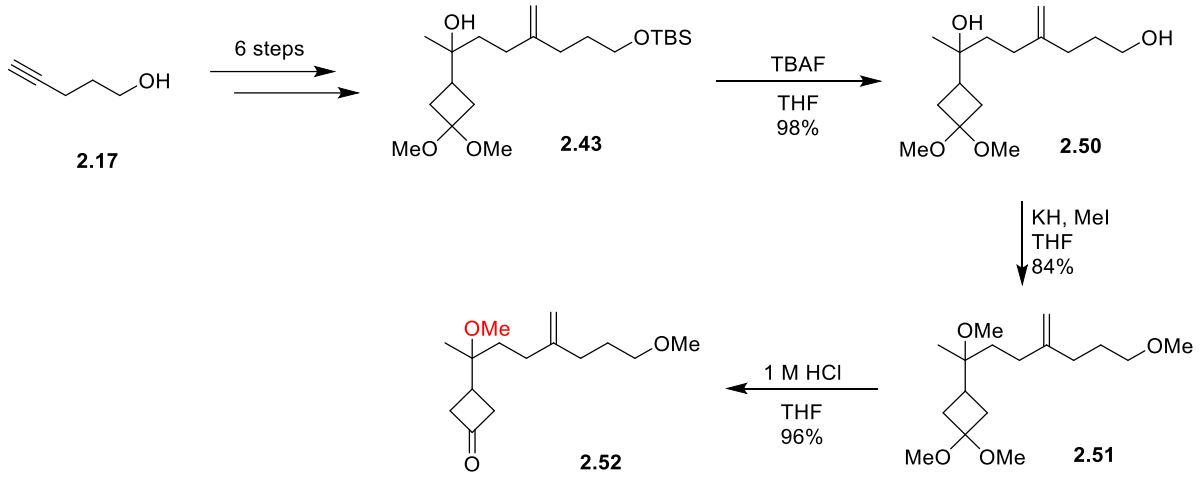


After getting cyclobutanone **2.52**, we screened the different catalyst, ligands and solvent (Table 2.12-2.14). However, no desired cyclized product **2.53** was captured under these conditions.

**Table 2.12.** Ligands Screening on "Cut-and-Sew" Reaction of Cyclobutanone **2.52**.

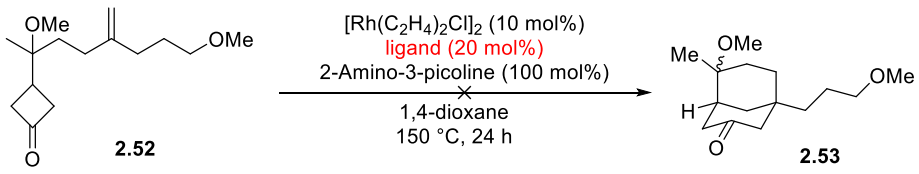


| Entry | Ligand | Result | Entry | Ligand | Result |
|---|---|---|---|---|---|
| 1 | SPhos | Decarbonylation | 7 | $P(4\text{-}C_6H_4CF_3)_3$ | N.D. |
| 2 | XPhos | N.R. | 8 | $P(3,5\text{-}C_6H_3(CF_3)_2)_3$ | N.D. |
| 3 | $PPh_3$ | N.D. | 9 | TFP | N.D. |
| 4 | $P(OPh)_3$ | N.D. | 10 | $AsPh_3$ | N.D. |
| 5 | $P(C_6F_5)_3$ | N.D. | 11 | IPr | Decarbonylation |
| 6 | $P(4\text{-}C_6H_4F)_3$ | N.D. | 12 | IMes | Decarbonylation |

**Table 2.13.** Catalysts Screening on "Cut-and-Sew" Reaction of Cyclobutanone **2.52**.

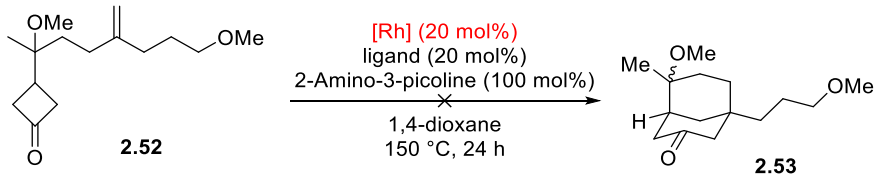


| Entry | [Rh] (20 mol%) | ligands (20 mol%) | Result |
|---|---|---|---|
| 1 | $[Rh(COD)Cl]_2$ | / | N.D. |
| 2 | $[Rh(COE)_2Cl]_2$ | / | N.D. |
| 3 | $[Rh(C_2H_4)_2Cl]_2$ | / | N.D. |
| 4 | $[Rh(COD)Cl]_2$ | $P(C_6F_5)_3$ | N.D. |
| 5 | $[Rh(COE)_2Cl]_2$ | $P(C_6F_5)_3$ | N.D. |
| 6 | $[Rh(C_2H_4)_2Cl]_2$ | $P(C_6F_5)_3$ | N.D. |

**Table 2.14.** Ligands Screening on "Cut-and-Sew" Reaction of Cyclobutanone **2.52** (Toluene as Solvent).

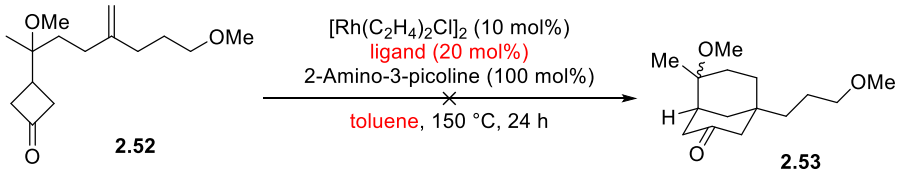


| Entry | Ligand | Result |
|---|---|---|
| 1 | / | N.R. |
| 2 | $PPh_3$ | N.R. |
| 3 | $P(OPh)_3$ | N.R. |
| 4 | $P(C_6F_5)_3$ | N.R. |
| 5 | $AsPh_3$ | N.R. |
| 6 | $P(3,5\text{-}C_6H_3(CF_3)_2)_3$ | N.R. |

Although screening of ligands with cationic rhodium also not provided promising results, a side product amide **2.54** was determined (Table 2.15). In this case, oxidative addition of rhodium into C−C bond delivered intermediate **2.56**, which was attacked by water to give intermediate **2.58**. A following protonation furnished amide **2.54**.

**Table 2.15.** Ligands Screening on "Cut-and-Sew" Reaction of Cyclobutanone **2.52** (Cationic Rhodium).

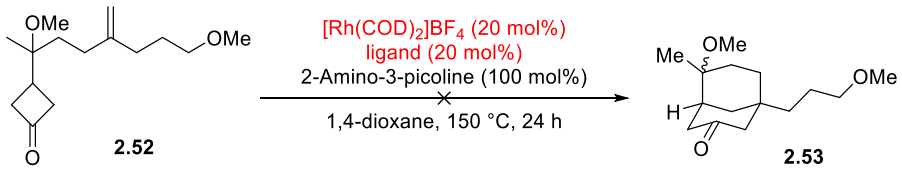


| Entry | Ligand | Result | Entry | Ligand | Result |
|---|---|---|---|---|---|
| 1 | dppm | N.D. | 9 | $P(OPh)_3$ | Decarbonylation |
| 2 | dppe | N.R. | 10 | $P(OMe)_3$ | Decarbonylation |
| 3 | dppp | Decarbonylation | 11 | $P(C_6F_5)_3$ | Decarbonylation |
| 4 | dppb | N.D. | 12 | $P(4\text{-}C_6H_4F)_3$ | N.D. |
| 5 | dppf | Decarbonylation | 13 | $P(4\text{-}C_6H_4CF_3)_3$ | N.D. |
| 6 | dpppe | N.D. | 14 | $P(3,5\text{-}C_6H_3(CF_3)_2)_3$ | N.D. |
| 7 | dfppe | N.R. | 15 | TFP | N.D. |
| 8 | $PPh_3$ | N.D. | 16 | $AsPh_3$ | N.R. |

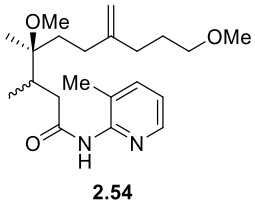


**Scheme 2.13.** Preparation of Methyl Ether Tethered Cyclobutanone **2.54**.

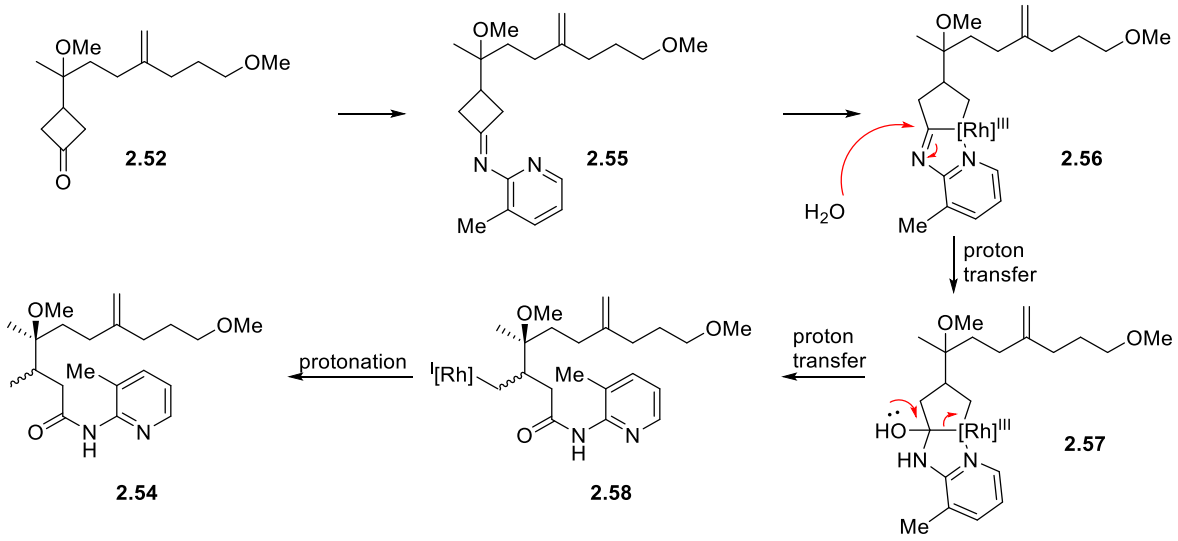

Comparing the reported examples and previous failed substrates (Scheme 2.14), the major difference is the linker between cyclobutanone and olefin. The reported linkers includes tosyl amine linker in **2.59**, malonic ester linker in **2.60** and benzene linker in **2.61**. All of these linker can make olefin part and cyclobutanone part to become closer, which reduces the activation enthalpy and entropy. Thus, we designed a new model substrate cyclobutanone **2.62**, which contains a rigid ester linker. Comparing to alkene linker in cyclobutanone **2.6**, ester linker in cyclobutanone **2.62** is proposed to have several advantages. First, the rigid tetra-substituted double bond could restrict the conformation, which make cyclobutanone and olefin to stay at the same side of the linker. Second, the steric repulsion between ester and olefin would further promote cyclobutanone part and olefin part to become closer. Third, the tetra-substituted double bond is relatively inert and hard to coordinate with transition metal catalyst, which inhibit side reaction.

**Scheme 2.14.** Design of Ester Linker.

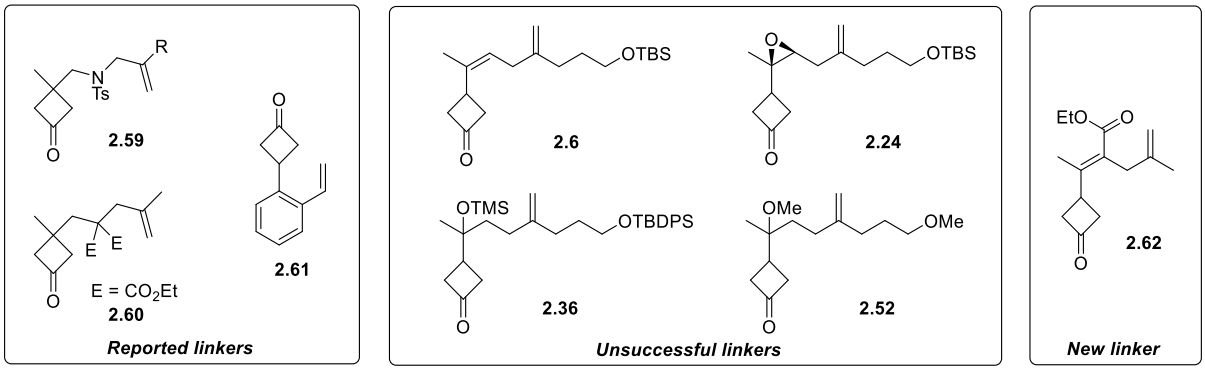


A convergent synthetic route was developed to synthesize cyclobutanone **2.62** (Scheme 2.15). On the one hand, (*E*)-enol triflate **2.65** was prepared from ethyl acetoacetate **2.63** through alkylation[14] and stereoselective enolization.[15] On the other hand, bromide **2.66** was obtained from carboxylic acid **2.37** by Hunsdiecker reaction,[16] which further protected to ketal **2.67**. Ketal **2.67** readily underwent copper-mediated coupling[17] with triflate **2.65** to give ketal **6.68** in 44% yield.

Finally, hydrolysis of ketal **2.68** provided the new substrate for "cut-and-sew" reaction, cyclobutanone **2.62** in 96% yield.

**Scheme 2.15.** Preparation of Cyclobutanone **2.62**.

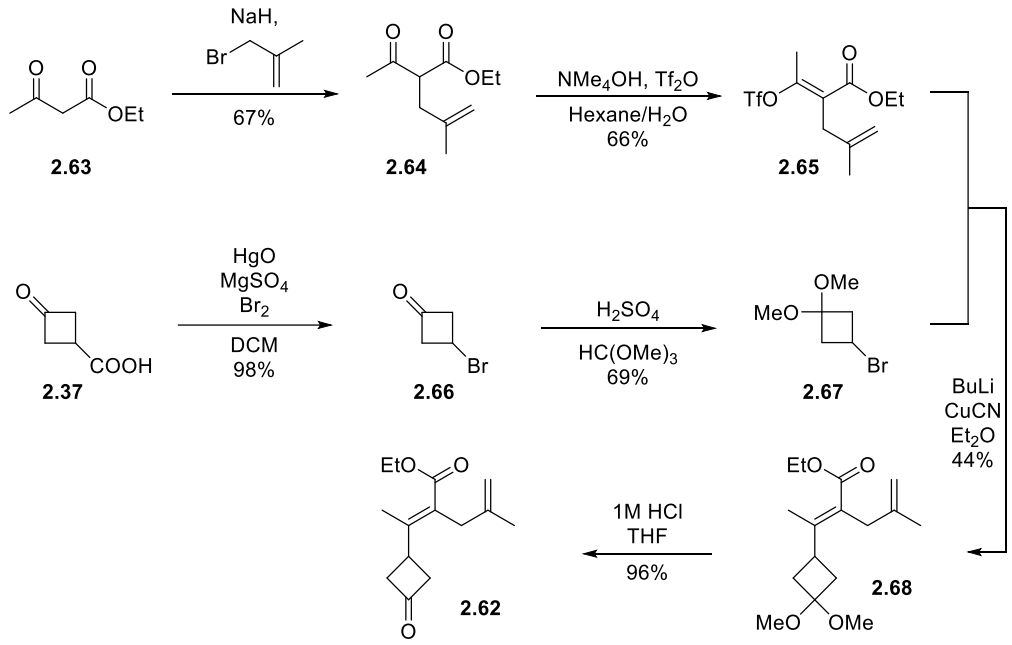


Due to the low yield of copper-mediated coupling between triflate **2.65** and bromide **2.67**, we decided to optimize the synthetic route to cyclobutanone **2.62**. Inspired by a report in literature,[18] we proposed that cyclobutanone **2.62** could be prepared by three-component coupling (Scheme 2.16). Bromide **2.67** was treated with $^{t}$BuLi to give alkyl lithium **2.69**, which underwent transmetalation with copper(I) salt to generate alkyl cuprate **2.70**. Cuprate **2.70** was readily inserted into ynoate **2.71** to deliver vinyl cuprate **2.72**, which was captured by methallyl bromide to give ketal **2.68**. Further deprotection of ketal **2.68** delivered cyclobutanone **2.62** (see scheme 2.15 for detail). 48% yield of ketal **2.68** was obtained after adjusting the reaction temperature, equivalence of regents and copper catalyst. The three-component coupling reaction enabled 4-step

synthesis of cyclobutanone **2.62**, in stead of 6 total steps in previous route. The new strategy also avoided the usage of highly toxic CuCN, and delivered higher yield of cyclobutanone **2.62**.

**Scheme 2.16.** Preparation of Ketal **2.68** through Three-Components Coupling.

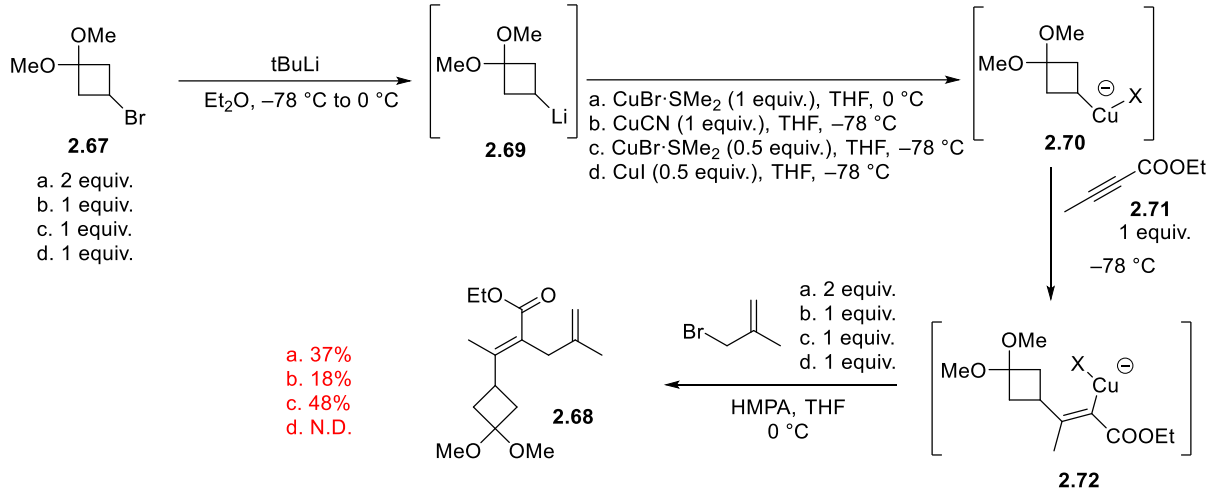


After successful preparation of cyclobutanone **2.62**, we started to explore the "cut-and-sew" reaction on this substrate. We first employ the reported condition,[11] which gave no reaction. Crude screening of ligands also did not provide any promising results (Table 2.16). However, we obtained the desired "cut-and-sew" product in 15% yield by increasing the temperature to 170 °C (Table 2.17).

**Table 2.16.** Initial Screening on "Cut-and-Sew" Reaction of Cyclobutanone **2.62**.

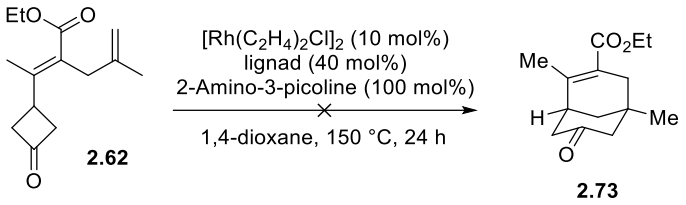


| Entry | Ligand | Result |
|---|---|---|
| 1 | $PPh_3$ | N.D. |
| 2 | $P(C_6F_5)_3$ | N.R. |
| 3 | $P(4\text{-}C_6H_4CF_3)_3$ | N.D. |
| 4 | TFP | N.D. |
| 5 | $P(3,5\text{-}C_6H_3(CF_3)_2)_3$ | N.R. |

**Table 2.17.** Temperature Screening on "Cut-and-Sew" Reaction of Cyclobutanone **2.62**.

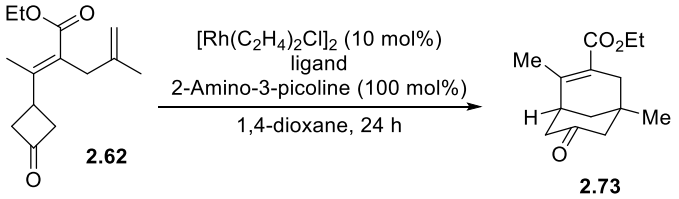


| Entry | Ligand | Temperature | Result |
|---|---|---|---|
| 1 | $P(3,5\text{-}C_6H_3(CF_3)_2)_3$ (20 mol%) | 160 °C | N.R. |
| 2 | $P(3,5\text{-}C_6H_3(CF_3)_2)_3$ (40 mol%) | 160 °C | N.R. |
| 3 | $P(3,5\text{-}C_6H_3(CF_3)_2)_3$ (20 mol%) | 170 °C | low conversion |
| 4 | $P(3,5\text{-}C_6H_3(CF_3)_2)_3$ (40 mol%) | 170 °C | 16% (27% SM) |

After confirming the structure of the "cut-and-sew" product, we started to optimize the reaction conditions. Screening of some electron-deficient ligands and Buchward ligands shown that the original used ligand ($P(3,5\text{-}C_6H_3(CF_3)_2)_3$) provided the highest yield (Table 2.18). Meanwhile, tri(2-furyl)phosphine also delivered the "cut-and-sew" product, but in a lower yield (entry 4, Table 2.18). Screening of the catalysts revealed that rhodium ethylene chloride is the optimized for this reaction (Table 2.19).

**Table 2.18.** Ligand Screening on "Cut-and-Sew" Reaction of Cyclobutanone **2.62**.

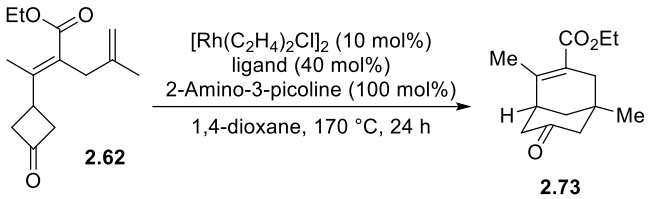


| Entry | Ligand | Yield |
|---|---|---|
| 1 | $P(3,5\text{-}C_6H_3(CF_3)_2)_3$ | 15% |
| 2 | $P(C_6F_5)_3$ | trace |
| 3 | $P(4\text{-}C_6H_4CF_3)_3$ | trace |
| 4 | TFP | <10% |
| 5 | $AsPh_3$ | trace |
| 6 | $PPh_2(C_6F_5)$ | trace |
| 7 | $P(OPh)_3$ | trace |
| 8 | SPhos | trace |
| 9 | XPhos | trace |

**Table 2.19.** Catalysts Screening on "Cut-and-Sew" Reaction of Cyclobutanone **2.62**.

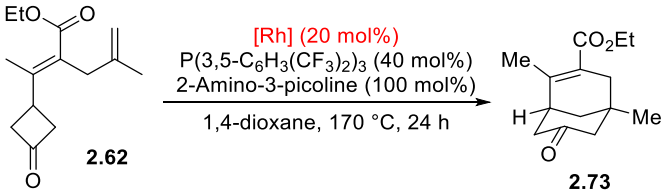


| Entry | [Rh] | Yield |
|---|---|---|
| 1 | $[Rh(COD)Cl]_2$ | trace |
| 2 | $[Rh(COE)_2Cl]_2$ | trace |
| 3 | $[Rh(C_2H_4)_2Cl]_2$ | trace |
| 4 | $[Rh(CO)_2Cl]_2$ | 11% (35% S.M.) |
| 5 | $[Rh(COD)OH]_2$ | trace |
| 6 | $[Rh(COD)_2]BF_4$ | trace |

The solvent effect was also explored for this reaction (Table 2.20). 1,4-dioxane, toluene, chlorobenzene and xylene all could deliver desired cyclized product. Among the solvents, chlorobenzene gave highest yield, but had a lower recovery of the starting materials. Since the mass balance of the "cut-and-sew" reaction under 170 °C is pretty low, we screened different

solvents at 150 °C (Table 2.21). Some aromatic solvents delivered the desired product 2.73 in low yield at 150 °C, including chlorobenzene, toluene, benzene and hexafluorobenzene. Among all these solvents, toluene gave the best BRSM yield, which was chosen as the standard solvent for the further condition screening.

**Table 2.20.** Solvent Screening on "Cut-and-Sew" Reaction of Cyclobutanone **2.62**.

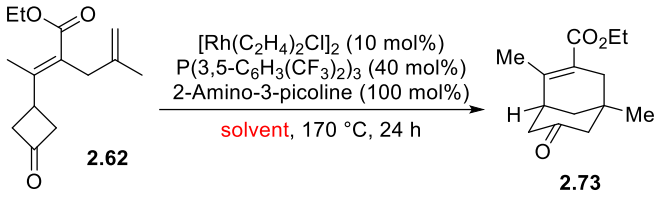


| Entry | Solvent | Yield |
|---|---|---|
| 1 | 1,4-dioxane | 16% (27% S.M.) |
| 2 | PhCl | 22% (15% S.M.) |
| 3 | toluene | 13% (43% S.M.) |
| 4 | xylene | 11% (0% S.M.) |
| 5 | DMF | trace |
| 6 | DMSO | trace |

**Table 2.21.** Solvent Screening on "Cut-and-Sew" Reaction of Cyclobutanone **2.62** (150 °C).

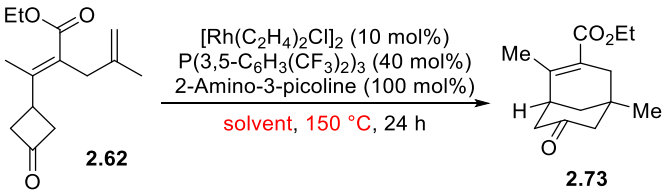


| Entry | Solvent | Yield |
|---|---|---|
| 1 | PhCl | 8% (47% S.M.) |
| 2 | toluene | 6% (80% S.M.) |
| 3 | DME | trace |
| 4 | benzene | 12% (14% S.M.) |
| 5 | $C_6F_6$ | 17% (15% S.M.) |
| 6 | PhF | trace |
| 7 | 1,2-difluorobenzene | trace |
| 8 | $PhCF_3$ | trace |
| 9 | 1,4-dioxane | trace |

Besides neutral rhodium, we also screening many conditions with cationic rhodium as catalyst. However, after testing diverse types of monodentate and bidentate ligands, no desired product was detected (Table 2.22). In most cases the starting material was decomposed with cationic rhodium catalyst. We tried to reduce reaction temperature to suppress decomposition, but the desired product was still not detected when the reaction temperature was decreased to 130 °C (Table 2.23).

**Table 2.22.** Ligands Screening on "Cut-and-Sew" Reaction of Cyclobutanone **2.62** (Cationic Rhodium).

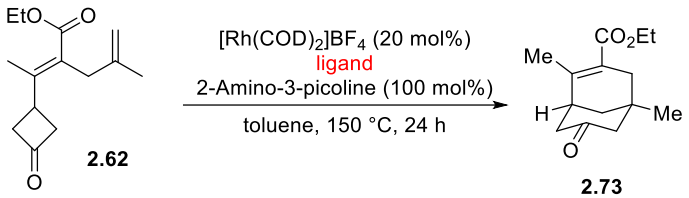


| Entry | Ligand | Yield | Entry | Ligand | Yield |
|---|---|---|---|---|---|
| 1 | SPhos (20 mol%) | N.D. | 11 | dfppe (20 mol%) | N.D. |
| 2 | XPhos (20 mol%) | N.D. | 12 | dppf (20 mol%) | N.D. |
| 3 | QPhos (20 mol%) | N.D. | 13 | BINAP (20 mol%) | N.D. |
| 4 | COD (40 mol%) | N.D. | 14 | dppbz (20 mol%) | trace |
| 5 | $PPh_3$ (40 mol%) | trace | 15 | DPEPhos (20 mol%) | trace |
| 6 | $P(2,4,6\text{-}C_6H_2(OMe)_3)_3$ (40 mol%) | N.D. | 16 | XantPhos (20 mol%) | N.D. |
| 7 | dppm (20 mol%) | N.D. | 17 | DTBM-SEGPhos (20 mol%) | N.D. |
| 8 | dppe (20 mol%) | N.D. | 18 | dCypm (20 mol%) | N.D. |
| 9 | dppp (20 mol%) | N.D. | 19 | dCype (20 mol%) | N.D. |
| 10 | dppb (20 mol%) | trace | 20 | dCypb (20 mol%) | N.D. |

**Table 2.23.** Ligands Screening on "Cut-and-Sew" Reaction of Cyclobutanone **2.62** (Cationic Rhodium, 130 °C).

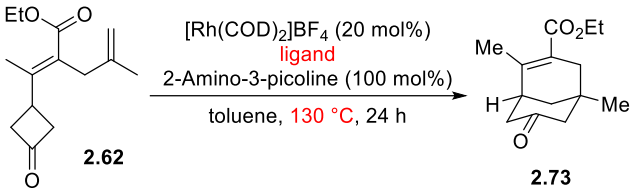


| Entry | Ligand | Yield |
|---|---|---|
| 1 | $PPh_3$ (20 mol%) | N.D. |
| 2 | dppb (20 mol%) | N.D. |
| 3 | dppbz (20 mol%) | N.D. |
| 4 | DPEPhos (40 mol%) | N.D. |

After screening the ligands for the cationic rhodium catalyst, our attention turned to the X ligand of rhodium, which could be prepared from the reaction between rhodium chloride and relative silver salts (Table 2.24). The rhodium acetylacetonate was found to be a promising catalyst for the "cut-and-sew" reaction of compound **2.62**, which delivered 14% yield of ketone **2.73** as well as 72% of cyclobutanone **2.62** recovery (entry 5, Table 2.24).

**Table 2.24.** Additives Screening on "Cut-and-Sew" Reaction of Cyclobutanone **2.62**.

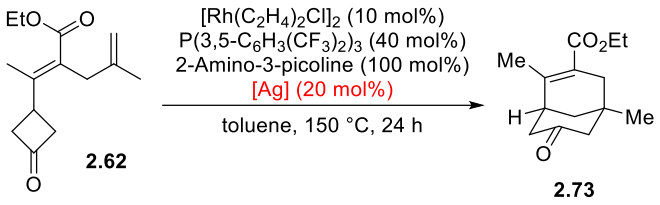


| Entry | [Ag] | Yield |
|---|---|---|
| 1 | AgOAc | N.D. |
| 2 | AgOBz | N.D. |
| 3 | Ag(TFA) | N.D. |
| 4 | Ag(lactate) | N.D. |
| 5 | Ag(acac) | 14% (72% SM) |
| 6 | Ag(TMHD) | N.D. |
| 7 | Ag(COD)(acac-$F_6$) | 10% (21% SM) |

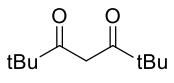

TMHD

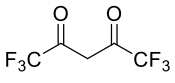

acac-$F_6$

As a brief summary at this stage, we have explored the linker effect in "cut-and-sew" reaction. Compared to benzocyclobutenones, intramolecular [4+2] cycloaddition with saturated cyclobutanones are generally more challenging due to (i) competing decarbonylation to form cyclopropanes and (ii) lack of rigid scaffolds to promote cyclization. Clearly, the linkers between cyclobutanones and olefins play a critical role in the "cut-and-sew" reaction, as they can provide favorable conformations for the desired cyclization. To date, only three kinds of linkers including benzo-, amide- and malonate-based ones (**Lk1**−**3**) have been succeeded in this type of annulation reactions (Scheme 2.17). A strong Thorpe-Ingold effect appears to be important for bridged-ring formation. In the context of penicibilaene synthesis, a number of carbon-based linkers were attempted in the proposed "cut-and-sew" reaction. Using the native trisubstituted alkene as the linker (**Lk4**), the olefin moiety proved to be labile and tended to isomerize under the reaction conditions. "Masked" alkenes, such as epoxide (**Lk5**), tertiary alcohol (**Lk6**) and ether (**Lk7**), were

also prepared; however, they proven to be either unstable or inactive for cyclization. Finally, the ester substituted alkenyl linker (**Lk8**) was found to be ideal. The conjugation and the electron-withdrawing feature of the ester moiety inhibited double-bond migration. The enhanced rigidity of the tetrasubstituted alkene and the buttressing effect between the methyl and the ester groups are expected to be factors that benefit the cyclization. More importantly, with the ester moiety, synthesis of the "cut-and-sew" precursor became much simpler.

**Scheme 2.17.** Linker Effect in the "cut-and-sew" reaction.

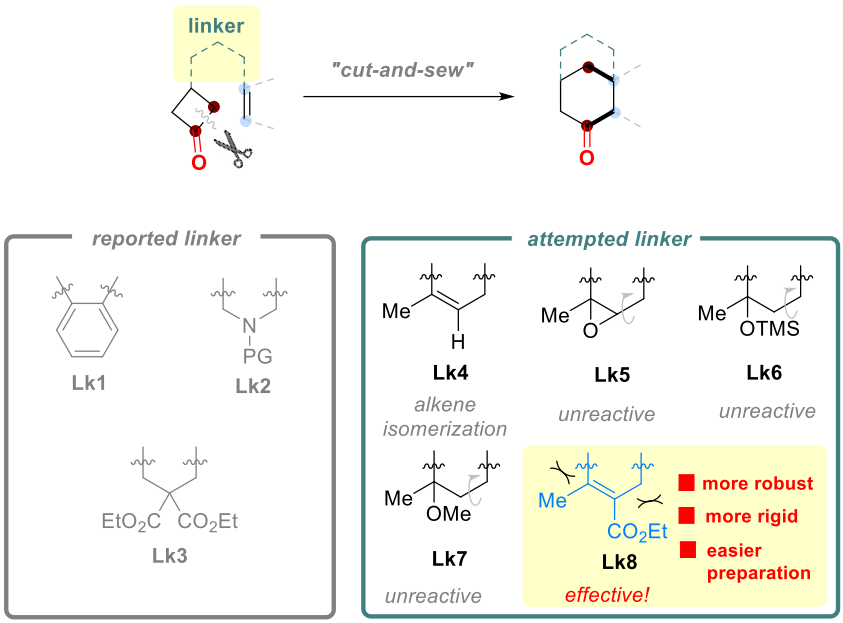


Encouraged by the promising preliminary result in model study, we then moved to synthesize of real substrate cyclobutanone **2.75**, which contained a ester linker (Scheme 2.18). Following the reported procedure,[19] silane **2.77** was prepared dibromide **2.76** through hydrosilylation and elimination (Scheme 2.19). Michael addition of methyl crotonate by Grignard reagent prepared from bromide **2.77** furnished ester **2.78**,[20] which was reduced by $LiAlH_4$ and protected by TBS to give silane **2.80**. Bromination of silane **2.80** by NBS delivered bromide **2.81**.[21] Finally,

cyclobutanone **2.75** was prepared via a three-component coupling among bromide **2.67**, ynoate **2.71** and bromide **2.81** followed by acid deprotection.

**Scheme 2.18.** Proposed Retrosynthetic Analysis Enabled by "Cut-and-Sew" Reaction of Ester Tethered Cyclobutanone.

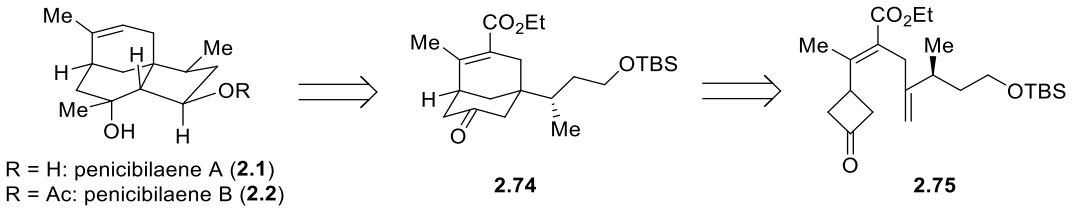


**Scheme 2.19.** Preparation of Cyclobutanone **2.75**.

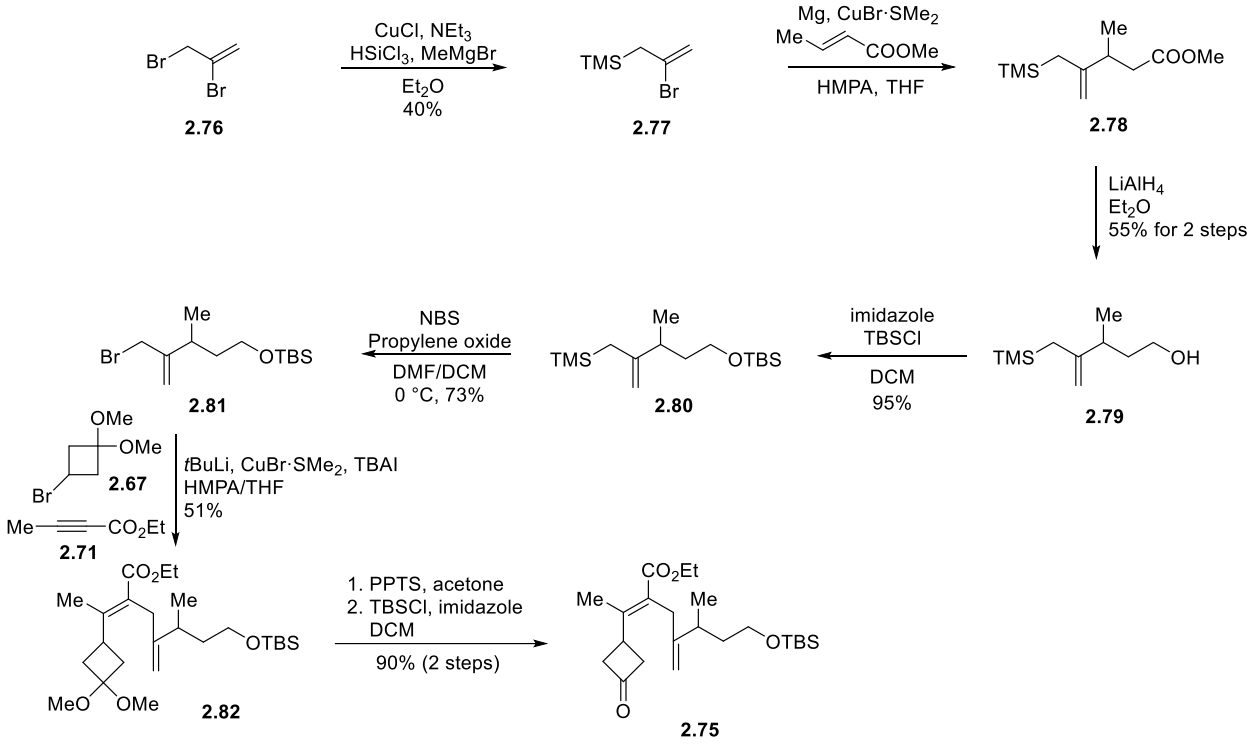


With cyclobutanone **2.75** in hand, we started to explore the "cut-and-sew" reaction based on this substrate. However, after trying all the conditions that worked for model substrate, we found that none of them delivered the desired cyclohexanone **2.74** (Table 2.25).

**Table 2.25.** Attempts on "Cut-and-Sew" Reaction of Cyclobutanone **2.75**.

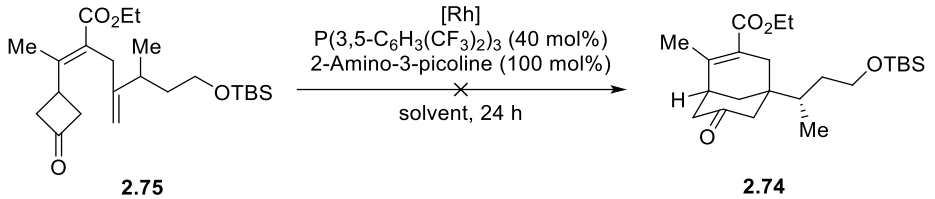


**2.75** **2.74**

| Entry | [Rh] | Solvent | Temperature | Result |
|---|---|---|---|---|
| 1 | $[Rh(C_2H_4)_2Cl]_2$ (10 mol%) | 1,4-dioxane | 170 °C | N.D. |
| 2 | $[Rh(C_2H_4)_2Cl]_2$ (10 mol%) | PhCl | 170 °C | N.D. |
| 3 | $[Rh(C_2H_4)_2Cl]_2$ (10 mol%) + Ag(acac) (20 mol%) | toluene | 150 °C | N.D. |
| 4 | $[Rh(C_2H_4)_2Cl]_2$ (10 mol%) + Ag(acac) (20 mol%) | toluene | 160 °C | N.D. |
| 5 | $Rh(acac)(C_2H_4)_2$ (20 mol%) | toluene | 160 °C | N.D. |

Comparing the real substrate cyclobutanone **2.75** and the model substrate cyclobutanone **2.62**, we proposed that the key factor to affect their reactivities is the steric hindrance of the alkene moiety. The tertiary carbon attached to alkene in cyclobutanone **2.75** was too bulky for the "cut-and-sew" reaction. Thus, we proposed to introduce the methyl group on the five-membered ring of penicibilaenes after "cut-and-sew" step. To test our hypothesis, cyclobutanone **2.91** was synthesized (Scheme 2.20). Protection of alcohol **2.83** by TBS gave iodide **2.84**, which was attacked by alcohol **2.85** to deliver allyl alcohol **2.86**.[22] Two-step bromination[22a] of alcohol **2.86** furnished bromide **2.89** along with deprotected bromide **2.88**, which could be reprotected to bromide **2.89**. Finally, three-component coupling of bromide **2.67**, ynoate **2.71** and bromide **2.89** following by deprotection accomplished cyclobutanone **2.91**. However, the "cut-and-sew" reaction still did not work on cyclobutanone **2.91** under standard conditions (Table 2.26).

**Scheme 2.20.** Preparation of Cyclobutanone **2.91**.

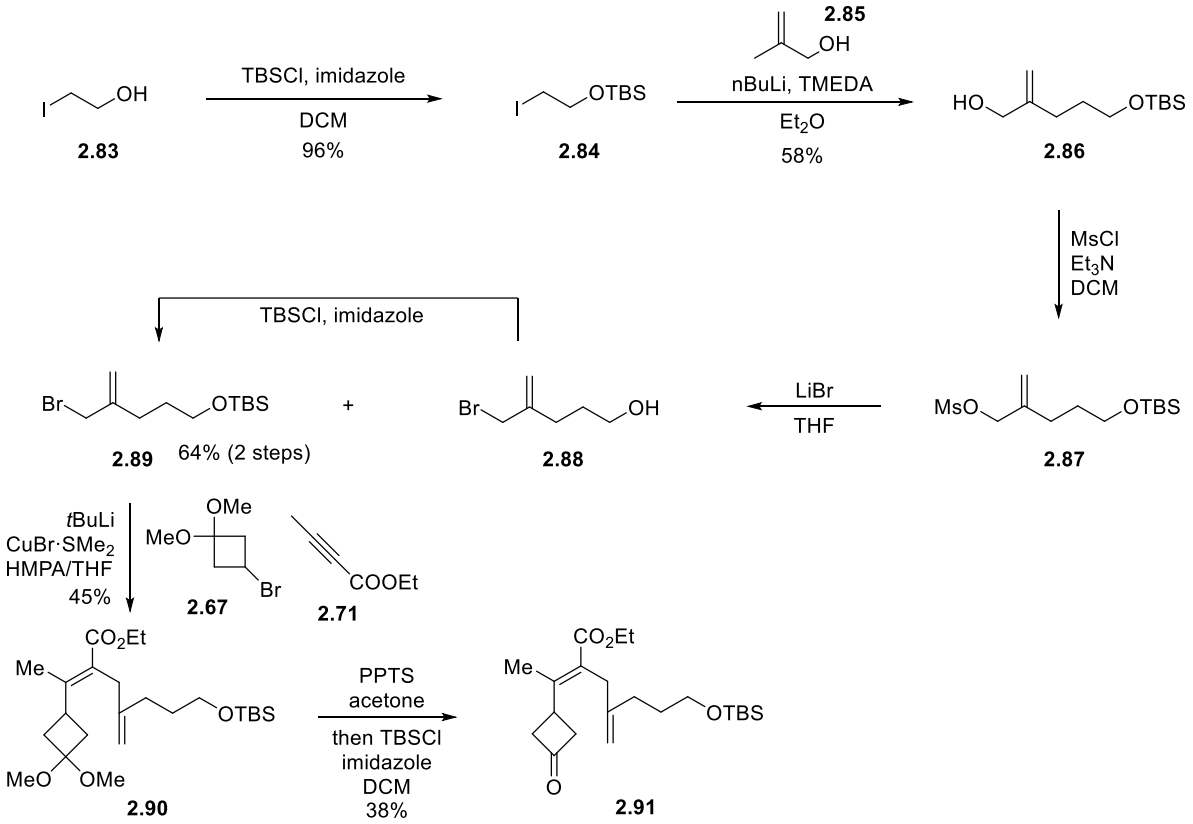


**Table 2.26.** Attempts on "Cut-and-Sew" Reaction of Cyclobutanone **2.91**.

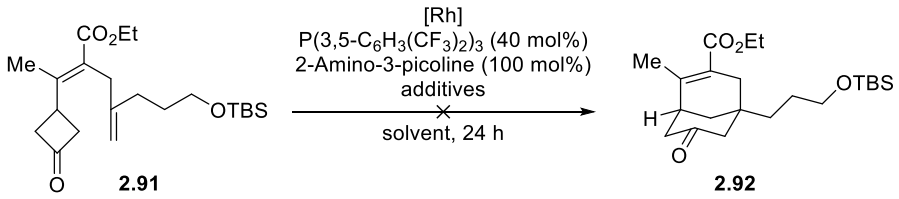


| Entry | [Rh] | Solvent | Temperature | Result |
|---|---|---|---|---|
| 1 | $[Rh(C_2H_4)_2Cl]_2$ (10 mol%) | 1,4-dioxane | 170 °C | N.D. |
| 2 | $[Rh(C_2H_4)_2Cl]_2$ (10 mol%) + Ag(acac) (20 mol%) | toluene | 150 °C | N.D. |

## 2.3. Second Generation Route

The failure of the "cut-and-sew" reaction on the real substrates cyclobutanone **2.75** and **2.91** pushes us to make some change on the synthetic route. Although trisubstituted alkenes are generally more challenging substrates for "cut-and-sew" reaction comparing with mono- or di-substituted alkene, the "cut-and-sew" reaction on cyclic alkene is less explored. Due to the internal ring strain (5.9 kcal/mol for cyclopentene),[23] cyclic alkene is proposed to be more reactive than linear alkene, which inspires us to design a "cut-and-sew" reaction between cyclobutanone and cyclopentene (Scheme 2.21). The "cut-and-sew" reaction in the second generation strategy constructs the all there rings in the natural product in a diastereoselective manner, which enables a more efficient way to synthesize penicibilaenes.

**Scheme 2.21.** The Second Generation Strategy to Synthesize Penicibilaenes.

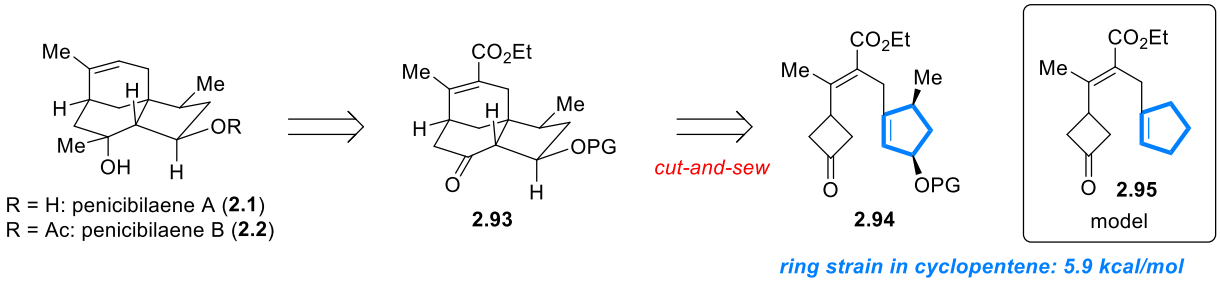


To test our hypothesis, cyclobutanone **2.95** was chosen as the model. Synthesis of cyclobutanone **2.95** was straightforward using three-component coupling method (Scheme 2.22). Ester **2.96** was treated with DIBAL-H and then $Br_2/PPh_3$ to deliver bromide **2.97**. Then the three-component coupling of bromide **2.67**, ynoate **2.71** and bromide **2.97** gave ketal **2.98**, which was further deprotected to afford cyclobutanone **2.95**.

**Scheme 2.22.** Preparation of Cyclobutanone **2.95**.

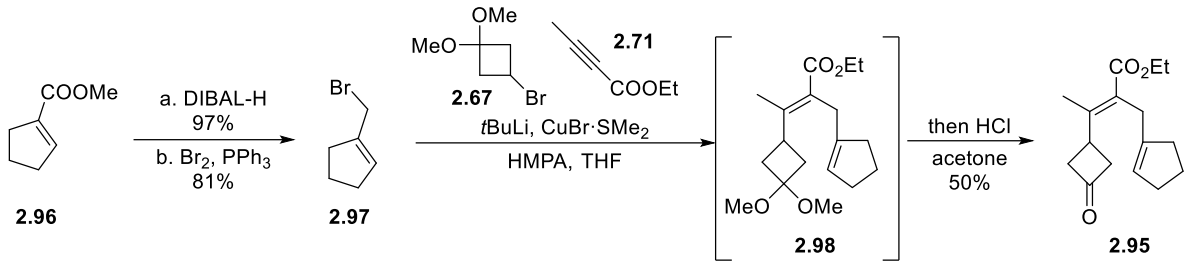


With cyclobutanone **2.95** in hand, we started to explore the "cut-and-sew" reaction of the new model (Table 2.27). Unfortunately, no desired product was detected under previous standard conditions (entry 1-5, Table 2.27). To our surprise, when $ZnCl_2$ was added into the reaction system, the desired product compound **2.99** was isolated in 12% to 13% yield (entry 6-7, Table 2.27). It was the first time to find that Lewis acid can promote "cut-and-sew" reaction between cyclobutanone and alkene. We proposed the roles of Lewis acid in this reaction are three folds: (i) Lewis acid could promote condensation between cyclobutanone and directing group, amino pyridine; (ii) Lewis acid could bind to the imine, which made α-C−C bond to be more electron-deficient and facilitate oxidative addition step; (iii) Lewis acid could help dissociation of phosphine ligand, which promoted migratory insertion step.

**Table 2.27.** "Cut-and-Sew" Reaction of Cyclobutanone **2.95**.

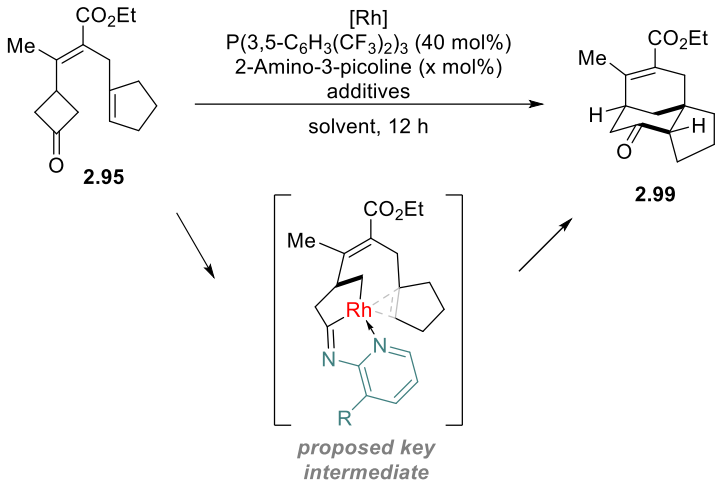


| Entry | [Rh] | Solvent | x mol% | additive | Temperature | Result |
|---|---|---|---|---|---|---|
| 1 | $[Rh(C_2H_4)_2Cl]_2$ (10 mol%) | 1,4-dioxane | 100 | / | 170 °C | N.D. |
| 2 | $[Rh(C_2H_4)_2Cl]_2$ (10 mol%) + Ag(acac) (20 mol%) | toluene | 100 | / | 150 °C | N.D. |
| 3 | $[Rh(C_2H_4)_2Cl]_2$ (10 mol%) | 1,4-dioxane | 20 | / | 170 °C | N.D. |
| 4 | $[Rh(C_2H_4)_2Cl]_2$ (10 mol%) + Ag(acac) (20 mol%) | toluene | 20 | / | 150 °C | N.D. |
| 5 | $[Rh(COD)Cl]_2$ (10 mol%) | 1,4-dioxane | 100 | / | 170 °C | N.D. |
| 6 | $[Rh(C_2H_4)_2Cl]_2$ (10 mol%) | 1,4-dioxane | 100 | $ZnCl_2$ (1 equiv.) | 170 °C | 13% |
| 7 | $[Rh(C_2H_4)_2Cl]_2$ (10 mol%) | 1,4-dioxane | 100 | $ZnCl_2$ (1 equiv.) | 150 °C | 12% (35% SM) |
| 8 | $[Rh(C_2H_4)_2Cl]_2$ (10 mol%) | 1,4-dioxane | 100 | $ZnCl_2$ (1 equiv.) | 130 °C | N.D. |

Due to the important role of Lewis acid in our "cut-and-sew" reaction, we screened more Lewis acid (Table 2.28). Only several Lewis acid delivered the desired product, and zinc triflate gave the highest yield (20%) among all the Lewis acid we screened (entry 5, Table 2.28).

**Table 2.28.** Lewis Acid Screening on "Cut-and-Sew" Reaction of Cyclobutanone **2.95**.

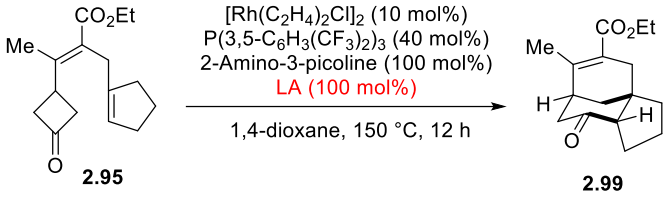


| Entry | LA | Yield |
|---|---|---|
| 1 | $CoCl_2$ | 15% (20% SM) |
| 2 | $CoBr_2$ | 14% (20% SM) |
| 3 | $Ni(OTf)_2$ | 7% (33% SM) |
| 4 | $ZnI_2$ | 8% (17% SM) |
| 5 | $Zn(OTf)_2$ | 20% (21% SM) |
| 6 | $Dy(OTf)_3$ | 6% (40% SM) |
| 7 | $Er(OTf)_3$ | 7% (37% SM) |

| | | | | | | | |
|---|---|---|---|---|---|---|---|
| LiOTf | $MgBr_2$•$OEt_2$ | $TiCl_4$ | $Cr(acac)_3$ | $Co(acac)_2$ | $AuCl_3$ | $AlCl_3$ | $CeCl_3$ |
| Li(acac) | $Mg(OTf)_2$ | $Ti(OiPr)_4$ | $MnCl_2$ | $NiCl_2$ | $ZnF_2$ | $In(OTf)_3$ | $Ce(OTf)_3$ |
| LiCl | $MgSO_4$ | $ZrF_4$ | $FeCl_3$ | $Ni(acac)_2$ | $ZnCl_2$•TMEDA | $InCl_3$ | $Pr(OTf)_3$ |
| LiBr | $Ca(OTf)_2$ | $ZrCl_4$•$^2$THF | $Fe(acac)_3$ | $CuCl_2$ | $Zn(OAc)_2$ | $BiCl_3$ | $Sm(OTf)_3$ |
| LiI | $CaCl_2$ | $Hf(acac)_4$ | $CoF_2$ | $Cu(OTf)_2$ | $B(OH)_3$ | $Bi(OTf)_3$ | $Eu(OTf)_3$ |
| $MgCl_2$ | $Sc(OTf)_3$ | $Cr(OAc)_3$ | $Co(OTf)_2$ | CuOTf | $BF_3$•$OEt_2$ | $La(OTf)_3$ | $Yb(OTf)_3$ |

**N.D. or trace**

To exclude the possibility that this reaction was catalyzed by acid rather than rhodium, some control experiments were conducted (Table 2.29). No desired product was detected without rhodium catalyst, directing group or ligand (entry 2-4, Table 2.29), which prove the key role of the rhodium catalyst. It also shown that the "cut-and-sew" reaction is not very sensitive to water. With the presence of 1 equivalent of water, the yield does not drop (entry 6, Table 2.29).

**Table 2.29.** Control Experiments on "Cut-and-Sew" Reaction of Cyclobutanone **2.95**.

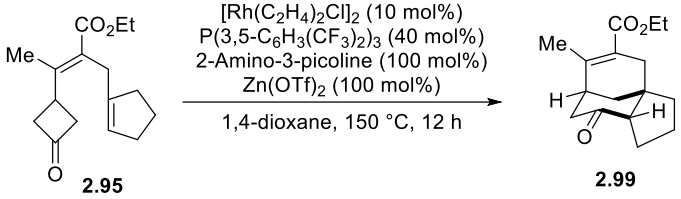


| Entry | conditions | yield |
|---|---|---|
| 1 | as above | 18% (17% SM) |
| 2 | w/o [Rh] | N.D. (85% SM) |
| 3 | w/o DG | N.D. (63% SM) |
| 4 | w/o ligand | N.D. (50% SM) |
| 5 | SPS dioxane | 18% (21% SM) |
| 6 | +1 equiv. $H_2O$ | 18% (26% SM) |

After confirming our "cut-and-sew" reaction was catalyzed by rhodium, we continued to optimize the reaction yield. We found that the yield and substrate recovery increased when the equivalence of the directing groups decreased (Table 2.30). As aniline derivatives, the amino pyridine directing groups not only could promote "cut-and-sew" reaction, but also cause some side reactions, such as aldol reaction. Decreasing the equivalence of directing groups may inhibit such side reactions. Since there are still some substrate remained after 12 hours, we tried to prolong the reaction time to increase the conversion (Table 2.31). The yield of the "cut-and-sew" reaction reached to 34% with 0.2 equivalent of directing groups after 48 hours (entry 6, Table 2.31).

**Table 2.30.** Directing Group Equivalence Screening on "Cut-and-Sew" Reaction of Cyclobutanone **2.95**.

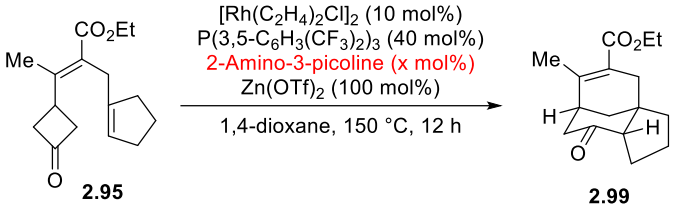


| Entry | x mol% | GC yield |
|---|---|---|
| 1 | 100 | 16% (14% SM) |
| 2 | 80 | 16% (14% SM) |
| 3 | 60 | 25% (18% SM) |
| 4 | 40 | 28% (24% SM) |
| 5 | 20 | 23% (35% SM) |

**Table 2.31.** Directing Group Equivalence and Reaction Time Screening on "Cut-and-Sew" Reaction of Cyclobutanone **2.95**.

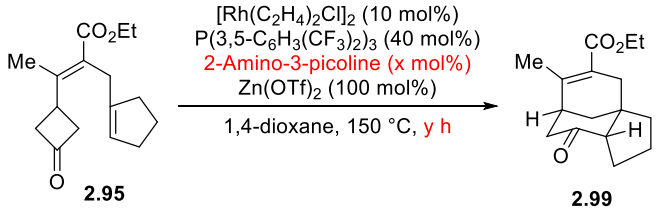


| Entry | x mol% | y h | GC yield |
|---|---|---|---|
| 1 | 40 | 12 | 21% (19% SM) |
| 2 | 20 | 12 | 24% (30% SM) |
| 3 | 40 | 24 | 22% (14% SM) |
| 4 | 20 | 24 | 26% (26% SM) |
| 5 | 40 | 48 | 29% (trace SM) |
| 6 | 20 | 48 | 34% (14% SM) |

After screening of the directing group equivalence, we moved to screen the species of the directing groups (Table 2.32). The structure of the directing groups had significant influence on the yield. By increasing the size of the 3-substituent on the directing group, the yield was enhanced accordingly. It is possible that, like the linker effect, the larger steric on the DG can provide a

more conformationally rigid intermediate that would be beneficial for the cyclization. However, further increasing the bulkiness on the C3 of DG, such as using 2-amino-3-trimethylsilylpyridine (**DG4**), only gave a trace amount of the product. Unlike the substituent on the C3 of DG, the substituent on the C5 position of DG inhibit the reactivity, which may due to larger bulkiness on C5 of DG inhibited rhodium catalyst coordination.

**Table 2.32.** Directing Group Screening on "Cut-and-Sew" Reaction of Cyclobutanone **2.95**.

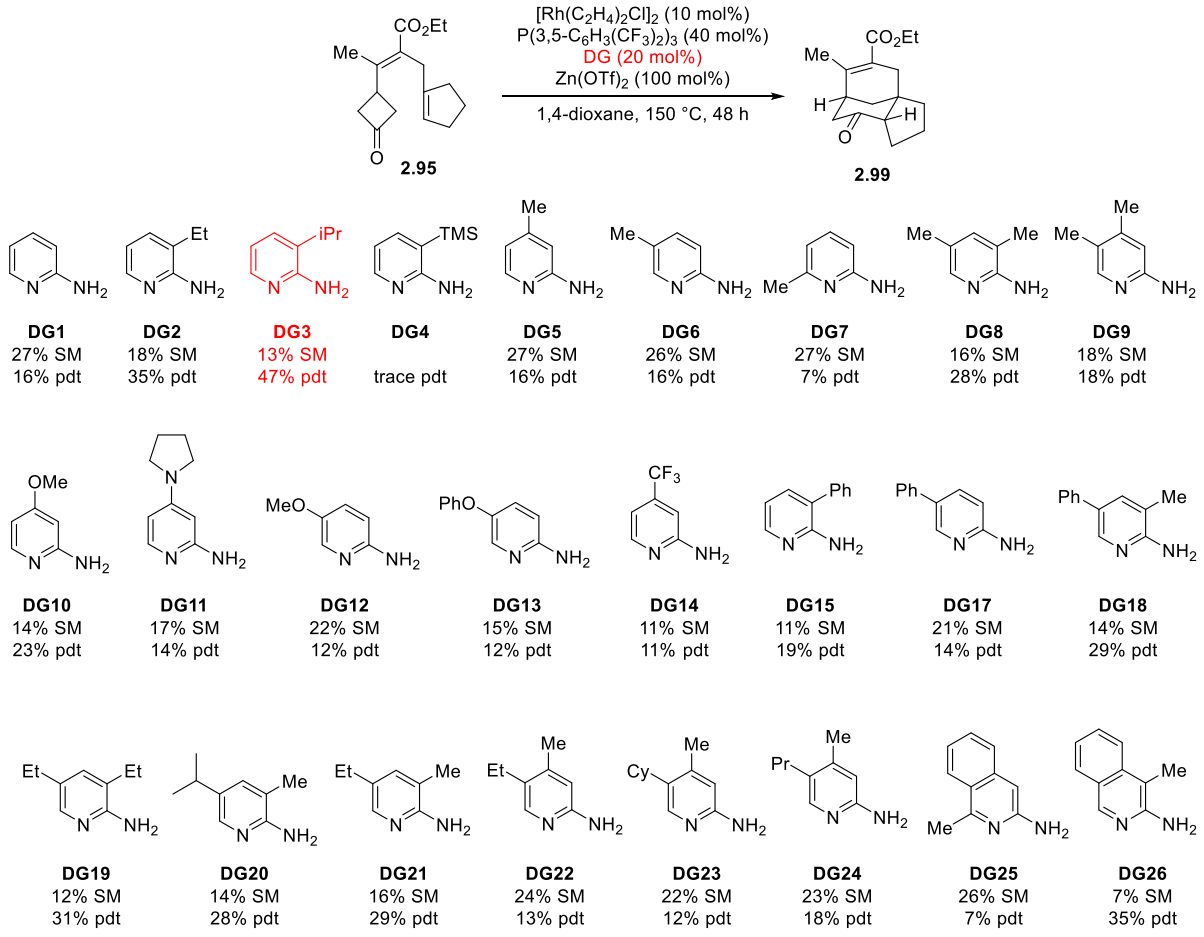


Besides Lewis acid, we also tested Brønsted acid on our "cut-and-sew" reaction. However, the typical Brønsted acids were failed to deliver any desired product (Table 2.33).

**Table 2.33.** Brønsted Acid Screening on "Cut-and-Sew" Reaction of Cyclobutanone **2.95**.

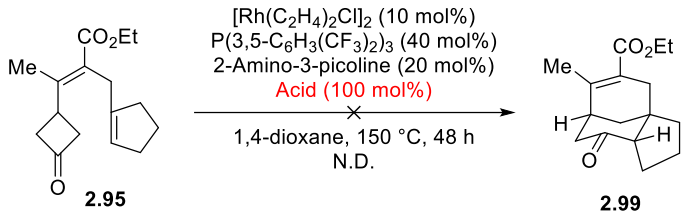


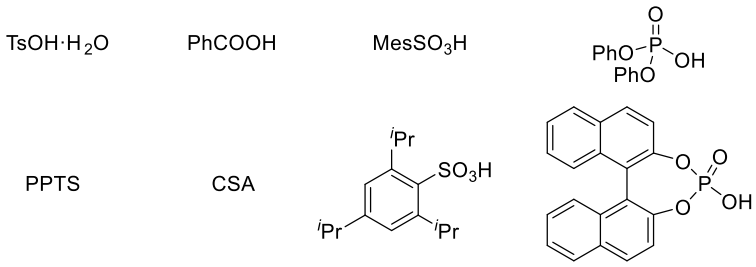


After screening different concentrations, we found that our "cut-and-sew" reaction is not sensitive to the concentration (Table 2.34). Both higher or lower concentrations than 0.1 M slightly decrease the yield. Besides concentration, we also screened different solvents (Table 2.35). The aromatic solvents generally were able to provide higher conversion comparing to 1,4-diaoxane. And the toluene gave the highest yield among these solvents (entry 2, table 2.35). Since aromatic solvents gave excellent conversion, we hope to suppress the side reactions and increase the yield by decreasing the reaction temperature (Table 2.36) or the loading of the catalyst (Table 2.37). However, although the mass balance become better under these conditions, the yields were dropped.

**Table 2.34.** Concentration Screening on "Cut-and-Sew" Reaction of Cyclobutanone **2.95**.

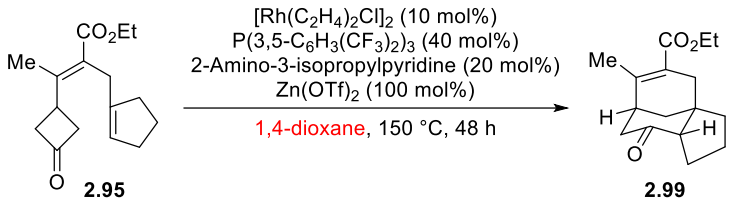


| Entry | Concentration | GC yield |
|---|---|---|
| 1 | 0.2 M | 39% (8% SM) |
| 2 | 0.1 M | 43% (17% SM) |
| 3 | 0.05 M | 40% (23% SM) |

**Table 2.35.** Solvent Screening on "Cut-and-Sew" Reaction of Cyclobutanone **2.95**.

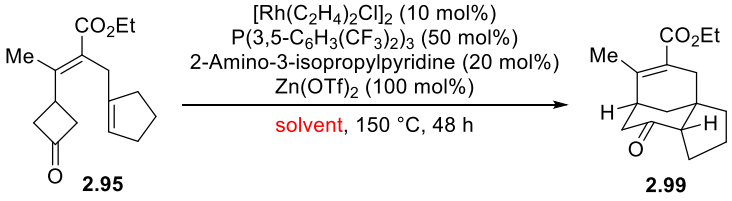


| Entry | solvent | GC yield |
|---|---|---|
| 1 | 1,4-dioxane | 39% (15% SM) |
| 2 | toluene | 48% (0% SM) |
| 3 | PhCl | 34% (0% sm) |
| 4 | PhF | 40% (0% SM) |
| 5 | 1,2-$C_6H_4F_2$ | 29% (0% SM) |
| 6 | 1,3-$C_6H_4F_2$ | 47% (0% SM) |
| 7 | 1,4-$C_6H_4F_2$ | 38% (0% SM) |
| 8 | $C_6F_6$ | 18% (0% SM) |

**Table 2.36.** Solvent Screening on "Cut-and-Sew" Reaction of Cyclobutanone **2.95** (140 °C).

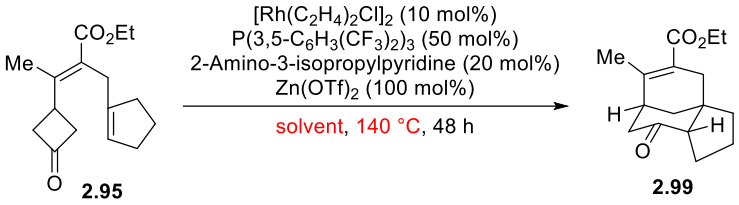


| Entry | solvent | GC yield |
|---|---|---|
| 1 | toluene | 38% (20% SM) |
| 2 | PhCl | 20% (22% SM) |
| 3 | PhF | 30% (26% sm) |
| 4 | 1,3-$C_6H_4F_2$ | 31% (23% SM) |
| 5 | 1,4-$C_6H_4F_2$ | 36% (35% SM) |

**Table 2.37.** Solvent Screening on "Cut-and-Sew" Reaction of Cyclobutanone **2.95** (5 mol% catalyst loading).

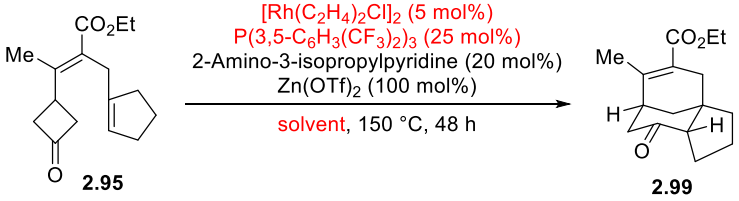


| Entry | solvent | GC yield |
|---|---|---|
| 1 | toluene | 44% (23% SM) |
| 2 | PhCl | 31% (20% SM) |
| 3 | PhF | 28% (37% sm) |
| 4 | 1,3-$C_6H_4F_2$ | 40% (33% SM) |
| 5 | 1,4-$C_6H_4F_2$ | 35% (43% SM) |

With the presence of the 2,6-di-*tert*-butylpyridine as a buffer, the gram-scale "cut-and-sew" reaction of cyclobutanone **2.95** was realized in 42% yield, which paved the way for the further synthesis (Scheme 2.22).

**Scheme 2.23.** Gram-Scale "Cut-and-Sew" Reaction of Cyclobutanone **2.95**.

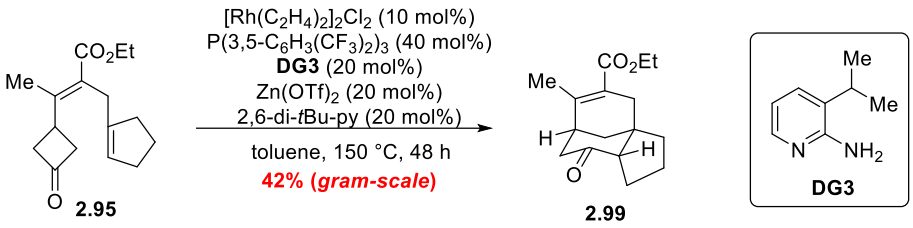


Besides cyclopentenyl moiety, mono- and 1,1-disubstituted alkenes can also be efficiently coupled to form bridged bicycles, which implied some generality of this method (entry 1-2, Table 2.38). However, cyclobutanone **2.104** contained a cyclohexene moiety only delivered trace amounts of desired product under standard condition (entry 3, Table 2.38), which possibly due to the high steric hinderance of the alkene part.

**Table 2.38.** Preliminary Substrate Scope of the "Cut-and-Sew" Reaction of Ester-Tethered Cyclobutanones.

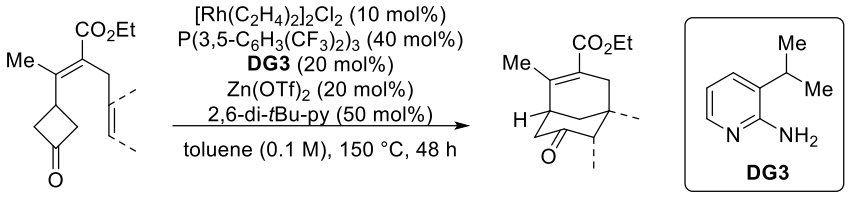


| Entry | Substrate | Product | Yield[b] |
|---|---|---|---|
| 1 | 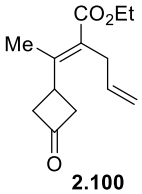 **2.100** | 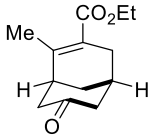 **2.101** | 85% |
| 2 | 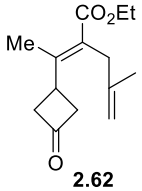 **2.62** | 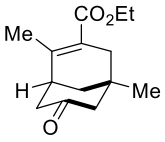 **2.73** | 64% |
| 3 | 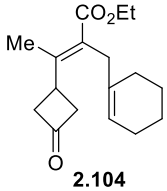 **2.104** | 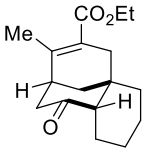 **2.105** | trace |

Encouraged by the promising result on model study, we started to synthesize the real substrate. The initial designed real substrate was cyclobutanone **2.94a**, which had both methyl and protected hydroxyl groups on the five-membered ring. Cyclobutanone **2.94a** was proposed to be synthesized from enone **2.108**, which planed to be prepared from enyne **2.107** through a Pauson-Khand reaction.[24] Enyne **2.107** was readily prepared from silyl chloride **2.106** in 21% yield. However, after trying the representative reported conditions of Pauson-Khand reaction, the best yield of

enone **2.108** we obtained is only 10% (Table 2.39). Due to the low yield of Pauson-Khand reaction on enyne **2.107**, we gave up this route.

**Table 2.39.** Preparation of Cyclobutanone **2.94a** through Pauson-Khand Reaction.

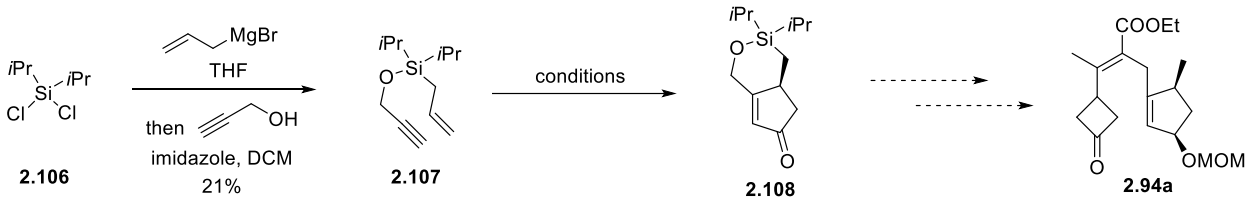


| Entry | Conditions | Result |
|---|---|---|
| 1 | $Co_2(CO)_8$ (1.1 equiv.), then NMO (10 equiv.), DCM, RT, overnight | 10% |
| 2 | $Co_2(CO)_8$ (3 mol%), TMTU (18 mol%), CO (1 atm), toluene, 70 °C, 3 h | N.D. |
| 3 | $Co_2(CO)_8$ (10 mol%), TMTU (60 mol%), CO (1 atm), toluene, 70 °C, 3 h | N.D. |
| 4 | $Co_2(CO)_8$ (10 mol%), TMTU (60 mol%), CO (1 atm), toluene, 90 °C, 3 h | N.D. |
| 5 | $Co_2(CO)_8$ (10 mol%), TMTU (60 mol%), CO (1 atm), toluene, 110 °C, 3 h | N.D. |
| 6 | $CoBr_2$ (10 mol%), TMTU (60 mol%), Zn (2 equiv.), CO (1 atm), toluene, 70 °C, 3 h | N.D. |
| 7 | $[Rh(CO)_2Cl]_2$ (2 mol%), CO (1 atm), xylene, 110 °C, 3 h | N.D. |
| 8 | $[Rh(CO)_2Cl]_2$ (2 mol%), CO (1 atm), PhCl, 150 °C, 3 h | N.D. |
| 9 | $[Rh(CO)_2Cl]_2$ (2 mol%), CO (3 atm), toluene, 150 °C, overnight | N.D. |
| 10 | $[Rh(COD)Cl]_2$ (2.5 mol%), dppp (10 mol%), cinnamaldhyde, 120 °C, 3 h | N.D. |
| 11 | $Mo(CO)_3(DMF)_3$ (1.1 equiv.), DCM, RT | N.D. |

Due to the difficulty of synthesizing cyclobutanone **2.94a**, we designed a new substrate, cyclobutanone **2.110**, for the key "cut-and-sew" reaction, which do not have methyl group on the five-membered ring (Scheme 2.24). We proposed that the methyl group on C ring could be introduced after "cut-and-sew" step.

**Scheme 2.24.** Total Synthesis of Penicibilaenes through "Cut-and-Sew" Reaction of Cyclobutanone **2.110**.

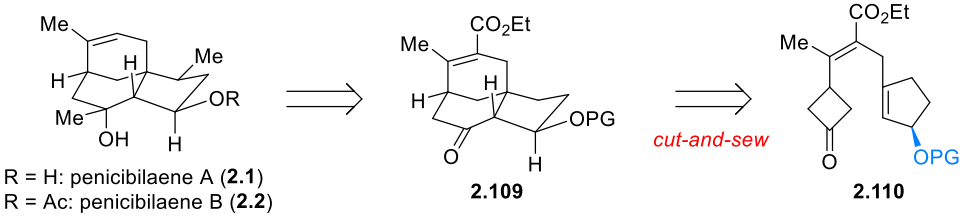

Preparation of cyclobutanone **2.110** also started from ester **2.96** (Scheme 2.25). Ester **2.96** was oxidized by $CrO_3$ to generate ketone **2.111**.[25] Luche reduction of ketone **2.111** delivered alcohol **2.112**, which was protected by benzyl group to give ester **2.113**. Ester **2.113** was treated with DIBAL-H to form alcohol **2.114**, followed by bromination to furnish bromide **2.115**. Three-component coupling of bromide **2.115** delivered ketal **2.116**. However, ketal **2.116** decomposed under typical mild conditions for ketal deprotection, which means that the allylic ether may not be stable under acidic condition. Considering the crucial rule of Lewis acid in our "cut-and-sew" reaction, we gave up this approach.

**Scheme 2.25.**Approach to Prepare Cyclobutanone **2.110**.

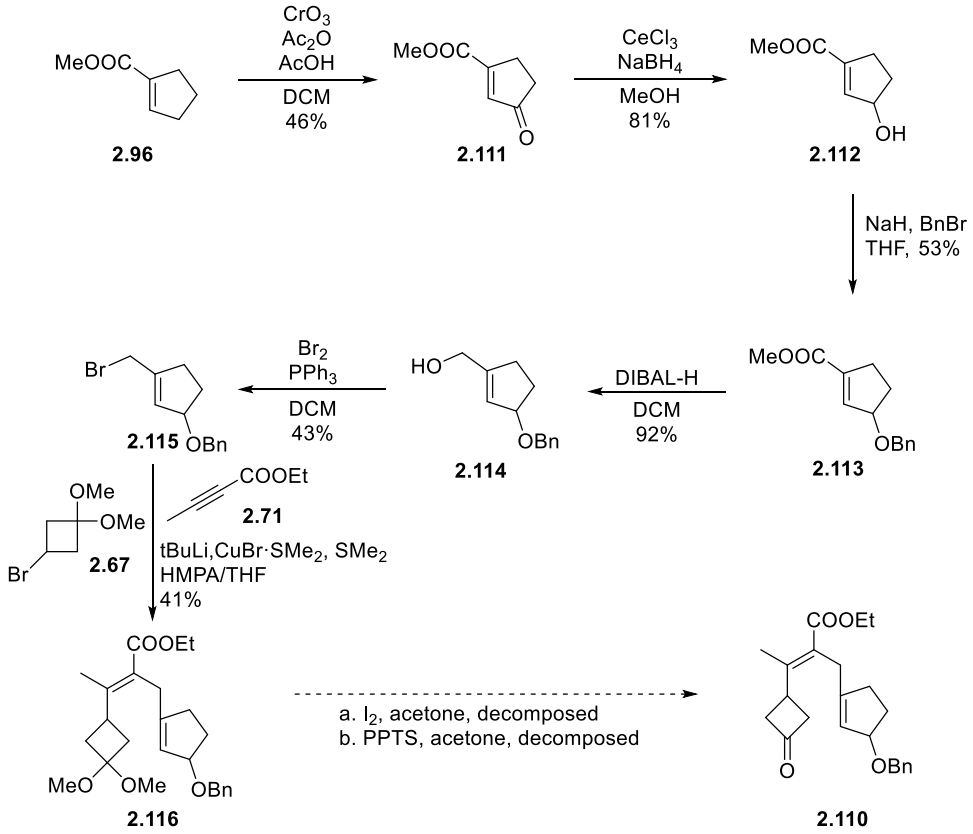


Since cyclobutanone **2.110** which contained allylic ether moiety was not stable in acid, we planned to introduce the oxygen on the five-membered ring after "cut-and-sew" reaction. Thus,

we designed a new real substrate, cyclobutanone **2.118**, which contained a methyl group on the five-membered ring (Scheme 2.26).

**Scheme 2.26.** Total Synthesis of Penicibilaenes through "Cut-and-Sew" Reaction of Cyclobutanone **2.118**.

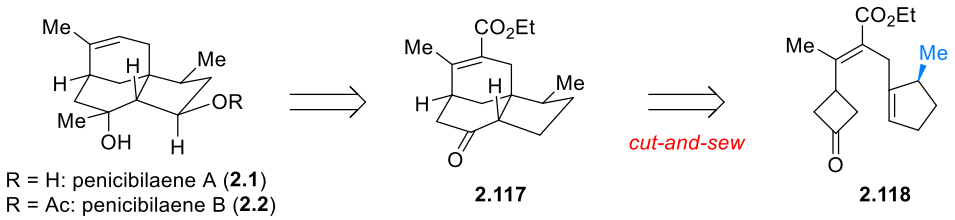


Our first attempt to synthesize new substrate started from ester **2.119** (Scheme 2.27). Methylation of ester **2.119** afforded ester **2.120**,[26] which readily underwent decarboxylation to deliver ketone **2.121**. After condensing with *p*-toluenesulfonyl hydrazide, ketone **2.121** was treated with base and then quenched by DMF to form aldehyde **2.123**. 1,2-Reduction of aldehyde **2.123** generated allylic alcohol **2.124**. However, after several attempts to optimize the Shapiro reaction of hydrazone **2.122**, the yield was still only 44%. Thus, we gave up this route.

**Scheme 2.27.** Preparation of Alcohol **2.124**.

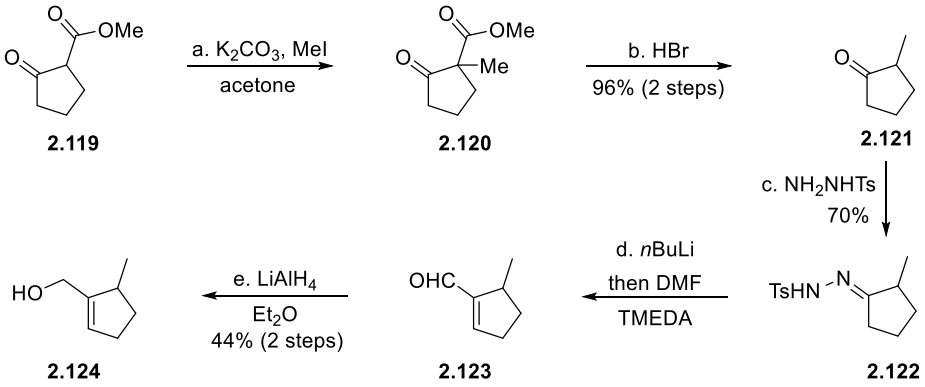

Another route to synthesize cyclobutanone **2.118** was developed from commercially available acetal **2.125** (Scheme 2.28). Following the reported procedure,[27] acetal **2.125** was treated with triethyl phosphonoacetate and base to give alcohol **2.126**, which underwent acetylation to deliver ester **2.127**. Michael addition and elimination of ester **2.127** furnished ester **2.128**,[28] which was reduced by DIBAL-H to give allylic alcohol **2.124**. comparing to previous route, the new strategy could synthesize alcohol **2.124** in higher yield and fewer steps. Bromination of alcohol **2.124** delivered bromide **2.129**, which underwent three-component coupling with bromide **2.67** and ynoate **2.71** to give ketal **2.130**. Finally, deprotection of ketal **2.130** delivered cyclobutanone **2.118** in 28% yield.

**Scheme 2.28.** Preparation of Cyclobutanone **2.118**.

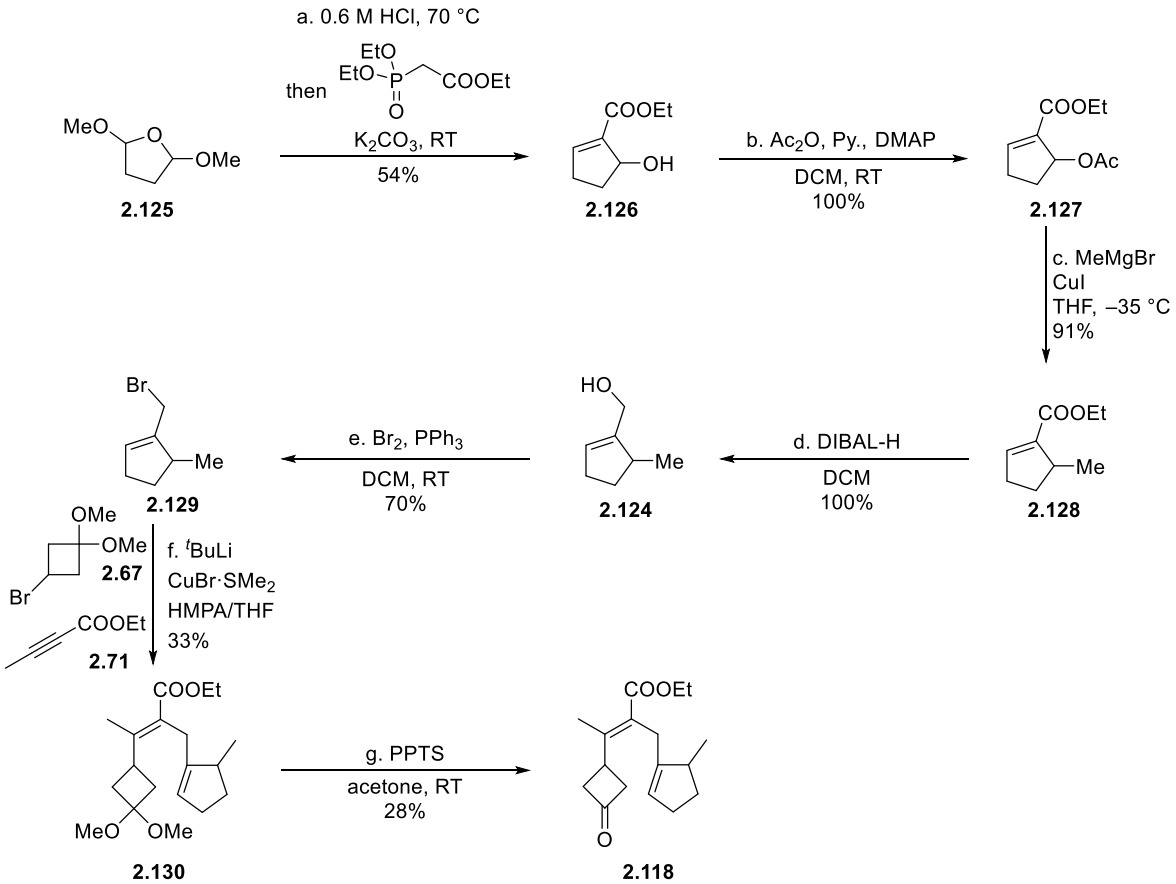

With cyclobutanone **2.118** in hand, we started to investigate "cut-and-sew" reaction of this substrate. 3% of desired product **2.117** was observed under standard condition (entry 1, Table 2.40). After screening of rhodium pre-catalysts, we found that Rh(COD)(acac) (entry 6, Table 2.40) and $Rh(CO)_2(acac)$ (entry 7, Table 2.40) delivered higher yield comparing to $[Rh(C_2H_4)_2Cl]_2$.

**Table 2.40.** Catalyst Screening on "Cut-and-Sew" Reaction of Cyclobutanone **2.118**.

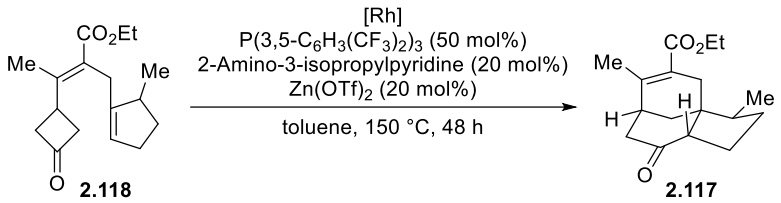


| Entry | [Rh] | SM% | pdt% |
|---|---|---|---|
| 1 | $[Rh(C_2H_4)_2Cl]_2$ (10 mol%) | 3% | 3% |
| 2 | $[Rh(COD)Cl]_2$ (10 mol%) | 5% | trace |
| 3 | $[Rh(COE)_2Cl]_2$ (10 mol%) | 2% | trace |
| 4 | $[Rh(CO)_2Cl]_2$ (10 mol%) | 2% | trace |
| 5 | $[Rh(1,5\text{-}HD)Cl]_2$ (10 mol%) | 0% | trace |
| 6 | Rh(COD)acac (20 mol%) | 0% | 7% |
| 7 | $Rh(CO)_2$acac (20 mol%) | 3% | 6% |

Besides rhodium pre-catalysts, different types of ligands were also tested (Table 2.41). However, NHC ligands was not able to generate any desired product. Phosphoramidite ligands and other electron-deficient ligands wither give trace amounts of ketone **2.117** or have low yield. We also examined the influence of the ligand equivalence on this reaction, and it seems that the equivalence of the ligand did not significantly affect the yield (Table 2.42).

**Table 2.41.** Ligands Screening on "Cut-and-Sew" Reaction of Cyclobutanone **2.118**.

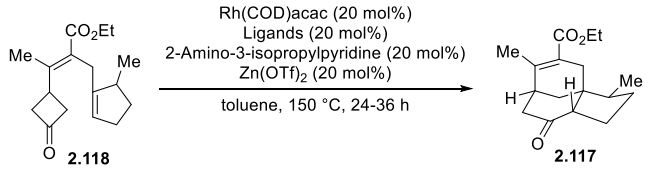


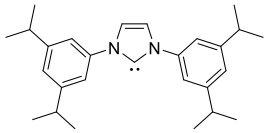

**IPr**
SM: 13%
pdt: trace
deCO: 5%

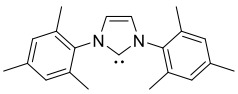

**IMes**
SM: 10%
pdt: trace
deCO: 19%

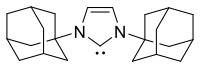

**IAd**
SM: 15%
pdt: trace
deCO: trace

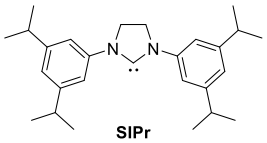

**SIPr**
SM: 19%
pdt: trace
deCO: trace

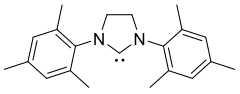

**SIMes**
SM: 7%
pdt: trace
deCO: 18%

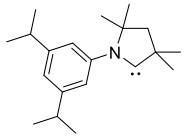

**MeCAAC**
SM: 17%
pdt: trace
deCO: 34%

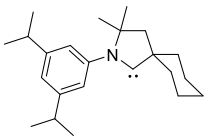

**CyCAAC**
SM: 10%
pdt: trace
deCO: 37%

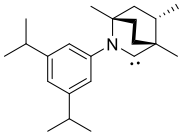

**BiCAAC**
SM: trace
pdt: trace
deCO: 53%

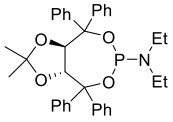

**L1**
SM: 5%
pdt: trace

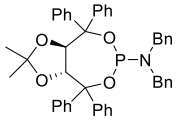

**L2**
SM: 4%
pdt: 5%

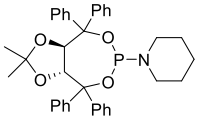

**L3**
SM: 5%
pdt: trace

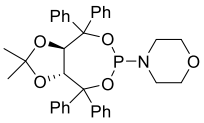

**L4**
SM: 6%
pdt: trace

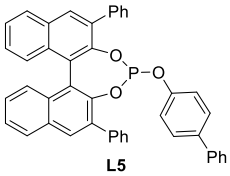

**L5**
SM: 12%
pdt: trace

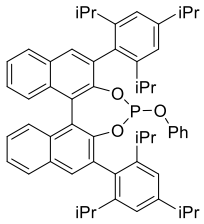

**L6**
SM: 10%
pdt: trace

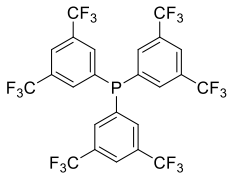

SM: 6%
pdt: 7%

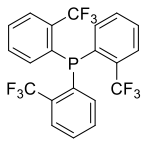

SM: 15%
pdt: trace
deCO: 5%*

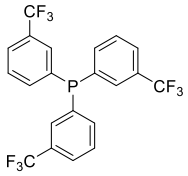

SM: 18%
pdt: trace
deCO: 5%*

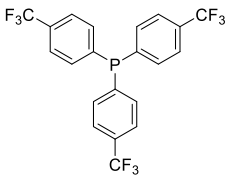

SM: 7%
pdt: trace
deCO: 2%*

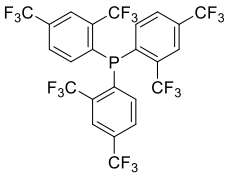

SM: 18%
pdt: trace
deCO: 5%*

$P(C_6F_5)_3$

SM: 44%
pdt: trace
deCO: 2%*

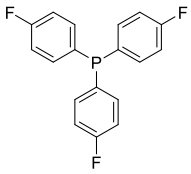

SM: 10%
pdt: trace
deCO: trace*

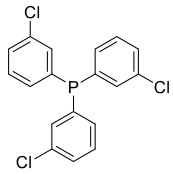

SM: 9%
pdt: trace
deCO: 2%*

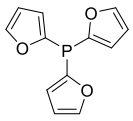

SM: trace
pdt: trace
deCO: trace*

*40 mol% ligand; adding 20 mol% 2,6-di-tBu-py

**Table 2.42.** Ligand Equivalence Screening on "Cut-and-Sew" Reaction of Cyclobutanone **2.118**.

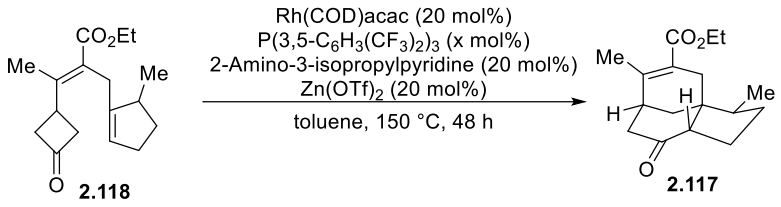


| Entry | x mol% | SM% | pdt% |
|---|---|---|---|
| 1 | 0 | 7% | trace |
| 2 | 20 | 6% | 9% |
| 3 | 40 | trace | 9% |
| 4 | 60 | trace | 9% |

In addition to ligands, we also screened several common solvents for "cut-and-sew" reaction (Table 2.43), However, among all the solvents, toluene still provided the best result. Since we always observed some double bonds migration side product, we proposed that zinc triflate can be hydrolyzed under reaction conditions and generated trace amounts of triflic acid, which could catalyze double bond migration. Thus, we tried to add some base to quench trace amounts of triflic acid and suppress the side reaction. After screening of some inorganic and organic bases, we found that adding base cannot further increase the yield (Table 2.44). We also screened Lewis acids (Table 2.45), concentration (Table 2.46) and directing groups (Table 2.47). Unfortunately, none of them could deliver a better yield.

**Table 2.43.** Solvent Screening on "Cut-and-Sew" Reaction of Cyclobutanone **2.118**.

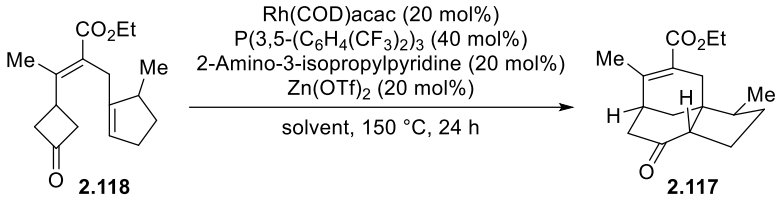


| Entry | solvent | SM% | pdt% |
|---|---|---|---|
| 1 | 1,4-dioxane | 22% | 3% |
| 2 | toluene | 17% | 5% |
| 3 | PhCl | 7% | trace |
| 4 | MeTHF | 14% | trace |
| 5 | 1,2-$C_6H_4F_2$ | 3% | 5% |
| 6 | 1,3-$C_6H_4F_2$ | 8% | 5% |
| 7 | 1,4-$C_6H_4F_2$ | 18% | 4% |

**Table 2.44.** Base Additives Screening on "Cut-and-Sew" Reaction of Cyclobutanone **2.118**.

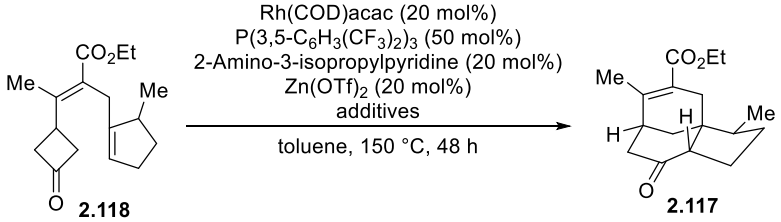


| Entry | Base | SM% | pdt% |
|---|---|---|---|
| 1 | MgO (100 mol%) | 34% | trace |
| 2 | $CaCO_3$ (100 mol%) | trace | 5% |
| 3 | $K_2HPO_4$ (100 mol%) | 25% | trace |
| 4 | 2,6-ditBu-py (100 mol%) | trace | 9% |
| 5 | $Zn(CO_3)_{0.4}(OH)_{1.2}$ (100 mol%) | trace | 7% |
| 6 | 2,6-di-tBu-py (20 mol%)* | 7% | 9% |
| 7 | DTBMP (20 mol%)* | 12% | 6% |
| 8 | pyridine (20 mol%)* | trace | trace |
| 9 | DIPEA (20 mol%)* | 12% | 5% |
| 10 | $NEt_3$ (20 mol%)* | 10% | 8% |
| 11 | 2,6-lutidine (20 mol%)* | 17% | 5% |
| 12 | * | 10% | 8% |

*40 mol% ligand

**Table 2.45.** Lewis Acids Screening on "Cut-and-Sew" Reaction of Cyclobutanone **2.118**.

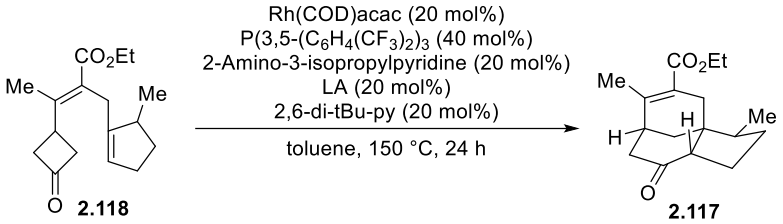


| Entry | LA | SM% | pdt% |
|---|---|---|---|
| 1 | $ZnCl_2$ | 31% | trace |
| 2 | $Zn(OTf)_2$ | 21% | 5% |
| 3 | $CoCl_2$ | 40% | trace |
| 4 | $CoBr_2$ | 39% | trace |
| 5 | $Er(OTf)_3$ | 9% | 5% |

**Table 2.46.** Concentration Screening on "Cut-and-Sew" Reaction of Cyclobutanone **2.118**.

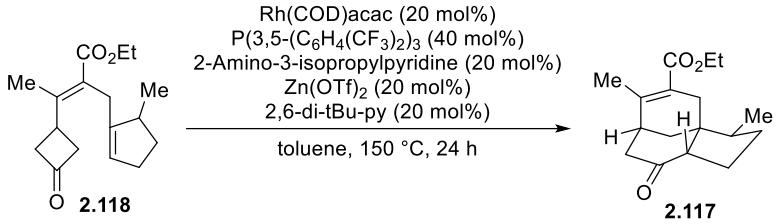


| Entry | concentration | SM% | pdt% | decarbonylation |
|---|---|---|---|---|
| 1 | 0.1 M | 8% | 7% | 5% |
| 2 | 0.05 M | 17% | 7% | 3% |
| 3 | 0.025 M | 10% | 5% | 2% |

**Table 2.47.** Directing Groups Screening on "Cut-and-Sew" Reaction of Cyclobutanone **2.118**.

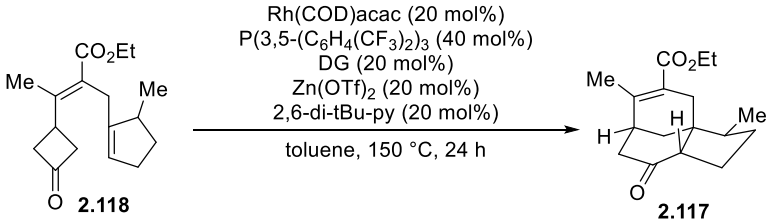


| Entry | DG | SM% | pdt% | decarbonylation |
|---|---|---|---|---|
| 1 | 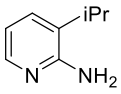 | 12% | 5% | 2% |
| 2 | 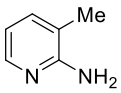 | 12% | 5% | 3% |
| 3 | 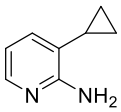 | 14% | 5% | 5% |
| 4 | 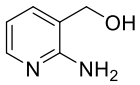 | 21% | trace | 6% |
| 5 | 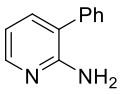 | 16% | 5% | 5% |
| 6 | 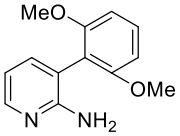 | 15% | trace | 5% |
| 7 | 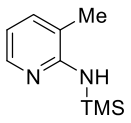 | 21% | trace | trace |

We analyzed the side products of the "cut-and-sew" reaction of cyclobutanone **2.118** (Scheme 2.29). It seems that major side reactions contained double bond-migration and decarbonylation. However, we failed to find a method to suppress these side reactions. Thus, we gave up the route.

**Scheme 2.29.** Side Products Analysis on "Cut-and-Sew" Reaction of Cyclobutanone **2.118**.

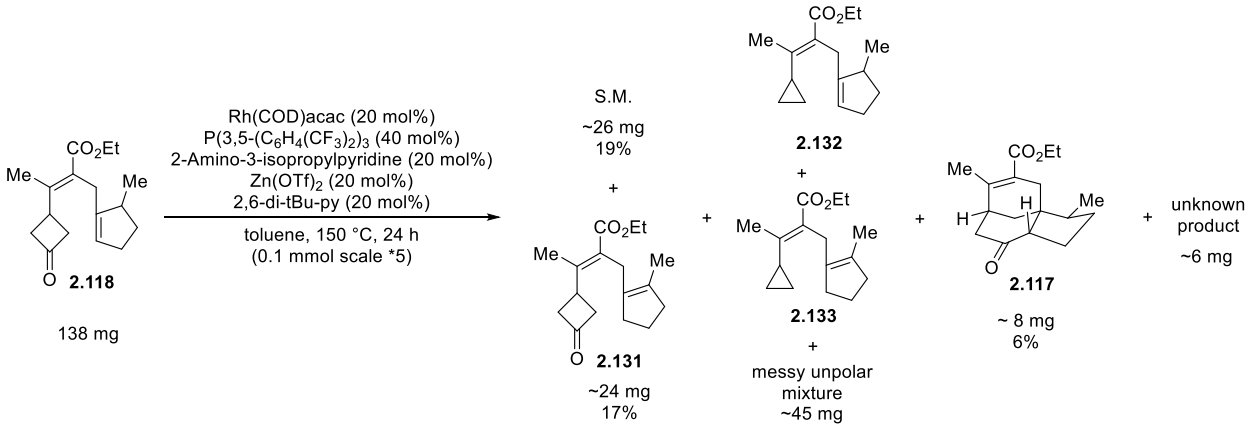


## 2.4. Third Generation Route

At this stage, we have confirmed that the success of the "cut-and-sew" reactions on ester-tethered cyclobutanone requires "naked" cyclopentenyl group, which means any substituents on the five-membered ring would inhibit "cut-and-sew" reaction. Thus, our third-generation route to penicibilaenes highlighted a "C−C/C−H" strategy, which in "C−C" stage we construct the skeleton of natural products by "cut-and-sew" reaction, and in "C−H" stage the substituents on the carbon backbone was introduced through *β*-functionalization. From the retrosynthetic viewpoint (Scheme 2.30), the C13 methyl group in penicibilaenes A (**2.1**) and B (**2.2**) could be introduced in the late stage via the *β*-functionalization from intermediate **2.134**. It can be further envisaged that the C4 oxygen functional group can also be installed via a similar *β*-functionalization from ketone **2.135**, and the C6 tertiary alcohol stereocenter can be introduced through an axial-selective carbonyl addition reaction. The core tricyclic skeleton in **2.135** is then expected to be constructed by the "cut-and-sew" reaction through C−C activation of cyclobutanone **2.99**. Finally, the precursor (**2.95**) for the "cut-and-sew" could be rapidly prepared via a Cu-mediated three-component coupling,

ultimately from three commercially available chemicals: cyclobutanone **2.37**, enoate **2.71** and ynoate **2.96**. It is noteworthy that an ester moiety is strategically introduced in the tricycle intermediate **2.99** because it can (i) greatly simplify substrate preparation and (ii) play a pivotal role in the "cut-and-sew" reaction.

**Scheme 2.30.** Retrosynthetic Analysis (Third Generation Route).

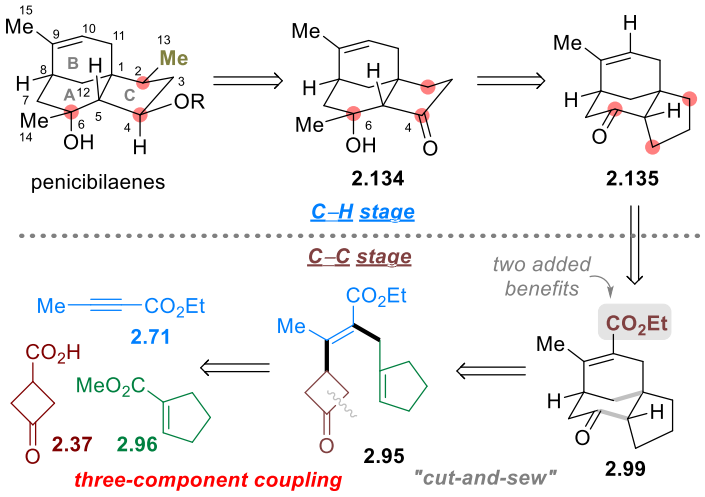


With ester **2.99** in hand, we started to explore the following transformations. Comparing ester **2.99** with penicibilaenes, we could find that all the three rings in the natural products has been established. We needed to introduce functional groups on the five membered ring, methylate the cyclohexanone to form tertiary alcohol, as well as remove the ester group on B ring. First, we explored how to remove the ester group. Hydrolysis of ester **2.99** is straightforward (Table 2.48). In this case, the harsh condition is required due to the extra stability of conjugated ester. The structure of carboxylic acid **2.136** was confirmed by XRD experiment.

**Table 2.48.** Hydrolysis of Ester **2.99**.

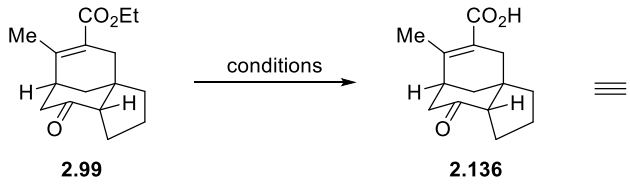


**2.99** **2.136**

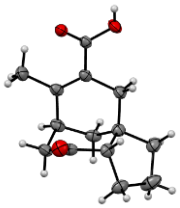

**X-ray**

| Entry | Conditions | yield |
|---|---|---|
| 1 | LiOH, THF/$H_2O$, RT | N.R. |
| 2 | LiOH, THF/$H_2O$, 50 °C, 2 days | 100% |
| 3 | LiOH, THF/$H_2O$, 70 °C, overnight | 99% |

The decarboxylation of carboxylic acid **2.136** is more challenging compared to hydroxylation. There are only few examples of decarboxylation of $\alpha,\beta$-unsaturated carboxylic acids in the literatures. Two general strategies for decarboxylation are transition metal catalysis[29] and radical approach,[30] and both methods were tested in our reaction. Transition metal catalysis approaches, such as silver- and gold-catalysis, were tried at the beginning. They have been reported to work well for decarboxylation of aryl carboxylic acid. However, no desired product was observed under these conditions (entry 1-2, Table 2.49). We then turned to radical approaches. Barton decarboxylation of carboxylic acid **2.136** delivered ketone **2.135** in 27% yield in the first trial (entry 3, Table 2.49). With this preliminary result in hand, we optimized this reaction by screening hydrogen atom source, Barton auxiliary reagents, solvents under thermos- or photo-conditions (entry 4-13, Table 2.49). We found that the Barton decarboxylation with AIBN as initiator, $^t$BuSH as HAT reagent and toluene as solvent gave the best yield as 62% (entry 13, Table 2.49). We also tested nickel-catalyzed decarboxylation developed by Baran group.[30b] However, this condition is not as good as Barton decarboxylation (entry 14, Table 2.49). We then tried one-step decarboxylation of carboxylic acid **2.136**. Two photo-induced Barton decarboxylation were examined (entry 15-16, Table 2.49), which delivered much lower yield comparing to two-step

procedure. Finally, we found that directly removing the solvent after condensation without quenching furnished ketone **2.135** in 53% yield, which is slightly lower than two-step procedure (entry 17, Table 2.49).

**Table 2.49.** Decarboxylation of Carboxylic Acid **2.136**.

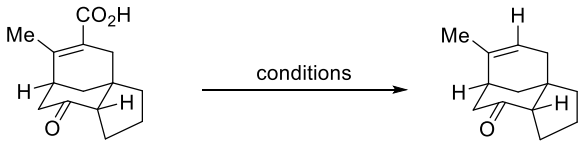


**2.136** **2.135**

| Entry | Conditions | yield |
|---|---|---|
| 1 | AgOAc, $K_2CO_3$, NMP, 140 °C, overnight | decomposed |
| 2 | Au(SIPr)OH, AdCOOH, toluene, 120 °C, 16 h | trace |
| 3 | EDC, **2.137**, DCM, RT, then tBuSH, THF, hv | 27% (two steps) |
| 4 | $PBu_3$, **2.138**, toluene, RT, then AIBN, $(TMS)_3SiH$, 80 °C | trace |
| 5 | $PBu_3$, **2.138**, $CHCl_3$, RT, then hv | 19% (two steps) |
| 6 | $PBu_3$, **2.138**, THF, RT, then tBuSH, hv | 38% (two steps) |
| 7 | $PBu_3$, **2.138**, DCM, RT, then tBuSH, hv | 11% (two steps) |
| 8 | EDC, **2.137**, then tBuSH, DCM, hv. | 32% (two steps) |
| 9 | EDC, **2.137**, then tBuSH, THF, hv. | 31% (two steps) |
| 10 | EDC, **2.137**, then tBuSH, MeCN, hv. | 32% (two steps) |
| 11 | EDC, **2.137**, then tBuSH, MeCN/$H_2O$, hv. | trace |
| 12 | EDC, **2.137**, then tBuSH, toluene, hv. | 33% (two steps) |
| 13 | EDC, **2.137**, then tBuSH, AIBN, toluene, 80 °C | 62% (two steps) |
| 14 | NHPI, DIC, DMAP, DCM, then $NiCl_2 \cdot 6H_2O$, $PhSiH_3$, Zn,THF/DMF/iPrOH | 16% |
| 15 | isopropyl chloroformate, NMM, then pyrithione, TEA, then tBuSH, hv. | n.d. |
| 16 | EDCI, **2.137**, DCM, then tBuSH, hv. | 30% (one step) |
| 17 | EDCI, **2.137**, DCM, then AIBN, tBuSH, toluene, 80 °C | 53% (one step) |

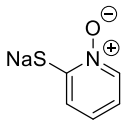


**2.137**

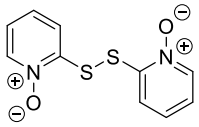


**2.138**

The structure of ketone **2.135** was confirmed unambiguously by XRD experiment of its derivative, hydrazone **2.139** (Scheme 2.31).

**Scheme 2.31.** X-Ray Structure of hydrazone **2.139**.

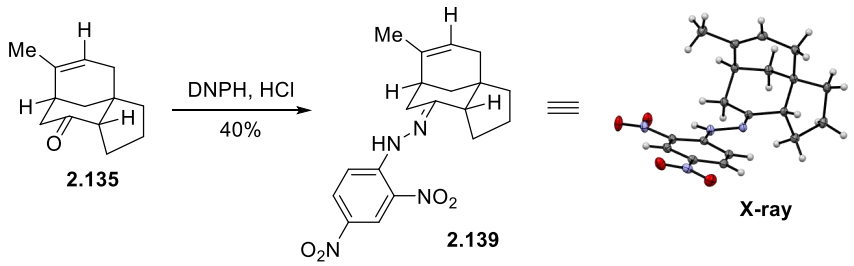


With ketone **2.135** in hand, we started to explore how to install functional group on the C ring. We firstly checked Schönecker−Baran Oxidation[31] to install hydroxyl group (Scheme 2.32). However, *α*-oxygenated product **2.142** instead of desired *β*-oxygenated product was observed, maybe due to the radical condition prefer to generate tertiary radical rather than secondary radical.

**Scheme 2.32.** Approach to Install Oxygen on C4 through Schönecker−Baran Oxidation.

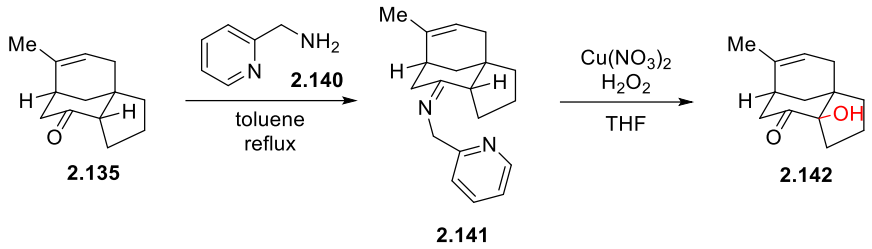


We also tested Sanford's method for ketone *β*-oxygenation, which utilized *O*-methyl oxime as directing group.[32] The *O*-methyl oxime **2.143** was readily prepared in one step from ester **2.99** (Scheme 2.33). However, all the typical reported conditions were not able to deliver the desired product **2.144** (Table 2.50). The rigid skeleton in compound **2.143** may prohibit the C−H activation step, since the organometallacycle formed after C−H activation was highly strained.

**Scheme 2.33.** Preparation of *O*-Methyl Oxime **2.143**.

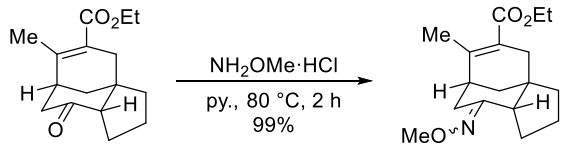


**2.99** **2.143**

**Table 2.50.** Approach to Install Oxygen on C4 through Sanford's C−H Oxygenation.

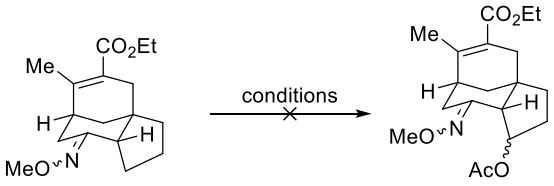


**2.143** **2.144**

| Entry | Conditions | Result |
|---|---|---|
| 1 | $Pd(OAc)_2$ (20 mmol%), PIDA (1.5 equiv.), AcOH/$Ac_2O$, 100 °C, 1 h | N.R. |
| 2 | $Pd(OAc)_2$ (20 mmol%), PIDA (1.5 equiv.), AcOH/$Ac_2O$, 100 °C, overnight | N.R. |
| 3 | $Pd(OAc)_2$ (20 mmol%), PIDA (1.5 equiv.), AcOH/$Ac_2O$, 90 °C, overnight | N.R. |
| 4 | $Pd(OAc)_2$ (20 mmol%), PIDA (1.5 equiv.), AcOH/$Ac_2O$, 80 °C, overnight | N.R. |
| 5 | $Pd(OAc)_2$ (1 equiv.), PIDA (1.5 equiv.), AcOH/$Ac_2O$, 100 °C, 1 h | N.R. |

Besides Schönecker−Baran Oxidation and Sanford C−H oxygenation, we also tried some other radical approaches based on 1,5-HAT (Scheme 2.34).[33] Unfortunately, none of them delivered the desired C−H oxygenated product.

**Scheme 2.34.** Approach to Install Oxygen on C4 through 1,5-HAT.

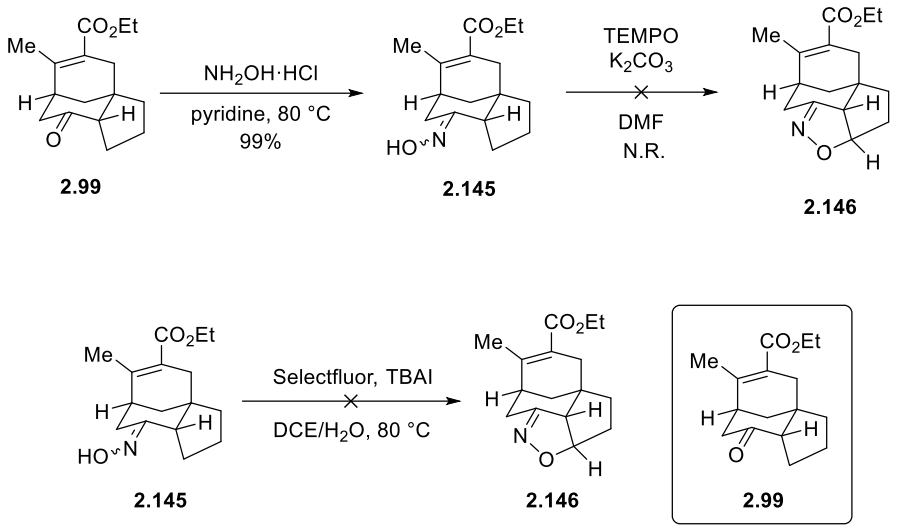


Besides trying C−H oxygenation based on ketone, we also investigated C−H oxygenation based on alcohol. We proposed that C−H oxygenation based on alcohol is more promising on account of the geometry of the molecule. Comparing the structure of ketone **2.135** and alcohol **2.148**, it is clear that the hydroxyl group in alcohol **2.148** is much more closer to the C−H bond which needed to be activated. In order to achieve methylation of ketone **2.135** in a diastereoselective manner, we screened diverse methods of ketone methylation (Table 2.51). More acidic methylation reagent such as $MeTiCl_3$ preferred to attack ketone from concave face to give axial alcohol **2.147** (entry 5, Table 2.51).[34] In contrast, methyl lithium favored to attack convex face of ketone **2.135** to deliver equatorial alcohol **2.148** (entry 8, Table 2.51). The configuration of alcohol **2.148** was confirmed by nOe analysis.

**Table 2.51.** Methylation of Ketone **2.135**.

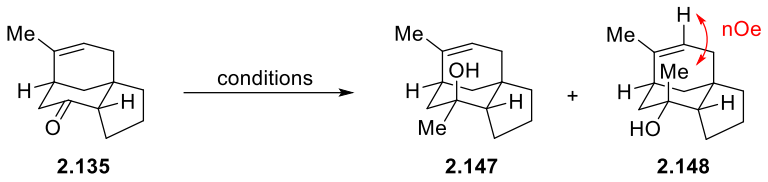


**2.135** **2.147** **2.148**

| Entry | Conditions | SM% | **2.147**% | **2.148**% | d.r. |
|---|---|---|---|---|---|
| 1 | MeLi, THF, -78 °C to r.t., 3 h | 28% | 9% | 52% | 1 : 5.8 |
| 2 | MeLi, $Et_2O$, -78 °C to r.t., 3 h | 29% | 21% | 45% | 1 : 2.1 |
| 3 | MeMgBr, THF, 0 °C to r.t., 16 h | 34% | 20% | 35% | 1 : 1.8 |
| 4 | MeMgBr, $Et_2O$, 0 °C to r.t., 16 h | 27% | 42% | 26% | 1.6 : 1 |
| 5 | $MeTiCl_3$, $Et_2O$, -78 °C to 0 °C, 3 h | 28% | 53% | 8% | 6.6 : 1 |
| 6 | $Yb(OTf)_3$, MeLi, THF, -78 °C, 1 h | 87% | / | / | / |
| 7 | MeLi, HMPA/THF, -78 °C to r.t., 3 h | 100% | / | / | / |
| 8 | MeLi, LiBr, THF, -78 °C to r.t., 16 h | 26% | 8% | 54% | 1 : 6.8 |

With alcohol **2.148** in hand, we tried to activate the C−H bond on C ring by Hartwig C−H hydroxylation,[35] which went through an one-pot three-step process (Scheme 2.35A). The first step is silylation of alcohol **2.148** to give silane **2.149**, which was directly used in the next step without further purification. Then an iridium catalyzed C−H silylation of silane **2.149** delivered siloxane **2.150**, followed by a Fleming−Tamao oxidation to furnish diol **2.151**. However, instead of activation of secondary C−H bond on the C ring, the C−H activation occurred on a less hindered methyl group to deliver undesired diol **2.151**. We tried to decrease the temperature of C−H silylation step to 100 °C, but diol **2.151** was still the only observed product (Scheme 2.35B).

Hartwig hydroxylation of other silane were also explored. We found that dimethyl silane **2.152** could be easily prepared in high yield (Scheme 2.35C). However, iridium catalyzed Hartwig C−H hydroxylation of silane **2.152** also delivered undesired diol **2.151**. We also tried rhodium catalyzed Hartwig C−H hydroxylation,[36] but only desilylation product **2.148** was observed under this condition (Scheme 2.35D).

**Scheme 2.35.** Approach to Install Oxygen on C4 through Hartwig C−H hydroxylation.

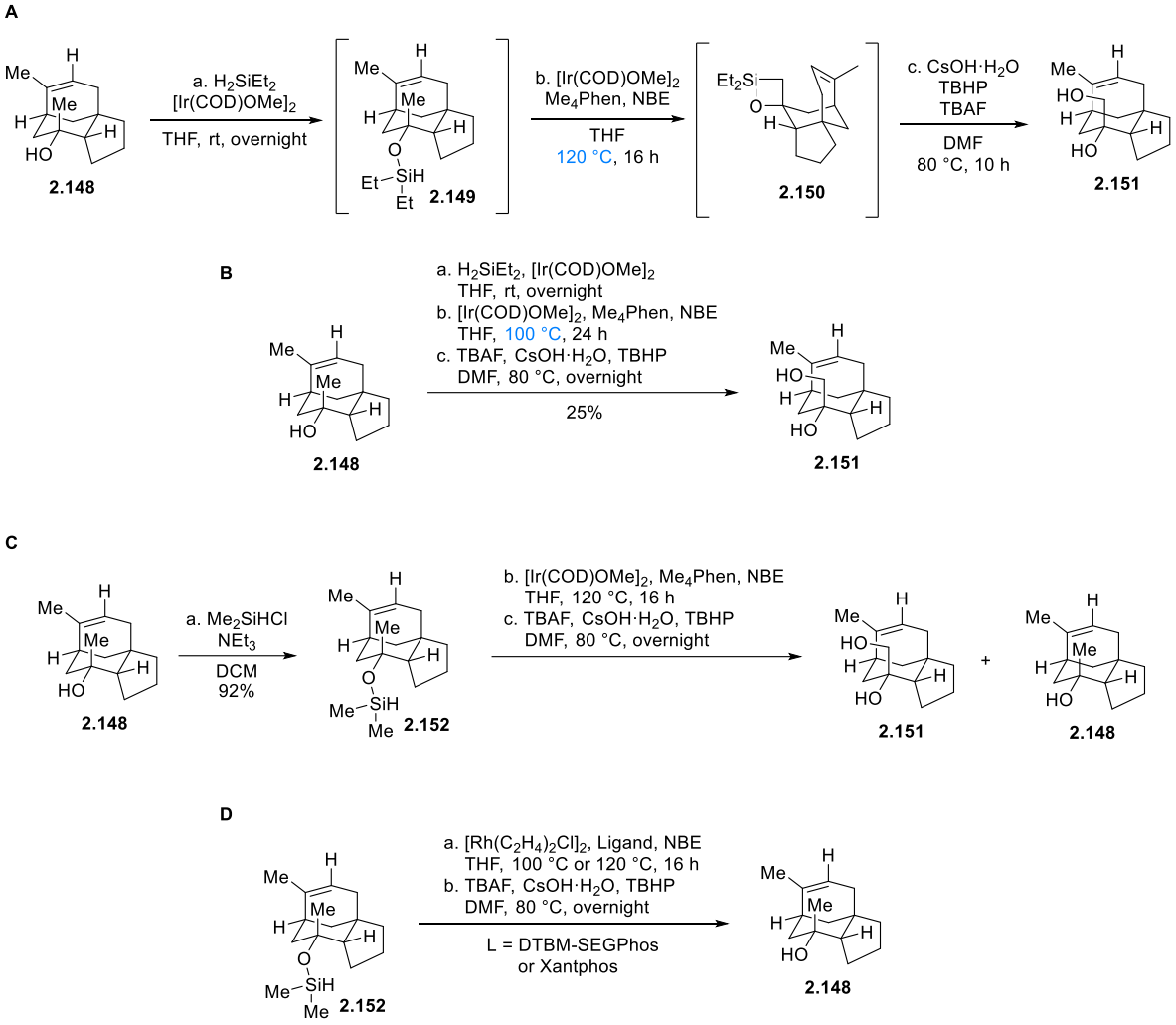


In addition to Hartwig C−H hydroxylation, Gevorgyan C−H functionalization based on 1,6-HAT was also examined. The silyl iodide in siloxane **2.154** was served as directing group in Gevorgyan's methods,[37] which was prepared form alcohol **2.148** in two steps (Scheme 2.36A). However, the 1,6-HAT did not happen in both desaturation (Scheme 2.36B) and amination (Scheme 2.36C).

**Scheme 2.36.** Approach to Install Oxygen on C4 through Gevorgyan C−H Functionalization.

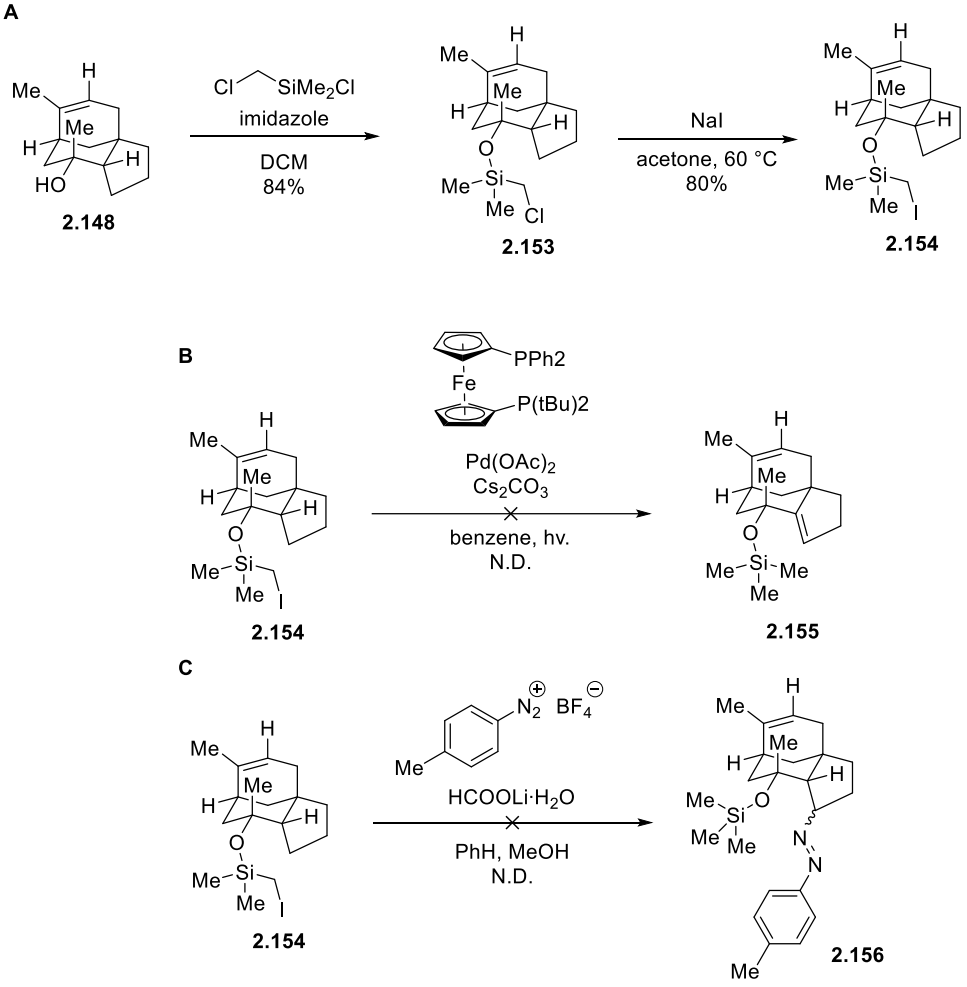


Since Hartwig C−H hydroxylation and Gevorgyan C−H functionalization cannot deliver the desired product on our substrate, we turned to explore Du Bois C−H amination.[38] We first tried to prepare sulfonyl amide **2.157** from tertiary alcohol **2.148**. However, instead of obtaining sulfonyl amide **2.157**, only the elimination product alkene **2.158** was observed under various conditions (Table 2.52).

**Table 2.52.** Attemps to Prepare sulfonyl amide **2.157**.

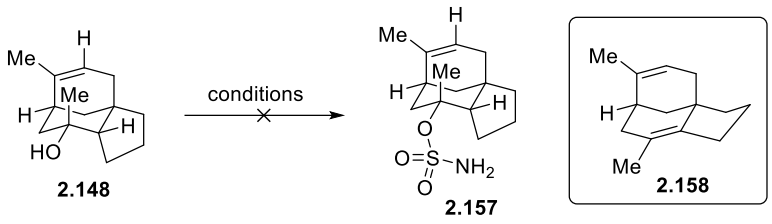


| Entry | Conditions | Result |
|---|---|---|
| 1 | MgO, $ClSO_2NCO$, HCOOH, MeCN/DMAc | n.d. |
| 2 | NaH, $ClSO_2NCO$, HCOOH, MeCN/DMF | n.d. |
| 3 | KH, $ClSO_2NCO$, HCOOH, MeCN/DMF | n.d. |
| 4 | $NEt_3$, $ClSO_2NCO$, HCOOH, DCM, 0 °C | n.d. |
| 5 | $NEt_3$, $ClSO_2NCO$, HCOOH, DCM, -78 °C | n.d. |
| 6 | $ClSO_2NH_2$, DMAc, 0 °C to RT | n.d. |

Then we paid our attention to prepare sulfonyl amide from secondary alcohol, which was harder to undergo elimination. The first challenge we encountered was how to selectively reduce ketone **2.135** to give equatorial alcohol **2.160**. Typical axial-reducing reagents, such as $LiAlH_4$, $LiBH_4$ and $NaBH_4$, were tested, but axial alcohol **2.159** was the favored product under these conditions (entry 1-7, Table 2.53). In contrast, bulky reducing reagent, L-selectride, exclusively underwent axial attack to deliver equatorial alcohol **2.150** (entry 10, Table 2.53), which indicate concave-convex selectivity is dominated in our substrate. Besides L-selectride, Meerwein−Ponndorf−Verley reduction also favored to give more thermodynamically stable equatorial alcohol **2.150** (entry 9, Table 2.53).

**Table 2.53.** Reduction of Ketone **2.135**.

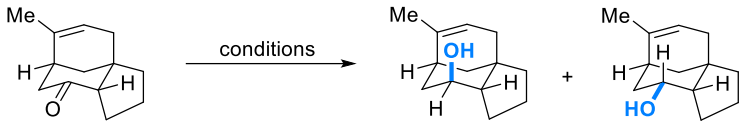


**2.135** **2.159** **2.160**

| Entry | Conditions | **2.159**%[a] | **2.160**%[a] | d.r. |
|---|---|---|---|---|
| 1 | $NaBH_4$, MeOH, 0 °C, 3 h | 16% | 5% | 3 : 1 |
| 2 | $LiBH_4$, THF, 0 °C, 3 h | 38% | 17% | 2.3 : 1 |
| 3 | $LiBH_4$, $Et_2O$, 0 °C, 3 h | 61% | 38% | 1.6 : 1 |
| 4 | $LiAlH_4$, THF, 0 °C, 3 h | 66% | 33% | 2 : 1 |
| 5 | $LiAlH_4$, $Et_2O$, 0 °C, 3 h | 67% | 32% | 2.1 : 1 |
| 6 | $LiBH_4$, $Et_2O$, -78 °C, 3 h | / | / | / |
| 7 | $NaBH_4$, $CeCl_3$, MeOH, -78 °C, 0.5 h | 54% | 45% | 1.2 : 1 |
| 8 | Mg, $HgCl_2$, EtOH | / | / | / |
| 9 | $Al(OiPr)_3$, iPrOH, 80 °C, 5 h | 17% | 67% | 1 : 3.8 |
| 10 | L-selectride, THF, -78 °C to 0 °C, 3 h | / | 99% (78%) | / |

[a]NMR yield; numbers in the parentheses are isolated yields

After establishing diastereoselective reduction of ketone **2.135**, we then tried to prepare sulfonyl amide **2.161** (Table 2.54). Sulfonyl amide **2.161** was obtained in 55% yield with MgO served as a base in the reaction condition (entry 3, Table 2.54). With sulfonyl amide **2.161** in hand, we next explored Du Bois C−H amination on this compound (Table 2.55). We observed that the nitrene could insert into either *β*-C−H bonds on C4 to deliver two diastereomers **2.162** and **2.163** in 2.5:1 diastereoselectivity (entry 1, Table 2.55). Utilizing $Rh_2(esp)_2$ as catalyst[38b] and adjusting the concentration increased the yield to 73% with 4.2:1 diastereoselectivity (entry 6, Table 2.55).

**Table 2.54.** Preparation of Sulfonyl Amide **2.161**.

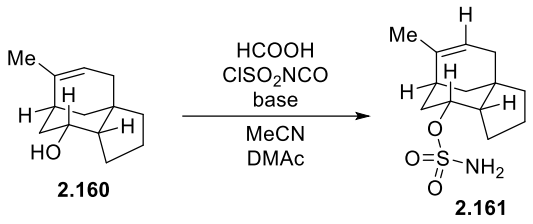


**2.160** **2.161**

| Entry | base | yield[a] |
|---|---|---|
| 1 | $NaHCO_3$ | 71% |
| 2 | $CaCO_3$ | 71% |
| 3 | MgO | 93% (55%) |
| 4 | $K_2CO_3$ | 69% |
| 5 | $K_2HPO_4$ | 88% |
| 6 | $NH_4HCO_3$ | 82% |

[a]NMR yield; numbers in the parentheses are isolated yields

**Table 2.55.** Du Bois C−H Amination of Sulfonyl Amide **2.161**.

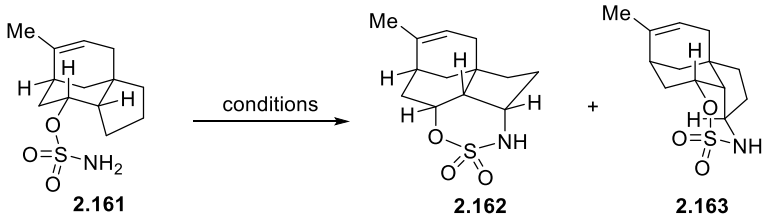


**2.161** **2.162** **2.163**

| Entry | Conditions | **2.162**% | **2.163**% | d.r. |
|---|---|---|---|---|
| 1 | $Rh_2(OAc)_4$ (5 mol%), PIDA (1.1 equiv.) MgO(3 equiv.), DCM (0.02 M), 40 °C, 3 h | 32% | 13% | 2.5 : 1 |
| 2 | $Rh_2(esp)_2$ (5 mol%), PIDA (1.1 equiv.) MgO(3 equiv.), DCM (0.02 M), 40 °C, 0.5 h | 59% | 12% | 5 : 1 |
| 3 | $Rh_2(esp)_2$ (5 mol%), PIDA (1.1 equiv.) MgO(3 equiv.), DCM (0.02 M), RT, 6 h | 57% | 17% | 3.3 : 1 |
| 4 | $Rh_2(esp)_2$ (2 mol%), PIDA (1.1 equiv.) MgO(3 equiv.), DCM (0.02 M), 40 °C, 1 h | 58% | 13% | 4.5 : 1 |
| 5 | $Rh_2(esp)_2$ (1 mol%), PIDA (1.1 equiv.) MgO(3 equiv.), DCM (0.02 M), 40 °C, 1 h | 55% | 15% | 3.7 : 1 |
| 6 | $Rh_2(esp)_2$ (2 mol%), PIDA (1.1 equiv.) MgO(3 equiv.), DCM (0.01 M), 40 °C, 1 h | 59% | 14% | 4.2 : 1 |

Reduction of the mixture of sulfonyl amide **2.162** and **2.163** by Red-Al[39] provided amine **2.164**. However, we were unable to convert amine **2.164** into ketone **2.165** after several trials (Table 2.56).[40]

**Table 2.56.** Attempts to Prepare Ketone **2.165**.

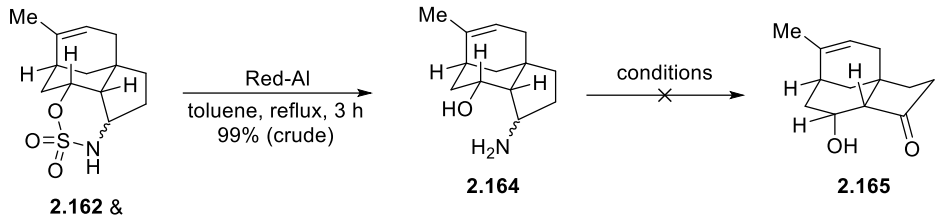


**2.162** & **2.163**

**2.164**

**2.165**

| Entry | Conditions | Result |
|---|---|---|
| 1 | PIDA, TEMPO, DCM | n.d. |
| 2 | DTBBQ, oxalic acid, MeOH/THF | n.d. |
| 3 | $Ru(BPY)_3$, $K_2S_2O_8$, $MeCN/H_2O$, *hv*. | decomposed |

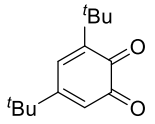


**DTBBQ**

The elimination product of sulfonylation, alkene **2.158** (Table 2.52), inspired us a new way to functionalize $\beta$-C−H bond. We proposed that the double bond would place at more substituted position when converting ketone to silyl enol ether, as the same regioselectivity in elimination of **2.148** (Table 2.52). The experiment results proved our hypothesis (Table 2.57). Silyl enol ether **2.166** was obtained in 77% yield from ketone **2.99** with DBU as base (entry 6, Table 2.57). A following selenoxide elimination of enol ether **2.166** afforded enone **2.167** (entry 5, Table 2.58).

**Table 2.57.** Preparation of Silyl Enol Ether **2.166**.

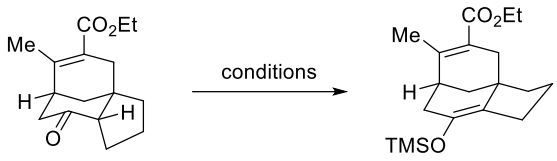


**2.99** **2.166**

| Entry | Conditions | Result |
|---|---|---|
| 1 | TMSCl, TBAI, NEt3, MeCN, RT | n.r. |
| 2 | TMSCl, TBAI, NEt3, DCM, RT | n.r. |
| 3 | TMSCl, KI, NEt3, DMF, RT | n.r. |
| 4 | TMSCl, TBAI, DIPEA, DCM, RT | n.r. |
| 5 | TMSCl, TBAI, proton sponge, DCM, RT | n.r. |
| 6 | TMSCl, TBAI, DBU, DCM, RT | 77% |

**Table 2.58.** Preparation of enone **2.167**.

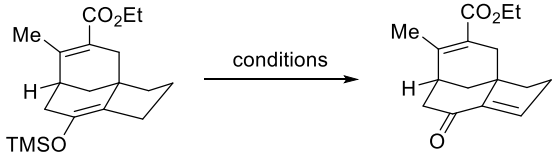


**2.166** **2.167**

| Entry | Conditions | Result |
|---|---|---|
| 1 | $Pd(OAc)_2$, diallyl carbonate, MeCN, RT, overnight | trace |
| 2 | $Pd_2(dba)_3$, diallyl carbonate, MeCN, RT, overnight | trace |
| 3 | $Pd(OAc)_2$, MeCN, RT, overnight | trace |
| 4 | $Pd(OAc)_2$, 2,6-di-tBu-py, MeCN, RT | 29% |
| 5 | PhSeCl, DCM, -78 °C to 0 °C, then $H_2O_2$, DCM, 0 °C | 76% |
| 6 | PhSeCl, DCM, -78 °C to 0 °C, then mCPBA, DCM, 0 °C | 44% |
| 7 | PhSeCl, 2,6-di-tBu-py, DCM, -78 °C to 0 °C, then mCPBA, DCM, 0 °C | 31% |

With enone **2.167** in hand, we planned to methylation of enone **2.167** to give tertiary alcohol **2.168**, followed by hydroboration-elimination to install oxygen on C4. However, methylation of ketone **2.167** delivered alcohol **2.169**, instead of alcohol **2.168** (Scheme 2.37), since ester in compound **2.167** is less sterically hindered than ketone. We then protected enone **2.167** by glycol, and tried hydroboration-oxidation of ketal **2.170** (Table 2.59). Unfortunately, no desired product alcohol **2.171** was observed after several trials.

**Scheme 2.37.** Methylation of Protection of Enone **2.167**.

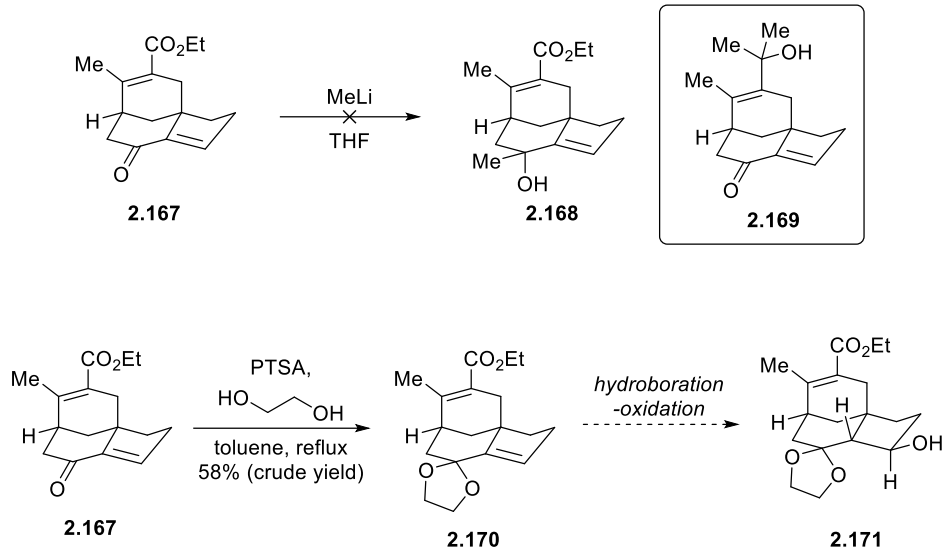


**Table 2.59.** Attemps on Hydroboration-Oxidation of Ketal **2.167**.

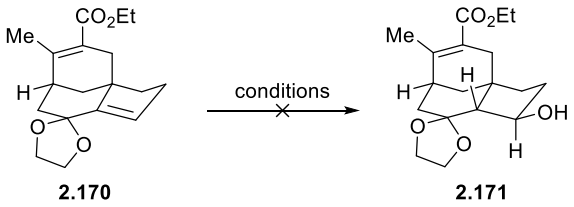


| Entry | Conditions | Result |
|---|---|---|
| 1 | $BH_3$·THF (3 equiv.), THF, then $NaBO_3$, $H_2O$ | decomposed |
| 2 | $BH_3$·THF (1 equiv.), THF, then $NaBO_3$, $H_2O$ | decomposed |
| 3 | $BH_3$·DMS (0.5 equiv.), THF, then $NaBO_3$, $H_2O$ | decomposed |
| 4 | 9-BBN (1.5 equiv.), THF, then $NaBO_3$, $H_2O$ | no reaction |

Like ketone **2.99**, ketone **2.135** could also be oxidized to enone. However, our previous optimized condition suffered from low reaction rate and moderate conversion. After condition screening (Table 2.60), we found that using *in-situ* generated trimethylsilyl iodide with HMDS as base gave enone **2.173** in 87% yield within 12 h (entry 7, Table 2.60).

**Table 2.60.** Desaturation of Ketone **2.135**.

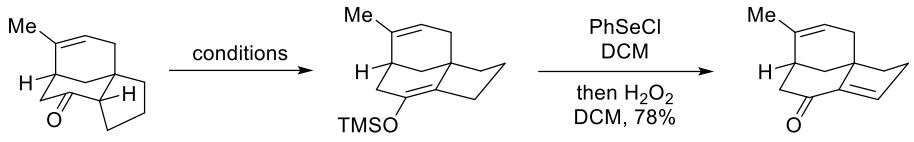


**2.135** **2.172** **2.173**

| Entry | Conditions | Result |
|---|---|---|
| 1 | TBAI. TMSCl, DBU, DCM | 68% |
| 2 | TBAI. TMSCl, DBU, THF | low conversion |
| 3 | TMSOTf, DBU, DCM | n.d. |
| 4 | TMSCl, NaI, HMDS, MeCN | 65% |
| 5 | TMSCl, NaI, DBU, MeCN | 55% |
| 6 | TMSCl, NaI, NEt3, MeCN | low conversion |
| 7 | TMSCl, NaI, HMDS, MeCN | 87% |

Although selenoxide elimination of ketone **2.135** delivered enol **2.173** in good yield, this transformation needed 3 steps. In the recent years, many methods to desaturate linear or cyclic ketone have been developed. However, in most cases the α-carbon of ketone was secondary instead of tertiary. The tertiary α-carbon in ketone **2.135** prevented interactions between substrate and reagent, which made one-step desaturation of ketone **2.135** to be pretty challenged. IBX dehydrogenation of ketone (entry 1, Table 2.61),[41] one-step selenium oxide elimination (entry 2, Table 2.61)[42] as well as bromination/elimination (entry 3-4, Table 2.61)[43] did not work on ketone **2.135**. To our surprise, palladium catalyzed Stahl oxidation[44] of ketone **2.135** delivered enone **2.173** in 8% yield (entry 7, Table 2.61).

**Table 2.61.** One-Step Desaturation of Ketone **2.135**.

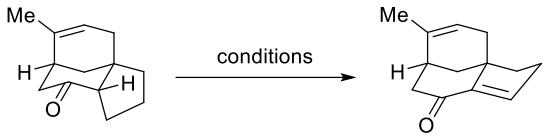


**2.135** **2.173**

| Entry | Conditions | Results |
|---|---|---|
| 1 | IBX, toluene/DMSO, 75 °C | decomposed |
| 2 | PhSeCl, EA, then $NaHCO_3$, $H_2O_2$ | n.d. |
| 3 | NBS, $CCl_4$, reflux, then aniline, RT | decomposed |
| 4 | $CuBr_2$, EA, $CHCl_3$, reflux | n.d. |
| 5 | $Pd(OAc)_2$, $Ag_2CO_3$, $O_2$, DMSO | n.r. |
| 6 | $Pd(TFA)_2(DMSO)_2$, $O_2$, AcOH, 80 °C | n.d. |
| 7 | $Pd(OAc)_2$, $O_2$, DMSO, 80 °C | 8% (69% SM) |

We then tried to optimize Stahl oxidation (Table 2.62). TFA was found to be a crucial additive for this reaction,[45] which increased the yield from 8% to 12% (entry 2, Table 2.62). We proposed that TFA could facilitate enolization of ketone **2.135**. Catalysts (entry 4-5, Table 2.62), other additives (entry 6-7, Table 2.62) and ligands[46] (entry 8-11, Table 2.62) were also screened, but not fruitful. Increasing palladium catalyst loading to 20 mol% increased the yield to 21% (entry 12, Table 2.62), but further raising the palladium catalyst loading to 100 mol% did not significantly increase the yield (entry 13, Table 2.62). Other catalyst loading, temperature and reaction time were also examined (Table 2.63). Finally, we found that 60 °C is the best temperature for this reaction, which delivered enone **2.173** in 42% NMR yield (38% isolated yield) using 30 mol% palladium acetate as catalyst (entry 7 & 9, Table 2.63).

**Table 2.62.** Optimization on Stahl Oxidation of Ketone **2.135** (Part I).

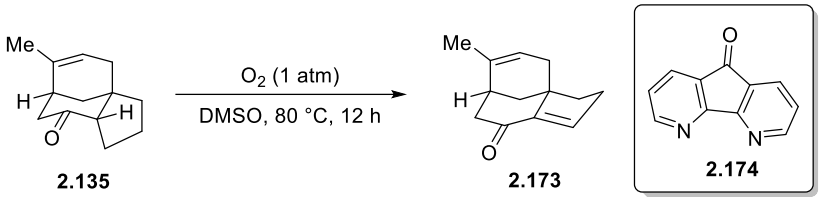


**2.135** **2.173** **2.174**

| Entry | Catalyst | Ligand | Additives | Concentration | yield |
|---|---|---|---|---|---|
| 1 | $Pd(TFA)_2$ (10 mol%)<br>$Pd(OAc)_2$ (10 mol%) | / | / | DMSO (0.05 M) | 7% (45% SM) |
| 2 | $Pd(OAc)_2$ (10 mol%) | / | TFA (1 equiv) | DMSO (0.05 M) | 12% (73% SM) |
| 3 | $Pd(OAc)_2$ (20 mol%) | / | TFA (3 equiv) | DMSO (0.05 M) | 14% (41% SM) |
| 4 | $Pd(TFA)_2$ (20 mol%) | / | TFA (1 equiv) | DMSO (0.05 M) | 17% (50% SM) |
| 5 | $Pd(OPiv)_2$ (20 mol%) | / | TFA (1 equiv) | DMSO (0.05 M) | N.D. |
| 6 | $Pd(OAc)_2$ (20 mol%) | / | PTSA (1 equiv) | DMSO (0.05 M) | 17% (34% SM) |
| 7 | $Pd(OAc)_2$ (20 mol%) | / | TMSOTf (1 equiv) | DMSO (0.05 M) | N.D. |
| 8 | $Pd(TFA)_2$ (10 mol%) | **2.174** (20 mol%) | / | DMSO (0.1 M) | 6% (78% SM) |
| 9 | $Pd(TFA)_2$ (20 mol%) | **2.174** (20 mol%) | / | DMSO (0.05 M) | 15% (61% SM) |
| 10 | $Pd(TFA)_2$ (20 mol%) | **2.174** (20 mol%) | TFA (1 equiv) | DMSO (0.05 M) | 14% (49% SM) |
| 11 | $Pd(TFA)_2$ (20 mol%) | **2.174** (20 mol%) | / | DMSO (0.2 M) | 13% (73% SM) |
| 12 | $Pd(OAc)_2$ (20 mol%) | / | TFA (1 equiv) | DMSO (0.2 M) | 21% (66% SM) |
| 13 | $Pd(OAc)_2$ (1 equiv) | / | TFA (1 equiv) | DMSO (0.05 M) | 23% (33% SM) |

**Table 2.63.** Optimization on Stahl Oxidation of Ketone **2.135** (Part II).

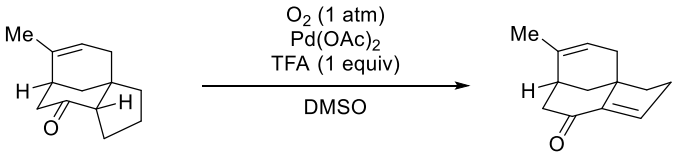


**2.135** **2.173**

| Entry | Catalyst loading | Temperature | Concentration | Time | yield |
|---|---|---|---|---|---|
| 1 | $Pd(OAc)_2$ (20 mol%*4) | 80 °C | 0.05 M | 24 h | 25% (25% SM) |
| 2 | $Pd(OAc)_2$ (20 mol%) | 60 °C | 0.05 M | 24 h | 28% (46% SM) |
| 3 | $Pd(OAc)_2$ (20 mol%) | 40 °C | 0.05 M | 24 h | 7% (52% SM) |
| 4 | $Pd(OAc)_2$ (30 mol%) | 60 °C | 0.05 M | 24 h | 40% (34% SM) |
| 5 | $Pd(OAc)_2$ (50 mol%) | 60 °C | 0.05 M | 24 h | 36% (26% SM) |
| 6 | $Pd(OAc)_2$ (30 mol%) | 60 °C | 0.05 M | 48 h | 37% (31% SM) |
| 7 | $Pd(OAc)_2$ (30 mol%) | 60 °C | 0.2 M | 24 h | 42% (31% SM) |
| 8 | $Pd(OAc)_2$ (30 mol%) | 60 °C | 0.2 M | 6 h | 35% (51% SM) |
| 9 | $Pd(OAc)_2$ (30 mol%) | 60 °C | 0.2 M | 24 h | 38% (15% SM, isolated yield) |

NHC-catalyzed *β*-silylation of enone **2.173** delivered ketone **2.175** in 29% yield (entry 1, Table 2.64).[47] the configuration of ketone **2.175** was confirmed by nOe analysis. Other silylation methods were also tested,[48] and copper catalyzed conjugated addition of $PhMe_2SiLi$ gave 80% yield of ketone **2.175** (entry 4, Table 2.64).[49] However, methylation of ketone **2.175** was failed under several typical conditions (Table 2.65), maybe due to the extra steric hinderance caused by the huge silyl group.

**Table 2.64.** Silylation of Enone **2.173**.

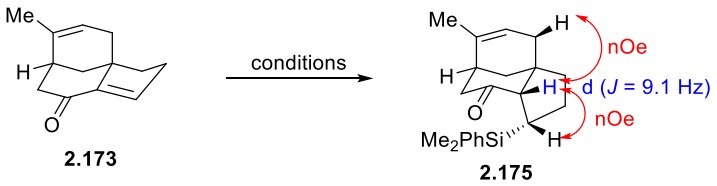


**2.173** **2.175**

| Entry | Conditions | Results |
|---|---|---|
| 1 | DBU, $PhMe_2SiB(pin)$, SIMes·HCl, $THF/H_2O$ | 29% (50% SM) |
| 2 | $PhMe_2SiB(pin)$, $CuSO_4$, 4-picoline, $H_2O$ | messy |
| 3 | Li, $PhMe_2SiCl$, $Et_2Zn$, THF | low conversion |
| 4 | Li, $PhMe_2SiCl$, CuCN, THF | 80% |

**Table 2.65.** Meylation of Ketone **2.175**.

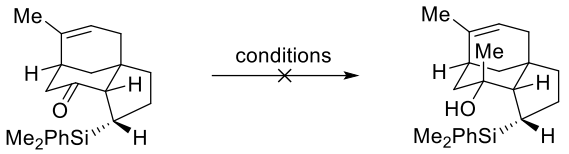


**2.175** **2.176**

| Entry | Conditions | Results |
|---|---|---|
| 1 | MeLi (1.5 equiv), THF, -78 °C | low conversion |
| 2 | MeLi (1.5 equiv), THF, 0 °C | messy |
| 3 | MeLi (3 equiv), THF, -78 °C | n.d. |
| 4 | MeMgBr (3 equiv), THF, 0 °C | n.d. |

Due to the failure of methylation of ketone **2.175**, we tried to oxidize *β*-silyl ketone **2.175** to *β*-hydroxyl ketone **2.177** firstly, which could make the carbonyl group to be less sterically hindered (Scheme 2.38). Fleming-Tamao oxidation of ketone **2.175** successfully furnished ketone **2.177** in

11% yield. Using $LaCl_3$ as a chelating reagent, methylation of ketone **2.177** was achieved to give diol **2.178** in 46% yield and as a single diastereomer under 2 mg scale.

**Scheme 2.38.** Oxidation of Ketone **2.175** and Methylation of Ketone **2.177**.

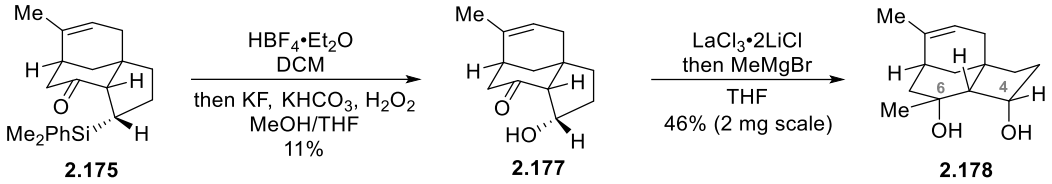


At this stage, we have proved that diol **2.178** could be obtained from ketone **2.177** (Scheme 2.38). However, Fleming-Tamao oxidation[50] of ketone **2.175** only gave 11% yield. Thus, an alternative method needed to be established to synthesize ketone **2.177** in high efficiency. Besides 1,4-silylation of enone, 1,4-boration of enone is also well established.[51] We found that boration of enone **2.173** followed by oxidation delivered ketone **2.177** in high yield and the same diastereo-selectivity as silylation (Scheme 2.39). This approach could also be realized in one step. Methylation[52] of ketone **2.177** furnished diol **2.178** in 88% yield as a single diastereomer.

**Scheme 2.39.** Preparation of Diol through Hoveyda *β*-Boration.

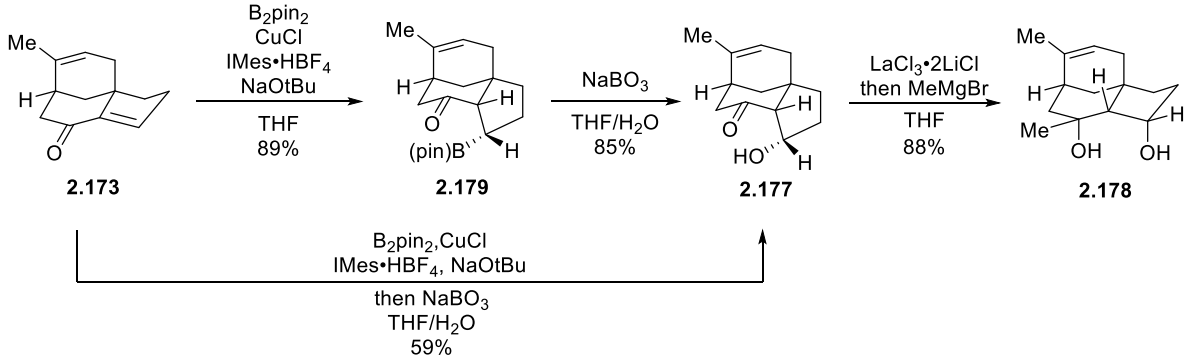


However, oxidation of diol **2.178** was challenged, since β-hydroxyl ketone **2.134** was easy to undergo dehydration to give enone **2.181**. IBX oxidation with DMSO as solvent (entry 1, Table

2.66) and DMP oxidation (entry 2, Table 2.66) only gave elimination product. Ley oxidation delivered desired ketone **2.134**, but the conversion of this reaction is low (entry 3, Table 2.66). Finally, we found IBX oxidation in ethyl acetate[53] afforded ketone **2.134** in 67% yield (entry 4, Table 2.66).

**Table 2.66.** Oxidation of Diol **2.178**.

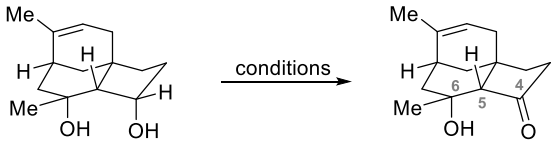


**2.178** **2.134**

| Entry | Conditions | Results |
|---|---|---|
| 1 | IBX, DMSO, 90 °C | **2.180** + **2.181** |
| 2 | DMP, NaHCO3, DCM, RT | **2.181** + **2.182** |
| 3 | TPAP, NMO, DCM, RT | **2.134** + **2.178** |
| 4 | IBX, EA, 80 °C | 93% **2.134** |

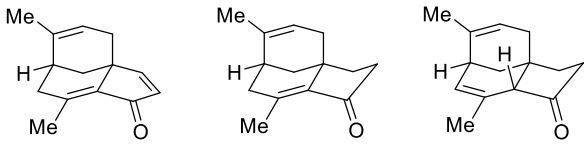


**2.180** **2.181** **2.182**

With ketone **2.134** in hand, we tried to synthesize enone **2.185** through Saegusa oxidation, which used silyl enol ether **2.183** as an intermediate. Different bases were tested to prepare silyl enol ether **2.183** (Table 2.67). However, silyl enol ether **2.183** was only formed in good selectivity when LDA was used as base (entry 1, Table 2.67). And the condition delivered enol ether **2.183** in 28% yield with 35% starting material recovery. Other strong base, such as LiHMDS (entry 2-3, Table 2.67), NaHMDS (entry 4, Table 2.67) and KHMDS (entry 5, Table 2.67), either gave poor selectivity between enol ether **2.183** and **2.184**, or only delivered enol ether **2.184**. The following Saegusa oxidation of enol ether **2.183** worked smoothly to deliver enone **2.185** in 99% yield

(Scheme 2.40). In contrast, Saegusa oxidation of silyl enol ether **2.184** gave very low conversion, which may due to the high steric hinderance caused by TMS protected tertiary alcohol.

**Table 2.67.** Preparation of Silyl Enol Ether **2.183**.

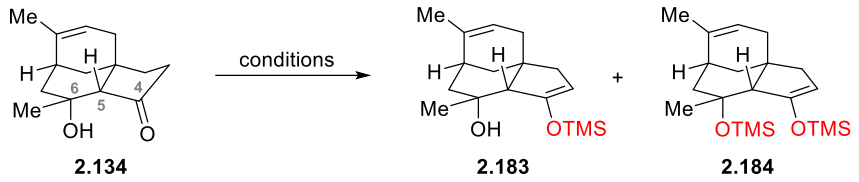


**2.134** **2.183** **2.184**

| Entry | Conditions | Results |
|---|---|---|
| 1 | $^{n}$BuLi, DIPA (distilled), THF, then TMSCl, -78 °C | 28% **2.183** + 35% **2.134** |
| 2 | LHMDS, THF, then TMSCl, -78 °C | low conversion |
| 3 | LHMDS, THF, then TMSCl, 0 °C | only **2.184** |
| 4 | NaHMDS, THF, then TMSCl, -78 °C | **2.134** + **2.183** + **2.184** |
| 5 | KHMDS, THF, then TMSCl, -78 °C | **2.183** (minor) + **2.184** (major) |

**Scheme 2.40.** Saegusa Oxidation of Silyl Enol Ether **2.183** and **2.184**.

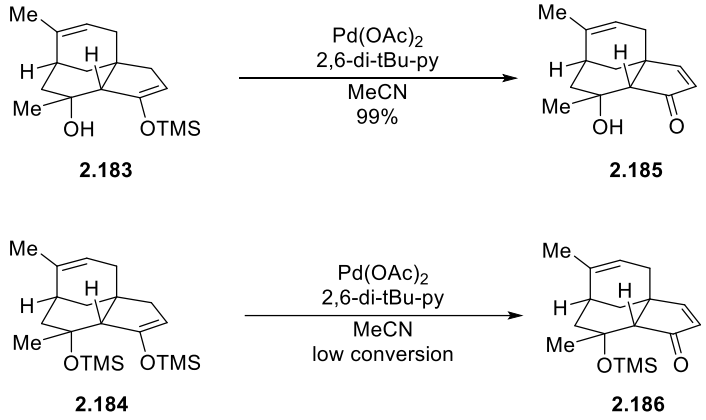


The two-step sequence to desaturate ketone **2.134** suffered from the low efficiency to form silyl enol ether **2.183**. Thus, we then moved to one-step desaturation of ketone **2.134**, which is highly challenged due to the presence of labile *β*-hydroxy group. We tested Ming's dehydrogenation (entry 1-5 Table 2.68),[54] Stahl's dehydrogenation (entry 6-7, Table 2.68),[44] Newhouse's dehydrogenation (entry 8-9, Table 2.68),[55] Nicolaou-Baran's hypervalent iodine (entry 10-11, Table 2.68),[41a, 41b] one-pot Saegusa oxidation (entry 12-13, Table 2.68) and one-pot

selenoxide elimination (entry 14, Table 2.68).[56] However, none of them gave the desired product. Eventually, using Mukaiyama's one-pot desaturation method[57] with N-*tert*-butyl phenylsulfinimidoyl chloride (**2.187**) as desaturation reagent delivered enone **2.185** in 51% yield without the need to protect C6 alcohol (entry 15, Table 2.68). The choice of base proved to be crucial in this reaction. Other lithium strong base such as LiHMDS and LiTMP gave much lower yield (entry 16-17, Table 2.68).

**Table 2.68.** One-Step Desaturation of Ketone **2.134**.

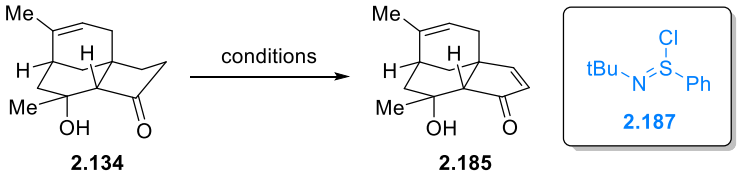


**2.134** **2.185**

| Entry | Conditions | Results |
|---|---|---|
| 1 | $Pt(COD)(TFA)_2$, BQ, BaO, PhCl, 80 °C | n.d. |
| 2 | $Pt(COD)Cl_2$, AgTFA, DAC, $Bu_2BOTf$, DIPEA, toluene | n.d. |
| 3 | CuTC, $CyPPh_2$, DTBP, benzene, 80 °C | n.d. |
| 4 | $Pt(COD)TFA_2$, DAC, $Bu_2BOTf$, DIPEA, toluene | n.d. |
| 5 | $Pd(TFA)_2$, DAC, $Bu_2BOTf$, DIPEA, toluene,50 °C | n.d. |
| 6 | $Pd(TFA)_2$, $O_2$, DMSO, 80 °C | n.d. |
| 7 | $Pd(OAc)_2$, $Cu(OAc)_2$, $O_2$, DMSO, 40 °C | n.d. |
| 8 | LiTMP, $ZnCl_2$, $[Pd(allyl)Cl]_2$, allylOPiv, THF | n.r. |
| 9 | LDA, $ZnCl_2$, $[Pd(allyl)Cl]_2$, allylOAc, THF | n.d. |
| 10 | IBX, MPO, DMSO, rt | n.r. |
| 11 | $HIO_3$, DMSO, 80 °C | n.d. |
| 12 | TMSOTf, PMP, DCM, then $Pd(OAc)_2$, MeCN | n.d. |
| 13 | $Bu_2BOTf$, 2,6-di-tBu-py, $Pd(OAc)_2$, MeCN | n.d. |
| 14 | LDA, PhSeBr, $NaIO_4$, THF | n.d. |
| 15 | LDA, then **2.187**, -78 °C | 51% |
| 16 | LHMDS, then **2.187**, -78 °C | trace |
| 17 | LiTMP, then **2.187**, -78 °C | 11% |

We then moved to investigate conjugated methylation of enone **2.185**. However, typical copper catalyzed or mediated methylation didn't give any desired product (entry 1-3, Table 2.69). Comparing with copper, nickel-mediated conjugated methylation[58] give desired ketone **2.188** in

52% yield, albeit in low diastereoselectivity (entry 6, Table 2.69). Later, we found that diastereoselective conjugated methylation of enone **2.185** was achieved when treated by stoichiometric amount of $CuBr{\cdot}SMe_2$ and methyl Grignard reagent,[59] which only generated convex-face methylation product ketone **2.188** (entry 9, Table 2.69).

**Table 2.69.** Conjugated Methylation of Enone **2.185**.

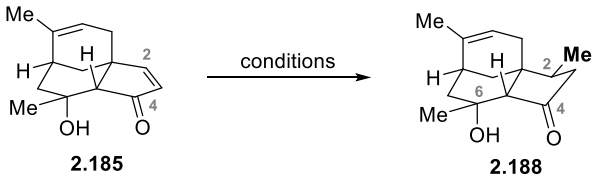


| Entry | Conditions | Result |
|---|---|---|
| 1 | MeLi, $CuBr{\bullet}SMe_2$, $Et_2O$ | n.r. |
| 2 | MeLi, CuI, $Et_2O$ | n.r. |
| 3 | MeMgBr, $CuBr{\bullet}SMe_2$, THF/HMPA, -40 °C to 0 °C | decomposed |
| 4 | $AlMe_3$, $Ni(acac)_2$ (0.2 equiv), THF | low conversion |
| 5 | $AlMe_3$, $Ni(acac)_2$ (0.5 equiv), THF | low conversion |
| 6 | $AlMe_3$, $Ni(acac)_2$ (1 equiv), THF | 52% (d.r. = 1.6:1) |
| 7 | $AlMe_3$, $Cu(OTf)_2$ (0.2 equiv), toluene | elimination |
| 8 | MeLi, $ZnBr_2$, $Ni(acac)_2$ (0.5 equiv), THF | n.d |
| 9 | $CuBr{\bullet}SMe_2$, MeMgBr, THF, -78 °C to 0 °C | 60% (d.r. > 20:1) |

In the end game, an alcohol directed *syn*-reduction[60] of ketone **2.188** by $NMe_4{\cdot}BH(OAc)_3$ delivered penicibilaene A (**2.1**) in 88% yield (Scheme 2.41). Penicibiaene B (**2.2**) can be further prepared from penicibilaene A in good yield via a chemo-selective acylation of the secondary alcohol.

**Scheme 2.41.** Synthesis of Penicibilaenes A and B.

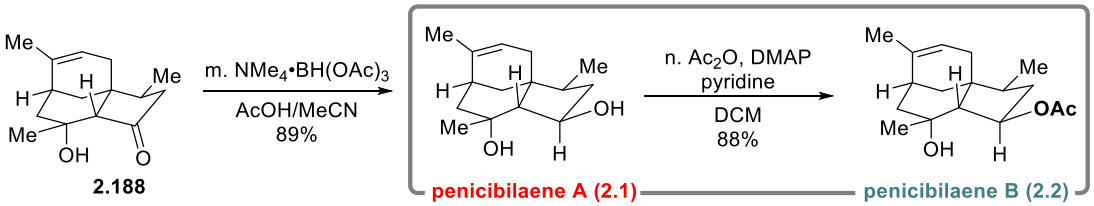

## 2.5. Conclusion

In summary, we have described the first total synthesis of penicibilaenes A (**2.1**) and B (**2.2**) in 13 and 14 steps, respectively, in the longest linear sequence from commercially available starting materials. The synthesis features a deconstructive formation of the tricyclic skeleton via C−C activation of cyclobutanones and the use of carbonyl desaturation relay to replace $\beta$-C−H bonds with the desired functional groups. Such a "C−C/C−H" approach may inspire alternative bond-disconnecting strategies for natural product syntheses. In addition, the discovery of a new linker system and a Lewis acid effect in the Rh-catalyzed "cut-and-sew" reaction between cyclobutanones and bulky alkenes could have broader implications on preparing other all-carbon bridged/fused rings.

(Some contents of this chapter were published in *J. Am. Chem. Soc.* **2021**, DOI: 10.1021/jacs.1c04335)

## 2.6. Experimental

### 2.6.1 General Information

Unless noted otherwise, all solvents were dried by filtration through a Pure-Solv MD-5 Solvent Purification System (Innovative Technology), all reactions were carried out under nitrogen atmosphere, all commercially available substrates were used without further purification. Thin layer chromatography (TLC) analysis was run on silica gel plates purchased from EMD Chemical (silica gel 60, F254). Infrared spectrum was recorded on a Nicolet iS5 FT-IR Spectrometer. Samples were scanned as neat liquids or dissolved in dichloromethane on potassium bromide (KBr)

salt plates. Frequencies were reported in reciprocal centimeters ($cm^{-1}$). High-resolution mass spectra (HRMS) were obtained on an Agilent 6224 TOF-MS spectrometer and were reported for the molecular ion $[M]^+$, $[M+Na]^+$, or $[M+H]^+$. Nuclear magnetic resonance (NMR) spectrum ($^1H$ NMR and $^{13}C$ NMR) were recorded with a 400 MHz Bruker Avance-III-HD nanobay spectrometer equipped with a BBFO SmartProbe (400 MHz for $^1H$, 101 MHz for $^{13}C$) or a 500 MHz Bruker Avance-III spectrometer equipped with a $^1H$ ($^{13}C$,$^{31}P$) TXI probe (500 MHz for $^1H$, 126 MHz for $^{13}C$). For $CDCl_3$ solutions, the chemical shifts were reported as parts per million (ppm) referenced to residual protium or carbon of the solvents: $CHCl_3$ δ H (7.26 ppm) and $CDCl_3$ δ C (77.00 ppm). For actone-D6 solutions, the chemical shifts were reported as parts per million (ppm) referenced to residual protium or carbon of the solvents: acetone-D6 δ H (2.05 ppm) and acetone-D6 δ C (29.84 ppm). Coupling constants were reported in Hertz (Hz). Data for $^1H$ NMR spectra were reported as following: chemical shift (δ, ppm), multiplicity (br = broad, s = singlet, d = doublet, t = triplet, q = quartet, dd = doublet of doublets, td = triplet of doublets, ddd = doublet of doublet of doublets, m = multiplet), coupling constant (Hz), and integration.

### 2.6.2 Experimental Procedure and Characterization Data

*Synthesis of compound **2.20***

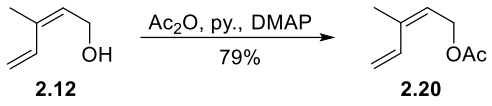

**2.12** **2.20**

To a solution of compound **2.12** (200 mg, 2.04 mmol) in DCM (10 mL) was added pyridine (250 μL, 3.06 mmol), $Ac_2O$ (230 μL, 2.45 mmol) and DMAP (25 mg, 0.20 mmol). After stirring at room temperature for 2 h, the reaction mixture was quenched by sat. $NH_4Cl$, extracted by DCM. The

organic phase was dried with $Na_2SO_4$ and concentrated under reduced pressure. The residue was purified by column chromatography (silica gel, hexane:EA = 15:1 to 10:1) to give compound **2.20** (227.1 mg, 79% yield) as a colorless oil.

$R_f$ = 0.6 (hexane:EA = 4:1)

**$^1$H NMR** (500 MHz, Chloroform-d) δ 6.75 (ddd, J = 17.2, 10.8, 0.9 Hz, 1H), 5.52 (t, J = 7.3 Hz, 1H), 5.33 (dt, J = 17.2, 1.0 Hz, 1H), 5.22 (dt, J = 10.8, 1.6 Hz, 1H), 4.72 (dd, J = 7.3, 1.1 Hz, 2H), 2.06 (s, 3H), 1.88 (q, J = 1.1 Hz, 3H).

*Synthesis of compound **2.22***

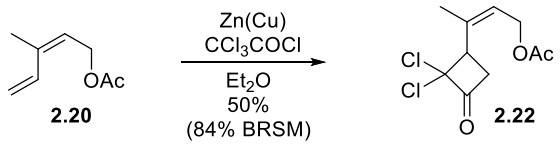


To a solution of compound **2.20** (50 mg, 0.36 mmol) in $Et_2O$ (4 mL) was added Zn(Cu) (71 mg, 1.08 mmol), $CCl_3COCl$ (100 μL, 0.9 mmol). After sonicating at room temperature for 1 h, the reaction mixture was quenched by saturated $NaHCO_3$ solution, then filtered through Celite, extracted by $Et_2O$. The organic phase was dried with $Na_2SO_4$ and concentrated under reduced pressure. The residue was purified by column chromatography (silica gel, hexane:EA = 15:1 to 10:1) to give the substrate **2.20** (14.0 mg) and compound **2.22** (36.2 mg, 40% yield, 56% BRSM) as yellow oil.

$R_f$ = 0.3 (hexane:EA = 4:1)

**$^1$H NMR** (500 MHz, Chloroform-d) δ 5.85 (ddt, J = 8.6, 5.6, 1.5 Hz, 1H), 4.90 – 4.80 (m, 1H), 4.52 (ddq, J = 13.0, 5.6, 1.5 Hz, 1H), 4.09 (t, J = 9.9 Hz, 1H), 3.54 – 3.39 (m, 2H), 2.07 (s, 3H), 1.86 (d, J = 1.6 Hz, 3H).

*Synthesis of compound **2.16***

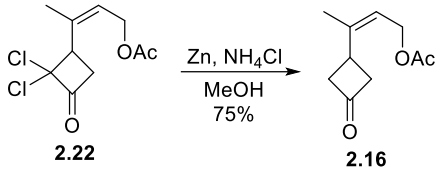


To a solution of compound **2.22** (10.6 g, 42.4 mmol) in MeOH (440 mL, 0.1 M) was added $NH_4Cl$ (22.5 g, 420 mmol) and Zn(Cu) powder (13.8 g, 210 mmol). After stirring at room temperature for 1 h, the reaction mixture was filtered through Celite. The organic phase was concentrated under reduced pressure. The residue was dilute in water and extracted by DCM. The organic phase was dried by $Na_2SO_4$ and concentrated under reduced pressure. The residue was purified by column chromatography (silica gel, hexane:EA = 20:1 to 10:1) to give the compound **2.16** (5.77 g, 75% yield) as colorless oil.

$R_f$ = 0.4 (hexane:EA = 2:1)

**$^1$H NMR** (500 MHz, Chloroform-d) δ 5.49 (tq, J = 7.1, 1.3 Hz, 1H), 4.62 (dd, J = 7.3, 1.0 Hz, 2H), 3.62 – 3.53 (m, 1H), 3.25 – 3.06 (m, 4H), 2.05 (s, 2H), 1.84 (q, J = 1.1 Hz, 3H).

*Synthesis of compound **2.6***

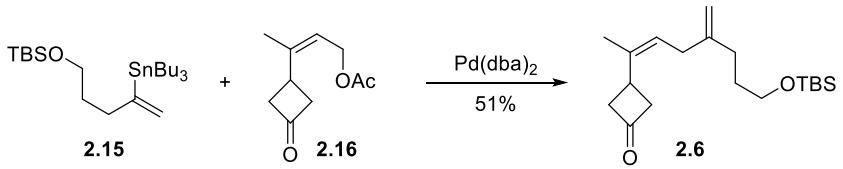


A flame dried flask was charged with LiCl (35 mg, 0.81 mmol), compound **2.15** (200 mg, 0.41 mmol), compound **2.16** (50 mg, 0.27 mmol), DMF (3 mL) and $Pd(dba)_2$ (16 mg, 0.027 mmol). The reaction mixture was degassed for 10 min with nitrogen buddle. After stirring at 70 °C for 2 h, the reaction mixture was quenched by water and extracted by ether. The organic phase was washed by brine, dried by $Na_2SO_4$ and concentrated under reduced pressure. The residue was purified by column chromatography (silica gel, hexane:EA = 100:1 to 50:1) to give the compound **2.6** (45.0 mg, 52% yield) as colorless oil.

$R_f$ = 0.4 (hexane:EA = 4:1)

**$^1$H NMR** (500 MHz, Chloroform-d) δ 5.34 (ddt, J = 8.7, 7.3, 1.3 Hz, 1H), 4.73 (ddd, J = 7.0, 2.0, 1.0 Hz, 2H), 3.62 (t, J = 6.5 Hz, 2H), 3.17 – 2.96 (m, 5H), 2.77 (d, J = 7.3 Hz, 2H), 2.09 – 2.03 (m, 2H), 1.70 – 1.68 (m, 3H), 1.68 – 1.63 (m, 2H), 0.89 (s, 9H), 0.05 (s, 6H).

**$^{13}$C NMR** (101 MHz, $CDCl_3$) δ 207.2, 148.3, 136.6, 125.3, 122.3, 109.5, 63.0, 51.2, 34.9, 34.7, 32.5, 31.4, 31.1, 26.1, 24.3, 18.8, 18.5, 14.3, -5.1.

*Synthesis of compound **2.24***

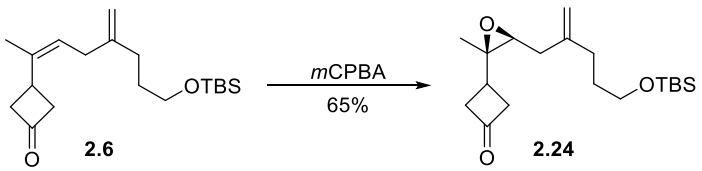

To a solution of compound **2.6** (45 mg, 0.14 mmol) in DCM (3 mL) was added *m*CPBA (34 mg, 0.20 mmol) at –10 °C. After stirring at –10 °C for 30 min, the reaction mixture was quenched by $NaHCO_3$ (sat. in $H_2O$) and $Na_2S_2O_3$ (sat. in $H_2O$) and extracted by DCM. The organic phase was washed by brine, dried by $Na_2SO_4$ and concentrated under reduced pressure. The residue was purified by column chromatography (silica gel, hexane:EA = 50:1 to 20:1) to give the compound **2.24** (30.7 mg, 65% yield) as colorless oil.

$R_f$ = 0.3 (hexane:EA = 4:1)

**$^1$H NMR** (500 MHz, Chloroform-d) δ 4.86 (s, 1H), 4.82 (s, 1H), 3.63 (t, J = 6.4 Hz, 2H), 3.08 – 3.04 (m, 2H), 2.87 – 2.78 (m, 3H), 2.70 (p, J = 8.0 Hz, 1H), 2.38 (dd, J = 15.6, 6.3 Hz, 1H), 2.25 (dd, J = 15.6, 6.2 Hz, 1H), 2.15 – 2.10 (m, 2H), 1.72 – 1.64 (m, 2H), 1.35 (s, 3H), 0.89 (s, 9H), 0.05 (s, 6H).

**$^{13}$C NMR** (101 MHz, CDCl3) δ 205.55, 145.73, 111.15, 62.75, 59.96, 49.05, 46.75, 35.33, 33.05, 30.98, 29.27, 26.10, 15.99, -5.13.

*Synthesis of compound **2.27***

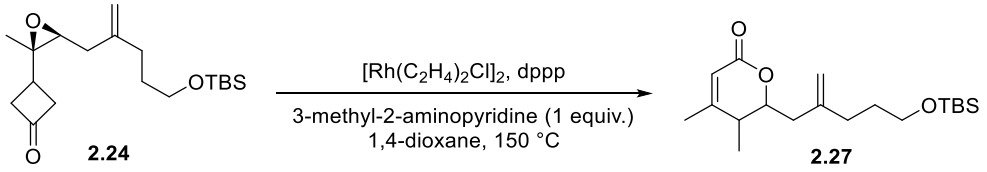


A flame dried vial was charged with $[Rh(C_2H_4)_2Cl]_2$ (1.2 mg, 0.003 mmol), dppp (2.7 mg, 0.0066 mmol), 3-methyl-2-amino-pyridine (3.2 mg, 0.03 mmol), compound **2.24** (10 mg, 0.03 mmol) and dioxane (0.5 mL) in glove box. Then the vial was sealed and removed from glovebox. The reaction

was stirred at 150 °C overnight, before cooled to room temperature. Then the solvent was removed under reduced pressure. The residue was purified by column chromatography (silica gel) to give the compound **2.27** as colorless oil.

**$^1$H NMR** (500 MHz, Chloroform-d) δ 5.75 (q, J = 1.4 Hz, 1H), 4.91 – 4.88 (m, 2H), 4.52 (td, J = 7.2, 3.0 Hz, 1H), 3.62 (t, J = 6.3 Hz, 2H), 2.55 (dd, J = 14.5, 7.1 Hz, 1H), 2.33 (dd, J = 14.6, 7.3 Hz, 1H), 2.17 – 2.07 (m, 3H), 1.99 (d, J = 1.4 Hz, 3H), 1.72 – 1.62 (m, 2H), 1.07 (d, J = 7.1 Hz, 3H), 0.89 (s, 9H), 0.04 (s, 6H).

**$^{13}$C NMR** (101 MHz, CDCl3) δ 163.89, 144.02, 115.86, 112.98, 78.06, 62.65, 38.02, 36.82, 32.26, 30.97, 26.09, 21.59, 18.47, 10.61, -5.14.

*Synthesis of compound **2.31***

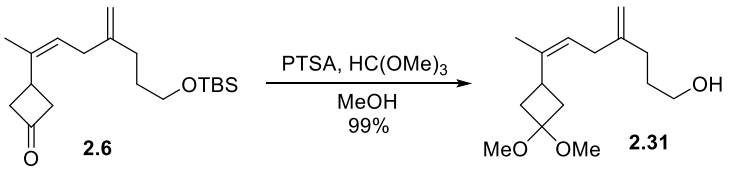


To a solution of compound **2.6** (400 mg, 1.24 mmol) in MeOH (12 mL) was added $HC(OMe)_3$ (0.4 mL, 3.7 mmol) and PTSA (23 mg, 0.12 mmol). After stirring at room temperature for 3 h, the reaction mixture was concentrated under reduced pressure. The residue was then diluted by DCM, quenched by $NaHCO_3$ (saturated in $H_2O$) and extracted by DCM. The organic phase was dried by $Na_2SO_4$ and concentrated under reduced pressure to give the crude compound **2.31** (327 mg, 1.29 mmol, 100% yield) as a colorless oil.

$R_f$ = 0.1 (hexane:EA = 4:1)

**$^1$H NMR** (500 MHz, Chloroform-d) δ 5.18 (tt, J = 7.3, 1.6 Hz, 1H), 4.75 (s, 2H), 3.66 (q, J = 6.3 Hz, 2H), 3.18 (s, 3H), 3.14 (s, 3H), 2.74 (d, J = 7.7 Hz, 2H), 2.67 – 2.62 (m, 1H), 2.37 – 2.30 (m, 2H), 2.09 (q, J = 8.8, 8.3 Hz, 2H), 1.95 (td, J = 9.4, 2.8 Hz, 2H), 1.77 – 1.68 (m, 2H), 1.59 (s, 3H), 1.39 (t, J = 5.6 Hz, 1H).

*Synthesis of compound **2.32***

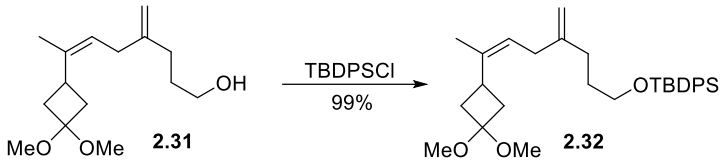


To a solution of compound **2.31** (327 mg, 1.3 mmol) in DCM (8 mL) was added imidazole (140 mg, 2.0 mmol) and TBDPSCl (440 mg, 1.6 mmol). After stirring at room temperature overnight, the reaction mixture was quenched by $NH_4Cl$ (saturated in $H_2O$) and extracted by DCM. The organic phase was dried by $Na_2SO_4$ and concentrated under reduced pressure. The residue was purified by column chromatography (silica gel) to give the compound **2.32** (680.3 mg, 1.4 mmol, 100% yield) as colorless oil.

$R_f$ = 0.6 (hexane:EA = 4:1)

**$^1$H NMR** (500 MHz, Chloroform-d) δ 7.69 (ddt, J = 24.3, 6.5, 1.6 Hz, 4H), 7.44 – 7.35 (m, 6H), 5.17 (tt, J = 7.3, 1.5 Hz, 1H), 4.73 – 4.66 (m, 2H), 3.67 (t, J = 6.4 Hz, 2H), 3.19 (s, 3H), 3.13 (s, 3H), 2.70 (d, J = 7.4 Hz, 2H), 2.66 – 2.60 (m, 1H), 2.37 – 2.29 (m, 2H), 2.08 (q, J = 6.9, 6.1 Hz, 2H), 1.94 (td, J = 9.4, 2.8 Hz, 2H), 1.74 – 1.67 (m, 2H), 1.56 (s, 3H), 1.05 (s, 9H).

*Synthesis of compound **2.33***

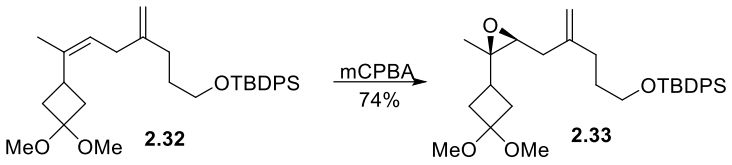


To a solution of compound **2.32** (680 mg, 1.38 mmol) in DCM (20 mL) was added *m*CPBA at –20 °C. After stirring at –20 °C for 2 h, the reaction mixture was quenched by $Na_2S_2O_3$ (saturated in $H_2O$) and $NaHCO_3$ (saturated in $H_2O$), extracted by DCM. The organic phase was washed by $NaHCO_3$ (saturated in $H_2O$), dried by $Na_2SO_4$ and concentrated under reduced pressure. The residue was purified by column chromatography (silica gel) to give the compound **2.33** (517.7 mg, 74% yield) as colorless oil.

$R_f$ = 0.5 (hexane:EA = 4:1)

**$^1$H NMR** (400 MHz, Chloroform-d) δ 7.69 (ddd, J = 20.9, 7.8, 1.7 Hz, 4H), 7.45 – 7.34 (m, 6H), 4.80 (s, 1H), 4.78 (s, 1H), 3.67 (t, J = 6.3 Hz, 2H), 3.16 (s, 3H), 3.11 (s, 3H), 2.77 (t, J = 6.3 Hz, 1H), 2.36 – 2.22 (m, 3H), 2.20 – 2.10 (m, 3H), 2.06 – 1.90 (m, 2H), 1.82 – 1.67 (m, 3H), 1.21 (s, 3H), 1.05 (s, 9H).

*Synthesis of compound **2.34***

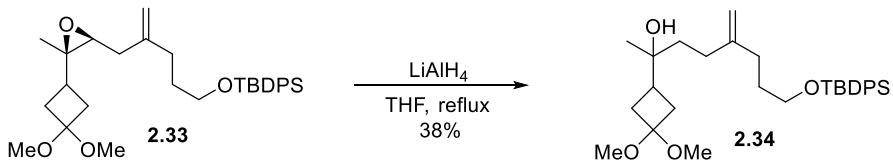

To a solution of compound **2.33** (518 mg, 1.02 mmol) in THF (10 mL) was added $LiAlH_4$ (116 mg, 3.06 mmol) at 0 °C. After stirring at 70 °C for 3 h, the reaction mixture was quenched by EA, then added water (120 μL), 15% NaOH (240 μL), water (360 μL) and filtered through Celite. The organic phase was concentrate under reduced pressure. The residue was purified by column chromatography (silica gel) to give the compound **2.34** (199.5 mg, 38% yield) as colorless oil.

$R_f$ = 0.3 (hexane:EA = 4:1)

**$^1$H NMR** (400 MHz, Chloroform-d) δ 7.69 – 7.63 (m, 4H), 7.46 – 7.35 (m, 6H), 4.71 (s, 1H), 4.70 (s, 1H), 3.67 (t, J = 6.4 Hz, 2H), 3.18 (s, 3H), 3.14 (s, 3H), 2.20 – 1.99 (m, 11H), 1.74 – 1.64 (m, 3H), 1.57 (s, 3H), 1.05 (s, 9H).

*Synthesis of compound **2.35***

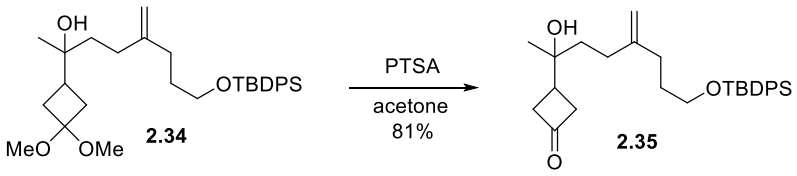


To a solution of compound **2.34** (50 mg, 0.10 mmol) in acetone (2 mL) was added PTSA (2 mg, 0.010 mmol) at room temperature. After stirring at room temperature overnight, the reaction mixture was concentrated under reduced pressure. The residue was diluted by DCM, quenched by $NaHCO_3$ (saturated in $H_2O$) and extracted by DCM. The organic phase was dried by $Na_2SO_4$ and concentrated under reduced pressure. The residue was purified by column chromatography (silica gel) to give the compound **2.35** (37.1 mg, 81% yield) as colorless oil.

$R_f$ = 0.3 (hexane:EA = 4:1)

**$^1$H NMR** (400 MHz, Chloroform-d) δ 7.70 – 7.63 (m, 4H), 7.46 – 7.34 (m, 6H), 4.74 (dd, J = 4.7, 1.6 Hz, 2H), 3.68 (t, J = 6.3 Hz, 2H), 3.17 – 3.06 (m, 2H), 2.97 – 2.81 (m, 2H), 2.42 (tt, J = 8.7, 7.5 Hz, 1H), 2.10 (dt, J = 14.8, 7.1 Hz, 5H), 1.75 – 1.61 (m, 4H), 1.22 (s, 3H), 1.05 (s, 9H).

*Synthesis of compound **2.36***

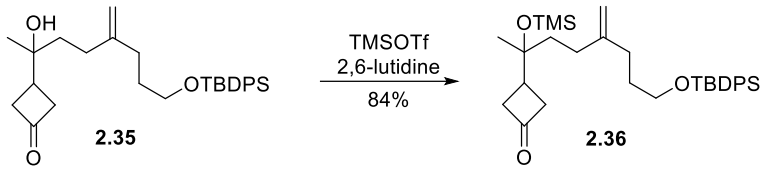


To a solution of compound **2.35** (80 mg, 0.17 mmol) in DCM (3.5 mL) was added 2,6-lutidine (70 μL, 0.60 mmol) and TMSOTf (70 μL, 0.38 mmol) at 0 °C. After stirring at 0 °C for 20 min, the reaction mixture was quenched by $NaHCO_3$ (saturated in $H_2O$) and extracted by DCM. The organic phase was dried by $Na_2SO_4$ and concentrated under reduced pressure. The residue was purified by column chromatography (silica gel, hexane:EA = 20:1 to 10:1) to give the compound **2.36** (76.7 mg, 84% yield) as colorless oil.

$R_f$ = 0.7 (hexane:EA = 4:1)

**$^1$H NMR** (400 MHz, Chloroform-d) δ 7.69 – 7.64 (m, 4H), 7.44 – 7.34 (m, 6H), 4.72 – 4.69 (m, 2H), 3.67 (t, J = 6.3 Hz, 2H), 3.14 – 3.00 (m, 2H), 2.90 – 2.72 (m, 2H), 2.36 (tt, J = 8.4, 7.0 Hz, 1H), 2.13 – 2.07 (m, 2H), 1.97 (t, J = 8.3 Hz, 2H), 1.74 – 1.61 (m, 4H), 1.23 (s, 3H), 1.05 (s, 9H), 0.12 (s, 9H).

**$^{13}$C NMR** (101 MHz, CDCl3) δ 207.92, 149.36, 135.70, 134.13, 129.70, 127.75, 109.05, 75.65, 63.65, 47.61, 47.37, 40.34, 33.26, 32.58, 31.52, 30.96, 27.00, 25.51, 19.37, 2.65.

*Synthesis of compound **2.38***

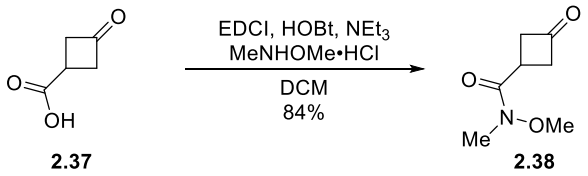


**2.37** **2.38**

To a solution of compound **11**(200 mg, 1.75 mmol) in DCM (9 mL) was added MeNHOMe·HCl (170 mg, 1.75 mmol), HOBt·$H_2O$ (300 mg, 1.93 mmol), EDCI (370 mg, 1.93 mmol) and $NEt_3$ (0.48 mL, 3.5 mmol) at room temperature. After stirring at RT for 10 h, the reaction mixture was quenched by $H_2O$ and extracted by DCM. The organic phase was dried by $Na_2SO_4$ and concentrated under reduced pressure. The residue was purified by column chromatography (silica gel, hexane:EA = 1:1) to give amide **2.38** (231.0 mg, 84% yield) as a colorless oil.

**$^1$H NMR** (400 MHz, Chloroform-*d*) δ 3.72 (s, 3H), 3.63 – 3.53 (m, 1H), 3.52 – 3.42 (m, 2H), 3.25 (s, 3H), 3.23 – 3.15 (m, 2H).

*Synthesis of compound **2.39***

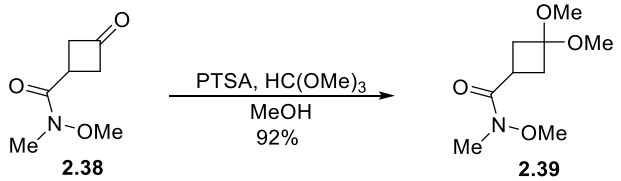


**2.38** **2.39**

To a solution of compound **2.38** (2.75 g, 17.5 mmol) in MeOH (170 mL) was added $HC(OMe)_3$ (5.8 mL, 52.5 mmol) and TsOH·$H_2O$ (330 mg, 1.75 mmol) at room temperature. After stirring at

room temperature for 3 h, the reaction mixture was concentrated under reduced pressure. The residue was diluted by DCM, quenched by $NaHCO_3$ (saturated in $H_2O$) and extracted by DCM. The organic phase was dried by $Na_2SO_4$ and concentrated under reduced pressure. The residue was purified by column chromatography (silica gel, hexane:EA = 1:1) to give ketal **2.39** (3.27 g, 92% yield) as a colorless oil.

**$^1$H NMR** (400 MHz, Chloroform-*d*) δ 3.66 (s, 3H), 3.19 (s, 3H), 3.19 (s, 3H), 3.14 – 3.17 (m, 4H), 2.40 (s, 2H), 2.38 (s, 2H).

*Synthesis of compound **2.40***

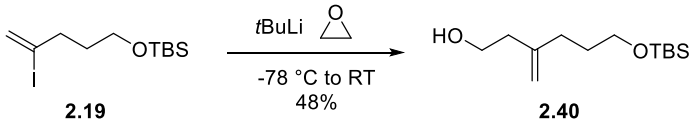


To a solution of compound **2.19** (1.0 g, 3.1 mmol) in THF (30 mL) was added *t*BuLi (1.7 M in pentane, 4 mL, 6.7 mmol) at −78 °C. After stirring at −78 °C for 30 min, the reaction mixture was added ethylene oxide (1.2 M in hexane, 5.2 mL, 6.2 mmol) at −78 °C. After stirring at room temperature for 1 h, the reaction mixture was quenched by saturated $NH_4Cl$ and extracted by EA. The organic phase was dried by $Na_2SO_4$ and concentrated under reduced pressure. The residue was purified by column chromatography (silica gel, hexane:EA = 10:1) to give alcohol **2.40** (0.36 g, 48% yield) as a colorless oil.

$R_f$ = 0.4 (hexane:EA = 2:1)

**$^1$H NMR** (500 MHz, Chloroform-*d*) δ 4.88 (q, *J* = 1.6 Hz, 1H), 4.85 – 4.81 (m, 1H), 3.72 (q, *J* = 6.1 Hz, 2H), 3.62 (t, *J* = 6.4 Hz, 2H), 2.31 (td, *J* = 6.3, 1.2 Hz, 2H), 2.09 (t, *J* = 7.8 Hz, 2H), 1.71 – 1.63 (m, 2H), 1.48 (t, *J* = 5.9 Hz, 1H), 0.89 (s, 9H), 0.05 (s, 6H).

*Synthesis of compound **2.41***

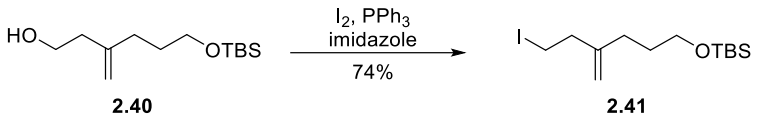


**2.40** **2.41**

To a solution of $PPh_3$ (130 mg, 0.49 mmol) in DCM (3 mL) was added $I_2$ (135 mg, 0.53 mmol). After stirring at room temperature for 30 min, the reaction mixture was added imidazole (36 mg, 0.53 mmol) and compound **2.40** (100 mg, 0.41 mmol) in DCM (1 mL) at 0 °C. After stirring at room temperature for 3 h, the reaction mixture was flashed through silica gel (hexane:EA = 10:1) and quenched by saturated $Na_2S_2O_3$. The organic phase was concentrated under reduced pressure to give compound **2.41** (145.8 mg, 74% yield) as a colorless oil.

$R_f$ = 0.9 (hexane:EA = 2:1)

**$^1$H NMR** (400 MHz, Chloroform-*d*) δ 4.87 (s, 1H), 4.79 (s, 1H), 3.61 (t, *J* = 6.3 Hz, 2H), 3.25 (t, *J* = 7.7 Hz, 2H), 2.60 (t, *J* = 7.6 Hz, 2H), 2.07 (t, *J* = 7.9 Hz, 2H), 1.69 – 1.60 (m, 2H), 0.89 (s, 9H), 0.05 (s, 6H).

*Synthesis of compound **2.42***

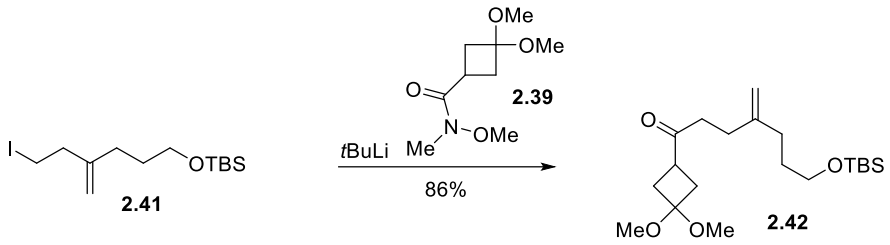


To a solution of compound **2.41** (550 mg, 1.15 mmol) in $Et_2O$ (8 mL) was added *t*BuLi (1.7 M in pentane, 1.4 mL, 2.4 mmol) at −78 °C. After stirring at −78 °C for 30 min, the reaction mixture was added compound **2.39** (260 mg, 1.26 mmol) in $Et_2O$ (2 mL) at −78 °C. After stirring at −78 °C for 10 min, the reaction mixture was warmed to room temperature slowly. After stirring at room temperature for 10 h, the reaction mixture was quenched by $NH_4Cl$ (saturated in $H_2O$) and extracted by $Et_2O$. The organic phase was dried by $Na_2SO_4$ and concentrated under reduced pressure. The residue was purified by column chromatography (silica gel, hexane:EA = 20:1) to give ketone **2.42** (367.0 mg, 86% yield) as a colorless oil.

$R_f$ = 0.5 (hexane:EA = 4:1)

**$^1$H NMR** (400 MHz, Chloroform-*d*) δ 4.74 (s, 1H), 4.68 (s, 1H), 3.60 (t, *J* = 6.4 Hz, 2H), 3.17 (s, 3H), 3.13 (s, 3H), 2.98 (p, *J* = 8.6 Hz, 1H), 2.58 – 2.53 (m, 2H), 2.38 – 2.26 (m, 6H), 2.08 – 2.03 (m, 2H), 1.69 – 1.60 (m, 2H), 0.89 (s, 9H), 0.04 (s, 6H).

*Synthesis of compound **2.43***

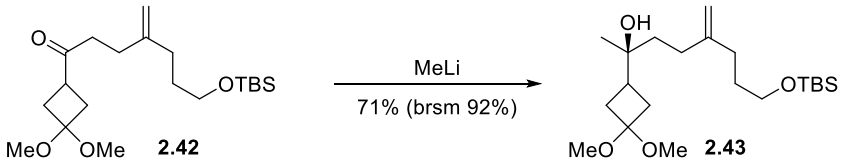

To a solution of compound **2.42** (370 mg, 1.0 mmol) in THF (10 mL) was added MeLi (1.6 M in $Et_2O$, 0.75 mL, 1.2 mmol) at −78 °C. After stirring at −78 °C for 30 min, the reaction mixture was quenched by saturated $NH_4Cl$ and extracted by $Et_2O$. The organic phase was dried by $Na_2SO_4$ and concentrated under reduced pressure. The residue was purified by column chromatography (silica gel, hexane:EA = 10:1) to recover compound **2.42** (84.8 mg) and give alcohol **2.43** (275.0 mg, 71% yield, 92% BRSM) as a colorless oil.

$\boldsymbol{R_f}$ = 0.4 (hexane:EA = 2:1)

**$^1$H NMR** (500 MHz, Chloroform-*d*) δ 4.72 (d, *J* = 4.5 Hz, 2H), 3.61 (t, *J* = 6.5 Hz, 2H), 3.18 (s, 3H), 3.14 (s, 3H), 2.18 – 2.12 (m, 4H), 2.09 – 2.03 (m, 6H), 1.68 – 1.62 (m, 2H), 1.46 (ddd, *J* = 13.6, 11.3, 5.8 Hz, 2H), 1.10 (s, 3H), 0.89 (s, 9H), 0.05 (s, 6H).

*Synthesis of compound **2.44***

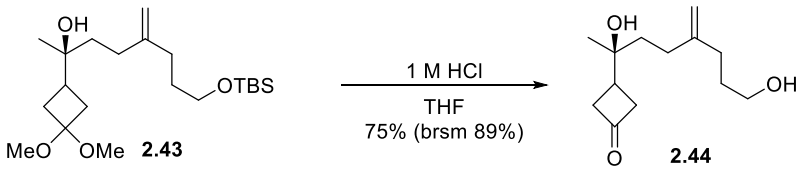


To a solution of compound **2.43** (275 mg, 0.71 mmol) in THF (6 mL) was added HCl (1 M in $H_2O$, 2 mL). After stirring at room temperature for 1 h, the reaction mixture was quenched by $NaHCO_3$ (saturated in $H_2O$) and extracted by EA. The organic phase was dried by $Na_2SO_4$ and concentrated under reduced pressure to give diol **2.44** (121.2 mg, 75% yield, 89% BRSM) as a colorless oil.

**$^1$H NMR** (400 MHz, Chloroform-*d*) δ 4.79 (s, 2H), 3.68 (t, *J* = 6.4 Hz, 2H), 3.17 – 3.09 (m, 2H), 2.99 – 2.83 (m, 2H), 2.44 (tt, *J* = 8.6, 7.4 Hz, 1H), 2.14 (dd, *J* = 9.4, 6.2 Hz, 4H), 1.77 – 1.64 (m, 4H), 1.23 (s, 3H).

*Synthesis of compound **2.35***

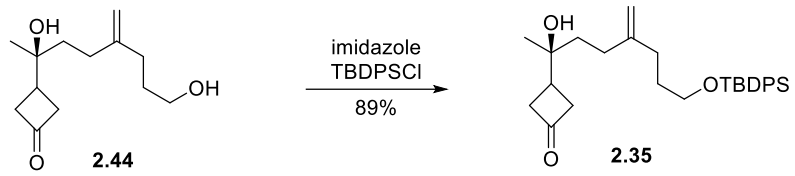


To a solution of compound **2.44** (120 mg, 0.53 mmol) in DCM (5 mL) was added imidazole (110 mg, 1.06 mmol) and TBDPSCl (210 μL, 0.80 mmol) at room temperature. After stirring at room temperature for 10 h, the reaction mixture was quenched by saturated $NH_4Cl$ and extracted by DCM. The organic phase was dried by $Na_2SO_4$ and concentrated under reduced pressure. The residue was purified by column chromatography (silica gel, hexane:EA = 20:1) to give alcohol **2.35** (219.5 mg, 89% yield) as a colorless oil.

**$^1$H NMR** (400 MHz, Chloroform-*d*) δ 7.69 – 7.64 (m, 4H), 7.46 – 7.34 (m, 6H), 4.77 – 4.72 (m, 2H), 3.68 (t, *J* = 6.3 Hz, 2H), 3.18 – 3.05 (m, 2H), 2.97 – 2.81 (m, 2H), 2.42 (p, *J* = 7.9 Hz, 1H), 2.17 – 2.02 (m, 4H), 1.75 – 1.63 (m, 4H), 1.22 (s, 3H), 1.05 (s, 9H).

*Synthesis of compound **2.51***

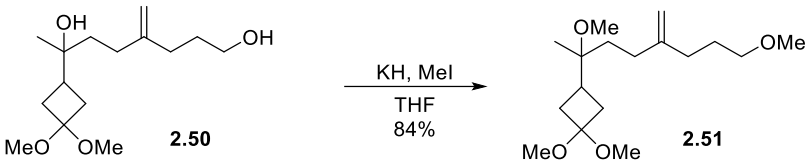


To a suspension of KH (0.69 g, 17.2 mmol) in THF (40 mL) was added Compound **23** (1.17 g, 4.3 mmol) in THF (10 mL) at 0 °C. After stirring at 0 °C for 1 h, the reaction mixture was added MeI (1.1 mL, 17.2 mmol) at 0 °C. After stirring at room temperature for 1 h, the reaction mixture was quenched by $NH_4Cl$ (saturated in $H_2O$) and extracted by $Et_2O$. The organic phase was dried by $Na_2SO_4$ and concentrated under reduced pressure. The residue was purified by column chromatography (silica gel, hexane:EA = 10:1) to give ketal **2.51** (1.09 g, 84% yield) as a colorless oil.

**$^1$H NMR** (500 MHz, Chloroform-*d*) δ 4.73 (d, *J* = 1.6 Hz, 1H), 4.71 (d, *J* = 1.6 Hz, 1H), 3.37 (t, *J* = 6.6 Hz, 2H), 3.33 (s, 3H), 3.17 (s, 3H), 3.16 (s, 3H), 3.13 (s, 3H), 2.25 (dt, *J* = 9.4, 8.5 Hz, 1H), 2.16 – 2.04 (m, 5H), 1.95 (ddd, *J* = 13.3, 10.3, 8.2 Hz, 3H), 1.74 – 1.67 (m, 2H), 1.55 (ddd, *J* = 10.3, 6.7, 5.3 Hz, 2H), 1.07 (s, 3H).

*Synthesis of compound **2.52***

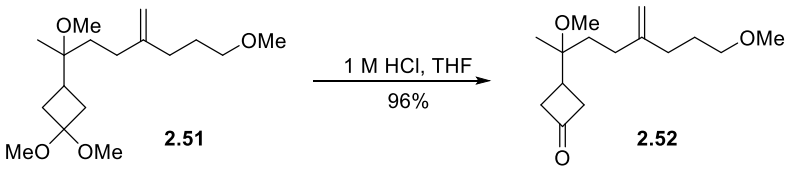


To a solution of compound **2.51** (1.08 g, 3.6 mmol) in THF (30 mL) was added HCl (1 M in $H_2O$, 10 mL) at room temperature. After stirring at RT for 3 h, the reaction mixture was quenched by

$NaHCO_3$ (saturated in $H_2O$) and extracted by $Et_2O$. The organic phase was dried by $Na_2SO_4$ and concentrated under reduced pressure. The residue was purified by column chromatography (silica gel, hexane:EA = 20:1) to give ketone **2.52** (0.88 g, 96% yield) as a colorless oil.

**$^1$H NMR** (400 MHz, Chloroform-*d*) δ 4.77 – 4.71 (m, 2H), 3.37 (t, *J* = 6.5 Hz, 2H), 3.33 (s, 3H), 3.21 (s, 3H), 3.19 – 3.03 (m, 2H), 2.95 – 2.79 (m, 2H), 2.53 (tt, *J* = 8.8, 7.3 Hz, 1H), 2.11 – 2.04 (m, 2H), 1.99 (tdd, *J* = 11.6, 10.6, 5.5, 2.7 Hz, 2H), 1.76 – 1.65 (m, 4H), 1.15 (s, 3H).

**$^{13}$C NMR** (101 MHz, $CDCl_3$) δ 207.98, 149.27, 109.11, 75.62, 72.46, 58.73, 49.46, 48.07, 47.51, 34.53, 32.72, 32.17, 30.63, 27.92, 19.90.

*Synthesis of compound **2.54***

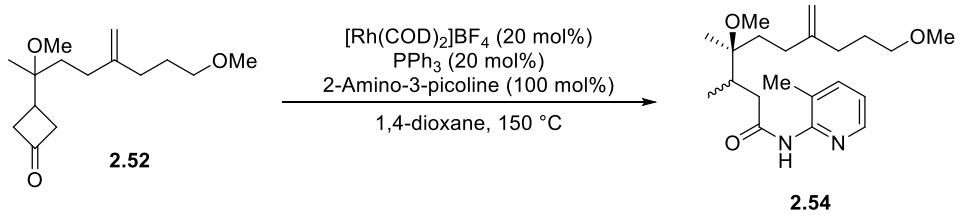


To a flame dried vial was added compound **2.52** (10 mg, 0.04 mmol), $[Rh(COD)_2]BF_4$ (3.2 mg, 0.008 mmol), $PPh_3$ (2.1 mg, 0.008 mmol), 2-amino-3-picoline (4 μL, 0.04 mmol) and 1,4-dioxane (0.5 mL) in the glove box. The vial was then sealed and moved out of the glove box. After stirring at 150 °C on a pi-block for 12 h, the reaction mixture was cooled to room temperature and concentrated under reduced pressure. The residue was purified by PTLC to give amide **2.54** as a colorless oil.

**$^1$H NMR** (400 MHz, Chloroform-*d*) δ 8.27 – 8.22 (m, 1H), 7.76 (s, 1H), 7.56 (ddd, *J* = 7.5, 1.8, 0.8 Hz, 1H), 7.10 (dd, *J* = 7.6, 4.8 Hz, 1H), 4.77 – 4.70 (m, 2H), 3.38 (t, *J* = 6.5 Hz, 2H), 3.33 (s, 3H), 3.17 (s, 3H), 2.71 (dd, *J* = 14.6, 3.2 Hz, 1H), 2.46 (ddd, *J* = 10.1, 6.8, 3.2 Hz, 1H), 2.27 (s, 3H), 2.12 – 2.06 (m, 3H), 1.77 – 1.68 (m, 3H), 1.63 – 1.55 (m, 3H), 1.13 (s, 3H), 1.02 (d, *J* = 6.8 Hz, 3H).

*Synthesis of compound **2.65***

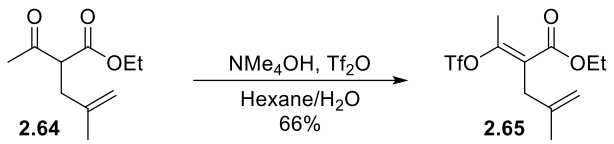


To a solution of compound **2.64** (100 mg, 0.54 mmol) in hexane (2.7 mL) was added $NMe_4OH·5H_2O$ (490 mg, 2.7 mmol) in $H_2O$ (2.8 mL) at 0 °C. After stirring at 0 °C for 30 min, the reaction mixture was added $Tf_2O$ (0.23 mL, 1.35 mmol) at 0 °C. After stirring at 0 °C for 10 min, the reaction mixture was diluted with water and extracted by $Et_2O$. The organic phase was dried by $Na_2SO_4$ and concentrated under reduced pressure. The residue was purified by column chromatography (silica gel, hexane:EA = 20:1) to enol triflate **2.65** (113.4 mg, 66% yield) as a colorless oil.

$R_f$ = 0.5 (hexane:EA = 5:1)

**$^1$H NMR** (400 MHz, Chloroform-*d*) δ 4.79 (q, *J* = 1.4 Hz, 1H), 4.68 – 4.65 (m, 1H), 4.23 (q, *J* = 7.1 Hz, 2H), 3.14 (s, 2H), 2.42 (d, *J* = 1.0 Hz, 3H), 1.74 (dd, *J* = 1.5, 0.8 Hz, 3H), 1.29 (t, *J* = 7.1 Hz, 3H).

*Synthesis of compound **2.67***

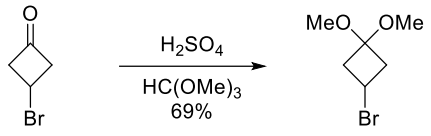


**2.66** **2.67**

To a solution of compound **2.66** (6.7 g, 44 mmol) in $HC(OMe)_3$ (15 mL, 135 mmol), $H_2SO_4$ was added (0.47 mL, 8.8 mmol) at 0 °C. After stirring at room temperature for 3 h, the reaction mixture was diluted with dichloromethane (100 mL), quenched with 1M HCl (50 mL), and extracted with dichloromethane (3 × 50 mL). The organic phase was dried with $Na_2SO_4$ and concentrated under reduced pressure. The residue was purified by column chromatography (silica gel, hexane:ethyl acetate = 10:1) to give bromide **2.67** (5.90 g, 69% yield for 2 steps) as a colorless oil.

**$R_f$** = 0.70 (hexane:ethyl acetate = 4:1)

**$^1$H NMR** (500 MHz, $CDCl_3$) δ 4.24 – 4.16 (m, 1H), 3.15 (s, 3H), 3.13 (s, 3H), 2.93 – 2.86 (m, 2H), 2.56 – 2.49 (m, 2H).

**$^{13}$C NMR** (126 MHz, $CDCl_3$) δ 100.5, 48.9, 48.8, 44.9, 32.9.

**IR (KBr)** $\nu_{max}$ = 2999, 2952, 2832, 1448, 1410, 1276, 1158, 1042, 859, 543 $cm^{-1}$

**HRMS (CI)** m/z calcd. for $C_6H_{11}{}^{79}BrO_2^+$ $[M]^+$: 193.9937, found 193.9980; m/z calcd. for $C_6H_{11}{}^{81}BrO_2^+$ $[M]^+$: 195.9917, found 195.9864

*Synthesis of compound **2.68***

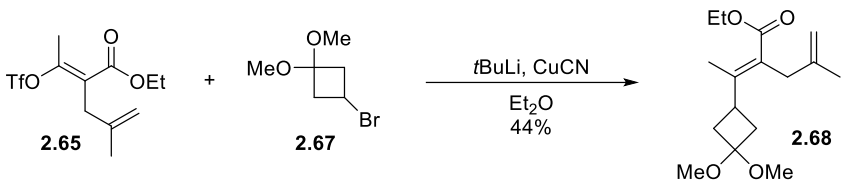


To a solution of compound **2.67** (460 mg, 2.4 mmol) in $Et_2O$ (10 mL) was added *t*BuLi (1.7 M in pentane, 3 mL, 5.1 mmol) at −78 °C. After stirring at −78 °C for 1 h, the reaction mixture was added CuCN (285 mg, 3.2 mmol) at −78 °C. After stirring at −78 °C for 30 min, the reaction mixture was added compound **2.65** (500 mg, 1.6 mmol) in THF (5 mL) at −78 °C. After stirring at −78 °C for 1 h, the reaction mixture was quenched with $NH_4Cl$ (saturated in $H_2O$) and extracted by $Et_2O$. The organic phase was dried with $Na_2SO_4$ and concentrated under reduced pressure. The residue was purified by column chromatography (silica gel, hexane:EA = 20:1) to give ketal **2.68** (194.4 mg, 44% yield) as a colorless oil.

**$R_f$** = 0.47 (hexane:ethyl acetate = 4:1)

**$^1$H NMR** (500 MHz, $CDCl_3$) δ 4.71 (s, 1H), 4.60 (s, 1H), 4.16 (q, *J* = 7.2 Hz, 2H), 3.20 – 3.11 (m, 7H), 3.00 (s, 2H), 2.33 – 2.26 (m, 2H), 2.14 – 2.07 (m, 2H), 1.97 (s, 3H), 1.70 (s, 3H), 1.26 (t, *J* = 7.1 Hz, 3H).

**$^{13}$C NMR** (101 MHz, $CDCl_3$) δ 169.8, 145.7, 143.3, 127.1, 110.7, 99.9, 60.1, 48.7, 48.3, 37.3, 36.0, 28.4, 22.7, 16.4, 14.2.

**IR (KBr)** $\nu_{max}$ = 2984, 2948, 1712, 1446, 1274, 1227, 1197, 1151, 1044 $cm^{-1}$

**HRMS (ESI):** m/z calcd for $C_{16}H_{27}O_4^+$ $[M+H]^+$: 283.1904, found 283.1902.

*Synthesis of compound **2.62***

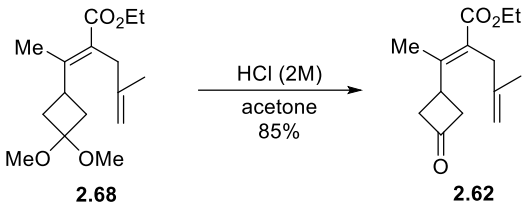


**2.68** **2.62**

To a solution of compound **2.68** (118.6 mg, 0.42 mmol) in acetone (8.5 mL), HCl (2 M in $H_2O$, 0.4 mL, 0.8 mmol) was added at room temperature. After stirring at room temperature for 12 h, the reaction mixture was quenched with $NaHCO_3$ (sat. in $H_2O$, 10 mL) and extracted with ethyl acetate (3 × 10 mL). The organic phase was washed with brine (sat. in $H_2O$, 20 mL) and dried with $Na_2SO_4$ and concentrated under reduced pressure. The residue was then purified by column chromatography (silica gel, hexane:ethyl acetate = 20:1) to give compound **2.62** (84.2 mg, 85% yield) as a colorless oil.

**$R_f$** = 0.50 (hexane:ethyl acetate = 4:1)

**$^1$H NMR** (500 MHz, $CDCl_3$) δ 4.76 (s, 1H), 4.63 (s, 1H), 4.19 (q, *J* = 7.2 Hz, 2H), 3.53 (p, *J* = 8.2 Hz, 1H), 3.21 – 3.10 (m, 4H), 3.09 (s, 2H), 2.02 (s, 3H), 1.73 (s, 3H), 1.28 (t, *J* = 7.1 Hz, 3H).

**$^{13}$C NMR** (101 MHz, $CDCl_3$) δ 205.9, 169.4, 144.1, 143.0, 128.3, 111.0, 60.4, 51.4, 37.5, 26.6, 22.7, 15.5, 14.2.

**IR (KBr)** $\nu_{max}$ = 2980, 2934, 1789, 1710, 1447, 1380, 1292, 1198, 1105, 1069 $cm^{-1}$

**HRMS (ESI):** m/z calcd for $C_{14}H_{21}O_3^+$ $[M+H]^+$: 237.1485, found 237.1485.

*Synthesis of compound **2.68***

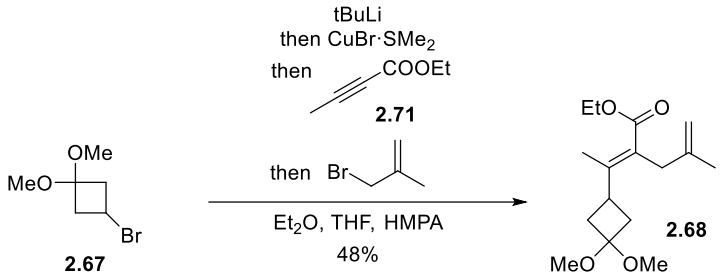


To a solution of compound **2.67** (50 mg, 0.26 mmol) in $Et_2O$ (0.5 mL) was added *t*BuLi (1.7 M in pentane, 0.3 mL, 0.55 mmol) at −78 °C. After stirring at −78 °C for 30 min, the reaction mixture was warmed to 0 °C and stirred at 0 °C for 5 min. In another flame dried flask, to a suspension of $CuBr{\cdot}SMe_2$ (30 mg, 0.143 mmol) in THF (2 mL) was added previous prepared alkyl lithium solution at −78 °C. After stirring at −78 °C for 10 min, the reaction mixture was added compound **2.71** (31 μL, 0.26 mmol) at −78 °C. After stirring at −78 °C for 30 min, the reaction mixture was added HMPA (0.5 mL) and 3-bromo-2-methylpropene (26 μL, 0.26 mmol) at −78 °C. After stirring at 0 °C for 2 h, the reaction was quenched by $NH_4Cl$ (sat.) and extracted by $Et_2O$. The organic phase was dried with $Na_2SO_4$ and concentrated under reduced pressure. The residue was purified by column chromatography (silica gel, hexane:EA = 20:1) to give compound **2.68** (34.9 mg, 48% yield) as a colorless oil.

The analytic data of compound **2.68** were the same as above.

*Synthesis of compound **2.73***

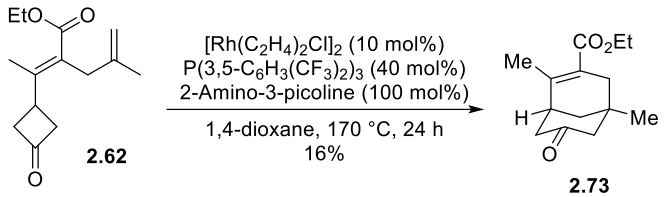


A flame dried vial was charged with compound **2.62** (20 mg, 0.085 mmol), $[Rh(C_2H_4)_2Cl]_2$ (3.3 mg, 0.0085 mmol), $P(3,5\text{-}C_6H_3(CF_3)_2)_3$ (22.8 mg, 0.034 mmol), 2-amino-3-picoline (8.6 μL, 0.085 mmol) and 1,4-dioxane (1.0 mL) in glove box. The vial was then sealed and removed from glovebox. After stirring at 170 °C for 24 h, the reaction mixture was concentrated under reduced pressure. The residue was purified by PTLC to give ketone **2.73** (3.1 mg, 15% yield) as a colorless oil.

$R_f$ = 0.6 (hexane:EA = 2:1)

**$^1$H NMR** (500 MHz, Chloroform-*d*) δ 4.14 (q, *J* = 7.1 Hz, 2H), 2.65 (q, *J* = 3.5 Hz, 1H), 2.44 (d, *J* = 3.9 Hz, 2H), 2.31 – 2.18 (m, 4H), 2.02 (t, *J* = 2.1 Hz, 3H), 1.87 – 1.78 (m, 2H), 1.27 (t, *J* = 7.2 Hz, 3H), 1.13 (s, 3H).

**$^{13}$C NMR** (126 MHz, $CDCl_3$) δ 209.66, 167.86, 147.12, 123.44, 60.14, 55.43, 43.88, 40.75, 40.20, 37.47, 33.88, 31.28, 20.58, 14.24.

**DEPT-135 NMR** (126 MHz, $CDCl_3$) δ 60.10, 55.38, 43.84, 40.70, 40.15, 37.41, 31.23, 20.54, 14.19.

*Synthesis of compound **2.78***

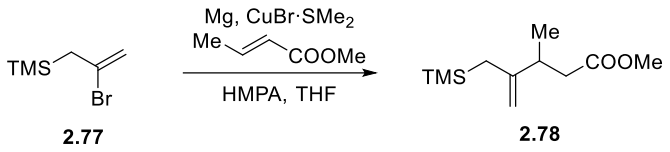


To a suspension of Mg (3.8 g, 155 mmol) in THF (20 mL) was added 1,2-dibromoethane (0.5 mL) at room temperature. After initiation, the reaction mixture was added compound **2.77** (15 g, 77.7 mmol) in THF (60 mL) slowly. After refluxing for 30 min, the solution was transferred to another flask charged with THF (50 mL) and HMPA (23 mL, 130 mmol). After cooling to −40 °C, the reaction mixture was added $CuBr{\cdot}SMe_2$ (0.4 g, 2 mmol), TMSCl (9.8 mL, 77.7 mmol) and methyl crotonate (5.5 mL, 51.8 mmol) in THF (40 mL) at −40 °C. After stirring at −40 °C for 1.5 h, the reaction mixture was warmed to room temperature. After stirring at room temperature for 1 h, the reaction mixture was quenched by $H_2O$ (100 mL) and HCl (1 M, 25 mL). The reaction mixture was then added pentane (100 mL) and extracted by $Et_2O$. The organic phase was washed by brine, dried with $Na_2SO_4$ and concentrated under reduced pressure. The residue was flashed through silica gel to give crude compound **2.78** (11.05 g, crude) as a colorless oil. The crude product could be directly used in next step without further purification.

$\boldsymbol{R_f}$ = 0.7 (hexane:EA = 5:1)

**$^1$H NMR** (500 MHz, Chloroform-*d*) δ 4.63 (t, *J* = 1.1 Hz, 1H), 4.56 (d, *J* = 1.1 Hz, 1H), 3.66 (s, 3H), 2.55 – 2.43 (m, 2H), 2.23 (dd, *J* = 14.5, 8.3 Hz, 1H), 1.54 (dd, *J* = 3.8, 1.0 Hz, 2H), 1.06 (d, *J* = 6.7 Hz, 3H), 0.03 (s, 9H).

*Synthesis of compound **2.79***

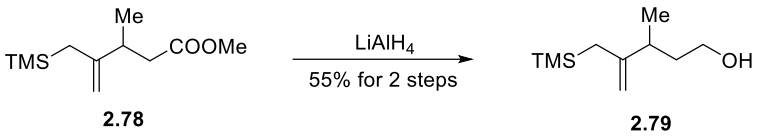


**2.78** **2.79**

To a suspension of $LiAlH_4$ (5.9 g, 154.5 mmol) in $Et_2O$ (500 mL) was added compound **2.78** (11 g, 51.5 mmol, crude) at 0 °C. After stirring at RT for 2 h, the reaction mixture was quenched by EA, added $H_2O$ (5.9 mL), NaOH (15% in $H_2O$, 11.8 mL) and $H_2O$ (17.7 mL). The reaction mixture was then filtered through Celite to give compound **2.79** (5.35 g, 55% yield for 2 steps) as a colorless oil.

$\boldsymbol{R_f}$ = 0.2 (hexane:EA = 5:1)

**$^1$H NMR** (400 MHz, Chloroform-*d*) δ 4.66 (dd, *J* = 1.6, 1.0 Hz, 1H), 4.60 – 4.56 (m, 1H), 3.72 – 3.59 (m, 2H), 1.74 (dt, *J* = 13.5, 6.8 Hz, 1H), 1.62 – 1.56 (m, 1H), 1.53 (d, *J* = 1.0 Hz, 2H), 1.04 (d, *J* = 6.9 Hz, 3H), 0.03 (s, 9H).

*Synthesis of compound **2.80***

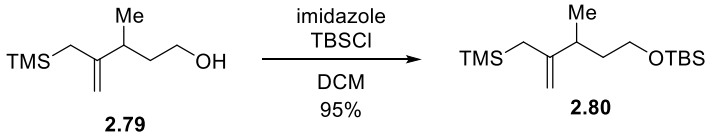


**2.79** **2.80**

To a solution of compound **2.79** (100 mg, 0.54 mmol) in DCM (3 mL) was added imidazole (74 mg, 1.08 mmol) and TBSCl (122 mg, 0.81 mmol) at room temperature. After stirring at room temperature for 30 min, the reaction mixture was quenched by $NH_4Cl$ (sat. in $H_2O$) and extracted by DCM. The organic phase was dried with $Na_2SO_4$ and concentrated under reduced pressure. The

residue was purified by column chromatography (silica gel, hexane:EA = 20:1) to give compound **2.80** (154.5 mg, 95% yield) as a colorless oil.

$R_f$ = 0.8 (hexane:EA = 5:1)

**$^1$H NMR** (500 MHz, Chloroform-*d*) δ 4.61 (dd, *J* = 1.6, 0.9 Hz, 1H), 4.54 (d, *J* = 1.5 Hz, 1H), 3.63 – 3.57 (m, 2H), 2.13 – 2.04 (m, 1H), 1.77 – 1.68 (m, 1H), 1.52 (d, *J* = 1.0 Hz, 2H), 1.43 (dddd, *J* = 13.5, 7.7, 6.7, 5.8 Hz, 1H), 1.01 (d, *J* = 6.9 Hz, 3H), 0.89 (s, 9H), 0.04 (s, 6H), 0.01 (s, 9H).

*Synthesis of compound **2.81***

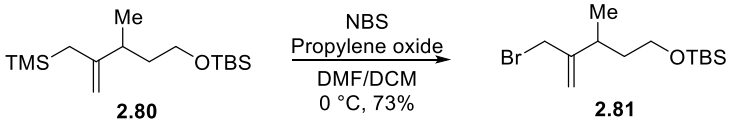


To a solusion of compound **2.80** (6.5 g, 22 mmol) in DCM (200 mL) and DMF (200 mL) was added propylene oxide (15.4 mL, 220 mmol) and NBS (11.8 g, 66 mmol) at −78 °C. After stirring at −78 °C for 30 min, the reaction mixture was warmed to 0 °C. After stirring at 0 °C for 30 min, the reaction mixture was poured into mixture of $NaHCO_3$ (sat. in $H_2O$) and $Na_2S_2O_3$ (sat. in $H_2O$) at 0 °C, extracted by $Et_2O$. The organic phase was dried with $Na_2SO_4$ and concentrated under reduced pressure. The residue was purified by column chromatography (silica gel, hexane:EA = 100:1) to give compound **2.81** (5.58 g, 73% yield) as a colorless oil.

$R_f$ = 0.46 (hexane:EA = 20:1)

**$^1$H NMR** (500 MHz, Chloroform-*d*) δ 5.21 (d, *J* = 0.9 Hz, 1H), 5.01 (s, 1H), 4.04 – 3.96 (m, 2H), 3.62 (t, *J* = 6.6 Hz, 2H), 2.54 (q, *J* = 6.9 Hz, 1H), 1.74 (dq, *J* = 13.4, 6.7 Hz, 1H), 1.61 – 1.55 (m, 1H), 1.11 (d, *J* = 6.9 Hz, 3H), 0.89 (s, 9H), 0.04 (d, *J* = 1.6 Hz, 6H).

*Synthesis of compound **2.82***

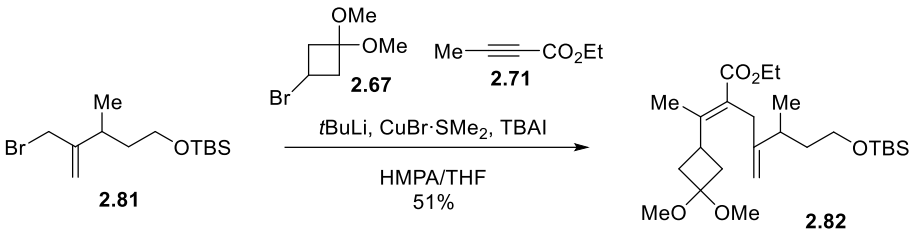


To a solution of compound **2.67** (630 mg, 3.25 mmol) in $Et_2O$ (5 mL) was added *t*BuLi (1.7 M in pentane, 4 mL, 6.8 mmol) at −78 °C. After stirring at −78 °C for 30 min, then reaction mixture was warmed to 0 °C and stirred at 0 °C for 5 min. In another flame dried flask, to a suspension of $CuBr{\cdot}SMe_2$ (360 mg, 1.8 mmol) in THF (30 mL) was added previous prepared alkyl lithium solution at −78 °C. After stirring at −78 °C for 10 min, the reaction mixture was added compound **2.71** (0.38 mL, 3.25 mmol) at −78 °C. After stirring at −78 °C for 30 min, the reaction mixture was added HMPA (8 mL) and compound **2.81** (1.0 g, 3.25 mmol) at −78 °C. After stirring at 0 °C for 2 h, the reaction mixture was quenched by $NH_4Cl$ (sat. in $H_2O$) and extracted by $Et_2O$. The organic phase was dried with $Na_2SO_4$ and concentrated under reduced pressure. The residue was purified by column chromatography (silica gel, hexane:EA = 20:1) to give compound **2.82** (0.75 g, 51% yield) as a colorless oil.

**$^1$H NMR** (400 MHz, Chloroform-*d*) δ 4.75 (dd, *J* = 1.5, 0.8 Hz, 1H), 4.57 (d, *J* = 1.6 Hz, 1H), 4.14 (q, *J* = 7.1 Hz, 2H), 3.58 (td, *J* = 6.8, 2.4 Hz, 2H), 3.16 (s, 3H), 3.14 (s, 3H), 3.10 (t, *J* = 9.0 Hz,

1H), 3.05 – 2.92 (m, 2H), 2.34 – 2.26 (m, 3H), 2.16 – 2.08 (m, 2H), 2.01 (d, *J* = 0.9 Hz, 3H), 1.76 – 1.65 (m, 1H), 1.49 (dt, *J* = 13.6, 6.8 Hz, 1H), 1.25 (t, *J* = 7.1 Hz, 3H), 1.05 (d, *J* = 6.9 Hz, 3H), 0.89 (s, 9H), 0.04 (s, 6H).

*Synthesis of compound **2.75***

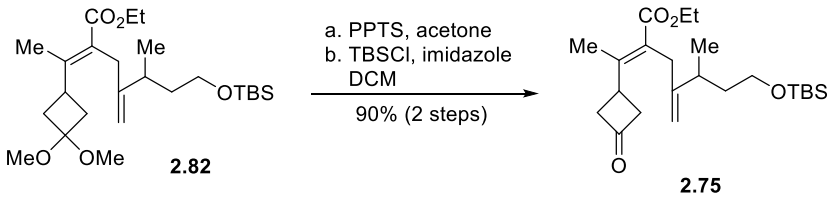


To a solution of compound **2.82** (4 g, 8.7 mmol) in acetone (200 mL) was added PPTS (0.2 g, 0.87 mmol) at room temperature. After stirring at room temperature for 3 h, the reaction mixture was quenched by $NaHCO_3$ (sat. in $H_2O$) and extracted by $Et_2O$. The organic phase was dried with $Na_2SO_4$ and concentrated under reduced pressure. Then the residue was diluted by DCM (100 mL), added imidazole (1.2 g, 17.4 mmol) and TBSCl (2.0 g, 13 mmol) at room temperature. After stirring at RT for 30 min, the reaction mixture was quenched by $NH_4Cl$ (sat.) and extracted by DCM. The organic phase was dried with $Na_2SO_4$ and concentrated under reduced pressure. The residue was purified by column chromatography (silica gel, hexane:EA = 20:1) to give compound **2.75** (3.20 g, 90% yield) as a colorless oil.

**$^1$H NMR** (500 MHz, Chloroform-*d*) δ 4.80 – 4.76 (m, 1H), 4.60 (d, *J* = 1.5 Hz, 1H), 4.17 (q, *J* = 7.1 Hz, 2H), 3.59 (td, *J* = 6.7, 1.5 Hz, 2H), 3.50 – 3.42 (m, 1H), 3.15 (s, 2H), 3.13 (s, 2H), 3.12 – 3.02 (m, 2H), 2.33 (q, *J* = 6.9 Hz, 1H), 2.06 (s, 3H), 1.70 (dq, *J* = 13.6, 6.8 Hz, 1H), 1.52 (dq, *J* =

13.7, 6.8 Hz, 1H), 1.27 (t, $J$ = 7.1 Hz, 3H), 1.06 (d, $J$ = 6.9 Hz, 3H), 0.89 (s, 9H), 0.04 (d, $J$ = 1.6 Hz, 6H).

**$^{13}$C NMR** (101 MHz, $CDCl_3$) δ 205.91, 169.13, 151.03, 145.02, 127.96, 108.96, 61.24, 60.35, 51.51, 51.47, 38.27, 36.59, 33.33, 26.75, 25.92, 19.81, 18.28, 15.56, 14.21, -5.30, -5.32.

*Synthesis of compound **2.90***

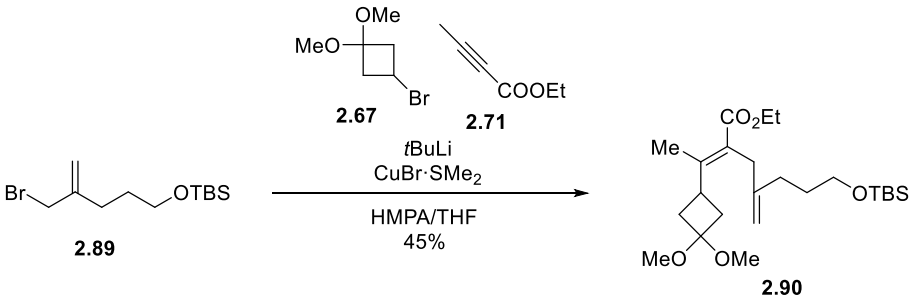


To a solution of compound **2.67** (1 g, 5.1 mmol) in $Et_2O$ (10 mL) was added *t*BuLi (1.7 M in pentane, 6.3 mL, 10.7 mmol) at −78 °C. After stirring at −78 °C for 30 min, the reaction mixture was warmed to 0 °C and stirred at 0 °C for 5 min. In another flame dried flask, to a suspension of $CuBr{\cdot}SMe_2$ (0.58 g, 2.8 mmol) in THF (40 mL) was added previous prepared alkyl lithium solution at −78 °C. After stirring at −78 °C for 10 min, the reaction mixture was added compound **2.71** (0.6 mL, 5.1 mmol) at −78 °C. After stirring at −78 °C for 30 min, the reaction mixture was added HMPA (10 mL) and compound **2.89** (1.5 g, 5.1 mmol) at −78 °C. After stirring at 0 °C for 2 h, the reaction mixture was quenched by $NH_4Cl$ (sat. in $H_2O$) and extracted by $Et_2O$. The organic phase was dried with $Na_2SO_4$ and concentrated under reduced pressure. The residue was purified by column chromatography (silica gel, hexane:EA = 20:1) to give compound **2.91** (1.02 g, 45% yield) as a colorless oil.

*Synthesis of compound **2.91***

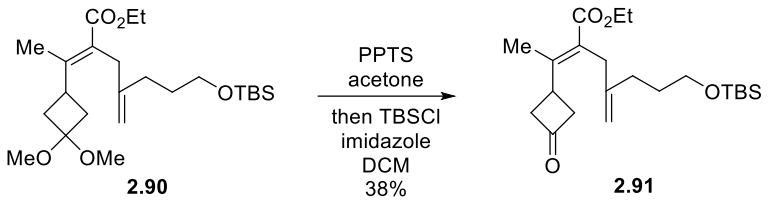


To a solution of compound **2.90** (1.02 g, 2.3 mmol) in acetone (50 mL) was added PPTS (58 mg, 0.23 mmol) at room temperature. After stirring at RT for 3 h, the reaction mixture was quenched by $NaHCO_3$ (sat.) and extracted by $Et_2O$. The organic phase was dried with $Na_2SO_4$ and concentrated under reduced pressure. The residue was diluted by DCM (25 mL), added imidazole (0.32 g, 4.6 mmol) and TBSCl (0.53 g, 3.5 mmol) at room temperature. After stirring at RT for 30 min, the reaction mixture was quenched by $NH_4Cl$ (sat. in $H_2O$) and extracted by DCM. The organic phase was dried with $Na_2SO_4$ and concentrated under reduced pressure. The residue was purified by column chromatography (silica gel, hexane:EA = 20:1) to give compound **2.91** (0.3448 g, 38% yield) as a colorless oil.

**$^1$H NMR** (500 MHz, Chloroform-*d*) δ 4.77 (d, *J* = 1.4 Hz, 1H), 4.65 (d, *J* = 1.7 Hz, 1H), 4.18 (q, *J* = 7.1 Hz, 2H), 3.61 (t, *J* = 6.4 Hz, 2H), 3.53 – 3.49 (m, 1H), 3.15 (ddt, *J* = 8.3, 3.4, 1.3 Hz, 4H), 3.10 (s, 2H), 2.10 – 2.04 (m, 2H), 2.03 (d, *J* = 0.9 Hz, 3H), 1.67 (ddt, *J* = 9.4, 7.6, 6.4 Hz, 2H), 1.28 (t, *J* = 7.2 Hz, 3H), 0.89 (s, 9H), 0.05 (s, 6H).

*Synthesis of compound **S2.1***

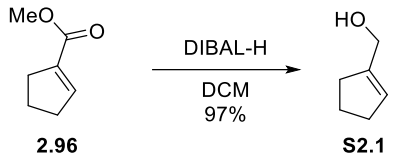


Following the literature reported procedure, a flask containing dichloromethane (600 mL) was cooled to −78 °C, then diisobutylaluminum hydride (DIBAL-H, 1M in hexane, 540 mL, 540 mmol) was added at −78 °C. Compound **2.96** (31.13 g, 247 mmol) was then added slowly to the reaction mixture. After being stirred at −78 °C for 2 h and 0 °C for 30 min, the reaction mixture was quenched with Rochelle salt (sat. in $H_2O$, 800 mL) and stirred at room temperature overnight. The mixture was extracted with dichloromethane (3 × 300 mL). The organic phase was dried with $Na_2SO_4$ and concentrated under reduced pressure. The residue was purified by column chromatography (silica gel, hexane:ethyl acetate = 10:1) to give compound **S2.1** (23.59 g, 97% yield) as a colorless oil.

Spectra matched with literature report.

*Synthesis of compound **2.97***

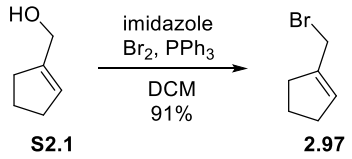


To a solution of $PPh_3$ (52 g, 198 mmol) in dichloromethane (800 mL), $Br_2$ was added (10.2 mL, 198 mmol) dropwise at 0 °C. Adding extra $PPh_3$ may be necessary at this stage, until the reaction mixture becomes colorless. After this, imidazole (14.6 g, 214 mmol) and compound **S2.1** (16.2 g,

165 mmol) were added slowly to the reaction mixture at 0 °C. After being stirred at room temperature overnight, the reaction mixture was quenched with $Na_2SO_3$ (sat. in $H_2O$, 400 mL) and extracted with dichloromethane (3 × 300 mL). The organic phase was dried with $Na_2SO_4$ and concentrated under reduced pressure. The residue was purified by column chromatography (silica gel, pure pentane) to give bromide **2.97** (24.25 g, 91% yield) as a colorless oil.

Spectra matched with literature report.

*Synthesis of compound **2.95***

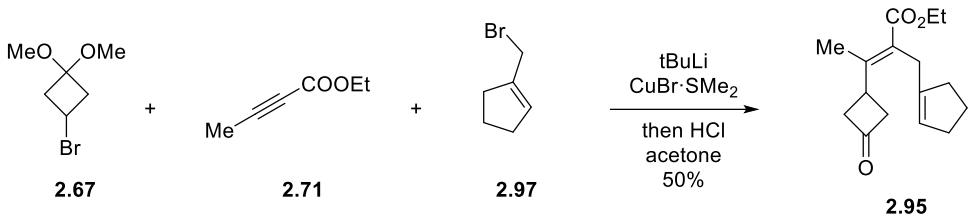


To a solution of compound **2.67** (3.9 g, 20 mmol) in $Et_2O$ (20 mL), $^t$BuLi was added (1.7 M in pentane, 25.6 mL, 41 mmol) at −78 °C, and stirred at −78 °C for 1 h. This alkyl lithium solution was added to a separate flask containing $CuBr{\cdot}SMe_2$ (4.1 g, 20 mmol) in tetrahydrofuran (THF, 100 mL) at −78 °C. After stirring at −78 °C for 10 min, compound **2.71** (2.24 g, 20 mmol) was added to the reaction mixture and stirred at −78 °C for an additional 30 min. Hexamethylphosphoramide (HMPA, 20 mL) and compound **2.97** (4.3 g, 22 mmol) were then added to the reaction mixture at −78 °C. After stirring at 0 °C for 2 h, the reaction mixture was treated with HCl (2 M in $H_2O$, 40 mL) and acetone (100 mL). The reaction was then stirred at room temperature overnight and quenched with $NaHCO_3$ (sat. in $H_2O$, 200 mL) and extracted with ethyl acetate (3 × 100 mL). The organic phase was washed with brine (sat. in $H_2O$, 3 × 200 mL),

dried with $Na_2SO_4$ and concentrated under reduced pressure. The residue was purified by column chromatography (silica gel, hexane:ethyl acetate = 20:1) to give compound **2.95** (2.65 g, 50% yield) as a colorless oil.

**$R_f$** = 0.28 (hexane:ethyl acetate = 4:1)

**$^1$H NMR** (500 MHz, $CDCl_3$) δ 5.30 (hept, J = 1.9 Hz, 1H), 4.20 (q, J = 7.1 Hz, 2H), 3.61 – 3.51 (m, 1H), 3.20 – 3.07 (m, 6H), 2.27 (tq, J = 7.2, 2.3 Hz, 2H), 2.24 – 2.19 (m, 2H), 2.01 (s, 3H), 1.86 (tt, J = 8.2, 6.7 Hz, 2H), 1.29 (t, J = 7.1 Hz, 3H).

**$^{13}$C NMR** (101 MHz, $CDCl_3$) δ 206.0, 169.6, 143.1, 141.7, 128.7, 125.0, 60.4, 51.4, 35.2, 32.3, 31.6, 26.5, 23.4, 15.5, 14.2.

**IR (KBr)** $\nu_{max}$ = 2932, 2846, 1789, 1710, 1446, 1381, 1289, 1214, 1189, 1101, 1064 $cm^{-1}$

**HRMS (ESI)** m/z calcd. for $C_{16}H_{23}O_3^+$ $[M+H]^+$: 263.1642, found 263.1610.

*Synthesis of compound **2.99***

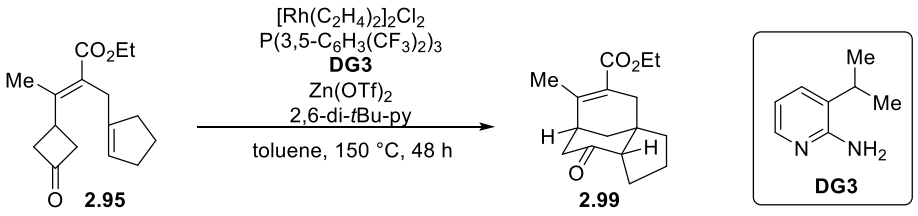


0.05 mmol scale procedure:

A flame dried 4 mL vial was charged with $P(3,5\text{-}C_6H_3(CF_3)_2)_3$ (16.8 mg, 0.025 mmol), **DG3** (1.4 mg, 0.01 mmol) and $Zn(OTf)_2$ (18.2 mg, 0.05 mmol) in glove box. After adding a solution of

compound **2.95** (13.1 mg, 0.05 mmol) and $[Rh(C_2H_4)_2Cl]_2$ (1.9 mg, 0.005 mmol) dissolved in toluene (0.5 mL), the vial was sealed and removed from glovebox. The reaction was stirred at 150 °C in a pi-block for 48 h, before being cooled to room temperature. Then the solvent was removed under reduced pressure to give ketone **2.99** (48% GC yield, 1-methylnaphthalene as internal standard).

Gram-scale procedure:

A flame dried glass pressure vessel was charged with $P(3,5\text{-}C_6H_3(CF_3)_2)_3$ (1.07 g, 1.6 mmol), **DG3** (109 mg, 0.8 mmol), $Zn(OTf)_2$ (290 mg, 0.8 mmol) and 2,6-di-*tert*-butylpyridine (380 mg, 2 mmol) in glove box. After adding a solution of compound **2.95** (1.05 g, 4 mmol) and $[Rh(C_2H_4)_2Cl]_2$ (155 mg, 0.4 mmol) in toluene (40 mL), the vessel was sealed and removed from glovebox. The reaction was then stirred at 150 °C in oil bath for 48 h before being cooled to room temperature. The reaction mixture was quenched with $NH_4Cl$ (sat. in $H_2O$, 50 mL) and extracted with ethyl acetate (3 × 50 mL). The organic phase was dried with $Na_2SO_4$ and concentrated under reduced pressure. The residue was then purified by column chromatography (silica gel, hexane:ethyl acetate = 20:1 to 10:1) to give compound **2.99** (0.87 g, combining 2 parallel reactions, 42% yield) as a colorless oil.

$\mathbf{R}_f$ = 0.40 (hexane:ethyl acetate = 2:1)

**$^1$H NMR** (500 MHz, $CDCl_3$) δ 4.15 (q, *J* = 7.1 Hz, 2H), 2.60 (dt, *J* = 4.0, 1.9 Hz, 1H), 2.56 (dd, *J* = 16.0, 5.6 Hz, 1H), 2.46 (dt, *J* = 17.6, 2.1 Hz, 1H), 2.36 (ddt, *J* = 16.0, 3.3, 1.6 Hz, 1H), 2.29 – 2.20 (m, 2H), 2.01 (t, *J* = 2.0 Hz, 3H), 1.98 (dq, *J* = 8.8, 5.2, 4.3 Hz, 1H), 1.91 – 1.80 (m, 3H), 1.78 – 1.72 (m, 1H), 1.64 – 1.59 (m, 3H), 1.27 (t, *J* = 7.1 Hz, 3H).

**$^{13}$C NMR** (101 MHz, $CDCl_3$) δ 213.1, 168.1, 147.5, 124.5, 60.2, 59.8, 44.4, 40.6, 40.25, 40.20, 39.7, 32.8, 29.6, 22.3, 20.4, 14.2.

**IR (KBr)** $\nu_{max}$ = 2934, 1708, 1448, 1371, 1238, 1208, 1094, 1056 $cm^{-1}$

**HRMS (ESI)** m/z calcd. for $C_{16}H_{23}O_3^+$ $[M+H]^+$: 263.1642, found 263.1643; $C_{16}H_{22}NaO_3^+$ $[M+Na]^+$: 285.1461, found 285.1460.

*Synthesis of compound **S2.2***

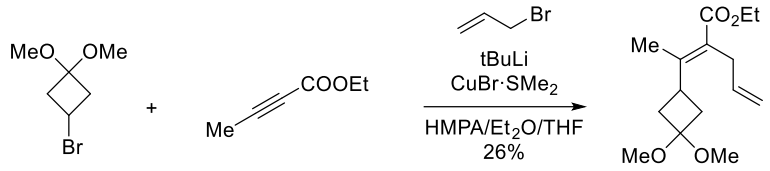


To a solution of compound **2.67** (195 mg, 1 mmol) in $Et_2O$ (1 mL), $^t$BuLi (1.6 M in pentane, 1.3 mL, 2.05 mmol) was added at −78 °C and stirred for 1 h. The previously prepared alkyl lithium solution was then added to another flask containing $CuBr{\cdot}SMe_2$ (205 mg, 1 mmol) suspended in tetrahydrofuran (THF, 5 mL) at −78 °C. After stirring at −78 °C for 10 min, compound **2.71** (112 mg, 1 mmol) was added, and the reaction mixture was stirred at −78 °C for 30 min. Hexamethylphosphoramide (HMPA, 1 mL) and allyl bromide (133 mg, 1.1 mmol) were then added to the reaction mixture at −78 °C. After stirring at 0 °C for 2 h, the reaction mixture was quenched with $NH_4Cl$ (sat. in $H_2O$, 10 mL) and extracted with ethyl acetate (3 × 5 mL). The organic phase was washed with brine (sat. in $H_2O$, 10 mL), dried with $NA_2SO_4$ and concentrated under reduced pressure. The residue was purified by column chromatography (silica gel, hexane:ethyl acetate = 20:1) to give compound **S2.2** (70.1 mg, 26% yield) as a colorless oil.

**$R_f$** = 0.50 (hexane:ethyl acetate = 4:1)

**$^1$H NMR** (500 MHz, $CDCl_3$) δ 5.76 (ddt, *J* = 17.2, 10.1, 6.0 Hz, 1H), 5.04 – 4.94 (m, 2H), 4.18 (q, *J* = 7.1 Hz, 2H), 3.23 – 3.18 (m, 1H), 3.18 (s, 3H), 3.14 (s, 3H), 3.08 – 3.04 (m, 2H), 2.36 – 2.29 (m, 2H), 2.14 – 2.07 (m, 2H), 1.97 (s, 3H), 1.28 (t, *J* = 7.1 Hz, 3H).

**$^{13}$C NMR** (101 MHz, $CDCl_3$) δ 169.6, 145.9, 135.7, 126.7, 115.3, 99.9, 60.2, 48.7, 48.4, 36.1, 33.6, 28.4, 16.5, 14.3.

**IR (KBr)** $\nu_{max}$ = 2982, 2949, 1712, 1445, 1274, 1202, 1152, 1043 $cm^{-1}$

**HRMS (ESI):** m/z calcd for $C_{15}H_{25}O_4^+$ $[M+H]^+$: 269.1747, found 269.1745.

*Synthesis of compound **2.100***

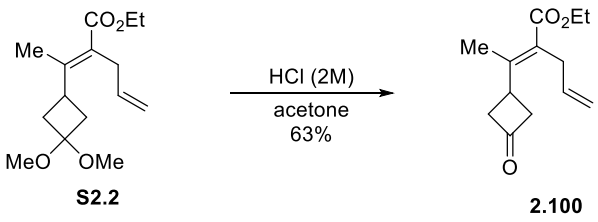


To a solution of compound **S2.2** (70.1 mg, 0.26 mmol) in acetone (5 mL), HCl (2 M in $H_2O$, 0.25 mL, 0.5 mmol) was added at room temperature. After stirring at room temperature for 12 h, the reaction mixture was quenched with $NaHCO_3$ (sat. in $H_2O$, 10 mL) and extracted with ethyl acetate (3 × 10 mL). The organic phase was then washed with brine (sat. in $H_2O$, 20 mL), dried with $Na_2SO_4$, and concentrated under reduced pressure. The residue was then purified by column

chromatography (silica gel, hexane:ethyl acetate = 20:1) to give compound **2.100** (36.4 mg, 63% yield) as a colorless oil.

**$R_f$** = 0.35 (hexane:ethyl acetate = 4:1)

**$^1$H NMR** (500 MHz, $CDCl_3$) δ 5.80 (ddd, *J* = 17.3, 10.8, 6.0 Hz, 1H), 5.07 – 4.98 (m, 2H), 4.21 (qd, *J* = 7.1, 2.0 Hz, 2H), 3.57 (dd, *J* = 9.3, 7.2 Hz, 1H), 3.23 – 3.08 (m, 6H), 2.02 (s, 3H), 1.30 (t, *J* = 7.2 Hz, 3H).

**$^{13}$C NMR** (101 MHz, $CDCl_3$) δ 205.8, 169.2, 144.1, 135.3, 127.9, 115.6, 60.5, 51.5, 33.7, 26.5, 15.6, 14.2.

**IR (KBr)** $\nu_{max}$ = 2980, 2932, 1789, 1710, 1446, 1381, 1286, 1207, 1106, 1053 $cm^{-1}$

**HRMS (ESI):** m/z calcd for $C_{13}H_{19}O_3^+$ $[M+H]^+$: 223.1329, found 223.1327.

*Synthesis of compound **2.101***

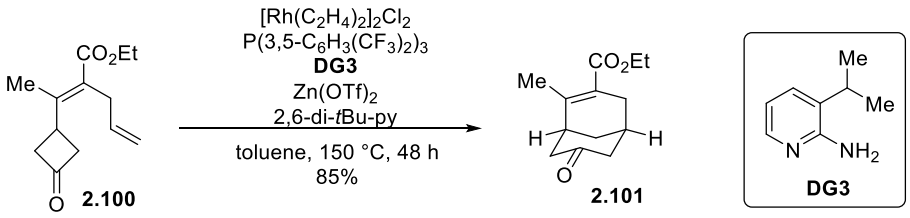


A flame dried 4 mL vial was charged with $P(3,5\text{-}C_6H_3(CF_3)_2)_3$ (13.4 mg, 0.02 mmol), **DG3** (1.4 mg, 0.01 mmol), $Zn(OTf)_2$ (3.6 mg, 0.01 mmol) and 2,6-di-*tert*-butylpyridine (5.6 μL, 0.025 mmol) in glove box. After adding a solution of compound **S5** (11 mg, 0.05 mmol) and $[Rh(C_2H_4)_2Cl]_2$ (1.9 mg, 0.005 mmol) dissolved in toluene (0.5 mL), the vial was sealed and removed from the

glove box. The reaction was stirred at 150 °C in a pi-block for 48 h, before it was cooled to room temperature. The reaction mixture was then concentrated under reduced pressure and the residue purified by column chromatography (silica gel, hexane:ethyl acetate = 10:1) to give compound **S6** (9.4 mg, 85% yield) as a colorless oil.

**$R_f$** = 0.31 (hexane:ethyl acetate = 2:1)

**$^1$H NMR** (500 MHz, $CDCl_3$) δ 4.14 (q, *J* = 7.2 Hz, 2H), 2.65 – 2.49 (m, 4H), 2.47 (d, *J* = 3.8 Hz, 2H), 2.30 (dd, *J* = 16.9, 4.4 Hz, 2H), 2.06 – 2.02 (m, 1H), 2.01 (s, 3H), 1.98 – 1.91 (m, 1H), 1.26 (t, *J* = 7.2 Hz, 3H).

**$^{13}$C NMR** (101 MHz, $CDCl_3$) δ 210.1, 168.0, 147.5, 122.9, 60.1, 48.7, 44.6, 38.9, 33.6, 29.7, 29.3, 20.8, 14.2.

**IR (KBr)** $\nu_{max}$ = 2927, 1712, 1639, 1437, 1372, 1238, 1196, 1063 $cm^{-1}$

**HRMS (ESI):** m/z calcd for $C_{13}H_{19}O_3^+$ $[M+H]^+$: 223.1329, found 223.1327; $C_{13}H_{18}NaO_3^+$ $[M+Na]^+$: 245.1148, found 245.1144.

*Synthesis of compound **2.73***

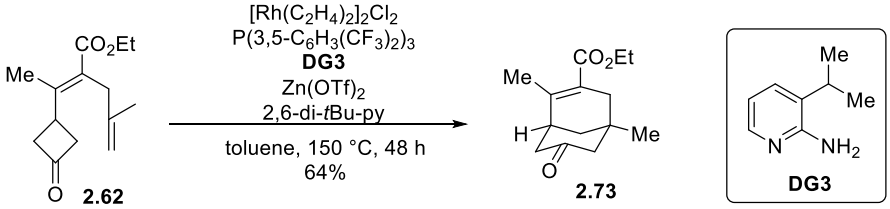

A flame dried 4 mL vial was charged with P(3,5-$C_6H_3(CF_3)_2)_3$ (13.4 mg, 0.02 mmol), **DG3** (1.4 mg, 0.01 mmol), $Zn(OTf)_2$ (3.6 mg, 0.01 mmol) and 2,6-di-*tert*-butylpyridine (5.6 µL, 0.025 mmol) in glove box. After adding a solution of compound **2.62** (11.8 mg, 0.05 mmol) and $[Rh(C_2H_4)_2Cl]_2$ (1.9 mg, 0.005 mmol) dissolved in toluene (0.5 mL), the vial was sealed and removed from the glove box. The reaction was stirred at 150 °C in a pi-block for 48 h, before being cooled to room temperature. The reaction mixture was then concentrated under reduced pressure and purified by column chromatography (silica gel, hexane:ethyl acetate = 10:1) to give compound **2.73** (7.6 mg, 64% yield) as a colorless oil.

Analytic data of compound **2.73** was the shown above.

*Synthesis of compound **DG4***

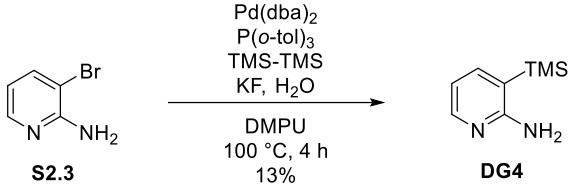

**S2.3** **DG4**

To a solution of compound **S2.3** (173 mg, 1 mmol) in *N*,*N*'-dimethylpropyleneurea (DMPU, 3.3 mL), bis(dibenzylideneacetone)palladium(0) ($Pd(dba)_2$, 17 mg, 0.03 mmol), tri(*o*-tolyl)phosphine (P(*o*-tol)$_3$, 27 mg, 0.09 mmol), KF (290 mg, 5 mmol), hexamethyldisilane (244 µL, 1.2 mmol) and $H_2O$ (36 µL, 2 mmol) were added at room temperature. After stirring at 100 °C for 4 h, the reaction mixture was quenched with $H_2O$ (10 mL) and extracted with ethyl acetate (3 × 10 mL). The organic phase was washed with brine (sat. in $H_2O$, 20 mL), dried with $Na_2SO_4$, and concentrated under

reduced pressure. The residue was then purified by column chromatography (silica gel, hexane:ethyl acetate = 4:1) to give compound **DG4** (20.9 mg, 13% yield) as a white solid.

$\mathbf{R_f}$ = 0.52 (pure ethyl acetate)

**$^1$H NMR** (500 MHz, $CDCl_3$) δ 8.05 (dd, *J* = 5.0, 2.0 Hz, 1H), 7.53 (dd, *J* = 7.1, 2.0 Hz, 1H), 6.64 (dd, *J* = 7.1, 5.0 Hz, 1H), 4.55 (s, 2H), 0.32 (s, 9H).

**$^{13}$C NMR** (126 MHz, $CDCl_3$) δ 161.7, 149.0, 143.9, 116.5, 114.2, -1.4.

**IR (KBr)** $\nu_{max}$ = 3495, 3395, 3308, 3175, 2955, 1607, 1566, 1427, 1252, 873, 839 $cm^{-1}$

**HRMS (ESI):** m/z calcd for $C_8H_{15}N_2Si^+$ $[M+H]^+$: 167.0999, found 167.1001.

**Melting point**: 48.0 – 48.8 °C

*Synthesis of compound **2.113***

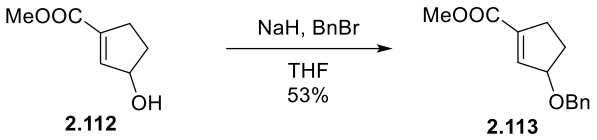


To a solution of compound **2.112** (2.4 g, 16.9 mmol) in THF (85 mL) was added NaH (0.81 g, 20.3 mmol) at 0 °C. After stirring at 0 °C for 20 min, the reaction mixture was added TBAI (0.6 g, 1.69 mmol) and BnBr (2.6 mL, 22.0 mmol) at 0 °C. After stirring at RT overnight, the reaction mixture was quenched by $NH_4Cl$ (sat. in $H_2O$) and extracted by $Et_2O$. The organic phase was dried with $Na_2SO_4$, and concentrated under reduced pressure. The residue was purified by column

chromatography (silica gel, hexane:EA = 10:1) to give compound **2.113** (2.09 g, 53% yield) as a colorless oil.

$R_f$ = 0.86 (hexane:EA = 2:1)

**$^1$H NMR** (500 MHz, Chloroform-*d*) δ 7.35 (d, *J* = 4.4 Hz, 4H), 7.32 – 7.27 (m, 1H), 6.80 (q, *J* = 2.1 Hz, 1H), 4.74 (ddtd, *J* = 7.4, 4.7, 2.3, 1.5 Hz, 1H), 4.56 (d, *J* = 1.8 Hz, 2H), 3.75 (s, 3H), 2.78 – 2.70 (m, 1H), 2.52 – 2.44 (m, 1H), 2.31 (dddd, *J* = 13.7, 8.7, 7.6, 4.1 Hz, 1H), 1.95 (dddd, *J* = 13.8, 9.1, 5.7, 4.9 Hz, 1H).

*Synthesis of compound **2.114***

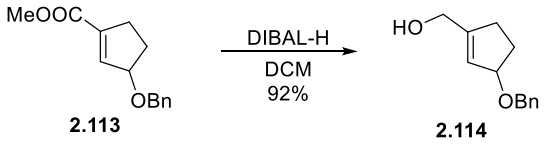


To a solution of DIBAL-H (1 M in THF, 20.7 mL, 20.7 mmol) in DCM (45 mL) was added compound **2.113** (2.09 g, 9.0 mmol) at the −78 °C. After stirring at −78 °C for 2 h, the reaction mixture was warmed to 0 °C. After stirring at 0 °C for 30 min, the reaction mixture was quenched by MeOH and added potassium sodium tartrate (sat. in $H_2O$, 50 mL). After stirring at RT for 2 h, the reaction mixture was extracted by DCM. The organic phase was dried with $Na_2SO_4$, and concentrated under reduced pressure. The residue was purified by column chromatography (silica gel, hexane:EA = 1:1) to give compound **2.114** (1.68 g, 92% yield) as a colorless oil.

$R_f$ = 0.15 (hexane:EA = 2:1)

**$^1$H NMR** (500 MHz, Chloroform-*d*) δ 7.36 – 7.32 (m, 4H), 7.28 (dt, *J* = 5.3, 2.2 Hz, 1H), 5.81 (q, *J* = 1.8 Hz, 1H), 4.68 – 4.62 (m, 1H), 4.59 – 4.48 (m, 2H), 4.30 – 4.17 (m, 2H), 2.54 – 2.46 (m, 1H), 2.30 – 2.20 (m, 2H), 1.99 – 1.91 (m, 1H).

*Synthesis of compound **2.115***

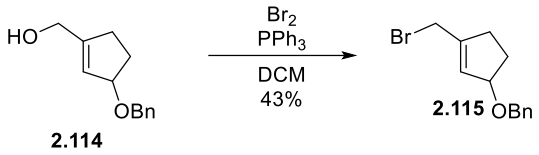


To a solution of $PPh_3$ (1.0 g, 3.8 mmol) in DCM (20 mL) was added $Br_2$ (0.2 mL, 3.8 mmol) dropwise at 0 °C. After stirring at 0 °C for 30 min, the reaction mixture was added imidazole (0.29 g, 4.2 mmol) and compound **2.114** (0.57 g, 2.8 mmol) at 0 °C. After stirring at RT overnight, the reaction mixture was quenched by $Na_2SO_3$ (sat. in $H_2O$) and extracted by DCM. The organic phase was dried with $Na_2SO_4$, and concentrated under reduced pressure. The residue was purified by column chromatography (silica gel, hexane:ether = 20:1) to give compound **2.115** (0.39 g, 52% yield) as a colorless oil.

$\boldsymbol{R_f}$ = 0.4 (hexane:EA = 5:1)

**$^1$H NMR** (400 MHz, Chloroform-*d*) δ 7.36 – 7.32 (m, 4H), 7.30 – 7.27 (m, 1H), 5.92 (dt, *J* = 2.0, 1.0 Hz, 1H), 4.66 (dddd, *J* = 5.1, 4.0, 2.1, 1.1 Hz, 1H), 4.57 – 4.47 (m, 2H), 4.05 (dddt, *J* = 11.6, 10.6, 9.8, 0.9 Hz, 2H), 2.62 – 2.51 (m, 1H), 2.47 – 2.38 (m, 1H), 2.31 (dddd, *J* = 13.5, 8.9, 7.3, 4.5 Hz, 1H), 2.02 – 1.92 (m, 1H).

*Synthesis of compound **2.116***

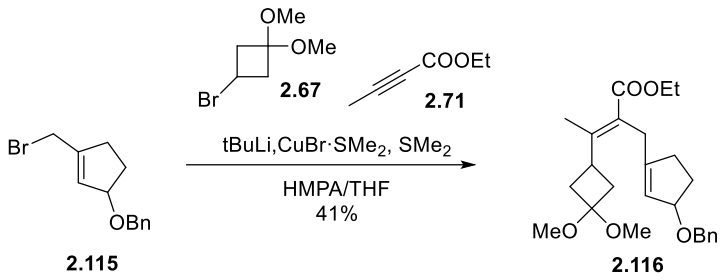


To a solution of compound **2.67** (150 mg, 0.75 mmol) in $Et_2O$ (1 mL) was added *t*BuLi (1.7 M in pentane, 0.93 mL, 1.58 mmol) at −78 °C. After stirring at −78 °C for 30 min, the reaction mixture was warmed to 0 °C and stirred at 0 °C for 5 min. In another flame dried flask, to a suspension of $CuBr{\cdot}SMe_2$ (85 mg, 0.41 mmol) in THF (5 mL) was added previous prepared alkyl lithium solution at −78 °C. After stirring at −78 °C for 10 min, the reaction mixture was added compound **2.71** (90 μL, 0.75 mmol) at −78 °C. After stirring at −78 °C for 30 min, the reaction mixture was added HMPA (1 mL) and compound **2.115** (200 mg, 0.75 mmol) at −78 °C and then warmed to 0 °C. After stirring at 0 °C for 2 h, the reaction mixture was quenched by $NH_4Cl$ (sat. in $H_2O$) and extracted by $Et_2O$. The organic phase was dried with $Na_2SO_4$, and concentrated under reduced pressure. The residue was purified by column chromatography (silica gel, hexane:EA = 20:1) to give compound **2.116** (127.7 mg, 41% yield) as a colorless oil.

**$^1$H NMR** (500 MHz, Chloroform-*d*) δ 7.34 – 7.29 (m, 4H), 7.26 – 7.22 (m, 1H), 5.49 (q, *J* = 1.8 Hz, 1H), 4.59 (ddt, *J* = 5.4, 3.6, 2.0 Hz, 1H), 4.51 – 4.42 (m, 2H), 4.16 (q, *J* = 7.1 Hz, 2H), 3.21 – 3.07 (m, 9H), 2.47 – 2.37 (m, 1H), 2.34 – 2.28 (m, 2H), 2.22 – 2.15 (m, 2H), 2.14 – 2.06 (m, 2H), 1.99 (s, 3H), 1.90 – 1.83 (m, 1H), 1.26 (t, *J* = 7.1 Hz, 3H).

*Synthesis of compound **2.124***

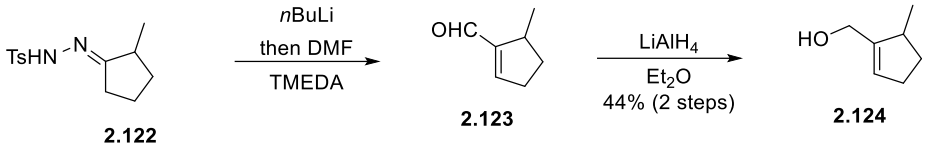


To a solution of compound **2.122** (15.4 g, 58 mmol) in TMEDA (85 mL, 580 mmol) was added *n*BuLi (1.6 M in hexane, 93 mL, 231 mmol) dropwise over 30 min at −78 °C. After stirring at RT for 1 h, the reaction mixture was cooled to 0 °C and added DMF (10 g, 139 mmol) at 0 °C. After stirring at 0 °C for 1 h, the reaction mixture was quenched by $H_2O$ and extracted by $Et_2O$. The organic phase was washed by HCl (1 M), $H_2O$, brine and dried with $Na_2SO_4$, and concentrated under reduced pressure to give crude compound **2.123**. The crude product could be directly used in next step without further purification.

To a suspension of $LiAlH_4$ (2.4 g, 64 mmol) in $Et_2O$ (500 mL) was added crude compound **2.123** at the 0 °C. After stirring at 0 °C for 1 h, the reaction mixture was quenched by EA, then added $H_2O$ (2.4 mL), NaOH (15% in $H_2O$, 4.8 mL) and $H_2O$ (7.2 mL). The reaction mixture was filtered through Celite to give compound **2.124** (2.88 g, 44% yield for 2 steps) as a colorless oil.

$\boldsymbol{R_f}$ = 0.6 (hexane:EA = 2:1)

**$^1$H NMR** (400 MHz, Chloroform-*d*) δ 5.60 (q, *J* = 1.9 Hz, 1H), 4.26 – 4.12 (m, 2H), 2.73 (ddddd, *J* = 9.0, 7.0, 4.7, 2.2, 1.2 Hz, 1H), 2.38 – 2.09 (m, 3H), 1.45 (dddd, *J* = 15.3, 9.0, 5.7, 2.9 Hz, 2H), 1.04 (d, *J* = 6.9 Hz, 3H).

*Synthesis of compound **2.124***

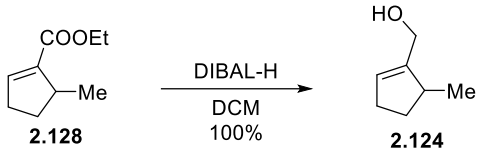


To a solution of DIBAL-H (1 M in THF, 69 mL, 69 mmol) in DCM (100 mL) was added compound **2.128** (4.6 g, 30 mmol) at the −78 °C. After stirring at −78 °C for 2 h, the reaction mixture was warmed to 0 °C. After stirring at 0 °C for 30 min, the reaction mixture was quenched by MeOH, then added potassium sodium tartrate (sat. in $H_2O$, 100 mL). After stirring at RT for 2 h, the reaction mixture was extracted by DCM. The organic phase was dried with $Na_2SO_4$, and concentrated under reduced pressure to give compound **2.124** (3.47 g, 100% yield) as a colorless oil.

The analytical data of compound **2.124** see above.

*Synthesis of compound **2.129***

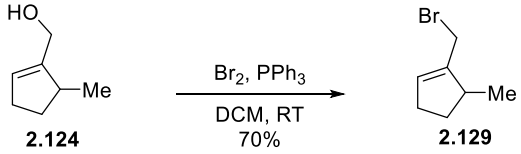


To a solution of $PPh_3$ (2.8 g, 10.7 mmol) in DCM (50 mL) was added $Br_2$ (0.55 mL, 10.7 mmol) dropwise at 0 °C. After stirring at 0 °C for 30 min, the reaction mixture was added imidazole (0.8 g, 11.6 mmol) and compound **2.124** (1 g, 8.9 mmol) at 0 °C. After stirring at RT overnight, the reaction mixture was quenched by $Na_2SO_3$ (sat. in $H_2O$) and extracted by DCM. The organic phase was dried with $Na_2SO_4$, and concentrated under reduced pressure. The residue was purified by

column chromatography (silica gel, pentane:ether = 100:1) to give compound **2.129** (1.10 g, 70% yield) as a colorless oil.

**$^1$H NMR** (400 MHz, Chloroform-*d*) δ 5.79 (t, *J* = 2.0 Hz, 1H), 4.11 (dt, *J* = 10.3, 0.7 Hz, 1H), 4.05 – 3.99 (m, 1H), 2.94 – 2.84 (m, 1H), 2.33 – 2.24 (m, 2H), 2.24 – 2.11 (m, 1H), 1.51 – 1.40 (m, 1H), 1.06 (d, *J* = 6.9 Hz, 3H).

*Synthesis of compound **2.130***

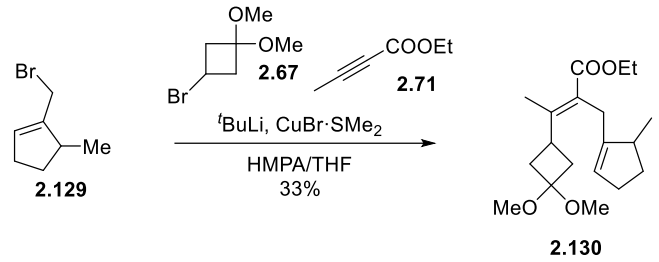


To a solution of compound **2.67** (0.5 g, 2.2 mmol) in $Et_2O$ (2.5 mL) was added *t*BuLi (1.7 M in pentane, 2.7 mL, 4.6 mmol) at −78 °C. After stirring at −78 °C for 30 min, the reaction mixture was warmed to 0 °C and stirred at 0 °C for 5 min. In another flame dried flask, to a suspension of $CuBr{\cdot}SMe_2$ (0.25 g, 1.2 mmol) in THF (13 mL) was added previous prepared alkyl lithium solution at −78 °C. After stirring at −78 °C for 10 min, the reaction mixture was added compound **2.71** (0.26 mL, 2.2 mmol) at −78 °C. After stirring at −78 °C for 30 min, the reaction mixture was added HMPA (3 mL) and compound **2.129** (0.43 g, 2.2 mmol) at −78 °C. After stirring at 0 °C for 2 h, the reaction mixture was quenched by $NH_4Cl$ (sat. in $H_2O$) and extracted by $Et_2O$. The organic phase was dried with $Na_2SO_4$, and concentrated under reduced pressure. The residue was purified

by column chromatography (silica gel, hexane:EA = 20:1) to give compound **2.130** (0.2359 g, 33% yield) as a colorless oil.

*Synthesis of compound **2.118***

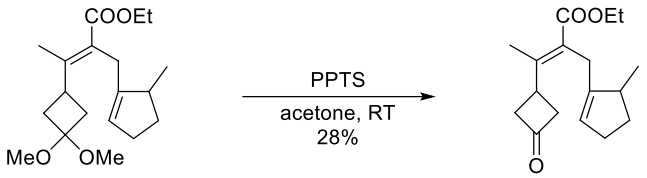


**2.130** **2.118**

To a solution of compound **2.130** (0.24 g, 0.73 mmol) in acetone (15 mL) was added PPTS (18 mg, 0.073 mmol) at room temperature. After stirring at RT overnight, the reaction mixture was quenched by $NaHCO_3$ (sat.) and extracted by $Et_2O$. The organic phase was dried with $Na_2SO_4$, and concentrated under reduced pressure. The residue was purified by column chromatography (silica gel, hexane:EA = 20:1) to give compound **2.118** (56.1 mg, 28% yield) as a colorless oil.

**$^1$H NMR** (500 MHz, Chloroform-*d*) δ 5.21 (q, *J* = 2.0 Hz, 1H), 4.18 (q, *J* = 7.2 Hz, 2H), 3.51 (p, *J* = 8.2 Hz, 1H), 3.13 (dt, *J* = 8.1, 1.6 Hz, 5H), 3.04 – 2.95 (m, 1H), 2.58 – 2.51 (m, 1H), 2.25 (dddd, *J* = 14.1, 9.4, 5.2, 2.7 Hz, 1H), 2.18 – 2.05 (m, 2H), 2.01 (s, 3H), 1.45 – 1.38 (m, 1H), 1.27 (t, *J* = 7.1 Hz, 3H), 1.02 (d, *J* = 7.0 Hz, 3H).

**$^{13}$C NMR** (101 MHz, $CDCl_3$) δ 206.12, 169.51, 145.97, 143.30, 128.72, 124.35, 60.34, 51.51, 51.41, 41.51, 32.84, 30.45, 29.58, 26.62, 19.25, 15.50, 14.21.

*Synthesis of compound **2.117***

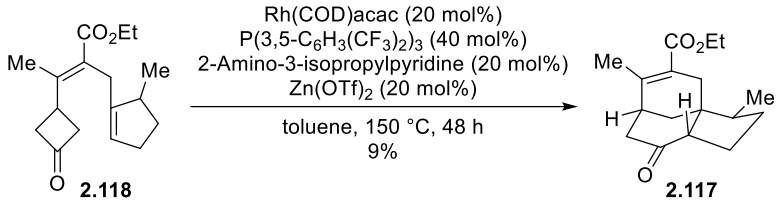


A flame dried vial was charged with compound **2.118** (13.8 mg, 0.05 mmol) Rh(COD)acac (3.1 mg, 0.01 mmol), P(3,5-$C_6H_3(CF_3)_2)_3$ (13.4 mg, 0.02 mmol), 2-amino-3-isopropylpyridine (1.4 mg, 0.01 mmol), $Zn(OTf)_2$ (3.6 mg, 0.01 mmol) and toluene (0.5 mL) in glove box. The vial was then sealed and moved out of glove box. After stirring at 150 °C for 24 h, the reaction mixture was cooled to room temperature and filtered through a short pad of silica gel to give compound **2.117** (9% NMR yield).

**$^1$H NMR** (400 MHz, $CDCl_3$) δ 4.18 (q, *J* = 7.1 Hz, 2H), 2.60 – 2.52 (m, 2H), 2.45 (t, *J* = 9.8 Hz, 1H), 2.37 (d, *J* = 15.5 Hz, 2H), 2.20 (d, *J* = 17.8 Hz, 1H), 2.11 – 2.04 (m, 1H), 2.01 (t, *J* = 2.0 Hz, 3H), 1.78 (td, *J* = 12.3, 11.1, 6.2 Hz, 2H), 1.68 (s, 2H), 1.46 – 1.35 (m, 3H), 1.29 (t, *J* = 7.1 Hz, 3H), 0.93 (d, *J* = 7.1 Hz, 3H).

*Synthesis of compound **2.136***

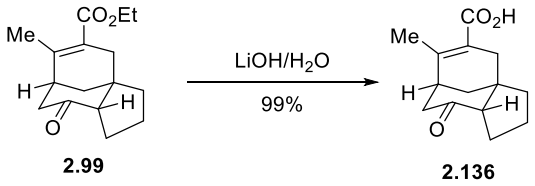


To a solution of compound **2.99** (320 mg, 1.22 mmol) in tetrahydrofuran (THF, 7.2 mL), $LiOH{\cdot}H_2O$ (160 mg, 3.7 mmol), water (2.4 mL) and methanol (2.4 mL) were added at room

temperature. After stirring at 70 °C overnight, the reaction mixture was extracted with $Et_2O$ (5 mL). The organic phase was discarded and to the aqueous phase 1M HCl was added until pH = 1 and extracted with dichloromethane (3 × 10 mL). The organic phase was dried with $Na_2SO_4$ and concentrated under reduced pressure to give crude compound **2.136** (283.3 mg, 99% yield) as a white solid. The crude compound **2.136** was directly used in next step without further purification.

**$R_f$** = 0.42 (pure ethyl acetate)

**$^1$H NMR** (500 MHz, $CDCl_3$) δ 2.66 (dq, *J* = 4.0, 1.9 Hz, 1H), 2.59 (dd, *J* = 16.2, 5.7 Hz, 1H), 2.48 (dt, *J* = 17.8, 2.0 Hz, 1H), 2.38 (dq, *J* = 16.1, 2.0 Hz, 1H), 2.31 – 2.23 (m, 2H), 2.10 (t, *J* = 2.0 Hz, 3H), 1.99 (ddt, *J* = 13.2, 8.6, 4.6 Hz, 1H), 1.93 – 1.80 (m, 3H), 1.80 – 1.73 (m, 1H), 1.64 (dd, *J* = 7.5, 5.2 Hz, 3H).

**$^{13}$C NMR** (101 MHz, $CDCl_3$) δ 213.0, 173.3, 151.9, 123.4, 59.7, 44.3, 40.8, 40.6, 40.0, 39.7, 32.6, 29.5, 22.3, 20.9.

**IR (KBr)** $\nu_{max}$ = 2932, 2626, 1704, 1629, 1449, 1415, 1273, 917, 732 $cm^{-1}$

**HRMS (ESI)** m/z calcd. for $C_{14}H_{19}O_3^+$ $[M+H]^+$: 235.1329, found 263.1330; $C_{14}H_{18}NaO_3^+$ $[M+Na]^+$: 257.1148, found 257.1150.

**Melting point**: 109.8 – 111.8 °C

*Synthesis of compound **2.135***

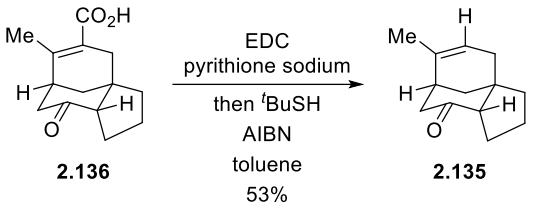


To a solution of compound **2.136** (66 mg, 0.28 mmol) in dichloromethane (2.8 mL), pyrithione sodium (51 mg, 0.34 mmol) and *N*-(3-Dimethylaminopropyl)-*N′*-ethylcarbodiimide hydrochloride (EDC, 65 mg, 0.34 mmol) were added at room temperature. After stirring at room temperature for 2 h, the reaction mixture was concentrated under reduced pressure. To the residue, toluene (5.6 mL), 2,2′-azobis(2-methylpropionitrile) (AIBN, 4.6 mg, 0.028 mmol), and $^t$BuSH (0.32 mL, 2.8 mmol) were added at room temperature. The solution was then bubbled with nitrogen gas for 20 min. Then, after stirring at 75 °C for 1 h, the resulting mixture was concentrated under reduced pressure. The residue was purified by column chromatography (silica gel, hexane:ethyl acetate = 20:1) to give compound **2.135** (28.4 mg, 53% yield) as a white solid.

**$R_f$** = 0.56 (hexane:ethyl acetate = 4:1)

**$^1$H NMR** (500 MHz, $CDCl_3$) δ 5.36 (dt, *J* = 4.9, 1.9 Hz, 1H), 2.51 (dd, *J* = 15.6, 5.0 Hz, 1H), 2.44 (t, *J* = 3.5 Hz, 1H), 2.33 – 2.24 (m, 2H), 2.20 (t, *J* = 9.6 Hz, 1H), 2.01 – 1.92 (m, 1H), 1.91 – 1.86 (m, 2H), 1.85 – 1.69 (m, 3H), 1.64 (dt, *J* = 2.8, 1.5 Hz, 3H), 1.63 – 1.56 (m, 2H), 1.52 (ddd, *J* = 12.9, 9.9, 8.1 Hz, 1H).

**$^{13}$C NMR** (101 MHz, $CDCl_3$) δ 214.3, 136.5, 121.6, 60.5, 44.9, 40.5, 39.6, 39.3, 37.2, 33.5, 29.6, 22.4, 21.5.

**IR (KBr)** $\nu_{max}$ = 2957, 2928, 2828, 1704, 1447, 1327, 1232, 1037, 931, 807 $cm^{-1}$

**HRMS (ESI)** m/z calcd. for $C_{13}H_{19}O^+$ $[M+H]^+$: 191.1430, found 191.1430.

**Melting point**: 45.0 – 46.2 °C

*Synthesis of compound **2.139***

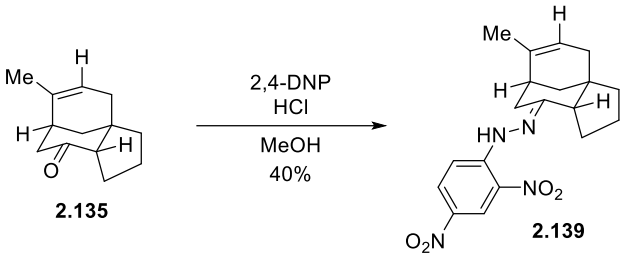


To a solution of compound **2.135** (8.1 mg, 0.043 mmol) in methanol (0.5 mL), 2,4-dinitrophenylhydrazine (2,4-DNP, 8.5 mg, 0.043 mmol) and HCl (conc. in $H_2O$, 2.6 µL, 0.043 mmol) were added at room temperature. After stirring at room temperature overnight, the reaction was quenched with $NaHCO_3$ (sat. in $H_2O$, 1 mL) and extracted with dichloromethane (3 × 1 mL). The organic phase was dried with $Na_2SO_4$ and concentrated under reduced pressure. The residue was purified by column chromatography (silica gel, hexane:ethyl acetate = 20:1) to give compound **2.139** (6.3 mg, 40% yield) as an orange solid.

$\mathbf{R_f}$ = 0.61 (hexane:ethyl acetate = 4:1)

**$^1$H NMR** (500 MHz, $CDCl_3$) δ 11.19 (s, 1H), 9.11 (d, *J* = 2.5 Hz, 1H), 8.27 (dd, *J* = 9.6, 2.6 Hz, 1H), 7.93 (d, *J* = 9.6 Hz, 1H), 5.39 (s, 1H), 2.77 (d, *J* = 15.3 Hz, 1H), 2.48 (t, *J* = 9.2 Hz, 2H), 2.36 – 2.23 (m, 2H), 2.00 – 1.88 (m, 2H), 1.88 – 1.79 (m, 3H), 1.79 – 1.74 (m, 1H), 1.66 (s, 3H), 1.62 – 1.56 (m, 3H).

**$^{13}$C NMR** (101 MHz, $CDCl_3$) δ 162.7, 145.3, 137.4, 135.2, 129.8, 128.7, 123.6, 122.5, 116.5, 54.6, 42.9, 39.8, 38.9, 36.6, 33.4, 31.3, 26.9, 21.74, 21.72.

**IR (KBr)** $\nu_{max}$ = 3321, 2928, 1619, 1591, 1518, 1426, 1336, 1136, 1074, 916, 831, 743 $cm^{-1}$

**HRMS (ESI)** m/z calcd. for $C_{19}H_{23}N_4O_4^+$ $[M+H]^+$: 371.1714, found 371.1716.

**Melting point**: 140.7 – 141.4 °C

*Synthesis of compound **2.141***

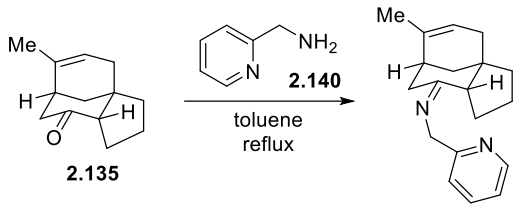


To a solution of Compound **2.135** (10 mg, 0.05 mmol) in toluene (1 mL) was added compound **2.140** (10 µL, 0.1 mmol) and PTSA (1.7 mg, 0.01 mmol) at room temperature. After stirring at 110 °C for 2 h, the reaction mixture was quenched by $NH_4Cl$ (sat. in $H_2O$) and extracted by diethyl ether. The organic phase was dried with $Na_2SO_4$ and concentrated under reduced pressure to give crude compound **2.141** as a yellow oil. The crude compound **2.141** was directly used in the next step without further purification.

*Synthesis of compound **2.142***

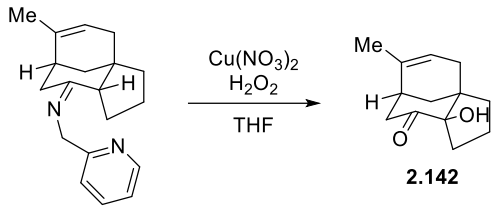


**2.141** **2.142**

To a solution of compound **2.141** (0.05 mmol) in THF (0.5 mL) was added $Cu(NO_3)_2 \cdot 3H_2O$ (13.3 mg, 0.055 mmol) at room temperature. After stirred at room temperature for 30 min, the reaction mixture was added $H_2O_2$ (30% in water, 26 μL, 0.25 mmol) dropwise at room temperature. After stirring at room temperature for 1 h, the reaction mixture was diluted by EA and quenched by $Na_2EDTA$ (sat. in $H_2O$). After stirring at room temperature overnight, the reaction mixture was extracted by EA. The organic phase was dried with $Na_2SO_4$ and concentrated under reduced pressure. The residue was purified by column chromatography (silica gel, hexane:EA = 10:1) to give compound **2.142** as a colorless oil.

**$^1$H NMR** (500 MHz, Chloroform-*d*) δ 5.35 – 5.28 (m, 1H), 3.84 (s, 1H), 2.77 (dd, *J* = 14.5, 4.7 Hz, 1H), 2.53 (dt, *J* = 14.5, 2.8 Hz, 1H), 2.48 (t, *J* = 3.3 Hz, 1H), 2.35 (ddd, *J* = 13.9, 9.8, 6.7 Hz, 2H), 2.04 (dt, *J* = 13.2, 2.2 Hz, 1H), 2.01 – 1.93 (m, 2H), 1.92 – 1.83 (m, 2H), 1.75 (dt, *J* = 13.2, 3.2 Hz, 2H), 1.71 – 1.54 (m, 4H).

**$^{13}$C NMR** (101 MHz, $CDCl_3$) δ 213.60, 135.19, 122.60, 86.37, 52.26, 41.15, 38.46, 38.43, 37.02, 36.46, 30.56, 29.68, 21.20, 20.47.

*Synthesis of compound **2.143***

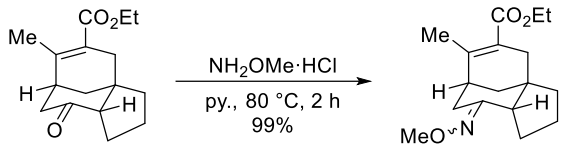


**2.99** **2.143**

To a solution of compound **2.99** (20 mg, 0.076 mmol) in pyridine (0.4 mL) was added $NH_2OMe{\cdot}HCl$ (9.5 mg, 0.11 mmol) at room temperature. After stirring at 80 °C for 2 h, the reaction mixture was cooled to room temperature and concentrated under reduced pressure. The residue was purified by column chromatography (silica gel, hexane:EA = 20:1) to give compound **2.143** (22.4 mg, 99% yield) as a colorless oil.

**$^1$H NMR** (500 MHz, Chloroform-*d*) δ 4.19 – 4.12 (m, 2H), 3.77 (d, *J* = 7.6 Hz, 3H), 3.19 (dt, *J* = 15.6, 2.6 Hz, 1H), 2.48 – 2.35 (m, 3H), 2.27 (t, *J* = 9.5 Hz, 1H), 2.20 – 2.12 (m, 1H), 2.02 (d, *J* = 2.2 Hz, 3H), 1.91 – 1.70 (m, 4H), 1.60 – 1.51 (m, 1H), 1.49 – 1.39 (m, 1H), 1.28 (td, *J* = 7.2, 0.8 Hz, 3H).

*Synthesis of compound **2.147***

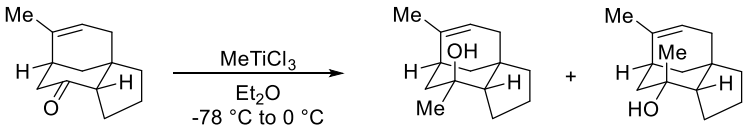


**2.135** **2.147** 53% **2.148** 8%

To a solution of $Et_2O$ (0.5 mL) was added $TiCl_4$ (1 M in DCM, 0.2 mL, 0.21 mmol) and MeLi (1.6 M in $Et_2O$, 0.13 mL. 0.21 mmol) slowly at the −78 °C. The reaction mixture was then added compound **2.135** (20 mg, 0.11 mmol) in $Et_2O$ (0.5 mL) at −30 °C. After stirring at 0 °C for 3 h, the reaction mixture was quenched by water and extracted by $Et_2O$. The organic phase was dried with

$Na_2SO_4$ and concentrated under reduced pressure to give compound **2.147** and **2.148** (61% NMR yield, d.r. = 6.6:1).

**$^1$H NMR** (500 MHz, Chloroform-*d*) δ 5.55 (tt, *J* = 2.8, 1.4 Hz, 1H), 2.30 (ddt, *J* = 18.1, 3.6, 1.8 Hz, 1H), 2.19 – 2.15 (m, 1H), 1.97 (ddt, *J* = 18.4, 3.9, 1.8 Hz, 1H), 1.84 (dq, *J* = 8.8, 5.1, 4.5 Hz, 1H), 1.79 (q, *J* = 1.9 Hz, 3H), 1.75 – 1.69 (m, 2H), 1.64 – 1.54 (m, 4H), 1.53 – 1.41 (m, 2H), 1.28 – 1.21 (m, 2H), 1.05 (s, 3H).

**$^{13}$C NMR** (101 MHz, $CDCl_3$) δ 142.59, 123.40, 72.44, 57.57, 40.72, 39.04, 38.42, 36.22, 35.56, 32.84, 29.21, 28.98, 22.23, 19.38.

*Synthesis of compound **2.148***

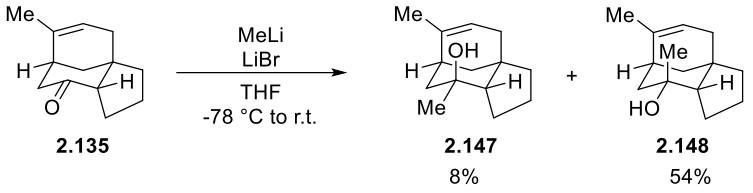


**2.135** **2.147** 8% **2.148** 54%

To a solution of compound **2.135** (20 mg, 0.11 mmol) in THF (0.5 mL) was added LiBr (14 mg, 0.16 mmol) at room temperature. The reaction mixture was then cooled to −78 °C, added MeLi (1.6 M in $Et_2O$, 0.1 mL. 0.16 mmol) slowly at the −78 °C. After stirring at 0 °C for 2 h, the reaction mixture was quenched by $NH_4Cl$ (sat. in $H_2O$) and extracted by $Et_2O$. The organic phase was dried with $Na_2SO_4$ and concentrated under reduced pressure to give compound **2.147** and **2.148** (62% NMR yield, d.r. = 1:6.8).

**$^1$H NMR** (500 MHz, Chloroform-*d*) δ 5.25 (dd, *J* = 4.6, 2.4 Hz, 1H), 2.22 – 2.15 (m, 1H), 1.99 (dt, *J* = 17.8, 2.4 Hz, 1H), 1.87 – 1.75 (m, 4H), 1.74 – 1.68 (m, 1H), 1.66 (q, *J* = 1.9 Hz, 4H), 1.62 – 1.50 (m, 4H), 1.46 – 1.38 (m, 1H), 1.34 (ddd, *J* = 12.1, 3.6, 1.7 Hz, 1H), 1.21 (s, 3H).

**$^{13}$C NMR** (101 MHz, $CDCl_3$) δ 139.58, 120.72, 71.97, 53.72, 41.60, 40.45, 40.21, 39.94, 35.20, 32.82, 31.45, 29.68, 26.98, 22.01.

**$^1$H NMR** (500 MHz, **Benzene-*d*$_6$**) δ 5.23 (dt, *J* = 4.9, 1.8 Hz, 1H), 2.12 – 2.07 (m, 1H), 1.98 (dt, *J* = 11.6, 2.2 Hz, 1H), 1.96 – 1.91 (m, 1H), 1.74 (ddd, *J* = 6.3, 3.8, 2.1 Hz, 1H), 1.73 – 1.65 (m, 3H), 1.61 (dt, *J* = 2.8, 1.7 Hz, 3H), 1.55 (s, 1H), 1.53 – 1.45 (m, 4H), 1.42 – 1.38 (m, 2H), 1.04 (s, 3H).

*Synthesis of compound **2.151***

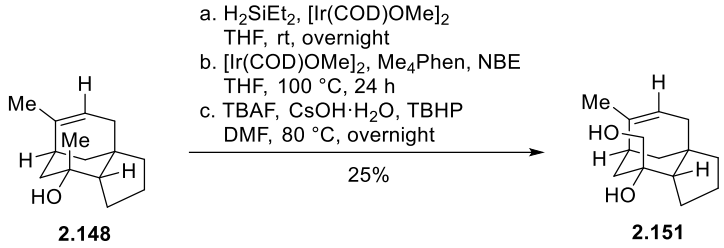

**2.148** **2.151**

In glovebox, to a solution of compound **2.148** (10 mg, 0.048 mmol) in THF (0.3 mL) was added $[Ir(COD)OMe]_2$ (0.2 mg, 0.00024 mmol) and $Et_2SiH_2$ (9.4 μL, 0.072 mmol) at room temperature. After stirring at room temperature overnight, the reaction mixture was concentrated under reduced pressure and placed under vacuum for 30 min to give crude mixture. The crude mixture was directly used in the next step.

To a solution of the crude mixture in THF (0.3 mL) was added NBE (5.5 mg, 0.058 mmol), $[Ir(COD)OMe]_2$ (1.3 mg, 0.0019 mmol) and $Me_4Phen$ (1.1 mg, 0.0048 mmol) at room temperature. After stirring at 100 °C for 24 h, the reaction mixture was concentrated under reduced pressure to give crude mixture. The crude mixture was directly used in the next step.

To a solution of the crude mixture in DMF (0.5 mL) was added $CsOH·H_2O$ (98 mg, 0.58 mmol), TBAF (1 M in THF, 0.24 mL, 0.24 mmol) and TBHP (5.5 M in decane, 0.12 mL, 0.67 mmol) at room temperature. After stirring at 80 °C overnight, the reaction mixture was quenched by $N_2SO_3$ (sat. in $H_2O$) and extracted by $Et_2O$. The organic phase was dried with $Na_2SO_4$ and concentrated under reduced pressure. The residue was purified by column chromatography (silica gel, hexane:EA = 10:1) to give compound **2.151** (2.7 mg, 25% yield) as a colorless oil.

**$^1$H NMR** (500 MHz, Chloroform-*d*) δ 5.29 (ddt, *J* = 4.3, 2.7, 1.3 Hz, 1H), 3.53 (d, *J* = 10.8 Hz, 1H), 3.45 (d, *J* = 10.8 Hz, 1H), 2.20 (dq, *J* = 5.6, 2.7 Hz, 1H), 2.11 (dq, *J* = 18.2, 2.3 Hz, 1H), 1.83 – 1.77 (m, 2H), 1.74 (ddd, *J* = 8.3, 4.6, 2.3 Hz, 1H), 1.72 – 1.64 (m, 7H), 1.61 – 1.52 (m, 2H), 1.50 – 1.42 (m, 1H), 1.31 (ddd, *J* = 12.2, 3.3, 1.7 Hz, 1H), 1.25 (s, 3H).

*Synthesis of compound **2.152***

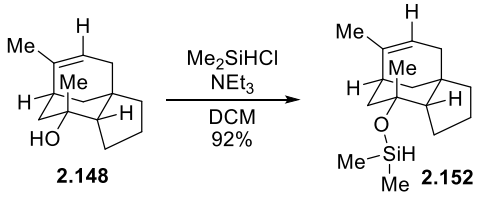


To a solution of compound **2.148** (20 mg, 0.097 mmol) in DCM (1 mL) was added $NEt_3$ (21 µL, 0.19 mmol) and $Me_2SiHCl$ (55 µL, 0.39 mmol) at room temperature. After stirring at room

temperature for 3 h, the reaction mixture was quenched by water and extracted by $Et_2O$. The organic phase was dried with $Na_2SO_4$ and concentrated under reduced pressure. The residue was purified by column chromatography (silica gel, hexane:EA = 100:1) to give compound **2.152** (23.6 mg, 92% yield) as a colorless oil.

**$^1$H NMR** (500 MHz, Chloroform-*d*) δ 5.22 – 5.17 (m, 1H), 4.75 (p, *J* = 2.8 Hz, 1H), 2.15 (d, *J* = 8.7 Hz, 1H), 1.99 (dd, *J* = 14.3, 8.5 Hz, 1H), 1.92 – 1.85 (m, 2H), 1.79 (dq, *J* = 4.9, 1.6 Hz, 1H), 1.77 – 1.69 (m, 2H), 1.64 (q, *J* = 1.8 Hz, 4H), 1.51 – 1.43 (m, 2H), 1.39 (dt, *J* = 14.3, 1.6 Hz, 1H), 1.37 – 1.33 (m, 1H), 1.29 (ddd, *J* = 11.8, 3.5, 1.4 Hz, 1H), 1.21 (s, 4H), 0.15 (t, *J* = 2.5 Hz, 6H).

*Synthesis of compound **2.153***

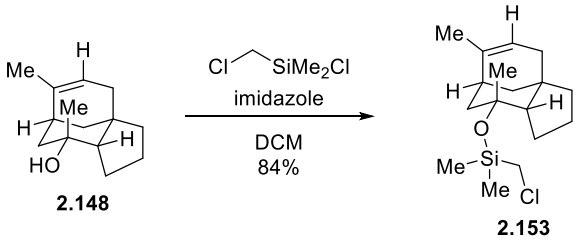


To a solution of compound **2.148** (30 mg, 0.15 mmol) in DCM (0.75 mL) was added imidazole (21 mg, 0.30 mmol) and $Me_2SiClCH_2Cl$ (30 μL, 0.23 mmol) at room temperature. After stirring at room temperature for 3 h, the reaction mixture was quenched by $NH_4Cl$ (sat. in $H_2O$) and extracted by $Et_2O$. The organic phase was dried with $Na_2SO_4$ and concentrated under reduced pressure. The residue was purified by column chromatography (silica gel, hexane:EA = 100:1) to give compound **2.153** (39.5 mg, 84% yield) as a colorless oil.

**$^1$H NMR** (500 MHz, Chloroform-*d*) δ 5.19 (dt, *J* = 3.9, 1.9 Hz, 1H), 2.75 (d, *J* = 4.4 Hz, 3H), 2.15 (d, *J* = 8.5 Hz, 1H), 1.92 (dd, *J* = 14.3, 8.6 Hz, 1H), 1.88 (dt, *J* = 11.5, 2.5 Hz, 2H), 1.79 (dt, *J* = 5.1, 1.8 Hz, 1H), 1.77 – 1.70 (m, 2H), 1.64 (q, *J* = 1.8 Hz, 3H), 1.51 – 1.39 (m, 4H), 1.32 (dddd, *J* = 13.1, 11.8, 3.8, 1.7 Hz, 2H), 1.20 (s, 3H), 0.25 – 0.21 (m, 6H).

*Synthesis of compound **2.154***

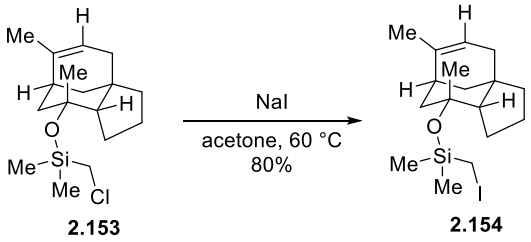

**2.153** **2.154**

To a solution of compound **2.153** (39.5 mg, 0.13 mmol) in acetone (0.7 mL) was added NaI (95 mg, 0.63 mmol) at room temperature. After stirring at 60 °C for 24 h, the reaction mixture was quenched by $Na_2S_2O_3$ (sat. in $H_2O$) and extracted by $Et_2O$. The organic phase was dried with $Na_2SO_4$ and concentrated under reduced pressure. The residue was purified by column chromatography (silica gel, hexane:EA = 100:1) to give compound **2.154** (42.1 mg, 80% yield) as a colorless oil.

**$^1$H NMR** (500 MHz, Chloroform-*d*) δ 5.19 (dt, *J* = 3.8, 1.9 Hz, 1H), 2.16 (d, *J* = 8.6 Hz, 1H), 2.02 (d, *J* = 2.3 Hz, 3H), 1.97 – 1.85 (m, 3H), 1.81 – 1.71 (m, 3H), 1.64 (dd, *J* = 2.6, 1.4 Hz, 3H), 1.52 – 1.36 (m, 5H), 1.31 (ddd, *J* = 11.8, 3.6, 1.4 Hz, 1H), 1.20 (s, 3H), 0.31 – 0.27 (m, 6H).

*Synthesis of compound **2.160***

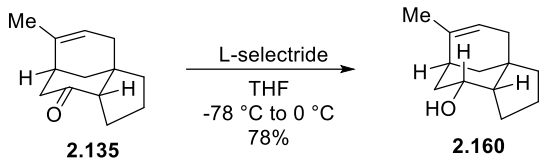


To a solution of compound **2.135** (37.5 mg, 0.20 mmol) in THF (2 mL) was added L-Selectride (1 M in THF, 0.3 mL. 0.2 mmol) slowly at the −78 °C. After stirring at −78 °C for 1 h, the reaction mixture was warmed to 0 °C. After stirring at 0 °C for 30 min, the reaction mixture was quenched by $NH_4Cl$ (sat. in $H_2O$) and extracted by $Et_2O$. The organic phase was dried with $Na_2SO_4$ and concentrated under reduced pressure. The residue was purified by column chromatography (silica gel, hexane:EA = 20:1 to 10:1) to give compound **2.160** (29.7 mg, 78% yield) as a white solid.

**$^1$H NMR** (500 MHz, $CDCl_3$) δ 5.36 (dt, *J* = 4.1, 2.3 Hz, 1H), 4.06 (dt, *J* = 11.7, 5.9 Hz, 1H), 2.22 (dt, *J* = 16.4, 3.2 Hz, 2H), 1.94 – 1.84 (m, 1H), 1.80 – 1.69 (m, 4H), 1.65 (q, *J* = 2.0 Hz, 3H), 1.54 (dt, *J* = 12.4, 2.1 Hz, 1H), 1.48 – 1.44 (m, 2H), 1.40 (td, *J* = 12.0, 3.7 Hz, 1H), 1.22 (dq, *J* = 11.0, 1.8 Hz, 1H), 0.86 (dddd, *J* = 17.2, 14.9, 7.6, 4.7 Hz, 2H).

*Synthesis of compound **2.161***

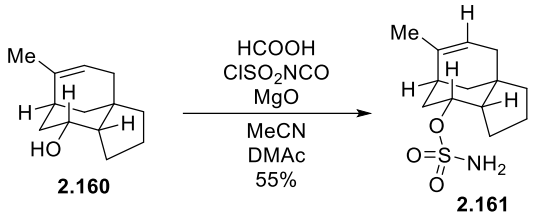


To a flame dried flask was charged chlorosulfonyl isocyanate (31 μL, 0.36 mmol) and formic acid (14 μL, 0.36 mmol) at 0 °C. After stirring vigorously at 0 °C for 10 min, the reaction mixture was added MeCN (0.5 mL) at 0 °C. After stirring at 0 °C for 30 min, the reaction mixture was warmed

to RT and stirring at RT for 10 h. In another flame dried flask, to a solution of compound **2.160** (14 mg, 0.073 mmol) in DMA (0.24 mL) was added MgO (29 mg, 0.73 mmol) and above solution at 0 °C. After stirring at RT for 2 h, the reaction mixture was quenched by water and extracted by $Et_2O$. The organic phase was dried with $Na_2SO_4$ and concentrated under reduced pressure. The residue was purified by column chromatography (silica gel, hexane:EA = 50:1) to give compound **2.161** (10.9 mg, 55% yield) as a white solid.

**$^1$H NMR** (500 MHz, $CDCl_3$) δ 5.45 (s, 1H), 5.01 (dt, *J* = 11.9, 6.2 Hz, 1H), 4.62 (s, 2H), 2.27 (d, *J* = 20.5 Hz, 2H), 2.16 (d, *J* = 7.8 Hz, 1H), 2.04 (s, 1H), 1.89 – 1.81 (m, 3H), 1.80 – 1.74 (m, 2H), 1.70 (d, *J* = 2.0 Hz, 4H), 1.52 – 1.48 (m, 2H), 1.29 (d, *J* = 11.7 Hz, 2H).

*Synthesis of compound **2.162** and **2.163***

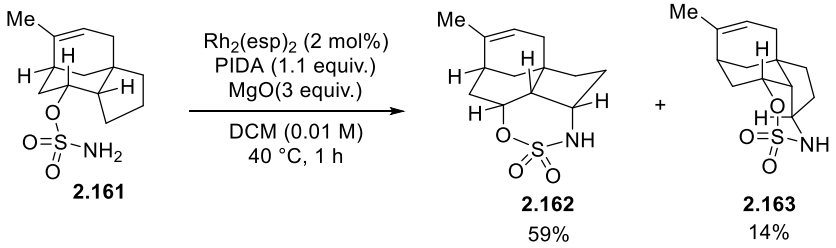


To a solution of compound **2.161** (5 mg, 0.018 mmol) in DCM (2 mL) was added MgO (2.2 mg, 0.054 mmol), PIDA (6.4 mg, 0.02 mmol) and $Rh_2(esp)_2$ (0.3 mg, 0.00036 mmol) at room temperature. After stirring at 40 °C for 3 h, the reaction mixture was cooled to RT, diluted with DCM and filtered through Celite. The organic phase concentrated under reduced pressure. The residue was purified by column chromatography (silica gel, hexane:EA = 10:1) to give compound **2.162** (59% NMR yield) as a white solid, and **2.163** (14% NMR yield) as a white solid.

Compound **2.162**:

**$^1$H NMR** (500 MHz, $CDCl_3$) δ 5.28 – 5.24 (m, 1H), 5.10 (td, *J* = 6.7, 4.4 Hz, 1H), 4.21 (qd, *J* = 7.2, 3.8 Hz, 1H), 4.05 (d, *J* = 7.6 Hz, 1H), 2.33 (ddt, *J* = 8.1, 4.2, 2.0 Hz, 1H), 2.11 (dddd, *J* = 16.4, 14.8, 7.0, 3.6 Hz, 3H), 2.05 – 1.99 (m, 1H), 1.89 – 1.80 (m, 2H), 1.78 – 1.69 (m, 2H), 1.67 (d, *J* = 2.2 Hz, 4H), 1.65 – 1.57 (m, 2H).

**$^{13}$C NMR** (126 MHz, $CDCl_3$) δ 138.48, 119.51, 81.66, 59.34, 44.85, 41.47, 38.99, 38.56, 32.75, 32.50, 32.39, 30.35, 21.73.

**DEPT-135 NMR** (126 MHz, $CDCl_3$) δ 119.55, 81.71, 59.38, 44.89, 41.50, 38.59, 32.79, 32.53, 32.43, 30.38, 21.77.

Compound **2.163**:

**$^1$H NMR** (500 MHz, $CDCl_3$) δ 5.41 (d, *J* = 4.4 Hz, 1H), 4.98 (dt, *J* = 13.4, 6.7 Hz, 1H), 4.24 (qd, *J* = 11.5, 7.5 Hz, 1H), 4.06 (d, *J* = 11.3 Hz, 1H), 2.37 – 2.29 (m, 2H), 2.28 – 2.13 (m, 3H), 1.88 (d, *J* = 17.0 Hz, 1H), 1.79 (dd, *J* = 12.0, 6.6 Hz, 2H), 1.70 – 1.63 (m, 5H), 1.60 (dd, *J* = 12.6, 2.3 Hz, 1H), 1.51 (d, *J* = 16.2 Hz, 1H).

*Synthesis of compound **2.166***

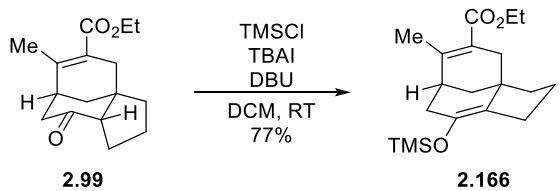


**2.99** **2.166**

To a solution of compound **2.99** (90 mg, 0.34 mmol) in DCM (3.4 mL) was added DBU (0.13 mL, 0.85 mmol), TMSCl (65 μL, 0.51 mmol) and TBAI (25 mg, 0.07 mmol) at room temperature. After stirring at RT for 24 h, the reaction mixture was quenched by pH = 7 buffer and extracted by diethyl ether. The organic phase was dried with $Na_2SO_4$ and concentrated under reduced pressure. The residue was purified by column chromatography (silica gel, hexane:EA = 20:1) to give compound **2.166** (87.8 mg, 77% yield) as a colorless oil.

**$^1$H NMR** (500 MHz, $CDCl_3$) δ 4.21 – 4.09 (m, 2H), 2.50 (s, 1H), 2.41 – 2.29 (m, 3H), 2.22 (dd, *J* = 14.9, 11.2 Hz, 1H), 2.08 – 2.01 (m, 4H), 1.96 (d, *J* = 16.4 Hz, 1H), 1.85 – 1.65 (m, 3H), 1.42 (td, *J* = 11.8, 8.6 Hz, 1H), 1.32 (dt, *J* = 11.7, 2.1 Hz, 1H), 1.29 – 1.24 (m, 4H), 0.13 (s, 9H).

*Synthesis of compound **2.167***

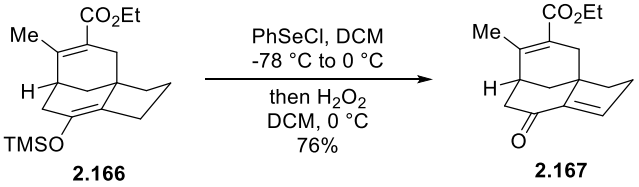

**2.166** **2.167**

To a solution of compound **2.166** (80 mg, 0.24 mmol) in DCM (2.4 mL) was added PhSeCl (56 mg, 0.29 mmol) at the −78 °C. After stirring at −78 °C for 1 h, the reaction mixture was warmed to 0 °C. After stirring at 0 °C for 30 min, the reaction mixture was quenched by $NaHCO_3$ (sat. in $H_2O$) and extracted by DCM. The organic phase was dried with $Na_2SO_4$ and concentrated under reduced pressure to give crude intermediate.

To a solution of the crude intermediate in DCM (2.4 mL) was added $H_2O_2$ (30% in $H_2O$, 74 μL, 0.72 mmol) at 0 °C. After stirring at 0 °C for 1 h, the reaction mixture was quenched by $Na_2S_2O_3$

(sat. in $H_2O$) and extracted by DCM. The organic phase was dried with $Na_2SO_4$ and concentrated under reduced pressure. The residue was purified by column chromatography (silica gel, hexane:EA = 10:1) to give compound **2.167** (42.3 mg, 76% yield) as a white solid.

**$^1$H NMR** (400 MHz, $CDCl_3$) δ 6.63 (dd, *J* = 3.5, 2.1 Hz, 1H), 4.14 (q, *J* = 7.1 Hz, 2H), 2.66 – 2.52 (m, 3H), 2.50 – 2.34 (m, 4H), 2.09 (t, *J* = 3.2 Hz, 1H), 2.05 (dd, *J* = 2.4, 1.7 Hz, 3H), 2.04 – 1.91 (m, 2H), 1.76 (dt, *J* = 12.5, 1.9 Hz, 1H), 1.27 (t, *J* = 7.1 Hz, 3H).

*Synthesis of compound **2.170***

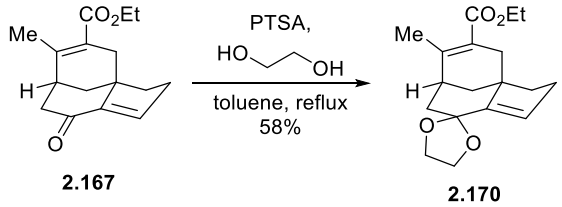


In Dean-Stark apparatus was charged compound **2.167** (118 mg, 0.45 mmol), toluene (10 mL), ethylene glycol (250 μL, 4.5 mmol) and PTSA (9 MG, 0.045 mmol) at room temperature. After refluxing for 10 h, the reaction mixture was quenched by $NaHCO_3$ (sat. in $H_2O$) and extracted by $Et_2O$. The organic phase was dried with $Na_2SO_4$ and concentrated under reduced pressure. The residue was purified by column chromatography (silica gel, hexane:EA = 10:1) to give compound **2.170** (79.1 mg, 58% yield) as a colorless oil.

**$^1$H NMR** (500 MHz, $CDCl_3$) δ 5.65 (t, *J* = 2.4 Hz, 1H), 4.22 – 4.13 (m, 2H), 3.96 – 3.87 (m, 2H), 3.85 – 3.77 (m, 2H), 2.53 – 2.25 (m, 4H), 2.09 (t, *J* = 2.1 Hz, 3H), 2.04 (q, *J* = 1.8 Hz, 2H), 1.91 – 1.82 (m, 3H), 1.76 (ddd, *J* = 11.9, 3.7, 2.0 Hz, 2H), 1.29 (t, *J* = 7.1 Hz, 3H).

*Synthesis of compound **2.172***

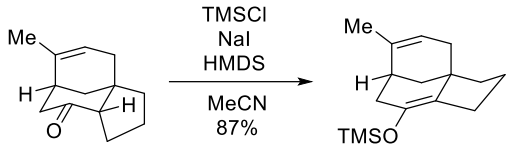


**2.135** **2.172**

To a solution of compound **2.135** (50 mg, 0.26 mmol) in acetonitrile (2.6 mL), hexamethyldisilazane (HMDS, 0.22 mL, 1.05 mmol), NaI (157 mg, 1.05 mmol), and chlorotrimethylsilane (TMSCl, 99 μL, 0.78 mmol) were added at room temperature. After stirring at room temperature for 12 h, the reaction mixture was quenched with pH = 7 buffer (aqueous, 5 mL) and extracted with $Et_2O$ (3 × 5 mL). The organic phase was then dried with $Na_2SO_4$ and concentrated under reduced pressure, then purified by column chromatography (silica gel, hexane:$Et_2O$ = 20:1) to give compound **2.172** (59.3 mg, 87% yield) as a colorless oil.

**$R_f$** = 0.77 (hexane:ethyl acetate = 10:1)

**$^1$H NMR** (500 MHz, $CDCl_3$) δ 5.24 (t, *J* = 3.9 Hz, 1H), 2.40 – 2.29 (m, 2H), 2.27 – 2.15 (m, 2H), 1.99 – 1.88 (m, 2H), 1.85 (d, *J* = 17.4 Hz, 1H), 1.79 (dd, *J* = 11.5, 3.9 Hz, 1H), 1.75 – 1.70 (m, 1H), 1.69 – 1.66 (m, 4H), 1.66 – 1.61 (m, 1H), 1.44 – 1.34 (m, 1H), 1.31 – 1.26 (m, 1H), 0.13 (s, 9H).

**$^{13}$C NMR** (101 MHz, $CDCl_3$) δ 140.6, 136.6, 124.3, 120.0, 40.8, 40.6, 37.5, 36.3, 36.2, 34.3, 25.4, 22.0, 21.8, 0.7.

**IR (KBr)** $\nu_{max}$ = 2955, 2913, 1699, 1348, 1251, 1209, 1165, 1004, 873, 842 $cm^{-1}$

**HRMS (ESI)** m/z calcd. for $C_{13}H_{17}O^+$ $[M+H]^+$: 189.1274, found 189.1280.

*Synthesis of compound **2.173***

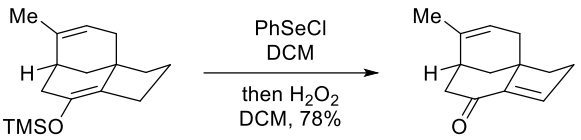


**2.172** **2.173**

To a solution of compound **2.172** (20 mg, 0.076 mmol) in dichloromethane (1.5 mL), PhSeCl (21 mg, 0.11 mmol) was added at −78 °C. After stirring at −78 °C for 30 min, the reaction mixture was warmed to 0 °C and stirred for 5 min. The reaction was then quenched with $NaHCO_3$ (sat. in $H_2O$, 2 mL) and extracted with dichloromethane (3 × 2 mL). The organic phase was dried with $Na_2SO_4$ and concentrated under reduced pressure. The residue was added dichloromethane (1.5 mL) and $H_2O_2$ (30% in $H_2O$, 40 μL, 0.38 mmol) at the 0 °C. After stirring at 0 °C for 1 h, the reaction was quenched with $Na_2S_2O_3$ (sat. in $H_2O$, 2 mL) and extracted with dichloromethane (3 × 2 mL). The organic phase was dried with $Na_2SO_4$ and concentrated under reduced pressure. The residue was purified by column chromatography (silica gel, hexane:$Et_2O$ = 20:1) to give compound **2.173** (11.2 mg, 78% yield) as a colorless oil.

**$R_f$** = 0.46 (hexane:ethyl acetate = 4:1)

**$^1$H NMR** (500 MHz, $CDCl_3$) δ 6.56 (t, *J* = 2.9 Hz, 1H), 5.35 – 5.27 (m, 1H), 2.60 – 2.48 (m, 2H), 2.46 (t, *J* = 3.5 Hz, 1H), 2.43 – 2.33 (m, 2H), 2.19 (dt, *J* = 17.5, 3.0 Hz, 1H), 2.10 (dt, *J* = 15.4, 3.1 Hz, 2H), 1.99 – 1.87 (m, 2H), 1.78 – 1.72 (m, 1H), 1.67 (d, *J* = 2.4 Hz, 3H).

**$^{13}$C NMR** (101 MHz, $CDCl_3$) δ 199.1, 149.4, 137.7, 136.5, 120.7, 46.3, 44.2, 41.0, 39.0, 38.1, 36.9, 29.9, 21.5.

**IR (KBr)** $\nu_{max}$ = 2921, 1683, 1612, 1436, 1328, 1261, 1221, 1048, 986, 919 $cm^{-1}$

**HRMS (CI)** m/z calcd. for $C_{16}H_{27}OSi^+$ $[M+H]^+$: 263.1826, found 263.1826.

*Synthesis of compound **2.173***

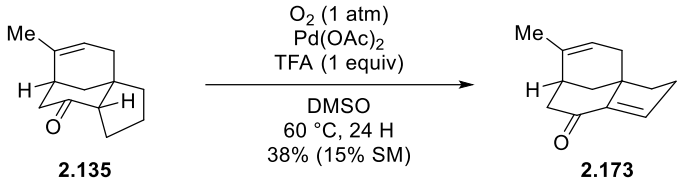


To a solution of compound **2.135** (49 mg, 0.26 mmol) in dimethyl sulfoxide (DMSO, 1.3 mL), trifluoroacetic acid (TFA, 20 μL, 0.26 mmol) and $Pd(OAc)_2$ (17 mg, 0.077 mmol) were added at room temperature. The solution was then bubbled with $O_2$ for 20 min. After stirring at 60 °C under $O_2$ atmosphere for 24 h, the reaction was quenched with $NaHCO_3$ (sat. in $H_2O$, 3 mL) and extracted with $Et_2O$ (3 × 3 mL). The organic phase was dried with $Na_2SO_4$ and concentrated under reduced pressure. The residue was then purified by column chromatography (silica gel, hexane:$Et_2O$ = 100:1) to give compound **2.173** (18.4 mg, 38% yield) and compound **2.135** (7.4 mg, 15% recovery).

Analytical data see above.

*Synthesis of compound **2.175***

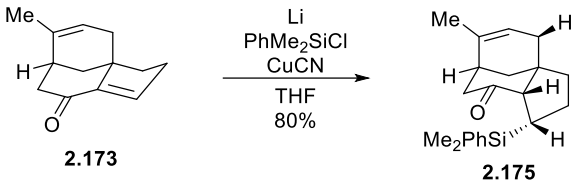


**2.173** **2.175**

To a flame dried 10 mL flask was charged $Me_2PhSiCl$ (195 mg, 1.14 mmol) and THF (2 mL) at room temperature. The mixture was added lithium (32 mg, 4.6 mmol) at 0 °C and stirred at 0 °C for 3 h. The obtained $Me_2PhSiLi$ solution was transferred to the suspension of CuCN (51 mg, 0.57 mmol) in THF (1 mL) at −78 °C. After stirring at 0 °C for 30 min, the reaction mixture was added compound **2.173** (72 mg, 0.38 mmol) in THF (1 mL) at −78 °C. After stirring at −78 °C for 30 min, the reaction mixture was warmed to 0 °C. After stirring at 0 °C for 30 min, the reaction mixture was quenched by $NH_4Cl$ (sat. in $H_2O$) and extracted by $Et_2O$. The organic phase was dried with $Na_2SO_4$ and concentrated under reduced pressure. The residue was then purified by column chromatography (silica gel, hexane:EA = 20:1) to give compound **2.175** (0.0990 g, 80% yield) as a colorless oil.

$\mathbf{R_f}$ = 0.53 (hexane:EA = 4:1)

**$^1$H NMR** (400 MHz, $CDCl_3$) δ 7.55 – 7.51 (m, 2H), 7.32 (dd, *J* = 4.9, 1.9 Hz, 3H), 5.39 (d, *J* = 4.9 Hz, 1H), 2.60 (d, *J* = 9.1 Hz, 1H), 2.30 (s, 1H), 2.24 – 2.16 (m, 2H), 2.11 (dd, *J* = 17.2, 7.6 Hz, 1H), 1.91 (dd, *J* = 17.1, 4.9 Hz, 1H), 1.71 (q, *J* = 6.0 Hz, 1H), 1.68 – 1.66 (m, 4H), 1.62 (dd, *J* = 11.7, 5.9 Hz, 1H), 1.50 – 1.40 (m, 2H), 1.39 – 1.30 (m, 2H), 0.40 (s, 3H), 0.29 (s, 3H).

*Synthesis of compound **2.177***

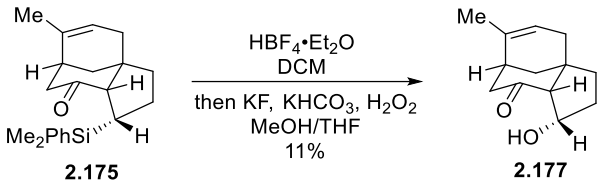


To a solution of compound **2.175** (28 mg, 0.086 mmol) in DCM (0.9 mL) was added $HBF_4 \cdot Et_2O$ (59 μL, 2.5 mmol) at the room temperature. After stirring at room temperature for 2 h, the reaction mixture was quenched by $NaHCO_3$ (sat. in $H_2O$) and extracted by DCM. The organic phase was dried with $Na_2SO_4$ and concentrated under reduced pressure to give crude intermediate.

To a solution of the crude intermediate in THF (0.43 mL) and MeOH (0.43 mL) was added $KHCO_3$ (17 mg, 0.17 mmol) and KF (9.9 mg, 0.17 mmol) at room temperature. After stirring at room temperature for 15 min, the reaction mixture was cooled to 0 °C and added $H_2O_2$ (30% in water, 130 μL, 1.3 mmol). After stirring at room temperature for 12 h, the reaction mixture was quenched by $Na_2S_2O_3$ (sat.) and extracted by $Et_2O$. The organic phase was dried with $Na_2SO_4$ and concentrated under reduced pressure. The residue was then purified by column chromatography (silica gel, hexane:$Et_2O$ = 4:1) to give compound **2.177** (2.0 mg, 11% yield) as a colorless oil.

**$R_f$** = 0.52 (hexane:ethyl acetate = 2:1)

**$^1$H NMR** (500 MHz, $CDCl_3$) δ 5.34 (dt, *J* = 5.1, 1.8 Hz, 1H), 4.60 (tt, *J* = 6.3, 3.2 Hz, 1H), 2.49 (dtd, *J* = 16.8, 2.2, 1.3 Hz, 1H), 2.43 (ddq, *J* = 6.1, 4.0, 2.0 Hz, 1H), 2.36 (dd, *J* = 16.9, 5.4 Hz, 1H), 2.27 (d, *J* = 3.6 Hz, 1H), 2.26 – 2.19 (m, 2H), 2.05 – 1.97 (m, 2H), 1.89 – 1.76 (m, 4H), 1.65 (dt, *J* = 2.8, 1.5 Hz, 3H), 1.59 – 1.54 (m, 1H).

**$^{13}$C NMR** (101 MHz, $CDCl_3$) δ 214.7, 137.5, 121.1, 76.1, 64.8, 44.9, 41.7, 41.2, 38.0, 36.0, 35.7, 33.0, 21.5.

**IR (KBr)** $\nu_{max}$ = 3432, 2912, 2828, 1692, 1445, 1330, 1220, 1112, 1039, 808, 564 $cm^{-1}$

**HRMS (ESI):** m/z calcd for $C_{13}H_{19}O_2^+$ $[M+H]^+$: 207.1380, found 207.1379.

*Synthesis of compound **2.179***

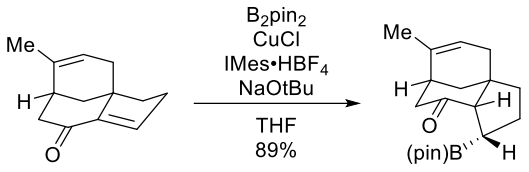


To a suspension of CuCl (28 mg, 0.28 mmol) in THF (15 mL) was added IMes·$HBF_4$ (110 mg, 0.28 mmol) and NaOtBu (54 mg, 0.56 mmol) at room temperature. After stirring at room temperature for 40 min, the reaction mixture was added compound **2.173** (0.2647 g, 1.4 mmol) and $B_2(pin)_2$ (460 mg, 1.82 mmol) in THF (15 mL) at 0 °C. After stirring at 0 °C for 2 h and at room temperature for 1 h, the reaction mixture was quenched by $NH_4Cl$ (sat. in $H_2O$) and extracted by $Et_2O$. The organic phase was dried with $Na_2SO_4$ and concentrated under reduced pressure. The residue was purified by column chromatography (silica gel, hexane:$Et_2O$ = 10:1) to give compound **2.179** (0.3956 g, 89% yield) as a colorless oil.

**$R_f$** = 0.39 (hexane:EA = 10:1, run twice)

**$^1$H NMR** (500 MHz, $CDCl_3$) δ 5.43 – 5.39 (m, 1H), 2.77 (d, *J* = 8.8 Hz, 1H), 2.44 – 2.31 (m, 3H), 2.19 (d, *J* = 17.2 Hz, 1H), 1.94 (dd, *J* = 17.2, 5.0 Hz, 1H), 1.76 – 1.68 (m, 5H), 1.62 – 1.59 (m, 1H), 1.52 – 1.45 (m, 2H), 1.40 (dd, *J* = 11.5, 6.3 Hz, 1H), 1.37 – 1.31 (m, 1H), 1.28 (s, 6H), 1.25 (s, 6H).

**$^{11}$B NMR** (128 MHz, $CDCl_3$) δ 33.28.

**$^{13}$C NMR** (101 MHz, $CDCl_3$) δ 214.79, 138.01, 121.85, 82.75, 61.02, 43.68, 41.77, 41.73, 41.67, 35.60, 35.16, 27.04, 24.94, 24.79, 21.67.

**DEPT-135** (101 MHz, $CDCl_3$) δ 121.81, 60.97, 41.72, 41.68, 41.63, 35.55, 35.11, 26.99, 24.89, 24.75, 21.62.

**IR (KBr)** $\nu_{max}$ = 2974, 2929, 1705, 1447, 1409, 1377, 1313, 1199, 1147, 1114, 968, 862 $cm^{-1}$

**HRMS (ESI):** m/z calcd for $C_{19}H_{29}BNaO_3^+$ $[M+Na]^+$: 339.2102, found 339.2105.

*Synthesis of compound **2.177***

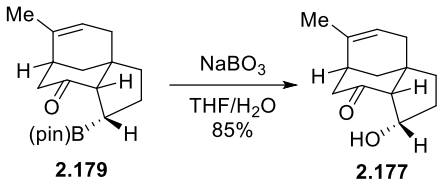


To a solution of compound **2.179** (0.3956 g, 1.25 mmol) in THF (12 mL) and $H_2O$ (12 mL) was added $NaBO_3 \cdot 4H_2O$ (0.58 g, 3.75 mmol) at the room temperature. After stirring at room temperature for 3 h, the reaction mixture was quenched by $Na_2S_2O_3$ (sat. in $H_2O$) and extracted by $Et_2O$. The organic phase was dried with $Na_2SO_4$ and concentrated under reduced pressure. The residue was then purified by column chromatography (silica gel, hexane:$Et_2O$ = 4:1) to give compound **2.177** (0.2340 g, 85% yield) as a colorless oil.

Analytic data of **2.177** see above.

*Synthesis of compound **2.177***

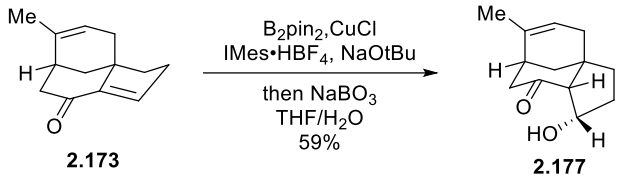


To a suspension of CuCl (0.5 mg, 0.0054 mmol) in tetrahydrofuran (THF, 0.25 mL), 1,3-Bis(2,4,6-trimethylphenyl)imidazolium tetrafluoroborate (IMes·$HBF_4$, 2 mg, 0.0054 mmol), and NaO$^t$Bu (1 mg, 0.0108 mmol) were added at room temperature. After stirring at room temperature for 40 min, a solution containing compound **2.173** (5 mg, 0.027 mmol) and bis(pinacolato)diboron ($B_2(pin)_2$, 9 mg, 0.035 mmol) in tetrahydrofuran (THF, 0.25 mL) was added to the reaction mixture. After stirring at 0 °C for 2 h and room temperature for 1 h, 0.5 mL $H_2O$ and $NaBO_3·4H_2O$ (12.5 mg, 0.081 mmol) were added to the reaction mixture and stirred at room temperature for 3 h. The reaction was then quenched with $Na_2S_2O_3$ (sat. in $H_2O$, 1 mL) and extracted with ethyl acetate (3 × 2 mL), and the organic phase was dried with $NA_2SO_4$ and concentrated under reduced pressure. The residue was purified by column chromatography (silica gel, hexane:$Et_2O$ = 4:1) to give compound **2.177** (3.3 mg, 59% yield) as a colorless oil.

Analytic data of **2.177** see above.

*Synthesis of compound **2.178***

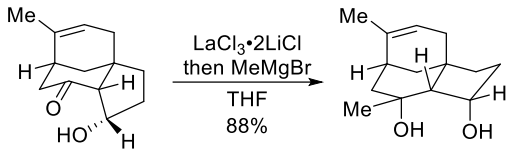


**2.177** **2.178**

To a solution of compound **2.177** (0.234 g, 1.13 mmol) in tetrahydrofuran (THF, 12 mL), $LaCl_3 \cdot LiCl$ (0.5 M in THF, 2.5 mL, 1.25 mmol) was added at 0 °C. After stirring at 0 °C for 1 h, MeMgBr (3M in $Et_2O$, 0.83 mL, 2.49 mmol) was added to the reaction mixture at 0 °C. After stirring at 0 °C for 30 min, the reaction was quenched with $NH_4Cl$ (sat. in $H_2O$, 10 mL). HCl (2M in water) was then added to the reaction mixture until all precipitate dissolved, and the resulting mixture was extracted with ethyl acetate (3 × 10 mL). The organic phase was washed with $NaHCO_3$ (sat. in $H_2O$, 30 mL) and brine (sat. in $H_2O$, 30 mL), dried with $Na_2SO_4$ and concentrated under reduced pressure. The residue was purified by column chromatography (silica gel, hexane:$Et_2O$ = 4:1) to give compound **2.178** (0.2202 g, 88% yield) as a white solid.

$\mathbf{R}_f$ = 0.36 (hexane:ethyl acetate = 2:1)

**$^1$H NMR** (500 MHz, $CDCl_3$) δ 5.27 (tt, *J* = 2.8, 1.4 Hz, 1H), 4.63 (td, *J* = 6.6, 3.3 Hz, 1H), 3.02 (d, *J* = 2.4 Hz, 1H), 2.81 (s, 1H), 2.25 (dd, *J* = 6.3, 2.9 Hz, 1H), 2.16 – 2.07 (m, 2H), 2.06 – 1.99 (m, 1H), 1.86 (dd, *J* = 13.6, 6.4 Hz, 1H), 1.75 – 1.69 (m, 3H), 1.67 (q, *J* = 1.9 Hz, 3H), 1.63 (d, *J* = 13.3 Hz, 1H), 1.54 (dd, *J* = 6.5, 1.3 Hz, 1H), 1.48 – 1.42 (m, 1H), 1.38 (s, 3H), 1.36 (dt, *J* = 3.2, 1.4 Hz, 1H).

**$^{13}$C NMR** (101 MHz, $CDCl_3$) δ 139.0, 121.1, 76.9, 73.2, 59.4, 41.6, 40.4, 40.3, 39.3, 35.7, 33.2, 33.1, 32.4, 21.9.

**IR (KBr)** $\nu_{max}$ = 3320, 2958, 2929, 2870, 1440, 1370, 1166, 1137, 1094, 1061, 1019, 920, 799 $cm^{-1}$

**HRMS (ESI):** m/z calcd for $C_{14}H_{22}NaO_2^+$ $[M+Na]^+$: 245,1512, found 245.1518.

**Melting point**: 88.3 – 89.6 °C

*Synthesis of compound **2.134***

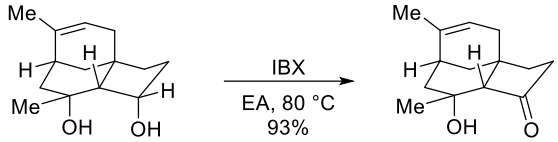


**2.178** **2.134**

To a solution of compound **2.178** (100 mg, 0.45 mmol) in ethyl acetate (9 mL), 2-iodoxybenzoic acid (IBX, 378 mg, 1.35 mmol) was added at room temperature. After stirring at 80 °C for 3 h, the reaction mixture was filtered through a short pad of silica gel and concentrated under reduced pressure. The residue was purified by column chromatography (silica gel, hexane:$Et_2O$ = 4:1) to give compound **2.134** (92.4 mg, 93% yield) as a white solid.

$\mathbf{R_f}$ = 0.40 (hexane:ethyl acetate = 2:1)

**$^1$H NMR** (500 MHz, $CDCl_3$) δ 5.64 (d, *J* = 1.7 Hz, 1H), 5.37 (ddd, *J* = 4.4, 2.8, 1.5 Hz, 1H), 2.42 – 2.31 (m, 2H), 2.31 – 2.23 (m, 2H), 2.11 – 2.03 (m, 2H), 1.83 – 1.78 (m, 1H), 1.78 – 1.66 (m, 5H), 1.57 (d, *J* = 5.0 Hz, 1H), 1.44 – 1.35 (m, 2H), 1.31 (s, 3H).

**$^{13}$C NMR** (101 MHz, $CDCl_3$) δ 222.7, 138.6, 121.6, 71.6, 64.2, 40.03, 39.97, 38.8, 35.8, 35.1, 33.5, 32.9, 30.8, 22.0.

**IR (KBr)** $\nu_{max}$ = 3444, 2922, 2867, 1704, 1439, 1406, 1367, 1154, 1137, 1040, 919, 895, 803 $cm^{-1}$

**HRMS (ESI):** m/z calcd for $C_{14}H_{21}O_2^+$ $[M+H]^+$: 221.1536, found 221.1532.

**Melting point**: 117.6 – 118.7 °C

*Synthesis of compound **2.183***

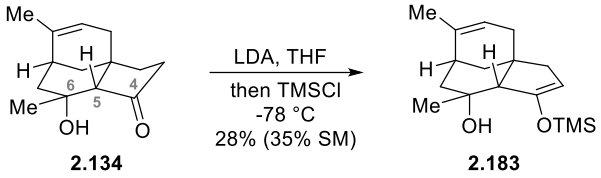


To a solution of DIPA (12 µL, 0.086 mmol) in THF (0.3 mL) was added *n*BuLi (2.5 M in hexane, 33 µL, 0.082 mmol) at the 0 °C and stirred at 0 °C for 30 min. In another flask, to a solution o f compound **2.134** (7.2 mg, 0.033 mmol) in THF (0.4 mL) was added the prepared LDA solution at −78. After stirring at −78 °C for 1 h, the reaction mixture was added TMSCl (12.3 µL, 0.1 mmol) at −78 °C. After stirring at −78 °C for 30 min, the reaction mixture was quenched by $NH_4Cl$ (sat. in $H_2O$) and extracted by $Et_2O$. The organic phase was dried with $Na_2SO_4$ and concentrated under reduced pressure. The residue was then purified by column chromatography (silica gel, hexane:$Et_2O$ = 10:1) to give compound **2.183** (2.7 mg, 28% yield) as a colorless oil and recycle compound **2.134** (2.5 mg, 35% recovery).

$\mathbf{R_f}$ = 0.84 (hexane:EA = 2:1)

**$^1$H NMR** (500 MHz, $CDCl_3$) δ 5.20 (dd, *J* = 4.4, 2.6 Hz, 1H), 4.82 (dt, *J* = 3.1, 1.6 Hz, 1H), 2.20 – 2.12 (m, 3H), 2.11 – 2.05 (m, 2H), 2.00 – 1.88 (m, 3H), 1.64 (dt, *J* = 2.8, 1.5 Hz, 3H), 1.54 (d, *J* = 1.6 Hz, 1H), 1.48 – 1.42 (m, 2H), 1.32 (s, 3H), 0.21 (s, 9H).

*Synthesis of compound **2.185***

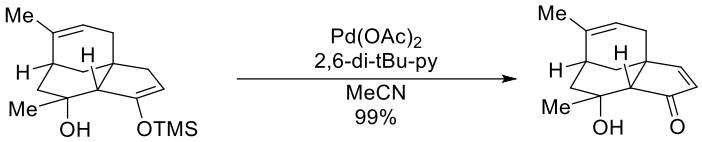


**2.183** **2.185**

To a solution of compound **2.183** (2.7 mg, 0.0092 mmol) in MeCN (0.2 mL) was added 2,6-di-$^t$Bu-py (6.3 μL, 0.028 mmol) and $Pd(OAc)_2$ (3.1 mg, 0.014 mmol) at the room temperature. After stirring at room temperature for 5 h, the reaction mixture was filtered through a short pad of silica gel and concentrated under reduced pressure. The residue was then purified by column chromatography (silica gel, hexane:$Et_2O$ = 2:1) to give compound **2.185** (2.1 mg, 99% yield) as a white solid.

**$R_f$** = 0.41 (hexane:ethyl acetate = 2:1)

**$^1$H NMR** (500 MHz, $CDCl_3$) δ 7.56 (d, *J* = 5.7 Hz, 1H), 6.13 (d, *J* = 5.6 Hz, 1H), 5.31 (dt, *J* = 4.9, 1.7 Hz, 1H), 2.35 – 2.25 (m, 2H), 2.21 (dt, *J* = 11.9, 2.2 Hz, 1H), 1.96 (dd, *J* = 14.9, 9.7 Hz, 1H), 1.92 (s, 1H), 1.69 (dt, *J* = 2.6, 1.5 Hz, 3H), 1.62 – 1.59 (m, 1H), 1.59 – 1.56 (m, 1H), 1.55 (s, 3H), 1.55 – 1.52 (m, 1H), 1.32 (s, 1H).

**$^{13}$C NMR** (101 MHz, $CDCl_3$) δ 211.2, 172.4, 141.0, 132.8, 118.6, 71.8, 59.1, 44.0, 42.4, 39.5, 32.8, 31.0, 28.9, 22.1.

**IR (KBr)** $\nu_{max}$ = 3432, 2961, 2921, 1698, 1675, 1584, 1443, 1384, 1125, 934, 804 $cm^{-1}$

**HRMS (ESI):** m/z calcd for $C_{14}H_{19}O_2^+$ $[M+H]^+$: 219.1380, found 219.1374.

**Melting point**: 146.0 – 146.6 °C

*Synthesis of compound **2.185***

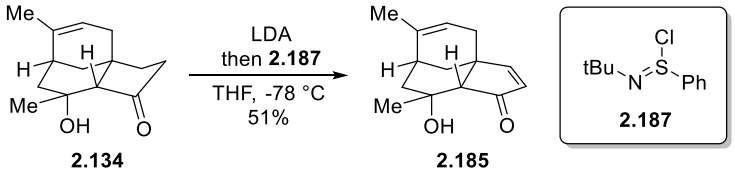


To a solution of diisopropyl amine (7.4 µL, 0.053 mmol) in tetrahydrofuran (THF, 0.1 mL), $^n$BuLi (2.5 M in THF, 20 µL, 0.051 mmol) was added at 0 °C and stirred for 1 h. This lithium diisopropylamide (LDA) solution was then added to another flask containing compound **2.134** (5 mg, 0.023 mmol) in tetrahydrofuran (THF, 0.1 mL) at −78 °C. After stirring at −78 °C for 30 min, freshly prepared compound **2.187** (1M in benzene, 35 µL, 0.035 mmol) was added to the reaction mixture.[61] After stirring at −78 °C for 30 min, the reaction was quenched with $NH_4Cl$ (sat. in $H_2O$, 1 mL) and extracted with ethyl acetate (3 × 1 mL). The organic phase was dried with $Na_2SO_4$ and concentrated under reduced pressure. The residue was then purified by column chromatography (silica gel, hexane:ethyl acetate = 10:1) to give compound **2.185** (51% NMR yield) as a white solid.

Analytically data of **2.185** see above.

*Synthesis of compound **2.188***

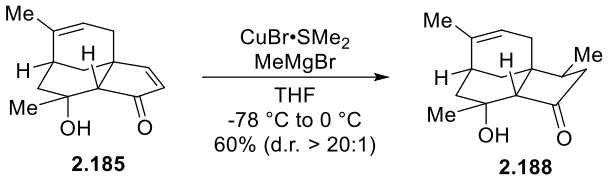


To a solution of compound **2.185** (4.5 mg, 0.021 mmol) in tetrahydrofuran (THF, 0.4 mL), $CuBr{\cdot}SMe_2$ (8.6 mg, 0.042 mmol) was added at room temperature. The mixture was then cooled to -78 °C and MeMgBr (3 M in $Et_2O$, 15 µL, 0.044 mmol) was added. After stirring at −78 °C for 1 h and 0 °C for 10 min, the reaction was quenched with $NH_4Cl$ (sat. in $H_2O$, 1 mL) and extracted with ethyl acetate (3 × 1 mL). The organic phase was dried with $Na_2SO_4$ and concentrated under reduced pressure. The residue was then purified by column chromatography (silica gel, hexane:ethyl acetate = 10:1) to give compound **2.188** (2.9 mg, 60% yield) as a white solid.

**$R_f$** = 0.58 (hexane:ethyl acetate = 2:1)

**$^1$H NMR** (500 MHz, $CDCl_3$) δ 5.38 (ddq, *J* = 4.3, 3.0, 1.5 Hz, 1H), 5.12 (d, *J* = 1.2 Hz, 1H), 2.61 (dd, *J* = 19.3, 8.3 Hz, 1H), 2.31 – 2.25 (m, 1H), 2.24 (s, 1H), 2.22 (dd, *J* = 5.7, 2.9 Hz, 1H), 2.06 – 1.93 (m, 3H), 1.82 – 1.74 (m, 1H), 1.69 (q, *J* = 1.9 Hz, 3H), 1.66 – 1.62 (m, 1H), 1.45 (dt, *J* = 3.1, 1.4 Hz, 2H), 1.33 (t, *J* = 0.8 Hz, 3H), 1.07 (d, *J* = 7.1 Hz, 3H).

**$^{13}$C NMR** (101 MHz, $CDCl_3$) δ 222.6, 138.5, 121.4, 71.5, 59.8, 44.5, 41.7, 40.7, 37.2, 35.7, 34.9, 30.8, 21.9, 15.7.

**IR (KBr)** $\nu_{max}$ = 3454, 2959, 2924, 1719, 1444, 1409, 1377, 1232, 1197, 1133, 1092, 899 $cm^{-1}$

**HRMS (CI):** m/z calcd for $C_{15}H_{23}O_2^+$ $[M+H]^+$: 235.1693, found 235.1690.

**Melting point**: 85.4 – 86.5 °C

*Synthesis of compound **2.1***

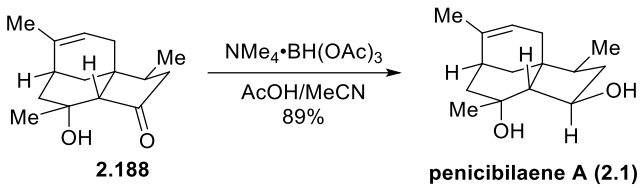


**2.188** **penicibilaene A (2.1)**

To a solution of compound **2.188** (6.7 mg, 0.029 mmol) in acetonitrile (0.3 mL) and acetic acid (0.3 mL), $NMe_4 \cdot NH(OAc)_3$ (23 mg, 0.086 mmol) was added at room temperature. After stirring at room temperature for 2 h, the reaction was quenched with $NaHCO_3$ (sat. in $H_2O$, 2 mL) and extracted with ethyl acetate (3 × 2 mL). The organic phase was dried with $Na_2SO_4$ and concentrated under reduced pressure. The residue was purified by column chromatography (silica gel, hexane:ethyl acetate = 4:1) to give compound **2.1** (6.0 mg, 89% yield) as a white solid.

$\mathbf{R_f}$ = 0.26 (hexane:ethyl acetate = 1:1)

**$^1$H NMR** (500 MHz, Acetone-D6) δ 5.23 (d, *J* = 4.9 Hz, 1H), 4.45 (p, *J* = 6.9 Hz, 1H), 3.41 (d, *J* = 5.3 Hz, 1H), 3.21 (s, 1H), 2.15 (d, *J* = 8.5 Hz, 1H), 2.10 – 2.04 (m, 3H), 2.04 – 1.97 (m, 2H), 1.93 – 1.86 (m, 1H), 1.90 – 1.83 (m, 2H), 1.78 – 1.70 (m, 1H), 1.73 – 1.65 (m, 2H), 1.63 (d, *J* = 2.0 Hz, 3H), 1.50 (d, *J* = 14.2 Hz, 1H), 1.46 (d, *J* = 6.2 Hz, 1H), 1.38 (td, *J* = 11.8, 8.6 Hz, 1H), 1.30 (ddd, *J* = 11.6, 4.0, 1.4 Hz, 1H), 1.26 (s, 3H), 0.89 (d, *J* = 7.0 Hz, 3H).

**$^{13}$C NMR** (101 MHz, Acetone-D6) δ 140.9, 120.7, 73.4, 71.3, 61.5, 42.6, 42.54, 42.48, 42.4, 36.0, 35.4, 33.3, 31.4, 22.2, 15.0.

**IR (KBr)** $\nu_{max}$ = 3359, 3300, 2963, 1913, 1443, 1411, 1142, 1113, 1036, 922, 861 $cm^{-1}$

**HRMS (ESI):** m/z calcd for $C_{15}H_{25}O_2^+$ $[M+H]^+$: 237.1849, found 237.1842.

**Melting point**: 159.3 – 160.0 °C

*Synthesis of compound **2.2***

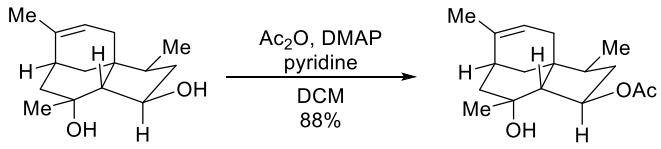

**penicibilaene A (2.1)** **penicibilaene B (2.2)**

To a solution of compound **2.1** (6.0 mg, 0.025 mmol) in dichloromethane (0.5 mL), pyridine (6.1 μL, 0.075 mmol), acetic anhydride ($Ac_2O$, 4.7 μL, 0.051 mmol), and 4-(dimethylamino)pyridine (DMAP, 0.3 mg, 0.0025 mmol) were added at room temperature. After stirring at room temperature for 24 h, the reaction was quenched with $NH_4Cl$ (sat. in $H_2O$, 1 mL) and extracted with dichloromethane (3 × 2 mL). The organic phase was dried with $Na_2SO_4$ and concentrated under reduced pressure. The residue was then purified by column chromatography (silica gel, hexane:ethyl acetate = 10:1) to give compound **2.2** (6.2 mg, 88% yield) as a white solid.

**$R_f$** = 0.76 (hexane:ethyl acetate = 1:1)

**$^1$H NMR** (500 MHz, $CDCl_3$) δ 5.36 (ddd, *J* = 8.7, 7.6, 6.0 Hz, 1H), 5.26 (d, *J* = 4.9 Hz, 1H), 2.31 (ddd, *J* = 12.8, 7.5, 5.8 Hz, 1H), 2.22 (d, *J* = 9.2 Hz, 1H), 2.05 (d, *J* = 17.0 Hz, 1H), 2.00 (s, 3H),

1.83 (dd, $J$ = 14.7, 9.1 Hz, 1H), 1.79 – 1.76 (m, 1H), 1.75 – 1.74 (m, 1H), 1.72 (d, $J$ = 6.1 Hz, 1H), 1.72 – 1.68 (m, 1H), 1.65 (dt, $J$ = 2.7, 1.5 Hz, 3H), 1.53 (dt, $J$ = 14.6, 1.3 Hz, 1H), 1.44 (ddd, $J$ = 11.8, 3.9, 1.5 Hz, 1H), 1.37 (td, $J$ = 12.4, 8.7 Hz, 1H), 1.15 (s, 3H), 1.13 (s, 1H), 0.91 (d, $J$ = 6.9 Hz, 3H).

**$^{13}$C NMR** (101 MHz, $CDCl_3$) δ 170.9, 140.3, 119.4, 75.5, 71.1, 56.8, 41.8, 41.7, 41.2, 38.3, 34.4, 34.2, 31.9, 30.3, 21.8, 21.4, 13.9.

**IR (KBr)** $\nu_{max}$ = 3505, 2958, 2926, 2886, 1736, 1719, 1458, 1375, 1271, 1245, 1114, 1030, 927, 805 $cm^{-1}$

**HRMS (ESI):** m/z calcd for $C_{17}H_{27}O_3^+$ $[M+H]^+$: 279.1955, found 237.1886; $C_{17}H_{26}NaO_3^+$ $[M+Na]^+$: 301.1774, found 301.1768.

**Melting point**: 122.8 – 123.5 °C

### 2.6.3 Comparison of Spectroscopic Data of the Natural and Synthetic Products

**Table 2.70.** Comparison of the $^{1}$H-NMR (Acetone-D6) Data of the Synthetic Penicibilaene A (**2.1**)

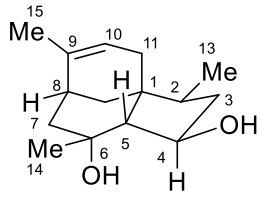

Penicibilaene A (**2.1**)

| No. | Wang's isolated natural penicibilaene (**2.1**)[7] $\delta$ $^{1}$H [ppm, mult, J (Hz)] 500 MHz | Our synthetic penicibilaene (**2.1**) $\delta$ $^{1}$H [ppm, mult, J (Hz)] 500 MHz |
|---|---|---|
| 2 | 1.69 (m, 1H) | 1.69 (m, 1H) |
| 3α | 2.07 (m, 1H) | 2.07 (m, 1H) |
| 3β | 1.38 (dt,11.7, 8.6, 1H) | 1.38 (dt, 11.8, 8.6, 1H) |
| 4 | 4.45 (m, 1H) | 4.45 (p, 6.9, 1H) |
| 5 | 1.46 (d, 6.2, 1H) | 1.46 (d, 6.2, 1H) |
| 7α | 1.86 (dd, 12.0, 4.8, 1H) | 1.86 (m, 1H) |
| 7β | 1.30 (dd, 12.0, 3.9, 1H) | 1.30 (ddd, J = 11.6, 4.0, 1.4 Hz, 1H) |
| 8 | 2.15 (dd, 4.8, 3.9, 1H) | 2.15 (d, 8.5, 1H) |
| 10 | 5.23 (dd, 3.1, 1.5, 1H) | 5.23 (d, 4.9 Hz, 1H) |
| 11α | 2.01 (d, 16.3, 1H) | 2.00 (m, 1H) |
| 11β | 1.74 (m, 1H) | 1.74 (m, 1H) |
| 12α | 1.90 (dd, 14.2, 5.6, 1H) | 1.89 (m, 1H) |
| 12β | 1.50 (d, 14.2, 1H) | 1.50 (d, 14.2, 1H) |
| 13 | 0.89 (d, 7.1, 3H) | 0.88 (d, 7.0, 3H) |
| 14 | 1.26 (s, 3H) | 1.26 (s, 3H) |
| 15 | 1.63 (br s, 3H) | 1.63 (d, 2.0, 3H) |
| 4-OH | 3.40 (d, 5.2, 1H) | 3.41 (d, 5.3, 1H) |
| 6-OH | 3.20 (s, 1H) | 3.21 (s, 1H) |

**Table 2.71.** Comparison of the $^{13}$C-NMR (Acetone-D6) Data of the Synthetic Penicibilaene A (**2.1**)

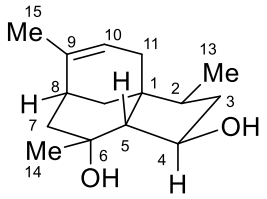

Penicibilaene A (**2.1**)

| No. | Wang's isolated natural penicibilaene (**2.1**)[7] δ $^{13}$C [ppm, mult, J (Hz)] 125 MHz | Our synthetic penicibilaene (**2.1**) $\delta$ $^{13}$C [ppm, mult, J (Hz)] 101 MHz |
|---|---|---|
| 1 | 42.58 | 42.54 |
| 2 | 42.62 | 42.60 |
| 3 | 42.5 | 42.5 |
| 4 | 73.4 | 73.4 |
| 5 | 61.5 | 61.5 |
| 6 | 71.3 | 71.3 |
| 7 | 33.3 | 33.3 |
| 8 | 36.1 | 36.0 |
| 9 | 140.9 | 140.9 |
| 10 | 120.7 | 120.7 |
| 11 | 35.4 | 35.4 |
| 12 | 42.4 | 42.4 |
| 13 | 15.0 | 15.0 |
| 14 | 31.4 | 31.4 |
| 15 | 22.2 | 22.2 |

**Table 2.72.** Comparison of the $^{1}$H-NMR ($CDCl_3$) Data of the Synthetic Penicibilaene B (**2.2**)

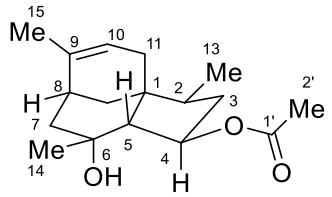

Penicibilaene B (**2.2**)

| No. | Wang's isolated natural penicibilaene (**2.2**)[7] $\delta$ $^{1}$H [ppm, mult, J (Hz)] 500 MHz | Our synthetic penicibilaene (**2.2**) $\delta$ $^{1}$H [ppm, mult, J (Hz)] 500 MHz |
|---|---|---|
| 2 | 1.80 (m, 1H) | 1.83 (dd, 14.7, 9.1, 1H) |
| 3α | 2.28 (ddd, 12.5, 7.1, 6.6, 1H) | 2.31 (ddd, 12.8, 7.5, 5.8, 1H) |
| 3β | 1.34 (dt, 12.5, 8.7, 1H) | 1.37 (dt, 12.4, 8.7, 1H) |
| 4 | 5.33 (ddd, 8.7, 6.6, 6.0, 1H) | 5.36 (ddd, 8.7, 7.6, 6.0, 1H) |
| 5 | 1.70 (d, 6.0, 1H) | 1.72 (d, 6.1, 1H) |
| 7α | 1.78 (dd, 11.9, 6.2, 1H) | 1.77 (m, 1H) |
| 7β | 1.41 (dd, 11.9, 2.5, 1H) | 1.44 (ddd, 11.8, 3.9, 1.5, 1H) |
| 8 | 2.18 (dd, 6.2, 2.5, 1H) | 2.22 (d, 9.2, 1H) |
| 10 | 5.24 (d, 4.2, 1H) | 5.26 (d, 4.9, 1H) |
| 11α | 2.02 (d, 16.0, 1H) | 2.05 (d, 17.0, 1H) |
| 11β | 1.70 (m, 1H) | 1.70 (m, 1H) |
| 12α | 1.75 (dd, 14.5, 6.3, 1H) | 1.75 (m, 1H) |
| 12β | 1.50 (d, 14.5, 1H) | 1.53 (dt, 14.6, 1.3, 1H) |
| 13 | 0.88 (d, 6.9, 3H) | 0.91 (d, 6.9, 3H) |
| 14 | 1.13 (s, 3H) | 1.15 (s, 3H) |
| 15 | 1.63 (m, 3H) | 1.65 (dt, 2.7, 1.5, 3H) |
| 2' | 1.97 (s, 3H) | 2.00 (s, 3H) |
| 6-OH | | 1.13 (s, 1H) |

**Table 2.73.** Comparison of the $^{1}$H-NMR ($CDCl_3$) Data of the Synthetic Penicibilaene B (**2.2**)

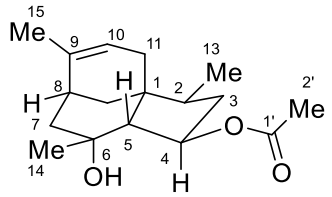

Penicibilaene B (**2.2**)

| No. | Wang's isolated natural penicibilaene (**2.2**)[7] $\delta$ $^{13}$C [ppm, mult, J (Hz)] 125 MHz | Our synthetic penicibilaene (**2.2**) $\delta$ $^{13}$C [ppm, mult, J (Hz)] 101 MHz |
|---|---|---|
| 1 | 41.5 | 41.2 |
| 2 | 42.1 | 41.8 |
| 3 | 38.6 | 38.3 |
| 4 | 75.8 | 75.5 |
| 5 | 57.1 | 56.8 |
| 6 | 71.3 | 71.1 |
| 7 | 32.2 | 31.9 |
| 8 | 34.7 | 34.4 |
| 9 | 140.5 | 140.3 |
| 10 | 119.7 | 119.4 |
| 11 | 34.4 | 34.2 |
| 12 | 41.9 | 41.7 |
| 13 | 14.1 | 13.9 |
| 14 | 30.5 | 30.3 |
| 15 | 22.1 | 21.8 |
| 1' | 171.1 | 170.9 |
| 2' | 21.6 | 21.4 |

### 2.6.4 Crystal Data and Structure Refinement

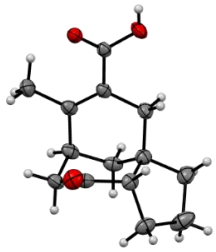

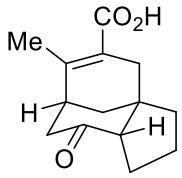


**2.136**

**CCDC #2078710**

| | |
|---|---|
| Identification code | mo_1019_SHO_YX_0m |
| Empirical formula | $C_{14}H_{18}O_3$ |
| Formula weight | 234.28 |
| Temperature/K | 100(2) |
| Crystal system | monoclinic |
| Space group | $P2_1/n$ |
| a/Å | 9.7164(6) |
| b/Å | 13.8970(8) |
| c/Å | 9.9583(6) |
| α/° | 90 |
| β/° | 115.861(2) |

| | |
|---|---|
| γ/° | 90 |
| Volume/Å$^3$ | 1210.00(13) |
| Z | 4 |
| $\rho_{calc}$g/cm$^3$ | 1.286 |
| μ/mm$^{-1}$ | 0.089 |
| F(000) | 504.0 |
| Crystal size/mm$^3$ | 0.586 × 0.574 × 0.332 |
| Radiation | MoKα (λ = 0.71073) |
| 2Θ range for data collection/° | 4.888 to 48.904 |
| Index ranges | -11 ≤ h ≤ 11, -16 ≤ k ≤ 16, -11 ≤ l ≤ 11 |
| Reflections collected | 19941 |
| Independent reflections | 2006 [$R_{int}$ = 0.0243, $R_{sigma}$ = 0.0106] |
| Data/restraints/parameters | 2006/0/156 |
| Goodness-of-fit on F$^2$ | 1.045 |
| Final R indexes [I>=2σ (I)] | $R_1$ = 0.0356, w$R_2$ = 0.0930 |

Final R indexes [all data] $R_1 = 0.0376$, $wR_2 = 0.0948$

Largest diff. peak/hole / e $Å^{-3}$ 0.22/-0.18

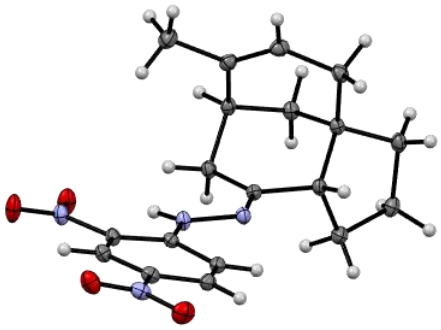

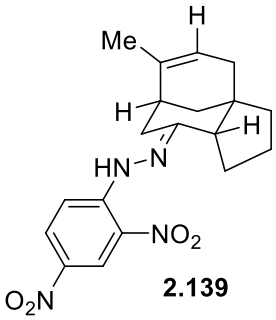


**2.139**

**CCDC #2078965**

| | |
|---|---|
| Identification code | xyb-3-286 |
| Empirical formula | $C_{19}H_{22}N_4O_4$ |
| Formula weight | 370.40 |
| Temperature/K | 100(2) |
| Crystal system | monoclinic |
| Space group | $P2_1/c$ |
| a/Å | 13.5093(13) |
| b/Å | 6.2144(6) |
| c/Å | 20.982(2) |
| α/° | 90 |
| β/° | 96.738(2) |

| | |
|---|---|
| γ/° | 90 |
| Volume/Å$^3$ | 1749.3(3) |
| Z | 4 |
| $\rho_{calc}$g/cm$^3$ | 1.406 |
| μ/mm$^{-1}$ | 0.101 |
| F(000) | 784.0 |
| Crystal size/mm$^3$ | 0.514 × 0.225 × 0.126 |
| Radiation | MoKα (λ = 0.71073) |
| 2Θ range for data collection/° | 4.66 to 61.44 |
| Index ranges | -19 ≤ h ≤ 19, -8 ≤ k ≤ 8, -30 ≤ l ≤ 30 |
| Reflections collected | 55097 |
| Independent reflections | 5423 [$R_{int}$ = 0.0328, $R_{sigma}$ = 0.0173] |
| Data/restraints/parameters | 5423/0/249 |
| Goodness-of-fit on F$^2$ | 1.043 |
| Final R indexes [I>=2σ (I)] | $R_1$ = 0.0401, $wR_2$ = 0.0995 |

Final R indexes [all data] $R_1 = 0.0497$, $wR_2 = 0.1051$

Largest diff. peak/hole / e $Å^{-3}$ 0.46/-0.17

### 2.6.5 NMR Spectra

**Figure 2.1.** $^{1}$H-NMR Spectrum of **2.20** in $CDCl_3$, 500 MHz

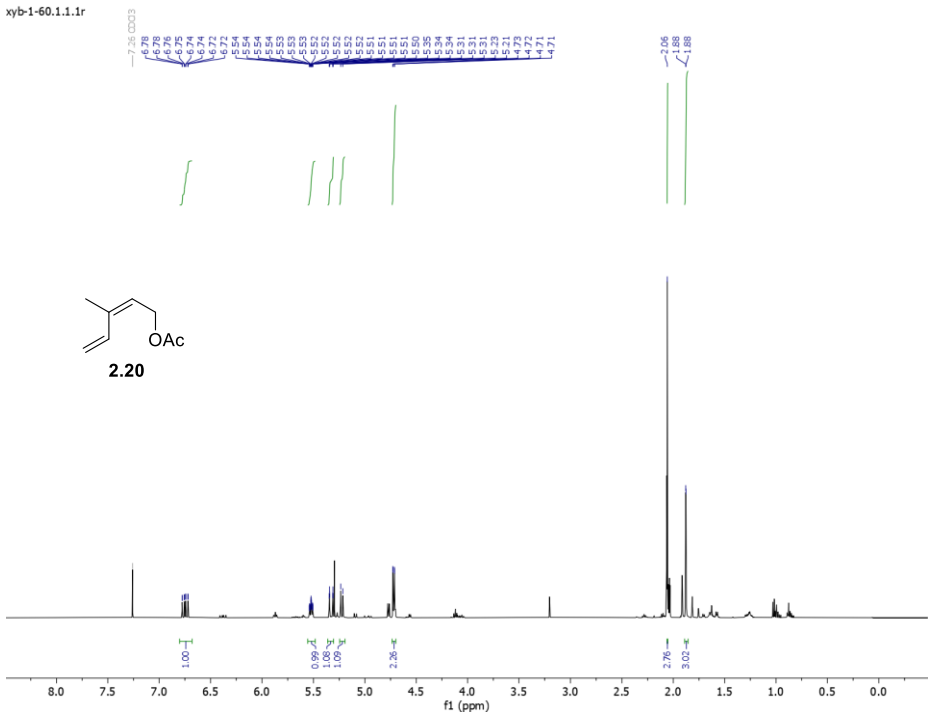


**Figure 2.2.** $^{1}$H-NMR Spectrum of **2.22** in $CDCl_3$, 500 MHz

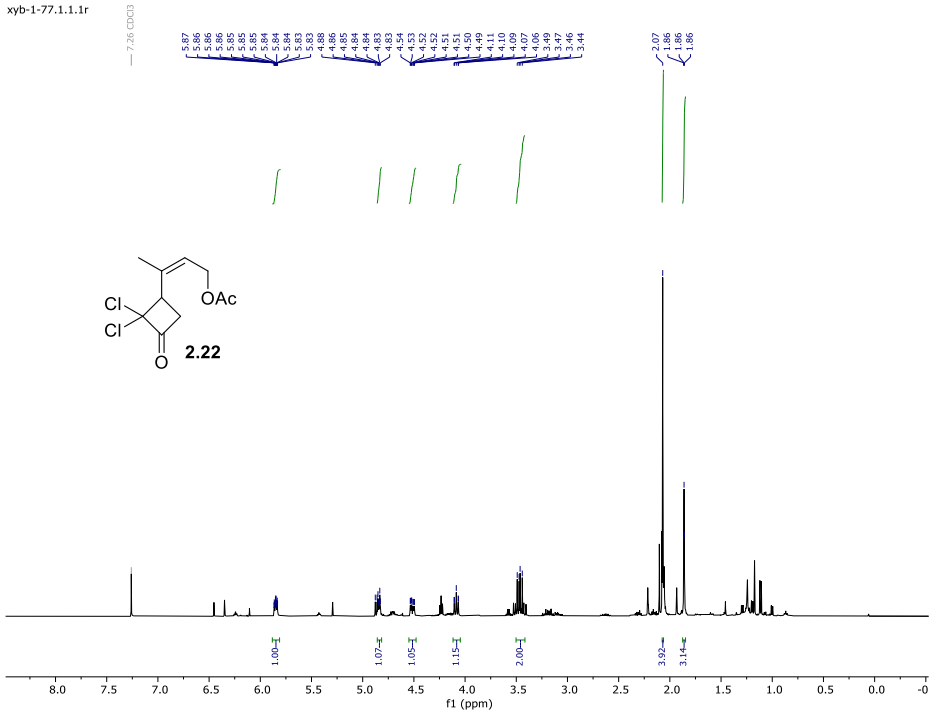

**Figure 2.3.** $^{1}$H-NMR Spectrum of **2.16** in $CDCl_3$, 500 MHz

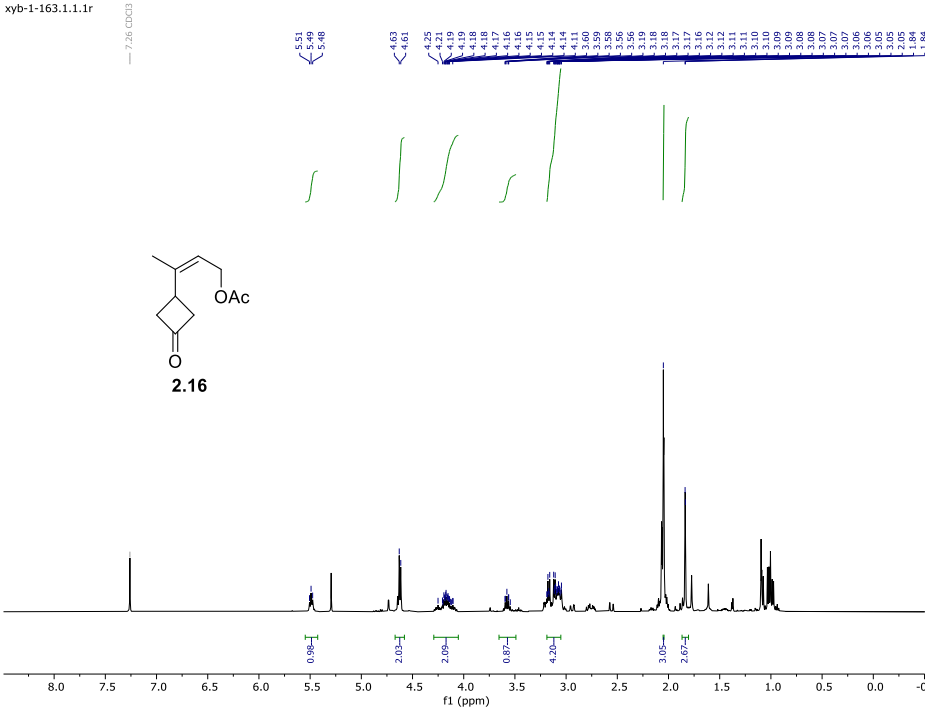


**Figure 2.4.** $^{1}$H-NMR Spectrum of **2.6** in $CDCl_3$, 500 MHz

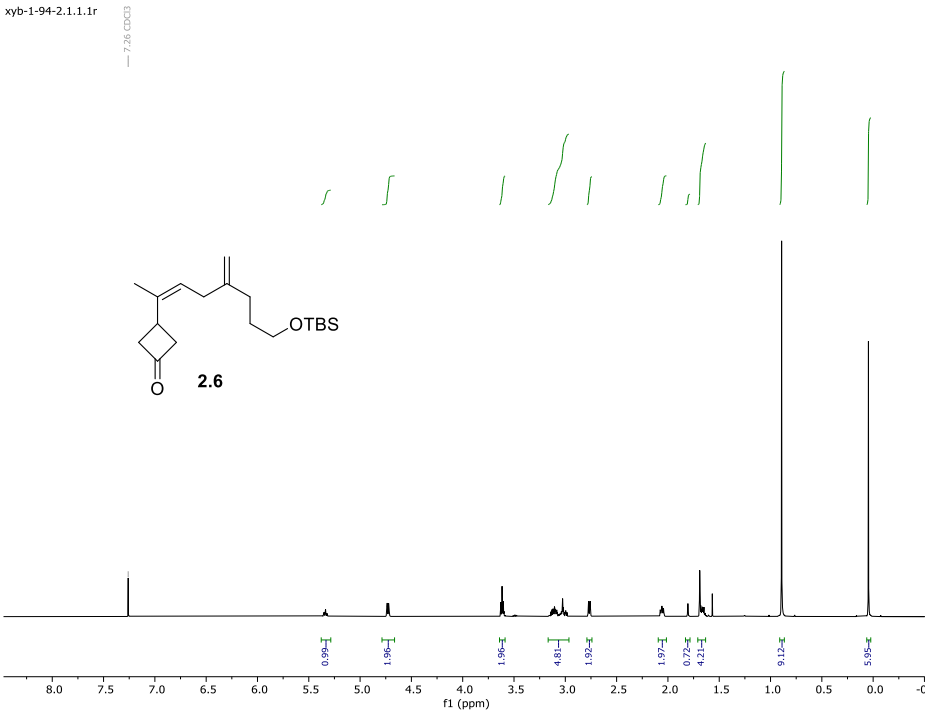

**Figure 2.5.** $^{13}$C-NMR Spectrum of **2.6** in $CDCl_3$, 101 MHz

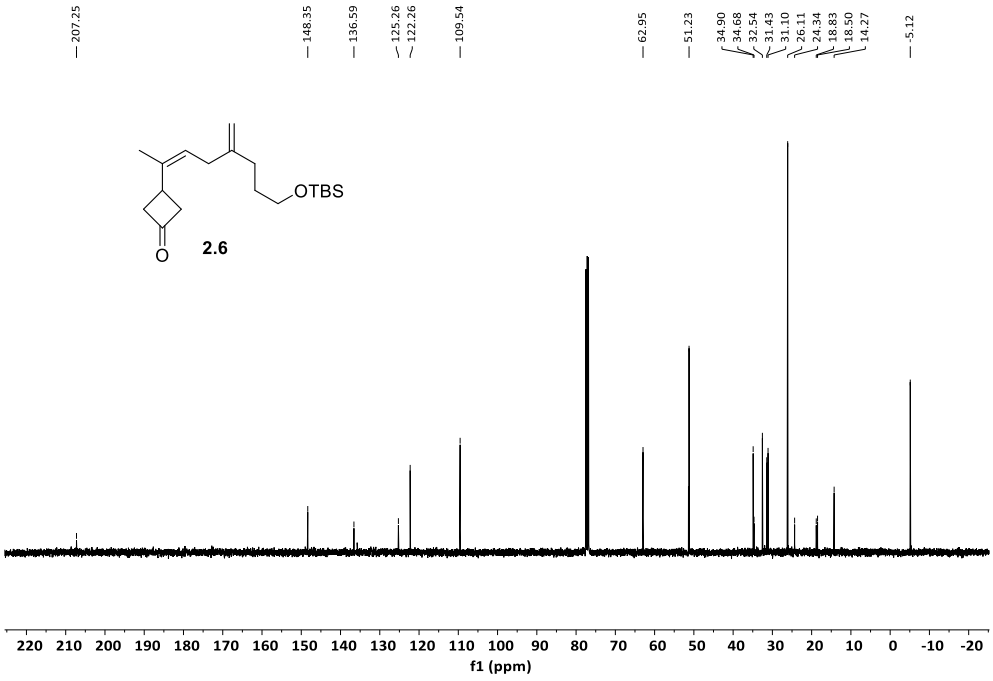


**Figure 2.6.** $^{1}$H-NMR Spectrum of **2.24** in $CDCl_3$, 500 MHz

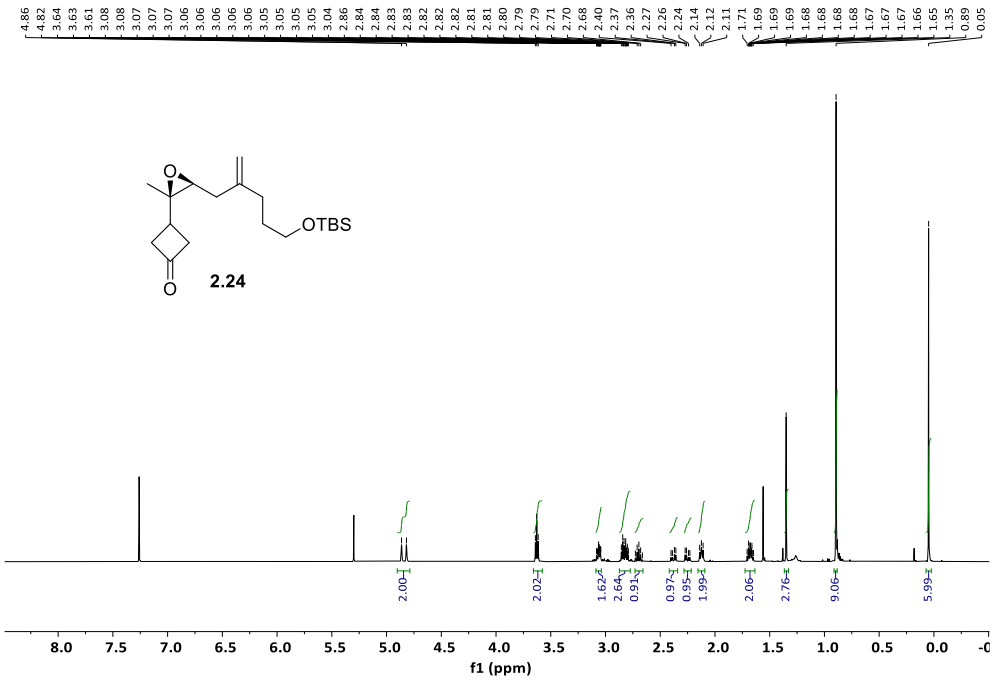

**Figure 2.7.** $^{13}$C-NMR Spectrum of **2.24** in $CDCl_3$, 101 MHz

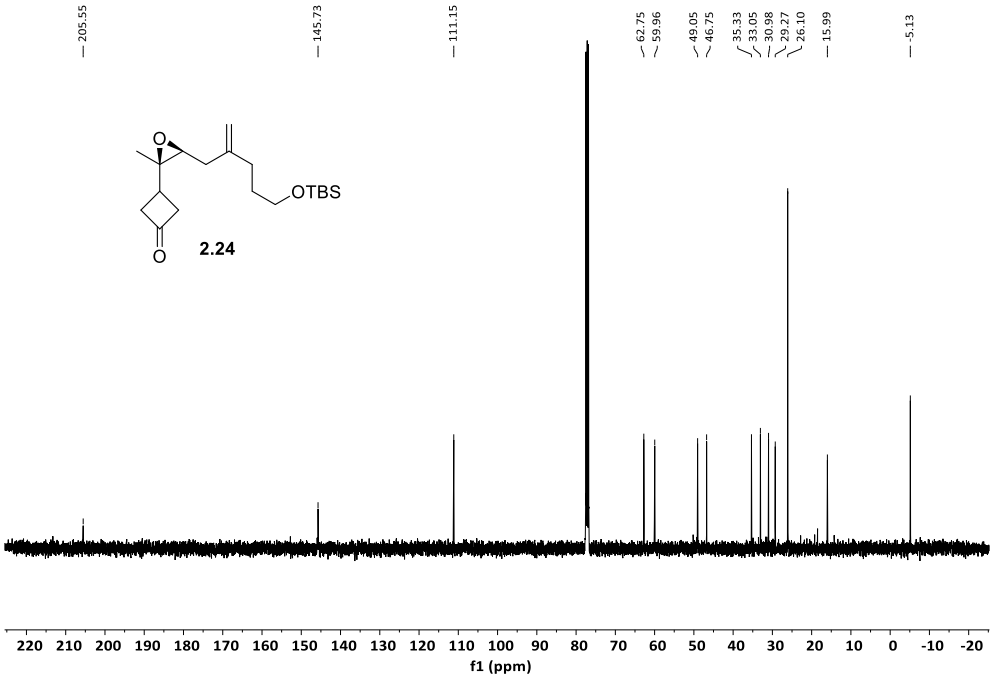


**Figure 2.8.** $^{1}$H-NMR Spectrum of **2.27** in $CDCl_3$, 500 MHz

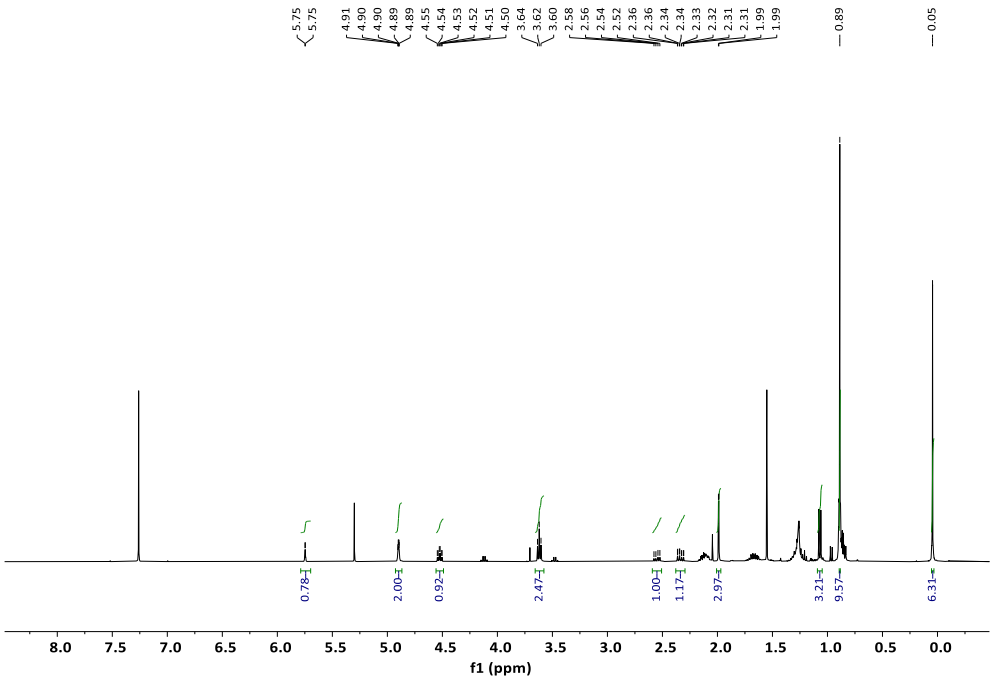

**Figure 2.9.** $^{13}$C-NMR Spectrum of **2.27** in $CDCl_3$, 101 MHz

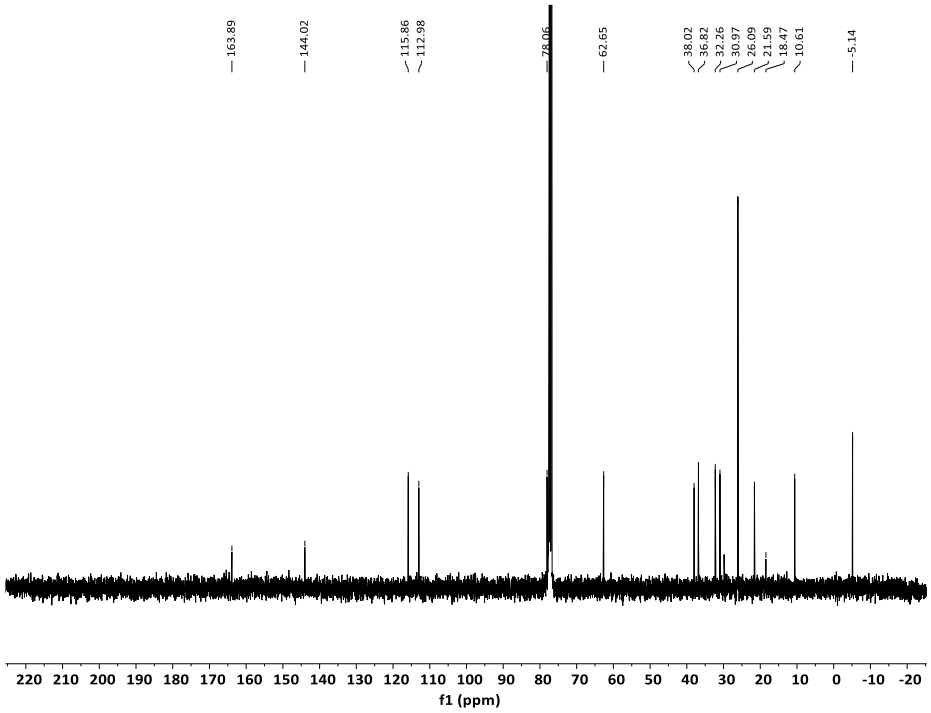


**Figure 2.10.** $^{1}$H-NMR Spectrum of **2.31** in $CDCl_3$, 500 MHz

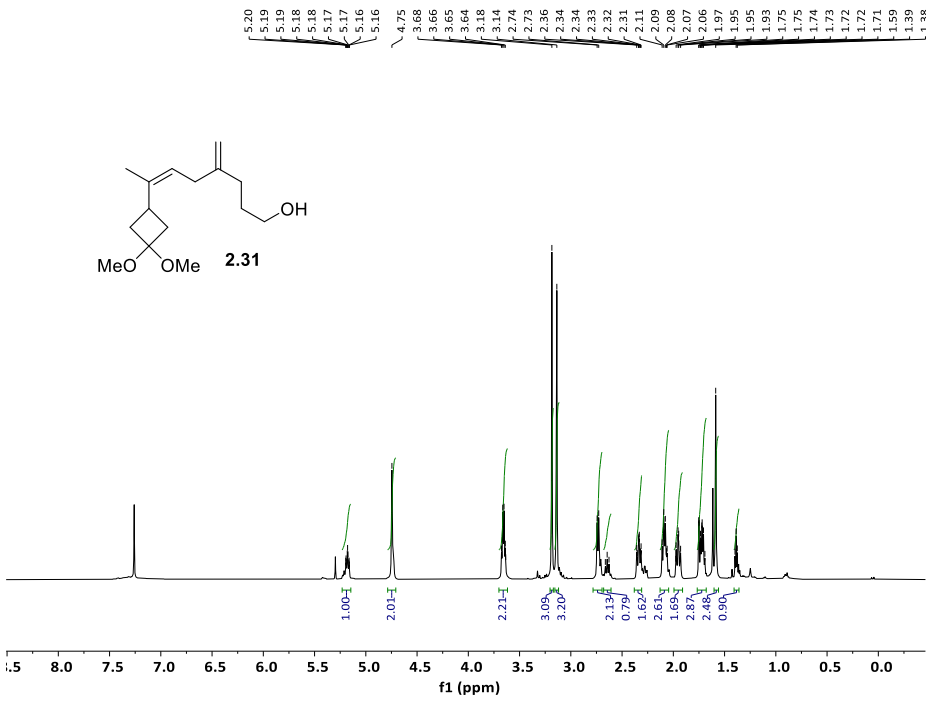

**Figure 2.11.** $^{1}$H-NMR Spectrum of **2.32** in $CDCl_3$, 500 MHz

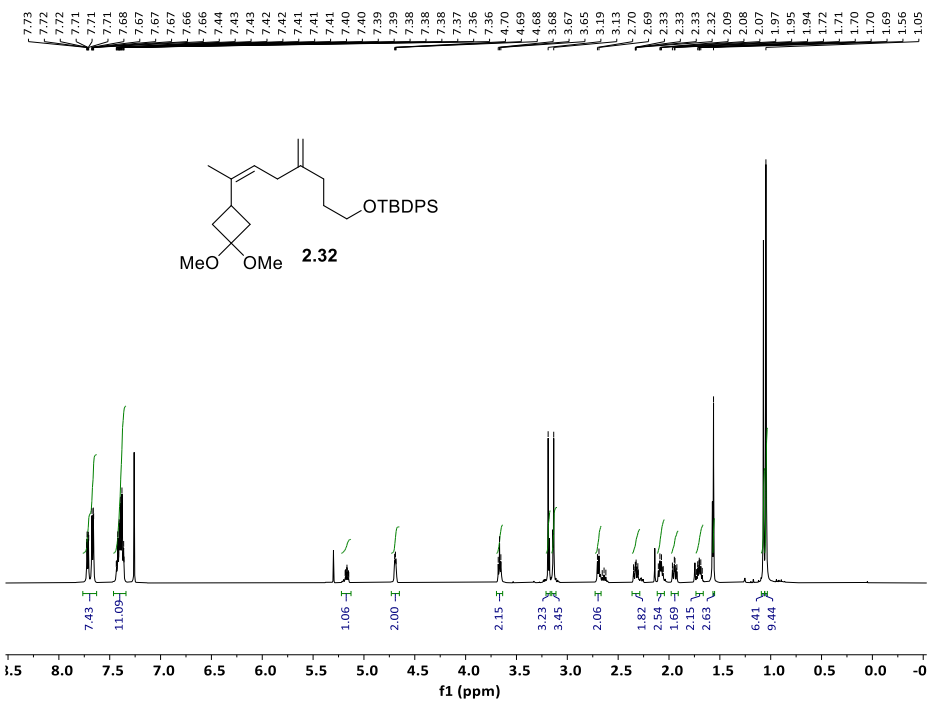


**Figure 2.12.** $^{1}$H-NMR Spectrum of **2.33** in $CDCl_3$, 500 MHz

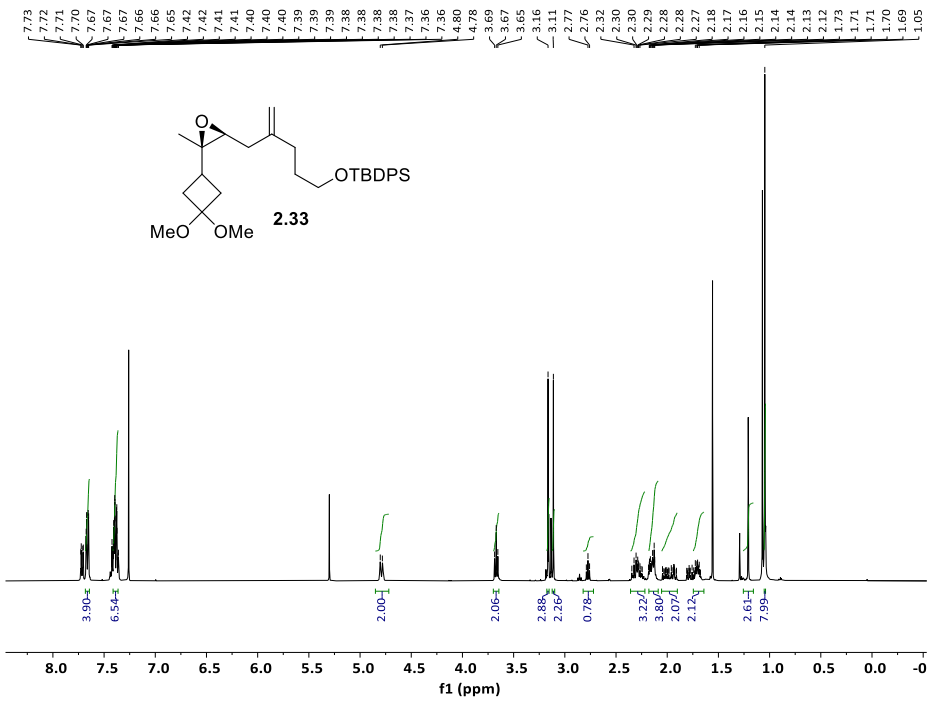

**Figure 2.13.** $^{1}$H-NMR Spectrum of **2.34** in $CDCl_3$, 500 MHz

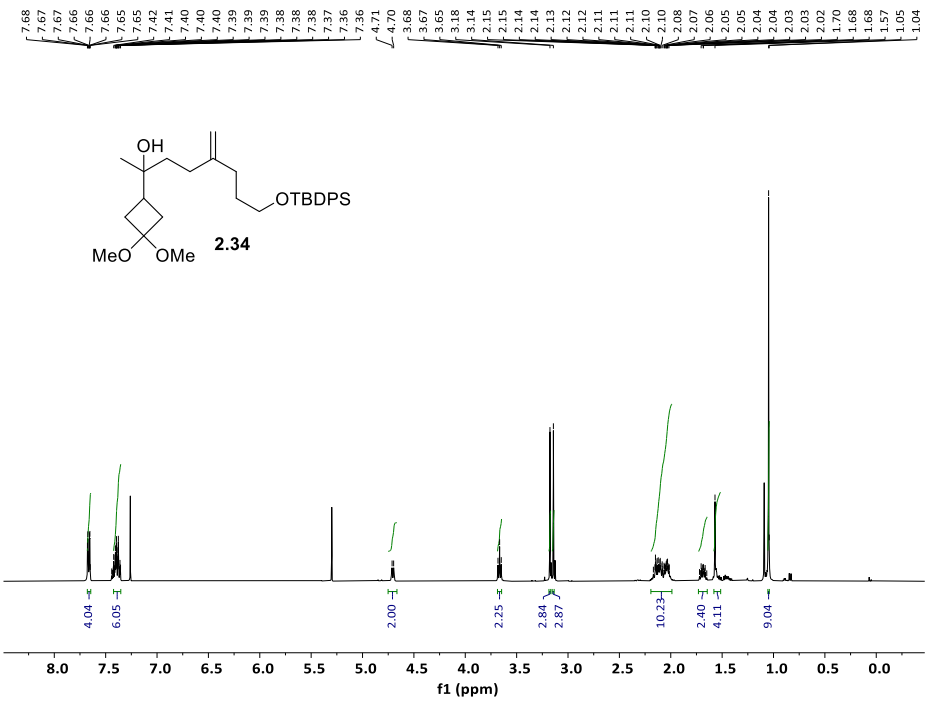


**Figure 2.14.** $^{1}$H-NMR Spectrum of **2.35** in $CDCl_3$, 500 MHz

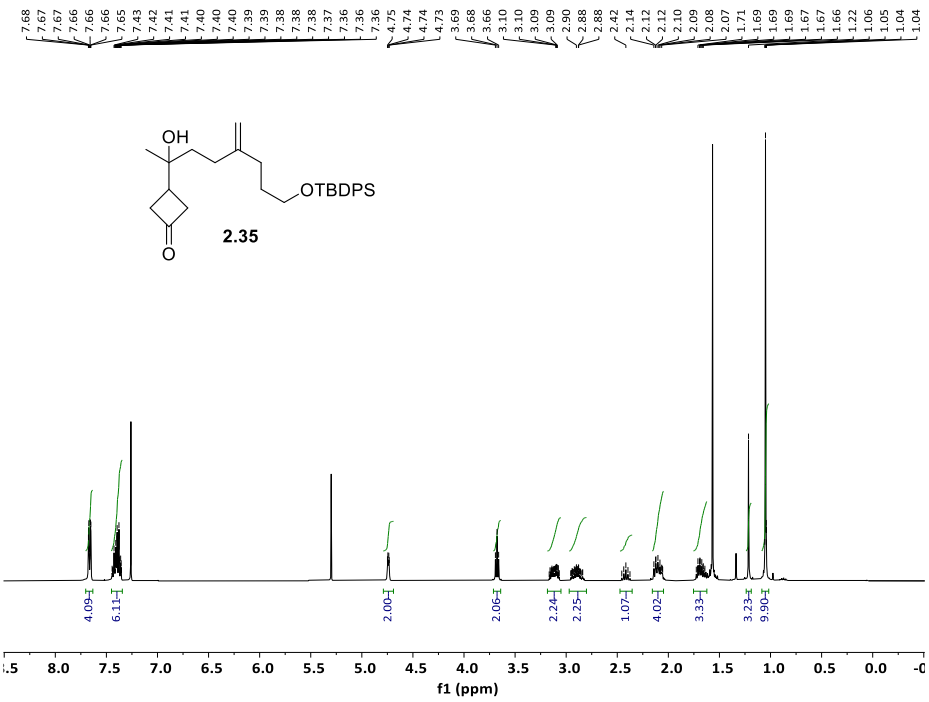

**Figure 2.15.** $^{1}$H-NMR Spectrum of **2.36** in $CDCl_3$, 500 MHz

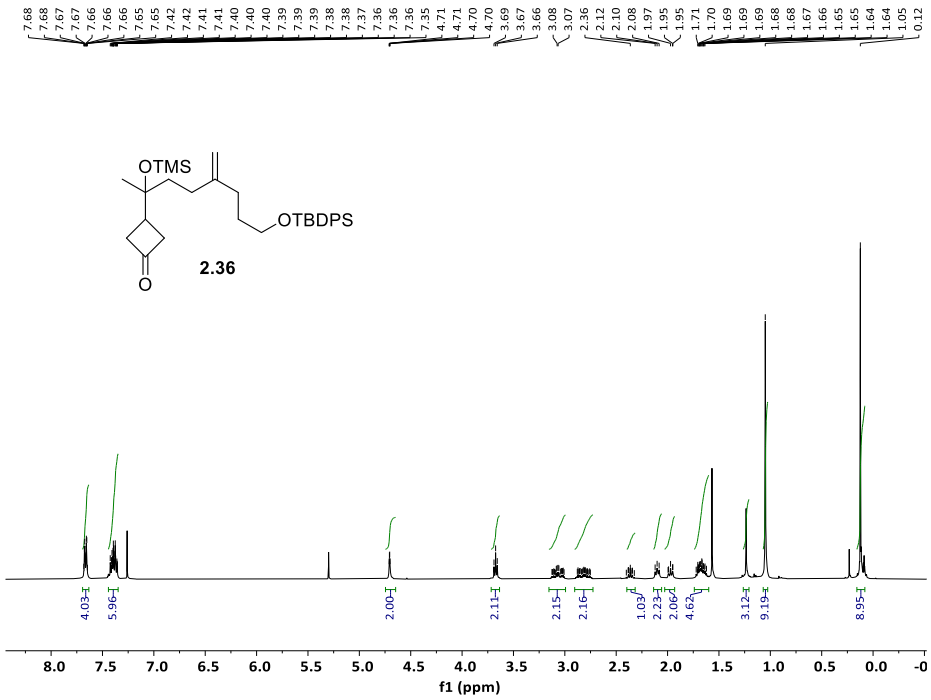


**Figure 2.16.** $^{13}$C-NMR Spectrum of **2.36** in $CDCl_3$, 101 MHz

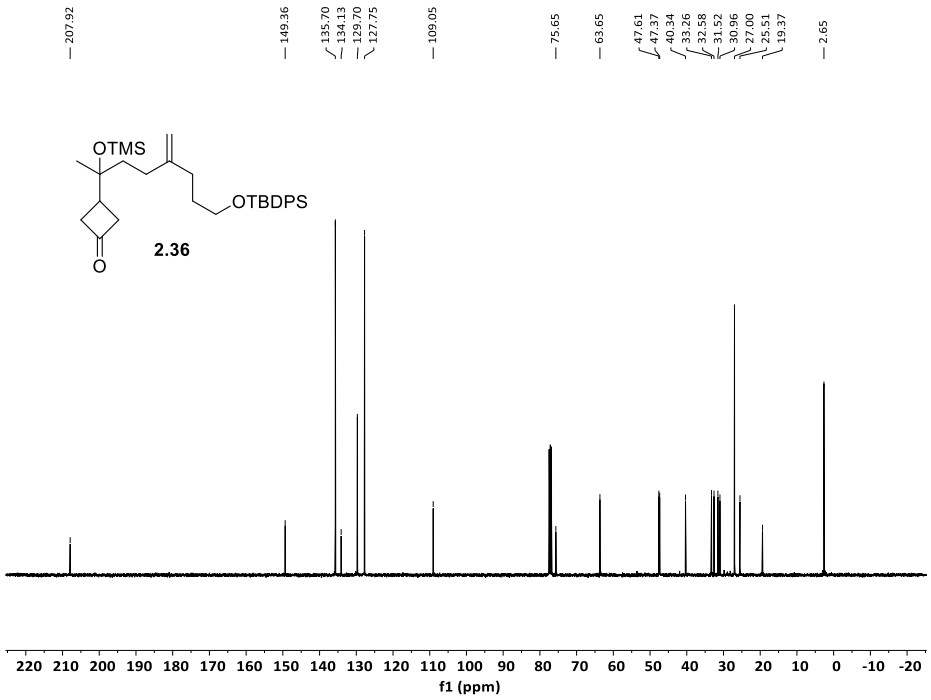

**Figure 2.17.** $^{1}$H-NMR Spectrum of **2.38** in $CDCl_3$, 500 MHz

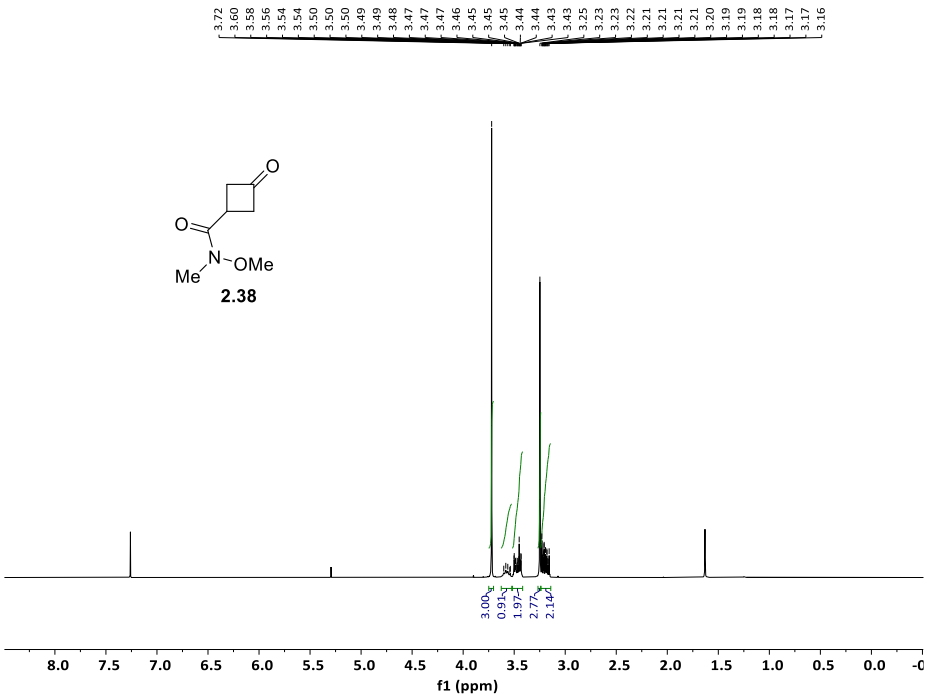


**Figure 2.18.** $^{1}$H-NMR Spectrum of **2.39** in $CDCl_3$, 500 MHz

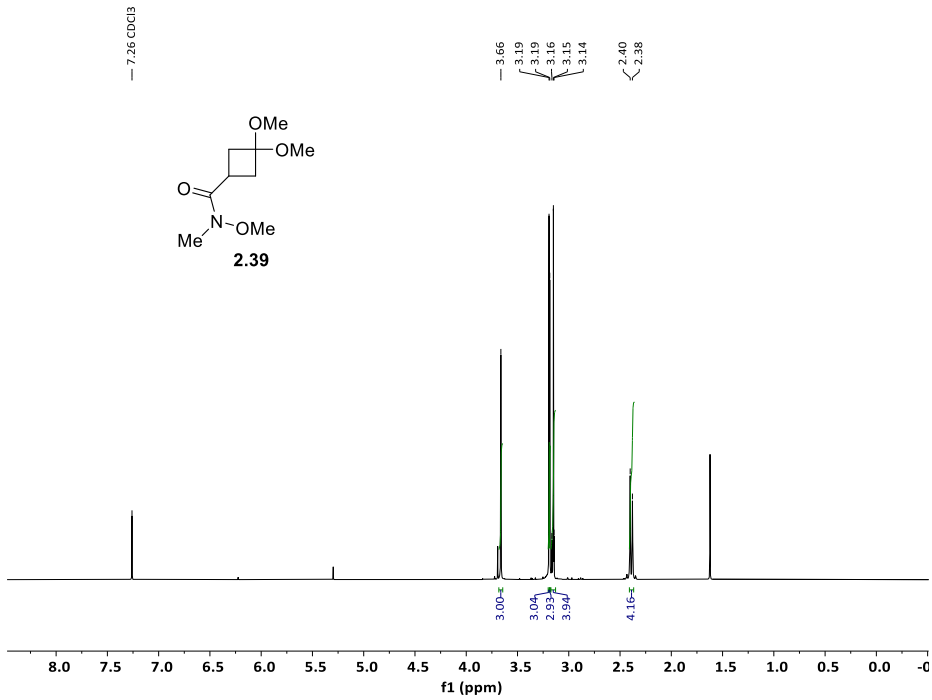

**Figure 2.19.** $^{1}$H-NMR Spectrum of **2.40** in $CDCl_3$, 500 MHz

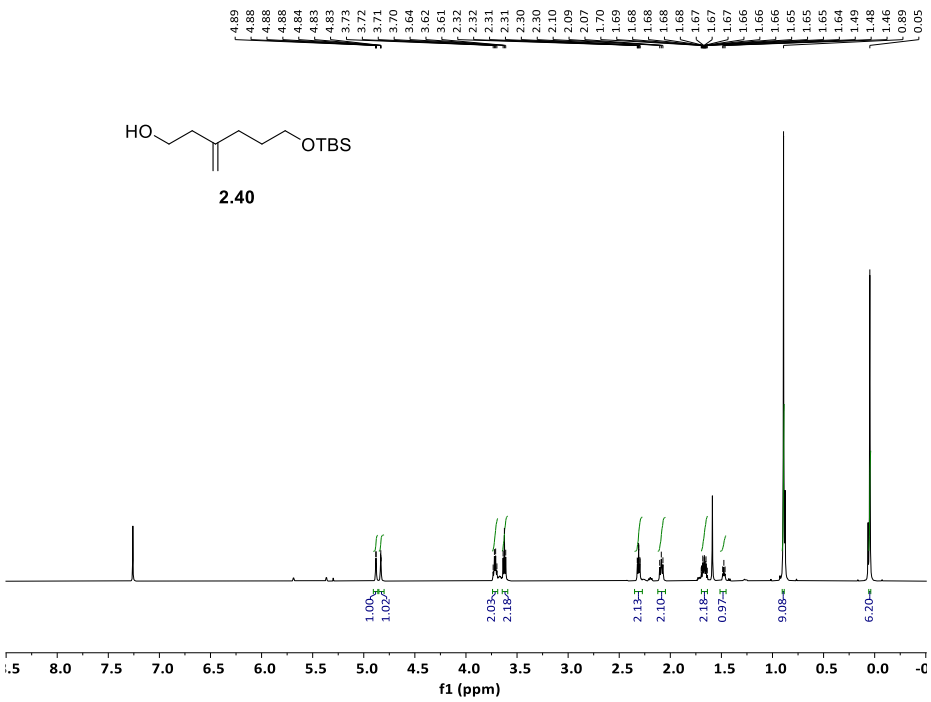


**Figure 2.20.** $^{1}$H-NMR Spectrum of **2.41** in $CDCl_3$, 500 MHz

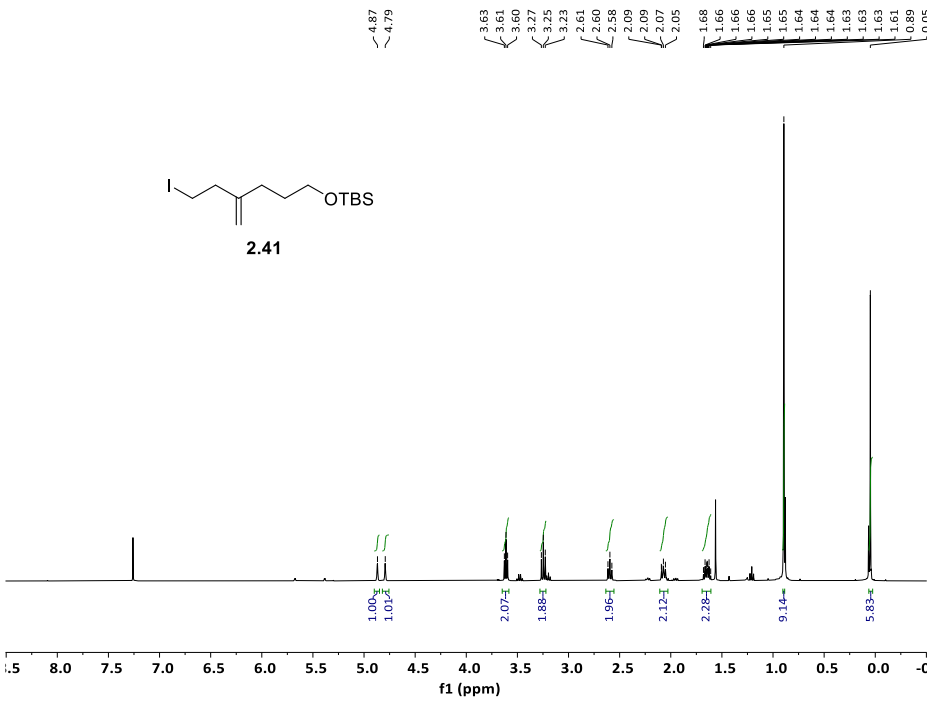

**Figure 2.21.** $^{1}$H-NMR Spectrum of **2.42** in $CDCl_3$, 500 MHz

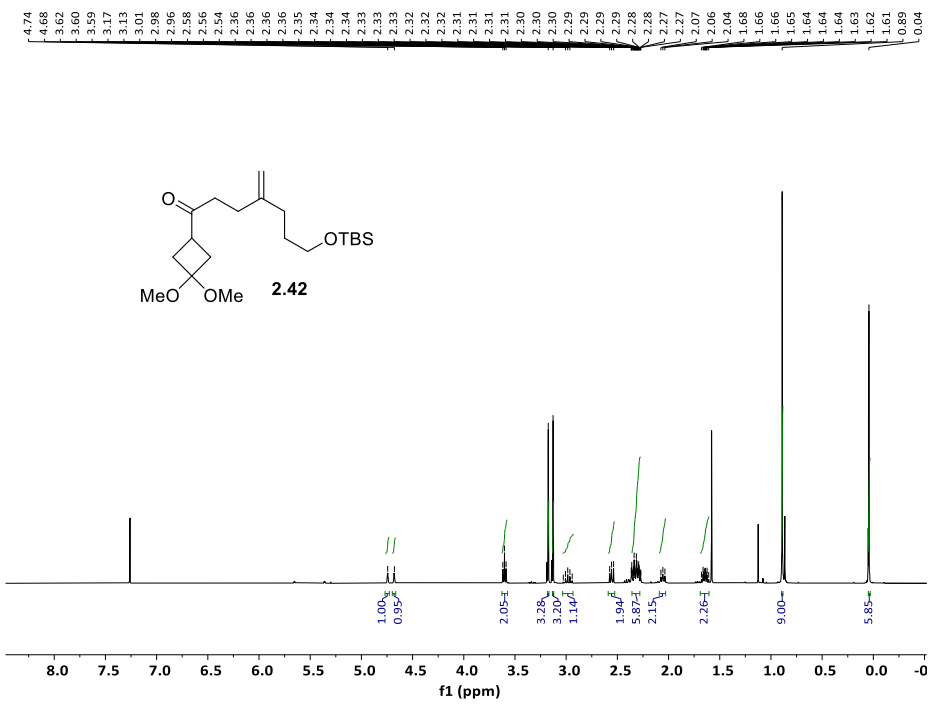


**Figure 2.22.** $^{1}$H-NMR Spectrum of **2.43** in $CDCl_3$, 500 MHz

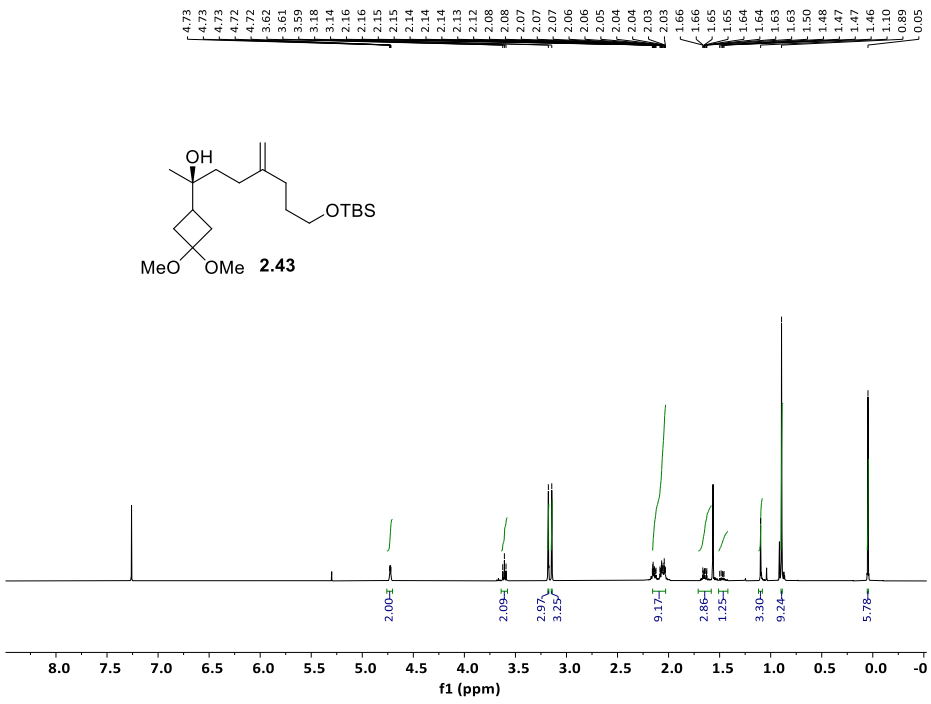

**Figure 2.23.** $^{1}$H-NMR Spectrum of **2.44** in $CDCl_3$, 500 MHz

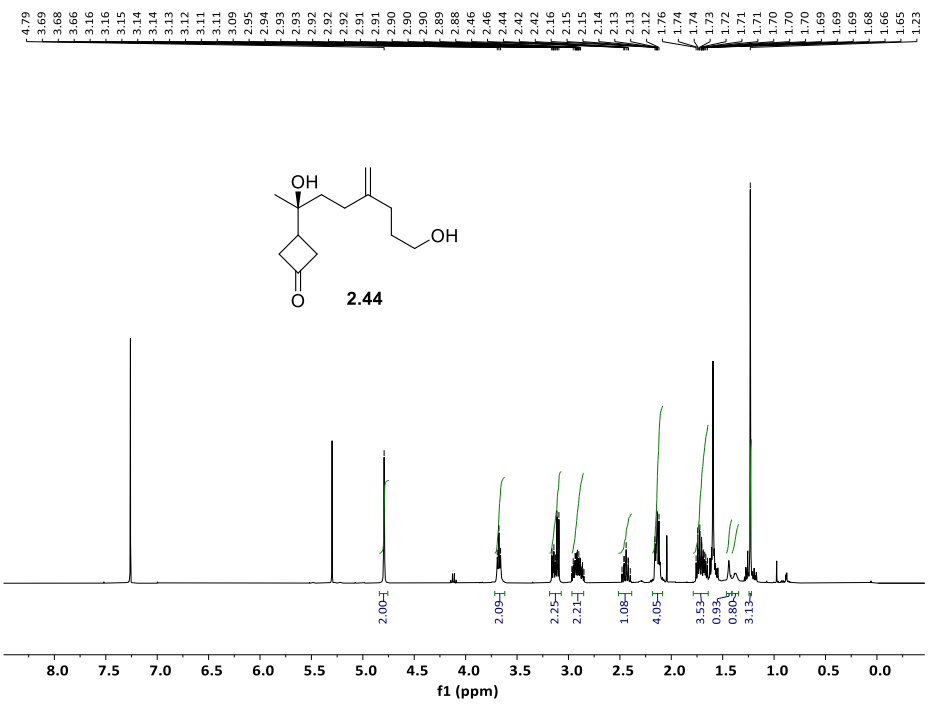


**Figure 2.24.** $^{1}$H-NMR Spectrum of **2.51** in $CDCl_3$, 500 MHz

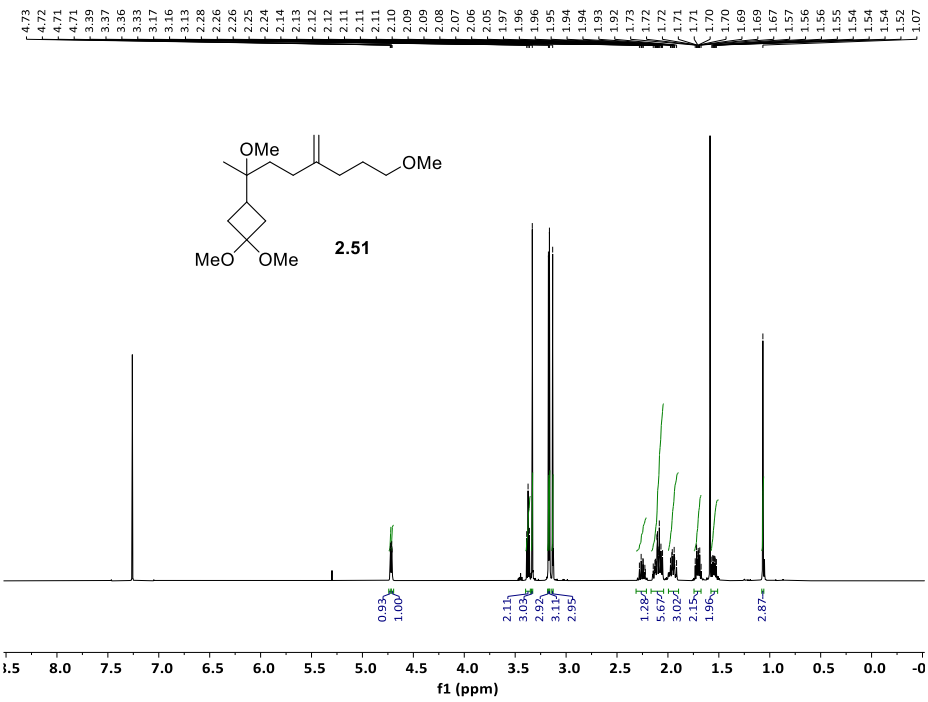

**Figure 2.25.** $^{1}$H-NMR Spectrum of **2.52** in $CDCl_3$, 500 MHz

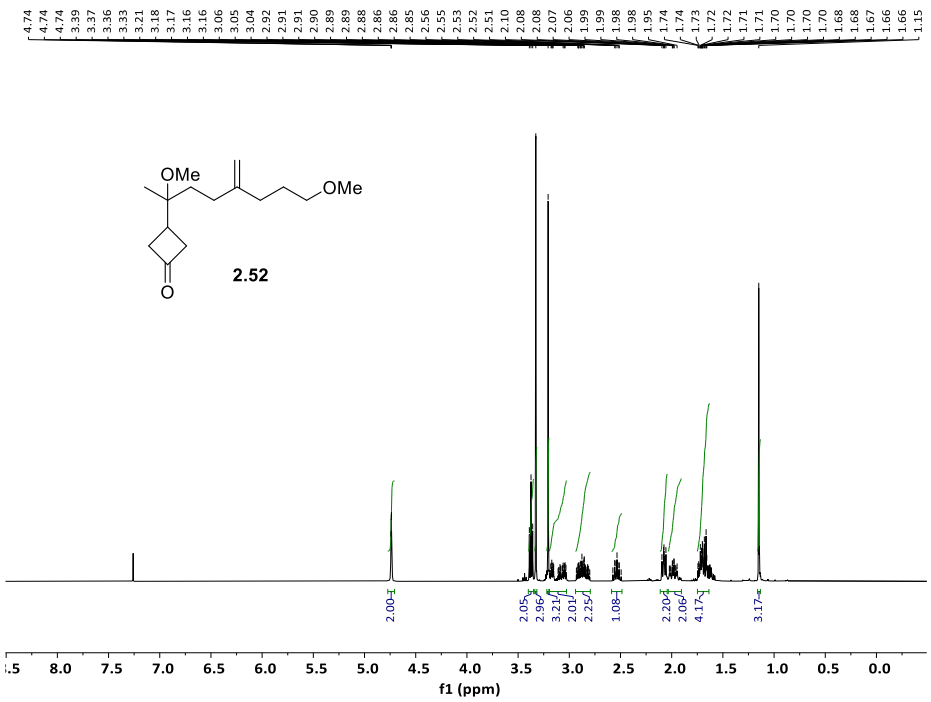


**Figure 2.26.** $^{13}$C-NMR Spectrum of **2.52** in $CDCl_3$, 101 MHz

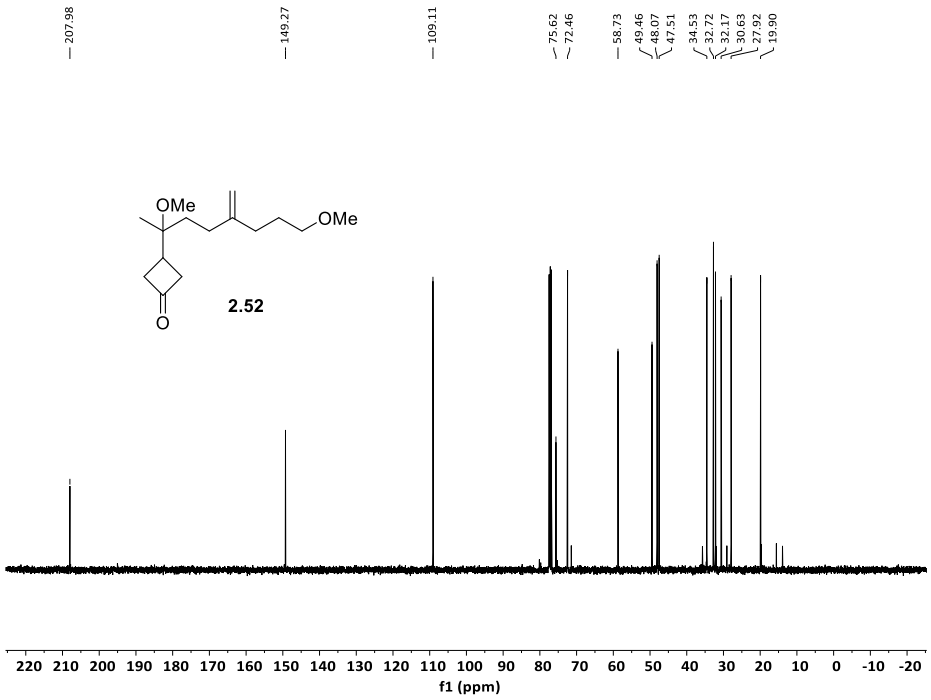

**Figure 2.27.** $^{1}$H-NMR Spectrum of **2.54** in $CDCl_3$, 500 MHz

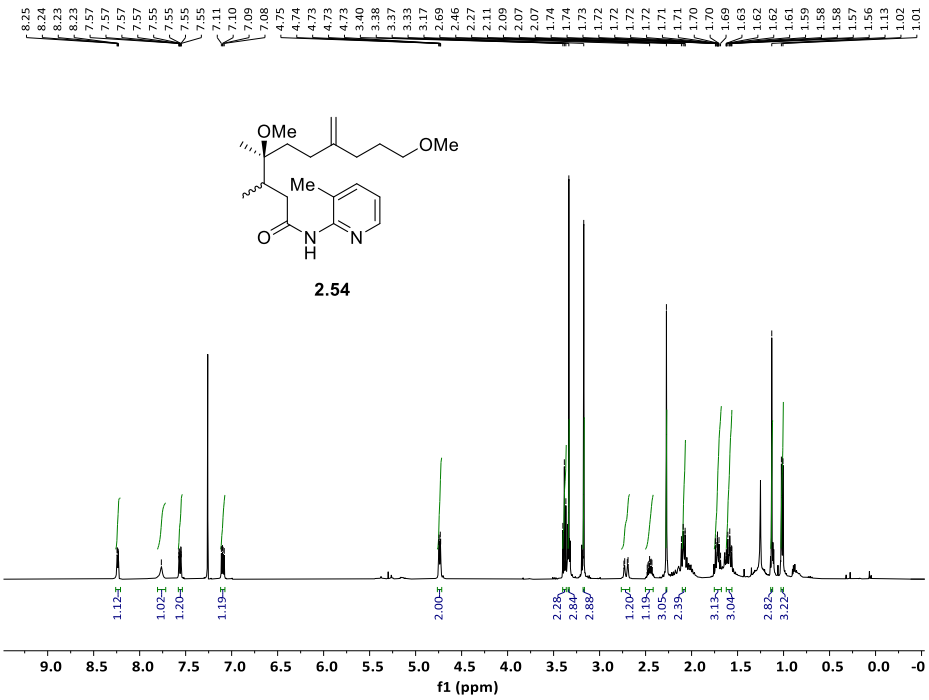


**Figure 2.28.** $^{1}$H-NMR Spectrum of **2.65** in $CDCl_3$, 500 MHz

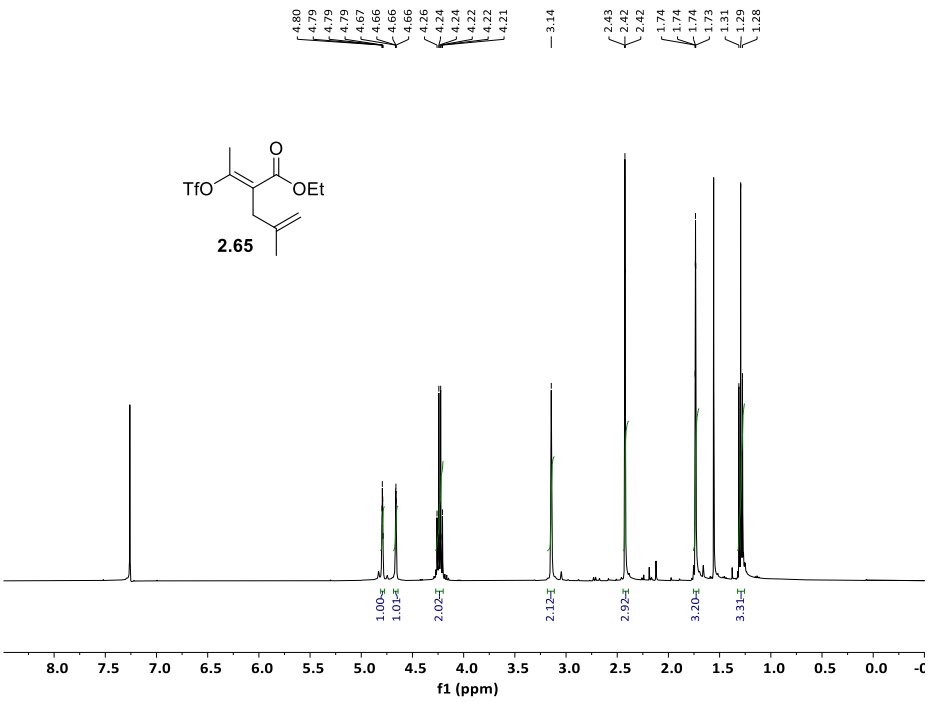

**Figure 2.29.** $^{1}$H-NMR Spectrum of **2.67** in $CDCl_3$, 500 MHz

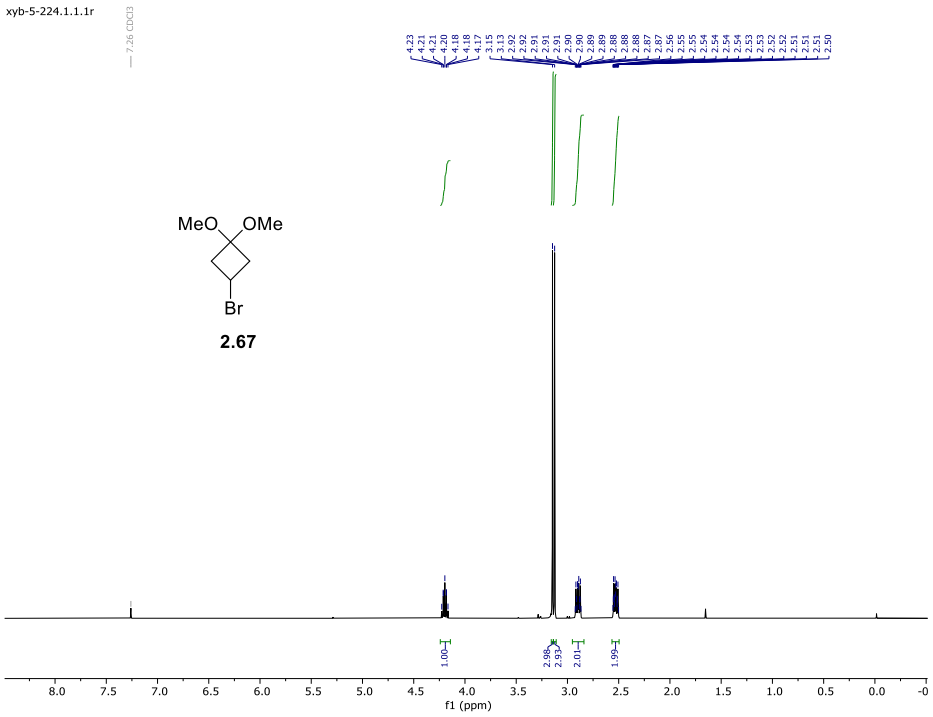


**Figure 2.30.** $^{13}$C-NMR Spectrum of **2.67** in $CDCl_3$, 126 MHz

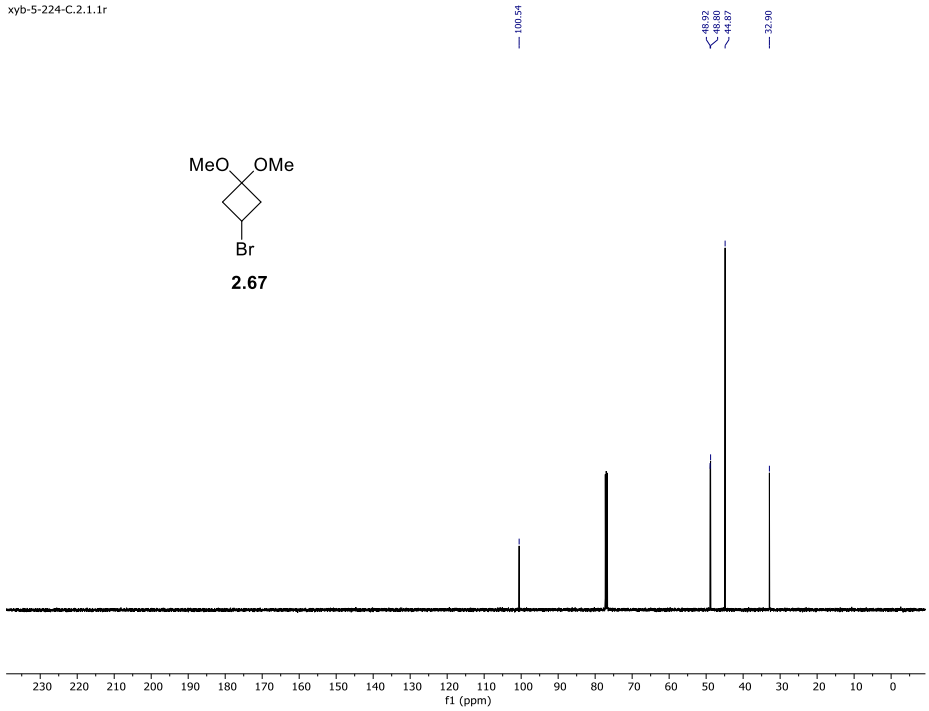

**Figure 2.31.** $^{1}$H-NMR Spectrum of **2.68** in $CDCl_3$, 500 MHz

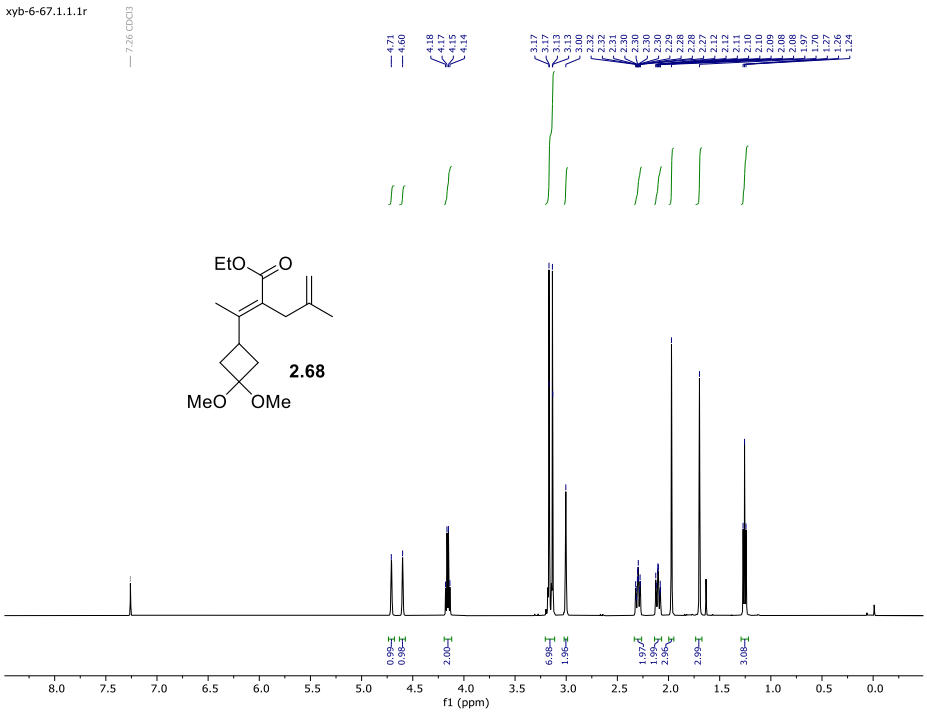


**Figure 2.32.** $^{13}$C-NMR Spectrum of **2.68** in $CDCl_3$, 101 MHz

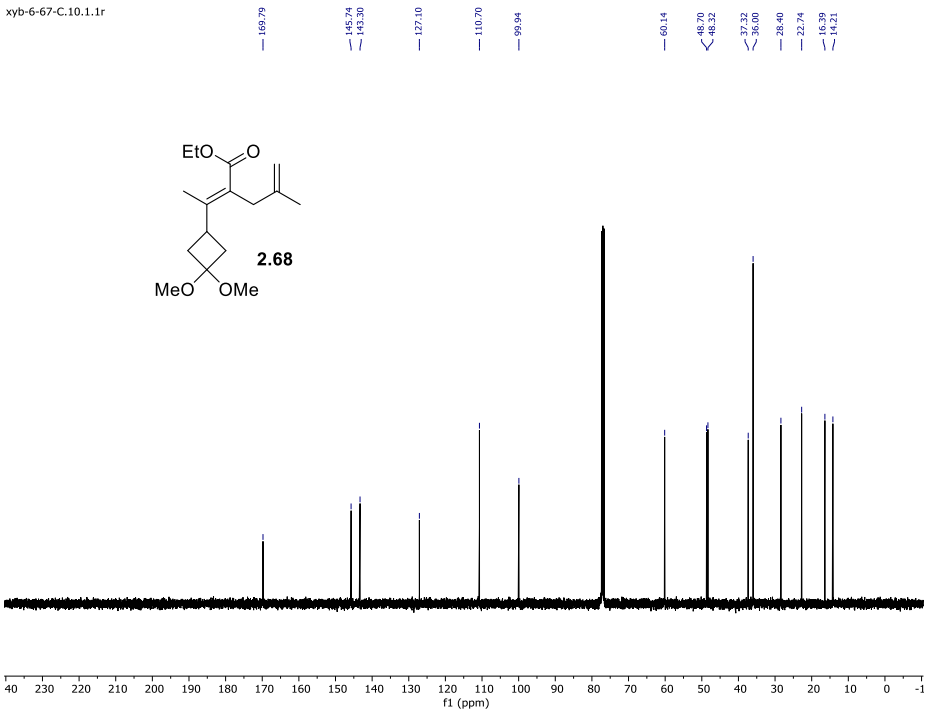

**Figure 2.33.** $^{1}$H-NMR Spectrum of **2.62** in $CDCl_3$, 500 MHz

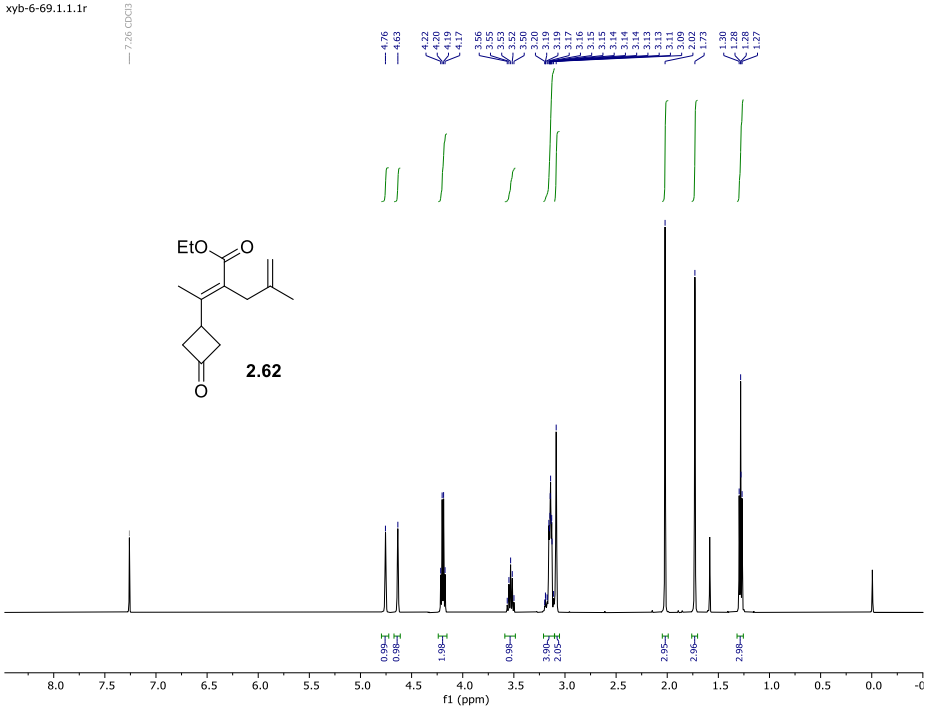


**Figure 2.34.** $^{13}$C-NMR Spectrum of **2.62** in $CDCl_3$, 101 MHz

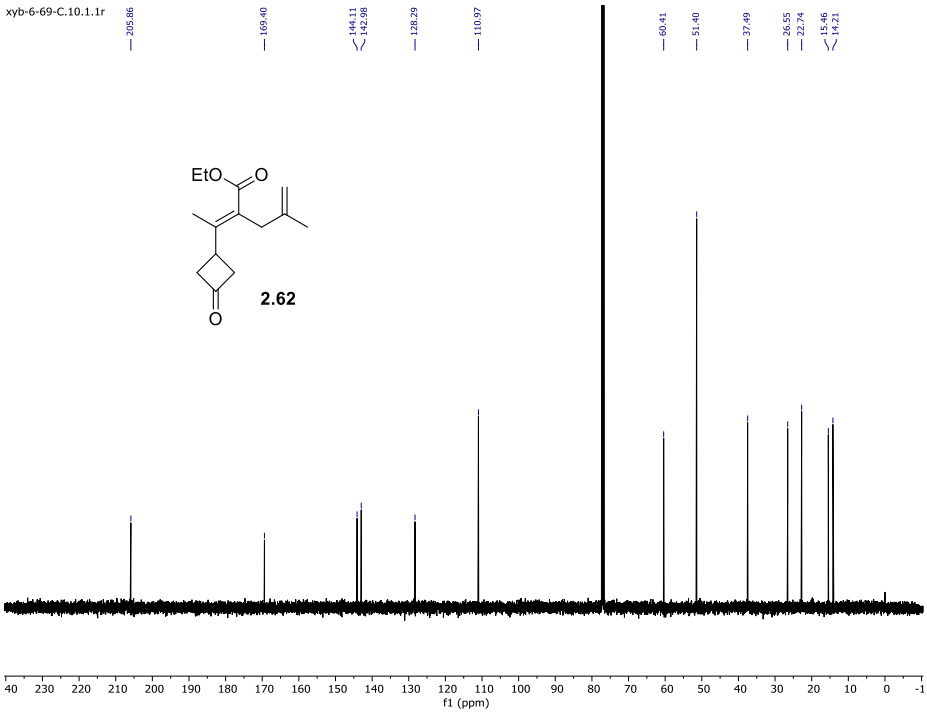

**Figure 2.35.** $^{1}$H-NMR Spectrum of **2.73** in $CDCl_3$, 500 MHz

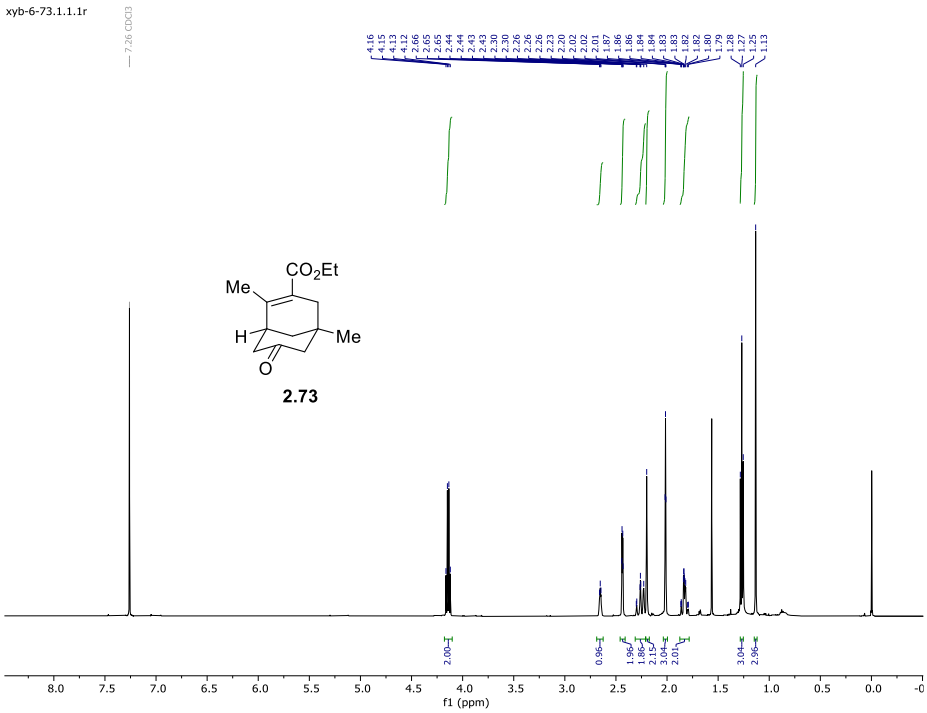


**Figure 2.36.** $^{13}$C-NMR Spectrum of **2.73** in $CDCl_3$, 101 MHz

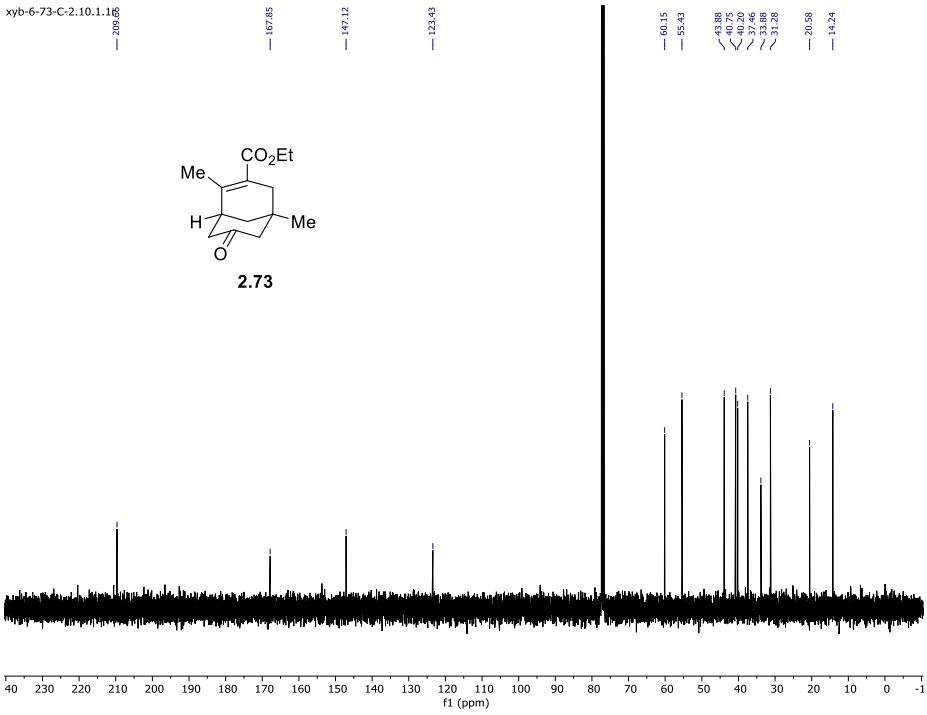

**Figure 2.37.** $^{1}$H-NMR Spectrum of **2.78** in $CDCl_3$, 500 MHz

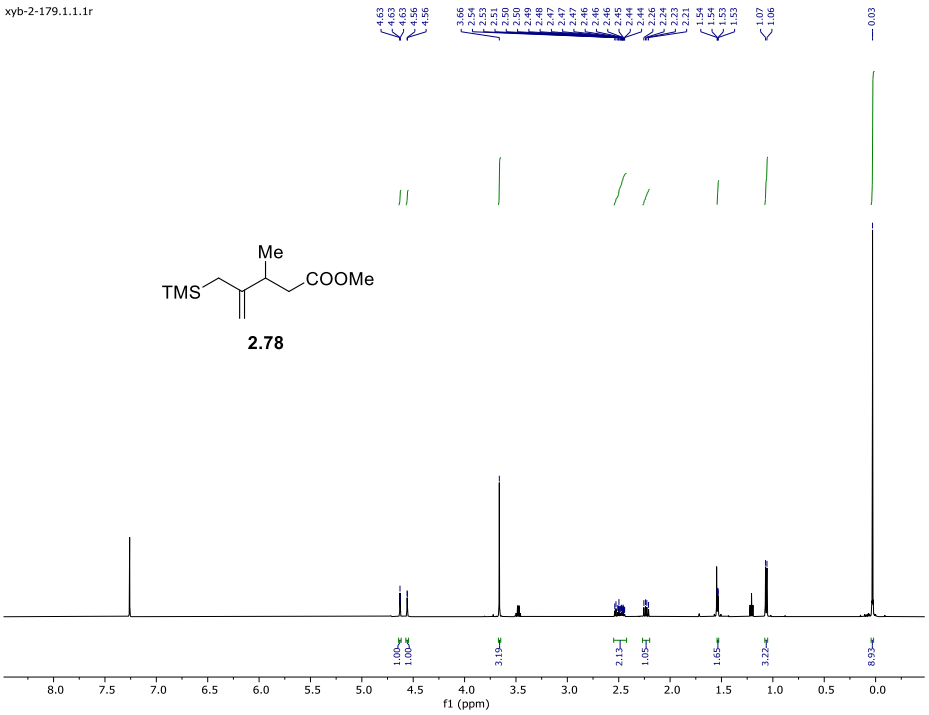


**Figure 2.38.** $^{1}$H-NMR Spectrum of **2.79** in $CDCl_3$, 500 MHz

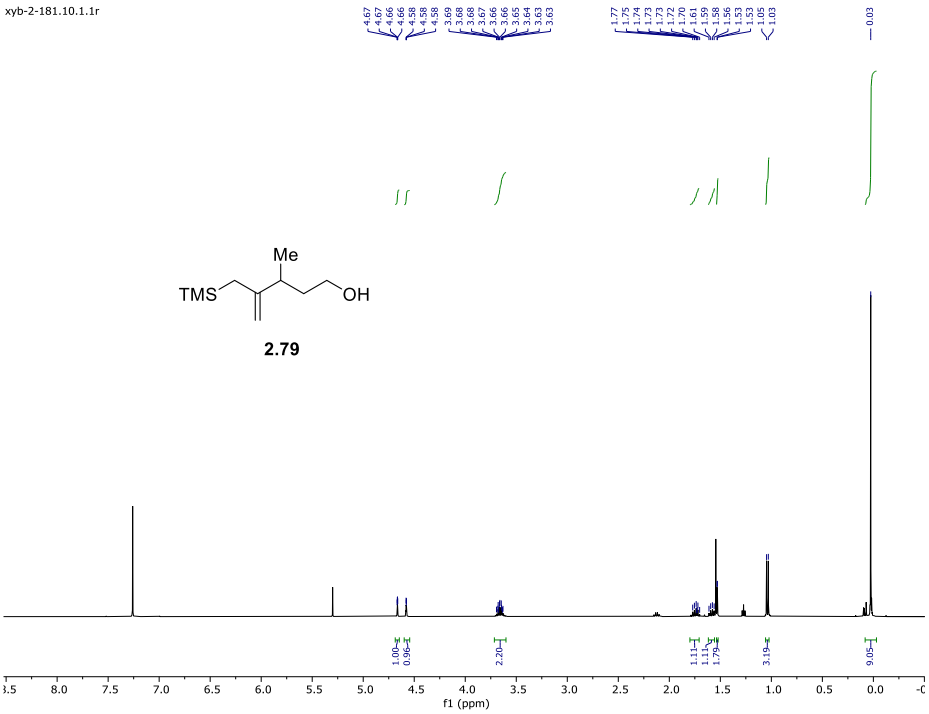

**Figure 2.39.** $^{1}$H-NMR Spectrum of **2.80** in $CDCl_3$, 500 MHz

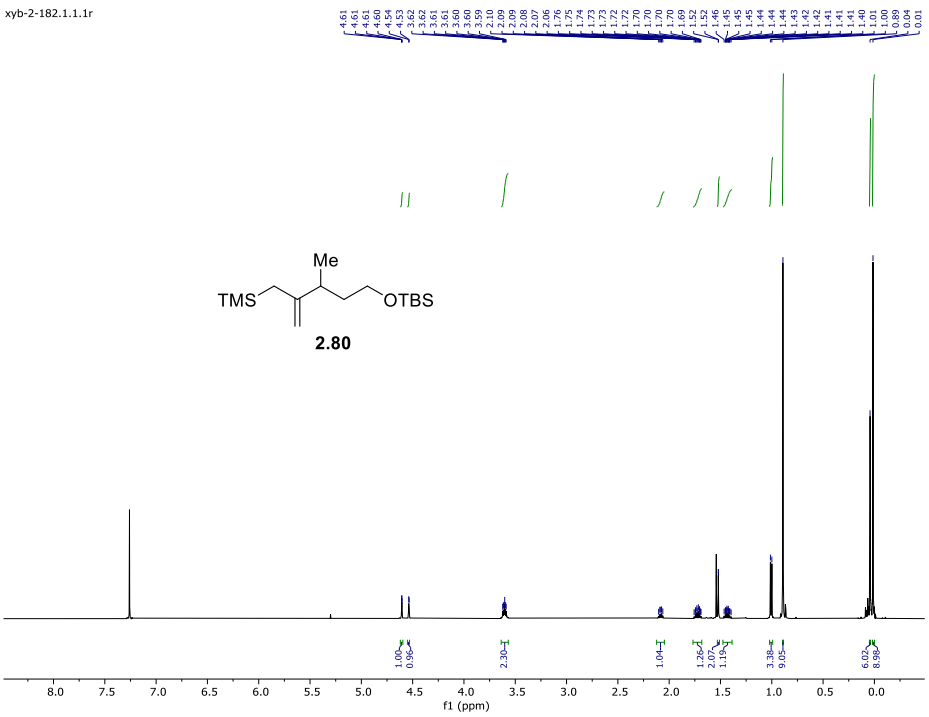


**Figure 2.40.** $^{1}$H-NMR Spectrum of **2.81** in $CDCl_3$, 500 MHz

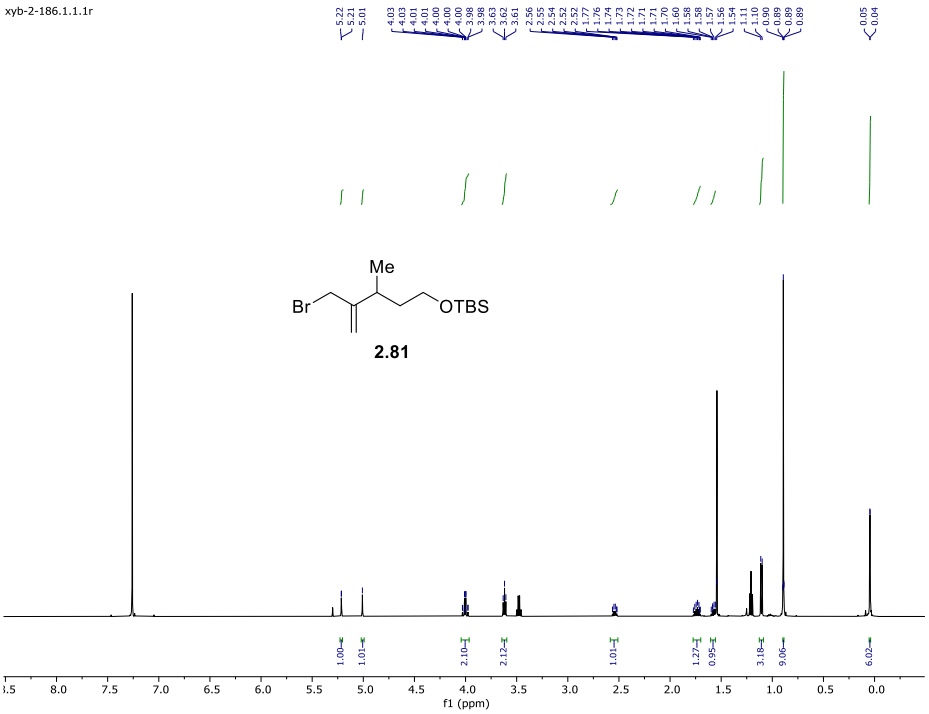

**Figure 2.41.** $^{1}$H-NMR Spectrum of **2.82** in $CDCl_3$, 500 MHz

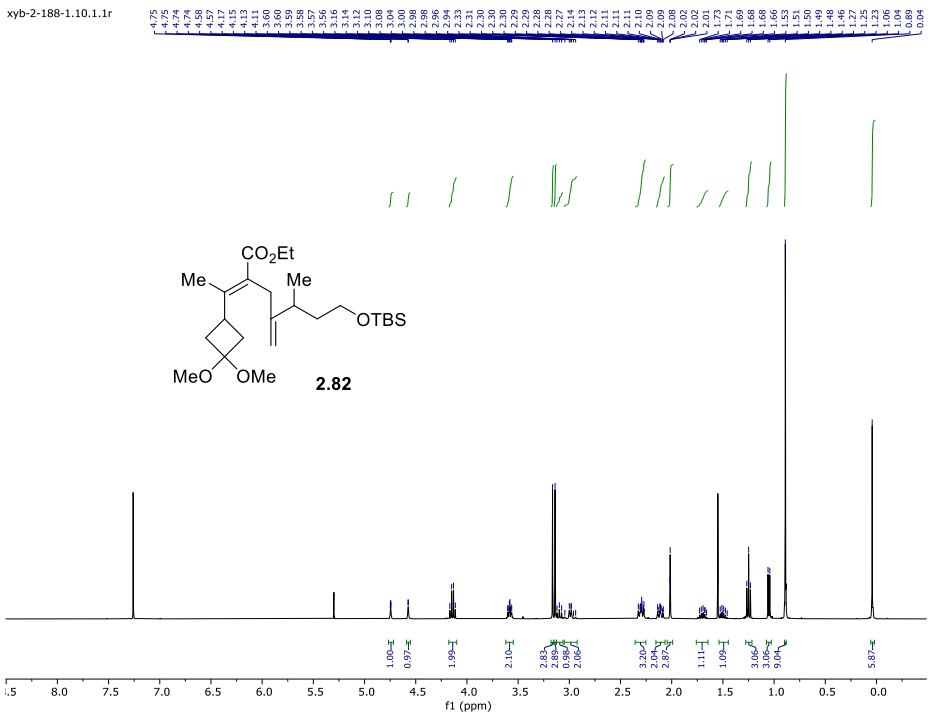


**Figure 2.42.** $^{1}$H-NMR Spectrum of **2.75** in $CDCl_3$, 500 MHz

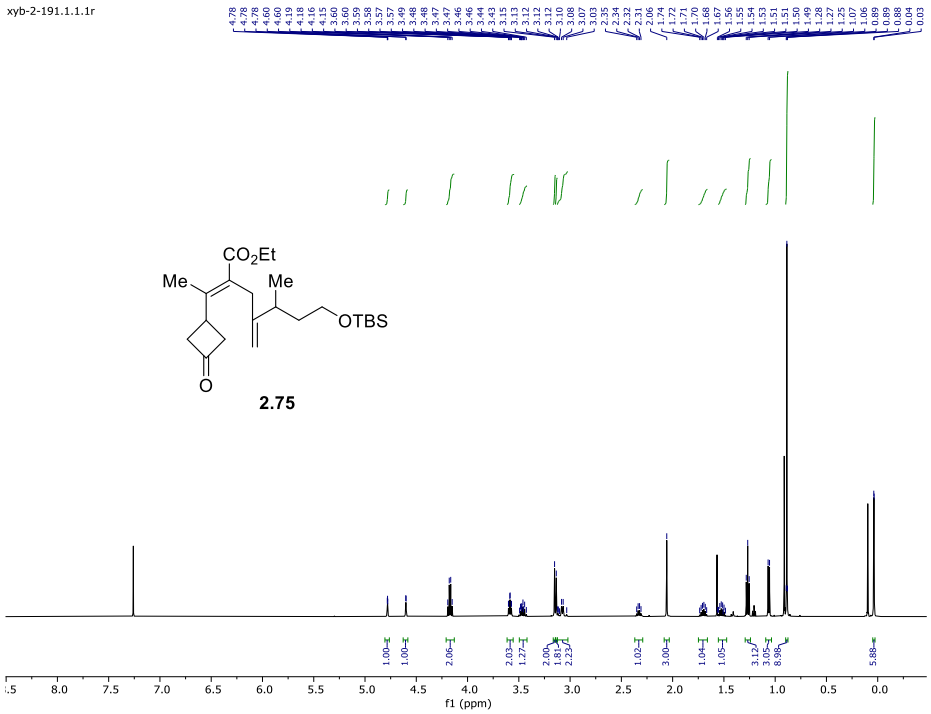

**Figure 2.43.** $^{13}$C-NMR Spectrum of **2.75** in $CDCl_3$, 101 MHz

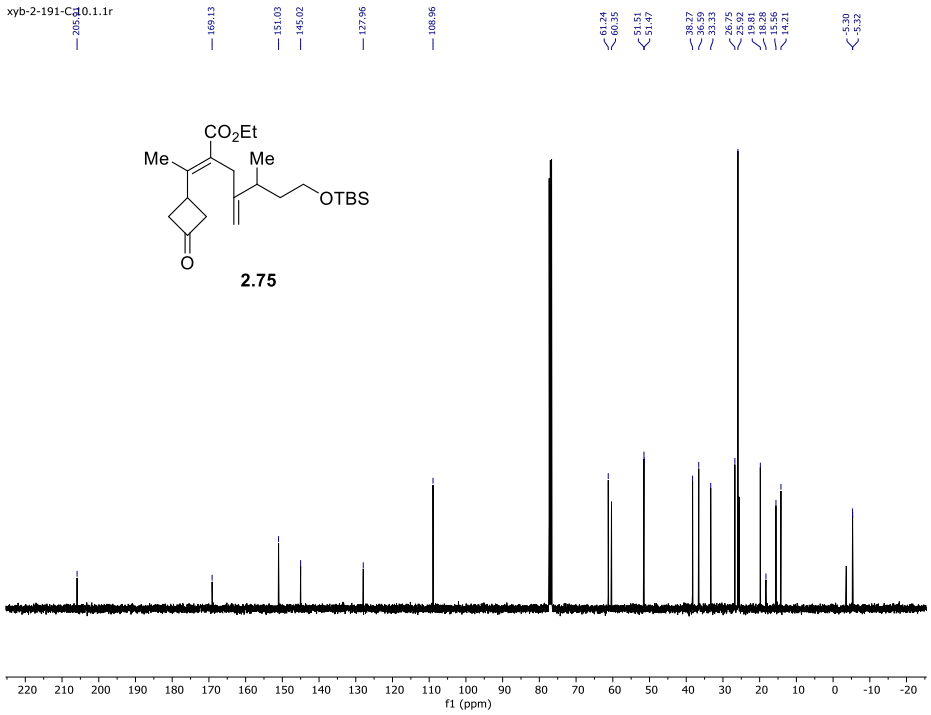


**Figure 2.44.** $^{1}$H-NMR Spectrum of **2.91** in $CDCl_3$, 500 MHz

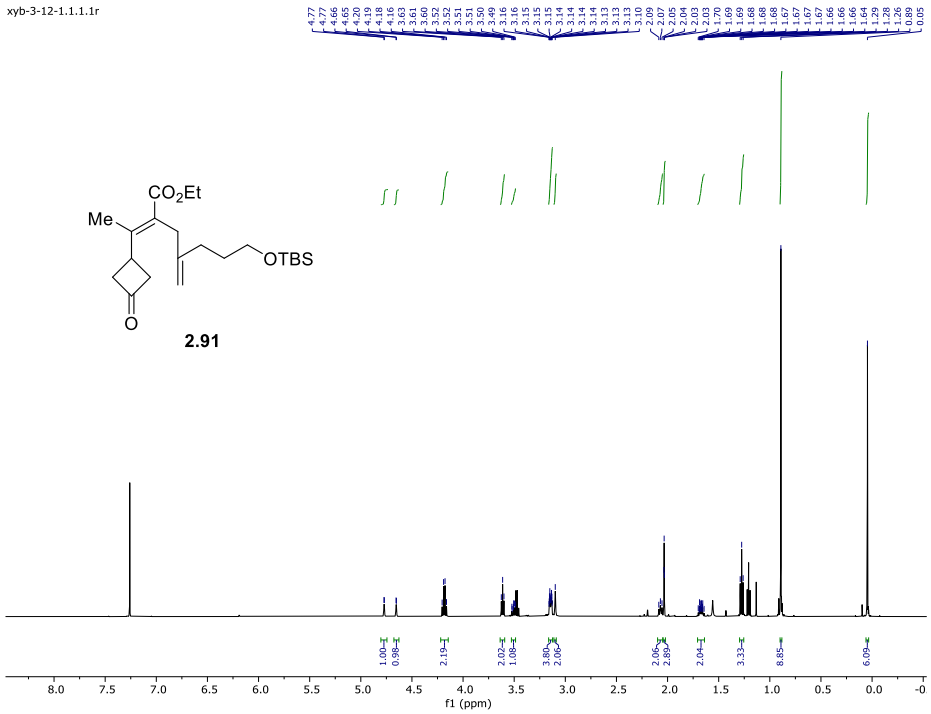

**Figure 2.45.** $^{1}$H-NMR Spectrum of **2.95** in $CDCl_3$, 500 MHz

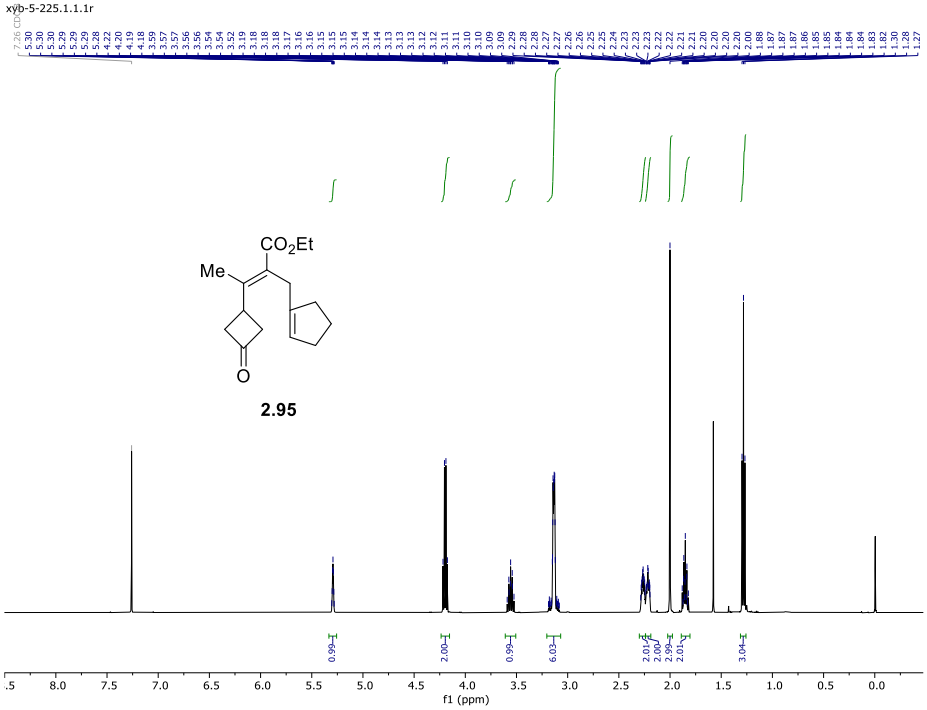


**Figure 2.46.** $^{13}$C-NMR Spectrum of **2.95** in $CDCl_3$, 101 MHz

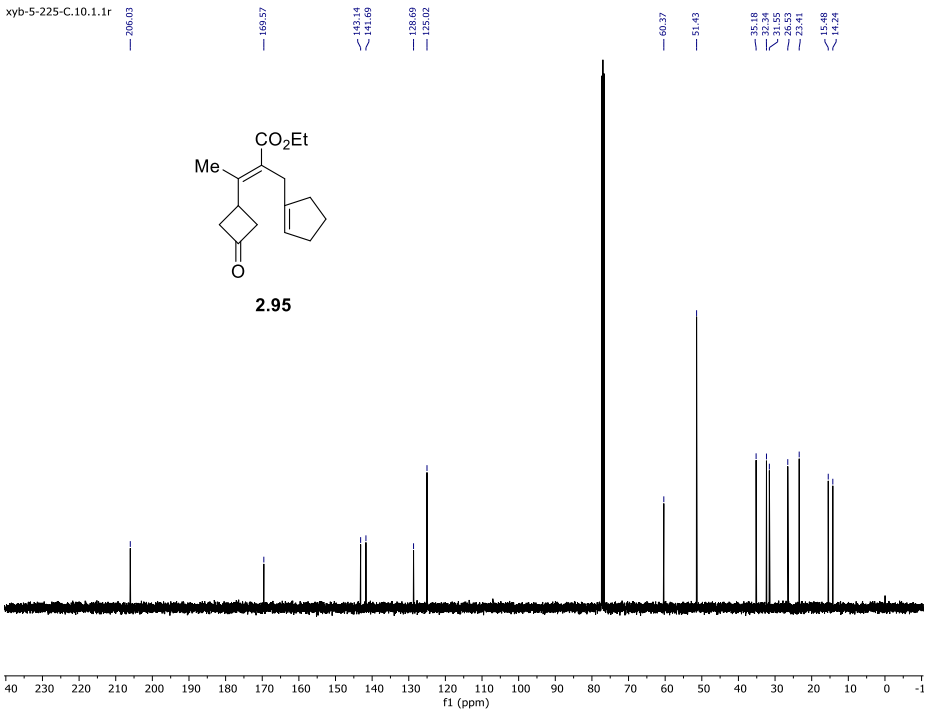

**Figure 2.47.** $^{1}$H-NMR Spectrum of **2.99** in $CDCl_3$, 500 MHz

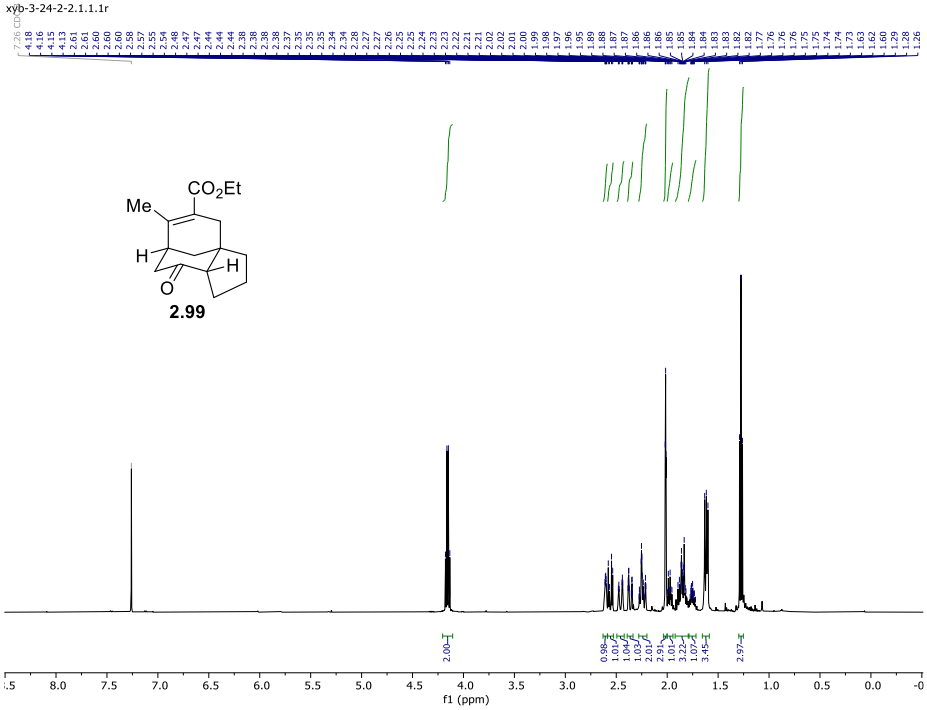


**Figure 2.48.** $^{13}$C-NMR Spectrum of **2.99** in $CDCl_3$, 101 MHz

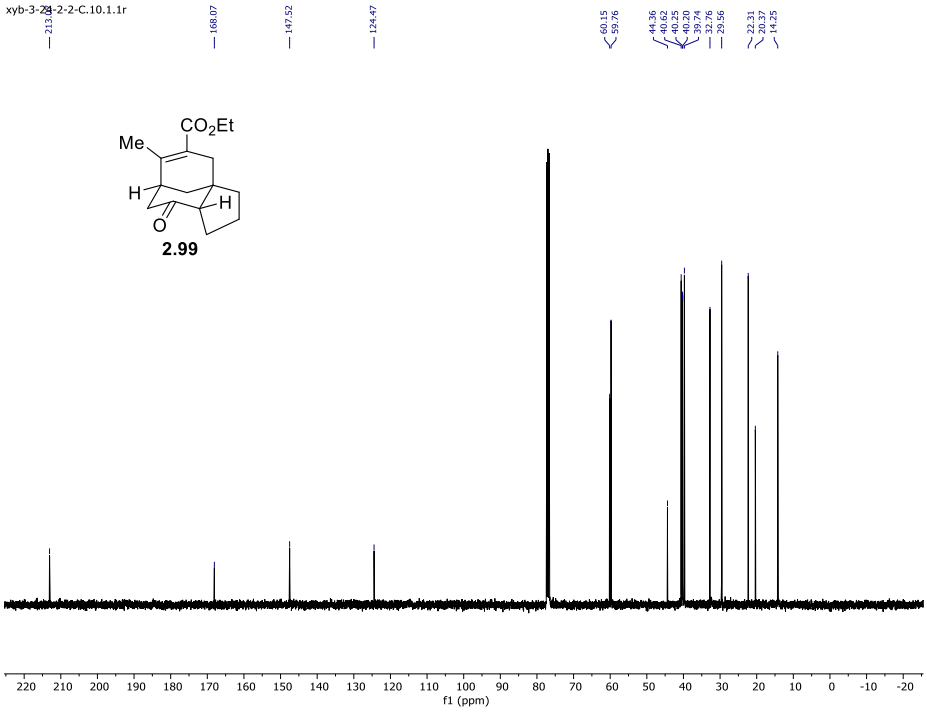

**Figure 2.49.** $^{1}$H-NMR Spectrum of **S2.2** in $CDCl_3$, 500 MHz

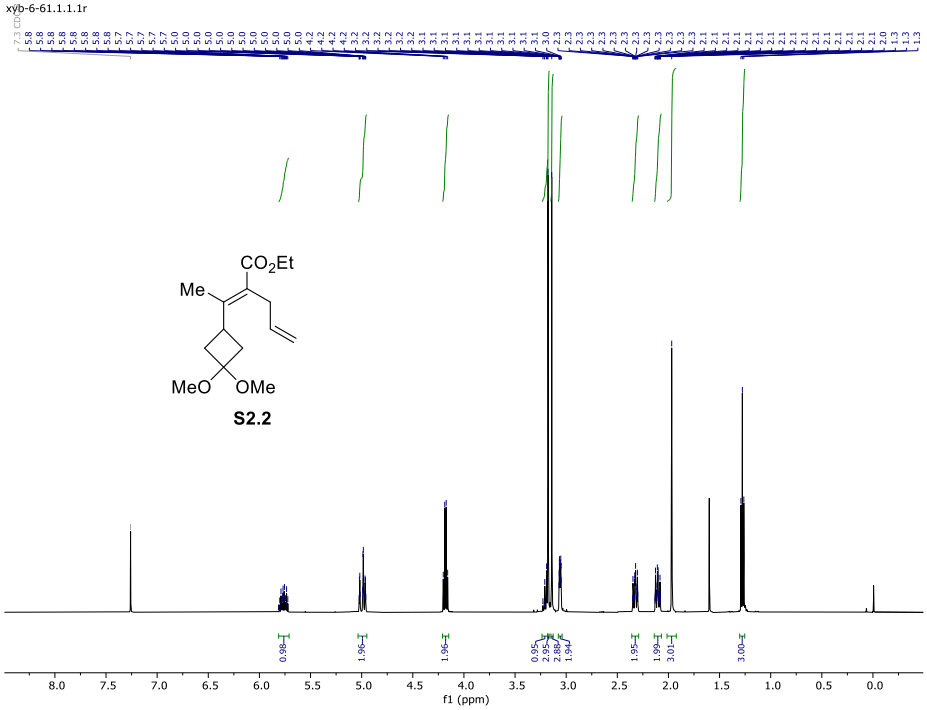


**Figure 2.50.** $^{13}$C-NMR Spectrum of **S2.2** in $CDCl_3$, 101 MHz

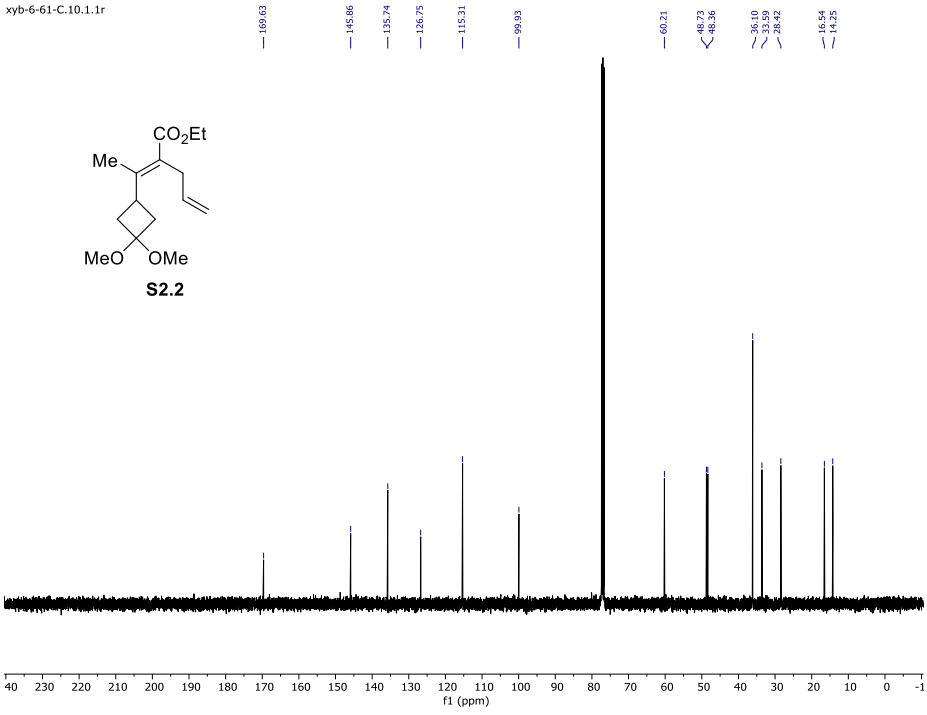

**Figure 2.51.** $^{1}$H-NMR Spectrum of **2.100** in $CDCl_3$, 500 MHz

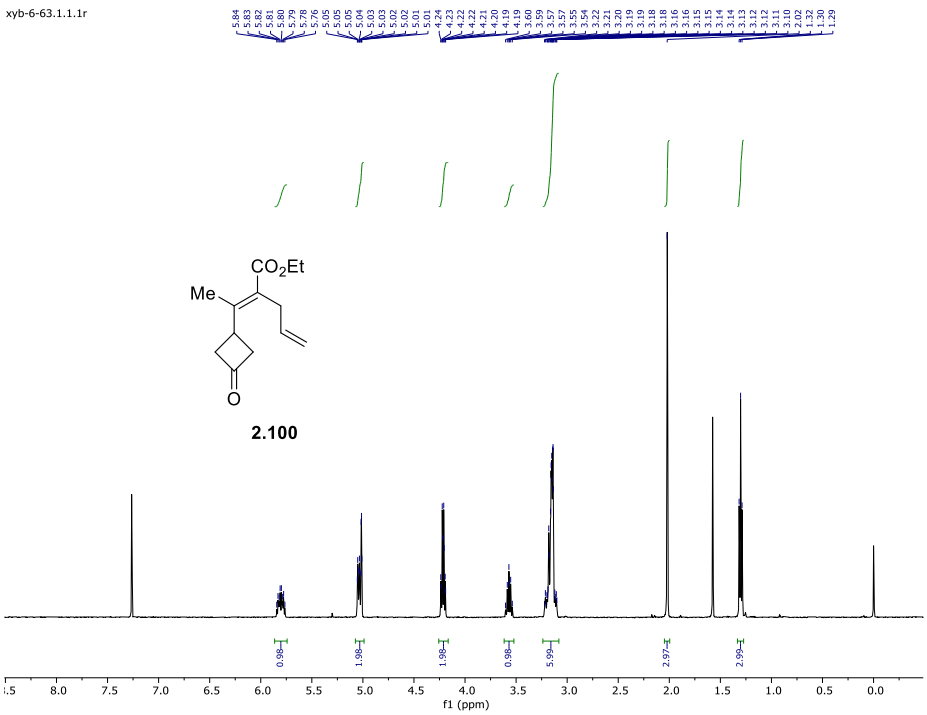


**Figure 2.52.** $^{13}$C-NMR Spectrum of **2.100** in $CDCl_3$, 101 MHz

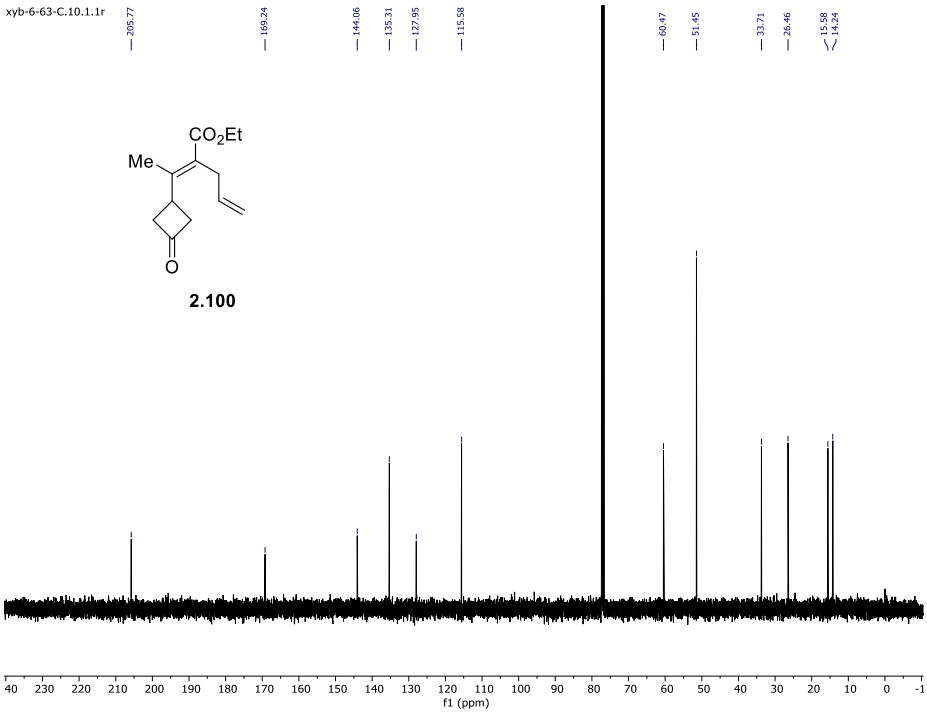

**Figure 2.53.** $^{1}$H-NMR Spectrum of **2.101** in $CDCl_3$, 500 MHz

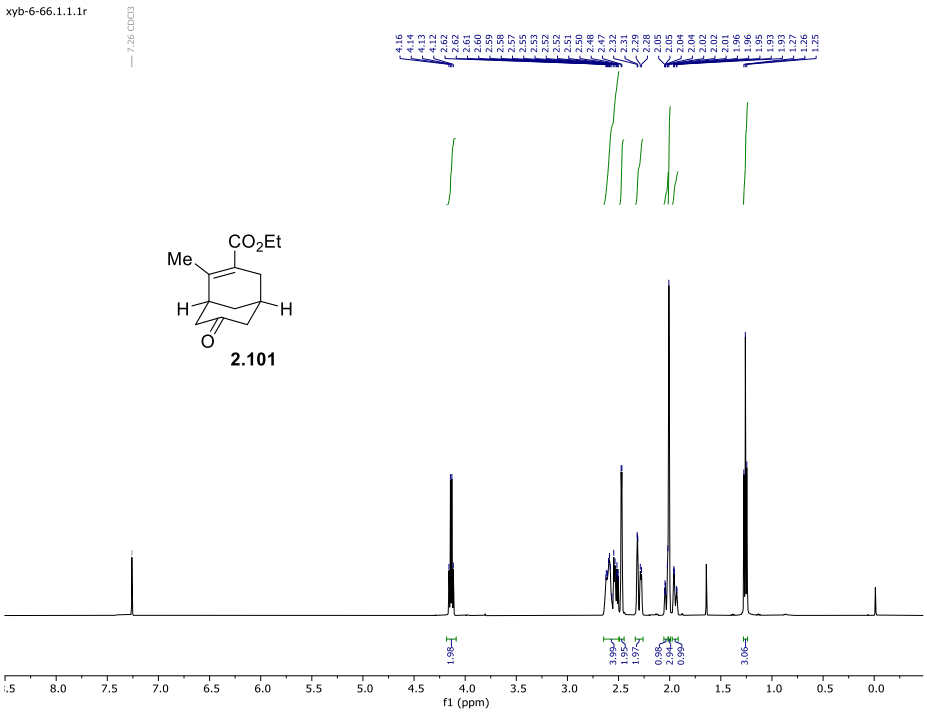


**Figure 2.54.** $^{13}$C-NMR Spectrum of **2.101** in $CDCl_3$, 101 MHz

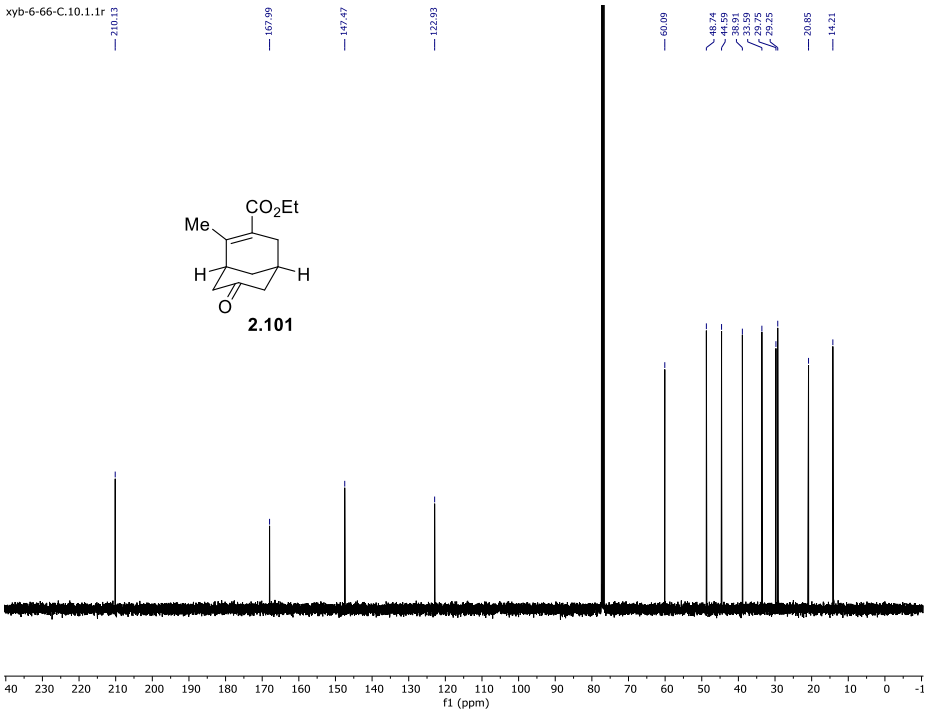

**Figure 2.55.** $^{1}$H-NMR Spectrum of **DG4** in $CDCl_3$, 500 MHz

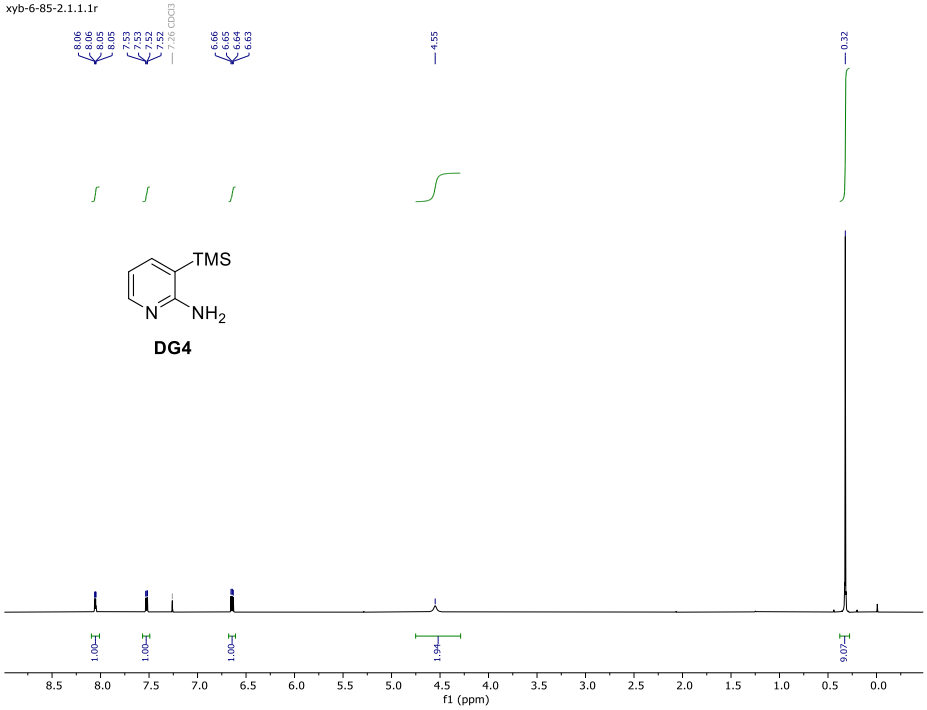


**Figure 2.56.** $^{13}$C-NMR Spectrum of **DG4** in $CDCl_3$, 101 MHz

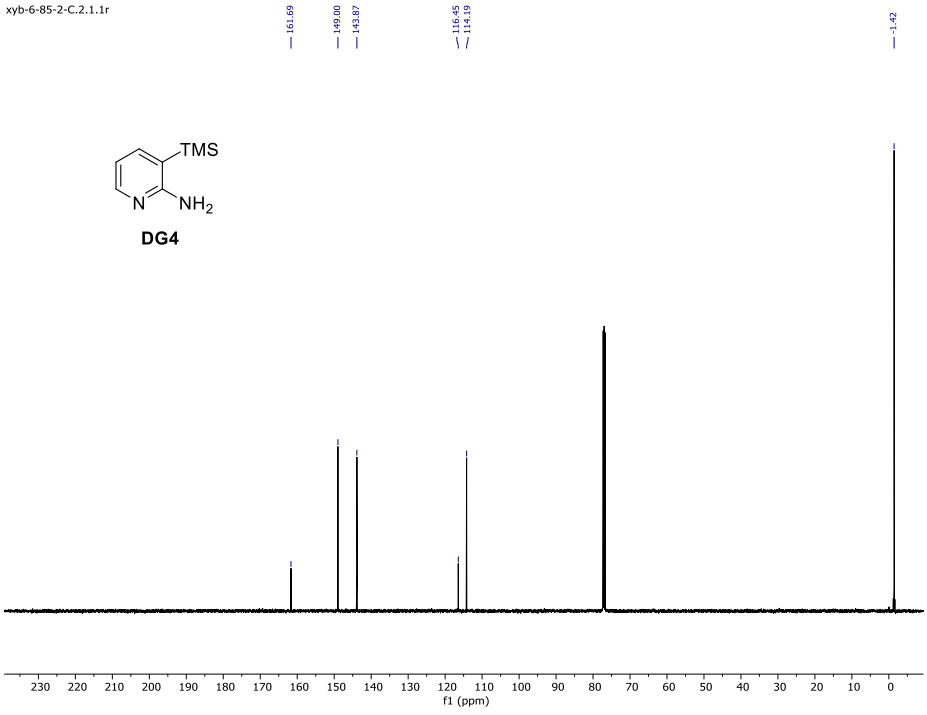

**Figure 2.57.** $^{1}$H-NMR Spectrum of **2.113** in $CDCl_3$, 500 MHz

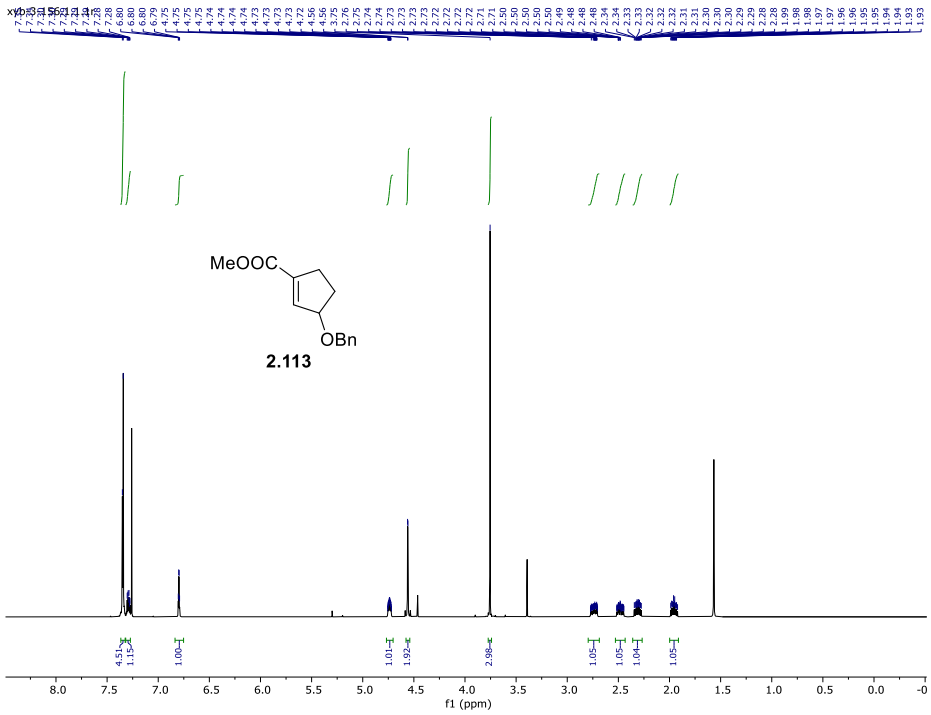


**Figure 2.58.** $^{1}$H-NMR Spectrum of **2.114** in $CDCl_3$, 500 MHz

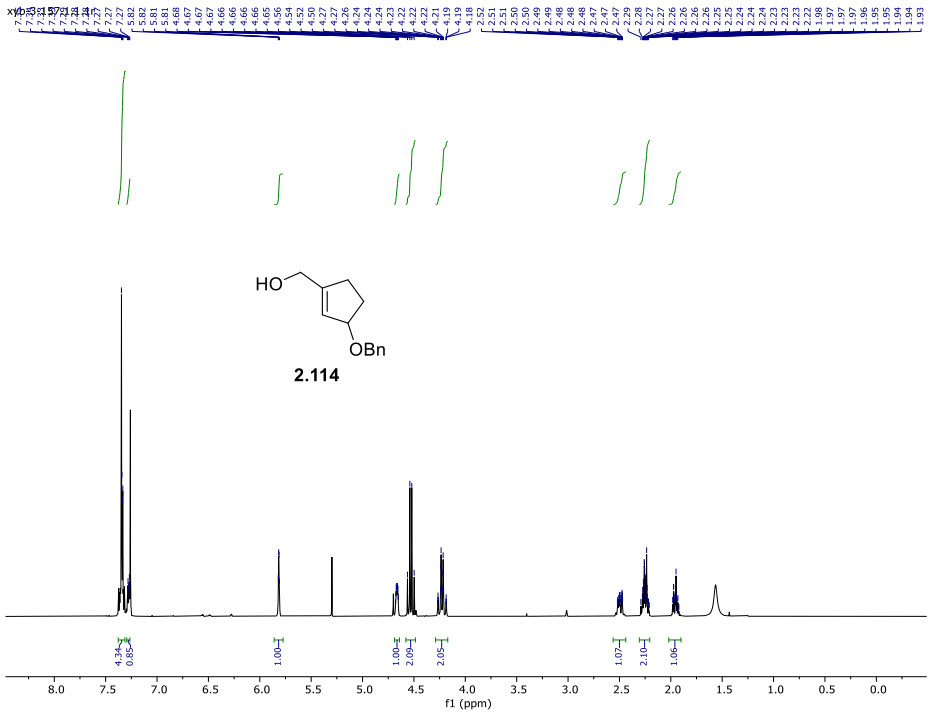

**Figure 2.59.** $^{1}$H-NMR Spectrum of **2.115** in $CDCl_3$, 500 MHz

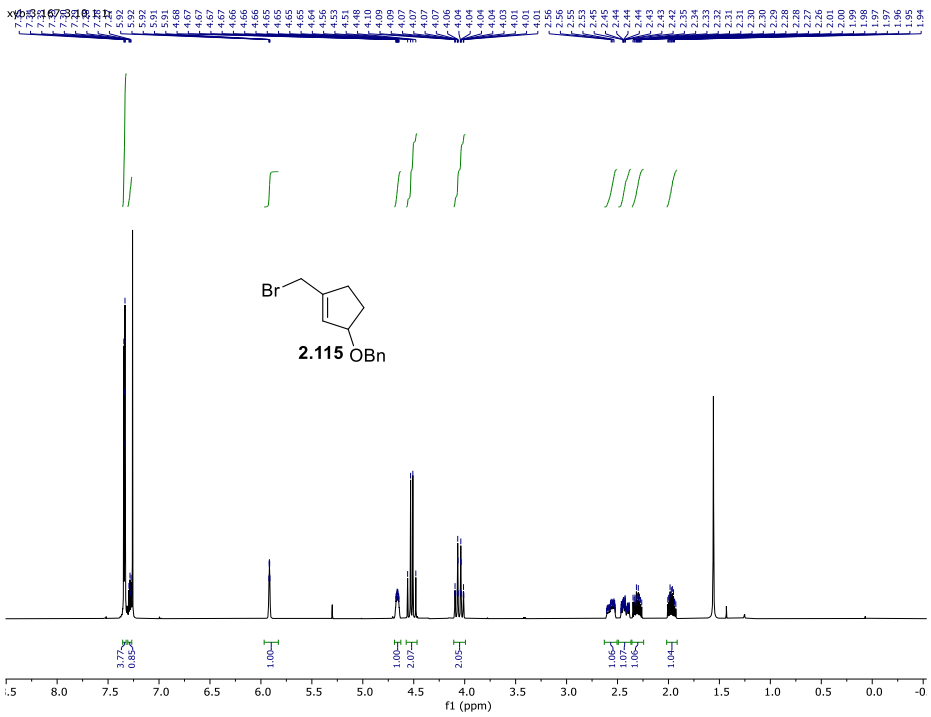


**Figure 2.60.** $^{1}$H-NMR Spectrum of **2.116** in $CDCl_3$, 500 MHz

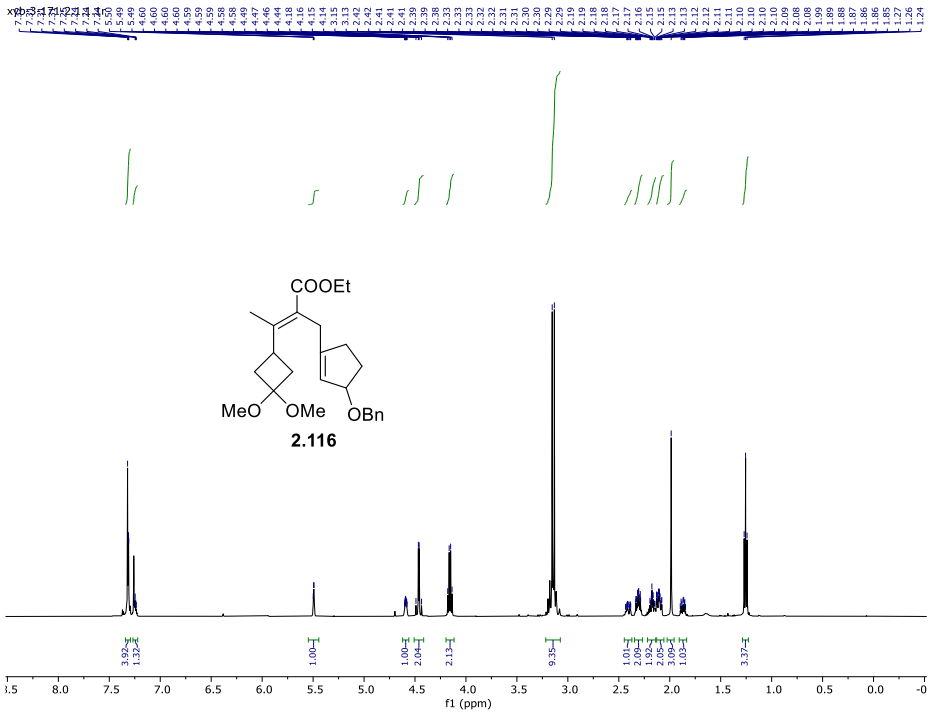

**Figure 2.61.** $^{1}$H-NMR Spectrum of **2.124** in $CDCl_3$, 500 MHz

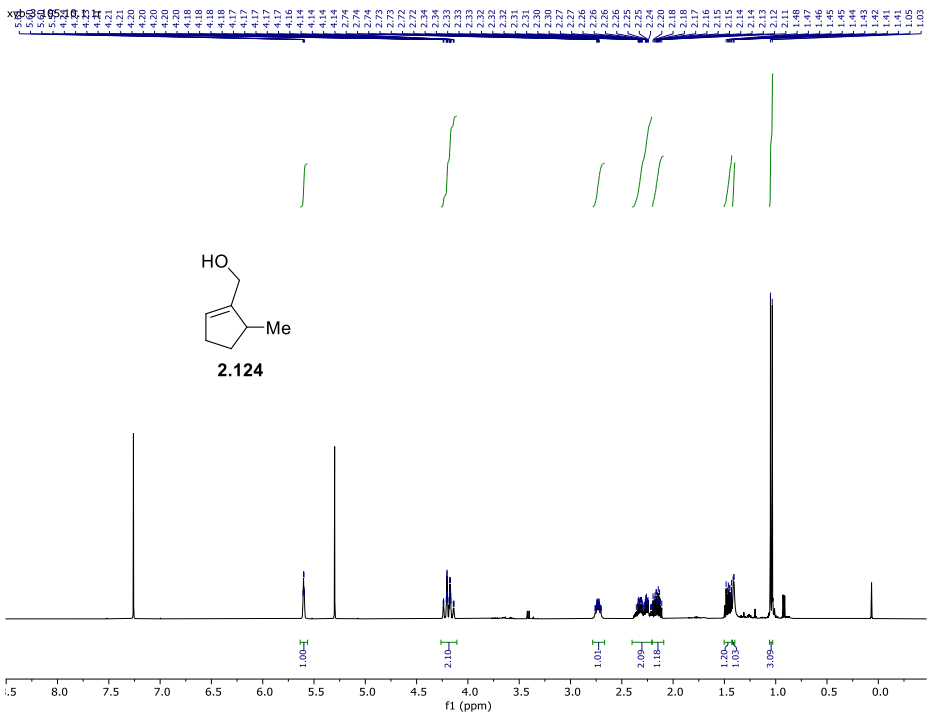


**Figure 2.62.** $^{1}$H-NMR Spectrum of **2.129** in $CDCl_3$, 500 MHz

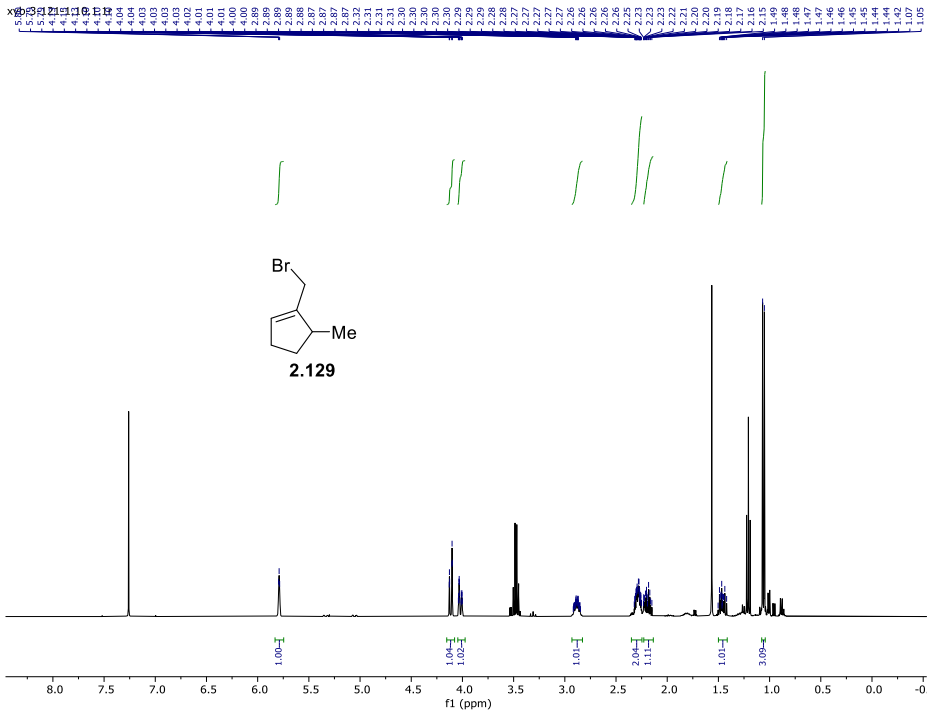

**Figure 2.63.** $^{1}$H-NMR Spectrum of **2.118** in $CDCl_3$, 500 MHz

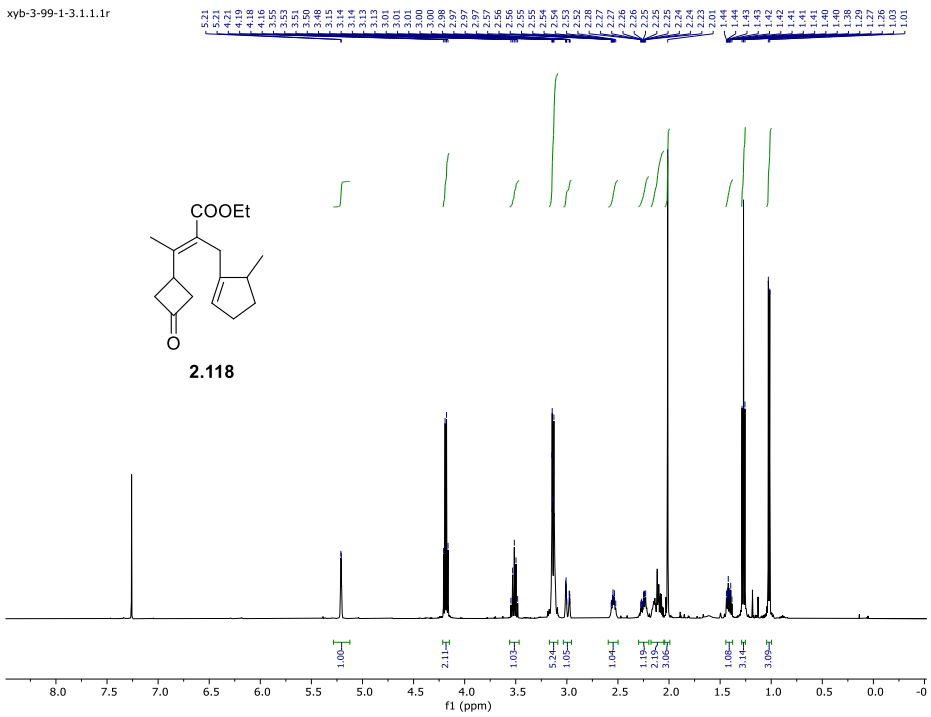


**Figure 2.64.** $^{13}$C-NMR Spectrum of **2.118** in $CDCl_3$, 101 MHz

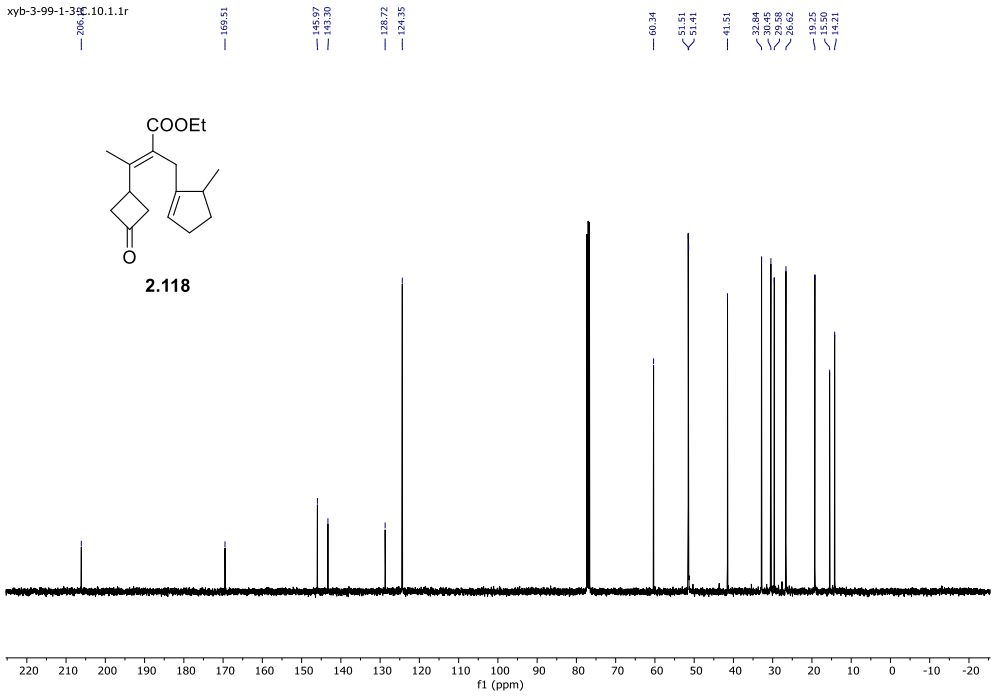

**Figure 2.65.** $^{1}$H-NMR Spectrum of **2.117** in $CDCl_3$, 500 MHz

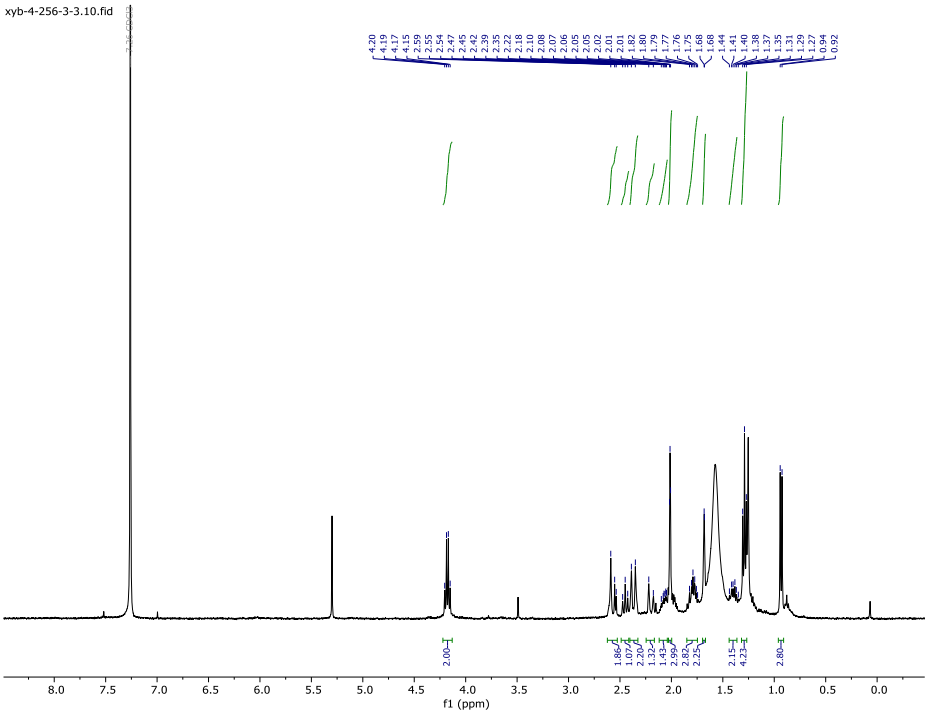


**Figure 2.66.** $^{1}$H-NMR Spectrum of **2.136** in $CDCl_3$, 500 MHz

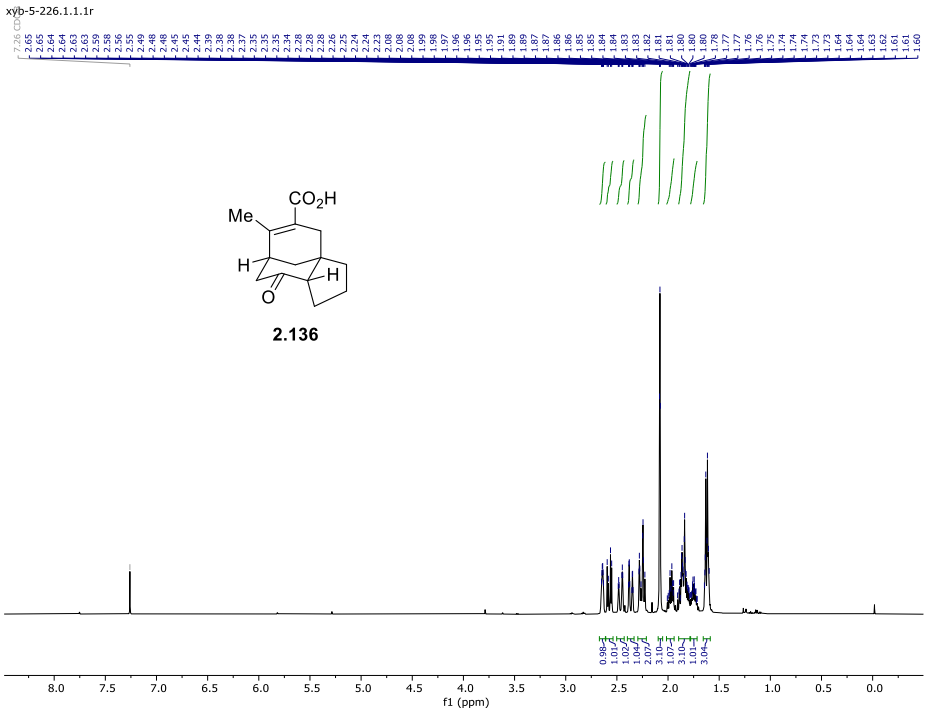

**Figure 2.67.** $^{13}$C-NMR Spectrum of **2.136** in $CDCl_3$, 101 MHz

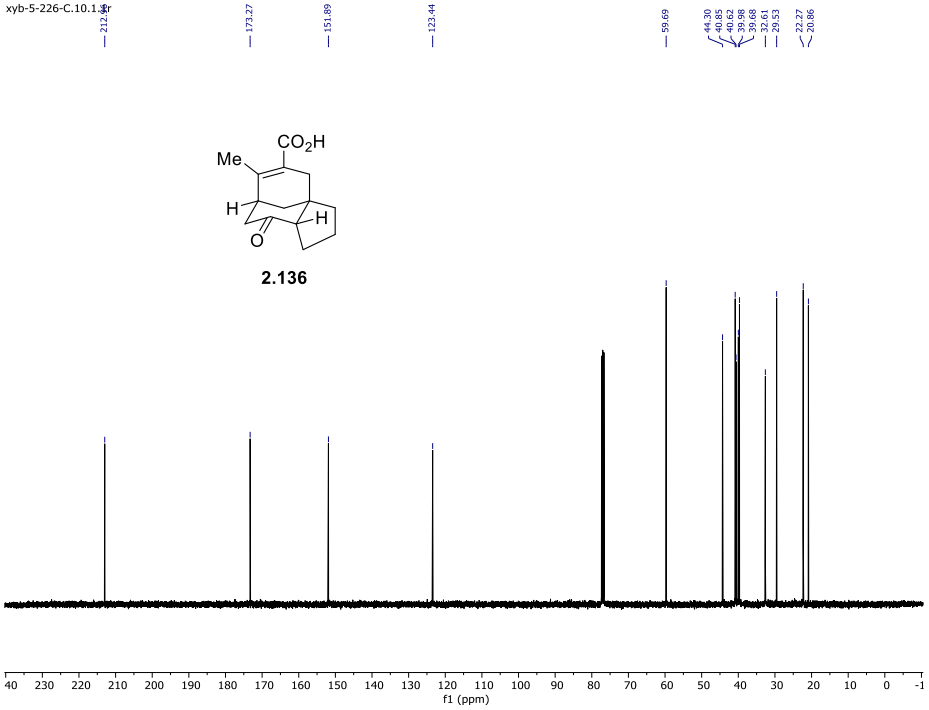


**Figure 2.68.** $^{1}$H-NMR Spectrum of **2.135** in $CDCl_3$, 500 MHz

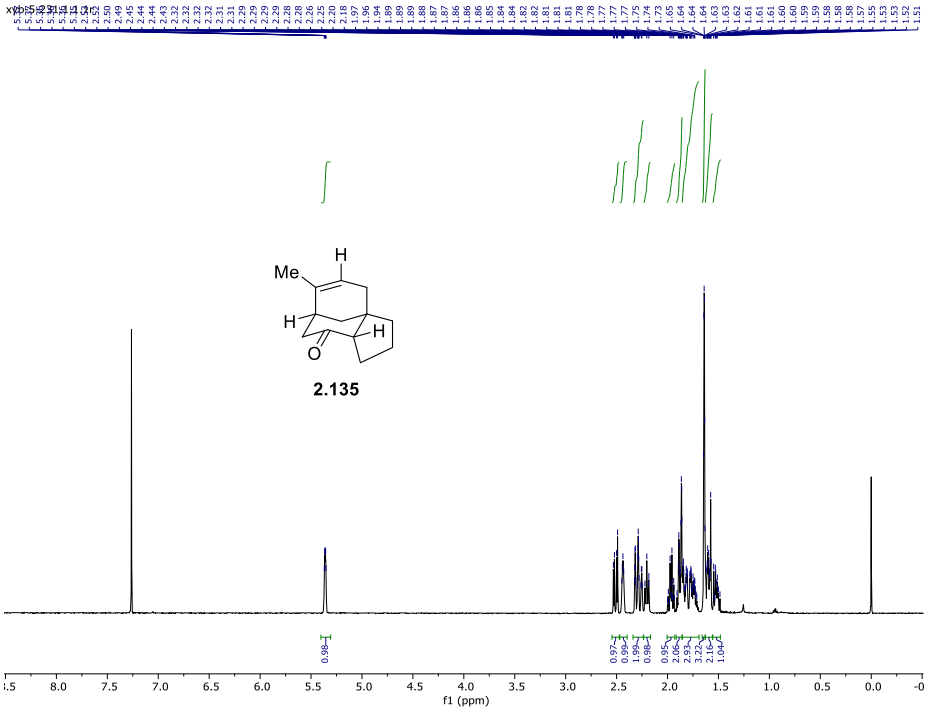

**Figure 2.69.** $^{13}$C-NMR Spectrum of **2.135** in $CDCl_3$, 101 MHz

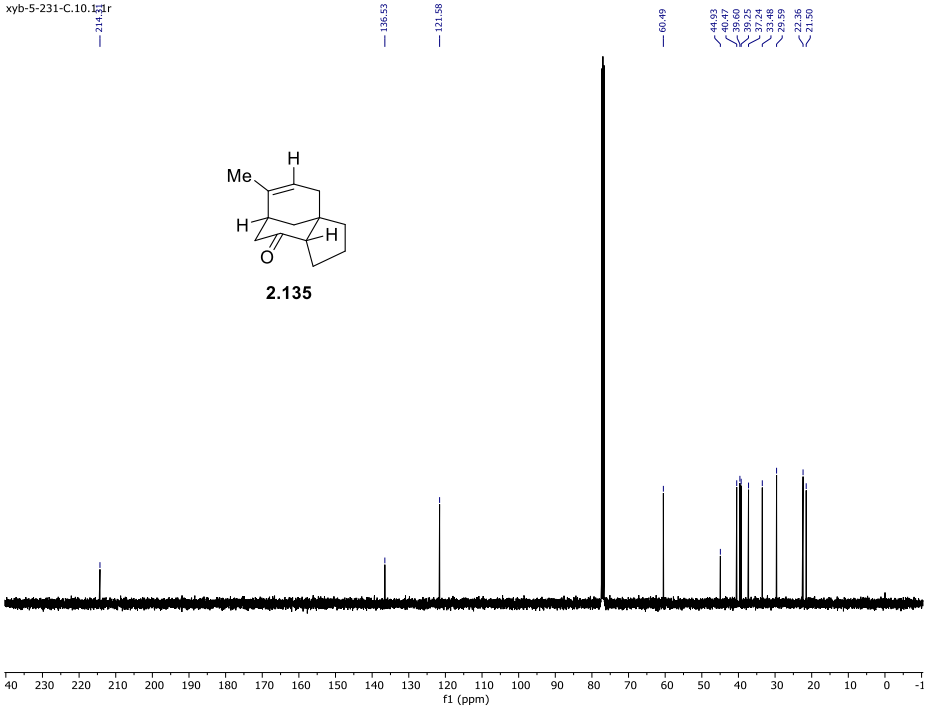


**Figure 2.70.** $^{1}$H-NMR Spectrum of **2.139** in $CDCl_3$, 500 MHz

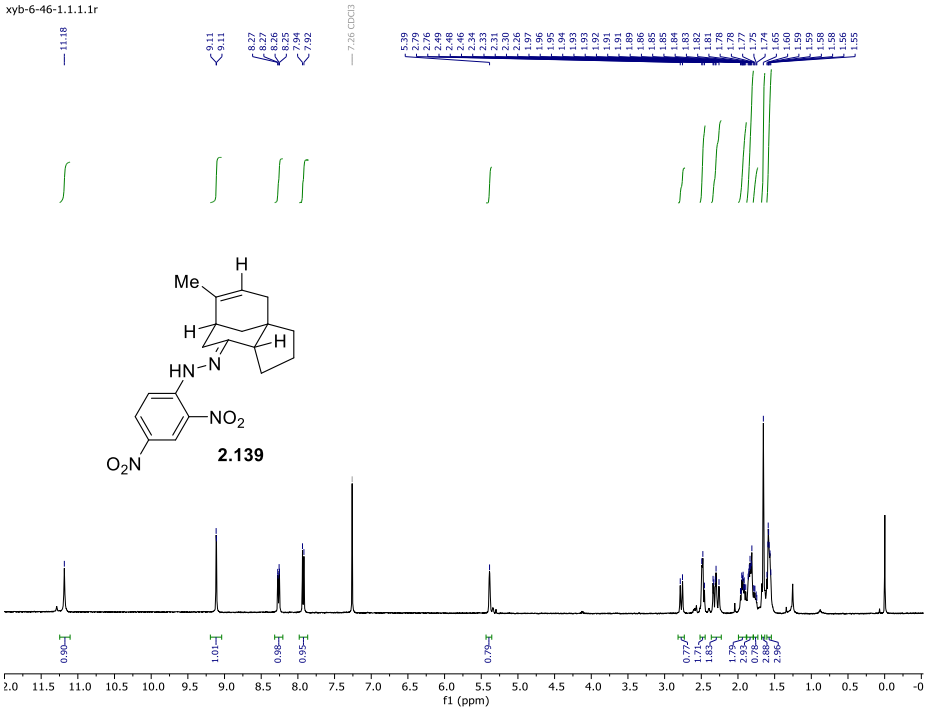

**Figure 2.71.** $^{13}$C-NMR Spectrum of **2.139** in $CDCl_3$, 101 MHz

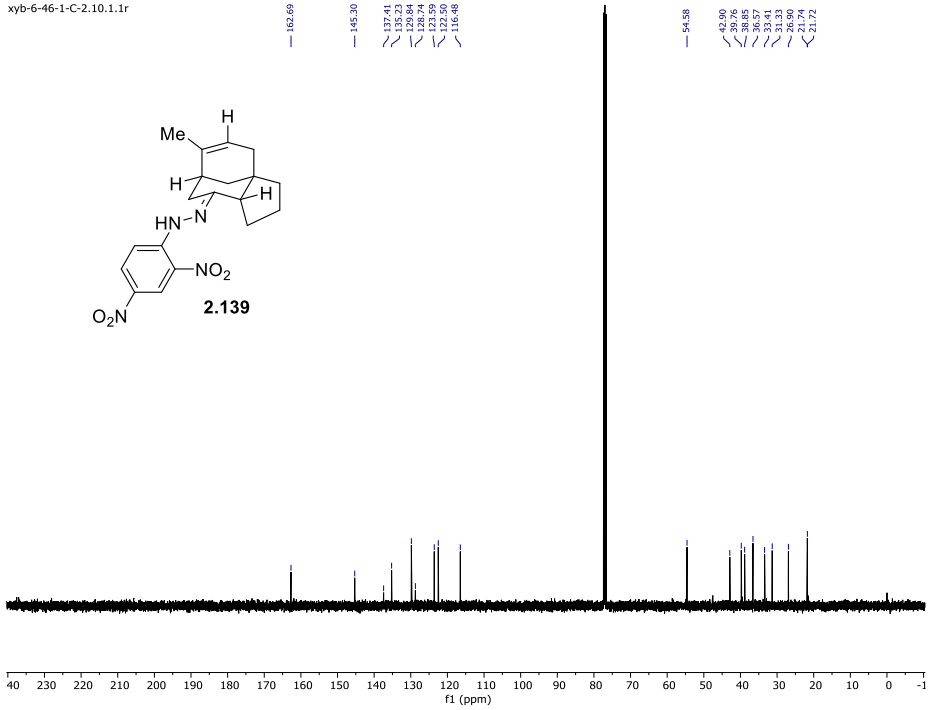


**Figure 2.72.** $^{1}$H-NMR Spectrum of **2.142** in $CDCl_3$, 500 MHz

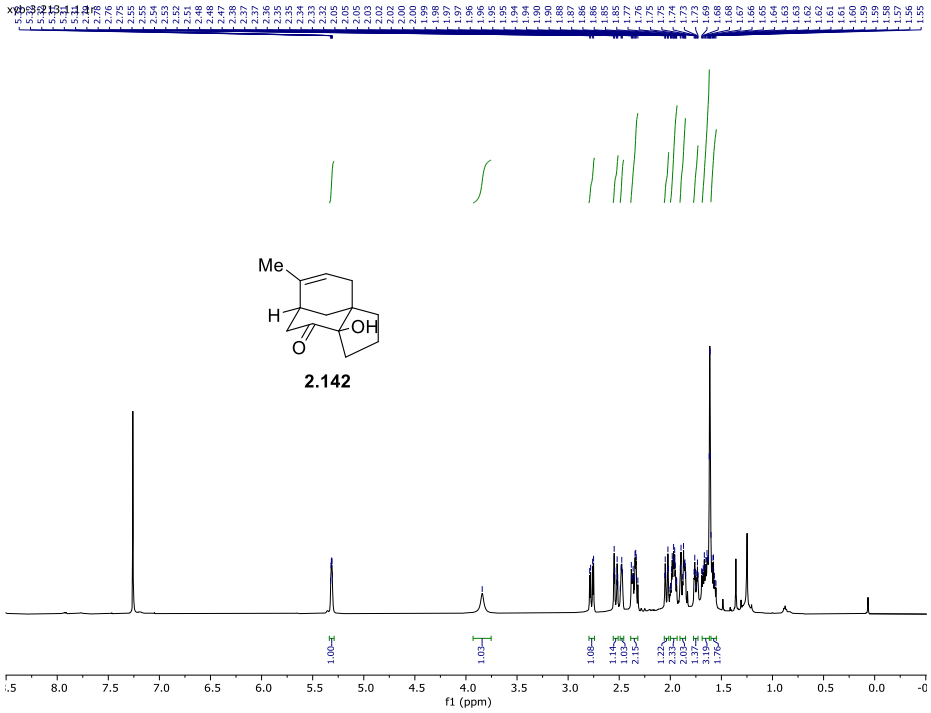

**Figure 2.73.** $^{13}$C-NMR Spectrum of **2.142** in $CDCl_3$, 101 MHz

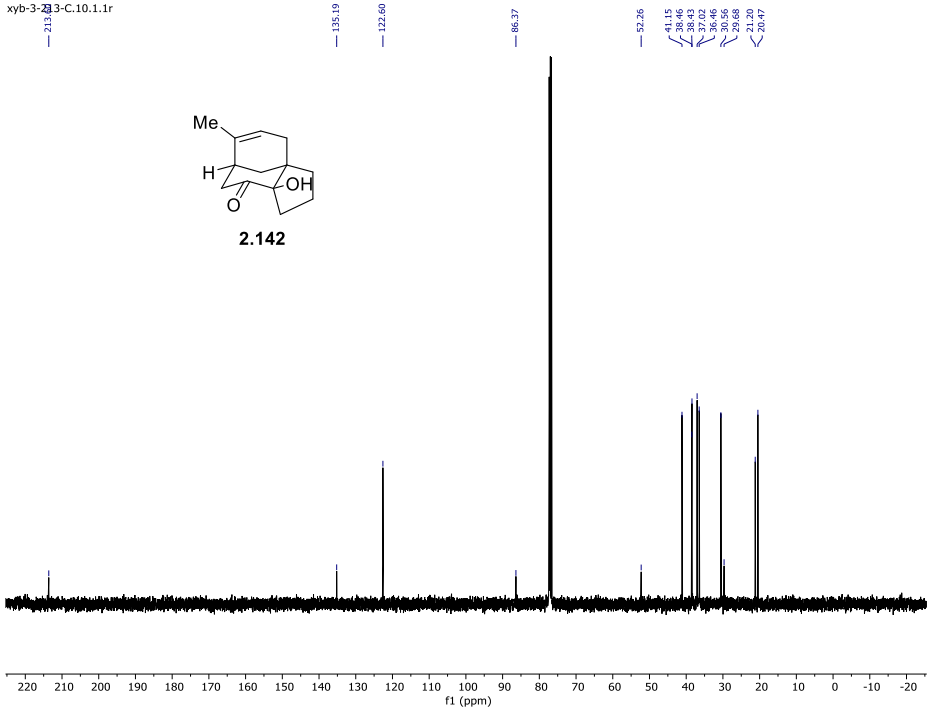


**Figure 2.74.** $^{1}$H-NMR Spectrum of **2.143** in $CDCl_3$, 500 MHz

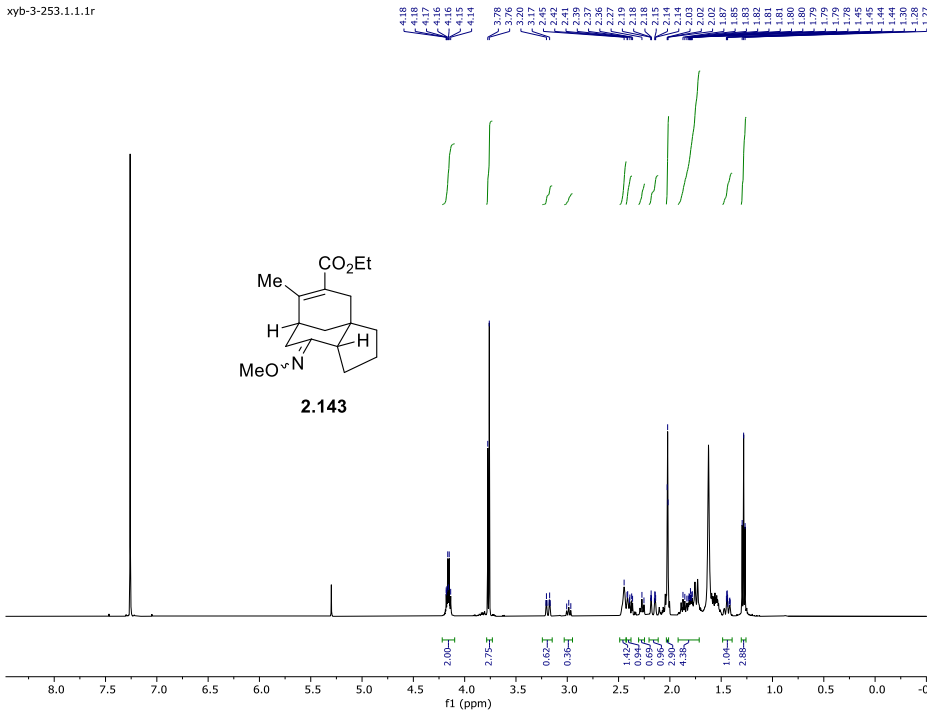

**Figure 2.75.** $^{1}$H-NMR Spectrum of **2.147** in $CDCl_3$, 500 MHz

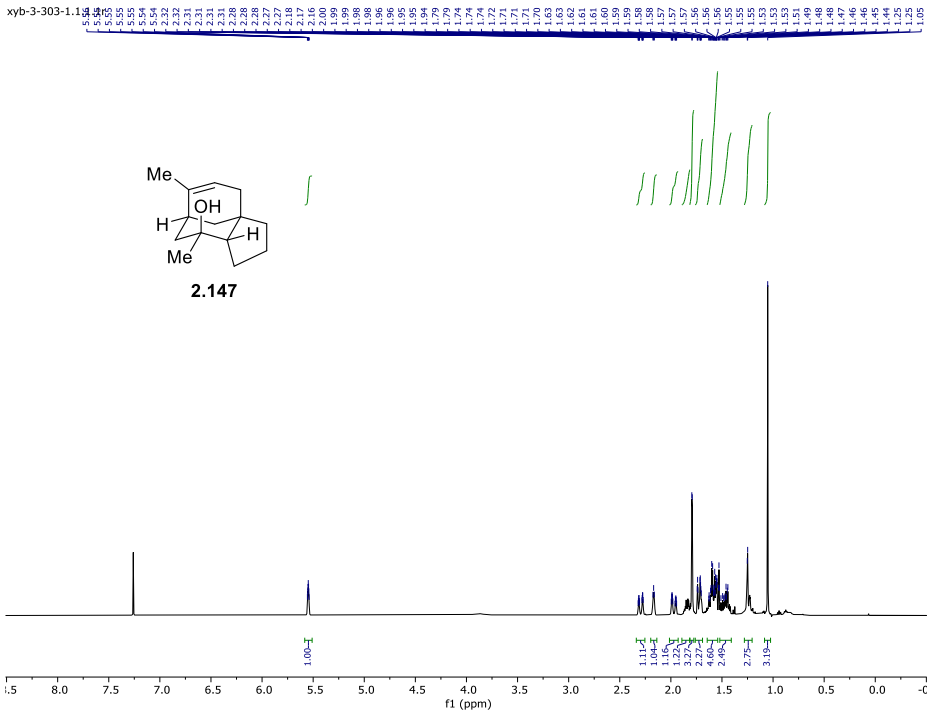


**Figure 2.76.** $^{13}$C-NMR Spectrum of **2.147** in $CDCl_3$, 101 MHz

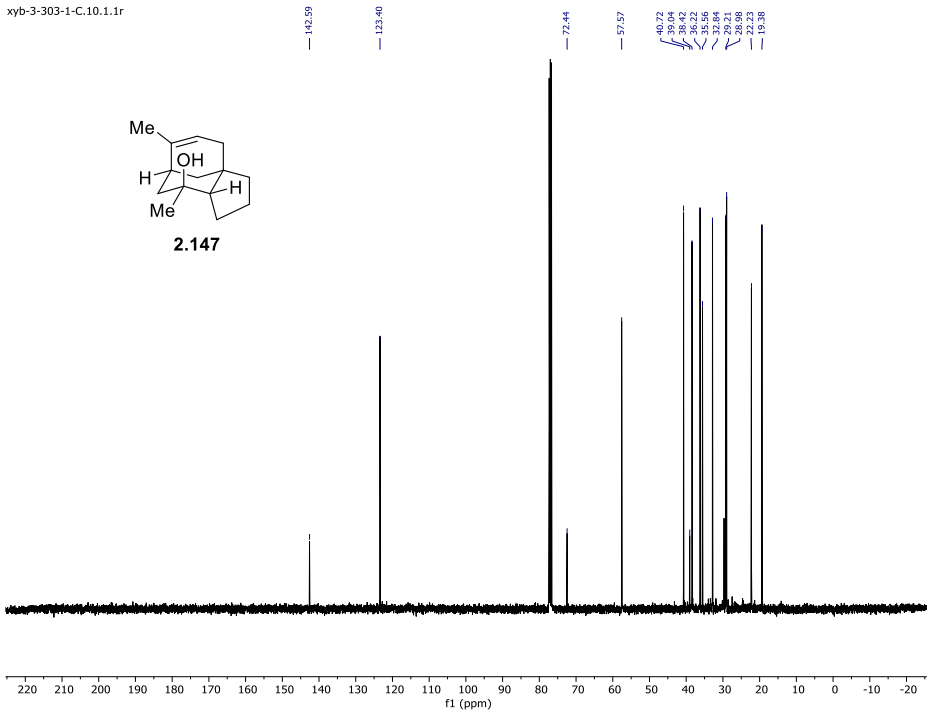

**Figure 2.77.** $^{1}$H-NMR Spectrum of **2.148** in $CDCl_3$, 500 MHz

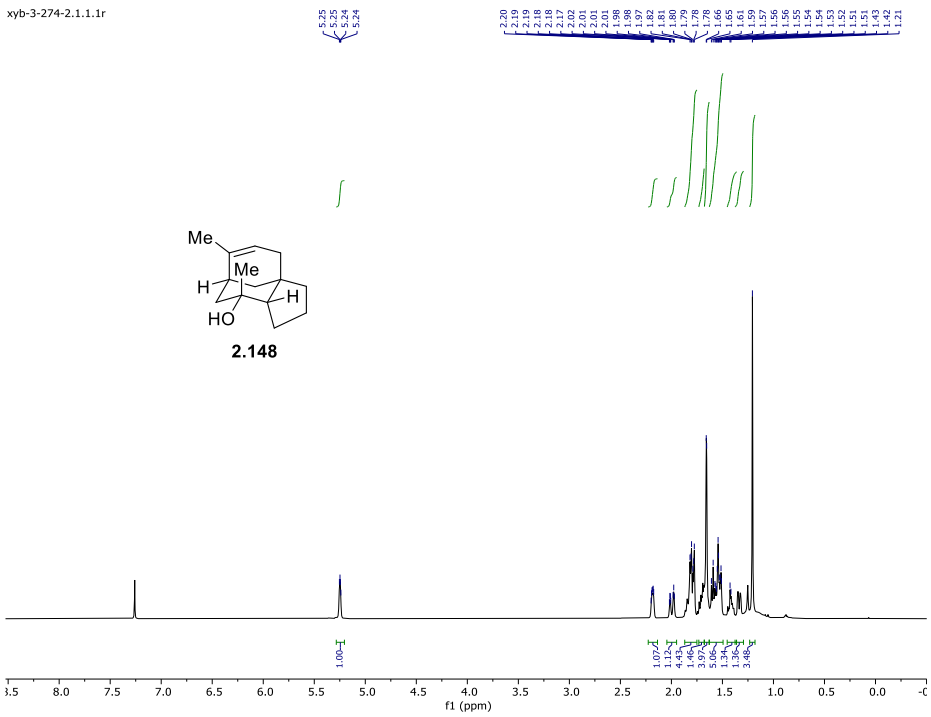


**Figure 2.78.** $^{13}$C-NMR Spectrum of **2.148** in $CDCl_3$, 101 MHz

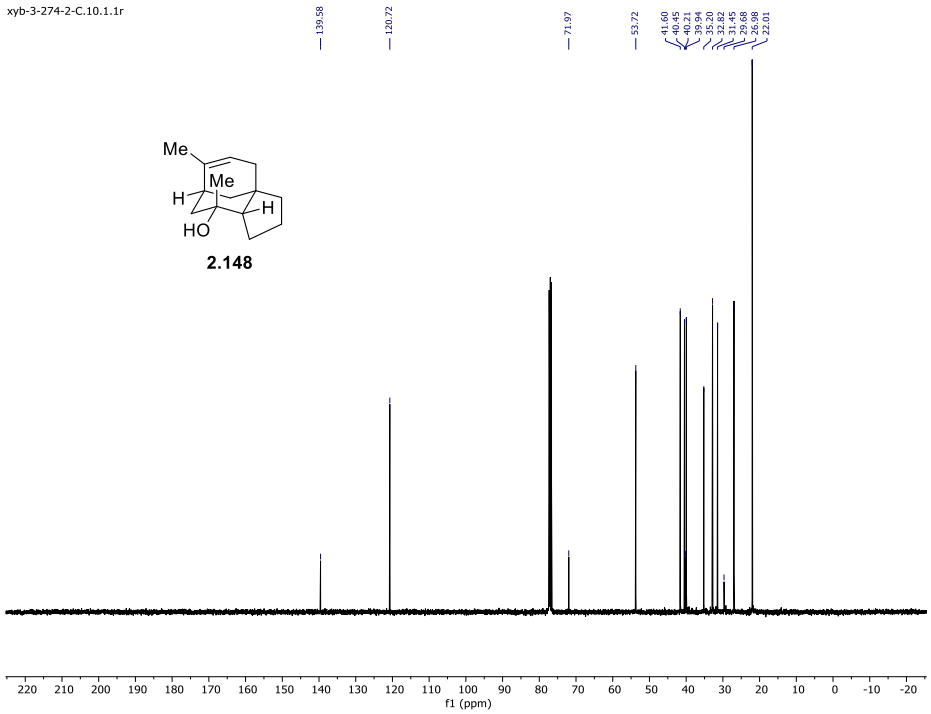

**Figure 2.79.** $^{1}$H-NMR Spectrum of **2.148** in $C_6D_6$, 500 MHz

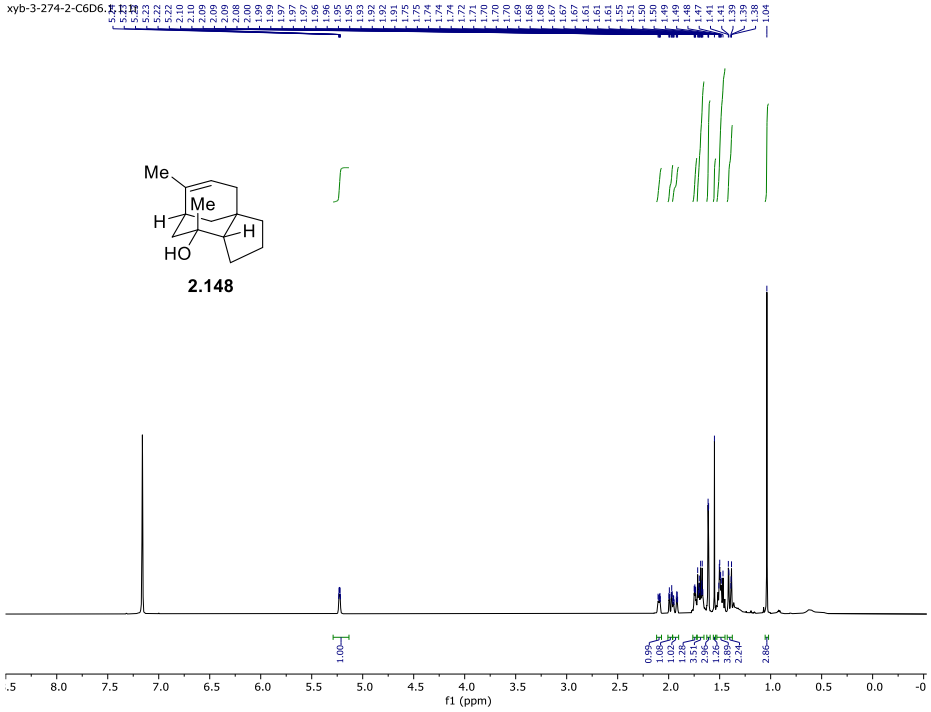


**Figure 2.80.** COSY Spectrum of **2.148** in $C_6D_6$

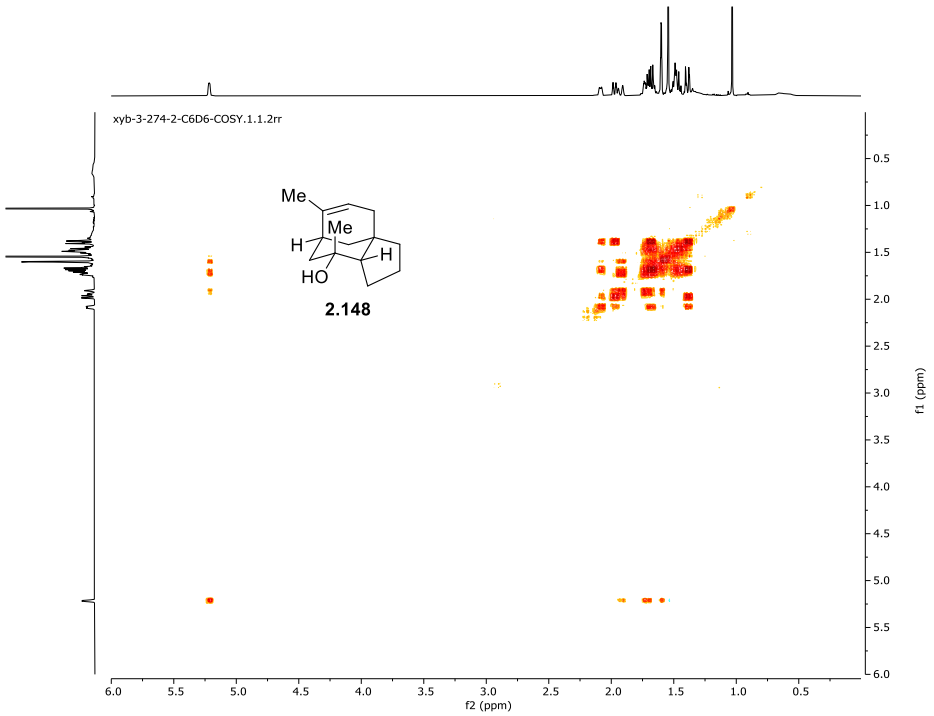

**Figure 2.81.** NOESY Spectrum of **2.148** in $C_6D_6$

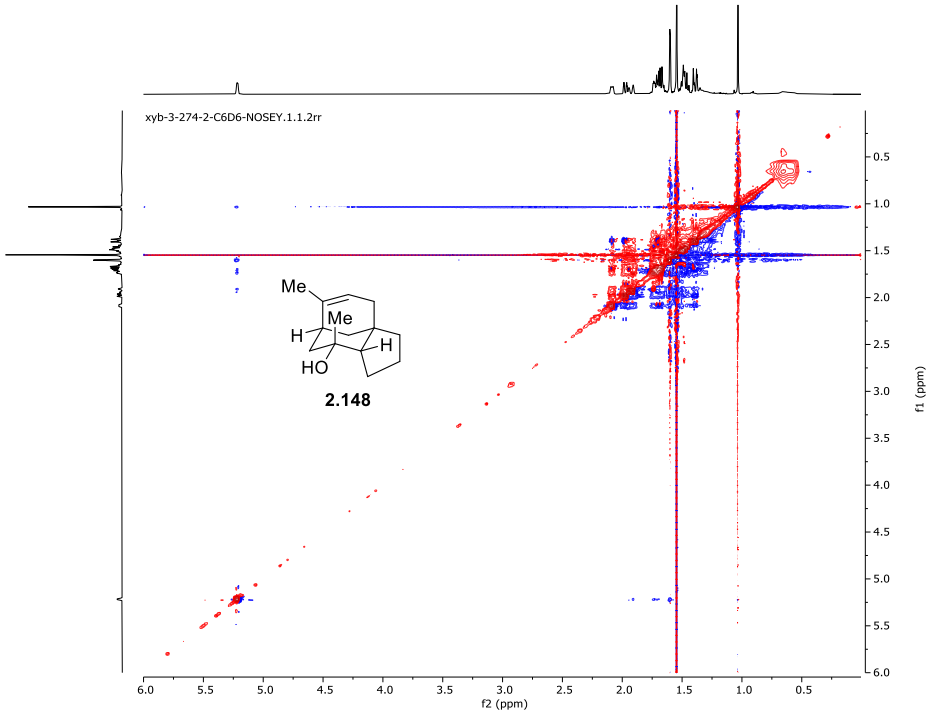


**Figure 2.82.** $^1$H-NMR Spectrum of **2.151** in $CDCl_3$, 500 MHz

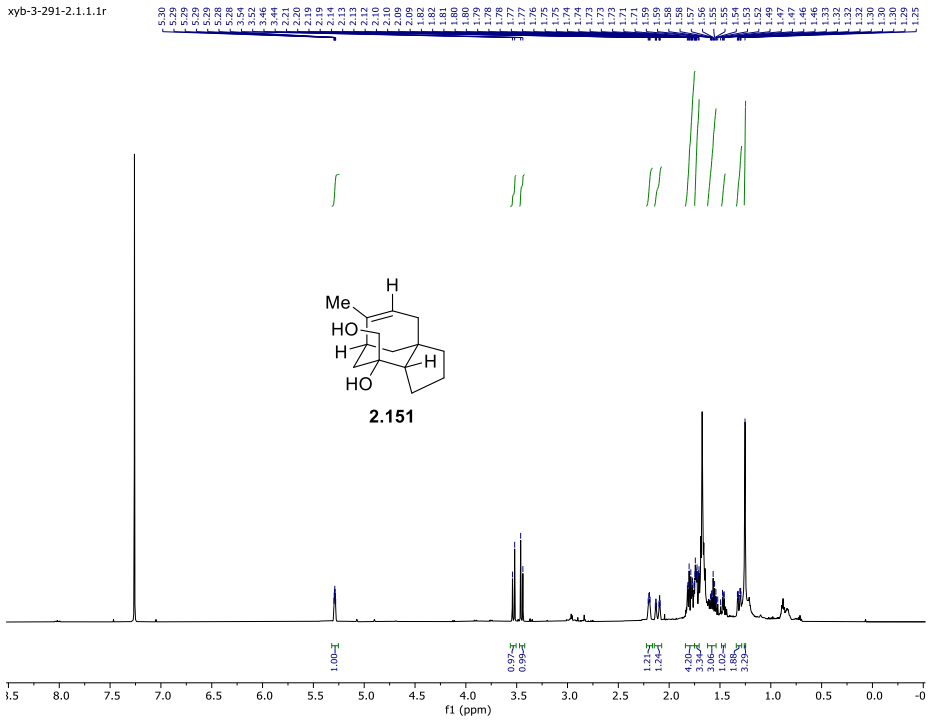

**Figure 2.83.** $^{1}$H-NMR Spectrum of **2.152** in $CDCl_3$, 500 MHz

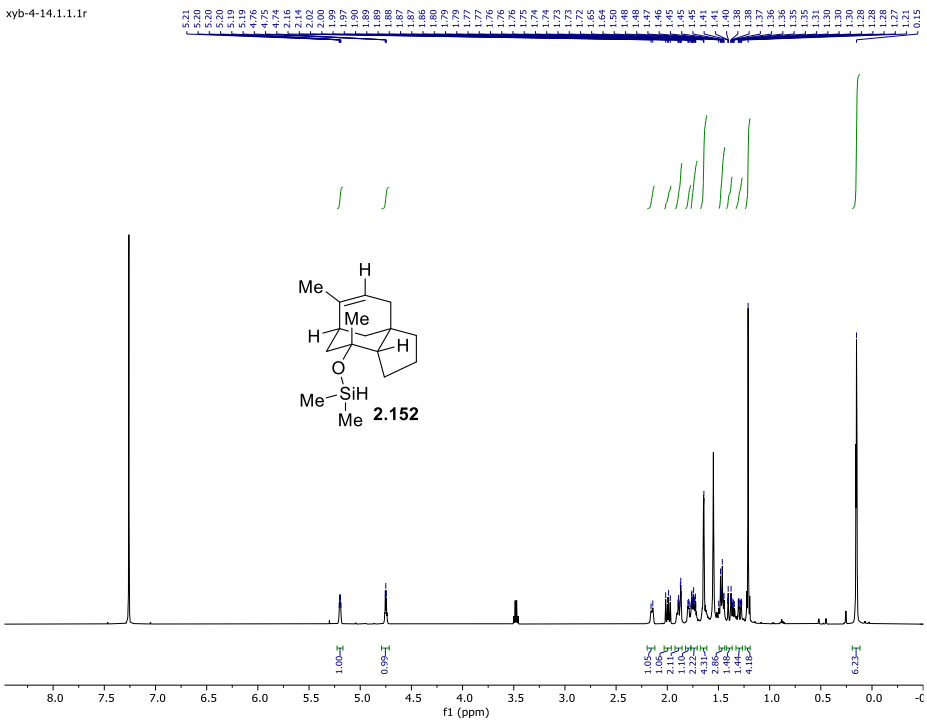


**Figure 2.84.** $^{1}$H-NMR Spectrum of **2.153** in $CDCl_3$, 500 MHz

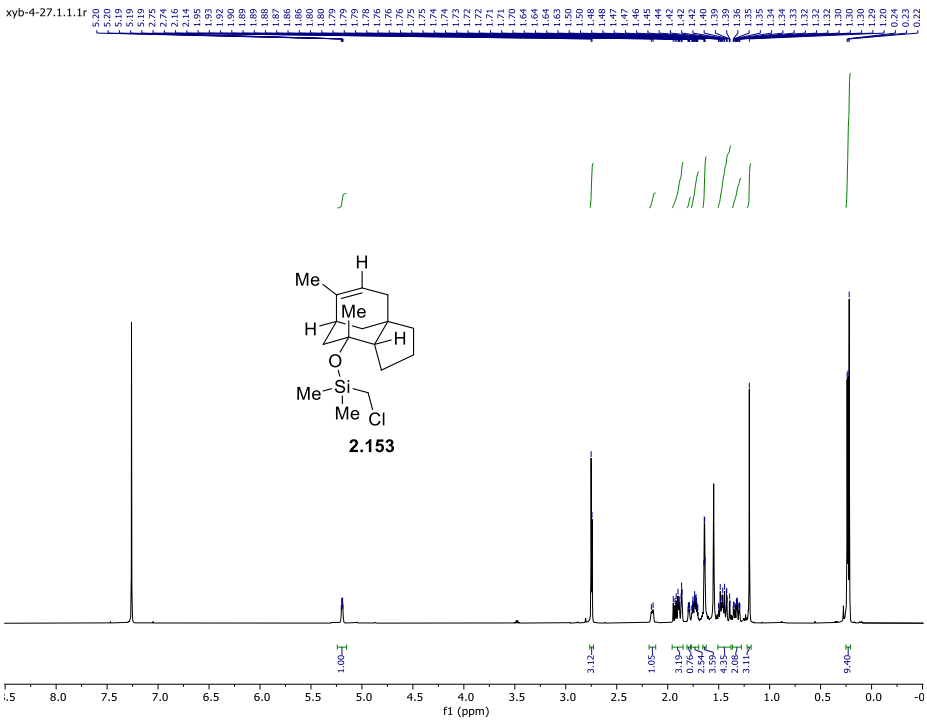

**Figure 2.85.** $^{1}$H-NMR Spectrum of **2.154** in $CDCl_3$, 500 MHz

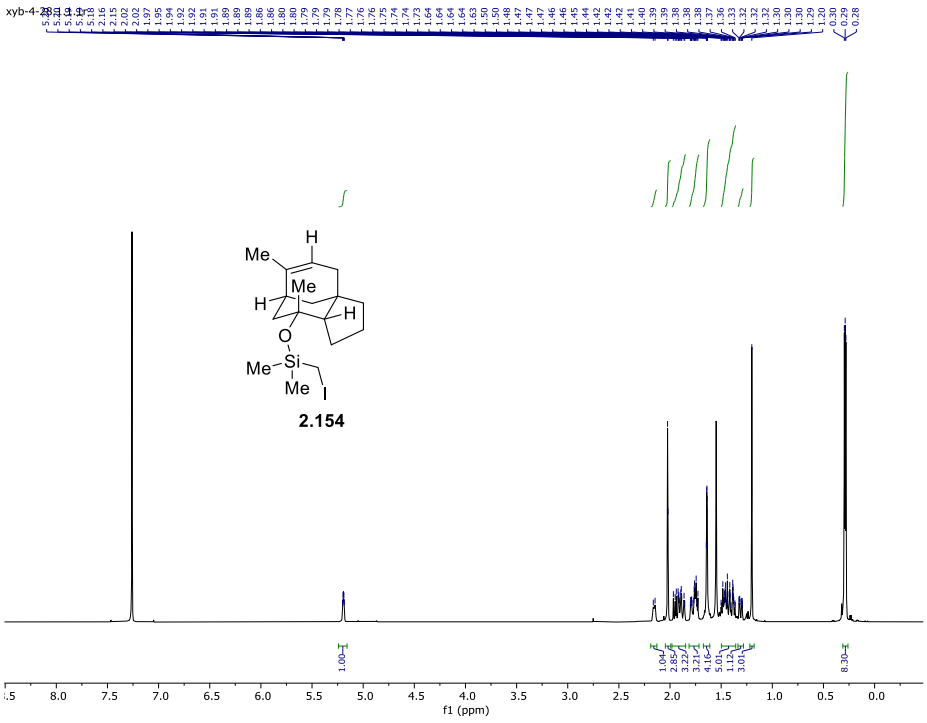


**Figure 2.86.** $^{1}$H-NMR Spectrum of **2.160** in $CDCl_3$, 500 MHz

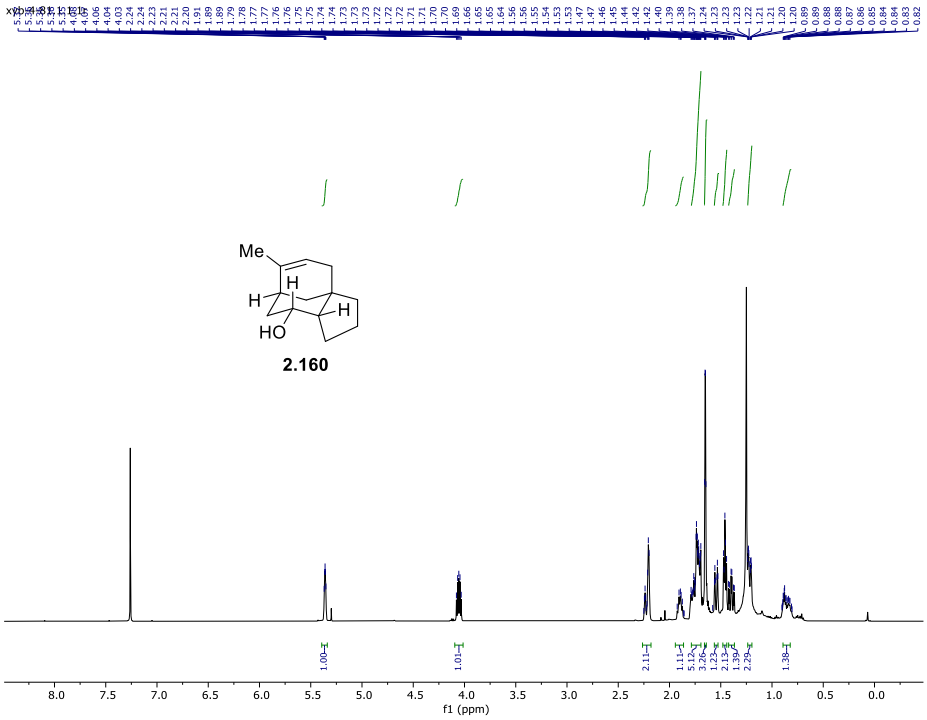

**Figure 2.87.** $^{1}$H-NMR Spectrum of **2.161** in $CDCl_3$, 500 MHz

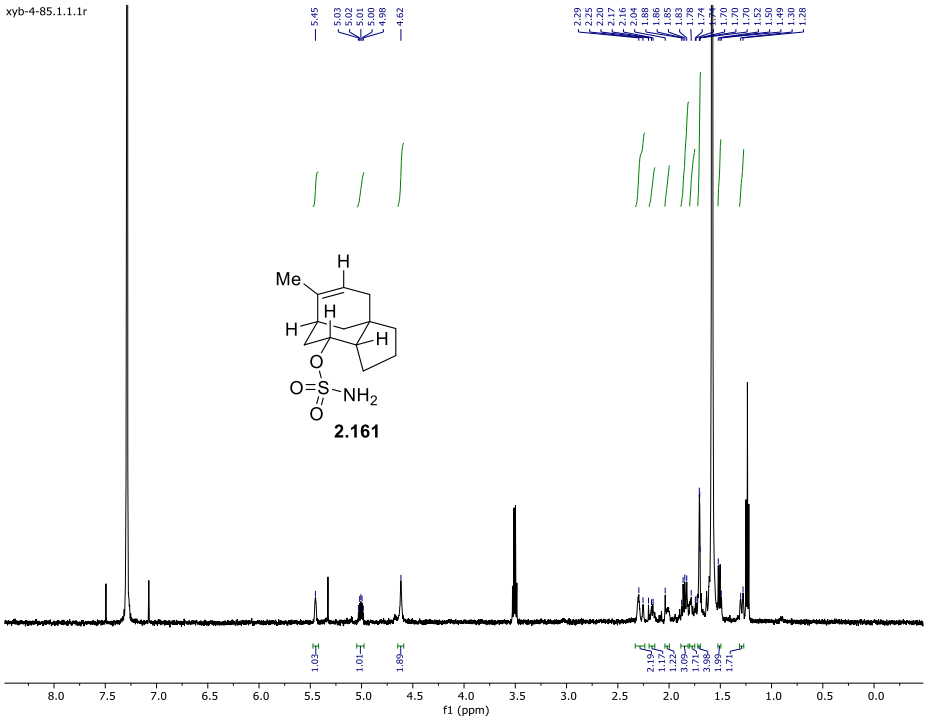


**Figure 2.88.** $^{1}$H-NMR Spectrum of **2.162** in $CDCl_3$, 500 MHz

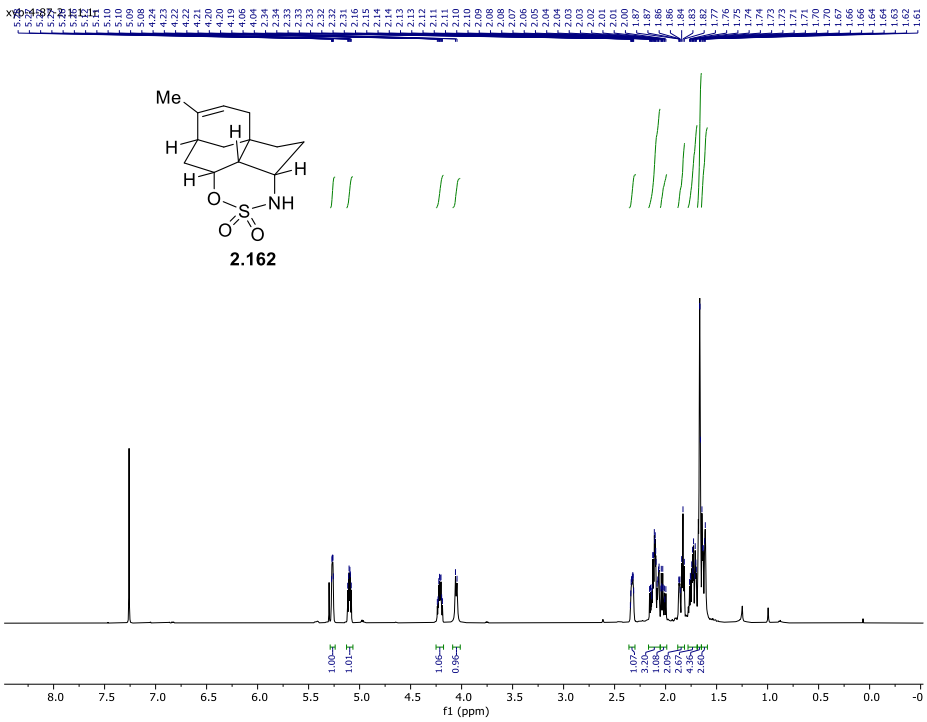

**Figure 2.89.** $^{13}$C-NMR Spectrum of **2.162** in $CDCl_3$, 101 MHz

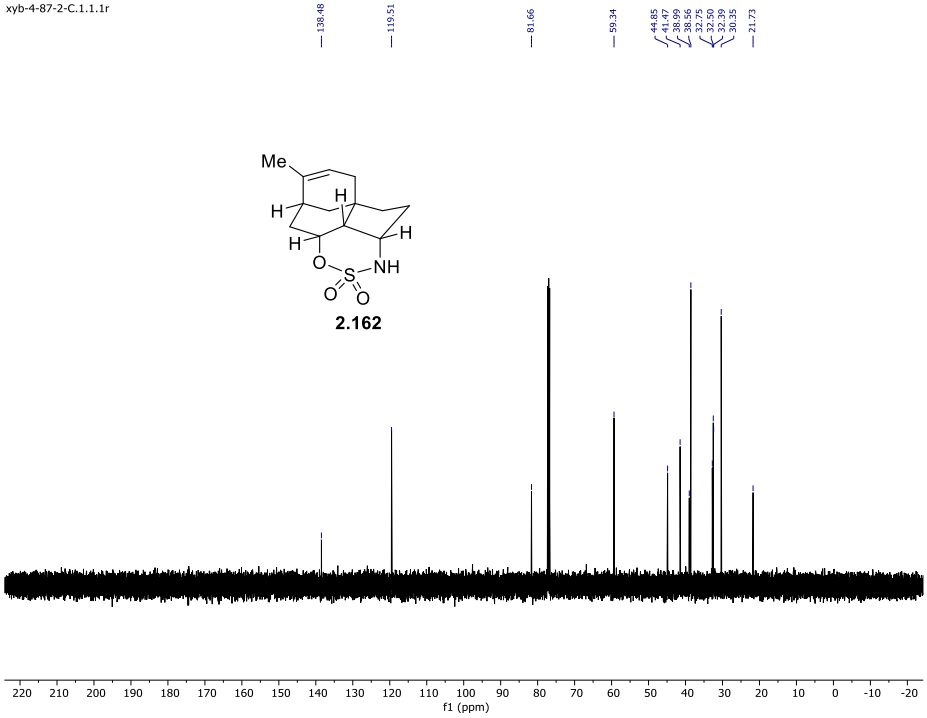


**Figure 2.90.** DEPT135-NMR Spectrum of **2.162** in $CDCl_3$, 126 MHz

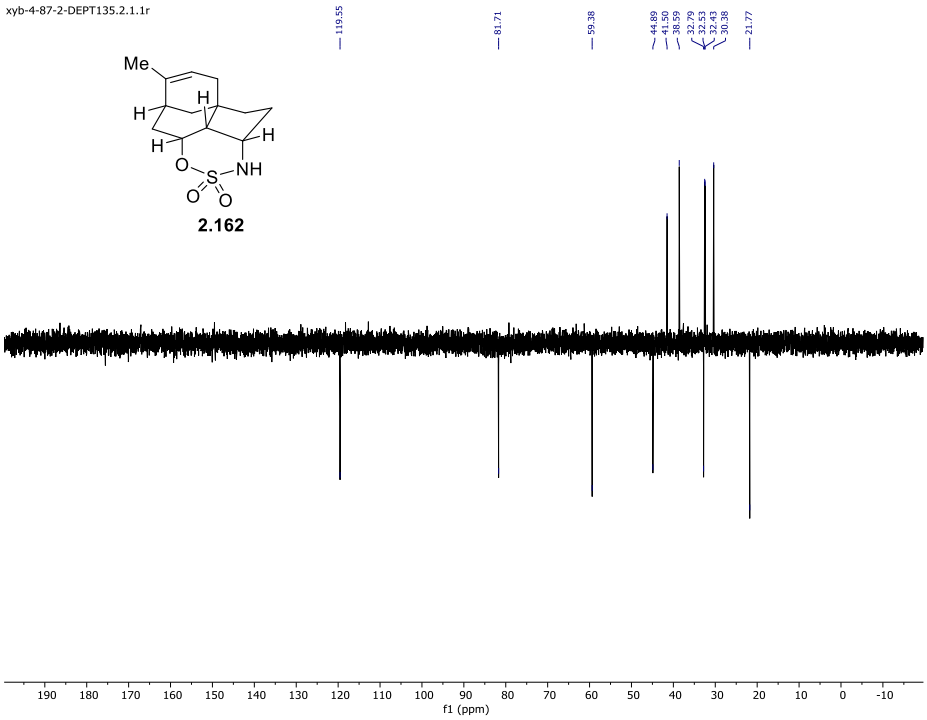

**Figure 2.91.** COSY-NMR Spectrum of **2.162** in $CDCl_3$, 126 MHz

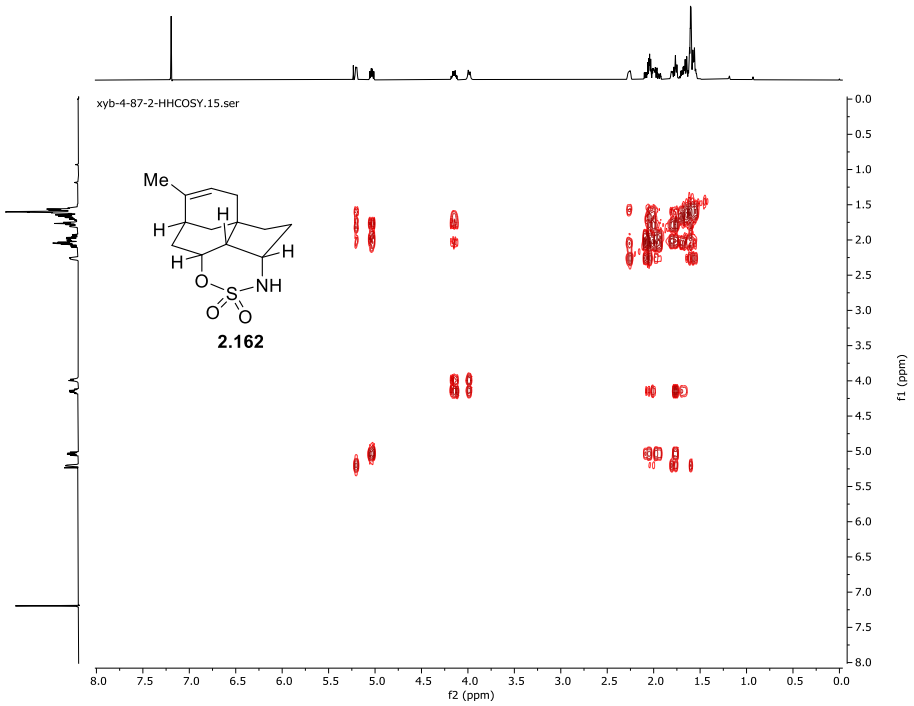


**Figure 2.92.** $^1$H-NMR Spectrum of **2.163** in $CDCl_3$, 500 MHz

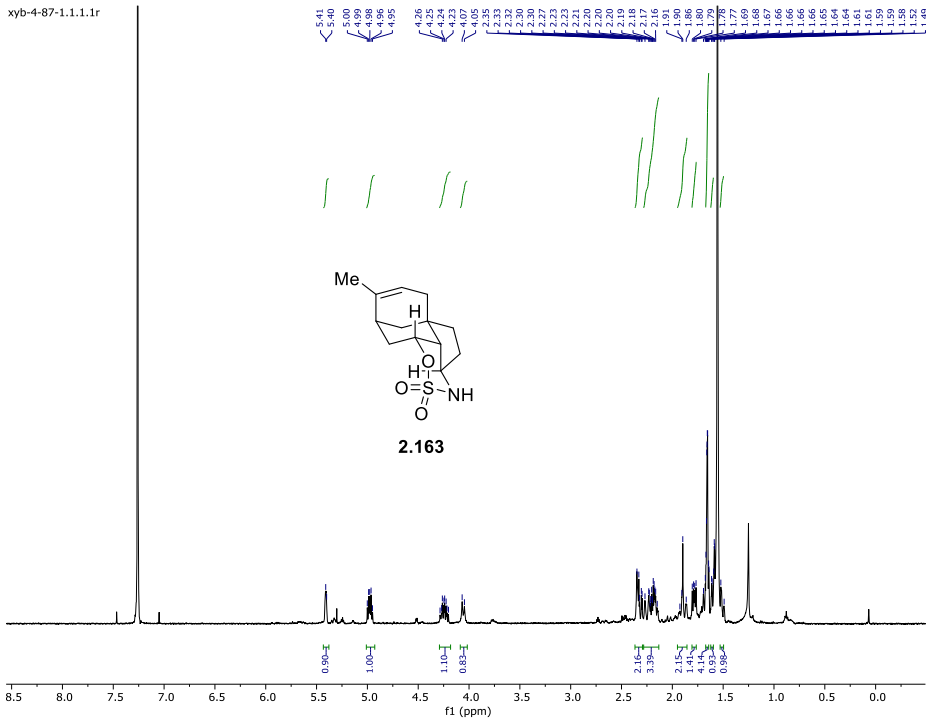

**Figure 2.93.** $^{1}$H-NMR Spectrum of **2.166** in $CDCl_3$, 500 MHz

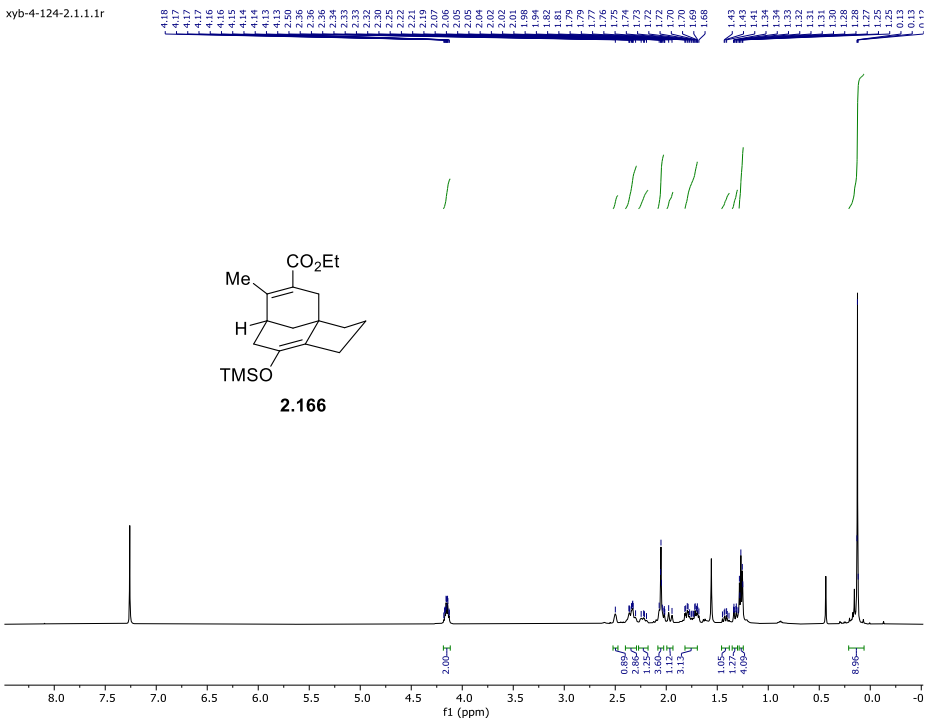


**Figure 2.94.** $^{1}$H-NMR Spectrum of **2.167** in $CDCl_3$, 500 MHz

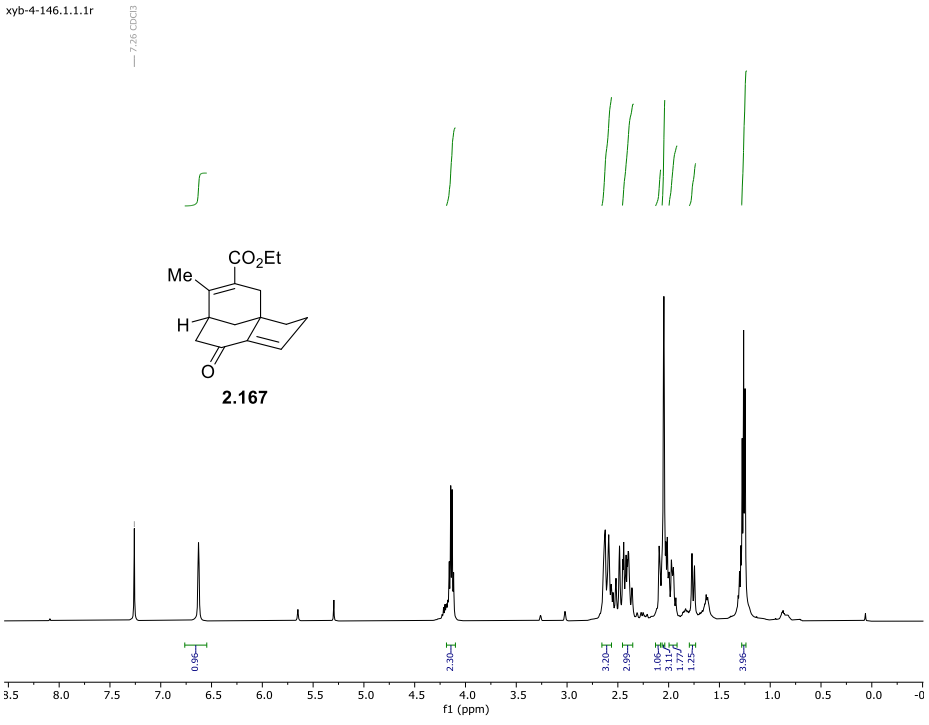

**Figure 2.95.** $^{1}$H-NMR Spectrum of **2.170** in $CDCl_3$, 500 MHz

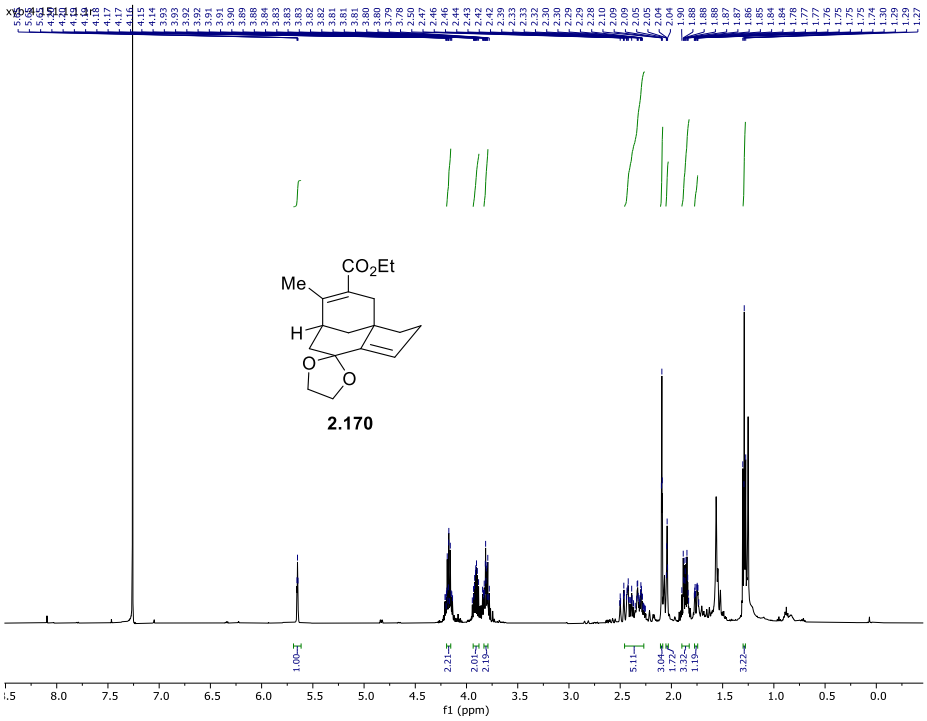


**Figure 2.96.** $^{1}$H-NMR Spectrum of **2.172** in $CDCl_3$, 500 MHz

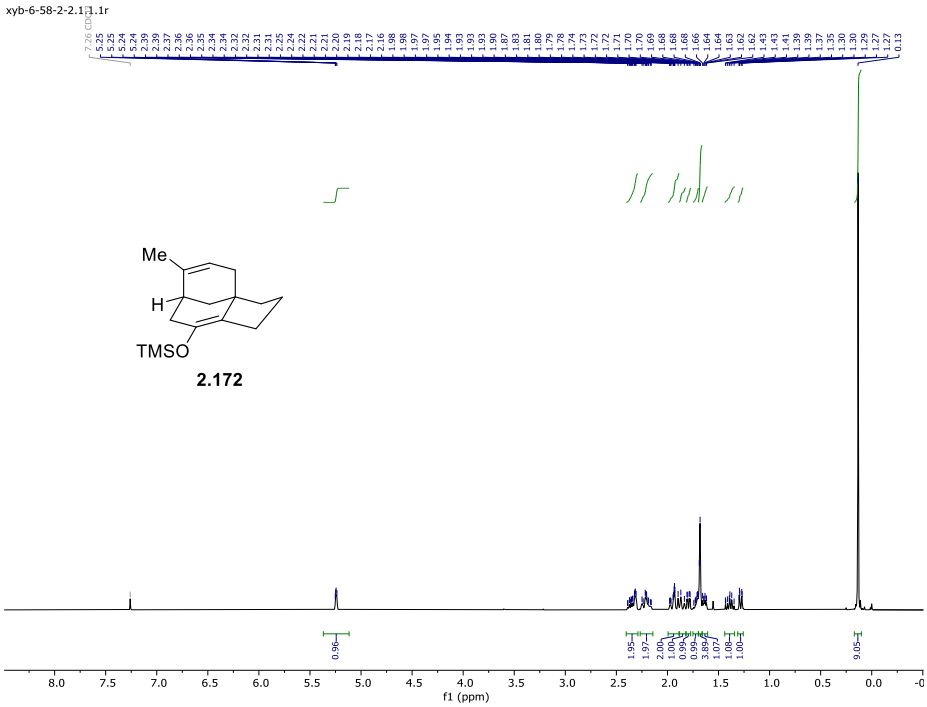

**Figure 2.97.** $^{13}$C-NMR Spectrum of **2.172** in $CDCl_3$, 101 MHz

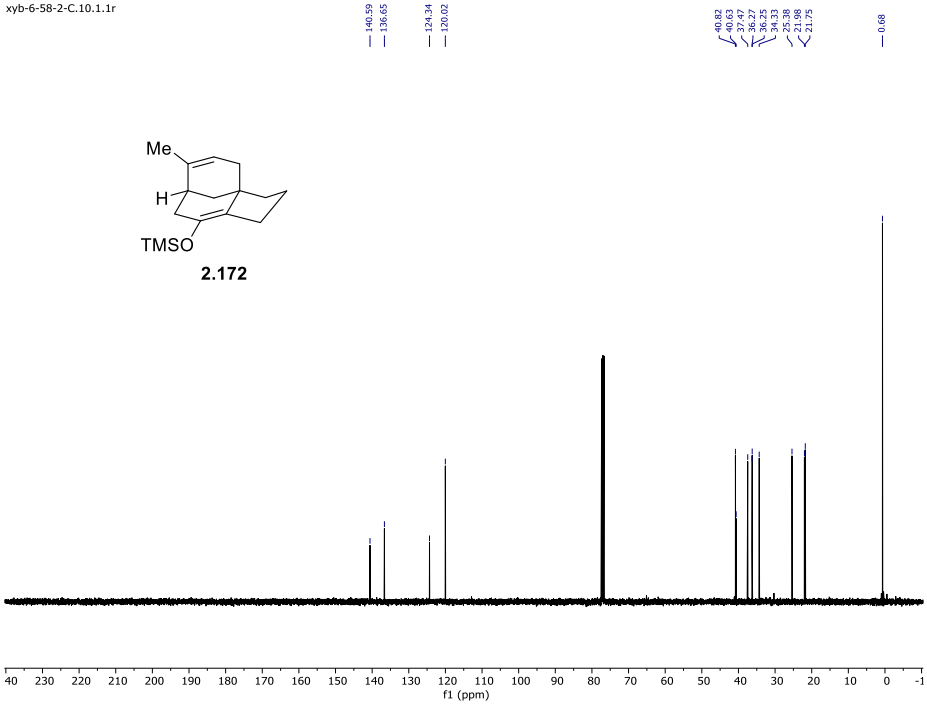


**Figure 2.98.** $^{1}$H-NMR Spectrum of **2.173** in $CDCl_3$, 500 MHz

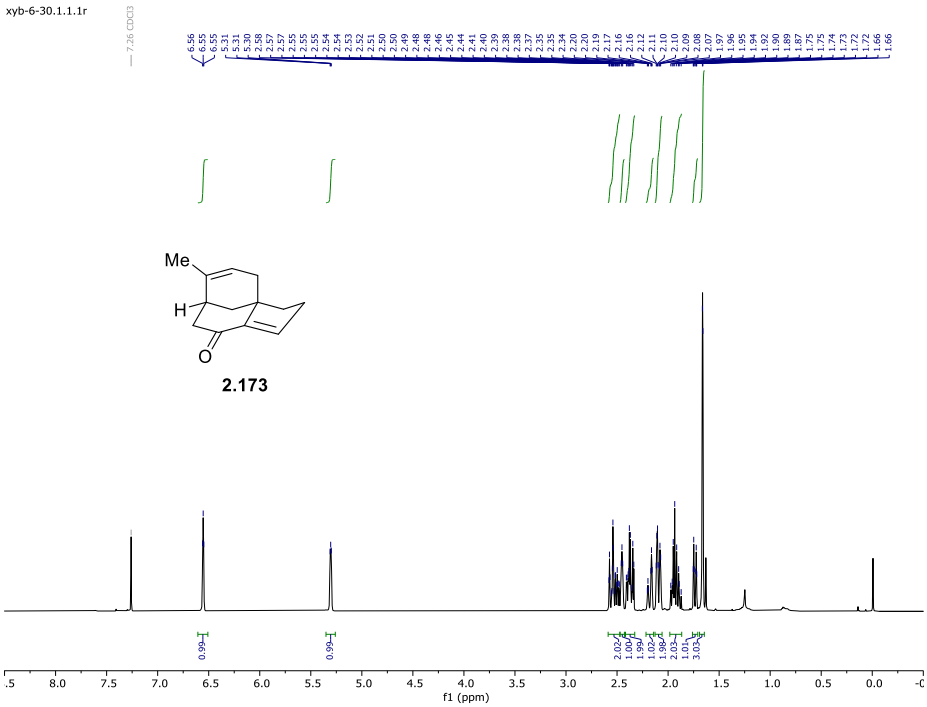

**Figure 2.99.** $^{13}$C-NMR Spectrum of **2.173** in $CDCl_3$, 101 MHz

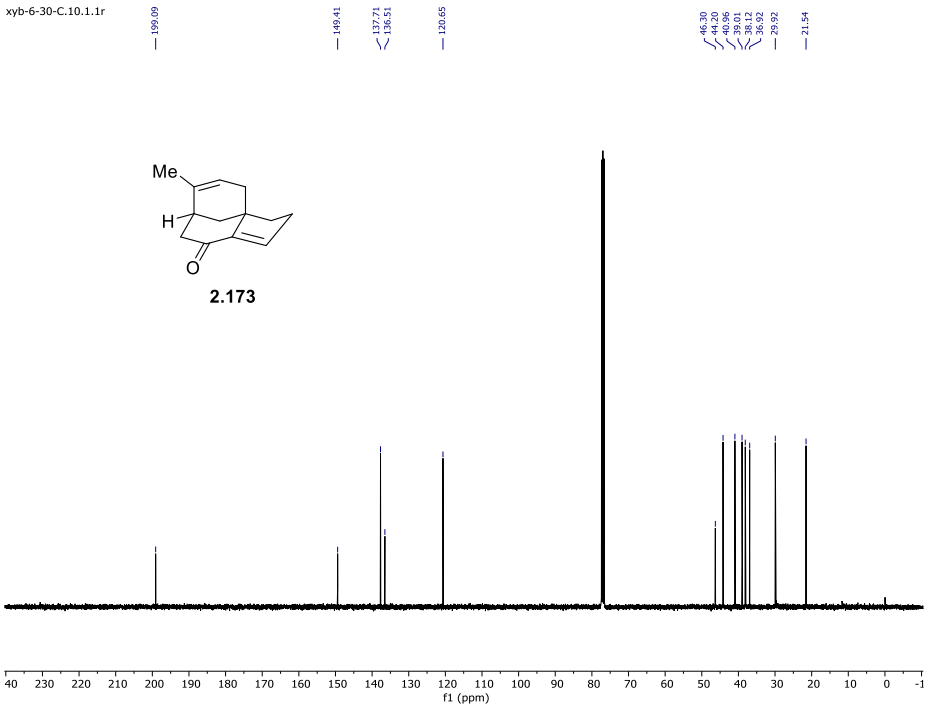


**Figure 2.100.** $^{1}$H-NMR Spectrum of **2.175** in $CDCl_3$, 500 MHz

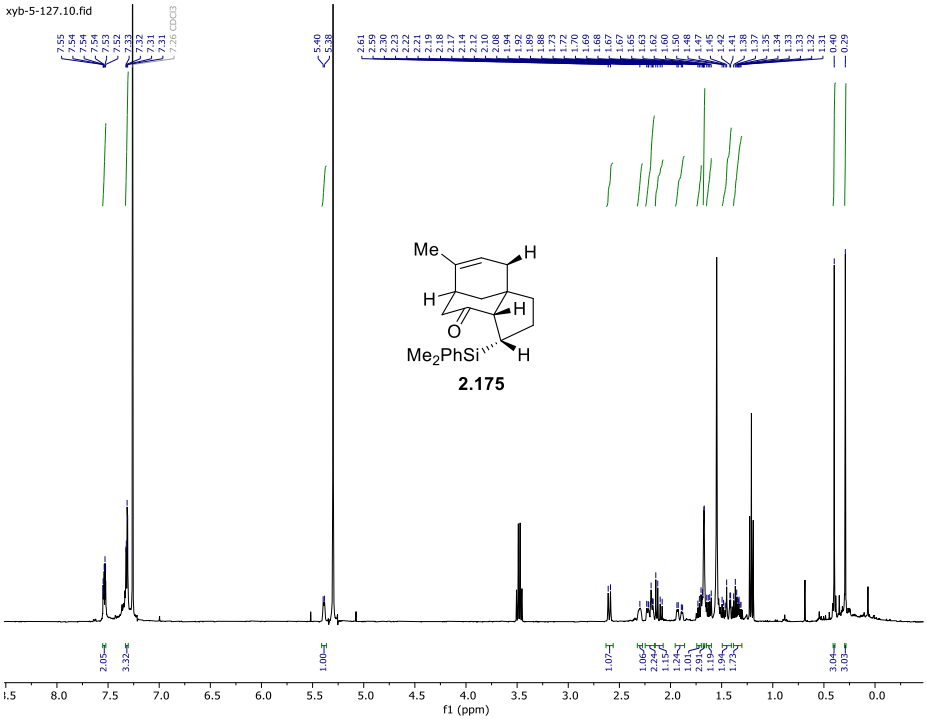

**Figure 2.101.** $^{1}$H-NMR Spectrum of **2.177** in $CDCl_3$, 500 MHz

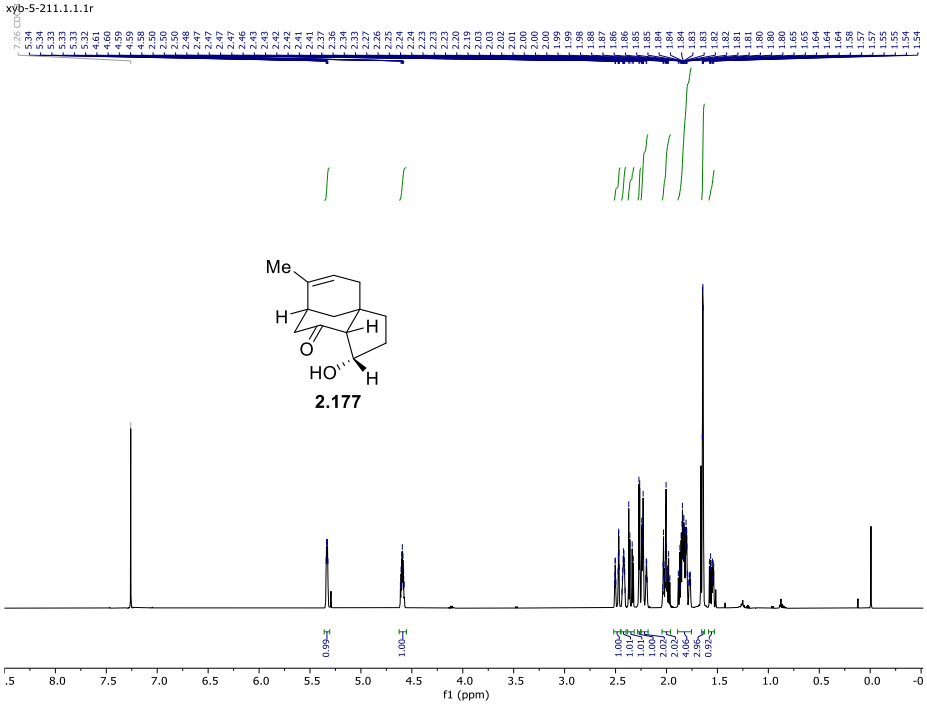


**Figure 2.102.** $^{13}$C-NMR Spectrum of **2.177** in $CDCl_3$, 101 MHz

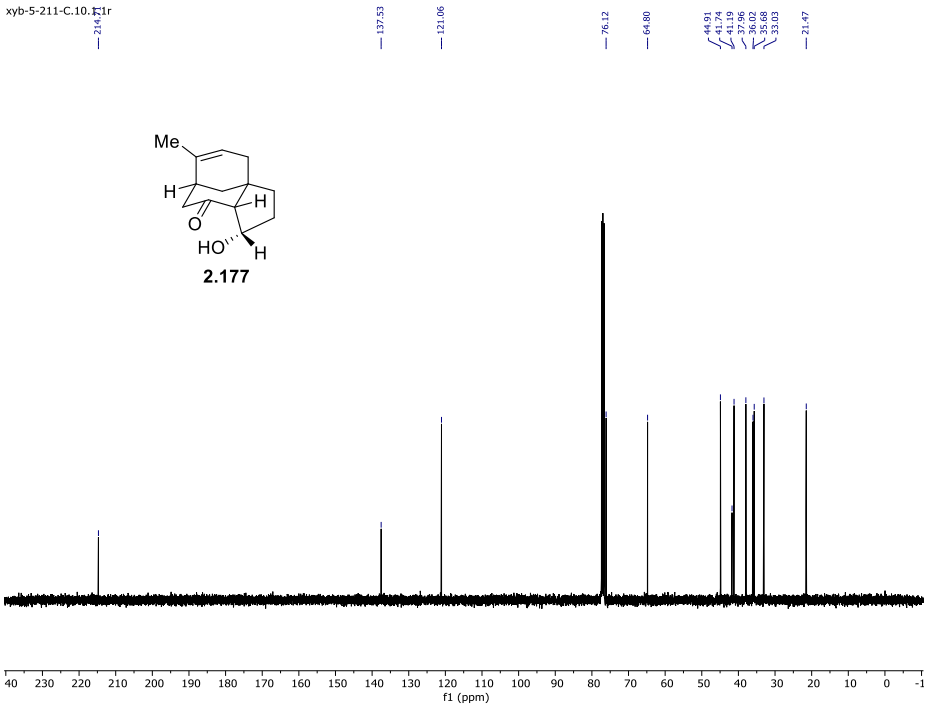

**Figure 2.103.** $^{1}$H-NMR Spectrum of **2.179** in $CDCl_3$, 500 MHz

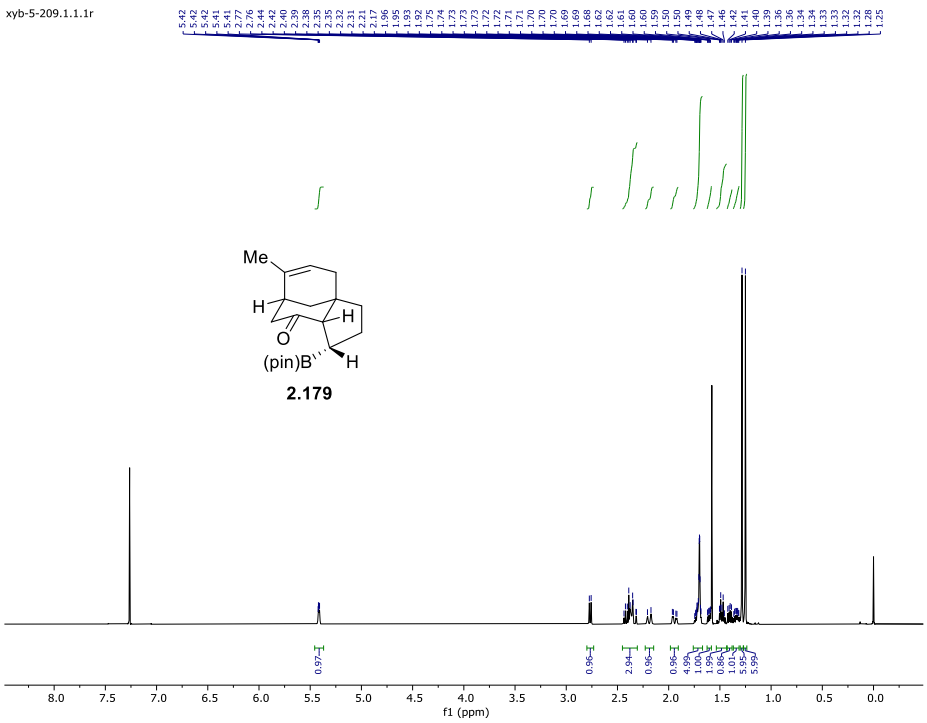


**Figure 2.104.** $^{13}$C-NMR Spectrum of **2.179** in $CDCl_3$, 101 MHz

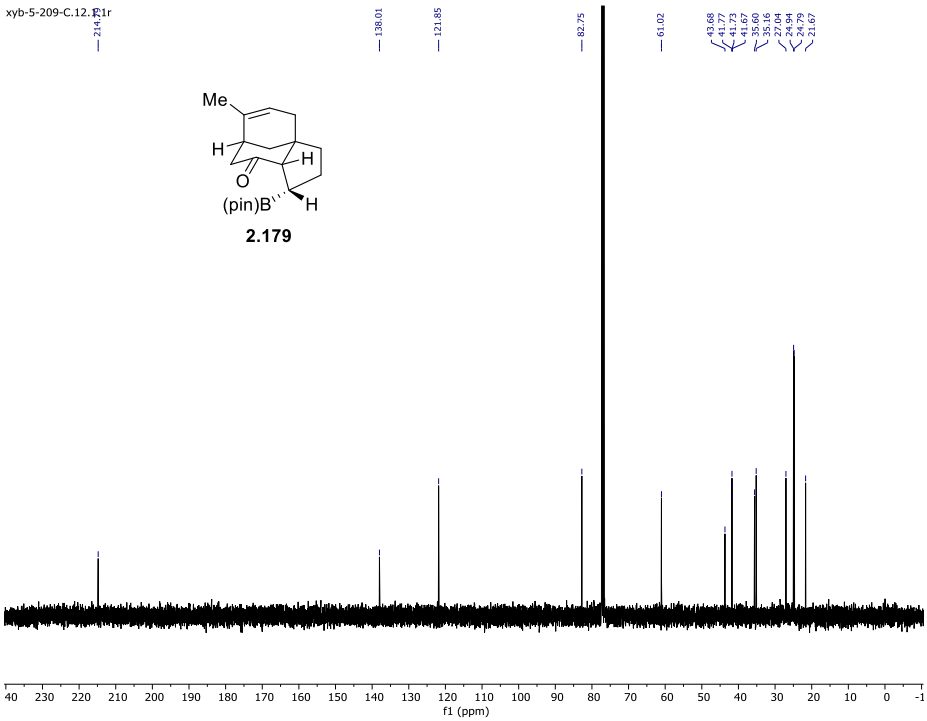

**Figure 2.105.** DEPT135-NMR Spectrum of **2.179** in $CDCl_3$, 101 MHz

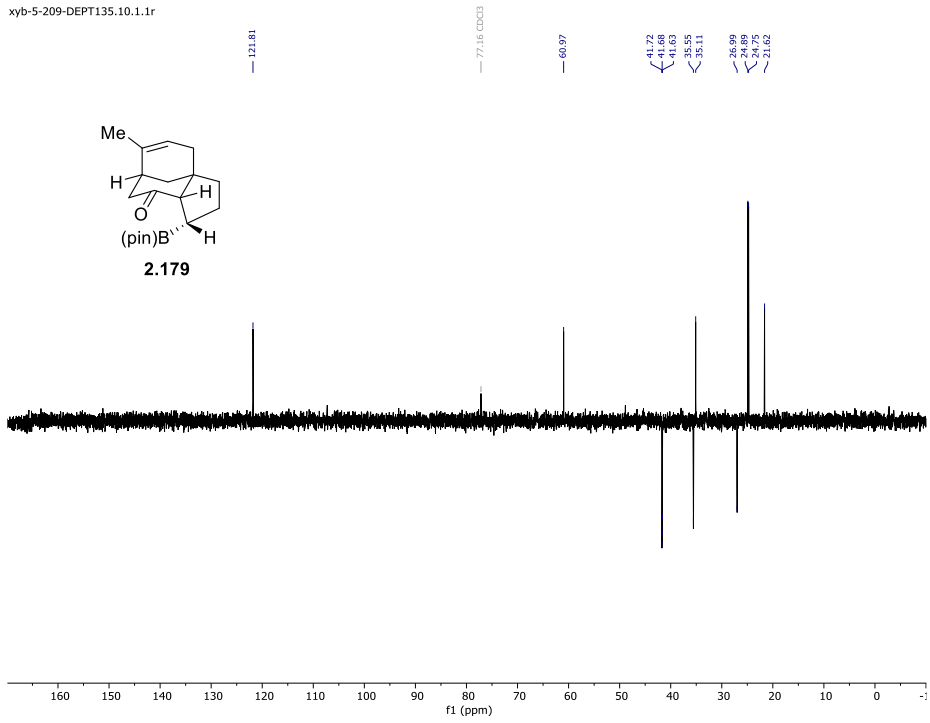


**Figure 2.106.** $^{11}B$-NMR Spectrum of **2.179** in $CDCl_3$, 128 MHz

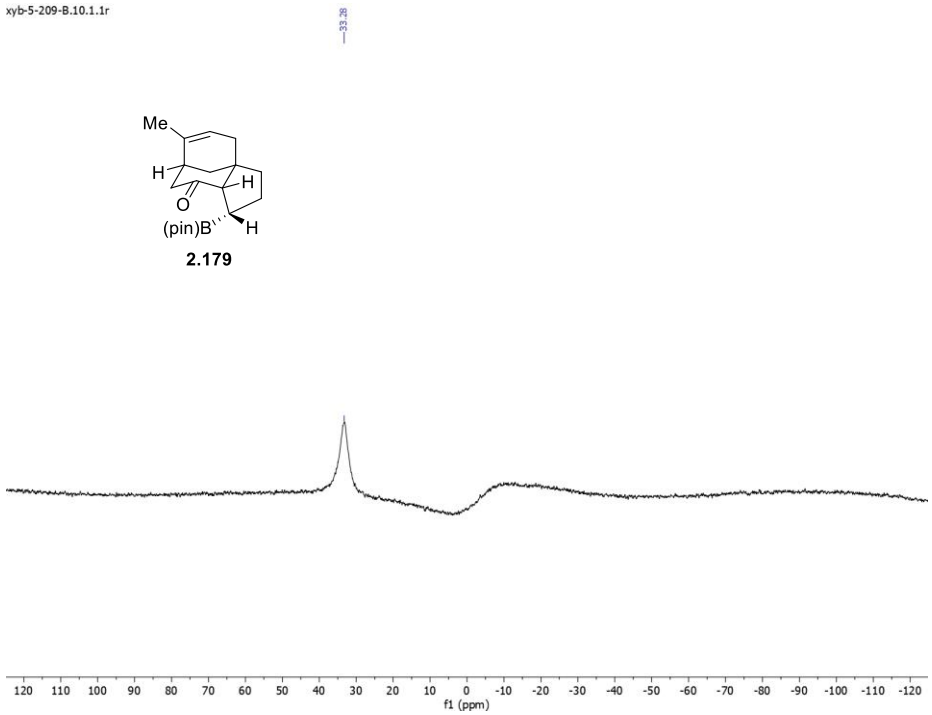

**Figure 2.107.** $^{1}$H-NMR Spectrum of **2.178** in $CDCl_3$, 500 MHz

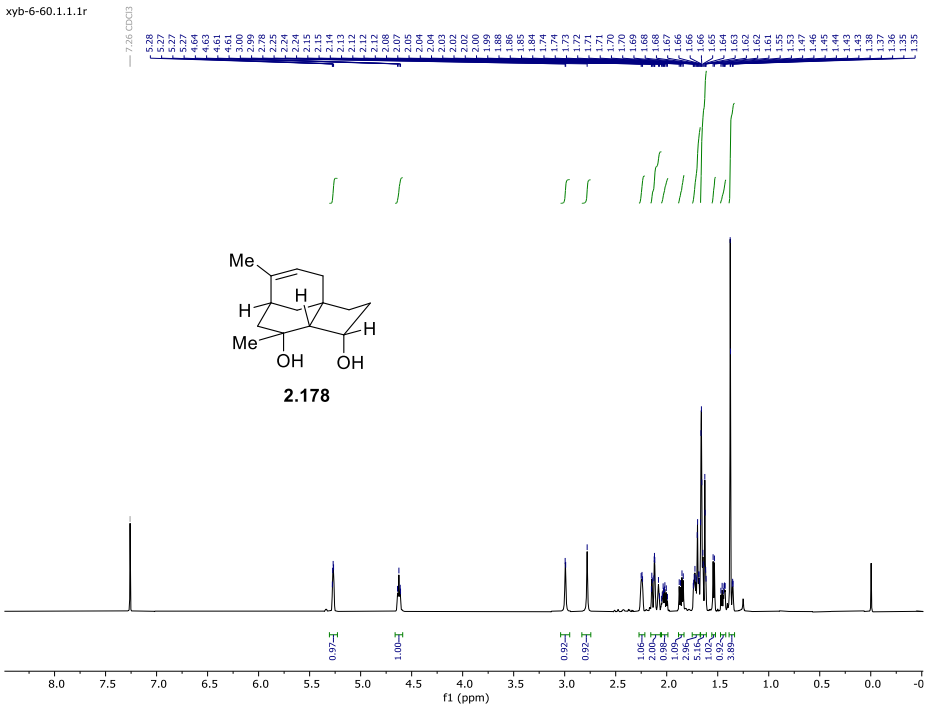


**Figure 2.108.** $^{13}$C-NMR Spectrum of **2.178** in $CDCl_3$, 101 MHz

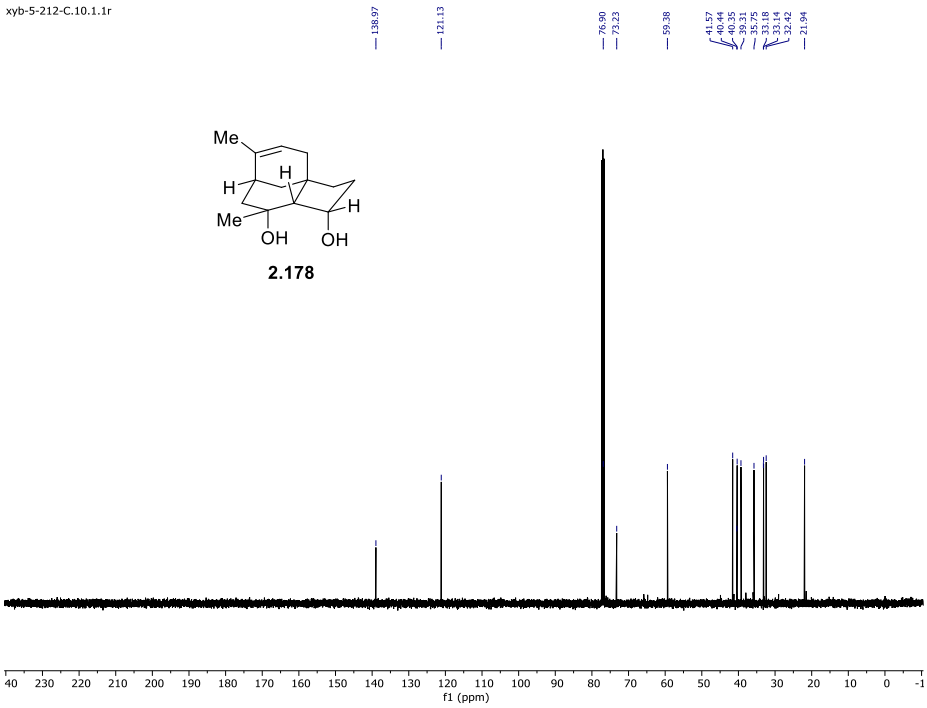

**Figure 2.109.** $^{1}$H-NMR Spectrum of **2.134** in $CDCl_3$, 500 MHz

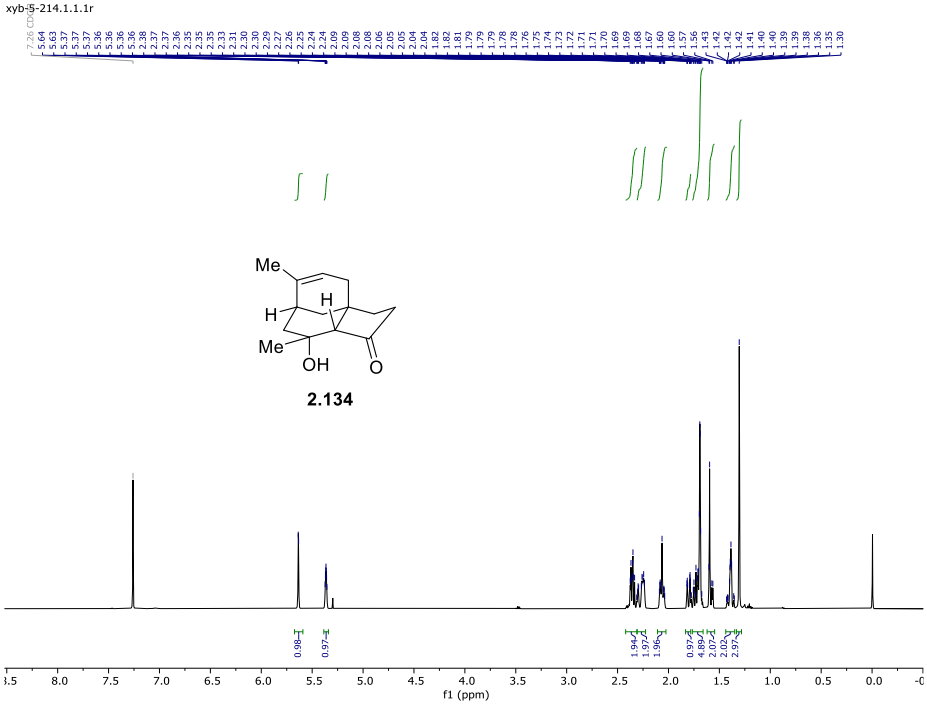


**Figure 2.110.** $^{13}$C-NMR Spectrum of **2.134** in $CDCl_3$, 101 MHz

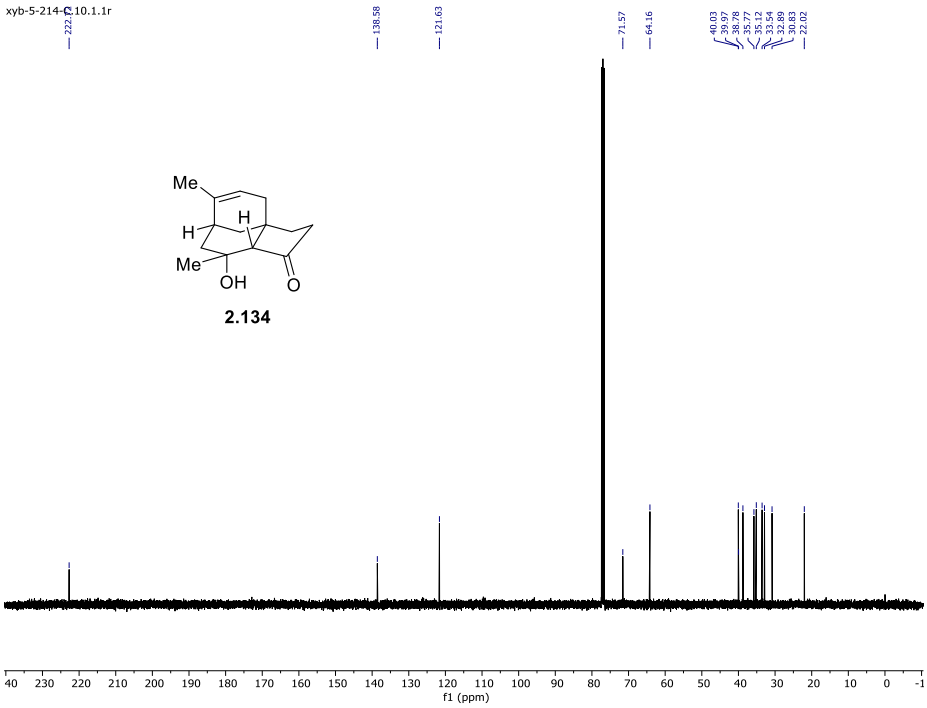

**Figure 2.111.** $^{1}$H-NMR Spectrum of **2.183** in $CDCl_3$, 500 MHz

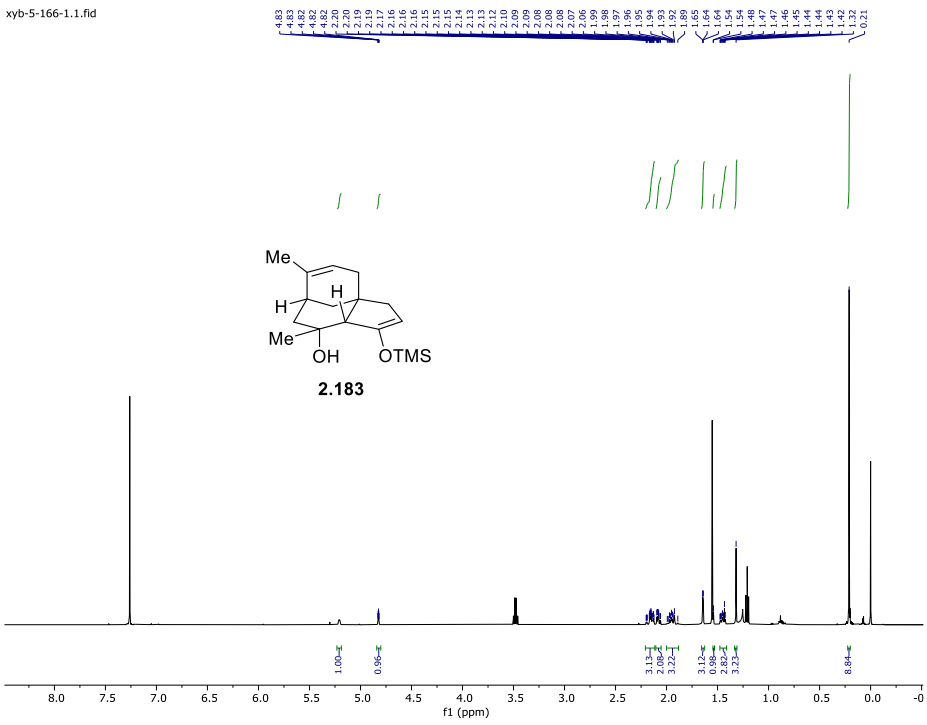


**Figure 2.112.** $^{1}$H-NMR Spectrum of **2.185** in $CDCl_3$, 500 MHz

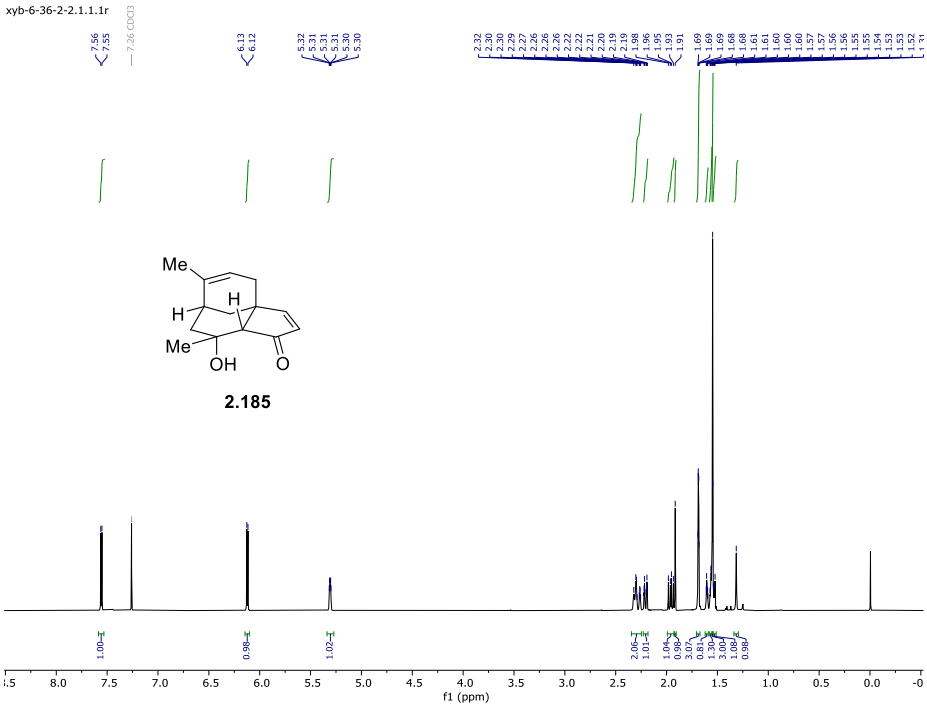

**Figure 2.113.** $^{13}$C-NMR Spectrum of **2.185** in $CDCl_3$, 101 MHz

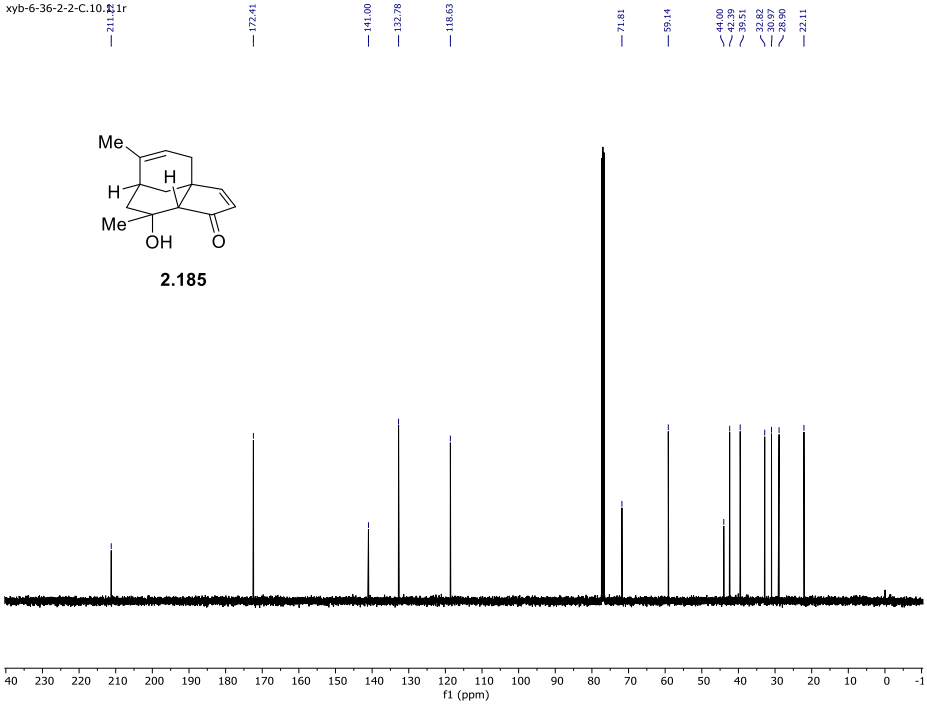


**Figure 2.114.** $^{1}$H-NMR Spectrum of **2.188** in $CDCl_3$, 500 MHz

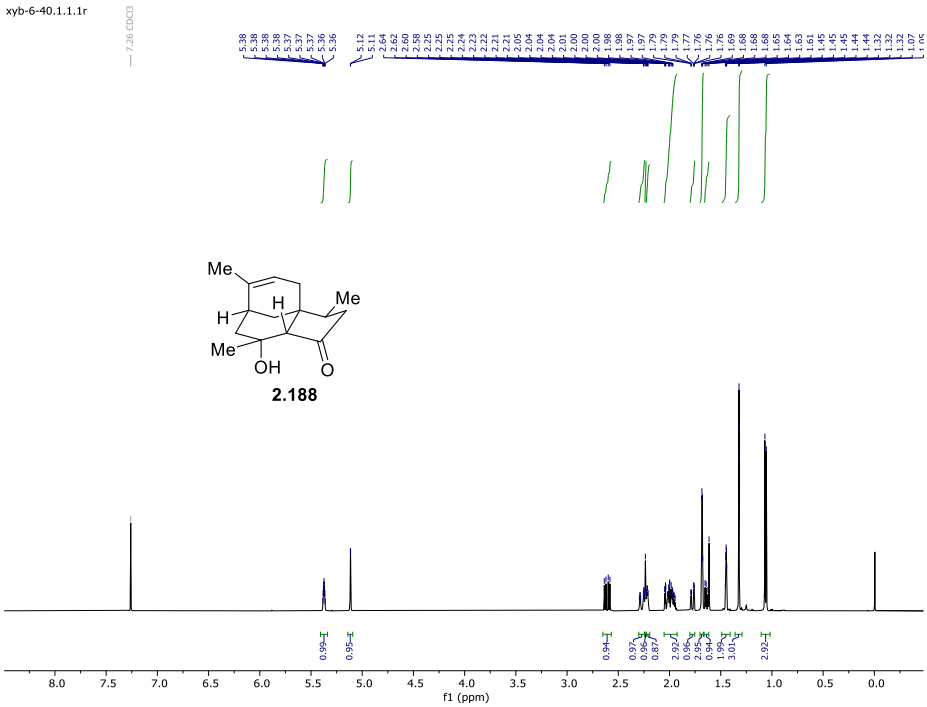

**Figure 2.115.** $^{13}$C-NMR Spectrum of **2.188** in $CDCl_3$, 101 MHz

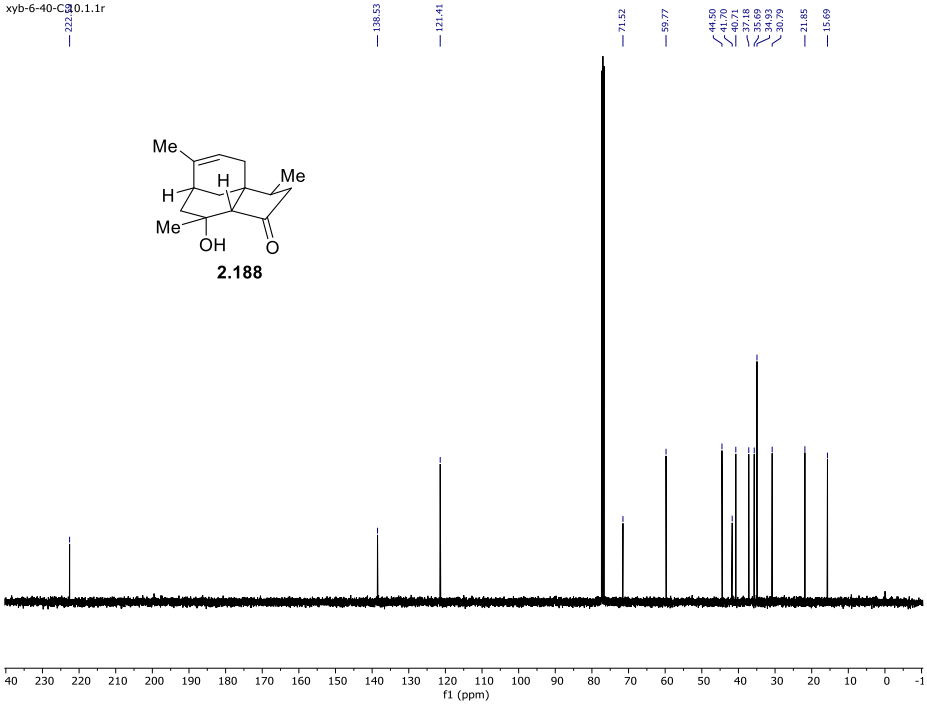


**Figure 2.116.** $^{1}$H-NMR Spectrum of **2.1** in acetone-D6, 500 MHz

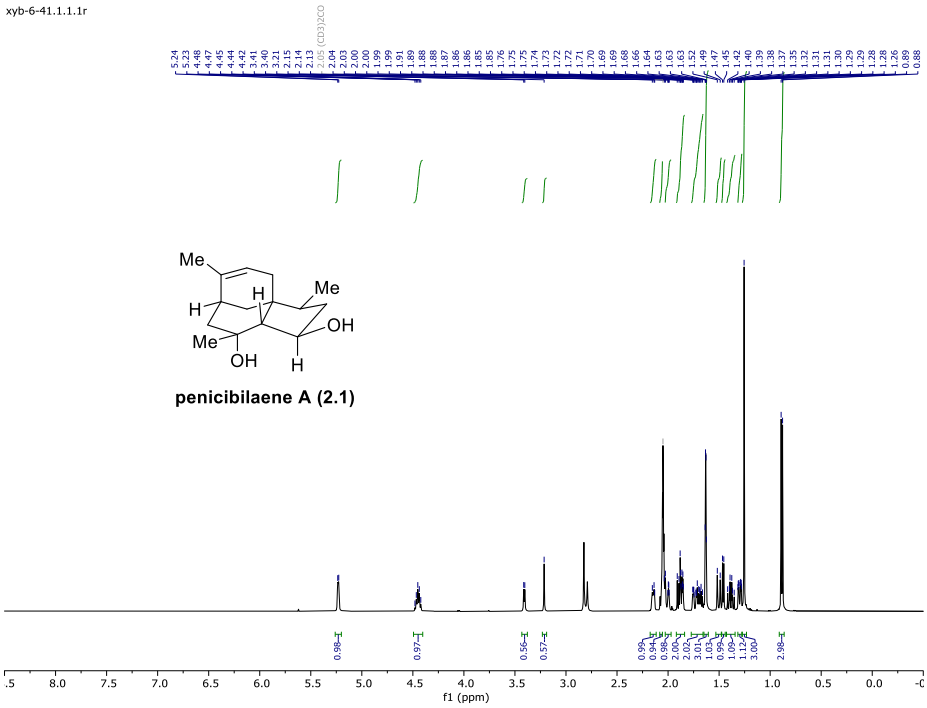

**Figure 2.117.** $^{13}$C-NMR Spectrum of **2.1** in acetone-D6, 101 MHz

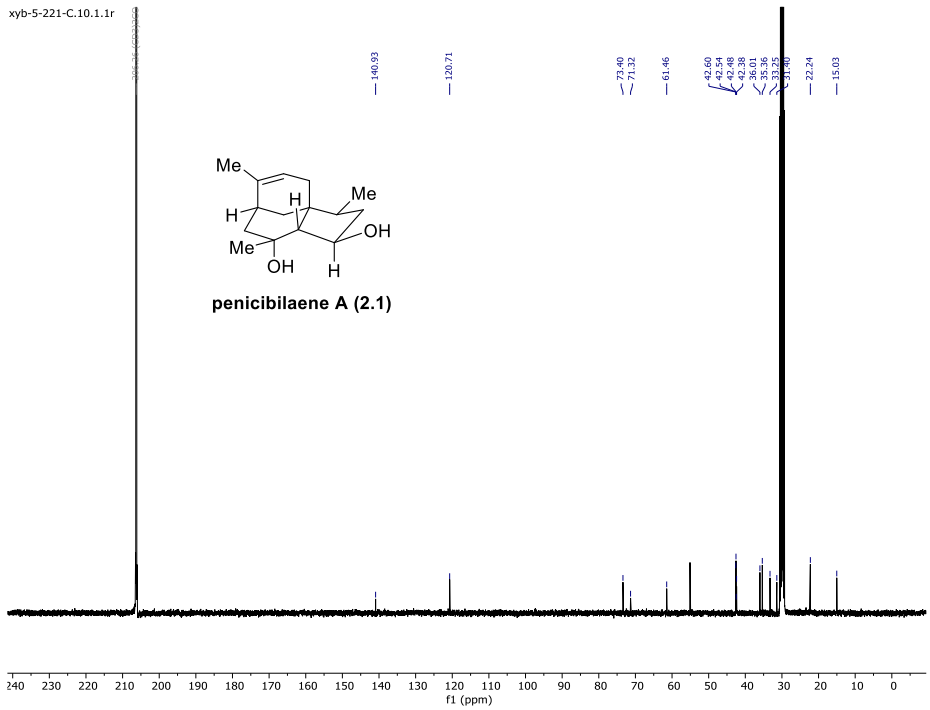


**Figure 2.118.** $^{1}$H-NMR Spectrum of **2.2** in $CDCl_3$, 500 MHz

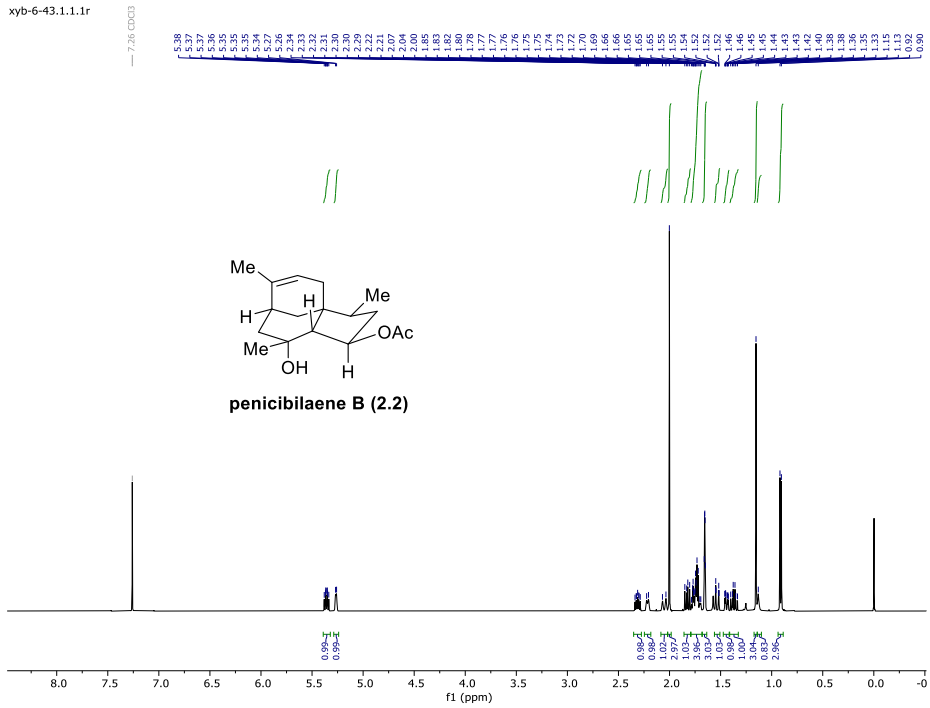

**Figure 2.118.** $^{13}$C-NMR Spectrum of **2.2** in $CDCl_3$, 101 MHz

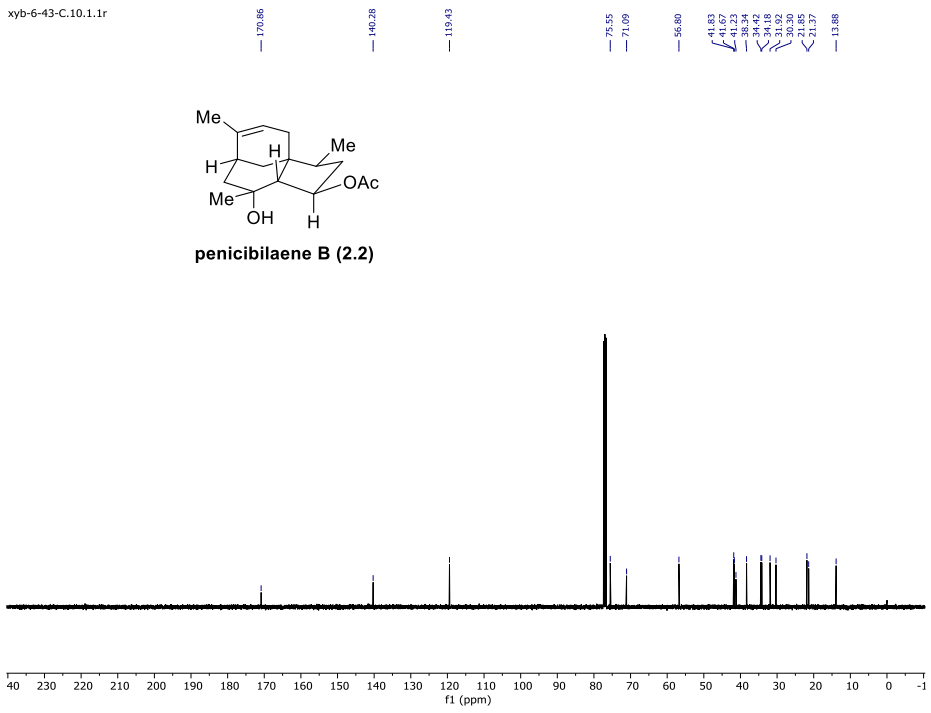


## 2.7. References


1. (a) Cherney, E. C.; Baran, P. S. Terpenoid-Alkaloids: Their Biosynthetic Twist of Fate and Total Synthesis. *Isr. J. Chem.* **2011,** *51*, 391-405. (b) Justicia, J.; Álvarez de Cienfuegos, L.; Campaña, A. G.; Miguel, D.; Jakoby, V.; Gansäuer, A.; Cuerva, J. M. Bioinspired terpene synthesis: a radical approach. *Chem. Soc. Rev.* **2011,** *40*, 3525-3537. (c) Urabe, D.; Asaba, T.; Inoue, M. Convergent Strategies in Total Syntheses of Complex Terpenoids. *Chem. Rev.* **2015,** *115*, 9207-9231. (d) Brill, Z. G.; Condakes, M. L.; Ting, C. P.; Maimone, T. J. Navigating the Chiral Pool in the Total Synthesis of Complex Terpene Natural Products. *Chem. Rev.* **2017,** *117*, 11753-11795.

2. (a) Chen, K.; Baran, P. S. Total synthesis of eudesmane terpenes by site-selective C–H oxidations. *Nature* **2009,** *459*, 824-828. (b) Ishihara, Y.; Baran, P. S. Two-Phase Terpene Total Synthesis: Historical Perspective and Application to the Taxol® Problem. *Synlett* **2010,** *2010*, 1733-1745. (c)

Foo, K.; Usui, I.; Götz, D. C. G.; Werner, E. W.; Holte, D.; Baran, P. S. Scalable, Enantioselective Synthesis of Germacrenes and Related Sesquiterpenes Inspired by Terpene Cyclase Phase Logic. *Angew. Chem., Int. Ed.* **2012,** *51*, 11491-11495. (d) Jørgensen, L.; McKerrall, S. J.; Kuttruff, C. A.; Ungeheuer, F.; Felding, J.; Baran, P. S. 14-Step Synthesis of (+)-Ingenol from (+)-3-Carene. *Science* **2013,** *341*, 878-882. (e) Wilde, N. C.; Isomura, M.; Mendoza, A.; Baran, P. S. Two-Phase Synthesis of (−)-Taxuyunnanine D. *J. Am. Chem. Soc.* **2014,** *136*, 4909-4912. (f) Kanda, Y.; Nakamura, H.; Umemiya, S.; Puthukanoori, R. K.; Murthy Appala, V. R.; Gaddamanugu, G. K.; Paraselli, B. R.; Baran, P. S. Two-Phase Synthesis of Taxol. *J. Am. Chem. Soc.* **2020,** *142*, 10526-10533.

3. (a) Jun, C.-H. Transition metal-catalyzed carbon–carbon bond activation. *Chem. Soc. Rev.* **2004,** *33*, 610-618. (b) Souillart, L.; Cramer, N. Catalytic C–C Bond Activations via Oxidative Addition to Transition Metals. *Chem. Rev.* **2015,** *115*, 9410-9464. (c) Deng, L.; Dong, G. Carbon–Carbon Bond Activation of Ketones. *Trends Chem.* **2020,** *2*, 183-198. (d) Murakami, M.; Ishida, N. Cleavage of Carbon–Carbon σ-Bonds of Four-Membered Rings. *Chem. Rev.* **2021,** *121*, 264-299.

4. (a) Xu, T.; Dong, G. Rhodium-Catalyzed Regioselective Carboacylation of Olefins: A C□C Bond Activation Approach for Accessing Fused-Ring Systems. *Angew. Chem., Int. Ed.* **2012,** *51*, 7567-7571. (b) Chen, P.-h.; Billett, B. A.; Tsukamoto, T.; Dong, G. "Cut and Sew" Transformations via Transition-Metal-Catalyzed Carbon–Carbon Bond Activation. *ACS Catal.* **2017,** *7*, 1340-1360.

5. (a) Huang, Z.; Lim, H. N.; Mo, F.; Young, M. C.; Dong, G. Transition metal-catalyzed ketone-directed or mediated C–H functionalization. *Chem. Soc. Rev.* **2015,** *44*, 7764-7786. (b) Hartwig, J. F. Catalyst-Controlled Site-Selective Bond Activation. *Acc. Chem. Res.* **2017,** *50*, 549-555. (c)

Huang, Z.; Dong, G. Site-Selectivity Control in Organic Reactions: A Quest To Differentiate Reactivity among the Same Kind of Functional Groups. *Acc. Chem. Res.* **2017,** *50*, 465-471.

6. (a) Murakami, M.; Ishida, N. Potential of Metal-Catalyzed C–C Single Bond Cleavage for Organic Synthesis. *J. Am. Chem. Soc.* **2016,** *138*, 13759-13769. (b) Wang, B.; Perea, M. A.; Sarpong, R. Transition Metal-Mediated C−C Single Bond Cleavage: Making the Cut in Total Synthesis. *Angew. Chem., Int. Ed.* **2020,** *59*, 18898-18919.

7. Meng, L.-H.; Li, X.-M.; Liu, Y.; Wang, B.-G. Penicibilaenes A and B, Sesquiterpenes with a Tricyclo[6.3.1.01,5]dodecane Skeleton from the Marine Isolate of Penicillium bilaiae MA-267. *Org. Lett.* **2014,** *16*, 6052-6055.

8. (a) Shing, T. K. M.; Zhu, X. Y.; Yeung, Y. Y. Studies towards Simalikalactone D and Quassimarin: Construction of an Advanced Pentacyclic Intermediate. *Chem. - Eur. J.* **2003,** *9*, 5489-5500. (b) Wu, Z.; Wouters, J.; Poulter, C. D. Isopentenyl Diphosphate Isomerase. Mechanism-Based Inhibition by Diene Analogues of Isopentenyl Diphosphate and Dimethylallyl Diphosphate. *J. Am. Chem. Soc.* **2005,** *127*, 17433-17438.

9. Gao, F.; Hoveyda, A. H. α-Selective Ni-Catalyzed Hydroalumination of Aryl- and Alkyl-Substituted Terminal Alkynes: Practical Syntheses of Internal Vinyl Aluminums, Halides, or Boronates. *J. Am. Chem. Soc.* **2010,** *132*, 10961-10963.

10. (a) Del Valle, L.; Stille, J. K.; Hegedus, L. S. Palladium-catalyzed coupling of allylic acetates with aryl- and vinylstannanes. *J. Org. Chem.* **1990,** *55*, 3019-3023. (b) Li, F.-X.; Ren, S.-J.; Li, P.-F.; Yang, P.; Qu, J. An Endo-Selective Epoxide-Opening Cascade for the Fast Assembly of the Polycyclic Core Structure of Marine Ladder Polyethers. *Angew. Chem., Int. Ed.* **2020,** *59*, 18473-18478. (c) Williams, D. R.; Gladen, P. T.; Pinchman, J. R. Total Synthesis of Neodolastane Diterpenes Trichoaurantianolides C and D. *J. Org. Chem.* **2015,** *80*, 5474-5493.

11. Ko, H. M.; Dong, G. Cooperative activation of cyclobutanones and olefins leads to bridged ring systems by a catalytic [4 + 2] coupling. *Nat. Chem.* **2014,** *6*, 739-744.

12. Deng, L.; Jin, L.; Dong, G. Fused-Ring Formation by an Intramolecular "Cut-and-Sew" Reaction between Cyclobutanones and Alkynes. *Angew. Chem., Int. Ed.* **2018,** *57*, 2702-2706.

13. (a) Deng, L.; Fu, Y.; Lee, S. Y.; Wang, C.; Liu, P.; Dong, G. Kinetic Resolution via Rh-Catalyzed C–C Activation of Cyclobutanones at Room Temperature. *J. Am. Chem. Soc.* **2019,** *141*, 16260-16265. (b) Hou, S.-H.; Yu, X.; Zhang, R.; Deng, L.; Zhang, M.; Prichina, A. Y.; Dong, G. Enantioselective Type II Cycloaddition of Alkynes via C–C Activation of Cyclobutanones: Rapid and Asymmetric Construction of [3.3.1] Bridged Bicycles. *J. Am. Chem. Soc.* **2020,** *142*, 13180-13189.

14. Modak, A.; Alegre-Requena, J. V.; de Lescure, L.; Rynders, K. J.; Paton, R. S.; Race, N. J. Homologation of Electron-Rich Benzyl Bromide Derivatives via Diazo C–C Bond Insertion. *J. Am. Chem. Soc.* **2022,** *144*, 86-92.

15. Munteanu, C.; Frantz, D. E. Palladium-Catalyzed Synthesis of Alkynes via a Tandem Decarboxylation/Elimination of (E)-Enol Triflates. *Org. Lett.* **2016,** *18*, 3937-3939.

16. Li, X.; Danishefsky, S. J. Cyclobutenone as a Highly Reactive Dienophile: Expanding Upon Diels−Alder Paradigms. *J. Am. Chem. Soc.* **2010,** *132*, 11004-11005.

17. Mu, Y.; Gibbs, R. A.; Eubanks, L. M.; Poulter, C. D. Cuprate-Mediated Synthesis and Biological Evaluation of Cyclopropyl- and tert-Butylfarnesyl Diphosphate Analogs. *J. Org. Chem.* **1996,** *61*, 8010-8015.

18. Zhu, N.; Hall, D. G. Effect of Additives on the Stereochemical Integrity and Reactivity of α-Alkoxycarbonyl Alkenylcopper Intermediates. Optimal Conditions for the Synthesis of Isomerically Pure Tetrasubstituted Alkenes. *J. Org. Chem.* **2003,** *68*, 6066-6069.

19. Gill, D.; Taylor, N. H.; Thomas, E. J. Synthesis of 2,6-cis-disubstituted 4-methylenetetrahydropyrans by oxy-Michael addition. *Tetrahedron* **2011,** *67*, 5034-5045.

20. Gampe, C. M.; Carreira, E. M. Total Syntheses of Guanacastepenes N and O. *Angew. Chem., Int. Ed.* **2011,** *50*, 2962-2965.

21. Williams, D. R.; Patnaik, S.; Plummer, S. V. Leucascandrolide A: A Second Generation Formal Synthesis. *Org. Lett.* **2003,** *5*, 5035-5038.

22. (a) Perreault, S.; Rovis, T. Enantioselective Synthesis of the Tricyclic Core of FR901483 Featuring a Rhodium-Catalyzed [2+2+2] Cycloaddition. *Synthesis* **2013,** *45*, 719-728. (b) Kitabayashi, Y.; Yokoshima, S.; Fukuyama, T. Total Synthesis of (−)-Lepistine. *Org. Lett.* **2014,** *16*, 2862-2864.

23. Anslyn, E. V.; Dougherty, D. A. *Modern physical organic chemistry*. University science books: 2006.

24. Gallagher, A. G.; Tian, H.; Torres-Herrera, O. A.; Yin, S.; Xie, A.; Lange, D. M.; Wilson, J. K.; Mueller, L. G.; Gau, M. R.; Carroll, P. J.; Martinez-Solorio, D. Access to Highly Functionalized Cyclopentenones via Diastereoselective Pauson–Khand Reaction of Siloxy-Tethered 1,7-Enynes. *Org. Lett.* **2019,** *21*, 8646-8651.

25. Aye, Y.; Davies, S. G.; Garner, A. C.; Roberts, P. M.; Smith, A. D.; Thomson, J. E. Parallel kinetic resolution of tert-butyl (RS)-3-oxy-substituted cyclopent-1-ene-carboxylates for the asymmetric synthesis of 3-oxy-substituted cispentacin and transpentacin derivatives. *Org. Biomol. Chem.* **2008,** *6*, 2195-2203.

26. Abraham, E.; Claridge, T. D. W.; Davies, S. G.; Odell, B.; Roberts, P. M.; Russell, A. J.; Smith, A. D.; Smith, L. J.; Storr, H. R.; Sweet, M. J.; Thompson, A. L.; Thomson, J. E.; Tranter, G. E.; Watkin, D. J. A systematic study of the solid state and solution phase conformational

preferences of β-peptides derived from C(3)-alkyl substituted transpentacin derivatives. *Tetrahedron: Asymmetry* **2011,** *22*, 69-100.

27. Candish, L.; Lupton, D. W. Concise formal synthesis of (−)-7-deoxyloganinvia N-heterocyclic carbene catalysed rearrangement of α,β-unsaturated enol esters. *Org. Biomol. Chem.* **2011,** *9*, 8182-8189.

28. Davies, S. G.; Garner, A. C.; Long, M. J. C.; Morrison, R. M.; Roberts, P. M.; Savory, E. D.; Smith, A. D.; Sweet, M. J.; Withey, J. M. Kinetic resolution and parallel kinetic resolution of methyl (±)-5-alkyl-cyclopentene-1-carboxylates for the asymmetric synthesis of 5-alkyl-cispentacin derivatives. *Org. Biomol. Chem.* **2005,** *3*, 2762-2775.

29. (a) Gooßen, L. J.; Linder, C.; Rodríguez, N.; Lange, P. P.; Fromm, A. Silver-catalysed protodecarboxylation of carboxylic acids. *Chem. Commun.* **2009**, 7173-7175. (b) Liu, C.; Qin, Z.-X.; Ji, C.-L.; Hong, X.; Szostak, M. Highly-chemoselective step-down reduction of carboxylic acids to aromatic hydrocarbons via palladium catalysis. *Chem. Sci.* **2019,** *10*, 5736-5742. (c) Cahiez, G.; Moyeux, A.; Gager, O.; Poizat, M. Copper-Catalyzed Decarboxylation of Aromatic Carboxylic Acids: En Route to Milder Reaction Conditions. *Adv. Synth. Catal.* **2013,** *355*, 790-796. (d) Gooßen, L. J.; Rodríguez, N.; Linder, C.; Lange, P. P.; Fromm, A. Comparative Study of Copper- and Silver-Catalyzed Protodecarboxylations of Carboxylic Acids. *ChemCatChem* **2010,** *2*, 430-442.

30. (a) Yamaguchi, K.; Kazuta, Y.; Abe, H.; Matsuda, A.; Shuto, S. Construction of a cis-Cyclopropane via Reductive Radical Decarboxylation. Enantioselective Synthesis of cis- and trans-1-Arylpiperazyl-2-phenylcyclopropanes Designed as Antidopaminergic Agents. *J. Org. Chem.* **2003,** *68*, 9255-9262. (b) Qin, T.; Malins, L. R.; Edwards, J. T.; Merchant, R. R.; Novak, A. J. E.; Zhong, J. Z.; Mills, R. B.; Yan, M.; Yuan, C.; Eastgate, M. D.; Baran, P. S. Nickel-

Catalyzed Barton Decarboxylation and Giese Reactions: A Practical Take on Classic Transforms. *Angew. Chem., Int. Ed.* **2017,** *56*, 260-265.

31. (a) Schönecker, B.; Zheldakova, T.; Liu, Y.; Kötteritzsch, M.; Günther, W.; Görls, H. Biomimetic Hydroxylation of Nonactivated CH2 Groups with Copper Complexes and Molecular Oxygen. *Angew. Chem., Int. Ed.* **2003,** *42*, 3240-3244. (b) See, Y. Y.; Herrmann, A. T.; Aihara, Y.; Baran, P. S. Scalable C–H Oxidation with Copper: Synthesis of Polyoxypregnanes. *J. Am. Chem. Soc.* **2015,** *137*, 13776-13779.

32. Desai, L. V.; Hull, K. L.; Sanford, M. S. Palladium-Catalyzed Oxygenation of Unactivated sp3 C−H Bonds. *J. Am. Chem. Soc.* **2004,** *126*, 9542-9543.

33. Zhu, X.; Wang, Y.-F.; Ren, W.; Zhang, F.-L.; Chiba, S. TEMPO-Mediated Aliphatic C–H Oxidation with Oximes and Hydrazones. *Org. Lett.* **2013,** *15*, 3214-3217.

34. Reetz, M. T.; Hugel, H.; Dresely, K. The relative reactivity of cyclic ketones towards methyltitanium reagents. *Tetrahedron* **1987,** *43*, 109-114.

35. Li, B.; Driess, M.; Hartwig, J. F. Iridium-Catalyzed Regioselective Silylation of Secondary Alkyl C–H Bonds for the Synthesis of 1,3-Diols. *J. Am. Chem. Soc.* **2014,** *136*, 6586-6589.

36. Karmel, C.; Li, B.; Hartwig, J. F. Rhodium-Catalyzed Regioselective Silylation of Alkyl C–H Bonds for the Synthesis of 1,4-Diols. *J. Am. Chem. Soc.* **2018,** *140*, 1460-1470.

37. (a) Kurandina, D.; Yadagiri, D.; Rivas, M.; Kavun, A.; Chuentragool, P.; Hayama, K.; Gevorgyan, V. Transition-Metal- and Light-Free Directed Amination of Remote Unactivated C(sp3)–H Bonds of Alcohols. *J. Am. Chem. Soc.* **2019,** *141*, 8104-8109. (b) Parasram, M.; Chuentragool, P.; Wang, Y.; Shi, Y.; Gevorgyan, V. General, Auxiliary-Enabled Photoinduced Pd-Catalyzed Remote Desaturation of Aliphatic Alcohols. *J. Am. Chem. Soc.* **2017,** *139*, 14857-14860.

38. (a) Espino, C. G.; Wehn, P. M.; Chow, J.; Du Bois, J. Synthesis of 1,3-Difunctionalized Amine Derivatives through Selective C−H Bond Oxidation. *J. Am. Chem. Soc.* **2001,** *123*, 6935-6936. (b) Espino, C. G.; Fiori, K. W.; Kim, M.; Du Bois, J. Expanding the Scope of C−H Amination through Catalyst Design. *J. Am. Chem. Soc.* **2004,** *126*, 15378-15379.

39. Duan, H.-X.; Zhang, Y.; Zhang, Z.-Z.; Wang, Y.-Q. C2-Symmetric 1,2-Diphenylethane-1,2-diamine-Derived Primary–Tertiary Diamine-Catalyzed Asymmetric Mannich Addition of Cyclic N-Sulfonyl Trifluoromethylated Ketimines. *J. Org. Chem.* **2020,** *85*, 11331-11339.

40. (a) Bansode, A. H.; Suryavanshi, G. Metal-free hypervalent iodine/TEMPO mediated oxidation of amines and mechanistic insight into the reaction pathways. *RSC Advances* **2018,** *8*, 32055-32062. (b) Klein, R. F. X.; Bargas, L. M.; Horak, V. Oxidative deamination of sec-alkyl primary amines with 3,5-di-tert-butyl-1,2-benzoquinone; a second look. *J. Org. Chem.* **1988,** *53*, 5994-5998. (c) Iqbal, N.; Cho, E. J. Formation of Carbonyl Compounds from Amines through Oxidative C□N Bond Cleavage using Visible Light Photocatalysis and Applications to N-PMB-Amide Deprotection. *Adv. Synth. Catal.* **2015,** *357*, 2187-2192.

41. (a) Nicolaou, K. C.; Montagnon, T.; Baran, P. S. Modulation of the Reactivity Profile of IBX by Ligand Complexation: Ambient Temperature Dehydrogenation of Aldehydes and Ketones to α,β-Unsaturated Carbonyl Compounds. *Angew. Chem., Int. Ed.* **2002,** *41*, 993-996. (b) Nicolaou, K. C.; Montagnon, T.; Baran, P. S. HIO3 and I2O5: Mild and Selective Alternative Reagents to IBX for the Dehydrogenation of Aldehydes and Ketones. *Angew. Chem., Int. Ed.* **2002,** *41*, 1386-1389. (c) Nicolaou, K. C.; Zhong, Y. L.; Baran, P. S. A New Method for the One-Step Synthesis of α,β-Unsaturated Carbonyl Systems from Saturated Alcohols and Carbonyl Compounds. *J. Am. Chem. Soc.* **2000,** *122*, 7596-7597.

42. Honda, T.; Rounds, B. V.; Gribble, G. W.; Suh, N.; Wang, Y.; Sporn, M. B. Design and synthesis of 2-cyano-3,12-dioxoolean-1,9-dien-28-oic acid, a novel and highly active inhibitor of nitric oxide production in mouse macrophages. *Bioorg. Med. Chem. Lett.* **1998,** *8*, 2711-2714.

43. Shimazaki, M.; Huang, Z.-H.; Goto, M.; Suzuki, N.; Ohta, A. Syntheses of 2-Cycloalken-1-ones. *Synthesis* **1990,** *1990*, 677-678.

44. Diao, T.; Stahl, S. S. Synthesis of Cyclic Enones via Direct Palladium-Catalyzed Aerobic Dehydrogenation of Ketones. *J. Am. Chem. Soc.* **2011,** *133*, 14566-14569.

45. Pan, G.-F.; Zhu, X.-Q.; Guo, R.-L.; Gao, Y.-R.; Wang, Y.-Q. Synthesis of Enones and Enals via Dehydrogenation of Saturated Ketones and Aldehydes. *Adv. Synth. Catal.* **2018,** *360*, 4774-4783.

46. Diao, T.; Wadzinski, T. J.; Stahl, S. S. Direct aerobic α,β-dehydrogenation of aldehydes and ketones with a Pd(TFA)2/4,5-diazafluorenone catalyst. *Chem. Sci.* **2012,** *3*, 887-891.

47. O'Brien, J. M.; Hoveyda, A. H. Metal-Free Catalytic C–Si Bond Formation in an Aqueous Medium. Enantioselective NHC-Catalyzed Silyl Conjugate Additions to Cyclic and Acyclic α,β-Unsaturated Carbonyls. *J. Am. Chem. Soc.* **2011,** *133*, 7712-7715.

48. (a) Kamakura, D.; Todoroki, H.; Urabe, D.; Hagiwara, K.; Inoue, M. Total Synthesis of Talatisamine. *Angew. Chem., Int. Ed.* **2020,** *59*, 479-486. (b) Calderone, J. A.; Santos, W. L. Copper(II)-Catalyzed Silyl Conjugate Addition to α,β-Unsaturated Conjugated Compounds: Brønsted Base-Assisted Activation of Si–B Bond in Water. *Org. Lett.* **2012,** *14*, 2090-2093.

49. Sharma, S.; Oehlschlager, A. C. Synthetic and mechanistic implications of ligand mixing in higher order mixed (trialkylsilyl)- and (trialkylstannyl)cuprates. *J. Org. Chem.* **1991,** *56*, 770-776.

50. Okamoto, K.; Tamura, E.; Ohe, K. Stereoselective Construction of 1,3-Disilylcyclopentane Derivatives by Scandium-Catalyzed [3+2] Cycloaddition of Allylsilanes to β-Silylenones. *Angew. Chem., Int. Ed.* **2014,** *53*, 10195-10199.

51. Lee, K.-s.; Zhugralin, A. R.; Hoveyda, A. H. Efficient C−B Bond Formation Promoted by N-Heterocyclic Carbenes: Synthesis of Tertiary and Quaternary B-Substituted Carbons through Metal-Free Catalytic Boron Conjugate Additions to Cyclic and Acyclic α,β-Unsaturated Carbonyls. *J. Am. Chem. Soc.* **2009,** *131*, 7253-7255.

52. (a) Krasovskiy, A.; Kopp, F.; Knochel, P. Soluble Lanthanide Salts (LnCl3·2 LiCl) for the Improved Addition of Organomagnesium Reagents to Carbonyl Compounds. *Angew. Chem., Int. Ed.* **2006,** *45*, 497-500. (b) Breitler, S.; Carreira, E. M. Total Synthesis of (+)-Crotogoudin. *Angew. Chem., Int. Ed.* **2013,** *52*, 11168-11171.

53. Boyko, Y. D.; Huck, C. J.; Ning, S.; Shved, A. S.; Yang, C.; Chu, T.; Tonogai, E. J.; Hergenrother, P. J.; Sarlah, D. Synthetic Studies on Selective, Proapoptotic Isomalabaricane Triterpenoids Aided by Computational Techniques. *J. Am. Chem. Soc.* **2021,** *143*, 2138-2155.

54. (a) Chen, M.; Rago, A. J.; Dong, G. Platinum-Catalyzed Desaturation of Lactams, Ketones, and Lactones. *Angew. Chem., Int. Ed.* **2018,** *57*, 16205-16209. (b) Chen, M.; Dong, G. Platinum-Catalyzed α,β-Desaturation of Cyclic Ketones through Direct Metal–Enolate Formation. *Angew. Chem., Int. Ed.* **2021,** *60*, 7956-7961.

55. (a) Huang, D.; Zhao, Y.; Newhouse, T. R. Synthesis of Cyclic Enones by Allyl-Palladium-Catalyzed α,β-Dehydrogenation. *Org. Lett.* **2018,** *20*, 684-687. (b) Chen, Y.; Huang, D.; Zhao, Y.; Newhouse, T. R. Allyl-Palladium-Catalyzed Ketone Dehydrogenation Enables Telescoping with Enone α,β-Vicinal Difunctionalization. *Angew. Chem., Int. Ed.* **2017,** *56*, 8258-8262. (c) Chen, Y.;

Romaire, J. P.; Newhouse, T. R. Palladium-Catalyzed α,β-Dehydrogenation of Esters and Nitriles. *J. Am. Chem. Soc.* **2015,** *137*, 5875-5878.

56. Mori, K. Pheromone synthesis. Part 264: Synthesis of the core 3-oxabicyclo[3.3.0]octane structures of gomadalactones A, B and C, the components of the contact sex pheromone of the white-spotted longicorn beetle, Anoplophora malasiaca. *Tetrahedron* **2019,** *75*, 3387-3398.

57. Mukaiyama, T.; Matsuo, J.-i.; Kitagawa, H. A New and One-Pot Synthesis of α,β-Unsaturated Ketones by Dehydrogenation of Various Ketones with N-tert-Butyl Phenylsulfinimidoyl Chloride. *Chem. Lett.* **2000,** *29*, 1250-1251.

58. Qu, Y.; Wang, Z.; Zhang, Z.; Zhang, W.; Huang, J.; Yang, Z. Asymmetric Total Synthesis of (+)-Waihoensene. *J. Am. Chem. Soc.* **2020,** *142*, 6511-6515.

59. Cao, M.-Y.; Ma, B.-J.; Lao, Z.-Q.; Wang, H.; Wang, J.; Liu, J.; Xing, K.; Huang, Y.-H.; Gan, K.-J.; Gao, W.; Wang, H.; Hong, X.; Lu, H.-H. Optically Active Flavaglines-Inspired Molecules by a Palladium-Catalyzed Decarboxylative Dearomative Asymmetric Allylic Alkylation. *J. Am. Chem. Soc.* **2020,** *142*, 12039-12045.

60. Evans, D. A.; Chapman, K. T.; Carreira, E. M. Directed reduction of .beta.-hydroxy ketones employing tetramethylammonium triacetoxyborohydride. *J. Am. Chem. Soc.* **1988,** *110*, 3560-3578.

61. Trost, B. M.; Masters, J. T.; Lumb, J. P.; Fateen, D. Asymmetric synthesis of chiral cycloalkenone derivatives via palladium catalysis. *Chem. Sci.* **2014,** *5*, 1354-1360.

# CHAPTER 3

## Catalytic Activation of Unstrained C(aryl)−C(alkyl) Bonds in 2,2'-Methylenediphenols

### 3.1. Introduction

Transition metal (TM)-catalyzed carbon−carbon σ-bond (C−C) activation has been emerging from organometallic curiosity to useful synthetic tools in organic chemistry.[1] While enormous progress has been achieved to date, one obstacle to realizing broadly applicable C−C activation methods is still the scope of C−C bonds that can be selectively activated.[1h] The current methods primarily rely on substrates with either high ring strain[1h, 1l] and/or polar functional groups, such as carbonyls,[1j] nitriles,[1c, 1m] imines,[1b] and alcohols[2]. In contrast, cleavage of *unstrained and nonpolar* C−C bonds remains underdeveloped.[1d, 1i, 1k] In particular, catalytic approaches to realize C(aryl)−C(alkyl) bond activation have been rare.[3] Conventional retro-Fridel−Craft reactions require very strong acids for dealkylation, which raises concerns on functional group tolerance.[4] The pioneer work by Milstein showed that C(alkyl)−C(aryl) bonds in pincer-type substrates can be cut via direct oxidative addition of a TM (Scheme 1A);[5] however, this reaction typically needs stoichiometric TMs because the product is also a strong chelating ligand, and the only report on the use of catalytic TM exhibited low efficiency.[5d] Alternatively, C(aryl)−C(alkyl) bonds can be

scissored under oxidative conditions, such as a suite of elegant methods based on oxidation-Schmidt rearrangement reported by Jiao (Scheme 1B).[6] Recently, through a β-aryl elimination process, Kakiuchi and co-workers realized the catalytic cleavage of C(allyl)−C(aryl) bonds, in which the heteroarene directing group (DG) and the olefin moiety play critical roles in the C−C activation (Scheme 1C).[7]

Encouraged by our recent reports on the catalytic cleavage of C(aryl)−C(aryl) bonds in unstrained biaryl compounds (Scheme 1D),[8] we wondered whether the C(alkyl)−C(aryl) bonds in 2,2'-methylenediphenols, a common linkage in phenolic resins, could be cleaved in a catalytic, oxidant-free and strong-acid-free manner. The success of this transformation could have implications on upcycling of phenolic resins, which remains an unsolved problem.[9] We thus proposed that, through installing phosphinites onto the phenol OH groups as an easily removable directing group (RDG),[1k] oxidative addition of TMs into the target $Csp^2$−$Csp^3$ bond may take place to form a 5/6 spiro-metallocycle. The subsequent hydrogenolysis is expected to generate two unsymmetrical mono-phenol products. Given that electron-rich phenol moieties can readily react with oxidants and acids, this RDG approach could be attractive for sensitive phenol substrates. Here, we describe our detailed development of a Rh-catalyzed hydrogenolysis of unstrained C(alkyl)−C(aryl) bonds in 2,2'-methylenediphenols.

**Scheme 3.1.** TM-mediated C(aryl)−C(alkyl) Bond Activation.

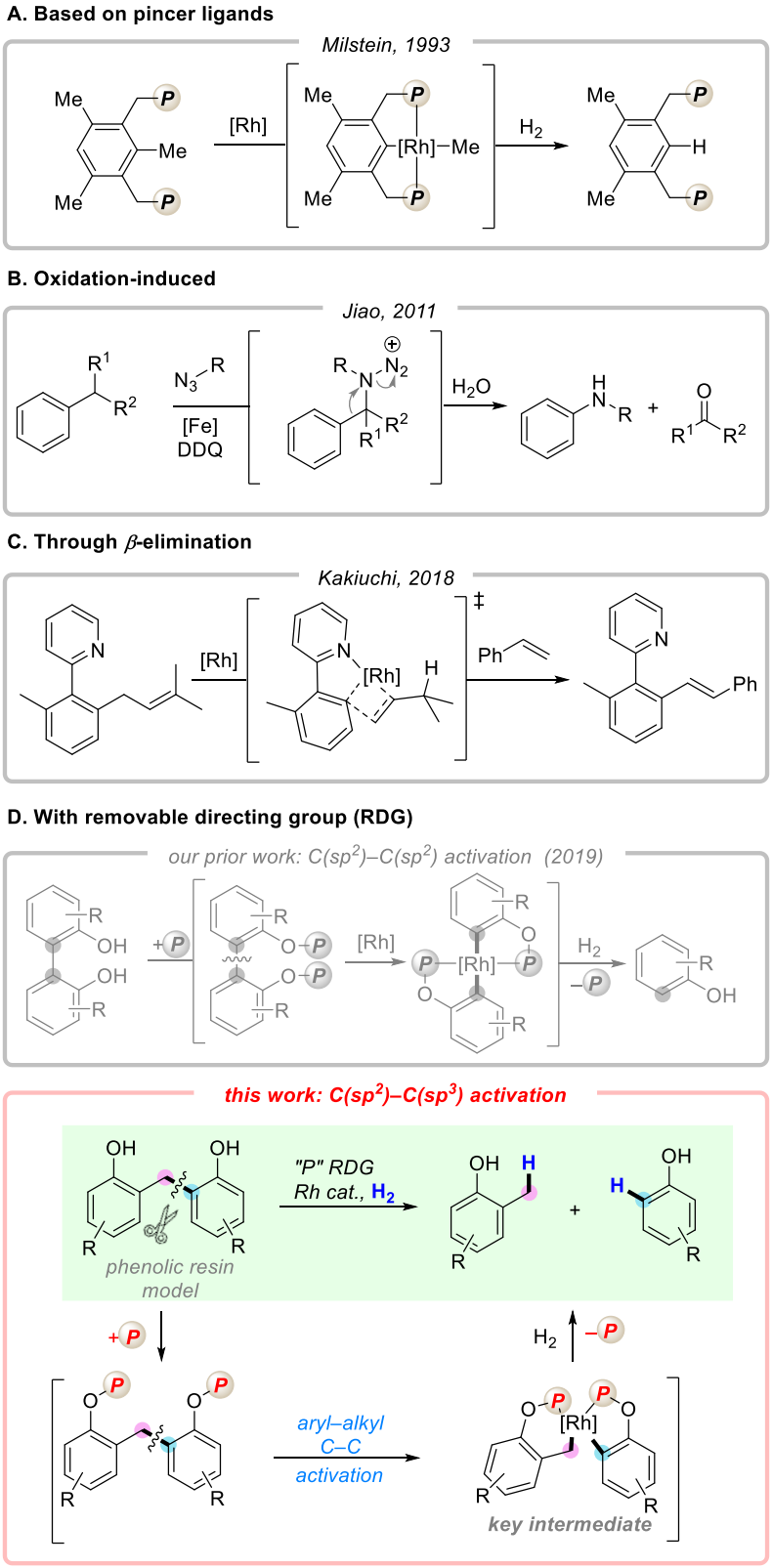

### 3.2. Discovery and Optimization

A number of challenges could be envisaged for the proposed RDG-enabled cleavage of C(alkyl)−C(aryl) bonds in 2,2'-methylenediphenols. First, the double-benzylic methylene C−H bonds could outcompete the less reactive C(alkyl)−C(aryl) bonds when reacting with the TM catalyst.[10] Second, comparing to C(aryl)−C(aryl) bonds, C(alkyl)−C(aryl) bonds are more directional, thus more difficult to coordinate well with TM catalysts. Third, considering that our prior C(aryl)−C(aryl) bond activations[8b] and the Milstein's pincer systems[5] all involve generating two 5-membered metallocycles, it is uncertain whether the proposed 5/6 spiro-metallocycle intermediate can actually be formed because such a mode of activation has not been reported previously.

To tackle these challenges, diphenol **3.1a**, representing a subunit of phenolic resin, was employed as the model substrate. Phosphinites were subsequently introduced to both phenol moieties as RDGs, due to their strong coordinative ability as well as the ease of installation and removal under mild conditions.[11] After a series of condition optimizations, to our delight, the aryl−alkyl linkage in phosphinite **3.2a** can indeed be effectively cleaved by employing 2.5 mol% of $[Rh(C_2H_4)_2Cl]_2$ as the catalyst and 150 psi of hydrogen gas as the reductant; after silica gel work up, the phosphinite RDGs were smoothly removed to afford monophenol products **3.3a** and **3.4a** in 87% and 85% yields, respectively (entry 1, Table 3.1). Control experiments were subsequently conducted to understand the role of each reactant. The reaction did not proceed without the rhodium catalyst, or hydrogen gas, or the RDG (entries 2-4, Table 3.1). Replacing the diisopropyl-derived phosphinite with the diphenyl one shut down the reactivity (entry 5, Table 3.1). Other reductants, such as silanes and boranes, were tested but giving no desired product (entries 6 and 7,

Table 3.1). A series of other rhodium catalysts were also surveyed (entries 8-11, Table 3.1). For example, Rh(I) hydride complexes, i.e., $RhH(PPh_3)_5$, exhibited comparable reactivity, while cationic rhodium species showed no reactivity. Other Rh(I) chloride complexes, such as $[Rh(COD)Cl]_2$ and Wilkinson's catalyst, also gave good yield, albeit slightly lower than $[Rh(C_2H_4)_2Cl]_2$. Other TM complexes including ruthenium, iridium, nickel, and palladium were also examined (entries 12-15, Table 3.1). Interestingly, a reasonably good yield was obtained with the iridium catalyst, showing promise for alternative metal-catalyzed C−C activation in the future. Switching the solvent to toluene led to somewhat lower efficiency (entry 16, Table 3.1) and more coordinative acetonitrile shut down the reaction (entry 17, Table 3.1).

**Table 3.1.** Control Experiments.

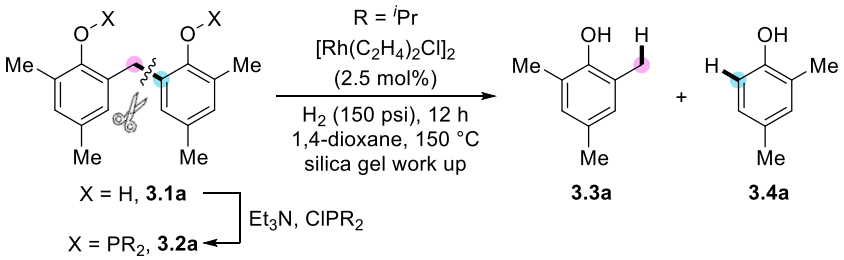


| Entry[a] | Variation from the standard condition | Yield[b] 3.3a | 3.4a | 3.1a |
|---|---|---|---|---|
| 1[c] | None | 87% | 85% | 0% |
| 2 | w/o catalyst | 0% | 0% | 91% |
| 3 | 150 psi Ar | 0% | 0% | 82% |
| 4 | **1a** as substrate | 0% | 0% | 94% |
| 5 | R = Ph instead of $^i$Pr | trace | trace | 51% |
| 6 | $PhMe_2SiH$ (4 equiv) | 0% | 0% | 57% |
| 7 | HB(pin) (4 equiv) | 0% | 0% | 93% |
| 8[c] | $RhH(PPh_3)_4$ (2.5 mol%) | 73% | 83% | 0% |
| 9 | $Rh(COD)_2BF_4$ (5 mol%) | 0% | 0% | 98% |
| 10[c,d] | $[Rh(COD)Cl]_2$ (2.5 mol%) | 79% | 74% | 0% |
| 11[c] | $Rh(PPh_3)_3Cl$ (2.5 mol%) | 76% | 68% | 0% |
| 12 | $Ru(COD)Cl_2$ (5 mol%) | 0% | 0% | 98% |
| 13[c,d] | $[Ir(COD)Cl]_2$ (2.5 mol%) | 54% | 57% | 30% |
| 14 | $Ni(COD)_2$ (5 mol%) | trace | trace | 62% |
| 15 | $Pd(PPh_3)_4$ (5 mol%) | 0% | 0% | 79% |
| 16[c] | toluene as solvent | 73% | 68% | 0% |
| 17 | MeCN as solvent | 0% | 0% | 98% |

[a]Unless otherwise mentioned, the reaction was run on 0.1 mmol scale. [b]Determined by $^1$H-NMR using dibromomethane as the internal standard. [c]Isolated yield. [d]0.3 mmol scale.

While relatively high pressure of hydrogen gas and high temperature were used in the standard conditions to ensure good yields of the reaction, the low limits of various reaction parameters have also been investigated (Table 3.2). First, lowering the $H_2$ pressure from 150 psi to 50 psi and dropping the reaction temperature from 150 °C to 100 °C only marginally affected the yield for substrate **3.2a** (entry 2, Table 3.2). Further reducing the reaction temperature to 70 °C

with 50 psi hydrogen pressure still afforded moderate reactivity (entries 3-6, table 3.2). To our delight, the catalyst loading could be decreased to as low as 0.5 mol% without significant erosion of the yields of **3.3a** and **3.4a** (entries 8-11, Table 3.2). Comparing to the prior pincer system,[5] the high catalysis efficiency of this transformation could likely be attributed to the fact that the products (monodentate ligands) are much weaker ligands than the substrates (chelating ligands). (The experiments in Table 3.2 is conducted by Dr. Jun Zhu)

**Table 3.2**. Exploring the Limits of the Hydrogenolysis of C(aryl)−C(alkyl) Bonds.[a]

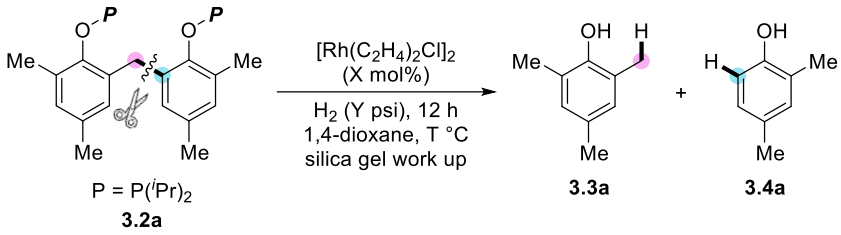


| Entry | X (mol%) | T (°C) | Y (psi) | Yield[b] 3.3a | 3.4a |
|---|---|---|---|---|---|
| 1[c,d] | 2.5 | 150 | 150 | 87% | 85% |
| 2 | 2.5 | 150 | 50 | 80% | 79% |
| 3 | 2.5 | 100 | 150 | 76% | 82% |
| 4 | 2.5 | 100 | 100 | 77% | 73% |
| 5 | 2.5 | 100 | 50 | 79% | 71% |
| 6 | 2.5 | 70 | 50 | 20% | 23% |
| 7 | 2.5 | 50 | 50 | trace | trace |
| 8 | 1.5 | 100 | 50 | 58% | 62% |
| 9 | 1.0 | 100 | 50 | 46% | 45% |
| 10 | 1.0 | 150 | 150 | 71% | 79% |
| 11 | 0.5 | 150 | 150 | 71% | 79% |

[a]Unless otherwise mentioned, the reaction was run on 0.3 mmol scale. [b]Determined by GC using tetradecane as the internal standard. [c]0.1 mmol scale. [d]Isolated yield.

### 3.3. Substrate Scope and Applications

Under the optimized conditions, the substrate scope was subsequently explored to understand the generality and robustness of the current catalytic system. First, alkyl groups at the 4,4'-positions could be well tolerated, though longer alkyl chains required a higher catalyst loading to achieve high yield (entries 1-5, Table 3.3). It is possible that longer alkyl chains may restrict free rotation of the target C–C bonds to some extent. Aryl and heteroaryl substituents at the 4,4'-positions also gave good yield (entries 6-14, Table 3.3). Additionally, common functional groups, such as ether, acetal, thioether, ketone and electron-rich heterocycles (furan and thiophene), were well tolerated under these conditions due to the strong-acid-free and oxidant-free features of this reaction. Moreover, halogens (chlorine and bromine) and ester-substituted 2,2'-methylenediphenols are competent substrates (entries 15-17, Table 3.3).

Substitution patterns on the phenol moieties have also been investigated. First, substitutions at the 5,5'-positions do not much impact the reaction yield (entries 12 and 18, Table 3.3). In addition, substitution at the ortho positions (6,6') and para position (4,4') proved to be not necessary for the desired reactivity (entry 19 and 20, Table 3.3), which is in sharp contrast to the case of cleaving the C(aryl)−C(aryl) bond in 2,2'-biphenols.[8b] The tolerance of hydrogen at the 6,6'-positions is critical for the proposed effective cleavage of phenolic resins (*vide infra*). On the other hand, besides OMe and methyl groups, aryl substituents at the 6,6'-positions also worked smoothly (entry 21, Table 3.3). It is exciting to note that substitution at the 3,3'-positions, which may significantly increase steric hinderance around the target C−C bond, still delivered the desired monophenol products. This again represents a distinct feature from the prior 2,2'-biphenol system,[8b] in which no substituents at the 3,3'-positions were tolerated. As expected, direct substitution on the methylene linker gave no reactivity (entry 23, Table 3.3), as the added ethyl

group vastly hindered metal coordination with the target C(aryl)−C(alkyl) bond. Finally, an unsymmetric substrate containing two aryl groups of different electronic properties was tested, which slightly favors cleavage at the more electron-deficient aryl side (entry 24, Table 3.3). (The preparation and C−C cleavage of compounds **3.2a**–**t**, **3.2u**, **3.2w**, **3.2x** are conducted by Dr. Jun Zhu).

**Table 3.3**. Substrate Scope.[a]

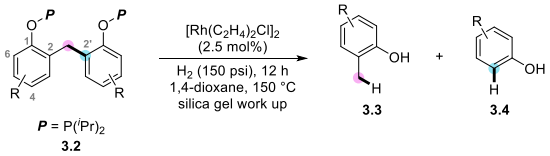


Entry 1

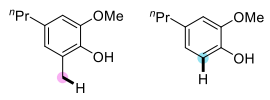

**3.3b**, 80% **3.4b**, 77%

Entry 2

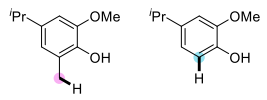

**3.3c**, 74% **3.4c**, 73%

Entry 3[b]

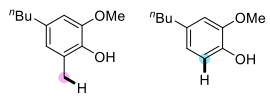

**3.3d**, 72% **3.4d**, 70%

Entry 4[b]

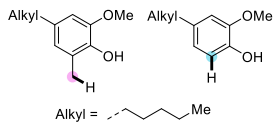

**3.3e**, 70% **3.4e**, 72%

Entry 5

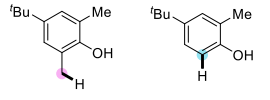

**3.3f**, 73% **3.4f**, 77%

Entry 6

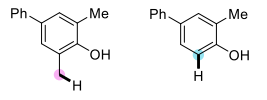

**3.3g**, 85% **3.4g**, 82%

Entry 7

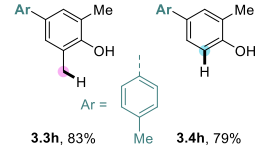

**3.3h**, 83% **3.4h**, 79%

Entry 8

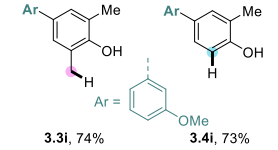

**3.3i**, 74% **3.4i**, 73%

Entry 9

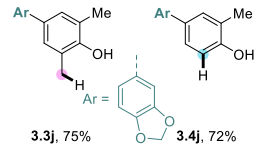

**3.3j**, 75% **3.4j**, 72%

Entry 10

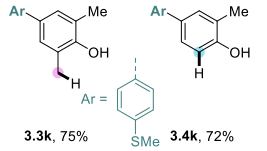

**3.3k**, 75% **3.4k**, 72%

Entry 11

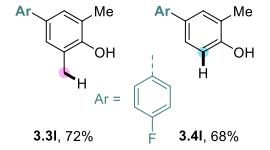

**3.3l**, 72% **3.4l**, 68%

Entry 12

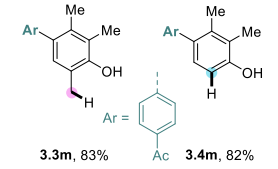

**3.3m**, 83% **3.4m**, 82%

Entry 13

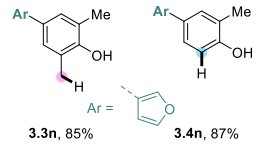

**3.3n**, 85% **3.4n**, 87%

Entry 14

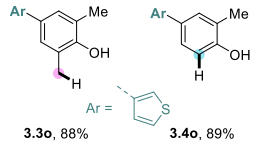

**3.3o**, 88% **3.4o**, 89%

Entry 15[c]

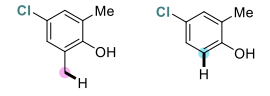

**3.3p**, 88% **3.4p**, 87%

Entry 16

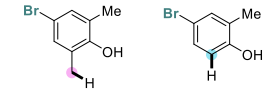

**3.3q**, 77% **3.4q**, 79%

Entry 17

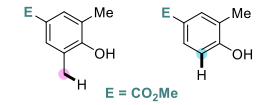

**3.3r**, 79% **3.4r**, 82%

Entry 18

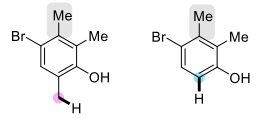

**3.3s**, 83% **3.4s**, 82%

Entry 19[b]

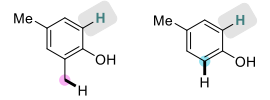

**3.4a**, 79% **3.4t**, 90%

Entry 20

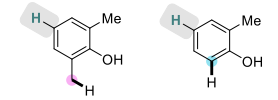

**3.3t'**, 72% **3.4t'**, 72%

Entry 21

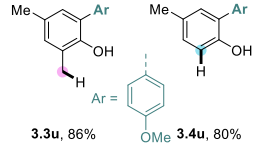

**3.3u**, 86% **3.4u**, 80%

Entry 22[b]

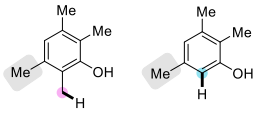

**3.3v**, 38% **3.4v**, 60%

Entry 23

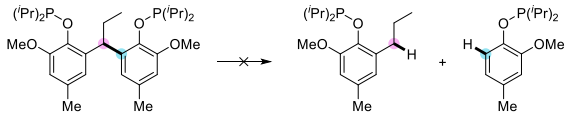

**3.2w**, N.P. **3.3w** **3.4w**

Entry 24

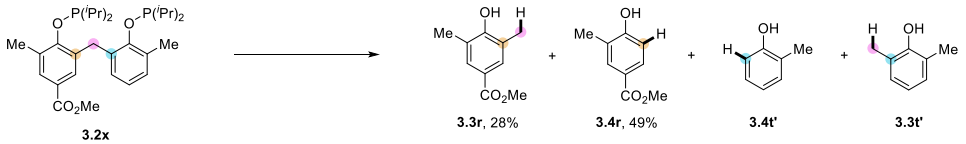

**3.2x**

**3.3r**, 28% **3.4r**, 49% **3.4t'** **3.3t'**

[a]Reaction conditions: **3.2** (0.3 mmol), $[Rh(C_2H_4)_2Cl]_2$ (0.0075 mmol) and $H_2$ (150 psi) in 1,4-dioxane (6 mL), 150 °C, 12 h. All yields are isolated yield unless otherwise mentioned. [b]5 mol% $[Rh(C_2H_4)_2Cl]_2$ (0.015 mmol) was used. [c]Determined by GC using tetradecane as the internal standard.

Regarding the synthetic utility of this transformation, the reaction was first found to be readily scalable, and even higher yields were obtained when it was carried out on a gram scale (Scheme 3.2A, conducted by Dr. Jun Zhu). In addition, a one-pot procedure was realized, in which free biphenol **3.1a** can be directly used as the substrate (Scheme 3.2B).

**Scheme 3.2.** Gram-Scale Synthesis and One-Pot Synthesis.

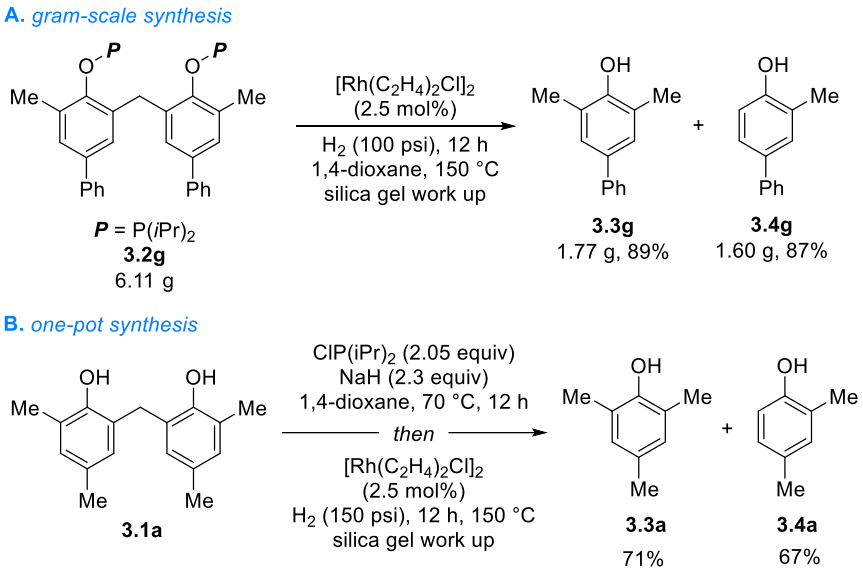


Encouraged by the scope and robustness of this reaction, we next studied degradation of methylenephenol oligomers, closer models for phenolic resins, with this method. As illustrated in Scheme 3.3, trimer **3.2y**, pentamer **3.2z** and heptamer **3.2aa** all reacted and provided moderate to good yield of the corresponding monomers. Note that dimer products were only formed in an appreciable amount with the heptamer substrate.

**Scheme 3.3.** C−C Cleavage of Oligomers.

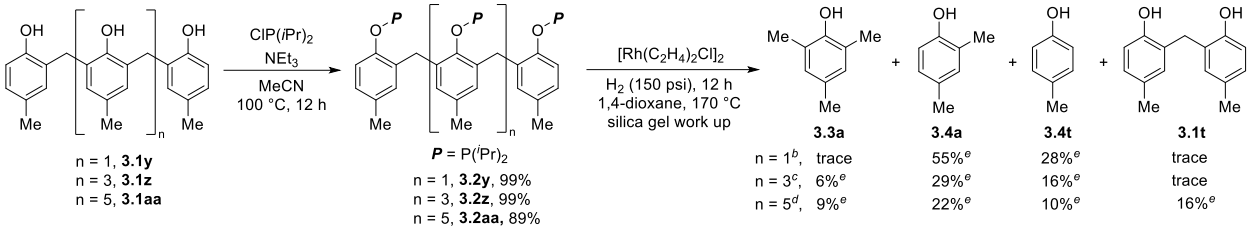


These results motivated us to explore catalytic hydrogenolysis of novolacs. Novolacs are phenol-formaldehyde resins with a formaldehyde to phenol molar ratio of less than one, containing 10-20 repeating units; they generally serve as prepolymers to thermoset materials. To the best of our knowledge, selective and catalytic methods to degrade novolacs to phenols remained unexplored.[9] As a preliminary result, linear novolacs **3.1ab**, prepared from p-cresol and formaldehyde,[12] underwent effective C−C cleavage reactions through the sequence of phosphination and hydrogenolysis to give 56% total yield of three monomers **3.3a**, **3.4a** and **3.4t** (Scheme 3.4A). Using the same approach, a commercially available random-linked phenol-formaldehyde novolacs **3.1ac** can also be effectively converted to a mixture of low-molecular-weight monomers, dimers, and oligomers detected by GC-MS (Scheme 3.4B).

**Scheme 3.4.** C−C Cleavage of Novolacs.

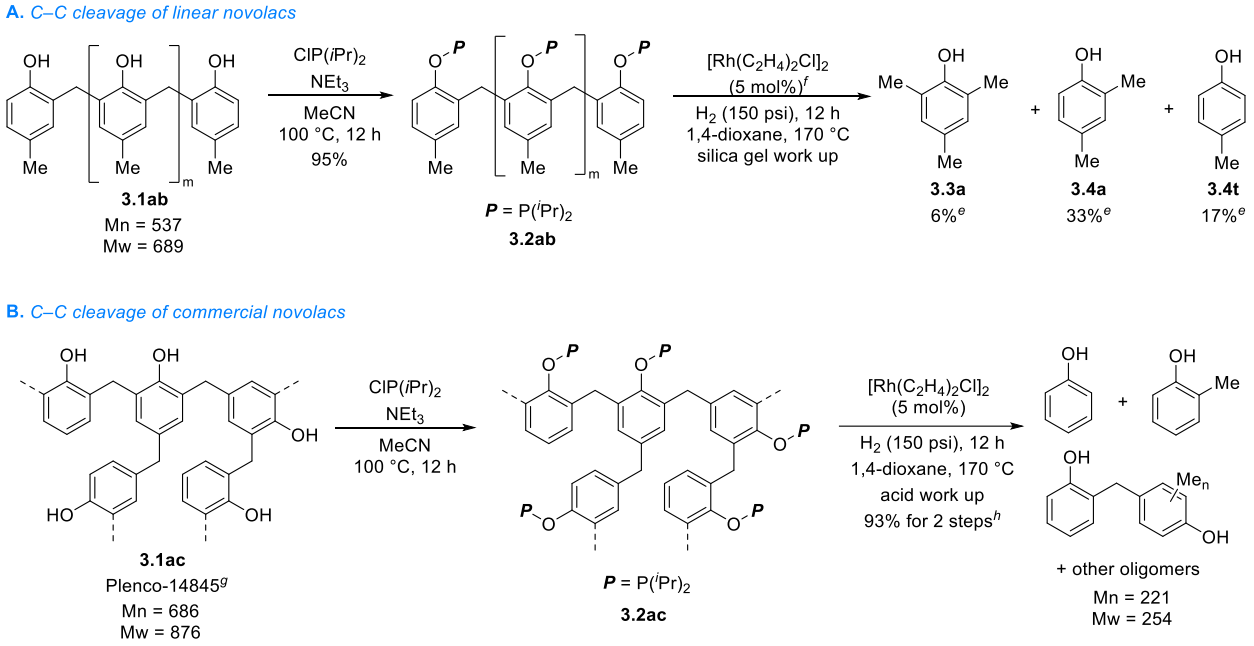


## 3.4. Mechanism Study

The mechanism for the Rh-catalyzed hydrogenolysis of 2,2'-methylenebiphenols was next explored. First, mixing 2,2'-methylenediphenol substrate **3.2g** with $[Rh(C_2H_4)_2Cl]_2$ at room temperature smoothly generated the corresponding complex [Rh(**3.2g**)Cl]$_2$ (Scheme 3.5), confirmed by X-ray crystallography (obtained by Dr. Jun Zhu), which suggests that bidentate coordination is indeed favorable and ligand substitution is facile in this system. Second, heating the mixture of **3.2g** and stoichiometric $RhH(PPh_3)_4$ or $RhCl(PPh_3)_3$ at 70 °C for 6 h afforded an orange solid (**3.5**) with C−H rhodation at the methylene position, showing that C−H activation of the methylene group is a relatively fast process.[10] The structure of complex **3.5** was unambiguously determined by X-ray crystallography (Scheme 3.6A, X-ray structure obtained by Dr. Jun Zhu). In addition, complex **3.5** was found to catalyze the desired C−C cleavage of **3.2g** efficiently (Scheme

3.6B), which indicates that either the C−H rhodation complex is an intermediate in the catalytic cycle or the C−H activation is a reversible but off-cycle process, similar to what was observed by Milstein and co-workers in the pincer system.[5b, 5c, 5g]

**Scheme 3.5.** Preparation of Intermediate [Rh(**3.2g**)Cl]$_2$.

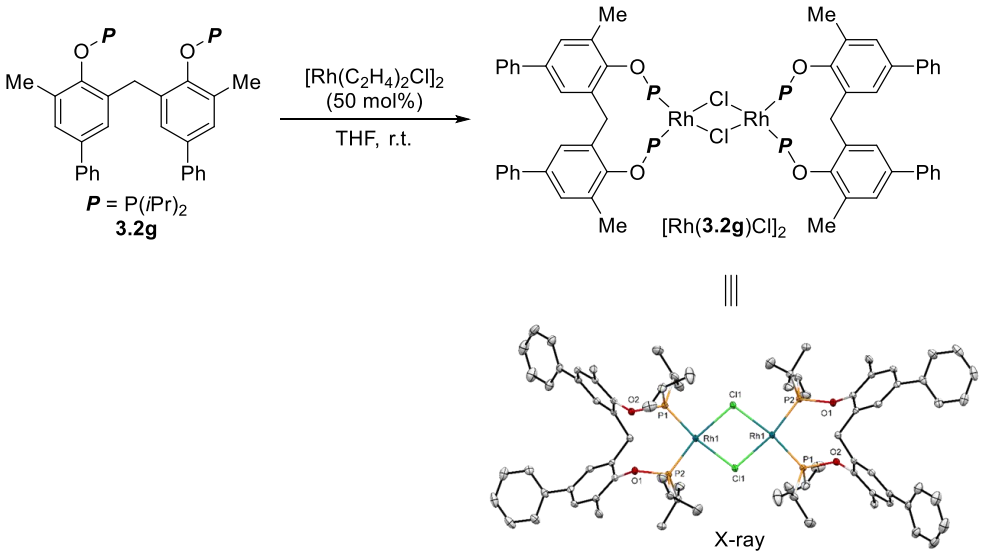

**Scheme 3.6.** Mechanism Studies on Complex **3.5**.

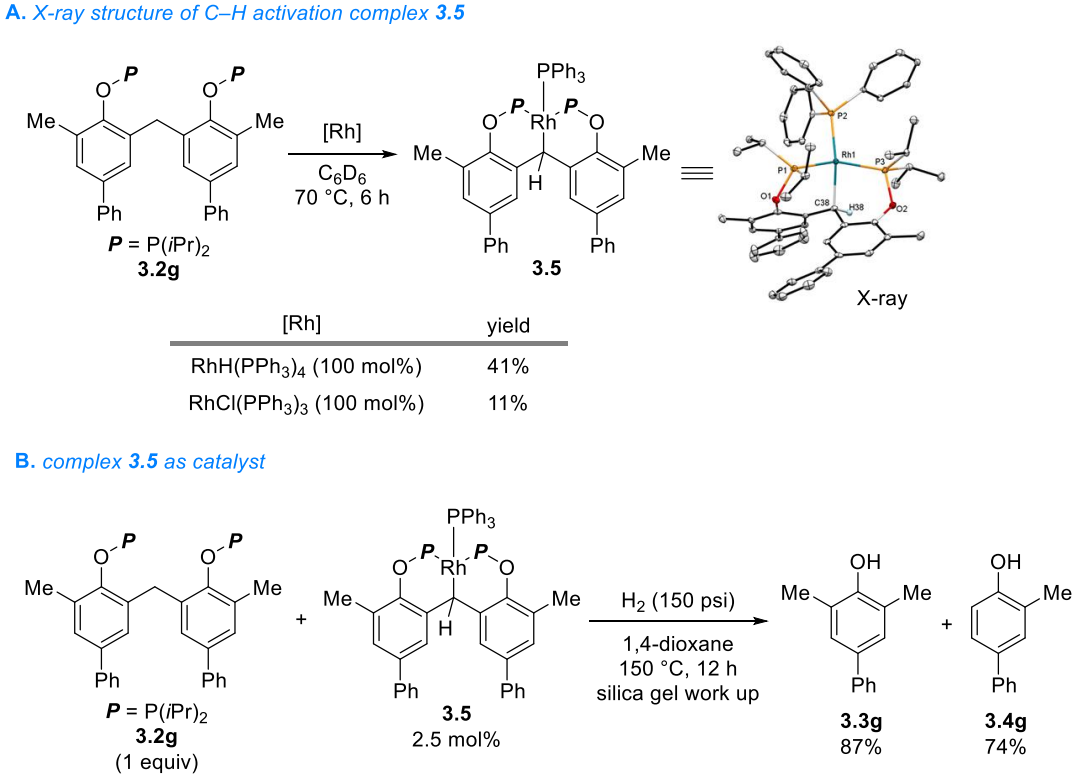


Moreover, running the catalytic reaction under 50 psi $D_2$ at 100 °C for 2 h afforded **3.3g-*d*** and **3.4g-*d*** in 40% and 42% yield, respectively (Scheme 3.7). Based on the NMR analysis, deuterium incorporation on the ortho-methyl of **3.3g-*d*** and the ortho hydrogen of **3.4g-*d*** were 91% and 90%, respectively, which suggests that H/D exchange on the methylene group is likely faster than the C−C activation process. Notably, the original methyl group in **3.3g-*d*** stayed untouched, indicating that the mono phosphinite-directed C−H activation was slower and less competitive than the C−C activation. The low deuteration ratio of the methylene group in recovered **3.1g** implies that (a) the C−H activation is indeed reversible and (b) ligand exchange between substrates is relatively slow.

**Scheme 3.7.** Deuterium Labeling.

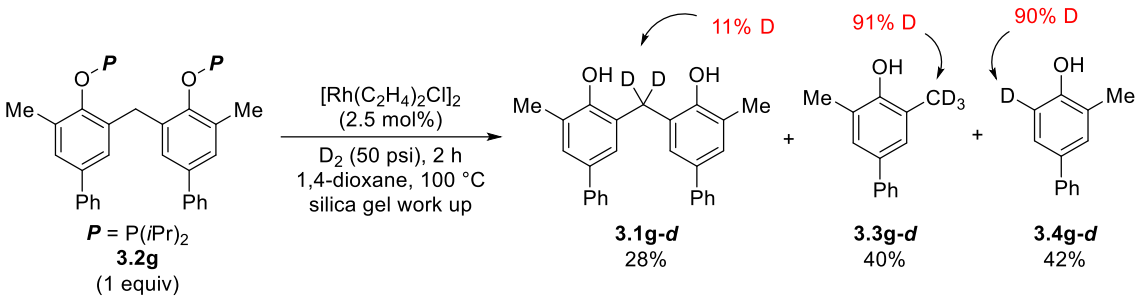


On the other hand, when a significantly higher loading of the rhodium catalyst was used, the yield of products **3.3a** and **3.4a** dropped to different extents; however, the high yield can be restored by adding a base (Table 3.4). According to our prior study,[8b] this observation suggests that a small amount of acid (HCl) may be generated, likely through catalyst activation by $H_2$ (*vide infra*). Finally, kinetic studies were conducted. Considering that the reaction proceeds too fast at the optimal temperature (150 °C), kinetic orders of the reactants were measured at a lower temperature (120 °C) in benzene-d6, and the initial rate method was applied (Scheme 3.8, conducted by Dr. Jun Zhu). The reaction was found to exhibit first-order dependence on the concentration of $[Rh(C_2H_4)_2Cl]_2$, zero-order dependence on the concentration of **3.2a** (0.0375 M – 0.100 M), and first-order dependence on the pressure of $H_2$. These results are consistent with the prior observations on the fast/strong binding between the substrate and the catalyst. Besides, the Hammett plot analysis shown the electron-deficient substituents on arene can promote the reaction, which support that the C−C bond oxidative addition can be included in rate-determine step.

**Table 3.4.** High Catalyst Loading Experiment.

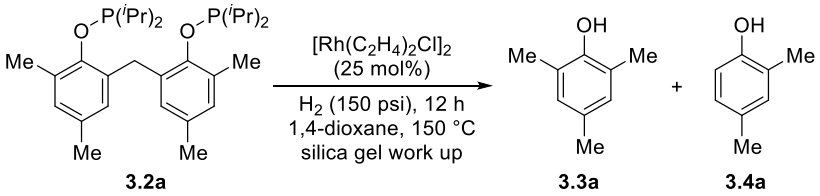


**3.2a** **3.3a** **3.4a**

| | 3.3a | 3.4a |
|---|---|---|
| without NaH | 85% | 65% |
| with NaH (1 equiv) | 87% | 84% |
| From Table 1, [Rh] (2.5 mol%) | 87% | 85% |

**Scheme 3.8.** Kenetic Order Measurement.

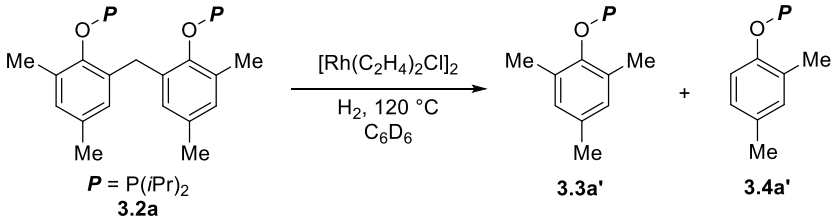


| | |
|---|---|
| **3.2a**: | Zero order |
| $[Rh(C_2H_4)_2Cl]_2$: | First order |
| $H_2$ pressure: | First order |

With the above mechanistic information in hand, at least two distinct pathways could be possible for the Rh-catalyzed hydrogenolysis of 2,2'-methylenebiphenols (Scheme 3.9 and 3.10). Based on our previous mechanistic study on the catalytic activation of aryl−aryl bonds in 2,2'-biphenols,[8b] a similar Rh-hydride-mediated "oxidative addition" catalytic cycle (path A, Scheme 3.9) can be proposed. In this proposal, the initially formed Rh−Cl complex was first converted to a Rh−H species by $H_2$, which then undergoes oxidative addition with the C(aryl)−C(alkyl) bond to give a 5/6 spiro rhodacycle (**3.8**). The subsequent C−H reductive elimination generated one monomer coordinating to the metal center (**3.9**). The following oxidative addition with $H_2$ and another C−H reductive elimination afforded another monomer with regeneration of the Rh−H catalyst. Alternatively, the catalytic cycle may involve rhodium carbene formation (path B, Scheme 3.10). Directed activation of the benzylic methylene linker would afford the fused 6,6-rhodacyle **3.7**, which could hypothetically undergo $\alpha$-aryl elimination[13] to deliver the 5,6-spiro rhodacycle

**3.12**. The subsequent C−H reductive elimination would generate one monomer, and the carbene species **3.13** could further react with $H_2$ to form the other monomer and close the catalytic cycle.

**Scheme 3.9.** Proposed Catalytic Cycles and Computed Energies (Path A).

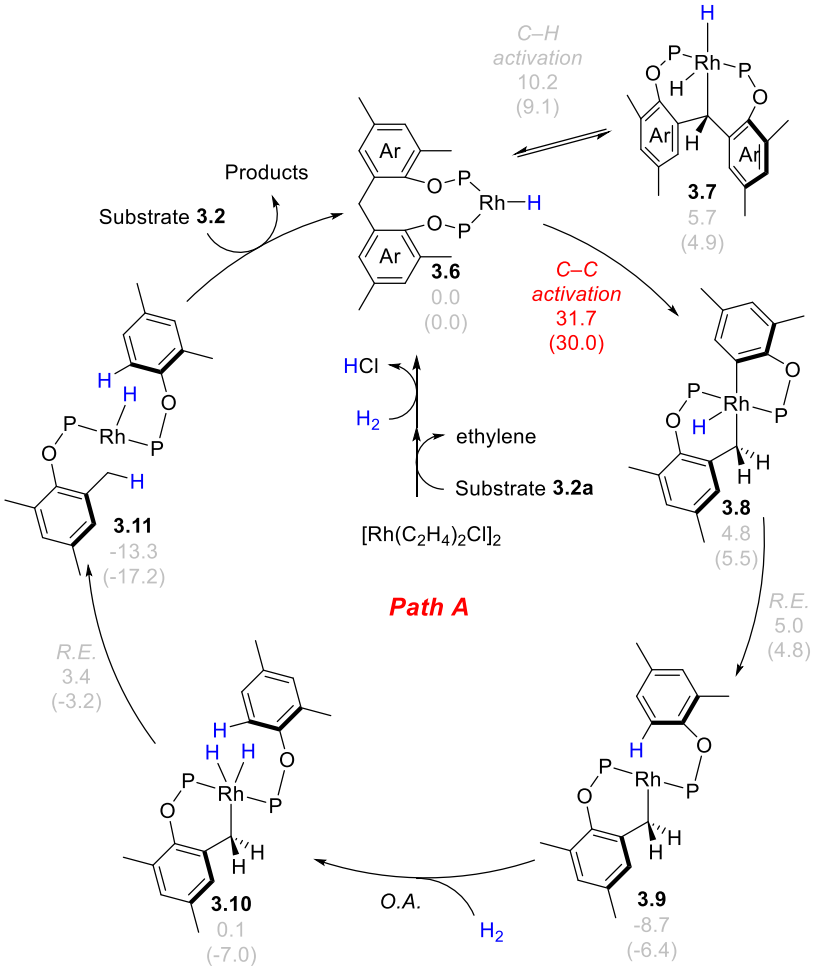

**Scheme 3.10.** Proposed Catalytic Cycles and Computed Energies (Path B).

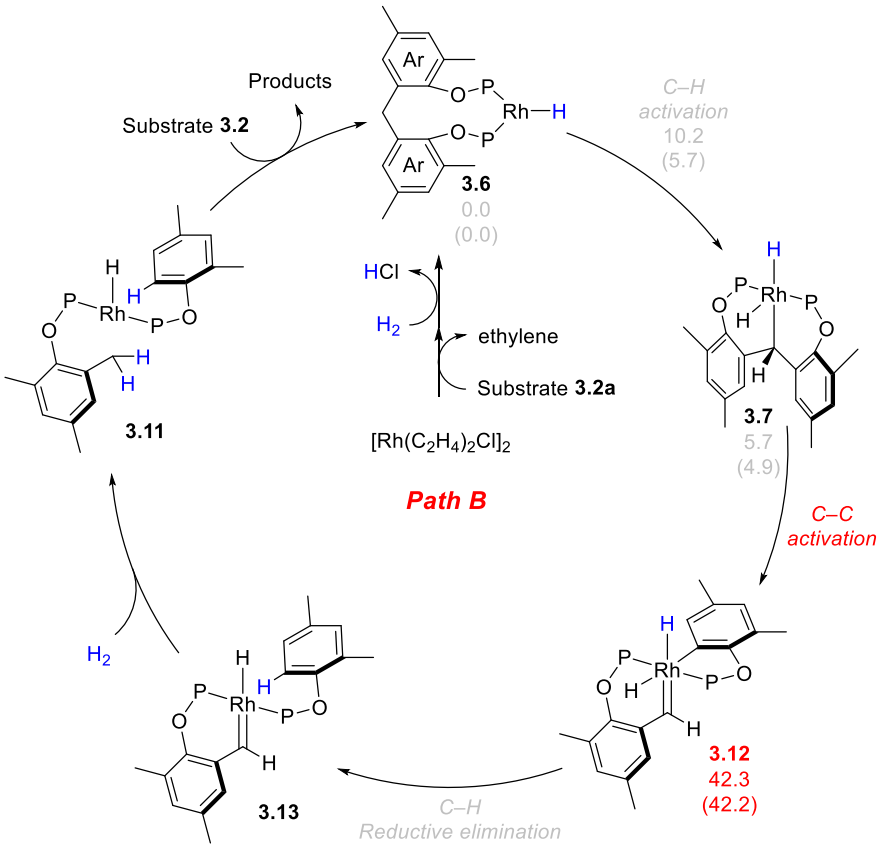


To differentiate these two mechanisms, a density functional theory (DFT) study was carried out (DFT calculation is conducted by Mr. Rui Zhang). As shown in Scheme 3.9, in Path A the direct C−C activation of **6** requires an activation barrier of 31.7 kcal/mol and is the turnover-limiting step (TLS). The subsequent two C−H reductive eliminations and $H_2$ coordination are facile and the whole process is exothermic by 16.0 kcal/mol. Compared with the C−C activation step, the methylene C–H activation has a much lower barrier (10.2 kcal/mol). However, as shown in Path B (Scheme 10), the following C−C activation of intermediate **3.7** via $\alpha$-aryl elimination is strongly disfavored, and the proposed carbene intermediate **3.12** appears to be highly unstable (42.3 kcal/mol uphill). Therefore, Path B is expected to be much less favorable than Path A. The isolation of the C−H activation product **3.5** (with additional ligands, see Scheme 3.3B) could be

attributed to the reversible nature of the C−H activation step, which is consistent with the experimentally observed H/D exchange in Scheme 3.3D. In addition, the DFT results correlate well with the kinetic data that support the C−C activation step being the TLS in Path A. Note that an alternative pathway involving Rh(I)−Cl-mediated direct oxidative addition into the C−C bond cannot be excluded at this stage.

### 3.5. Conclusion

In summary, we have developed the rhodium-catalyzed activation of nonpolar and unstrained C(aryl)−C(alkyl) bonds in 2,2'-methylenediphenols through the RDG strategy. Hydrogen is used as the reductant and mono phenols are generated as the products. The reaction exhibits good functional group tolerance and a broader substrate scope than the activation of the prior biaryl systems. It is also readily scalable and can be operated with a low catalyst loading, which is benefited from forming less coordinative products. Notably, initial promising results have been obtained on the catalytic hydrogenolysis of the methylene linkages in phenolic resins, such as linear or commercial novolacs, using this method. Given that this has been an underexplored area, the efficiency and practicality of this approach remain to be further improved. The detailed mechanistic study reveals a pathway involving direct oxidative addition of Rh(I) into the C(aryl)−C(alkyl) bond with the methylene C−H activation being a competitive but reversible side-reaction. The knowledge gained on the RDG-enabled 5/6 spirocyclic metallocycle formation could have various implications for activation of other inert C−C bonds beyond this work. Efforts on extending the reaction to substrates other than 2,2'-methylenediphenols are ongoing.

(Some contents of this chapter were published in *J. Am. Chem. Soc.* **2022**, DOI: 10.1021/jacs.1c13342)

### 3.6. Experimental

Unless noted otherwise, all solvents were dried by filtration through a Pure-Solv MD-5 Solvent Purification System (Innovative Technology), all reactions were carried out under nitrogen atmosphere, all commercially available substrates were used without further purification. Thin layer chromatography (TLC) analysis was run on silica gel plates purchased from EMD Chemical (silica gel 60, F254). Infrared spectrum was recorded on a Nicolet iS5 FT-IR Spectrometer. Samples were scanned as neat liquids or dissolved in dichloromethane on potassium bromide (KBr) salt plates. Frequencies were reported in reciprocal centimeters ($cm^{-1}$). High-resolution mass spectra (HRMS) were obtained on an Agilent 6224 TOF-MS spectrometer and were reported for the molecular ion $[M]^+$, $[M+Na]^+$, or $[M+H]^+$. MALDI-TOF mass spectra were obtained on a Bruker Ultraflextreme MALDI-Tof-Tof. X-ray diffraction data were collected at 100(2) K on a Bruker-Nonius Kappa CCD or Agilent SuperNova AtlasS2 CCD. Nuclear magnetic resonance (NMR) spectrum ($^1H$ NMR and $^{13}C$ NMR) were recorded with a 400 MHz Bruker Avance-III-HD nanobay spectrometer equipped with a BBFO SmartProbe (400 MHz for $^1H$, 101 MHz for $^{13}C$) or a 500 MHz Bruker Avance-III spectrometer equipped with a $^1H$ ($^{13}C$,$^{31}P$) TXI probe (500 MHz for $^1H$, 126 MHz for $^{13}C$). For $CDCl_3$ solutions, the chemical shifts were reported as parts per million (ppm) referenced to residual protium or carbon of the solvents: $CHCl_3$ δ H (7.26 ppm) and $CDCl_3$ δ C (77.00 ppm). For benzene-D6 solutions, the chemical shifts were reported as parts per million (ppm) referenced to residual protium or carbon of the solvents: acetone-D6 δ H (7.16 ppm) and acetone-D6 δ C (128.06 ppm). Coupling constants were reported in Hertz (Hz). Data for $^1H$ NMR

spectra were reported as following: chemical shift (δ, ppm), multiplicity (br = broad, s = singlet, d = doublet, t = triplet, q = quartet, dd = doublet of doublets, td = triplet of doublets, ddd = doublet of doublet of doublets, m = multiplet), coupling constant (Hz), and integration.

*General procedure for preparation of phenol **3.4***

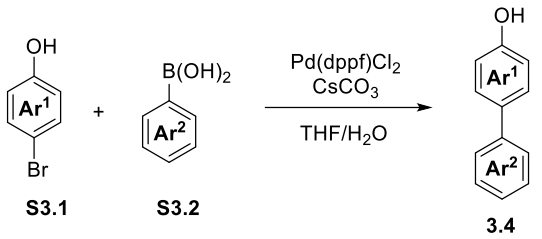


**General procedure:** To a solution of phenol **S3.1** (1 equiv) in THF (~50 mL/25 mmol), boronic acid **S3.2** (1.5 equiv), Pd(dppf)$Cl_2$ (1 mol%), $Cs_2CO_3$ (2 equiv) and $H_2O$ (~25 mmol/20 mL) were added at room temperature. The reaction mixture was then heated to reflux. After refluxing for 12 h, the reaction mixture was quenched with HCl (1 M in $H_2O$) and extracted with dichloromethane (3 times). The organic phase was dried with $Na_2SO_4$ and concentrated under reduced pressure. The mixture was purified by column chromatography (silica gel) to give pure compound **3.4**.

*Preparation of compound **3.4i***

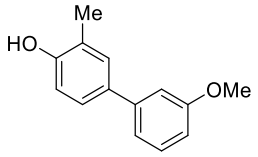


**3.4i**

4-Bromo-2-methylphenol (5.0 g) and 3-methoxyphenylboronic acid (6.09 g) was subjected to the general procedure to afford 3.8 g of **3.4i** with 67% yield as a colorless oil.

Analytical data see below.

*Preparation of compound **3.4j***

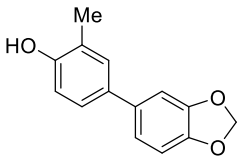


**3.4j**

4-Bromo-2-methylphenol (5.0 g) and 3,4-(Methylenedioxy)phenylboronic acid (6.65 g) was subjected to the general procedure to afford 4.0 g of **3.4j** with 66% yield as a white solid.

Analytical data see below.

*Preparation of compound **3.4l***

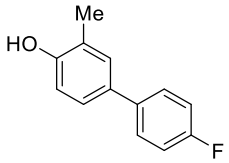


**3.4l**

4-Bromo-2-methylphenol (5.0 g) and 4-fluorophenylboronic acid (5.61 g) was subjected to the general procedure to afford 4.5 g of **3.4l** with 83% yield as a white solid.

Analytical data see below.

*Preparation of compound **3.4n***

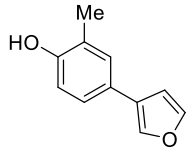


**3.4n**

4-Bromo-2-methylphenol (3.5 g) and 3-furanylboronic acid (3.14 g) was subjected to the general procedure to afford 2.0 g of **3.4n** with 61% yield as a pale yellow solid.

Analytical data see below.

(Preparation of compounds **3.4i**, **3.4j**, **3.4l**, **3.4n** is conducted by Dr. Jun Zhu)

*General procedure for preparation of compound **3.1***

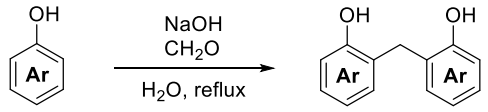


**3.4** **3.1**

**General procedure:** To a solution of NaOH (1.2 equiv) in $H_2O$ (1 mmol/mL), phenol **3.4** (1 equiv) and $CH_2O$ (37% in $H_2O$, 2.5 equiv) were added at room temperature, and the reaction mixture was then heated to reflux. After refluxing for 2 h, the reaction mixture was quenched with HCl (1 M in

$H_2O$) and extracted with dichloromethane (3 times). The organic phase was then dried with $Na_2SO_4$ and concentrated under reduced pressure. The mixture was purified by column chromatography (silica gel) to give compound **3.1**.

*Preparation of compound **3.1b***

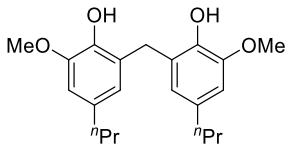


**3.1b**

2-Methoxy-4-propylphenol (5.0 g) was subjected to the general procedure and the product was purified by column chromatography (silica gel, hexane:ethyl acetate = 10:1) to afford 0.825 g of **3.1b** with 16% yield as a white solid.

**$R_f$** = 0.37 (hexane : ethyl acetate = 2:1)

**$^1$H NMR** (400 MHz, $CDCl_3$) δ 6.61 (d, *J* = 1.9 Hz, 2H), 6.54 (d, *J* = 2.0 Hz, 2H), 5.99 (s, 2H), 3.93 (s, 2H), 3.83 (s, 6H), 2.50 – 2.40 (m, 4H), 1.62 – 1.51 (m, 4H), 0.90 (t, *J* = 7.3 Hz, 6H).

**$^{13}$C NMR** (101 MHz, $CDCl_3$) δ 146.4, 141.0, 134.0, 126.1, 122.4, 109.1, 55.9, 37.8, 29.4, 24.8, 13.8.

**IR** (KBr) $\nu_{max}$ = 3267, 2957, 1593, 1501, 1464, 1295, 1141, 1067, 908, 842, 734 $cm^{-1}$.

**HRMS (MIX)** m/z calcd. for $C_{21}H_{27}O_4^-$ $[M-H]^-$: 343.1915, found 343.1932.

**Melting point**: 102.4 – 103.7 °C

*Preparation of compound **3.1c***

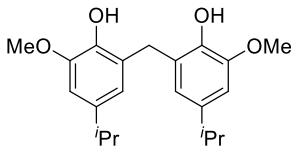


**3.1c**

4-Isopropyl-2-methoxyphenol[14] (5.0 g) was subjected to the general procedure and the product was purified by column chromatography (silica gel, hexane:ethyl acetate = 10:1) to afford 2.22 g of **3.1c** with 43% yield as a white solid.

**$R_f$** = 0.33 (hexane : ethyl acetate = 2:1)

**$^1$H NMR** (400 MHz, $CDCl_3$) δ 6.68 (d, *J* = 2.0 Hz, 2H), 6.59 (d, *J* = 2.0 Hz, 2H), 6.04 (s, 2H), 3.95 (s, 2H), 3.83 (s, 6H), 2.78 (hept, *J* = 6.9 Hz, 2H), 1.19 (d, *J* = 6.9 Hz, 12H).

**$^{13}$C NMR** (101 MHz, $CDCl_3$) δ 146.4, 141.1, 140.2, 126.1, 120.4, 107.1, 55.9, 33.8, 29.6, 24.2.

**IR** (KBr) $\nu_{max}$ = 3540, 2958, 1604, 1501, 1462, 1289, 1220, 1089, 947, 843 $cm^{-1}$.

**HRMS (ESI)** m/z calcd. for $C_{21}H_{27}O_4^-$ $[M-H]^-$: 343.1915, found 343.1934.

**Melting point**: 70.8 – 72.2 °C

*Preparation of compound **3.1d***

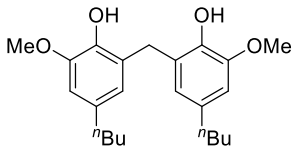


**3.1d**

4-butyl-2-methoxyphenol[8b] (3.0 g) was subjected to the general procedure and the product was purified by column chromatography (silica gel, hexane:ethyl acetate = 10:1) to afford 1.62 g of **3.1d** with 52% yield as a white solid.

**$R_f$** = 0.10 (hexane : ethyl acetate = 5:1)

**$^1$H NMR** (400 MHz, $CDCl_3$) δ 6.60 (d, *J* = 1.9 Hz, 2H), 6.54 (d, *J* = 1.9 Hz, 2H), 5.99 (s, 2H), 3.93 (s, 2H), 3.83 (s, 6H), 2.54 – 2.42 (m, 4H), 1.53 (tt, *J* = 9.1, 6.9 Hz, 4H), 1.32 (h, *J* = 7.3 Hz, 4H), 0.90 (t, *J* = 7.3 Hz, 6H).

**$^{13}$C NMR** (101 MHz, $CDCl_3$) δ 146.4, 141.0, 134.2, 126.1, 122.3, 109.1, 55.9, 35.4, 33.9, 29.4, 22.3, 13.9.

**IR** (KBr) $\nu_{max}$ = 3286, 2929, 1602, 1500, 1464, 1291, 1142, 1070, 909, 844, 733 $cm^{-1}$.

**HRMS (ESI)** molecular weight peak not found despite extensive efforts.

**Melting point**: 90.8 – 91.8 °C

*Preparation of compound **3.1e***

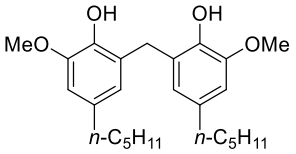


**3.1e**

2-Methoxy-4-pentylphenol[8b] (3.0 g) was subjected to the general procedure and the product was purified by column chromatography (silica gel, hexane:ethyl acetate = 10:1) to afford 1.70 g of **3.1e** with 55% yield as a white solid.

$\mathbf{R_f}$ = 0.17 (hexane : ethyl acetate = 5:1)

**$^1$H NMR** (400 MHz, $CDCl_3$) δ 6.61 (d, *J* = 1.9 Hz, 2H), 6.54 (d, *J* = 2.0 Hz, 2H), 6.00 (s, 2H), 3.93 (s, 2H), 3.83 (s, 6H), 2.52 – 2.42 (m, 4H), 1.54 (p, *J* = 7.4 Hz, 4H), 1.40 – 1.21 (m, 8H), 0.87 (t, *J* = 6.9 Hz, 6H).

**$^{13}$C NMR** (101 MHz, $CDCl_3$) δ 146.4, 141.0, 134.2, 126.1, 122.3, 109.1, 55.9, 35.6, 31.5, 31.4, 29.4, 22.5, 14.0.

**IR** (KBr) $\nu_{max}$ = 3544, 3289, 2928, 1603, 1500, 1464, 1290, 1141, 1071, 909, 734 $cm^{-1}$.

**HRMS (ESI)** molecular weight peak not found despite extensive efforts.

**Melting point**: 89.3 – 90.4 °C

*Preparation of compound **3.1g***

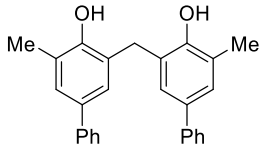


**3.1g**

3-Methyl-[1,1'-biphenyl]-4-ol[8b] (3.0 g) was subjected to the general procedure and the product was purified by column chromatography (silica gel, hexane:ethyl acetate = 10:1) to afford 1.3 g of **3.1g** with 42% yield as a white solid.

**$R_f$** = 0.38 (hexane : ethyl acetate = 2:1)

**$^1$H NMR** (400 MHz, $CDCl_3$) δ 7.54 – 7.47 (m, 4H), 7.43 – 7.35 (m, 6H), 7.31 – 7.25 (m, 2H), 7.24 – 7.20 (m, 2H), 6.16 (s, 2H), 4.05 (s, 2H), 2.30 (s, 6H).

**$^{13}$C NMR** (101 MHz, $CDCl_3$) δ 150.8, 140.9, 134.3, 128.6, 128.3, 127.2, 126.8, 126.6, 126.5, 124.3, 31.5, 16.2.

**IR** (KBr) $\nu_{max}$ = 3278, 3033, 1476, 1389, 1237, 1180, 763, 698 $cm^{-1}$.

**HRMS (ESI)** molecular weight peak not found despite extensive efforts.

**Melting point**: 146.5 – 147.7 °C

*Preparation of compound **3.1h***

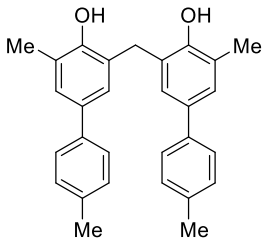


**3.1h**

3,4'-dimethyl-[1,1'-biphenyl]-4-ol[15] (3.0 g) was subjected to the general procedure and the product was purified by column chromatography (silica gel, hexane:ethyl acetate = 20:1) to afford 1.1 g of **3.1h** with 36% yield as a white solid.

**$R_f$** = 0.31 (hexane : ethyl acetate = 4:1)

**$^1$H NMR** (400 MHz, $CDCl_3$) δ 7.43 – 7.38 (m, 4H), 7.36 (d, *J* = 2.3 Hz, 2H), 7.23 – 7.14 (m, 6H), 6.20 (s, 2H), 4.03 (s, 2H), 2.36 (s, 6H), 2.28 (s, 6H).

**$^{13}$C NMR** (101 MHz, $CDCl_3$) δ 150.5, 138.1, 136.3, 134.2, 129.3, 128.1, 127.0, 126.7, 126.5, 124.3, 31.5, 21.0, 16.2.

**IR** (KBr) $\nu_{max}$ = 3279, 2919, 1478, 1378, 1210, 1181, 907, 819, 776, 731 $cm^{-1}$.

**HRMS (ESI)** molecular weight peak not found despite extensive efforts.

**Melting point**: 167.7 – 168.6 °C

*Preparation of compound **3.1i***

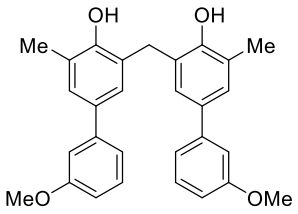


**3.1i**

3'-methoxy-3-methyl-[1,1'-biphenyl]-4-ol (**3.4i**, 3.0 g) was subjected to the general procedure and the product was purified by column chromatography (silica gel, hexane:ethyl acetate:dichloromethane = 7:1:1) to afford 1.73 g of **3.1i** with 56% yield as a white solid.

**$R_f$** = 0.29 (hexane : ethyl acetate = 7:1)

**$^1$H NMR** (400 MHz, $CDCl_3$) δ 7.37 (d, *J* = 2.3 Hz, 2H), 7.29 (t, *J* = 7.9 Hz, 2H), 7.24 – 7.17 (m, 2H), 7.12 – 7.06 (m, 2H), 7.03 (dd, *J* = 2.5, 1.6 Hz, 2H), 6.83 (ddd, *J* = 8.2, 2.6, 0.9 Hz, 2H), 6.36 (s, 2H), 4.03 (s, 2H), 3.83 (s, 6H), 2.26 (s, 6H).

**$^{13}$C NMR** (101 MHz, $CDCl_3$) δ 159.8, 150.8, 142.4, 134.1, 129.6, 128.2, 127.2, 126.6, 124.4, 119.4, 112.6, 112.0, 55.2, 31.4, 16.2.

**IR** (KBr) $\nu_{max}$ = 3399, 2939, 1600, 1579, 1478, 1230, 1164, 1048, 909, 777, 734 $cm^{-1}$.

**HRMS (ESI)** molecular weight peak not found despite extensive efforts.

**Melting point**: 136.2 – 137.3 °C

*Preparation of compound **3.1j***

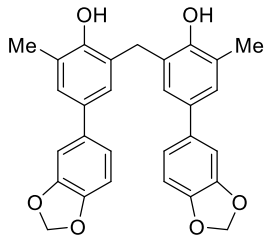


**3.1j**

4-(benzo[d][1,3]dioxol-5-yl)-2-methylphenol (**3.4j**, 3.0 g) was subjected to the general procedure and the product was purified by column chromatography (silica gel, hexane:acetone = 10:1) to afford 1.2 g of **3.1j** with 39% yield as a white solid.

$\mathbf{R}_f$ = 0.33 (hexane : ethyl acetate = 4:1)

**$^1$H NMR** (400 MHz, $CDCl_3$) δ 7.29 (d, *J* = 2.4 Hz, 2H), 7.17 – 7.12 (m, 2H), 6.98 (d, *J* = 1.8 Hz, 2H), 6.96 (dd, *J* = 8.0, 1.8 Hz, 2H), 6.84 (d, *J* = 8.0 Hz, 2H), 6.11 (s, 2H), 5.97 (s, 4H), 4.01 (s, 2H), 2.29 (s, 6H).

**$^{13}$C NMR** (101 MHz, $CDCl_3$) δ 150.5, 148.0, 146.6, 135.4, 134.0, 128.0, 127.0, 126.4, 124.3, 120.2, 108.5, 107.5, 101.0, 31.5, 16.2.

**IR** (KBr) $\nu_{max}$ = 3407, 2883, 1475, 1233, 1182, 1038, 931, 733 $cm^{-1}$.

**HRMS (ESI)** molecular weight peak not found despite extensive efforts.

**Melting point**: 192.9 – 193.8 °C

*Preparation of compound **3.1k***

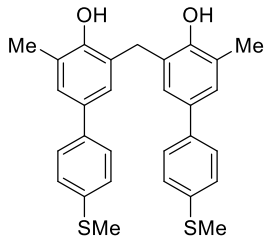


**3.1k**

3-methyl-4'-(methylthio)-[1,1'-biphenyl]-4-ol[8b] (2.0 g) was subjected to the general procedure and the product was purified by column chromatography (silica gel, hexane:acetone = 10:1) to afford 0.56 g of **3.1k** with 27% yield as a white solid.

**$R_f$** = 0.33 (hexane : ethyl acetate = 4:1)

**$^1$H NMR** (400 MHz, $CDCl_3$) δ 7.46 – 7.39 (m, 4H), 7.34 (d, *J* = 2.3 Hz, 2H), 7.28 (d, *J* = 8.3 Hz, 4H), 7.21 – 7.17 (m, 2H), 6.22 (s, 2H), 4.02 (s, 2H), 2.49 (s, 6H), 2.29 (s, 6H).

**$^{13}$C NMR** (101 MHz, $CDCl_3$) δ 150.7, 137.8, 136.7, 133.5, 128.0, 127.2, 127.1, 126.9, 126.5, 124.5, 31.4, 16.2, 16.1.

**IR** (KBr) $\nu_{max}$ = 3357, 2916, 1474, 1386, 1315, 1213, 1182, 1074, 908, 823, 776, 732 $cm^{-1}$.

**HRMS (ESI)** molecular weight peak not found despite extensive efforts.

*Preparation of compound **3.1l***

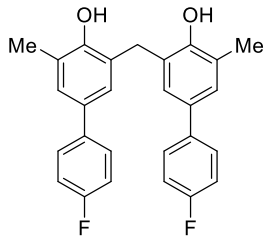


**3.1l**

4'-Fluoro-3-methyl-[1,1'-biphenyl]-4-ol (**3.4l**, 3.0 g) was subjected to the general procedure and the product was purified by column chromatography (silica gel, hexane:ethyl acetate:dichloromethane = 7:1:1) to afford 1.43 g of **3.1l** with 46% yield as a white solid.

**$R_f$** = 0.28 (hexane : ethyl acetate = 7:1)

**$^1$H NMR** (400 MHz, DMSO) δ 8.68 (s, 2H), 7.61 – 7.45 (m, 4H), 7.30 – 7.14 (m, 8H), 3.99 (s, 2H), 2.24 (s, 6H).

**$^{13}$C NMR** (101 MHz, DMSO) δ 162.2 (d, *J* = 242.9 Hz), 152.4, 137.0 (d, *J* = 3.0 Hz), 130.4, 128.1, 127.8 (d, *J* = 8.0 Hz), 126.9, 126.2, 124.9, 115.4 (d, *J* = 21.2 Hz), 30.6, 16.9.

**$^{19}$F NMR** (376 MHz, DMSO) δ -117.1.

**IR** (KBr) $\nu_{max}$ = 3253, 1601, 1514, 1478, 1389, 1218, 1160, 1097, 835, 776 $cm^{-1}$.

**HRMS (ESI)** molecular weight peak not found despite extensive efforts.

**Melting point**: 166.0 – 166.7 °C

*Preparation of compound **3.1m***

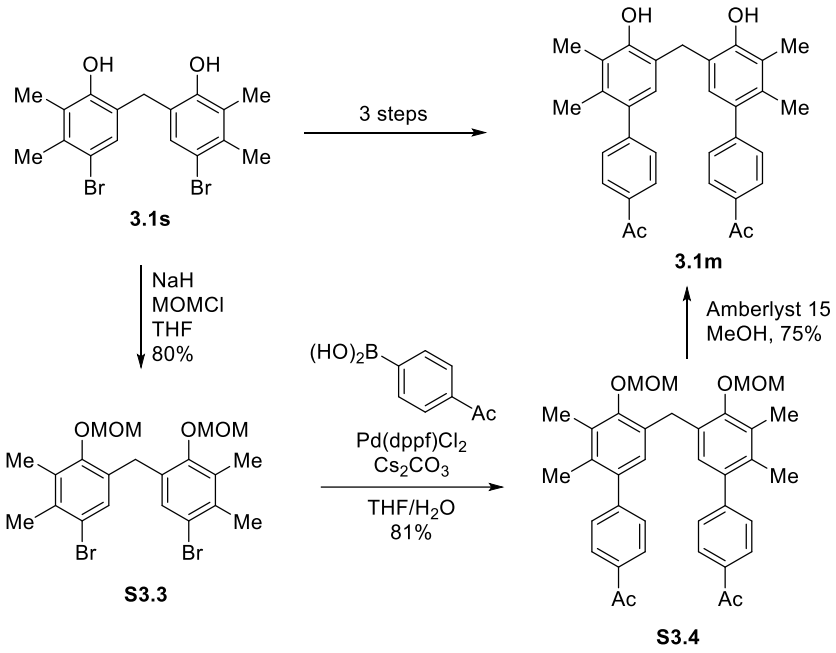


To a solution of compound **3.1s** (1.0 g, 2.4 mmol, see entry *Preparation of compound **3.1s*** for preparation) in THF (20 mL), NaH (60 % dispersion in mineral oil, 242 mg, 6.0 mmol) was added at 0 °C. After being stirred at 0 °C for 30 min, chloromethyl methyl ether (0.46 mL, 6.0 mmol) was added to the reaction mixture. After being stirred at room temperature for 12 h, the reaction mixture was quenched with $NH_4Cl$ (saturated in $H_2O$, 20 mL) and extracted with ethyl acetate (20 mL×3). The organic phase was then dried with $Na_2SO_4$ and concentrated under reduced pressure. The mixture was purified by column chromatography (silica gel, hexane:ethyl acetate = 20:1) to give compound **S3.3** (0.97 g, 80% yield).

To a solution of compound **S3.3** (1.2 g, 2.39 mmol) in THF (9 mL), 4-acetylphenylboronic acid (1.18 g, 7.17 mmol), $Pd(dppf)Cl_2$ (97.6 mg, 0.12 mmol), $Cs_2CO_3$ (2.34 g, 7.17 mmol) and $H_2O$ (1 mL) were added at room temperature, and the reaction mixture was then heated to 90 °C. After being stirred at 90 °C for 12 h, the reaction mixture was quenched with HCl (1 M in $H_2O$, 5 mL) and extracted with dichloromethane (5 mL×3). The organic phase was then dried with $Na_2SO_4$ and

concentrated under reduced pressure. The mixture was purified by column chromatography (silica gel, hexane:ethyl acetate = 20:1) to give compound **S3.4** (1.1 g, 81% yield).

To a solution of compound **S3.4** (1.1 g, 1.9 mmol) in methanol (20 mL), Amberlyst 15 (0.93 g) was added at room temperature, and the reaction mixture was then heated to reflux. After refluxing for 3 h, the reaction mixture was filtered through Celite, then dried with $Na_2SO_4$ and concentrated under reduced pressure. The mixture was purified by column chromatography (silica gel, hexane:ethyl acetate = 10:1) to give compound **3.1m** (0.70 g, 75% yield) as a white solid.

$\mathbf{R_f}$ = 0.13 (hexane : ethyl acetate = 2:1)

**$^1$H NMR** (400 MHz, $CDCl_3$) δ 8.05 – 7.88 (m, 4H), 7.38 – 7.28 (m, 4H), 6.99 (s, 2H), 6.41 (s, 2H), 3.96 (s, 2H), 2.63 (s, 6H), 2.24 (s, 6H), 2.12 (s, 6H).

**$^{13}$C NMR** (101 MHz, $CDCl_3$) δ 197.9, 150.7, 147.5, 135.2, 134.3, 133.7, 129.9, 128.8, 128.1, 123.8, 123.4, 31.3, 26.6, 17.5, 12.5.

**IR** (KBr) $\nu_{max}$ = 3314, 1667, 1601, 1475, 1355, 1268, 1182, 1090, 959, 836, 732 $cm^{-1}$.

**HRMS (ESI)** m/z calcd. for $C_{33}H_{31}O_4^-$ $[M-H]^-$: 491.2228, found 491.2237.

**Melting point**: decomposed while heating.

*Preparation of compound **3.1n***

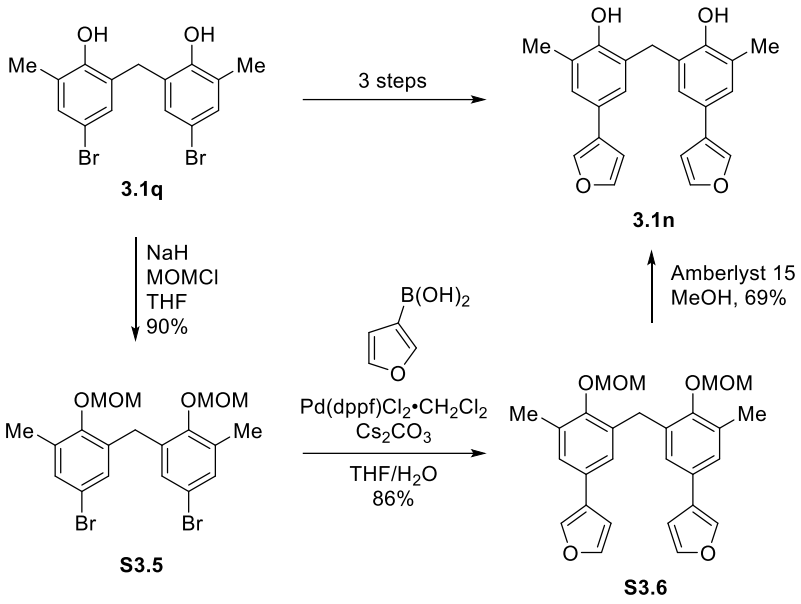


To a solution of compound **3.1q** (1.0 g, 2.6 mmol, see entry *Preparation of compound **3.1q*** for preparation) in THF (20 mL), NaH (60 % dispersion in mineral oil, 260 mg, 6.5 mmol) was added at 0 °C. After being stirred at 0 °C for 30 min, chloromethyl methyl ether (0.50 mL, 6.5 mmol) was added to the reaction mixture. After being stirred at room temperature for 12 h, the reaction mixture was quenched with $NH_4Cl$ (saturated in $H_2O$, 20 mL) and extracted with ethyl acetate (20 mL×3). The organic phase was then dried with $Na_2SO_4$ and concentrated under reduced pressure. The mixture was purified by column chromatography (silica gel, hexane:ethyl acetate = 20:1) to give compound **S3.5** (1.10 g, 90% yield).

To a solution of compound **S3.5** (2.0 g, 4.22 mmol) in THF (8 mL), 3-furanylboronic acid (1.42 g, 12.7 mmol), $Pd(dppf)Cl_2 \cdot CH_2Cl_2$ (172 mg, 0.21 mmol), $Cs_2CO_3$ (4.12 g, 12.65 mmol) and $H_2O$ (2 mL) was added at room temperature, and the reaction mixture was then heated to 90 °C. After being stirred at 90 °C for 12 h, the reaction mixture was quenched with HCl (1 M in $H_2O$, 5 mL) and extracted with dichloromethane (5 mL×3). The organic phase was then dried with $Na_2SO_4$ and

concentrated under reduced pressure. The mixture was purified by column chromatography (silica gel, hexane:ethyl acetate = 20:1) to give compound **S3.6** (1.62 g, 86% yield).

To a solution of compound **S3.6** (1.62 g, 3.61 mmol) in methanol (36 mL), Amberlyst 15 (1.77 g) was added at room temperature, and the reaction mixture was then heated to reflux. After refluxing for 3 h, the reaction mixture was filtered though Celite, then dried with $Na_2SO_4$ and concentrated under reduced pressure. The mixture was purified by column chromatography (silica gel, hexane:ethyl acetate = 20:1) to give compound **3.1n** (1.05 g, 69% yield) as a white solid.

$\mathbf{R_f}$ = 0.33 (hexane : ethyl acetate = 2:1)

**$^1$H NMR** (400 MHz, $CDCl_3$) δ 7.68 – 7.58 (m, 2H), 7.43 (t, *J* = 1.7 Hz, 2H), 7.25 – 7.22 (m, 2H), 7.15 – 7.10 (m, 2H), 6.62 (dd, *J* = 1.9, 0.9 Hz, 2H), 6.06 (s, 2H), 3.96 (s, 2H), 2.26 (s, 6H).

**$^{13}$C NMR** (101 MHz, $CDCl_3$) δ 150.4, 143.4, 137.7, 127.2, 126.4, 126.1, 126.0, 125.4, 124.5, 109.0, 31.3, 16.1.

**IR** (KBr) $\nu_{max}$ = 3433, 3296, 1507, 1480, 1454, 1316, 1191, 1159, 1108, 1022, 873, 776 $cm^{-1}$.

**HRMS (ESI)** m/z calcd. for $C_{23}H_{19}O_4^-$ $[M-H]^-$: 359.1289, found 359.1304.

**Melting point**: 174.9 – 176.0 °C.

*Preparation of compound **3.1o***

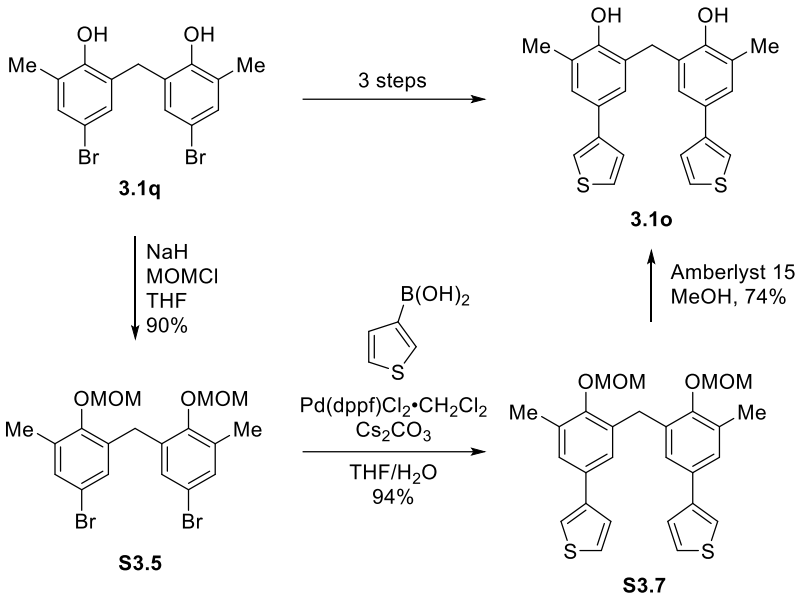


To a solution of compound **S3.5** (2.0 g, 4.22 mmol, see entry *Preparation of compound **3.1n*** for preparation) in THF (8 mL), 3-thienylboronic acid (1.62 g, 12.7 mmol), Pd(dppf)$Cl_2$·$CH_2Cl_2$ (172 mg, 0.21 mmol), $Cs_2CO_3$ (4.12 g, 12.65 mmol) and $H_2O$ (2 mL) was added at room temperature, and the reaction mixture was then heated to 90 °C. After being stirred at 90 °C for 12 h, the reaction mixture was quenched with HCl (1 M in $H_2O$, 5 mL) and extracted with dichloromethane (5 mL×3). The organic phase was then dried with $Na_2SO_4$ and concentrated under reduced pressure. The mixture was purified by column chromatography (silica gel, hexane:ethyl acetate = 20:1) to give compound **S3.7** (1.9 g, 94% yield).

To a solution of compound **S3.7** (1.9 g, 3.95 mmol) in methanol (40 mL), Amberlyst 15 (1.94 g) was added at room temperature, and the reaction mixture was then heated to reflux. After refluxing for 3 h, the reaction mixture was filtered through Celite, then dried with $Na_2SO_4$ and concentrated under reduced pressure. The mixture was purified by column chromatography (silica gel, hexane:ethyl acetate = 20:1) to give compound **3.1o** (1.22 g, 74% yield) as a white solid.

**$R_f$** = 0.36 (hexane : ethyl acetate = 2:1)

**$^1$H NMR** (400 MHz, $CDCl_3$) δ 7.36 (d, *J* = 2.2 Hz, 2H), 7.33 (d, *J* = 3.8 Hz, 2H), 7.31 – 7.20 (m, 6H), 6.10 (s, 2H), 3.99 (s, 2H), 2.27 (s, 6H).

**$^{13}$C NMR** (101 MHz, $CDCl_3$) δ 150.5, 142.1, 129.1, 127.7, 126.6, 126.4, 125.9, 124.4, 119.1, 31.4, 16.1.

**IR** (KBr) $\nu_{max}$ = 3416, 1482, 1354, 1230, 1188, 1165, 773 729 $cm^{-1}$.

**HRMS (ESI)** m/z calcd. for $C_{23}H_{19}O_2S_2^-$ $[M-H]^-$: 391.0832, found 391.0864.

**Melting point**: 177.8 – 178.7 °C.

*Preparation of compound **3.1p***

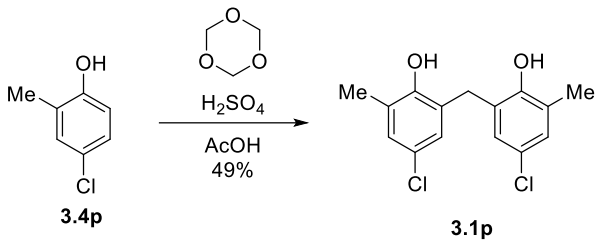


Compound **3.1p** was prepared following literature reported procedure.[16] 4-Chloro-2-methylphenol (7.13 g) was subjected to the reported procedure to afford 3.5 g of **3.1p** with 49% yield as a white solid.

**$R_f$** = 0.38 (hexane : ethyl acetate = 2:1)

**$^1$H NMR** (400 MHz, $CDCl_3$) δ 7.07 (d, $J$ = 2.6 Hz, 2H), 7.02 – 6.95 (m, 2H), 5.90 (s, 2H), 3.83 (s, 2H), 2.21 (s, 6H).

**$^{13}$C NMR** (101 MHz, $CDCl_3$) δ 149.7, 129.1, 128.0, 127.2, 125.7, 125.5, 30.6, 16.0.

**IR** (KBr) $\nu_{max}$ = 3328, 1473, 1443, 1379, 1266, 1215, 949, 861, 776 $cm^{-1}$.

**HRMS (ESI)** m/z calcd. for $C_{15}H_{13}Cl_2O_2^-$ $[M-H]^-$: 295.0298, found 295.0303.

**Melting point**: decomposed while heating.

*Preparation of compound **3.1q***

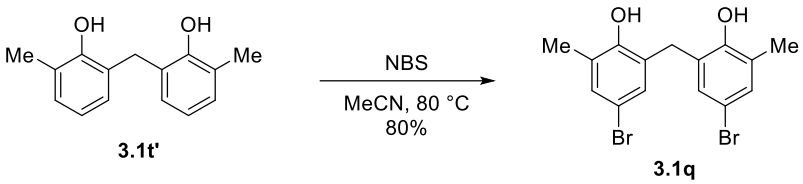


To a solution of compound **3.1t'**[17] (4.0 g, 17.5 mmol) in MeCN (100 mL), *N*-bromosuccinimide (6.39 g, 35.9 mmol) was added at 0 °C, and the reaction mixture was then heated to 80 °C. After being stirred at 80 °C for 2 h, the reaction mixture was cooled to room temperature, quenched with $Na_2S_2O_3$ (saturated in $H_2O$, 50 mL), and extracted with ethyl acetate (100 mL×3). The organic phase was then dried with $Na_2SO_4$ and concentrated under reduced pressure. The mixture was purified by column chromatography (silica gel, hexane:ethyl acetate = 10:1) to give compound **3.1q** (5.4 g, 80% yield) as a white solid.

**$R_f$** = 0.70 (hexane : ethyl acetate = 2:1)

**$^1$H NMR** (400 MHz, $CDCl_3$) δ 7.20 – 7.10 (m, 2H), 6.91 (d, $J$ = 2.1 Hz, 2H), 5.95 (s, 2H), 3.94 (s, 2H), 2.22 (s, 6H).

**$^{13}$C NMR** (101 MHz, $CDCl_3$) δ 147.6, 131.3, 130.7, 130.6, 127.2, 110.2, 31.3, 20.3.

**IR** (KBr) $\nu_{max}$ = 3281, 1476, 1449, 1274, 1206, 1175, 1155, 1106, 921, 859, 826, 753 $cm^{-1}$.

**HRMS (ESI)** m/z calcd. for $C_{15}H_{13}{}^{79}Br^{81}BrO_2^-$ $[M-H]^-$: 384.9267, found 384.9288.

**Melting point**: 156.7 – 157.8 °C

*Preparation of compound **3.1r***

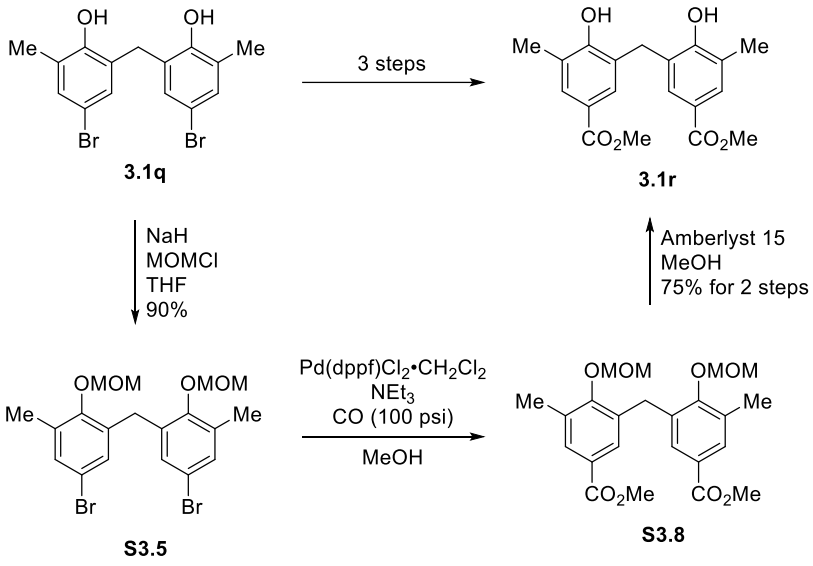


To a flame-dried Q-tube, compound **S3.5** (2.0 g, 4.22 mmol, see entry *Preparation of compound **3.1n*** for preparation), $Pd(dppf)Cl_2 \cdot CH_2Cl_2$ (172 mg, 0.21 mmol), triethyl amine (1.8 mL, 12.66 mmol) and MeOH (20 mL) was added at room temperature. The reaction vessel was then charged with 100 psi CO and heated to 100 °C. After being stirred at 100 °C for 12 h, the reaction mixture

was filtered through Celite, and the solution was concentrated under reduced pressure. The mixture was purified by column chromatography (silica gel, hexane:ethyl acetate = 4:1) to give compound **S3.8.**

To a solution of compound **S3.8** (previous step obtained) in methanol (30 mL), Amberlyst 15 (1.5 g) was added at room temperature, and the reaction mixture was then heated to reflux. After refluxing for 3 h, the reaction mixture was filtered through Celite, then concentrated under reduced pressure and purified by recrystallization (methanol) to give compound **3.1r** (1.1 g, 75% yield for 2 steps) as a white solid.

**$R_f$** = 0.22 (hexane : ethyl acetate = 2:1)

**$^1$H NMR** (500 MHz, DMSO) δ 9.38 (s, 2H), 7.60 (d, *J* = 2.3 Hz, 2H), 7.49 (d, *J* = 2.3 Hz, 2H), 3.94 (s, 2H), 3.74 (s, 6H), 2.22 (s, 6H).

**$^{13}$C NMR** (126 MHz, DMSO) δ 166.3, 157.8, 130.2, 129.5, 127.1, 124.4, 120.2, 51.6, 30.1, 16.7.

**IR** (KBr) $\nu_{max}$ = 3409, 1681, 1594, 1446, 1322, 1305, 1264, 1205, 768 $cm^{-1}$.

**HRMS (ESI)** m/z calcd. for $C_{19}H_{19}O_6^-$ $[M-H]^-$: 343.1187, found 343.1213.

**Melting point**: decomposed while heating.

*Preparation of compound **3.1s***

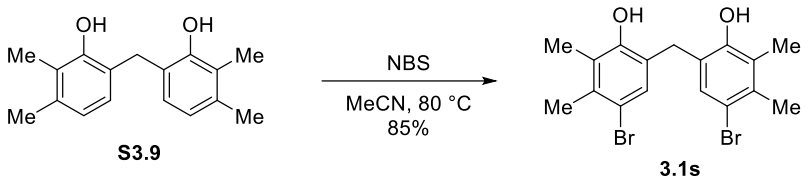


To a solution of compound **S3.9**[18] (3.0 g, 11.7 mmol) in MeCN (30 mL), *N*-bromosuccinimide (4.37 g, 24.6 mmol) was added at 0 °C, and the reaction mixture was then heated to 80 °C. After being stirred at 80 °C for 2 h, the reaction mixture was cooled to room temperature, quenched with $Na_2S_2O_3$ (saturated in $H_2O$, 50 mL) and extracted with ethyl acetate (50 mL×3). The organic phase was then dried with $Na_2SO_4$ and concentrated under reduced pressure. The mixture was purified by column chromatography (silica gel, hexane:ethyl acetate = 10:1) to give compound **3.1s** (4.1 g, 85% yield) as a white solid.

**$R_f$** = 0.51 (hexane : ethyl acetate = 2:1)

**$^1$H NMR** (400 MHz, $CDCl_3$) δ 7.29 (s, 2H), 5.98 (s, 2H), 3.79 (s, 2H), 2.39 – 2.26 (m, 6H), 2.25 – 2.13 (m, 6H).

**$^{13}$C NMR** (101 MHz, $CDCl_3$) δ 150.0, 135.6, 131.0, 125.2, 124.5, 116.6, 30.6, 19.9, 13.2.

**IR** (KBr) $\nu_{max}$ = 3458, 3289, 2937, 1464, 1408, 1348, 1271, 1184, 1085, 921, 882, 792 $cm^{-1}$.

**HRMS (ESI)** m/z calcd. for $C_{17}H_{17}{}^{79}Br^{81}BrO_2^-$ $[M-H]^-$: 412.9580, found 412.9534.

**Melting point**: 195.0 – 195.6 °C

*Preparation of compound **3.1u***

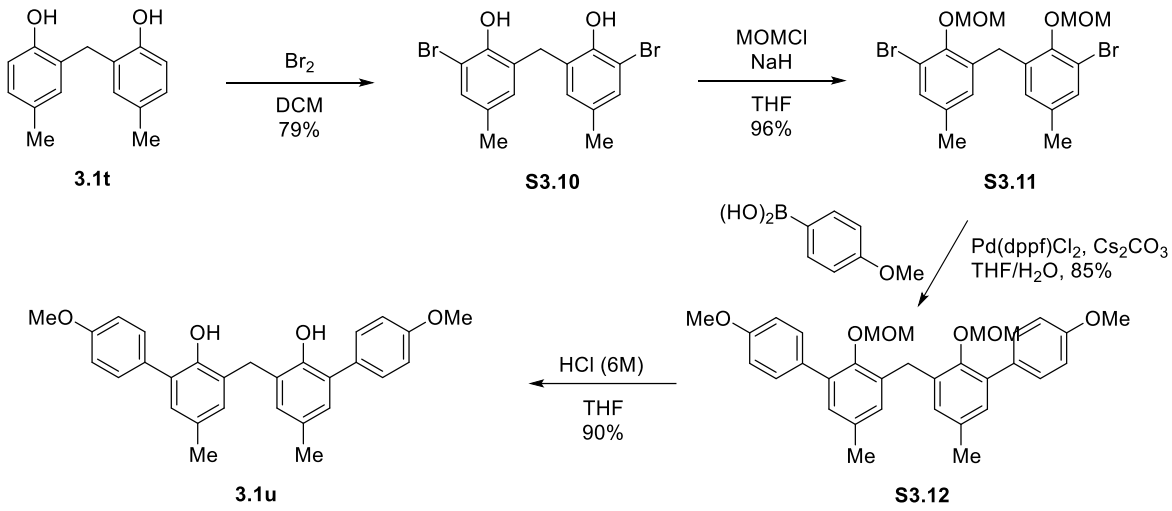


To a solution of compound **3.1t**[19] (3.0 g, 13.14 mmol) in dichloromethane (50 mL), bromine (1.42 mL, 27.6 mmol) was added at 0 °C. After being stirred at room temperature for 3 h, the reaction mixture was quenched with $Na_2S_2O_3$ (saturated in $H_2O$, 50 mL) and extracted with dichloromethane (50 mL×3). The organic phase was then dried with $Na_2SO_4$ and concentrated under reduced pressure. The mixture was purified by column chromatography (silica gel, hexane:ethyl acetate = 10:1) to give compound **S3.10** (4.0 g, 79% yield).

To a solution of compound **S3.10** (4.0 g, 10.4 mmol) in THF (50 mL), NaH (60 % dispersion in mineral oil, 1.04 g, 25.9 mmol) was added at 0 °C. After being stirred at 0 °C for 30 min, chloromethyl methyl ether (2.09 g, 25.9 mmol) was added to the reaction mixture. After being stirred at room temperature for 4 h, the reaction mixture was quenched with $NH_4Cl$ (saturated in $H_2O$, 40 mL) and extracted with diethyl ether (50 mL×3). The organic phase was then dried with $Na_2SO_4$ and concentrated under reduced pressure. The mixture was purified by column chromatography (silica gel, hexane:ethyl acetate = 20:1) to give compound **S3.11** (4.7 g, 96% yield).

To a solution of compound **S3.11** (1.0 g, 2.11 mmol) in THF (6 mL), 4-methoxyphenylboronic acid (0.96 g, 6.33 mmol), $Pd(dppf)Cl_2 \cdot CH_2Cl_2$ (86 mg, 0.11 mmol), $Cs_2CO_3$ (2.75 g, 8.44 mmol) and $H_2O$ (1.5 mL) were added at room temperature, and the reaction mixture was then heated to 90 °C. After being stirred at 90 °C for 12 h, the reaction mixture was quenched with HCl (1 M in $H_2O$, 5 mL) and extracted with dichloromethane (5 mL×3). The organic phase was then dried with $Na_2SO_4$ and concentrated under reduced pressure. The mixture was purified by column chromatography (silica gel, hexane:ethyl acetate = 20:1) to give compound **S3.12** (0.95 g, 85% yield).

To a solution of compound **S3.12** (0.95 g, 1.8 mmol) in THF (20 mL), HCl (6 M in $H_2O$, 1 mL) was added at room temperature. After being stirred at room temperature for 12 h, the reaction mixture was diluted with $H_2O$ (20 mL), extracted with ethyl acetate (20 mL×3). The organic phase was then dried with $Na_2SO_4$ and concentrated under reduced pressure, then purified by column chromatography (silica gel, hexane:ethyl acetate = 20:1) to give compound **3.1u** (0.71 g, 90% yield) as a white solid.

$\mathbf{R_f}$ = 0.51 (hexane : ethyl acetate = 2:1)

**$^1$H NMR** (400 MHz, $CDCl_3$) δ 7.41 – 7.33 (m, 4H), 7.08 (d, *J* = 2.2 Hz, 2H), 6.99 – 6.93 (m, 4H), 6.93 – 6.87 (m, 2H), 6.26 (s, 2H), 3.97 (s, 2H), 3.82 (s, 6H), 2.29 (s, 6H).

**$^{13}$C NMR** (101 MHz, $CDCl_3$) δ 159.0, 147.5, 130.3, 130.3, 130.0, 129.9, 129.3, 128.3, 126.8, 114.3, 55.3, 31.1, 20.6.

**IR** (KBr) $\nu_{max}$ = 3408, 2933, 1608, 1513, 1470, 1290, 1248, 1178, 1033, 909, 833, 732 $cm^{-1}$.

**HRMS (ESI)** m/z calcd. for $C_{29}H_{27}O_4^-$ $[M-H]^-$: 439.1915, found 439.1929.

**Melting point**: 70.3 – 71.8 °C

*Preparation of compound **3.1v***

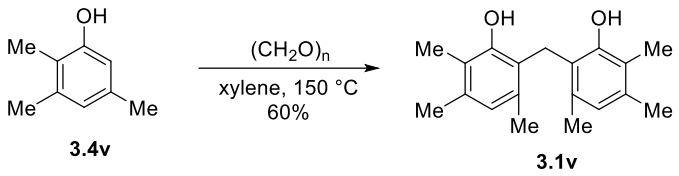


To a solution of 2,3,5-trimethylphenol (20 g, 147 mmol) in xylene (100 mL), paraformaldehyde (2.2 g, 73 mmol) was added at room temperature. The reaction mixture was then heated to 150 °C. After being stirred at 150 °C for 12 h, the reaction mixture was quenched with HCl (1 M in $H_2O$, 50 mL) and extracted with ethyl acetate (50 mL×3). The organic phase was then dried with $Na_2SO_4$ and concentrated under reduced pressure. The mixture was purified by column chromatography (silica gel, hexane:ethyl acetate = 10:1) to give compound **3.1v** (12.5 g, 60% yield).

$\mathbf{R}_f$ = 0.65 (hexane : ethyl acetate = 2:1)

**$^1$H NMR** (400 MHz, $CDCl_3$) δ 6.62 (s, 2H), 5.60 (s, 2H), 3.95 (s, 2H), 2.33 (s, 6H), 2.19 (s, 6H), 2.05 (s, 6H).

**$^{13}$C NMR** (101 MHz, $CDCl_3$) δ 152.6, 135.9, 134.4, 124.7, 120.8, 120.6, 25.1, 20.1, 19.8, 11.6.

**IR** (KBr) $\nu_{max}$ = 3431, 2914, 1562, 1464, 1404, 1298, 1258, 1201, 1170, 1080, 1045, 857 cm$^{-1}$.

**HRMS (ESI)** m/z calcd. for $C_{19}H_{23}O_2^-$ $[M-H]^-$: 283.1704, found 283.1728.

**Melting point**: 177 – 179 °C

*Preparation of compound **3.1w***

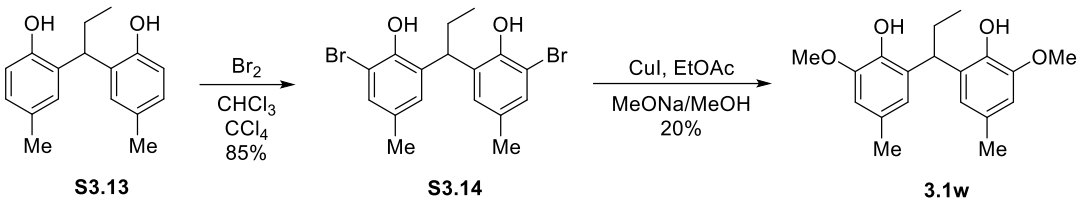


To a solution of compound **S3.13**[20] (3.0 g, 11.7 mmol) in chloroform (10 mL) and $CCl_4$ (10 mL), bromine (3.74 g, 23.4 mmol) in chloroform (10 mL) was added dropwise at 0 °C. After being stirred at room temperature for 30 min, the reaction mixture was quenched with $Na_2S_2O_3$ (saturated in $H_2O$, 20 mL) and extracted with dichloromethane (20 mL×3). The organic phase was then dried with $Na_2SO_4$ and concentrated under reduced pressure. The mixture was purified by column chromatography (silica gel, hexane:ethyl acetate = 20:1) to give compound **S3.14** (4.1 g, 85% yield).

To a solution of compound **S3.14** (4.1 g, 9.9 mmol) in ethyl acetate (1.2 mL), CuI (1.9 g, 9.9 mmol) and MeONa (25 wt.% in methanol, 10 mL) were added at room temperature, and the reaction mixture was then heated to 70 °C. After being stirred at 70 °C for 12 h, the reaction mixture was quenched with HCl (2 M in $H_2O$, 50 mL) and extracted with ethyl acetate (50 mL×3). The organic phase was then dried with $Na_2SO_4$ and concentrated under reduced pressure. The mixture was purified by column chromatography (silica gel, hexane:ethyl acetate = 10:1) to give compound **3.1w** (0.63 g, 20% yield).

**$R_f$** = 0.32 (hexane : ethyl acetate = 2:1)

**$^1$H NMR** (400 MHz, $CDCl_3$) δ 6.69 – 6.63 (m, 2H), 6.51 (d, *J* = 1.9 Hz, 2H), 5.96 (s, 2H), 4.47 (t, *J* = 7.7 Hz, 1H), 3.81 (s, 6H), 2.26 (s, 6H), 2.04 (p, *J* = 7.4 Hz, 2H), 0.91 (t, *J* = 7.3 Hz, 3H).

**$^{13}$C NMR** (101 MHz, $CDCl_3$) δ 146.4, 140.8, 130.1, 128.8, 120.0, 109.5, 55.8, 37.8, 27.0, 21.4, 12.6.

**IR** (KBr) $\nu_{max}$ = 3320, 2967, 2938, 1592, 1498, 1462, 1352, 1297, 1203, 1149, 1070, 838 cm$^{-1}$.

**HRMS (ESI)** molecular weight peak not found despite extensive efforts.

**Melting point**: 161.0 – 162.1 °C

*Preparation of compound **3.1x***

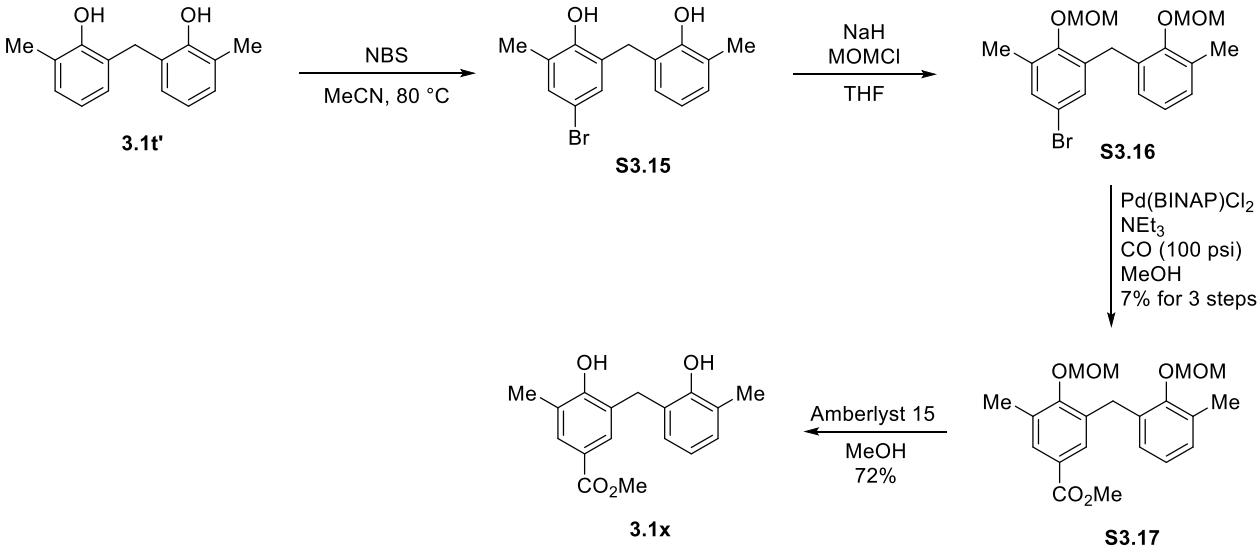


To a solution of compound **3.1t'**[17] (500 mg, 2.19 mmol) in MeCN (10 mL), *N*-bromosuccinimide (390 mg, 2.19 mmol) was added at 0 °C, and the reaction mixture was then heated to 80 °C. After being stirred at 80 °C for 2 h, the reaction mixture was cooled to room temperature, quenched with

$Na_2S_2O_3$ (saturated in $H_2O$, 10 mL) and extracted with ethyl acetate (10 mL×3). The organic phase was then dried with $Na_2SO_4$ and concentrated under reduced pressure. The mixture was purified by column chromatography (silica gel, hexane:ethyl acetate = 10:1) to give crude compound **S3.15** (mixture of **3.1t'**, monobromide and dibromide)..

To a solution of compound **S3.15** (crude product from previous step) in THF (10 mL), NaH (60 % dispersion in mineral oil, 0.22 g, 5.5 mmol) was added at 0 °C. After being stirred at 0 °C for 30 min, chloromethyl methyl ether (0.44 g, 5.5 mmol) was added to the reaction mixture. After being stirred at room temperature for 4 h, the reaction mixture was quenched with $NH_4Cl$ (saturated in $H_2O$, 10 mL) and extracted with diethyl ether (10 mL×3). The organic phase was then dried with $Na_2SO_4$ and concentrated under reduced pressure. The mixture was purified by column chromatography (silica gel, hexane:ethyl acetate = 20:1) to give crude compound **S3.16** (mixture monobromide and dibromide).

To a flame-dried Q-tube, compound **S3.16** (crude product from previous step), $Pd(BINAP)Cl_2$ (24 mg, 0.03 mmol), triethyl amine (54 µL, 0.39 mmol) and MeOH (2 mL) were added at room temperature. The reaction vessel was then charged with 100 psi CO and heated to 120 °C. After being stirred at 120 °C for 12 h, the CO was released and the reaction mixture was filtered through Celite, and the solution was concentrated under reduced pressure. The mixture was purified by column chromatography (silica gel, hexane:ethyl acetate = 10:1) to give compound **S3.17** (60 mg, 7% yield for 3 steps)**.**

To a solution of compound **S3.17** (60 mg, 0.16 mmol) in methanol (2 mL), Amberlyst 15 (80 mg) was added at room temperature, and the reaction mixture was then heated to reflux. After refluxing for 3 h, the reaction mixture was filtered through Celite, then concentrated under reduced pressure

and purified by recrystallization (hexane/dichloromethane) to give compound **3.1x** (33 mg, 72% yield) as a white solid.

**$R_f$** = 0.29 (hexane : ethyl acetate = 2:1)

**$^1$H NMR** (400 MHz, $CDCl_3$) δ 7.85 (t, *J* = 1.8 Hz, 1H), 7.68 (d, *J* = 2.1 Hz, 1H), 7.28 (s, 1H), 7.16 (d, *J* = 7.6 Hz, 1H), 6.99 (d, *J* = 7.5 Hz, 1H), 6.82 (td, *J* = 7.5, 1.5 Hz, 1H), 5.88 (s, 1H), 3.94 (s, 2H), 3.87 (d, *J* = 1.5 Hz, 3H), 2.25 (s, 3H), 2.22 (s, 3H).

**$^{13}$C NMR** (101 MHz, $CDCl_3$) δ 167.3, 156.2, 150.2, 131.0, 130.3, 129.5, 128.7, 126.3, 125.9, 124.8, 123.4, 122.0, 121.6, 51.9, 30.9, 16.1, 15.9.

**IR** (KBr) $\nu_{max}$ = 3360, 2951, 1692, 1602, 1471, 1436, 1323, 1295, 1214, 1022, 909, 772 $cm^{-1}$.

**HRMS (ESI)** molecular weight peak not found despite extensive efforts.

(Preparation of compounds **3.1c**–**e**, **3.1g**–**s**, **3.1u**–**x** is conducted by Dr. Jun Zhu).

*General Procedure for preparation of compound **3.2***

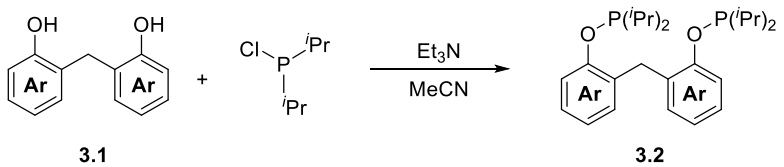


**3.1** **3.2**

**<u>General procedure:</u>** To a flame dried 40 mL vial charged with a stir bar, diphenol **3.1** (1.0 equiv.) was dissolved in dry MeCN (10 mL/500 mg), 4 equiv. of dry $Et_3N$ was added in one portion. 2.1

equiv. of chloro-diisopropylphosphine was then added dropwise at room temperature. The mixture was heated to 70 °C under $N_2$ atmosphere overnight. Upon completion of the reaction, the reaction mixture was extracted with pentane or hexane in glovebox and concentrated to give the corresponding phosphinites, which were pure enough for the C−C activation reactions. (The phosphinites were sensitive to moisture and must be stored in the glovebox. HRMS could not be obtained.)

*Preparation of compound **3.2a***

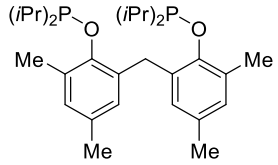


**3.2a**

6,6'-methylenebis(2,4-dimethylphenol)[21] (500 mg) was subjected to the general procedure to afford 505 mg of **3.2a** with 53% yield as a white solid.

**$^1$H NMR** (500 MHz, $C_6D_6$) δ 6.85 (s, 2H), 6.74 (s, 2H), 4.60 (s, 2H), 2.45 (s, 6H), 2.00 (s, 6H), 1.97 – 1.87 (m, 4H), 1.16 (dd, J = 11.0, 7.0 Hz, 6H), 1.05 (dd, J = 13.0, 7.0 Hz, 6H).

**$^{13}$C NMR** (125 MHz, $C_6D_6$) δ 152.3, 132.4, 131.9, 130.7, 130.0, 129.0, 32.8 (t, J = 7.2 Hz), 29.1 (d, J = 23.2 Hz), 20.7, 18.9 (d, J = 9.0 Hz), 17.8 (d, J = 16.5 Hz), 17.7 (d, J = 12.3 Hz).

**$^{31}$P NMR** (202 MHz, $C_6D_6$) δ 155.5.

**IR (NaCl)** $\nu_{max}$ = 2954, 2924, 2867, 1467, 1382, 1362, 1300, 1264, 1214, 1142, 1013 $cm^{-1}$.

**Melting point** 70 – 72 °C.

*Preparation of compound **3.2b***

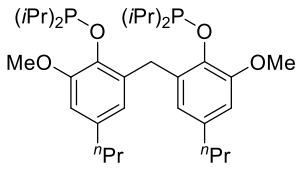


**3.2b**

6,6'-methylenebis(2-methoxy-4-propylphenol) (500 mg) was subjected to the general procedure to afford 743 mg of **3.2b** with 89% yield as a white solid.

**$^{1}$H NMR** (500 MHz, $C_6D_6$) δ 6.70 (s, 2H), 6.47 (d, J = 2.0 Hz, 2H), 4.53 (s, 2H), 3.45 (s, 6H), 2.33 (t, J = 7.5 Hz, 4H), 2.08 – 1.92 (m, 2H), 1.57 – 1.40 (m, 4H), 1.30 (dd, J = 11.0, 7.0 Hz, 12H), 1.17 (dd, J = 13.5, 7.0 Hz, 12H), 0.82 (t, J = 7.0 Hz, 6H).

**$^{13}$C NMR** (125 MHz, $C_6D_6$) δ 151.2, 144.3 (d, J = 4.0 Hz). 136.8, 133.1, 123.2, 111.7, 55.5, 38.2, 31.5, 29.3 (d, J = 22.8 Hz), 25.1, 18.0 (d, J = 17.5 Hz), 17.8 (d, J = 12.6 Hz), 14.0.

**$^{31}$P NMR** (202 MHz, $C_6D_6$) δ 160.3.

**IR (NaCl)** $\nu_{max}$ = 2956, 2868, 2836, 1585, 1485, 1460, 1424, 1383, 1350, 1334, 1305, 1271, 1255, 1226, 1183, 1148, 1100 $cm^{-1}$.

**Melting point** 56 – 58 °C.

*Preparation of compound **3.2c***

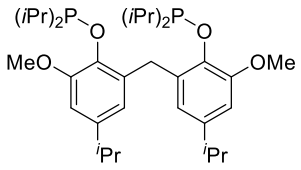


**3.2c**

6,6'-methylenebis(4-isopropyl-2-methoxyphenol) (500 mg) was subjected to the general procedure to afford 510 mg of **3.2c** with 61% yield as a white solid.

**$^{1}$H NMR** (500 MHz, $C_6D_6$) δ 6.78 (s, 2H), 6.55 (d, J = 2.0 Hz, 2H), 4.54 (s, 2H), 3.46 (s, 6H), 2.67 – 2.55 (m, 2H), 2.04 – 1.92 (m, 4H), 1.29 (dd, J = 11.0, 7.0 Hz, 12H), 1.17 (dd, J = 13.5, 7.5 Hz, 12H), 1.12 (d, J = 6.5 Hz, 12H).

**$^{13}$C NMR** (125 MHz, $C_6D_6$) δ 151.3, 144.3 (d, J = 4.0 Hz), 143.0, 133.1, 121.1, 109.7, 55.5, 34.3, 31.7, 29.3 (d, J = 22.6 Hz), 24.3, 18.0 (d, J = 17.5 Hz), 17.8 (d, J = 12.5 Hz).

**$^{31}$P NMR** (202 MHz, $C_6D_6$) δ 160.1.

**IR (NaCl)** $\nu_{max}$ = 2957, 2867, 2835, 1585, 1481, 1463, 1424, 1383, 1361, 1337, 1297, 1270, 1220, 1189, 1169, 1134 $cm^{-1}$.

**Melting point** 58 – 60 °C.

*Preparation of compound **3.2d***

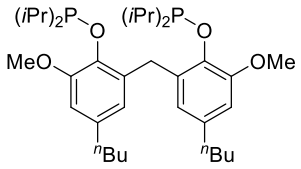


**3.2d**

6,6'-methylenebis(2-methoxy-4-propylphenol) (500 mg) was subjected to the general procedure to afford 603 mg of **3.2d** with 74% yield as a colorless oil.

**$^{1}$H NMR** (500 MHz, $C_6D_6$) δ 6.69 (s, 2H), 6.53 (d, J = 1.7 Hz, 2H), 4.53 (s, 2H), 3.46 (s, 6H), 2.41 – 2.28 (m, 4H), 2.05 – 1.92 (m, 2H), 1.57 – 1.38 (m, 8H), 1.34 – 1.23 (m, 6H), 1.21 – 1.09 (m, 18H), 0.80 (t, J = 7.4 Hz, 6H).

**$^{13}$C NMR** (125 MHz, $C_6D_6$) δ 151.3, 144.4, 141.7, 133.0, 121.7, 110.2, 55.5, 41.9, 31.6, 29.4, 29.2, 22.3, 18.0 (d, J = 17.5 Hz), 17.9 (d, J = 12.3 Hz), 12.5.

**$^{31}$P NMR** (202 MHz, $C_6D_6$) δ 160.0.

**IR (NaCl)** $\nu_{max}$ = 2955, 2929, 2867, 1585, 1482, 1464, 1423, 1380, 1362, 1339, 1299, 1249, 1220, 1148 cm$^{-1}$.

*Preparation of compound **3.2e***

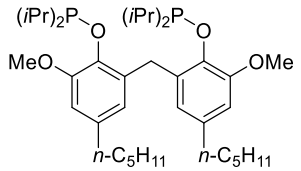


**3.2e**

6,6'-methylenebis(2-methoxy-4-pentylphenol) (500 mg) was subjected to the general procedure to afford 625 mg of **3.2e** with 79% yield as a colorless oil.

**$^1$H NMR** (500 MHz, $CDCl_3$) δ 6.56 (s, 2H), 6.39 (s, 2H), 4.06 (s, 2H), 3.82 (s, 6H), 2.42 (t, J = 7.7 Hz, 4H), 2.01 – 1.89 (m, 4H), 1.56 – 1.43 (m, 4H), 1.34 – 1.21 (m, 8H), 1.20 – 1.05 (m, 24H), 0.86 (t, J = 7.0 Hz, 6H).

**$^{13}$C NMR** (125 MHz, $CDCl_3$) δ 150.2, 143.2, 143.2, 136.6, 132.3, 122.5, 110.9, 55.6, 35.6, 31.4, 31.2, 30.5, 28.8, 28.7, 22.5, 17.6 (d, J = 13.3 Hz), 17.5 (d, J = 8.8 Hz), 14.0.

**$^{31}$P NMR** (202 MHz, $CDCl_3$) δ 160.5.

**IR (NaCl)** $\nu_{max}$ = 2954, 2928, 2866, 1585, 1482, 1464, 1422, 1380, 1362, 1295, 1215, 1147, 1100 $cm^{-1}$.

*Preparation of compound **3.2f***

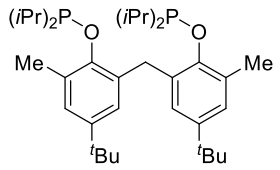


**3.2f**

6,6'-methylenebis(4-(tert-butyl)-2-methylphenol)[22] (500 mg) was subjected to the general procedure to afford 620 mg of **3.2f** with 74% yield as a colorless oil.

**$^1$H NMR** (500 MHz, $C_6D_6$) δ 7.13 (s, 2H), 7.10 (s, 2H), 4.68, (s, 2H), 2.52 (s, 6H), 1.92 (hept, 4H, J = 7.0 Hz), 1.21, (s, 18H), 1.16 (dd, 12H, J = 11.5, 7.0 Hz), 1.05 (dd, 12 H, J = 13.5, 7.0 Hz)

**$^{13}$C NMR** (125 MHz, $C_6D_6$) δ 152.4, 145.1, 132.0, 128.3, 128.0 (d, J = 24.4 Hz), 126.7 (d, J = 19.3 Hz), 34.2, 33.2 (t, J = 7.1 Hz), 31.7, 29.1 (d, J = 22.9 Hz), 19.3 (d, J = 9.1 Hz), 17.8 (t, J = 5.3 Hz)

**$^{31}$P NMR** (202 MHz, $C_6D_6$) δ 154.9.

*Preparation of compound **3.2g***

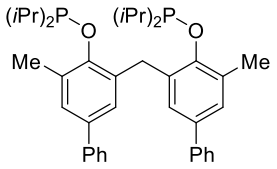


**3.2g**

5,5"-methylenebis(3-methyl-[1,1'-biphenyl]-4-ol) (500 mg) was subjected to the general procedure to afford 402.0 mg of **3.2g** with 50% yield as a white solid.

**$^{1}$H NMR** (500 MHz, $CDCl_3$) δ 7.47 (d, J = 7.5 Hz, 4H), 7.35 (t, J = 7.5 Hz, 4H), 7.27 – 7.26 (m, 4H), 7.12 (d, J = 2.0 Hz), 4.38 (s, 2H), 2.47 (s, 6H), 2.10 – 1.97 (m, 4H), 1.23 – 1.08 (m, 24H).

**$^{13}$C NMR** (125 MHz, $CDCl_3$) δ 153.6, 141.0, 135.1, 132.3, 129.2, 128.5, 128.3, 127.5, 126.8, 126.5, 32.4 (t, J = 5.9 Hz), 28.8 (d, J = 22.3 Hz) 18.9 (d, J = 10.0 Hz), 17.6 (d, J = 12.9 Hz) 17.5 (d, J = 9.3 Hz).

**$^{31}$P NMR** (202 MHz, $CDCl_3$) δ 157.4.

**IR** (NaCl) $\nu_{max}$ = 3060, 3030, 2954, 2925, 2867, 1601, 1574, 1465, 1403, 1382, 1365, 1323, 1303, 1264, 1231, 1167 $cm^{-1}$.

**Melting point** 112 – 114 °C.

*Preparation of compound **3.2h***

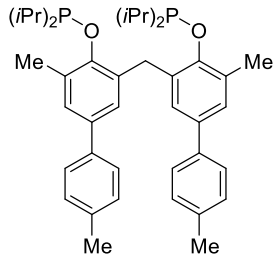


**3.2h**

5,5''-methylenebis(3,4'-dimethyl-[1,1'-biphenyl]-4-ol) (500 mg) was subjected to the general procedure to afford 672.0 mg of **3.2h** with 86% yield as a white solid.

**$^{1}$H NMR** (500 MHz, $CDCl_3$) δ 7.35 (d, J = 8.0 Hz, 4H), 7.19 (s, 2H), 7.15 (d, J = 7.8 Hz, 4H), 7.06 (s, 2H), 4.32 (s, 2H), 2.45 (s, 6H), 2.34 (s, 6H), 2.04 – 2.01 (m, 4H), 1.16 – 1.11 (m, 24H).

**$^{13}$C NMR** (125 MHz, $CDCl_3$) δ 153.3, 138.2, 136.1, 135.0, 132.3, 129.2, 129.1, 128.0, 127.3, 126.6, 32.4 (d, J = 5.9 Hz), 28.8 (d, J = 22 Hz), 21.0, 18.9 (d, J = 10.0 Hz), 17.6 (d, J = 10.8 Hz) 17.5 (d, J = 7.3 Hz).

**$^{31}$P NMR** (202 MHz, $CDCl_3$) δ 157.1.

**IR** (NaCl) $\nu_{max}$ = 3023, 2955, 2924, 2867, 1516, 1468, 1382, 1362, 1323, 1303, 1231, 1212, 1167 $cm^{-1}$.

**Melting point** 118 − 120 °C.

*Preparation of compound **3.2i***

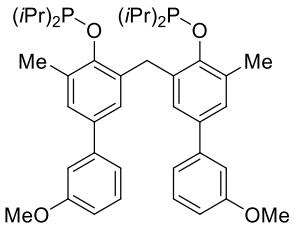


**3.2i**

5,5''-methylenebis(3'-methoxy-3-methyl-[1,1'-biphenyl]-4-ol) (500 mg) was subjected to the general procedure to afford 521.0 mg of **3.2i** with 68% yield as an amorphous foam.

**$^{1}$H NMR** (500 MHz, $C_6D_6$) δ 7.50 (s, 2H), 7.31 (d, J = 1.4 Hz, 2H), 7.11 (d, J = 7.8 Hz, 2H), 7.06 (t, J = 7.8 Hz, 2H), 6.72 (dd, J = 8.0, 1.5 Hz, 2H), 4.78 (s, 2H), 3.30 (s, 6H), 2.49 (s, 6H), 1.98 – 1.85 (m, 4H), 1.22 – 1.11 (m, 12H), 1.10 – 0.96 (m, 12H).

**$^{13}$C NMR** (125 MHz, $CDCl_3$) δ 159.8, 153.7, 142.6, 134.9, 132.2, 129.4, 129.2, 128.3, 127.5, 119.3, 112.3, 112.2, 55.2, 32.4 (t, J = 5.2 Hz), 28.8 (d, J = 22.3 Hz), 18.9 (d, J = 9.7 Hz), 17.6 (d, J = 15.0 Hz), 17.5 (d, J = 11.6 Hz).

**$^{31}$P NMR** (202 MHz, $C_6D_6$) δ 157.2.

**IR** (NaCl) $\nu_{max}$ = 2955, 2867, 2835, 1576, 1470, 1396, 1383, 1362, 1308, 1282, 1243, 1155, 1090, 1050 $cm^{-1}$.

*Preparation of compound **3.2j***

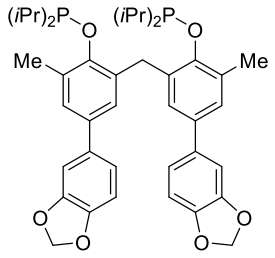

**3.2j**

6,6'-methylenebis(4-(benzo[d][1,3]dioxol-5-yl)-2-methylphenol) (500 mg) was subjected to the general procedure to afford 534.0 mg of **3.2j** with 60% yield as an amorphous foam.

**$^{1}$H NMR** (400 MHz, $CDCl_3$) δ 7.17 (d, J = 2.0 Hz, 2H), 7.02 (d, J = 2.0 Hz, 2H), 6.98 – 6.93 (m, 2H), 6.94 (d, J = 1.8 Hz, 2H), 6.82 (dd, J = 8.4, 0.8 Hz, 1H), 5.94 (s, 2H), 4.32 (s, 2H), 2.45 (s, 6H), 2.07 – 1.99 (m, 4H), 1.17 – 1.09 (m, 24H).

**$^{13}$C NMR** (100 MHz, $CDCl_3$) δ 153.3, 147.8, 146.4, 135.5, 134.8, 132.3, 129.2, 128.0, 127.1, 120.1, 108.3, 107.4, 100.9, 32.3 (t, J = 6.3 Hz), 28.8 (d, J = 22 Hz), 18.8 (d, J = 9.8 Hz), 17.6 (d, J = 12.5 Hz), 17.5 (d, J = 7.9 Hz).

**$^{31}$P NMR** (202 MHz, $CDCl_3$) δ 157.4.

**IR** (NaCl) $\nu_{max}$ = 2956, 2927, 2868, 2775, 1607, 1580, 1505, 1469, 1410, 1382, 1363, 1337, 1306, 1264, 1238, 1172 $cm^{-1}$.

*Preparation of compound **3.2k***

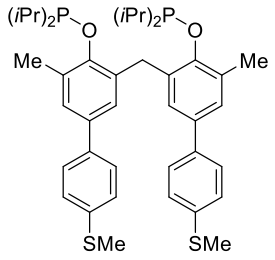


**3.2k**

5,5''-methylenebis(3-methyl-4'-(methylthio)-[1,1'-biphenyl]-4-ol) (500 mg) was subjected to the general procedure to afford 559 mg of **3.2k** with 75% yield as a white solid.

**$^{1}$H NMR** (500 MHz, $CDCl_3$) δ 7.38 (d, J = 8.2 Hz, 4H), 7.23 (d, J = 8.2 Hz, 4H), 7.19 (s, 2H), 7.04 (s, 2H), 4.32 (s, 2H), 2.48 (s, 6H), 2.45 (s, 6H), 2.08 – 1.97 (m, 4H), 1.18 – 1.06 (m, 24H).

**$^{13}$C NMR** (126 MHz, $CDCl_3$) δ 153.6, 138.0, 136.5, 134.3, 132.3, 129.3, 128.0, 127.1, 127.1, 127.0, 32.4 (t, J = 6.6 Hz), 28.8 (d, J = 22.0 Hz), 18.9 (d, J = 9.6 Hz), 17.6 (d, J = 12.8 Hz), 17.5 (d, J = 9.0 Hz), 16.1.

**$^{31}$P NMR** (202 MHz, $CDCl_3$) δ 157.6.

**IR** (NaCl) $\nu_{max}$ = 3022, 2955, 2922, 2866, 1597, 1467, 1382, 1319, 1232, 1168, 1098, 1075, 1013 $cm^{-1}$.

**Melting point** 143 – 145 °C.

*Preparation of compound **3.2l***

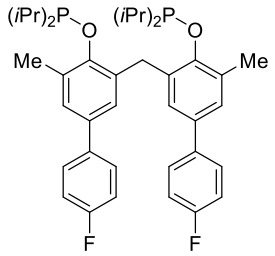


**3.2l**

5,5''-methylenebis(4'-fluoro-3-methyl-[1,1'-biphenyl]-4-ol) (500 mg) was subjected to the general procedure to afford 510 mg of **3.2l** with 65% yield as a white solid.

**$^{1}$H NMR** (500 MHz, $CDCl_3$) δ 7.45 – 7.39 (m, 4H), 7.19 (s, 2H), 7.08 – 7.00 (m, 6H), 4.36 (s, 2H), 2.48 (s, 6H), 2.11 – 1.97 (m, 4H), 1.22 – 1.08 (m, 24H).

**$^{13}$C NMR** (125 MHz, $CDCl_3$) δ 163.0, 161.0, 153.6, 137.1 (d, $J$ = 2.9 Hz), 134.1, 132.4, 129.4, 128.2 (d, $J$ = 7.5 Hz), 127.3, 115.3 (d, J = 20.9 Hz), 32.4, 28.9 (d, J = 22.3 Hz), 18.9 (d, J = 9.9 Hz), 17.6 (d, $J$ = 14.8 Hz), 17.4 (d, $J$ = 11.9 Hz).

**$^{31}$P NMR** (202 MHz, $CDCl_3$) δ 157.8.

**$^{19}$F NMR** (470 MHz, $CDCl_3$) δ -116.8.

**IR** (NaCl) $\nu_{max}$ = 2957, 2927, 2868, 1601, 1513, 1469, 1383, 1363, 1322, 1226, 1158, 1097, 1080 $cm^{-1}$

**Melting point** 100 – 102 °C.

*Preparation of compound **3.2m***

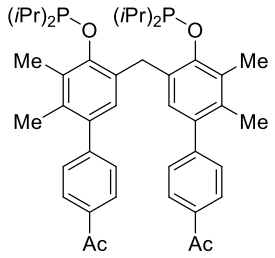


**3.2m**

1,1'-(methylenebis(4'-hydroxy-5',6'-dimethyl-[1,1'-biphenyl]-3',4-diyl))bis(ethan-1-one) (500 mg, 1.31 mmol) was subjected to the general procedure to afford 510 mg of **3.2m** with 65% yield as a white solid.

**$^{1}$H NMR** (400 MHz, $CDCl_3$) δ 7.93 (d, *J* = 8.5 Hz, 4H), 7.29 (d, *J* = 8.5 Hz, 4H), 6.68 (d, *J* = 5.2 Hz, 2H), 4.33 (s, 2H), 2.62 (s, 6H), 2.29 (s, 6H), 2.10 (s, 6H), 2.07 – 1.96 (m, 4H), 1.17 – 1.06 (m, 24H).

**$^{13}$C NMR** (100 MHz, $CDCl_3$) δ 197.9, 153.6, 147.9, 135.4, 135.1, 133.1, 129.9, 129.5, 129.0, 128.5, 127.9, 32.3 (t, *J* = 5.9 Hz), 28.7 (d, *J* = 22.4 Hz), 26.6, 17.7 (d, *J* = 6.5 Hz), 17.5 (d, *J* = 3.6 Hz), 14.8 (d, *J* = 6.7 Hz).

**$^{31}$P NMR** (202 MHz, $CDCl_3$) δ158.7.

**IR** (NaCl) $\nu_{max}$ = 2958, 2928, 2868, 1683, 1604, 1465, 1397, 1357, 1320, 1267, 1218, 1182, 1153, 1087, 1017 $cm^{-1}$.

**Melting point** 153 – 155 °C.

*Preparation of compound **3.2n***

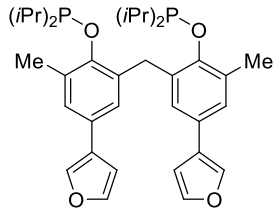

**3.2n**

6,6'-methylenebis(4-(furan-3-yl)-2-methylphenol) (400 mg) was subjected to the general procedure to afford 410 mg of **3.2n** with 62% yield as a colorless oil.

**$^{1}$H NMR** (500 MHz, $CDCl_3$) δ 7.56 (s, 2H), 7.39 (d, $J$ = 1.4 Hz, 2H), 7.13 (s, 2H), 6.96 (s, 2H), 6.55 (s, 2H), 4.29 (s, 2H), 2.44 (s, 6H), 2.09 – 1.96 (m, 4H), 1.22 – 1.06 (m, 24H).

**$^{13}$C NMR** (126 MHz, $CDCl_3$) δ 153.1, 143.3, 137.8, 132.3, 129.4, 127.1, 126.4, 126.3, 126.2, 108.9, 32.2 (t, $J$ = 6.9 Hz), 28.8 (d, $J$ = 22.1 Hz), 18.7 (d, $J$ = 9.5 Hz), 17.6 (d, $J$ = 16.1 Hz), 17.4 (d, $J$ = 12.1 Hz).

**$^{31}$P NMR** (202 MHz, $CDCl_3$) δ 157.6.

**IR** (NaCl) $\nu_{max}$ = 3034, 2955, 2927, 2867, 1575, 1508, 1466, 1382, 1354, 1331, 1310, 1238, 1179, 1107 $cm^{-1}$.

*Preparation of compound **3.2o***

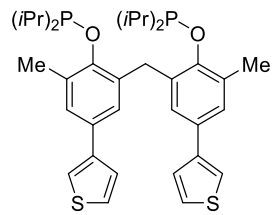

**3.2o**

6,6'-methylenebis(2-methyl-4-(thiophen-3-yl)phenol) (400 mg) was subjected to the general procedure to afford 330 mg of **3.2o** with 51% yield as a colorless oil.

**$^1$H NMR** (500 MHz, $CDCl_3$) δ 7.31 – 7.27 (m, 2H), 7.23 (d, $J$ = 3.4 Hz, 6H), 7.05 (s, 2H), 4.30 (s, 2H), 2.44 (s, 6H), 2.08 – 1.95 (m, 4H), 1.21 – 1.05 (m, 24H).

**$^{13}$C NMR** (125 MHz, $CDCl_3$) δ 153.3, 142.2, 132.3, 130.0, 129.3, 127.6, 126.8, 126.3, 125.7, 119.0, 32.3 (t, $J$ = 6.2 Hz), 28.8 (d, $J$ = 21.9 Hz), 18.8 (d, $J$ = 9.5 Hz), 17.6 (d, $J$ = 17.1 Hz), 17.4 (d, $J$ = 12.8 Hz).

**$^{31}$P NMR** (202 MHz, $CDCl_3$) δ 157.6.

**IR** (NaCl) $\nu_{max}$ = 3090, 3034, 2954, 2926, 2866, 1583, 1531, 1473, 1407, 1382, 1361, 1297, 1231, 1204, 1156 $cm^{-1}$.

*Preparation of compound **3.2p***

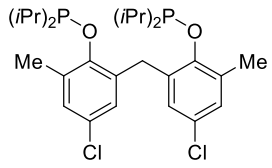


**3.2p**

6,6'-methylenebis(4-chloro-2-methylphenol) (500 mg) was subjected to the general procedure to afford 330 mg of **3.2p** with 51% yield as a white solid.

**$^1$H NMR** (500 MHz, $CDCl_3$) δ 6.97 (d, $J$ = 2.2 Hz, 2H), 6.70 (d, $J$ = 2.3 Hz, 2H), 4.18 (d, $J$ = 18.8 Hz, 2H), 2.35 (s, 6H), 2.04 – 1.90 (m, 4H), 1.20 – 1.01 (m, 24H).

**$^{13}$C NMR** (125 MHz, $CDCl_3$) δ 152.5, 133.1, 131.0, 129.4, 128.2, 127.0, 32.2 (t, *J* = 6.6 Hz), 28.8 (d, *J* = 22.2 Hz), 18.6 (d, *J* = 9.8 Hz), 17.5 (d, *J* = 16.1 Hz), 17.3 (d, *J* = 11.8 Hz).

**$^{31}$P NMR** (202 MHz, $CDCl_3$) δ 159.6.

**IR** (NaCl) $\nu_{max}$ = 2955, 2928, 2868, 1582, 1463, 1382, 1361, 1320, 1263, 1208, 1186, 1146 $cm^{-1}$.

**Melting point** 93 – 95 °C.

*Preparation of compound **3.2q***

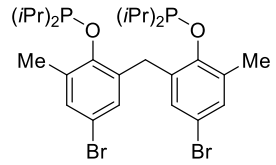


**3.2q**

6,6'-methylenebis(4-bromo-2-methylphenol) (500 mg) was subjected to the general procedure to afford 646 mg of **3.2q** with 81% yield as a white solid.

**$^{1}$H NMR** (500 MHz, $CDCl_3$) δ 7.14 (d, *J* = 1.3 Hz, 2H), 6.87 (s, 2H), 4.18 (s, 2H), 2.38 (s, 6H), 2.04 – 1.92 (m, 4H), 1.17 – 1.02 (m, 24H).

**$^{13}$C NMR** (125 MHz, $CDCl_3$) δ 153.0, 133.5, 132.3, 131.4, 131.1, 114.8, 32.1 (t, *J* = 7.1 Hz), 28.8 (d, *J* = 22.4 Hz), 18.5 (d, *J* = 9.9 Hz), 17.5 (d, *J* = 15.6 Hz), 17.3 (d, *J* = 11.9 Hz).

**$^{31}$P NMR** (202 MHz, $CDCl_3$) δ 159.7.

**IR** (NaCl) $\nu_{max}$ = 2953, 2918, 2888, 2868, 1585, 1574, 1462, 1431, 1421, 1380, 1319, 1283, 1258, 1206 $cm^{-1}$.

**Melting point** 135 – 137 °C.

*Preparation of compound **3.2r***

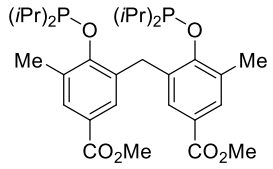


**3.2r**

Dimethyl 5,5'-methylenebis(4-hydroxy-3-methylbenzoate) (400 mg) was subjected to the general procedure to afford 320 mg of **3.2r** with 48% yield as a colorless oil.

**$^{1}$H NMR** (500 MHz, $CDCl_3$) δ 7.70 (s, 2H), 7.44 (s, 2H), 4.26 (s, 2H), 3.80 (s, 6H), 2.41 (s, 6H), 2.04 – 1.91 (m, 4H), 1.16 – 1.01 (m, 24H).

**$^{13}$C NMR** (125 MHz, $CDCl_3$) δ 167.0, 158.1, 131.6, 131.5, 130.4, 129.2, 124.0, 51.7, 32.4 (t, $J$ = 6.9 Hz), 29.0 (d, $J$ = 22.3 Hz), 18.8 (d, $J$ = 10.4 Hz), 17.4 (d, $J$ = 16.1 Hz), 17.2 (d, $J$ = 11.4 Hz).

**$^{31}$P NMR** (202 MHz, $CDCl_3$) δ 161.1.

**IR** (NaCl) $\nu_{max}$ = 2962, 2932, 2871, 1715, 1604, 1464, 1434, 1312, 1203, 1141, 1018 $cm^{-1}$.

*Preparation of compound **3.2s***

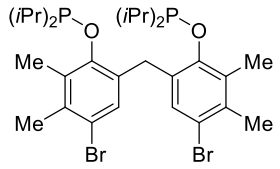


**3.2s**

6,6'-methylenebis(4-bromo-2,3-dimethylphenol) (500 mg) was subjected to the general procedure to afford 684 mg of **3.2s** with 88% yield as a white solid.

**$^{1}$H NMR** (500 MHz, $CDCl_3$) δ 6.95 (s, 2H), 4.19 (s, 2H), 2.33 (s, 6H), 2.31 (s, 6H), 2.05 – 1.94 (m, 4H), 1.16 – 1.04 (m, 24H).

**$^{13}$C NMR** (125 MHz, $CDCl_3$) δ 153.0, 135.3, 131.5, 130.7, 130.0, 118.6, 31.9 (t, $J$ = 8.8 Hz), 28.7 (d, $J$ = 22.7 Hz), 20.0, 17.6 (d, $J$ = 15.3 Hz), 17.5 (d, $J$ = 11.6 Hz), 15.7 (d, $J$ = 6.6 Hz).

**$^{31}$P NMR** (202 MHz, $CDCl_3$) δ 160.8.

**IR** (NaCl) $\nu_{max}$ = 2956, 2922, 2868, 1589, 1555, 1461, 1395, 1313, 1252, 1218, 1205, 1192, 1141 $cm^{-1}$.

**Melting point** 90 – 92 °C.

*Preparation of compound **3.2t***

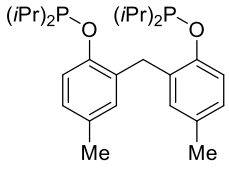


**3.2t**

2,2'-methylenebis(4-methylphenol)[19] (300 mg) was subjected to the general procedure to afford 550 mg of **3.2t** with 92% yield as a white solid.

**$^1$H NMR** (400 MHz, $C_6D_6$) δ 7.57 (dd, *J* = 8.2, 3.9 Hz, 2H), 6.94 (d, *J* = 9.5 Hz, 2H), 6.90 (d, *J* = 8.2 Hz, 2H), 4.27 (s, 2H), 2.05 (s, 6H), 1.84 – 1.70 (m, 4H), 1.18 – 1.06 (m, 12H), 1.04 – 0.92 (m, 12H).

**$^{13}$C NMR** (101 MHz, $C_6D_6$) δ 155.4 (d, *J* = 8.5 Hz), 131.6, 130.3, 130.1, 116.5, 116.2, 31.3, 28.5 (d, *J* = 18.0 Hz), 20.6, 17.9 (d, *J* = 19.9 Hz), 17.2 (d, *J* = 8.8 Hz).

**$^{31}$P NMR** (202 MHz, $C_6D_6$) δ 141.4.

**IR** (NaCl) $\nu_{max}$ = 2953, 2925, 2866, 1609, 1494, 1464, 1381, 1363, 1323, 1214, 1151, 1120, 1100 $cm^{-1}$.

**Melting point** 83 – 85 °C.

*Preparation of compound **3.2t'***

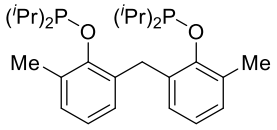


**3.2t'**

6,6'-methylenebis(2-methylphenol)[17] (457 mg) was subjected to the general procedure to afford 818.9 mg of **3.2t'** with 89% yield as a colorless oil.

**$^1$H NMR** (500 MHz, $C_6D_6$) δ 6.96 (dd, *J* = 7.6, 1.8 Hz, 2H), 6.93 (dd, *J* = 7.5, 1.8 Hz, 2H), 6.80 (td, *J* = 7.5, 0.8 Hz, 2H), 4.63 (s, 2H), 2.44 (s, 6H), 1.89 (heptd, *J* = 7.1, 3.2 Hz, 4H), 1.12 (dd, *J* = 11.3, 7.0 Hz, 12H), 1.02 (dd, *J* = 13.6, 7.2 Hz, 12H).

**$^{13}$C NMR** (126 MHz, $C_6D_6$) δ 154.5 (d, *J* = 1.7 Hz), 132.6, 130.0, 129.5, 129.4 (d, *J* = 1.9 Hz), 123.1 (d, *J* = 1.2 Hz), 33.1 (t, *J* = 7.7 Hz), 29.1 (d, *J* = 22.9 Hz), 18.9 (d, *J* = 9.1 Hz), 17.8, 17.7, 17.6, 17.5.

**$^{31}$P NMR** (202 MHz, $C_6D_6$) δ 156.5.

**IR** (NaCl) $\nu_{max}$ = 2955, 2927, 2867, 1590, 1463, 1382, 1255, 1205, 1091, 868, 763 cm$^{-1}$.

*Preparation of compound **3.2u***

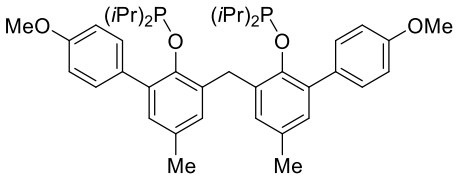


**3.2u**

3,3"-methylenebis(4'-methoxy-5-methyl-[1,1'-biphenyl]-2-ol) (500 mg) was subjected to the general procedure to afford 648 mg of **3.2u** with 85% yield as an amporphous foam.

**$^1$H NMR** (400 MHz, $C_6D_6$) δ 7.62 – 7.56 (m, 4H), 7.06 (s, 4H), 6.96 – 6.89 (m, 4H), 4.94 (s, 2H), 3.37 (s, 6H), 2.09 (s, 6H), 1.72 – 1.58 (m, 4H), 1.09 (dd, *J* = 11.5, 7.0 Hz, 12H), 0.93 (dd, *J* = 13.2, 7.2 Hz, 12H).

**$^{13}$C NMR** (101 MHz, $C_6D_6$) δ 159.3, 151.3, 134.8 (d, *J* = 2.2 Hz), 133.1, 133.1, 132.4, 131.9, 131.4, 130.4, 128.6, 113.7, 54.8, 33.5 (t, *J* = 11.2 Hz), 28.8 (d, *J* = 23.9 Hz), 20.9, 18.1 (d, *J* = 13.1 Hz), 17.7 (d, *J* = 15.7 Hz).

**$^{31}$P NMR** (162 MHz, $C_6D_6$) δ 160.9.

**IR** (NaCl) $\nu_{max}$ = 2953, 2928, 2866, 2835, 1610, 1575, 1514, 1457, 1401, 1382, 1363, 1289, 1246, 1212, 1175 $cm^{-1}$.

*Preparation of compound **3.2v***

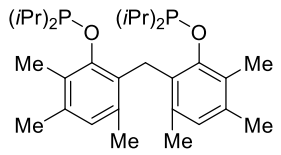


**3.2v**

6,6'-methylenebis(2,3,5-trimethylphenol) (500 mg) was subjected to the general procedure to afford 410 mg of **3.2v** with 45% yield as a white solid.

**$^{1}$H NMR** (400 MHz, $C_6D_6$) δ 6.56 (s, 2H), 4.67 (s, 2H), 2.40 (s, 6H), 2.06 (s, 6H), 2.14 – 1.96 (m, 4H), 2.05 (s, 6H), 1.22 (dd, *J* = 11.0, 7.0 Hz, 12H), 1.12 (dd, *J* = 13.4, 7.2 Hz, 12H).

**$^{13}$C NMR** (101 MHz, $C_6D_6$) δ 154.4, 135.8, 135.4, 129.7, 127.7, 124.8, 29.0 (d, *J* = 23.8 Hz), 27.6 (t, *J* = 4.9 Hz), 20.1, 19.9, 18.1 (d, *J* = 16.3 Hz), 17.9, 14.8 (d, *J* = 9.3 Hz).

**$^{31}$P NMR** (162 MHz, $C_6D_6$) δ 159.0.

**IR** (NaCl) $\nu_{max}$ = 3009, 2953, 2867, 1607, 1563, 1459, 1399, 1382, 1370, 1291, 1264, 1238, 1215, 1154 $cm^{-1}$.

**Melting point** 127 – 129 °C.

*Preparation of compound **3.2w***

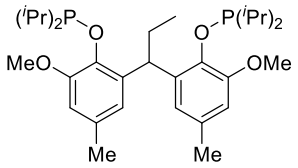


**3.2w**

6,6'-(propane-1,1-diyl)bis(2-methoxy-4-methylphenol) (500 mg) was subjected to the general procedure to afford 578 mg of **3.2w** with 67% yield as a colorless oil.

**$^1$H NMR** (400 MHz, $C_6D_6$) δ 6.82 (d, *J* = 2.0 Hz, 2H), 6.42 (d, *J* = 2.0 Hz, 2H), 5.02 (t, *J* = 7.7 Hz, 1H), 3.42 (s, 6H), 2.32 – 2.17 (m, 4H), 2.17 – 2.05 (m, 8H), 1.43 – 1.11 (m, 24H), 1.09 (t, *J* = 4.4 Hz, 3H).

**$^{13}$C NMR** (101 MHz, $C_6D_6$) δ 150.9 (d, *J* = 1.8 Hz), 144.2 (d, *J* = 4.3 Hz), 136.0 (d, *J* = 1.9 Hz), 130.9, 121.9, 112.8, 55.7 (d, *J* = 1.8 Hz), 40.3, 29.5 (d, *J* = 24.2 Hz), 29.1 (d, *J* = 22.7 Hz), 28.5, 21.4, 18.4 (d, *J* = 16.0 Hz), 18.2 (d, *J* = 18.1 Hz), 18.1 (d, *J* = 13.8 Hz), 17.8 (d, *J* = 16.2 Hz), 13.3.

**$^{31}$P NMR** (162 MHz, $C_6D_6$) δ 161.0.

**IR** (NaCl) $\nu_{max}$ = 2952, 2867, 2835, 1585, 1464, 1418, 1381, 1363, 1311, 1217, 1187, 1149, 1113 $cm^{-1}$.

*Preparation of compound **3.2x***

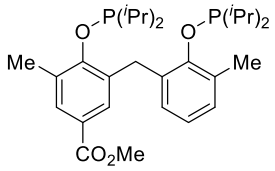


**3.2x**

Methyl 4-hydroxy-3-(2-hydroxy-3-methylbenzyl)-5-methylbenzoate (300 mg) was subjected to the general procedure to afford 410 mg of **3.2x** with 75% yield as a colorless oil.

**$^{1}$H NMR** (500 MHz, $C_6D_6$) δ 8.01 (s, 2H), 6.90 (t, *J* = 6.6 Hz, 2H), 6.77 (t, *J* = 7.5 Hz, 1H), 4.60 (s, 2H), 3.42 (s, 3H), 2.41 (s, 3H), 2.35 (s, 3H), 1.93 – 1.75 (m, 4H), 1.17 – 1.09 (m, 6H), 1.08 – 0.89 (m, 18H).

**$^{13}$C NMR** (125 MHz, $C_6D_6$) δ 166.6, 158.6, 154.3, 132.8, 132.1, 131.9, 131.5, 130.2, 129.7, 129.5, 129.0, 125.2, 123.1, 51.3, 33.2 (t, *J* = 7.6 Hz), 29.3 (d, *J* = 22.7 Hz), 29.2 (d, *J* = 22.7 Hz), 18.9 (d, *J* = 3.7 Hz), 18.8 (d, *J* = 2.4 Hz), 17.7 (d, *J* = 16.1 Hz), 17.6 (d, *J* = 10.0 Hz), 17.5 (d, *J* = 5.7 Hz), 17.4 (d, *J* = 11.4 Hz).

**$^{31}$P NMR** (202 MHz, $C_6D_6$) δ 160.3, 156.6.

**IR** (NaCl, $cm^{-1}$) 2954, 2928, 2868, 1721, 1603, 1463, 1433, 1382, 1363, 1308, 1278, 1253, 1233, 1199.

(Preparation of compounds **3.2a** – **t**, **3.2u** – **x** is conducted by Dr. Jun Zhu).

*General procedure for C−C bond cleavage*

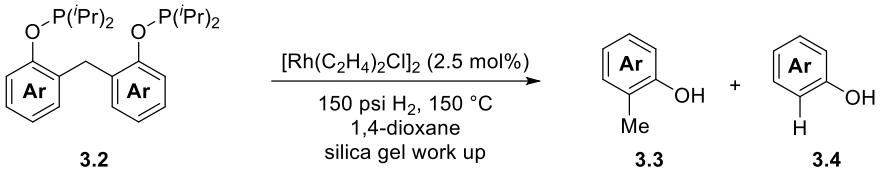


**3.2** **3.3** **3.4**

**General procedure**: To a Q-tube charged with a stir bar, substrate **3.2** (0.3 mmol), $[Rh(C_2H_4)_2Cl]_2$ (2.9 mg, 2.5 mol%) and 1,4-dioxane (6.0 mL) were added in the glovebox. The Q-tube was then resembled and taken out of the glovebox. The reaction mixture was flushed with hydrogen gas for 10 times and then charged with 150 psi $H_2$ followed by heating to 150 °C in a pre-heated oil bath for 24 h. After the reaction was completed, the $H_2$ pressure was released and the solvent was removed under vacuum. ~ 2 mL of dichloromethane and ~ 200 mg of silica gel were added and reconcentrated to give the silica gel containing the crude product which was further purified by silica gel chromatography to afford the corresponding phenols.

*Preparation of compounds **3.3a** and **3.4a***

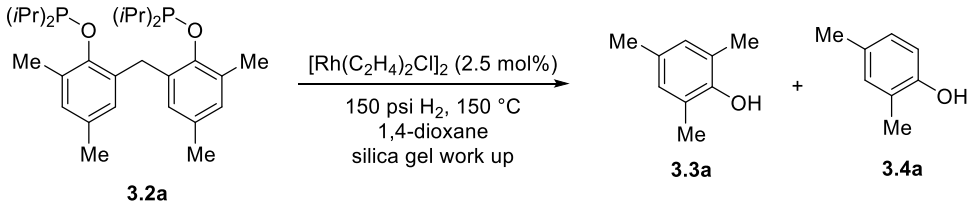


**3.2a** **3.3a** **3.4a**

The reaction was run on 0.1 mmol scale. The product was purified by column chromatography (silica gel, hexane:ethyl acetate = 20:1).

**3.3a**: white solid (11.8 mg, 87% yield).

$\mathbf{R_f}$ = 0.46 (hexane : ethyl acetate = 8:1)

**$^1$H NMR** (400 MHz, $CDCl_3$) δ 6.78 (s, 2H), 4.44 (s, 1H), 2.21 (s, 3H), 2.20 (s, 6H).

**$^{13}$C NMR** (101 MHz, $CDCl_3$) δ 149.8, 129.3, 129.1, 122.8, 20.3, 15.8.

Analytic data match the literature.[23]

**3.4a**: colorless oil (10.4 mg, 85% yield).

$\mathbf{R_f}$ = 0.37 (hexane : ethyl acetate = 8:1)

**$^1$H NMR** (400 MHz, $CDCl_3$) δ 6.92 (d, *J* = 2.2 Hz, 1H), 6.86 (ddt, *J* = 8.0, 2.3, 0.7 Hz, 1H), 6.65 (d, *J* = 8.0 Hz, 1H), 4.61 (s, 1H), 2.24 (s, 3H), 2.21 (s, 3H).

**$^{13}$C NMR** (101 MHz, $CDCl_3$) δ 151.4, 131.6, 129.9, 127.4, 123.4, 114.7, 20.4, 15.6.

Analytic data match the literature.[24]

*Preparation of compounds **3.3b** and **3.4b***

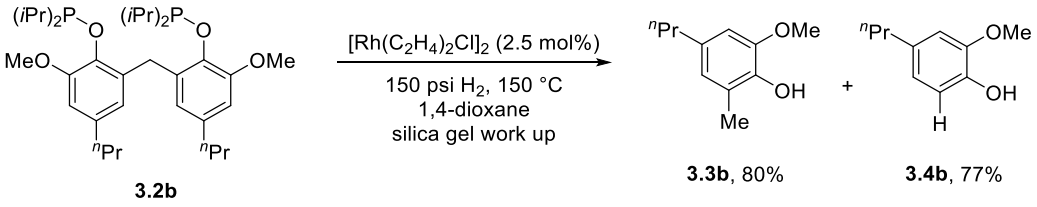


**3.2b** **3.3b**, 80% **3.4b**, 77%

The product was purified by column chromatography (silica gel, hexane:ethyl acetate = 20:1).

**3.3b**: Pale yellow oil (40.3 mg, 80% yield).

$\mathbf{R_f}$ = 0.43 (hexane : ethyl acetate = 5:1)

**$^1$H NMR** (500 MHz, $CDCl_3$) δ 6.58 (s, 1H), 6.56 (s, 1H), 5.55 (s, 1H), 3.87 (s, 3H), 2.50 (t, *J* = 7.7 Hz, 2H), 2.25 (s, 3H), 1.70 – 1.55 (m, 2H), 0.95 (t, *J* = 7.3 Hz, 3H).

**$^{13}$C NMR** (125 MHz, $CDCl_3$) δ 145.9, 141.6, 133.6, 123.3, 122.8, 108.4, 55.9, 37.8, 24.9, 15.4, 13.8.

**IR** (film) $\nu_{max}$ = 3550, 2958, 2929, 2871, 1607, 1504, 1464, 1428, 1365, 1339, 1297, 1236, 1218, 1151, 1097, 1001 $cm^{-1}$.

**HRMS (ESI)** m/z calcd. for $C_{11}H_{17}O_2^+$ $[M+H]^+$: 181.1223, found 181.1219.

**3.4b**: Colorless oil (38.4 mg, 77% yield).

$\mathbf{R_f}$ = 0.30 (hexane : ethyl acetate = 5:1)

**$^1$H NMR** (500 MHz, $CDCl_3$) δ 6.84 (d, *J* = 7.7 Hz, 1H), 6.72 – 6.65 (m, 2H), 5.49 (s, 1H), 3.88 (s, 3H), 2.53 (t, *J* = 7.6 Hz, 2H), 1.69 – 1.57 (m, 2H), 0.95 (t, *J* = 7.3 Hz, 3H).

**$^{13}$C NMR** (125 MHz, $CDCl_3$) δ 146.2, 143.5, 134.7, 120.9, 114.0, 111.0, 55.8, 37.7, 24.8, 13.8.

Analytic data match the literature.[25]

*Preparation of compounds **3.3c** and **3.4c***

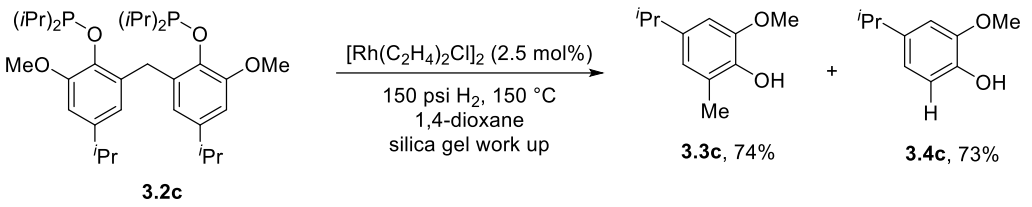


The product was purified by column chromatography (silica gel, hexane:ethyl acetate = 25:1).

**3.3c:** Pale yellow oil (40.1 mg, 74% yield).

$\mathbf{R}_f$ = 0.44 (hexane : ethyl acetate = 5:1)

**$^1$H NMR** (500 MHz, $CDCl_3$) δ 6.63 (s, 1H), 6.61 (s, 1H), 5.56 (s, 1H), 3.89 (s, 3H), 2.90 – 2.74 (m, 1H), 2.27 (s, 3H), 1.24 (d, $J$ = 7.0 Hz, 6H).

**$^{13}$C NMR** δ (125 MHz, $CDCl_3$) 146.0, 141.6, 139.9, 123.3, 120.7, 106.5, 55.9, 33.8, 24.3, 15.5.

**IR** (film) $\nu_{max}$ = 3550, 2959, 2869, 1606, 1506, 1464, 1427, 1382, 1362, 1324, 1295, 1261, 1220, 1175, 1134, 1095, 1069 $cm^{-1}$.

**HRMS (ESI)** m/z calcd. for $C_{11}H_{17}O_2^+$ $[M+H]^+$: 181.1223, found 181.1279.

**3.4c:** Pale yellow oil (36.3 mg, 73% yield).

$\mathbf{R}_f$ = 0.33 (hexane : ethyl acetate = 5:1)

**$^1$H NMR** (500 MHz, $CDCl_3$) δ 6.88 – 6.83 (m, 1H), 6.77 – 6.71 (m, 2H), 5.49 (s, 1H), 3.90 (s, 3H), 2.85 (m, 1H), 1.24 (d, $J$ = 7.0 Hz, 6H).

**$^{13}$C NMR** (125 MHz, $CDCl_3$) δ 146.3, 143.5, 141.0, 118.7, 114.1, 109.0, 55.8, 33.8, 24.2.

Analytic data match the literature.[14]

*Preparation of compounds **3.3d** and **3.4d***

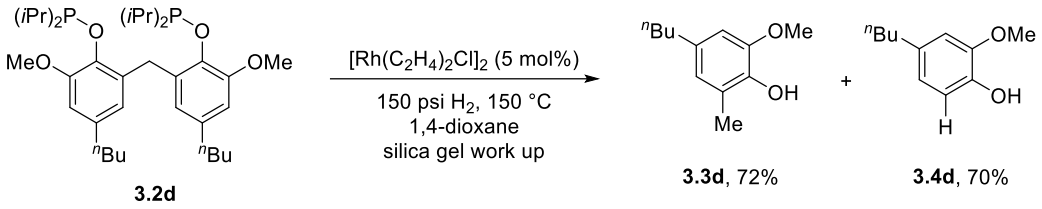


This example was run with 5 mol% $[Rh(C_2H_4)_2Cl]_2$. The product was purified by column chromatography (silica gel, hexane:ethyl acetate = 50:1).

**3.3d:** Pale yellow oil (41.7 mg, 72% yield).

$\mathbf{R_f}$ = 0.54 (hexane : ethyl acetate = 7:1)

**$^1$H NMR** (500 MHz, $CDCl_3$) δ 6.58 (s, 1H), 6.56 (s, 1H), 5.55 (s, 1H), 3.88 (s, 3H), 2.56 – 2.48 (m, 2H), 2.25 (s, 3H), 1.64 – 1.53 (m, 2H), 1.44 – 1.32 (m, 2H), 0.95 (t, $J$ = 7.4 Hz, 3H).

**$^{13}$C NMR** (125 MHz, $CDCl_3$) 145.9, 141.6, 133.6, 123.3, 122.8, 108.4, 55.9, 37.8, 24.9, 15.4, 13.8.

**IR** (film) $\nu_{max}$ = 3551, 2956, 2928, 2856, 1607, 1504, 1464, 1428, 1363, 1330, 1296, 1234, 1218, 1151, 1097, 1005 $cm^{-1}$.

**HRMS (ESI)** m/z calcd. for $C_{12}H_{19}O_2^+$ $[M+H]^+$: 195.1380, found 195.1397.

**3.4d:** Pale yellow oil (37.9 mg, 70% yield).

$\mathbf{R_f}$ = 0.43 (hexane : ethyl acetate = 7:1)

**$^1$H NMR** (500 MHz, $CDCl_3$) δ 6.84 (d, *J* = 7.7 Hz, 1H), 6.72 – 6.63 (m, 2H), 5.48 (s, 1H), 3.88 (s, 3H), 2.61 – 2.47 (m, 2H), 1.66 – 1.52 (m, 2H), 1.43 – 1.30 (m, 2H), 0.94 (t, *J* = 7.4 Hz, 3H).

**$^{13}$C NMR** (125 MHz, $CDCl_3$) 146.2, 143.4, 134.9, 120.9, 114.0, 110.9, 55.8, 35.3, 34.0, 22.3, 13.9.

Analytic data match the literature.[8b]

*Preparation of compounds **3.3e** and **3.4e***

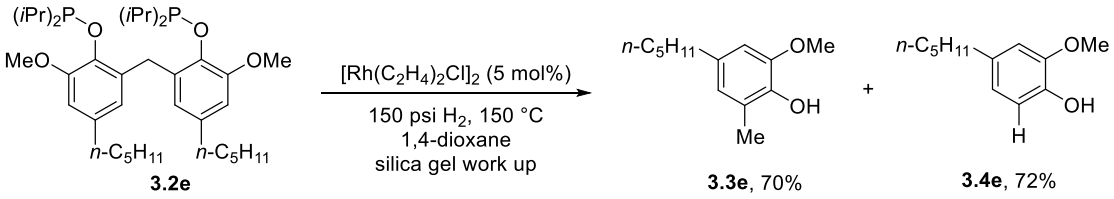


This reaction was run with 5 mol% $[Rh(C_2H_4)_2Cl]_2$. The product was purified by column chromatography (silica gel, hexane:ethyl acetate = 40:1).

**3.3e:** Pale yellow oil (43.9 mg, 70% yield).

**$R_f$** = 0.46 (hexane : ethyl acetate = 7:1)

**$^1$H NMR** (500 MHz, $CDCl_3$) δ 6.58 (s, 1H), 6.56 (s, 1H), 5.55 (s, 1H), 3.88 (s, 3H), 2.58 – 2.45 (m, 2H), 2.25 (s, 3H), 1.66 – 1.55 (m, 2H), 1.42 – 1.29 (m, 4H), 0.92 (t, *J* = 6.7 Hz, 3H).

**$^{13}$C NMR** (126 MHz, $CDCl_3$) δ 145.9, 141.5, 133.8, 123.3, 122.8, 108.4, 55.9, 35.7, 31.6, 31.6, 22.6, 15.4, 14.0.

**IR** (film) $\nu_{max}$ = 3552, 2928, 2856, 1607, 1504, 1464, 1428, 1364, 1332, 1295, 1241, 1218, 1188, 1151, 1099, 1002 $cm^{-1}$.

**HRMS (ESI)** m/z calcd. for $C_{13}H_{21}O_2^+$ $[M+H]^+$: 209.1536, found: 209.1541.

**3.4e:** Pale yellow oil (41.9 mg, 72% yield).

$\mathbf{R_f}$ = 0.38 (hexane : ethyl acetate = 7:1)

**$^1$H NMR** (500 MHz, $CDCl_3$) δ 6.84 (d, *J* = 7.7 Hz, 1H), 6.72 – 6.66 (m, 2H), 5.49 (s, 1H), 3.89 (s, 3H), 2.57 – 2.52 (m, 2H), 1.66 – 1.54 (m, 2H), 1.41 – 1.28 (m, 4H), 0.91 (t, *J* = 6.8 Hz, 3H).

**$^{13}$C NMR** (125 MHz, $CDCl_3$) δ 146.2, 143.4, 134.9, 120.9, 114.1, 110.9, 55.8, 35.6, 31.5, 22.5, 14.0.

Analytic data match the literature.[8b]

*Preparation of compounds **3.3f** and **3.4f***

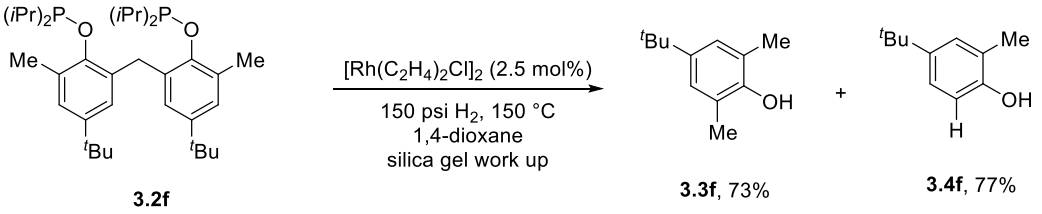


The product was purified by column chromatography (silica gel, hexane:ethyl acetate = 25:1).

**3.3f:** White solid (39.3 mg, 73% yield).

$\mathbf{R_f}$ = 0.50 (hexane : ethyl acetate = 7:1)

**$^1$H NMR** (500 MHz, $CDCl_3$) δ 7.02 (s, 2H), 4.50 (s, 1H), 2.27 (s, 6H), 1.31 (s, 9H).

**$^{13}$C NMR** (125 MHz, $CDCl_3$) δ 149.9, 142.9, 125.5, 122.3, 33.9, 31.6, 16.1.

Analytic data match the literature.[26]

**3.4f:** Pale yellow oil (39.1 mg, 77% yield).

**$R_f$** = 0.42 (hexane : ethyl acetate = 7:1)

**$^1$H NMR** (500 MHz, $CDCl_3$) δ 7.17 (d, *J* = 2.0 Hz, 1H), 7.12 (dd, *J* = 8.3, 2.3 Hz, 1H), 6.73 (d, *J* = 8.3 Hz, 1H), 4.71 (s, 1H), 2.28 (s, 3H), 1.31 (s, 9H).

**$^{13}$C NMR** (125 MHz, $CDCl_3$) δ 151.4, 143.5, 128.0, 123.8, 122.9, 114.4, 34.0, 31.5, 16.0.

**IR** (film) $\nu_{max}$ = 3389, 3029, 2963, 2868, 1611, 1511, 1463, 1411, 1393, 1363, 1275, 1202, 1128, 1104 $cm^{-1}$.

**HRMS (ESI)** m/z calcd. for $C_{11}H_{17}O^+$ $[M+H]^+$: 165.1274, found 165.1258.

*Preparation of compounds **3.3g** and **3.4g***

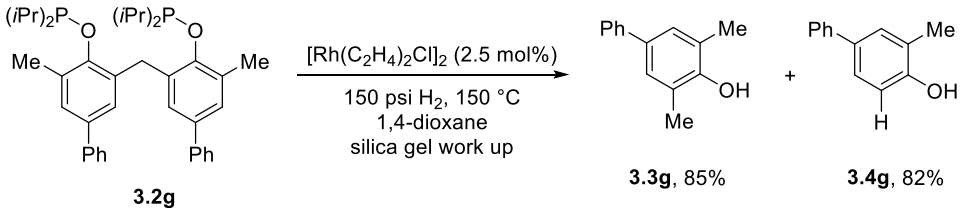


**3.2g** **3.3g**, 85% **3.4g**, 82%

The product was purified by column chromatography (silica gel, hexane:ethyl acetate = 40:1).

**3.3g:** White solid (50.6 mg, 85% yield).

$\mathbf{R_f}$ = 0.41 (hexane : ethyl acetate = 7:1)

**$^1$H NMR** (500 MHz, $CDCl_3$) δ 7.60 (d, *J* = 7.3 Hz, 2H), 7.46 (t, *J* = 7.7 Hz, 2H), 7.34 (t, *J* = 7.4 Hz, 1H), 7.28 (s, 2H), 4.70 (s, 1H), 2.37 (s, 6H).

**$^{13}$C NMR** (125 MHz, $CDCl_3$) δ 151.8, 141.1, 133.4, 128.6, 127.4, 126.7, 126.5, 123.3, 16.0.

Analytic data match the literature.[27]

**3.4g:** White solid (45.2 mg, 82% yield).

$\mathbf{R_f}$ = 0.31 (hexane : ethyl acetate = 7:1)

**$^1$H NMR** (500 MHz, $CDCl_3$) δ 7.57 (dd, *J* = 8.1, 0.9 Hz, 2H), 7.43 (t, *J* = 7.7 Hz, 2H), 7.40 (d, *J* = 1.7 Hz, 1H), 7.37 – 7.30 (m, 2H), 6.86 (d, *J* = 8.2 Hz, 1H), 4.82 (s, 1H), 2.34 (s, 3H).

**$^{13}$C NMR** (125 MHz, $CDCl_3$) δ 153.3, 140.9, 134.0, 129.8, 128.6, 126.7, 126.6, 125.8, 124.0, 115.2, 15.9.

Analytic data match the literature.[8b]

*Preparation of compounds **3.3h** and **3.4h***

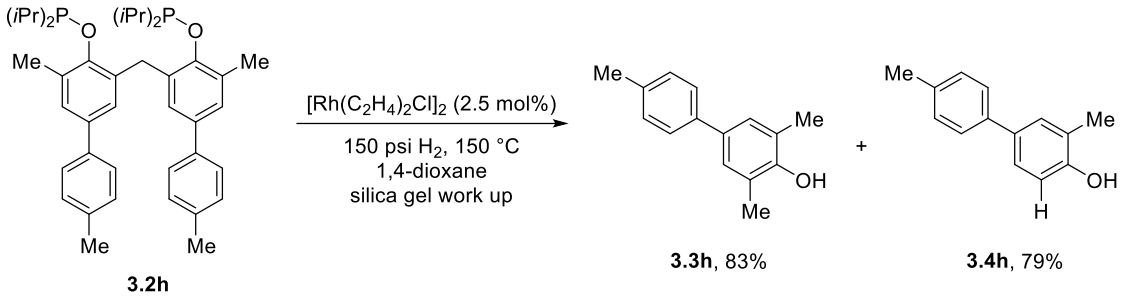


The product was purified by column chromatography (silica gel, hexane:ethyl acetate:dichloromethane = 50:1:1).

**3.3h:** White solid (52.8 mg, 83% yield).

$\mathbf{R}_f$ = 0.50 (hexane : ethyl acetate = 5:1)

**$^1$H NMR** (400 MHz, $CDCl_3$) δ 7.34 (s, 1H), 7.32 (s, 1H), 7.11 (t, *J* = 3.9 Hz, 4H), 4.53 (s, 1H), 2.28 (s, 3H), 2.20 (s, 6H).

**$^{13}$C NMR** (101 MHz, $CDCl_3$) δ 151.6, 138.2, 136.1, 133.3, 129.3, 127.1, 126.5, 123.2, 21.0, 16.0.

Analytic data match the literature.[28]

**3.4h:** White solid (47.2 mg, 79% yield).

$\mathbf{R}_f$ = 0.42 (hexane : ethyl acetate = 5:1)

**$^1$H NMR** (400 MHz, $CDCl_3$) δ 7.51 (d, *J* = 8.1 Hz, 2H), 7.43 (d, *J* = 2.1 Hz, 1H), 7.37 (dd, *J* = 8.2, 2.3 Hz, 1H), 7.29 (d, *J* = 8.3 Hz, 2H), 6.88 (d, *J* = 8.2 Hz, 1H), 4.92 (s, 1H), 2.45 (s, 3H), 2.38 (s, 3H).

**$^{13}$C NMR** (101 MHz, $CDCl_3$) δ 153.1, 138.0, 136.2, 133.9, 129.6, 129.4, 126.5, 125.6, 123.9, 115.2, 21.0, 15.9.

Analytic data match the literature.[15]

*Preparation of compounds **3.3i** and **3.4i***

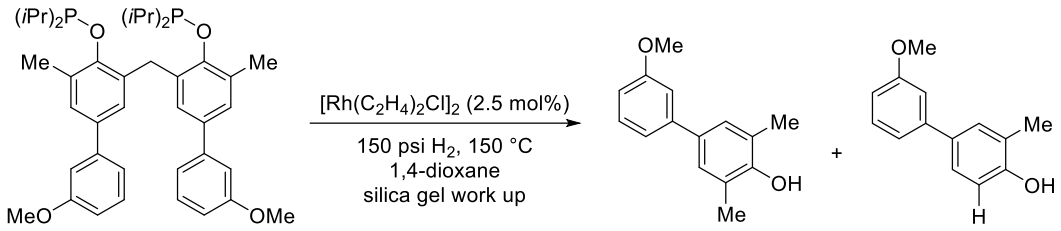


**3.2i** **3.3i**, 74% **3.4i**, 73%

The product was purified by column chromatography (silica gel, hexane:ethyl acetate:dichloromethane = 30:1:1).

**3.3i:** White solid (50.5 mg, 74% yield).

$\mathbf{R}_f$ = 0.44 (hexane : ethyl acetate = 4:1)

**$^1$H NMR** (500 MHz, $CDCl_3$) δ 7.36 (t, *J* = 7.9 Hz, 1H), 7.26 (s, 2H), 7.16 (t, *J* = 9.7 Hz, 1H), 7.12 (s, 1H), 6.89 (dd, *J* = 8.0, 1.5 Hz, 1H), 4.75 (s, 1H), 3.90 (s, 3H), 2.35 (s, 6H).

**$^{13}$C NMR** (125 MHz, $CDCl_3$) δ 159.8, 151.9, 142.6, 133.2, 129.6, 127.4, 123.2, 119.3, 112.4, 111.9, 55.3, 16.0. (unknown)

**IR** (film) $\nu_{max}$ = 3564, 3488, 3028, 2937, 2836, 1606, 1579, 1500, 1479, 1437, 1399, 1318, 1283, 1255, 1230, 1202, 1186, 1163, 1091, 1048 $cm^{-1}$.

**HRMS (ESI)** m/z calcd. for $C_{15}H_{17}O_2^+$ $[M+H]^+$: 229.1223, found 229.1218.

**Melting point** 48 - 50 °C.

**3.4i:** Colorless oil (46.9 mg, 73% yield).

$\mathbf{R_f}$ = 0.36 (hexane : ethyl acetate = 4:1)

**$^1$H NMR** (500 MHz, $CDCl_3$) δ 7.37 (s, 1H), 7.36 – 7.29 (m, 2H), 7.14 (d, *J* = 7.6 Hz, 1H), 7.09 (s, 1H), 6.89 – 6.85 (m, 1H), 6.84 (d, *J* = 8.2 Hz, 1H), 4.91 (s, 1H), 3.87 (s, 3H), 2.33 (s, 3H).

**$^{13}$C NMR** (125 MHz, $CDCl_3$) δ 159.8, 153.5, 142.5, 133.7, 129.8, 129.6, 125.8, 124.0, 119.3, 115.2, 112.5, 112.0, 55.3, 15.9.

**IR** (film) $\nu_{max}$ = 3410, 3027, 3000, 2940, 2836, 1609, 1579, 1513, 1481, 1465, 1436, 1402, 1317, 1270, 1233, 1162, 1121, 1093, 1058, 1040 $cm^{-1}$.

**HRMS (ESI)** m/z calcd. for $C_{14}H_{15}O_2^+$ $[M+H]^+$: 215.1067, found 215.1067.

*Preparation of compounds **3.3j** and **3.4j***

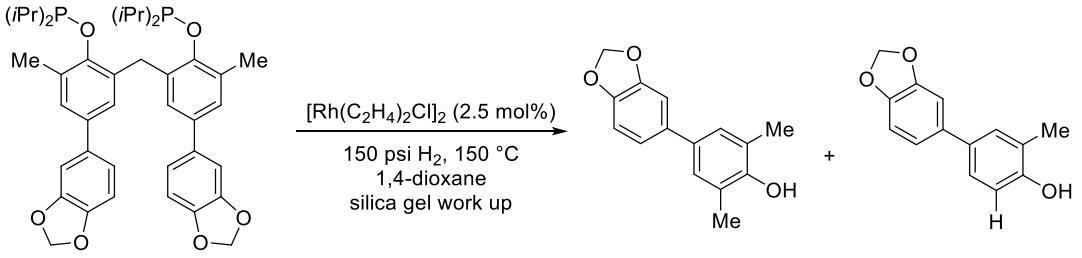


**3.2j** **3.3j**, 75% **3.4j**, 72%

The product was purified by column chromatography (silica gel, hexane:ethyl acetate:dichloromethane = 30:1:1).

**3.3j:** White solid (54.6 mg, 75% yield).

$\mathbf{R_f}$ = 0.57 (hexane : ethyl acetate = 4:1)

**$^1$H NMR** (400 MHz, $CDCl_3$) δ 7.15 (s, 2H), 7.00 (dd, *J* = 13.1, 5.0 Hz, 2H), 6.86 (d, *J* = 8.0 Hz, 1H), 5.98 (s, 2H), 4.66 (s, 1H), 2.31 (s, 6H).

**$^{13}$C NMR** (125 MHz, $CDCl_3$) δ 151.5, 147.9, 146.4, 135.6, 133.1, 127.1, 123.2, 120.0, 108.4, 107.4, 101.0, 16.0.

**IR** (film) $\nu_{max}$ = 3537, 2914, 1603, 1499, 1478, 1443, 1379, 1341, 1314, 1235, 1184, 1136, 1108, 1040 $cm^{-1}$.

**HRMS (ESI)** m/z calcd. for $C_{15}H_{15}O_3^+$ $[M+H]^+$: 243.1016, found 243.1020.

**Melting point** 106 − 108 °C.

**3.4j:** White solid (49.3 mg, 72% yield).

$\mathbf{R_f}$ = 0.43 (hexane : ethyl acetate = 4:1)

**$^1$H NMR** (500 MHz, $CDCl_3$) δ 7.15 (s, 2H), 7.04 – 6.97 (m, 2H), 6.85 (d, *J* = 8.0 Hz, 1H), 5.98 (s, 2H), 4.66 (s, 1H), 2.31 (s, 6H).

**$^{13}$C NMR** (125 MHz, $CDCl_3$) δ 153.1, 148.0, 146.5, 135.4, 133.7, 129.6, 125.5, 124.0, 120.0, 115.2, 108.5, 107.4, 101.0, 15.9.

**IR** (film) $\nu_{max}$ = 3467, 3026, 2894, 1607, 1500, 1482, 1444, 1412, 1340, 1233, 1194, 1172, 1116, 1040 $cm^{-1}$.

**HRMS (ESI)** m/z calcd. for $C_{14}H_{13}O_3^+$ $[M+H]^+$: 229.0859, found 229.0854.

**Melting point** 97 − 99 °C.

*Preparation of compounds **3.3k** and **3.4k***

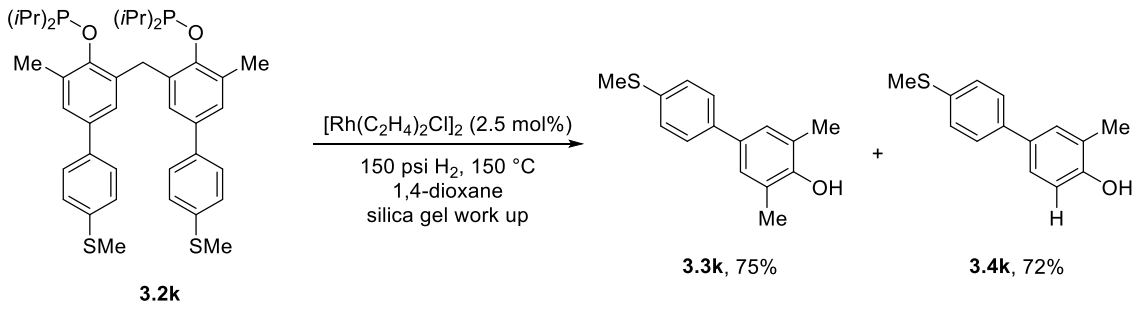


The product was purified by column chromatography (silica gel, hexane:ethyl acetate = 25:1).

**3.3k:** White solid (61.1 mg, 75% yield).

$\mathbf{R_f}$ = 0.44 (hexane : ethyl acetate = 6:1)

**$^1$H NMR** (500 MHz, $CDCl_3$) δ 7.48 (d, *J* = 8.2 Hz, 2H), 7.32 (d, *J* = 8.2 Hz, 2H), 7.22 (s, 2H), 4.71 (s, 1H), 2.53 (s, 3H), 2.32 (s, 6H).

**$^{13}$C NMR** (125 MHz, $CDCl_3$) δ 151.8, 138.0, 136.4, 132.6, 127.0, 123.3, 16.1, 16.0.

**IR** (film) $\nu_{max}$ = 3424, 2971, 2919, 2853, 1597, 1474, 1423, 1386, 1350, 1319, 1301, 1223, 1182, 1115, 1095, 1075, 1026, 1012 $cm^{-1}$.

**HRMS (ESI)** m/z calcd. for $C_{15}H_{17}OS^+$ $[M]^+$: 244.0916, found 244.0912.

**Melting point** 135 − 137 °C.

**3.4k:** White solid (57.1 mg, 72% yield).

$\mathbf{R}_f$ = 0.35 (hexane : ethyl acetate = 6:1)

**$^1$H NMR** (500 MHz, $CDCl_3$) δ 7.48 (d, *J* = 8.3 Hz, 2H), 7.40 – 7.27 (m, 4H), 6.84 (d, *J* = 8.2 Hz, 1H), 4.96 (s, 1H), 2.53 (s, 3H), 2.33 (s, 3H).

**$^{13}$C NMR** (125 MHz, $CDCl_3$) δ 153.3, 137.8, 136.5, 133.2, 129.5, 127.1, 127.0, 125.4, 124.1, 115.3, 16.0, 15.9. Analytic data match the literature.[8b]

*Preparation of compounds **3.3l** and **3.4l***

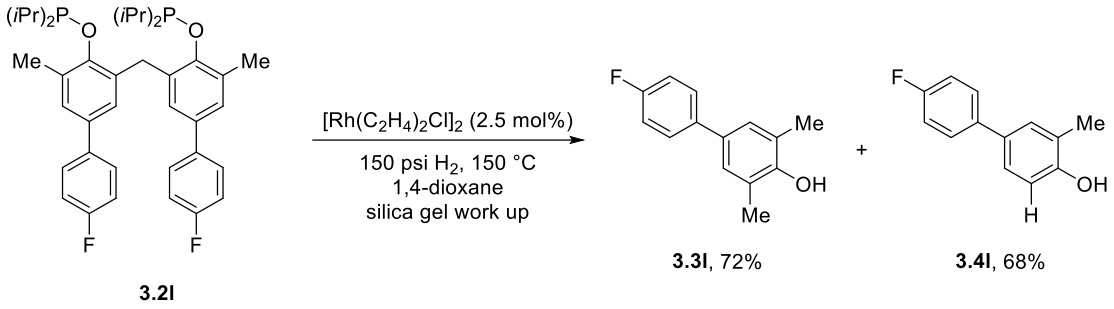


**3.2l**

**3.3l**, 72%

**3.4l**, 68%

The product was purified by column chromatography (silica gel, hexane:ethyl acetate:dichloromethane = 50:1:1).

**3.3l:** White solid (46.7 mg, 72% yield).

$\mathbf{R}_f$ = 0.51 (hexane : ethyl acetate = 6:1)

**$^1$H NMR** (500 MHz, $CDCl_3$) δ 7.53 – 7.46 (m, 2H), 7.18 (s, 2H), 7.13 – 7.06 (m, 2H), 4.68 (s, 1H), 2.33 (s, 6H).

**$^{13}$C NMR** (125 MHz, $CDCl_3$) δ 162.0 (d, *J* = 244.0 Hz), 151.8, 137.2 (d, *J* = 2.8 Hz), 132.4, 128.2 (d, *J* = 7.9 Hz), 127.2, 123.3, 115.4 (d, *J* = 21.1 Hz), 16.0.

**$^{19}$F NMR** (470 MHz, $CDCl_3$) δ -117.0.

Analytic data match the literature.[29]

**3.4l:** White solid (41.4 mg, 68% yield).

**$R_f$** = 0.40 (hexane : ethyl acetate = 6:1)

**$^{1}$H NMR** (500 MHz, $CDCl_3$) δ 7.54 – 7.47 (m, 2H), 7.35 (d, *J* = 1.7 Hz, 1H), 7.29 (dd, *J* = 8.4, 1.9 Hz, 1H), 7.17 – 7.08 (m, 2H), 6.87 (d, *J* = 8.2 Hz, 1H), 4.87 (s, 1H), 2.35 (s, 3H).

**$^{13}$C NMR** (125 MHz, $CDCl_3$) δ 162.0 (d, *J* = 244.3 Hz), 153.3, 137.0 (d, *J* = 2.9 Hz), 133.0, 129.7, 128.2 (d, *J* = 7.9 Hz), 125.6, 124.1, 115.4 (d, *J* = 21.3 Hz), 115.3, 15.8.

**$^{19}$F NMR** (470 MHz, $CDCl_3$) δ -116.8.

**IR** (KBr) $\nu_{max}$ = 3313, 1601, 1497, 1454, 1400, 1229, 1175, 1126, 843, 815 $cm^{-1}$.

**HRMS (ESI)** m/z calcd. for $C_{13}H_{11}FO^+$ $[M]^+$: 202.0794, found 202.0784.

**Melting point** 128 − 130 °C.

*Preparation of compounds **3.3m** and **3.4m***

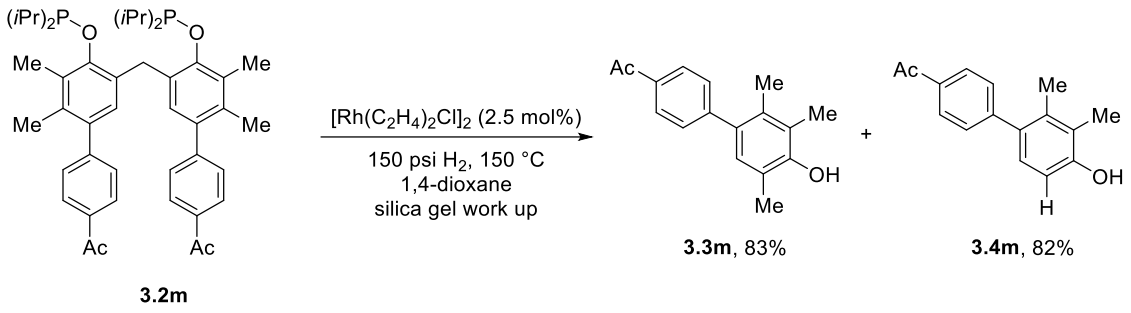


**3.2m**

**3.3m**, 83%

**3.4m**, 82%

The product was purified by column chromatography (silica gel, hexane:ethyl acetate:dichloromethane = 10:1:1).

**3.3m:** White solid (63.5 mg, 83% yield).

$\mathbf{R}_f$ = 0.47 (hexane : ethyl acetate = 3:1)

**$^1$H NMR** (400 MHz, $CDCl_3$) δ 7.99 (d, *J* = 8.1 Hz, 2H), 7.38 (d, *J* = 8.1 Hz, 2H), 6.88 (s, 1H), 4.91 (s, 1H), 2.65 (s, 3H), 2.28 (s, 3H), 2.26 (s, 3H), 2.16 (s, 3H).

**$^{13}$C NMR** (100 MHz, $CDCl_3$) δ 198.0, 151.7, 147.8, 135.1, 133.4, 132.7, 129.9, 129.0, 128.1, 122.6, 120.1, 26.6, 17.4, 15.8, 12.3.

**IR** (film) $\nu_{max}$ = 3389, 2923, 2855, 1668, 1602, 1556, 1509, 1472, 1399, 1362, 1285, 1274, 1253, 1222, 1200, 1157, 1112, 1092, 1015 $cm^{-1}$.

**HRMS (ESI)** m/z calcd. for $C_{17}H_{19}O_2^+$ $[M+H]^+$: 255.1380, found 255.1383.

**Melting point** 182 − 184 °C.

**3.4m:** Pale yellow solid (59.1 mg, 82% yield).

$\mathbf{R}_f$ = 0.39 (hexane : ethyl acetate = 3:1)

**$^1$H NMR** (400 MHz, $CDCl_3$) δ 8.05 – 7.95 (m, 2H), 7.41 – 7.33 (m, 2H), 6.96 (d, *J* = 8.2 Hz, 1H), 6.74 (d, *J* = 8.2 Hz, 1H), 5.23 (s, 1H), 2.66 (s, 3H), 2.26 (s, 3H), 2.18 (s, 3H).

**$^{13}$C NMR** (100 MHz, $CDCl_3$) δ 198.3, 153.4, 147.9, 135.5, 135.1, 133.9, 129.9, 128.2, 127.6, 123.2, 112.4, 26.6, 17.5, 12.0.

**IR** (film) $\nu_{max}$ = 3375, 2923, 2854, 1665, 1603, 1588, 1558, 1484, 1457, 1400, 1359, 1276, 1200, 1183, 1063, 1016 $cm^{-1}$.

**HRMS (ESI)** m/z calcd. for $C_{16}H_{17}O_2^+$ $[M+H]^+$: 241.1223, found 241.1226.

**Melting point** 157 − 159 °C.

*Preparation of compounds **3.3n** and **3.4n***

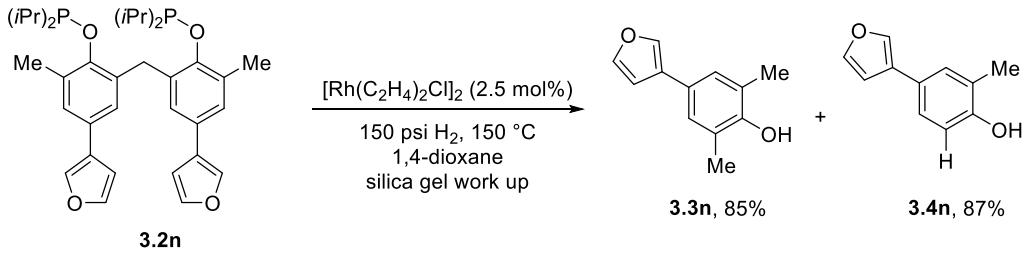


The product was purified by column chromatography (silica gel, hexane:ethyl acetate = 30:1).

**3.3n:** Pale yellow solid (47.8 mg, 85% yield).

**$R_f$** = 0.53 (hexane : ethyl acetate = 6:1)

**$^1$H NMR** (500 MHz, $CDCl_3$) δ 7.65 (s, 1H), 7.46 (s, 1H), 7.13 (s, 2H), 6.66 (s, 1H), 4.66 (s, 1H), 2.29 (s, 6H).

**$^{13}$C NMR** (125 MHz, $CDCl_3$) δ 151.4, 143.3, 137.5, 126.2, 124.5, 123.3, 108.9, 15.9.

**IR** (film) $\nu_{max}$ = 3296, 2946, 2918, 1511, 1483, 1438, 1422, 1387, 1365, 1348, 1331, 1241, 1191, 1163, 1107, 1065, 1026 $cm^{-1}$.

**HRMS (ESI)** m/z calcd. for $C_{12}H_{13}O_2^+$ $[M+H]^+$: 189.0910, found 189.0924.

**Melting point** 95 − 97 °C.

**3.4n:** Pale yellow solid (45.7 mg, 87% yield).

$\mathbf{R_f}$ = 0.44 (hexane : ethyl acetate = 6:1)

**$^1$H NMR** (500 MHz, $CDCl_3$) δ 7.66 (s, 1H), 7.47 (s, 1H), 7.28 (s, 1H), 7.22 (d, *J* = 8.2 Hz, 1H), 6.79 (d, *J* = 8.2 Hz, 1H), 6.66 (s, 1H), 4.94 (s, 1H), 2.30 (s, 3H).

**$^{13}$C NMR** (125 MHz, $CDCl_3$) δ 152.9, 143.4, 137.6, 128.6, 126.1, 125.1, 124.6, 124.1, 115.2, 108.9, 15.8.

**IR** (film) $\nu_{max}$ = 3333, 3134, 3019, 2928, 1515, 1492, 1352, 1246, 1179, 1162, 1125, 1096, 1058, 1021 $cm^{-1}$.

**HRMS (ESI)** m/z calcd. for $C_{11}H_{11}O_2^+$ $[M+H]^+$: 175.0754, found 175.0766.

**Melting point** 92 − 94 °C.

*Preparation of compounds **3.3o** and **3.4o***

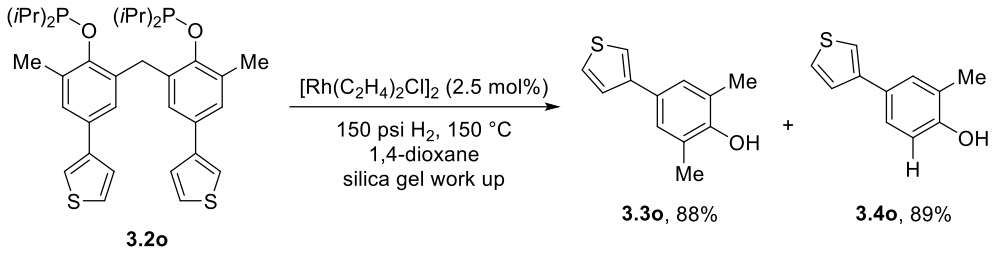


The product was purified by column chromatography (silica gel, hexane:ethyl acetate = 30:1).

**3.3o:** White solid (53.8 mg, 88% yield).

$\mathbf{R_f}$ = 0.42 (hexane : ethyl acetate = 6:1)

**$^1$H NMR** (500 MHz, $CDCl_3$) δ 7.39 – 7.31 (m, 3H), 7.25 (s, 2H), 4.67 (s, 1H), 2.31 (s, 6H).

**$^{13}$C NMR** (125 MHz, $CDCl_3$) δ 151.5, 142.2, 128.2, 126.7, 126.3, 125.8, 123.2, 118.7, 16.0.

**IR** (film) $\nu_{max}$ = 3333, 3134, 3019, 2928, 1515, 1492, 1352, 1246, 1179, 1162, 1125, 1096, 1058, 1021 $cm^{-1}$.

**HRMS (ESI)** m/z calcd. for $C_{12}H_{13}OS^+$ $[M+H]^+$: 205.0682, found 205.0674.

**Melting point** 101 − 103 °C.

**3.4o:** White solid (51.0 mg, 89% yield).

$\mathbf{R_f}$ = 0.33 (hexane : ethyl acetate = 6:1)

**$^1$H NMR** (400 MHz, $CDCl_3$) δ 7.44 – 7.28 (m, 5H), 6.81 (d, $J$ = 8.2 Hz, 1H), 4.87 (s, 1H), 2.32 (s, 3H).

**$^{13}$C NMR** (101 MHz, $CDCl_3$) δ 153.1, 142.1, 129.2, 128.9, 126.3, 126.0, 125.2, 124.0, 118.8, 115.2, 15.8.

**IR** (film) $\nu_{max}$ = 3326, 3103, 3026, 1611, 1537, 1507, 1492, 1457, 1398, 1384, 1352, 1243, 1205, 1165, 1121, 1086, 1048 $cm^{-1}$.

**HRMS (ESI)** m/z calcd. for $C_{11}H_{11}OS^+$ $[M+H]^+$: 191.0525, found 191.0532.

**Melting point** 118 − 120 °C.

*Preparation of compounds **3.3p** and **3.4p***

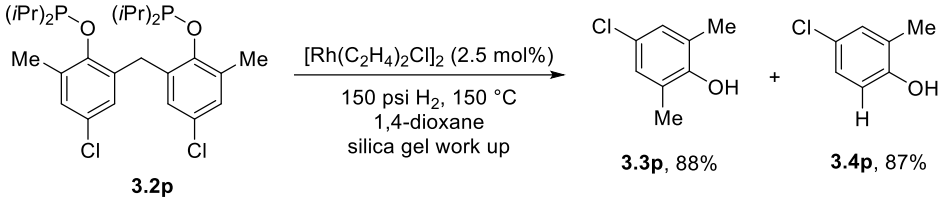


Products **3.3p** and **3.4p** was found inseparable from chromatography on silica gel, their yields were determined by GC-Fid.

Upon completion of the reaction, $H_2$ pressure was released and the reaction mixture was transferred to a 20 mL vial, the solvent was then removed under reduced pressure to afford a yellow residue which was dissolved in ~5 mL of dichloromethane and passed through a short silca gel pad (~10 cm). The short silica gel pad was flushed with ~25 mL dichloromethane, the combined filtrate was concentrated under reduced pressure to afford a yellow oil as the crude product. 20.1 mg of tetradecane and 25 mL of EtOAc were added to the crude mixture to afford a yellow solution which was subjected to gas chromatography (GC) analysis to determine the yield.

*Preparation of compounds **3.3q** and **3.4q***

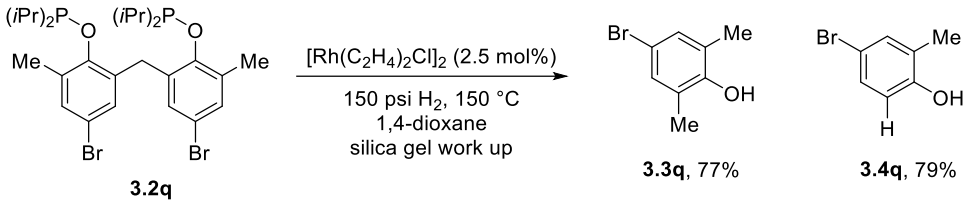


The product was purified by column chromatography (silica gel, hexane:ethyl acetate = 20:1).

**3.3q:** White solid (46.3 mg, 77% yield).

$\mathbf{R}_f$ = 0.45 (hexane : ethyl acetate = 4:1)

**$^1$H NMR** (500 MHz, $CDCl_3$) δ 7.10 (s, 2H), 4.56 (s, 1H), 2.22 (s, 3H).

**$^{13}$C NMR** (125 MHz, $CDCl_3$) δ 151.2, 131.0, 125.1, 112.0, 15.7.

Analytic data match the literature.[30]

**3.4q:** Pale yellow solid (44.3 mg, 79% yield).

$\mathbf{R}_f$ = 0.39 (hexane : ethyl acetate = 4:1)

**$^1$H NMR** (500 MHz, $CDCl_3$) δ 7.24 (d, $J$ = 1.6 Hz, 1H), 7.17 (dd, $J$ = 8.5, 2.0 Hz, 1H), 6.65 (d, $J$ = 8.5 Hz, 1H), 4.81 (s, 1H), 2.22 (s, 3H).

**$^{13}$C NMR** (125 MHz, $CDCl_3$) δ 152.9, 133.5, 129.7, 126.2, 116.5, 112.5, 15.6.

Analytic data match the literature.[31]

*Preparation of compounds **3.3r** and **3.4r***

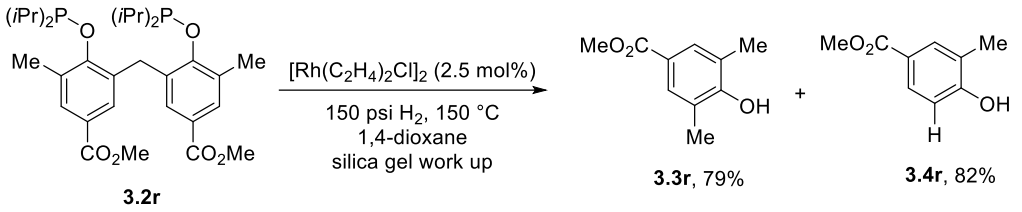


The product was purified by column chromatography (silica gel, hexane:ethyl acetate = 10:1).

**3.3r:** White solid (42.6 mg, 79% yield).

$\mathbf{R}_f$ = 0.38 (hexane : ethyl acetate = 3:1)

**$^1$H NMR** (500 MHz, $CDCl_3$) δ 7.69 (s, 2H), 5.50 (s, 1H), 3.87 (s, 3H), 2.27 (s, 6H).

**$^{13}$C NMR** (125 MHz, $CDCl_3$) δ 167.4, 156.6, 130.4, 123.0, 121.7, 51.8, 15.8.

Analytic data match the literature.[32]

**3.4r:** White solid (40.8 mg, 82% yield).

$\mathbf{R}_f$ = 0.31 (hexane : ethyl acetate = 3:1)

**$^1$H NMR** (500 MHz, $CDCl_3$) δ 7.84 (s, 1H), 7.78 (d, $J$ = 8.4 Hz, 1H), 6.84 (d, $J$ = 8.4 Hz, 1H), 6.63 (s, 1H), 3.89 (s, 3H), 2.27 (s, 3H).

**$^{13}$C NMR** (125 MHz, $CDCl_3$) δ 167.8, 158.7, 132.8, 129.4, 124.2, 121.9, 114.7, 52.0, 15.7.

Analytic data match the literature.[32]

*Preparation of compounds **3.3s** and **3.4s***

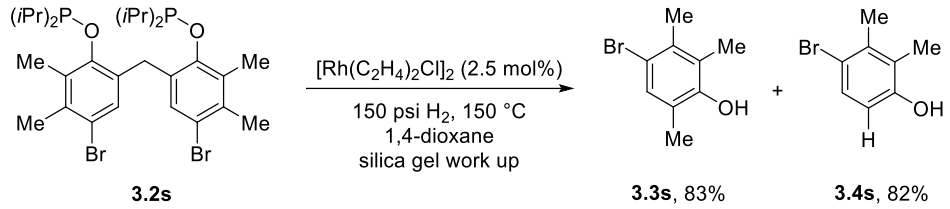


The product was purified by column chromatography (silica gel, hexane:ethyl acetate = 30:1).

**3.3s:** White solid (53.9 mg, 83% yield).

$\mathbf{R}_f$ = 0.45 (hexane : ethyl acetate = 6:1)

**$^1$H NMR** (500 MHz, $CDCl_3$) δ 7.19 (s, 1H), 4.59 (s, 1H), 2.34 (s, 3H), 2.22 (s, 3H), 2.20 (s, 3H).

**$^{13}$C NMR** (125 MHz, $CDCl_3$) δ 151.1, 134.5, 131.0, 123.7, 122.0, 115.6, 19.7, 15.6, 13.0.

Analytic data match the literature.[33]

**3.4s:** White solid (49.8 mg, 82% yield).

$\mathbf{R}_f$ = 0.38 (hexane : ethyl acetate = 6:1)

**$^1$H NMR** (500 MHz, $CDCl_3$) δ 7.27 (d, $J$ = 8.7 Hz, 1H), 6.55 (d, $J$ = 8.6 Hz, 1H), 4.81 (s, 1H), 2.39 (s, 3H), 2.25 (s, 3H).

**$^{13}$C NMR** (101 MHz, $CDCl_3$) δ 152.6, 137.4, 129.8, 124.6, 116.3, 113.9, 19.9, 12.9.

Analytic data match the literature.[8b]

*Preparation of compounds **3.4a** and **3.4t***

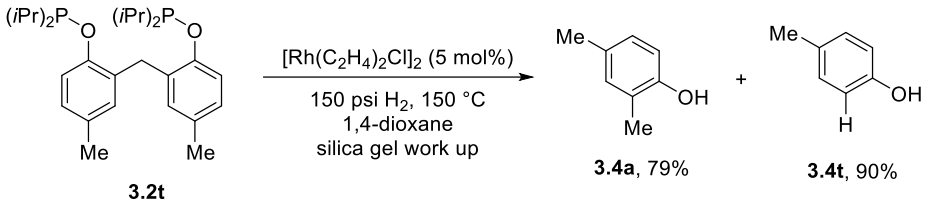


The product was purified by column chromatography (silica gel, pentane:ethyl acetate = 30:1).

**3.4a**: colorless oil (29.1 mg, 79% yield).

Data of **3.4a** match the one obtained from substrate **3.2a**.

**3.4t**: white solid (29.3 mg, 90% yield).

$\mathbf{R}_f$ = 0.34 (hexane : ethyl acetate = 5:1)

**$^1$H NMR** (400 MHz, $CDCl_3$) δ 7.08 – 6.95 (m, 2H), 6.72 (d, $J$ = 8.5 Hz, 2H), 4.95 (s, 1H), 2.26 (s, 3H).

**$^{13}$C NMR** (101 MHz, $CDCl_3$) δ 153.1, 130.1, 130.0, 115.1, 20.4.

Analytic data match the literature.[34]

*Preparation of compounds **3.3t'** and **3.4t'***

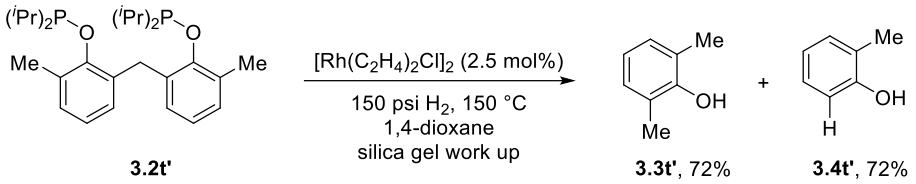


**3.2t'** **3.3t'**, 72% **3.4t'**, 72%

The product was purified by column chromatography (silica gel, pentane:ethyl acetate = 30:1).

**3.3t'**: white solid (26.4 mg, 72% yield).

$\mathbf{R}_f$ = 0.45 (hexane : ethyl acetate = 4:1)

**$^1$H NMR** (500 MHz, $CDCl_3$) δ 6.97 (d, *J* = 7.5 Hz, 2H), 6.75 (t, *J* = 7.5 Hz, 1H), 4.59 (s, 1H), 2.24 (s, 6H).

**$^{13}$C NMR** (126 MHz, $CDCl_3$) δ 152.1, 128.6, 122.9, 120.2, 15.8.

Analytic data match the literature.[35]

**3.4t'**: colorless oil (23.3 mg, 72% yield).

$\mathbf{R}_f$ = 0.39 (hexane : ethyl acetate = 4:1)

**$^1$H NMR** (500 MHz, $CDCl_3$) δ 7.14 – 7.10 (m, 1H), 7.08 (td, *J* = 7.7, 1.7 Hz, 1H), 6.84 (td, *J* = 7.4, 1.2 Hz, 1H), 6.76 (dd, *J* = 8.0, 1.2 Hz, 1H), 4.73 (s, 1H), 2.25 (s, 3H).

**$^{13}$C NMR** (126 MHz, $CDCl_3$) δ 153.7, 131.0, 127.1, 123.7, 120.7, 114.9, 15.7.

Analytic data match the literature. [23]

*Preparation of compounds **3.3u** and **3.4u***

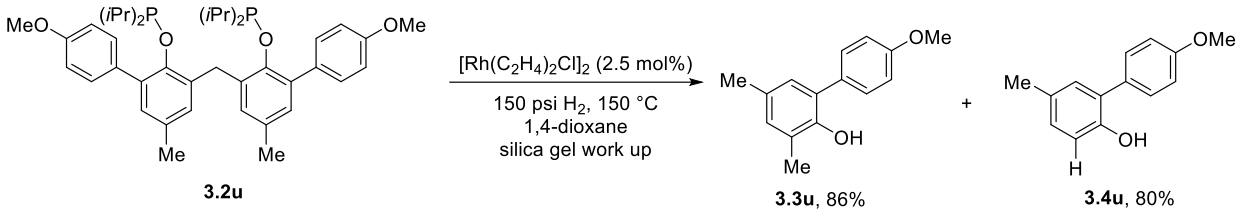


The product was purified by column chromatography (silica gel, pentane:ethyl acetate = 30:1).

**3.3u**: Pale yellow oil (58.6 mg, 86% yield)

$\mathbf{R_f}$ = 0.52 (hexane : ethyl acetate = 4:1)

**$^1$H NMR** (400 MHz, $CDCl_3$) δ 7.44 – 7.35 (m, 2H), 7.07 – 6.99 (m, 2H), 6.96 (d, *J* = 2.2 Hz, 1H), 6.89 (d, *J* = 2.3 Hz, 1H), 4.67 (s, 1H), 3.87 (s, 3H), 2.31 (s, 3H), 2.30 (s, 3H).

**$^{13}$C NMR** (100 MHz, $CDCl_3$) δ 159.2, 148.4, 130.8, 130.2, 129.6, 129.1, 128.1, 127.1, 124.2, 114.6, 55.3, 20.4, 16.1.

Analytic data match the literature.[36]

**3.4u:** White solid (51.2 mg, 80% yield)

$\mathbf{R_f}$ = 0.32 (hexane : ethyl acetate = 4:1)

**$^1$H NMR** (400 MHz, $CDCl_3$) δ 7.44 – 7.38 (m, 2H), 7.10 – 6.98 (m, 4H), 6.92 – 6.85 (m, 1H), 4.72 (s, 1H), 3.87 (s, 3H), 2.33 (s, 3H).

**$^{13}$C NMR** (100 MHz, $CDCl_3$) δ 159.1, 150.2, 130.7, 130.2, 129.8, 129.4, 129.2, 127.5, 115.5, 114.6, 55.3, 20.4.

Analytic data match the literature.[37]

*Preparation of compounds **3.3v** and **3.4v***

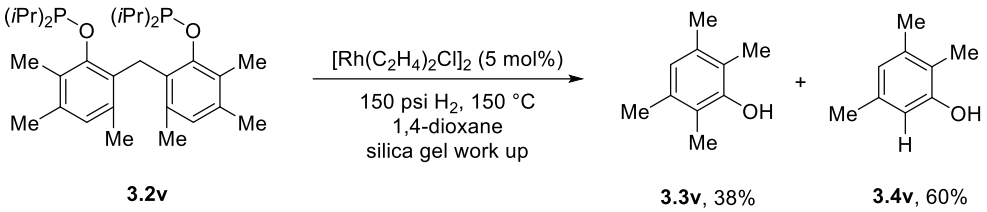


**3.2v** **3.3v**, 38% **3.4v**, 60%

This example was run with 5 mol% $[Rh(C_2H_4)_2Cl]_2$. The product was purified by column chromatography (silica gel, pentane:ethyl acetate = 30:1).

**3.3v**: white solid (16.9 mg, 38% yield)

$\mathbf{R_f}$ = 0.48 (hexane : ethyl acetate = 4:1)

**$^1$H NMR** (500 MHz, $CDCl_3$) δ 6.60 (s, 1H), 4.59 (s, 1H), 2.22 (s, 6H), 2.14 (s, 6H).

**$^{13}$C NMR** (101 MHz, $CDCl_3$) δ 151.7, 134.3, 123.5, 118.9, 19.8, 11.6.

Analytic data match the literature.[38]

**3.4v**: white solid (24.7 mg, 60% yield)

$\mathbf{R_f}$ = 0.40 (hexane : ethyl acetate = 4:1)

**$^1$H NMR** (500 MHz, $CDCl_3$) δ 6.64 – 6.60 (m, 1H), 6.49 – 6.45 (m, 1H), 4.68 (s, 1H), 2.26 (d, *J* = 1.4 Hz, 6H), 2.14 (s, 3H).

**$^{13}$C NMR** (101 MHz, $CDCl_3$) δ 153.3, 138.0, 135.8, 123.2, 119.2, 113.3, 20.8, 20.0, 11.1.

**IR** (KBr) $\nu_{max}$ = 3293, 2922, 1623, 1457, 1306, 1080, 839, 583 $cm^{-1}$.

**HRMS (ESI)** m/z calcd. for $C_9H_{13}O^+$ $[M+H]^+$: 137.0961, found 137.0953.

**Melting point** 93.4 – 94.3 °C.

*Preparation of compounds **3.3r** and **3.4r***

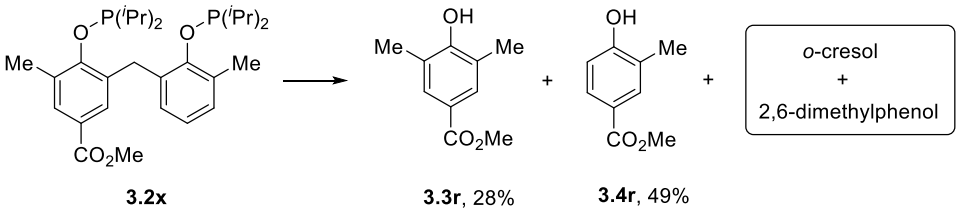


The product was purified by column chromatography (silica gel, hexane:ethyl acetate = 40:1).

**3.3r:** White solid (15.3 mg, 28% yield).

Data of **3r** match the one obtained from substrate **3.2r**.

**3.4r:** White solid (24.4 mg, 49% yield).

Data of **3.4r** match the one obtained from substrate **3.2r**.

(C−C cleavage of compounds **3.2b** – **t**, **3.2u**, **3.2w**, **3.2x** is conducted by Dr. Jun Zhu).

*Preparation of compounds **3.3g** and **3.4g** in gram scale (Conducted by Dr. Jun Zhu)*

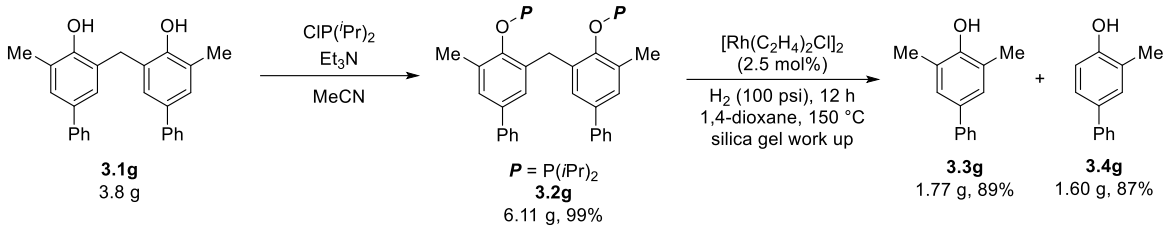


To a 100 mL sealed tube charged with a stir bar, **3.1g** (3.8 g, 10.0 mmol) and 50 mL of dry $CH_3CN$ were added in glove box to afford a suspension. $Et_3N$ (4.05 g, 40.0 mmol) was then added to the suspension to afford a colorless clear solution. To the clear solution, chloro-diisopropylphosphine (3.20 g, 11.04 mmol) was then added dropwise. The sealed tube was then resembled and transferred out of the glovebox. The reaction mixture was heated at 70 °C overnight. Upon completion of the reaction, the mixture was transferred to glovebox, and the solvent was removed under reduced pressure to afford the crude **3.2g** with triethylamine hydrochloride. The crude mixture was suspended in dry benzene (30 mL) and filtered to remove triethylamine hydrochloride. The residue was subsequently washed by dry benzene (10 mL *3). The combined filtrate was concentrated under reduced pressure to afford **3.2g** (6.11 g, 99% yield) as white solid, which was used directly in the next step.

To a 350 mL Q-tube charged with a stir bar, **3.2g** (6.11 g, 10.0 mmol) from the previous step, $[Rh(C_2H_4)_2Cl]_2$ (97.2 mg, 0.25 mmol) and 100 mL dry 1,4-dioxane were added in the glovebox. The Q-tube was then resembled and taken out of the glovebox. The reaction mixture was subjected to the freeze-pump-thaw technique by following the standard procedure three times. The Q-tube was then charged by 100 psi $H_2$ and heated at 150 °C in a pre-heated oil bath for 12 h. (*Caution: the pressure inside may increase to 130 psi during the heating*). Upon completion of the reaction, the Q-tube was taken out of the oil bath and cooled to room temperature. The hydrogen gas pressure was then released. The reaction mixture was concentrated under reduced pressure to

afford a yellow crude residue. To the crude residue, ~50 mL dichloromethane and 5.0 g silica gel were added to afford a silica gel slurry. The slurry was subjected to reduced pressure to remove dichloromethane to deliver silica gel containing the products, which was further purified by column chromatography on silica gel using hexane/EtOAc (9:1) as eluent to afford **3.3g** (1.77 g, 89% yield) and **3.4g** (1.60 g, 87% yield).

*One-pot preparation of compounds **3.3a** and **3.4a***

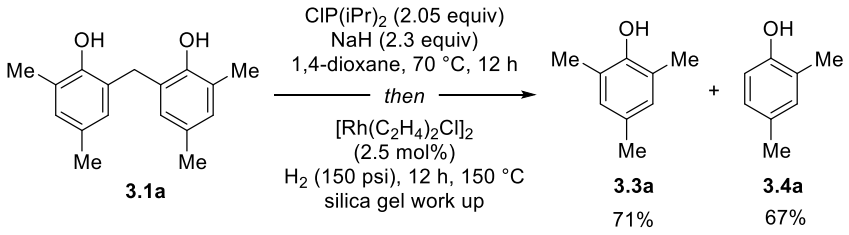


To a Q-tube charged with a stir bar, substrate **3.1a** (77 mg, 0.3 mmol), NaH (17 mg, 0.69 mmol), ClP($^i$Pr)$_2$ (94 mg, 0.62 mmol) and 1,4-dioxane (6.0 mL) were added in the glovebox. The Q-tube was then resembled and taken out of the glovebox. The reaction mixture was heated to 70 °C and stirred for 12 h. Then the Q-tube was taken into the glovebox, and [Rh($C_2H_4$)$_2$Cl]$_2$ (3 mg, 0.0075 mmol) was added to the Q-tube. The Q-tube was then resembled and taken out of the glovebox. The reaction mixture was flushed with hydrogen gas for 10 times and then charged with 150 psi $H_2$ followed by heating to 150 °C in a pre-heated oil bath for 12 h. After the reaction was completed, the $H_2$ pressure was released and the solvent was removed under vacuum. To the mixture, ~ 2 mL of dichloromethane and ~ 200 mg of silica gel were added and reconcentrated to give the silica gel containing the crude product which was further purified by silica gel chromatography to afford compound **3.3a** (29.2 mg, 71%) and compound **3.4a** (24.7 mg, 67%).

*General procedure for preparation of phenol oligomers*

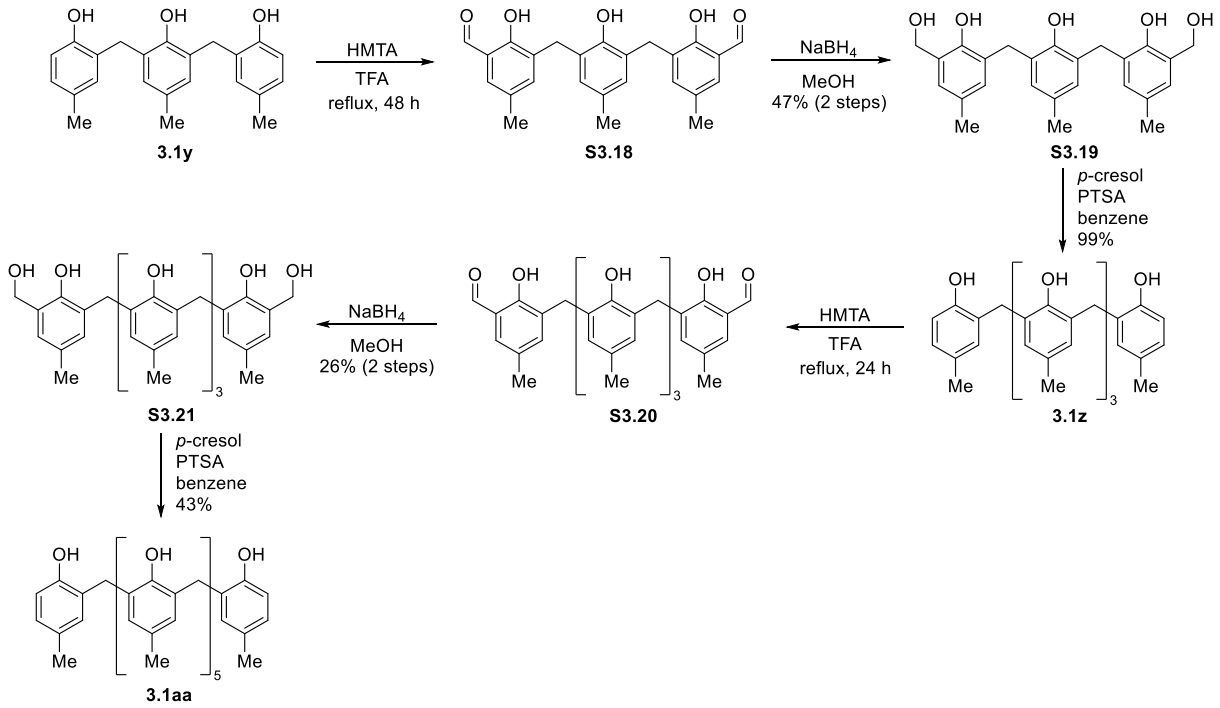


*Preparation of compounds **S3.18***

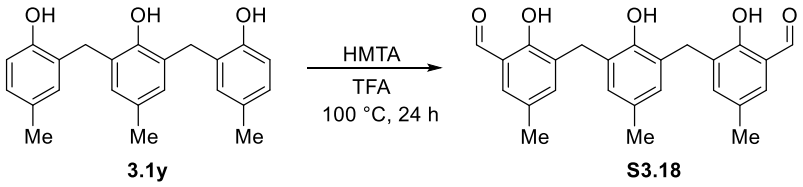


To a solution of compound **3.1y** (3.48 g, 10 mmol) in trifluoroacetic acid (17 mL), hexamethylenetetramine (8.4 g, 60 mmol) was added at 0 °C, and the reaction mixture was then heated to 100 °C. After being stirred at 100 °C for 24 h, $H_2O$ (60 mL) was added to the reaction mixture, and the reaction mixture was cooled to 80 °C. After being stirred at 80 °C for 4 h, the

reaction mixture cooled to room temperature and filtered through a glass funnel. The solid remained in the funnel was washed with $H_2O$ (3 × 10 mL) to give compound **S3.18** (5.4095 g, crude) as a yellow solid. The crude compound **S3.18** could be directly used as substrate in next step without further purification.

*Preparation of compounds **S3.19***

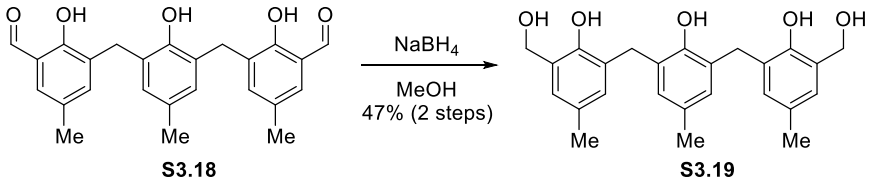

**S3.18** **S3.19**

To a solution of compound **S3.18** (2.7 g, crude) in MeOH (50 mL), $NaBH_4$ (0.76 g, 20 mmol) was added at 0 °C, and the reaction mixture was then warm to room temperature. After being stirred at room temperature for 12 h, the reaction mixture was quenched with HCl (2 M in $H_2O$, 30 mL) and extracted with ethyl acetate (3 × 50 mL). The organic phase was then dried with $Na_2SO_4$ and concentrated under reduced pressure. Then the mixture was purified by column chromatography (silica gel, hexane:ethyl acetate = 1:1) to give compound **S3.19** (0.9699 g, 47% for 2 steps) as a white solid.

**$R_f$** = 0.56 (hexane : ethyl acetate = 1:1)

**$^1$H NMR** (500 MHz, DMSO) δ 8.45 (s, 3H), 6.89 (d, *J* = 2.2 Hz, 2H), 6.71 (d, *J* = 2.3 Hz, 2H), 6.64 (s, 2H), 5.29 (s, 2H), 4.55 (s, 4H), 3.81 (s, 4H), 2.14 (s, 6H), 2.06 (s, 3H).

**$^{13}$C NMR** (101 MHz, DMSO) δ 149.6, 149.6, 129.0, 128.4, 128.0, 127.9, 127.7, 127.6, 127.4, 125.8, 59.9, 29.7, 20.4.

**IR** (KBr) $\nu_{max}$ = 3278, 2918, 2870, 1483, 1381, 1234, 1154, 1026, 863 cm$^{-1}$.

**HRMS (ESI)** m/z calcd. for $C_{25}H_{28}NaO_5^+$ $[M+Na]^+$: 431.1829, found 431.1830.

**Melting point:** decomposed while heating.

*Preparation of compounds **3.1z***

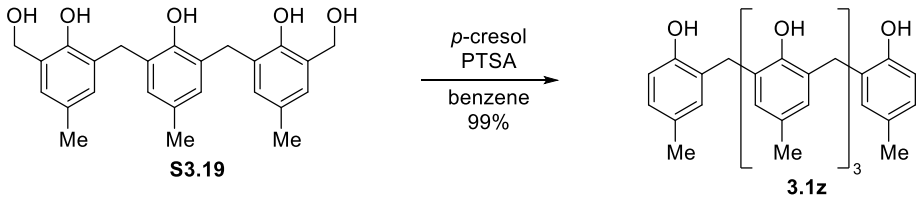


To a solution of compound **S3.19** (0.50 g, 1.22 mmol) in benzene (12 mL) in a Dean–Stark apparatus, *p*-cresol (0.53 g, 4.90 mmol) and *p*-toluenesulfonic acid (12 mg, 0.061 mmol) was added at room temperature, and the reaction mixture was heated to reflux. After refluxing for 2 h, the reaction mixture was concentrated under reduced pressure. The mixture was purified by column chromatography (silica gel, hexane:ethyl acetate = 10:1) to give compound **3.1z** (0.7077 g, 99% yield) as a white solid.

**$R_f$** = 0.41 (hexane:ethyl acetate = 2:1)

**$^1$H NMR** (500 MHz, $CDCl_3$) δ 9.19 (s, 2H), 9.14 (s, 1H), 8.87 (s, 2H), 7.08 (d, *J* = 2.2 Hz, 2H), 6.97 (d, *J* = 2.2 Hz, 2H), 6.91 – 6.87 (m, 6H), 6.81 (d, *J* = 8.1 Hz, 2H), 3.81 (s, 4H), 3.71 (s, 4H), 2.24 (s, 6H), 2.22 (d, *J* = 0.7 Hz, 6H), 2.20 (s, 3H).

**$^{13}$C NMR** (101 MHz, $CDCl_3$) δ 149.8, 147.5, 147.4, 131.3, 130.9, 130.9, 130.6, 129.8, 129.6, 128.5, 127.4, 127.0, 127.0, 126.8, 116.0, 31.6, 31.6, 20.5, 20.5, 20.4.

**IR** (KBr) $\nu_{max}$ = 3229, 3014, 2920, 1502, 1482, 1453, 1234, 909, 813, 733 $cm^{-1}$.

**HRMS (ESI)** m/z calcd. for $C_{39}H_{40}NaO_5^+$ $[M+Na]^+$: 611.2768, found 611.2774.

**Melting point** 137.0 – 138.7 °C.

*Preparation of compounds **S3.20***

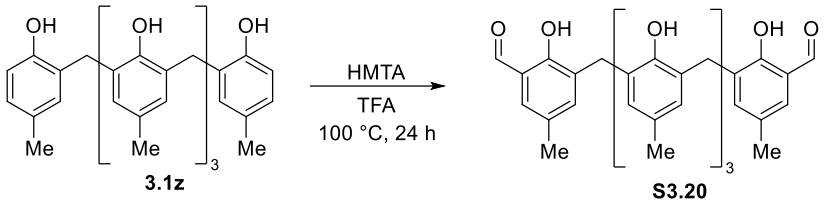


To a solution of compound **3.1z** (250 mg, 0.42 mmol) in trifluoroacetic acid (0.7 mL), hexamethylenetetramine (360 mg, 2.5 mmol) was added at 0 °C, and the reaction mixture was then heated to 100 °C. After being stirred at 100 °C for 24 h, $H_2O$ (2 mL) was added to the reaction mixture, and the reaction mixture was cooled to 80 °C. After being stirred at 80 °C for 4 h, the reaction mixture cooled to room temperature and filtered through a glass funnel. The solid remained in the funnel was washed with $H_2O$ (3 × 3 mL) to give compound **S3.20** (0.3244 g, crude)

as a yellow solid. The crude compound **S3.20** could be directly used as substrate in next step without further purification.

*Preparation of compounds **S3.21***

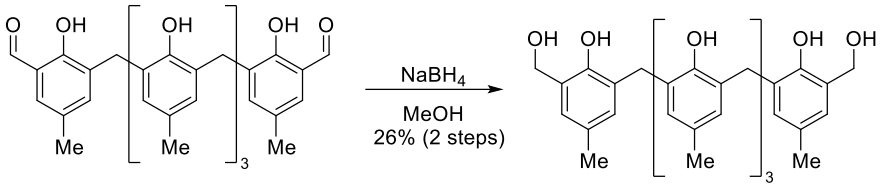


**S3.20** **S3.21**

To a solution of compound **S3.20** (0.32 g, crude) in MeOH (4.2 mL), $NaBH_4$ (112 mg, 2.94 mmol) was added at 0 °C, and the reaction mixture was then warm to room temperature. After being stirred at room temperature for 12 h, the reaction mixture was quenched with HCl (2 M in $H_2O$, 4 mL) and extracted with ethyl acetate (3 × 10 mL). The organic phase was then dried with $Na_2SO_4$ and concentrated under reduced pressure. The mixture was purified by column chromatography (silica gel, hexane:ethyl acetate = 1:1) to give compound **S3.21** (0.0746 g, 26% for 2 steps) as a white solid.

$\mathbf{R_f}$ = 0.32 (hexane:ethyl acetate = 1:1)

**$^1$H NMR** (500 MHz, $CDCl_3$) δ 9.30 (s, 3H), 9.14 (s, 2H), 6.97 (d, *J* = 2.2 Hz, 2H), 6.90 (d, *J* = 3.8 Hz, 6H), 6.70 (d, *J* = 2.2 Hz, 2H), 4.77 (s, 4H), 3.80 (s, 4H), 3.74 (s, 4H), 2.21 (s, 9H), 2.19 (s, 6H).

**$^{13}$C NMR** (101 MHz, $CDCl_3$) δ 149.9, 147.4, 147.3, 130.7, 130.6, 129.9, 129.6, 129.6, 129.5, 127.5, 127.4, 127.3, 127.3, 127.1, 125.4, 64.1, 31.7, 31.1, 20.5, 20.5, 20.4.

**IR** (KBr) $\nu_{max}$ = 3220, 3012, 2917, 1483, 1451, 1380, 1233, 1157, 909, 858, 733 $cm^{-1}$.

**HRMS (ESI)** m/z calcd. for $C_{41}H_{44}NaO_7^+$ $[M+Na]^+$: 671.2979, found 671.2974.

**Melting point** decomposed while heating.

*Preparation of compounds **3.1aa***

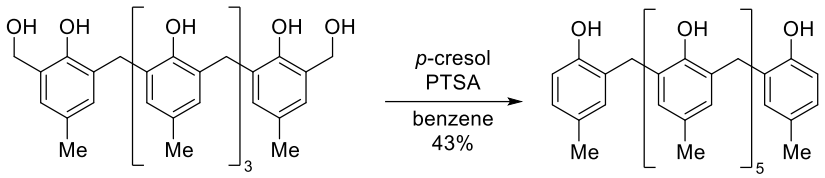


S3.21 3.1aa

To a solution of compound **S3.21** (27 mg, 0.04 mmol) in benzene (0.4 mL), *p*-cresol (17 mg, 0.16 mmol) and *p*-toluenesulfonic acid (0.4 mg, 0.002 mmol) was added at room temperature, and the reaction mixture was heated to reflux. After refluxing for 2 h, the reaction mixture was concentrated under reduced pressure. The mixture was purified by column chromatography (silica gel, hexane:ethyl acetate = 10:1) to give compound **3.1aa** (14.2 mg, 43% yield) as a white solid.

$\mathbf{R_f}$ = 0.35 (hexane:ethyl acetate = 2:1)

**$^1$H NMR** (500 MHz, $CDCl_3$) δ 10.17 (s, 1H), 10.07 (s, 2H), 9.77 (s, 2H), 9.46 (s, 2H), 7.08 (d, *J* = 2.2 Hz, 2H), 7.01 (d, *J* = 2.2 Hz, 2H), 6.96 (d, *J* = 2.2 Hz, 4H), 6.94 (d, *J* = 2.1 Hz, 2H), 6.92 (s, 2H), 6.79 (dd, *J* = 8.1, 2.2 Hz, 2H), 6.71 (d, *J* = 8.2 Hz, 2H), 3.93 (s, 4H), 3.82 (s, 4H), 3.80 (s, 4H), 2.26 (s, 6H), 2.24 (s, 6H), 2.22 (s, 6H), 2.21 (s, 3H).

**$^{13}$C NMR** (126 MHz, $CDCl_3$) δ 149.2, 147.3, 147.1, 146.9, 131.2, 131.1, 131.0, 131.0, 129.8, 129.7, 129.6, 129.5, 128.4, 128.2, 128.1, 128.1, 127.9, 127.6, 127.4, 116.8, 32.1, 32.0, 31.7, 20.5.

**IR** (KBr) $\nu_{max}$ = 3169, 3014, 2921, 1501, 1482, 1451, 1234, 909, 732 $cm^{-1}$.

**HRMS (ESI)** m/z calcd. for $C_{55}H_{57}O_7^+$ $[M+H]^+$: 829.4099, found 829.4094.

*Preparation of compounds **3.1ab***

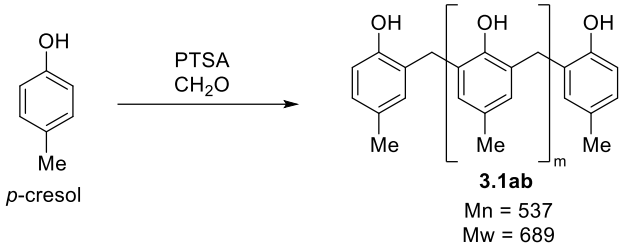


To a mixture of *p*-cresol (2.70 g, 25 mmol) and formaldehyde (37 wt.% in $H_2O$, 1.77 mL, 23.75 mmol), *p*-toluenesulfonic acid (95 mg, 0.5 mmol) was added at room temperature, and the reaction mixture was heated to 100 °C. After being stirred at 100 °C for 12 h, the reaction mixture was filter through a glass funnel, and then washed with hot water (3 × 20 mL). The residue was dissolved in DCM (100 mL) and dried by $Na_2SO_4$. The solution was concentrated under reduced pressure to give compound **3.1ab** (2.966 g, 99% yield) as a white solid.

Molecular weight of compound **3.1ab** was measured by GPC-MALS

**Figure 3.1.** GPC-MALS Chromatography of Compound **3.1ab**.

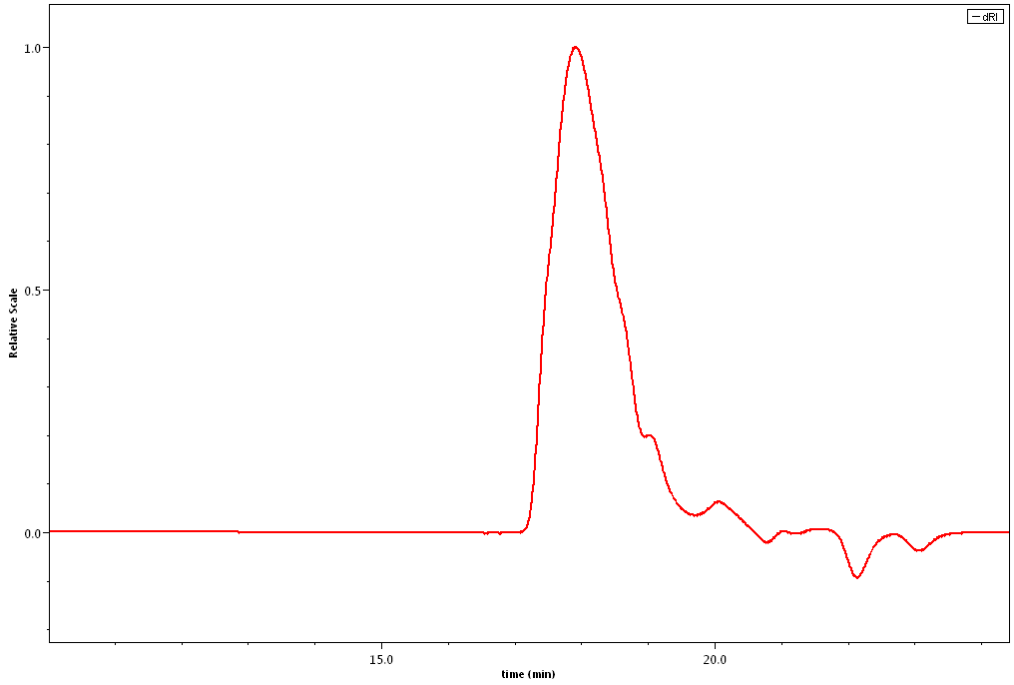


**Table 3.5.** Molecular Weight of Compound **3.1ab**.

| | |
|---|---|
| Sample concentration (mg/ml) | 6.4 |
| $M_n$ (kDa) | 0.537 |
| Uncertainty | 7.1% |
| $M_w$ (kDa) | 0.689 |
| Uncertainty | 4.98% |
| Polydispersity (Mw/Mn) | 1.284 |
| Uncertainty | 8.67% |
| rh(v)(avg) (nm) | 1.1 |
| Uncertainty | 0.1% |
| Mass fraction (%) | 100 |
| dn/dc (mL/g) | 0.335 |

**Figure 3.2.** MALDI-TOF Spectra of Compound **3.1ab**.

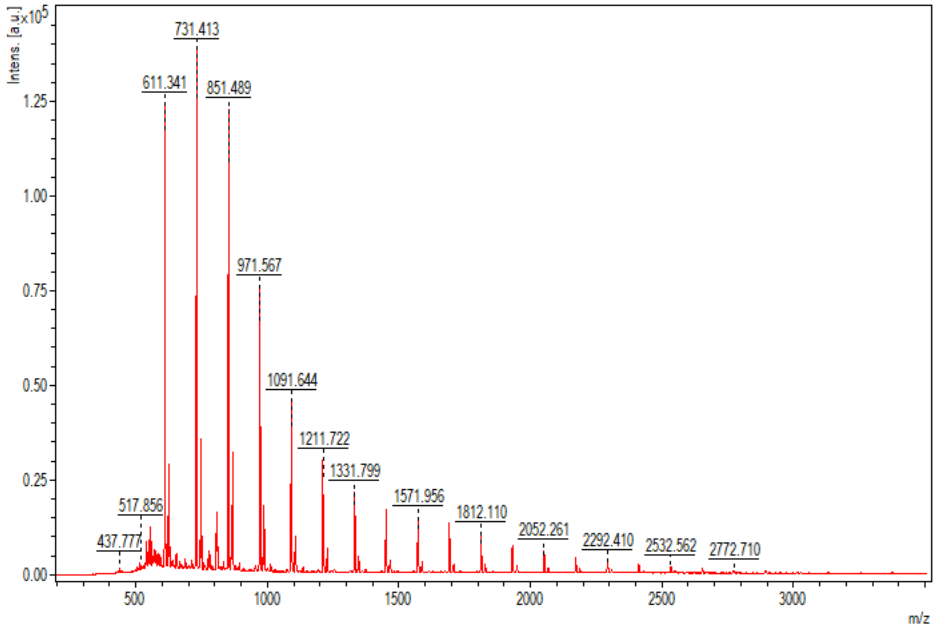


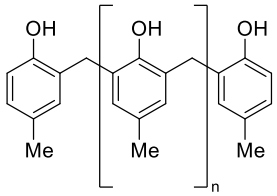


**3.1ab**

n = 3, m/z calcd. for $C_{39}H_{40}NaO_5^+$ $[M+Na]^+$: 611.277, found 611.341;

n = 4, m/z calcd. for $C_{47}H_{48}NaO_6^+$ $[M+Na]^+$: 731.334, found 731.413;

n = 5, m/z calcd. for $C_{55}H_{56}NaO_7^+$ $[M+Na]^+$: 851.392, found 851.489;

n = 6, m/z calcd. for $C_{63}H_{64}NaO_8^+$ $[M+Na]^+$: 971.449, found 971.567;

n = 7, m/z calcd. for $C_{71}H_{72}NaO_9^+$ $[M+Na]^+$: 1091.507, found 1091.644;

n = 8, m/z calcd. for $C_{79}H_{80}NaO_{10}^+$ $[M+Na]^+$: 1211.564, found 1211.722;

n = 9, m/z calcd. for $C_{87}H_{88}NaO_{11}^+$ $[M+Na]^+$: 1331.622, found 1331.799;

n = 11, m/z calcd. for $C_{103}H_{104}NaO_{13}^+$ $[M+Na]^+$: 1571.737, found 1571.956;

n = 13, m/z calcd. for $C_{119}H_{120}NaO_{15}^+$ $[M+Na]^+$: 1811.852, found 1812.110;

n = 15, m/z calcd. for $C_{135}H_{136}NaO_{17}^+$ $[M+Na]^+$: 2051.967, found 2052.261;

n = 17, m/z calcd. for $C_{151}H_{152}NaO_{19}^+$ $[M+Na]^+$: 2292.082, found 2292.410;

n = 19, m/z calcd. for $C_{167}H_{168}NaO_{21}^+$ $[M+Na]^+$: 2532.197, found 2532.562;

*Preparation of compounds **3.2y***

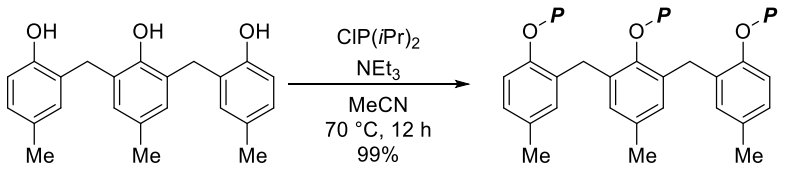


**3.1y** **3.2y**

To a flame dried 8 mL vial charged with a stir bar, compound **3.1y** (70 mg, 0.2 mmol), dry MeCN (3 mL) and dry $Et_3N$ (166 µL, 1.2 mmol) were added. Chloro-diisopropylphosphine (95 mg, 0.62 mmol) was then added dropwise at room temperature. The mixture was heated and stirred at 70 °C under $N_2$ atmosphere for 12 h. Upon completion of the reaction, the reaction mixture was extracted with hexane in glovebox and concentrated to give the compound **3.2y** (0.1374 g, 99% yield), which were pure enough for the next C−C activation reactions.

**$^1$H NMR** (500 MHz, $C_6D_6$) δ 7.60 (dd, *J* = 8.3, 4.0 Hz, 2H), 7.03 (d, *J* = 2.3 Hz, 2H), 6.92 (dd, *J* = 8.4, 2.3 Hz, 2H), 6.82 (s, 2H), 4.51 (s, 4H), 2.10 (s, 6H), 1.97 (pd, *J* = 7.1, 3.1 Hz, 2H), 1.91 (s, 3H), 1.79 (pd, *J* = 7.1, 3.0 Hz, 4H), 1.20 (dd, *J* = 11.3, 7.0 Hz, 6H), 1.14 (dd, *J* = 10.6, 7.0 Hz, 12H), 1.08 – 0.98 (m, 18H).

**$^{13}$C NMR** (126 MHz, $C_6D_6$) δ 155.4, 155.4, 152.0, 152.0, 132.0, 132.0, 132.0, 130.4, 130.4, 130.4, 130.3, 129.9, 116.4, 116.2, 32.2, 32.2, 29.3, 29.1, 28.6, 28.5, 20.7, 20.7, 18.0, 17.9, 17.8, 17.8, 17.7, 17.3, 17.3.

**$^{31}$P NMR** (162 MHz, $C_6D_6$) δ 156.4, 141.1.

**IR** (KBr) $\nu_{max}$ = 2953, 2926, 2867, 1494, 1461, 1217, 1127, 846, 810, 695, 665 cm$^{-1}$.

*Preparation of compounds **3.2z***

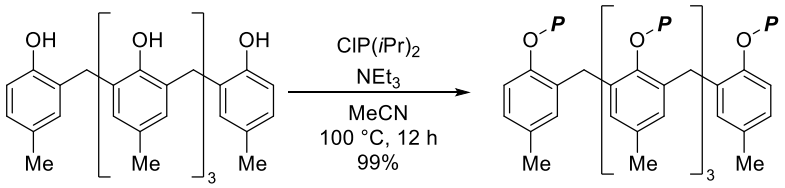


3.1z

3.2z

To a flame dried 8 mL vial charged with a stir bar, compound **3.1z** (71 mg, 0.12 mmol), dry MeCN (3 mL) and dry $Et_3N$ (166 µL, 1.2 mmol) were added. Chloro-diisopropylphosphine (101 mg, 0.66 mmol) was then added dropwise at room temperature. The mixture was heated and stirred at 100 °C under $N_2$ atmosphere for 12 h. Upon completion of the reaction, the reaction mixture was extracted with benzene in glovebox and concentrated to give the compound **3.2y** (0.1399 g, 99% yield), which were pure enough for the next C−C activation reactions.

**$^1$H NMR** (500 MHz, $C_6D_6$) δ 7.59 (dd, *J* = 8.3, 3.9 Hz, 2H), 7.02 (d, *J* = 2.3 Hz, 2H), 6.93 (dd, *J* = 9.3, 7.0 Hz, 6H), 6.83 (d, *J* = 2.3 Hz, 2H), 4.75 (s, 4H), 4.53 (s, 4H), 2.09 (s, 6H), 2.04 – 1.99 (m, 9H), 1.96 (s, 6H), 1.80 (pd, *J* = 7.1, 2.9 Hz, 4H), 1.25 (dt, *J* = 10.9, 5.3 Hz, 18H), 1.15 – 1.01 (m, 42H).

**$^{13}$C NMR** (101 MHz, $C_6D_6$) δ 155.4, 155.3, 152.3, 152.1, 132.4, 132.4, 132.1, 132.0, 130.4, 130.4, 130.3, 129.9, 128.6, 116.4, 116.2, 33.1, 33.0, 32.3, 32.2, 29.4, 29.4, 29.2, 29.1, 28.7, 28.5, 21.0, 20.9, 20.8, 18.0, 18.0, 18.0, 17.9, 17.9, 17.8, 17.8, 17.8, 17.4, 17.3.

**$^{31}$P NMR** (162 MHz, $C_6D_6$) δ 157.1, 156.6, 141.0.

*Preparation of compound **3.2aa***

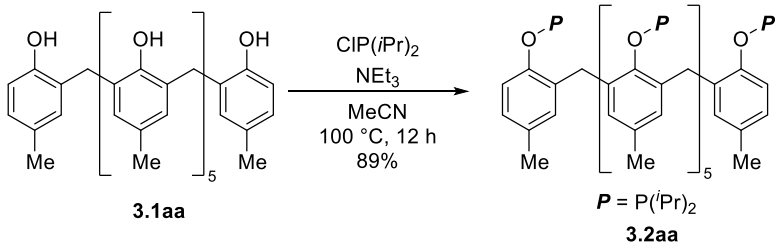


To a flame dried 4 mL vial charged with a stir bar, compound **3.1aa** (26 mg, 0.031 mmol), dry MeCN (1 mL) and dry $Et_3N$ (60 μL, 0.43 mmol) was added. Chloro-diisopropylphosphine (36 mg, 0.24 mmol) was then added dropwise at room temperature. The mixture was heated and stirred at 100 °C under $N_2$ atmosphere for 12 h. Upon completion of the reaction, the reaction mixture was extracted with benzene in glovebox and concentrated to give the compound **3.2aa** (0.0453 g, 89% yield), which were pure enough for the next C−C activation reactions.

**$^1$H NMR** (500 MHz, $C_6D_6$) δ 7.61 (dd, *J* = 8.3, 4.0 Hz, 2H), 7.03 (d, *J* = 2.3 Hz, 2H), 6.98 – 6.90 (m, 10H), 6.85 (d, *J* = 2.3 Hz, 2H), 4.80 (s, 4H), 4.77 (s, 4H), 4.55 (s, 4H), 2.09 (s, 6H), 2.06 (dd, *J* = 6.9, 2.5 Hz, 4H), 2.01 (d, *J* = 6.3 Hz, 15H), 1.96 (s, 6H), 1.80 (ddp, *J* = 10.1, 7.1, 2.9 Hz, 4H), 1.28 – 1.22 (m, 32H), 1.16 – 1.08 (m, 40H), 1.03 (dd, *J* = 15.5, 7.2 Hz, 12H).

**$^{13}$C NMR** (126 MHz, $C_6D_6$) δ 155.4, 155.4, 152.3, 152.1, 132.5, 132.5, 132.2, 132.2, 132.1, 132.0, 130.4, 130.4, 129.9, 116.4, 116.2, 33.1, 33.0, 32.3, 32.2, 29.4, 29.3, 29.2, 29.2, 28.6, 28.5, 21.0, 20.9, 20.7, 18.0, 18.0, 17.9, 17.9, 17.9, 17.8, 17.8, 17.8, 17.3, 17.3.

**$^{31}$P NMR** (202 MHz, $C_6D_6$) δ 157.3, 157.3, 156.9, 141.2.

*C−C activation of compound **3.2y***

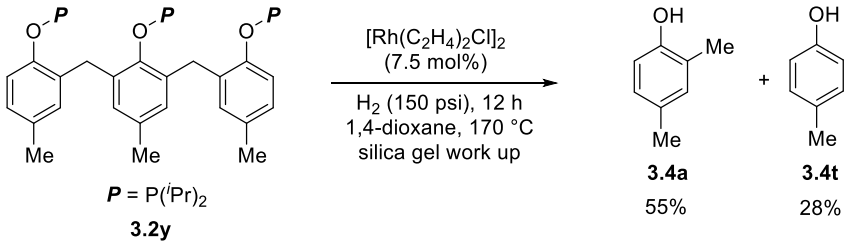


To a Q-tube charged with a stir bar, substrate **3.2y** (137.4 mg, 0.2 mmol), $[Rh(C_2H_4)_2Cl]_2$ (5.8 mg, 0.015 mmol) and 1,4-dioxane (6.0 mL) were added in the glovebox. The Q-tube was then resembled and taken out of the glovebox. The reaction mixture was flushed with hydrogen gas for 10 times and then charged with 150 psi $H_2$ followed by heating to 170 °C in a pre-heated oil bath for 12 h. After the reaction was completed, the $H_2$ pressure was released and the solvent was removed under vacuum. To the mixture, ~ 2 mL of dichloromethane and ~ 200 mg of silica gel were added and reconcentrated to give the silica gel containing the crude product which was further

purified by column chromatography (silica gel, hexane:ethyl acetate = 20:1) to afford compound **3.4a** and **3.4b** (58.9 mg in total, molar ratio **3.4a**:**3.4b** = 1.96:1 determined by $^1$H-NMR, yield of **3.4a** = 55%, yield of **3.4b** = 28%). All the yields were calculated based on the total phenol units, the ideal total yield is 100%.

*C−C activation of compound **3.2z***

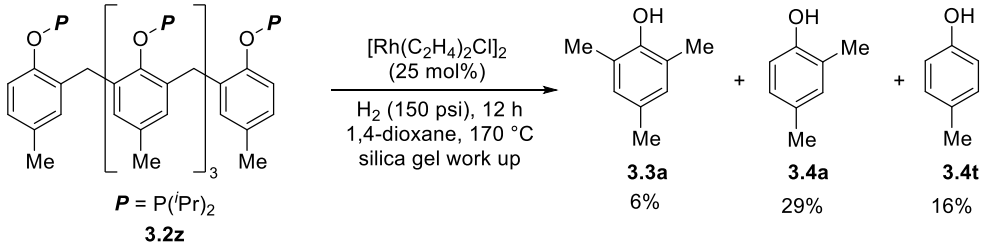


To a Q-tube charged with a stir bar, substrate **3.2z** (139.9 mg, 0.12 mmol), $[Rh(C_2H_4)_2Cl]_2$ (11.7 mg, 0.03 mmol) and 1,4-dioxane (6.0 mL) were added in the glovebox. The Q-tube was then resembled and taken out of the glovebox. The reaction mixture was flushed with hydrogen gas for 10 times and then charged with 150 psi $H_2$ followed by heating to 170 °C in a pre-heated oil bath for 12 h. After the reaction was completed, the $H_2$ pressure was released and the solvent was removed under vacuum. To the mixture, ~ 2 mL of dichloromethane and ~ 200 mg of silica gel were added and reconcentrated to give the silica gel containing the crude product which was further purified by column chromatography (silica gel, hexane:ethyl acetate = 20:1) to afford compound **3.3a** (4.6 mg, 6% yield), compound **3.4a** (20.9 mg, 29% yield) and compound **3.4t** (10.5 mg, 16% yield). All the yields were calculated based on the total phenol units, the ideal total yield is 100%.

*C−C activation of compound **3.2aa***

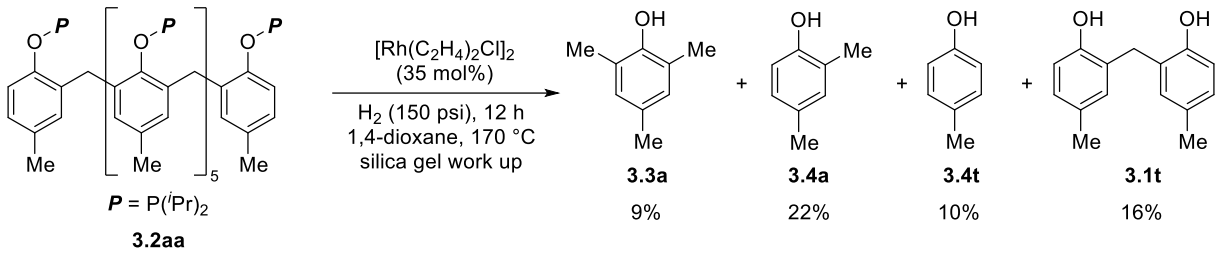


To a Q-tube charged with a stir bar, substrate **3.2aa** (45 mg, 0.027 mmol), $[Rh(C_2H_4)_2Cl]_2$ (3.7 mg, 0.0096 mmol) and 1,4-dioxane (2 mL) were added in the glovebox. The Q-tube was then resembled and taken out of the glovebox. The reaction mixture was flushed with hydrogen gas for 10 times and then charged with 150 psi $H_2$ followed by heating to 170 °C in a pre-heated oil bath for 12 h. After the reaction was completed, the $H_2$ pressure was released and the solvent was removed under vacuum. To the mixture, ~ 2 mL of dichloromethane and ~ 50 mg of silica gel were added and reconcentrated to give the silica gel containing the crude product which was further purified by column chromatography (silica gel, hexane:ethyl acetate = 20:1) to afford compound **3.3a** (2.3 mg, 9% yield), compound **3.4a** (5.0 mg, 22% yield), compound **3.4t** (2.0 mg, 10% yield) and compound **3.1t** (3.5 mg, 16% yield). All the yields were calculated based on the total phenol units, the ideal total yield is 100%.

Compound **3.1t**

**$R_f$** = 0.44 (hexane:ethyl acetate = 2:1)

**$^1$H NMR** (400 MHz, $CDCl_3$) δ 7.12 (s, 2H), 7.07 (d, *J* = 2.2 Hz, 2H), 6.90 – 6.83 (m, 2H), 6.69 (d, *J* = 8.1 Hz, 2H), 3.84 (s, 2H), 2.25 (s, 6H).

**$^{13}$C NMR** (101 MHz, $CDCl_3$) δ 150.1, 131.2, 130.7, 128.4, 126.6, 115.8, 30.9, 20.5.

Analytic data match the literature.[39]

*C−C activation of linear novolacs*

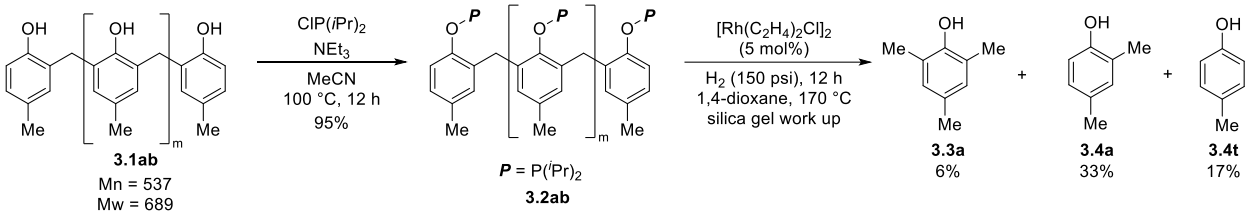


To a flame dried 8 mL vial charged with a stir bar, compound **3.1ab** (72 mg, 0.6 mmol, counted by the total phenol units), dry MeCN (3 mL) and dry $Et_3N$ (166 µL, 1.2 mmol) was added. Chloro-diisopropylphosphine (96 mg, 0.63 mmol) was then added dropwise at room temperature. The mixture was heated and stirred at 100 °C under $N_2$ atmosphere for 12 h. Upon completion of the reaction, the reaction mixture was extracted with benzene in glovebox and concentrated to give the compound **3.2ab** (crude, 0.1343 g, 95% yield, calculated based on phenol unit). The crude compound **3.2ab** was directly used in next step without further purification.

To a Q-tube charged with a stir bar, substrate **3.2ab** (134.3 mg, 0.57 mmol), $[Rh(C_2H_4)_2Cl]_2$ (11 mg, 0.028 mmol) and 1,4-dioxane (6 mL) were added in the glovebox. The Q-tube was then resembled and taken out of the glovebox. The reaction mixture was flushed with hydrogen gas for 10 times and then charged with 150 psi $H_2$ followed by heating to 170 °C in a pre-heated oil bath for 12 h. After the reaction was completed, the $H_2$ pressure was released and the solvent was removed under vacuum. To the mixture, ~ 2 mL of dichloromethane and ~ 200 mg of silica gel were added and reconcentrated to give the silica gel containing the crude product which was further purified by column chromatography (silica gel, hexane:ethyl acetate = 20:1) to afford compound

**3.3a** (4.4 mg, 6% yield), compound **3.4a** (23.1 mg, 56% yield), and compound **3.4t** (10.3 mg, 17% yield). All the yields were calculated based on the total phenol units, the ideal total yield is 100%.

*C−C activation of random novolacs*

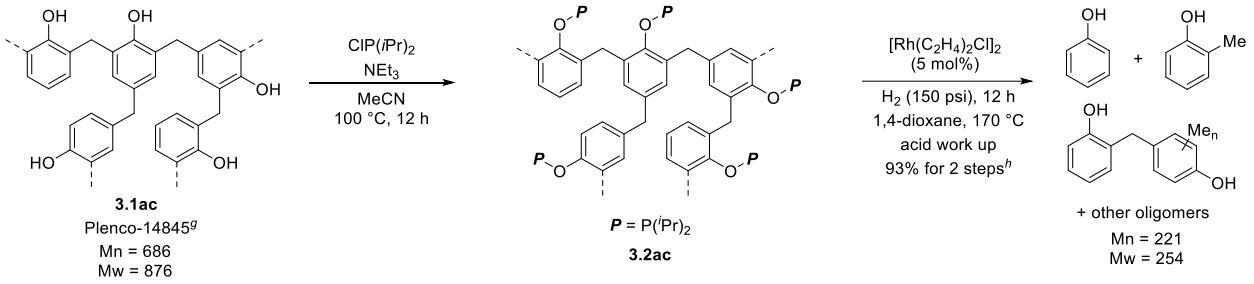


To a flame dried 8 mL vial charged with a stir bar, compound **3.1ac** (64 mg, 0.6 mmol, counted by the total phenol units), dry MeCN (3 mL) and dry $Et_3N$ (166 μL, 1.2 mmol) were added. Chloro-diisopropylphosphine (96 mg, 0.63 mmol) was then added dropwise at room temperature. The mixture was heated and stirred at 100 °C under $N_2$ atmosphere for 12 h. Upon completion of the reaction, the reaction mixture was extracted with benzene in glovebox and concentrated to give the compound **3.2ac** (crude, 0.1102 g). The crude compound **3.2ac** was directly used in next step without further purification.

To a Q-tube charged with a stir bar, substrate **3.2ac** (110.2 mg), $[Rh(C_2H_4)_2Cl]_2$ (9.7 mg, 0.025 mmol) and 1,4-dioxane (5 mL) were added in the glovebox. The Q-tube was then resembled and taken out of the glovebox. The reaction mixture was flushed with hydrogen gas for 10 times and then charged with 150 psi $H_2$ followed by heating to 170 °C in a pre-heated oil bath for 12 h. After the reaction was completed, the $H_2$ pressure was released and HCl (2M in $H_2O$, 3 mL) was added to the reaction mixture. After being stirred at room temperature for 30 min, the reaction mixture

was extracted by $Et_2O$ (3 × 10 mL). the organic phase was dried with $Na_2SO_4$ and concentrated under reduced pressure to give a mixture of monomer, dimer and oligomer of phenols (59.3 mg, 93% yield, calculated by weight ratio between product mixture and starting material compound **3.1ac**). The average molecular weight of product mixture was determined by GPC-MALS, and the component in the mixture was analyzed by GC-MS.

Compound **3.1ac**:

Sample donated by Plastics Engineering Co.

**Figure 3.3.** GPC-MALS Chromatography of Compound **3.1ac**.

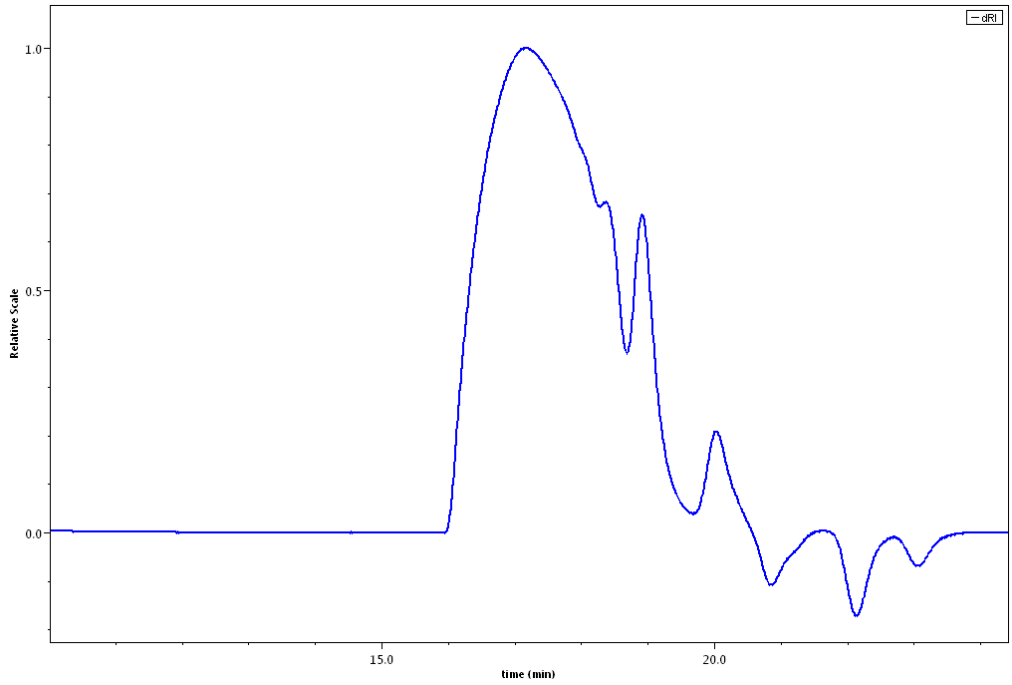

**Table 3.6.** Molecular Weight of Compound **3.1ac**.

| | |
|---|---|
| Sample concentration (mg/ml) | 8.1 |
| Mn (kDa) | 0.686 |
| Uncertainty | 11.99% |
| Mw (kDa) | 0.876 |
| Uncertainty | 6.83% |
| Polydispersity (Mw/Mn) | 1.278 |
| Uncertainty | 13.80% |
| rh(v)(avg) (nm) | 1.2 |
| Uncertainty | 0.1% |
| Mass fraction (%) | 100 |
| dn/dc (mL/g) | 0.3755 |

**Product mixture:**

Molecular weight measured by GPC-MALS:

**Figure 3.4.** GPC-MALS Chromatography of Product Mixture.

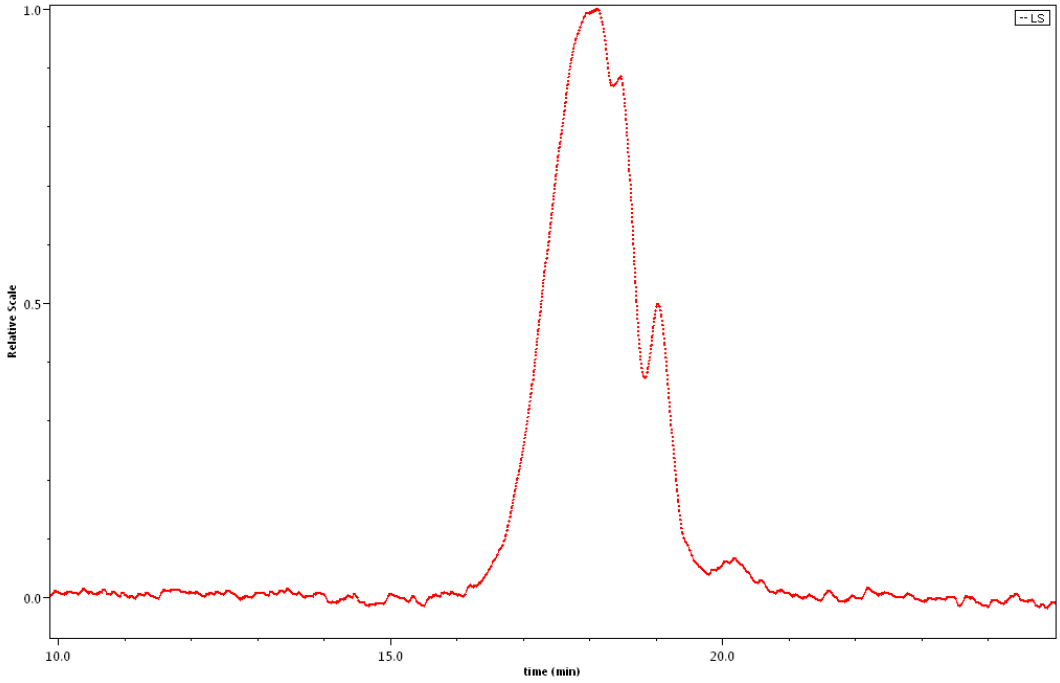


**Table 3.7.** Molecular Weight of Product Mixture.

| | |
|---|---|
| Sample concentration (mg/ml) | 9.9 |
| Mn (kDa) | 0.221 |
| Uncertainty | 14.51% |
| Mw (kDa) | 0.254 |
| Uncertainty | 11.72% |
| Polydispersity (Mw/Mn) | 1.146 |
| Uncertainty | 18.66% |
| rh(v)(avg) (nm) | 0.8 |
| Uncertainty | 0.1% |
| Mass fraction (%) | 100 |
| dn/dc (mL/g) | 0.5278 |

Components analyzed by GC-MS:

**Figure 3.5.** General GC-MS Chromatography of Product Mixture.

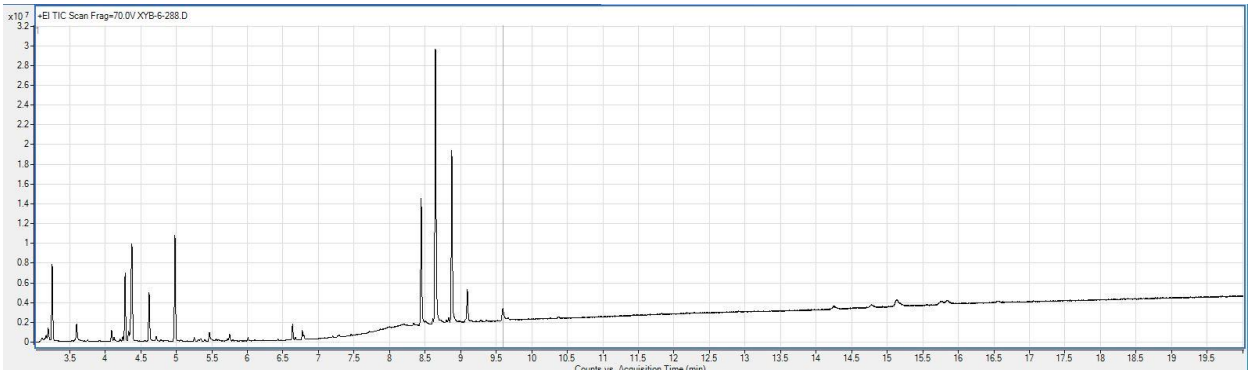


**Figure 3.6.** Mass Spectra of Peak A (Retention Time = 4.600 min).

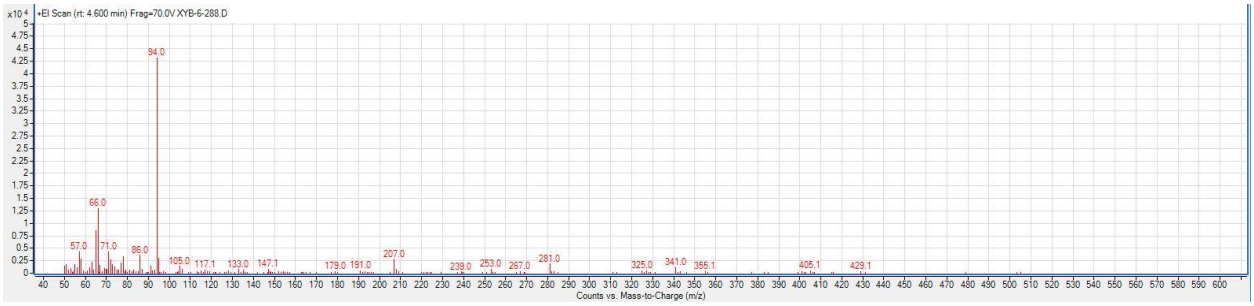


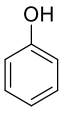


m/z calcd. for $C_6H_6O^+$ $[M]^+$: 94.0, found 94.0.

**Figure 3.7.** Mass Spectra of Peak B (Retention Time = 4.977 min).

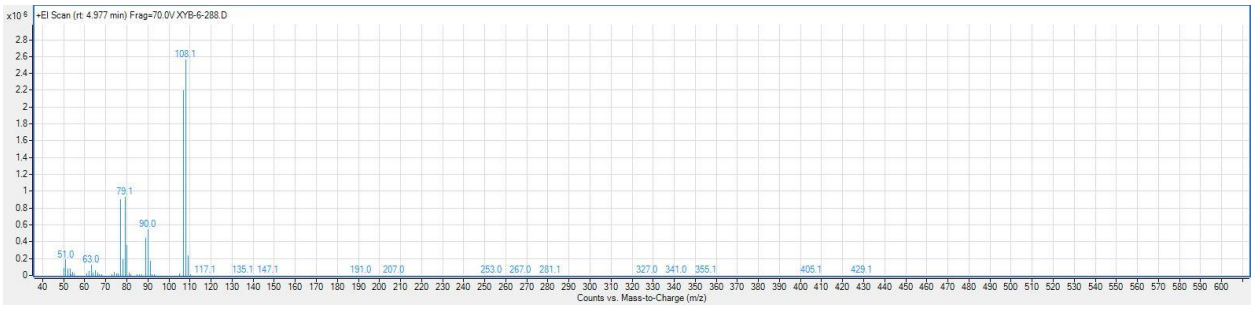

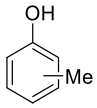


m/z calcd. for $C_7H_8O^+$ $[M]^+$: 108.1, found 108.1.

**Figure 3.8.** Mass Spectra of Peak C (Retention Time = 8.441 min).

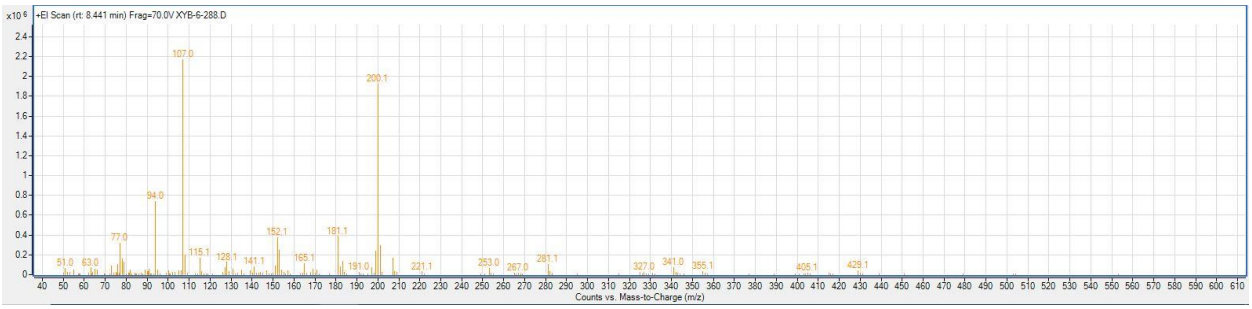


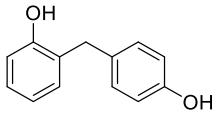


m/z calcd. for $C_{13}H_{12}O_2^+$ $[M]^+$: 200.1, found 200.1.

**Figure 3.9.** Mass Spectra of Peak D (Retention Time = 8.645 min).

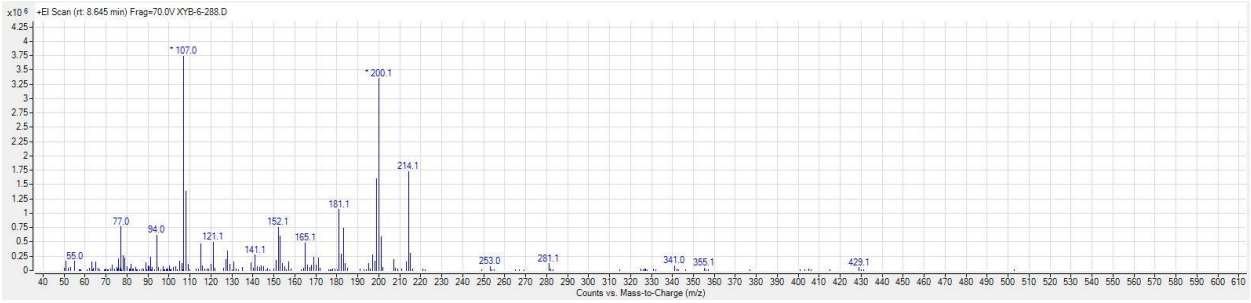


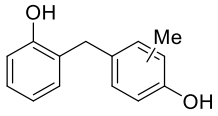


m/z calcd. for $C_{14}H_{14}O_2^+$ $[M]^+$: 214.1, found 214.1.

**Figure 3.10.** Mass Spectra of Peak E (Retention Time = 8.875 min).

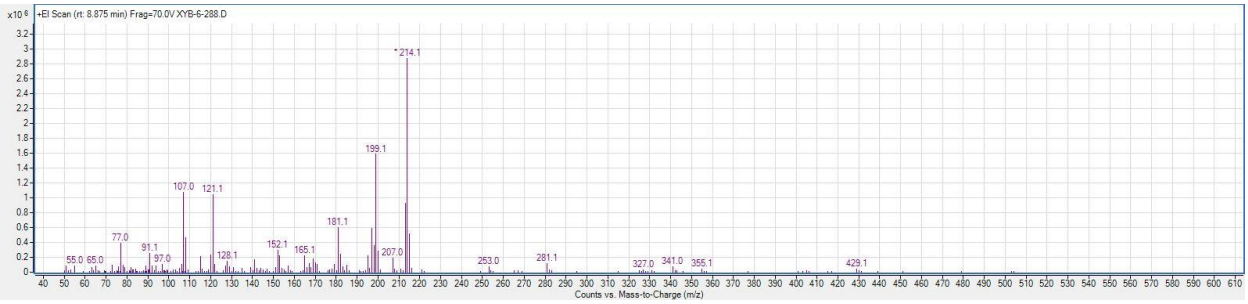


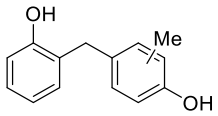


m/z calcd. for $C_{14}H_{14}O_2^+$ $[M]^+$: 214.1, found 214.1.

**Figure 3.11.** Mass Spectra of Peak F (Retention Time = 9.099 min).

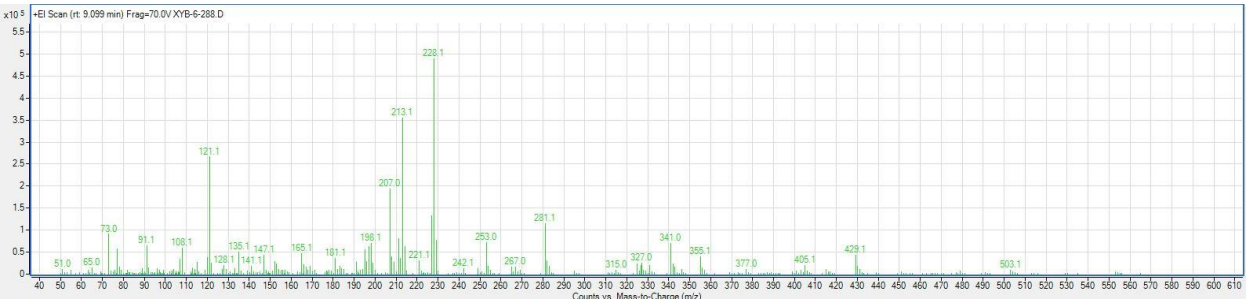


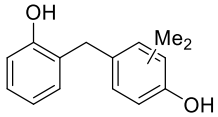


m/z calcd. for $C_{15}H_{16}O_2^+$ $[M]^+$: 228.1, found 228.1.

No phosphorus peak was detected by $^{31}$P-NMR in the crude NMR of the product mixture

**Figure 3.12.** $^{31}$P-NMR Spectrum of the Product Mixture in $CDCl_3$, 162 MHz, 8 scans

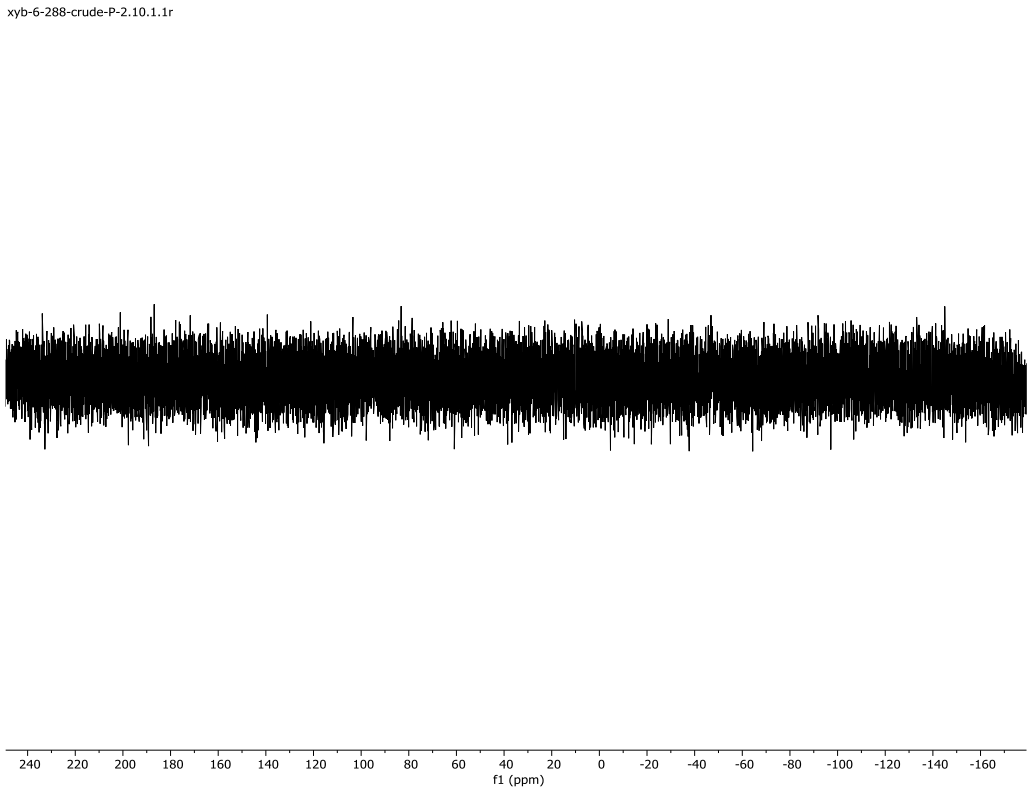


*Preparation of complex [Rh(**3.2g**)Cl]$_2$*

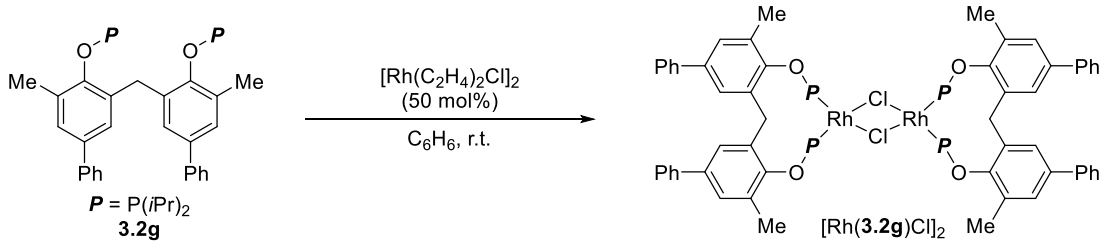


To a flame dried 4 mL vial charged with a stir bar, a solution of compound **3.2g** (31 mg, 0.05 mmol) in dry benzene (0.5 mL) and $[Rh(C_2H_4)_2Cl]_2$ (9.7 mg, 0.025 mmol) was added in the glovebox at room temperature. After being stirred at room temperature for 4 h, the reaction mixture was treated with methanol (2 mL) and then filtered through a glass funnel. The solid remained in the funnel

was washed with methanol (2 × 1 mL) to give compound [Rh(**3.2g**)Cl]$_2$ (10.1 mg, 27% yield) as an orange solid.

**$^1$H NMR** (500 MHz, $C_6D_6$) δ 7.45 (d, *J* = 2.5 Hz, 4H), 7.43 – 7.39 (m, 8H), 7.17 (s, 2H), 7.14 (s, 2H), 7.11 – 7.06 (m, 4H), 6.83 (d, *J* = 2.7 Hz, 4H), 6.31 (d, *J* = 12.8 Hz, 2H), 3.75 (d, *J* = 12.9 Hz, 2H), 2.88 – 2.74 (m, 4H), 2.59 – 2.47 (m, 4H), 2.13 (s, 12H), 1.99 (s, 12H), 1.91 (q, *J* = 6.9 Hz, 12H), 1.62 (s, 12H), 0.91 – 0.81 (m, 12H).

**$^{13}$C NMR** (126 MHz, $C_6D_6$) δ 152.7, 141.0, 137.1, 135.8, 131.0, 128.9, 127.2, 127.1, 126.6, 123.0, 40.6, 34.6, 32.5, 22.8, 20.8, 19.8, 18.3, 16.3.

**$^{31}$P NMR** (202 MHz, $C_6D_6$) δ 182.7 (d, *J* = 232.3 Hz).

*Preparation of complex **3.5***

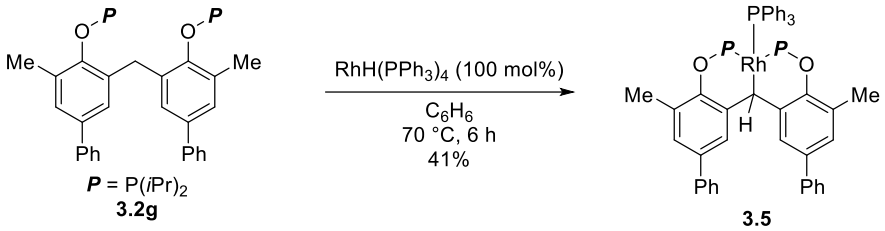


To a flame dried 4 mL vial charged with a stir bar, a solution of compound **3.2g** (15.3 mg, 0.025 mmol) in dry benzene (0.5 mL) and RhH(PPh$_3$)$_4$ (28.8 mg, 0.025 mmol) were added in the glovebox at room temperature. After being stirred at 70 °C for 6 h, the reaction mixture was treated with methanol (2 mL) and then filtered through a glass funnel. The solid remained in the funnel was washed with methanol (2 × 1 mL) to give complex **3.5** (9.9 mg, 41% yield) as an orange solid.

**$^1$H NMR** (500 MHz, $C_6D_6$) δ 7.74 (t, *J* = 7.9 Hz, 6H), 7.66 (dd, *J* = 12.0, 7.6 Hz, 4H), 7.36 (d, *J* = 2.5 Hz, 3H), 7.29 (d, *J* = 3.7 Hz, 2H), 7.25 (t, *J* = 7.6 Hz, 4H), 7.02 (d, *J* = 6.7 Hz, 5H), 6.92 (d, *J* = 7.0 Hz, 6H), 4.97 (d, *J* = 13.8 Hz, 1H), 2.46 (s, 3H), 2.42 (s, 3H), 2.03 – 1.95 (m, 2H), 1.57 (dd, *J* = 17.3, 7.3 Hz, 3H), 1.40 (t, *J* = 8.0 Hz, 3H), 1.22 – 1.17 (m, 6H), 1.09 – 1.03 (m, 6H), 0.96 (dd, *J* = 9.4, 6.8 Hz, 3H), 0.67 – 0.60 (m, 2H), 0.54 (dd, *J* = 15.6, 7.1 Hz, 3H).

**$^{31}$P NMR** (202 MHz, $C_6D_6$) δ 196.2 (dd, *J* = 188, 25 Hz), 188.1 (dd, *J* = 187, 23 Hz), 32.5 (dt, *J* = 140, 24 Hz)

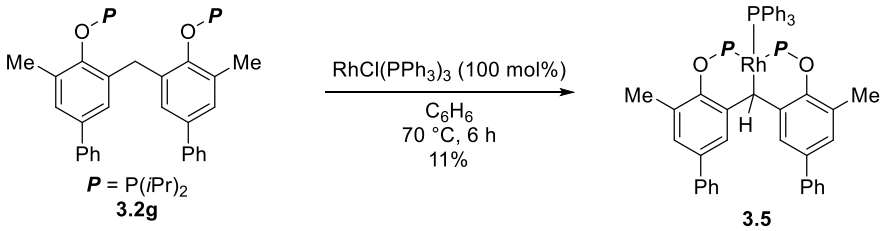


To a flame dried 4 mL vial charged with a stir bar, compound **3.2g** (15.3 mg, 0.025 mmol) in dry benzene (0.5 mL) and $RhCl(PPh_3)_3$ (23.1 mg, 0.025 mmol) were added in the glovebox at room temperature. After being stirred at 70 °C for 6 h, the reaction mixture was treated with methanol (2 mL) and then filtered through a glass funnel. The solid remained in the funnel was washed with methanol (2 × 1 mL) to give complex **3.5** (2.8 mg, 11% yield) as an orange solid.

*Complex **3.5** as catalyst*

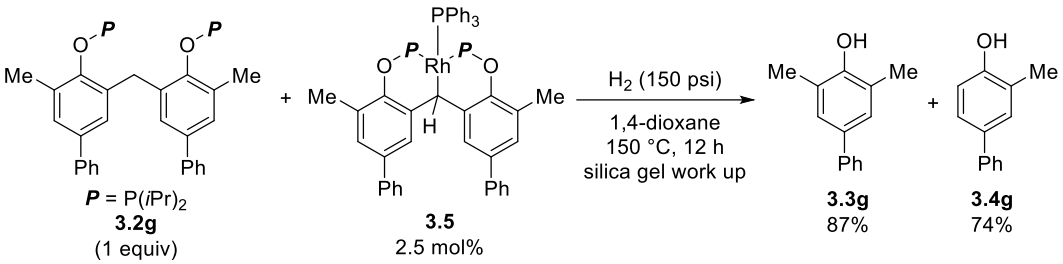


To a Q-tube charged with a stir bar, substrate **3.2g** (61.2 mg, 0.1 mmol), complex **3.5** (2.5 mg, 0.0025 mmol) and 1,4-dioxane (2 mL) were added in the glovebox. The Q-tube was then resembled and taken out of the glovebox. The reaction mixture was flushed with hydrogen gas for 10 times and then charged with 150 psi $H_2$ followed by heating to 150 °C in a pre-heated oil bath for 12 h. After the reaction was completed, the $H_2$ pressure was released and the solvent was removed under vacuum. To the mixture, ~ 2 mL of dichloromethane and ~ 200 mg of silica gel were added and reconcentrated to give the silica gel containing the crude product which was further purified by column chromatography (silica gel, hexane:ethyl acetate = 20:1) to afford compound **3.3g** (17.6 mg, 87% yield) and compound **3.4g** (13.9 mg, 74% yield).

*Deuterium labeling experiment*

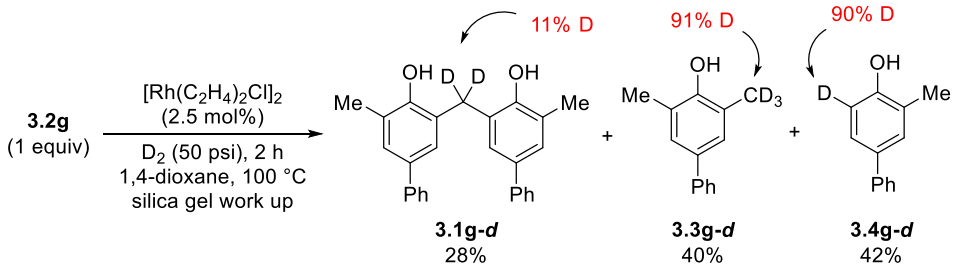


To a Q-tube charged with a stir bar, substrate **3.2g** (184 mg, 0.3 mmol), $[Rh(C_2H_4)_2Cl]_2$ (2.9 mg, 0.0075 mmol) and 1,4-dioxane (6.0 mL) were added in the glovebox. The Q-tube was then

resembled and taken out of the glovebox. The reaction mixture was flushed with hydrogen gas for 10 times and then charged with 50 psi $D_2$ followed by heating to 100 °C in a pre-heated oil bath for 2 h. After the reaction was completed, the $H_2$ pressure was released and the solvent was removed under vacuum. To the mixture, ~ 2 mL of dichloromethane and ~ 200 mg of silica gel were added and reconcentrated to give the silica gel containing the crude product which was further purified by silica gel chromatography to afford compound **3.1g-*d*** (51.7 mg, 28%), compound **3.3g-*d*** (23.6 mg, 40%) and compound **3.4g-*d*** (23.8 mg, 42%)

*High-loading catalyst experiment (without NaH)*

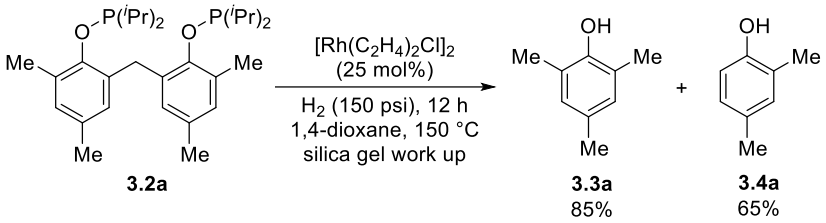


**3.2a** **3.3a** 85% **3.4a** 65%

To a Q-tube charged with a stir bar, substrate **3.2a** (48.9 mg, 0.1 mmol), $[Rh(C_2H_4)_2Cl]_2$ (9.7 mg, 0.025 mmol) and 1,4-dioxane (2.0 mL) were added in the glovebox. The Q-tube was then resembled and taken out of the glovebox. The reaction mixture was flushed with hydrogen gas for 10 times and then charged with 150 psi $H_2$ followed by heating to 150 °C in a pre-heated oil bath for 12 h. After the reaction was completed, the $H_2$ pressure was released and the solvent was removed under vacuum. To the mixture, ~ 2 mL of dichloromethane and ~ 200 mg of silica gel were added and reconcentrated to give the silica gel containing the crude product which was further purified by silica gel chromatography to afford compound **3.3a** (11.6 mg, 85%) and compound **3.4a** (8.0 mg, 65%).

*High-loading catalyst experiment (with NaH)*

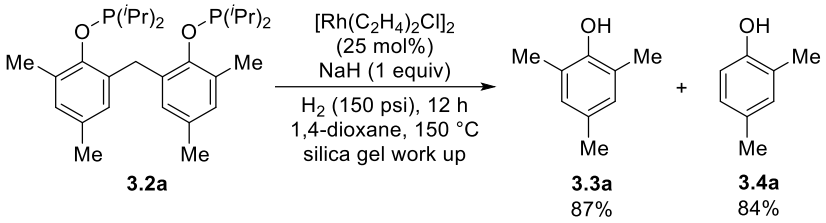


**3.2a** **3.3a** 87% **3.4a** 84%

To a Q-tube charged with a stir bar, substrate **3.2a** (48.9 mg, 0.1 mmol), $[Rh(C_2H_4)_2Cl]_2$ (9.7 mg, 0.025 mmol), NaH (2.4 mg, 0.1 mmol) and 1,4-dioxane (2.0 mL) were added in the glovebox. The Q-tube was then resembled and taken out of the glovebox. The reaction mixture was flushed with hydrogen gas for 10 times and then charged with 150 psi $H_2$ followed by heating to 150 °C in a pre-heated oil bath for 12 h. After the reaction was completed, the $H_2$ pressure was released and the solvent was removed under vacuum. To the mixture, ~ 2 mL of dichloromethane and ~ 200 mg of silica gel were added and reconcentrated to give the silica gel containing the crude product which was further purified by silica gel chromatography to afford compound **3.3a** (11.8 mg, 87%) and compound **3.4a** (10.3 mg, 84%).

## 3.7. NMR Spectra

**Figure 3.13.** $^{1}$H-NMR Spectrum of **3.1b** in $CDCl_3$, 400 MHz

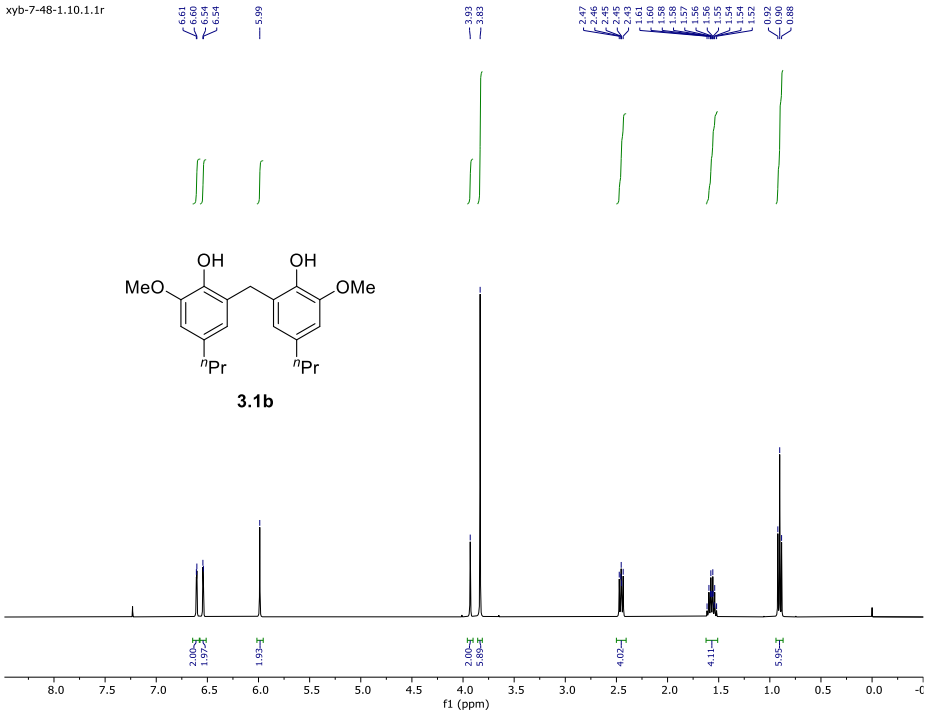


**Figure 3.14.** $^{13}$C-NMR Spectrum of **3.1b** in $CDCl_3$, 101 MHz

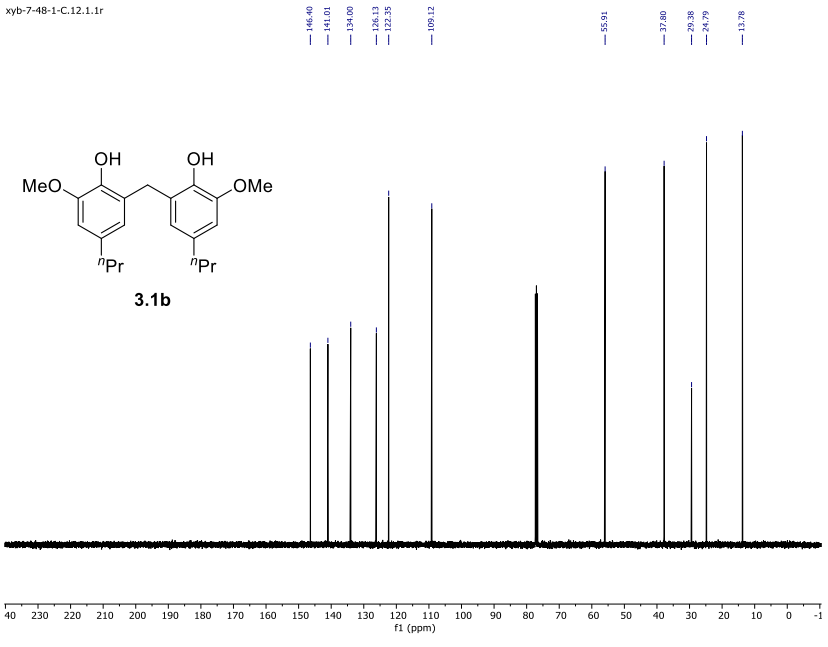

**Figure 3.15.** $^{1}$H-NMR Spectrum of **3.1c** in $CDCl_3$, 400 MHz

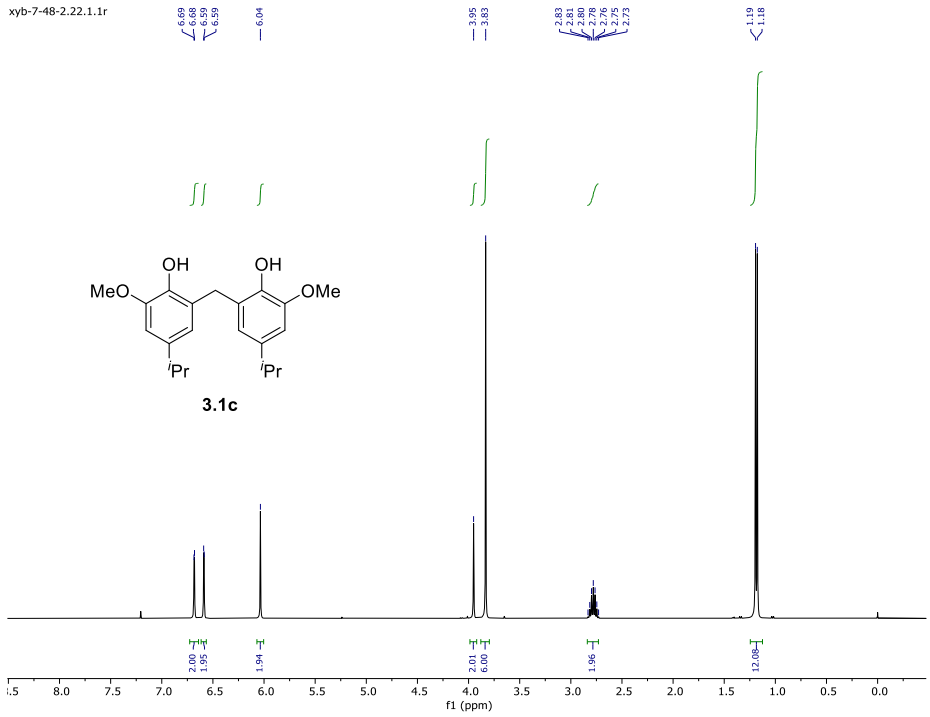


**Figure 3.16.** $^{13}$C-NMR Spectrum of **3.1c** in $CDCl_3$, 101 MHz

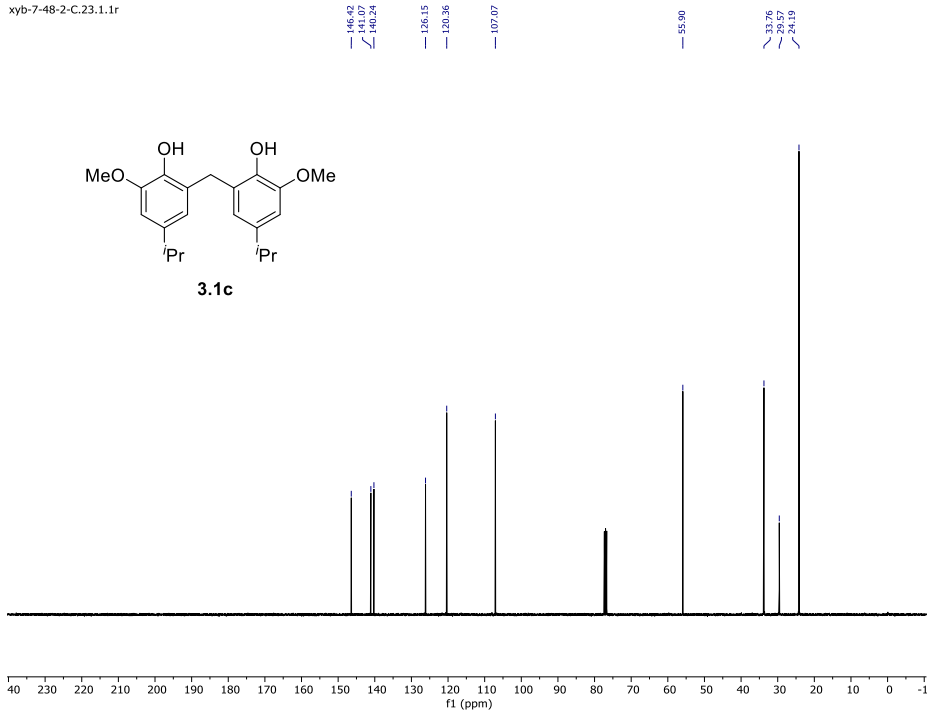

**Figure 3.17.** $^{1}$H-NMR Spectrum of **3.1d** in $CDCl_3$, 400 MHz

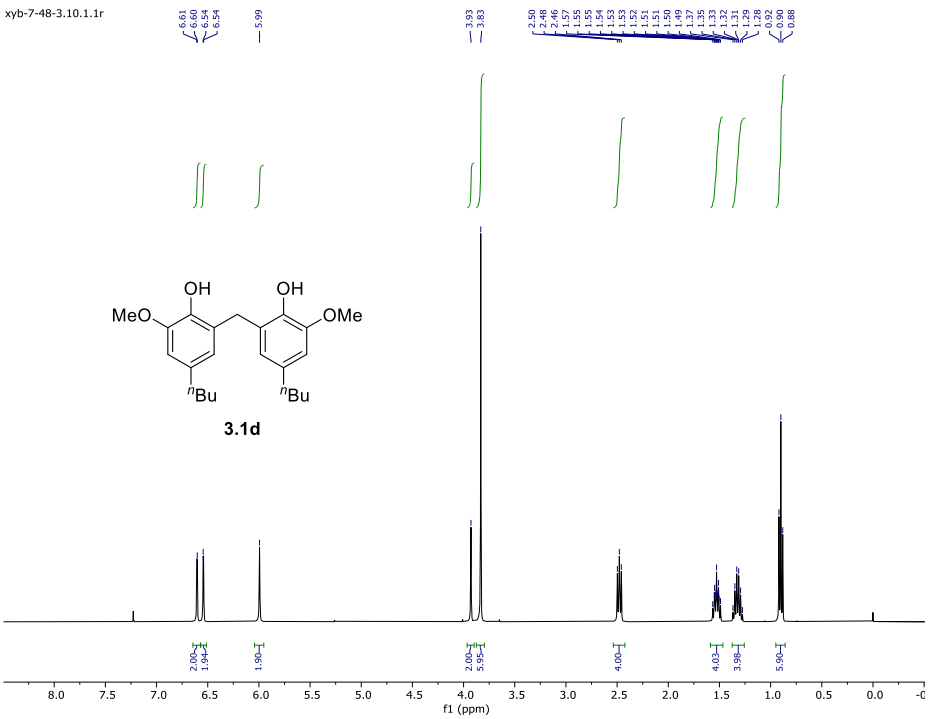


**Figure 3.18.** $^{13}$C-NMR Spectrum of **3.1d** in $CDCl_3$, 101 MHz

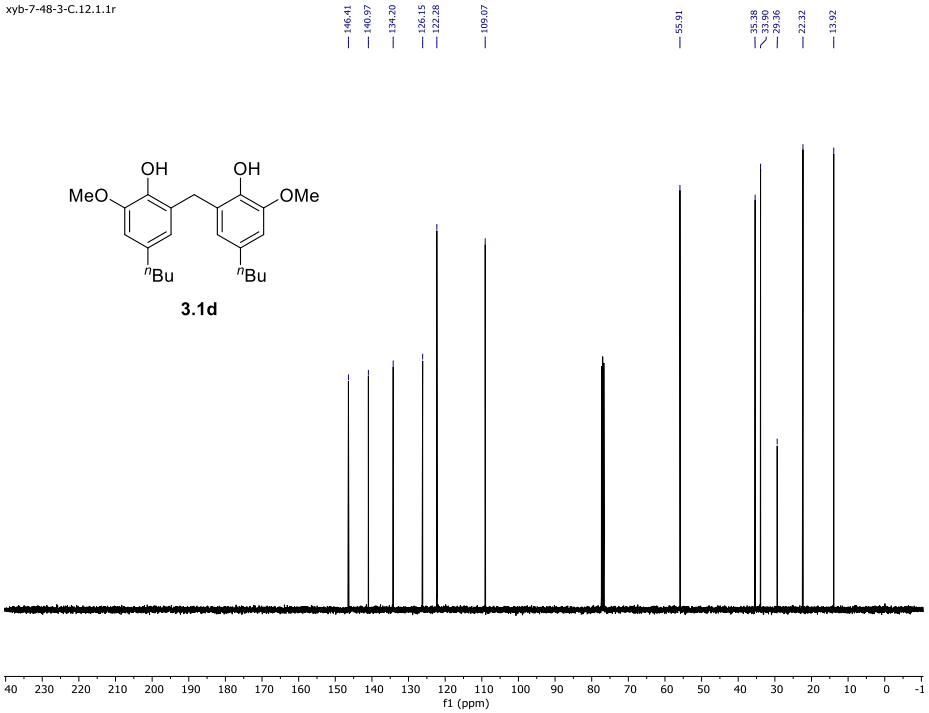

**Figure 3.19.** $^{1}$H-NMR Spectrum of **3.1e** in $CDCl_3$, 400 MHz

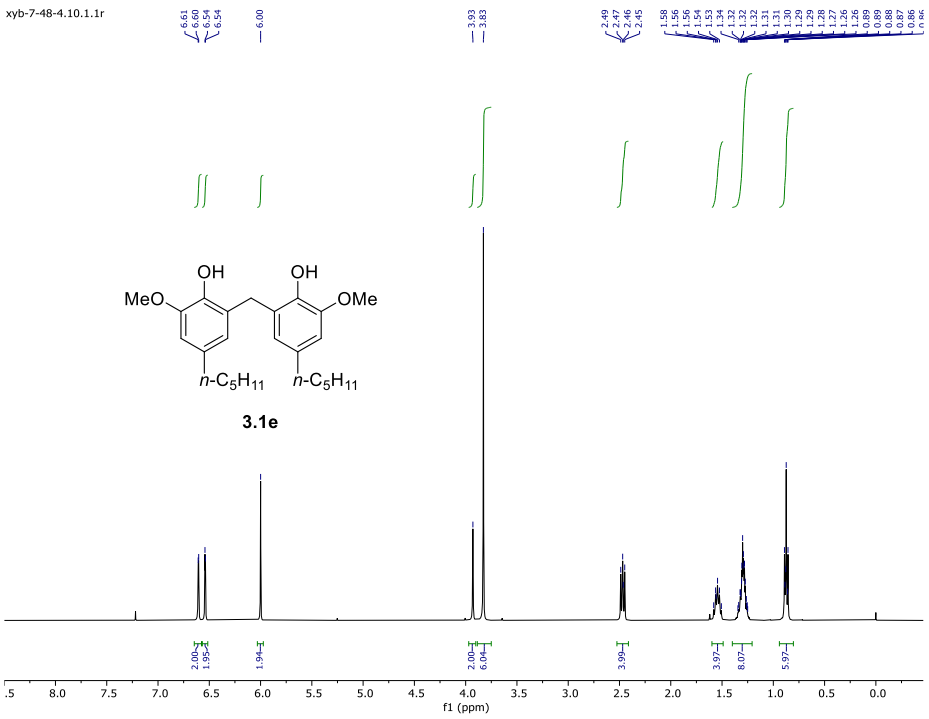


**Figure 3.20.** $^{13}$C-NMR Spectrum of **3.1e** in $CDCl_3$, 101 MHz

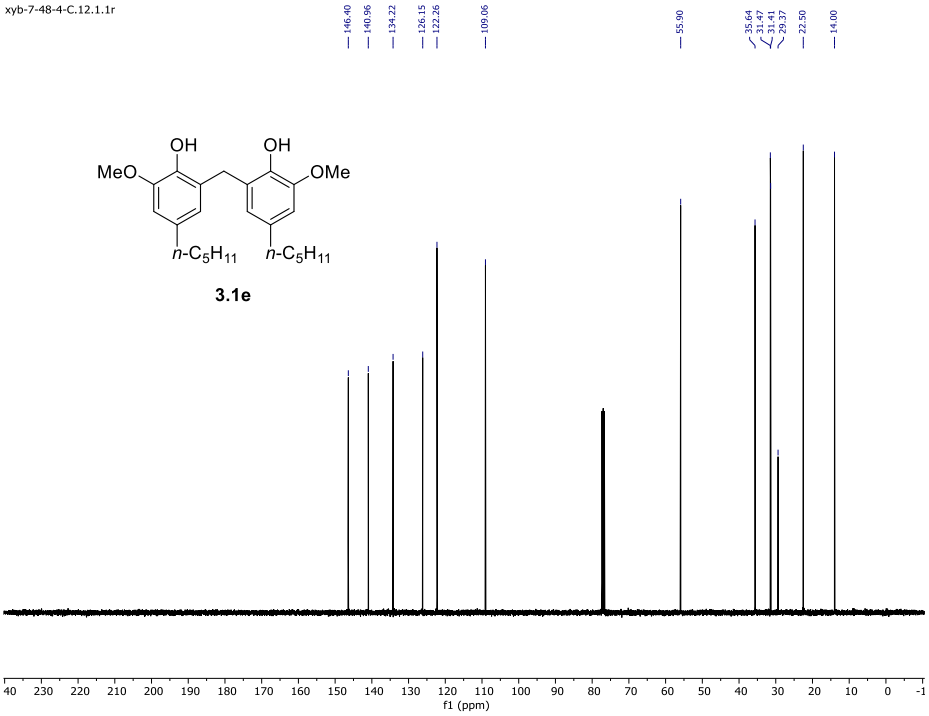

**Figure 3.21.** $^{1}$H-NMR Spectrum of **3.1g** in $CDCl_3$, 400 MHz

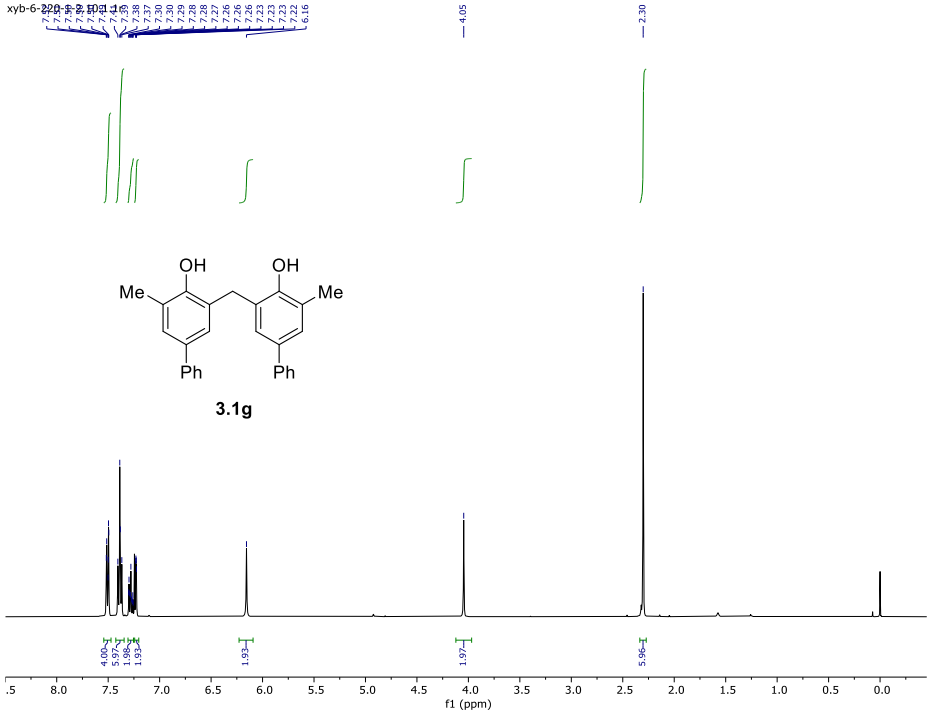


**Figure 3.22.** $^{13}$C-NMR Spectrum of **3.1g** in $CDCl_3$, 101 MHz

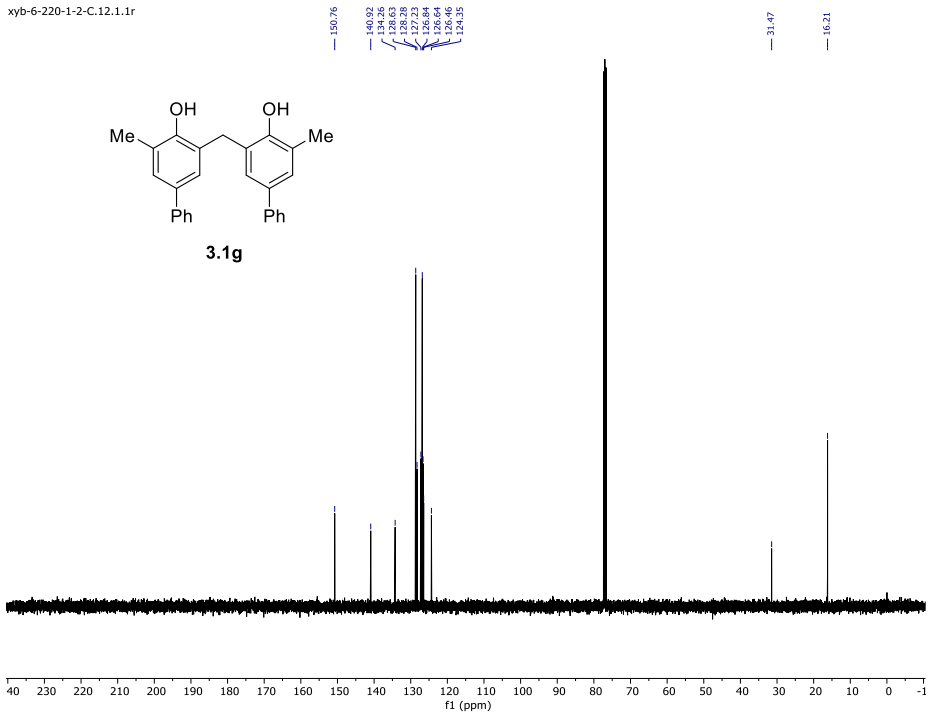

**Figure 3.23.** $^{1}$H-NMR Spectrum of **3.1h** in $CDCl_3$, 400 MHz

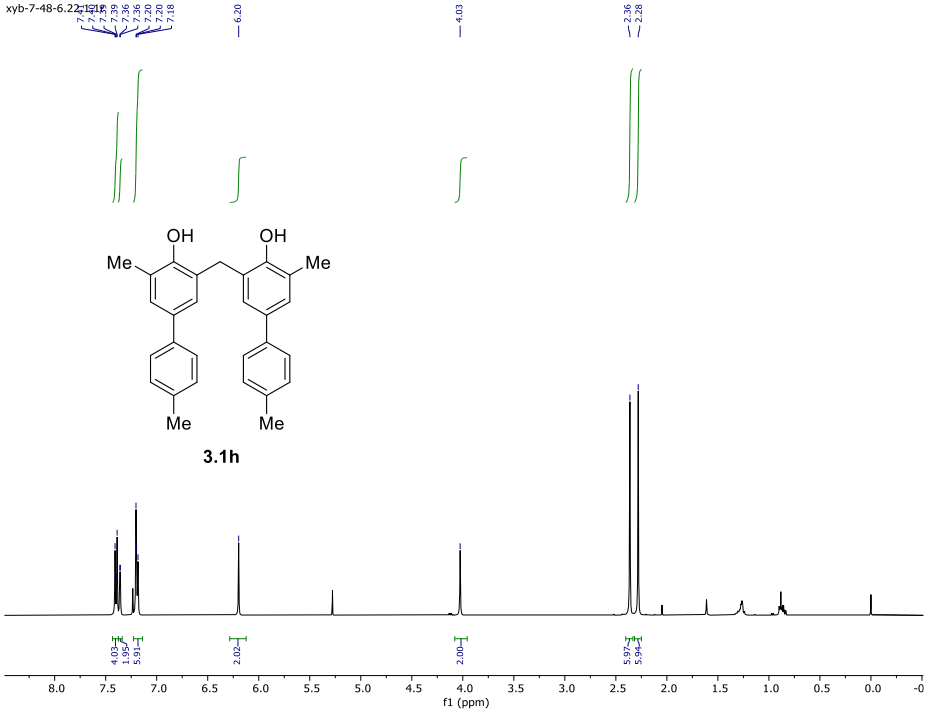


**Figure 3.24.** $^{13}$C-NMR Spectrum of **3.1h** in $CDCl_3$, 101 MHz

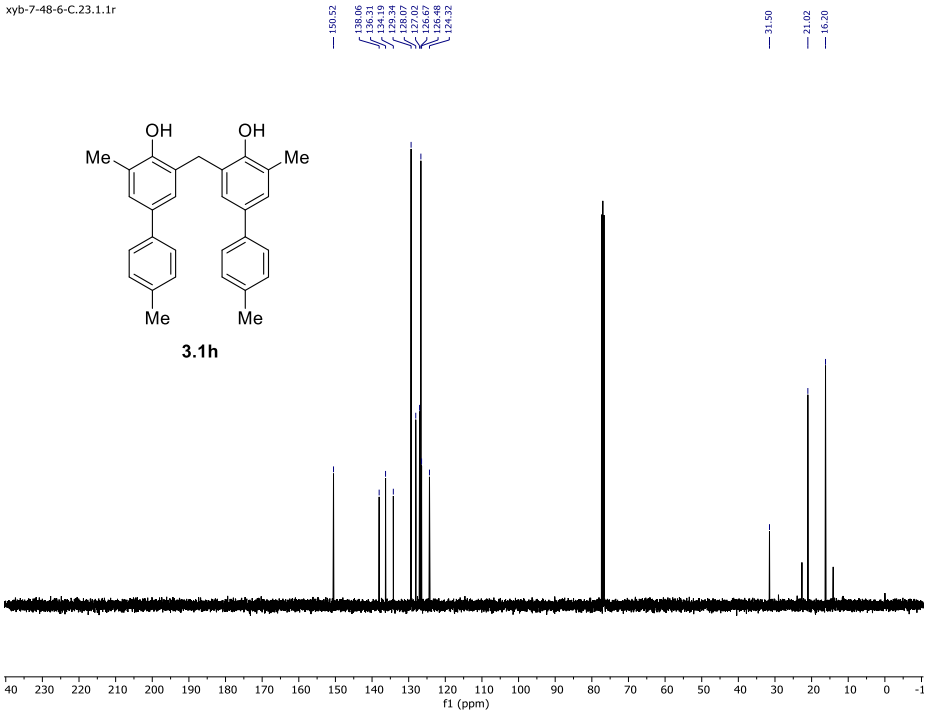

**Figure 3.25.** $^{1}$H-NMR Spectrum of **3.1i** in $CDCl_3$, 400 MHz

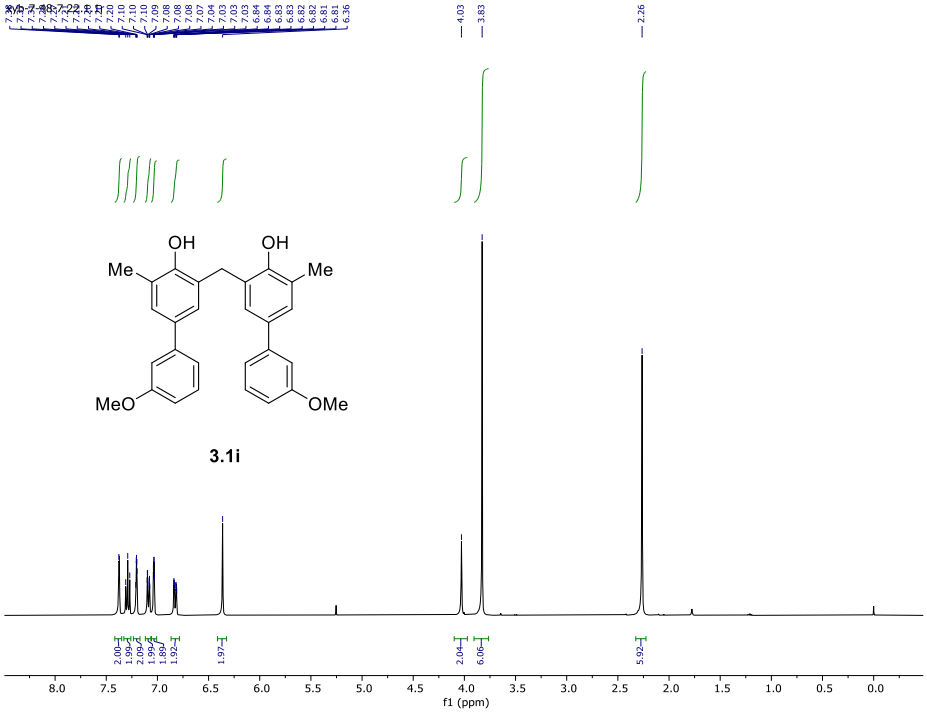


**Figure 3.26.** $^{13}$C-NMR Spectrum of **3.1i** in $CDCl_3$, 101 MHz

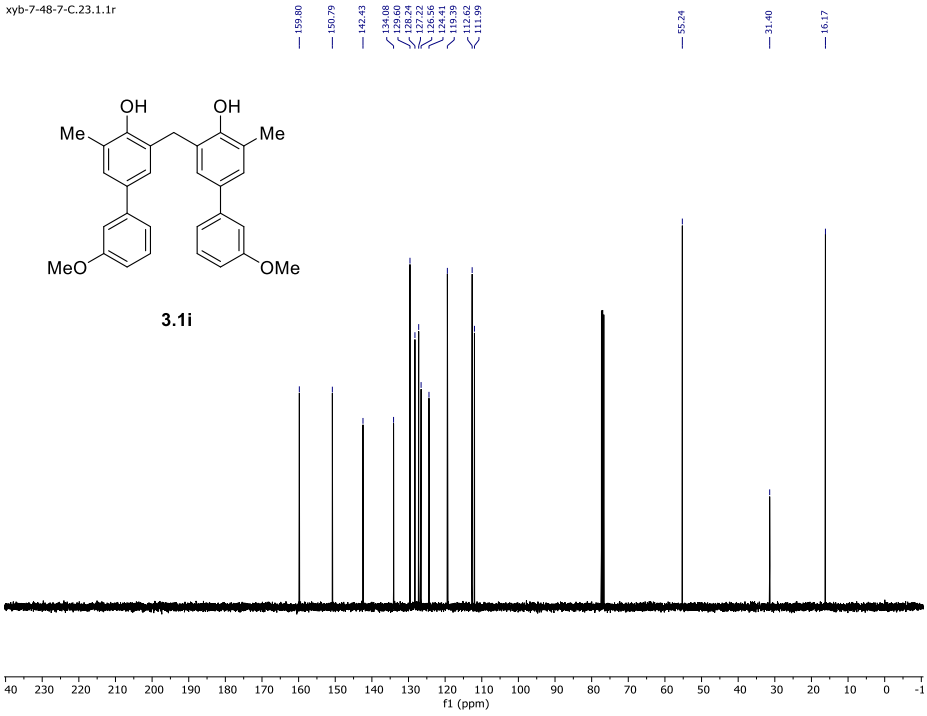

**Figure 3.27.** $^{1}$H-NMR Spectrum of **3.1j** in $CDCl_3$, 400 MHz

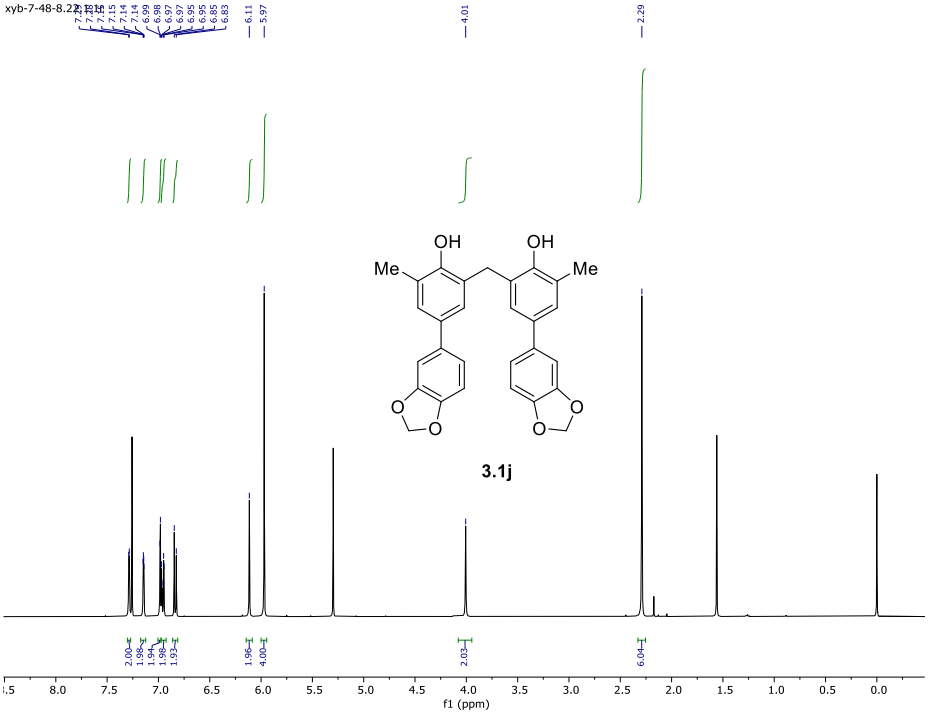


**Figure 3.28.** $^{13}$C-NMR Spectrum of **3.1j** in $CDCl_3$, 101 MHz

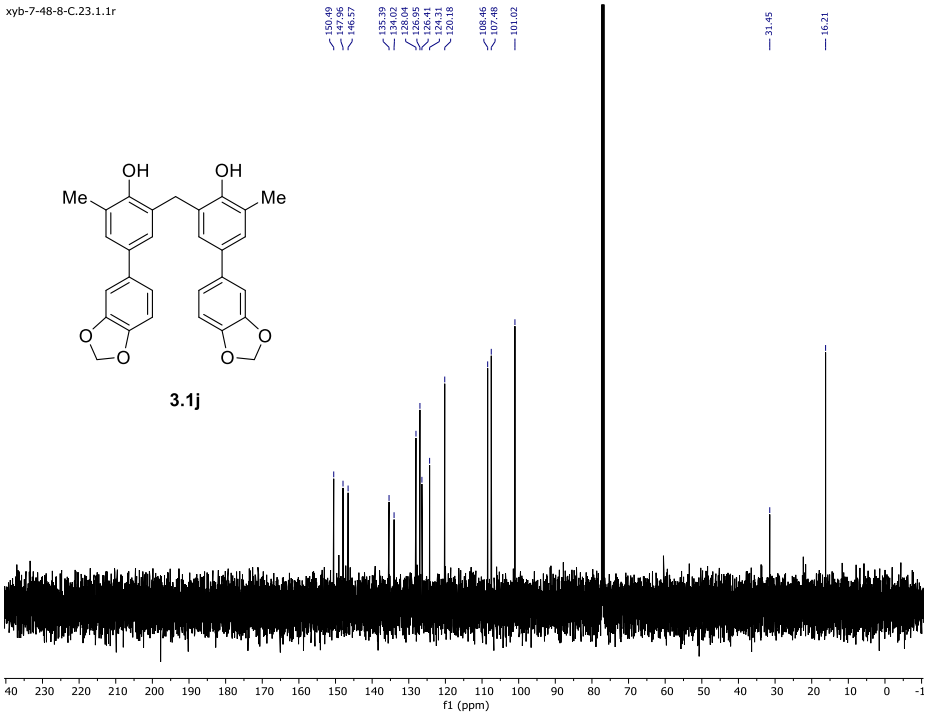

**Figure 3.29.** $^{1}$H-NMR Spectrum of **3.1k** in $CDCl_3$, 400 MHz

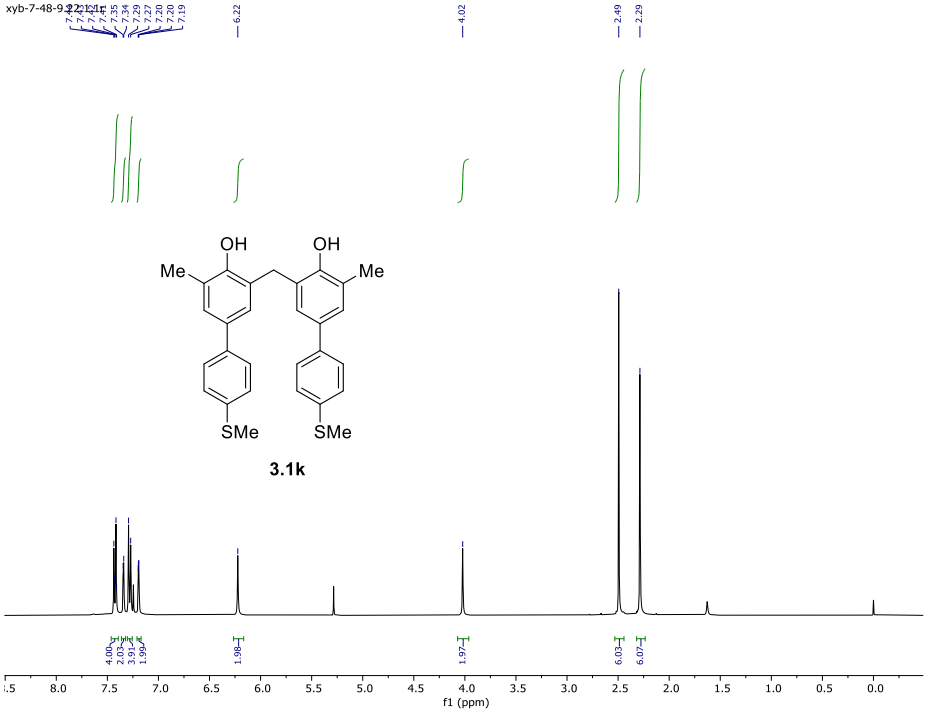


**Figure 3.30.** $^{13}$C-NMR Spectrum of **3.1k** in $CDCl_3$, 101 MHz

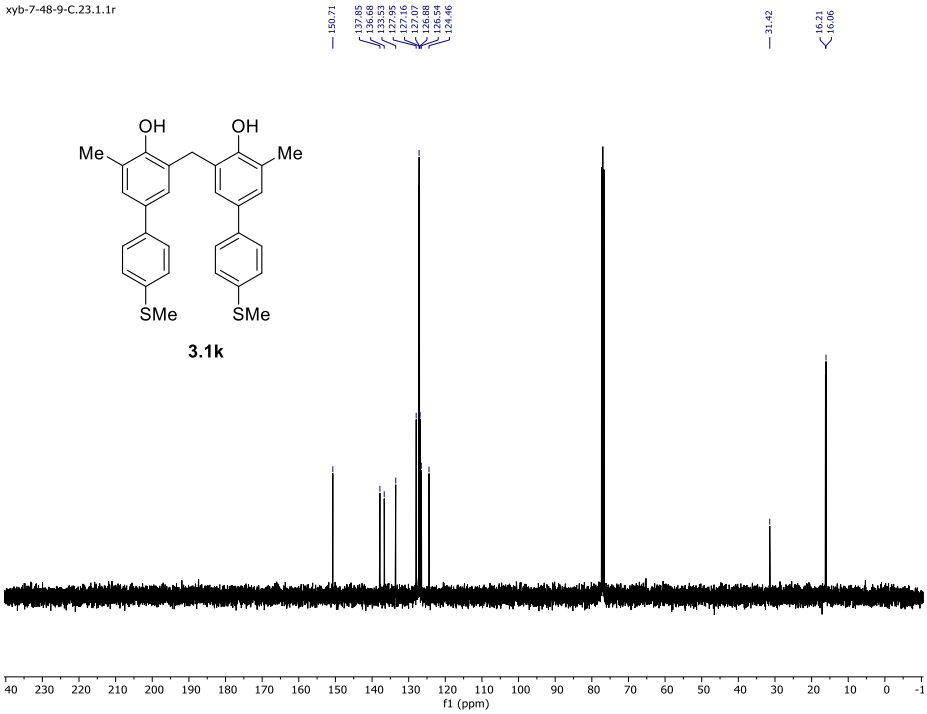

**Figure 3.31.** [1]H-NMR Spectrum of **3.1l** in DMSO-d6, 400 MHz

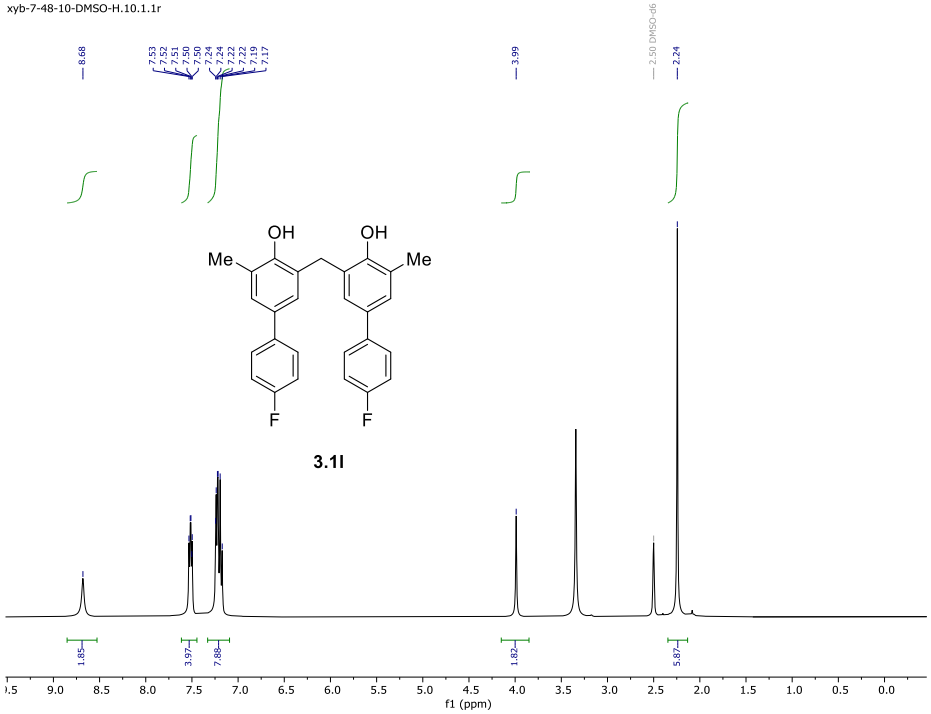


**Figure 3.32.** [13]C-NMR Spectrum of **3.1l** in DMSO-d6, 101 MHz

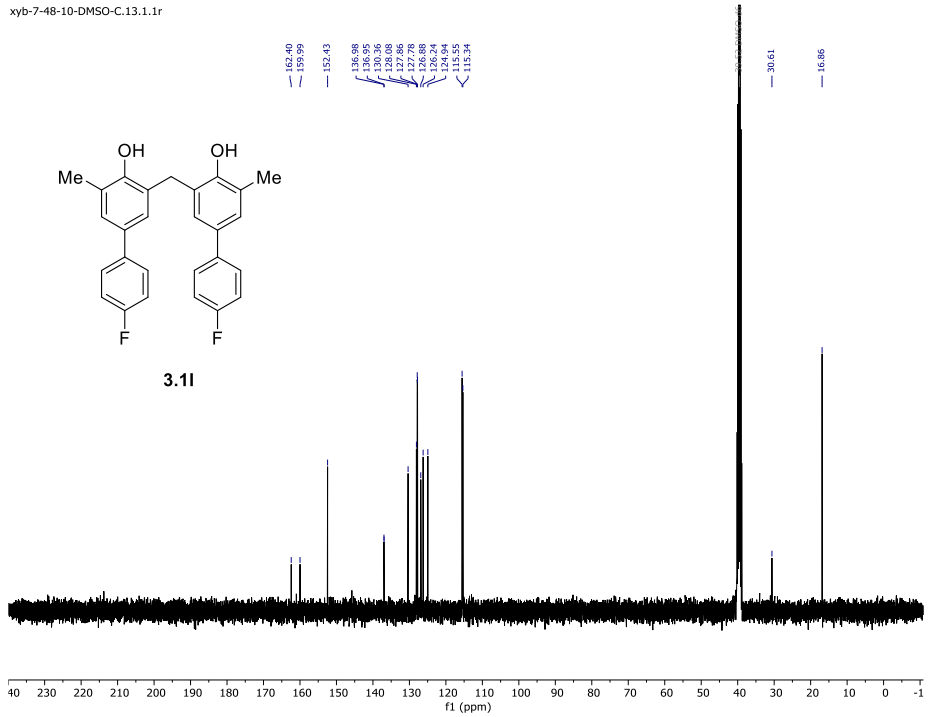

**Figure 3.33.** $^{19}$F-NMR Spectrum of **3.1l** in DMSO-d6, 376 MHz

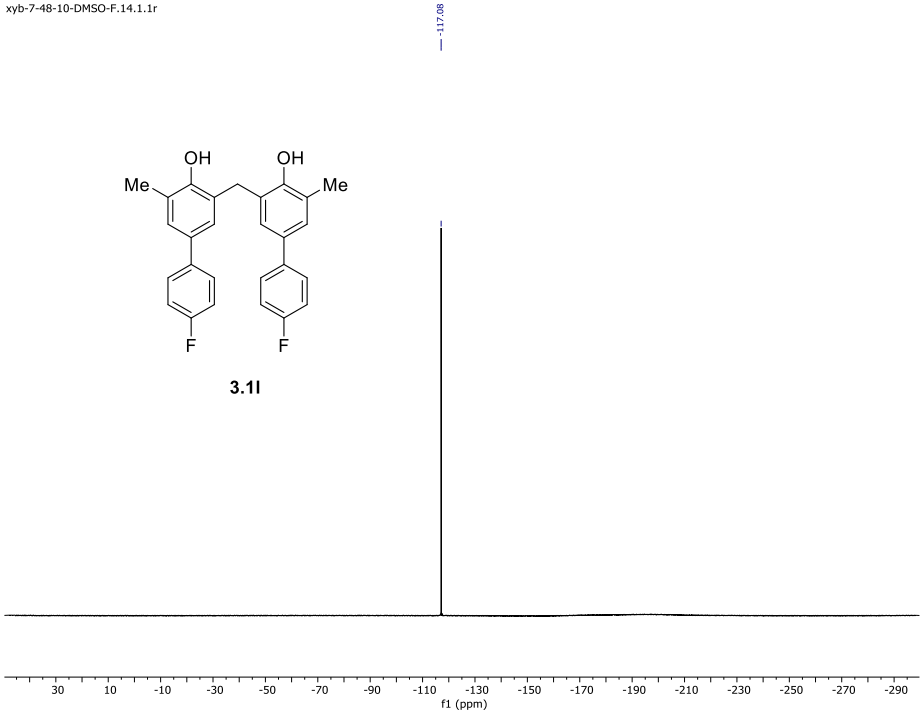

**Figure 3.34.** $^{1}$H-NMR Spectrum of **3.1m** in $CDCl_3$, 400 MHz

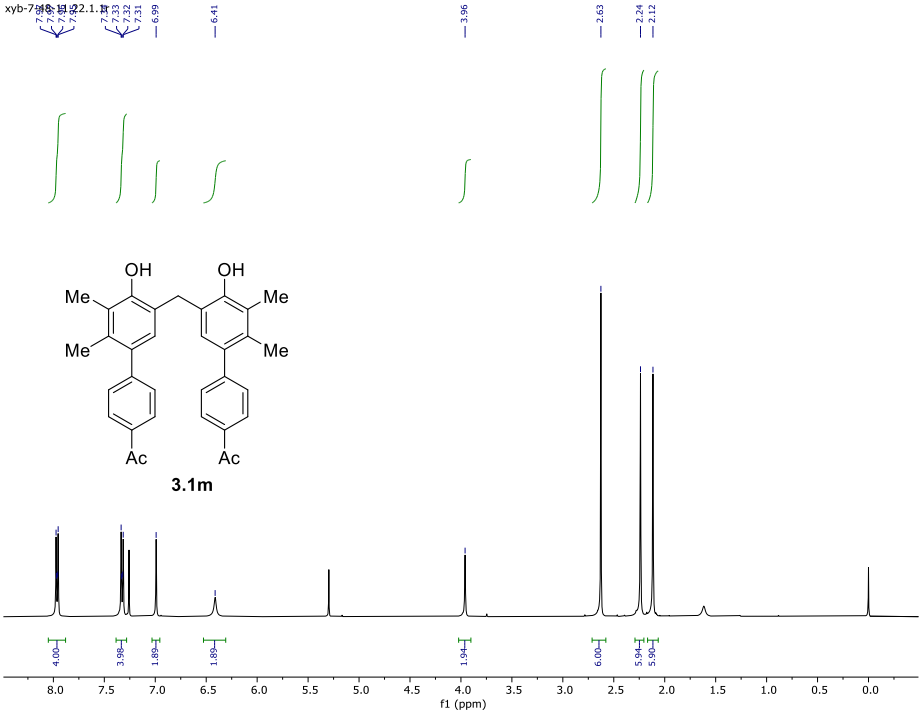


**Figure 3.35.** $^{13}$C-NMR Spectrum of **3.1m** in $CDCl_3$, 101 MHz

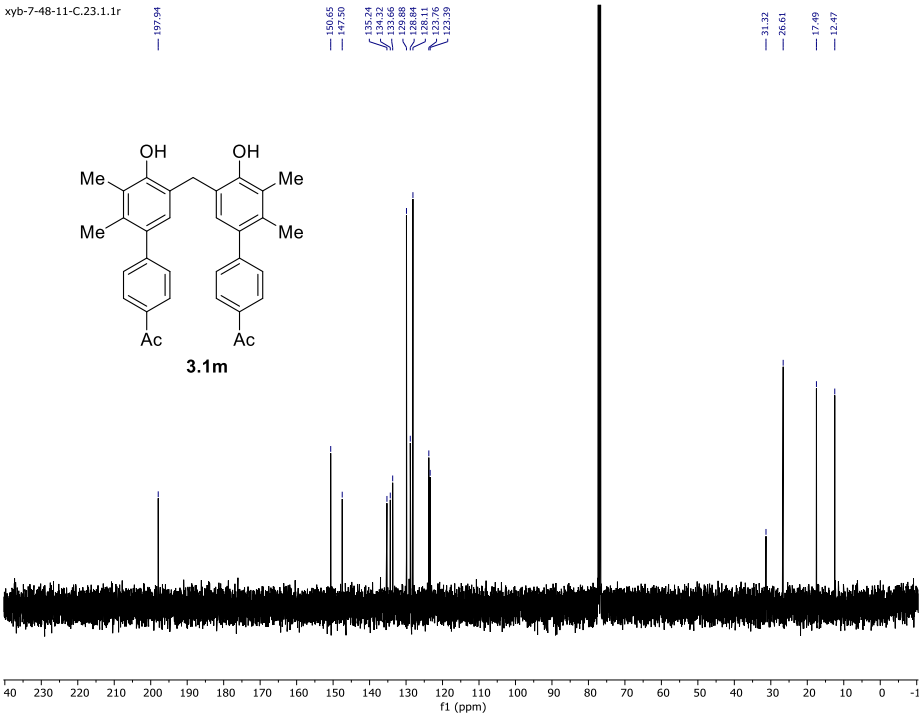

**Figure 3.36.** $^{1}$H-NMR Spectrum of **3.1n** in $CDCl_3$, 400 MHz

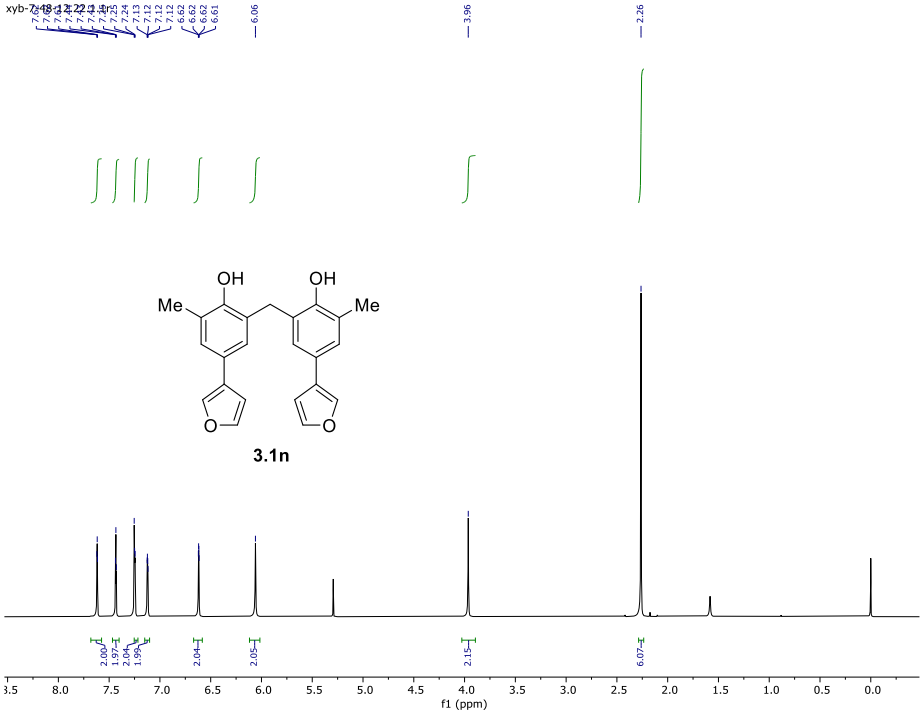


**Figure 3.37.** $^{13}$C-NMR Spectrum of **3.1n** in $CDCl_3$, 101 MHz

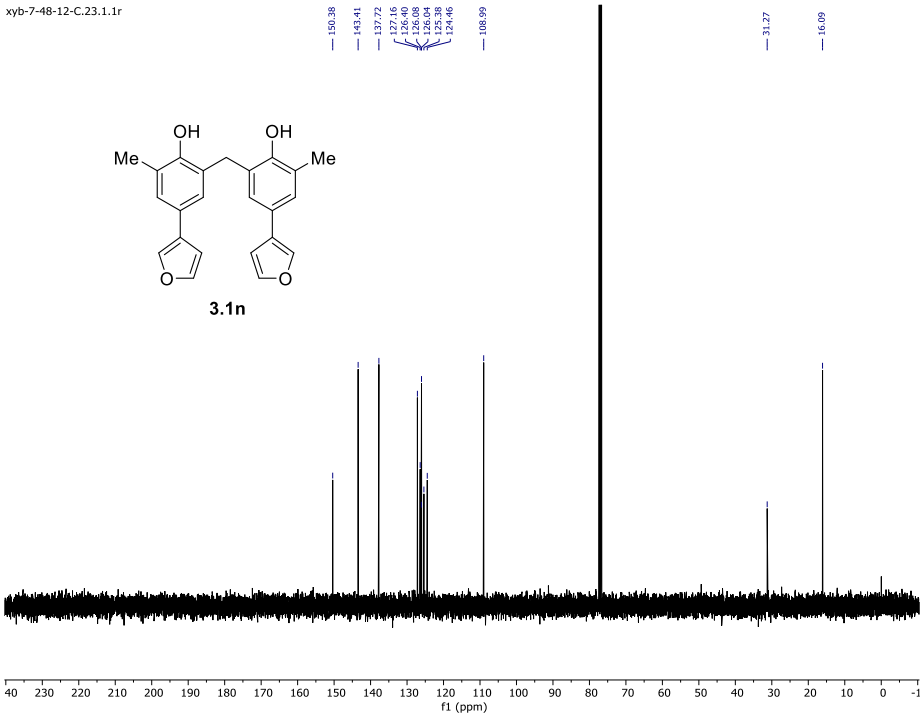

**Figure 3.38.** $^{1}$H-NMR Spectrum of **3.1o** in $CDCl_3$, 400 MHz

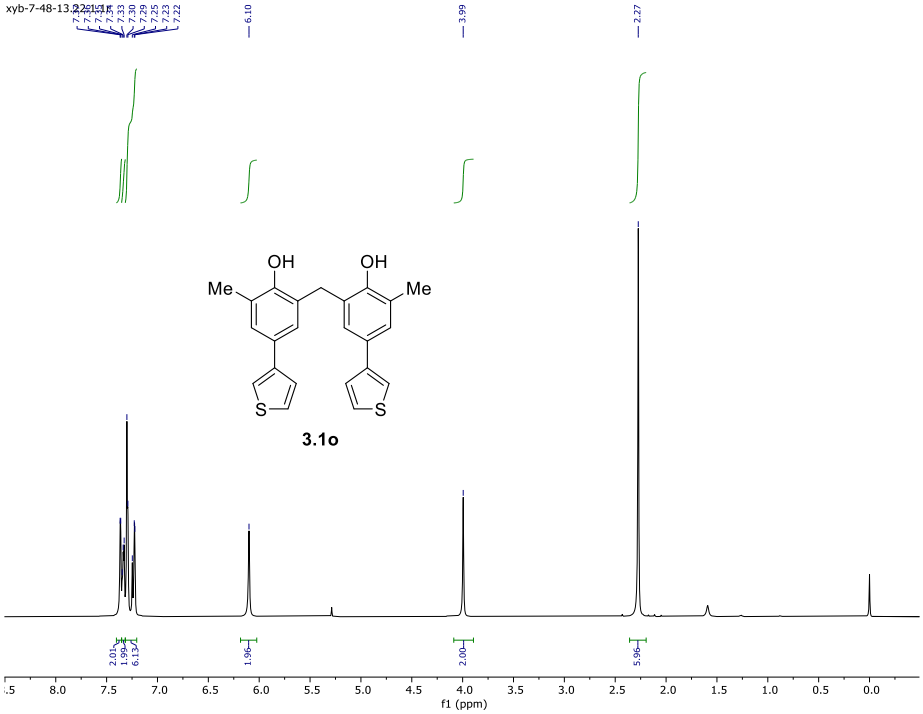


**Figure 3.39.** $^{13}$C-NMR Spectrum of **3.1o** in $CDCl_3$, 101 MHz

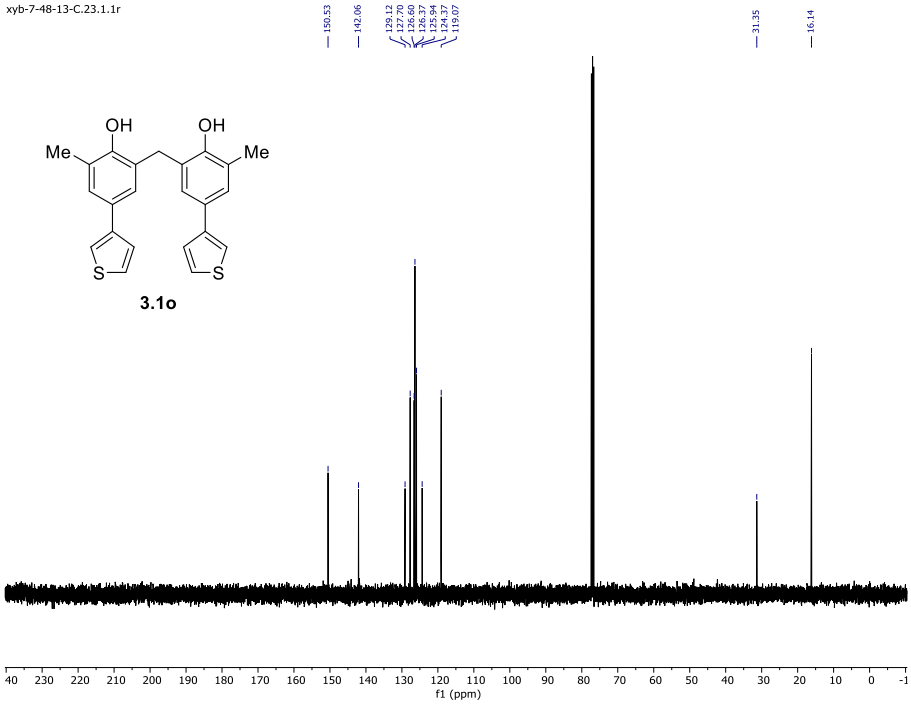

**Figure 3.40.** $^{1}$H-NMR Spectrum of **3.1p** in $CDCl_3$, 400 MHz

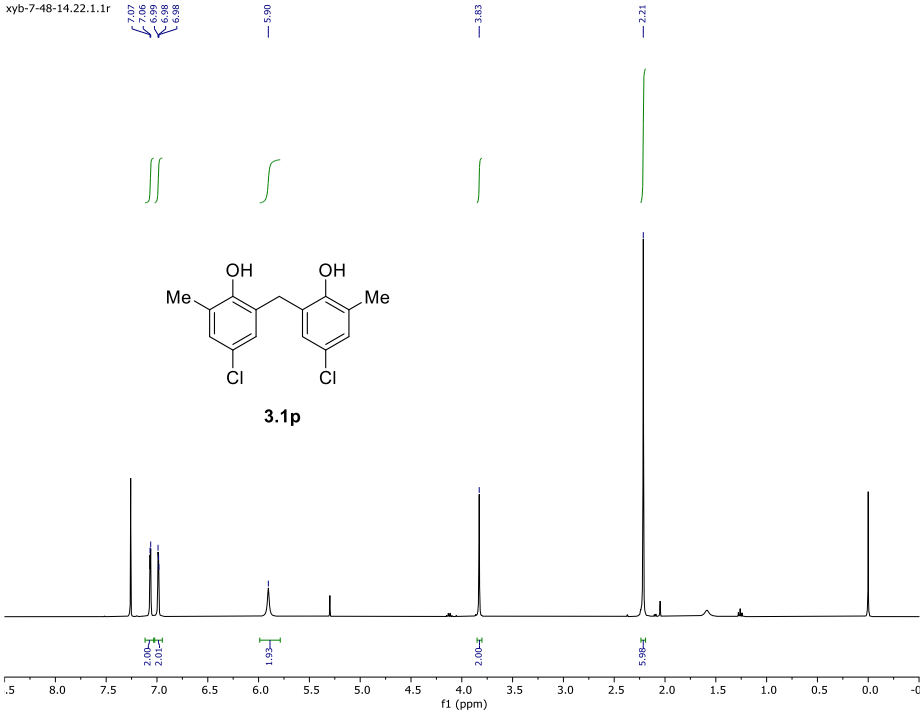


**Figure 3.41.** $^{13}$C-NMR Spectrum of **3.1p** in $CDCl_3$, 101 MHz

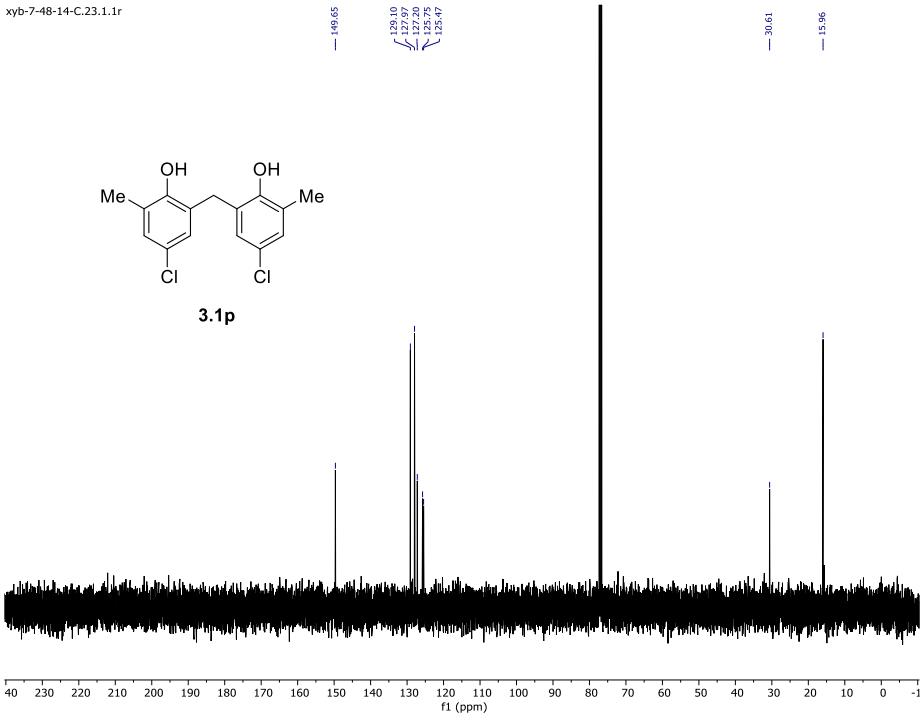

**Figure 3.42.** $^{1}$H-NMR Spectrum of **3.1q** in $CDCl_3$, 400 MHz

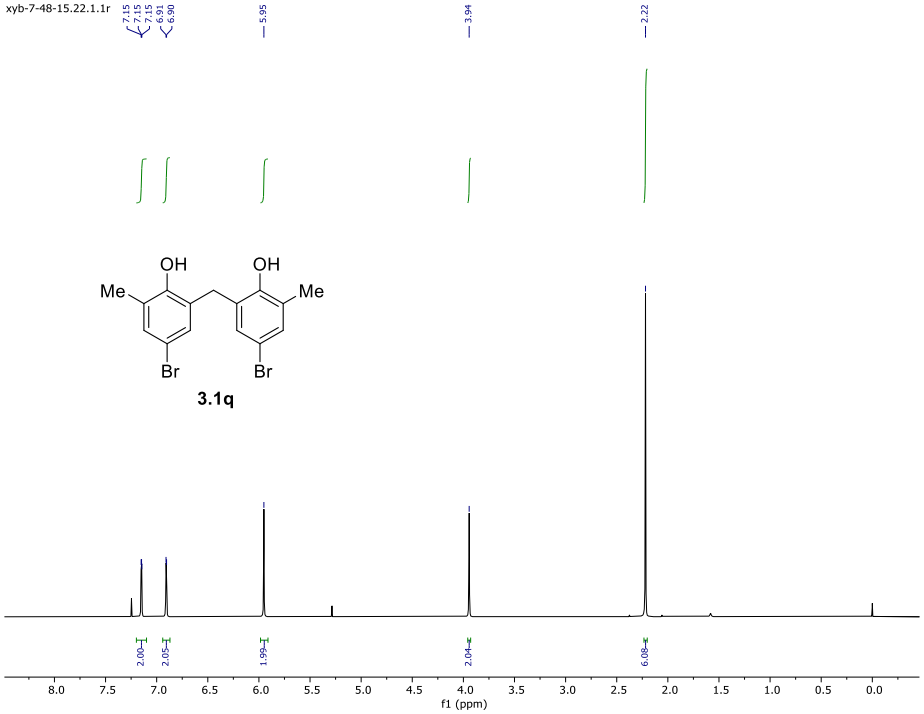


**Figure 3.43.** $^{13}$C-NMR Spectrum of **3.1q** in $CDCl_3$, 101 MHz

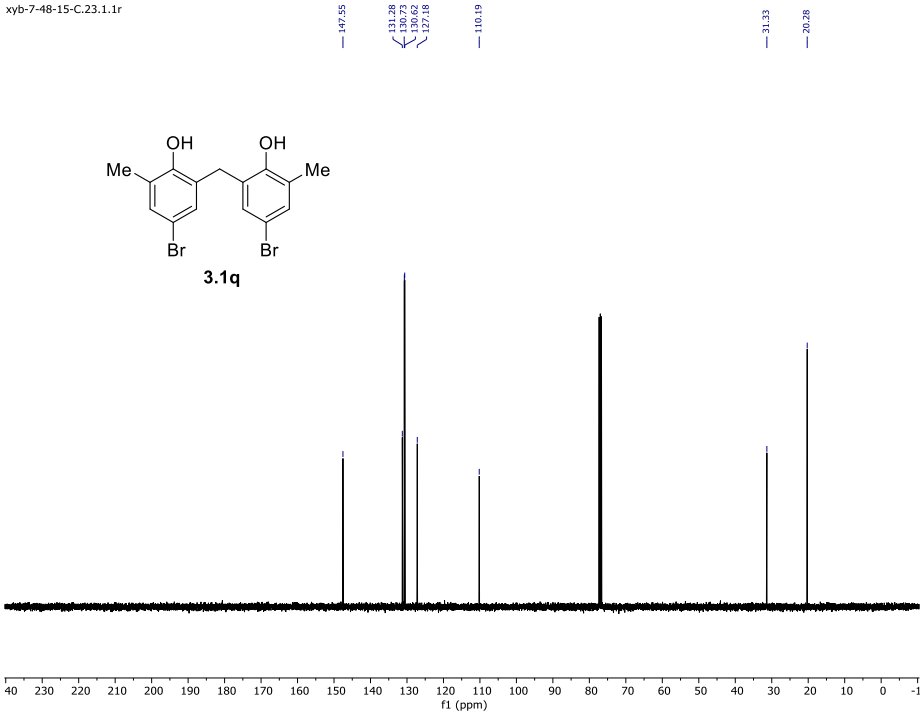

**Figure 3.44.** $^{1}$H-NMR Spectrum of **3.1r** in DMSO-d6, 500 MHz

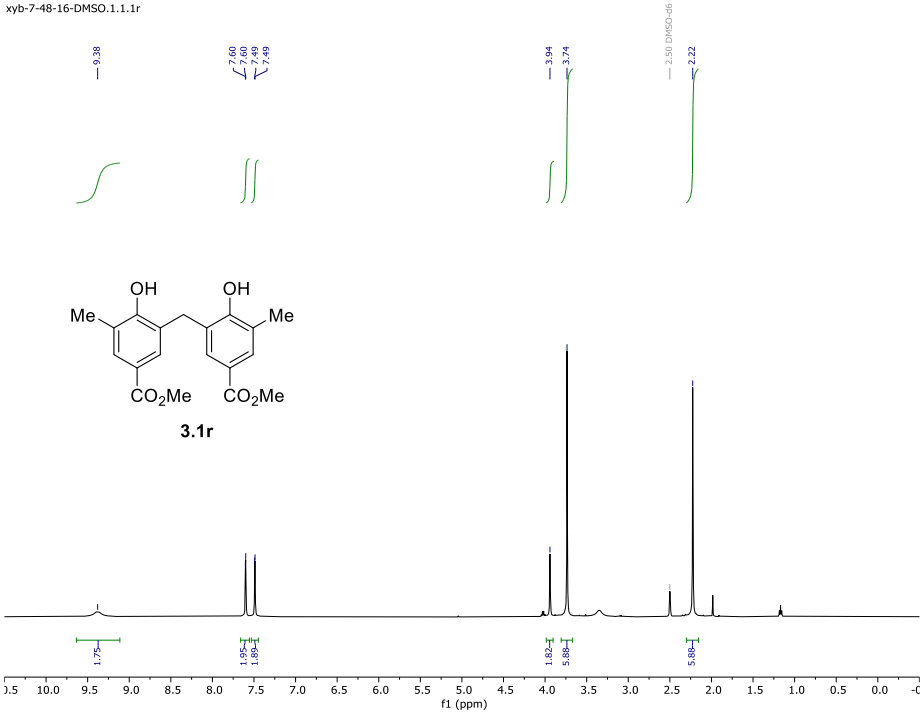


**Figure 3.45.** $^{13}$C-NMR Spectrum of **3.1r** in DMSO-d6, 126 MHz

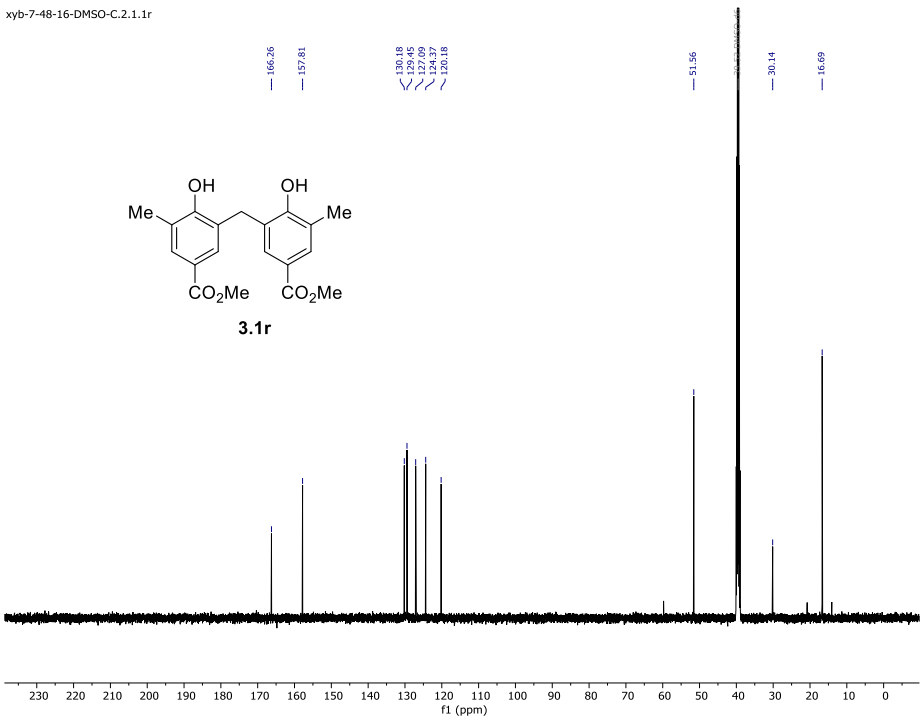

**Figure 3.46.** $^{1}$H-NMR Spectrum of **3.1s** in $CDCl_3$, 400 MHz

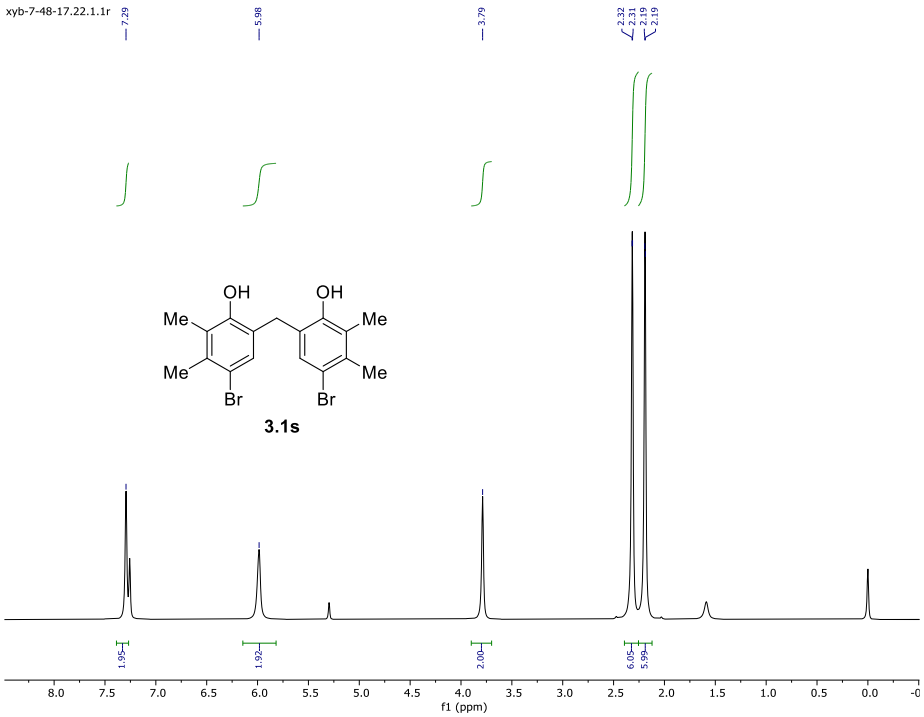


**Figure 3.47.** $^{13}$C-NMR Spectrum of **3.1s** in $CDCl_3$, 101 MHz

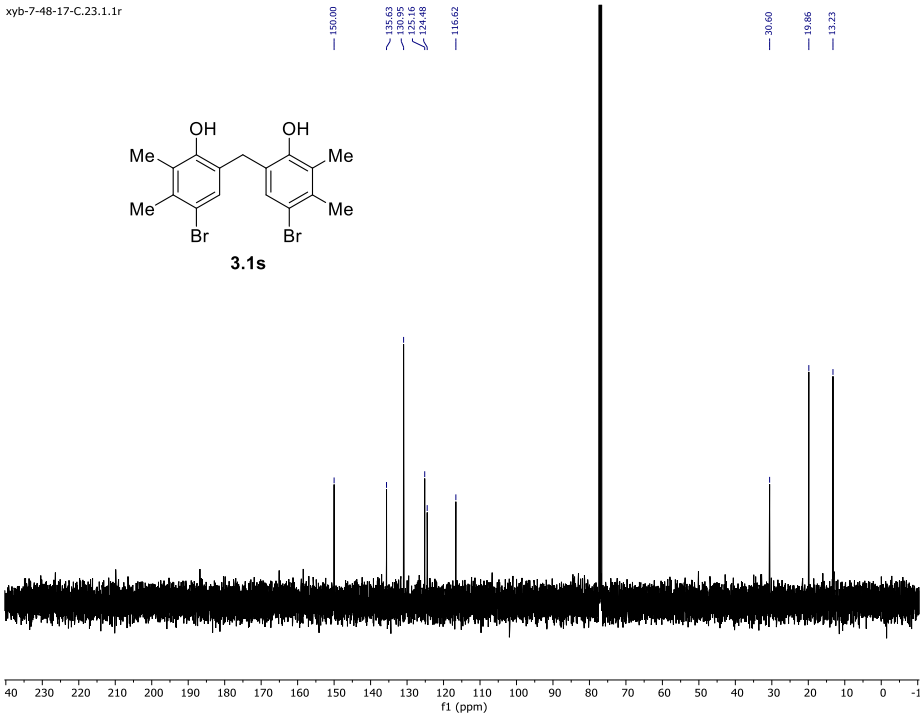

**Figure 3.48.** $^{1}$H-NMR Spectrum of **3.1u** in $CDCl_3$, 400 MHz

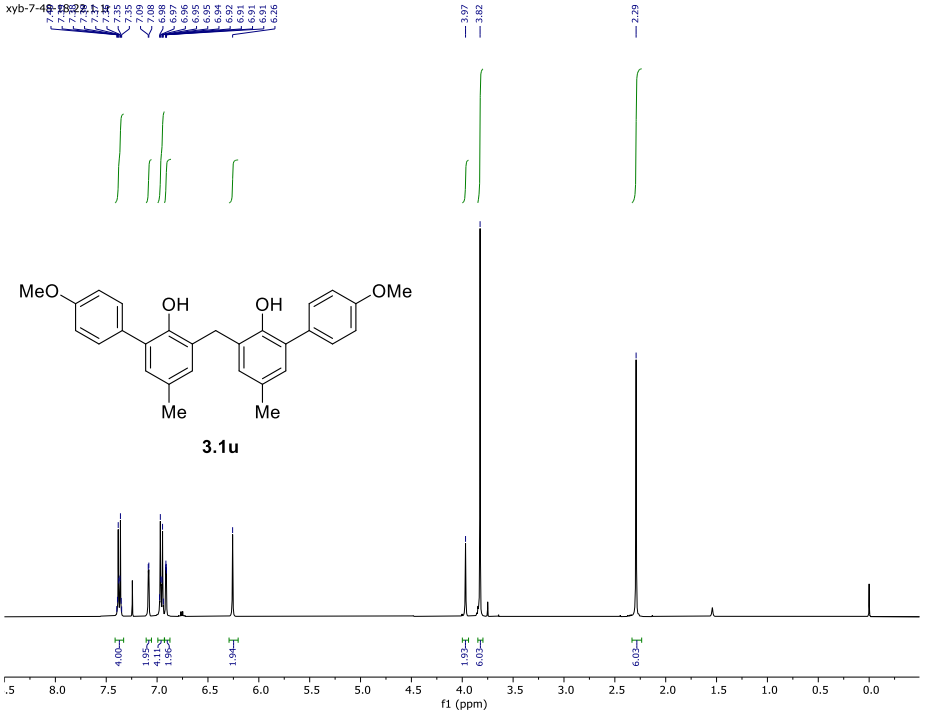


**Figure 3.49.** $^{13}$C-NMR Spectrum of **3.1u** in $CDCl_3$, 101 MHz

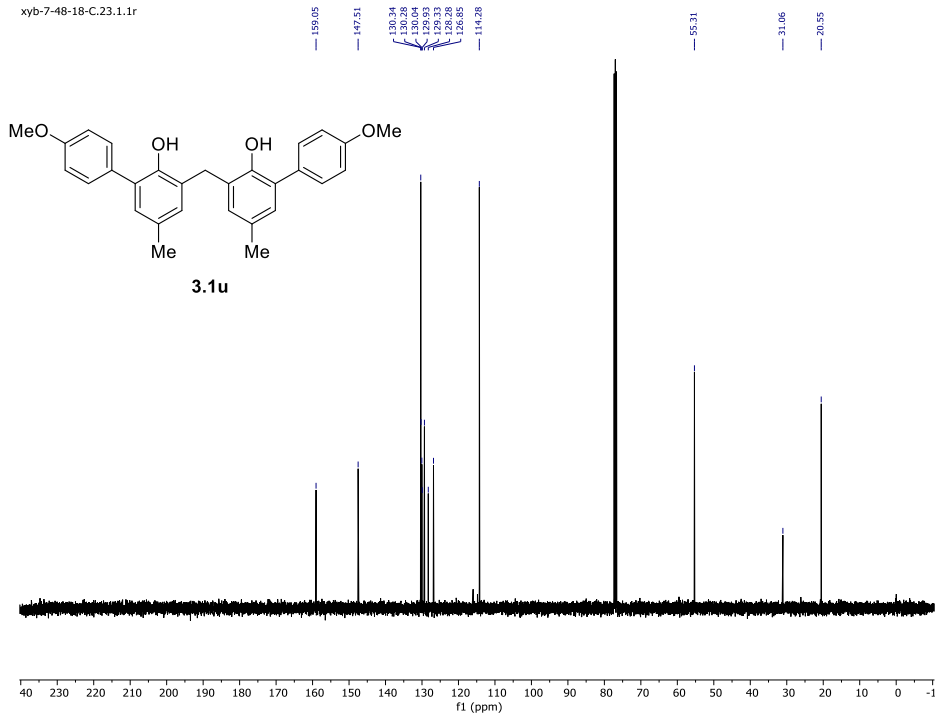

**Figure 3.50.** $^{1}$H-NMR Spectrum of **3.1v** in $CDCl_3$, 400 MHz

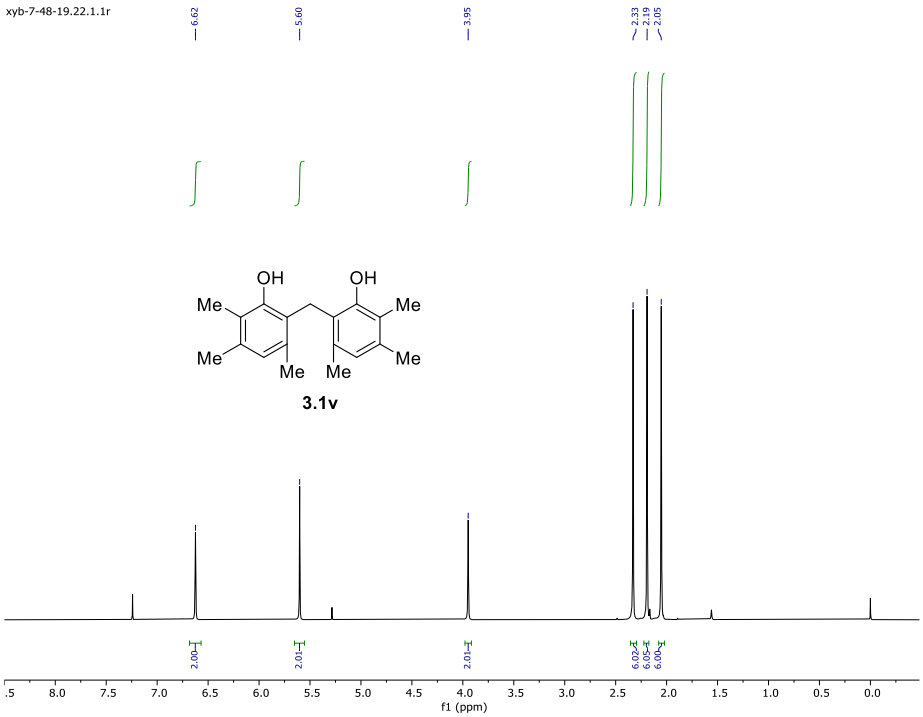


**Figure 3.51.** $^{13}$C-NMR Spectrum of **3.1v** in $CDCl_3$, 101 MHz

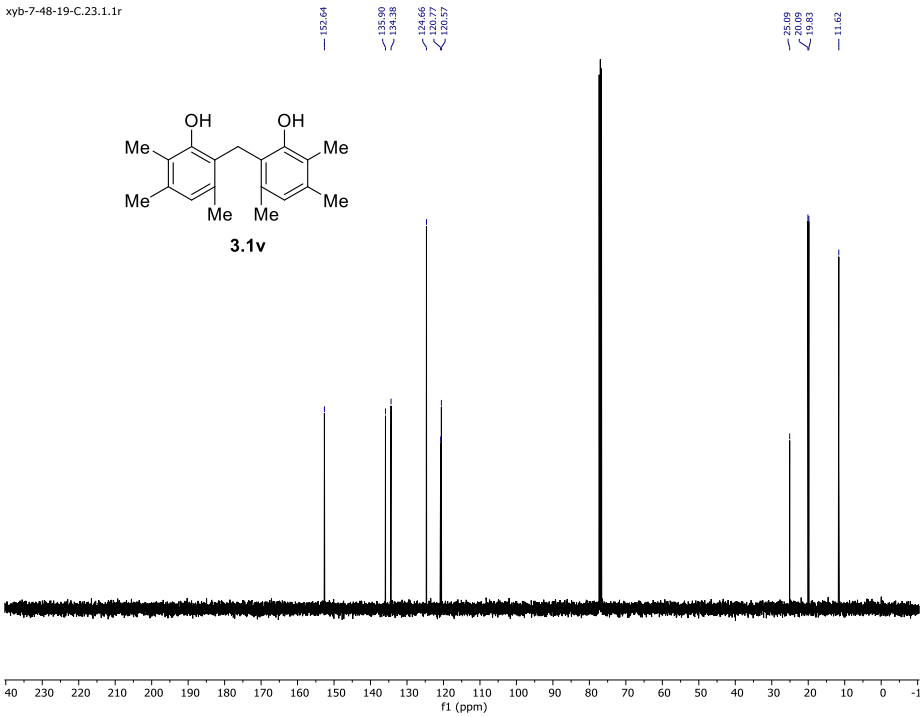

**Figure 3.52.** $^{1}$H-NMR Spectrum of **3.1w** in $CDCl_3$, 400 MHz

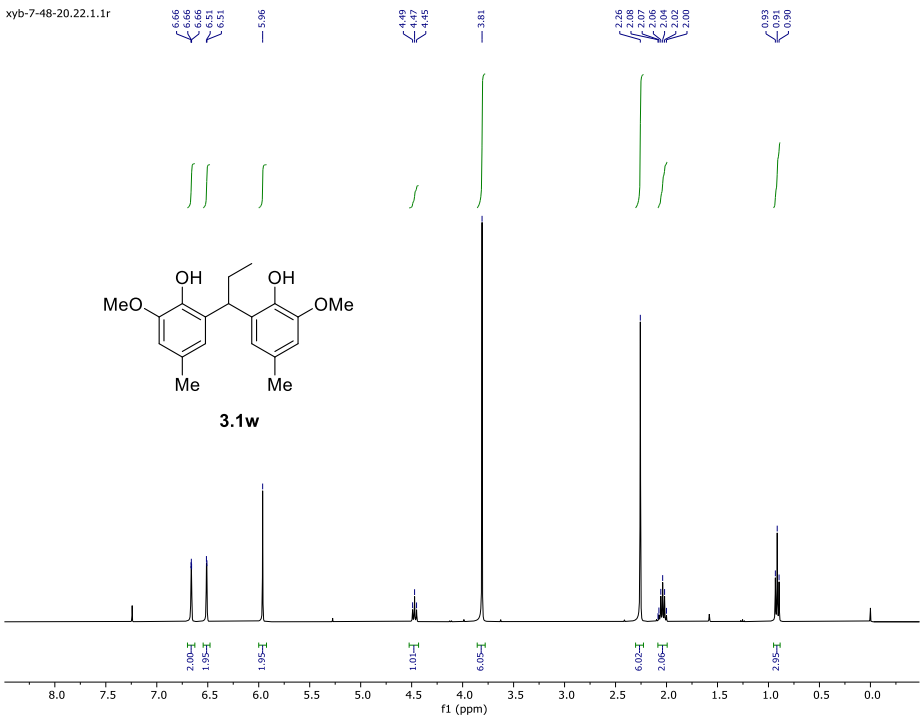


**Figure 3.53.** $^{13}$C-NMR Spectrum of **3.1w** in $CDCl_3$, 101 MHz

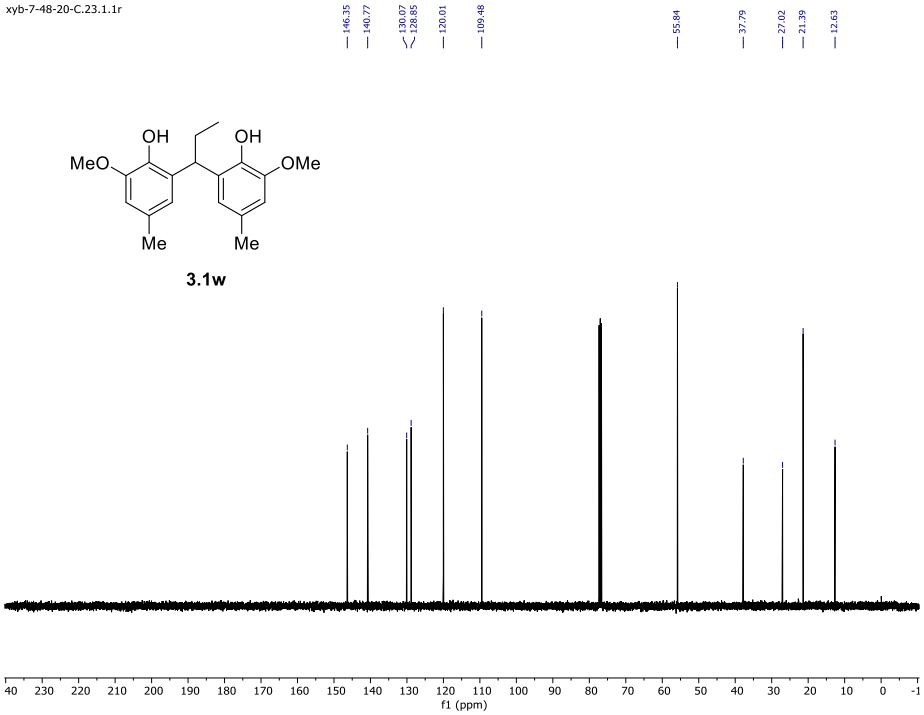

**Figure 3.54.** $^{1}$H-NMR Spectrum of **3.1x** in $CDCl_3$, 400 MHz

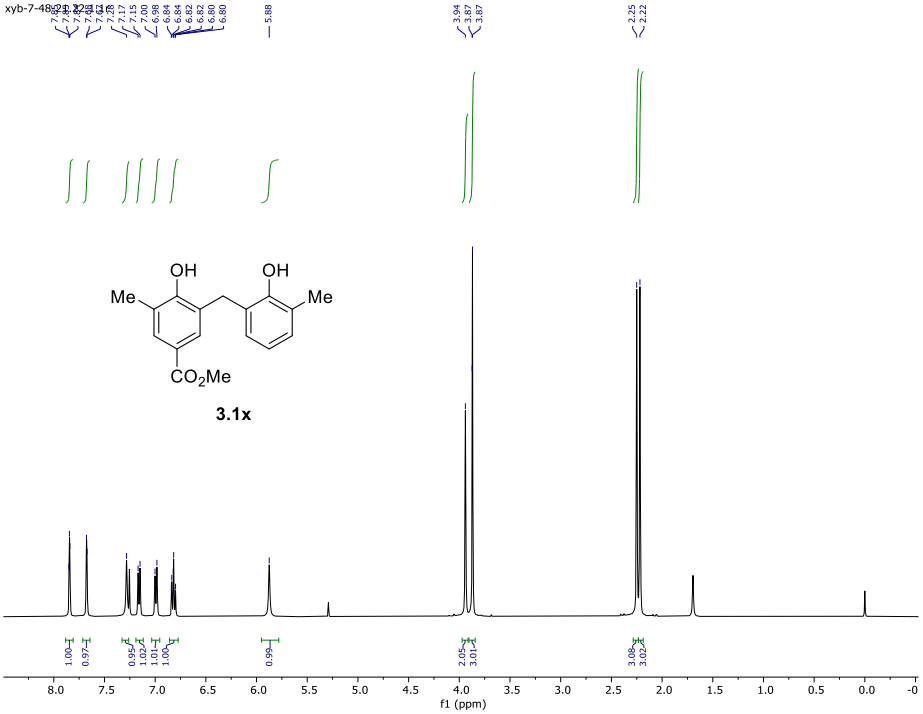


**Figure 3.55.** $^{13}$C-NMR Spectrum of **3.1x** in $CDCl_3$, 101 MHz

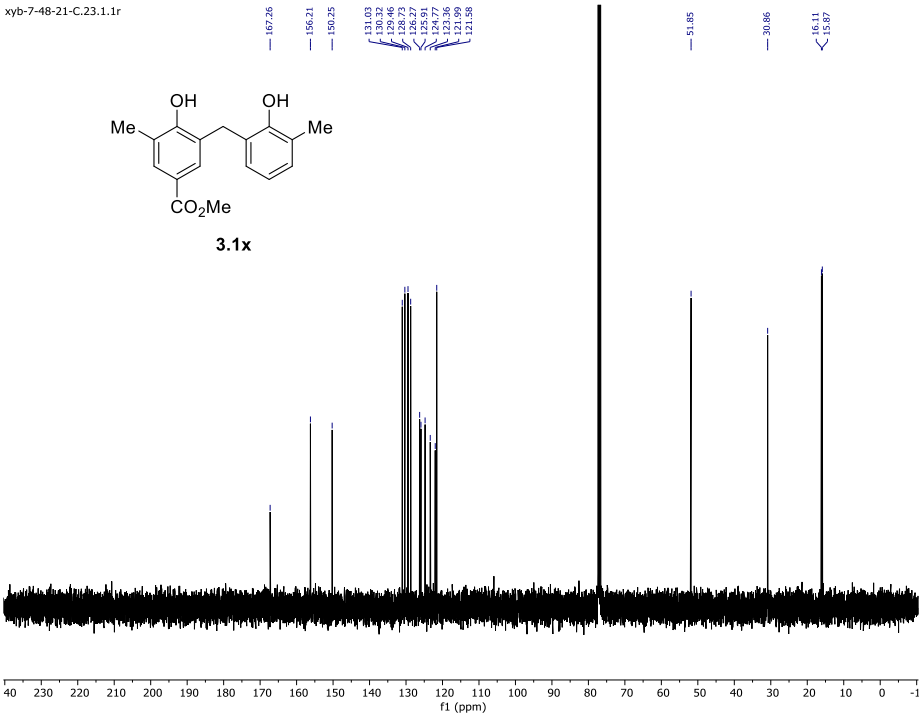

**Figure 3.56.** $^{1}$H-NMR Spectrum of **3.2a** in $C_6D_6$, 500 MHz

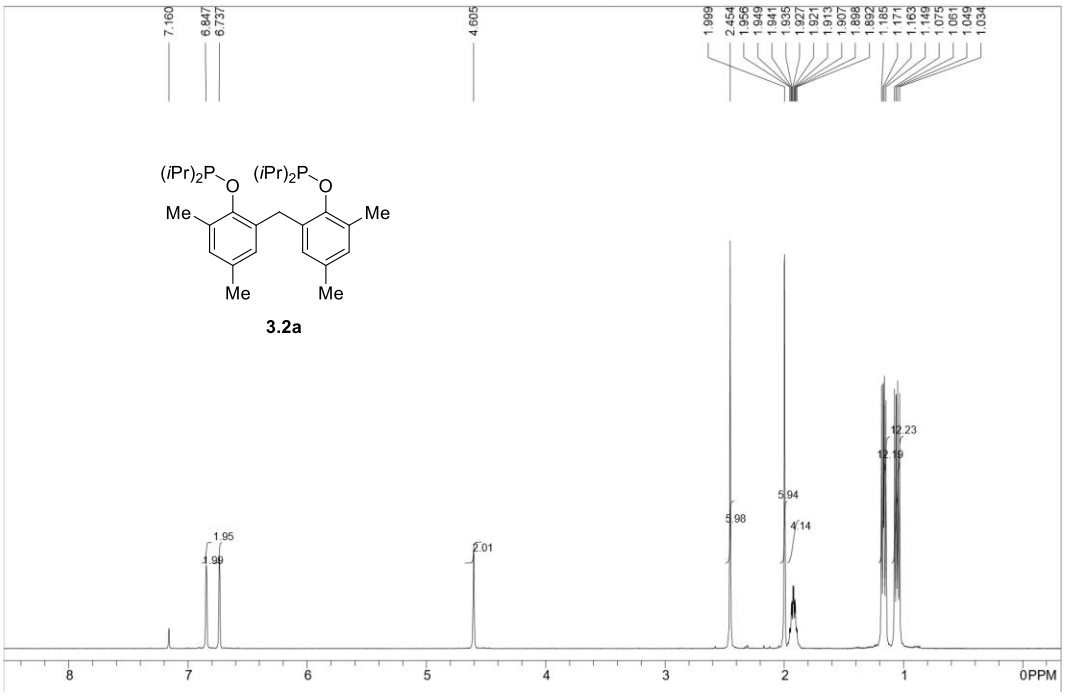


**Figure 3.57.** $^{13}$C-NMR Spectrum of **3.2a** in $C_6D_6$, 125 MHz

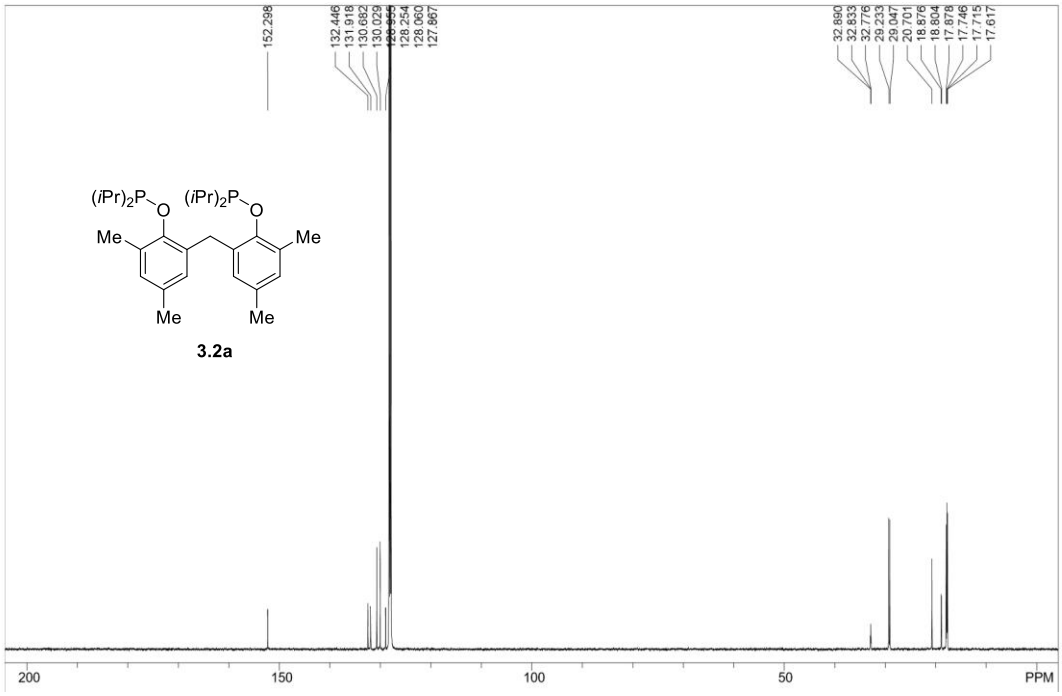

**Figure 3.58.** $^{31}$P-NMR Spectrum of **3.2a** in $C_6D_6$, 202 MHz

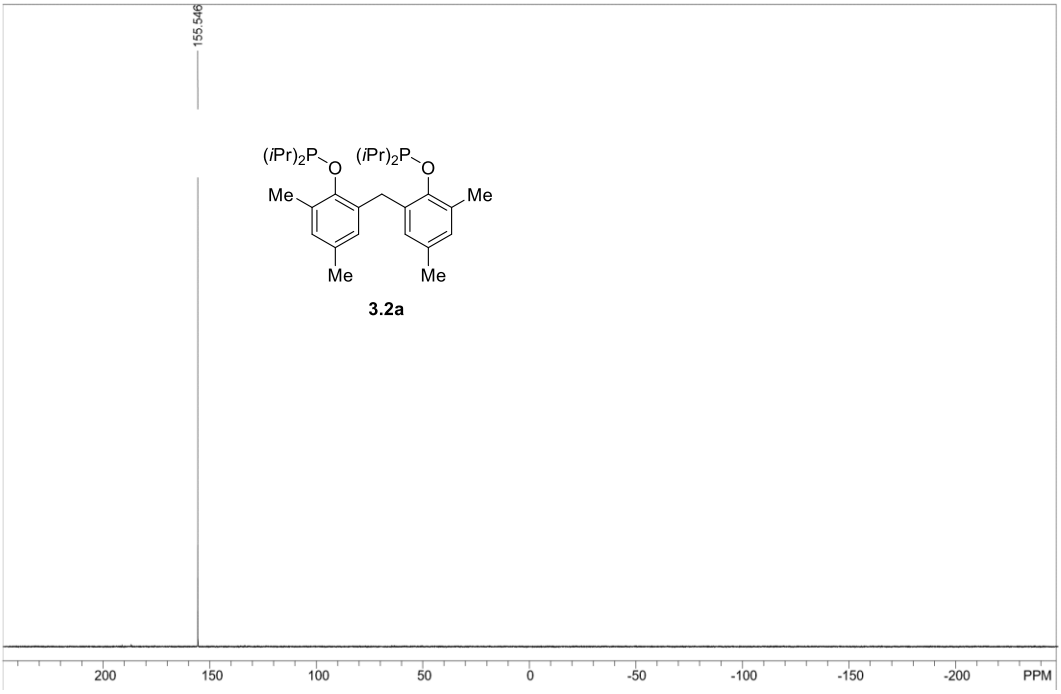

**Figure 3.59.** $^{1}$H-NMR Spectrum of **3.2b** in $C_6D_6$, 500 MHz

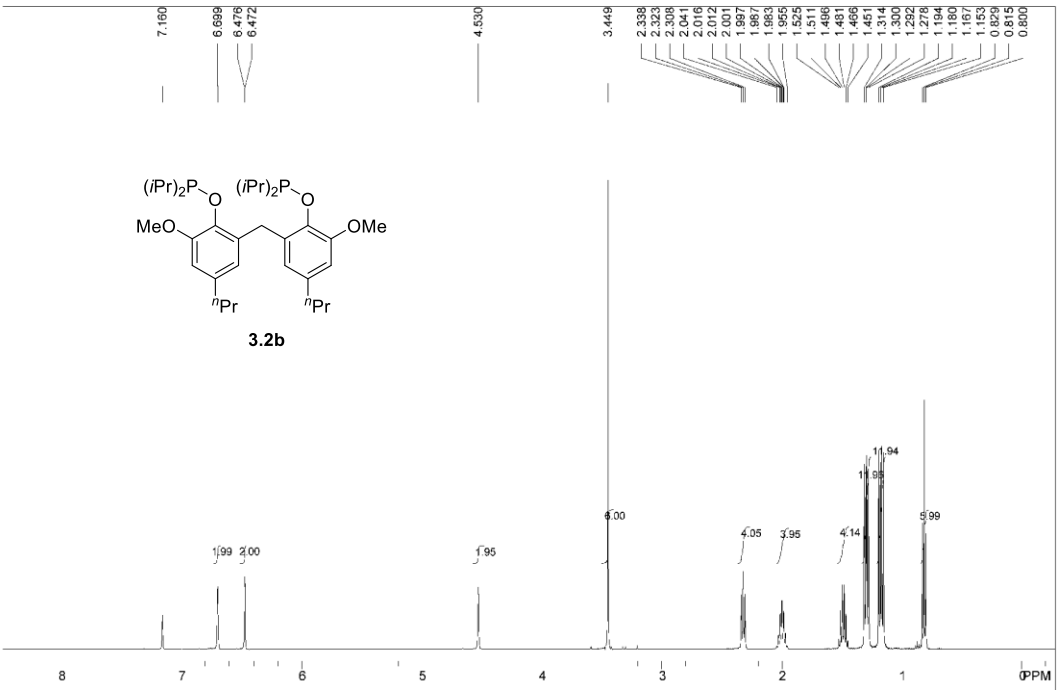


**Figure 3.60.** $^{13}$C-NMR Spectrum of **3.2b** in $C_6D_6$, 125 MHz

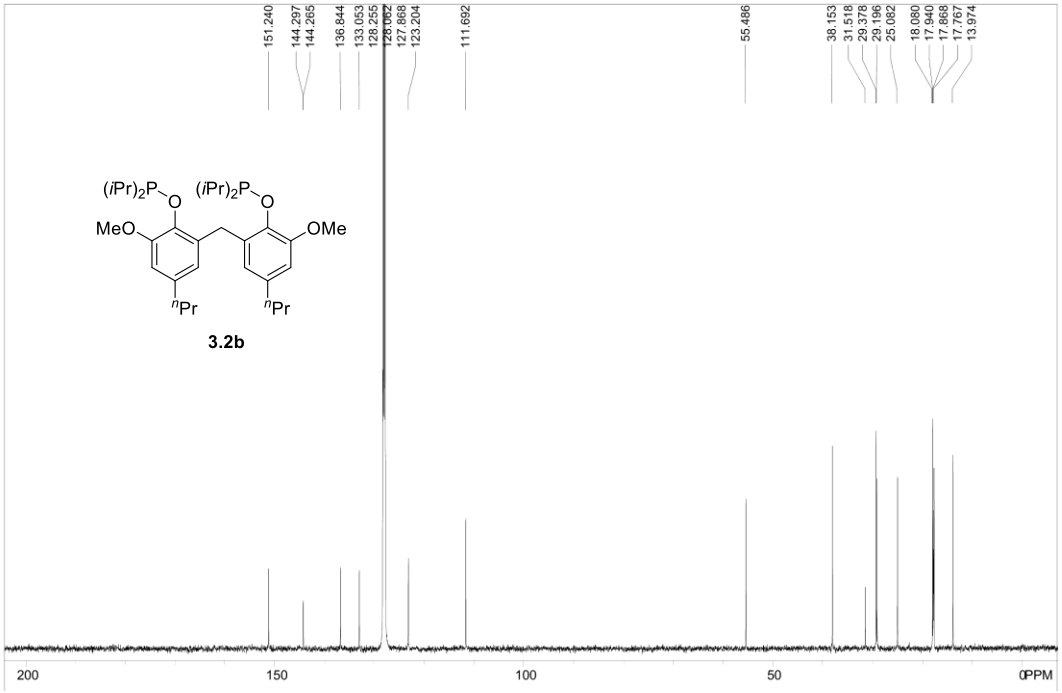

**Figure 3.61.** $^{31}$P-NMR Spectrum of **3.2b** in $C_6D_6$, 202 MHz

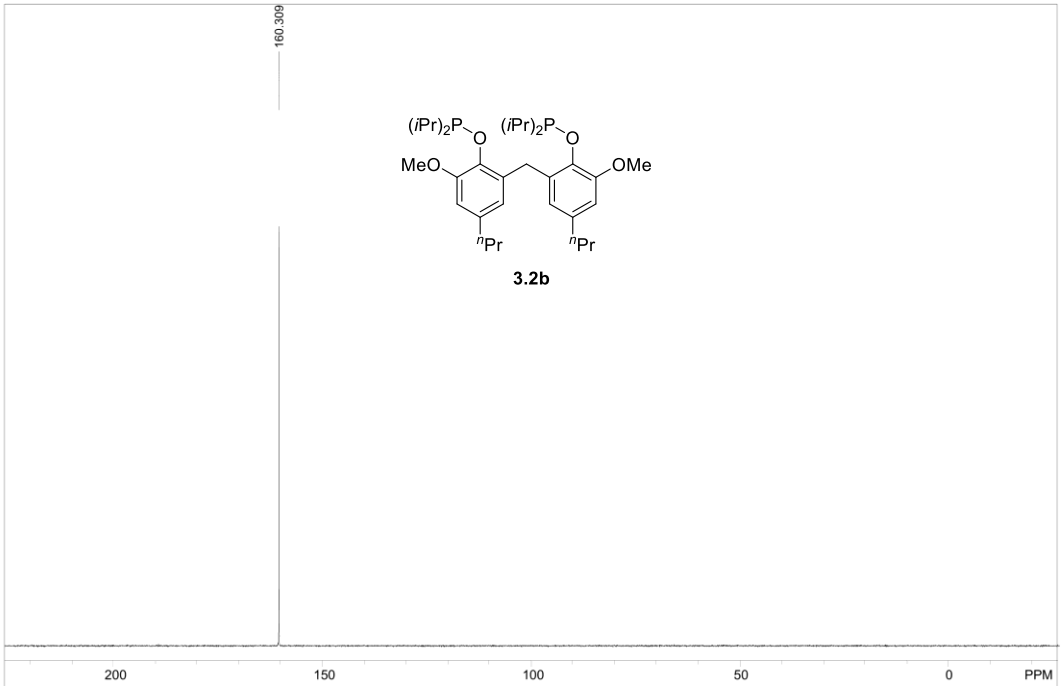

**Figure 3.62.** $^{1}$H-NMR Spectrum of **3.2c** in $C_6D_6$, 500 MHz

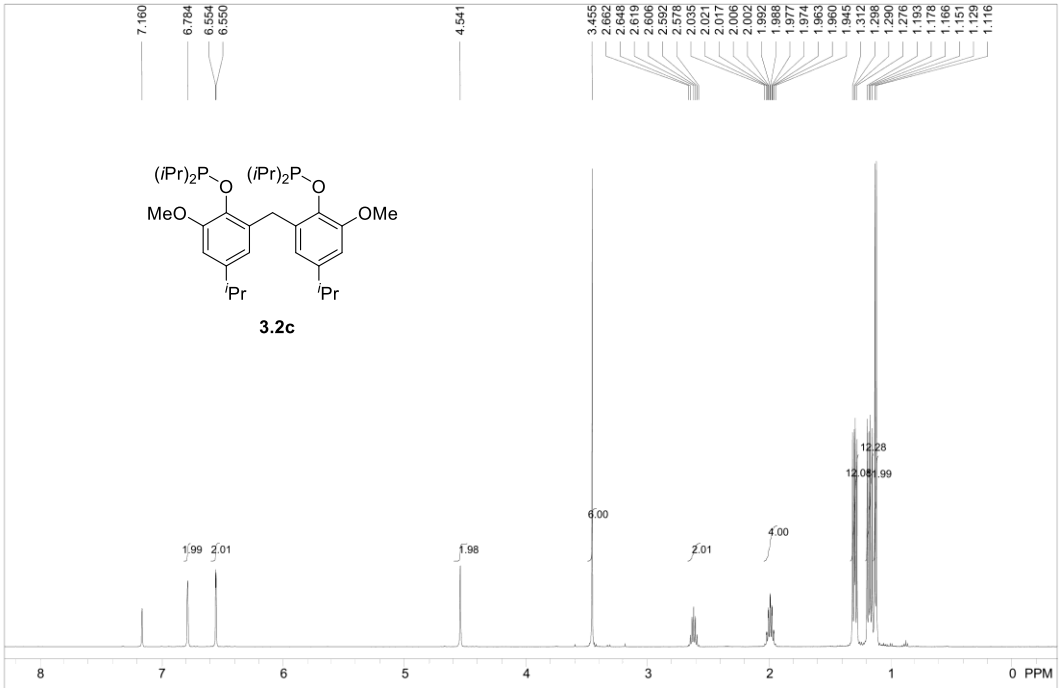


**Figure 3.63.** $^{13}$C-NMR Spectrum of **3.2c** in $C_6D_6$, 125 MHz

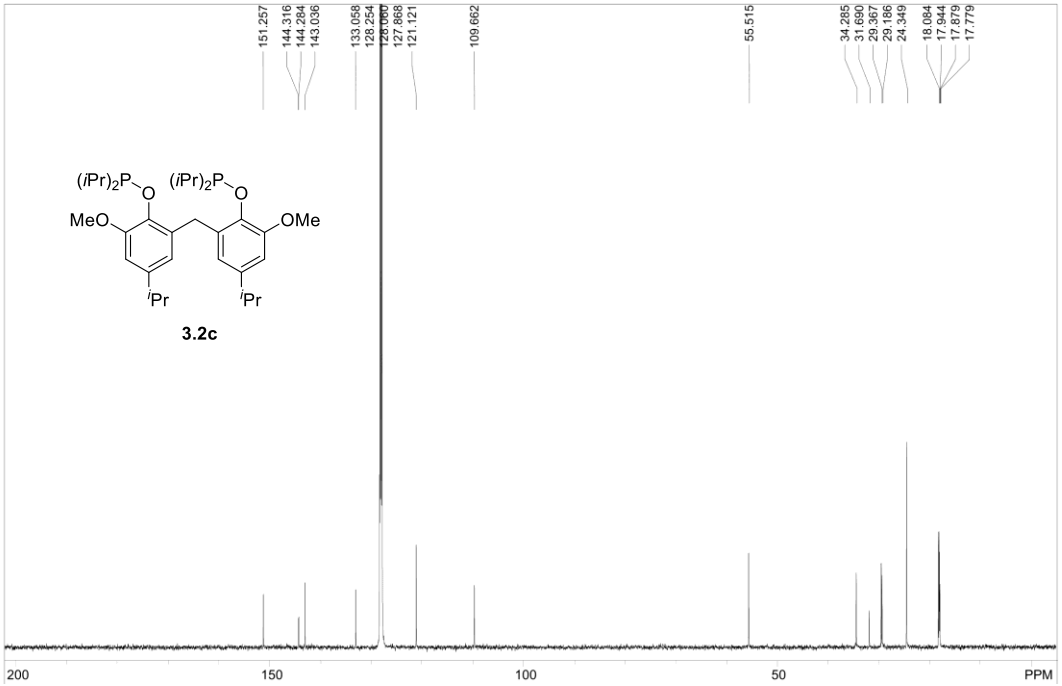

**Figure 3.64.** $^{31}$P-NMR Spectrum of **3.2c** in $C_6D_6$, 202 MHz

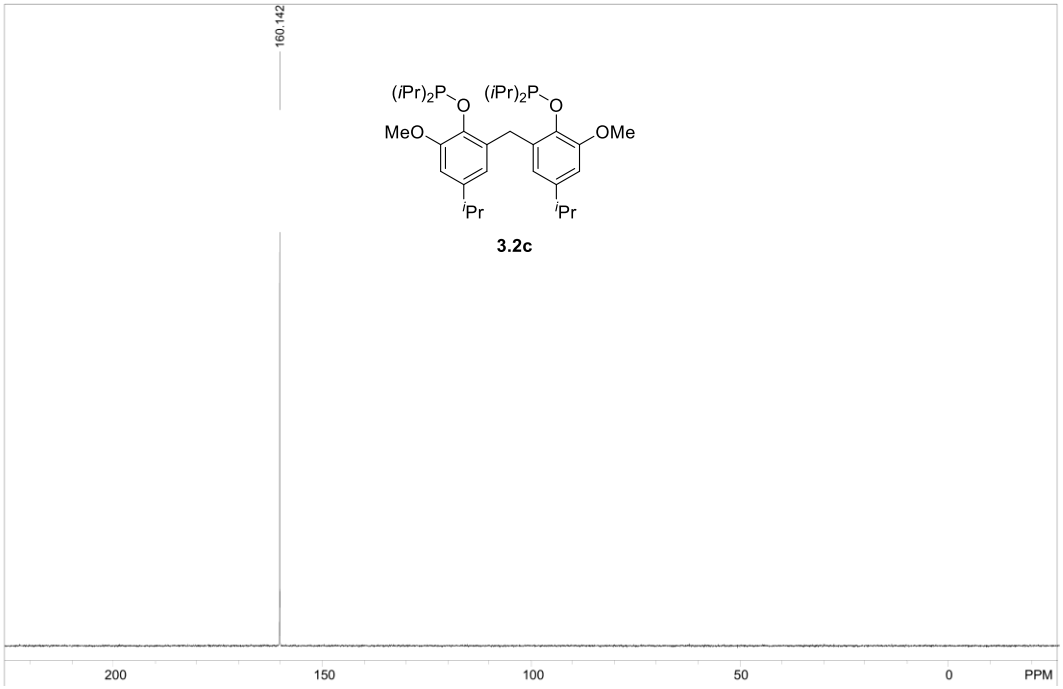

**Figure 3.65.** $^{1}$H-NMR Spectrum of **3.2d** in $C_6D_6$, 500 MHz

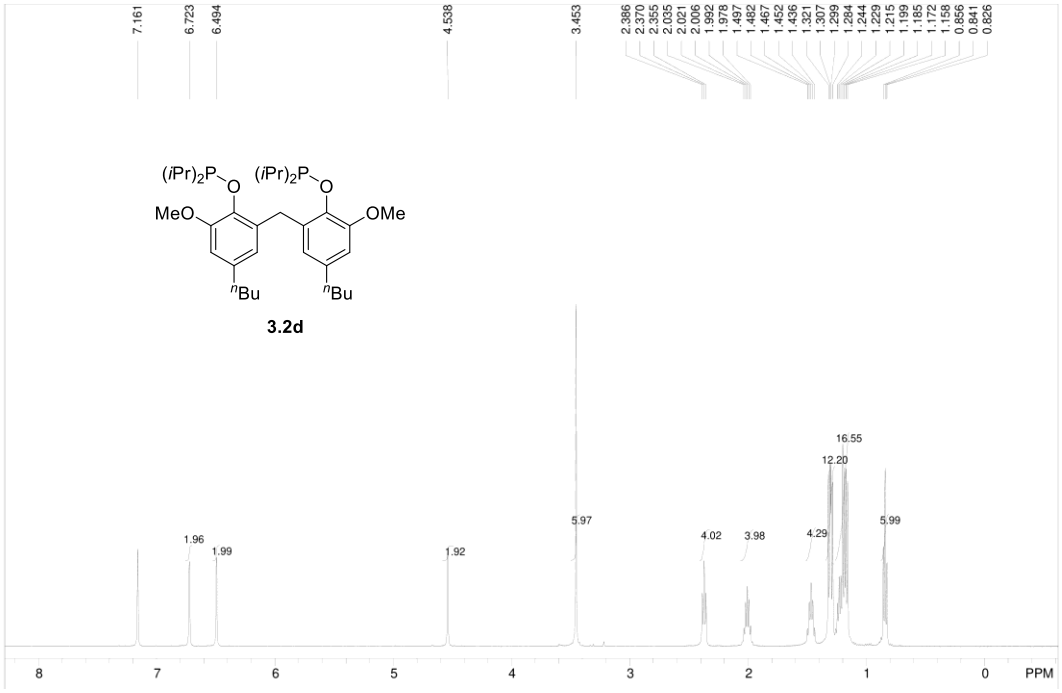


**Figure 3.66.** $^{13}$C-NMR Spectrum of **3.2d** in $C_6D_6$, 125 MHz

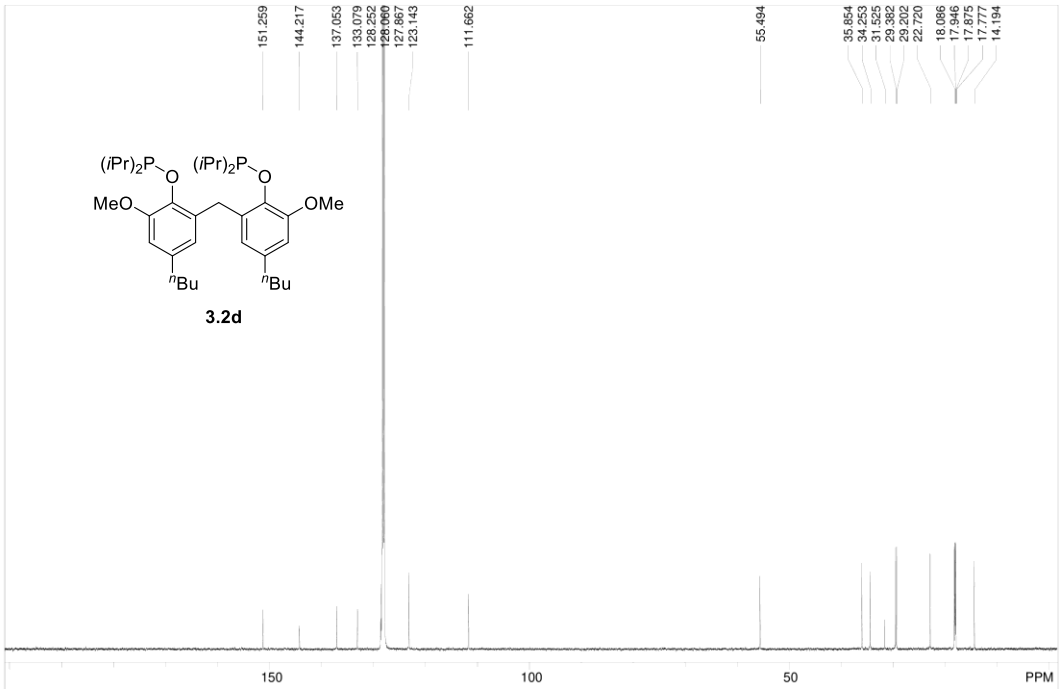

**Figure 3.67.** $^{31}$P-NMR Spectrum of **3.2d** in $C_6D_6$, 202 MHz

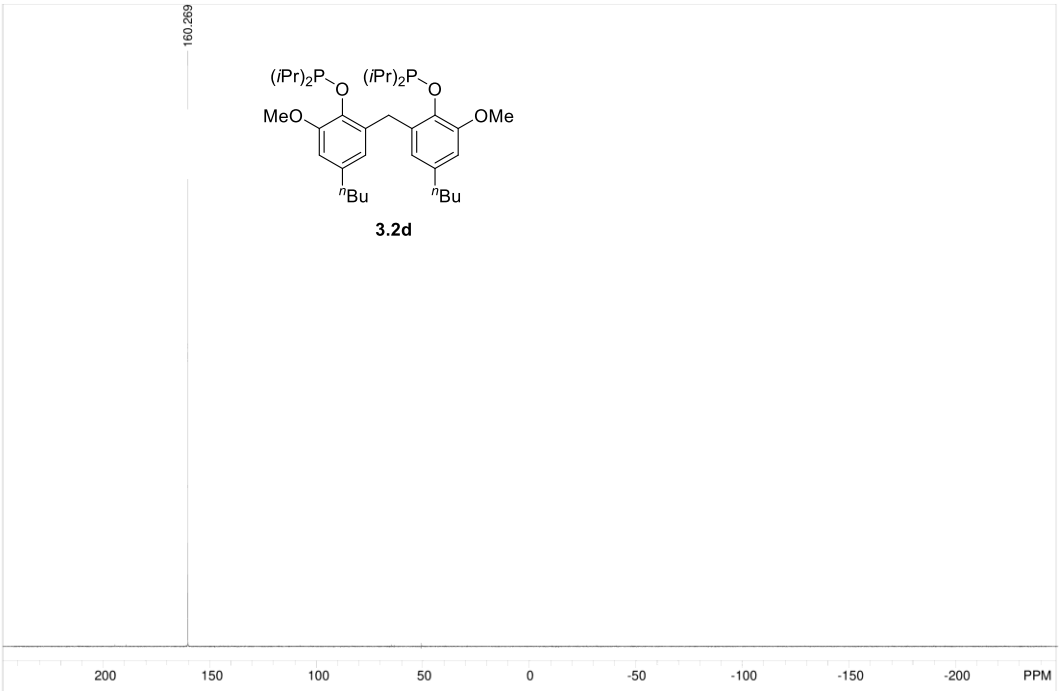

**Figure 3.68.** $^{1}$H-NMR Spectrum of **3.2e** in $CDCl_3$, 500 MHz

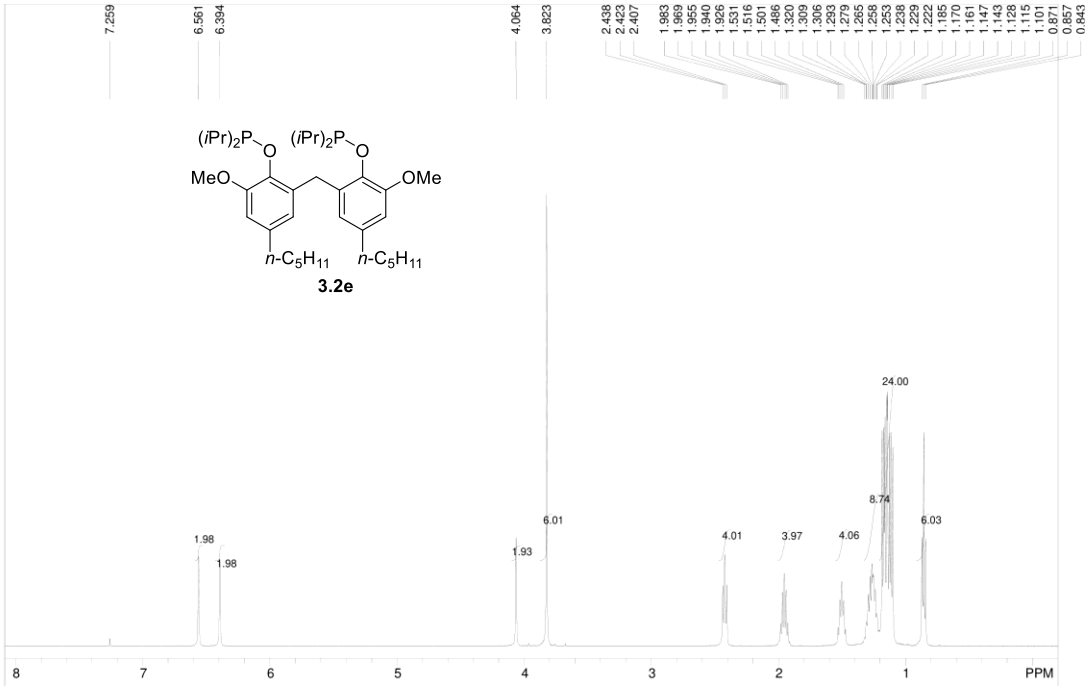


**Figure 3.69.** $^{13}$C-NMR Spectrum of **3.2e** in $CDCl_3$, 125 MHz

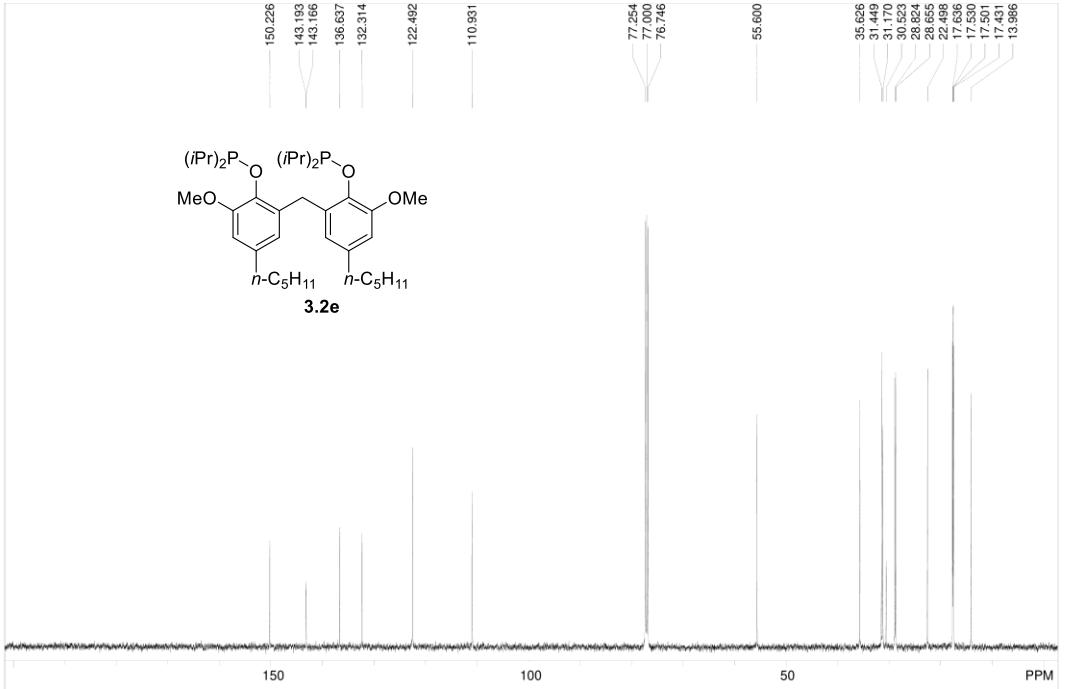

**Figure 3.70.** $^{31}$P-NMR Spectrum of **3.2e** in $CDCl_3$, 202 MHz

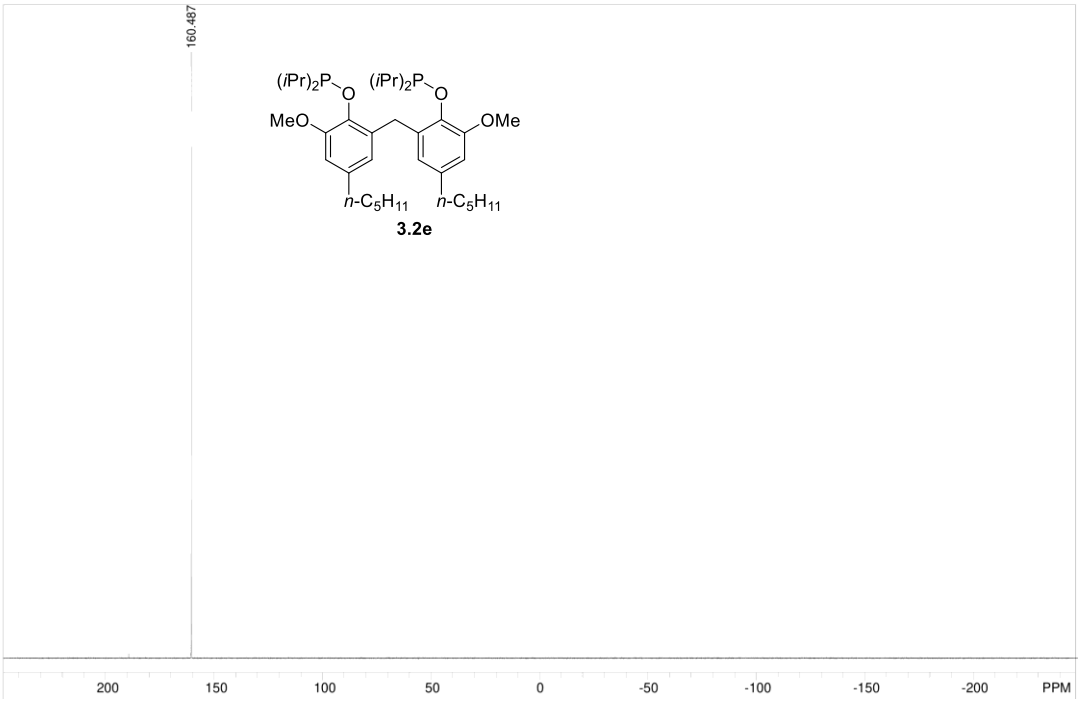

**Figure 3.71.** $^{1}$H-NMR Spectrum of **3.2f** in $C_6D_6$, 500 MHz

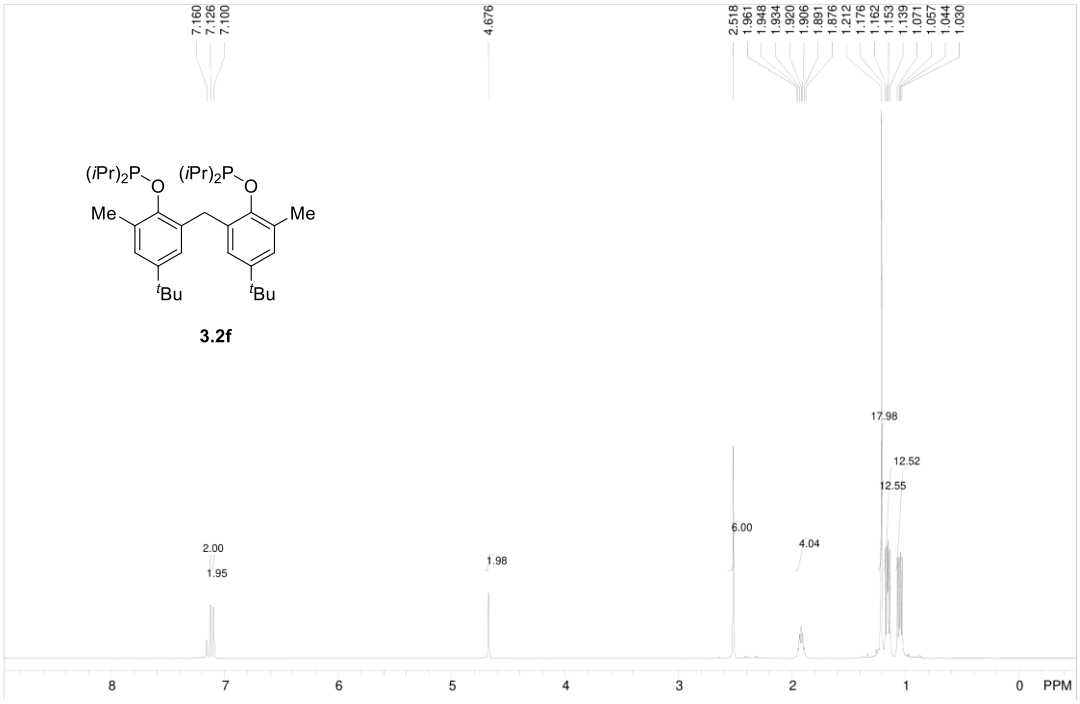


**Figure 3.72.** $^{13}$C-NMR Spectrum of **3.2f** in $C_6D_6$, 125 MHz

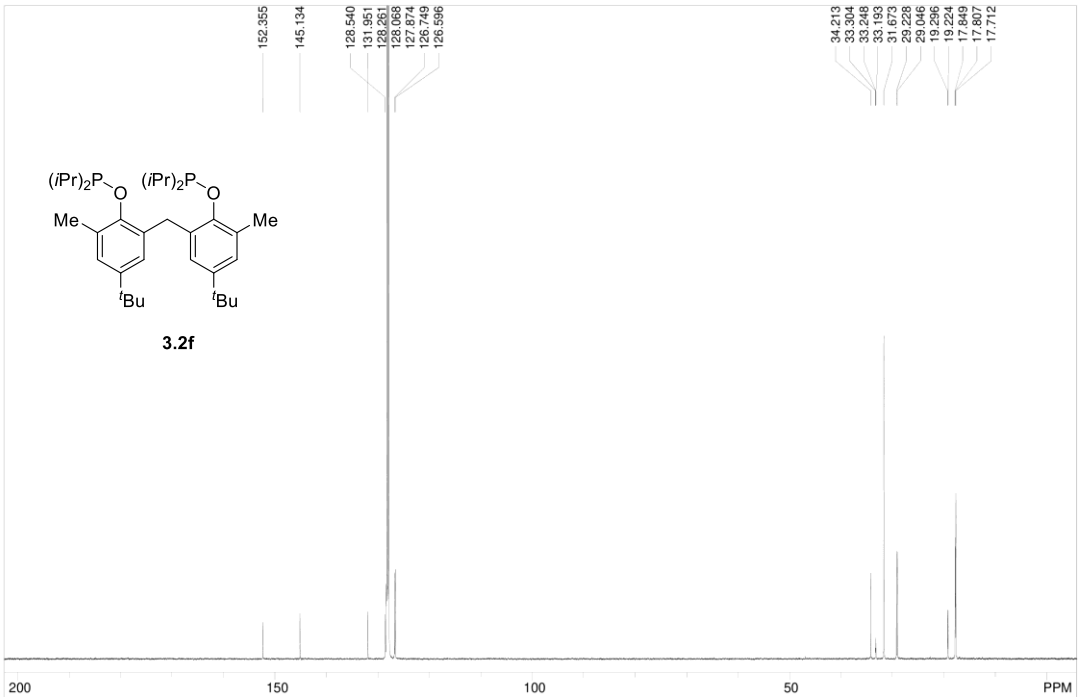

**Figure 3.73.** $^{31}$P-NMR Spectrum of **3.2f** in $C_6D_6$, 202 MHz

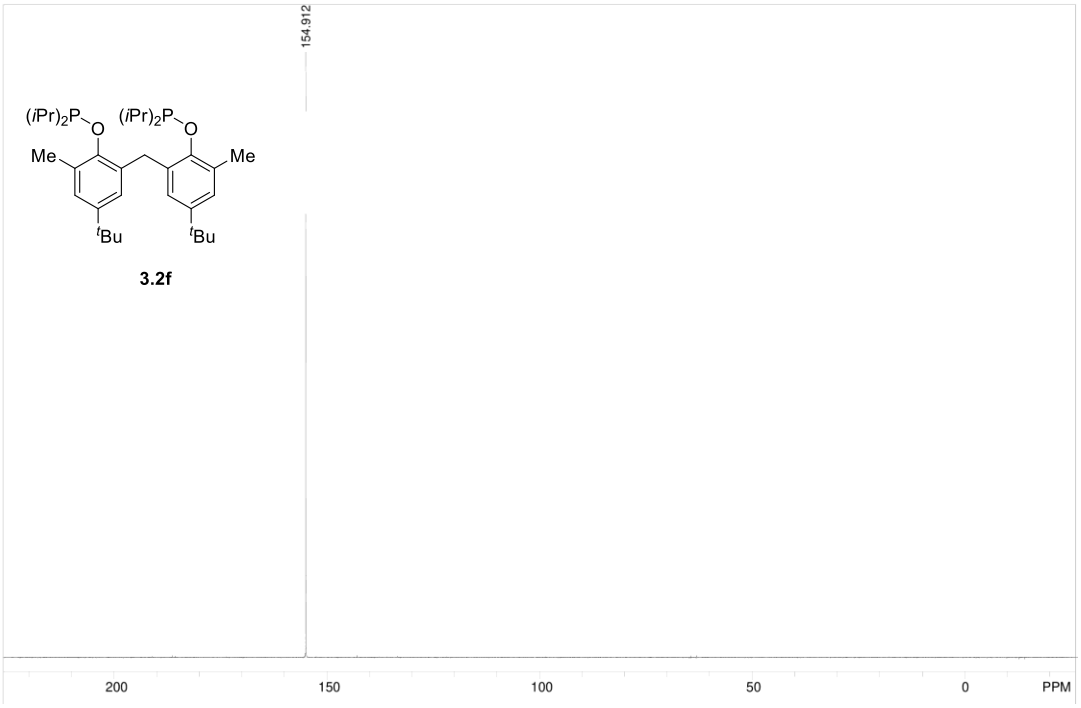

**Figure 3.74.** $^{1}$H-NMR Spectrum of **3.2g** in $CDCl_3$, 500 MHz

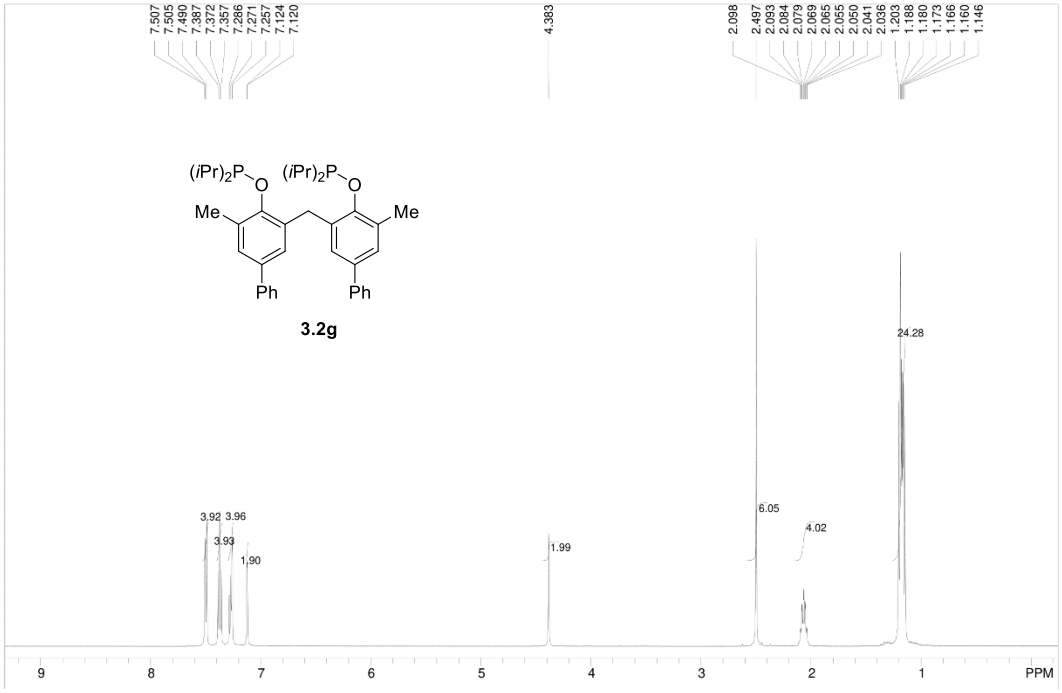


**Figure 3.75.** $^{13}$C-NMR Spectrum of **3.2g** in $CDCl_3$, 125 MHz

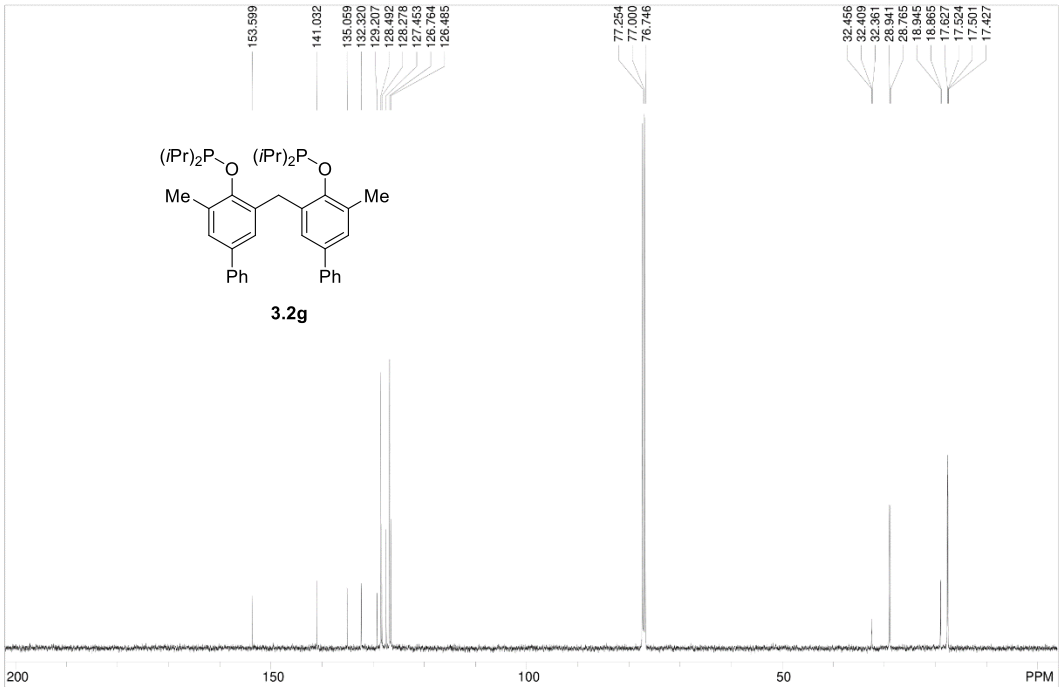

**Figure 3.76.** $^{31}$P-NMR Spectrum of **3.2g** in $CDCl_3$, 202 MHz

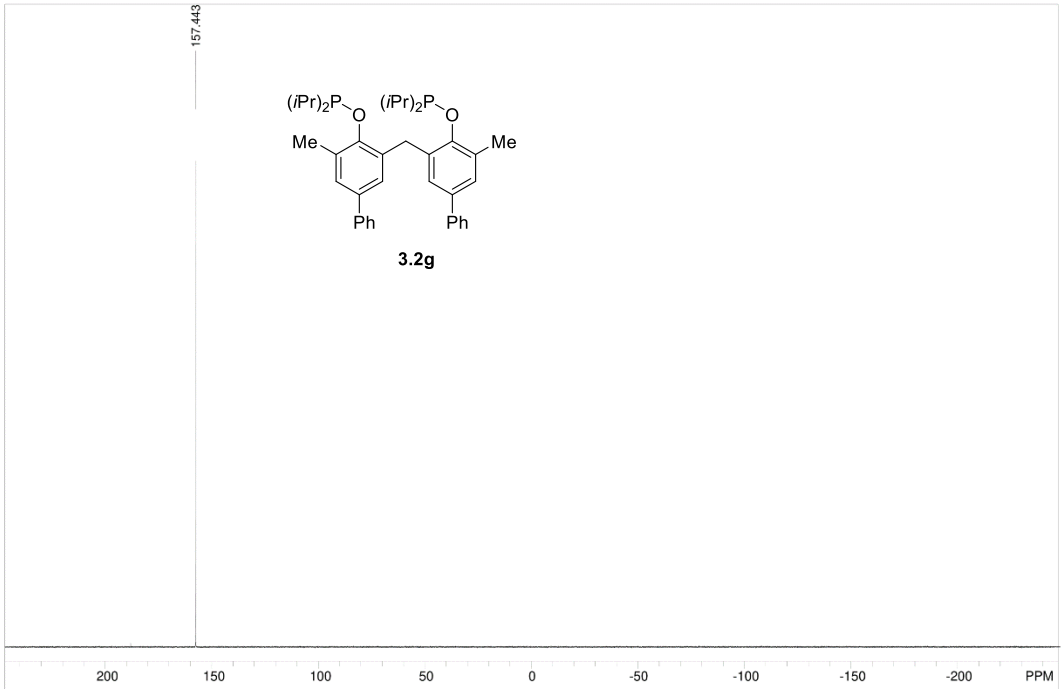

**Figure 3.77.** $^{1}$H-NMR Spectrum of **3.2h** in $CDCl_3$, 500 MHz

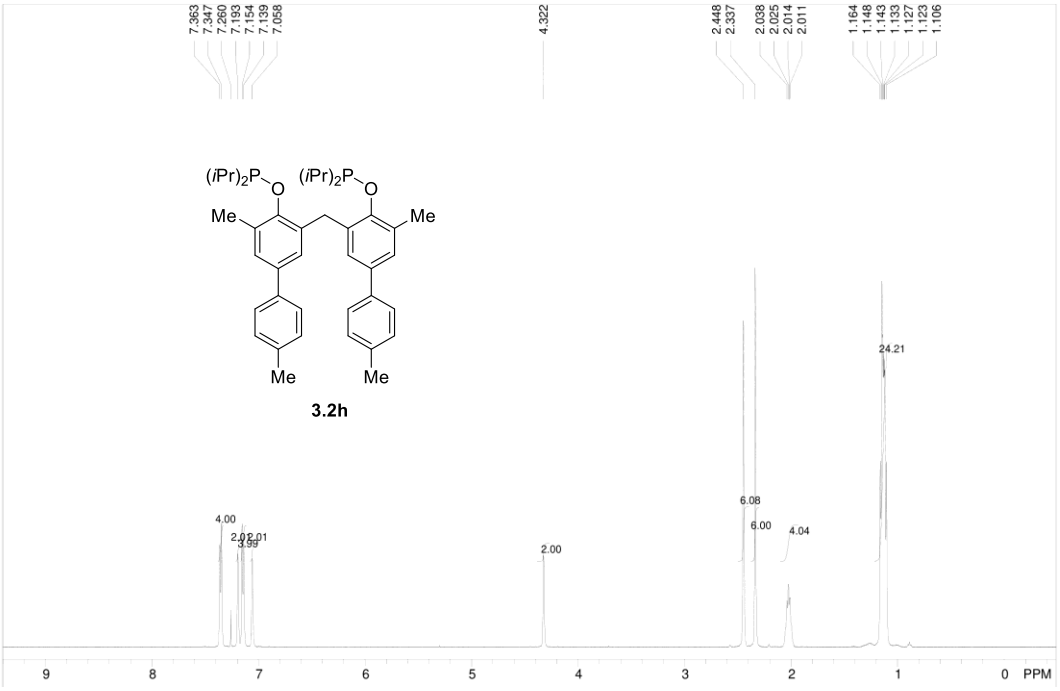


**Figure 3.78.** $^{13}$C-NMR Spectrum of **3.2h** in $CDCl_3$, 125 MHz

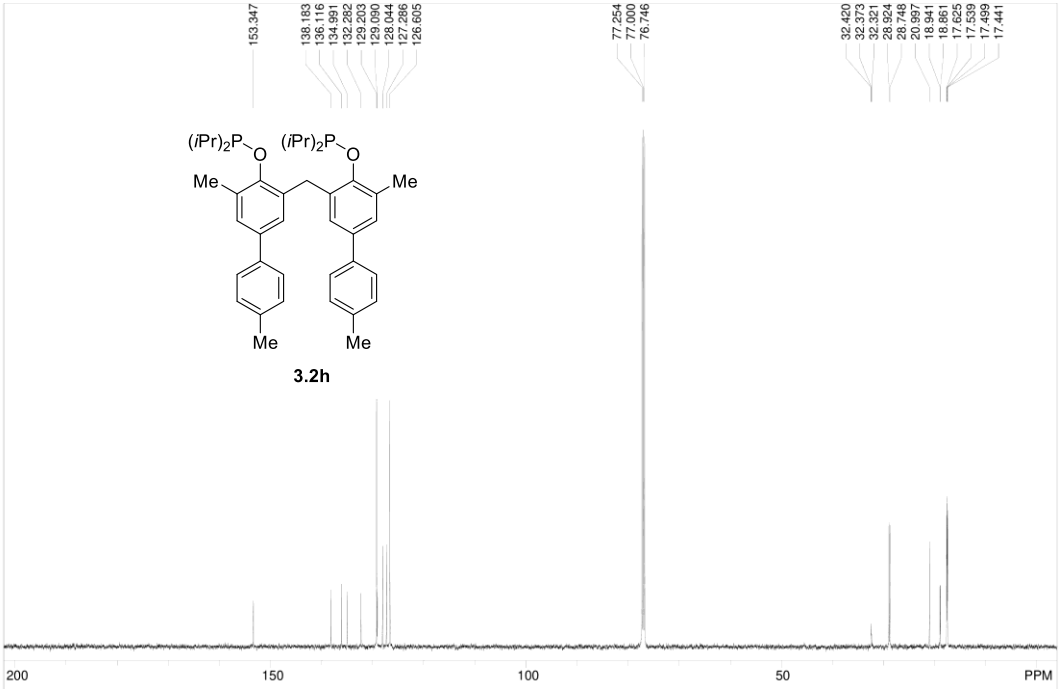

**Figure 3.79.** $^{31}$P-NMR Spectrum of **3.2h** in $CDCl_3$, 202 MHz

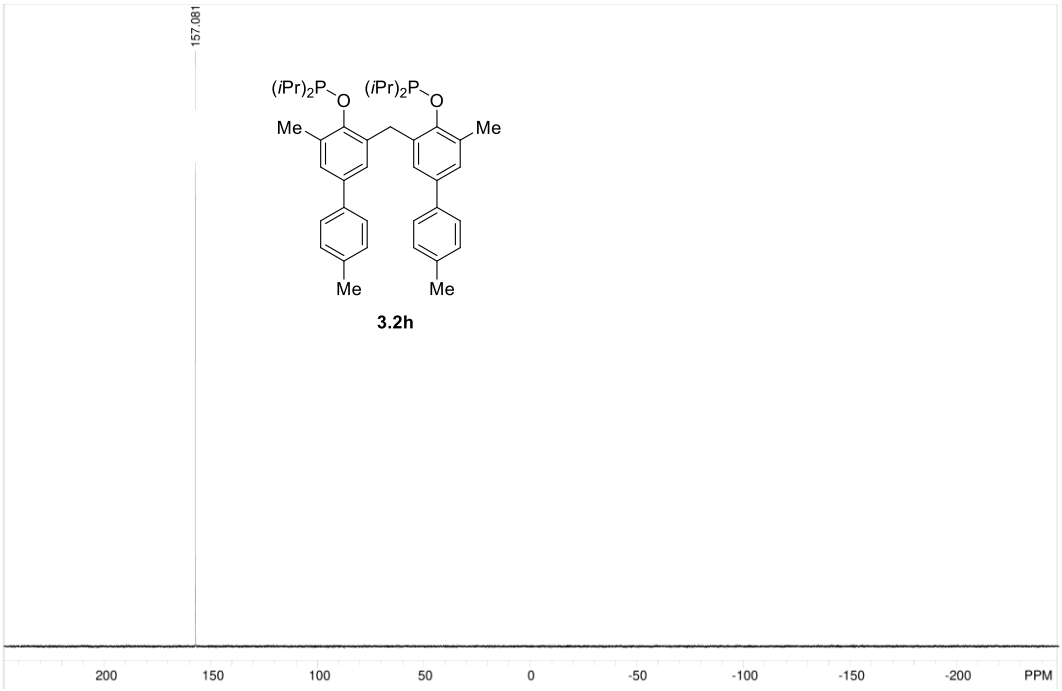

**Figure 3.80.** $^{1}$H-NMR Spectrum of **3.2i** in $C_6D_6$, 500 MHz

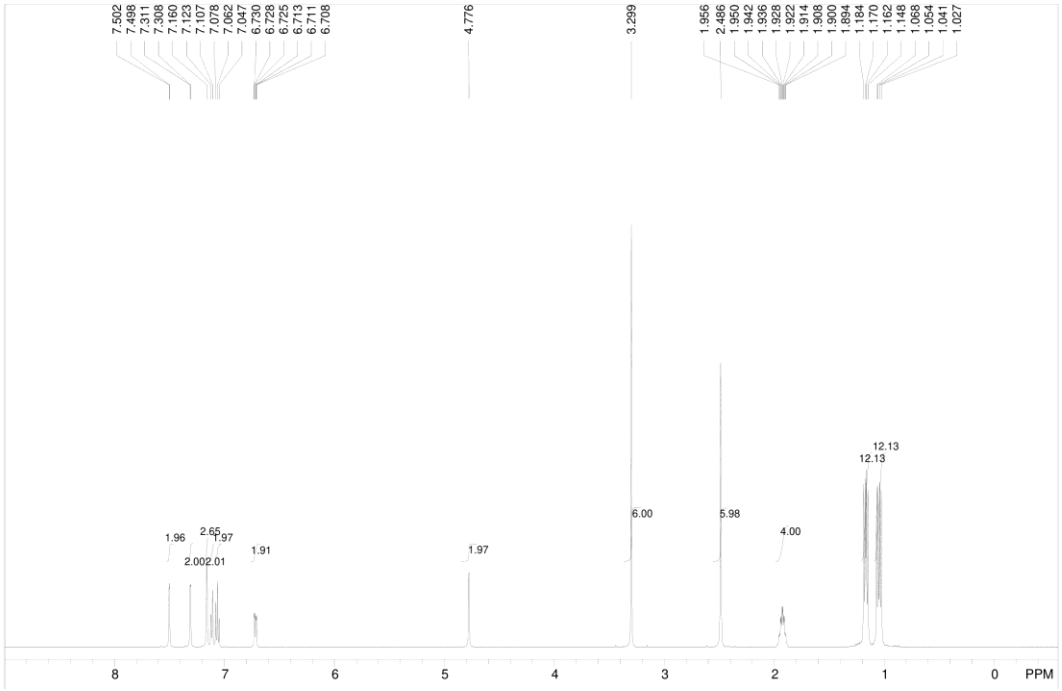


**Figure 3.81.** $^{13}$C-NMR Spectrum of **3.2i** in $C_6D_6$, 125 MHz

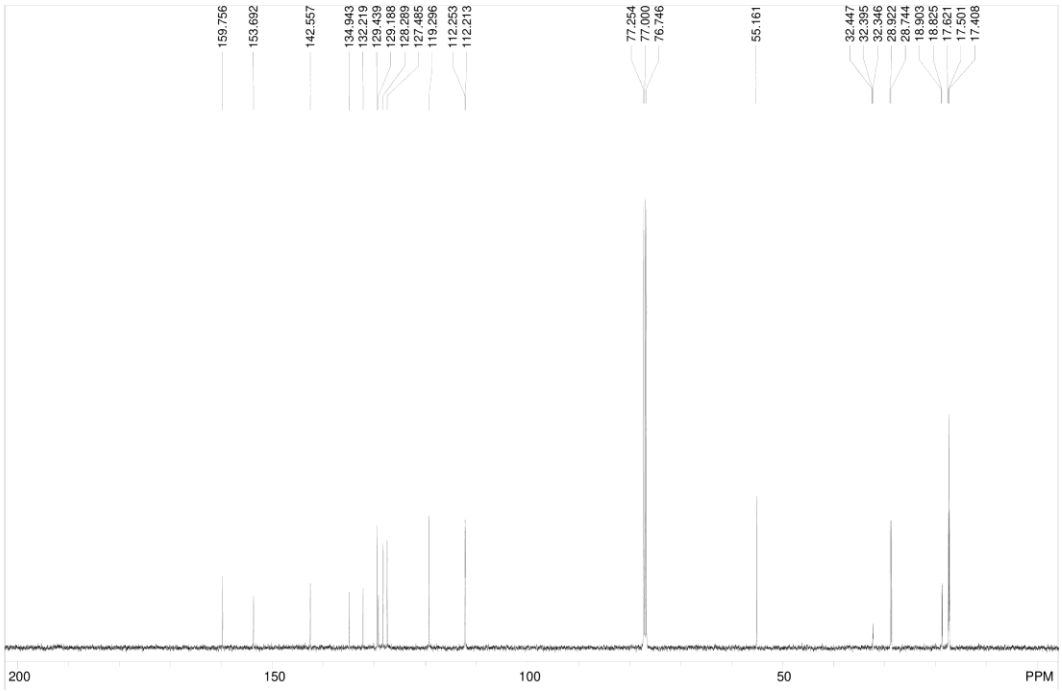

**Figure 3.82.** $^{31}$P-NMR Spectrum of **3.2i** in $C_6D_6$, 202 MHz

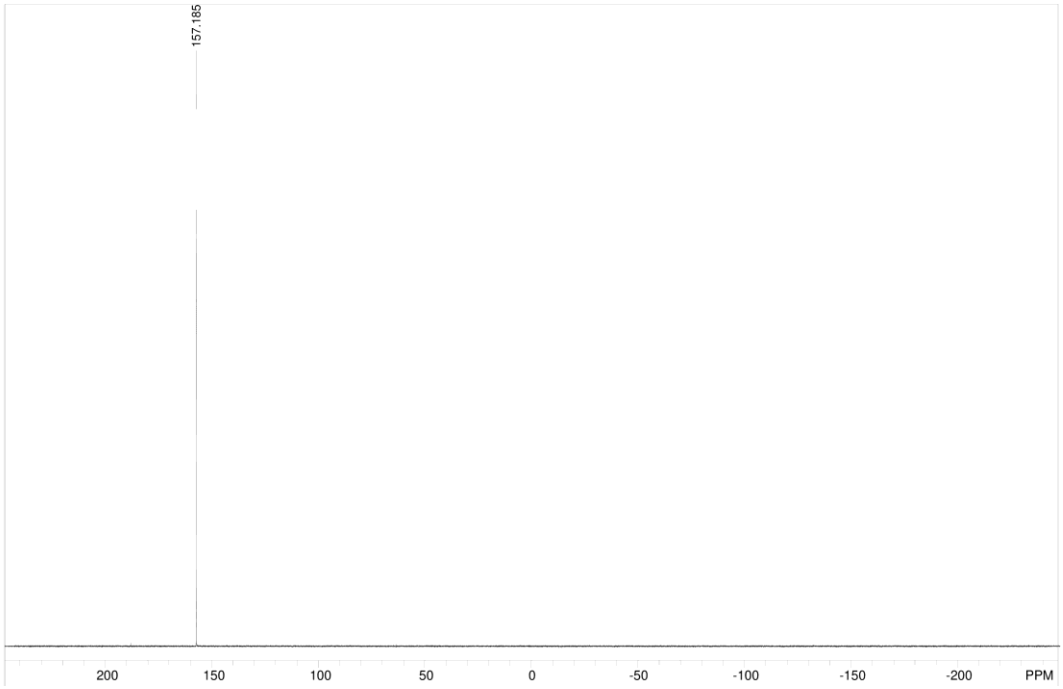

**Figure 3.83.** $^{1}$H-NMR Spectrum of **3.2j** in $CDCl_3$, 400 MHz

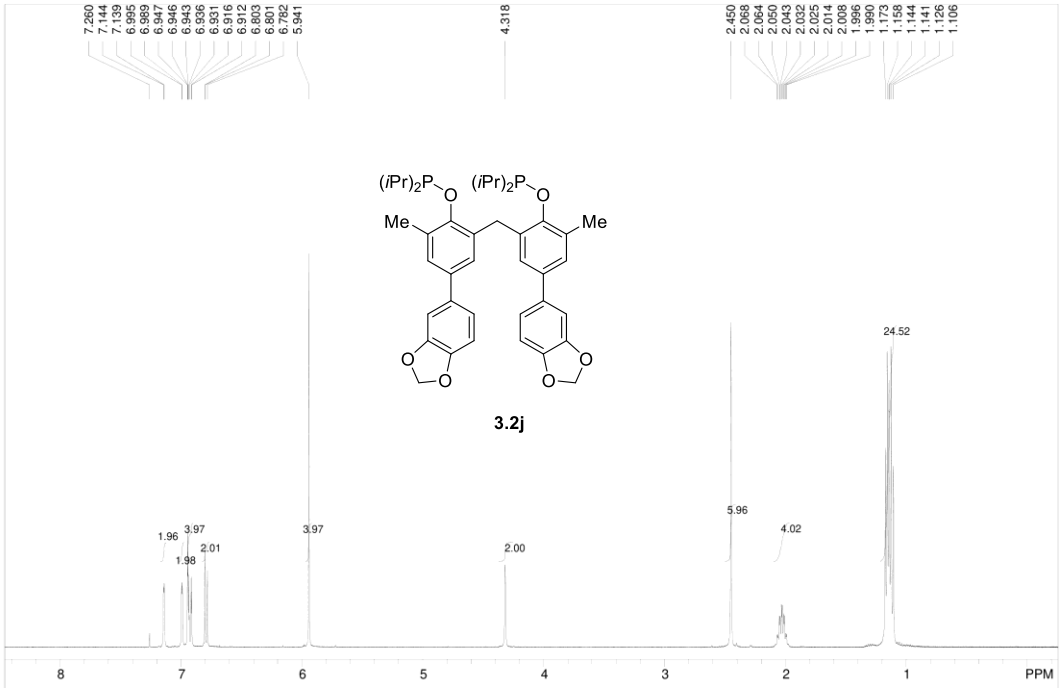


**Figure 3.84.** $^{13}$C-NMR Spectrum of **3.2j** in $CDCl_3$, 100 MHz

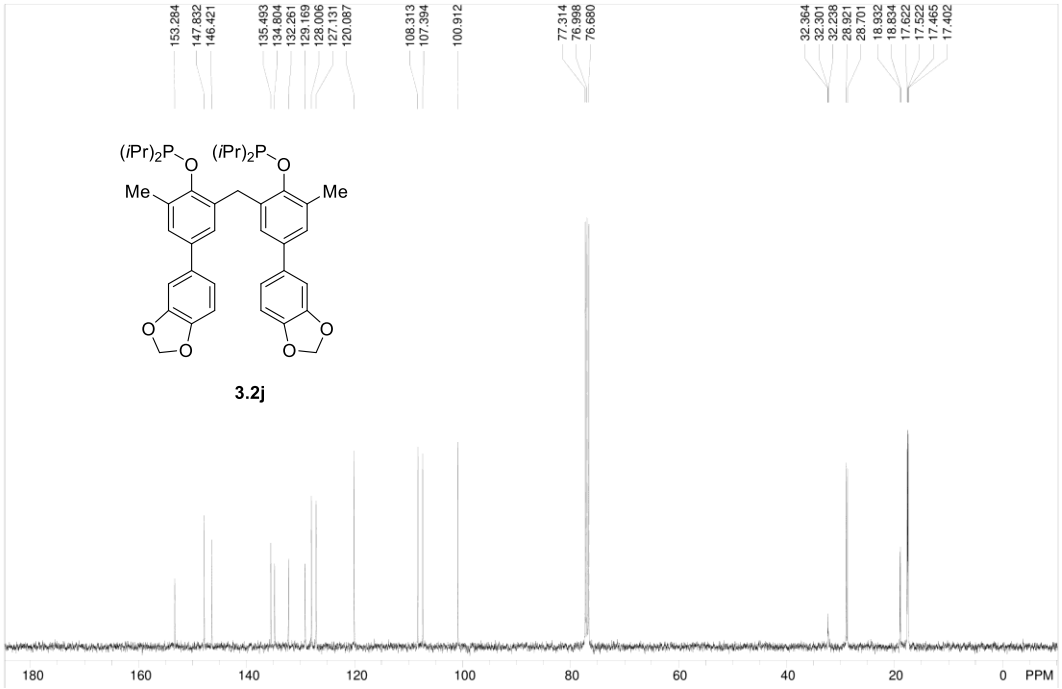

**Figure 3.85.** $^{31}$P-NMR Spectrum of **3.2j** in $CDCl_3$, 202 MHz

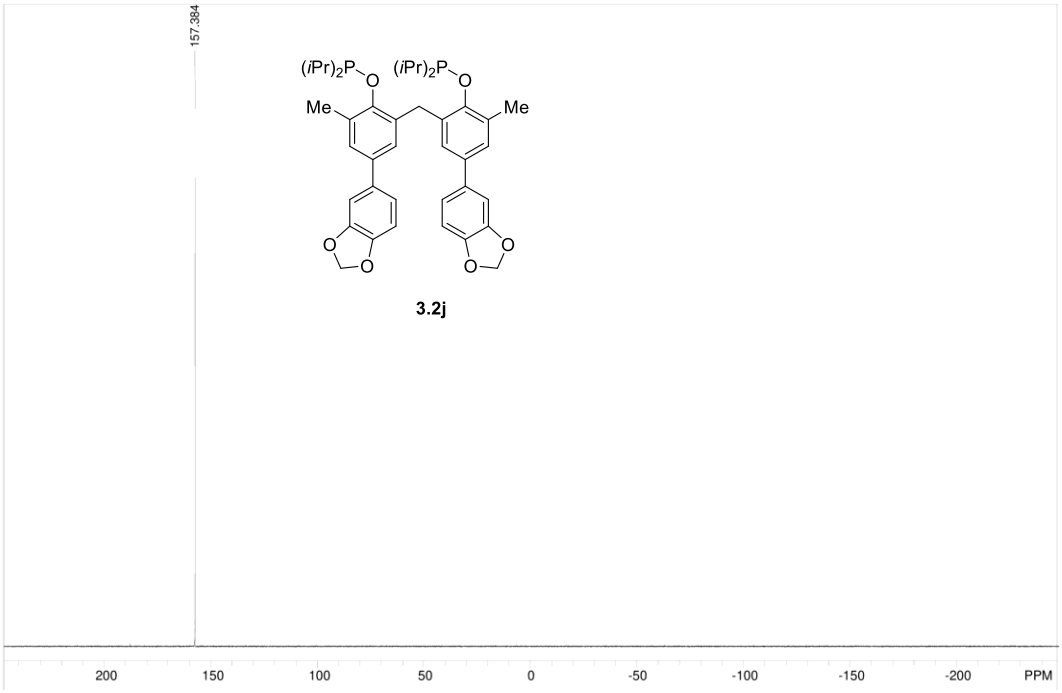

**Figure 3.86.** $^{1}$H-NMR Spectrum of **3.2k** in $CDCl_3$, 500 MHz

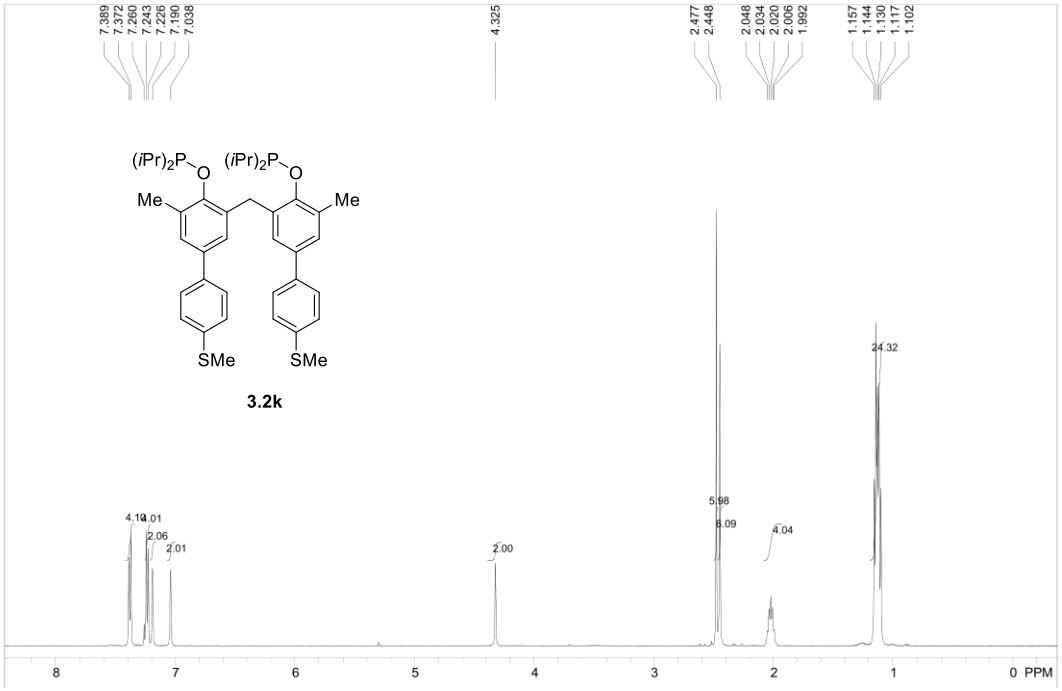


**Figure 3.87.** $^{13}$C-NMR Spectrum of **3.2k** in $CDCl_3$, 126 MHz

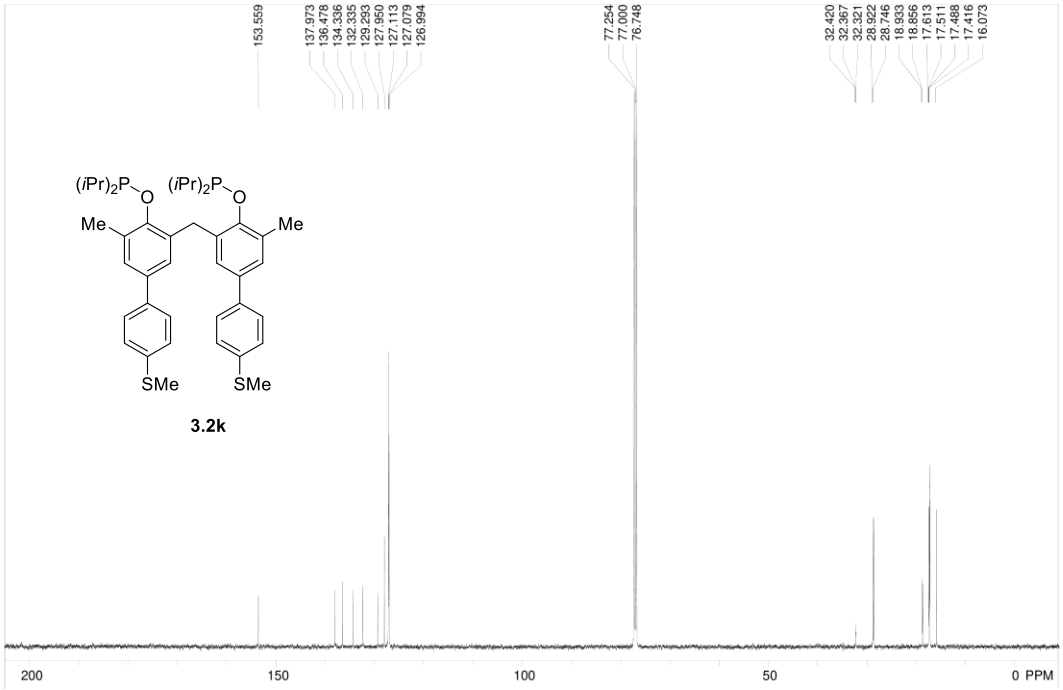

**Figure 3.88.** $^{31}$P-NMR Spectrum of **3.2k** in $CDCl_3$, 202 MHz

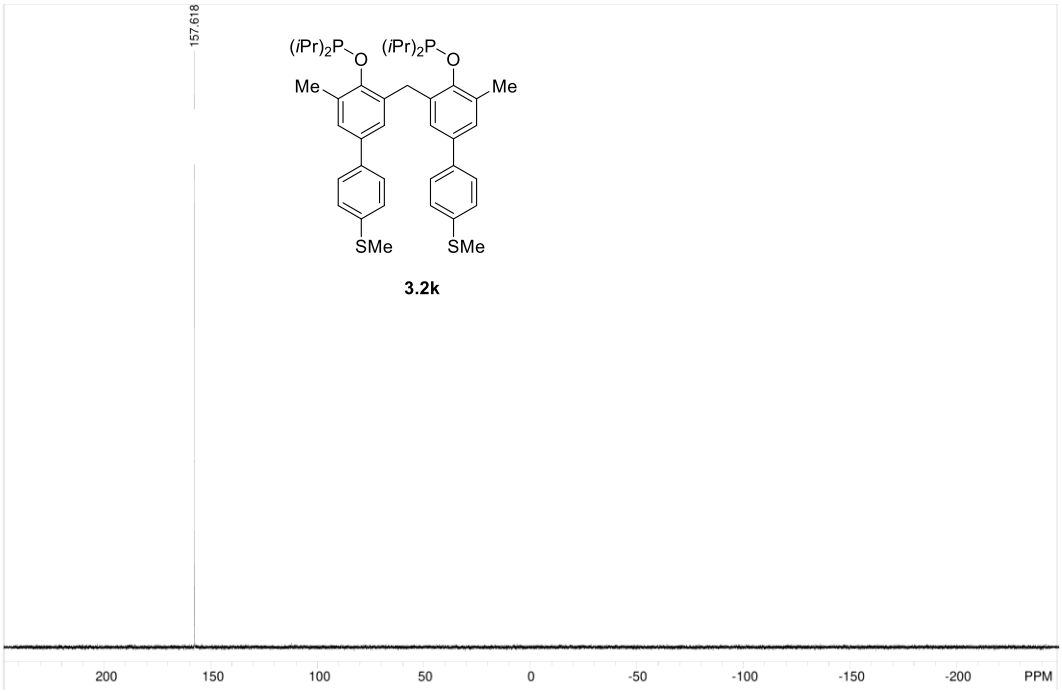

**Figure 3.89.** $^{1}$H-NMR Spectrum of **3.2l** in $CDCl_3$, 500 MHz

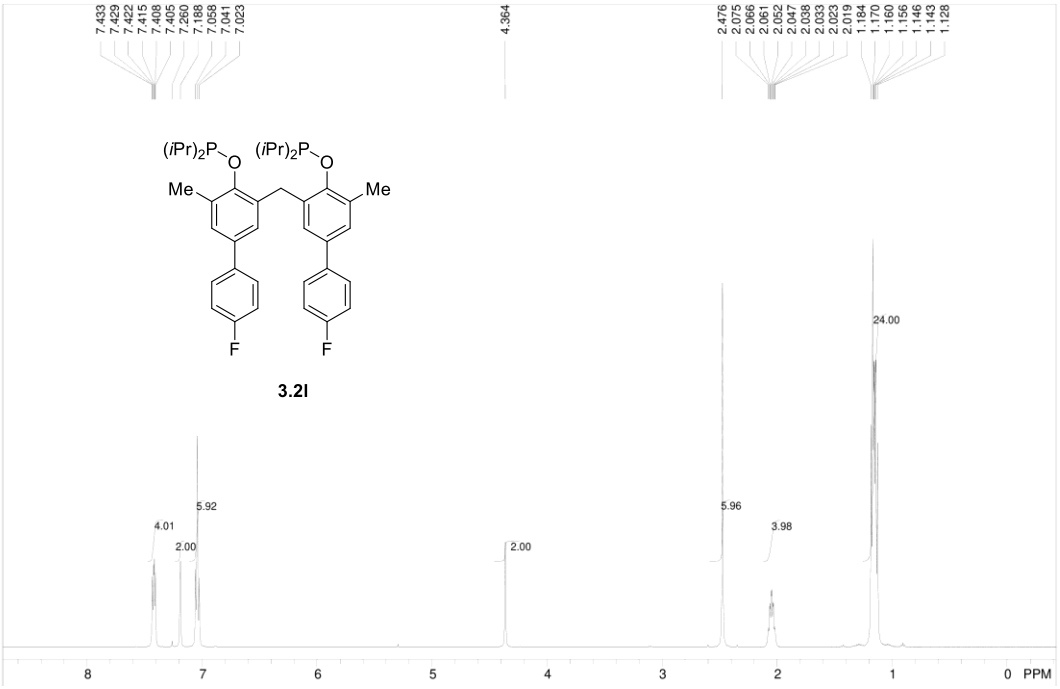


**Figure 3.90.** $^{13}$C-NMR Spectrum of **3.2l** in $CDCl_3$, 126 MHz

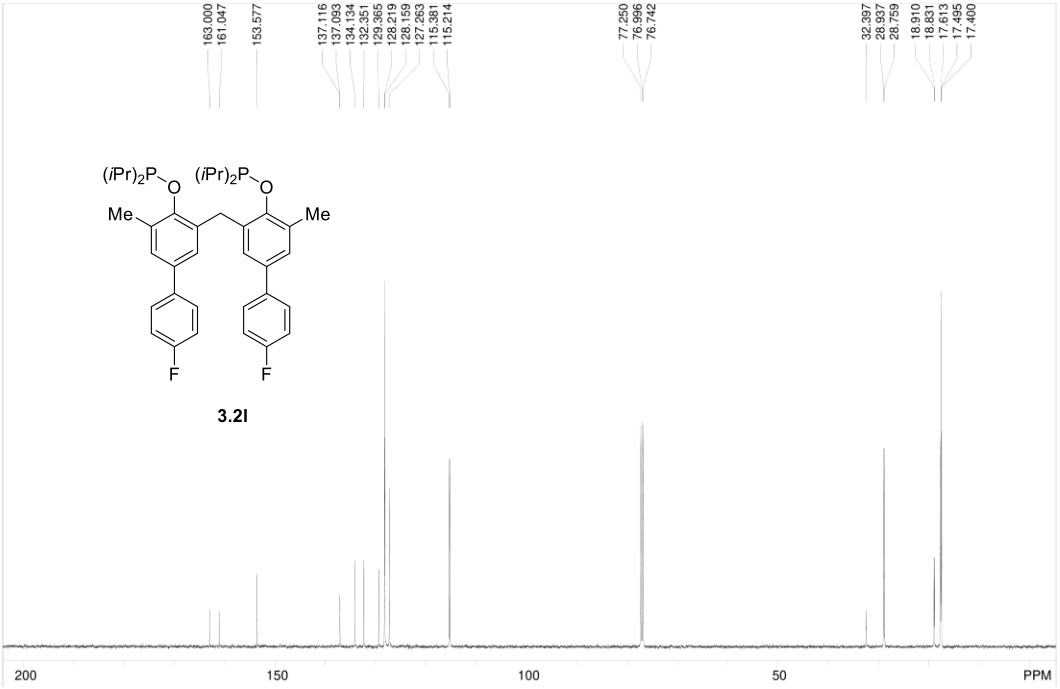

**Figure 3.91.** $^{19}$F-NMR Spectrum of **3.2l** in $CDCl_3$, 470 MHz

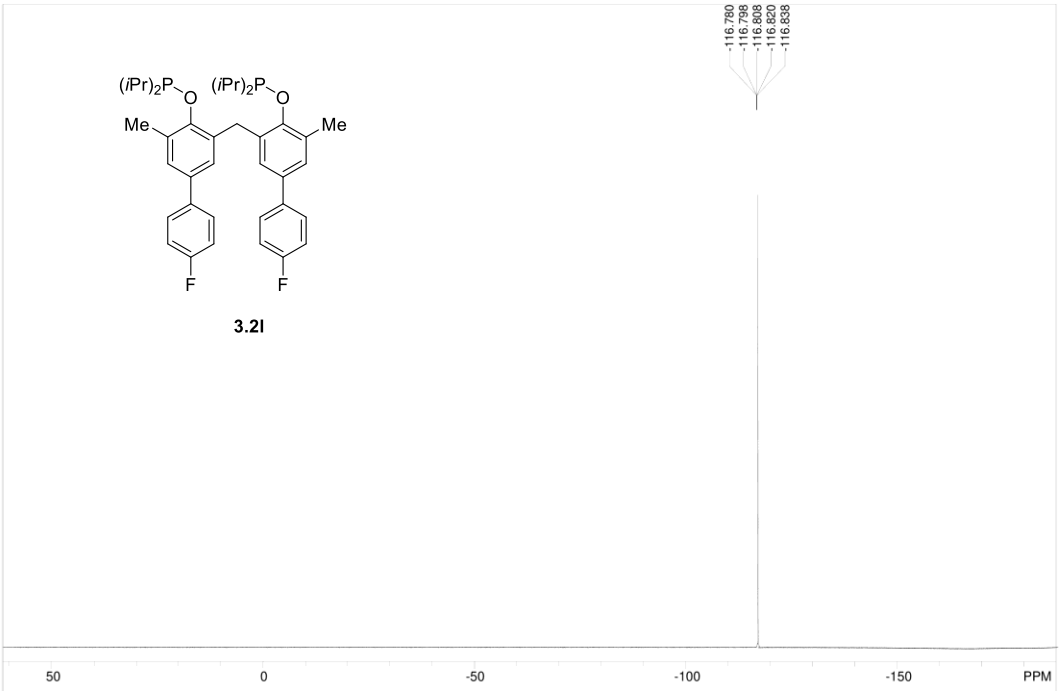


**Figure 3.92.** $^{31}$P-NMR Spectrum of **3.2l** in $CDCl_3$, 202 MHz

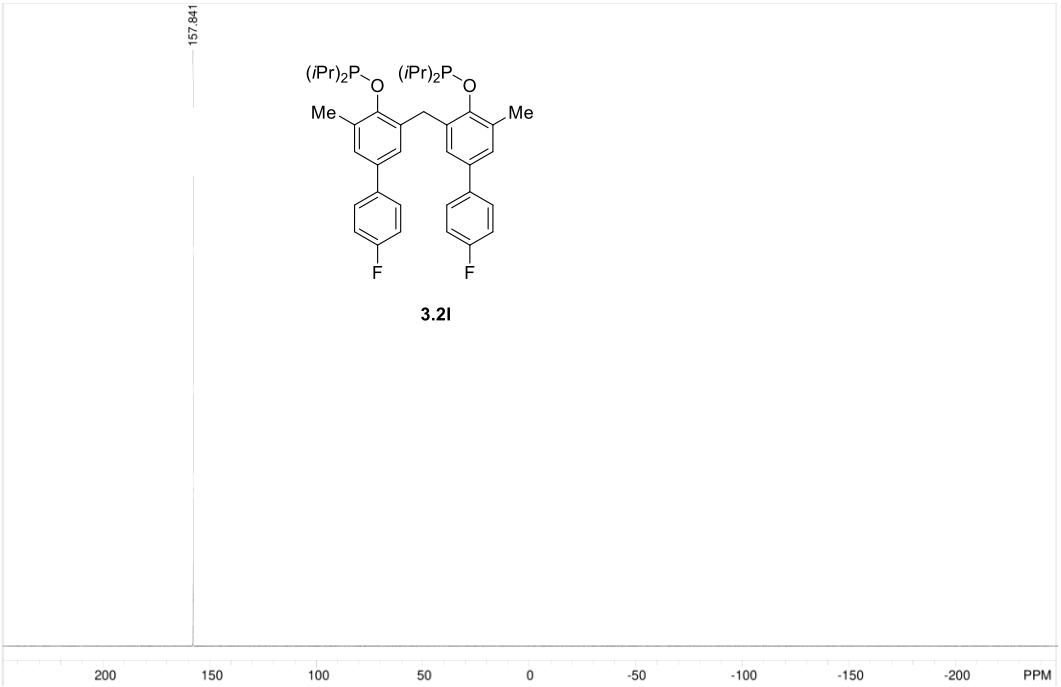

**Figure 3.93.** $^{1}$H-NMR Spectrum of **3.2m** in $CDCl_3$, 400 MHz

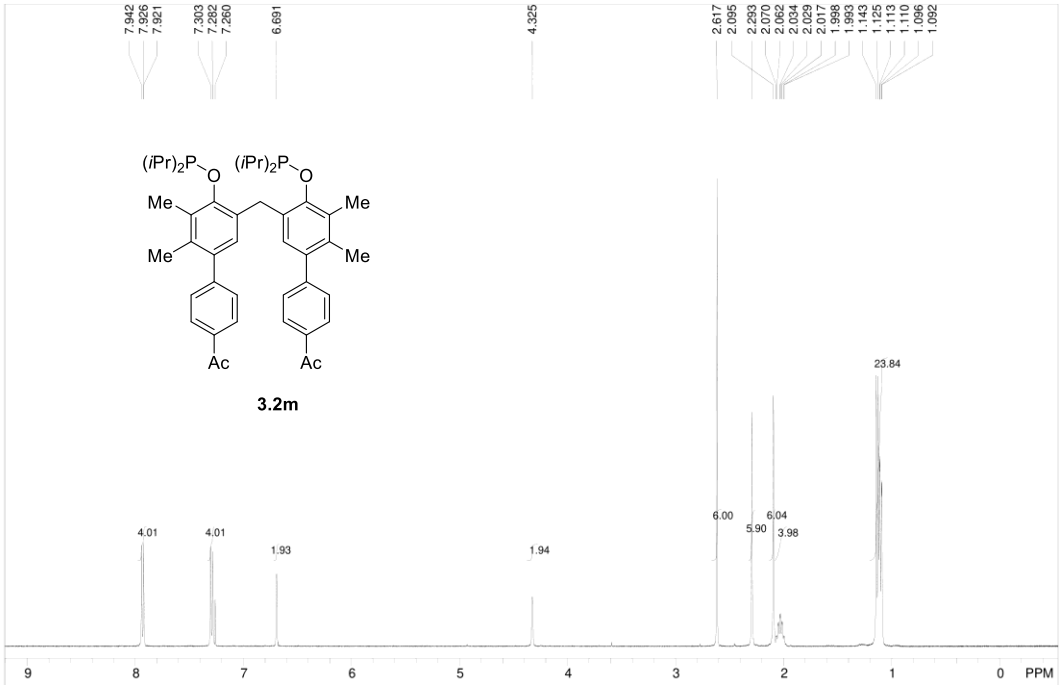


**Figure 3.94.** $^{13}$C-NMR Spectrum of **3.2m** in $CDCl_3$, 101 MHz

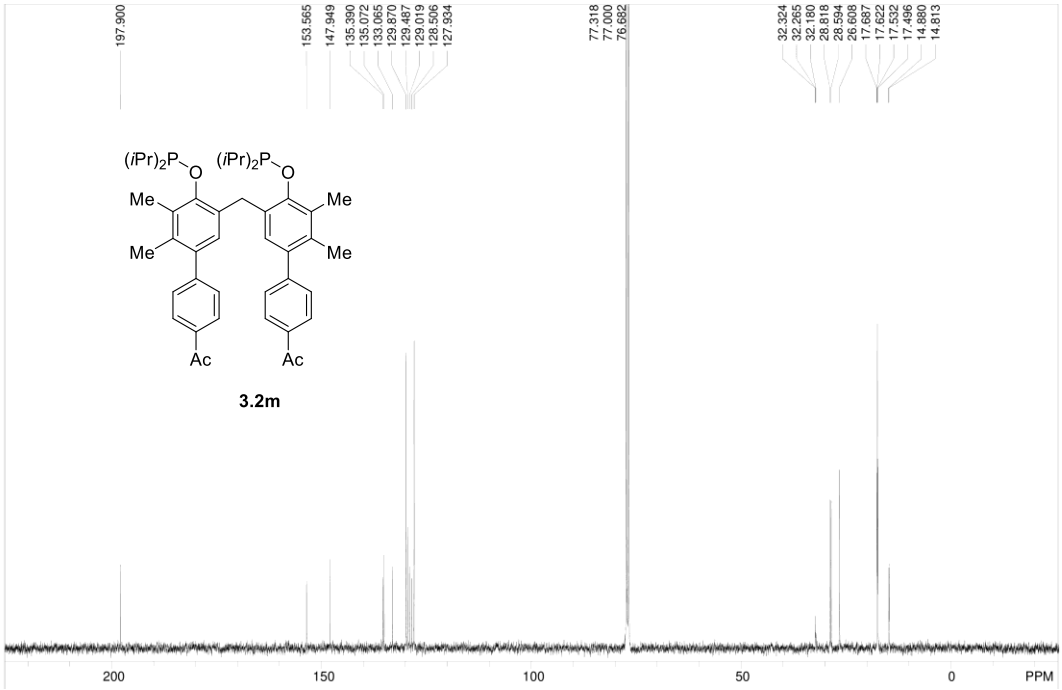

**Figure 3.95.** $^{31}$P-NMR Spectrum of **3.2m** in $CDCl_3$, 202 MHz

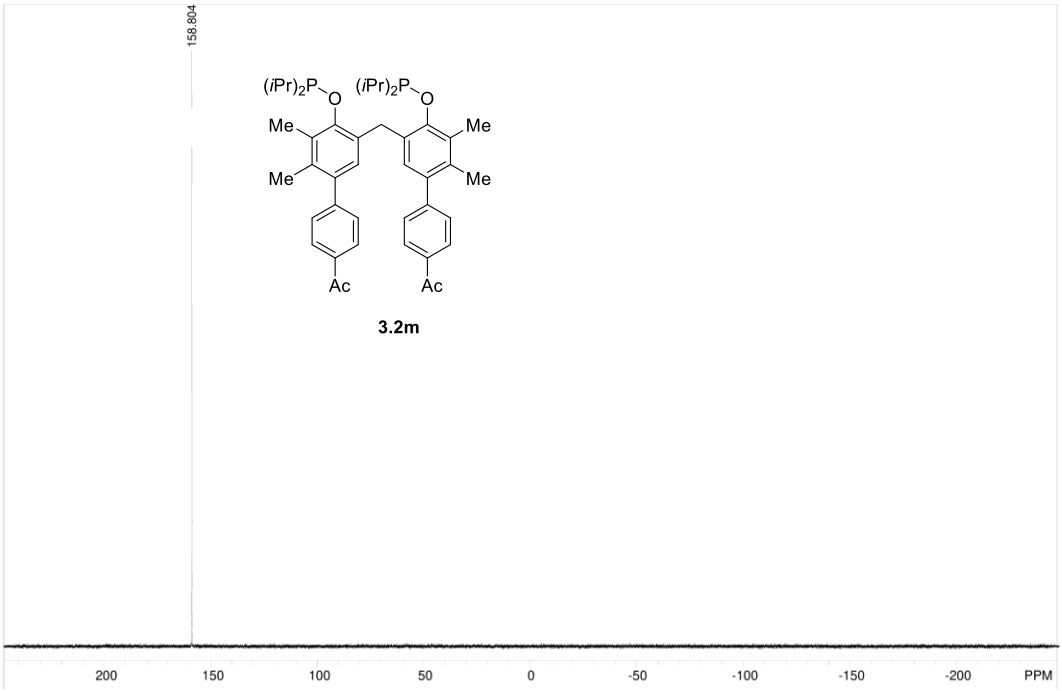

**Figure 3.96.** $^{1}$H-NMR Spectrum of **3.2n** in $CDCl_3$, 500 MHz

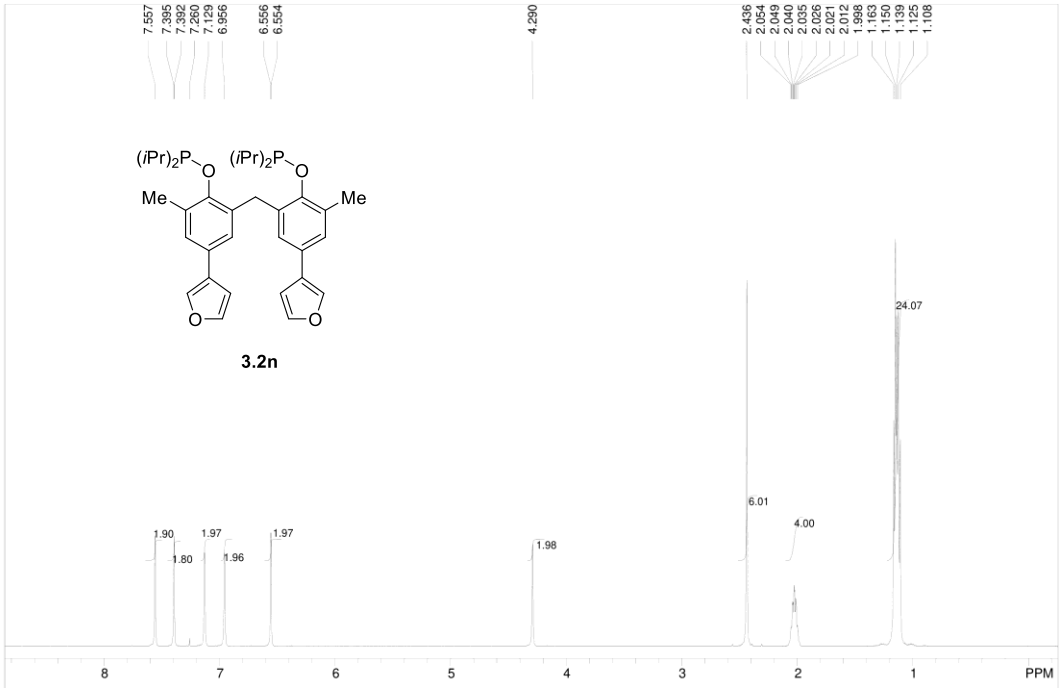


**Figure 3.97.** $^{13}$C-NMR Spectrum of **3.2n** in $CDCl_3$, 126 MHz

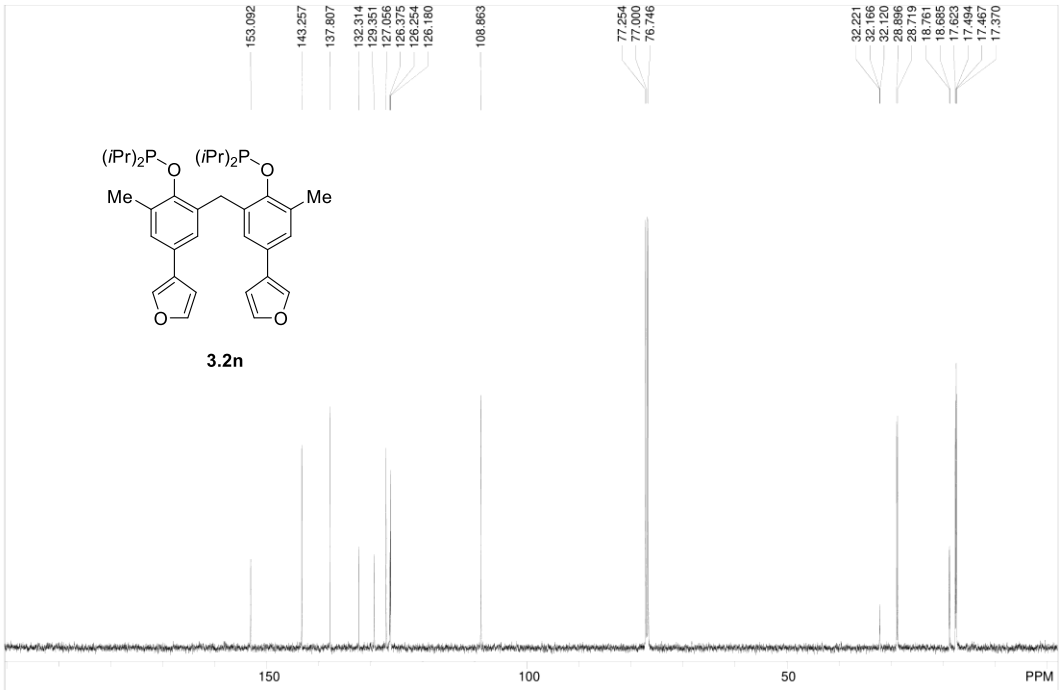

**Figure 3.98.** $^{31}$P-NMR Spectrum of **3.2n** in $CDCl_3$, 202 MHz

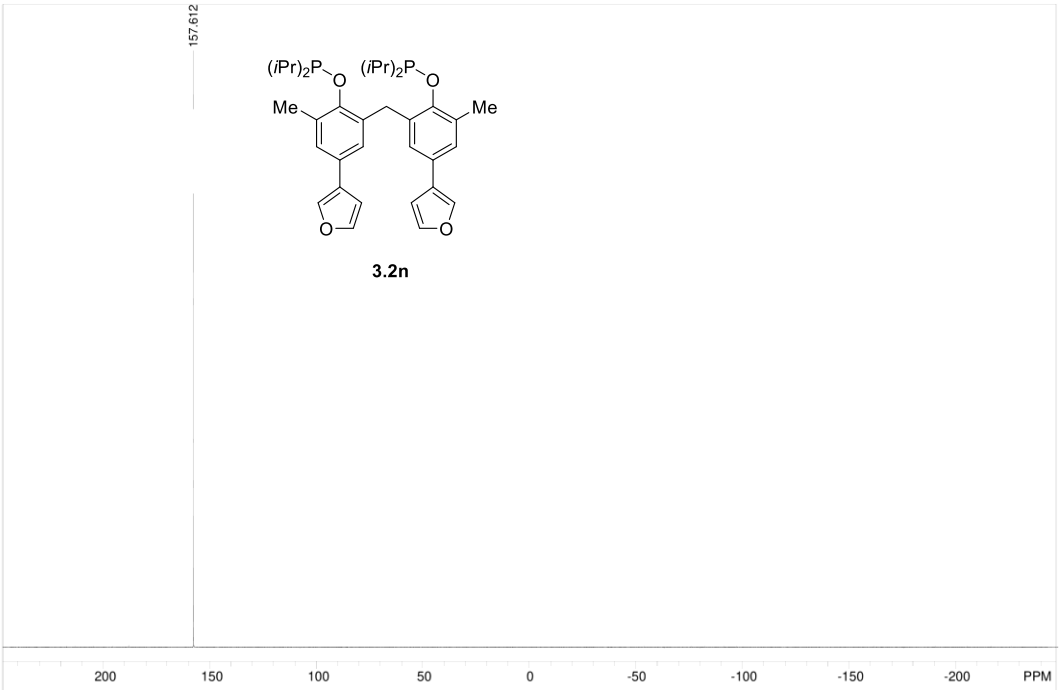

**Figure 3.99.** $^{1}$H-NMR Spectrum of **3.2o** in $CDCl_3$, 500 MHz

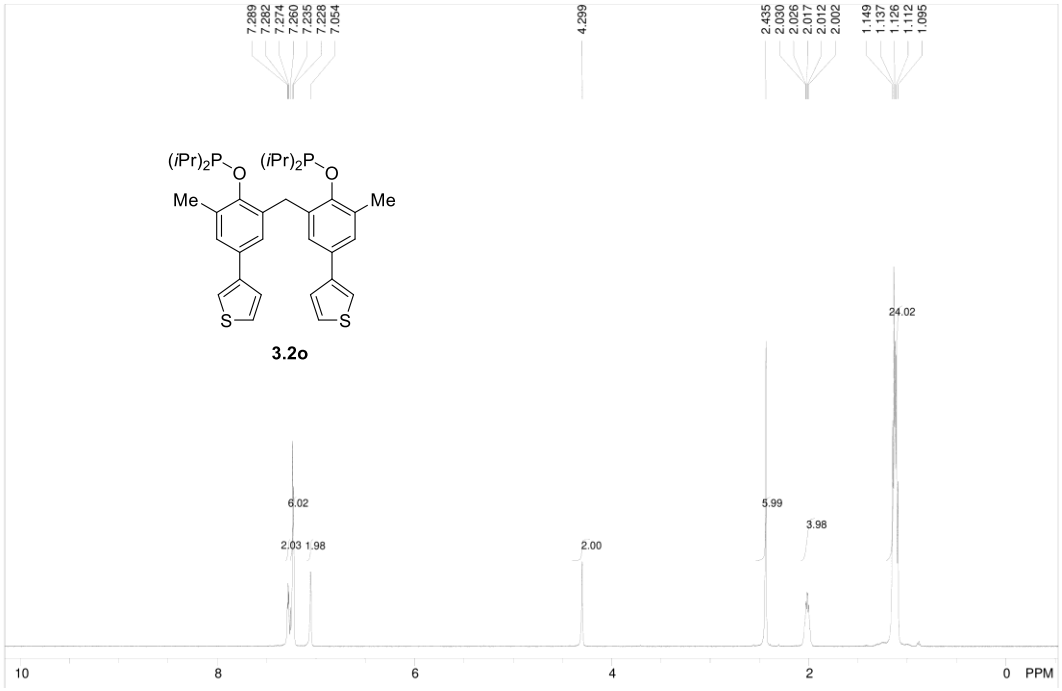


**Figure 3.100.** $^{13}$C-NMR Spectrum of **3.2o** in $CDCl_3$, 126 MHz

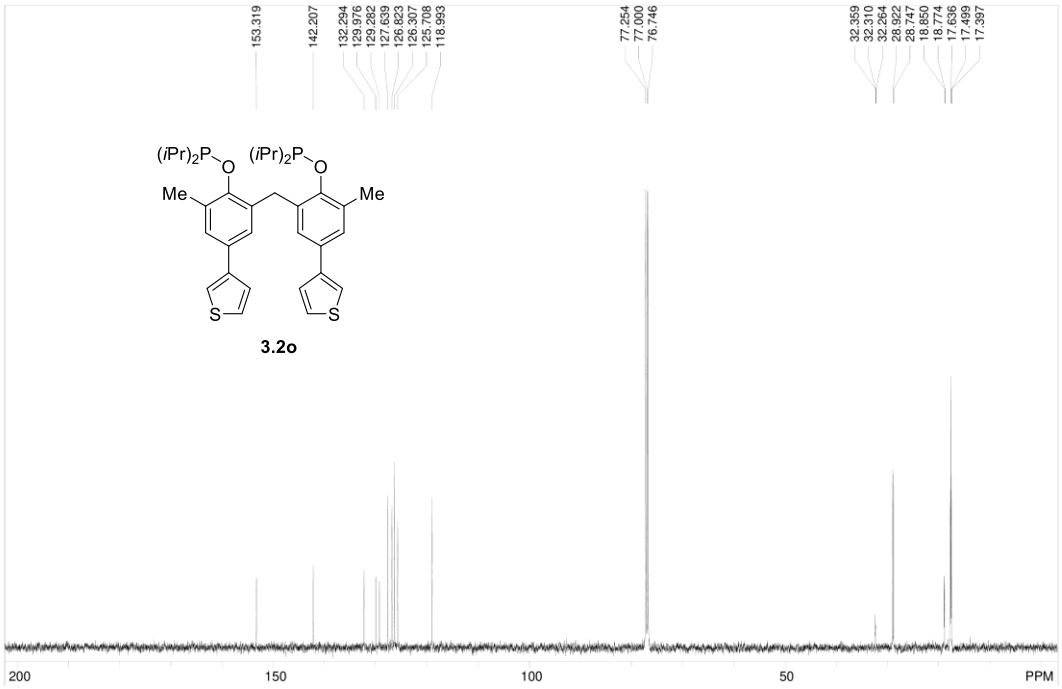

**Figure 3.101.** $^{31}$P-NMR Spectrum of **3.2o** in $CDCl_3$, 202 MHz

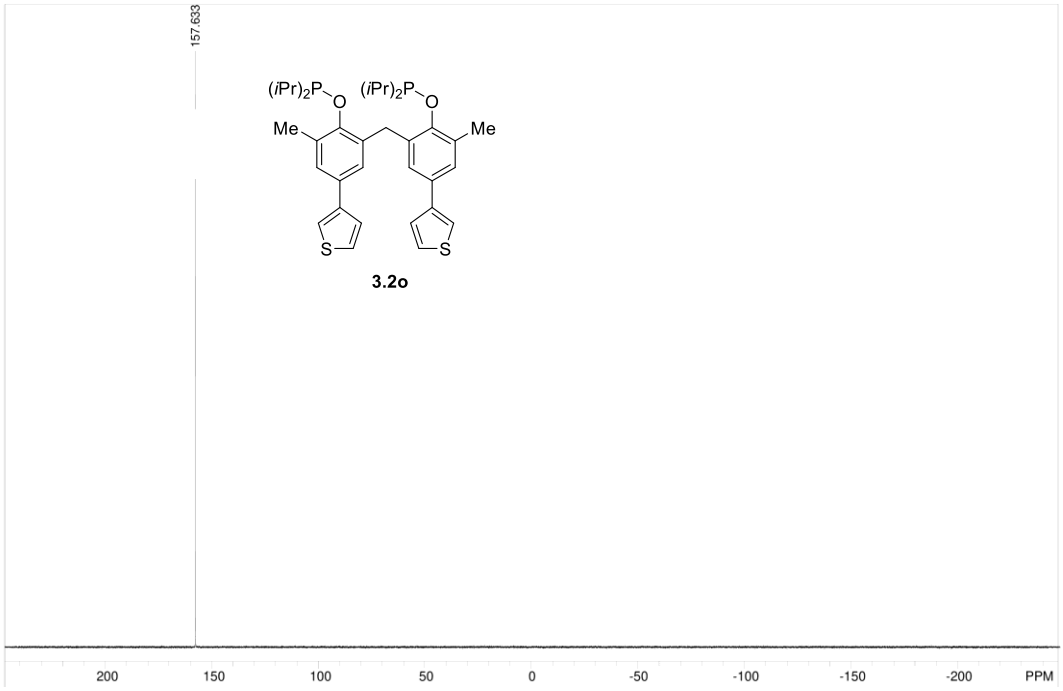

**Figure 3.102.** $^{1}$H-NMR Spectrum of **3.2p** in $CDCl_3$, 500 MHz

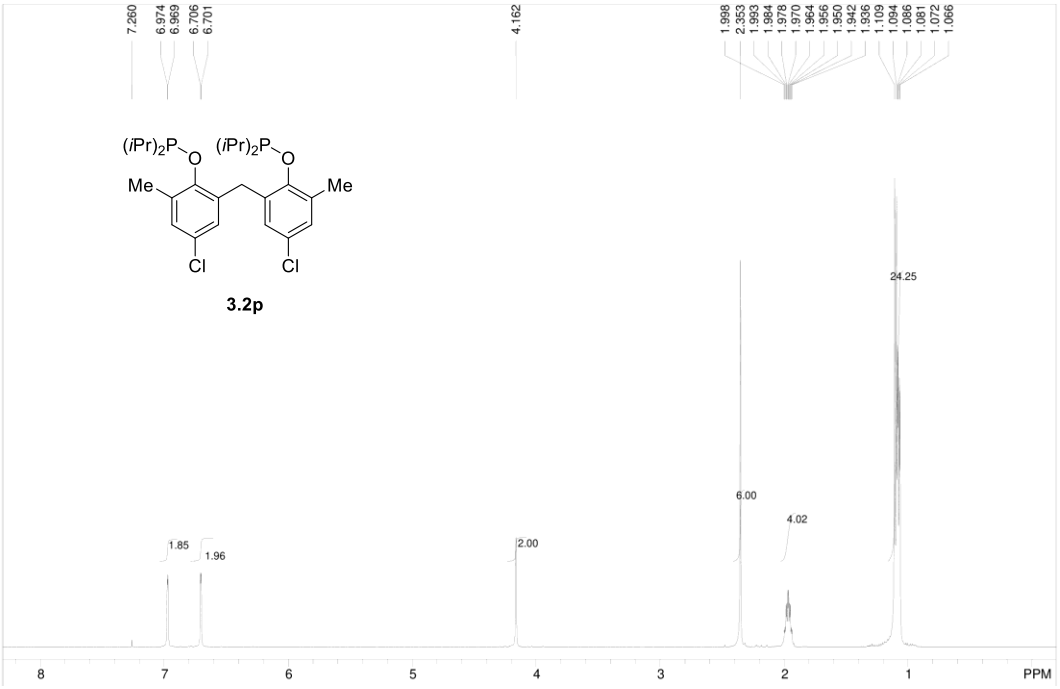


**Figure 3.103.** $^{13}$C-NMR Spectrum of **3.2p** in $CDCl_3$, 126 MHz

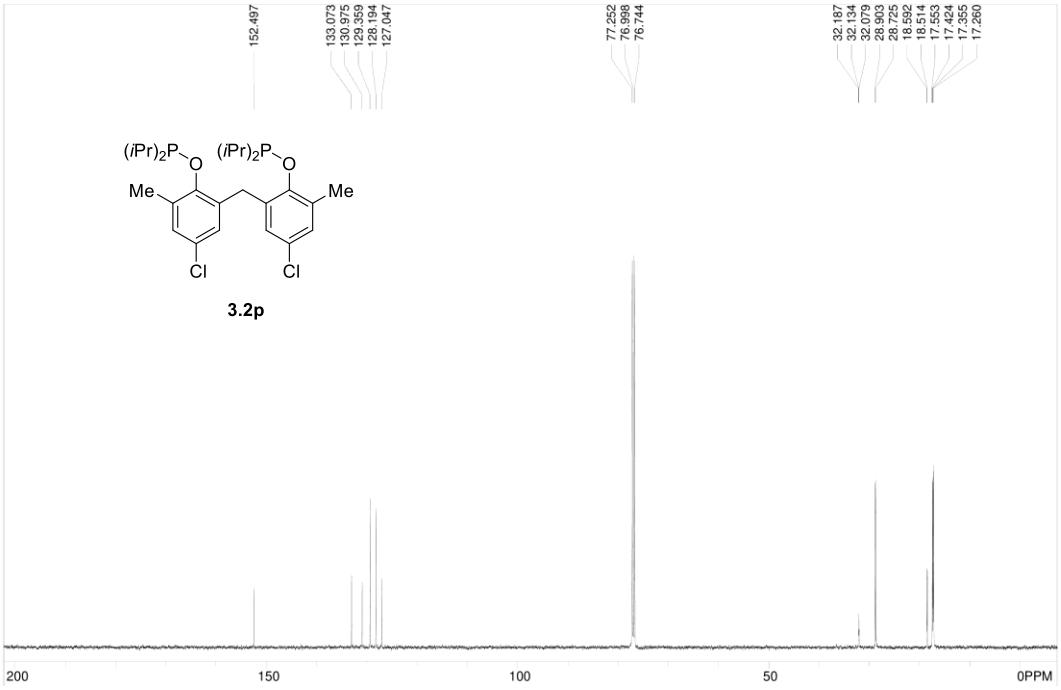

**Figure 3.104.** $^{31}$P-NMR Spectrum of **3.2p** in $CDCl_3$, 202 MHz

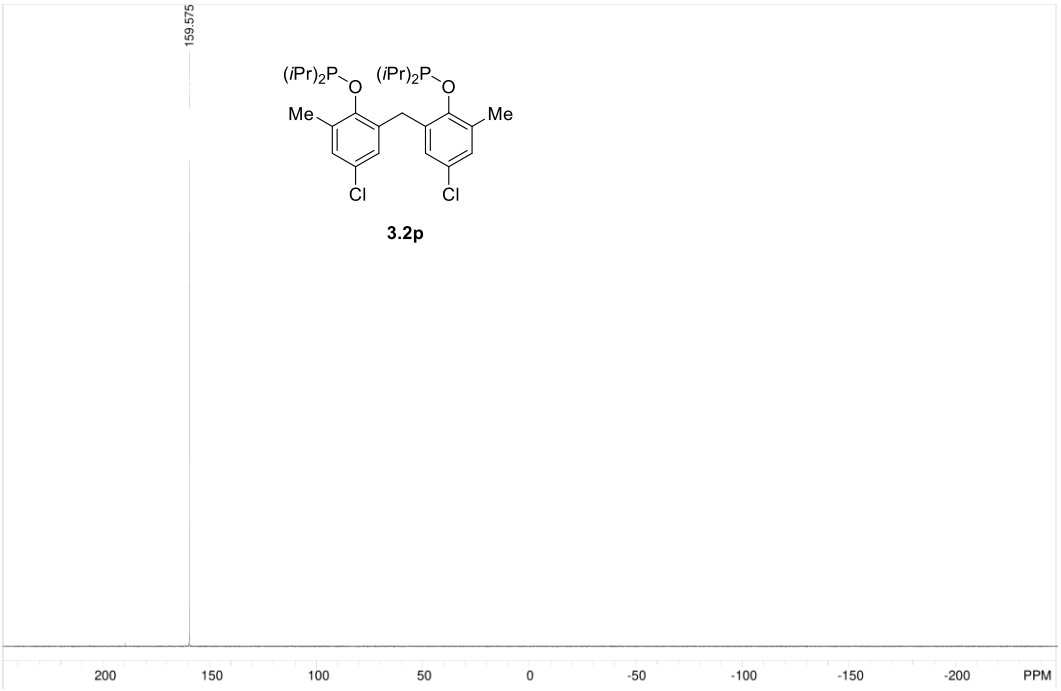

**Figure 3.105.** $^{1}$H-NMR Spectrum of **3.2q** in $CDCl_3$, 500 MHz

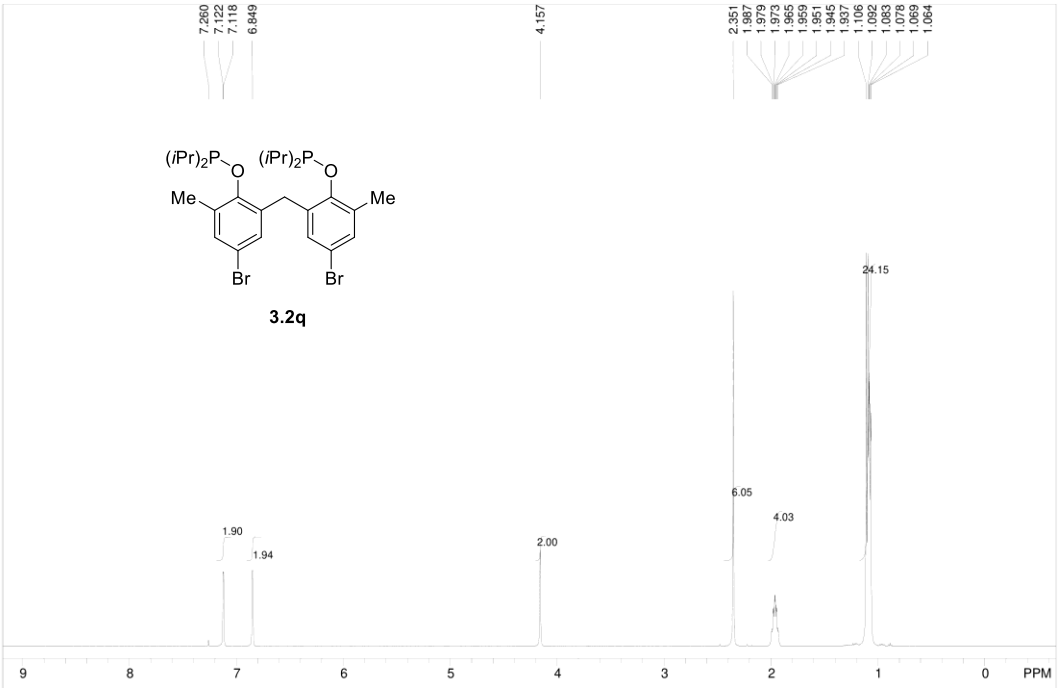


**Figure 3.106.** $^{13}$C-NMR Spectrum of **3.2q** in $CDCl_3$, 126 MHz

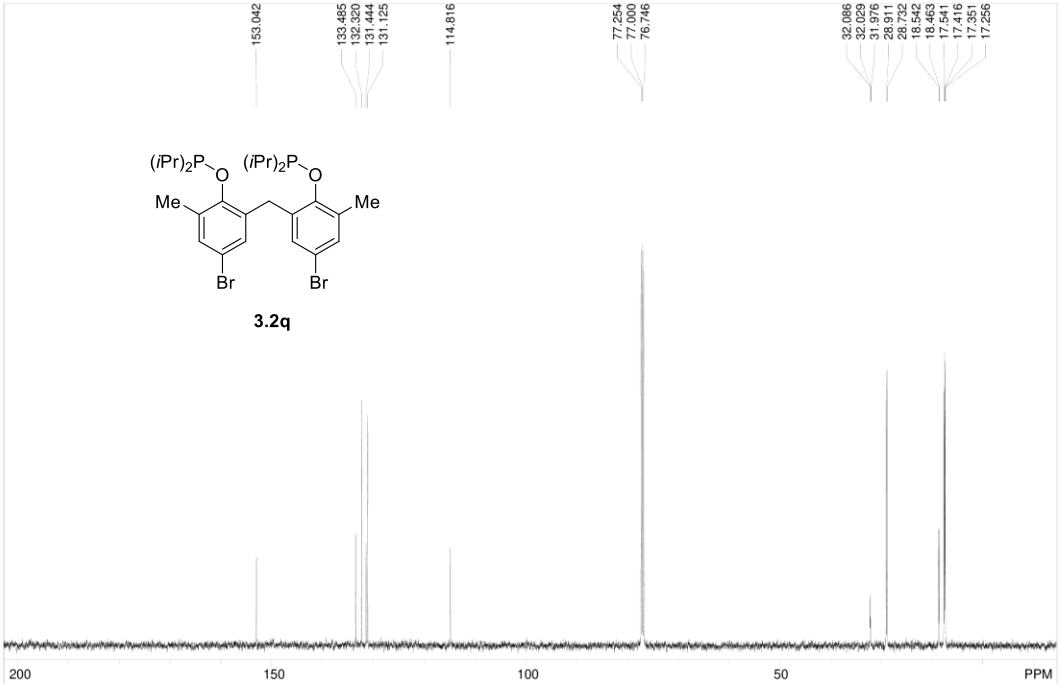

**Figure 3.107.** $^{31}$P-NMR Spectrum of **3.2q** in $CDCl_3$, 202 MHz

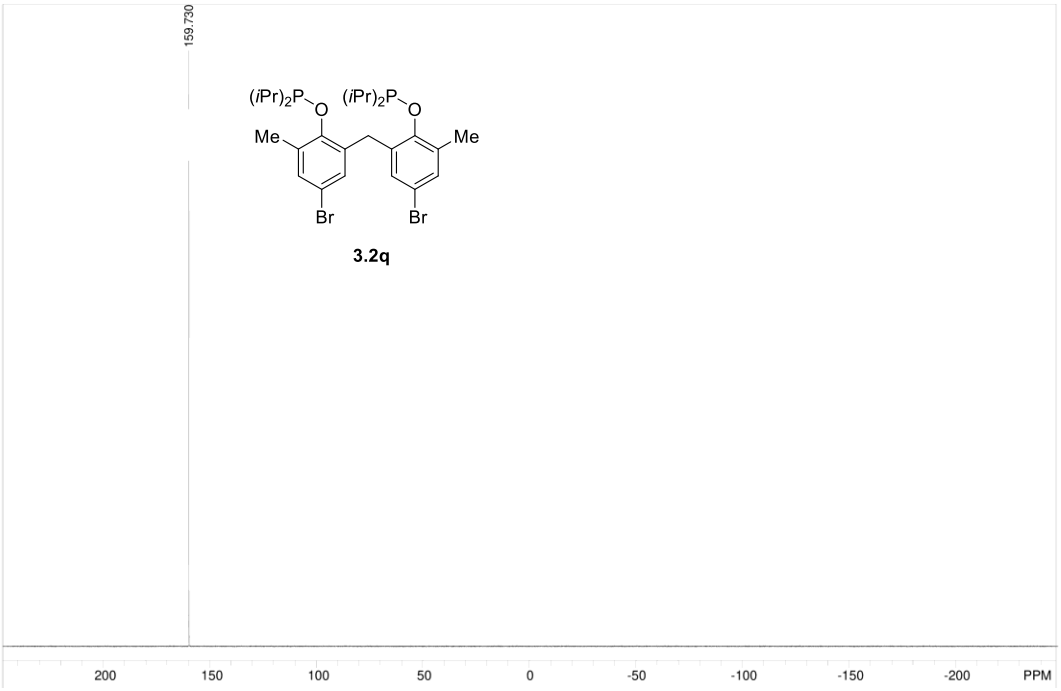

**Figure 3.108.** $^{1}$H-NMR Spectrum of **3.2r** in $CDCl_3$, 500 MHz

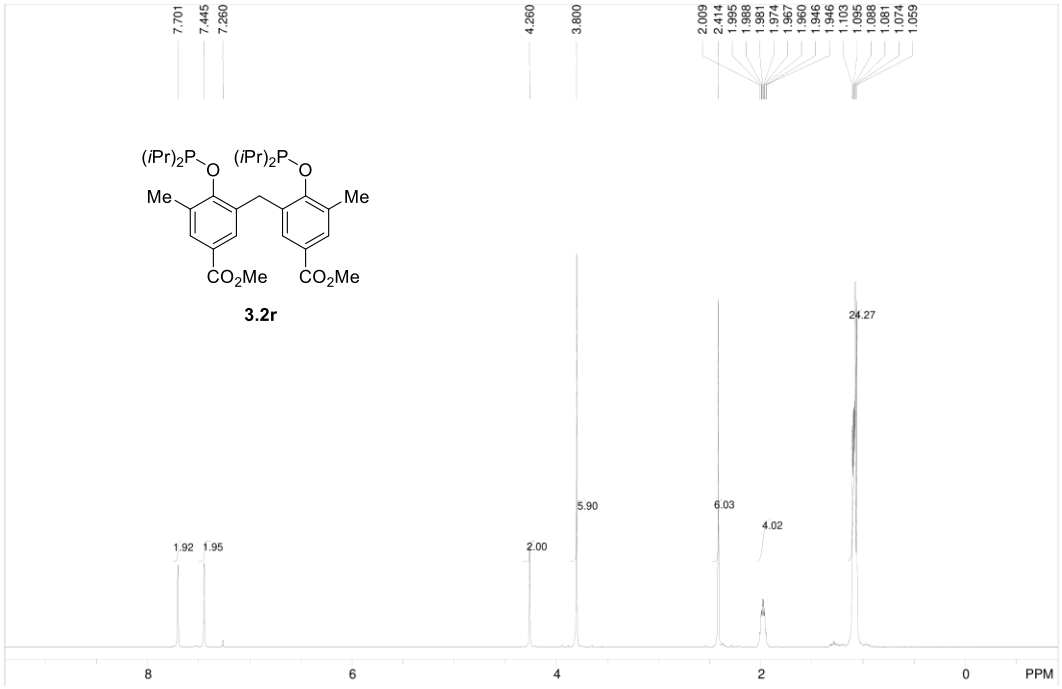


**Figure 3.109.** $^{13}$C-NMR Spectrum of **3.2r** in $CDCl_3$, 126 MHz

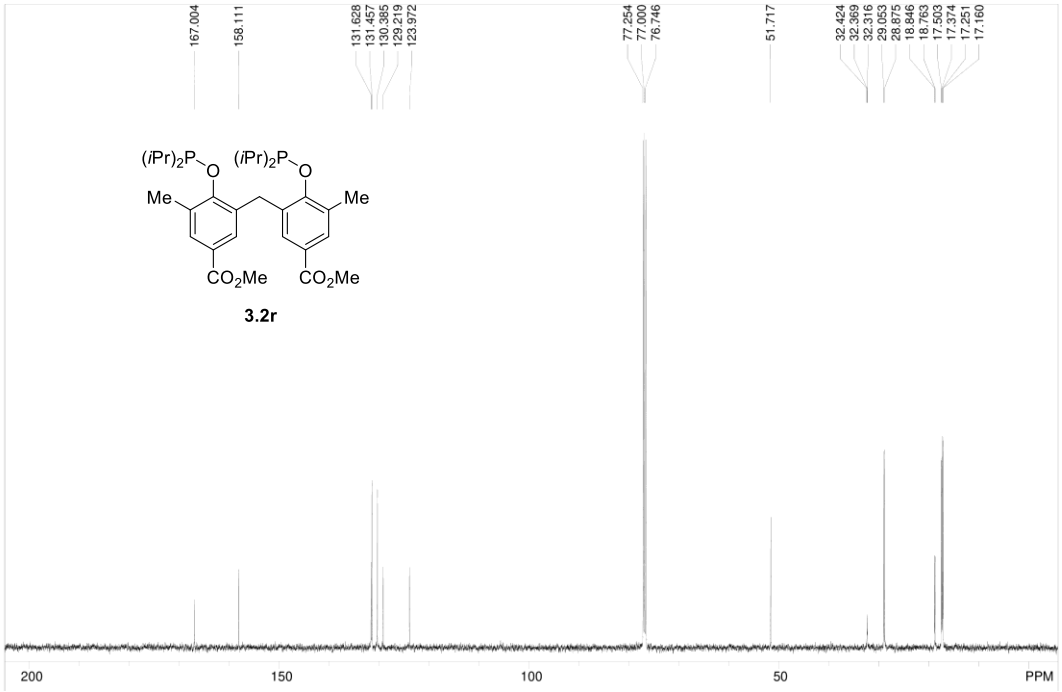

**Figure 3.110.** $^{31}$P-NMR Spectrum of **3.2r** in $CDCl_3$, 202 MHz

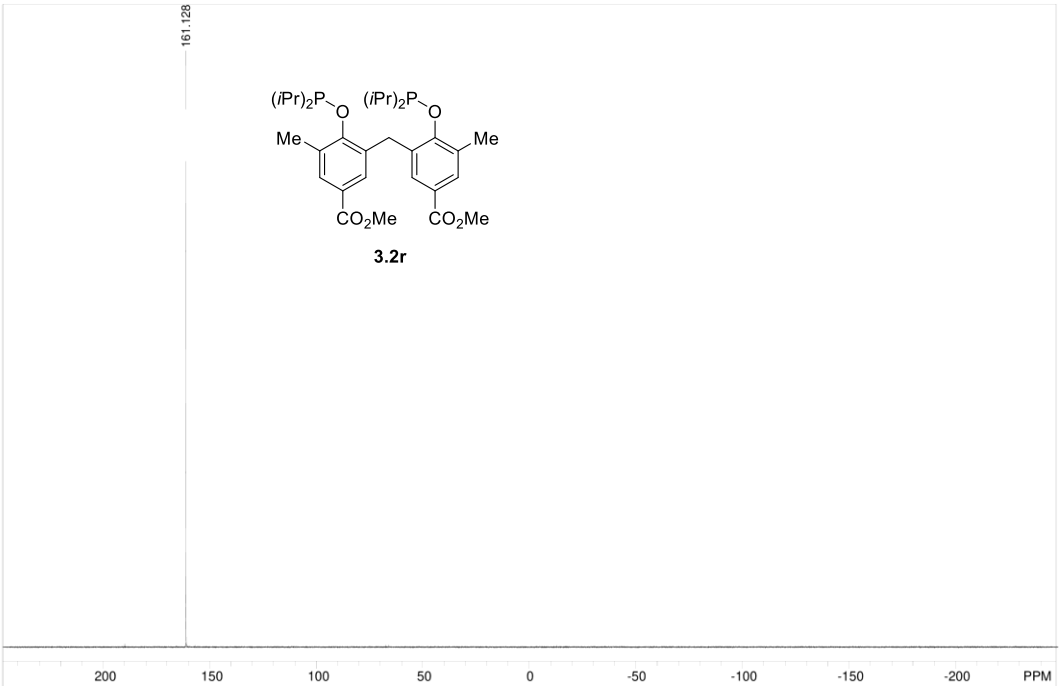

**Figure 3.111.** $^{1}$H-NMR Spectrum of **3.2s** in $CDCl_3$, 500 MHz

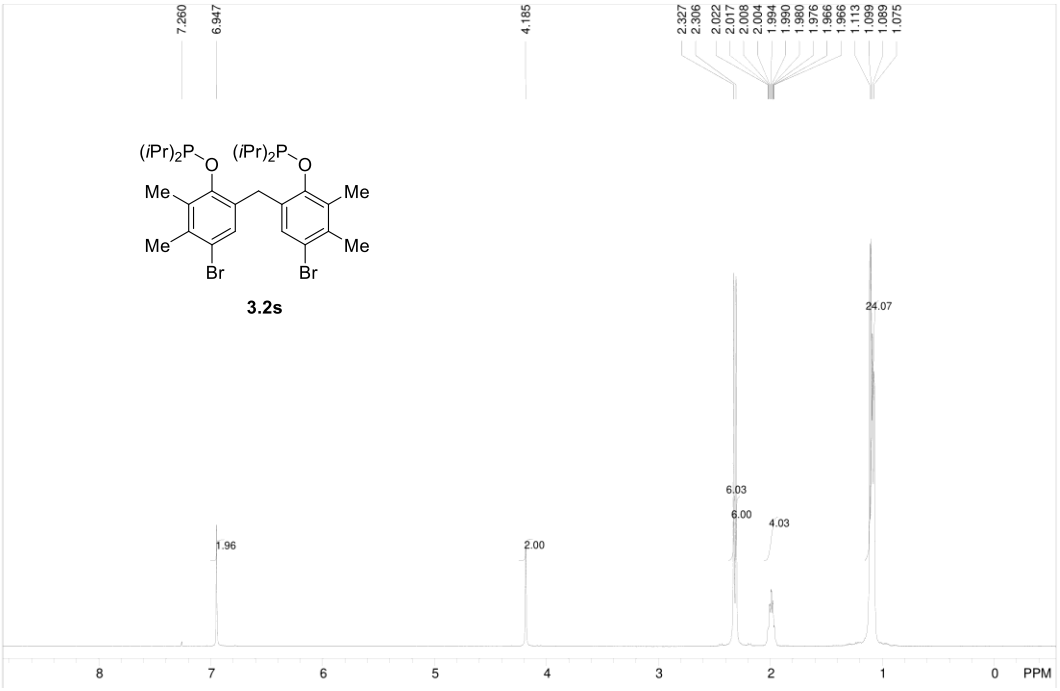


**Figure 3.112.** $^{13}$C-NMR Spectrum of **3.2s** in $CDCl_3$, 126 MHz

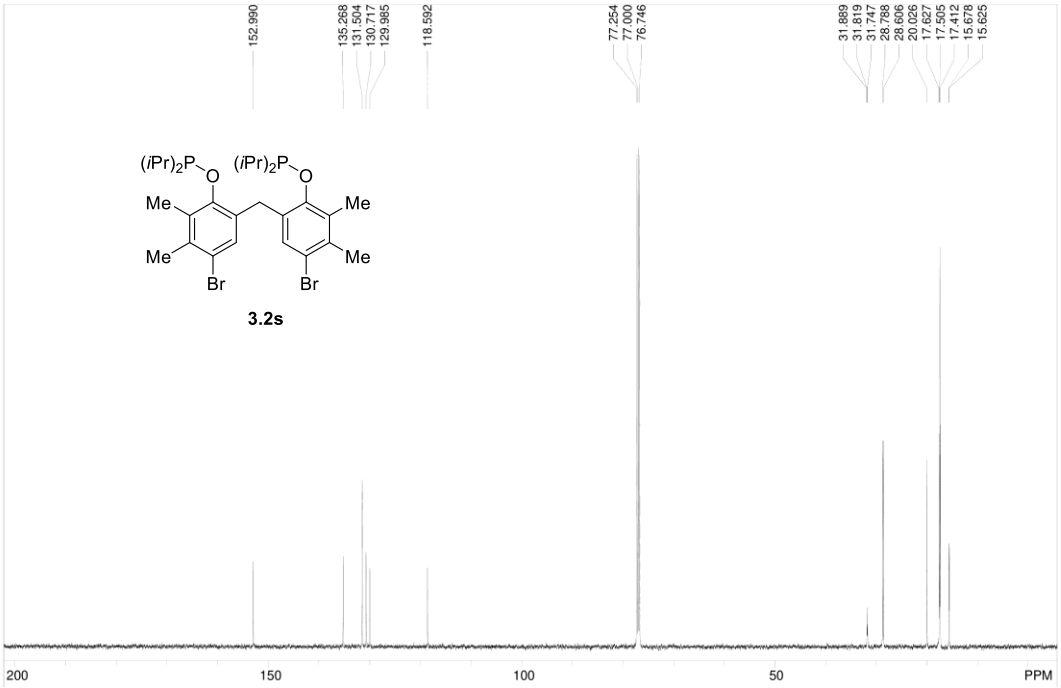

**Figure 3.113.** $^{31}$P-NMR Spectrum of **3.2s** in $CDCl_3$, 202 MHz

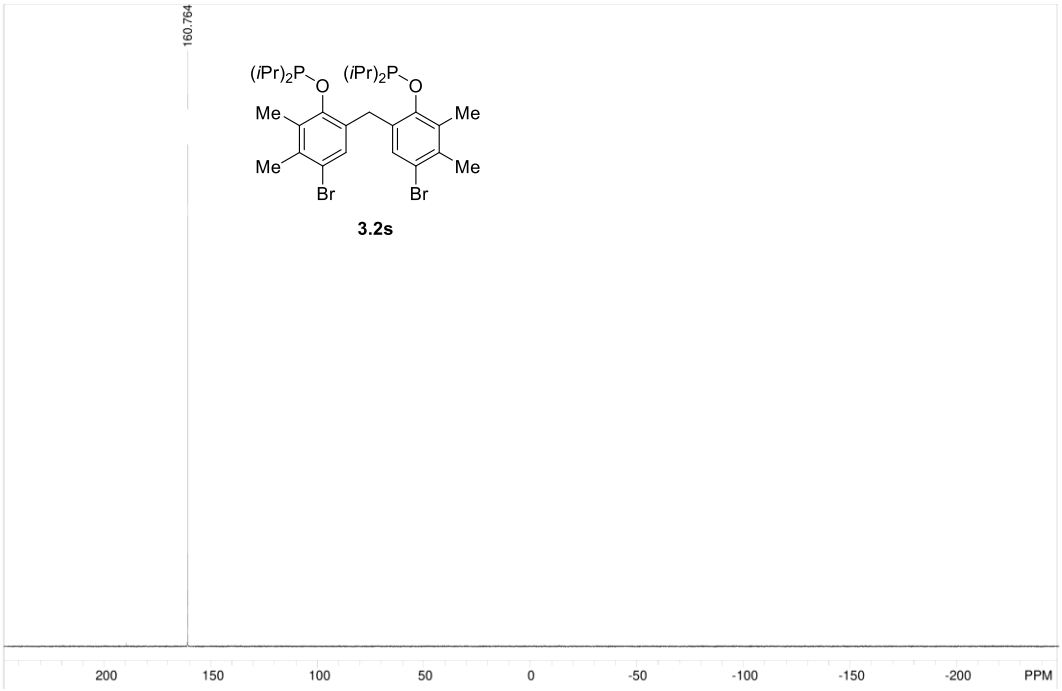

**Figure 3.114.** $^{1}$H-NMR Spectrum of **3.2t** in $C_6D_6$, 400 MHz

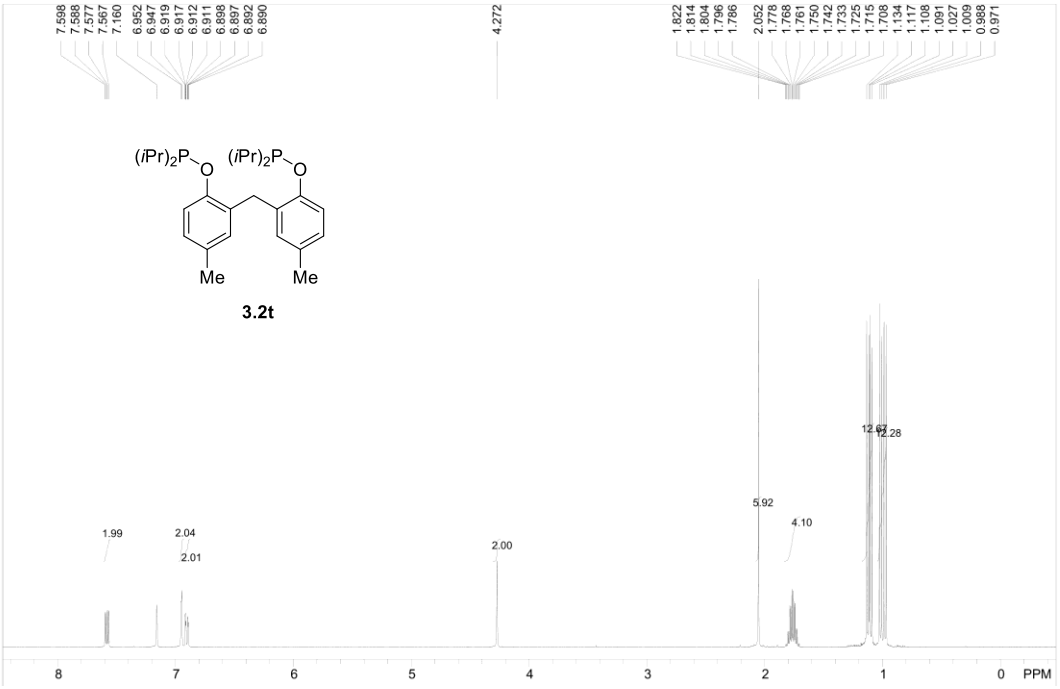


**Figure 3.115.** $^{13}$C-NMR Spectrum of **3.2t** in $C_6D_6$, 101 MHz

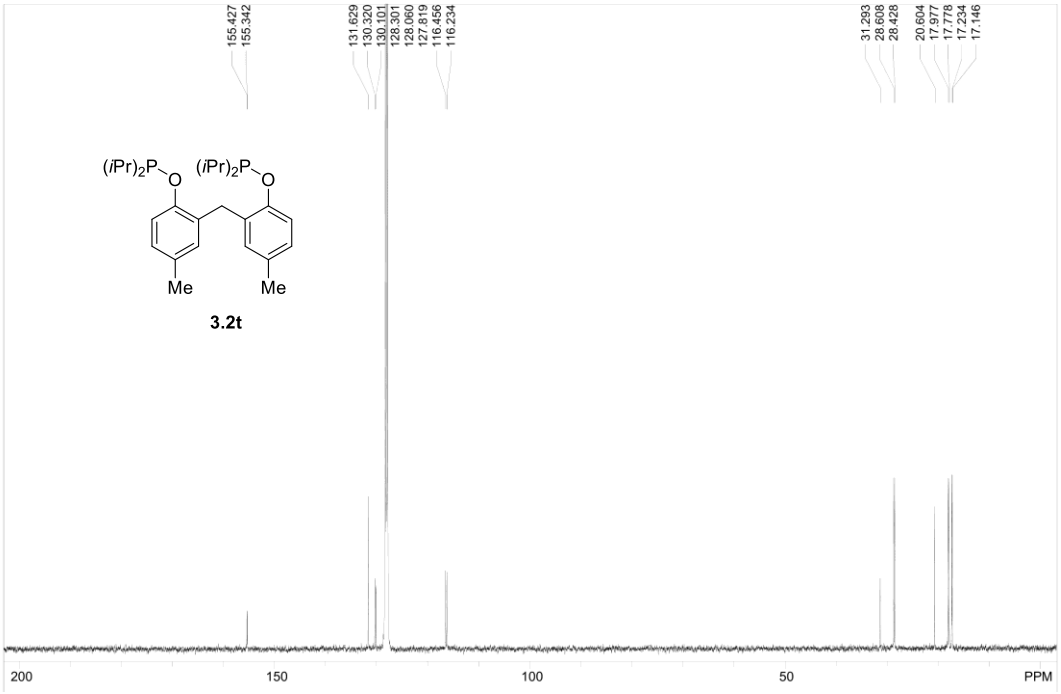

**Figure 3.116.** $^{31}$P-NMR Spectrum of **3.2t** in $C_6D_6$, 202 MHz

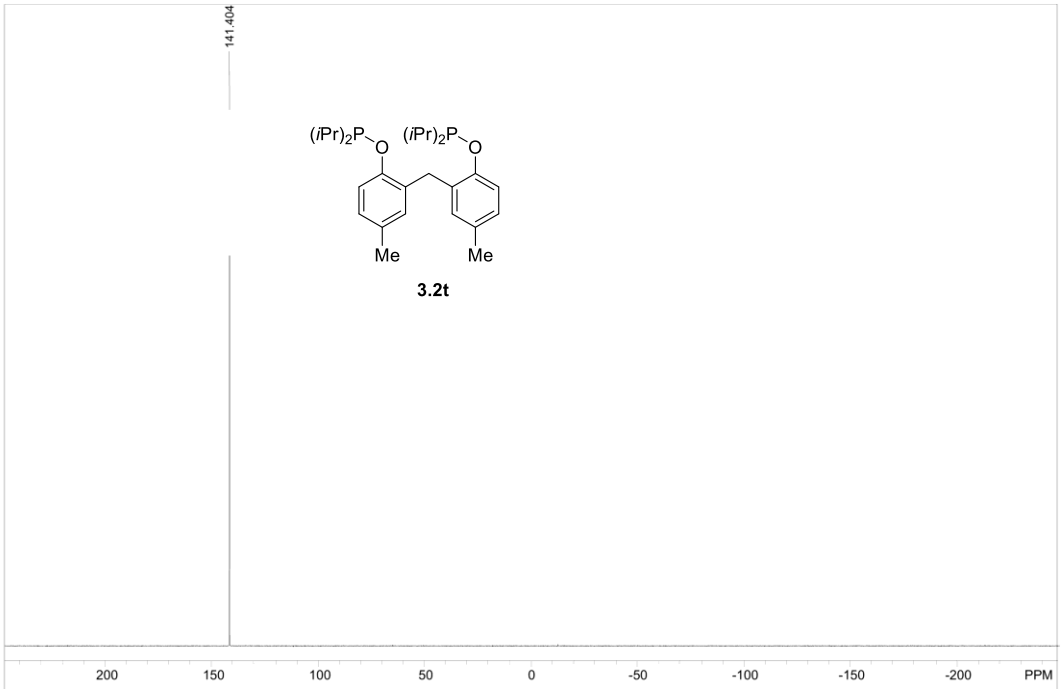

**Figure 3.117.** $^{1}$H-NMR Spectrum of **3.2t'** in $C_6D_6$, 500 MHz

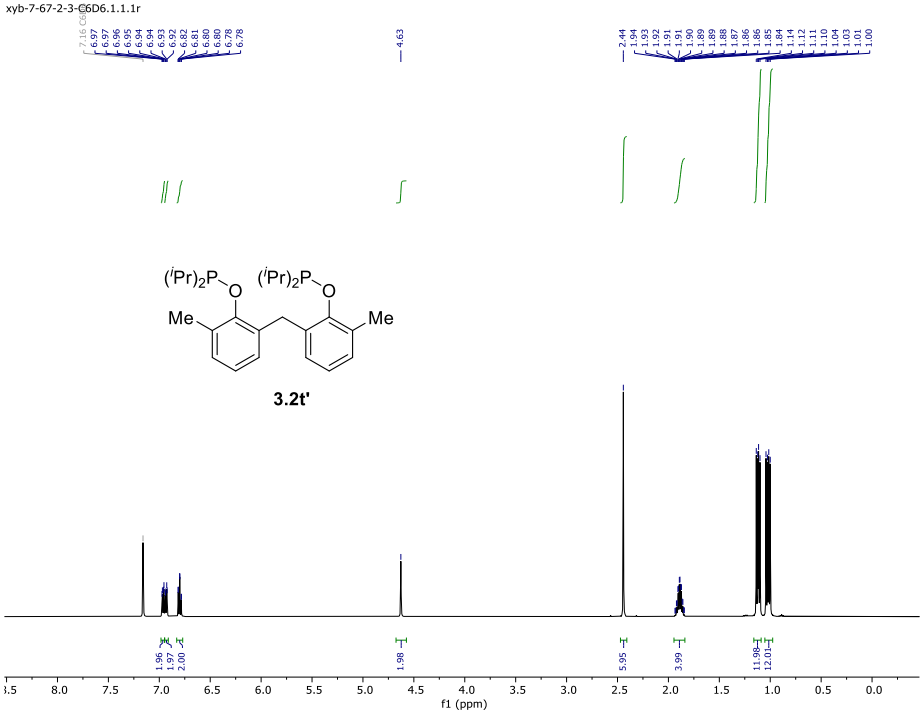


**Figure 3.118.** $^{13}$C-NMR Spectrum of **3.2t'** in $C_6D_6$, 126 MHz

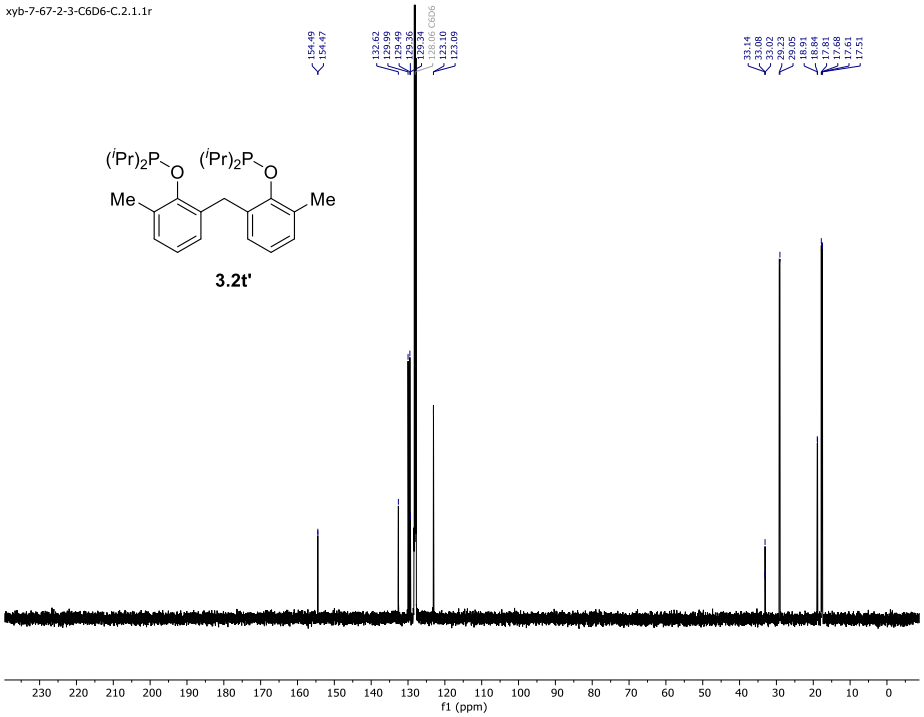

**Figure 3.119.** $^{31}$P-NMR Spectrum of **3.2t'** in $C_6D_6$, 202 MHz

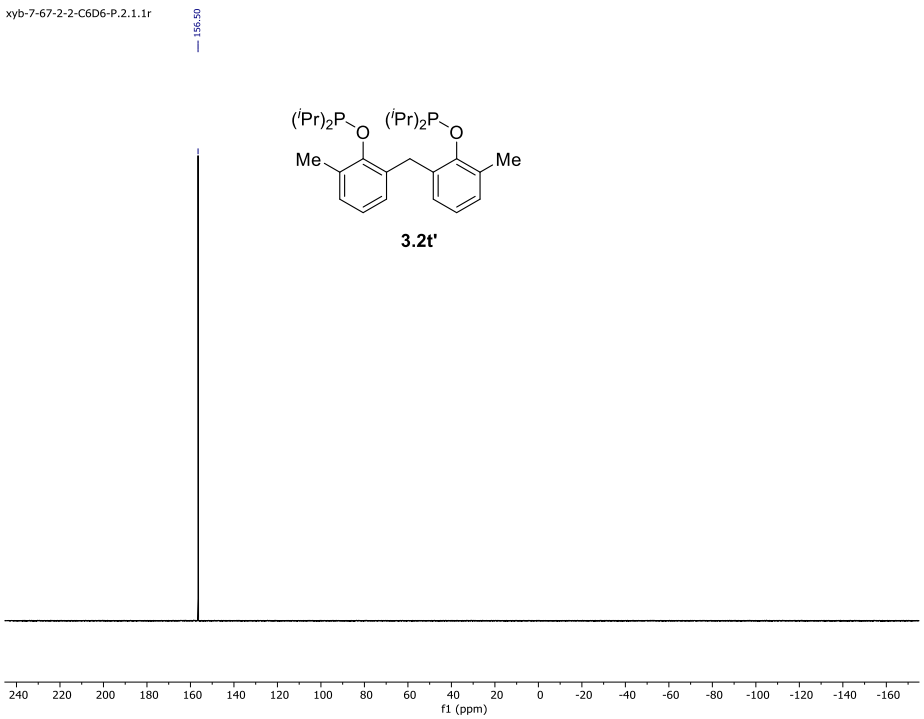

**Figure 3.120.** $^{1}$H-NMR Spectrum of **3.2u** in $C_6D_6$, 400 MHz

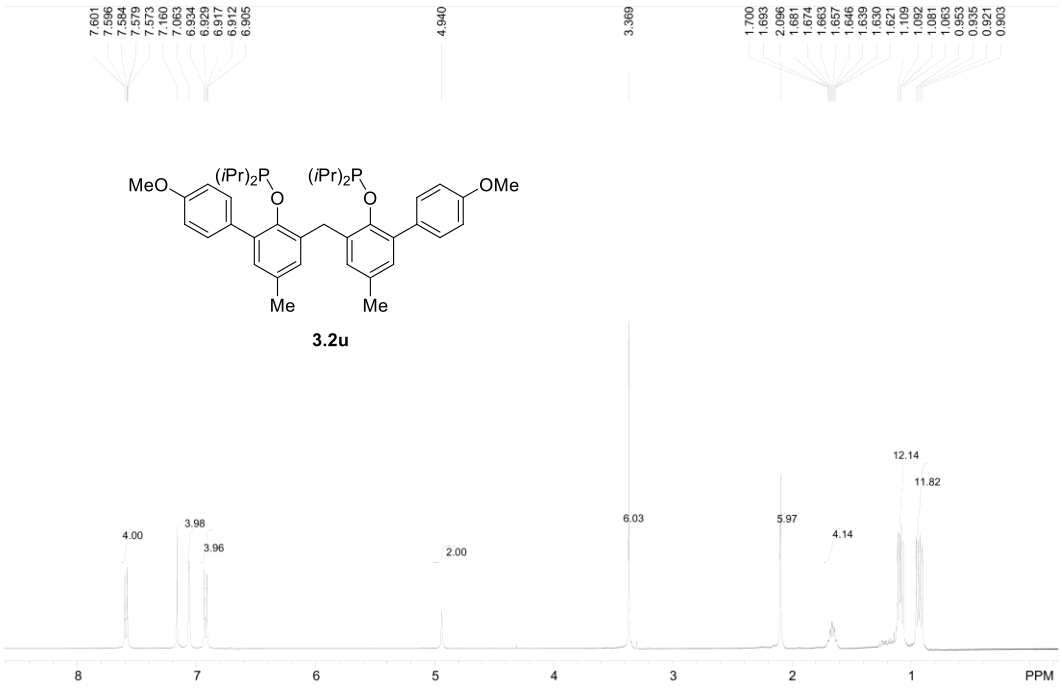


**Figure 3.121.** $^{13}$C-NMR Spectrum of **3.2u** in $C_6D_6$, 101 MHz

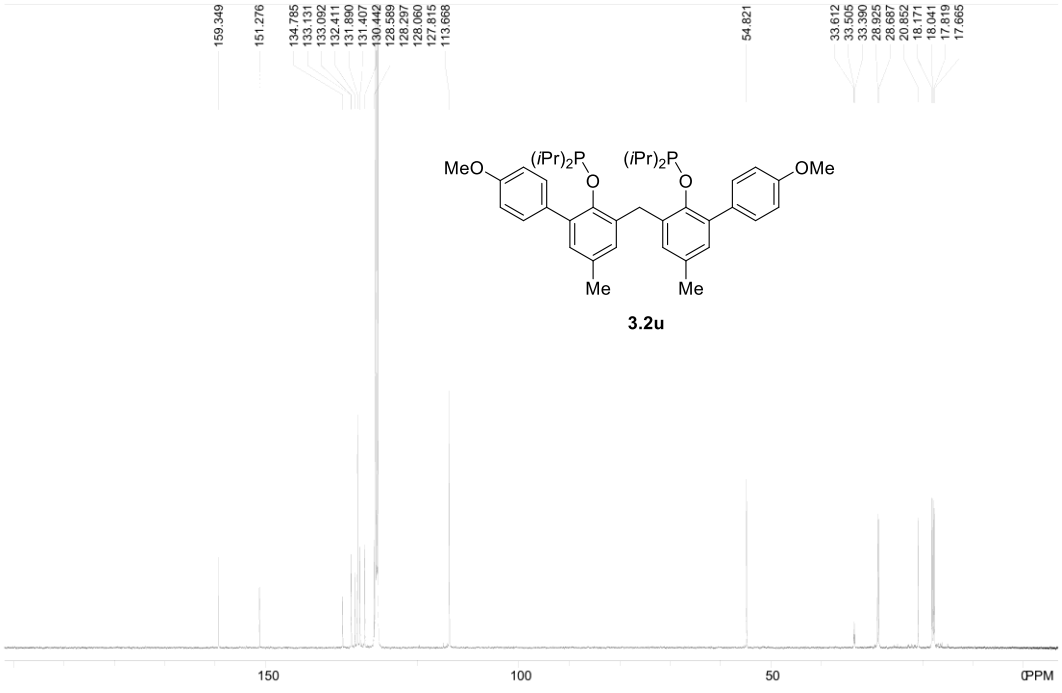

**Figure 3.122.** $^{31}$P-NMR Spectrum of **3.2u** in $C_6D_6$, 162 MHz

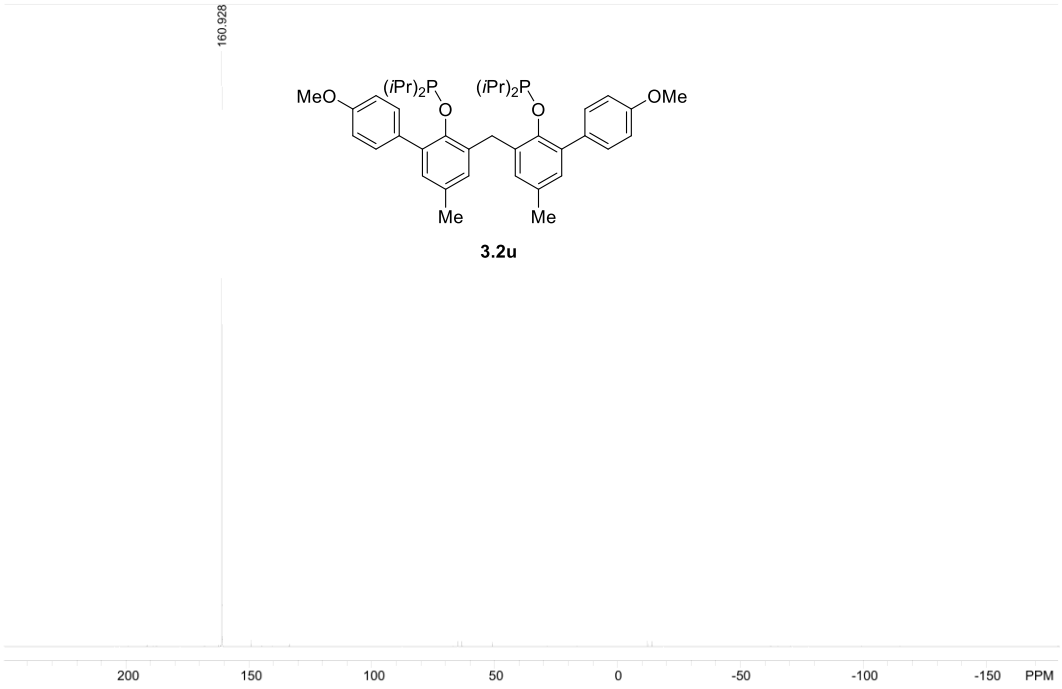

**Figure 3.123.** $^{1}$H-NMR Spectrum of **3.2v** in $C_6D_6$, 400 MHz

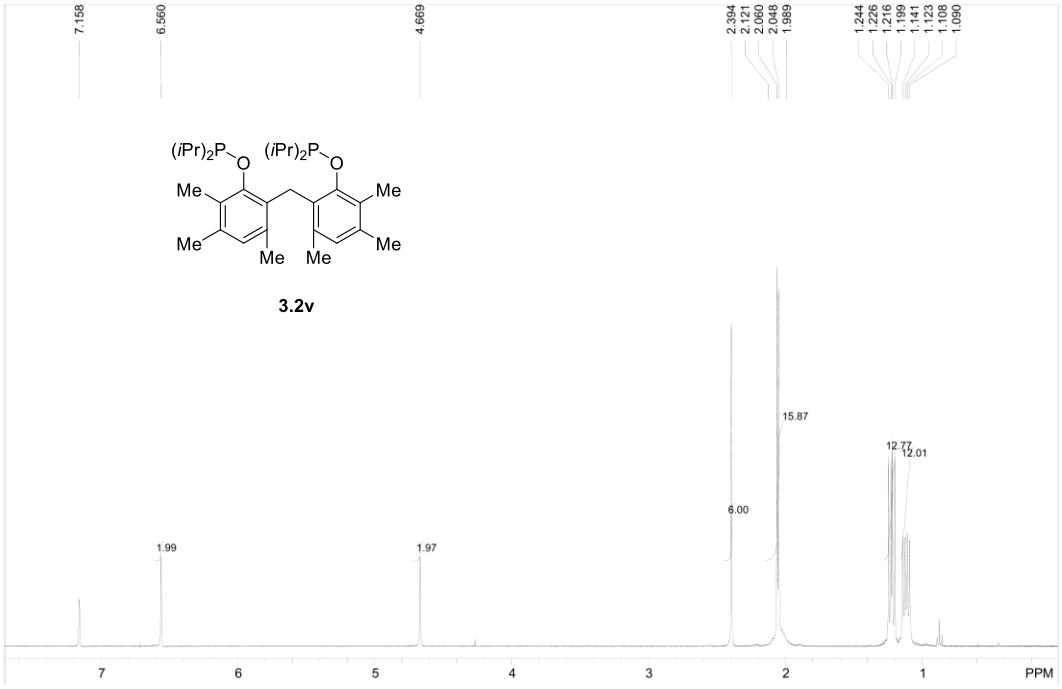


**Figure 3.124.** $^{13}$C-NMR Spectrum of **3.2v** in $C_6D_6$, 101 MHz

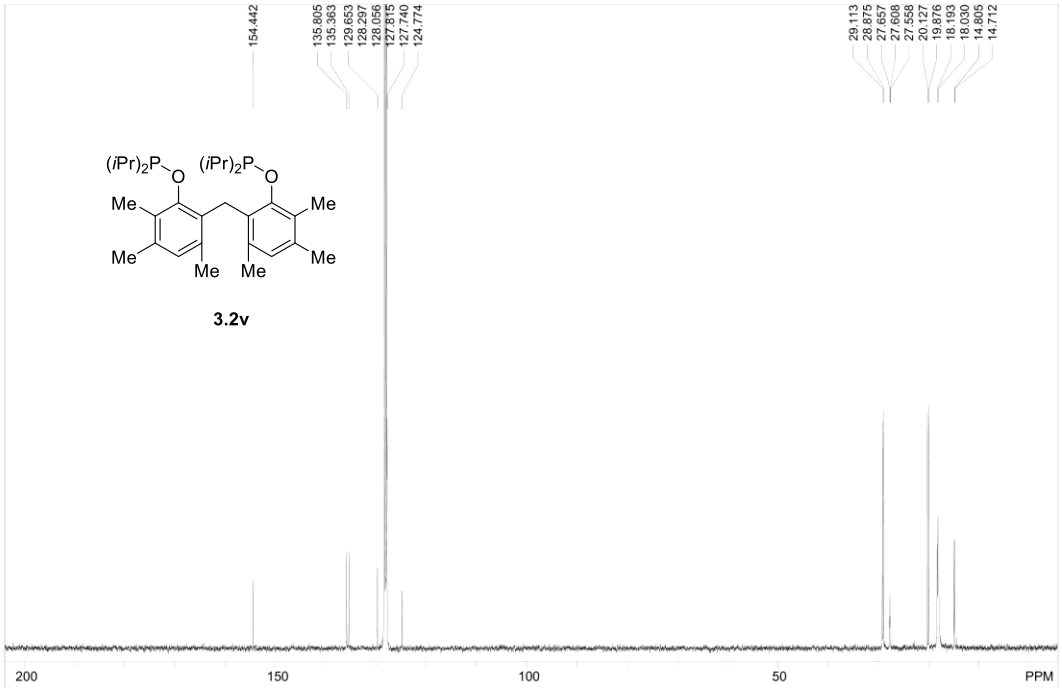

**Figure 3.125.** $^{31}$P-NMR Spectrum of **3.2v** in $C_6D_6$, 162 MHz

**Figure 3.126.** $^{1}$H-NMR Spectrum of **3.2w** in $C_6D_6$, 400 MHz

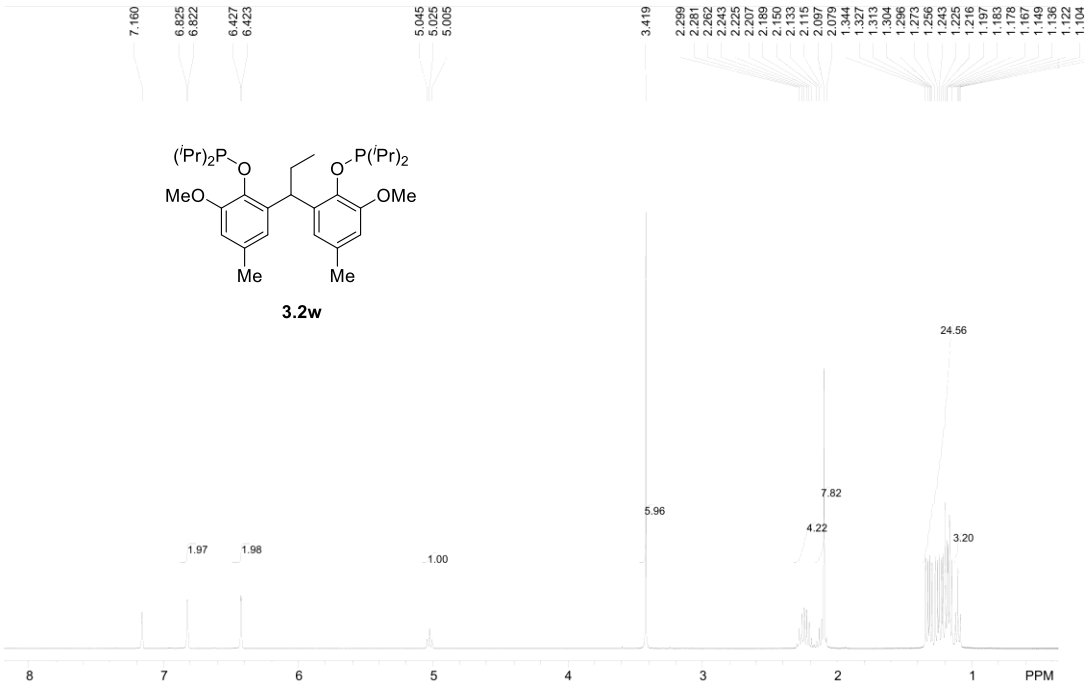


**Figure 3.127.** $^{13}$C-NMR Spectrum of **3.2w** in $C_6D_6$, 101 MHz

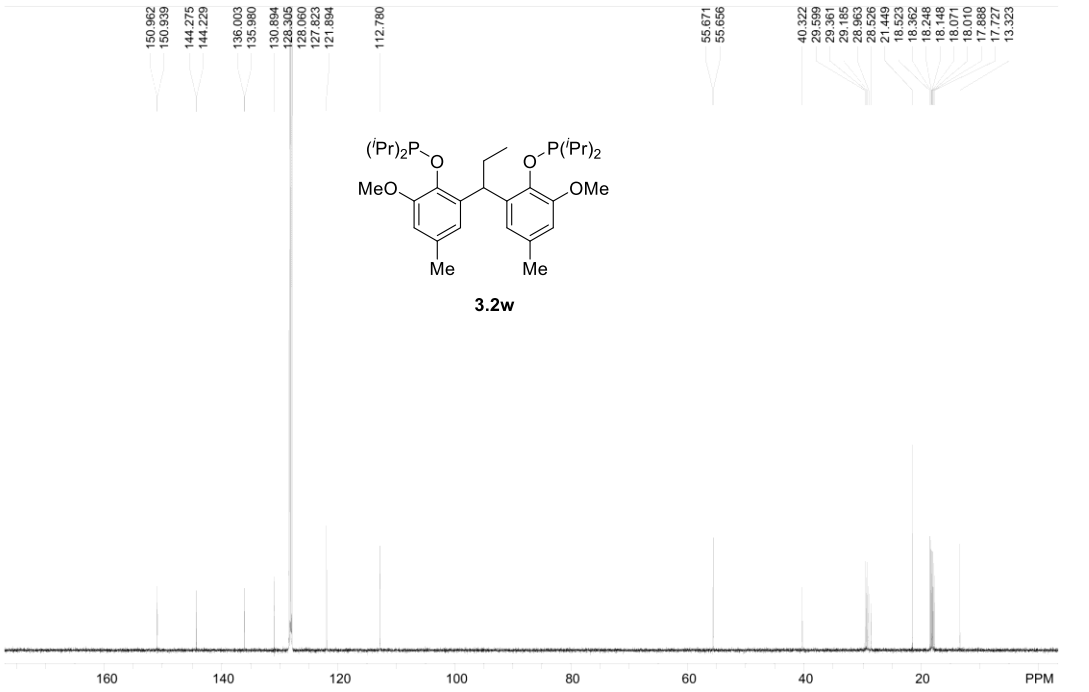

**Figure 3.128.** $^{31}$P-NMR Spectrum of **3.2w** in $C_6D_6$, 162 MHz

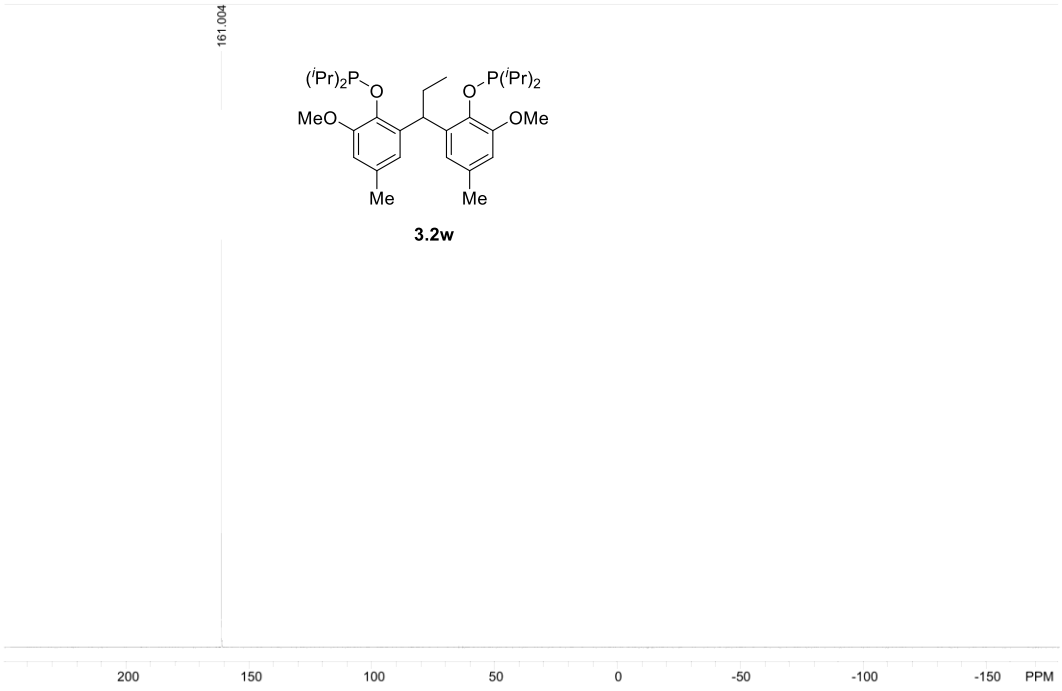

**Figure 3.129.** $^{1}$H-NMR Spectrum of **3.2x** in $C_6D_6$, 500 MHz

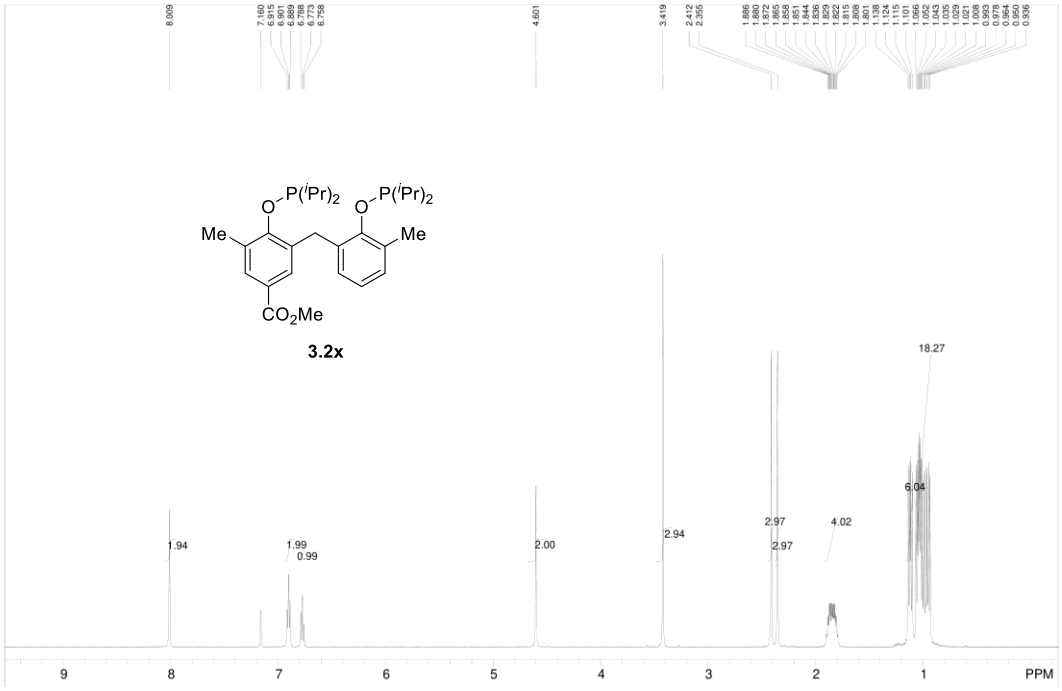


**Figure 3.130.** $^{13}$C-NMR Spectrum of **3.2x** in $C_6D_6$, 126 MHz

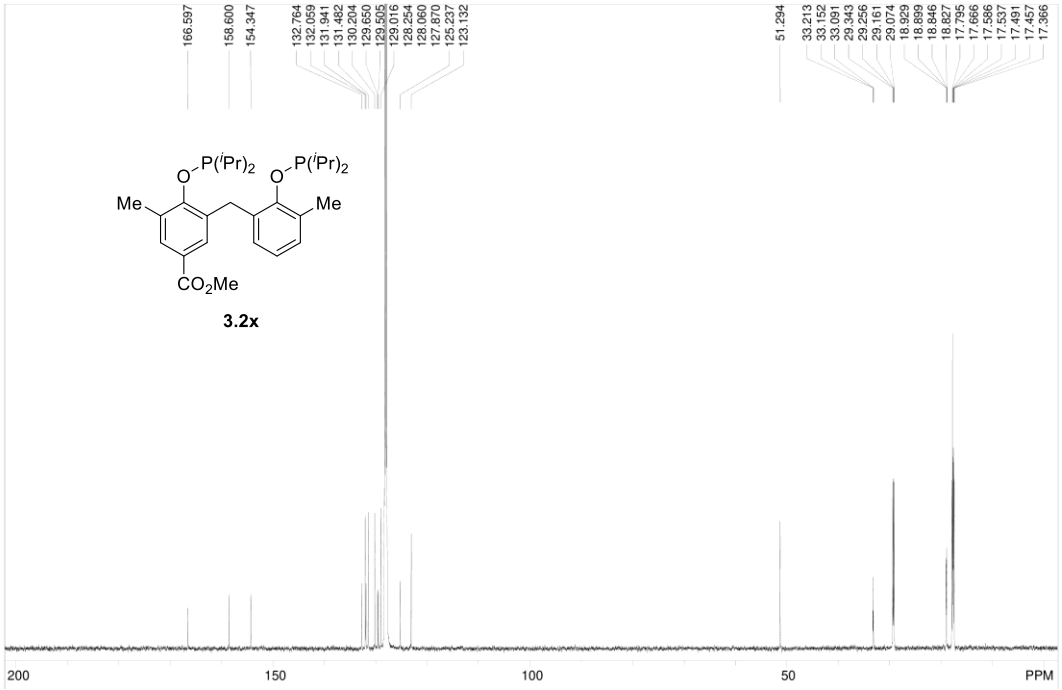

**Figure 3.131.** $^{31}$P-NMR Spectrum of **3.2x** in $C_6D_6$, 202 MHz

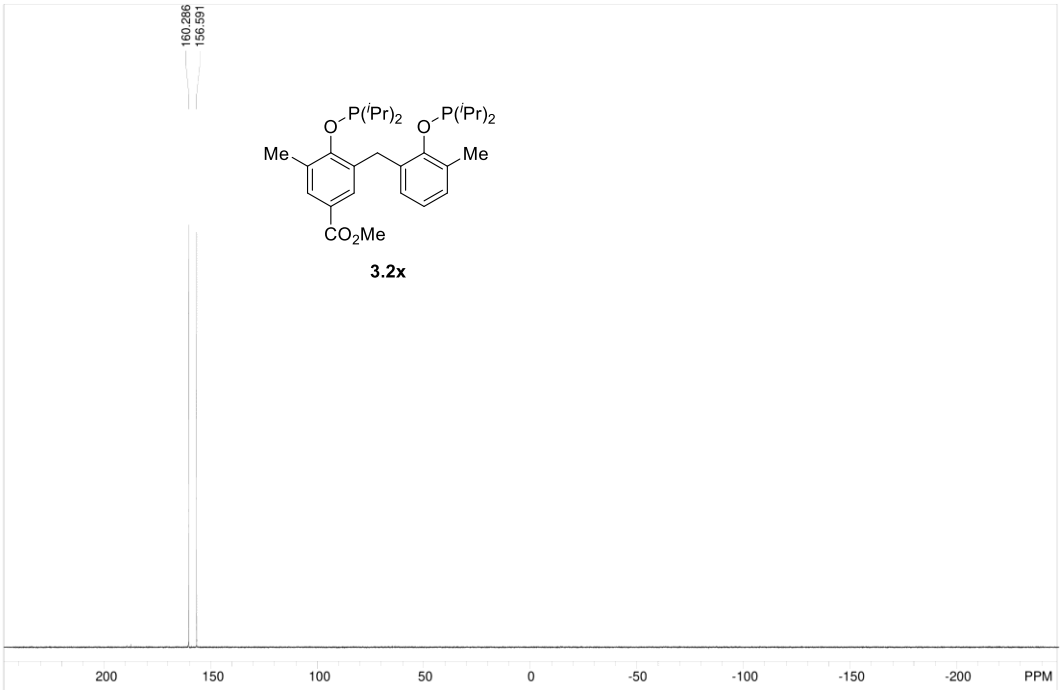

**Figure 3.132.** $^{1}$H-NMR Spectrum of **3.3a** in $CDCl_3$, 400 MHz

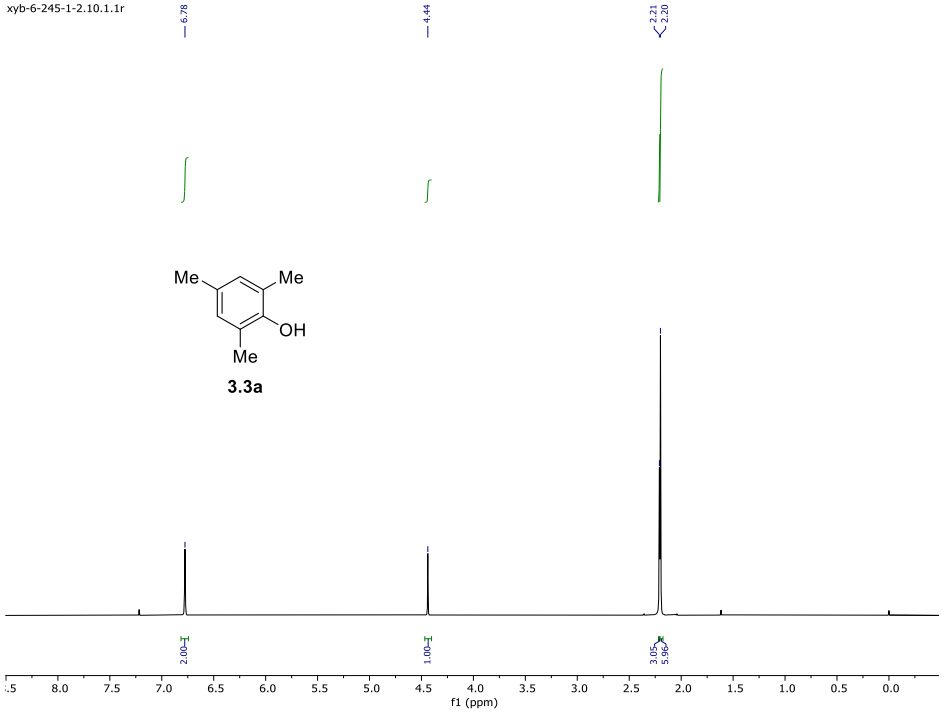


**Figure 3.133.** $^{13}$C-NMR Spectrum of **3.3a** in $CDCl_3$, 101 MHz

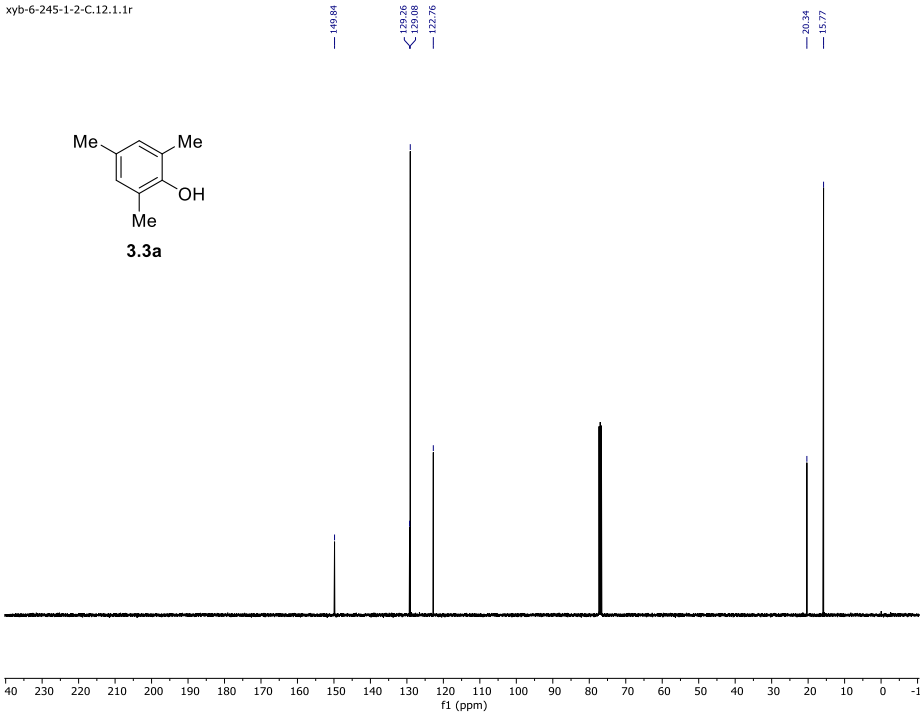

**Figure 3.134.** $^{1}$H-NMR Spectrum of **3.4a** in $CDCl_3$, 400 MHz

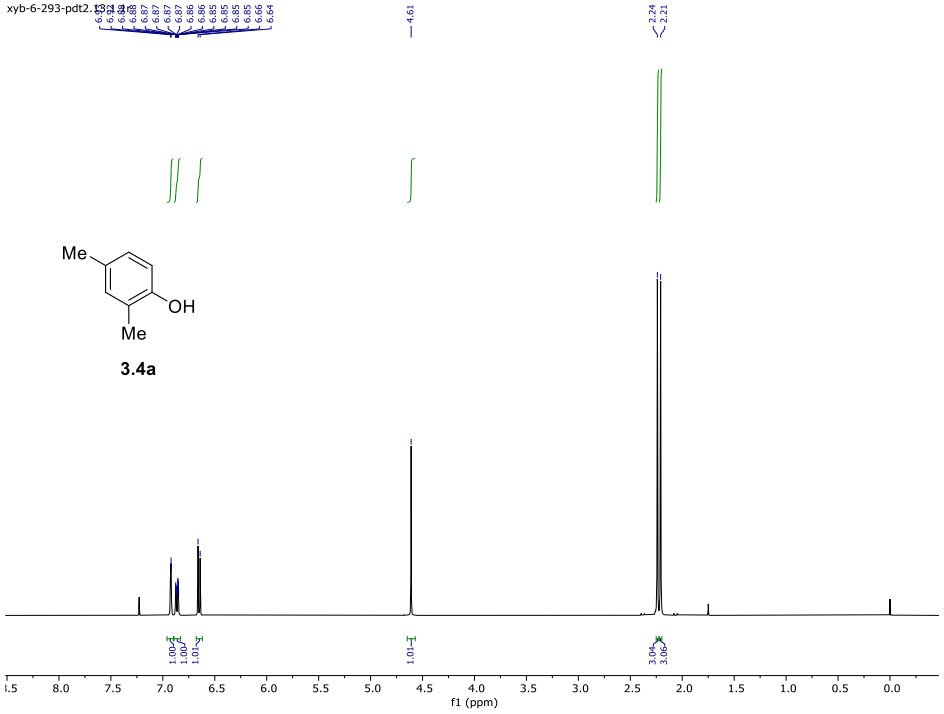


**Figure 3.135.** $^{13}$C-NMR Spectrum of **3.4a** in $CDCl_3$, 101 MHz

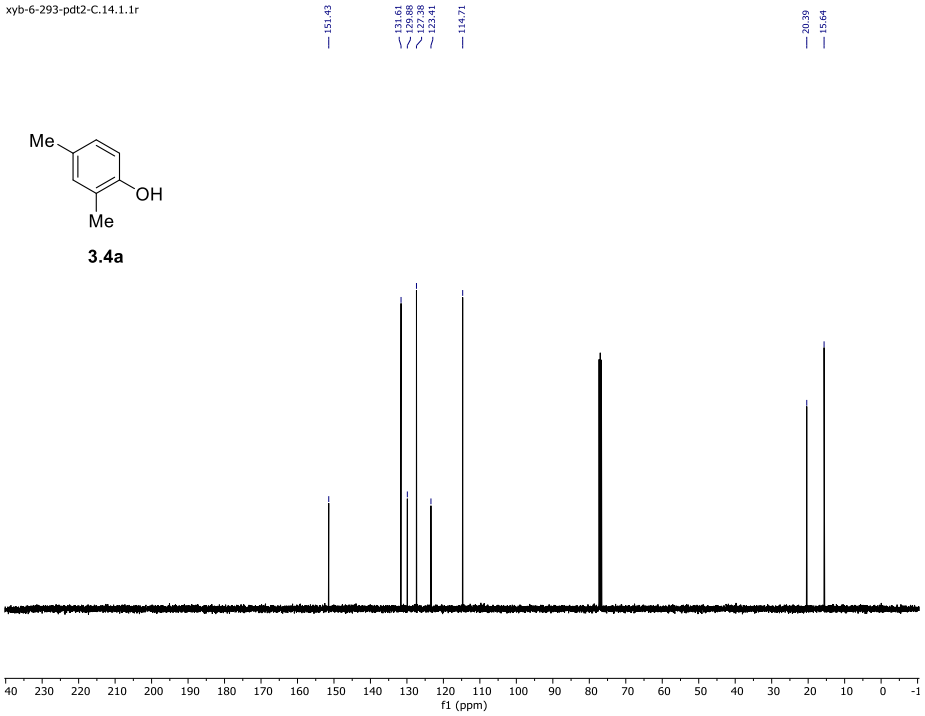

**Figure 3.136.** $^{1}$H-NMR Spectrum of **3.3b** in $CDCl_3$, 500 MHz

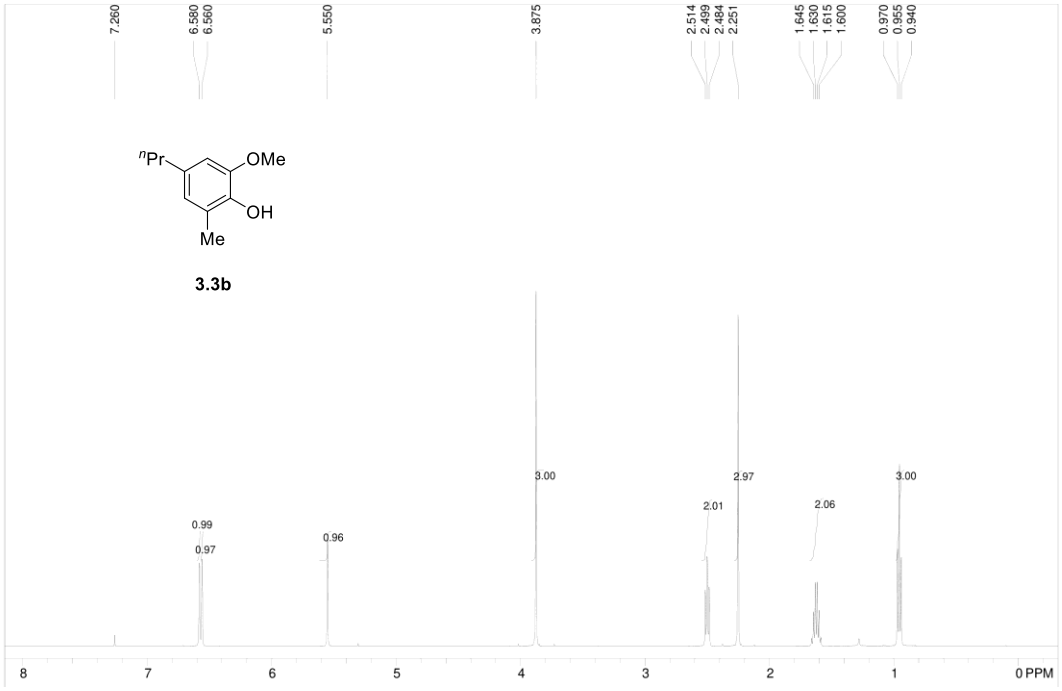


**Figure 3.137.** $^{13}$C-NMR Spectrum of **3.3b** in $CDCl_3$, 126 MHz

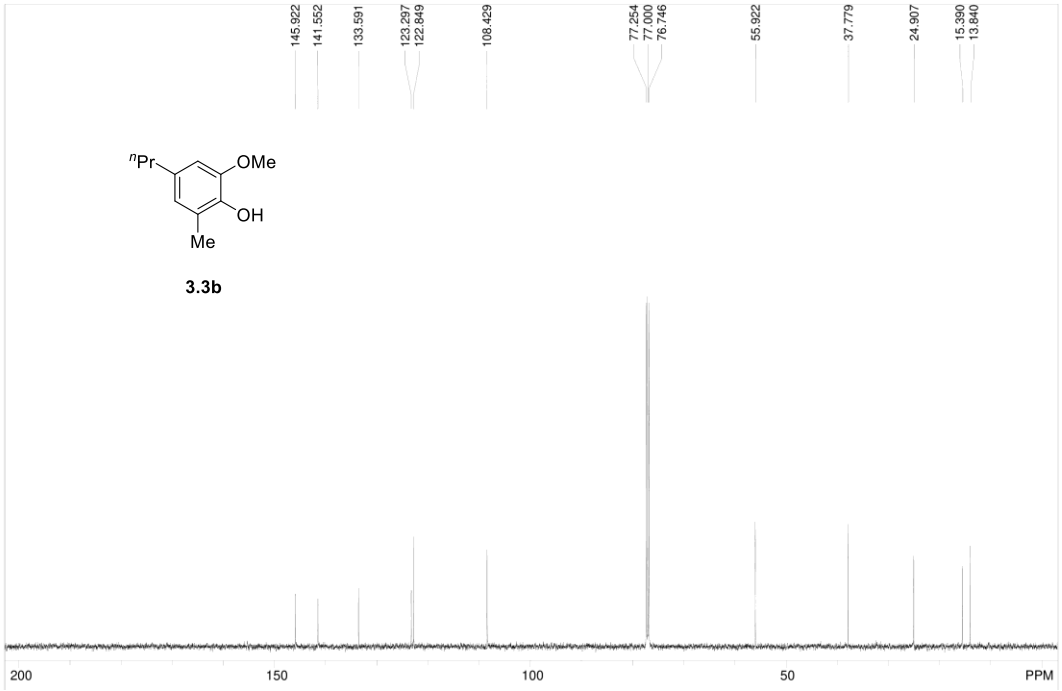

**Figure 3.138.** $^{1}$H-NMR Spectrum of **3.4b** in $CDCl_3$, 500 MHz

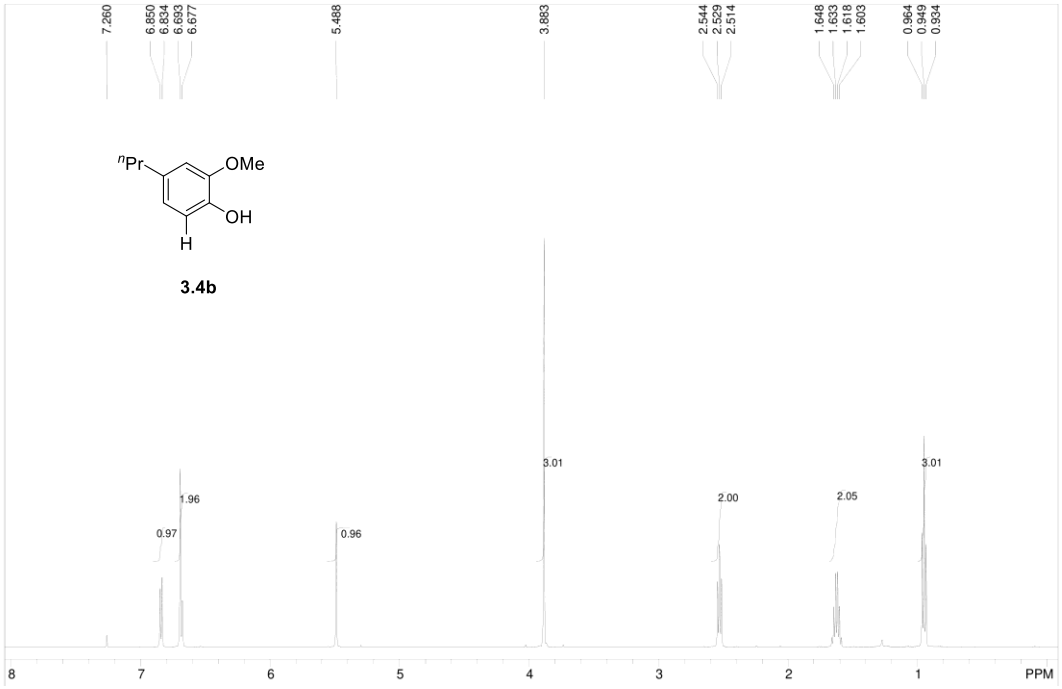


**Figure 3.139.** $^{13}$C-NMR Spectrum of **3.4b** in $CDCl_3$, 126 MHz

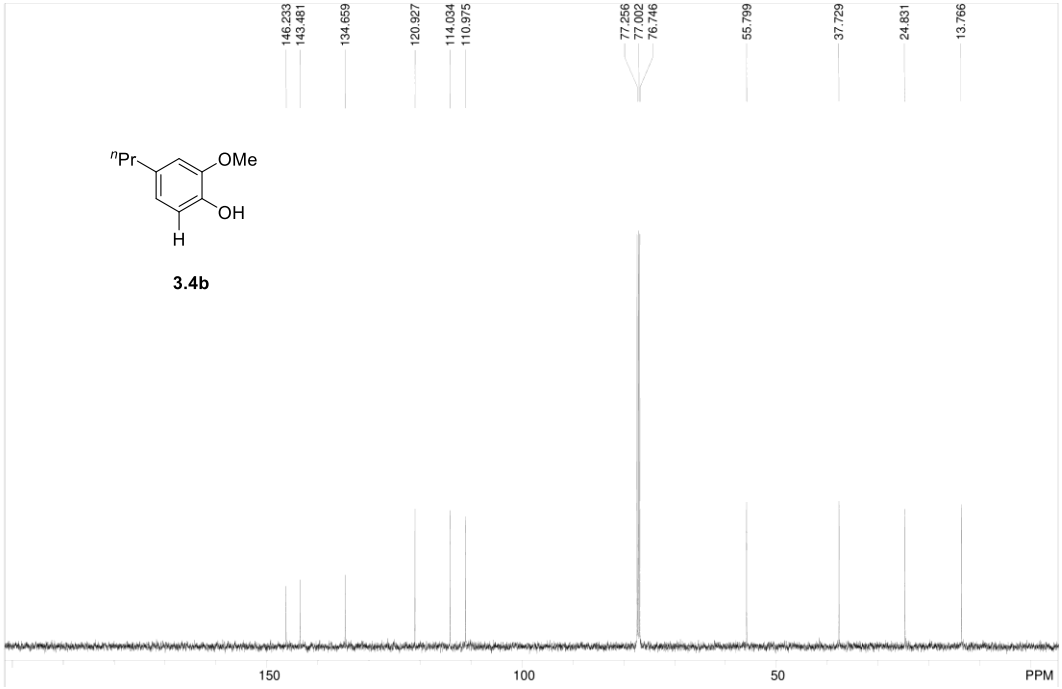

**Figure 3.140.** $^{1}$H-NMR Spectrum of **3.3c** in $CDCl_3$, 500 MHz

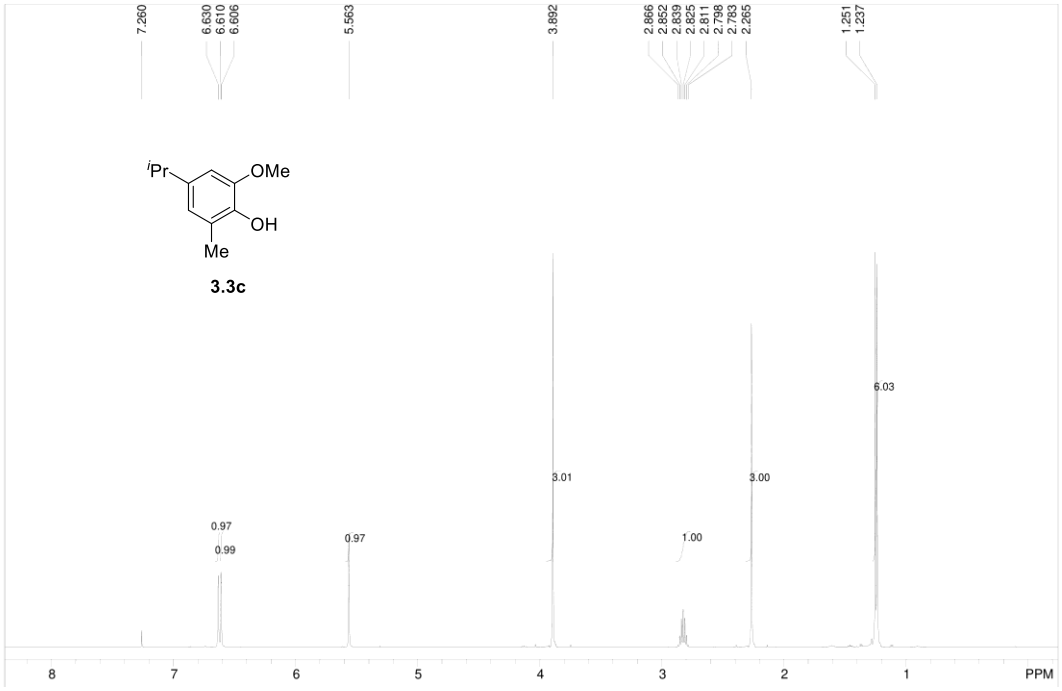


**Figure 3.141.** $^{13}$C-NMR Spectrum of **3.3c** in $CDCl_3$, 126 MHz

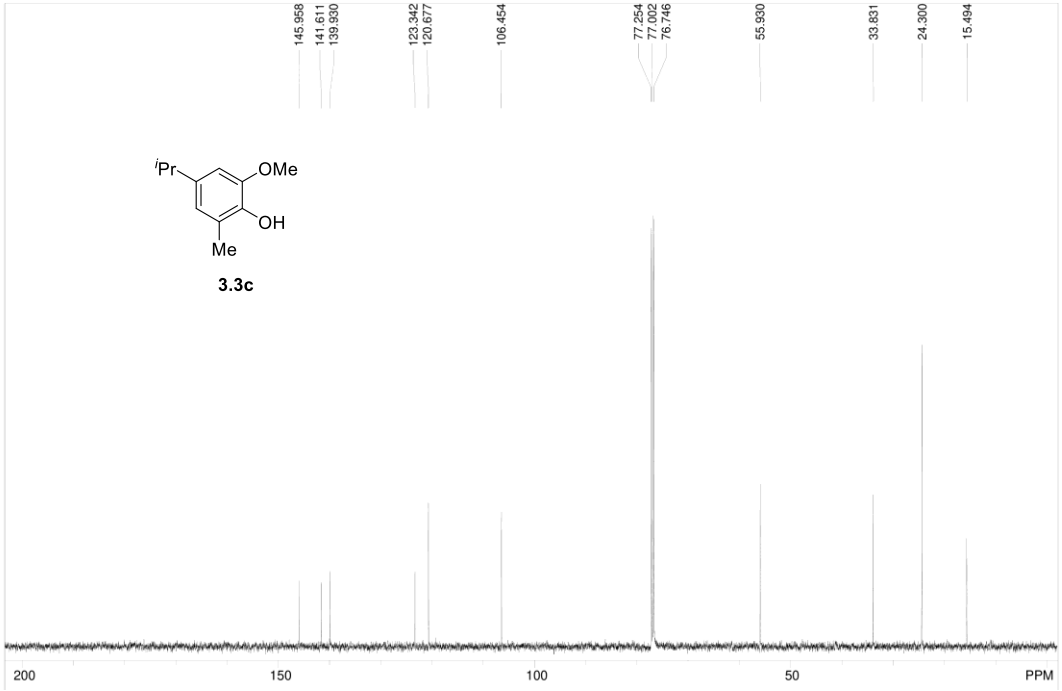

**Figure 3.142.** $^{1}$H-NMR Spectrum of **3.4c** in $CDCl_3$, 500 MHz

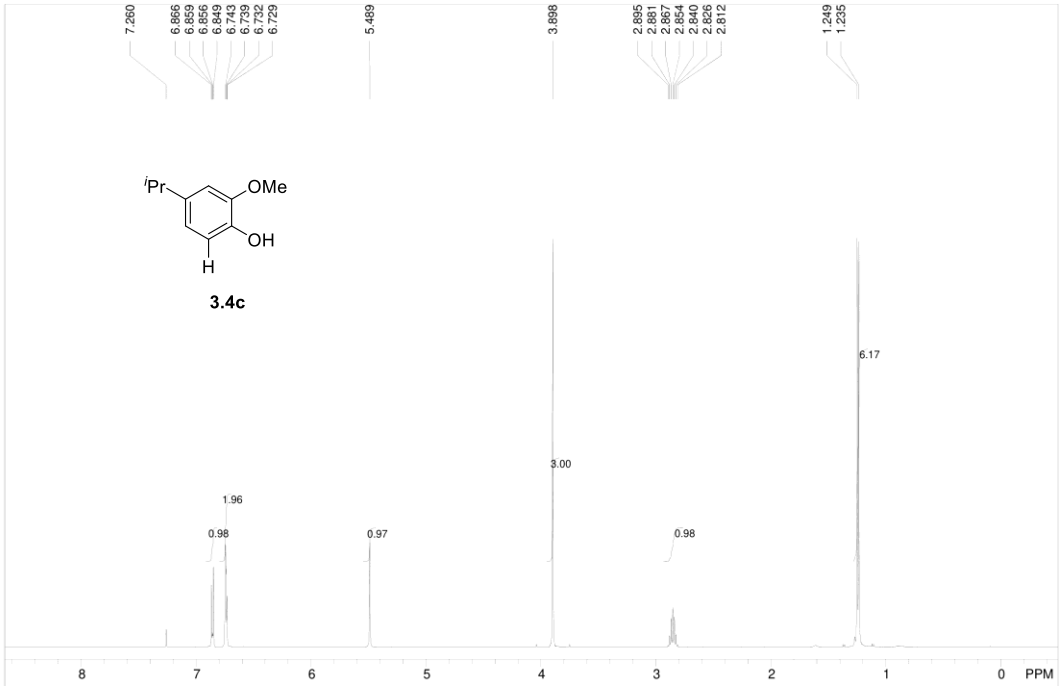


**Figure 3.143.** $^{13}$C-NMR Spectrum of **3.4c** in $CDCl_3$, 126 MHz

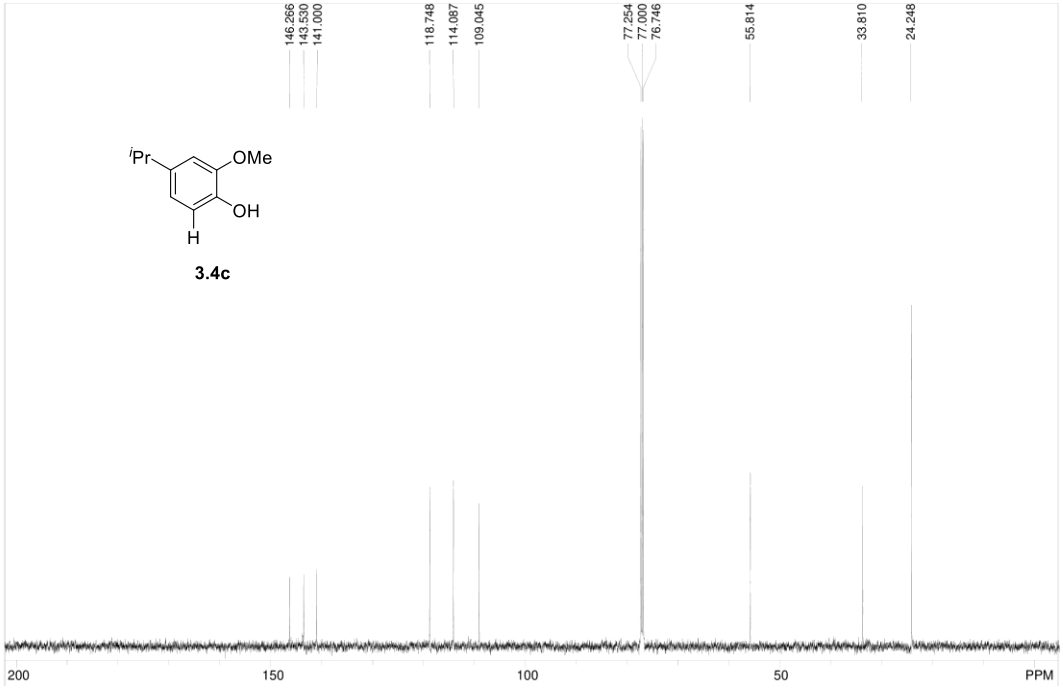

**Figure 3.144.** $^{1}$H-NMR Spectrum of **3.3d** in $CDCl_3$, 500 MHz

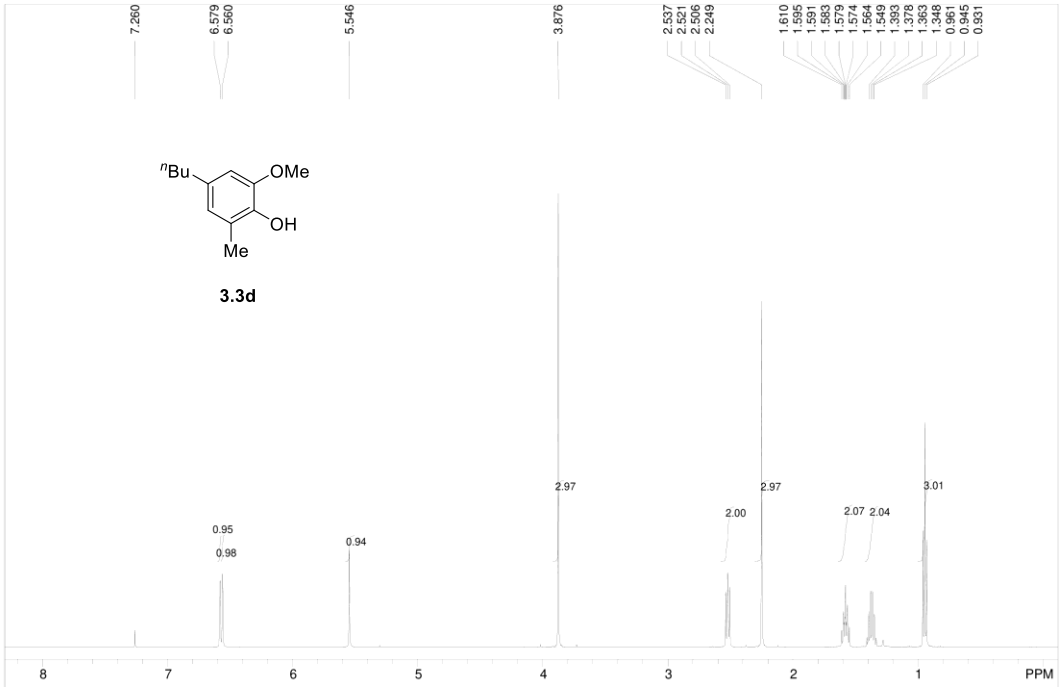


**Figure 3.145.** $^{13}$C-NMR Spectrum of **3.3d** in $CDCl_3$, 126 MHz

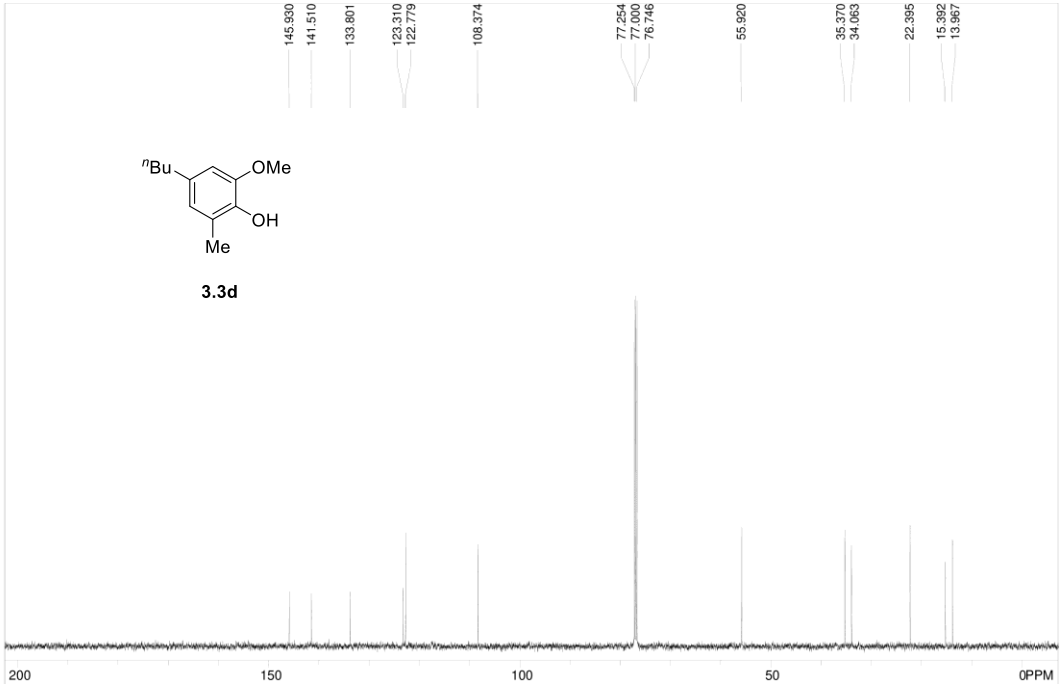

**Figure 3.146.** $^{1}$H-NMR Spectrum of **3.4d** in $CDCl_3$, 500 MHz

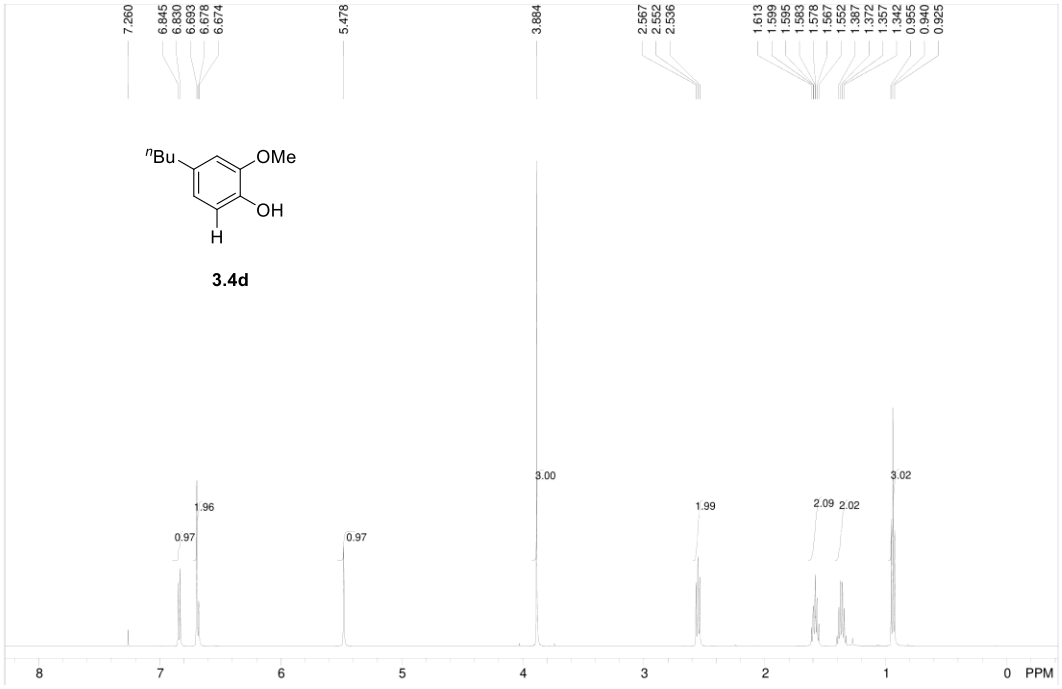


**Figure 3.147.** $^{13}$C-NMR Spectrum of **3.4d** in $CDCl_3$, 126 MHz

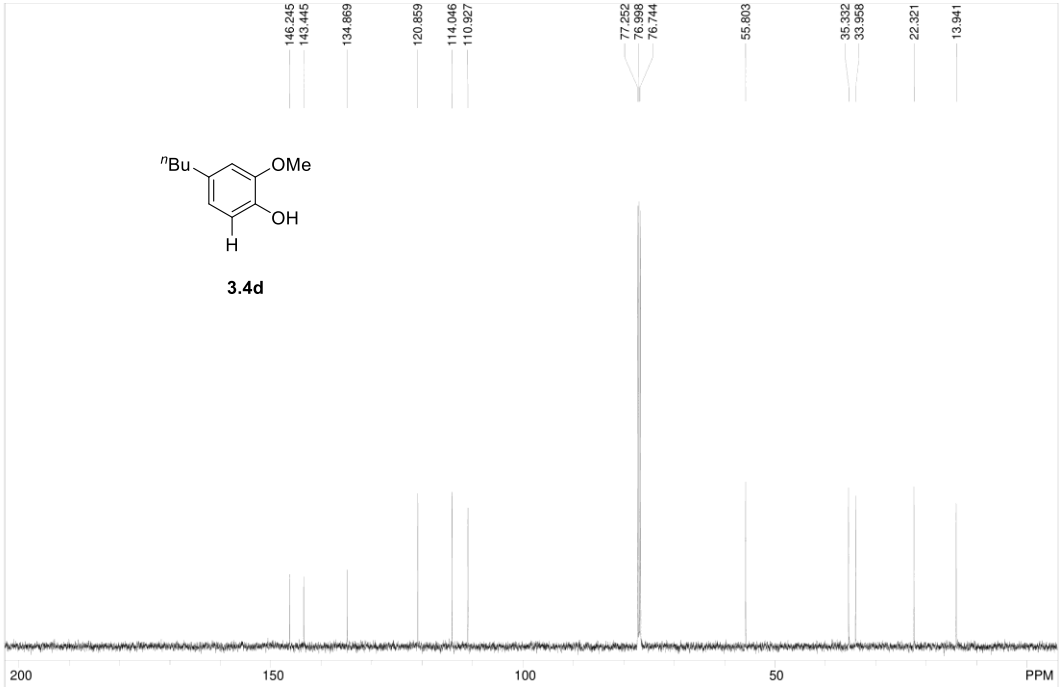

**Figure 3.148.** $^{1}$H-NMR Spectrum of **3.3e** in $CDCl_3$, 500 MHz

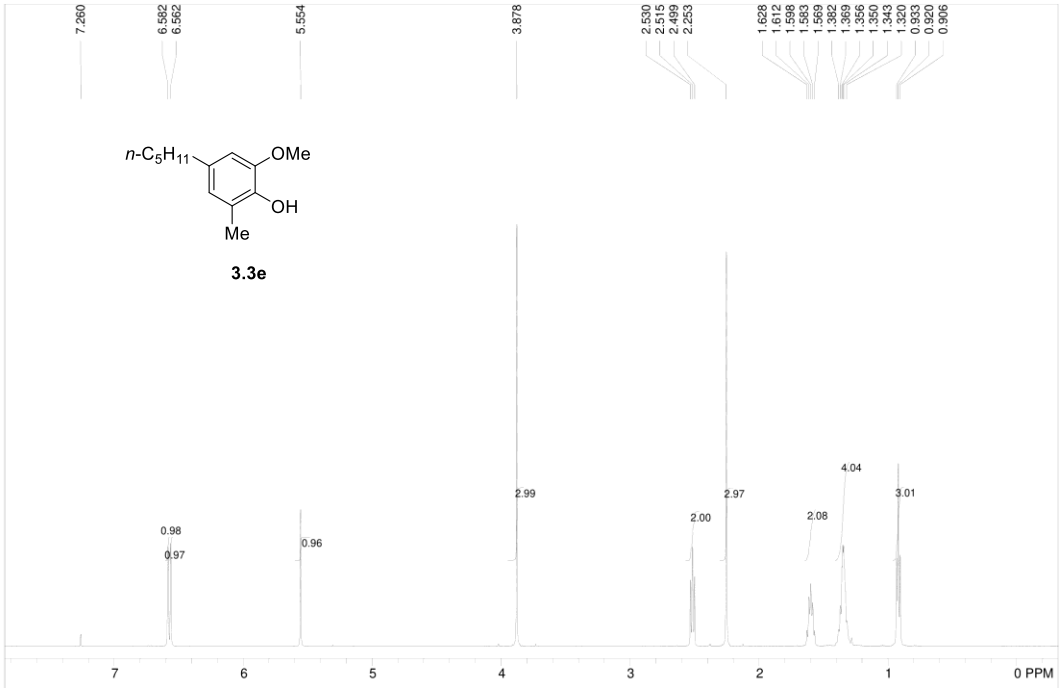


**Figure 3.149.** $^{13}$C-NMR Spectrum of **3.3e** in $CDCl_3$, 126 MHz

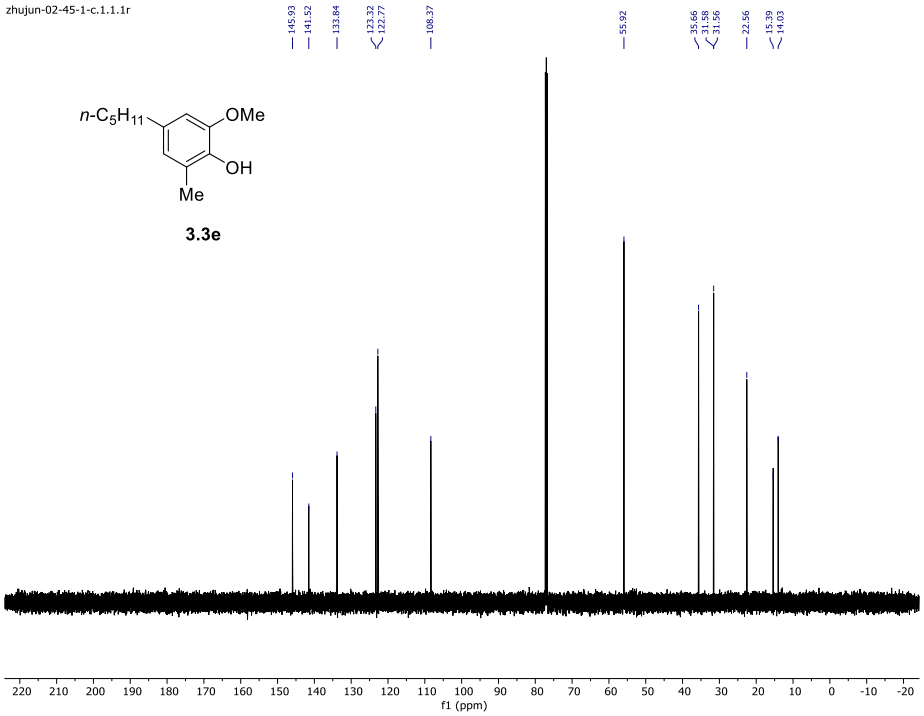

**Figure 3.150.** $^{1}$H-NMR Spectrum of **3.4e** in $CDCl_3$, 500 MHz

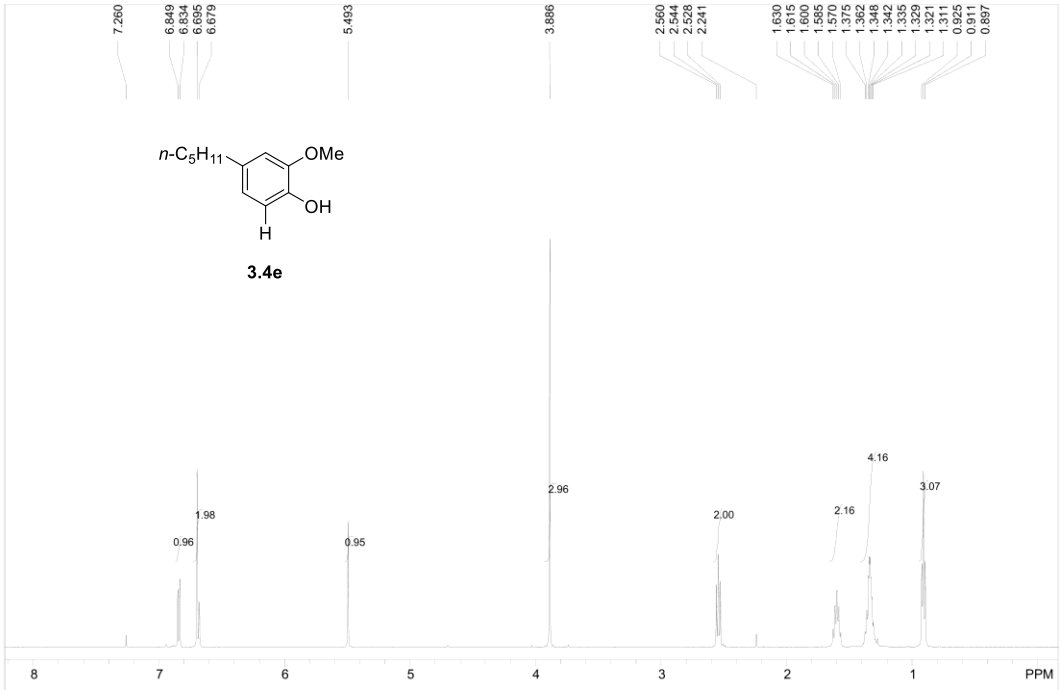


**Figure 3.151.** $^{13}$C-NMR Spectrum of **3.4e** in $CDCl_3$, 126 MHz

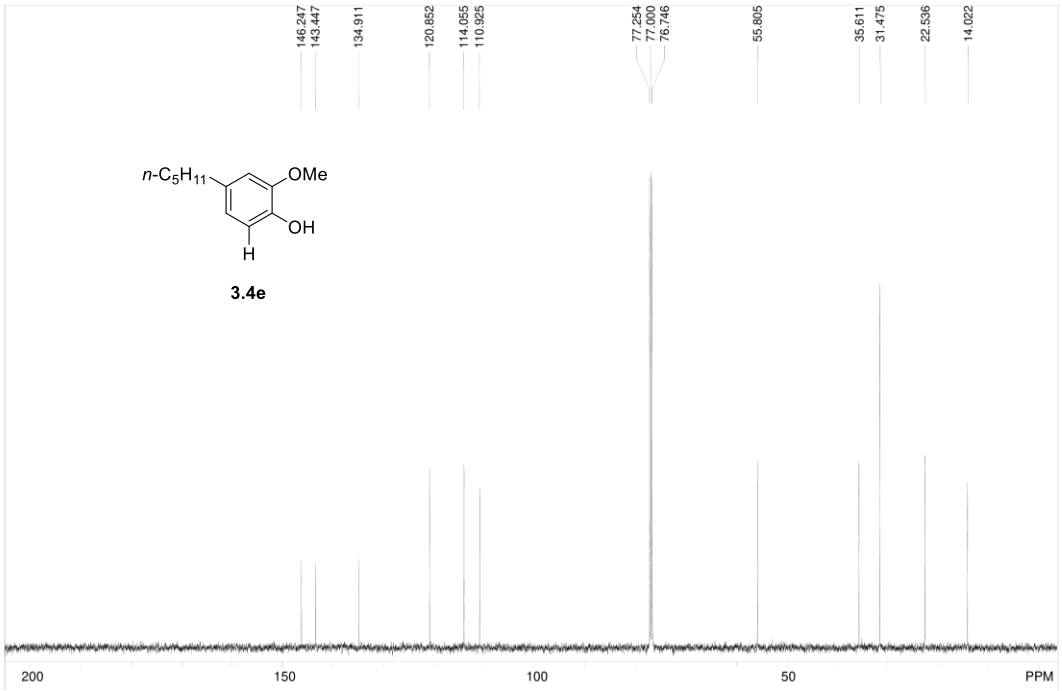

**Figure 3.152.** $^{1}$H-NMR Spectrum of **3.3f** in $CDCl_3$, 500 MHz

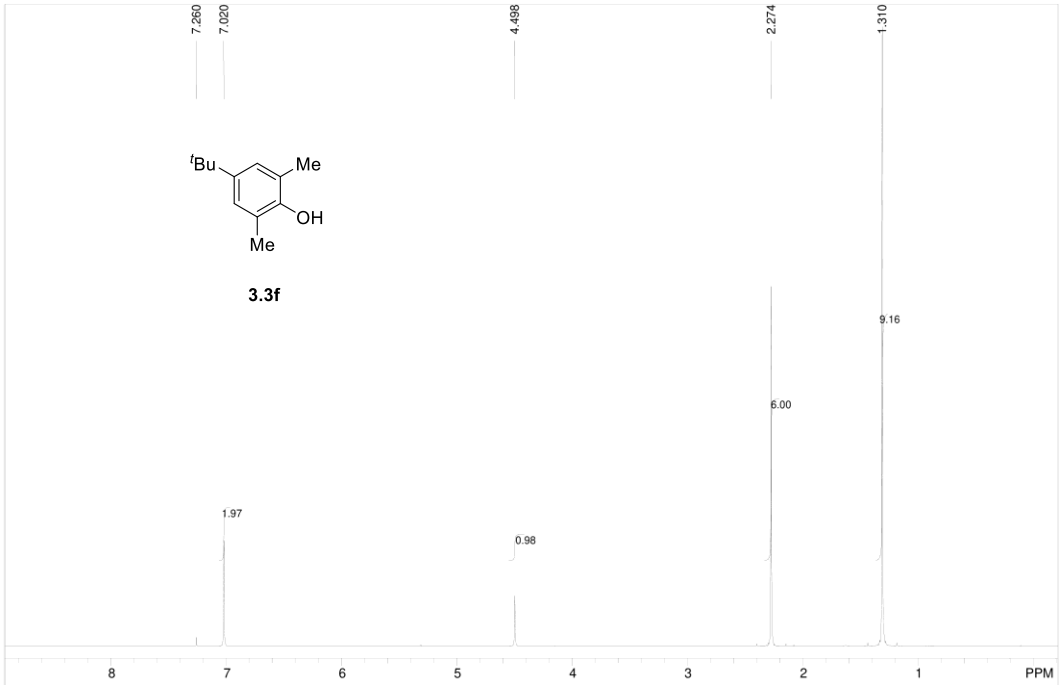


**Figure 3.153.** $^{13}$C-NMR Spectrum of **3.3f** in $CDCl_3$, 126 MHz

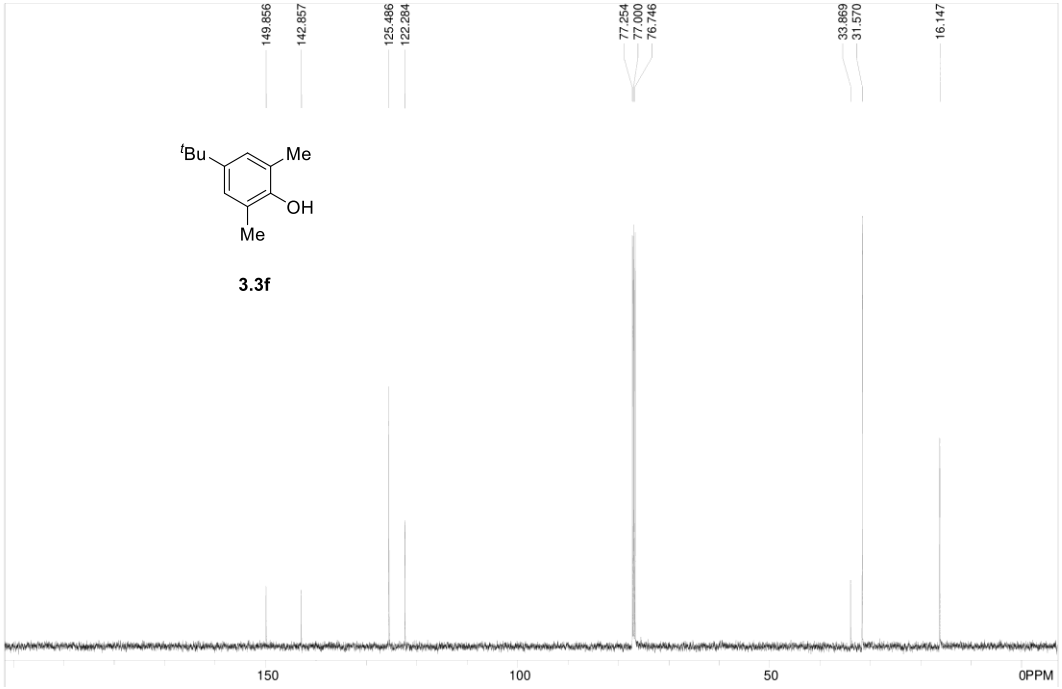

**Figure 3.154.** $^{1}$H-NMR Spectrum of **3.4f** in $CDCl_3$, 500 MHz

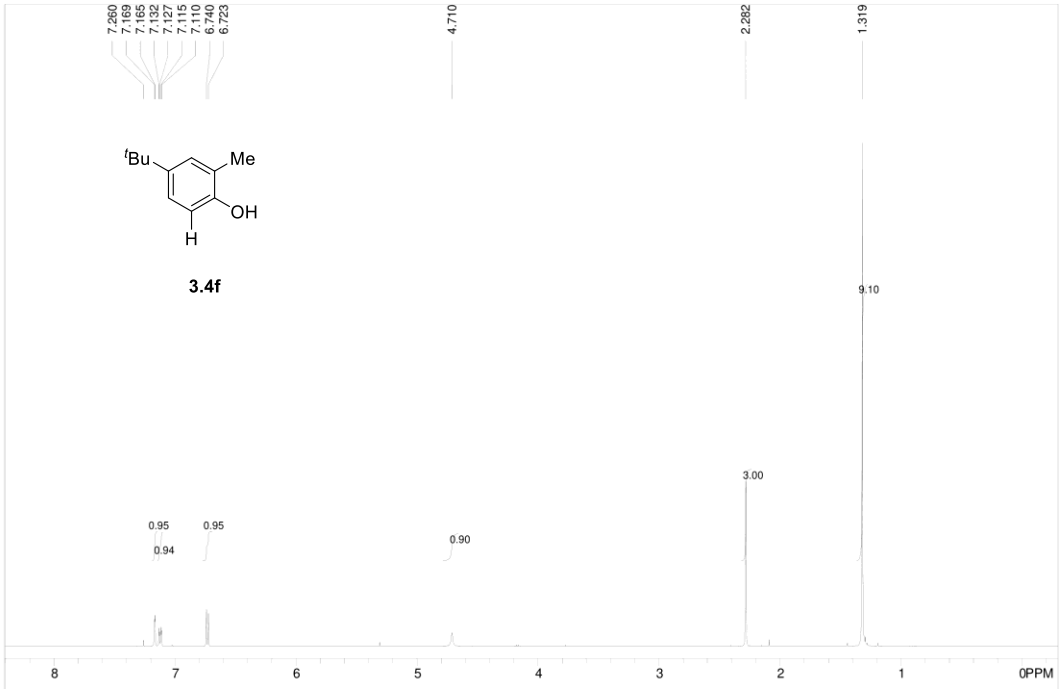


**Figure 3.155.** $^{13}$C-NMR Spectrum of **3.4f** in $CDCl_3$, 126 MHz

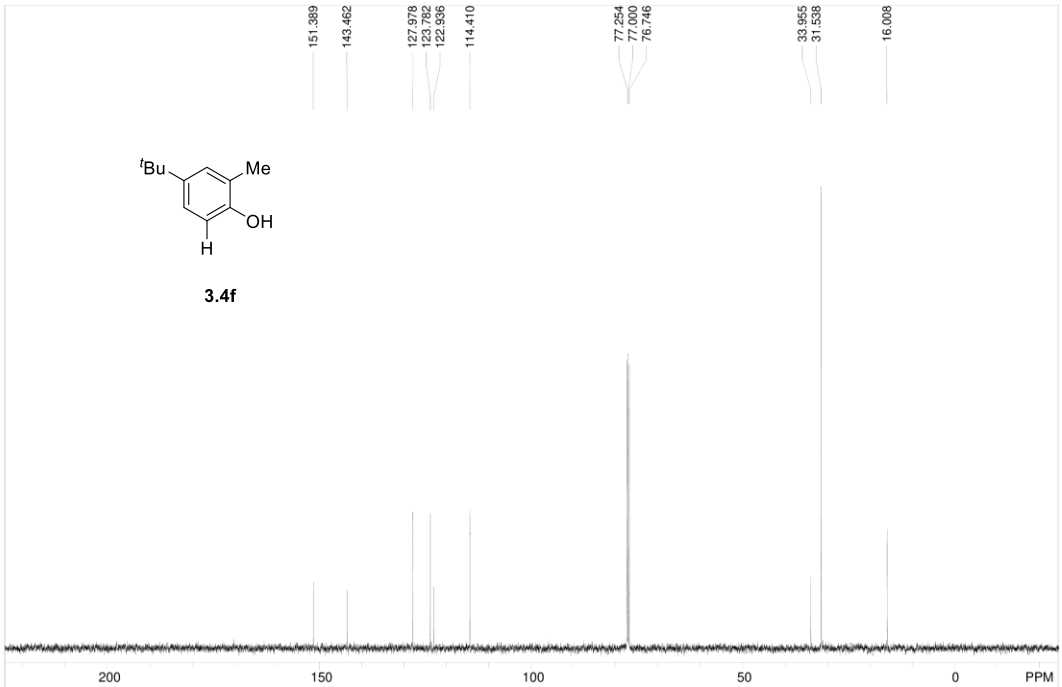

**Figure 3.156.** $^{1}$H-NMR Spectrum of **3.3g** in $CDCl_3$, 500 MHz

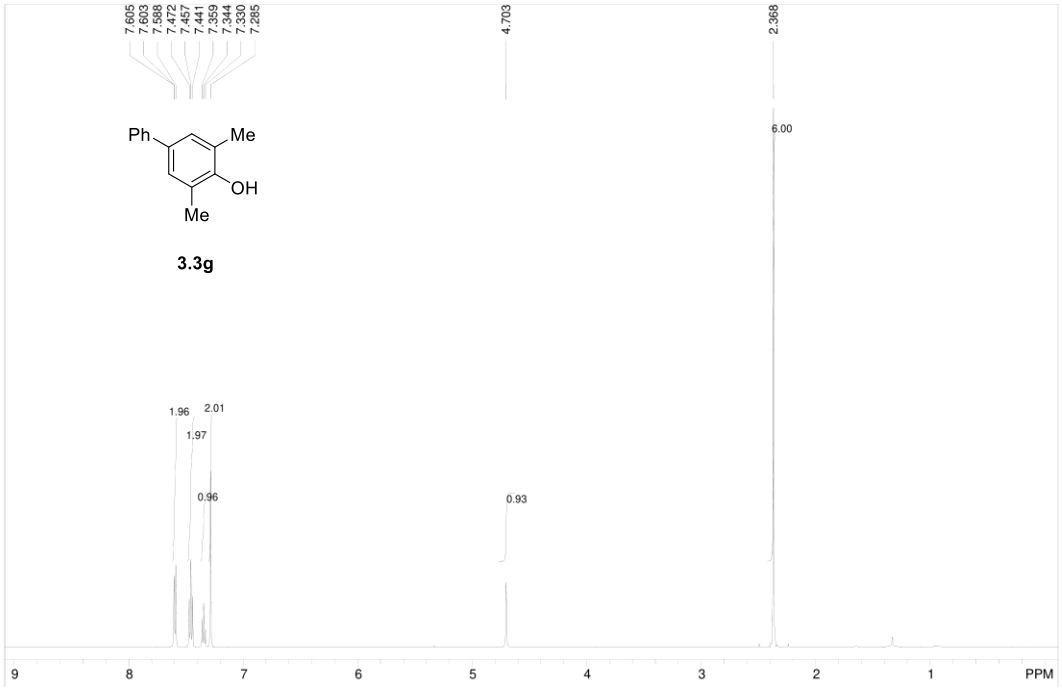


**Figure 3.157.** $^{13}$C-NMR Spectrum of **3.3g** in $CDCl_3$, 126 MHz

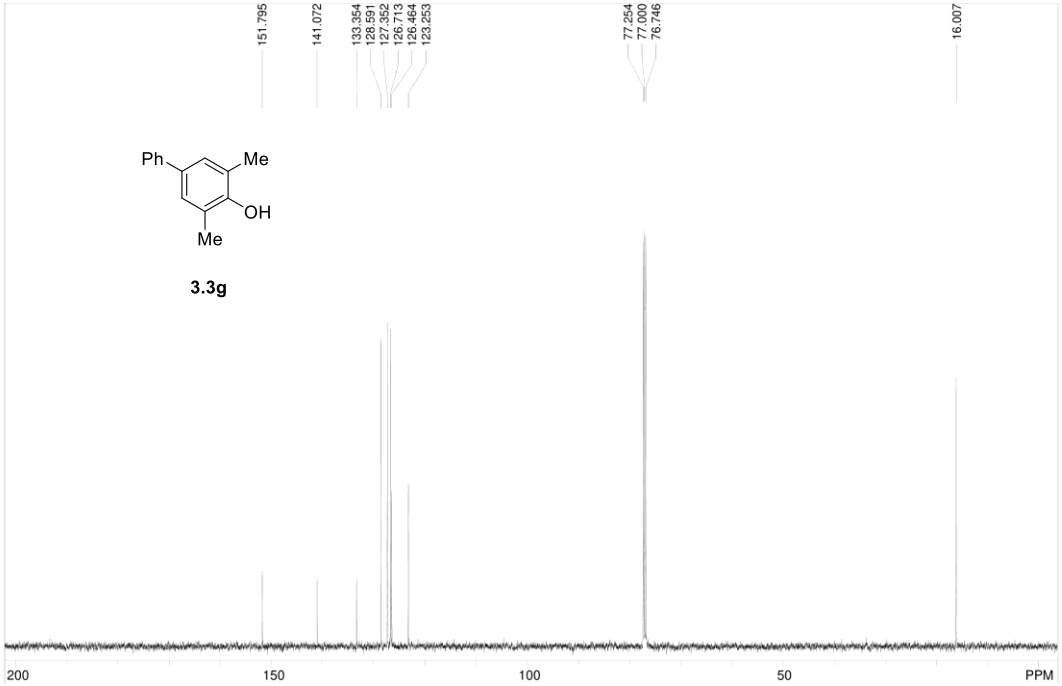

**Figure 3.158.** $^{1}$H-NMR Spectrum of **3.4g** in $CDCl_3$, 500 MHz

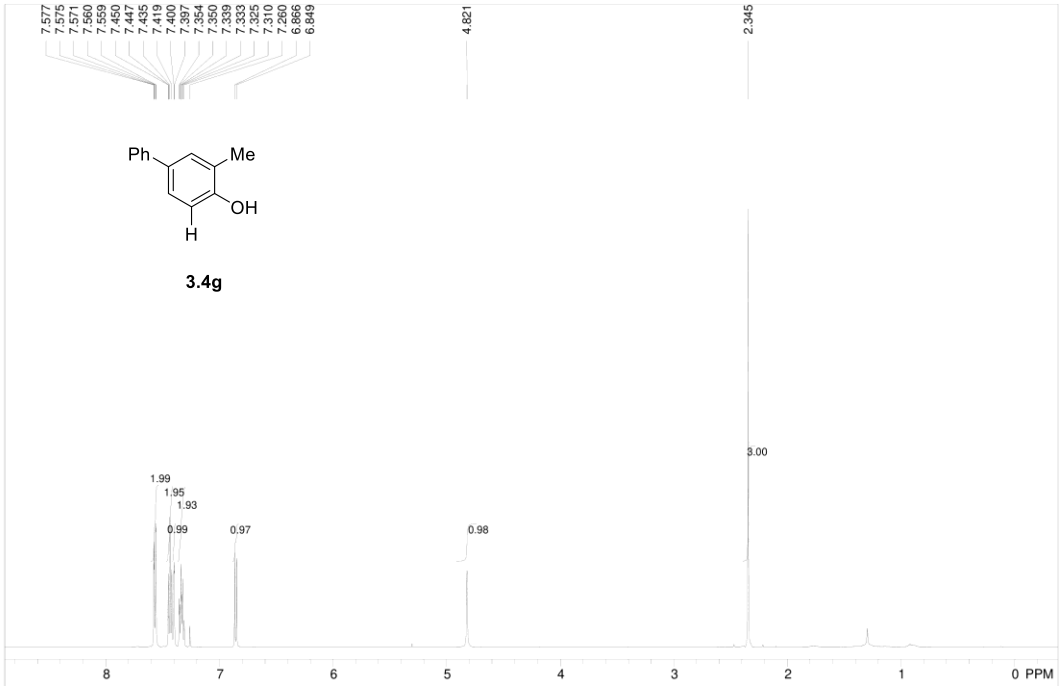


**Figure 3.159.** $^{13}$C-NMR Spectrum of **3.4g** in $CDCl_3$, 126 MHz

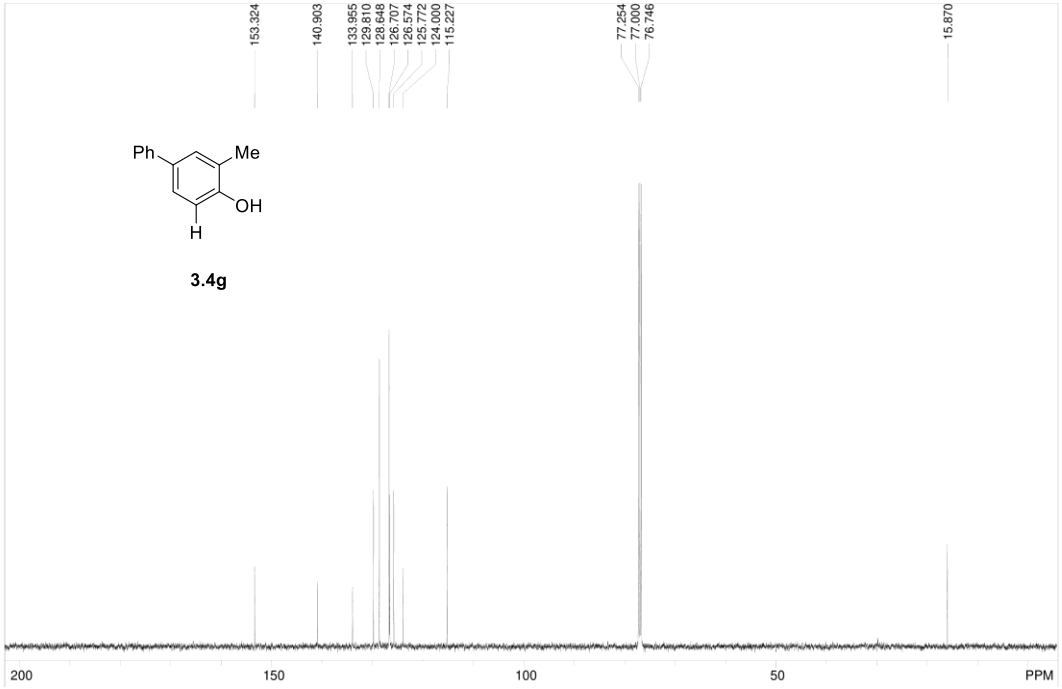

**Figure 3.160.** $^{1}$H-NMR Spectrum of **3.3h** in $CDCl_3$, 400 MHz

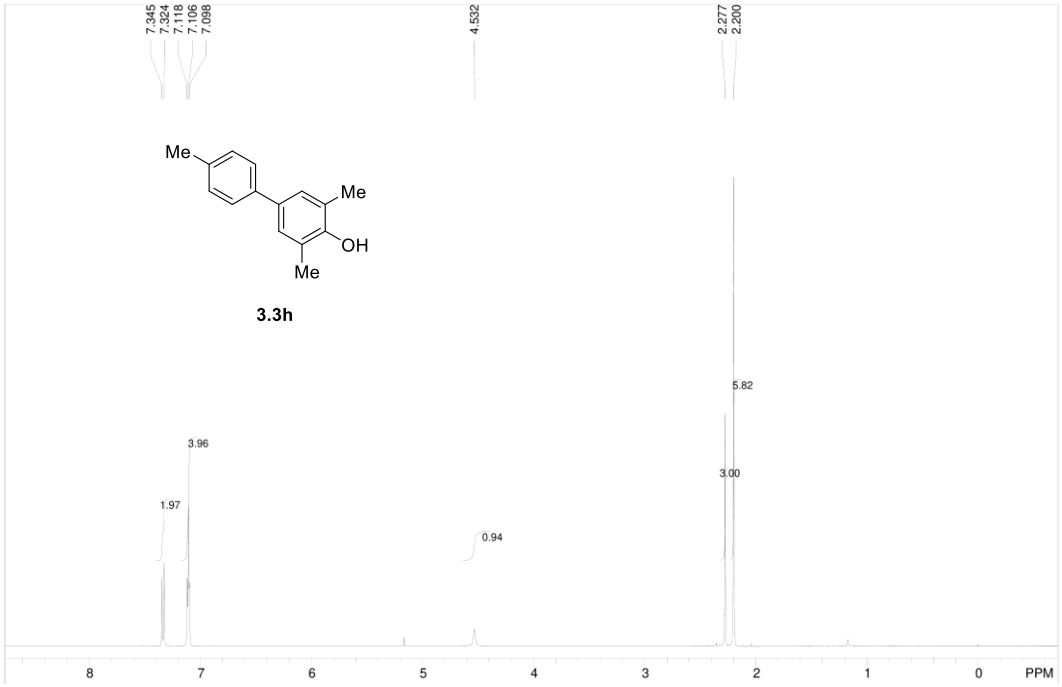


**Figure 3.161.** $^{13}$C-NMR Spectrum of **3.3h** in $CDCl_3$, 101 MHz

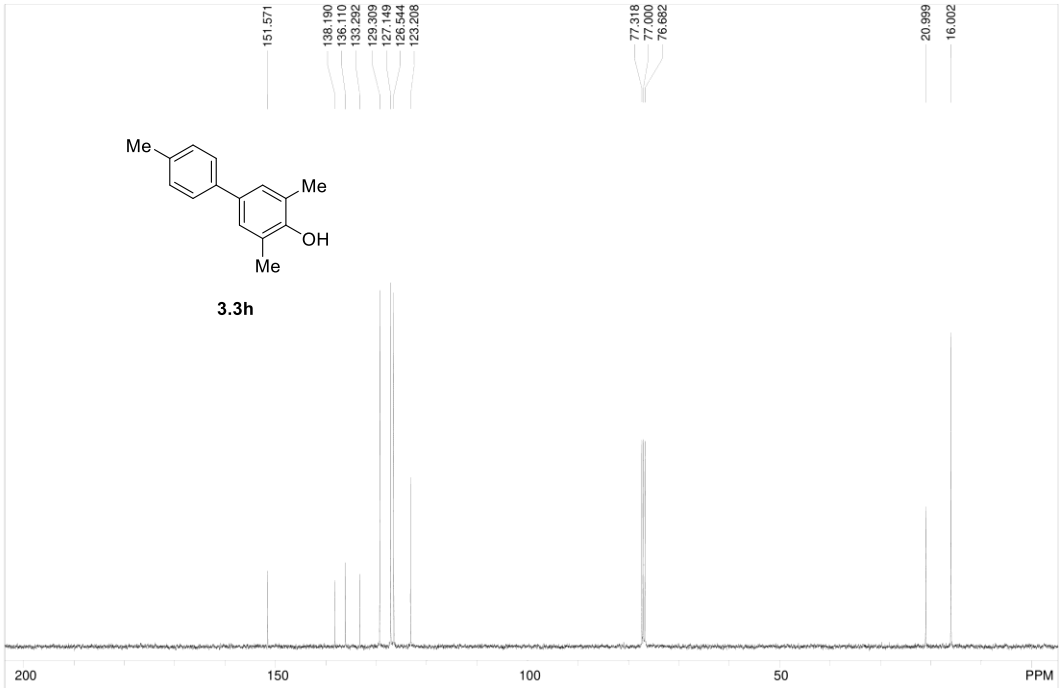

**Figure 3.162.** $^{1}$H-NMR Spectrum of **3.4h** in $CDCl_3$, 400 MHz

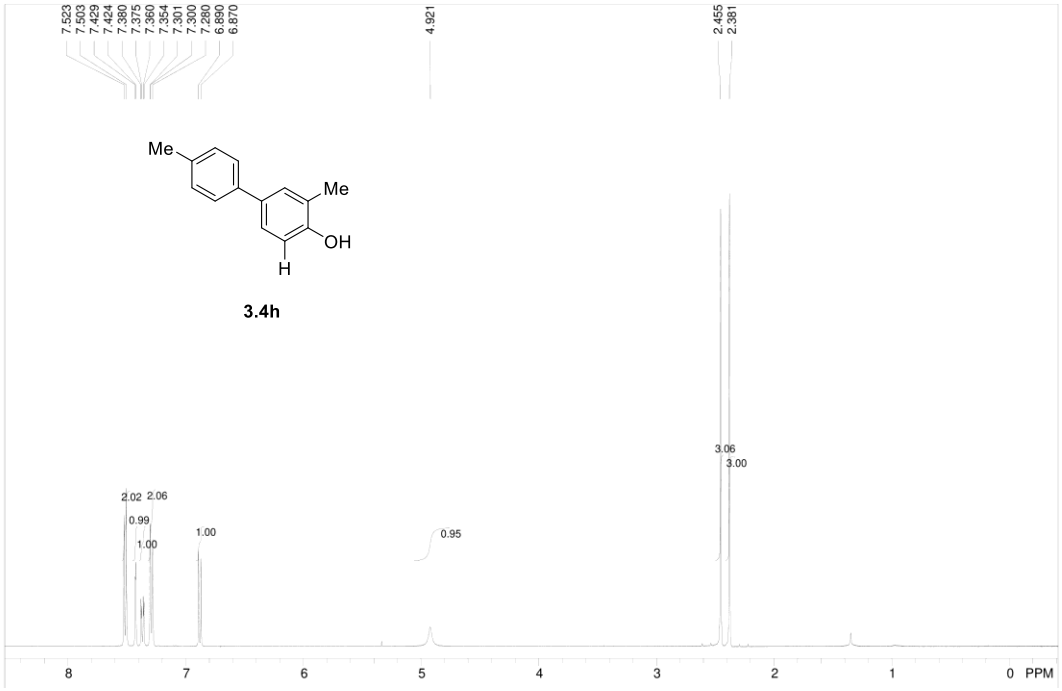


**Figure 3.163.** $^{13}$C-NMR Spectrum of **3.4h** in $CDCl_3$, 101 MHz

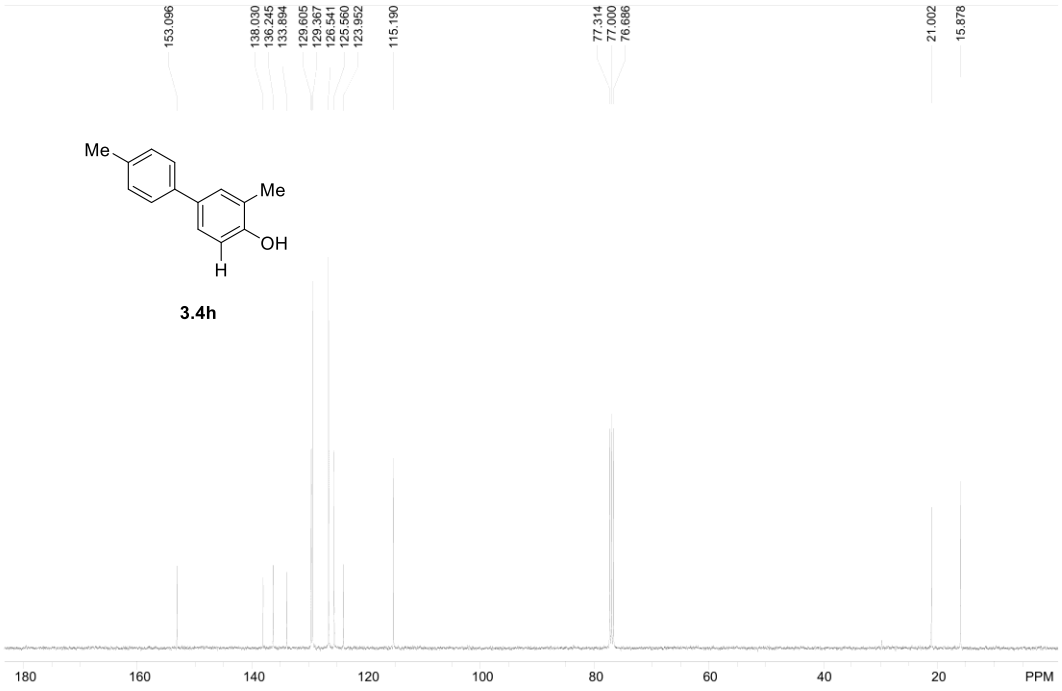

**Figure 3.164.** $^{1}$H-NMR Spectrum of **3.3i** in $CDCl_3$, 500 MHz

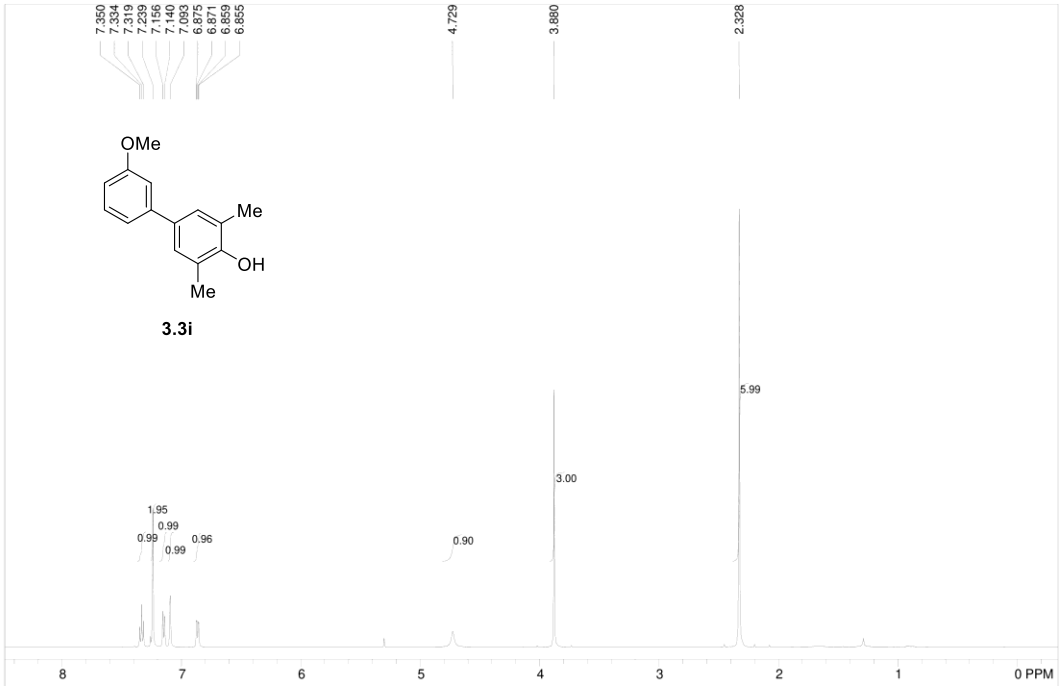


**Figure 3.165.** $^{13}$C-NMR Spectrum of **3.3i** in $CDCl_3$, 126 MHz

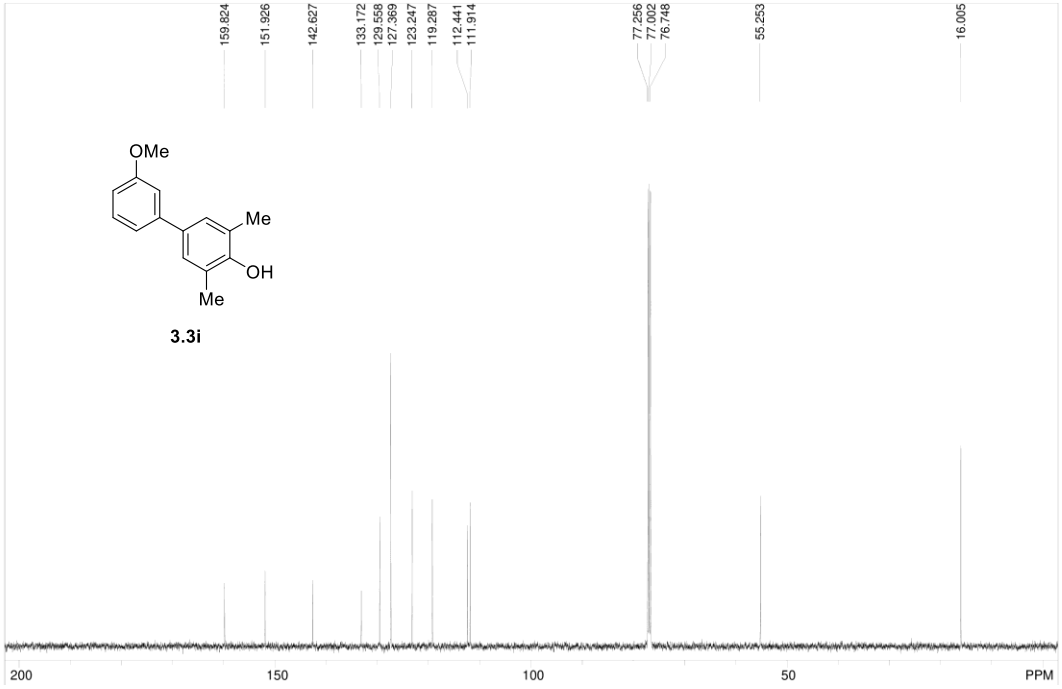

**Figure 3.166.** $^{1}$H-NMR Spectrum of **3.4i** in $CDCl_3$, 500 MHz

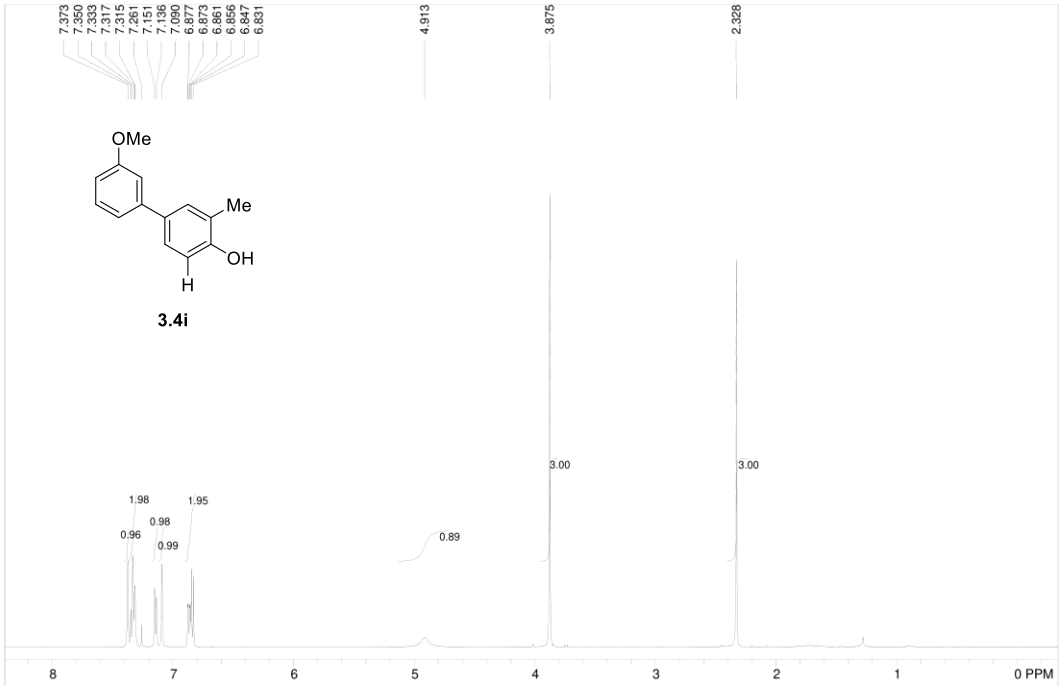


**Figure 3.167.** $^{13}$C-NMR Spectrum of **3.4i** in $CDCl_3$, 126 MHz

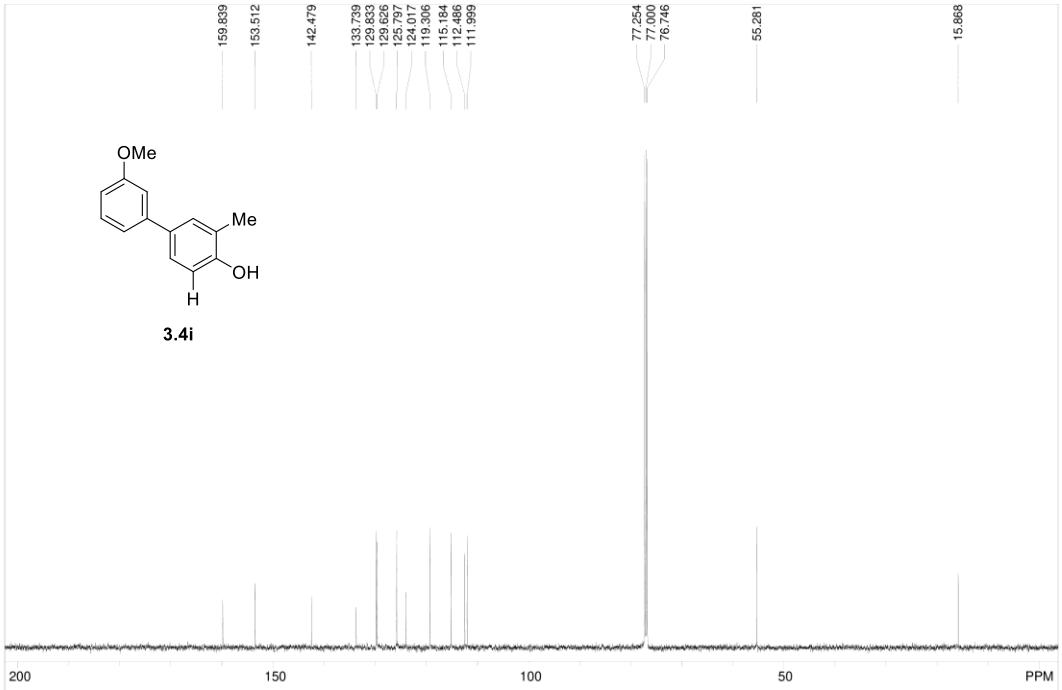

**Figure 3.168.** $^{1}$H-NMR Spectrum of **3.3j** in $CDCl_3$, 500 MHz

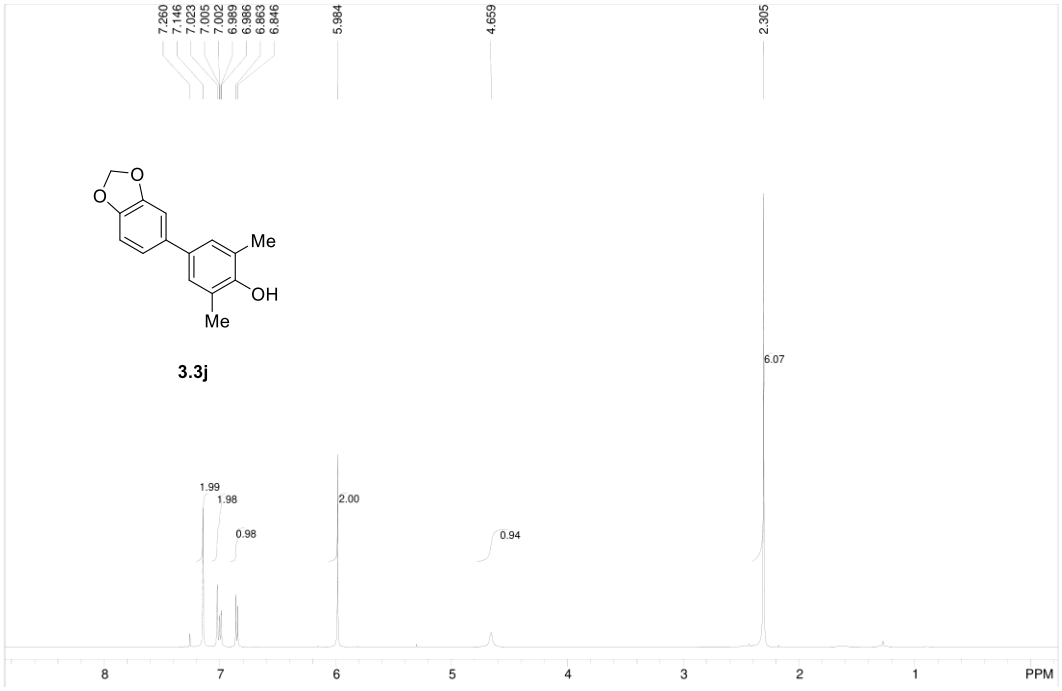


**Figure 3.169.** $^{13}$C-NMR Spectrum of **3.3j** in $CDCl_3$, 126 MHz

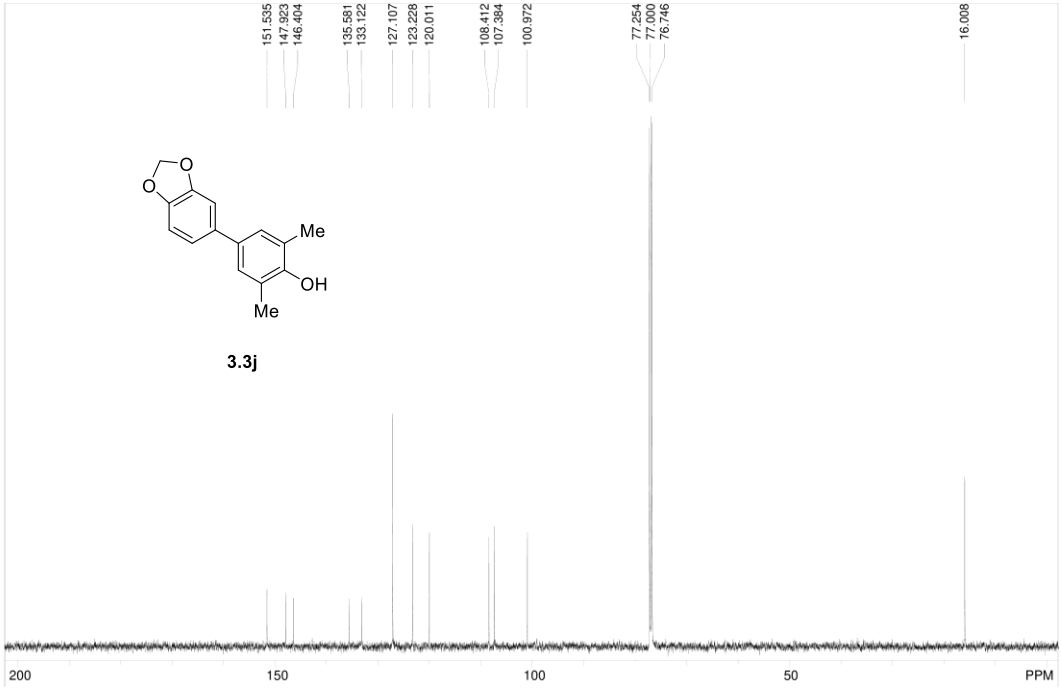

**Figure 3.170.** $^{1}$H-NMR Spectrum of **3.4j** in $CDCl_3$, 400 MHz

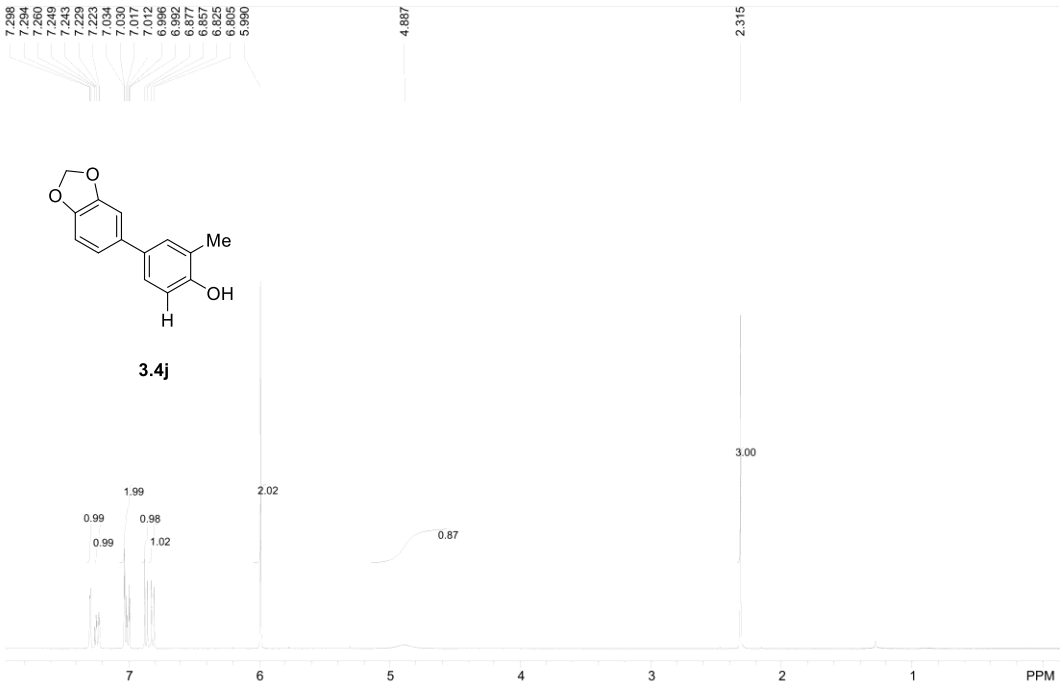


**Figure 3.171.** $^{13}$C-NMR Spectrum of **3.4j** in $CDCl_3$, 126 MHz

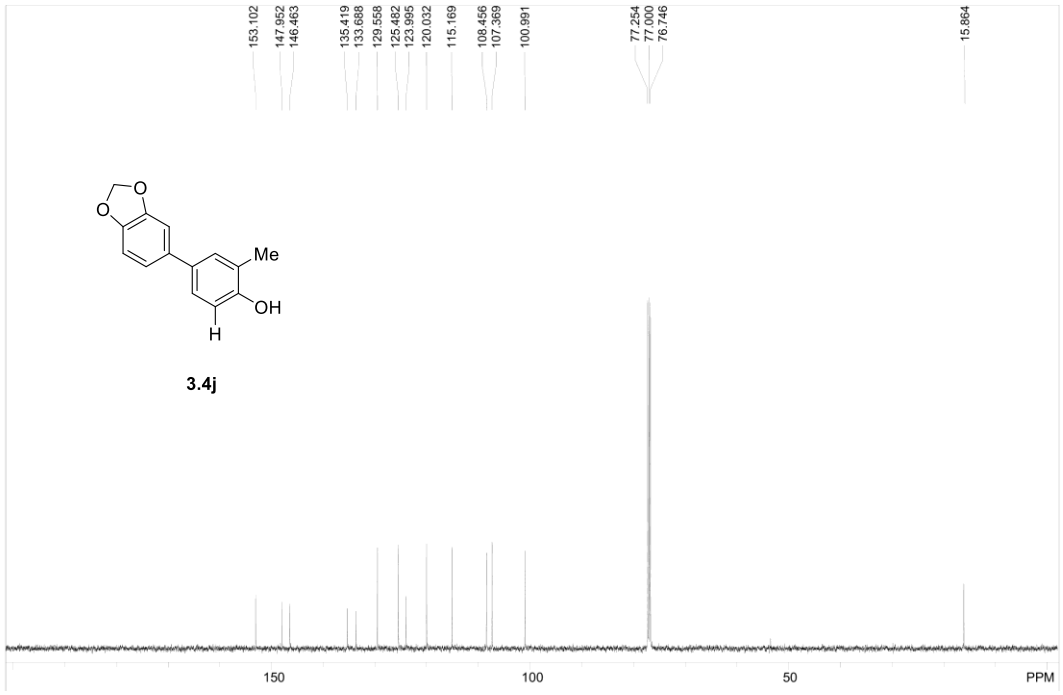

**Figure 3.172.** $^{1}$H-NMR Spectrum of **3.3k** in $CDCl_3$, 500 MHz

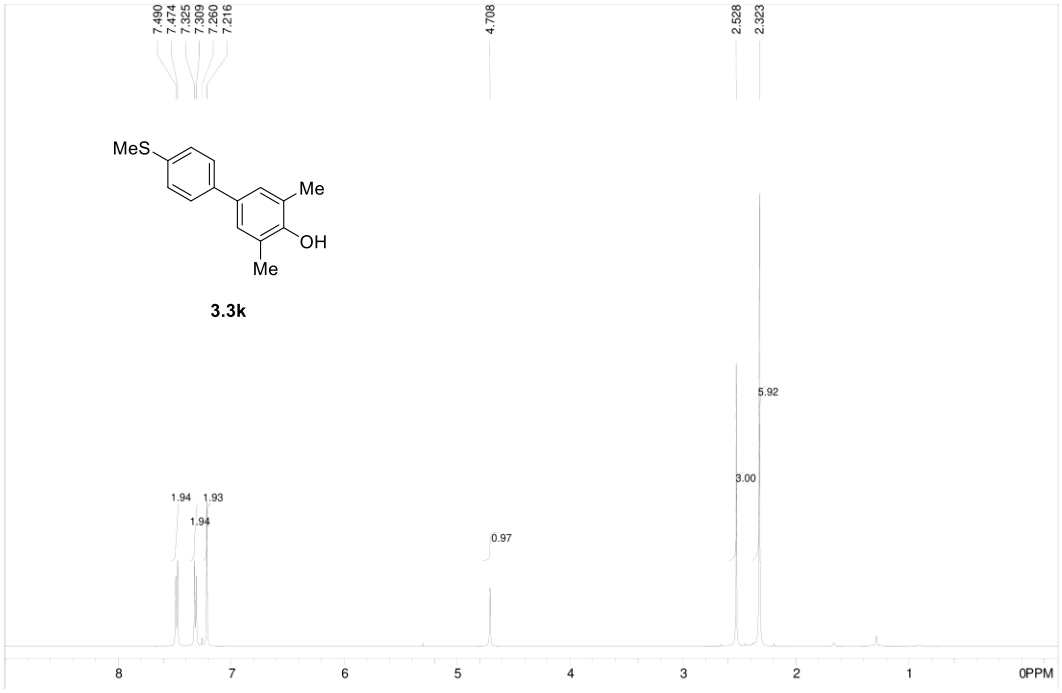


**Figure 3.173.** $^{13}$C-NMR Spectrum of **3.3k** in $CDCl_3$, 126 MHz

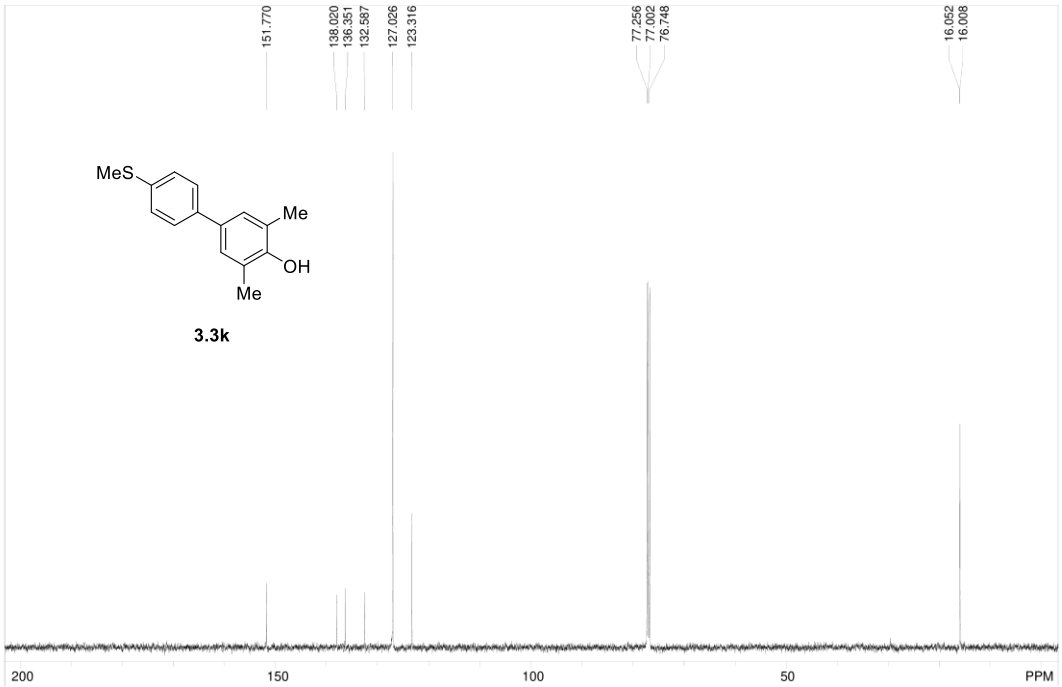

**Figure 3.174.** $^{1}$H-NMR Spectrum of **3.4k** in $CDCl_3$, 500 MHz

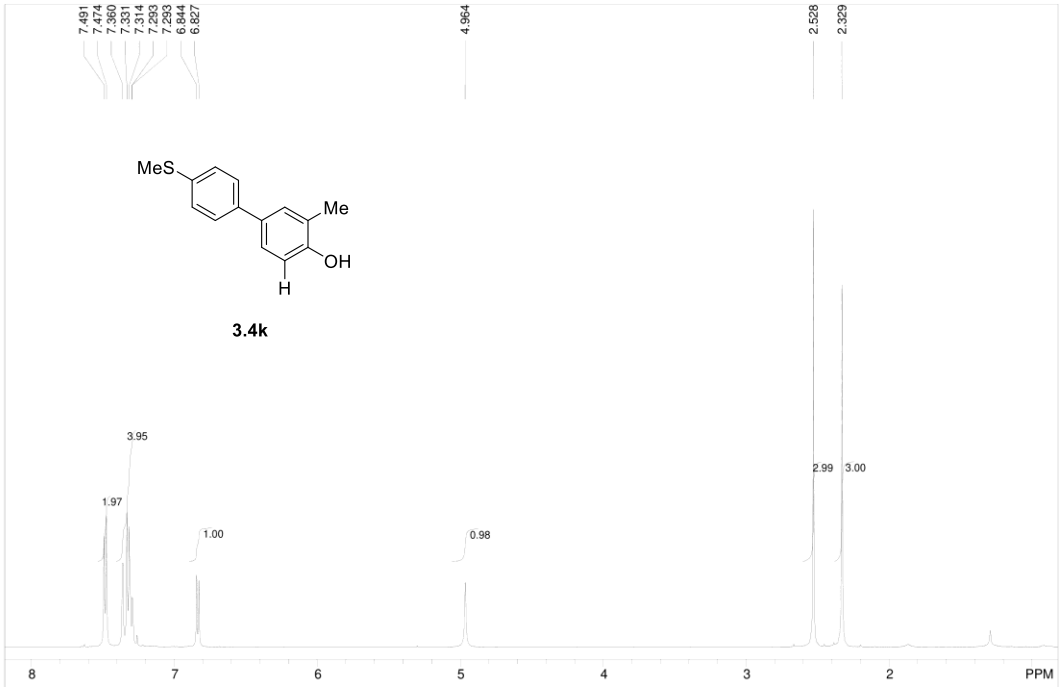


**Figure 3.175.** $^{13}$C-NMR Spectrum of **3.4k** in $CDCl_3$, 126 MHz

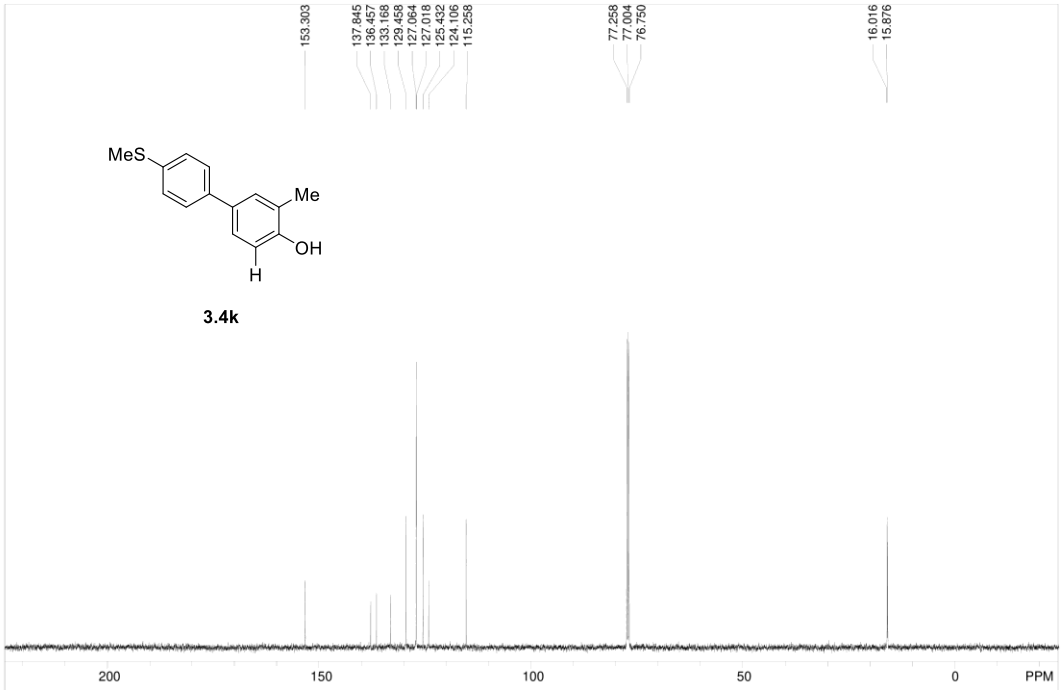

**Figure 3.176.** $^{1}$H-NMR Spectrum of **3.3l** in $CDCl_3$, 500 MHz

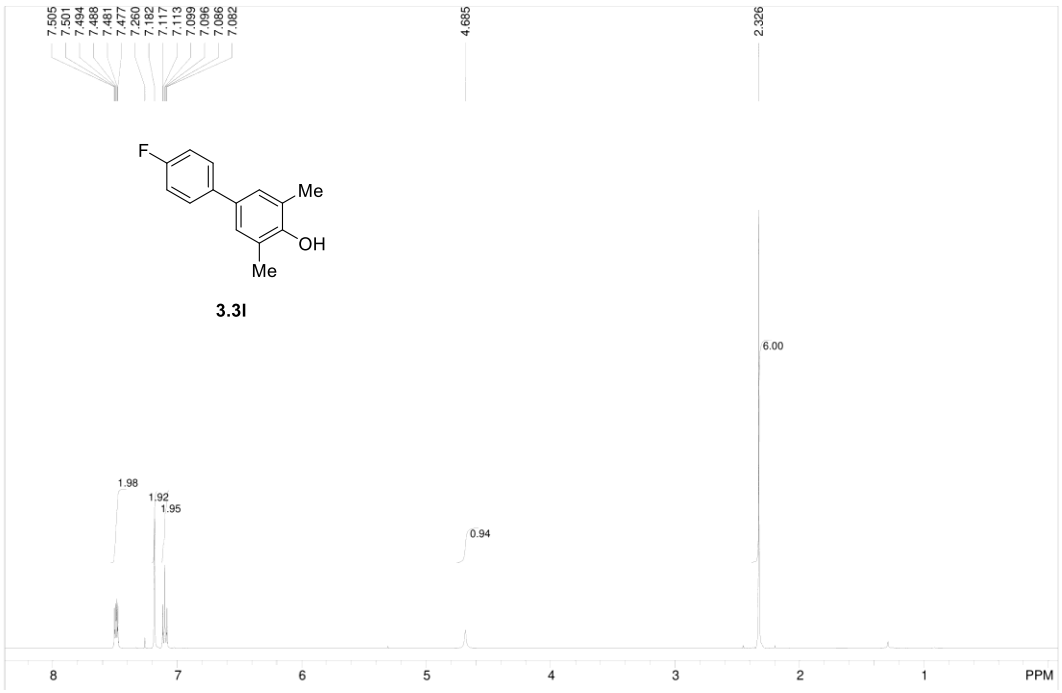


**Figure 3.177.** $^{13}$C-NMR Spectrum of **3.3l** in $CDCl_3$, 126 MHz

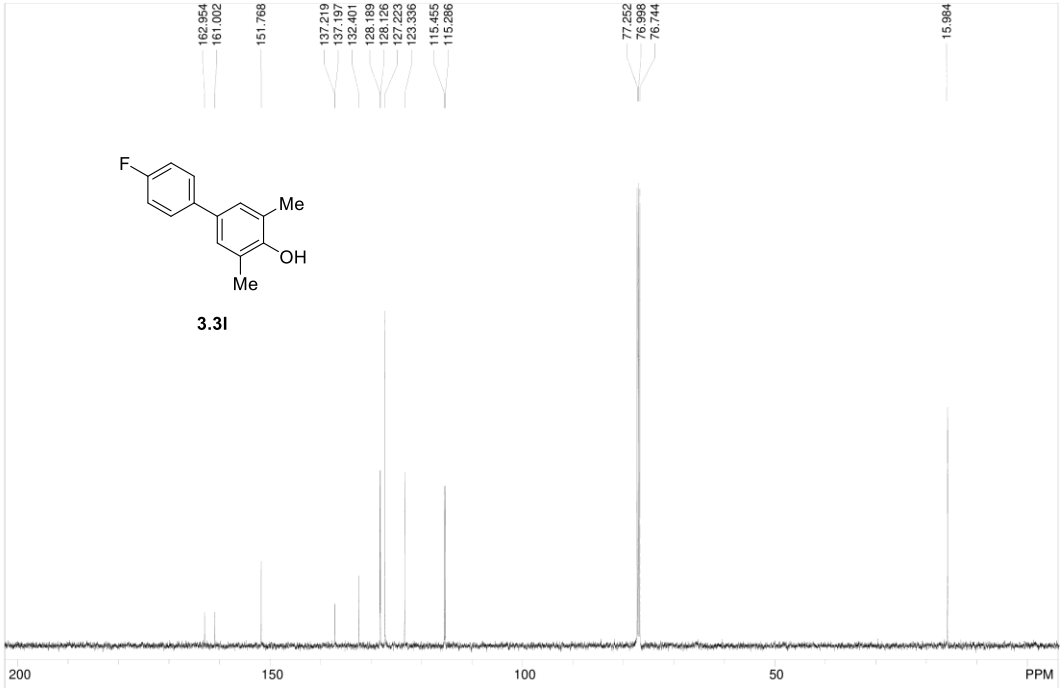

**Figure 3.178.** $^{19}$F-NMR Spectrum of **3.3l** in $CDCl_3$, 470 MHz

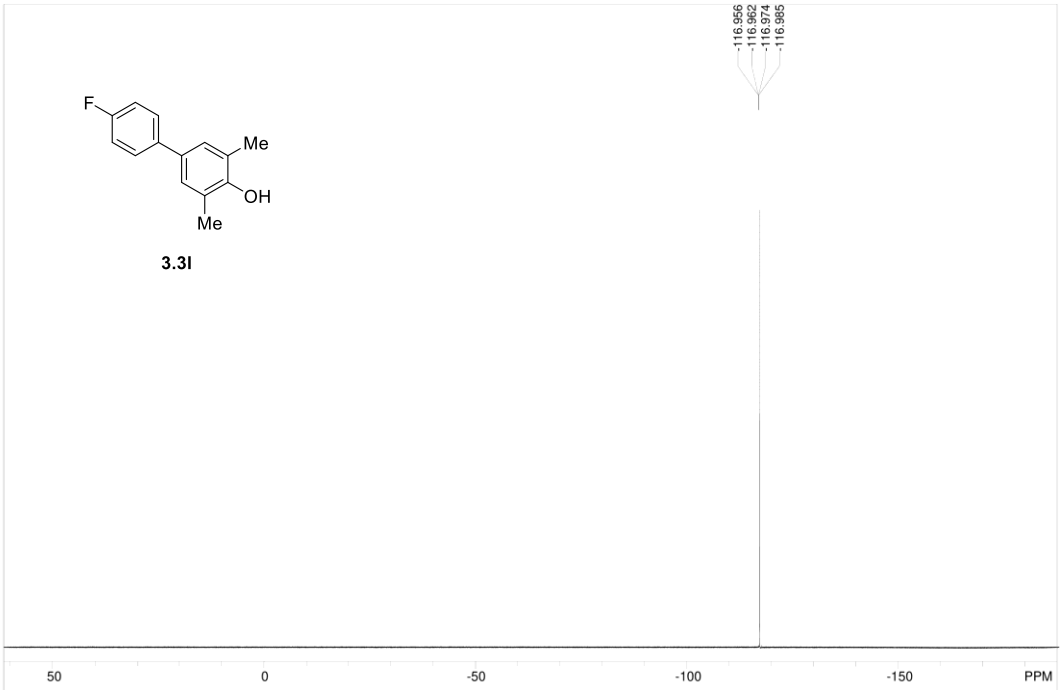

**Figure 3.179.** $^{1}$H-NMR Spectrum of **3.4l** in $CDCl_3$, 500 MHz

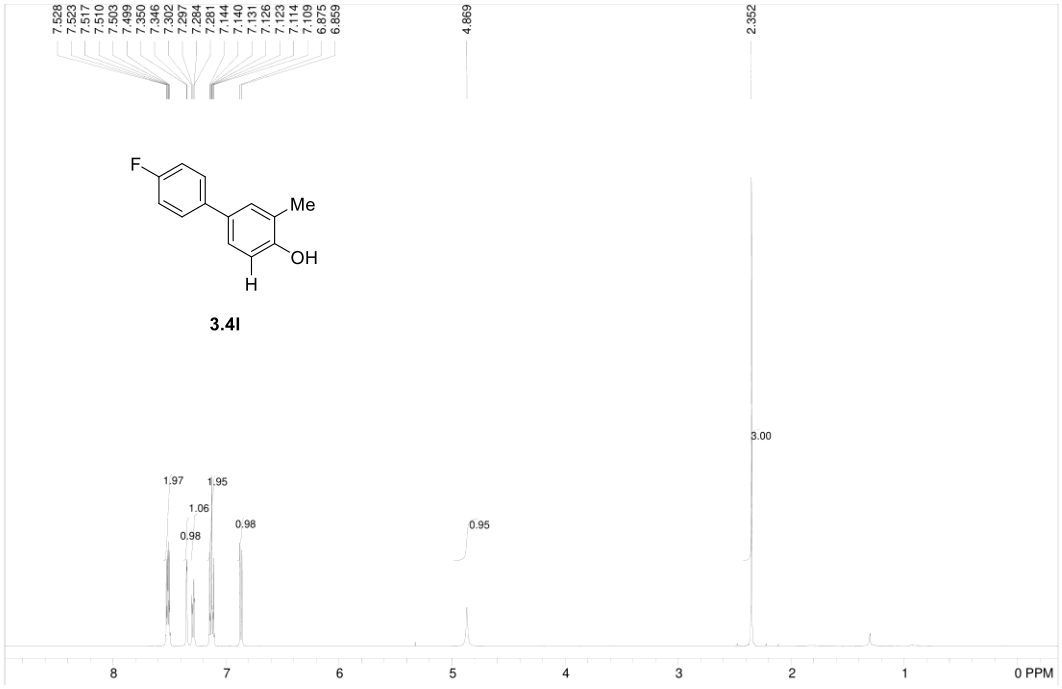


**Figure 3.180.** $^{13}$C-NMR Spectrum of **3.4l** in $CDCl_3$, 126 MHz

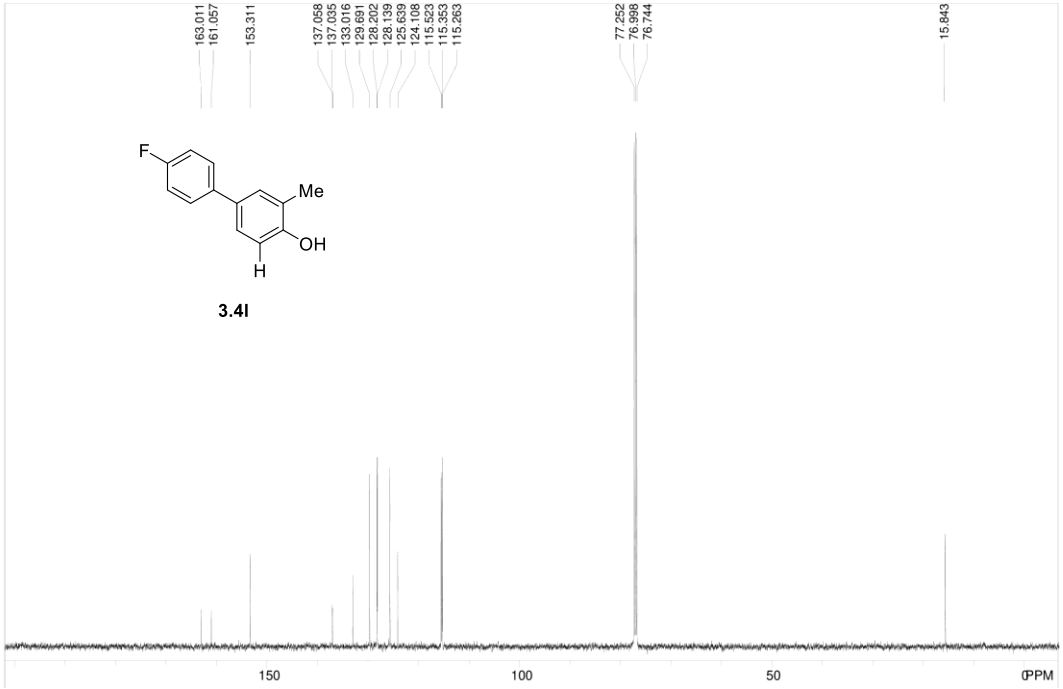

**Figure 3.181.** $^{19}$F-NMR Spectrum of **3.4l** in $CDCl_3$, 470 MHz

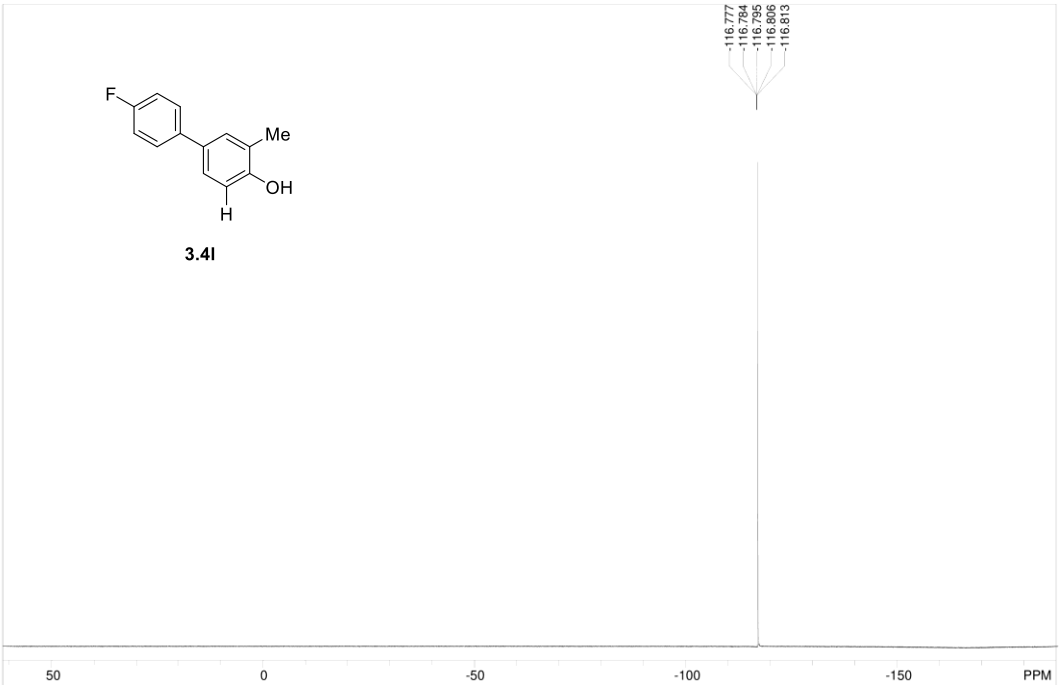

**Figure 3.182.** $^{1}$H-NMR Spectrum of **3.3m** in $CDCl_3$, 400 MHz

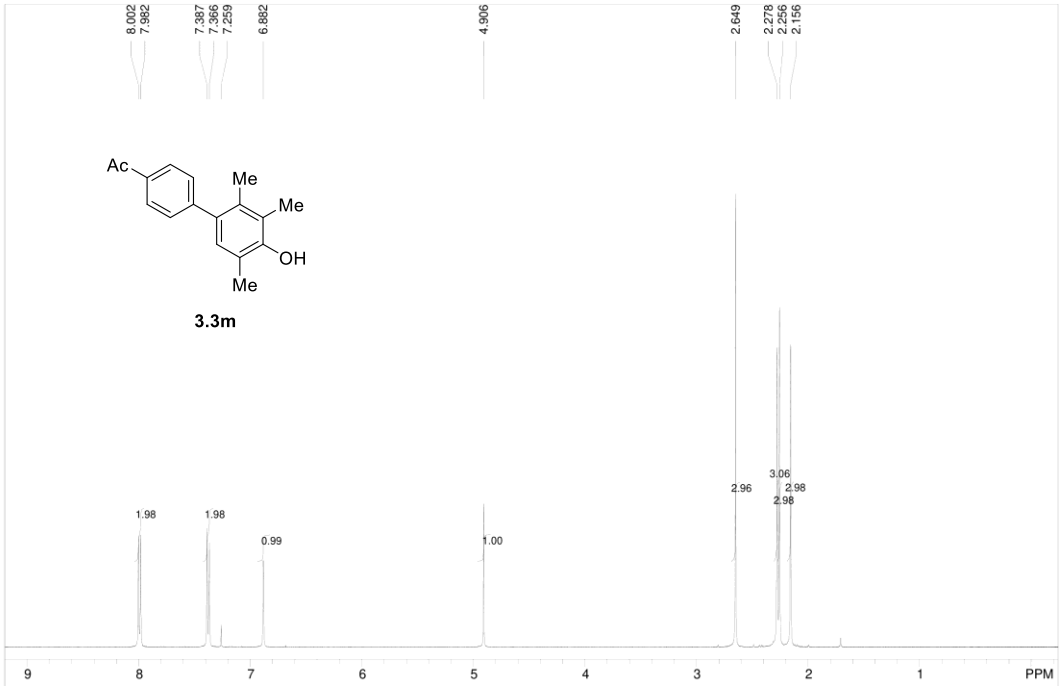


**Figure 3.183.** $^{13}$C-NMR Spectrum of **3.3m** in $CDCl_3$, 101 MHz

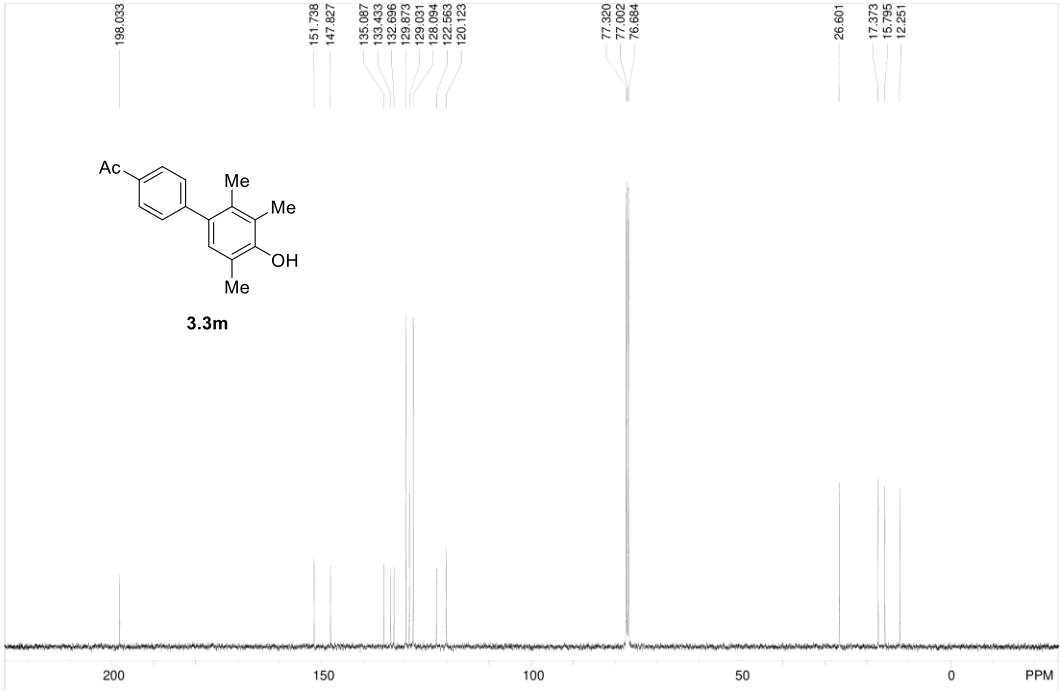

**Figure 3.184.** $^{1}$H-NMR Spectrum of **3.4m** in $CDCl_3$, 400 MHz

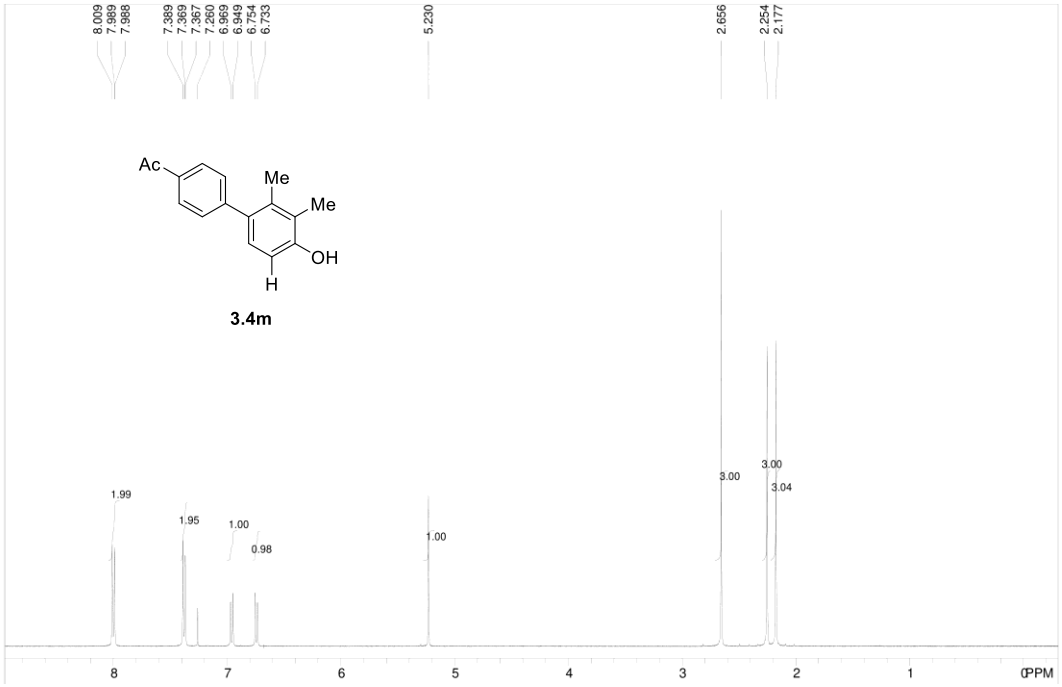


**Figure 3.185.** $^{13}$C-NMR Spectrum of **3.4m** in $CDCl_3$, 101 MHz

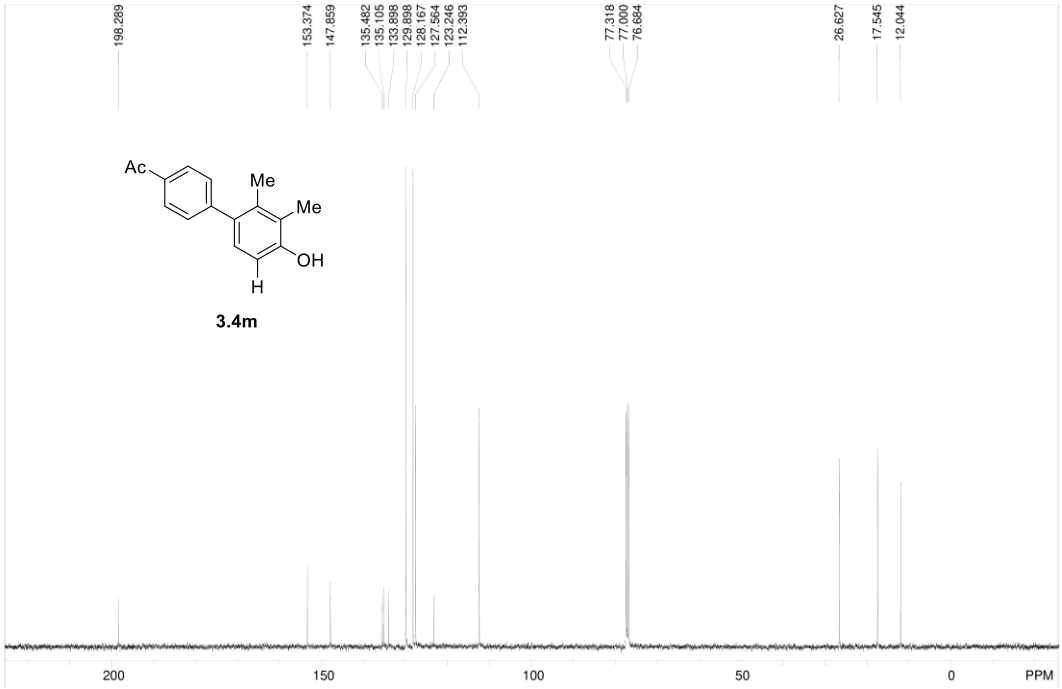

**Figure 3.186.** $^{1}$H-NMR Spectrum of **3.3n** in $CDCl_3$, 500 MHz

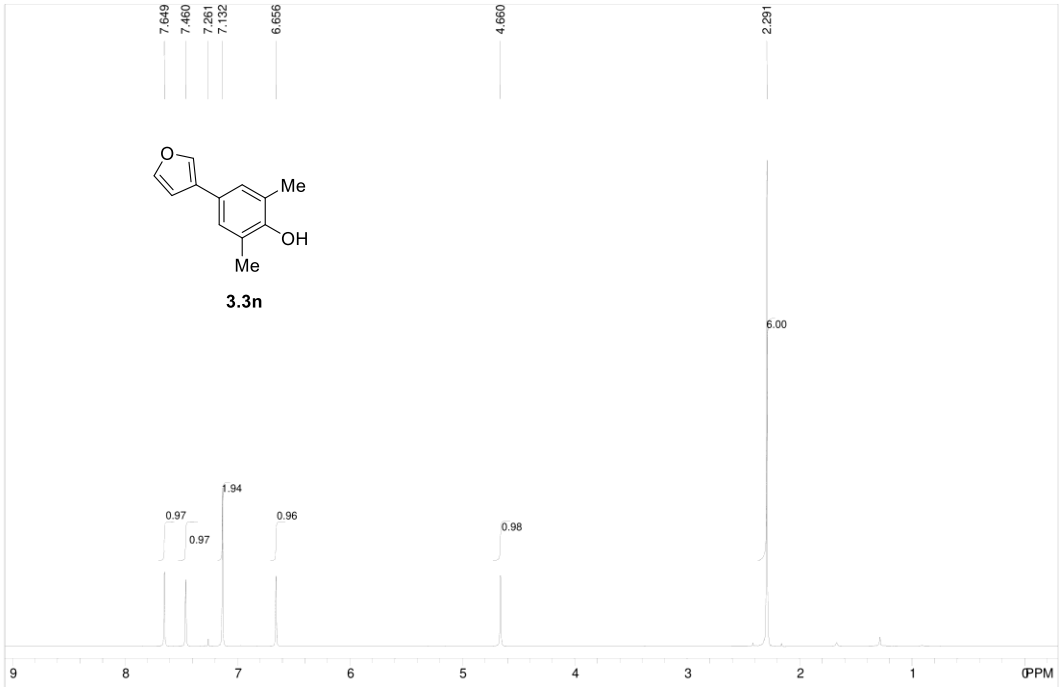


**Figure 3.187.** $^{13}$C-NMR Spectrum of **3.3n** in $CDCl_3$, 126 MHz

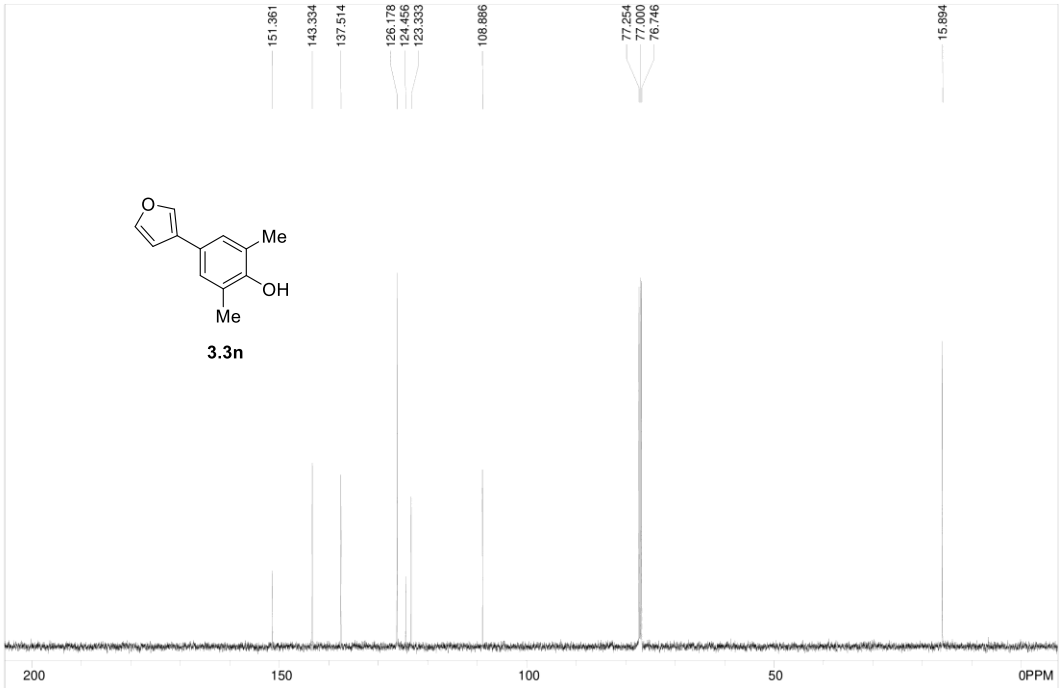

**Figure 3.188.** $^{1}$H-NMR Spectrum of **3.4n** in $CDCl_3$, 500 MHz

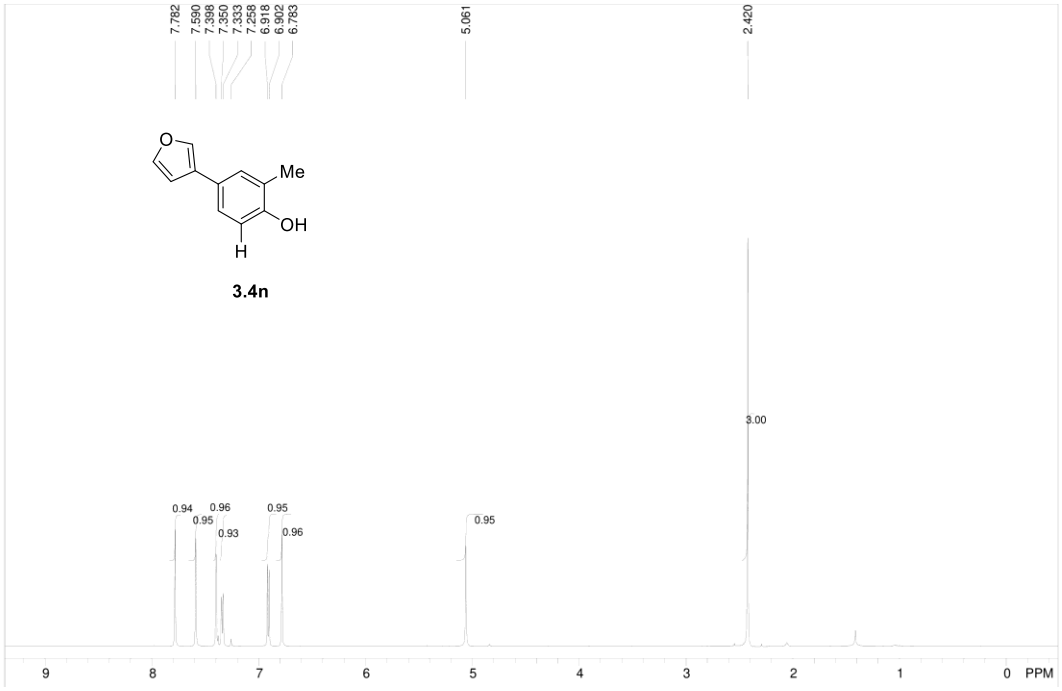


**Figure 3.189.** $^{13}$C-NMR Spectrum of **3.4n** in $CDCl_3$, 126 MHz

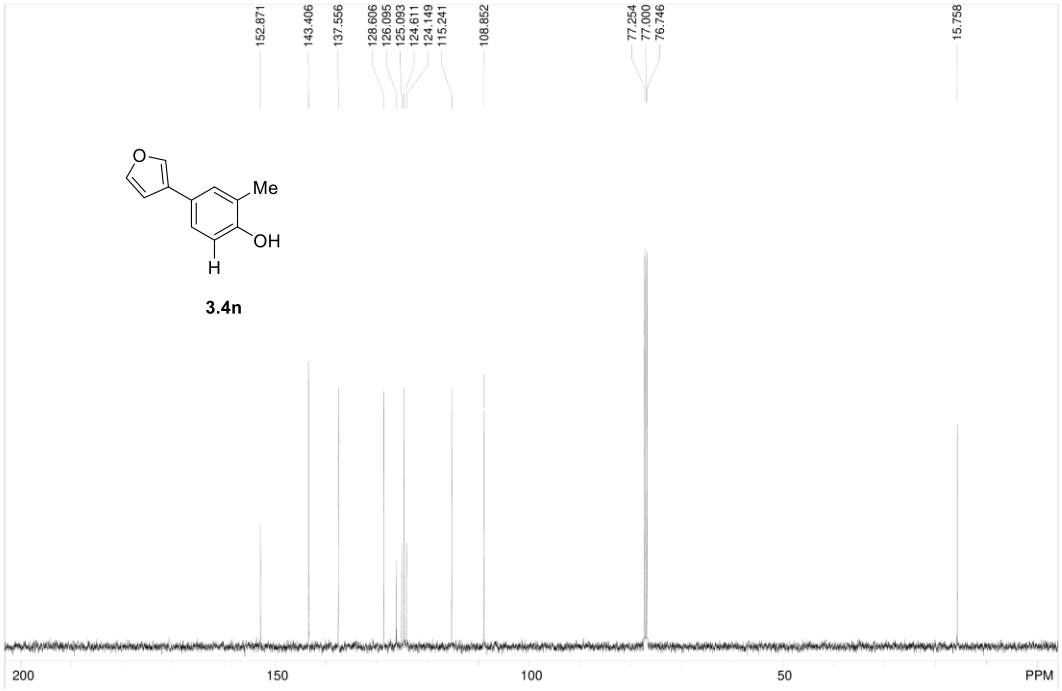

**Figure 3.190.** $^{1}$H-NMR Spectrum of **3.3o** in $CDCl_3$, 500 MHz

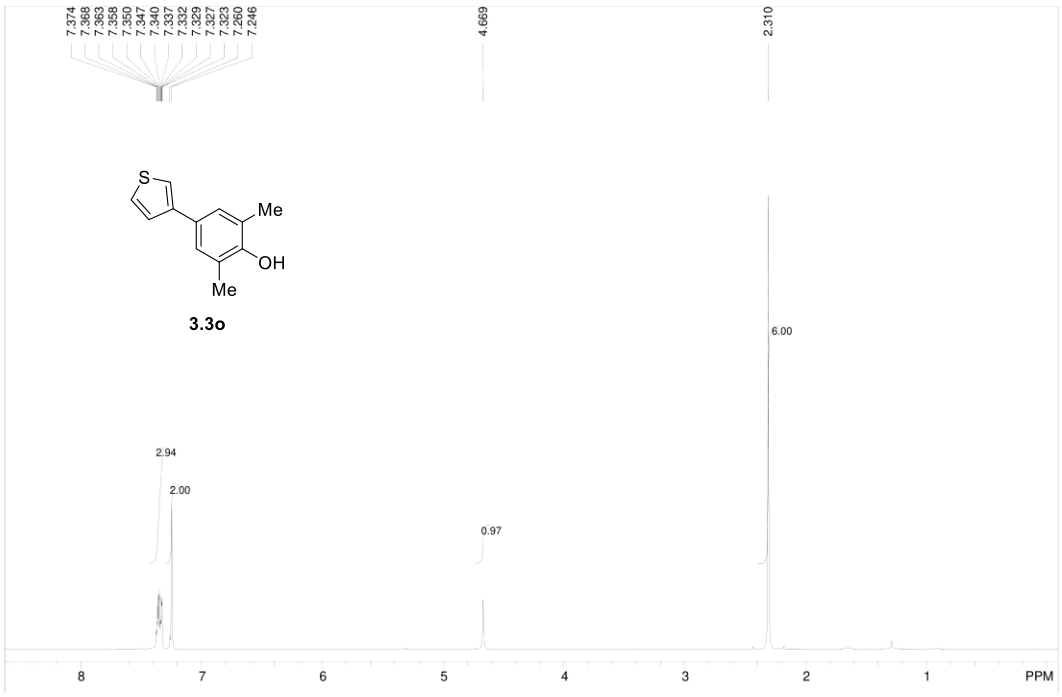


**Figure 3.191.** $^{13}$C-NMR Spectrum of **3.3o** in $CDCl_3$, 126 MHz

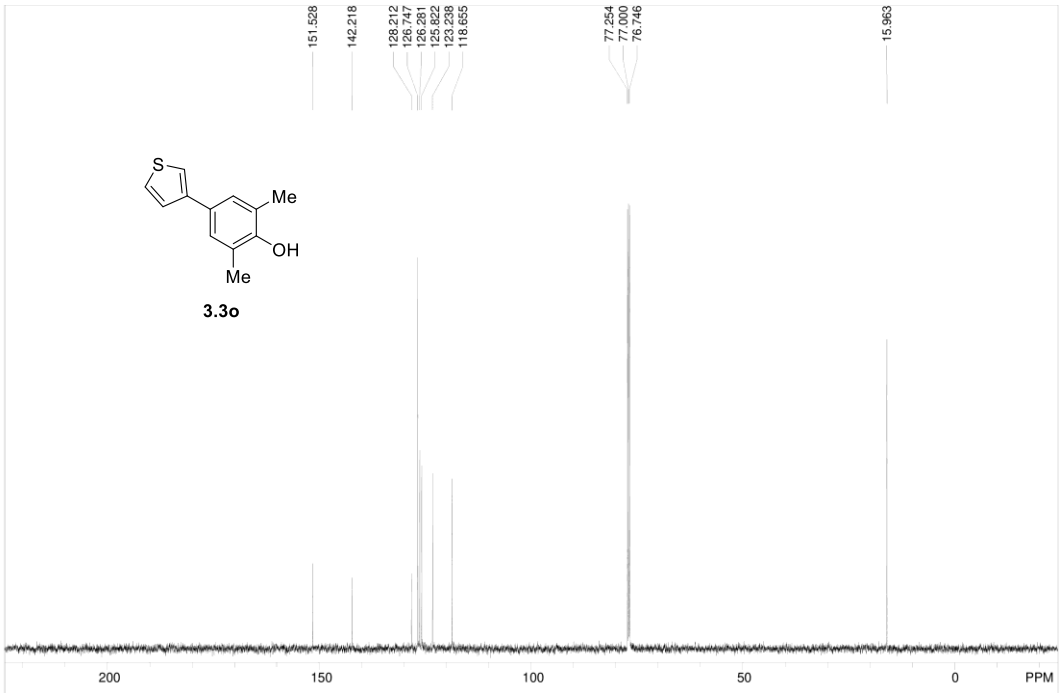

**Figure 3.192.** $^{1}$H-NMR Spectrum of **3.4o** in $CDCl_3$, 400 MHz

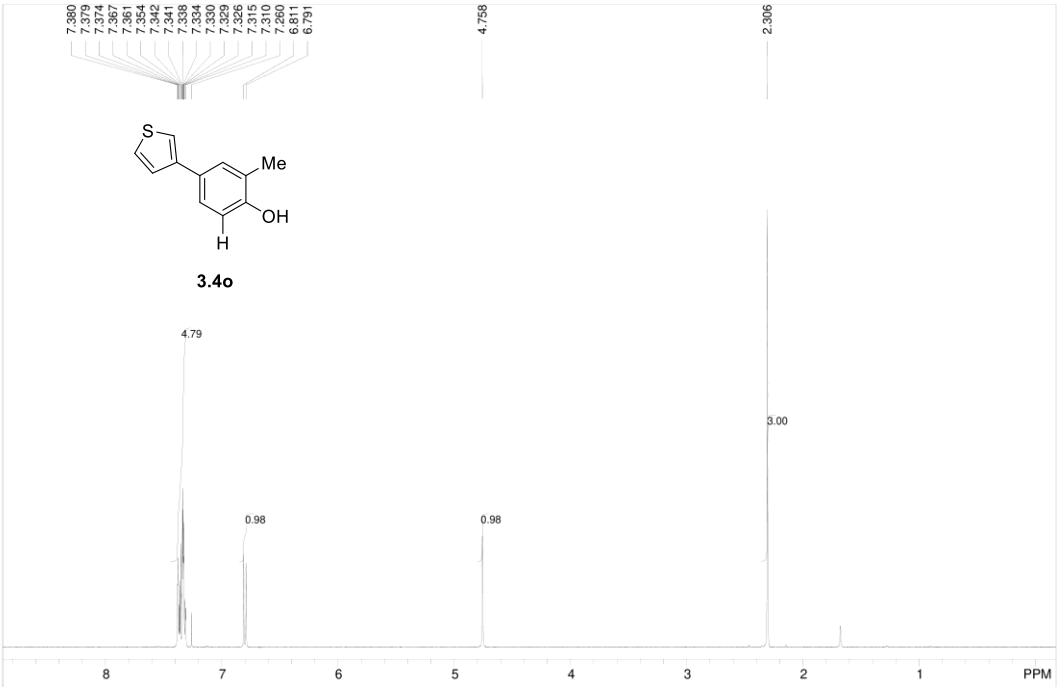


**Figure 3.193.** $^{13}$C-NMR Spectrum of **3.4o** in $CDCl_3$, 101 MHz

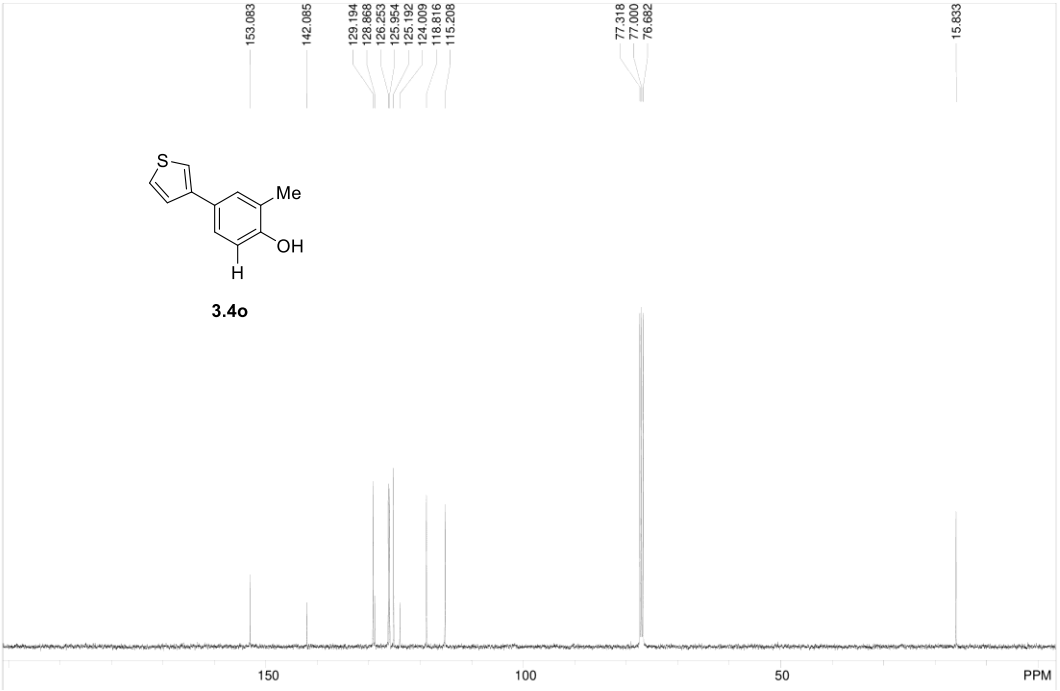

**Figure 3.194.** $^{1}$H-NMR Spectrum of **3.3q** in $CDCl_3$, 500 MHz

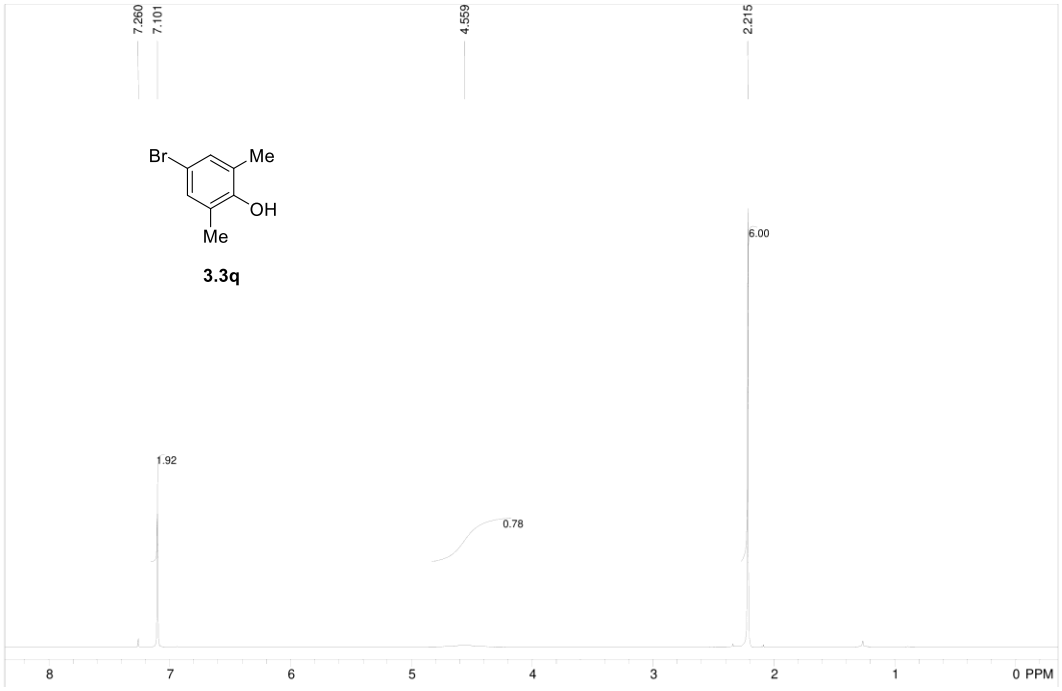


**Figure 3.195.** $^{13}$C-NMR Spectrum of **3.3q** in $CDCl_3$, 126 MHz

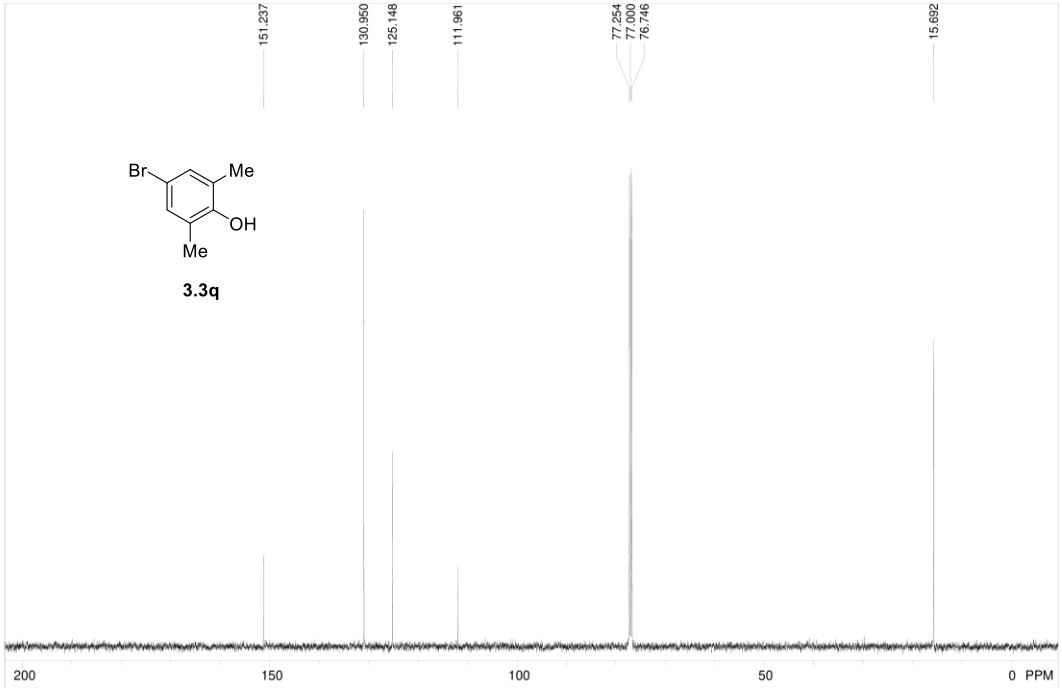

**Figure 3.196.** $^{1}$H-NMR Spectrum of **3.4q** in $CDCl_3$, 500 MHz

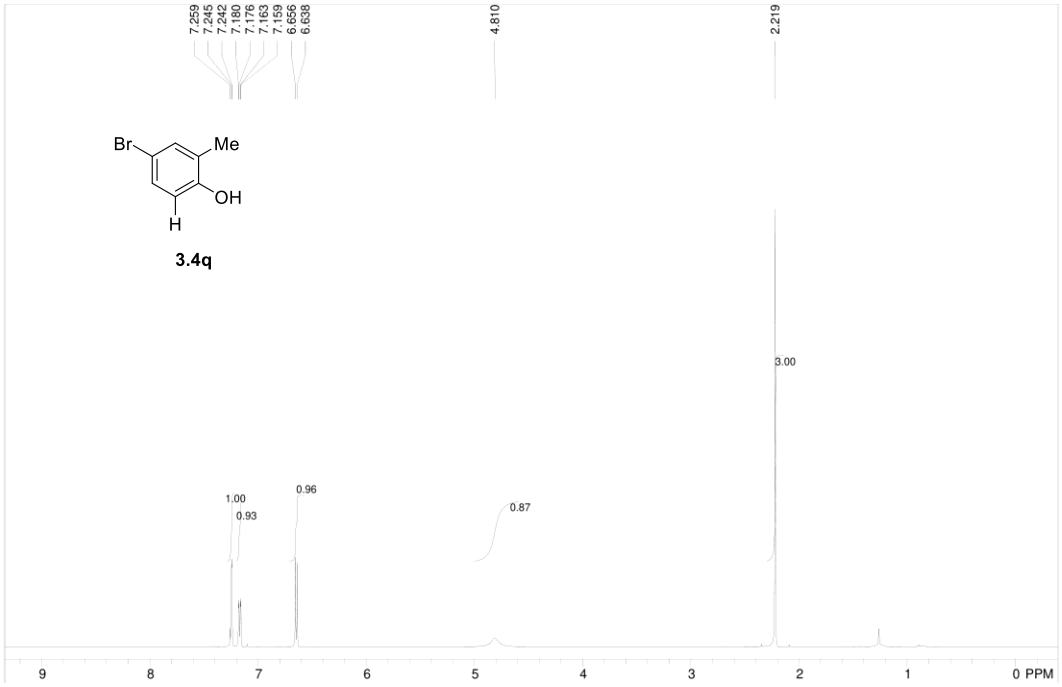


**Figure 3.197.** $^{13}$C-NMR Spectrum of **3.4q** in $CDCl_3$, 126 MHz

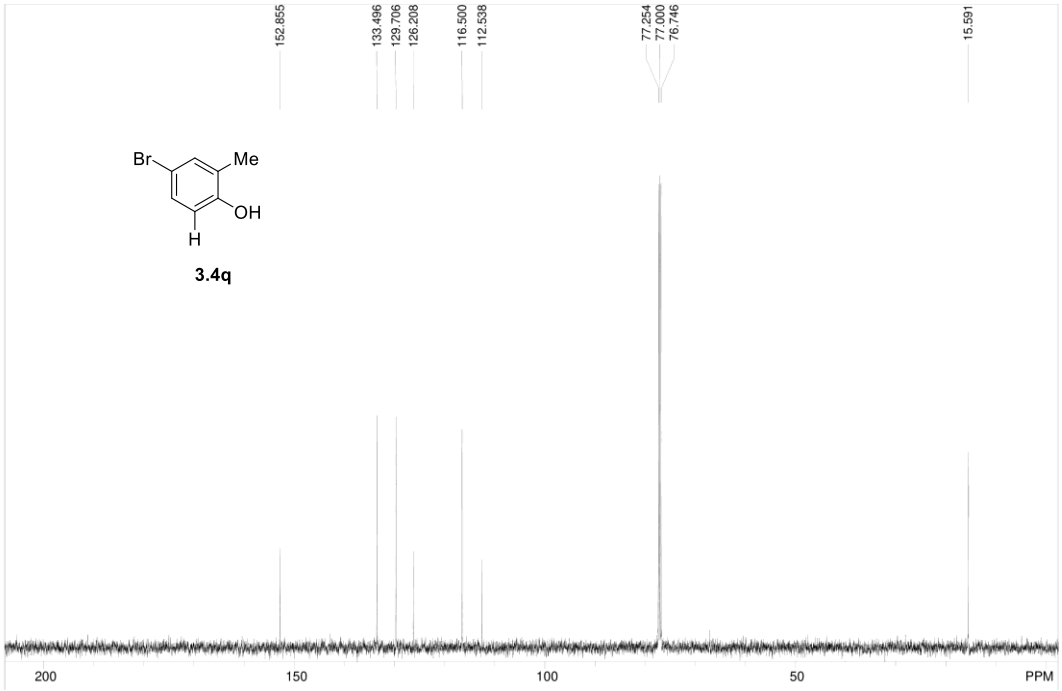

**Figure 3.198.** $^{1}$H-NMR Spectrum of **3.3r** in $CDCl_3$, 500 MHz

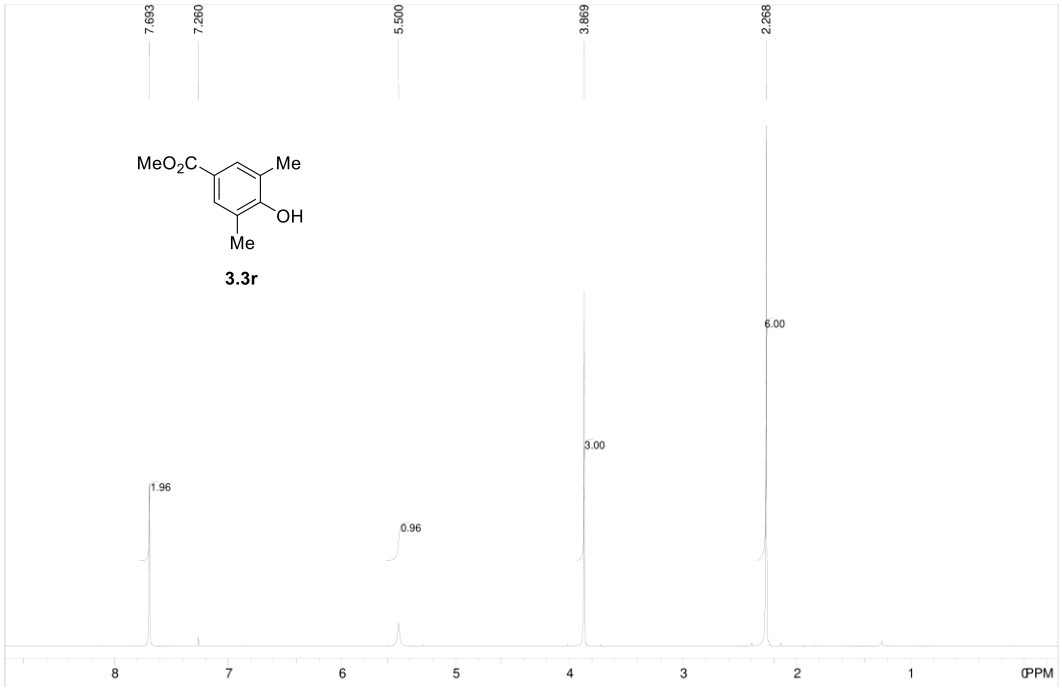


**Figure 3.199.** $^{13}$C-NMR Spectrum of **3.3r** in $CDCl_3$, 126 MHz

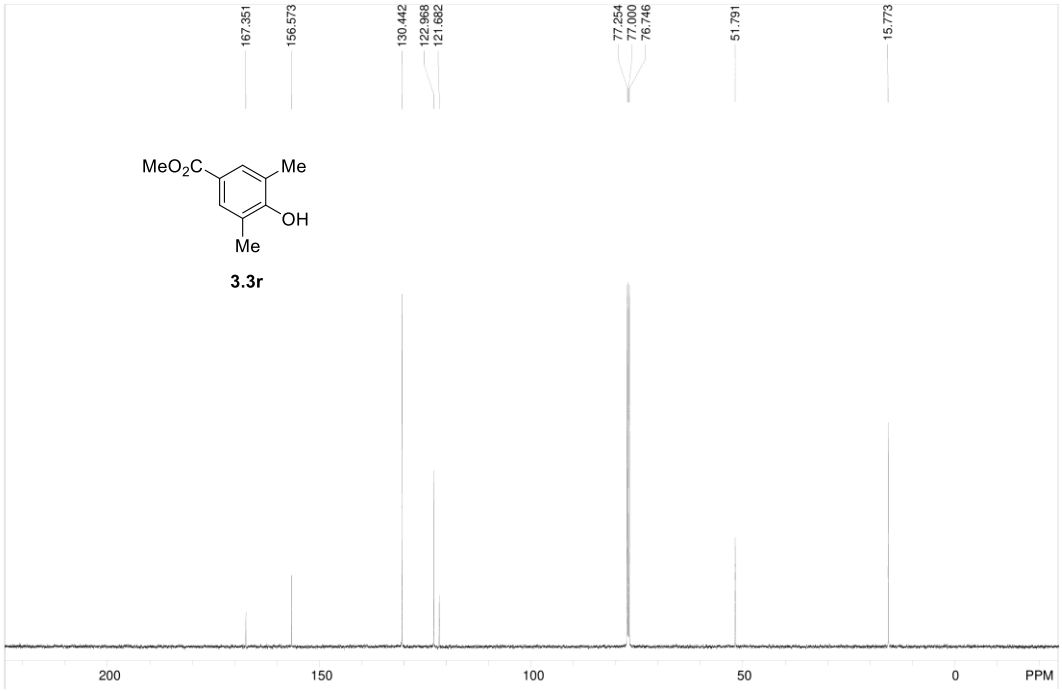

**Figure 3.200.** $^{1}$H-NMR Spectrum of **3.4r** in $CDCl_3$, 500 MHz

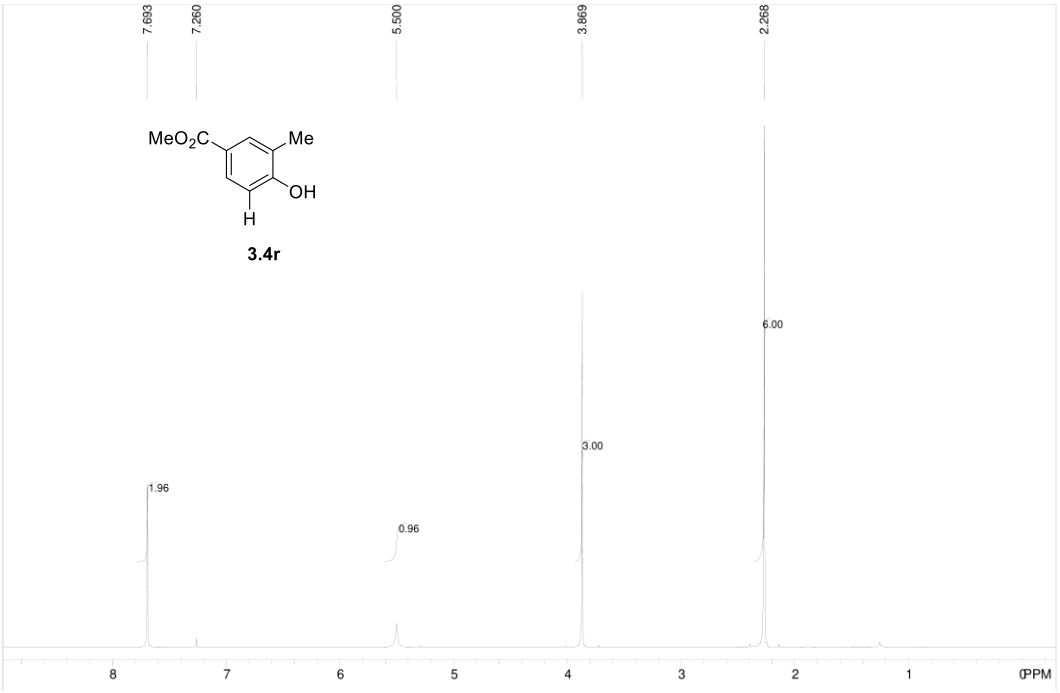


**Figure 3.201.** $^{13}$C-NMR Spectrum of **3.4r** in $CDCl_3$, 126 MHz

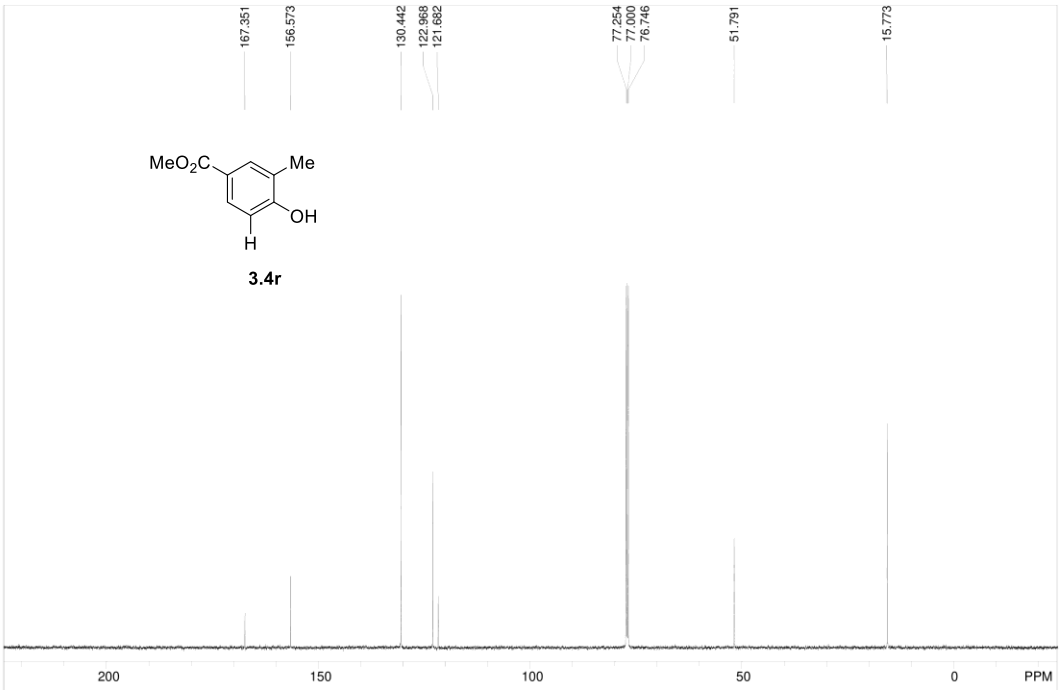

**Figure 3.202.** $^{1}$H-NMR Spectrum of **3.3s** in $CDCl_3$, 500 MHz

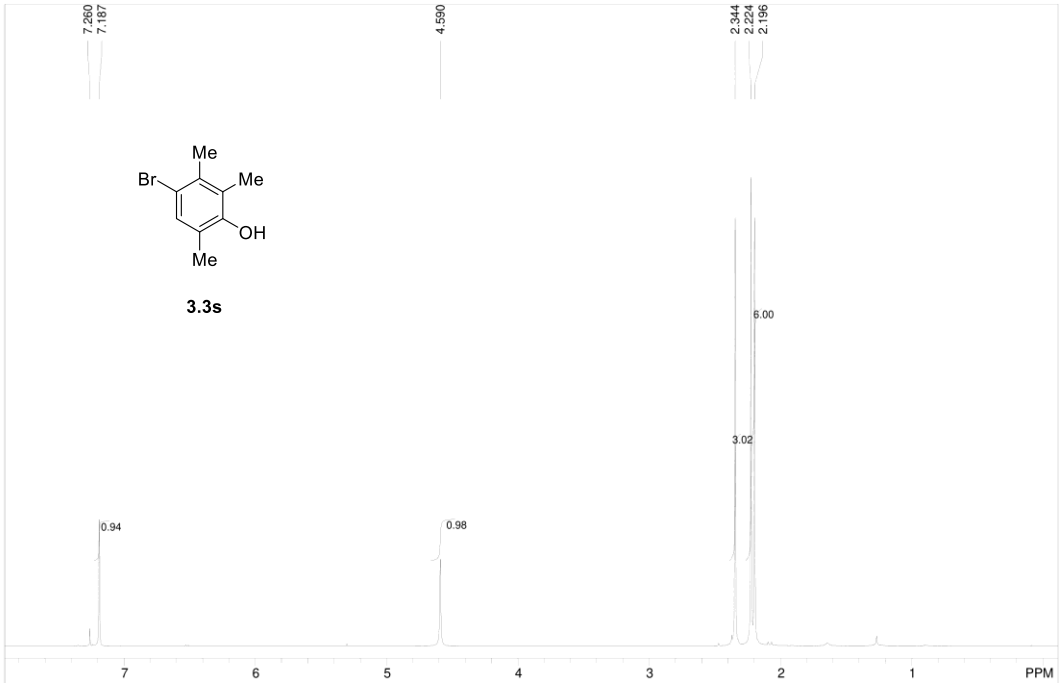


**Figure 3.203.** $^{13}$C-NMR Spectrum of **3.3s** in $CDCl_3$, 126 MHz

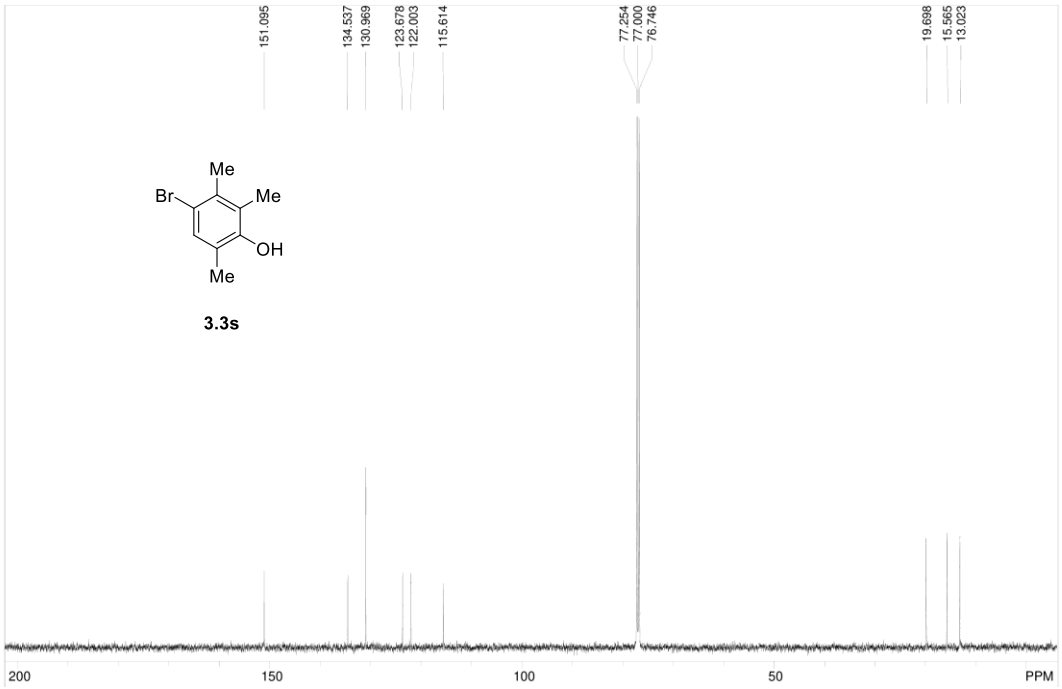

**Figure 3.204.** $^{1}$H-NMR Spectrum of **3.4s** in $CDCl_3$, 500 MHz

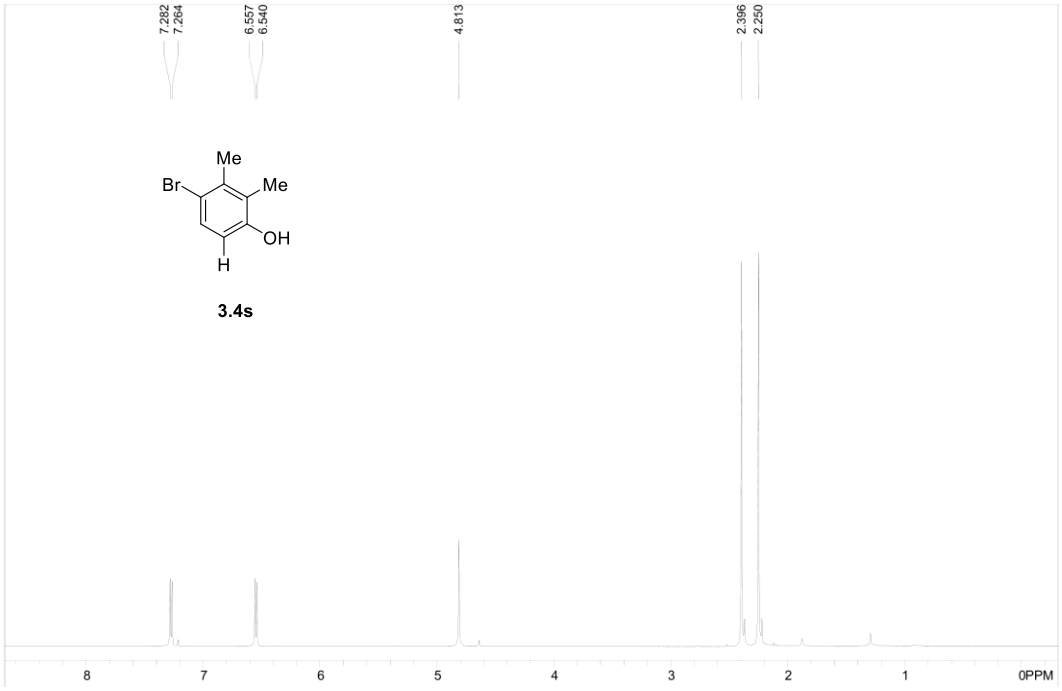


**Figure 3.205.** $^{13}$C-NMR Spectrum of **3.4s** in $CDCl_3$, 101 MHz

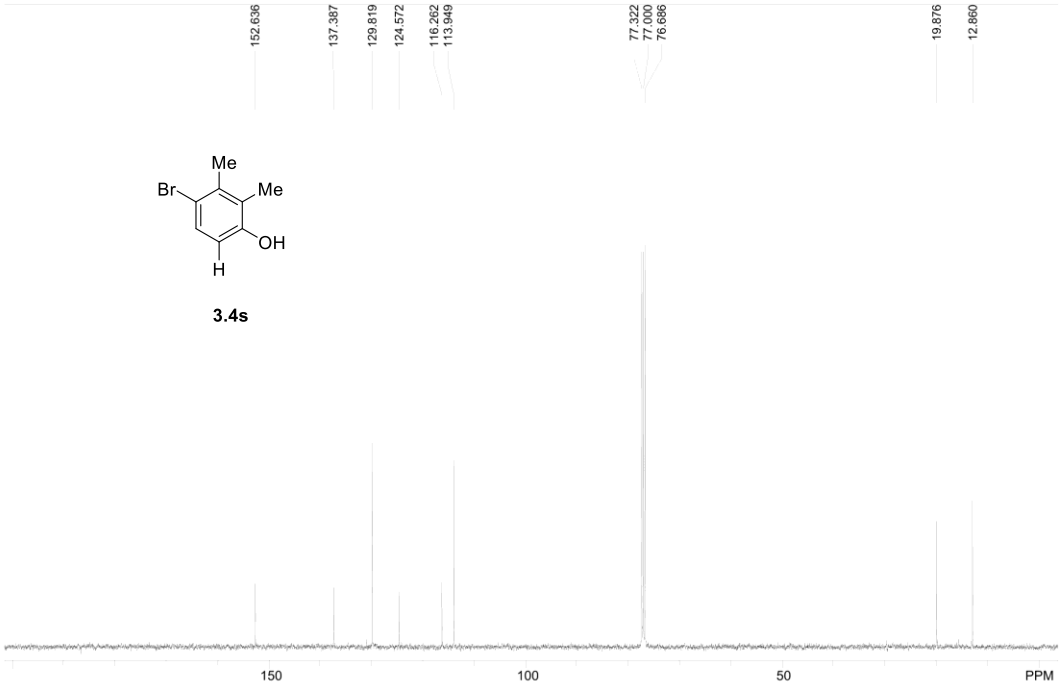

**Figure 3.206.** $^{1}$H-NMR Spectrum of **3.4t** in $CDCl_3$, 400 MHz

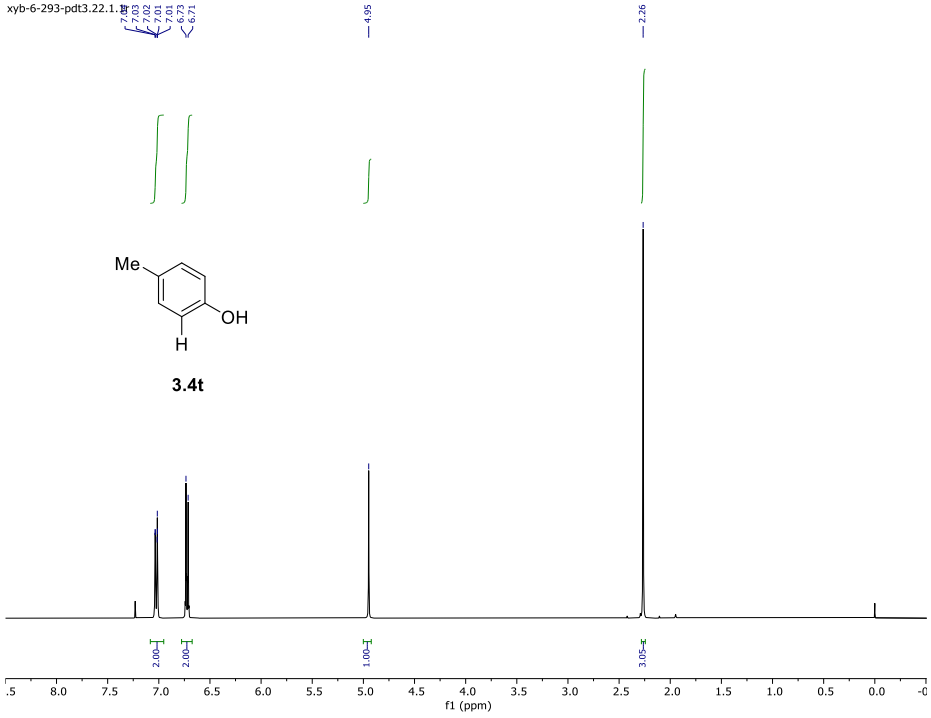


**Figure 3.207.** $^{13}$C-NMR Spectrum of **3.4t** in $CDCl_3$, 101 MHz

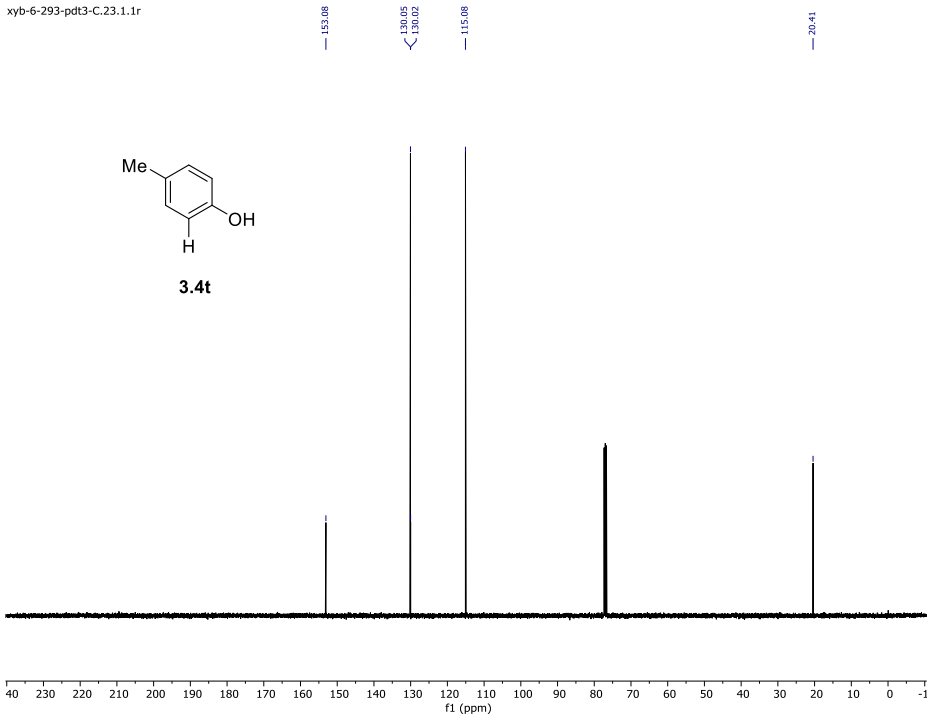

**Figure 3.208.** $^{1}$H-NMR Spectrum of **3.3t'** in $CDCl_3$, 500 MHz

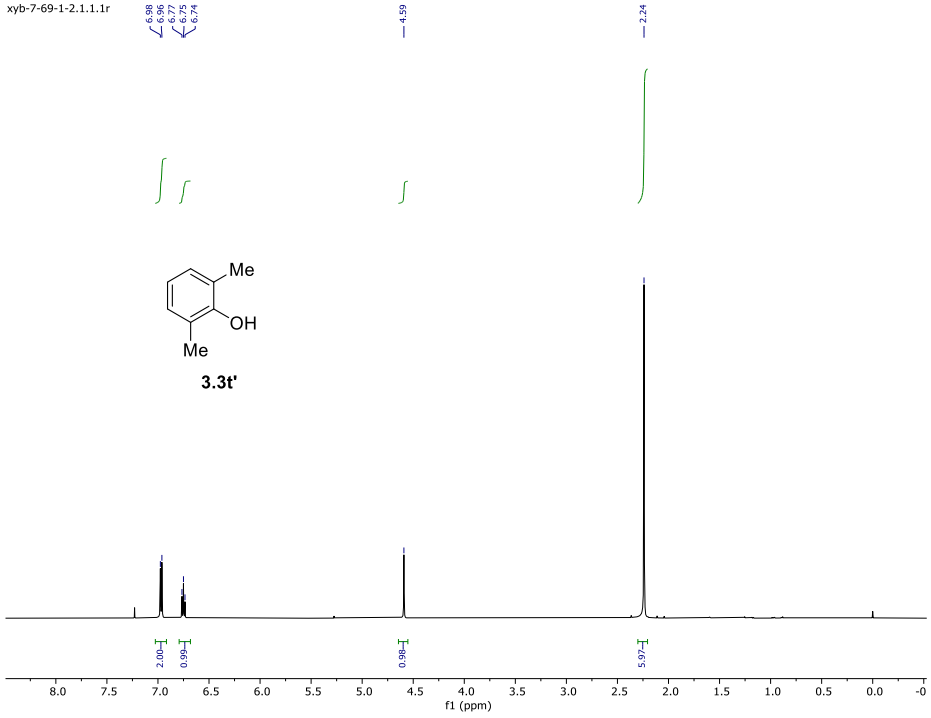


**Figure 3.209.** $^{13}$C-NMR Spectrum of **3.3t'** in $CDCl_3$, 126 MHz

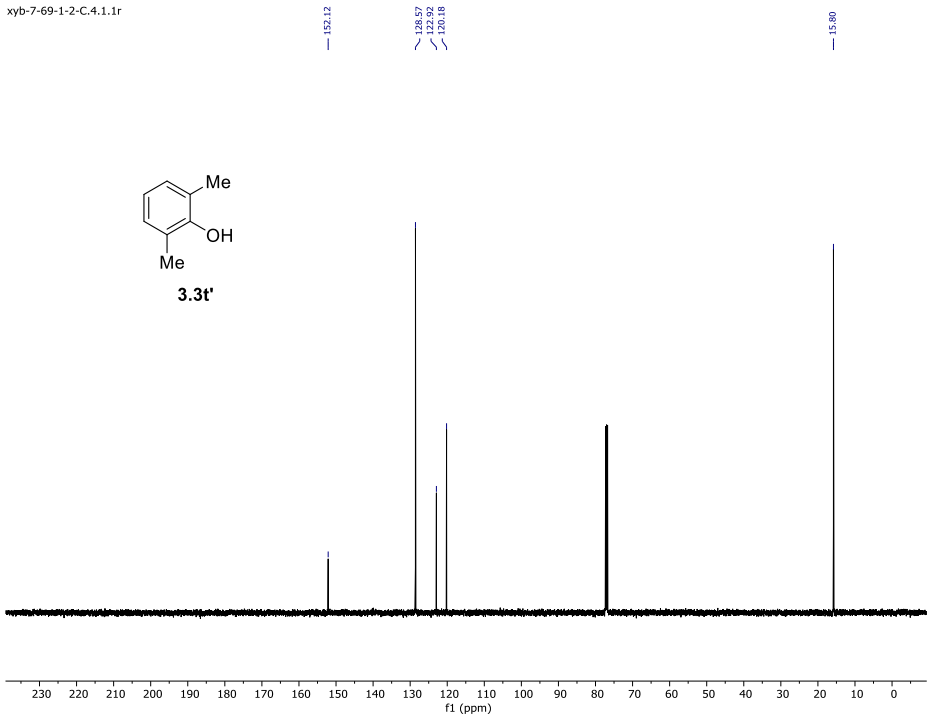

**Figure 3.210.** $^{1}$H-NMR Spectrum of **3.4t'** in $CDCl_3$, 500 MHz

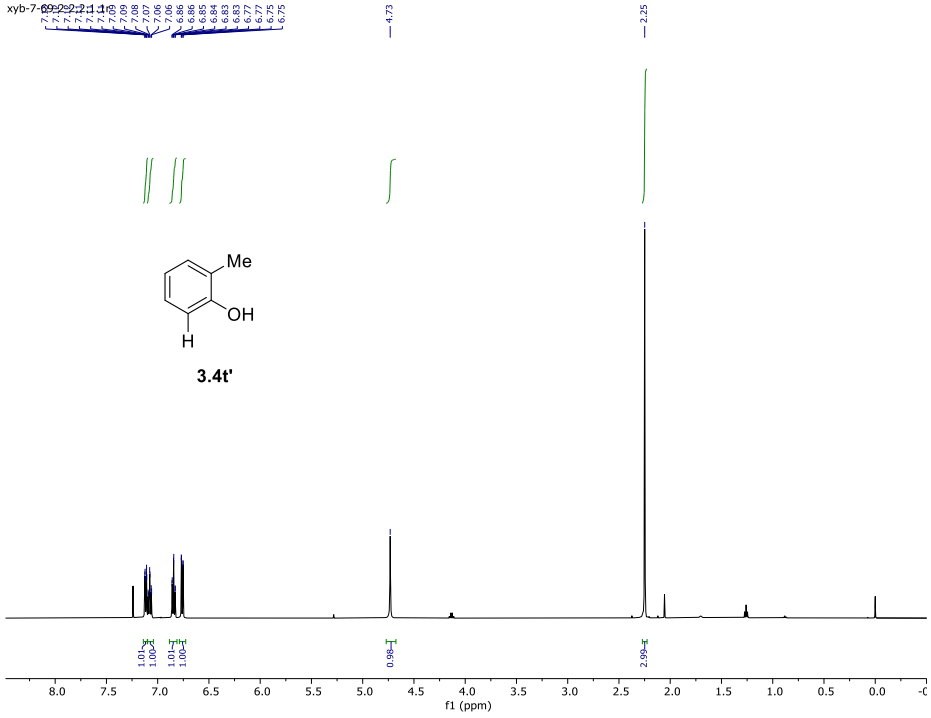


**Figure 3.211.** $^{13}$C-NMR Spectrum of **3.4t'** in $CDCl_3$, 126 MHz

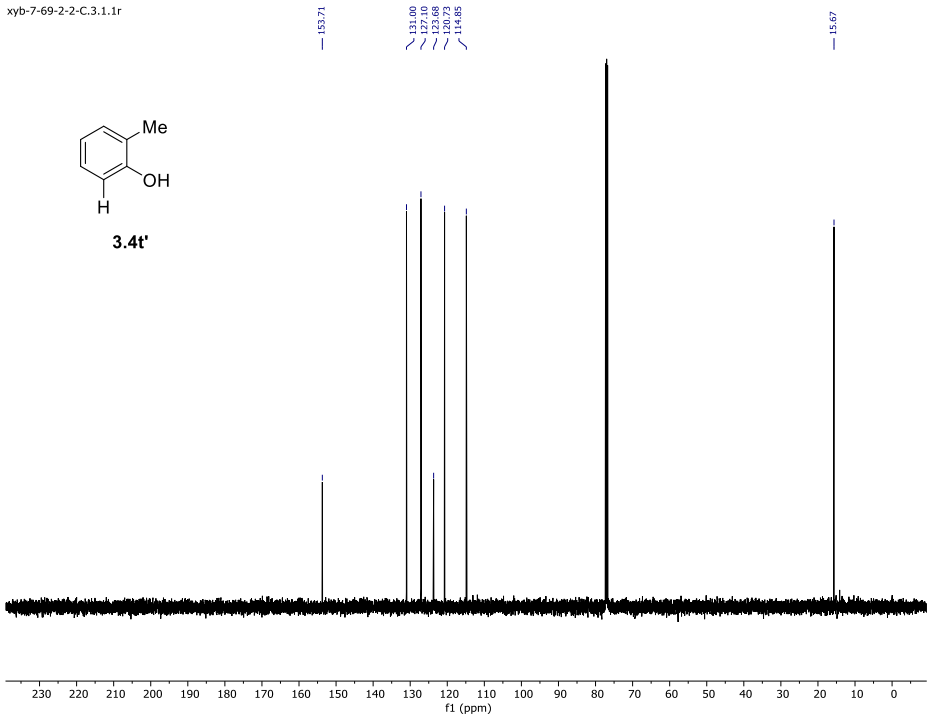

**Figure 3.212.** $^{1}$H-NMR Spectrum of **3.3u** in $CDCl_3$, 400 MHz

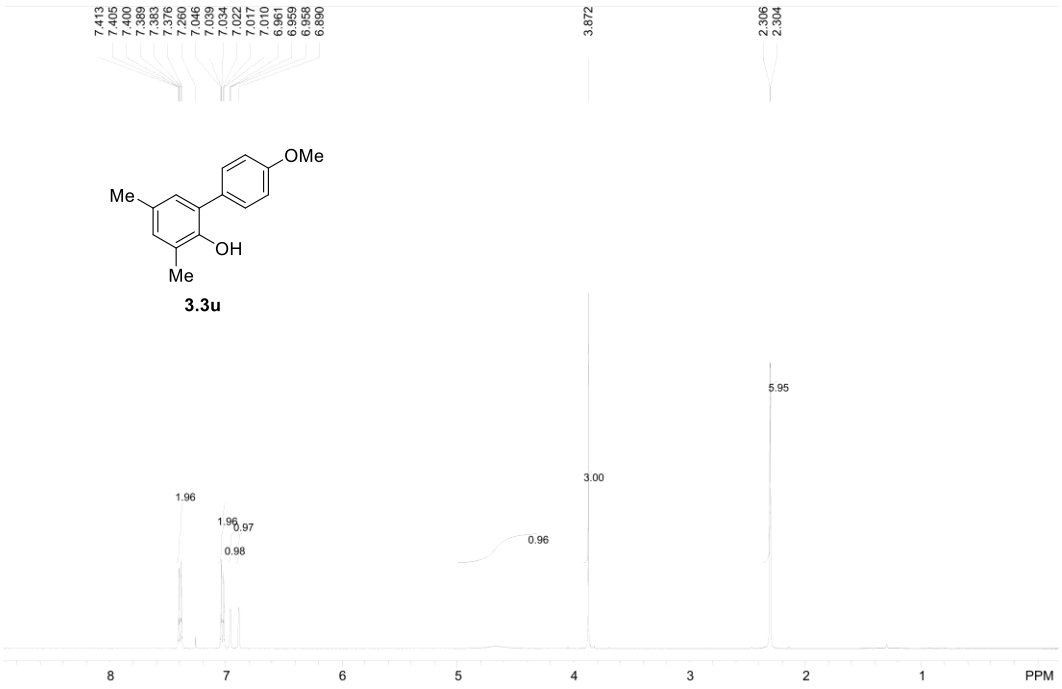


**Figure 3.213.** $^{13}$C-NMR Spectrum of **3.3u** in $CDCl_3$, 101 MHz

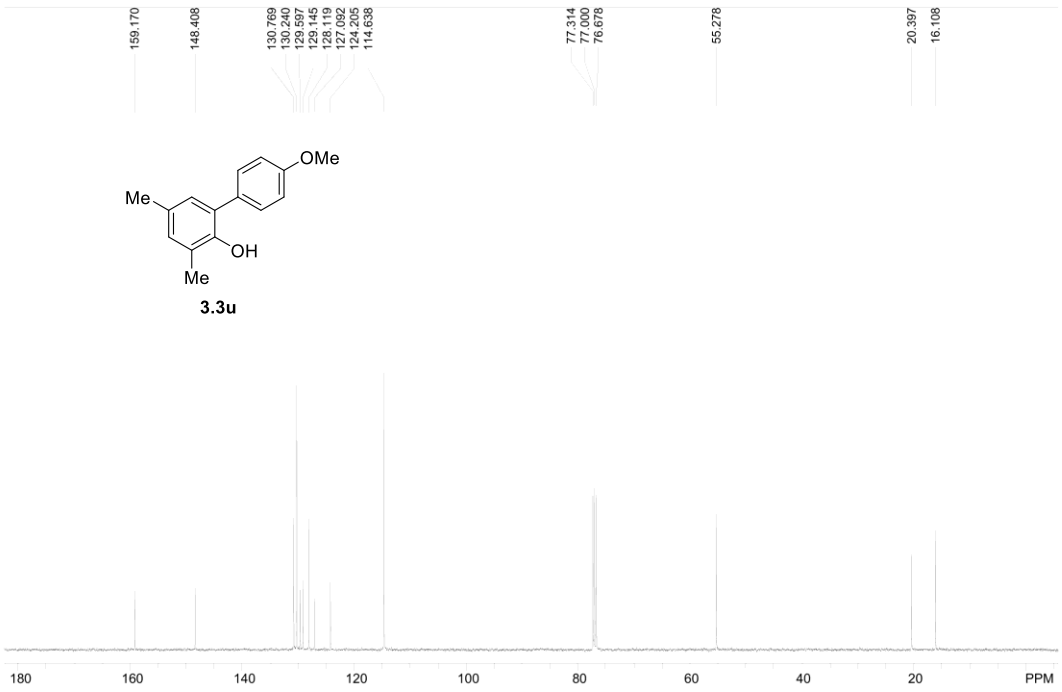

**Figure 3.214.** $^{1}$H-NMR Spectrum of **3.4u** in $CDCl_3$, 400 MHz

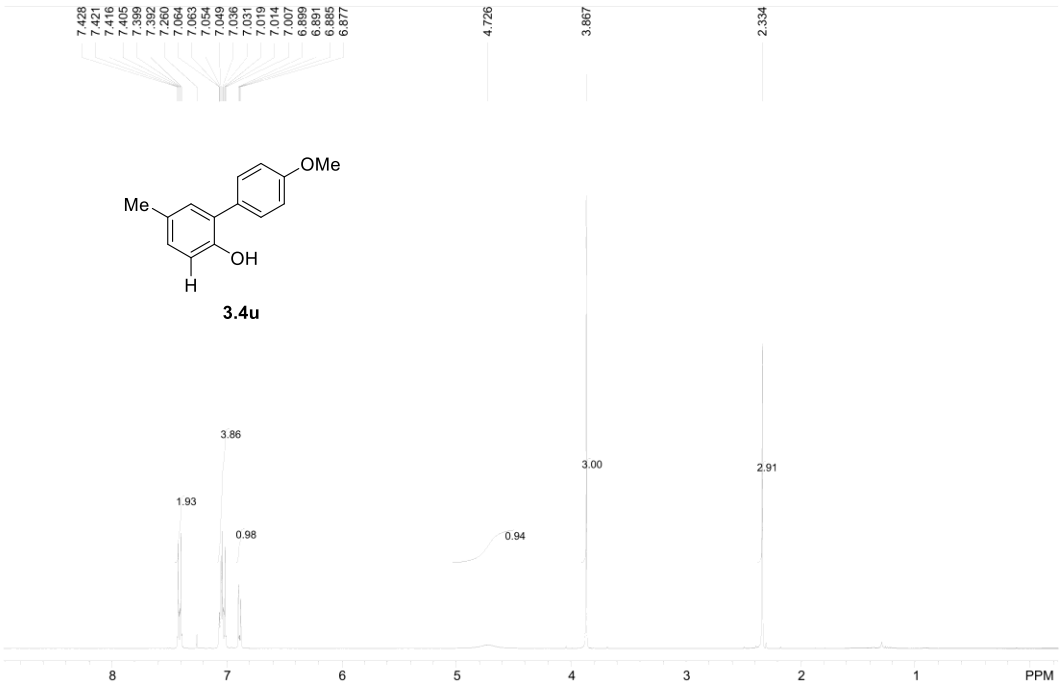


**Figure 3.215.** $^{13}$C-NMR Spectrum of **3.4u** in $CDCl_3$, 101 MHz

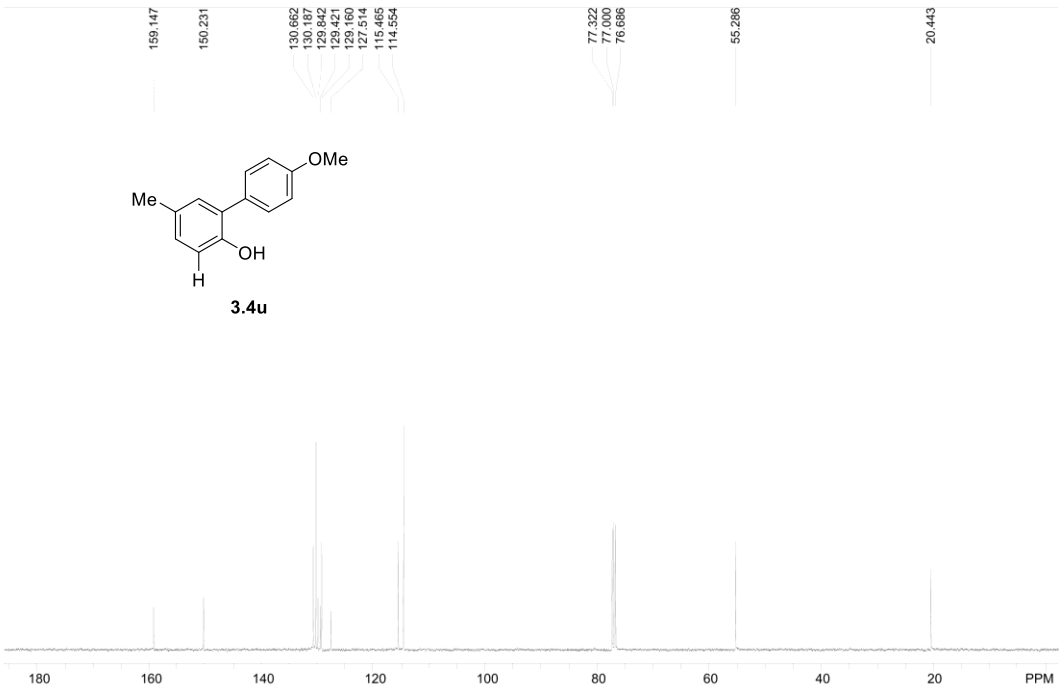

**Figure 3.216.** $^{1}$H-NMR Spectrum of **3.3v** in $CDCl_3$, 500 MHz

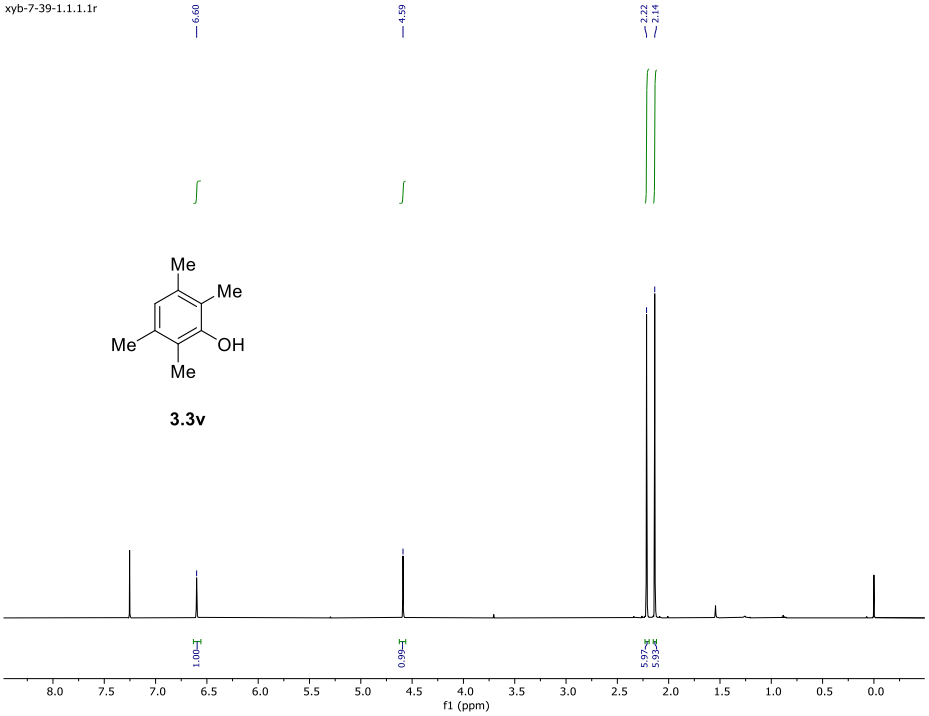


**Figure 3.217.** $^{13}$C-NMR Spectrum of **3.3v** in $CDCl_3$, 101 MHz

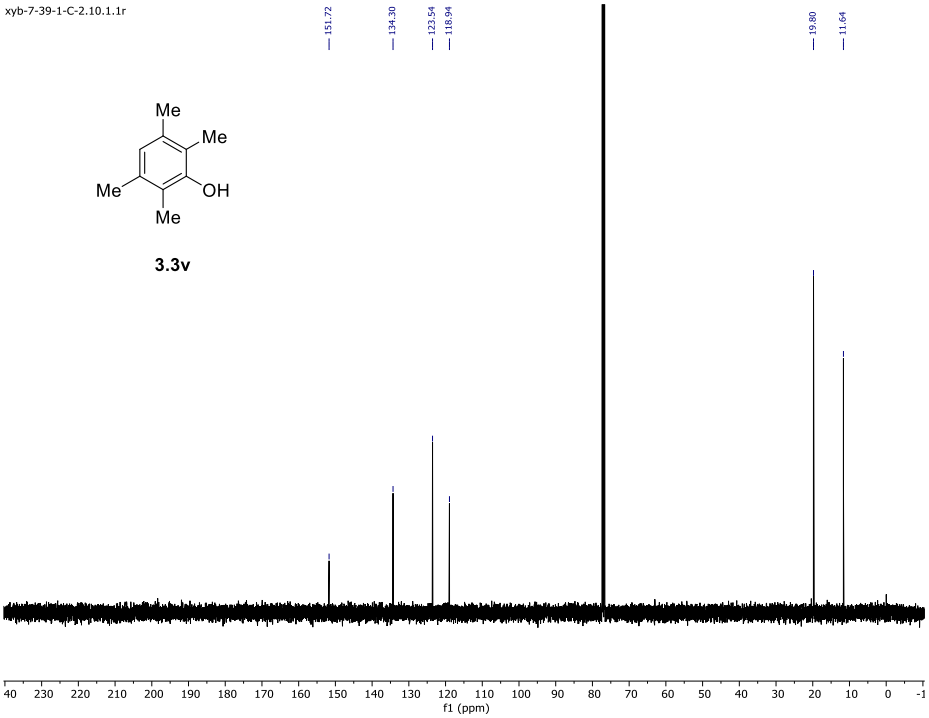

**Figure 3.218.** $^{1}$H-NMR Spectrum of **3.4v** in $CDCl_3$, 500 MHz

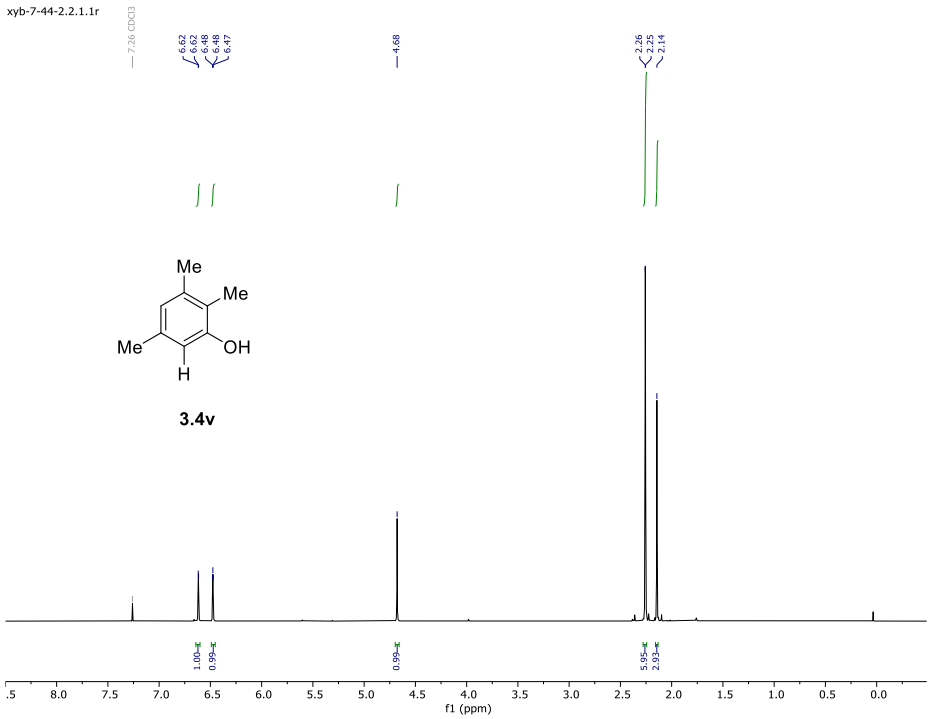


**Figure 3.219.** $^{13}$C-NMR Spectrum of **3.4v** in $CDCl_3$, 101 MHz

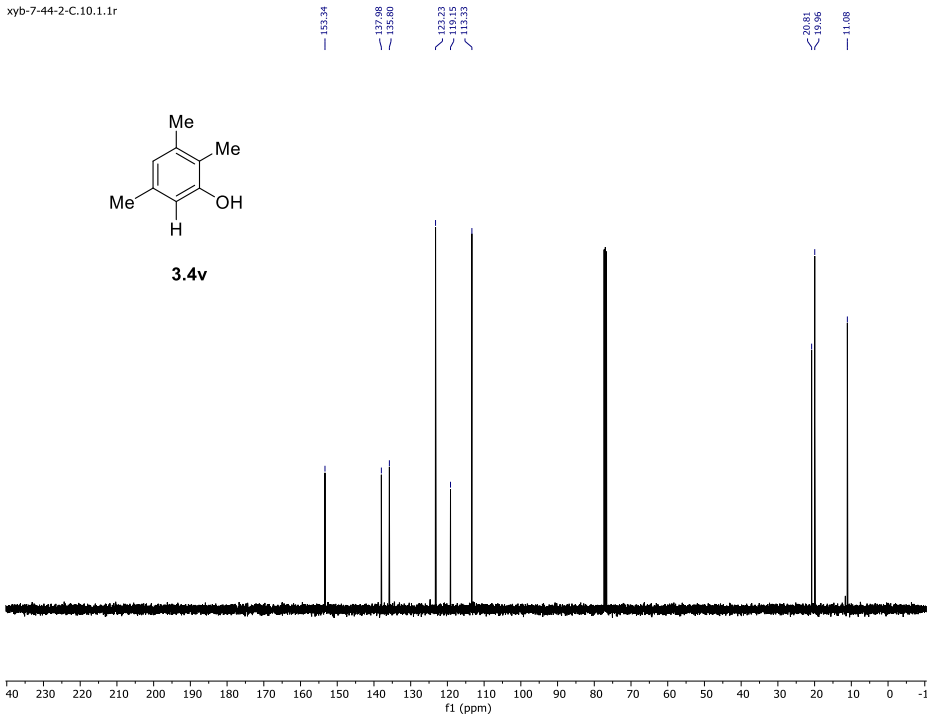

**Figure 3.220.** [1]H-NMR Spectrum of **S3.19** in DMSO-d6, 500 MHz

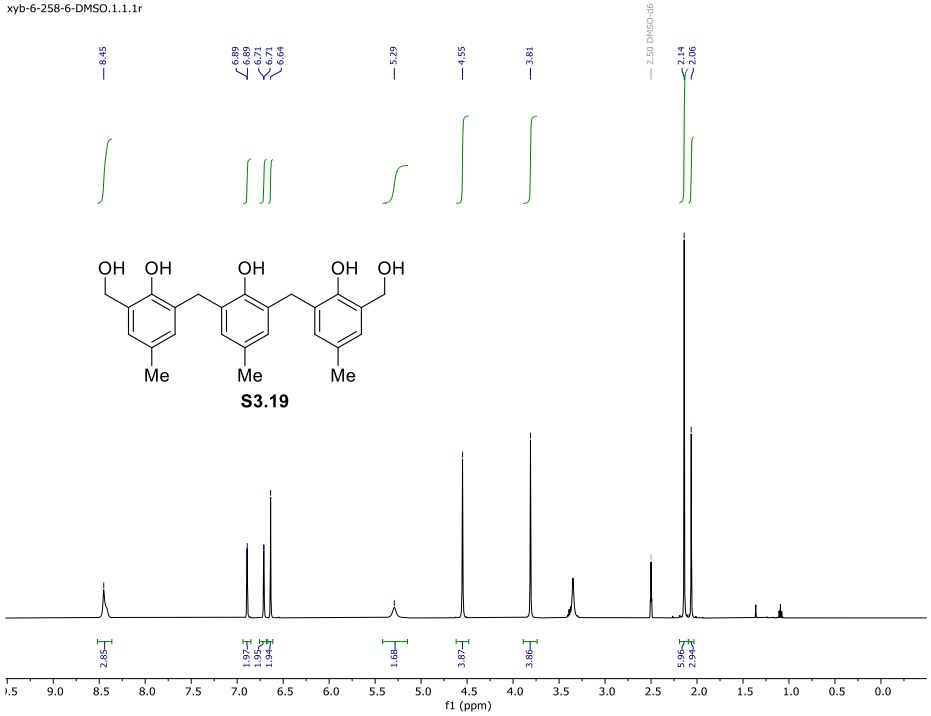


**Figure 3.221.** [13]C-NMR Spectrum of **S3.19** in DMSO-d6, 101 MHz

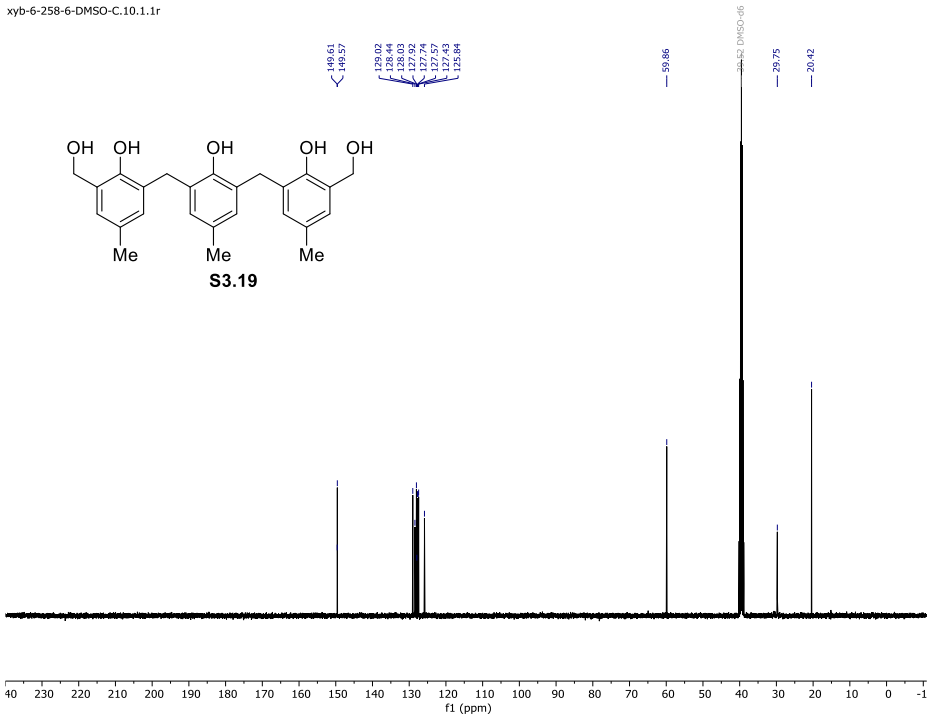

**Figure 3.222.** $^{1}$H-NMR Spectrum of **3.1z** in $CDCl_3$, 500 MHz

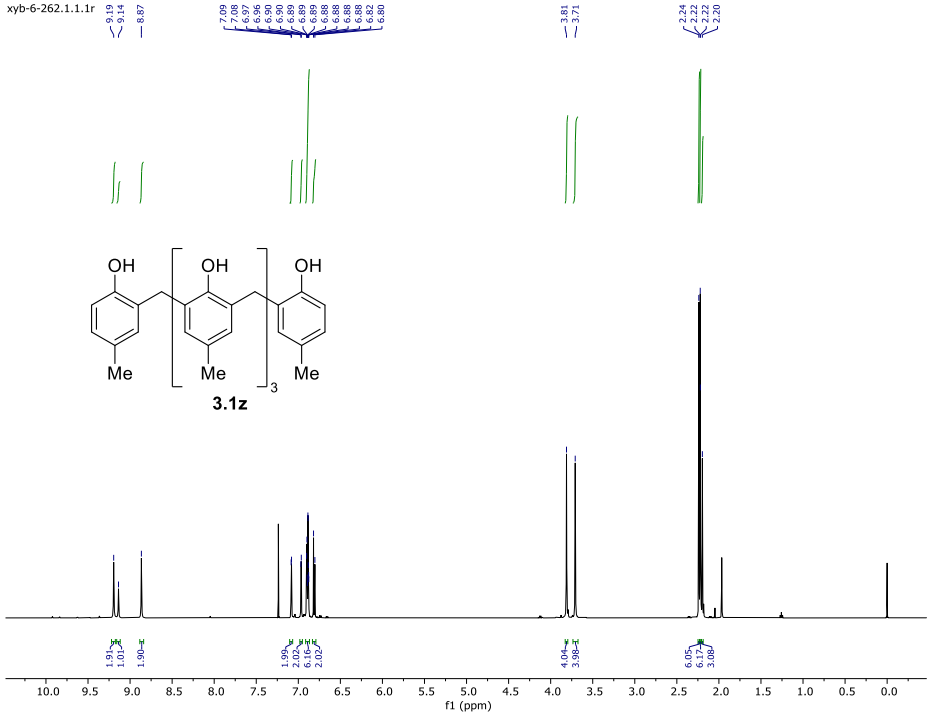


**Figure 3.223.** $^{13}$C-NMR Spectrum of **3.1z** in CDCl3, 101 MHz

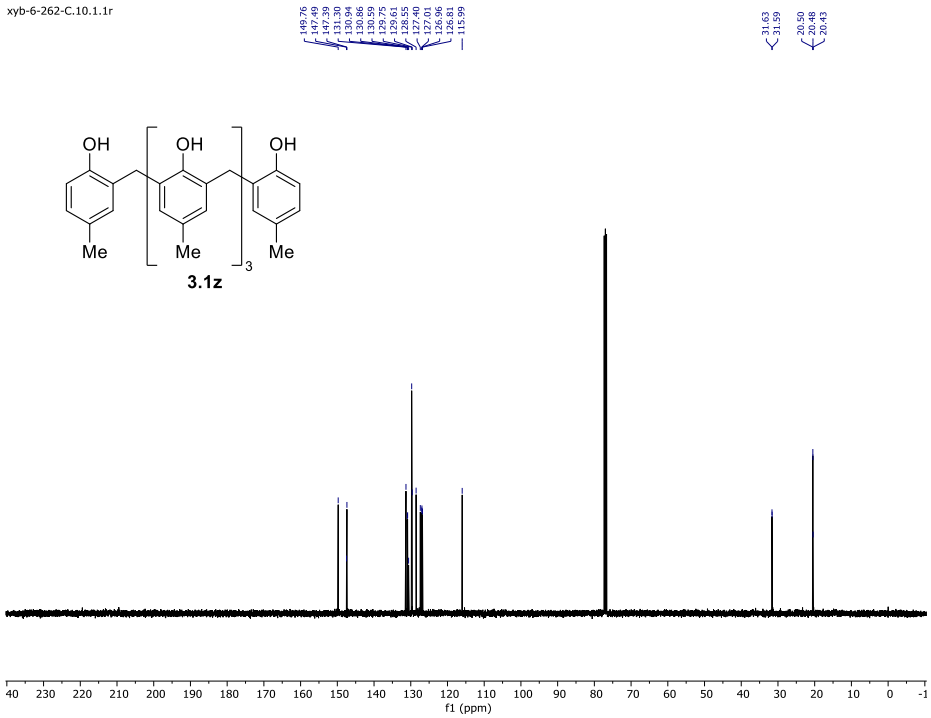

**Figure 3.224.** $^{1}$H-NMR Spectrum of **S3.21** in $CDCl_3$, 500 MHz

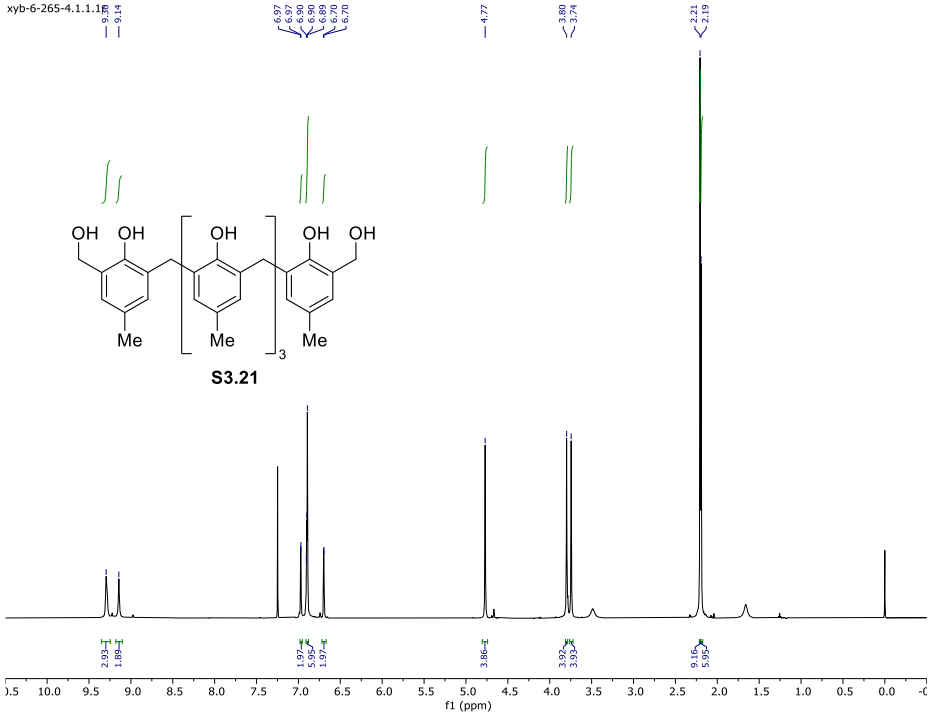


**Figure 3.225.** $^{13}$C-NMR Spectrum of **S3.21** in CDCl3, 101 MHz

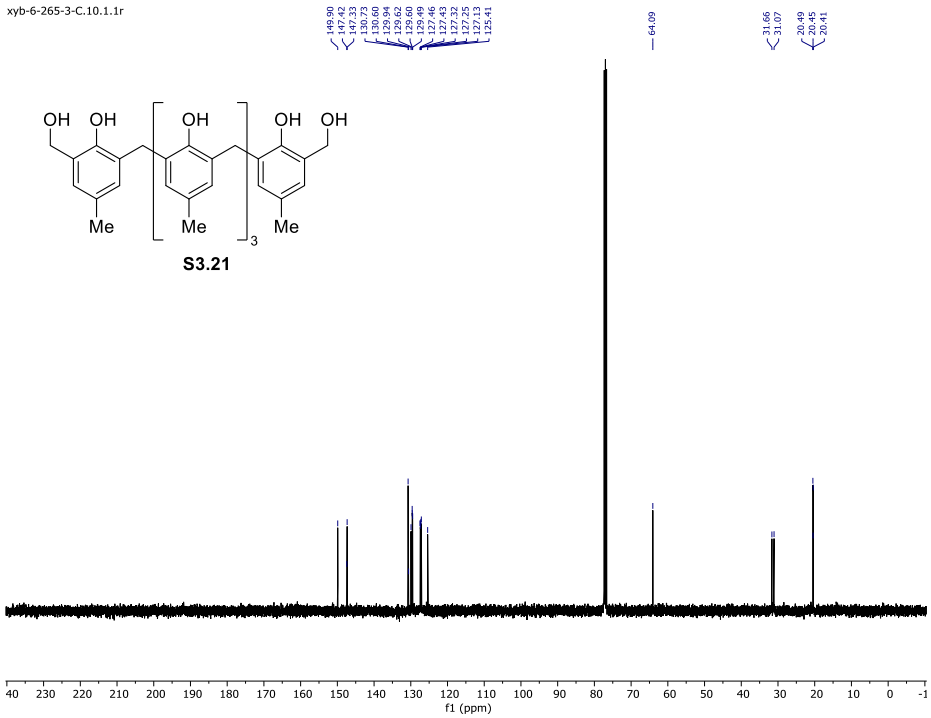

**Figure 3.226.** $^{1}$H-NMR Spectrum of **3.1aa** in $CDCl_3$, 500 MHz

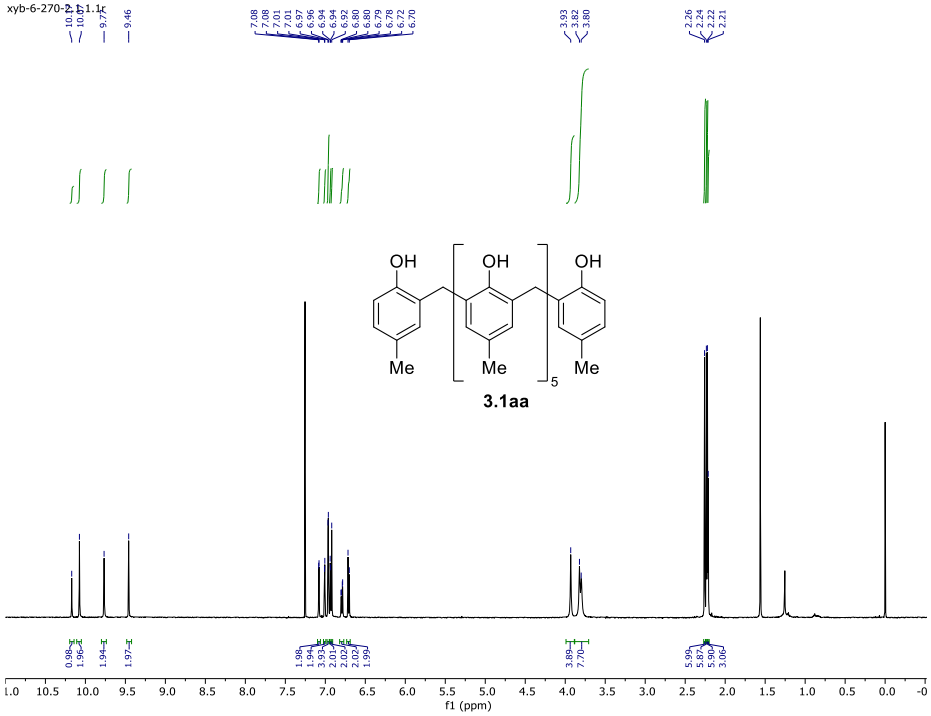


**Figure 3.227.** $^{13}$C-NMR Spectrum of **3.1aa** in $CDCl_3$, 101 MHz

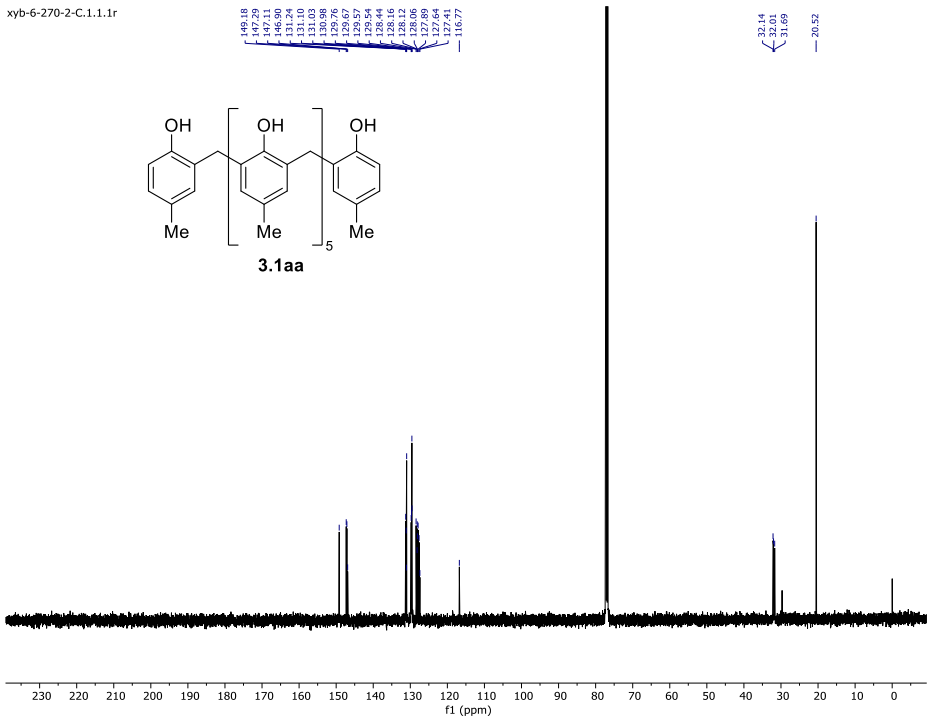

**Figure 3.228.** $^{1}$H-NMR Spectrum of **3.2y** in $C_6D_6$, 500 MHz

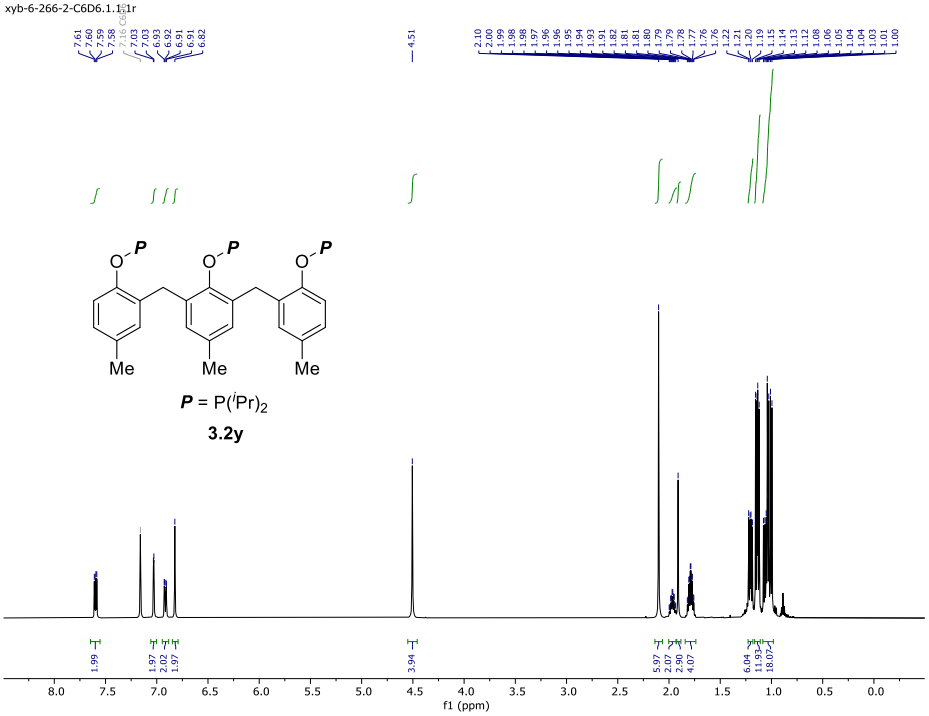


**Figure 3.229.** $^{13}$C-NMR Spectrum of **3.2y** in $C_6D_6$, 126 MHz

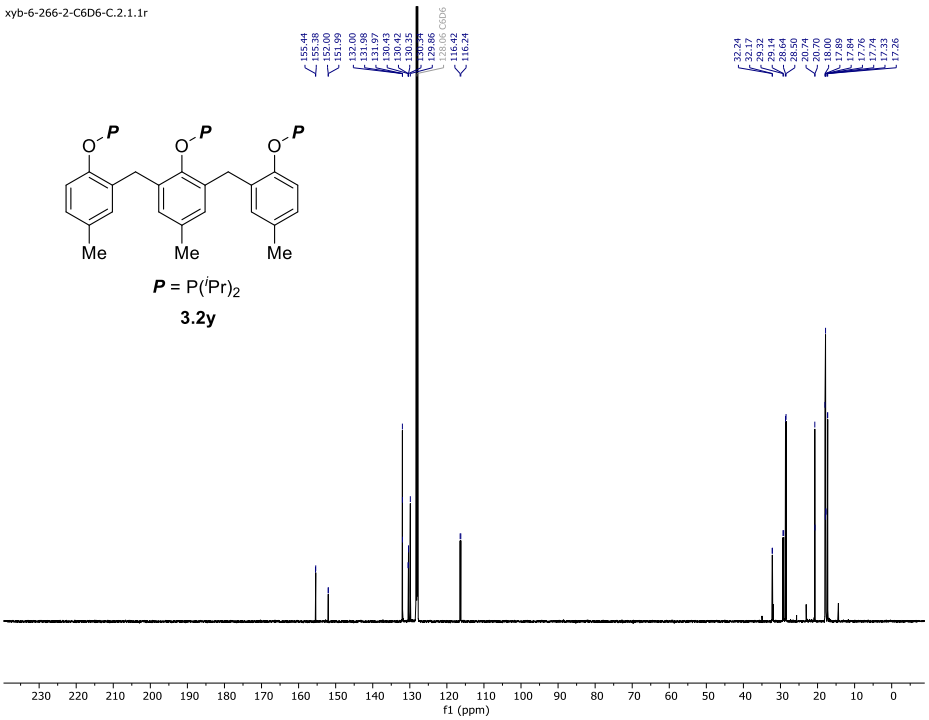

**Figure 3.230.** $^{31}$P-NMR Spectrum of **3.2y** in $C_6D_6$, 162 MHz

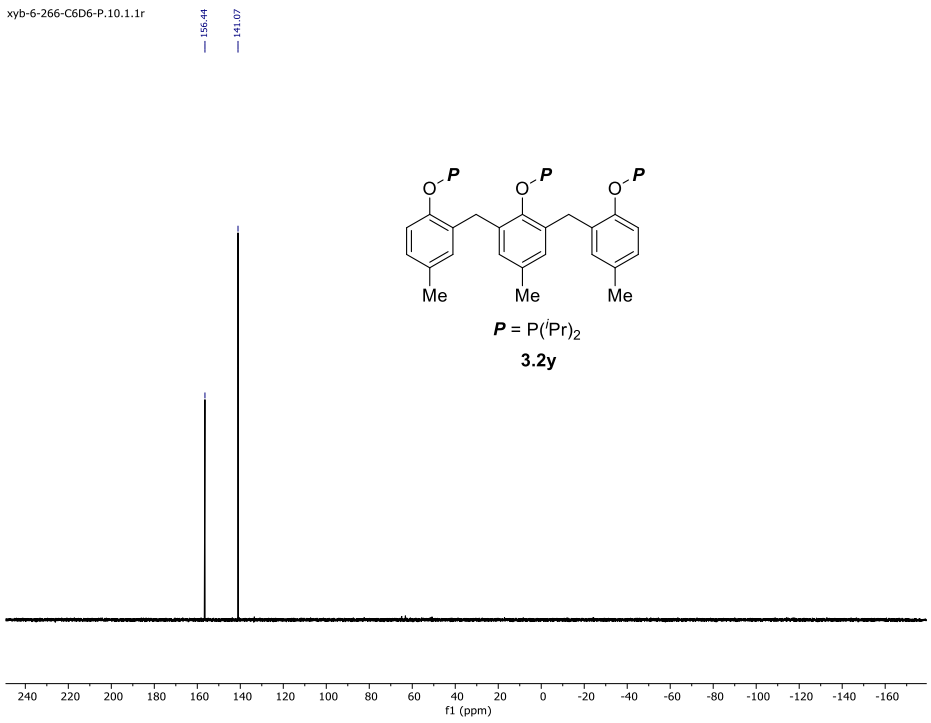

**Figure 3.231.** $^{1}$H-NMR Spectrum of **3.2z** in $C_6D_6$, 500 MHz

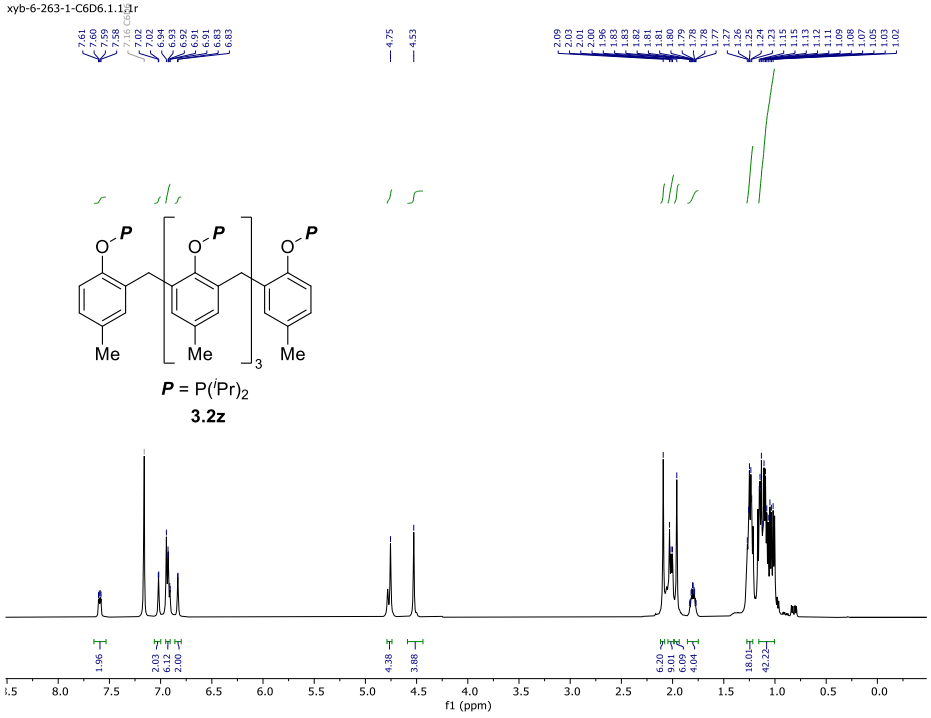


**Figure 3.232.** $^{13}$C-NMR Spectrum of **3.2z** in $C_6D_6$, 101 MHz

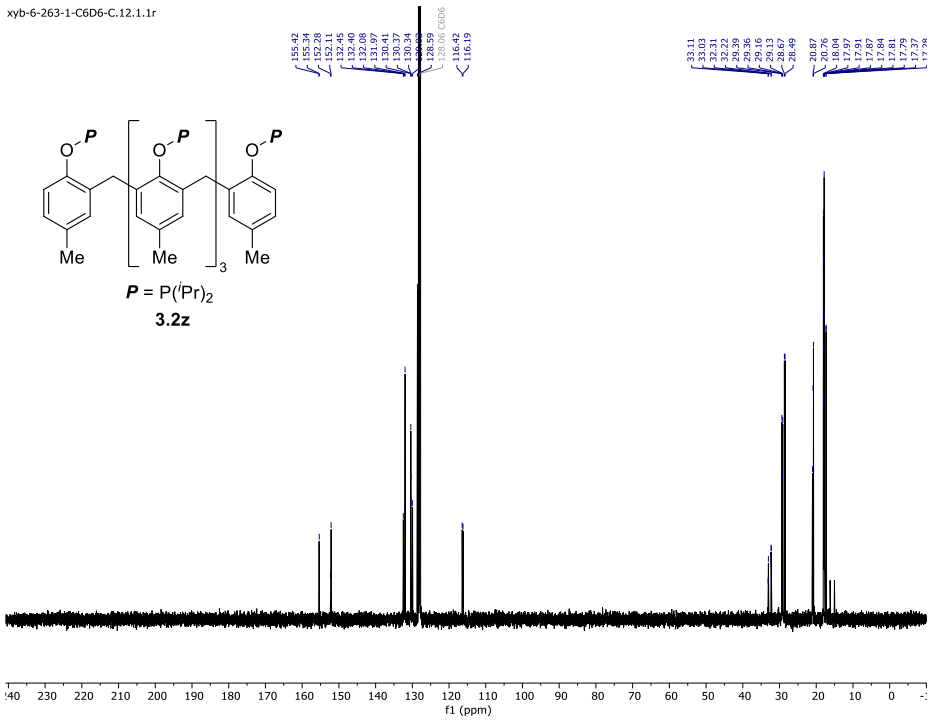

**Figure 3.233.** $^{31}$P-NMR Spectrum of **3.2z** in $C_6D_6$, 162 MHz

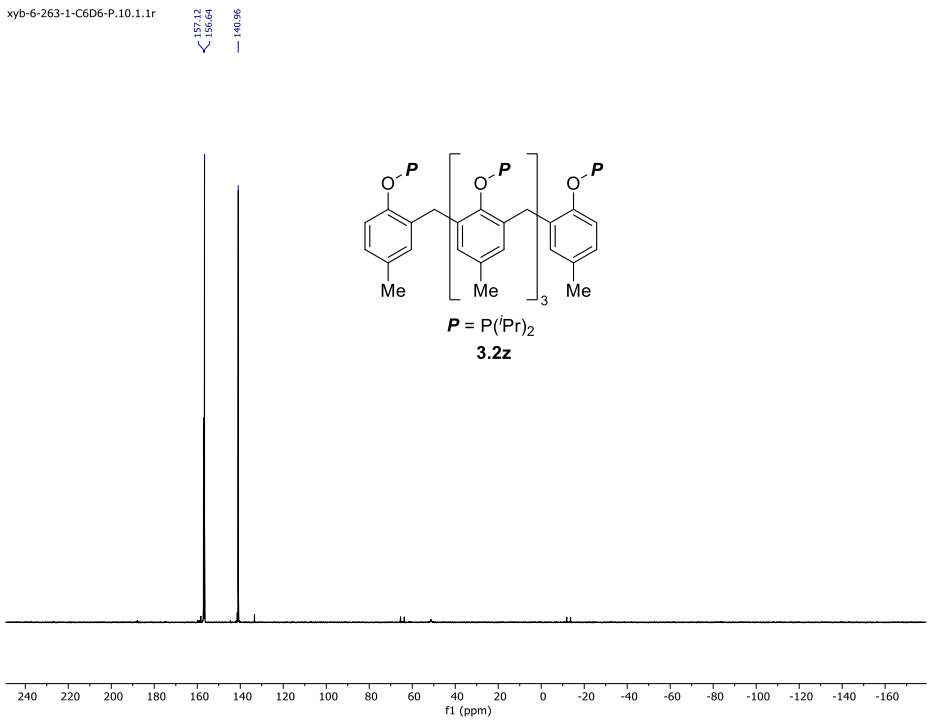

**Figure 3.234.** $^{1}$H-NMR Spectrum of **3.2aa** in $C_6D_6$, 500 MHz

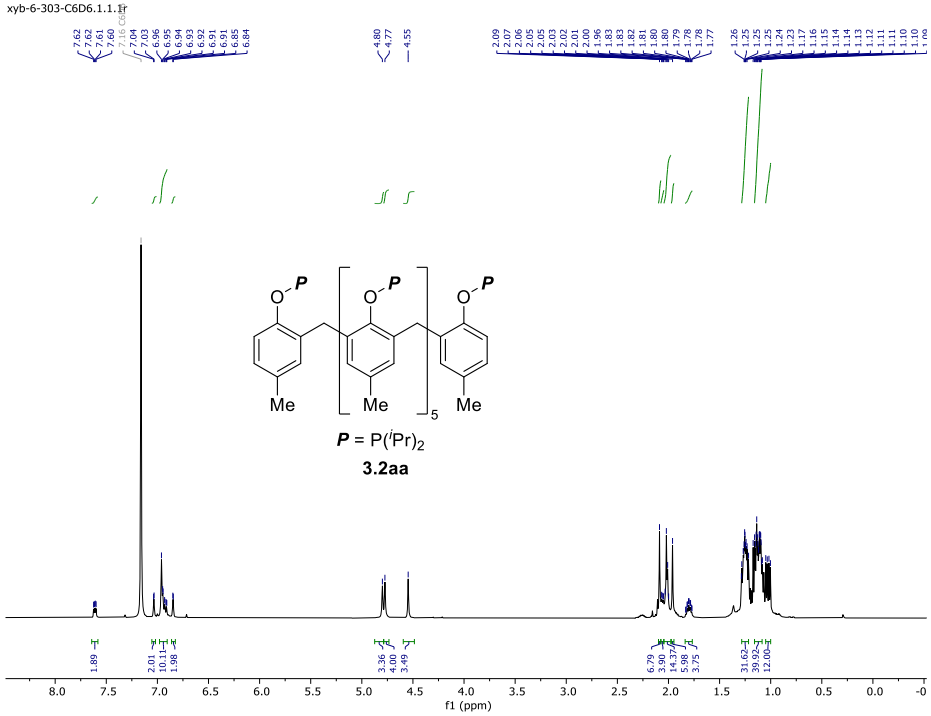


**Figure 3.235.** $^{13}$C-NMR Spectrum of **3.2aa** in $C_6D_6$, 126 MHz

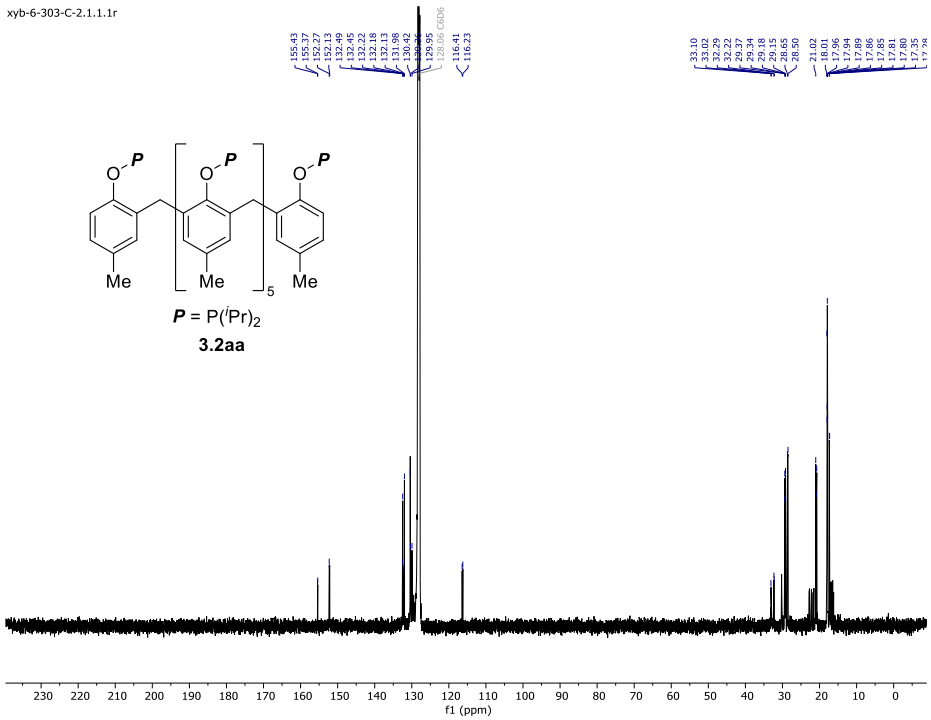

**Figure 3.236.** $^{31}$P-NMR Spectrum of **3.2aa** in $C_6D_6$, 202 MHz

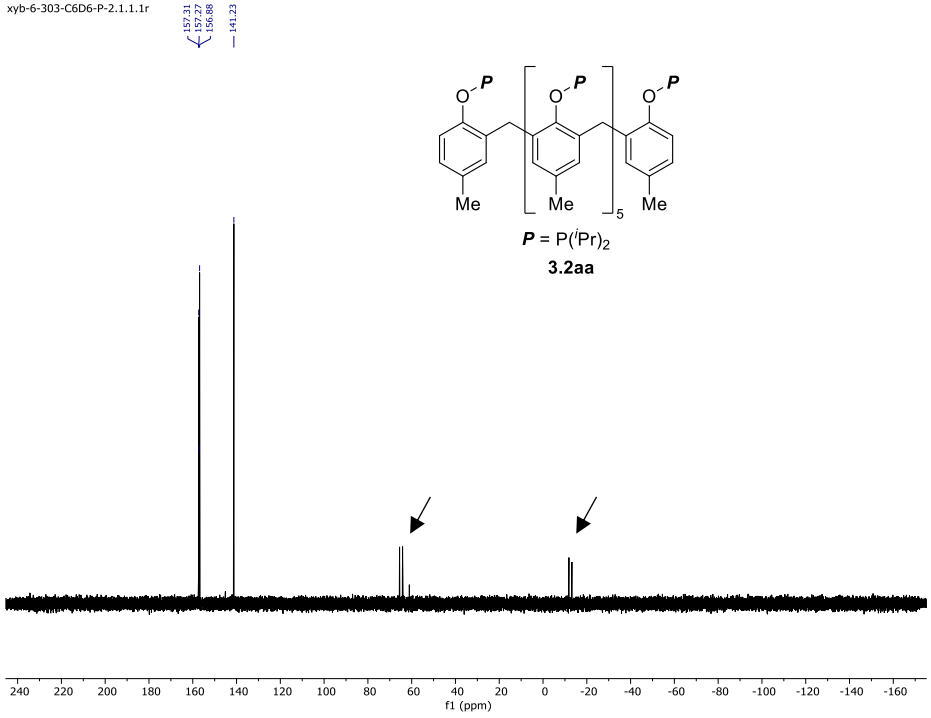

**Figure 3.237.** $^{1}$H-NMR Spectrum of **3.1t** in $CDCl_3$, 400 MHz

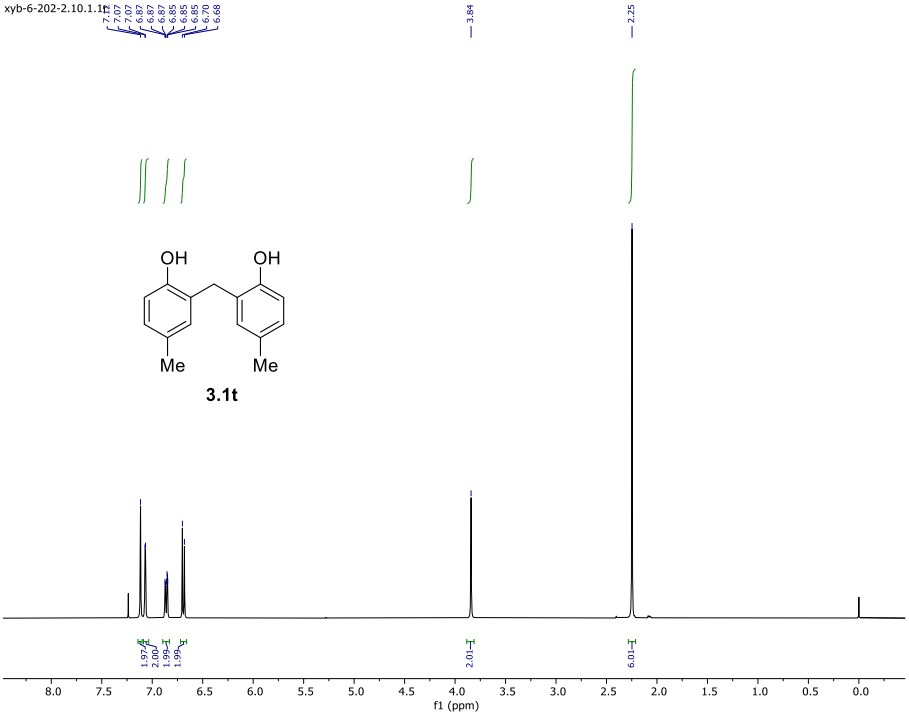


**Figure 3.238.** $^{13}$C-NMR Spectrum of **3.1t** in $CDCl_3$, 101 MHz

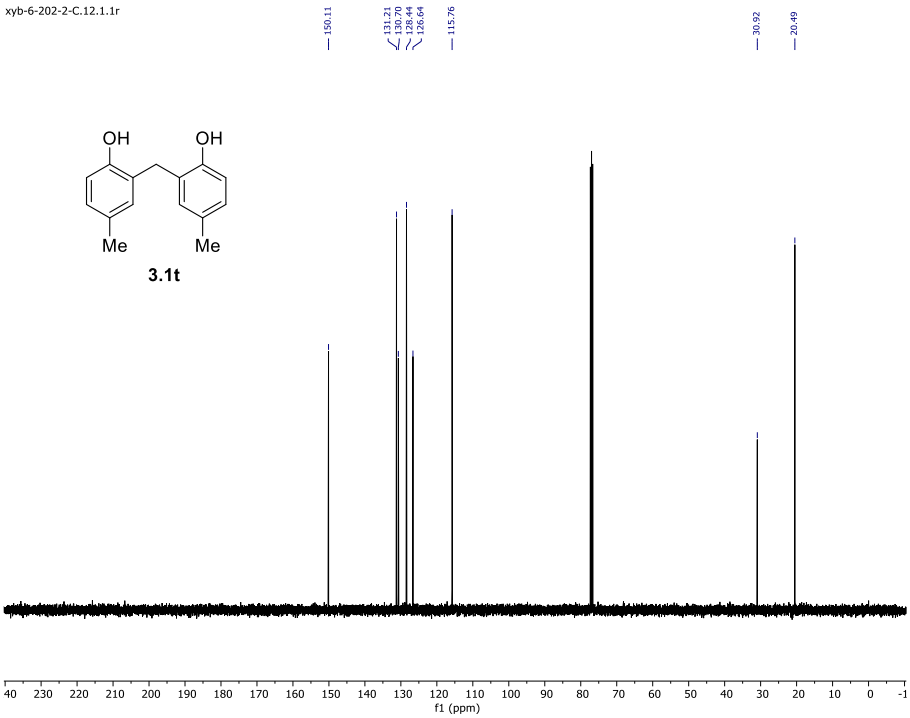

**Figure 3.239.** $^{1}$H-NMR Spectrum of **[Rh(3.2g)Cl]$_2$** in $C_6D_6$, 500 MHz

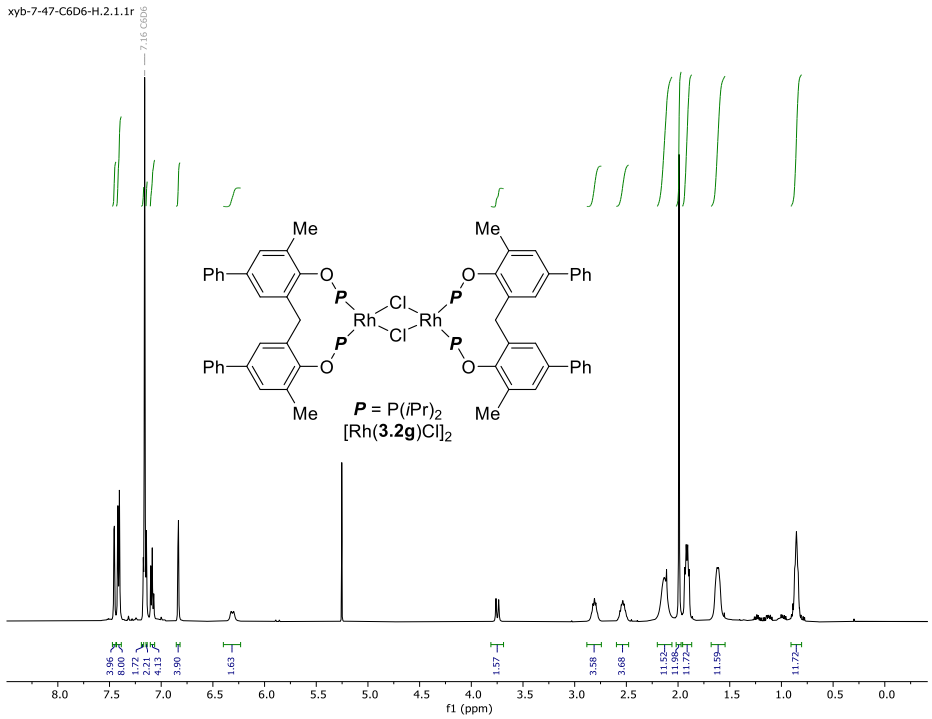


**Figure 3.240.** $^{13}$C-NMR Spectrum of **[Rh(3.2g)Cl]$_2$** in $C_6D_6$, 126 MHz

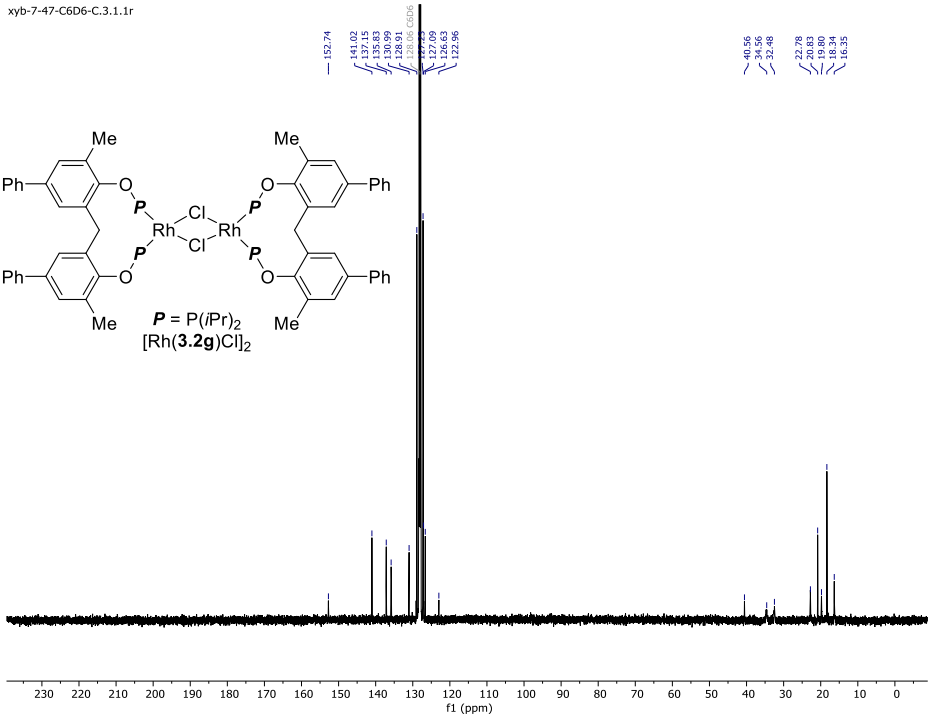

**Figure 3.241.** $^{31}$P-NMR Spectrum of **[Rh(3.2g)Cl]$_2$** in $C_6D_6$, 202 MHz

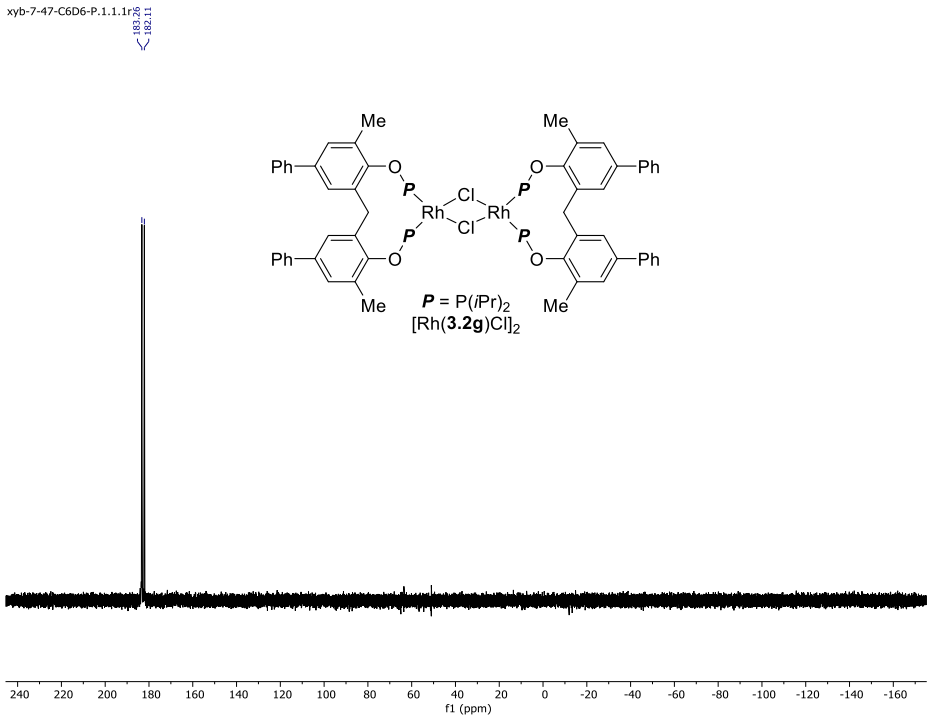

**Figure 3.242.** $^{1}$H-NMR Spectrum of **3.5** in $C_6D_6$, 500 MHz

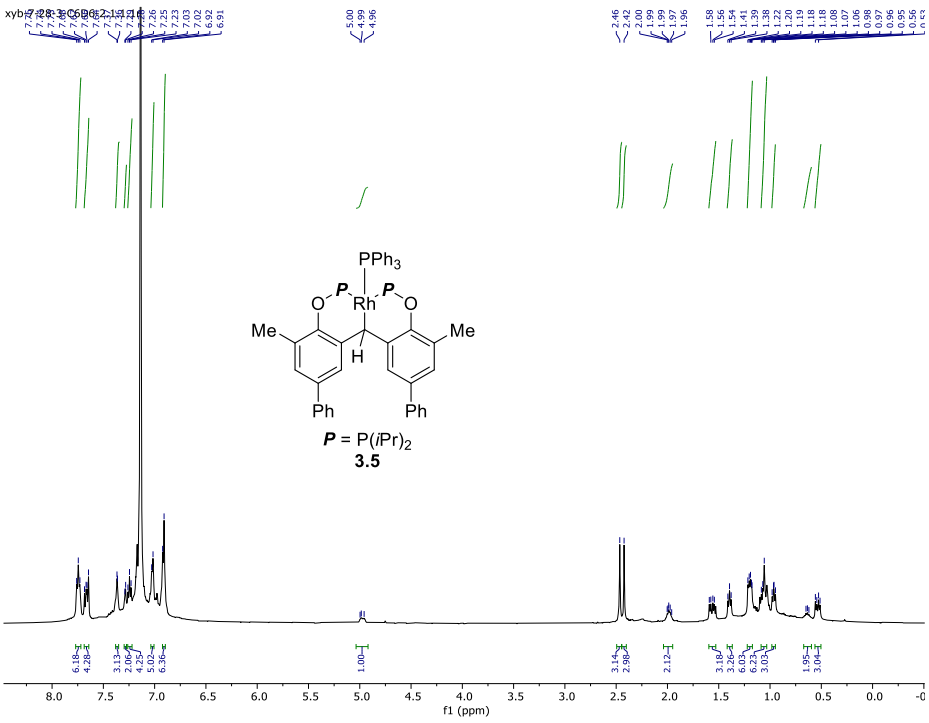


**Figure 3.243.** $^{31}$P-NMR Spectrum of **3.5** in $C_6D_6$, 202 MHz

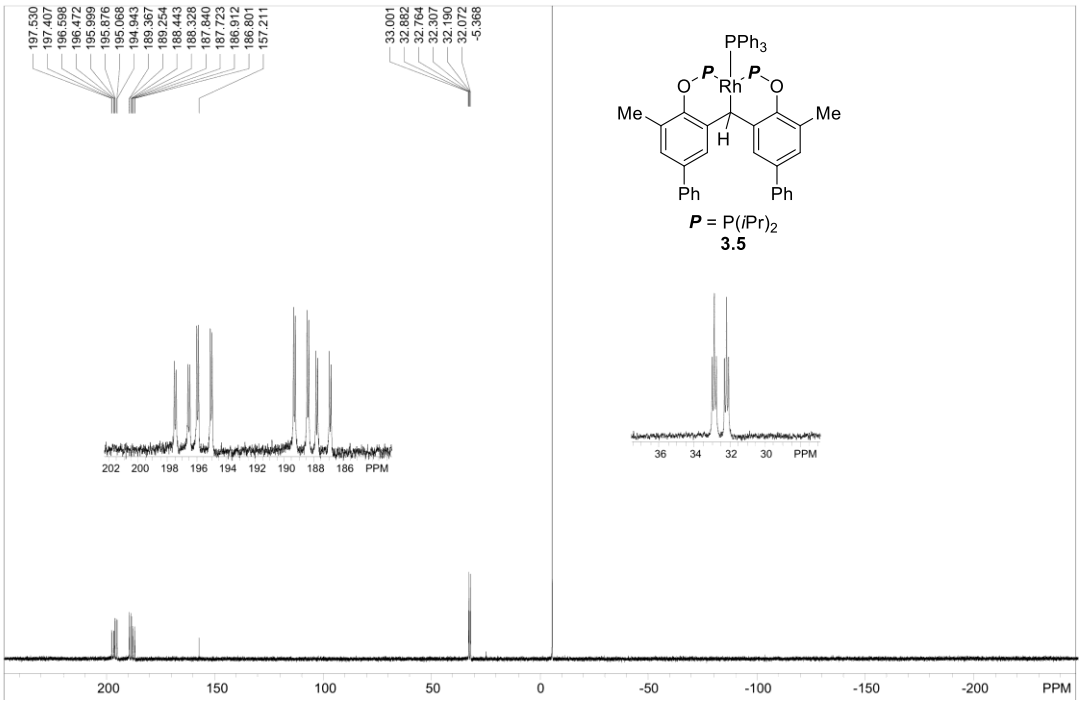

**Figure 3.244.** $^{1}$H-NMR Spectrum of **3.1g-*d*** in $CDCl_3$, 400 MHz

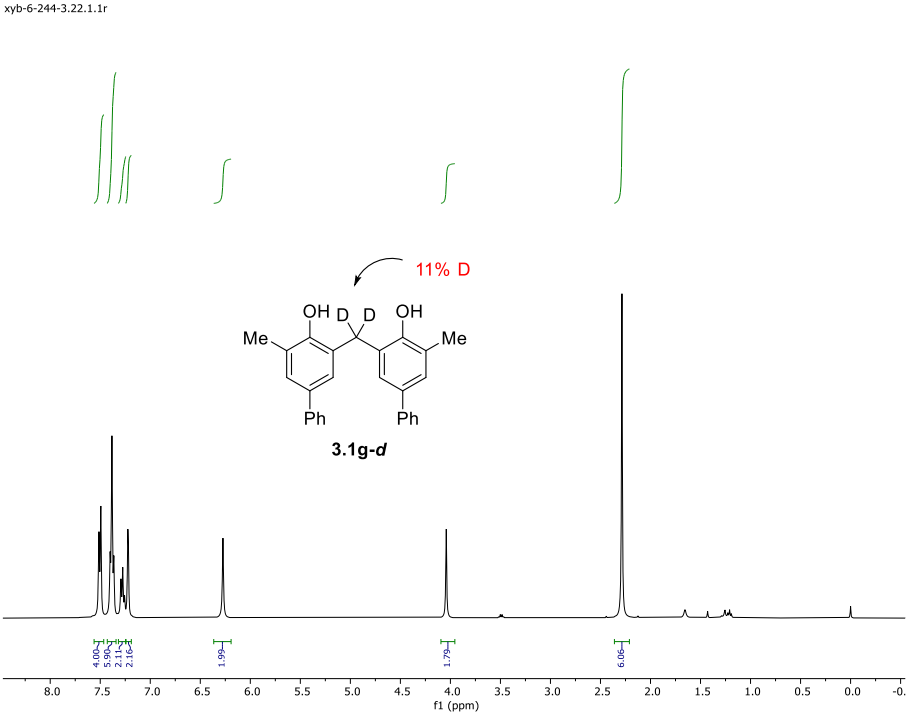


**Figure 3.245.** $^{13}$C-NMR Spectrum of **3.1g-*d*** in $CDCl_3$, 101 MHz

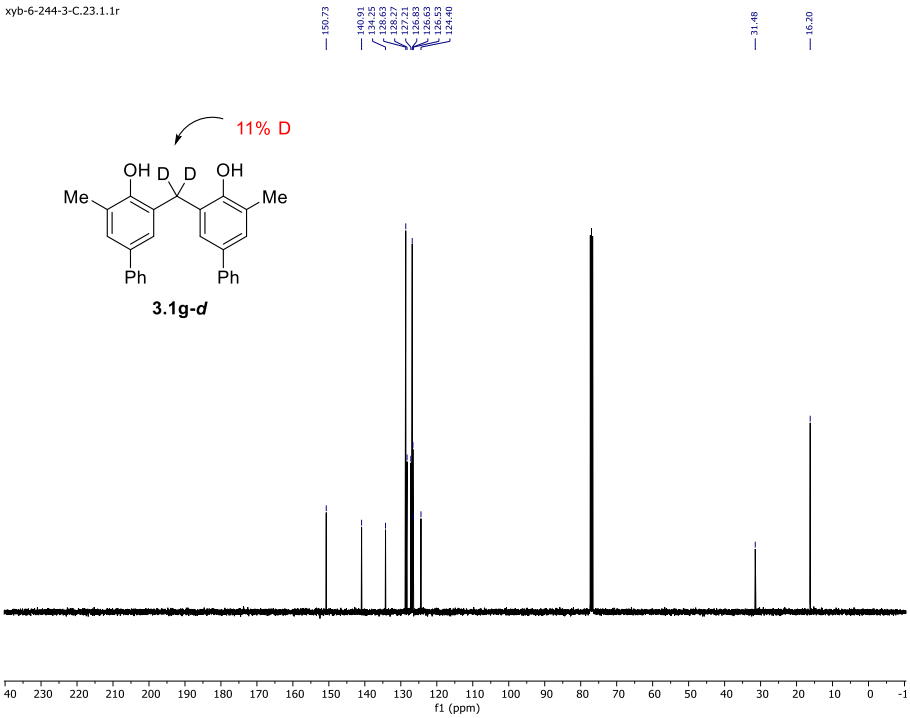

**Figure 3.246.** $^{1}$H-NMR Spectrum of **3.3g-*d*** in $CDCl_3$, 400 MHz

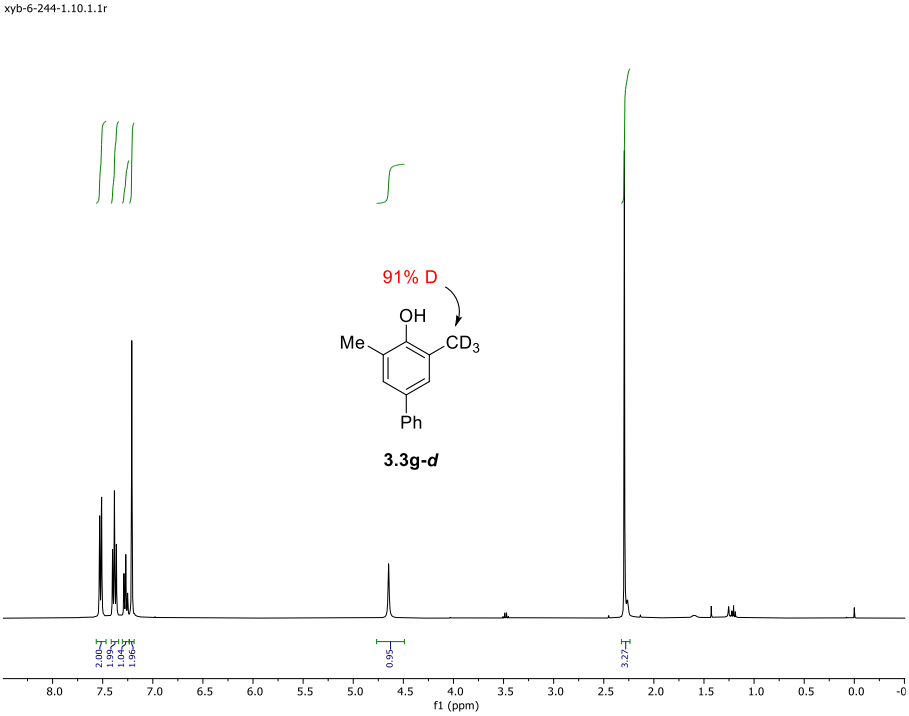


**Figure 3.247.** $^{13}$C-NMR Spectrum of **3.3g-*d*** in $CDCl_3$, 101 MHz

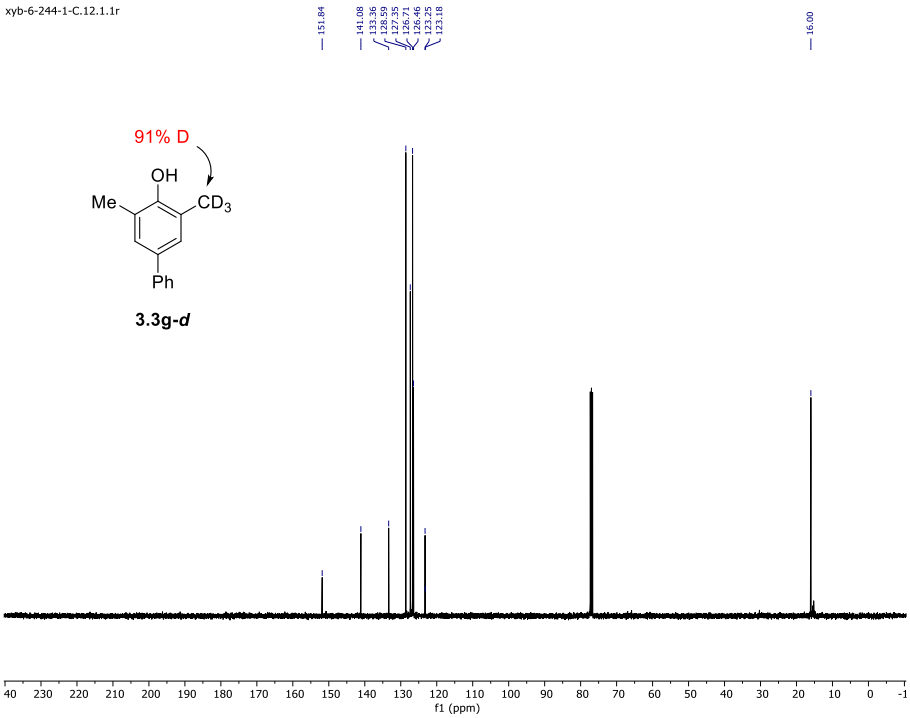

**Figure 3.248.** $^{1}$H-NMR Spectrum of **3.4g-*d*** in $CDCl_3$, 400 MHz

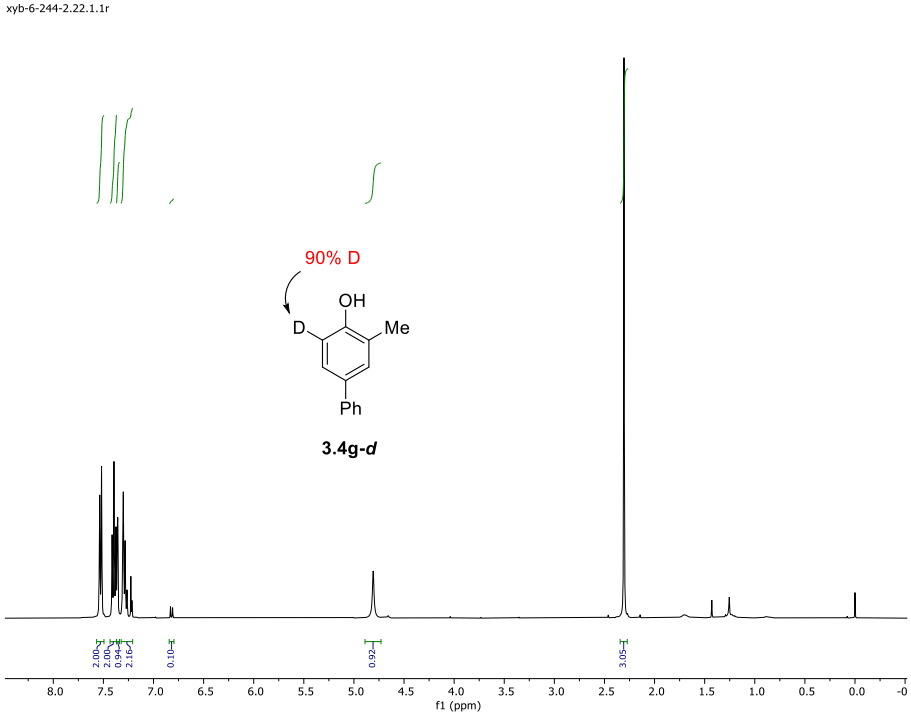


**Figure 3.249.** $^{13}$C-NMR Spectrum of **3.4g-*d*** in $CDCl_3$, 101 MHz

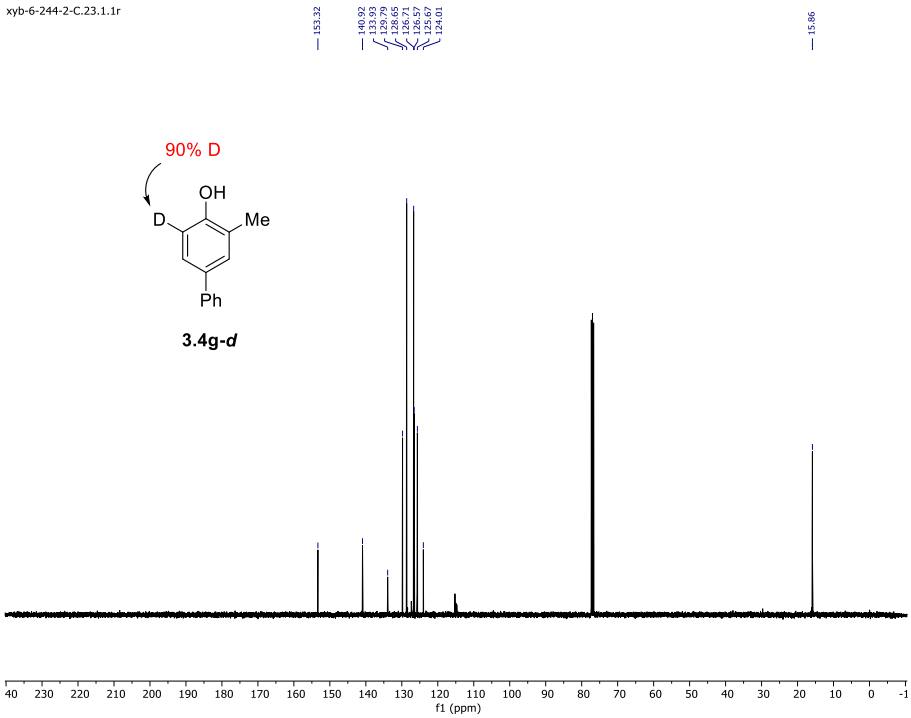

(The NMR spectra of compounds **3.2a**–**x**, **3.3b**–**o**, **3.3q**–**s**, **3.3u**, **3.4b**–**o**, **3.4q**–**s**, **3.4u** and $^{31}$P-NMR spectra of compound **3.5** were collected by Dr. Jun Zhu).

### 3.8. References


1. (a) van der Boom, M. E.; Milstein, D. Cyclometalated Phosphine-Based Pincer Complexes: Mechanistic Insight in Catalysis, Coordination, and Bond Activation. *Chem. Rev.* **2003,** *103*, 1759-1792. (b) Jun, C.-H. Transition metal-catalyzed carbon–carbon bond activation. *Chem. Soc. Rev.* **2004,** *33*, 610-618. (c) Tobisu, M.; Chatani, N. Catalytic reactions involving the cleavage of carbon–cyano and carbon–carbon triple bonds. *Chem. Soc. Rev.* **2008,** *37*, 300-307. (d) Chen, F.; Wang, T.; Jiao, N. Recent Advances in Transition-Metal-Catalyzed Functionalization of Unstrained Carbon–Carbon Bonds. *Chem. Rev.* **2014,** *114*, 8613-8661. (e) Souillart, L.; Cramer, N. Catalytic C–C Bond Activations via Oxidative Addition to Transition Metals. *Chem. Rev.* **2015,** *115*, 9410-9464. (f) Murakami, M.; Ishida, N. Potential of Metal-Catalyzed C–C Single Bond Cleavage for Organic Synthesis. *J. Am. Chem. Soc.* **2016,** *138*, 13759-13769. (g) Chen, P.-h.; Billett, B. A.; Tsukamoto, T.; Dong, G. "Cut and Sew" Transformations via Transition-Metal-Catalyzed Carbon–Carbon Bond Activation. *ACS Catal.* **2017,** *7*, 1340-1360. (h) Fumagalli, G.; Stanton, S.; Bower, J. F. Recent Methodologies That Exploit C–C Single-Bond Cleavage of Strained Ring Systems by Transition Metal Complexes. *Chem. Rev.* **2017,** *117*, 9404-9432. (i) Song, F.; Gou, T.; Wang, B.-Q.; Shi, Z.-J. Catalytic activations of unstrained C–C bond involving organometallic intermediates. *Chem. Soc. Rev.* **2018,** *47*, 7078-7115. (j) Deng, L.; Dong, G. Carbon–Carbon Bond Activation of Ketones. *Trends Chem.* **2020,** *2*, 183-198. (k) Xia, Y.; Dong, G. Temporary or removable directing groups enable activation of unstrained C–C bonds. *Nat. Rev. Chem.* **2020,** *4*, 600-614. (l) Murakami, M.; Ishida, N. Cleavage of Carbon–Carbon σ-Bonds of

Four-Membered Rings. *Chem. Rev.* **2021,** *121*, 264-299. (m) Nakao, Y. Metal-mediated C–CN Bond Activation in Organic Synthesis. *Chem. Rev.* **2021,** *121*, 327-344.

2. Lutz, M. D. R.; Morandi, B. Metal-Catalyzed Carbon–Carbon Bond Cleavage of Unstrained Alcohols. *Chem. Rev.* **2021,** *121*, 300-326.

3. (a) Rybtchinski, B.; Milstein, D. Metal Insertion into C−C Bonds in Solution. *Angew. Chem., Int. Ed.* **1999,** *38*, 870-883. (b) Dai, P.-F.; Wang, H.; Cui, X.-C.; Qu, J.-P.; Kang, Y.-B. Recent progress in C(aryl)–C(alkyl) bond cleavage of alkylarenes. *Org. Chem. Front.* **2020,** *7*, 896-904.

4. (a) Roberts, R. M.; Baylis, E. K.; Fonken, G. J. Alkylbenzenes. XII. Dealkylation and Fragmentation Reactions Induced by Aluminum Chloride-Water. *J. Am. Chem. Soc.* **1963,** *85*, 3454-3458. (b) Roberts, R. M.; Chen, H. H.-F.; Junhasavasdikul, B. New Friedel-Crafts chemistry. 34. Production of branched alkanes by acid-catalyzed dealkylation of linear alkylbenzenes. *J. Org. Chem.* **1978,** *43*, 2977-2982. (c) Macknight, E.; McClelland, R. A. A photochemical retro-Friedel–Crafts alkylation. Rapid rearrangement of cyclohexadienyl cations. *Can. J. Chem.* **1996,** *74*, 2518-2527.

5. (a) Gozin, M.; Weisman, A.; Ben-David, Y.; Milstein, D. Activation of a carbon–carbon bond in solution by transition-metal insertion. *Nature* **1993,** *364*, 699-701. (b) Liou, S.-Y.; Gozin, M.; Milstein, D. Directly Observed Oxidative Addition of a Strong Carbon-Carbon Bond to a Soluble Metal Complex. *J. Am. Chem. Soc.* **1995,** *117*, 9774-9775. (c) Rybtchinski, B.; Vigalok, A.; Ben-David, Y.; Milstein, D. A Room Temperature Direct Metal Insertion into a Nonstrained Carbon−Carbon Bond in Solution. C−C vs C−H Bond Activation. *J. Am. Chem. Soc.* **1996,** *118*, 12406-12415. (d) Liou, S.-Y.; E. van der Boom, M.; Milstein, D. Catalytic selective cleavage of a strong C–C single bond by rhodium in solution. *Chem. Commun.* **1998**, 687-688. (e) Rybtchinski, B.; Milstein, D. Solvent-Controlled Selectivity toward Exclusive C−C or C−H Bond Activation by

a Cationic Metal Center. *J. Am. Chem. Soc.* **1999,** *121*, 4528-4529. (f) van der Boom, M. E.; Ben-David, Y.; Milstein, D. Formation of Difluoromethylene−Arenium Complexes by Consecutive Aryl−CF3 C−C Bond Activation and C−F Bond Cleavage. *J. Am. Chem. Soc.* **1999,** *121*, 6652-6656. (g) Gandelman, M.; Vigalok, A.; Konstantinovski, L.; Milstein, D. The First Observation and Kinetic Evaluation of a Single Step Metal Insertion into a C−C Bond. *J. Am. Chem. Soc.* **2000,** *122*, 9848-9849.

6. (a) Qin, C.; Zhou, W.; Chen, F.; Ou, Y.; Jiao, N. Iron-Catalyzed C□H and C□C Bond Cleavage: A Direct Approach to Amides from Simple Hydrocarbons. *Angew. Chem., Int. Ed.* **2011,** *50*, 12595-12599. (b) Qin, C.; Shen, T.; Tang, C.; Jiao, N. FeCl2-Promoted Cleavage of the Unactivated C□C Bond of Alkylarenes and Polystyrene: Direct Synthesis of Arylamines. *Angew. Chem., Int. Ed.* **2012,** *51*, 6971-6975. (c) Liu, J.; Qiu, X.; Huang, X.; Luo, X.; Zhang, C.; Wei, J.; Pan, J.; Liang, Y.; Zhu, Y.; Qin, Q.; Song, S.; Jiao, N. From alkylarenes to anilines via site-directed carbon–carbon amination. *Nat. Chem.* **2019,** *11*, 71-77.

7. Onodera, S.; Ishikawa, S.; Kochi, T.; Kakiuchi, F. Direct Alkenylation of Allylbenzenes via Chelation-Assisted C–C Bond Cleavage. *J. Am. Chem. Soc.* **2018,** *140*, 9788-9792.

8. (a) Zhu, J.; Chen, P.-h.; Lu, G.; Liu, P.; Dong, G. Ruthenium-Catalyzed Reductive Cleavage of Unstrained Aryl–Aryl Bonds: Reaction Development and Mechanistic Study. *J. Am. Chem. Soc.* **2019,** *141*, 18630-18640. (b) Zhu, J.; Wang, J.; Dong, G. Catalytic activation of unstrained C(aryl)–C(aryl) bonds in 2,2′-biphenols. *Nat. Chem.* **2019,** *11*, 45-51. (c) Zhu, J.; Zhang, R.; Dong, G. Orthogonal cross-coupling through intermolecular metathesis of unstrained C(aryl)–C(aryl) single bonds. *Nat. Chem.* **2021,** *13*, 836-842.

9. (a) Benjamin, B. M.; Raaen, V. F.; Maupin, P. H.; Brown, L. L.; Collins, C. J. Thermal cleavage of chemical bonds in selected coal-related structures. *Fuel* **1978,** *57*, 269-272. (b) Allen, D. T.;

Gavalas, G. R. Reactions of methylene and ether bridges. *Fuel* **1984,** *63*, 586-592. (c) Tagaya, H.; Suzuki, Y.-i.; Kadokawa, J.-i.; Karasu, M.; Chiba, K. Decomposition of Model Compounds of Phenol Resin Waste with Supercritical Water. *Chem. Lett.* **1997,** *26*, 47-48. (d) Suzuki, Y.-i.; Tagaya, H.; Asou, T.; Kadokawa, J.-i.; Chiba, K. Decomposition of Prepolymers and Molding Materials of Phenol Resin in Subcritical and Supercritical Water under an Ar Atmosphere. *Ind. Eng. Chem. Res.* **1999,** *38*, 1391-1395. (e) Ozaki, J.-i.; Djaja, S. K. I.; Oya, A. Chemical Recycling of Phenol Resin by Supercritical Methanol. *Ind. Eng. Chem. Res.* **2000,** *39*, 245-249.

10. (a) Comanescu, C. C.; Iluc, V. M. Synthesis and Reactivity of a Nucleophilic Palladium(II) Carbene. *Organometallics* **2014,** *33*, 6059-6064. (b) Arras, J.; Speth, H.; Mayer, H. A.; Wesemann, L. Different Coordination Modes of the Ph2PCsp3PPh2 Pincer Ligand in Rhodium Complexes as a Consequence of Csp3–H Metal Interaction. *Organometallics* **2015,** *34*, 3629-3636. (c) Logan, J. R.; Piers, W. E.; Borau-Garcia, J.; Spasyuk, D. M. Ligand Attachment Chemistry in the Preparation of PCsp3P and PCsp2P Complexes of Rhodium. *Organometallics* **2016,** *35*, 1279-1286.

11. (a) Lewis, L. N.; Smith, J. F. Catalytic carbon-carbon bond formation via ortho-metalated complexes. *J. Am. Chem. Soc.* **1986,** *108*, 2728-2735. (b) Bedford, R. B.; Coles, S. J.; Hursthouse, M. B.; Limmert, M. E. The Catalytic Intermolecular Orthoarylation of Phenols. *Angew. Chem., Int. Ed.* **2003,** *42*, 112-114.

12. Opaprakasit, P.; Scaroni, A.; Painter, P. Intramolecular hydrogen bonding and calixarene-like structures in p-cresol/formaldehyde resins. *J. Mol. Struct.* **2001,** *570*, 25-35.

13. Karimzadeh-Younjali, M.; Wendt, O. F. α- and β-Eliminations in Transition Metal Complexes: Strategies to Cleave Unstrained C−C and C−F Bonds. *Helv. Chim. Acta* **2021,** *104*, e2100114.

14. Kirste, A.; Schnakenburg, G.; Waldvogel, S. R. Anodic Coupling of Guaiacol Derivatives on Boron-Doped Diamond Electrodes. *Org. Lett.* **2011,** *13*, 3126-3129.

15. Imahori, T.; Tokuda, T.; Taguchi, T.; Takahata, H. An Alternative Approach to para-C–H Arylation of Phenol: Palladium-Catalyzed Tandem γ-Arylation/Aromatization of 2-Cyclohexen-1-one Derivatives. *Org. Lett.* **2012,** *14*, 1172-1175.

16. Beaver, D. J.; Stoffel, P. J. Preparation of Substituted Bis-phenols. *J. Am. Chem. Soc.* **1952,** *74*, 3410-3411.

17. Bagnacani, V.; Sansone, F.; Donofrio, G.; Baldini, L.; Casnati, A.; Ungaro, R. Macrocyclic Nonviral Vectors: High Cell Transfection Efficiency and Low Toxicity in a Lower Rim Guanidinium Calix[4]arene. *Org. Lett.* **2008,** *10*, 3953-3956.

18. Song, G.-S.; Heo, Y.-J.; Baek, J. J.; Lee, H.; Bae, G. Y.; Choi, K. H.; Koh, W.-G.; Shin, G. The improved photosensitivity of photosensitive polyimides containing o-nitrobenzyl ether groups induced by the addition of photoacid generator. *Journal of Polymer Science* **2021,** *59*, 340-352.

19. Sartori, G.; Bigi, F.; Maggi, R.; Porta, C. Metal-template ortho-regioselective mono- and bis-de-tert-butylation of poly-tert-butylated phenols. *Tetrahedron Lett.* **1994,** *35*, 7073-7076.

20. Grüttner, C.; Böhmer, V.; Assmus, R.; Scherf, S. A convenient and general synthesis of alkanediyl diphenols. *J. Chem. Soc., Perkin Trans. 1* **1995**, 93-94.

21. Chutayothin, P.; Ishida, H. Polymerization of p-cresol, formaldehyde, and piperazine and structure of monofunctional benzoxazine-derived oligomers. *Polymer* **2011,** *52*, 3897-3904.

22. Aoki, M.; Nakashima, K.; Kawabata, H.; Tsutsui, S.; Shinkai, S. Molecular design and characterizations of new calixarene-based gelators of organic fluids. *Journal of the Chemical Society, Perkin Transactions 2* **1993**, 347-354.

23. Castro-Godoy, W. D.; Schmidt, L. C.; Argüello, J. E. A Green Alternative for the Conversion of Arylboronic Acids/Esters into Phenols Promoted by a Reducing Agent, Sodium Sulfite. *Eur. J. Org. Chem.* **2019,** *2019*, 3035-3039.

24. Paul, R.; Ali, M. A.; Punniyamurthy, T. Copper-Catalyzed Hydroxylation of Aryl Halides with Tetrabutylammonium Hydroxide: Synthesis of Substituted Phenols and Alkyl Aryl Ethers. *Synthesis* **2010,** *2010*, 4268-4272.

25. Maier, T. M.; Sandl, S.; Melzl, P.; Zweck, J.; Jacobi von Wangelin, A.; Wolf, R. Heterogeneous Olefin Hydrogenation Enabled by a Highly-Reduced Nickel(−II) Catalyst Precursor. *Chem. - Eur. J.* **2020,** *26*, 6113-6117.

26. Furukawa, T.; Tobisu, M.; Chatani, N. C–H Functionalization at Sterically Congested Positions by the Platinum-Catalyzed Borylation of Arenes. *J. Am. Chem. Soc.* **2015,** *137*, 12211-12214.

27. Johnson, S. M.; Connelly, S.; Wilson, I. A.; Kelly, J. W. Toward Optimization of the Linker Substructure Common to Transthyretin Amyloidogenesis Inhibitors Using Biochemical and Structural Studies. *J. Med. Chem.* **2008,** *51*, 6348-6358.

28. Bos, P. H.; Antalek, M. T.; Porco, J. A.; Stephenson, C. R. J. Tandem Dienone Photorearrangement–Cycloaddition for the Rapid Generation of Molecular Complexity. *J. Am. Chem. Soc.* **2013,** *135*, 17978-17982.

29. Dyadyuk, A.; Sudheendran, K.; Vainer, Y.; Vershinin, V.; Shames, A. I.; Pappo, D. Direct Synthesis of Polyaryls by Consecutive Oxidative Cross-Coupling of Phenols with Arenes. *Org. Lett.* **2016,** *18*, 4324-4327.

30. Song, S.; Sun, X.; Li, X.; Yuan, Y.; Jiao, N. Efficient and Practical Oxidative Bromination and Iodination of Arenes and Heteroarenes with DMSO and Hydrogen Halide: A Mild Protocol for Late-Stage Functionalization. *Org. Lett.* **2015,** *17*, 2886-2889.

31. Kavala, V.; Naik, S.; Patel, B. K. A New Recyclable Ditribromide Reagent for Efficient Bromination under Solvent Free Condition. *J. Org. Chem.* **2005,** *70*, 4267-4271.

32. Hackl, M. W.; Lakemeyer, M.; Dahmen, M.; Glaser, M.; Pahl, A.; Lorenz-Baath, K.; Menzel, T.; Sievers, S.; Böttcher, T.; Antes, I.; Waldmann, H.; Sieber, S. A. Phenyl Esters Are Potent Inhibitors of Caseinolytic Protease P and Reveal a Stereogenic Switch for Deoligomerization. *J. Am. Chem. Soc.* **2015,** *137*, 8475-8483.

33. Schmidt, R.; Stolle, A.; Ondruschka, B. Aromatic substitution in ball mills: formation of aryl chlorides and bromides using potassium peroxomonosulfate and NaX. *Green Chem.* **2012,** *14*, 1673-1679.

34. Pan, W.; Li, C.; Zhu, H.; Li, F.; Li, T.; Zhao, W. A mild and practical method for deprotection of aryl methyl/benzyl/allyl ethers with HPPh2 and tBuOK. *Org. Biomol. Chem.* **2021,** *19*, 7633-7640.

35. Zhong, Y.; Yuan, L.; Huang, Z.; Gu, W.; Shao, Y.; Han, W. Unexpected hydrazine hydrate-mediated aerobic oxidation of aryl/ heteroaryl boronic acids to phenols in ambient air. *RSC Advances* **2014,** *4*, 33164-33167.

36. Zhang, Q.; Chang, X.; Peng, L.; Guo, C. Asymmetric Lewis Acid Catalyzed Electrochemical Alkylation. *Angew. Chem., Int. Ed.* **2019,** *58*, 6999-7003.

37. Fuchs, A.; Baur, R.; Schoeder, C.; Sigel, E.; Müller, C. E. Structural analogues of the natural products magnolol and honokiol as potent allosteric potentiators of GABAA receptors. *Biorg. Med. Chem.* **2014,** *22*, 6908-6917.

38. Eliasen, A. M.; Thedford, R. P.; Claussen, K. R.; Yuan, C.; Siegel, D. A Protocol To Generate Phthaloyl Peroxide in Flow for the Hydroxylation of Arenes. *Org. Lett.* **2014,** *16*, 3628-3631.

39. Ingenfeld, B.; Straub, S.; Frömbgen, C.; Lützen, A. Synthesis of Monofunctionalized Calix[5]arenes. *Synthesis* **2018,** *50*, 676-684.

# CHAPTER 4

# Mono-Directed Catalytic Activation of Unstrained C(Aryl)−C(Alkyl) Bonds in α-Methyl Phenols

## 4.1. Introduction

Transition metal catalyzed C−C bond activation has become a useful tool in organic synthesis.[1] A deconstructive strategy to synthesize complex natural products with diverse scaffold is developed in recent years based on the C−C bond activation.[2] However, most work on C−C bond activation is still based on the substrates with high ring strain[1g, 1k] or polar functional groups,[1c, 1i, 1l] which limit the application of C−C bond activation. Activation and functionalization of non-polar and unstrained C−C bond remains to be a challenge for the organic chemist.

Milstein and co-workers found that the unstrained C(aryl)−C(alkyl) bond in pincer type ligands could be cleaved and hydrogenated mediated by transition metal (Scheme 4.1).[3] Their detailed mechanism study proved that the C(aryl)−C(alkyl) bond activation went through directly oxidative addition of the transition metal.[3b, 3g] However, their method typically required stoichiometric amount of transition metal to realize this transformation. For contrast, the only

catalytic case shown low efficiency, which caused by the competitive coordination between substrate and product.[3d]

Inspired by Milstein's pioneer work, our group developed the catalytic activation of unstrained C(aryl)−C(aryl) bonds.[4] Since the product of this reaction become monodentate ligand, which is less competitive for metal center coordination, our reaction shown very high turn-over number. In 2022, we extend this reaction to C(aryl)−C(alkyl) bonds activation, which also shown high catalytic efficiency to give unsymmetric mono-phenols (See Section 3 for details).[5]

**Scheme 4.1.** Bidentate Ligand Chelation-Assisted Unstained C−C Bond Activation via Oxidative Addition.

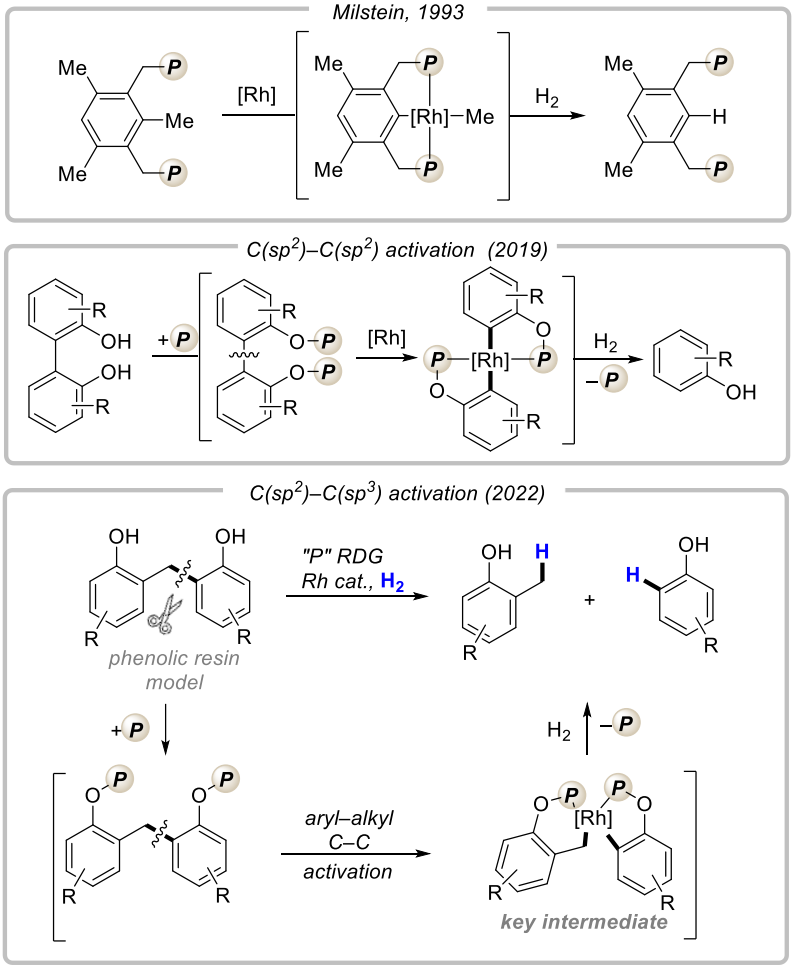


However, current methods of unstained C−C bond activation majorly relay on substate with bidentate directing groups. The bidentate directing group can facilitate the C−C activation in two aspects, including: (i) forming stable fused bicyclic or spiro-cyclic metallocycle after oxidative addition; (ii) promoting the ligand exchange between product-metal complex and substrate driven by entropy, which increase the catalytic efficiency. Although bidentate directing group can make the C−C activation process become easier, it also restrict the scope and application of this method. In 2001, Milstein group tested their C−C activation condition on substrate with monodentate

phosphine directing group, but they cannot detected C−C bond activation product (Scheme 4.2).[6] For instead, the only observe product is C−H activation product. In 2002, Whittlesey group found that the methyl group in IMes ligand of a ruthenium complex could be cleaved upon heating.[7] To our knowledge, this work represents the first example of unstrained C−C bond activation of monodentate ligand. The following calculation study shown that the key intermediate contains only one IMes ligand on metal center, and the strong electron-donating NHC ligand is crucial for C−C activation.[8] In 2018, Kakiuchi group reported an elegant Rh-catalyzed C(aryl)−C(allyl) bond activation via $\beta$-carbon elimination.[9] In this work, both pyridine directing group and allyl group are essential to realize this transformation.

**Scheme 4.2.** Monodentate Ligand Chelation-Assisted Unstained C−C Bond Activation.

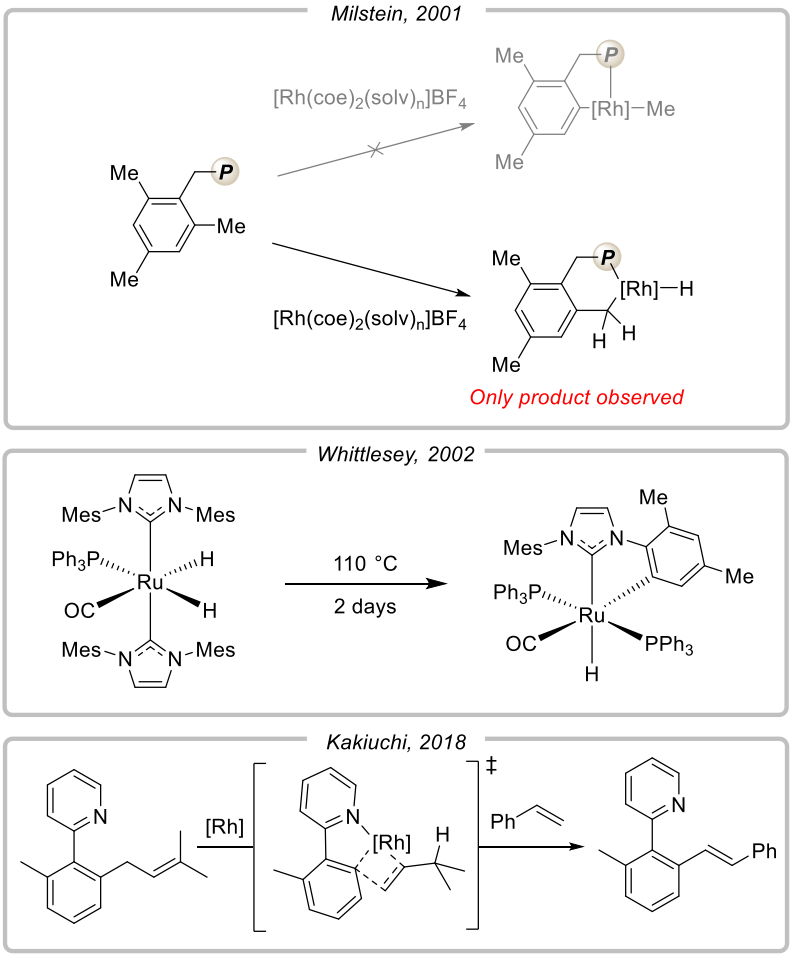


To overcome the current limitation on unstained C−C bond activation, we proposed that through installation of phosphinite directing group, the α-C−C bond of phenols could be cleaved by hydrogenation (Scheme 4.3). The NHC-coordinated transition metal was expected to be sufficient electron-rich to undergo oxidative addition into C−C bond, and the subsequential hydrogenation would generate α-unsubstituted phenol.

**Scheme 4.3.** Mono-Directed Catalytic C−C Activation.

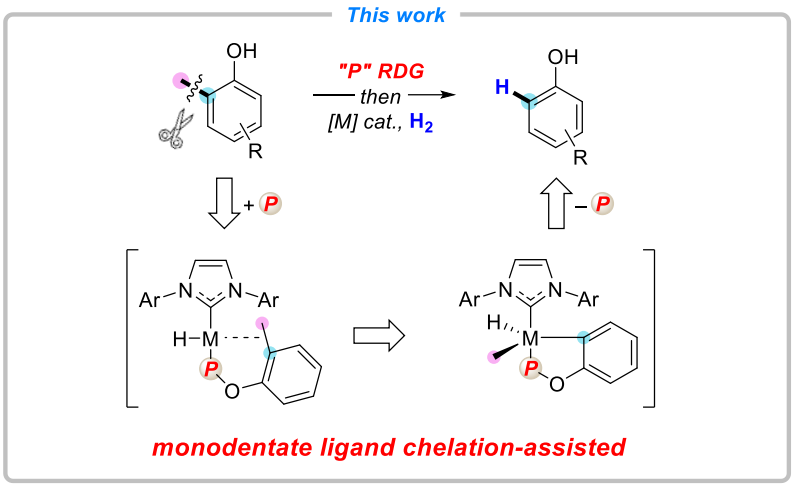


## 4.2. Discovery and Optimization

Preparation of phosphinite **4.2a** worked smoothly under standard condition in 93% yield (Scheme 4.4). With phosphinite **4.2a** in hand, we started to explore the key C−C cleavage reaction. We firstly tested the combination between different transition metal catalysts and NHC ligands, such as rhodium, ruthenium and iridium catalyst with IMes and IPr ligands (Table 4.1). However, no desired product was observed under these conditions.

**Scheme 4.4.** Preparation of Phosphinite **4.2a**.

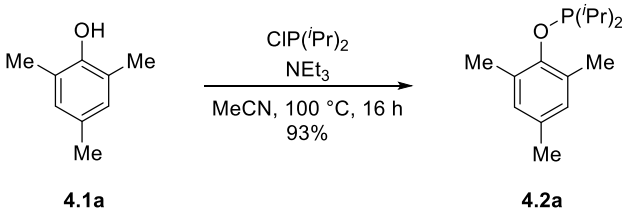


**4.1a** **4.2a**

**Table 4.1.** Catalysts Screening on C−C Activation of Phosphinite **4.2a**.

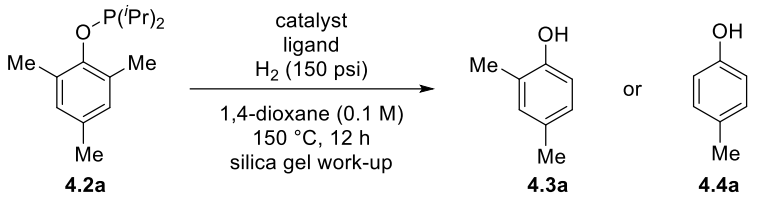


**4.2a** **4.3a** **4.4a**

| Entry | Catalyst | Ligand | Result |
|---|---|---|---|
| 1 | $[Rh(C_2H_4)_2Cl]_2$ (5 mol%) | IPr (10 mol%) or IMes (10 mol%) | n.r. |
| 2 | $Rh(PPh_3)_4H$ (2.5 mol%) | IPr (10 mol%) or IMes (10 mol%) | n.r. |
| 3 | $Ru(COD)Cl_2$ (10 mol%) | IPr (10 mol%) or IMes (10 mol%) | n.r. |
| 4 | Ru(*p*-cymene)($PCy_3$)HCl (5 mol%) | IPr (10 mol%) or IMes (10 mol%) | n.r. |
| 5 | Ru(*p*-cymene)($PCy_3$)$H_2$ (5 mol%) | IPr (10 mol%) or IMes (10 mol%) | n.r. |
| 6 | Ru(COD)(COT) (5 mol%) | IPr (10 mol%) or IMes (10 mol%) | n.r. |
| 7 | $[Ir(COD)Cl]_2$ (2.5 mol%) | IPr (10 mol%) or IMes (10 mol%) | n.r. |

Inspired by Whittlesey's work,[7] we proposed that we can increase the bulkiness of the phosphinite to avoid multiple coordination, which would inhibit C−C activation. Thus, we designed phosphinite **4.5a**, which bearing two *tert*-butyl groups. The preparation of phosphinite **4.5a** is not as simple as phosphinite **4.2a**, due to the huge steric hindrance of di-*tert*-butylchlorophosphine. After condition screening, we found that the desired phosphinite **4.5a** could be obtained in high yield using sodium hydride as base and DMF as solvent (entry 5, Table 4.2). And a 68% yield of phosphinite **4.5a** was got under gram-scale at an elevated temperature (entry 6, Table 4.2).

**Table 4.2.** Preparation of Phosphinite **4.5a**.

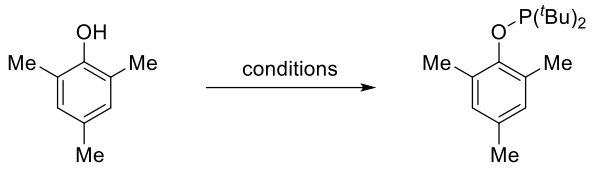


**4.1a** **4.5a**

| Entry | Conditions | Result |
|---|---|---|
| 1 | $ClP(^tBu)_2$, $NEt_3$, MeCN, 100 °C, 16 h | n.d. |
| 2 | $ClP(^tBu)_2$, $NEt_3$, DMF, 100 °C, 16 h | low conversion |
| 3 | NaH, $ClP(^tBu)_2$, 1,4-dioxane, 100 °C, 16 h | 66% (~85% purity) |
| 4 | NaH, $ClP(^tBu)_2$, THF, 100 °C, 16 h | not pure |
| 5 | NaH, $ClP(^tBu)_2$, DMF, 100 °C, 16 h | 95% |
| 6 | NaH, $ClP(^tBu)_2$, KI, DMF, 120 °C, 16 h | 68% (gram scale) |

To our surprise, the first trial on C−C cleavage of phosphinite **4.5a** gave the desired product **4.3a** in 14% yield with 22% yield of unreacted phenol **4.1a**, which proved our original hypothesis (entry 2, Table 4.3). We tried to decrease the temperature to 100 °C to prevent decomposition (entry 3-4, Table 4.3). However, only trace amount of phenol **4.3a** was observed under 100 °C.

**Table 4.3.** Initial Attempts on C−C Activation of Phosphinite **4.5a**.

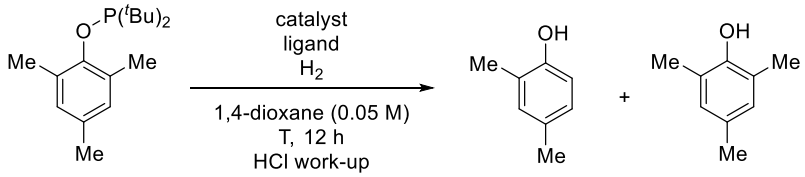


**4.5a** **4.3a** **4.1a**

| Entry | Catalyst | Ligand | Temperature | $H_2$ pressure | Result |
|---|---|---|---|---|---|
| 1 | $[Rh(C_2H_4)_2Cl]_2$ (2.5 mol%) | IPr (5 mol%) | 150 °C | 150 psi | trace **4.3a** |
| 2 | $[Rh(C_2H_4)_2Cl]_2$ (2.5 mol%) | IMes (5 mol%) | 150 °C | 150 psi | 14% **4.3a** + 22% **4.1a** |
| 3 | $[Rh(C_2H_4)_2Cl]_2$ (2.5 mol%) | IPr (5 mol%) | 100 °C | 100 psi | trace **4.3a** |
| 4 | $[Rh(C_2H_4)_2Cl]_2$ (2.5 mol%) | IMes (5 mol%) | 100 °C | 100 psi | trace **4.3a** |

With this preliminary result in hand, we started to screen different metal pre-catalysts. The first-row metal catalysts were unreactive for our reaction (entry 1-5, Table 4.4). Ruthenium

catalysts were found to be effective for this transformation (entry 6-14, Table 4.4), in which [Ru(*p*-cymene)$Cl_2$]$_2$ was found to be optimized catalyst to give 25% yield of phenol **4.3a** (entry 9, Table 4.4). It worth to notice that all the ruthenium dihydride catalysts did not deliver the desired C−C cleavage product (entry 8, 12, 14, Table 4.4), which may indicate ruthenium dihydride is not an intermediate in the catalytic cycle. Rhodium catalysts were also able to deliver phenol 4.3a, although in a slightly diminished yield (entry 15-17, Table 4.4). Other transition metal catalysts, such as palladium (entry 18, Table 4.4), iridium (entry 19, Table 4.4) and platinum (entry 20, Table 4.4), were unfruitful for this transformation.

**Table 4.4.** Catalysts Screening on C−C Activation of Phosphinite **4.5a**.

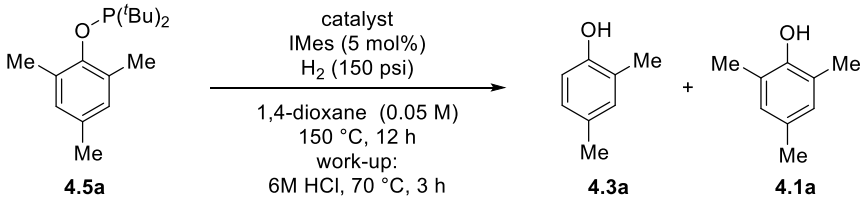


**4.5a** **4.3a** **4.1a**

| Entry | catalyst | **4.3a** | **4.1a** | Entry | catalyst | **4.3a** | **4.1a** |
|---|---|---|---|---|---|---|---|
| 1 | $FeCl_2$ (5 mol%) | n.d. | 100% | 11 | $Ru(PPh_3)_3(CO)HCl$ (5 mol%) | n.d. | 99% |
| 2 | $CoCl_2$ (5 mol%) | n.d. | 97% | 12 | $Ru(PPh_3)_3(CO)H_2$ (5 mol%) | n.d. | 98% |
| 3 | $CoCl(PPh_3)_3$ (5 mol%) | n.d. | 100% | 13 | $Ru(PPh_3)_3Cl_2$ (5 mol%) | n.d. | 97% |
| 4 | $Ni(COD)_2$ (5 mol%) | n.d. | 99% | 14 | $Ru(PPh_3)_4H_2$ (5 mol%) | n.d. | 92% |
| 5 | $NiCl_2$•DME (5 mol%) | n.d. | 98% | 15 | $[Rh(COD)Cl]_2$ (2.5 mol%) | 15% | 85% |
| 6 | $Ru(COD)Cl_2$ (5 mol%) | 16% | 80% | 16 | $Rh(OAc)_3$ (5 mol%) | 10% | 84% |
| 7 | Ru(p-cymene)($PCy_3$)HCl (5 mol%) | 5% | 89% | 17 | $Rh(acac)_3$ (5 mol%) | 7% | 88% |
| 8 | Ru(p-cymene)($PCy_3$)$H_2$ (5 mol%) | n.d. | 94% | 18 | $Pd(COD)Cl_2$ (5 mol%) | n.d. | 87% |
| 9 | $[Ru(p\text{-cymene})Cl_2]_2$ (2.5 mol%) | 25% | 75% | 19 | $[Ir(COD)Cl]_2$ (2.5 mol%) | n.d. | 91% |
| 10 | $Ru(PPh_3)_3HCl$•toluene (5 mol%) | n.d. | 99% | 20 | $Pt(COD)Cl_2$ (5 mol%) | n.d. | 87% |

Besides transition metal catalyst, different reaction temperature were also examined (Table 4.5). A slightly higher yield was obtained under 130 °C. We also screened different ligands for this reaction (Table 4.6). However, IMes is still the optimized one among all the NHC ligands we tested.

**Table 4.5.** Temperature Screening on C–C Activation of Phosphinite **4.5a**.

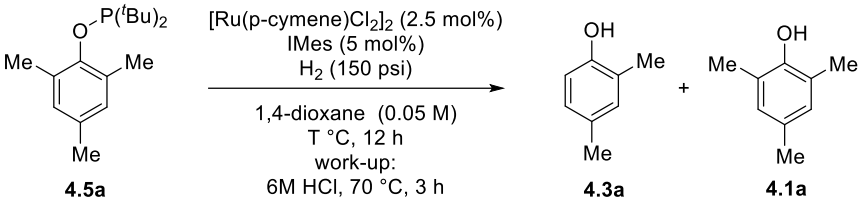


**4.5a** **4.3a** **4.1a**

| Entry | Temperature | **4.3a** | **4.1a** |
|---|---|---|---|
| 1 | 170 °C | 17% | 82% |
| 2 | 150 °C | 20% | 77% |
| 3 | 130 °C | 24% | 72% |
| 4 | 110 °C | 19% | 78% |

**Table 4.6.** Ligands Screening on C−C Activation of Phosphinite **4.5a**.

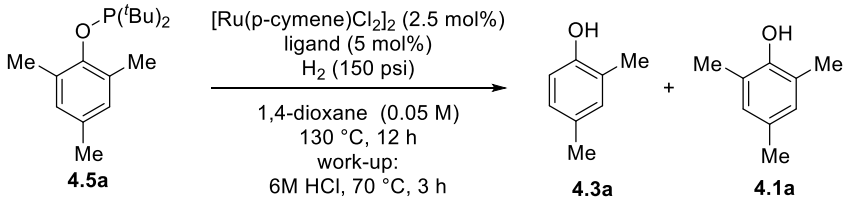


| Entry | ligand | **4.3a** | **4.1a** | Entry | ligand | **4.3a** | **4.1a** |
|---|---|---|---|---|---|---|---|
| 1 | / | 17% | 77% | 9 | SIPr | 17% | 79% |
| 2 | IMes | 25% | 75% | 10 | MeIPr | 11% | 83% |
| 3 | IMes (Sigma) | 31% | 62% | 11 | MeSIPr | 8% | 85% |
| 4 | NHC 1 | 30% | 69% | 12 | super IPr* | 16% | 78% |
| 5 | H,Me-IMes | 27% | 73% | 13 | CyCAAC | 19% | 76% |
| 6 | NHC 2 | 17% | 77% | 14 | MeCAAC | 20% | 80% |
| 7 | IMxy$^{Me}$ | 10% | 88% | 15 | BICAAC | 18% | 75% |
| 8 | IPr | 20% | 74% | 16 | MeICy | 23% | 77% |

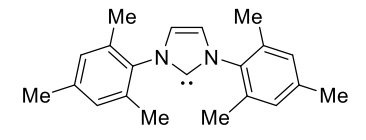

IMes

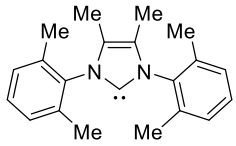

NHC-1

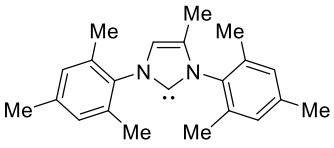

H,Me-IMes

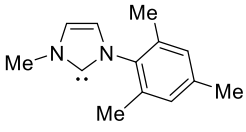

NHC-2

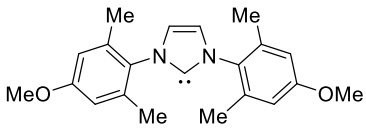

IMxy$^{Me}$

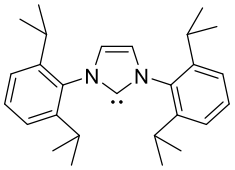

IPr

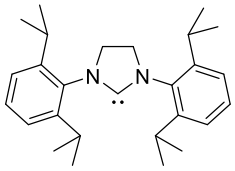

SIPr

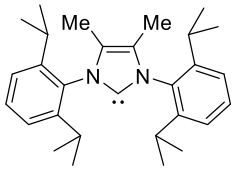

MeIPr

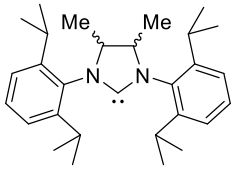

MeSIPr

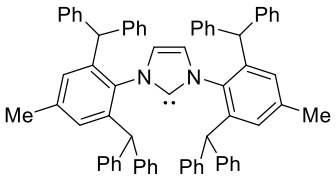

Super IPr*

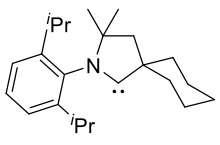

Cy-CAAC

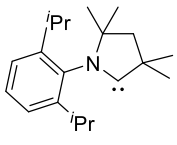

Me-CAAC

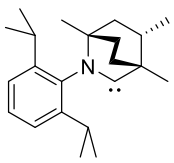

BICAAC

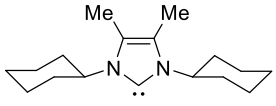

MeICy

Solvent was found to be crucial for C−C activation reactions. After increasing the catalyst loading to 5 mol%, we examined some representative solvent on this reaction. Comparing to 1,4-dioxane, other ether-type solvent such as THF and MeTHF delivered a lower conversion (entry 1-3, Table 4.7). Aromatic solvent such as benzene and toluene was found to be the optimized solvent for this transformation, which delivered 45% − 46% yield (entry 4-5, Table 4.7). Considering the toxicity of benzene and similar yields between benzene and toluene, we picked toluene as our optimized solvent. Halogenated benzene is not as good as the unsubstituted benzene or toluene (entry 6-8, Table 4.7). As our expected, strong coordinative solvent such as acetonitrile killed this reaction (entry 9, Table 4.7).

**Table 4.7.** Solvent Screening on C−C Activation of Phosphinite **4.5a**.

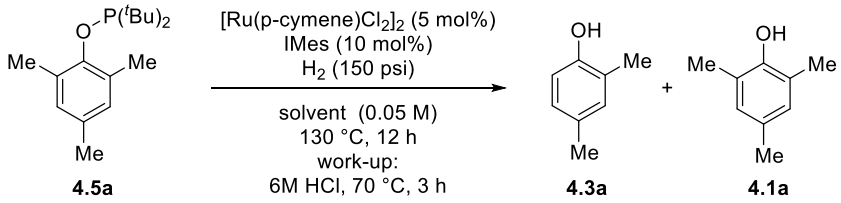


| Entry | Solvent | **4.3a** | **4.1a** |
|---|---|---|---|
| 1 | THF | 35% | 65% |
| 2 | MeTHF | 32% | 65% |
| 3 | 1,4-dioxane | 42% | 50% |
| 4 | benzene | 46% | 51% |
| 5 | toluene | 45% | 51% |
| 6 | PhCl | 17% | 73% |
| 7 | PhF | 9% | 91% |
| 8 | 1,2-DFB | 10% | 82% |
| 9 | MeCN | n.d. | 37% |

We then explored different reaction time, reaction temperature and concentration. Longer reaction time did not increase the reaction yield (entry 1-3, Table 4.8). Since we observed ruthenium black generated after 12 hours, we proposed to decrease the reaction temperature to

suppress catalyst decomposition. Unfortunately, lower reaction temperature did not deliver the promising results (entry 4-6, Table 4.8). Besides temperature, lower or higher concentration was not able to increase the yield (entry 7-9, Table 4.8).

**Table 4.8.** Reaction Time, Temperature and Concentration Screening on C−C Activation of Phosphinite **4.5a**.

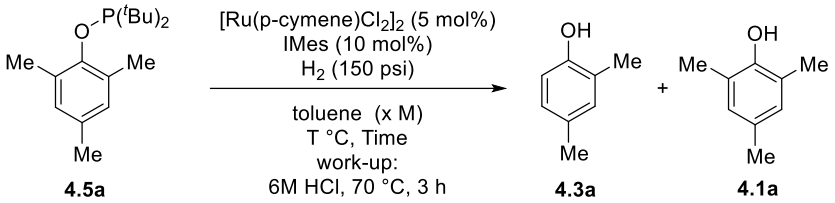


| Entry | Time | Temperature | Concentration | **4.3a** | **4.1a** |
|---|---|---|---|---|---|
| 1 | 12 h | 130 °C | 0.05 M | 45% | 51% |
| 2 | 24 h | 130 °C | 0.05 M | 41% | 49% |
| 3 | 48 h | 130 °C | 0.05 M | 43% | 53% |
| 4 | 12 h | 120 °C | 0.05 M | 43% | 40% |
| 5 | 12 h | 110 °C | 0.05 M | 30% | 54% |
| 6 | 12 h | 100 °C | 0.05 M | 24% | 57% |
| 7 | 12 h | 130 °C | 0.025 M | 38% | 61% |
| 8 | 12 h | 130 °C | 0.1 M | 37% | 60% |
| 9 | 12 h | 130 °C | 0.2 M | 41% | 50% |

Based on our previous mechanism study on ruthenium catalyzed reductive cleavage of C(aryl)−C(aryl) bond, the real catalyst for this transformation might be ruthenium hydride chloride. Thus, HCl would be generated when converting $RuL_nCl_2$ to $RuL_nHCl$, which can destroy phosphinite **4.5a**. We tried to adding some base to absorb the HCl generated during the reaction (entry 1-3, Table 4.9). However, extra base cannot increase the reaction yield. We also tested silver salt additives to convert chloride in the catalyst into other anions (entry 4-9, Table 4.9). Although adding silver salts did not provide a higher yield for this reaction, we surprisedly found that adding 10 mol% $AgBF_4$ also get 43% yield of phenol **4.3a**.

**Table 4.9.** Additives Screening on C−C Activation of Phosphinite **4.5a**.

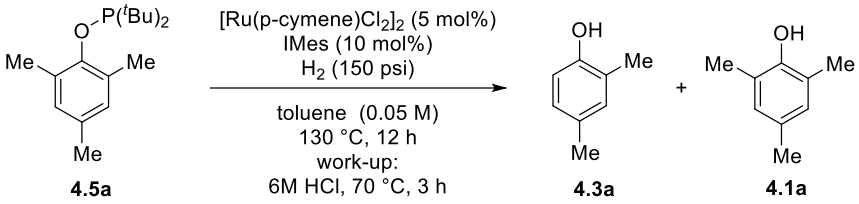


| Entry | Additives | A | B |
|---|---|---|---|
| 1 | 2,6-di-tBu-py (0.5 equiv) | 34% | 52% |
| 2 | $Cs_2CO_3$ (0.5 equiv) | 27% | 66% |
| 3 | NaH (0.5 equiv) | n.d. | 83% |
| 4 | AgOAc (10 mol%) | 16% | 81% |
| 5 | AgOAc (20 mol%) | n.d. | 91% |
| 6 | $AgBF_4$ (10 mol%) | 43% | 46% |
| 7 | $AgSbF_6$ (10 mol%) | 34% | 60% |
| 8 | $AgNTf_2$ (10 mol%) | 40% | 58% |
| 9 | NaBArF (10 mol%) | 42% | 52% |

Since we found cationic ruthenium can also catalyze this reaction, we then screened some ligands (Table 4.10) and temperature (Table 4.11) based on cationic ruthenium catalyst. However, other ligands and reaction temperatures did not provide a better result.

**Table 4.10.** Ligands Screening on C−C Activation of Phosphinite **4.5a** (Cationic Ruthenium).

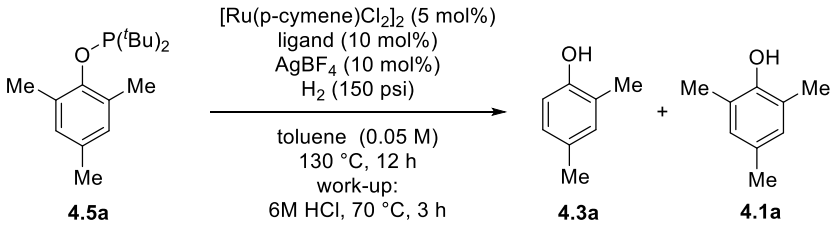


| Entry | ligand | 4.3a | 4.1a |
|---|---|---|---|
| 1 | / | n.d. | 98% |
| 2 | SIMes | n.d. | 94% |
| 3 | MeIMes | 28% | 71% |
| 4 | IPr | 10% | 86% |
| 5 | dppe | N.R. | |
| 6 | dppp | N.R. | |
| 7 | DPEphos | N.R. | |

**Table 4.11.** Temperature Screening on C−C Activation of Phosphinite **4.5a** (Cationic Ruthenium).

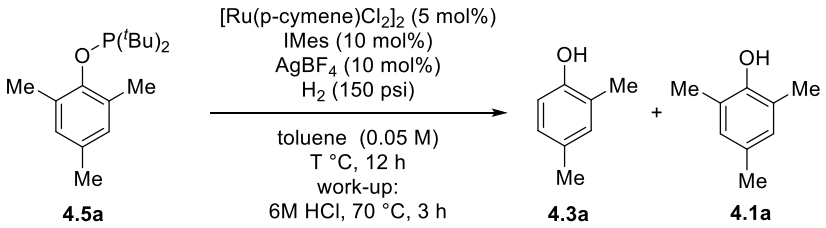


**4.5a** **4.3a** **4.1a**

| Entry | Temperature | **4.3a** | **4.1a** |
|---|---|---|---|
| 1 | 160 °C | 36% | 62% |
| 2 | 150 °C | 38% | 62% |
| 3 | 140 °C | 42% | 58% |
| 4 | 130 °C | 43% | 46% |
| 5 | 120 °C | 28% | 65% |
| 6 | 110 °C | 14% | 83% |
| 7 | 100 °C | 15% | 85% |

Since we have proven that *tert*-butyl phosphinite delivered a better result comparing with *iso*-propyl phosphinite, we are wondering if the better yield could be obtained using a more electron-rich and bulky phosphinite. Thus, we synthesized adamentyl phosphinite **4.6a** (Scheme 4.5). However, the C−C cleavage reaction on phosphinite **4.6a** didn't provide a better yield (entry 1, Table 4.12). But it is interesting that no desired product 4.3a was observed when treating adamentyl phosphinite **4.6a** with cationic ruthenium catalyst (entry 2, Table 4.12).

**Scheme 4.5.** Preparation of Phosphinite **4.6a**.

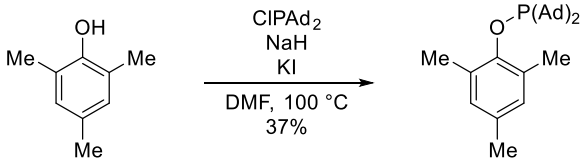


**4.1a** **4.6a**

**Table 4.12.** C−C Activation of Phosphinite **4.6a**.

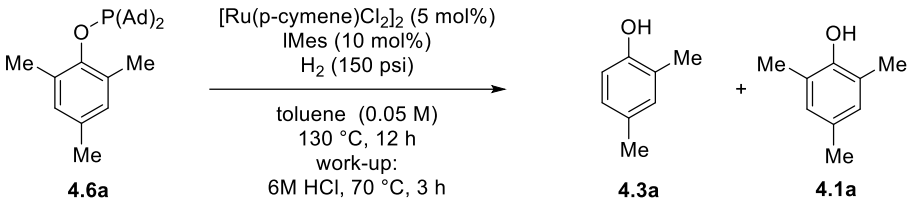


| Entry | Additives | **4.3a** | **4.1a** |
|---|---|---|---|
| 1 | / | 44% | 51% |
| 2 | $AgBF_4$ (10 mol%) | n.d. | 98% |

We then moved to explore more additives, such as extra halide salts (entry 1-3, Table 4.13), Lewis acid (entry 4-6, Table 4.13), silver fluoride (entry 7, Table 4.13), $\eta^6$-ligands (entry 8-10, Table 4.13) and triphenylphosphine oxide (entry 11, Table 4.13). However, none of them delivered fruitful result. Other reductants, including secondary alcohol (entry 1, 4, 6, Table 4.14), silane (entry 2, Table 4.14), borane (entry 3, Table 4.14) and Hantzsch ester (entry 5, Table 4.14) were tested. However all these reductants give no or low conversion.

**Table 4.13.** Additives Screening on C−C Activation of Phosphinite **4.5a** (Part 2).

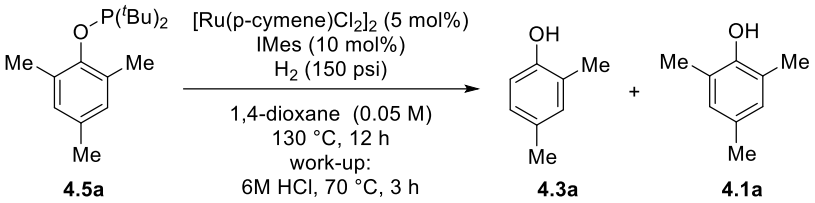


| Entry | Additives | **5.3a** | **5.1a** |
|---|---|---|---|
| 1 | LiCl (1 equiv) | 44% | 49% |
| 2 | LiBr (1 equiv) | 42% | 38% |
| 3 | NaI (1 equiv) | 24% | 65% |
| 4 | $ZnCl_2$ (1 equiv) | 36% | 42% |
| 5 | $ZnBr_2$ (1 equiv) | 35% | 47% |
| 6 | $ZnI_2$ (1 equiv) | 22% | 62% |
| 7 | AgF (20 mol%) | 38% | 47% |
| 8 | Anisole (1 equiv) | 43% | 48% |
| 9 | 1,4-dimethoxybenzene (1 equiv) | 35% | 51% |
| 10 | 1,3,5-trimethoxybenzene (1 equiv) | 38% | 49% |
| 11 | $POPh_3$ (1 equiv) | 38% | 43% |

**Table 4.14.** Reductant Screening on C−C Activation of Phosphinite **4.5a**.

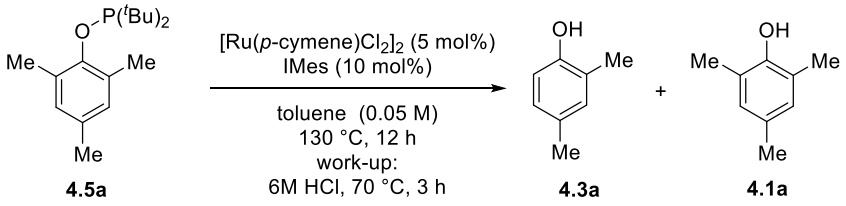


| Entry | Reductant | **4.3a** | **4.1a** |
|---|---|---|---|
| 1 | *i*PrOH | 5% | 71% |
| 2 | $PhSiH_3$ | N.R. | |
| 3 | Catecholborane | N.R. | |
| 4 | cyclopentanol | low conversion | |
| 5 | Hantzsch ester | low conversion | |
| 6 | cyclohexanol | low conversion | |

To avoid the decomposition of catalyst, we tested our reaction using bidentate NHC ligands, which can chelate the metal center and stabilize the metal catalyst (Scheme 4.6). However, these bidentate NHC ligands did not delivered higher yield comparing to simple IMes ligand.

**Scheme 4.6.** C−C Activation of Phosphinite **4.5a** with bidentate NHC ligands.

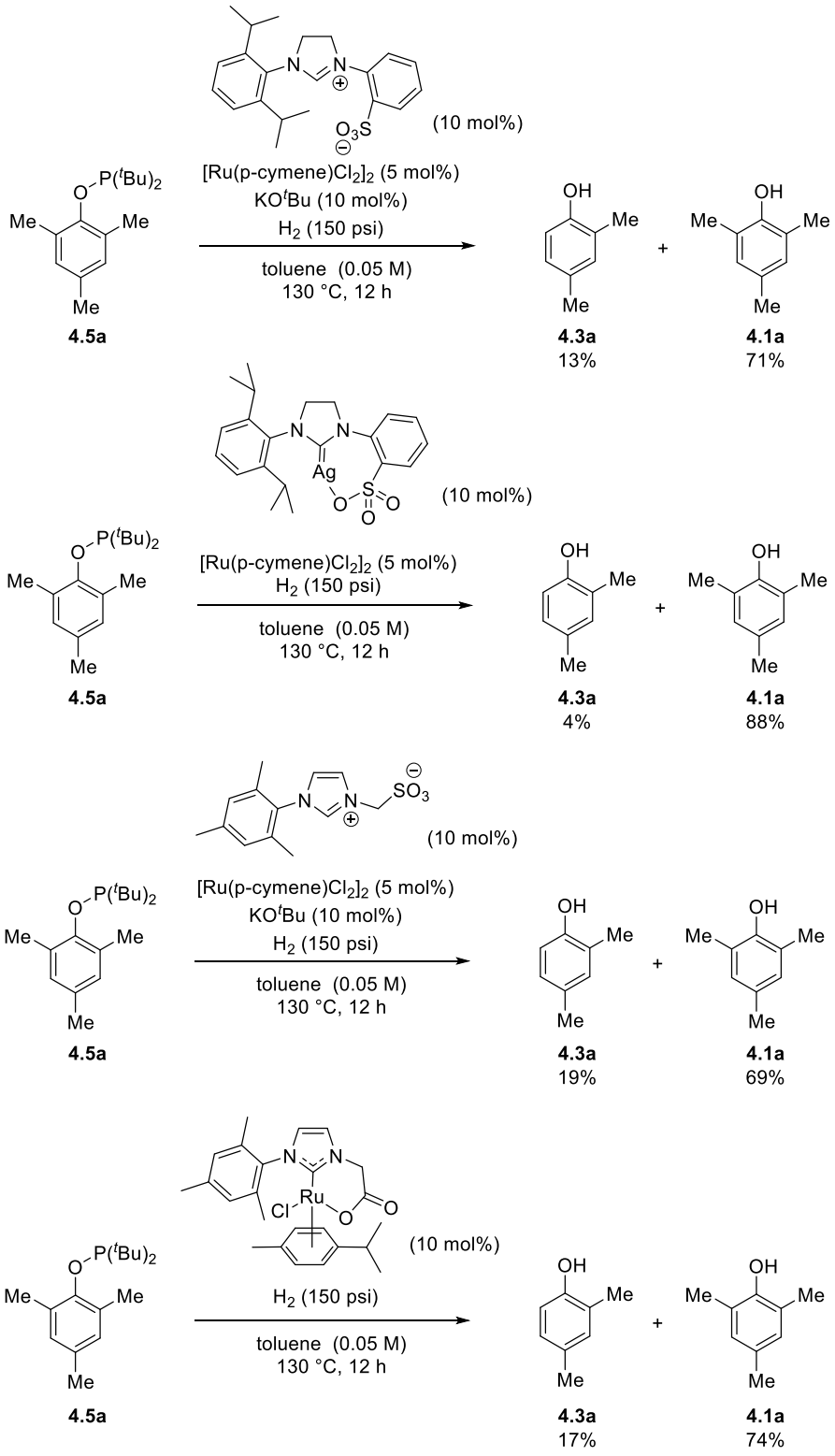

We also explored the kinetic profile of this reaction (Table 4.15). The experimental result clearly shown that the reaction stopped after 3 hours, which may cause by catalyst decomposition (Figure 4.1). The kinetic study also explained why the reaction yield remained the same when we lengthen the reaction time to 24 or 48 hours.

**Table 4.15.** Kinetic Studies on C–C Activation of Phosphinite **4.5a**.

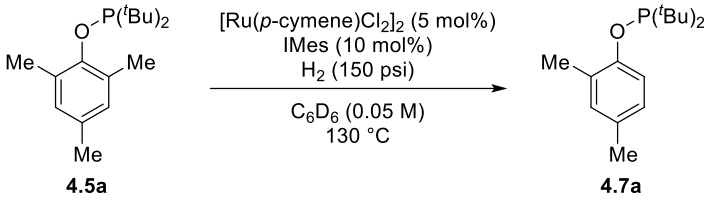


| Entry | Time | Yield |
|---|---|---|
| 1 | 1 h | 22% |
| 2 | 2 h | 36% |
| 3 | 3 h | 40% |
| 4 | 4 h | 40% |
| 5 | 5 h | 40% |
| 6 | 6 h | 40% |

**Figure 4.1.** Kinetic Profile on C–C Activation of Phosphinite **4.5a**.

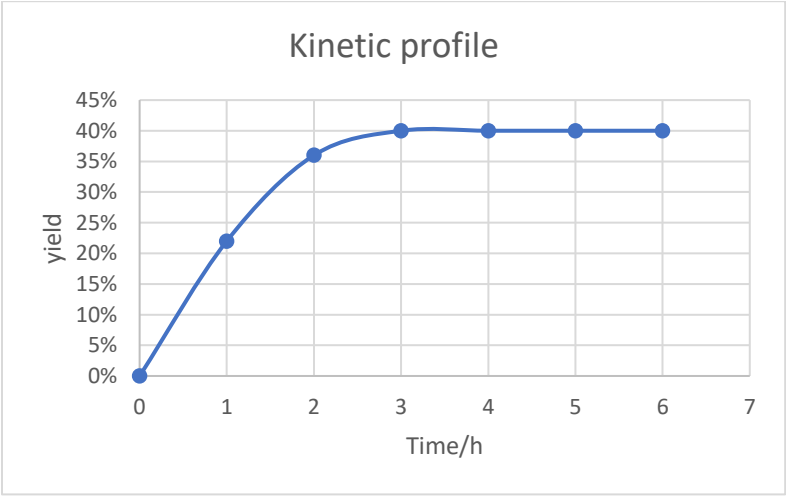

We proposed that adding some extra ligands into the reaction system may prevent catalyst decomposition. However, extra ligands such as pyridine or electron-deficient phosphine inhibit the reactivity (entry 2-5, Table 4.16). To our surprise, we found that adding 10 mol% $^t$BuOK increase the reaction yield to 53% (entry 6, Table 4.16). However, further increasing the equivalence of $^t$BuOK inhibited the reactivity (entry 7-8, Table 4.16), which indicated the key intermediate in this reaction is $RuL_nHCl$. Other bases did not work as well as $^t$BuOK (entry 9-10, Table 4.16). We also tested adding extra η6-ligands based on current optimized condition, which was not fruitful (Table 4.17).

**Table 4.16.** Additives Screening on C−C Activation of Phosphinite **4.5a** (Part 3).

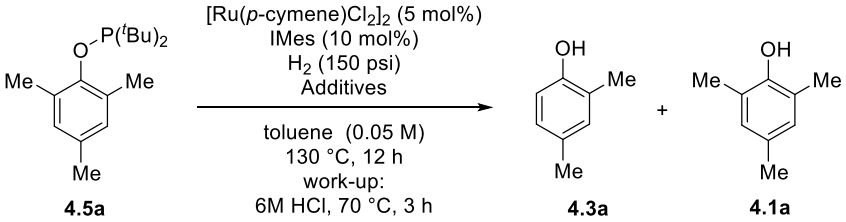


| Entry | Additives | **4.3a** | **4.1a** |
|---|---|---|---|
| 1 | / | 36% | 44% |
| 2 | pyridine (40 mol%) | 7% | 60% |
| 3 | pyridine (20 mol%) | 25% | 66% |
| 4 | pyridine (10 mol%) | 37% | 50% |
| 5 | $P(3,5\text{-}C_6H_3(CF_3)_2)_3$ (10 mol%) | 7% | 83% |
| 6 | *t*BuOK (10 mol%) | 53% | 40% |
| 7 | *t*BuOK (20 mol%) | 15% | 66% |
| 8 | *t*BuOK (30 mol%) | 8% | 62% |
| 9 | *t*BuONa (10 mol%) | 8% | 78% |
| 10 | *t*BuOLi (10 mol%) | 43% | 43% |

**Table 4.17.** Additives Screening on C−C Activation of Phosphinite **4.5a** (Part 4).

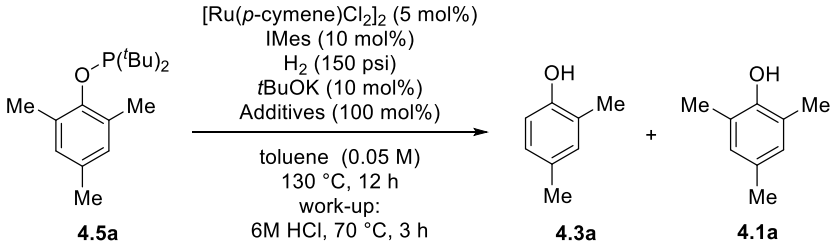


**4.5a** **4.3a** **4.1a**

| Entry | Additives | **4.3a** | **4.1a** |
|---|---|---|---|
| 1 | p-cymene | 51% | 33% |
| 2 | mesitylene | 48% | 35% |
| 3 | 1,2,4,5-tetramethylbenzene | 53% | 34% |

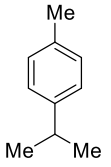


p-cymene

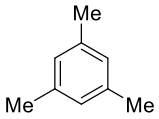


mesitylene

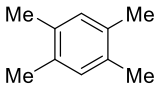


1,2,4,5-tetramethylbenzene

The yield of this reaction could be further increased to 59% when increasing the ruthenium catalyst loading to 10 mol% (entry 1, Table 4.18). Adding silver salt to remove the chloride in this reaction did not further increase the yield (entry 2, Table 4.18). Other base such as NaOMe and NaH also did not work well for this reaction (entry 3-4, Table 4.18). We surprisedly found that adding the catalysts in two batches further increased the yield to 69% (Scheme 4.7).

**Table 4.18.** Additives Screening on C−C Activation of Phosphinite **4.5a** (Part 5).

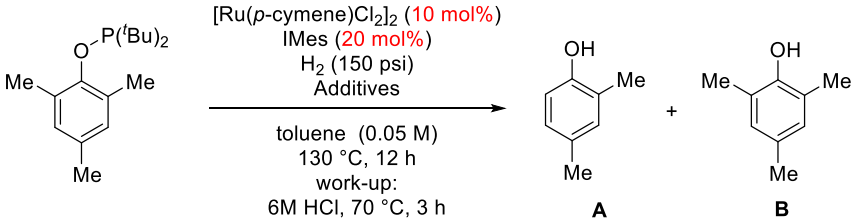


| Entry | Additives | A | B |
|---|---|---|---|
| 1 | *t*BuOK (20 mol%) | 59% | 30% |
| 2 | $AgBF_4$ (20 mol%) / $^t$BuOK (20 mol%) | 51% | 28% |
| 3 | NaOMe (20 mol%) | 18% | 65% |
| 4 | NaH (20 mol%) | 37% | 50% |

**Scheme 4.7.** C−C Activation of Phosphinite **4.5a** (Adding Catalyst in Two Batches).

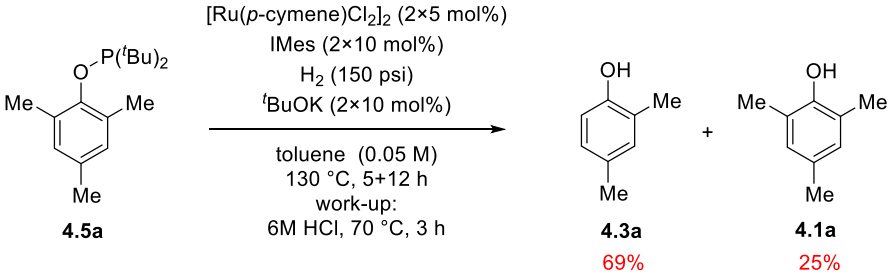


Besides phosphinite **4.5a**, we also tested our method on para-phenyl phosphite **4.5b** (see Scheme 4.8 for preparation). For C−C cleavage of phosphinite **4.5b**, we found that the mixed solvent between toluene and 1,4-dioxane can slightly increase the yield and the reproducibility, which may due to the better solubility of $^t$BuOK in 1,4-dioxane than in tolune (Table 4.19).

**Scheme 4.8.** Preparation of Phosphinite **4.5b**.

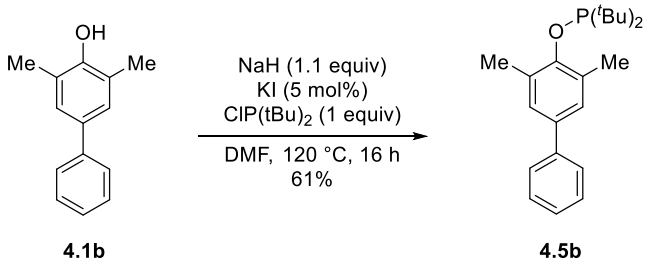

**Table 4.19.** Solvent Screening on C−C Activation of Phosphinite **4.5b**.

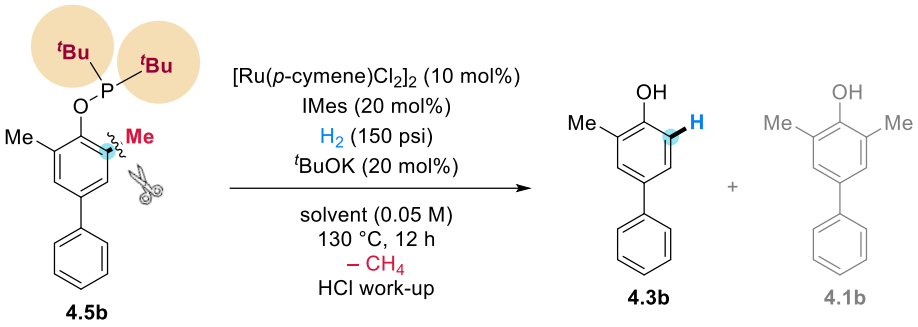


| Entry | Solvent | 4.3b | 4.1b |
|---|---|---|---|
| 1 | toluene | 78% | 20% |
| 2 | toluene/1,4-dioxane (9:1) | 23% | 68% |
| **3** | **toluene/1,4-dioxane (3:1)** | **81%** | 17% |
| 4 | toluene/1,4-dioxane (1:1) | 78% | 16% |
| 5 | toluene/1,4-dioxane (1:3) | 72% | 17% |
| 6 | toluene/1,4-dioxane (1:9) | 61% | 26% |

With optimized condition in hand, we started to explore the substrate scope of this reaction (Scheme 4.9). *Para*-methyl (**4.5a**), phenyl (**4.5b**) and tolyl phosphinites (**4.5e**) all worked well under standard condition, to give 65% - 78% yields of C−C cleavage product. The standard condition can also tolerate fluoride in substrate **4.5c**, which delivered 71% yield of phenol **4.3c**. The exploration of the scope on other substrates is still ongoing.

**Scheme 4.9.** Preliminary Substrate Scope.

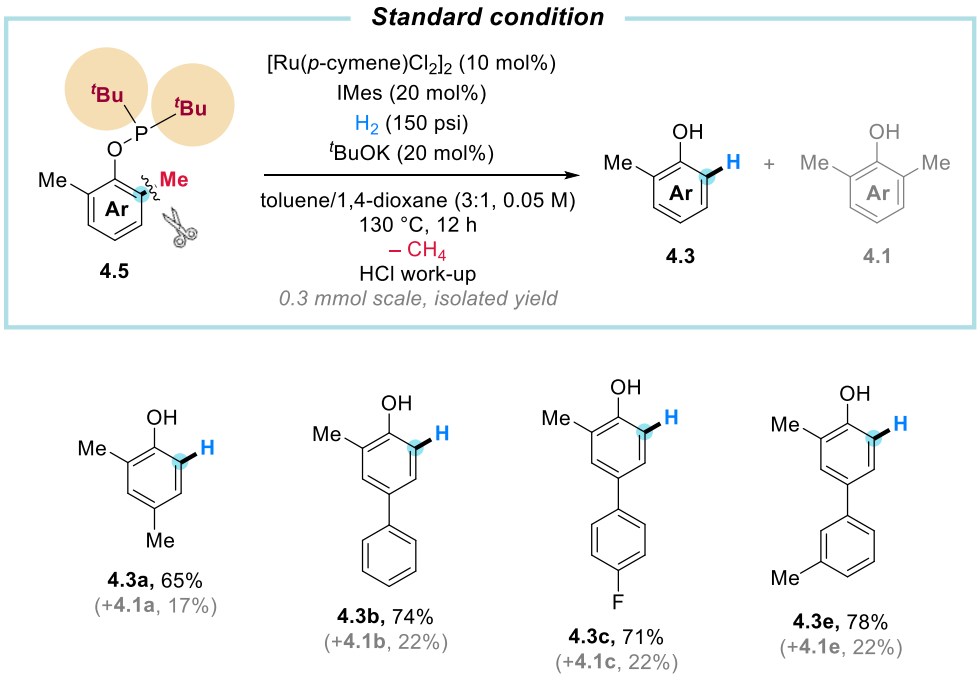


## 4.3. Conclusion

In summary, we have realized mono-directed ruthenium catalyzed nonpolar and unstrained C(aryl)−C(alkyl) bonds in *ortho*-methyl phenols. Hydrogen gas was applied as a reductant in this reaction to deliver demethylated phenols. The key designs to realize this challenged nonpolar and unstrained C−C bond activation includes: (i) Using phosphinite as a removable direction group to promote reversible coordination of the metal center; (ii) Using *tert*-butyl phosphinite to prevent multiple coordination of phosphinite; (iii) Applying the NHC ligand as a strong electron-donating ligand, which promote oxidation addition of C−C bond; (iv) Utilizing catalytic amounts of $^{t}$BuOK

to promote the formation of key $RuL_nHCl$ species and remove in-situ generated hydrochloride acid. The investigations of substrate scope and mechanism of this reaction are still ongoing.

### 4.4. Experimental

Unless noted otherwise, all solvents were dried by filtration through a Pure-Solv MD-5 Solvent Purification System (Innovative Technology), all reactions were carried out under nitrogen atmosphere, all commercially available substrates were used without further purification. Thin layer chromatography (TLC) analysis was run on silica gel plates purchased from EMD Chemical (silica gel 60, F254). Infrared spectrum was recorded on a Nicolet iS5 FT-IR Spectrometer. Samples were scanned as neat liquids or dissolved in dichloromethane on potassium bromide (KBr) salt plates. Frequencies were reported in reciprocal centimeters ($cm^{-1}$). High-resolution mass spectra (HRMS) were obtained on an Agilent 6224 TOF-MS spectrometer and were reported for the molecular ion $[M]^+$, $[M+Na]^+$, or $[M+H]^+$. MALDI-TOF mass spectra were obtained on a Bruker Ultraflextreme MALDI-Tof-Tof. X-ray diffraction data were collected at 100(2) K on a Bruker-Nonius Kappa CCD or Agilent SuperNova AtlasS2 CCD. Nuclear magnetic resonance (NMR) spectrum ($^1H$ NMR and $^{13}C$ NMR) were recorded with a 400 MHz Bruker Avance-III-HD nanobay spectrometer equipped with a BBFO SmartProbe (400 MHz for $^1H$, 101 MHz for $^{13}C$) or a 500 MHz Bruker Avance-III spectrometer equipped with a $^1H$ ($^{13}C$,$^{31}P$) TXI probe (500 MHz for $^1H$, 126 MHz for $^{13}C$). For $CDCl_3$ solutions, the chemical shifts were reported as parts per million (ppm) referenced to residual protium or carbon of the solvents: $CHCl_3$ δ H (7.26 ppm) and $CDCl_3$ δ C (77.00 ppm). For benzene-D6 solutions, the chemical shifts were reported as parts per million (ppm) referenced to residual protium or carbon of the solvents: acetone-D6 δ H (7.16 ppm) and acetone-D6 δ C (128.06 ppm). Coupling constants were reported in Hertz (Hz). Data for $^1H$ NMR

spectra were reported as following: chemical shift (δ, ppm), multiplicity (br = broad, s = singlet, d = doublet, t = triplet, q = quartet, dd = doublet of doublets, td = triplet of doublets, ddd = doublet of doublet of doublets, m = multiplet), coupling constant (Hz), and integration.

*General procedure for preparation of phenol **4.1***

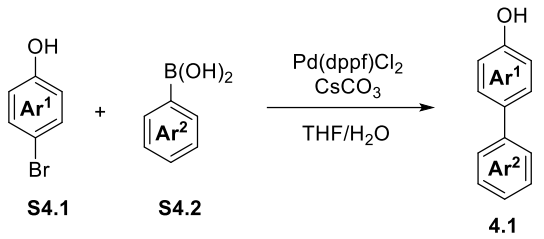


**General procedure:** To a solution of phenol **S4.1** (1 equiv) in THF (~50 mL/25 mmol), boronic acid **S4.2** (1.5 equiv), Pd(dppf)$Cl_2$ (1 mol%), $Cs_2CO_3$ (2 equiv) and $H_2O$ (~25 mmol/20 mL) were added at room temperature. The reaction mixture was then heated to reflux. After refluxing for 12 h, the reaction mixture was quenched with HCl (1 M in $H_2O$) and extracted with dichloromethane (3 times). The organic phase was dried with $Na_2SO_4$ and concentrated under reduced pressure. The mixture was purified by column chromatography (silica gel) to give pure compound **4.1**.

*Preparation of compound **4.1c***

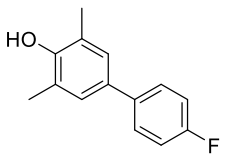


**4.1c**

4-Bromo-2,6-xylenol (2.01 g) and 4-fluorophenylboronic acid (2.10 g) was subjected to the general procedure and recrystallized in $CHCl_3$/hexane to afford 1.30 g of **4.1c** with 60% yield as a yellow needle crystal.

$R_f$ = 0.43 (hexane : ethyl acetate = 4:1)

**$^1$H NMR** (500 MHz, $CDCl_3$) δ 7.52 – 7.38 (m, 2H), 7.15 (s, 2H), 7.07 (t, *J* = 8.7 Hz, 2H), 4.65 (s, 1H), 2.30 (s, 6H).

**$^{13}$C NMR** (101 MHz, $CDCl_3$) δ 162.0 (d, *J* = 245.2 Hz), 151.8, 137.2 (d, *J* = 3.2 Hz), 132.4, 128.2 (d, *J* = 7.9 Hz), 127.2, 123.3, 115.4 (d, *J* = 21.3 Hz), 16.0.

**$^{19}$F NMR** (376 MHz, $CDCl_3$) δ -117.0.

**Melting point**: 116 – 118 °C

Analytic data match the literature.[5]

*Preparation of compound **4.1d***

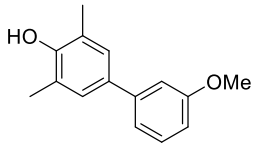


**4.1d**

4-Bromo-2,6-xylenol (2.01 g) and 3-methoxyphenylboronic acid (2.28 g) was subjected to the general procedure to afford 1.55 g of **4.1d** with 68% yield as a white solid.

**$^1$H NMR** (500 MHz, $CDCl_3$) δ 7.31 (t, *J* = 7.9 Hz, 1H), 7.21 (d, *J* = 0.8 Hz, 2H), 7.12 (ddd, *J* = 7.7, 1.7, 0.9 Hz, 1H), 7.06 (dd, *J* = 2.6, 1.7 Hz, 1H), 6.84 (ddd, *J* = 8.2, 2.6, 0.9 Hz, 1H), 4.67 (s, 1H), 3.85 (s, 3H), 2.30 (d, *J* = 0.7 Hz, 6H).

**$^{13}$C NMR** (101 MHz, $CDCl_3$) δ 159.8, 151.9, 142.6, 133.2, 129.6, 127.4, 123.2, 119.3, 112.4, 111.9, 55.3, 16.0.

Analytic data match the literature.[5]

*Preparation of compound **4.1e***

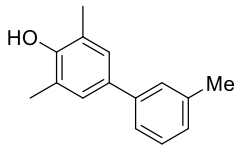


**4.1e**

4-Bromo-2,6-xylenol (2.01 g) and *m*-Tolylboronic acid (2.04 g) was subjected to the general procedure to afford 2.01 g of **4.1e** with 95% yield as a yellow oil.

$R_f$ = 0.34 (hexane : ethyl acetate = 4:1)

**$^1$H NMR** (400 MHz, $CDCl_3$) δ 7.37 – 7.31 (m, 2H), 7.28 (td, *J* = 7.4, 0.7 Hz, 1H), 7.21 (s, 2H), 7.13 – 7.04 (m, 1H), 4.65 (s, 1H), 2.40 (d, *J* = 0.8 Hz, 3H), 2.30 (d, *J* = 0.7 Hz, 6H).

**$^{13}$C NMR** (101 MHz, $CDCl_3$) δ 151.7, 141.1, 138.1, 133.5, 128.5, 127.5, 127.4, 127.2, 123.8, 123.2, 21.5, 16.0.

*General Procedure for preparation of compound **4.5***

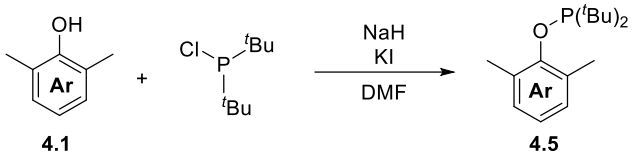


**General procedure:** To a 40 mL sealed tube charged with a stir bar, phenol **4.1** (1.0 equiv.) was dissolved in dry DMF (10 mL/5 mmol), 5 mol% KI and 1.1 equiv. of NaH was added slowly. After stirring under room temperature for 10 minutes, 1.1 equiv. of di-*tert*-butylchlorophosphine was then added dropwise at room temperature. The mixture was heated to 120 °C under $N_2$ atmosphere overnight. Upon completion of the reaction, the reaction mixture was extracted with pentane in glovebox, washed with acetonitrile and concentrated to give the corresponding phosphinites, which were pure enough for the C−C activation reactions. (The phosphinites were sensitive to moisture and must be stored in the glovebox. HRMS could not be obtained.)

*Preparation of compound **4.5a***

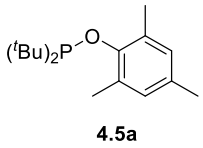


**4.5a**

2,4,6-Trimethylphenol (1.36 g) was subjected to the general procedure to afford 1.90 g of **4.5a** with 68% yield as a white solid.

**$^1$H NMR** (500 MHz, $C_6D_6$) δ 6.73 (s, 2H), 2.65 (s, 3H), 2.38 (d, $J$ = 38.3 Hz, 3H), 2.13 (s, 3H), 1.15 (s, 9H), 1.13 (s, 9H).

**$^{13}$C NMR** (126 MHz, $C_6D_6$) δ 153.0, 152.9, 131.7, 130.8, 130.0, 36.5, 36.3, 27.7, 27.6, 21.4, 20.5, 18.3.

**$^{31}$P NMR** (202 MHz, $C_6D_6$) δ 160.6.

*Preparation of compound **4.5b***

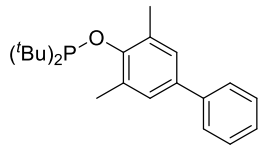


**4.5b**

4-Phenyl-2,6-dimethylphenol (0.99 g) was subjected to the general procedure to afford 1.04 g of **4.5b** with 61% yield as a white solid.

**$^{1}$H NMR** (500 MHz, $C_6D_6$) δ 7.55 – 7.48 (m, 2H), 7.28 – 7.19 (m, 4H), 7.16 – 7.11 (m, 1H), 2.69 (s, 3H), 2.42 (dd, $J$ = 42.8, 0.7 Hz, 3H), 1.16 (s, 9H), 1.13 (s, 9H).

**$^{31}$P NMR** (202 MHz, $C_6D_6$) δ 162.0.

*Preparation of compound **4.5c***

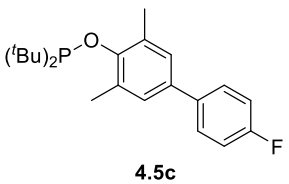


**4.5c**

Compound **4.1c** (0.54 g) was subjected to the general procedure to afford 0.6032 g of **4.5c** with 67% yield as a white solid.

**$^{1}$H NMR** (500 MHz, $C_6D_6$) δ 7.27 – 7.20 (m, 2H), 7.08 (s, 2H), 6.92 – 6.84 (m, 2H), 2.69 (s, 3H), 2.38 (s, 3H), 1.16 (s, 9H), 1.14 (s, 9H).

**$^{13}$C NMR** (126 MHz, $C_6D_6$) δ 162.6 (d, $J$ = 245.0 Hz), 154.75, 154.73, 137.5 (d, $J$ = 3.3 Hz), 134.0, 129.7, 128.7 (d, $J$ = 7.7 Hz), 115.7 (d, $J$ = 21.1 Hz), 36.6, 36.3, 27.7, 27.6, 21.7, 18.5.

**$^{31}$P NMR** (202 MHz, $C_6D_6$) δ 162.1.

**$^{19}$F NMR** (470 MHz, $C_6D_6$) δ -116.7.

*Preparation of compound **4.5e***

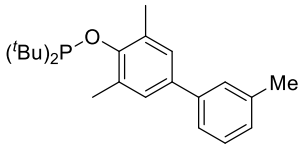


**4.5e**

Compound **4.1e** (0.53 g) was subjected to the general procedure to afford 0.5943 g of **4.5c** with 67% yield as a white solid.

**$^{1}$H NMR** (500 MHz, $C_6D_6$) δ 7.43 – 7.37 (m, 2H), 7.27 (s, 2H), 7.24 – 7.19 (m, 1H), 7.04 – 6.96 (m, 1H), 2.70 (s, 3H), 2.39 (s, 3H), 2.21 (s, 3H), 1.16 (s, 9H), 1.14 (s, 9H).

**$^{13}$C NMR** (126 MHz, $C_6D_6$) δ 154.7, 154.7, 141.5, 138.2, 135.3, 129.9, 128.9, 127.7, 124.5, 36.6, 36.3, 27.7, 27.6, 21.9, 21.6, 18.6.

**$^{31}$P NMR** (202 MHz, $C_6D_6$) δ 161.7.

*General procedure for C−C bond cleavage*

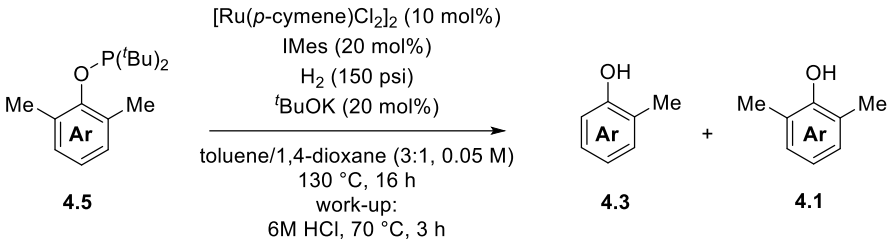


**4.5** **4.3** **4.1**

**General procedure**: To a flame dried 4 mL vial charged with a stir bar, IMes (18.3 mg, 0.060 mmol), [Ru(*p*-cymene)$Cl_2$]$_2$ (18.4 mg, 0.030 mmol) and 1,4-dioxane (1.5 mL) were added in glovebox. After stirring at room temperature for 5 minutes, $^t$BuOK (6.7 mg, 0.060 mmol) was added to the vial. The catalyst solution was stirred for another 10 minutes. To a Q-tube charged with a stir bar, phosphinite **4.5** (0.3 mmol), previous prepared catalyst solution (1.5 mL), and toluene (4.5 mL) were added in the glovebox. The Q-tube was then resembled and taken out of the glovebox. The reaction mixture was flushed with hydrogen gas for 10 times and then charged with 150 psi $H_2$ followed by heating to 130 °C in a pre-heated oil bath for 16 h.. After the reaction was completed, the $H_2$ pressure was released. The reaction mixture was then charged with HCl (3 mL, 6 M in $H_2O$). After stirring at 70 °C for 3 h under $N_2$ atmosphere, the reaction mixture was extracted by dichloromethane (10 mL × 3). The organic phase was concentrated under reduced pressure. The residue was purified by column chromatography (silica gel) to give pure compound **4.3** and **4.1**.

*Preparation of compounds **4.3a***

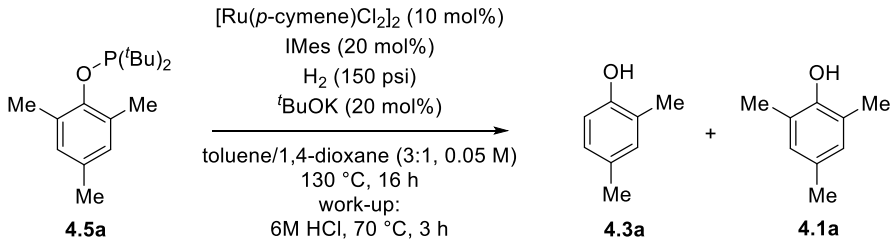


Compound **4.5a** (84.1 mg) was subjected to the general procedure to afford 23.7 mg of **4.3a** with 65% yield as a white solid and 6.8 mg **4.1a** with 17% yield as a white solid.

Analytical data of compound **4.3a**:

$R_f$ = 0.37 (hexane : ethyl acetate = 4:1)

**$^1$H NMR** (500 MHz, $CDCl_3$) δ 6.95 (d, *J* = 2.2 Hz, 1H), 6.89 (dd, *J* = 8.1, 2.2 Hz, 1H), 6.68 (d, *J* = 8.1 Hz, 1H), 4.76 (s, 1H), 2.27 (s, 3H), 2.24 (s, 3H).

**$^{13}$C NMR** (126 MHz, $CDCl_3$) δ 151.5, 131.6, 129.8, 127.4, 123.4, 114.7, 20.4, 15.6.

Analytic data match the literature.[5]

Analytical data of compound **4.1a**:

$R_f$ = 0.43 (hexane : ethyl acetate = 4:1)

**$^1$H NMR** (500 MHz, $CDCl_3$) δ 6.79 (s, 2H), 4.45 (s, 1H), 2.22 (d, *J* = 2.5 Hz, 9H).

**$^{13}$C NMR** (126 MHz, $CDCl_3$) δ 149.9, 129.3, 129.1, 122.7, 20.4, 15.8.

Analytic data match the literature.[5]

*Preparation of compounds **4.3b***

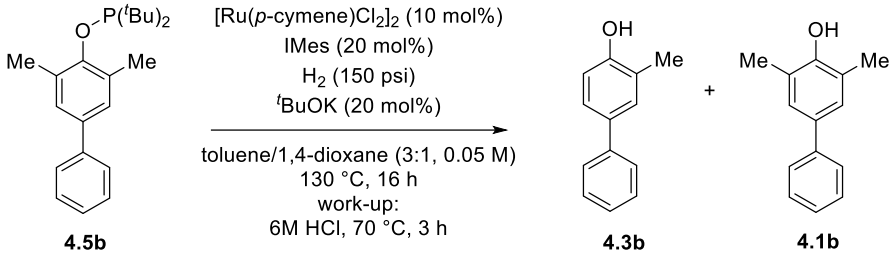


Compound **4.5b** (102.8 mg) was subjected to the general procedure to afford 40.8 mg of **4.3b** with 74% yield as a white solid and 12.9 mg **4.1b** with 22% yield as a white solid.

Analytical data of compound **4.3b**:

$R_f$ = 0.31 (hexane : ethyl acetate = 4:1)

**$^1$H NMR** (500 MHz, $CDCl_3$) δ 7.65 – 7.53 (m, 2H), 7.44 (t, *J* = 7.7 Hz, 2H), 7.41 (d, *J* = 2.3 Hz, 1H), 7.38 – 7.29 (m, 2H), 6.86 (d, *J* = 8.2 Hz, 1H), 4.98 (s, 1H), 2.35 (s, 3H).

**$^{13}$C NMR** (126 MHz, $CDCl_3$) δ 153.3, 140.9, 133.9, 129.8, 128.6, 126.7, 126.6, 125.7, 124.0, 115.2, 15.9.

Analytic data match the literature.[5]

Analytical data of compound **4.1b**:

$R_f$ = 0.40 (hexane : ethyl acetate = 4:1)

**$^1$H NMR** (500 MHz, $CDCl_3$) δ 7.57 – 7.49 (m, 2H), 7.39 (dd, *J* = 8.5, 7.0 Hz, 2H), 7.31 – 7.25 (m, 1H), 7.22 (s, 2H), 4.66 (s, 1H), 2.31 (s, 6H).

**$^{13}$C NMR** (126 MHz, $CDCl_3$) δ 151.8, 141.1, 133.4, 128.6, 127.4, 126.7, 126.5, 123.3, 16.0.

Analytic data match the literature.[5]

*Preparation of compounds **4.3c***

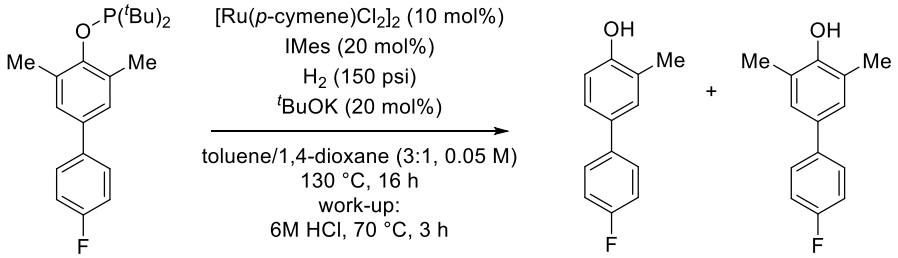


**4.5c** **4.3c** **4.1c**

Compound **4.5c** (108.1 mg) was subjected to the general procedure to afford 42.9 mg of **4.3c** with 71% yield as a white solid and 14.0 mg **4.1c** with 22% yield as a white solid.

Analytical data of compound **4.3c**:

$R_f$ = 0.33 (hexane : ethyl acetate = 4:1)

**$^1$H NMR** (400 MHz, $CDCl_3$) δ 7.50 – 7.42 (m, 2H), 7.29 (d, *J* = 2.4 Hz, 1H), 7.26 – 7.21 (m, 1H), 7.11 – 7.04 (m, 2H), 6.81 (d, *J* = 8.2 Hz, 1H), 4.87 (s, 1H), 2.30 (s, 3H).

**$^{13}$C NMR** (101 MHz, $CDCl_3$) δ 162.0 (d, *J* = 245.4 Hz), 153.3, 137.1 (d, *J* = 3.3 Hz), 133.0, 129.7, 128.2 (d, *J* = 8.0 Hz), 125.6, 124.1, 115.5, 115.3 (d, *J* = 6.8 Hz), 15.9.

**$^{19}$F NMR** (376 MHz, $CDCl_3$) δ -116.8.

Analytic data match the literature.[5]

Analytical data of compound **4.1c** see above.

*Preparation of compounds **4.3e***

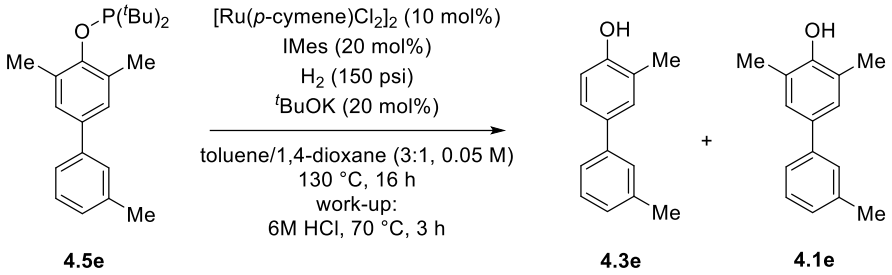


Compound **4.5e** (106.9 mg) was subjected to the general procedure to afford 46.7 mg of **4.3e** with 78% yield as a white solid and 14.2 mg **4.1e** with 22% yield as a yellow oil.

Analytical data of compound **4.3e**:

$R_f$ = 0.37 (hexane : ethyl acetate = 4:1)

**$^1$H NMR** (400 MHz, $CDCl_3$) δ 7.33 (dt, *J* = 10.2, 2.1 Hz, 3H), 7.30 – 7.24 (m, 2H), 7.10 (dd, *J* = 7.5, 1.8 Hz, 1H), 6.79 (d, *J* = 8.2 Hz, 1H), 4.93 (s, 1H), 2.39 (s, 3H), 2.29 (s, 3H).

**$^{13}$C NMR** (101 MHz, $CDCl_3$) δ 153.3, 140.9, 138.2, 134.0, 129.8, 128.5, 127.5, 127.3, 125.7, 124.0, 123.8, 115.2, 21.5, 15.9.

Analytical data of compound **4.1e** see above.

## 4.5. NMR Spectra

**Figure 4.2.** $^{1}$H-NMR Spectrum of **4.1c** in $CDCl_3$, 500 MHz

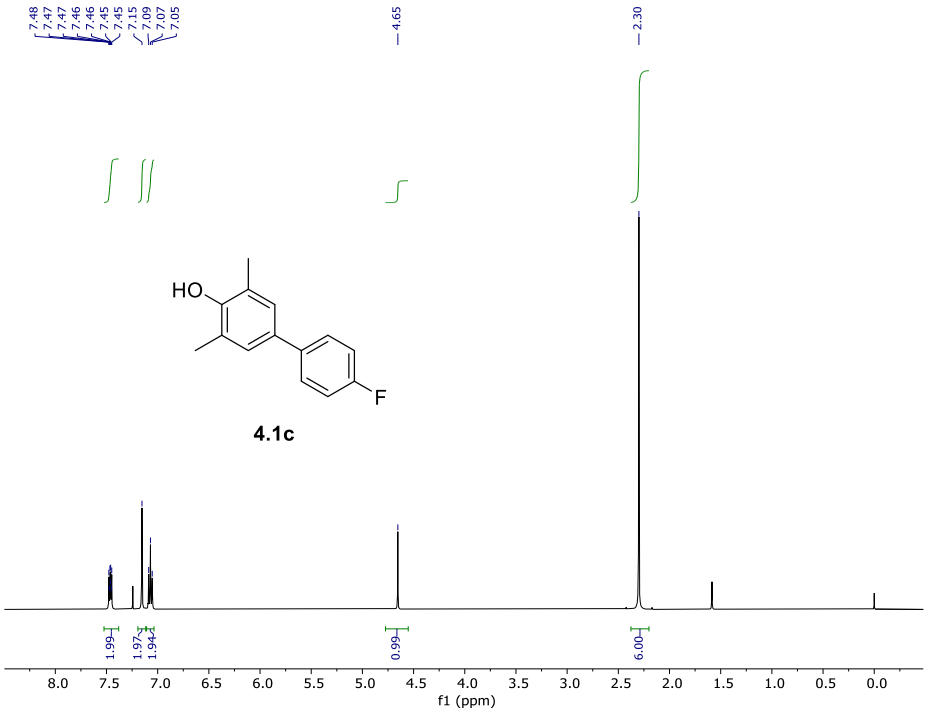


**Figure 4.3.** $^{13}$C-NMR Spectrum of **4.1c** in $CDCl_3$, 101 MHz

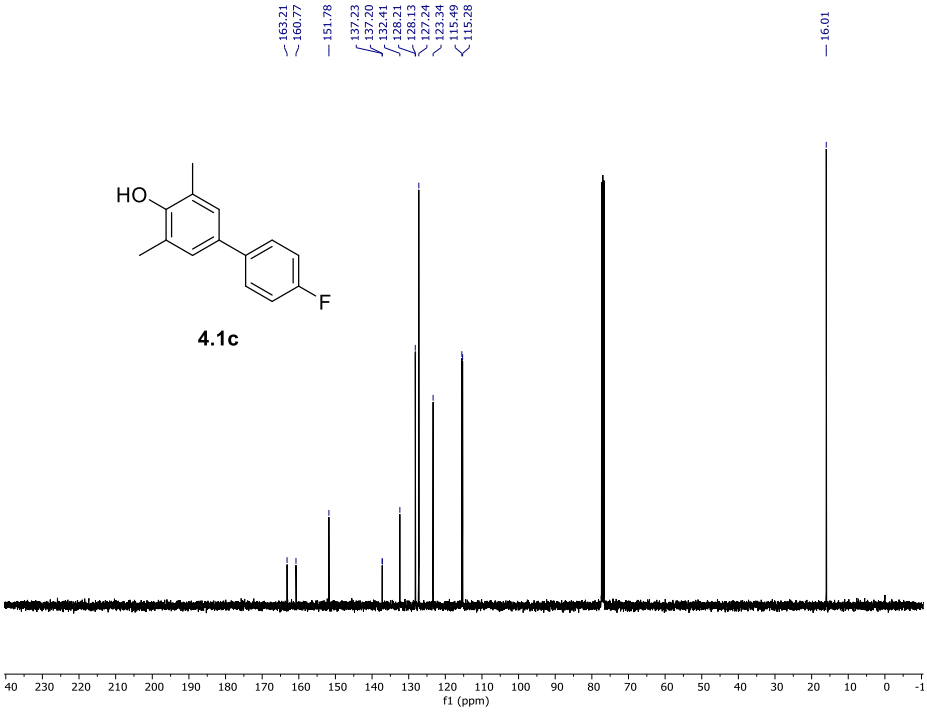

**Figure 4.4.** $^{19}$F-NMR Spectrum of **4.1c** in $CDCl_3$, 376 MHz

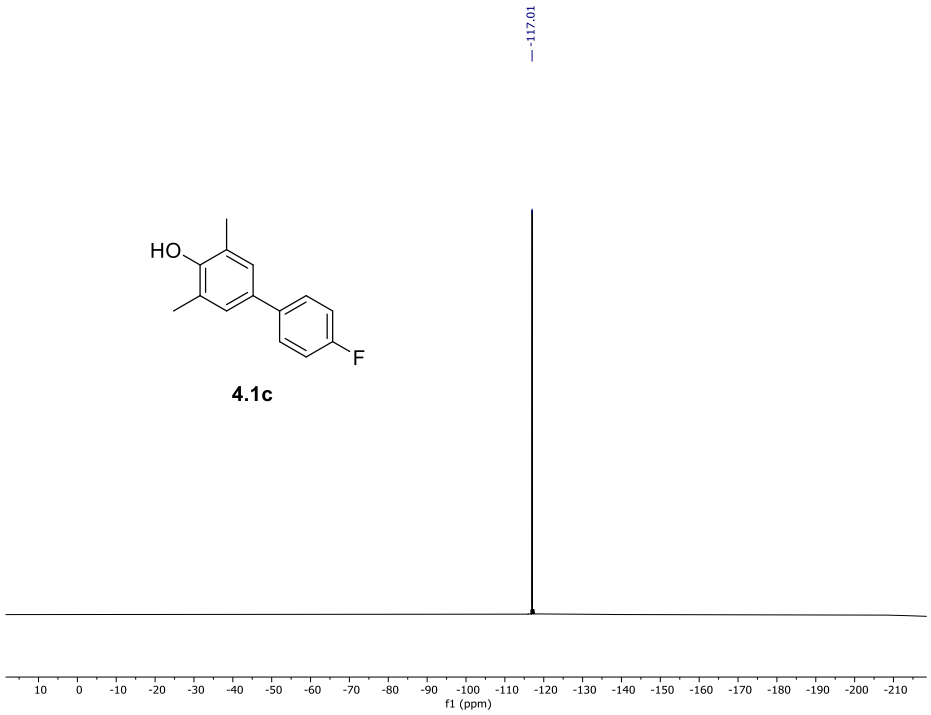

**Figure 4.5.** $^{1}$H-NMR Spectrum of **4.1d** in $CDCl_3$, 500 MHz

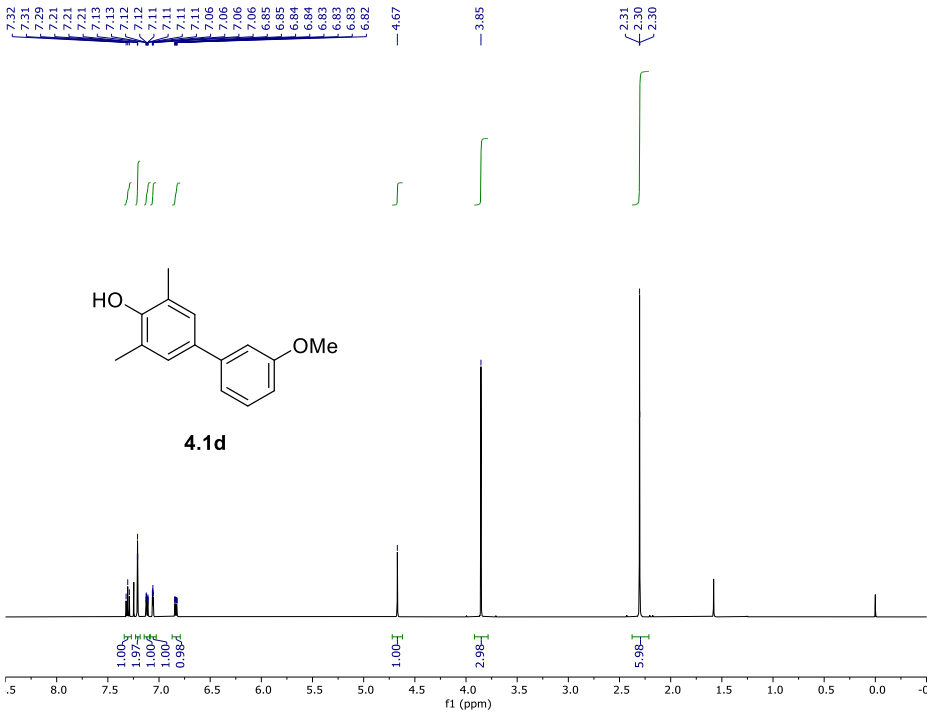


**Figure 4.6.** $^{13}$C-NMR Spectrum of **4.1d** in $CDCl_3$, 101 MHz

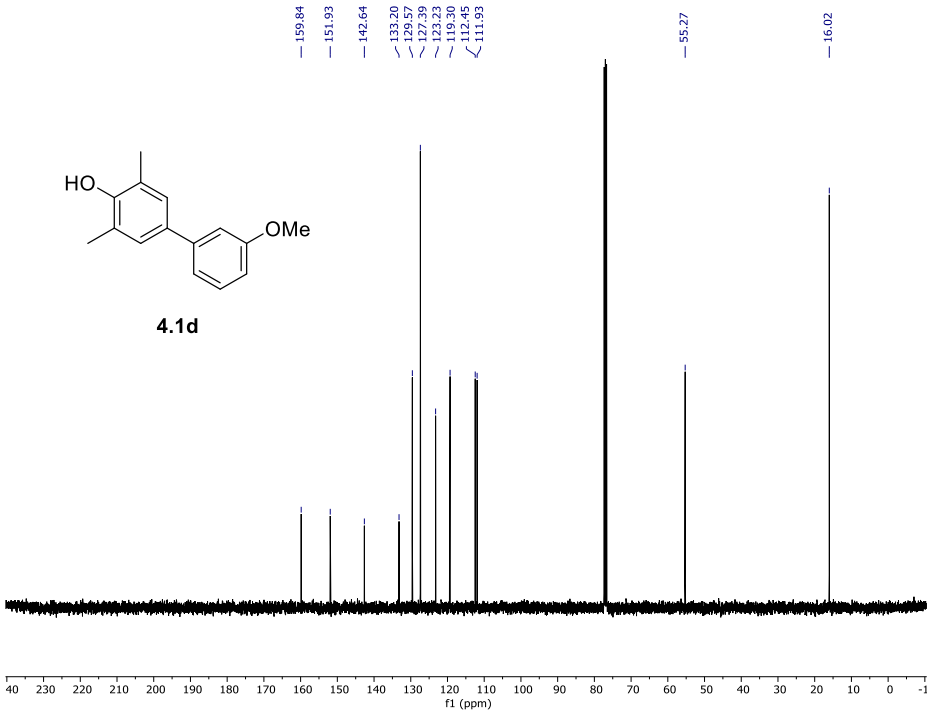

**Figure 4.7.** $^{1}$H-NMR Spectrum of **4.1e** in $CDCl_3$, 400 MHz

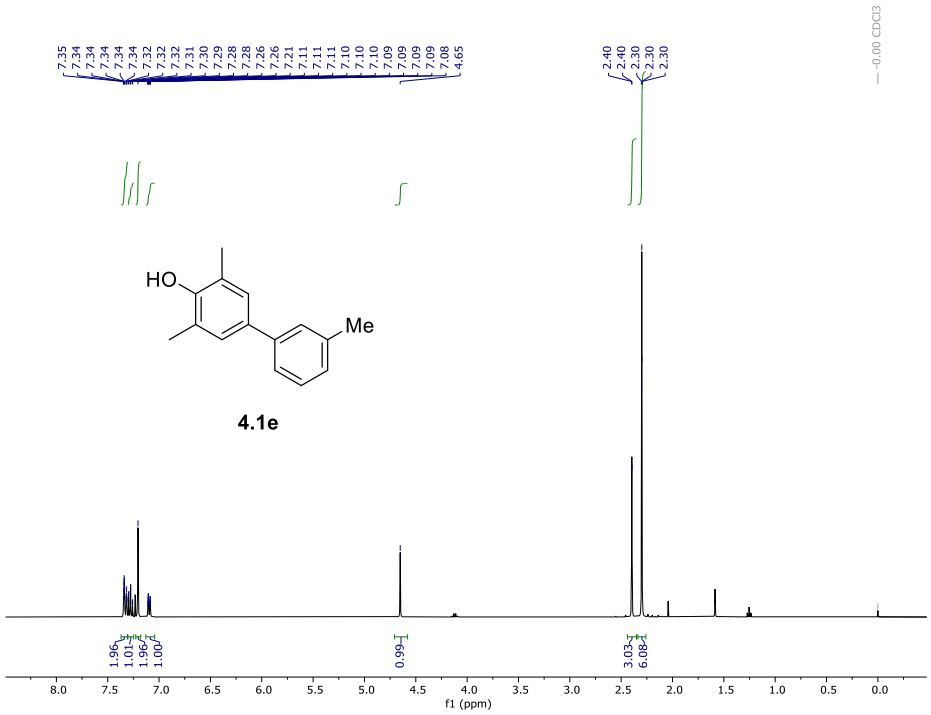


**Figure 4.8.** $^{13}$C-NMR Spectrum of **4.1e** in $CDCl_3$, 101 MHz

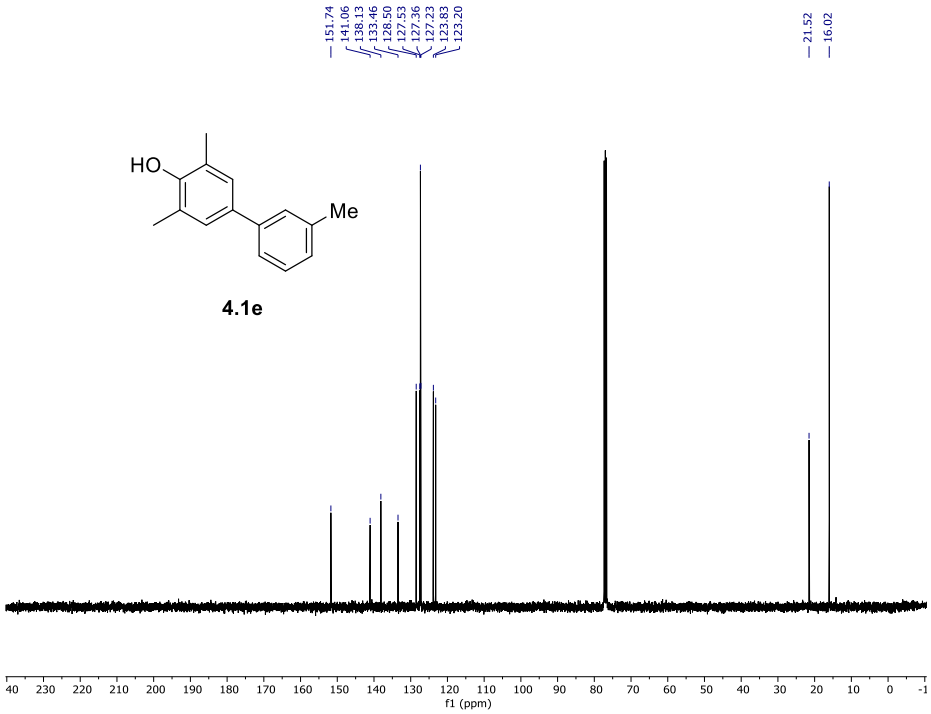

**Figure 4.9.** $^{1}$H-NMR Spectrum of **4.5a** in $C_6D_6$, 500 MHz

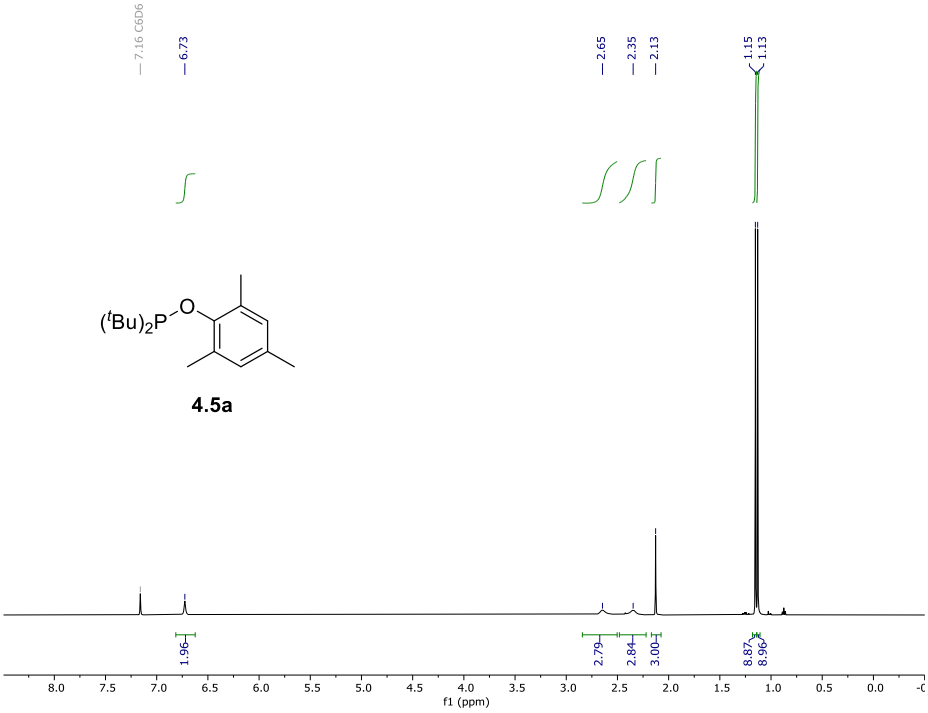


**Figure 4.10.** $^{13}$C-NMR Spectrum of **4.5a** in $C_6D_6$, 126 MHz

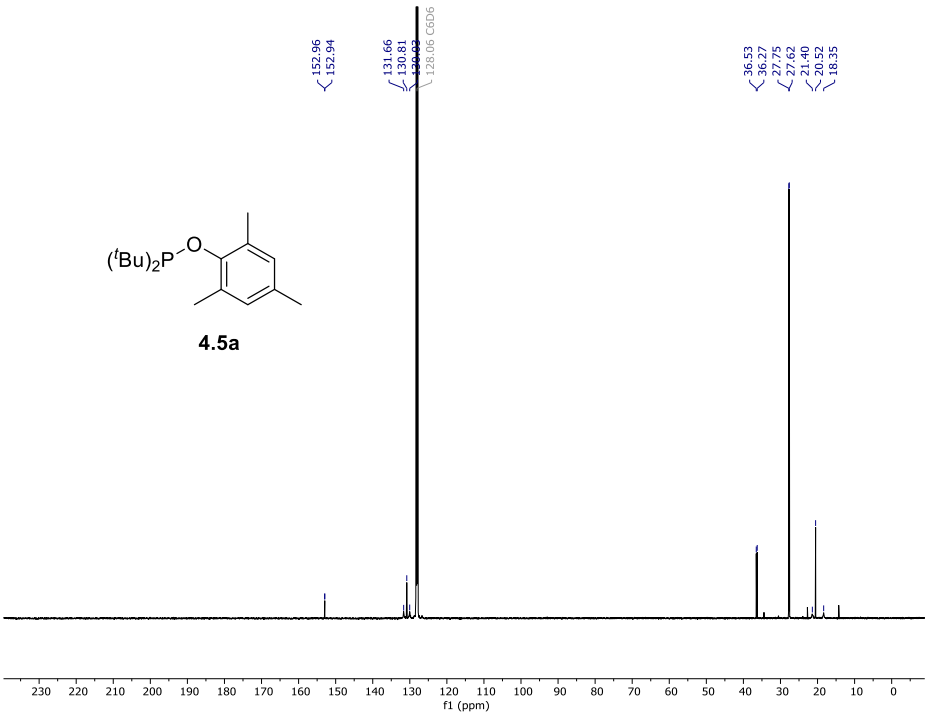

**Figure 4.11.** $^{31}$P-NMR Spectrum of **4.5a** in $C_6D_6$, 202 MHz

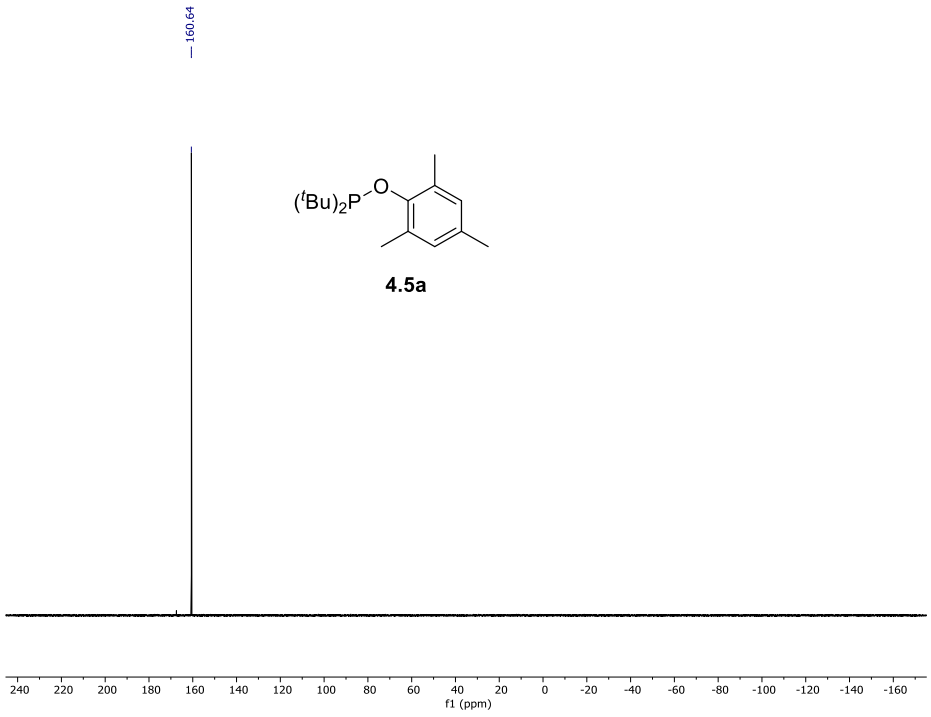

**Figure 4.12.** $^{1}$H-NMR Spectrum of **4.5b** in $C_6D_6$, 500 MHz

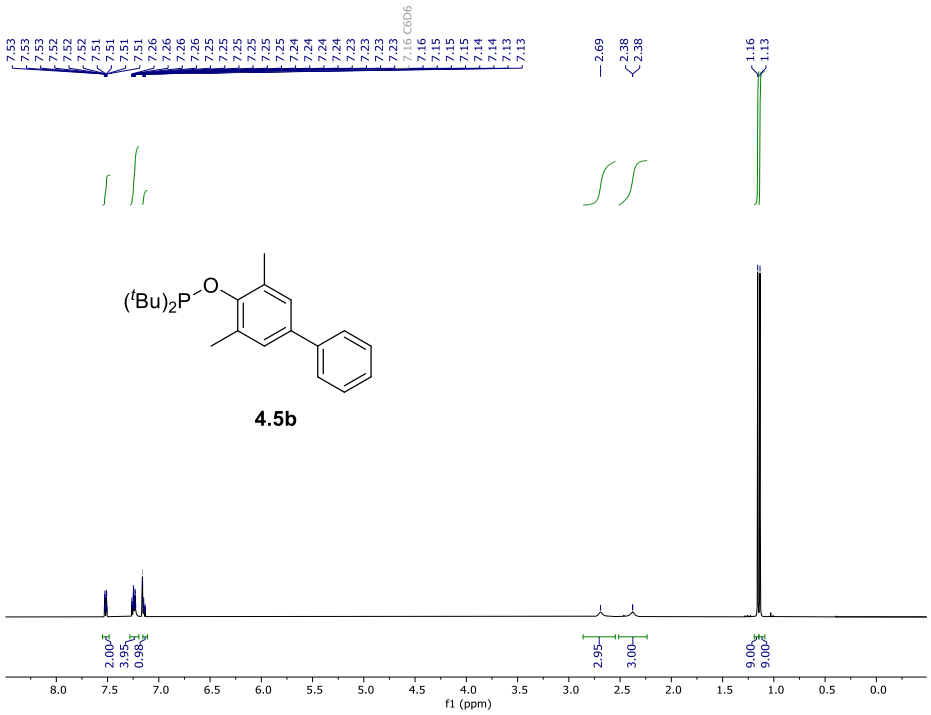


**Figure 4.13.** $^{31}$P-NMR Spectrum of **4.5b** in $C_6D_6$, 202 MHz

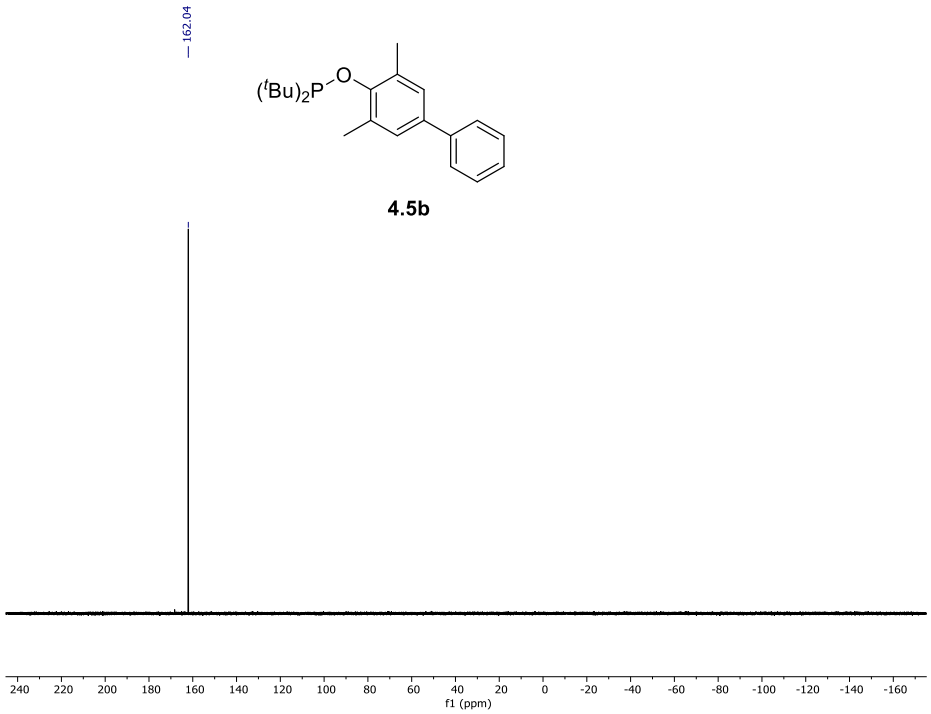

**Figure 4.14.** $^{1}$H-NMR Spectrum of **4.5c** in $C_6D_6$, 500 MHz

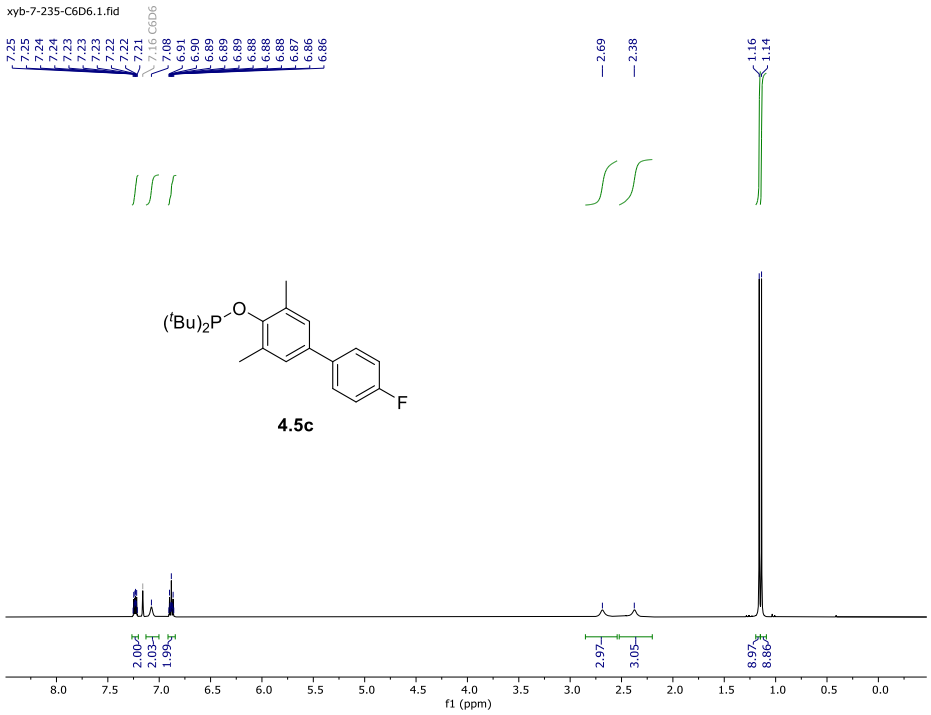


**Figure 4.15.** $^{13}$C-NMR Spectrum of **4.5c** in $C_6D_6$, 126 MHz

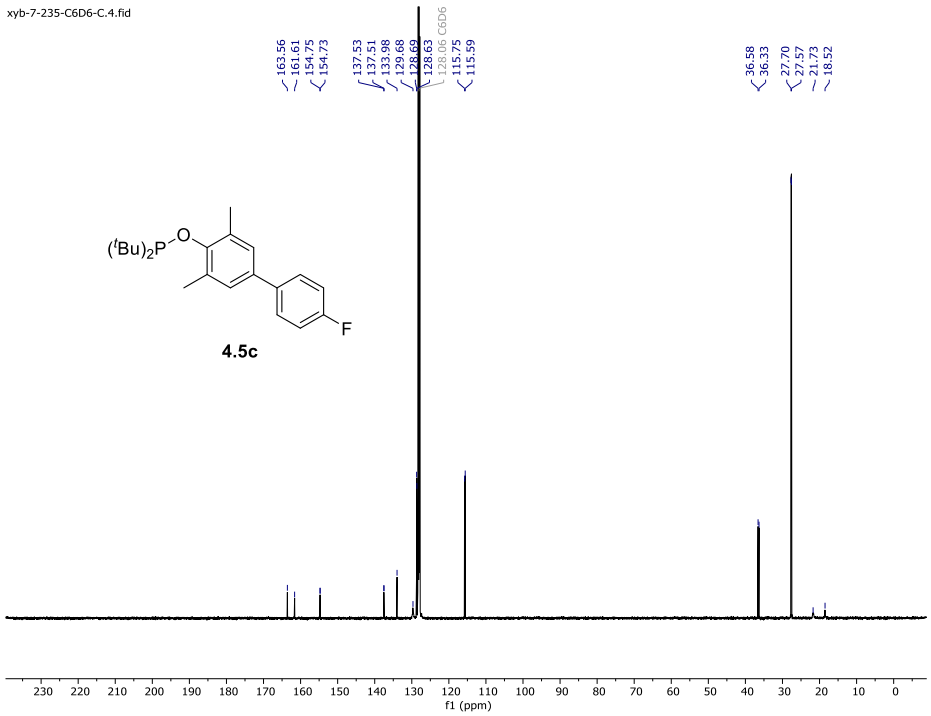

**Figure 4.16.** $^{31}$P-NMR Spectrum of **4.5c** in $C_6D_6$, 202 MHz

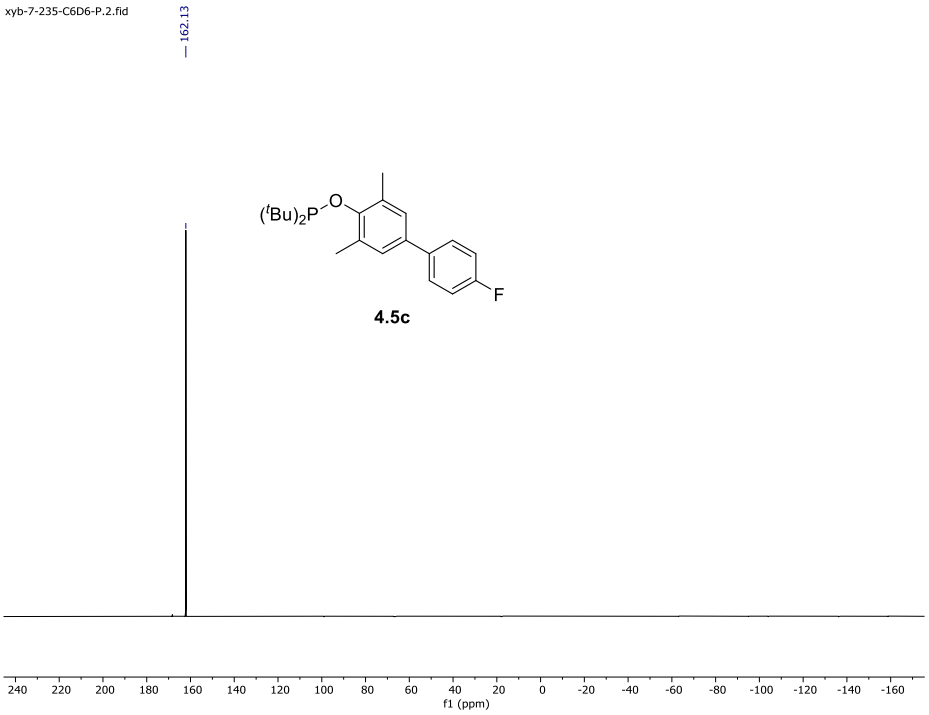


**Figure 4.17.** $^{19}$F-NMR Spectrum of **4.5c** in $C_6D_6$, 470 MHz

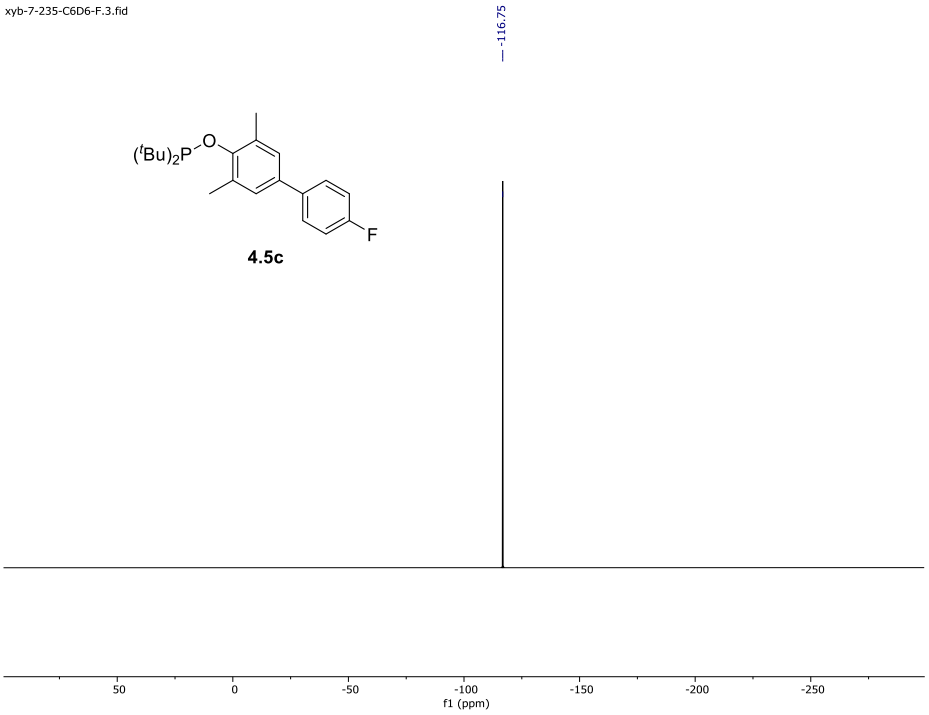

**Figure 4.18.** $^{1}$H-NMR Spectrum of **4.5e** in $C_6D_6$, 500 MHz

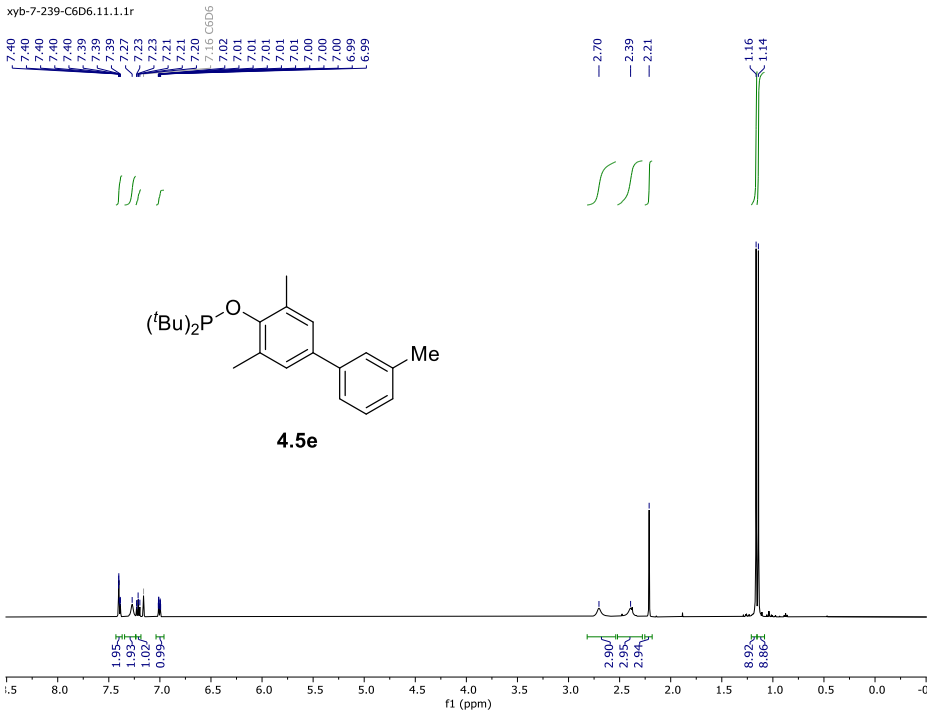


**Figure 4.19.** $^{13}$C-NMR Spectrum of **4.5e** in $C_6D_6$, 126 MHz

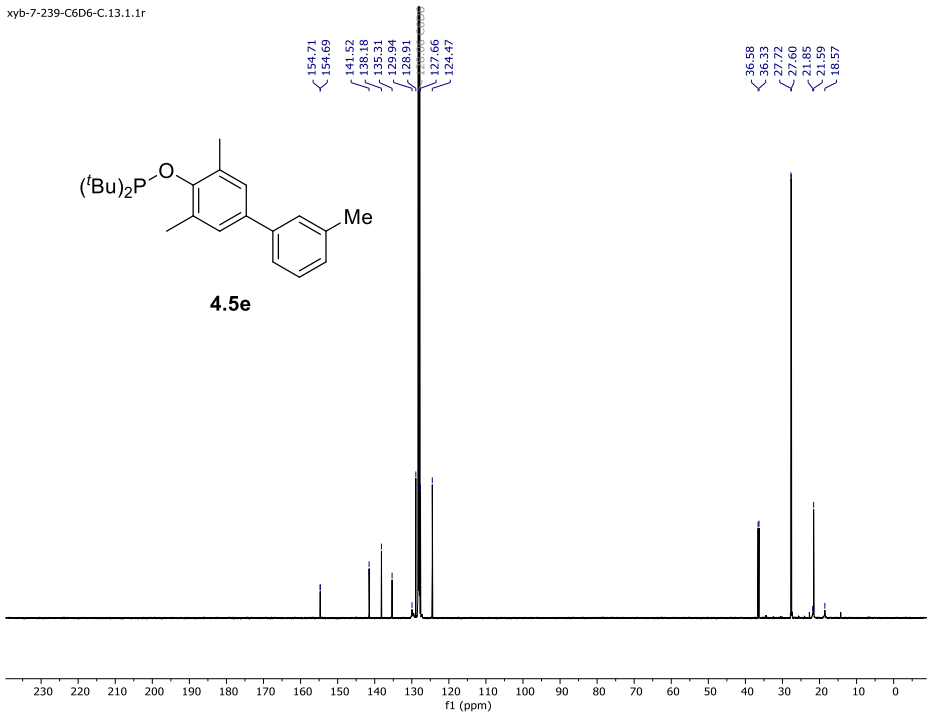

**Figure 4.20.** $^{31}$P-NMR Spectrum of **4.5e** in $C_6D_6$, 202 MHz

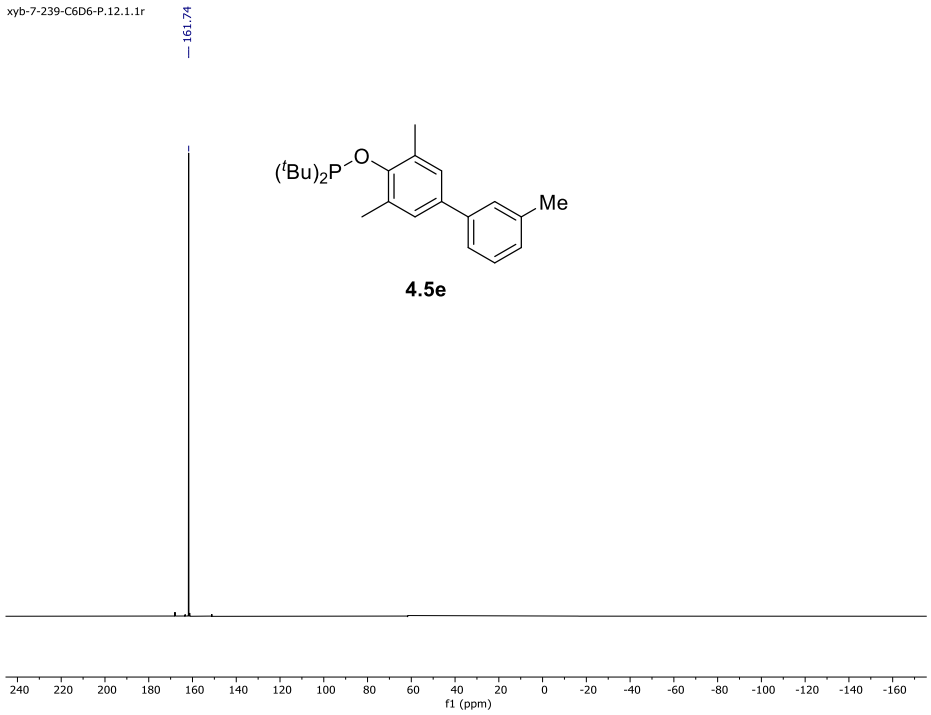

**Figure 4.21.** $^{1}$H-NMR Spectrum of **4.3a** in $CDCl_3$, 500 MHz

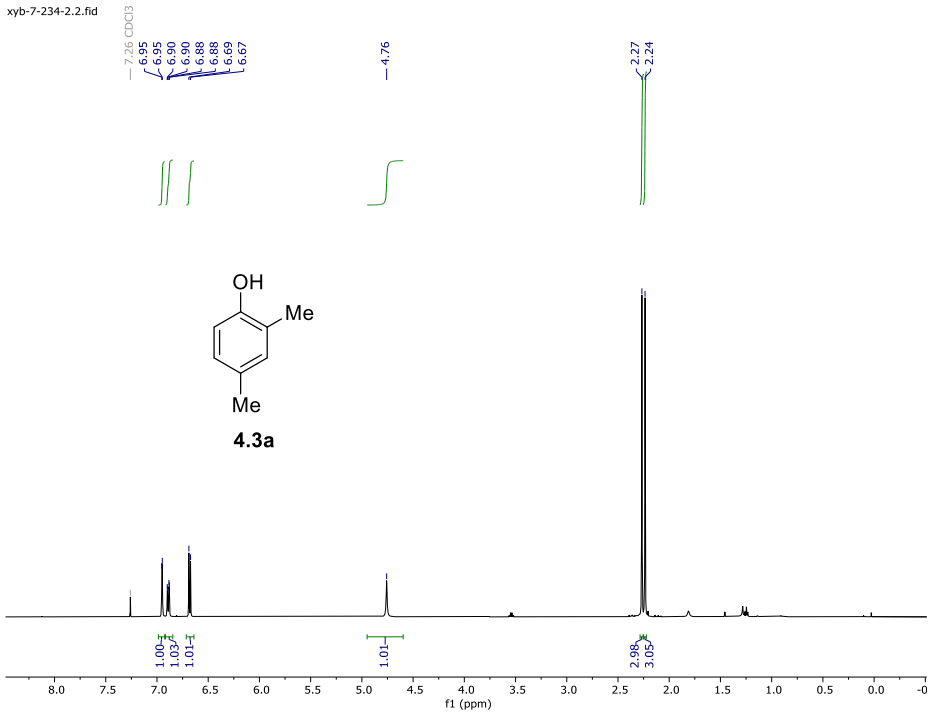


**Figure 4.22.** $^{13}$C-NMR Spectrum of **4.3a** in $CDCl_3$, 126 MHz

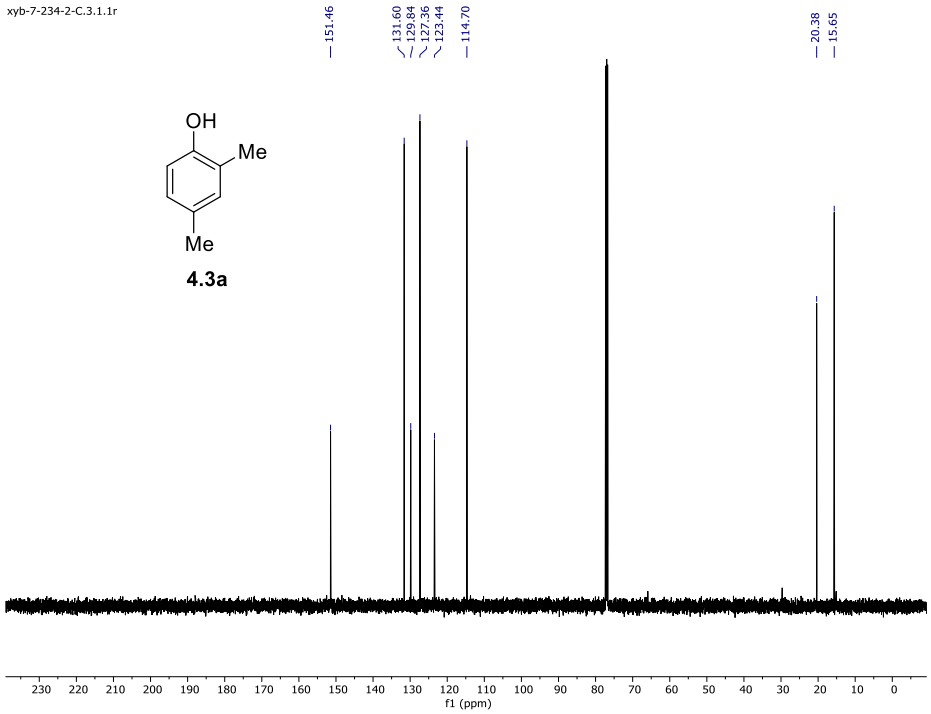

**Figure 4.23.** $^{1}$H-NMR Spectrum of **4.1a** in $CDCl_3$, 500 MHz

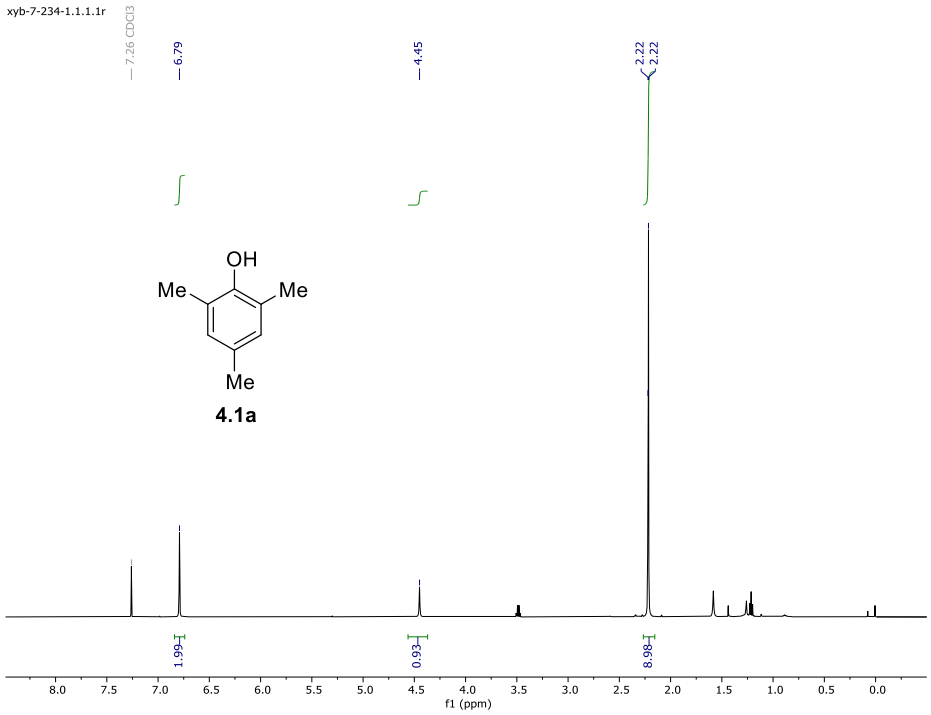


**Figure 4.24.** $^{13}$C-NMR Spectrum of **4.1a** in $CDCl_3$, 126 MHz

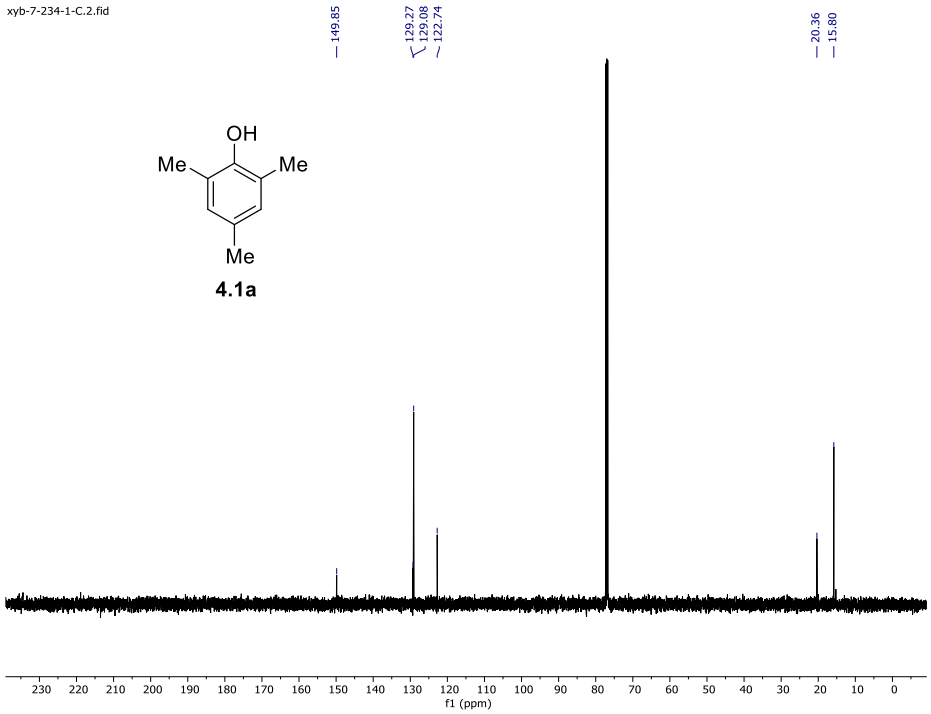

**Figure 4.25.** $^{1}$H-NMR Spectrum of **4.3b** in $CDCl_3$, 500 MHz

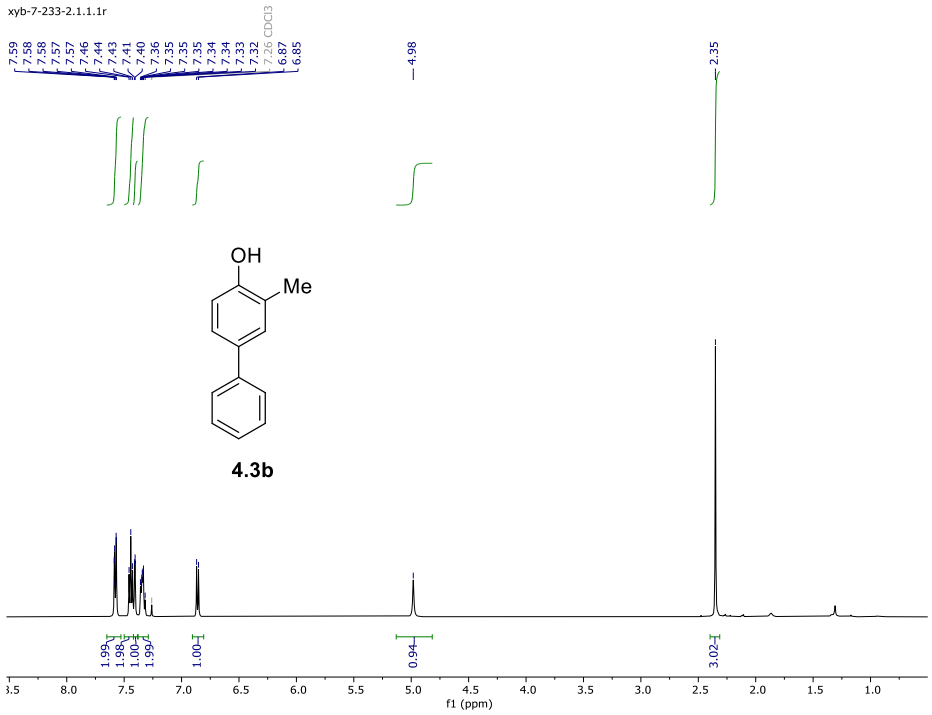


**Figure 4.26.** $^{13}$C-NMR Spectrum of **4.3b** in $CDCl_3$, 126 MHz

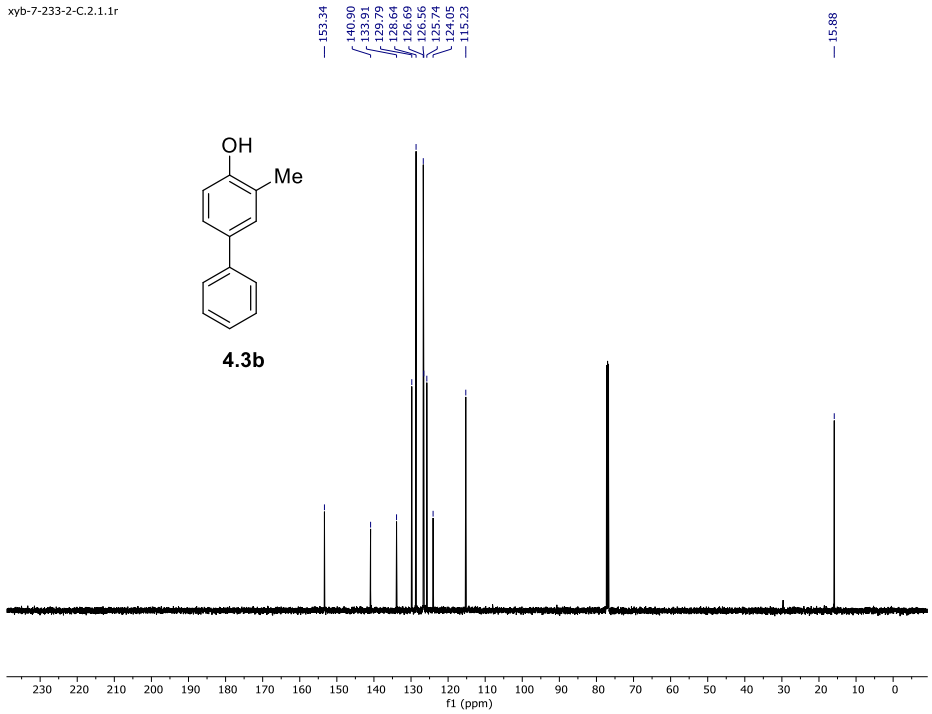

**Figure 4.27.** $^{1}$H-NMR Spectrum of **4.1b** in $CDCl_3$, 500 MHz

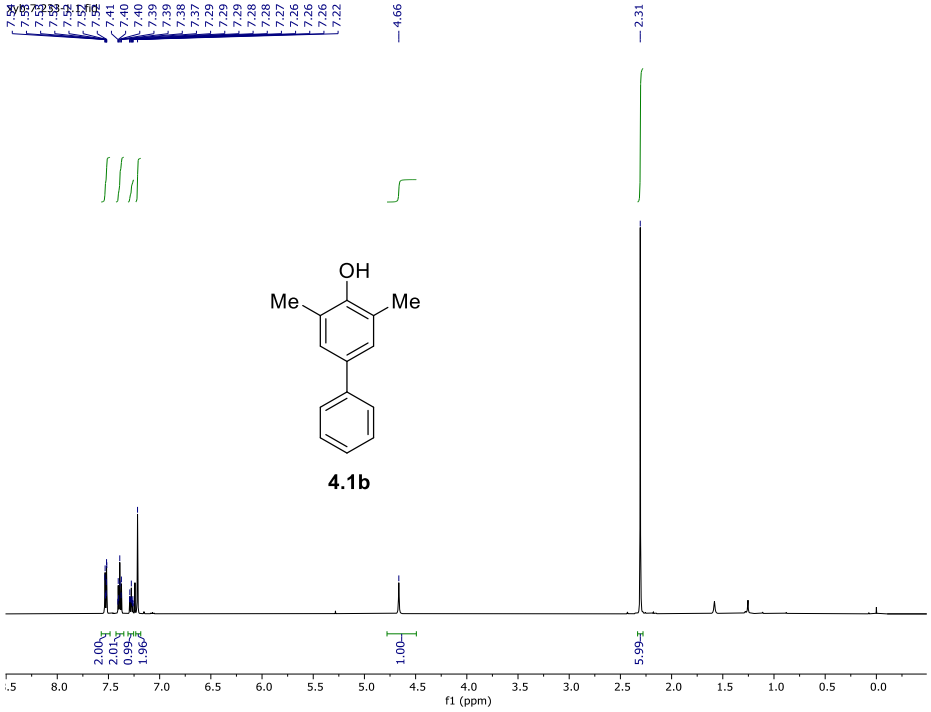


**Figure 4.28.** $^{13}$C-NMR Spectrum of **4.1b** in $CDCl_3$, 126 MHz

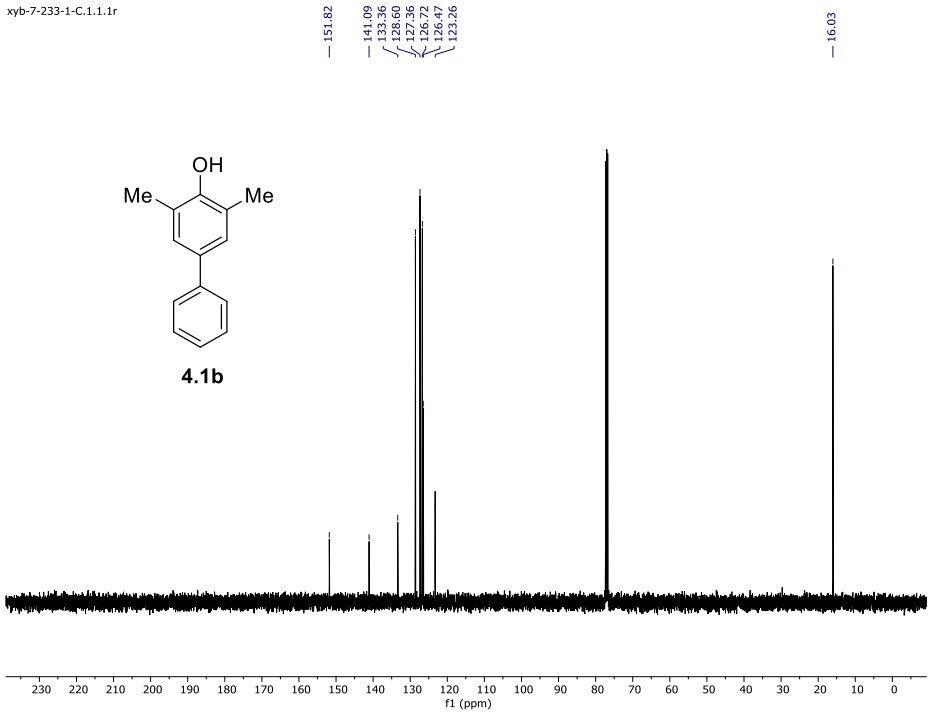

**Figure 4.29.** $^{1}$H-NMR Spectrum of **4.3c** in $CDCl_3$, 400 MHz

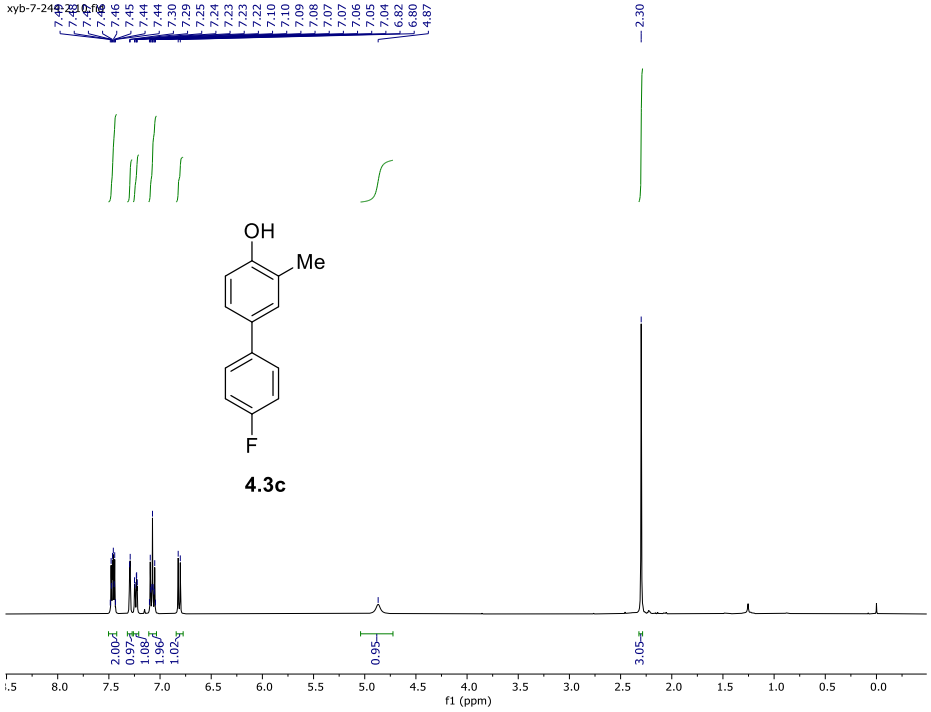


**Figure 4.30.** $^{13}$C-NMR Spectrum of **4.3c** in $CDCl_3$, 101 MHz

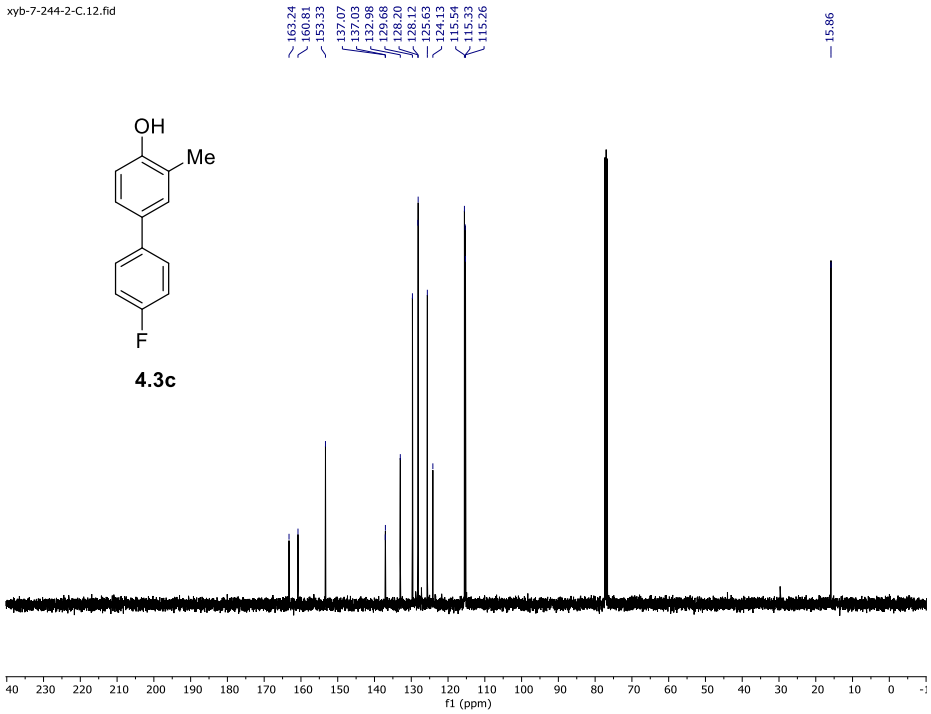

**Figure 4.31.** $^{19}$F-NMR Spectrum of **4.3c** in $CDCl_3$, 376 MHz

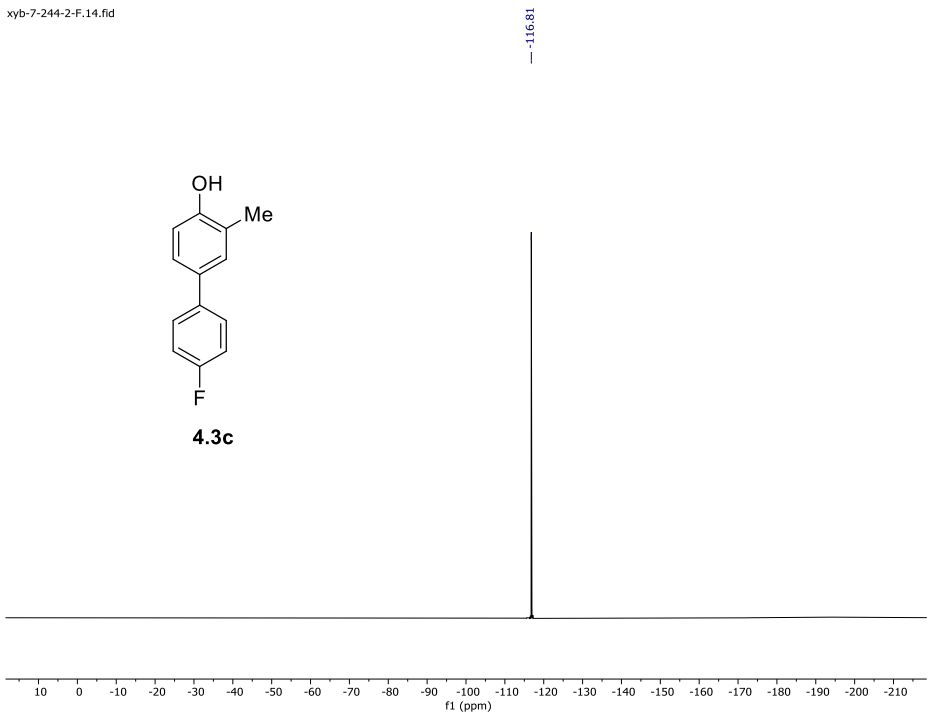

**Figure 4.32.** $^{1}$H-NMR Spectrum of **4.3e** in $CDCl_3$, 400 MHz

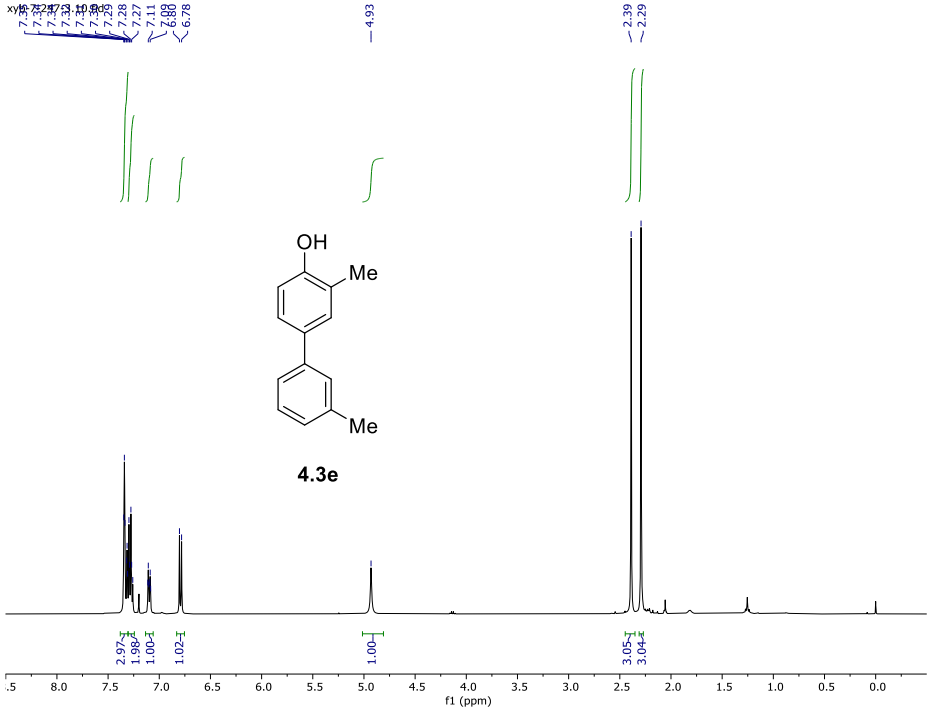


**Figure 4.33.** $^{13}$C-NMR Spectrum of **4.3e** in $CDCl_3$, 101 MHz

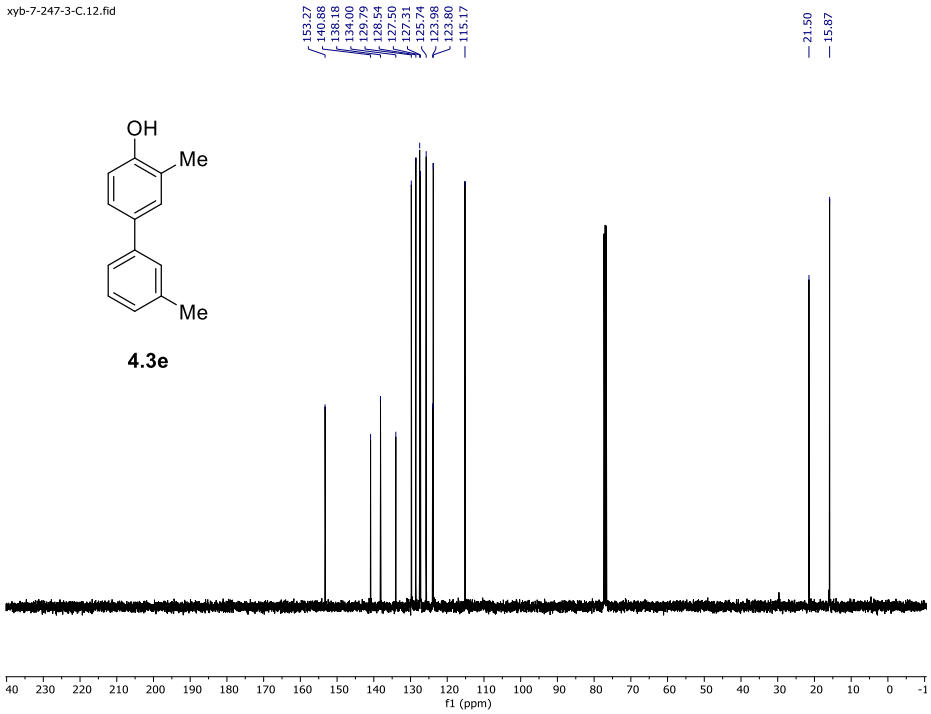

**4.6. References**

1. (a) van der Boom, M. E.; Milstein, D. Cyclometalated Phosphine-Based Pincer Complexes: Mechanistic Insight in Catalysis, Coordination, and Bond Activation. *Chem. Rev.* **2003,** *103*, 1759-1792. (b) Jun, C.-H. Transition metal-catalyzed carbon–carbon bond activation. *Chem. Soc. Rev.* **2004,** *33*, 610-618. (c) Tobisu, M.; Chatani, N. Catalytic reactions involving the cleavage of carbon–cyano and carbon–carbon triple bonds. *Chem. Soc. Rev.* **2008,** *37*, 300-307. (d) Chen, F.; Wang, T.; Jiao, N. Recent Advances in Transition-Metal-Catalyzed Functionalization of Unstrained Carbon–Carbon Bonds. *Chem. Rev.* **2014,** *114*, 8613-8661. (e) Souillart, L.; Cramer, N. Catalytic C–C Bond Activations via Oxidative Addition to Transition Metals. *Chem. Rev.* **2015,** *115*, 9410-9464. (f) Chen, P.-h.; Billett, B. A.; Tsukamoto, T.; Dong, G. "Cut and Sew" Transformations via Transition-Metal-Catalyzed Carbon–Carbon Bond Activation. *ACS Catal.* **2017,** *7*, 1340-1360. (g) Fumagalli, G.; Stanton, S.; Bower, J. F. Recent Methodologies That Exploit C–C Single-Bond Cleavage of Strained Ring Systems by Transition Metal Complexes. *Chem. Rev.* **2017,** *117*, 9404-9432. (h) Song, F.; Gou, T.; Wang, B.-Q.; Shi, Z.-J. Catalytic activations of unstrained C–C bond involving organometallic intermediates. *Chem. Soc. Rev.* **2018,** *47*, 7078-7115. (i) Deng, L.; Dong, G. Carbon–Carbon Bond Activation of Ketones. *Trends Chem.* **2020,** *2*, 183-198. (j) Xia, Y.; Dong, G. Temporary or removable directing groups enable activation of unstrained C–C bonds. *Nat. Rev. Chem.* **2020,** *4*, 600-614. (k) Murakami, M.; Ishida, N. Cleavage of Carbon–Carbon σ-Bonds of Four-Membered Rings. *Chem. Rev.* **2021,** *121*, 264-299. (l) Nakao, Y. Metal-mediated C–CN Bond Activation in Organic Synthesis. *Chem. Rev.* **2021,** *121*, 327-344.

2. (a) Murakami, M.; Ishida, N. Potential of Metal-Catalyzed C–C Single Bond Cleavage for Organic Synthesis. *J. Am. Chem. Soc.* **2016,** *138*, 13759-13769. (b) Wang, B.; Perea, M. A.;

Sarpong, R. Transition Metal-Mediated C−C Single Bond Cleavage: Making the Cut in Total Synthesis. *Angew. Chem., Int. Ed.* **2020,** *59*, 18898-18919.

3. (a) Gozin, M.; Weisman, A.; Ben-David, Y.; Milstein, D. Activation of a carbon–carbon bond in solution by transition-metal insertion. *Nature* **1993,** *364*, 699-701. (b) Liou, S.-Y.; Gozin, M.; Milstein, D. Directly Observed Oxidative Addition of a Strong Carbon-Carbon Bond to a Soluble Metal Complex. *J. Am. Chem. Soc.* **1995,** *117*, 9774-9775. (c) Rybtchinski, B.; Vigalok, A.; Ben-David, Y.; Milstein, D. A Room Temperature Direct Metal Insertion into a Nonstrained Carbon−Carbon Bond in Solution. C−C vs C−H Bond Activation. *J. Am. Chem. Soc.* **1996,** *118*, 12406-12415. (d) Liou, S.-Y.; E. van der Boom, M.; Milstein, D. Catalytic selective cleavage of a strong C–C single bond by rhodium in solution. *Chem. Commun.* **1998**, 687-688. (e) Rybtchinski, B.; Milstein, D. Solvent-Controlled Selectivity toward Exclusive C−C or C−H Bond Activation by a Cationic Metal Center. *J. Am. Chem. Soc.* **1999,** *121*, 4528-4529. (f) van der Boom, M. E.; Ben-David, Y.; Milstein, D. Formation of Difluoromethylene−Arenium Complexes by Consecutive Aryl−CF3 C−C Bond Activation and C−F Bond Cleavage. *J. Am. Chem. Soc.* **1999,** *121*, 6652-6656. (g) Gandelman, M.; Vigalok, A.; Konstantinovski, L.; Milstein, D. The First Observation and Kinetic Evaluation of a Single Step Metal Insertion into a C−C Bond. *J. Am. Chem. Soc.* **2000,** *122*, 9848-9849.

4. (a) Zhu, J.; Wang, J.; Dong, G. Catalytic activation of unstrained C(aryl)–C(aryl) bonds in 2,2′-biphenols. *Nat. Chem.* **2019,** *11*, 45-51. (b) Zhu, J.; Chen, P.-h.; Lu, G.; Liu, P.; Dong, G. Ruthenium-Catalyzed Reductive Cleavage of Unstrained Aryl–Aryl Bonds: Reaction Development and Mechanistic Study. *J. Am. Chem. Soc.* **2019,** *141*, 18630-18640. (c) Zhu, J.; Zhang, R.; Dong, G. Orthogonal cross-coupling through intermolecular metathesis of unstrained C(aryl)–C(aryl) single bonds. *Nat. Chem.* **2021,** *13*, 836-842.

5. Zhu, J.; Xue, Y.; Zhang, R.; Ratchford, B. L.; Dong, G. Catalytic Activation of Unstrained C(Aryl)–C(Alkyl) Bonds in 2,2′-Methylenediphenols. *J. Am. Chem. Soc.* **2022,** *144*, 3242-3249.

6. Rybtchinski, B.; Oevers, S.; Montag, M.; Vigalok, A.; Rozenberg, H.; Martin, J. M. L.; Milstein, D. Comparison of Steric and Electronic Requirements for C−C and C−H Bond Activation. Chelating vs Nonchelating Case. *J. Am. Chem. Soc.* **2001,** *123*, 9064-9077.

7. Jazzar, R. F. R.; Macgregor, S. A.; Mahon, M. F.; Richards, S. P.; Whittlesey, M. K. C−C and C−H Bond Activation Reactions in N-Heterocyclic Carbene Complexes of Ruthenium. *J. Am. Chem. Soc.* **2002,** *124*, 4944-4945.

8. Diggle, R. A.; Macgregor, S. A.; Whittlesey, M. K. Computational Study of C−C Activation of 1,3-Dimesitylimidazol-2-ylidene (IMes) at Ruthenium: The Role of Ligand Bulk in Accessing Reactive Intermediates. *Organometallics* **2008,** *27*, 617-625.

9. Onodera, S.; Ishikawa, S.; Kochi, T.; Kakiuchi, F. Direct Alkenylation of Allylbenzenes via Chelation-Assisted C–C Bond Cleavage. *J. Am. Chem. Soc.* **2018,** *140*, 9788-9792.